FOURTH EDITION

GAS TURBINE ENGINEERING HANDBOOK

MEHERWAN P. BOYCE



Copyrighted Materials
Copyright © 2012 Elsevier Retrieved from www.knovel.com

Gas Turbine Engineering Handbook

Fourth Edition

Meherwan P. Boyce

Managing Partner, The Boyce Consultancy
Fellow, American Society of Mechanical Engineers
Fellow, Institute of Diesel and Gas Turbine Engineers, U.K.



ELSEVIER

AMSTERDAM • BOSTON • HEIDELBERG • LONDON
NEW YORK • OXFORD • PARIS • SAN DIEGO
SAN FRANCISCO • SINGAPORE • SYDNEY • TOKYO
Butterworth-Heinemann is an imprint of Elsevier



Butterworth-Heinemann is an imprint of Elsevier
225 Wyman Street, Waltham, MA, 02451, USA
The Boulevard, Langford Lane, Kidlington, Oxford, OX5 1GB, UK

Fourth Edition 2012

Copyright © 2012 Elsevier Inc. All rights reserved.

No part of this publication may be reproduced, stored in a retrieval system or transmitted in any form or by any means electronic, mechanical, photocopying, recording or otherwise without the prior written permission of the publisher.

Permissions may be sought directly from Elsevier's Science & Technology Rights Department in Oxford, UK: phone: (+44) 1865 843830, fax: (+44) 1865 853333, e-mail: permissions@elsevier.com. Alternatively you can submit your request online by visiting the Elsevier web site at http://elsevier.com/locate/permissions, and selecting *Obtaining permission to use Elsevier material*.

Notice
No responsibility is assumed by the publisher for any injury and/or damage to persons or property as a matter of products liability, negligence or otherwise, or from any use or operation of any methods, products, instructions or ideas contained in the material herein. Because of rapid advances in the medical sciences, in particular, independent verification of diagnoses and drug dosages should be made.

British Library Cataloguing in Publication Data
A catalogue record for this book is available from the British Library.

Library of Congress Cataloging-in-Publication Data
A catalog record for this book is availabe from the Library of Congress.

ISBN: 978-0-12-383842-1

For information on all Butterworth-Heinemann publications visit our Web site at *www.elsevierdirect.com*

Printed and bound in United States of America
11 12 13 14 15 10 9 8 7 6 5 4 3 2 1

Working together to grow libraries in developing countries
www.elsevier.com | www.bookaid.org | www.sabre.org
ELSEVIER BOOK AID International Sabre Foundation

Copyrighted Materials
Copyright © 2012 Elsevier Retrieved from www.knovel.com

Preface to the Fourth Edition

The fourth edition of the *Gas Turbine Engineering Handbook* discusses the advancement in the areas of design, fabrication, installation, operation, and maintenance of gas turbines. This edition is written to better answer today's problems in the design, fabrication, installation, operation, and maintenance of gas turbines. This book has addressed most of the new developments and maintenance practices, in areas such as lubrication and controls for gas turbines over the past four years.

The use of gas turbines in the petrochemical, power generation, and offshore industries has mushroomed in the past few years. The power industry in the past 10 years has embraced the combined cycle power plants, and the new high-efficiency gas turbines are at the center of this growth segment of the industry. However, owing to the spiraling costs of natural gas, many of these plants designed for base load service have been cycled on a daily basis from part loads of 50% to full load, and in many cases, have had to be shutdown at weekends. The new maintenance chapters, with their case histories, should be of great assistance to the engineers in the field who have to operate their plant at other than design conditions of base loaded operation. Investigation into operation of these plants on other fuels is also covered in this edition.

In the first chapter, nearly 90 pages are devoted to the history of gas turbines and the details in the advancement in many of the major components in gas turbines. It is a summary of the major components in a gas turbine and their development over the years.

This edition also provides the basic fluid mechanics and thermodynamics for the young engineering graduate or undergraduate student who is being exposed to the field of turbomachinery for the first time. This book is very useful as a textbook for undergraduate or graduate turbomachinery courses as well as for in-house company training programs related to the petrochemical, power generation, and offshore industries. The fourth edition is not only an update of this technology in gas turbines but also provides a clearer understanding of the basic thermodynamics, cycles, and fluid mechanic relationships of turbines, as outlined in Chapters 2 and 3 based on the comments from many of the students who have used this book at the undergraduate level. These chapters with new figures and relationships have made it easier to understand the complex thermodynamics and fluid mechanic relationships, and also the new cycles, which have been introduced.

In this edition, chapters have been totally rewritten in the areas of combustors, axial and radial turbine expanders, and gear systems. The new chapter on combustors deals with the combustion problems with DLN combustors and the problems associated with these combustors such as flashback problems. The emphasis on low NO_x

emissions from gas turbines has led to the development of a new breed of Dry Low NO_x combustors, and their problems are dealt with in detail in this edition.

Hot gas turbine expanders, both axial and radial, have been dealt with in great detail in this edition. The new expanded chapter on radial turbines gives the reader much more insights into the design of these radial gas expanders and radial turbines. These turbines are getting more important as plant gases are being used to power turbines in refineries and other chemical plants.

The author thanks Ms. Lisa Ford, Director of Engineering, Power Transmission Division, Lufkin Industries Inc., who helped to rewrite this chapter so that the readers are exposed to the latest in gear technology as used in gas turbines. Detailed descriptions of the tools that make these gears and the gear characteristics are given in this expanded chapter.

This book deals with case histories of gas turbines from deterioration of the performance of gas turbines to failures encountered in all the major components of the gas turbine. The chapter on Maintenance Techniques has been completely rewritten and updated. These chapters deal with Long-Term Service Agreements (LTSAs), which have become the major service agreements for new advanced gas turbines, as lending institutions have more faith in the original equipment manufacturer for dealing with problems. Special maintenance tables have been added, so that the reader can troubleshoot problems on gas turbines they may encounter in the field.

The new advanced gas turbines have firing temperatures of 2600 °F (1427 °C) and pressure ratios exceeding 40:1 in aircraft gas turbines and over 30:1 in industrial turbines. This has led to the enhancement of axial flow compressor design; to fully understand the operating mechanics of these high-pressure-ratio axial-flow compressors, the reader must carefully read Chapter 7. The chapter covers in detail the advent of surge and describes in great detail the different mechanisms of surge, rotating stall, and choke flow conditions in the compressor of gas turbines.

Advances in materials and coatings have spurred the technology of compressor and turbine design, and the new editions have treated this new area in great detail. The last two editions have dealt with an upgrade in the design and maintenance of advanced gas turbines and with most of the applicable codes in the area of both performance and mechanical standards.

The last two new editions have been written with the experienced engineer in mind who is working in power plants and in petrochemical and offshore installations. These two editions should help him or her to understand more clearly problems encountered in the field and how to prevent them.

This new edition will give the manufacturer a glimpse of some of the problems associated with gas turbines in the field and help users to achieve maximum performance efficiency and high availability of their gas turbines.

I have been involved in the research, design, operation, and maintenance of gas turbines since the early 1960s. I have had the privilege of teaching courses at the graduate and undergraduate levels at the University of Oklahoma and Texas A&M University, and have lectured at universities in the United Kingdom, Japan, and India, and now, in general, in the industry. There have been over 4500 students through my courses, designed for the engineer in the field, representing over 520 companies from around

the world. They have used the book, and their comments and my field troubleshooting experiences have been very influential in the updating of material in these four editions. The enthusiasm of the students associated with these courses gave me the inspiration to undertake this endeavor. The many courses I have taught over the past 40 years have been an educational experience for me, and, I hope, have been satisfying for my students. The discussions that resulted from my association as a consultant to the power, petrochemical, and aviation industries with highly professional individuals have been a major contribution to both my personal and professional life as well as to this new edition of the book. In this edition, I have tried to assimilate the subject matter of various papers (and sometimes diverse views) into a comprehensive, unified treatment of gas turbines. Many illustrations, curves, and tables are employed to broaden the understanding of the descriptive text. I have provided extensive new charts that can be used to diagnose problems. In addition, the references direct the reader to sources of information that will help to investigate and solve specific problems. I hope that this book will serve as a reference text after it has accomplished its primary objective of introducing the reader to the broad subject of gas turbines.

I thank the many engineers whose published work and discussions I have had the privilege of using in the book, and whose articles make a cornerstone to this work. The Turbomachinery Symposium, which I have had the distinct honor of founding and chairing for eight years, and the proceedings of the Symposium have contributed many interesting technology issues from a design and maintenance point of view to this book. Special thanks to my colleagues on the Advisory Committee of the Texas A&M University Turbomachinery Symposium, of which I have been a member for 40 years, and to Dr. Dara Childs, who is now the chairman of the Advisory Committee.

My very special thanks to my wife, Zarine, for her readiness to help and her constant encouragement throughout this project.

I sincerely hope that my readers from all over the world, who have made this the most read book in the field over the past 35 years, find this new edition as interesting as the past three editions. I hope that my 50 years of experience in the field will be beneficial to all who read this book.

Meherwan P. Boyce
Houston, Texas

Preface to the Third Edition

Gas Turbine Engineering Handbook discusses the design, fabrication, installation, operation, and maintenance of gas turbines. The third edition is not only an updating of the technology in gas turbines, which has seen a great leap forward in the 2000s, but also a rewriting of various sections to better answer today's problems in the design, fabrication, installation, operation, and maintenance of gas turbines. The third edition has added a new chapter that examines the case histories of gas turbines from deterioration of the performance of gas turbines to failures encountered in all the major components of the gas turbine. The chapter on Maintenance Techniques has been completely rewritten and updated. The revised chapter deals with Long Term Service Agreements (LTSAs), and special maintenance tables have been added so that you can troubleshoot problems on gas turbines that you may encounter.

The new advanced gas turbines have firing temperatures of 2600 °F (1427 °C), and pressure ratios exceeding 40:1 in aircraft gas turbines, and over 30:1 in industrial turbines. This has led to the rewriting of Chapter 7, to fully understand the operating mechanics of these high pressure ratio axial-flow compressors. The chapter covers in detail the advent of surge, and describes in great detail the different mechanisms of surge, rotating stall, and choke flow conditions in the compressor of the gas turbine. Advances in materials and coatings have spurred this technology, and the new edition has treated this new area in great detail. The emphasis on low NO_x emissions from gas turbines has led to the development of a new breed of Dry Low NO_x combustors, and their problems are dealt with in depth in this new edition. The third edition deals with an upgrade in the design and maintenance of advanced gas turbines and deals with most of the applicable codes both in the area of performance and mechanical standards.

The new edition has been written with the experienced engineer in mind who is working in power plants, and in petrochemical and offshore installations. This edition should help him or her understand more clearly problems encountered in the field, and how to prevent them.

The book also provides the basic fluid mechanics and thermodynamics for the young engineering graduate or undergraduate student who is being exposed to the turbomachinery field for the first time. The book is very useful as a textbook for undergraduate or graduate turbomachinery courses as well as for in-house company training programs related to the petrochemical, power generation, and offshore industries.

The use of gas turbines in the petrochemical, power generation, and offshore industries has mushroomed in the past few years. The power industry in the past ten years has embraced the combined cycle power plants, and the new high-efficiency gas turbines are at the center of this growth segment of the industry. However, due to the

spiraling costs of natural gas, many of these plants designed for base load service have been cycled on a daily basis from part loads of 50% to full load, and in many cases have had to be shutdown on weekends. The new maintenance chapters, with their case histories, should be of great assistance to the engineers in the field who have to operate their plant at other than design conditions of base loaded operation. Investigation of operating these plants on other fuels is also handled in this edition.

The book will give the manufacturer a glimpse of some of the problems associated with gas turbines in the field and help users to achieve maximum performance efficiency and high availability of their gas turbines.

I have been involved in the research, design, operation, and maintenance of gas turbines since the early 1960s. I have also taught courses at the graduate and undergraduate level at the University of Oklahoma and Texas A&M University, and now, in general, to the industry. There have been over 4000 students through my courses designed for the engineer in the field, representing over 450 companies from around the world. They have used the book, and their comments and my field troubleshooting experience have been very influential in the updating of material in this edition. The enthusiasm of the students associated with these courses gave me the inspiration to undertake this endeavor. The many courses I have taught over the past 35 years have been an educational experience for me as well as for the students. The discussions and consultations that resulted from my association as a consultant to the power, petrochemical, and aviation industries with highly professional individuals have been a major contribution to both my personal and professional life as well as to this new edition of the book.

In this edition I have tried to assimilate the subject matter of various papers (and sometimes diverse views) into a comprehensive, unified treatment of gas turbines. Many illustrations, curves, and tables are employed to broaden the understanding of the descriptive text. I have provided extensive new charts that can be used to diagnose problems. In addition, the references direct you to sources of information that will help you investigate and solve your specific problems. I hope that this book will serve as a reference text after it has accomplished its primary objective of introducing you to the broad subject of gas turbines.

I wish to thank the many engineers whose published work and discussions have been a cornerstone to this work. The Turbomachinery Symposium, of which I had the distinct honor and pleasure of founding and chairing for eight years, and the proceedings of the Symposium, have contributed many interesting technology issues from both a design and maintenance point of view. A special thanks also goes to my colleagues on the Advisory Committee of the Texas A&M University Turbomachinery Symposium, of which I have been a member for 34 years, and to Dr. Dara Childs, who is now the chairman of the Advisory Committee.

I wish to acknowledge and give a very special thanks to my wife, Zarine, for her readiness to help and her constant encouragement throughout this project. A special thanks also to my secretary and executive assistant Donna Masters for the hours she has spent working with me on this new edition.

I sincerely hope that this new edition will be educational and will enable you to get a new updated look at gas turbine technology and enhanced maintenance practices, while retaining the basic theory that governs the development of gas turbines.

Meherwan P. Boyce
Houston, Texas
September 2005

Preface to the Second Edition

Gas Turbine Engineering Handbook discusses the design, fabrication, installation, operation, and maintenance of gas turbines. The second edition is not only an updating of the technology in gas turbines, which has seen a great leap forward in the 1990s, but also a rewriting of various sections to better answer today's problems in the design, fabrication, installation, operation, and maintenance of gas turbines. The new advanced gas turbines have firing temperatures of 2600 °F (1427 °C), and pressure ratio's exceeding 40:1 in aircraft gas turbines, and over 30:1 in industrial turbines. Advances in materials and coatings have spurred this technology, and the new edition has treated this new area in great detail. The emphasis on low NO_x emissions from gas turbines has led to the development of a new breed of dry low NO_x combustors, which are dealt with in depth in this new edition. The second edition deals with an upgrade of most of the applicable codes both in the area of performance and mechanical standards.

The book has been written to provide an overall view for the experienced engineer working in a specialized aspect of the subject and for the young engineering graduate or undergraduate student who is being exposed to the turbomachinery field for the first time. The book will be very useful as a textbook for undergraduate turbomachinery courses as well as for in-house company training programs related to the petrochemical, power generation, and offshore industries.

The use of gas turbines in the petrochemical, power generation, and offshore industries has mushroomed in the past few years. In the past 10 years, the power industry has embraced the Combined Cycle Power Plants and the new high efficiency gas turbines are at the center of this growth segment of the industry. This has also led to the rewriting of Chapters 1 and 2. It is to these users and manufacturers of gas turbines that this book is directed. The book will give the manufacturer a glimpse of some of the problems associated with his equipment in the field and help the user to achieve maximum performance efficiency and high availability of his gas turbines.

I have been involved in the research, design, operation, and maintenance of gas turbines since the early 1960s. I have also taught courses at the graduate and undergraduate level at the University of Oklahoma and Texas A&M University, and now, in general, to the industry. There have been over 3,000 students through my courses designed for the engineer in the field representing over 400 companies from around the world. Companies have used the book, and their comments have been very influential in the updating of material in the second edition. The enthusiasm of the students associated with these courses gave me the inspiration to undertake this endeavor. The many courses I have taught over the past 25 years have been an educational experience for me as well as for the students. The Texas A&M University Turbomachinery

Symposium, which I had the privilege to organize and chair for over eight years and be part of the Advisory Committee for 30 years, is a great contributor to the operational and maintenance sections of this book. The discussions and consultations that resulted from my association with highly professional individuals have been a major contribution to both my personal and professional life as well as to this book.

In this book, I have tried to assimilate the subject matter of various papers (and sometimes diverse views) into a comprehensive, unified treatment of gas turbines. Many illustrations, curves, and tables are employed to broaden the understanding of the descriptive text. Mathematical treatments are deliberately held to a minimum so that the reader can identify and resolve any problems before he is ready to execute a specific design. In addition, the references direct the reader to sources of information that will help him to investigate and solve his specific problems. It is hoped that this book will serve as a reference text after it has accomplished its primary objective of introducing the reader to the broad subject of gas turbines.

I wish to thank the many engineers whose published work and discussions have been a cornerstone to this work. I especially thank all my graduate students and former colleagues on the faculty of Texas A&M University without whose encouragement and help this book would not be possible. Special thanks go to the Advisory Committee of the Texas A&M University Turbomachinery Symposium and Dr. M. Simmang, Chairman of the Texas A&M University Department of Mechanical Engineering, who were instrumental in the initiation of the manuscript.

I wish to acknowledge and give special thanks to my wife, Zarine, for her readiness to help and her constant encouragement throughout this project.

I sincerely hope that this new edition will be as interesting to read as it was for me to write and that it will be a useful reference to the fast-growing field of turbomachinery.

Finally, I would like to add that the loss of my friend and mentor Dr. C.M. Simmang who has written the foreword to the first edition of this book is a deep loss not only to me but also to the engineering educational community and to many of his students from Texas A&M University.

Meherwan P. Boyce
Houston, Texas

Preface to the First Edition

Gas Turbine Engineering Handbook discusses the design, fabrication, installation, operation, and maintenance of gas turbines. The book has been written to provide an overall view for the experienced engineer working in a specialized aspect of the subject and for the young engineering graduate or undergraduate student who is being exposed to the turbomachinery field for the first time. The book will be very useful as a textbook for undergraduate turbomachinery courses as well as for in-house company training programs related to the petrochemical, power generation, and offshore industries.

The use of gas turbines in the petrochemical, power generation, and offshore industries has mushroomed in the past few years. It is to these users and manufacturers of gas turbines that this book is directed. The book will give the manufacturer a glimpse of some of the problems associated with his equipment in the field and help the user to achieve maximum performance efficiency and high availability of his gas turbines.

I have been involved in the research, design, operation, and maintenance of gas turbines since the early 1960s. I have also taught courses at the graduate and undergraduate level at the University of Oklahoma and Texas A&M University, and now, in general, to the industry. The enthusiasm of the students associated with these courses gave me the inspiration to undertake this endeavor. The many courses I have taught over the past 15 years have been an educational experience for me as well as for the students. The Texas A&M University Turbomachinery Symposium, which I had the privilege to organize and chair for seven years, is a great contributor to the operational and maintenance sections of this book. The discussions and consultations that resulted from my association with highly professional individuals have been a major contribution to both my personal and professional life as well as to this book.

In this book, I have tried to assimilate the subject matter of various papers (and sometimes diverse views) into a comprehensive, unified treatment of gas turbines. Many illustrations, curves, and tables are employed to broaden the understanding of the descriptive text. Mathematical treatments are deliberately held to a minimum so that the reader can identify and resolve any problems before he is ready to execute a specific design. In addition, the references direct the reader to sources of information that will help him to investigate and solve his specific problems. It is hoped that this book will serve as a reference text after it has accomplished its primary objective of introducing the reader to the broad subject of gas turbines.

I wish to thank the many engineers whose published work and discussions have been a cornerstone to this work. I especially thank all my graduate students and

former colleagues on the faculty of Texas A&M University without whose encouragement and help this book would not be possible. Special thanks go to the Advisory Committee of the Texas A&M University Turbomachinery Symposium and Dr. C.M. Simmang, Chairman of the Texas A&M University Department of Mechanical Engineering, who were instrumental in the initiation of the manuscript, and to Janet Broussard for the initial typing of the manuscript. Acknowledgment is also gratefully made of the competent guidance of William Lowe and Scott Becken of Gulf Publishing Company. Their cooperation and patience facilitated the conversion of the raw manuscript to the finished book. Lastly, I wish to acknowledge and give special thanks to my wife, Zarine, for her readiness to help and her constant encouragement throughout this project.

I sincerely hope that this book will be as interesting to read as it was for me to write and that it will be a useful reference to the fast-growing field of turbomachinery.

Meherwan P. Boyce
Houston, Texas

Copyrighted Materials
Copyright © 2012 Elsevier Retrieved from www.knovel.com

Contents

Preface to the Fourth Edition **xix**
Preface to the Third Edition **xxiii**
Preface to the Second Edition **xxvii**
Preface to the First Edition **xxix**
Foreword to the First Edition **xxxi**
About the Author **xxxiii**

Part I Design: Theory and Practice **1**

1 An Overview of Gas Turbines **3**
Gas Turbine Cycle in the Combined Cycle or Cogeneration Mode **3**
Gas Turbine Performance **6**
Gas Turbine Design Considerations **11**
Categories of Gas Turbines **15**
Frame Type Heavy-Duty Gas Turbines **16**
Aircraft-Derivative Gas Turbines **30**
Industrial-Type Gas Turbines **39**
Small Gas Turbines **42**
Vehicular Gas Turbines **44**
Microturbines **50**
Major Gas Turbine Components **51**
Compressors **51**
Regenerators/Recuperators **57**
Fuel Type **59**
Combustors **61**
Environmental Effects **62**
Turbine Expander Section **76**
Radial-Inflow Turbine **76**
Mixed-Flow Turbine **77**
Axial-Flow Turbines **78**
Materials **80**
Coatings **83**
Gas Turbine Heat Recovery **83**
Supplementary Firing of Heat Recovery Systems **85**
Instrumentation and Controls **87**

2 Theoretical and Actual Cycle Analyses 89
The Brayton Cycle **89**
Regeneration Effect **92**
Increasing the Work Output of the Simple-Cycle Gas Turbine **95**
Intercooling and Reheating Effects **95**
Actual Cycle Analysis **98**
The Simple Cycle **98**
The Split-Shaft Simple Cycle **100**
The Regenerative Cycle **101**
The Inter-cooled Simple Cycle **102**
The Reheat Cycle **103**
The Inter-cooled Regenerative Reheat Cycle **105**
The Steam Injection Cycle **105**
The Evaporative Regenerative Cycle **109**
The Brayton–Rankine Cycle **110**
Summation of Cycle Analysis **113**
A General Overview of Combined-Cycle Plants **114**
Compressed Air Energy Storage Cycle **121**
Power Augmentation **122**
Inlet Cooling **122**
Injection of Compressed Air, Steam, or Water **124**
Inlet Cooling Techniques **124**
Evaporative Cooling of the Turbine **124**
Refrigerated Inlets for the Gas Turbines **125**
Combination of Evaporative and Refrigerated Inlet Systems **127**
Thermal Energy Storage Systems **128**
Injection of Compressed Air, Steam, or Water for Increasing Power **128**
Mid-Compressor Flashing of Water **128**
Injection of Humidified and Heated Compressed Air **129**
Combination of Evaporative Cooling and Steam Injection **131**
Summation of the Power Augmentation Systems **132**
Bibliography **137**

3 Compressor and Turbine Performance Characteristics 139
Aerothermodynamics of Turbomachinery **139**
Ideal Gas **140**
Dry- and Wet-bulb Temperatures **144**
Optical and Radiation Pyrometers **148**
Ideal Gas Laws **149**
Compressibility Effect **150**
Aerothermal Equations **153**
Continuity Equation **153**
Momentum Equation **154**
Energy Equation **156**

Efficiencies 157
Adiabatic Thermal Efficiency 158
Polytropic Efficiency 161
Dimensional Analysis 163
Compressor Performance Characteristics 166
Turbine Performance Characteristics 167
Gas Turbine Performance Computation 167
Bibliography 176

4 Performance and Mechanical Standards 177
Major Variables for a Gas Turbine Application 177
Type of Application 177
Plant Location and Site Configuration 179
Plant Type 180
Gas Turbine Size and Efficiency 180
Type of Fuel 180
Enclosures 183
Plant Operation Mode: Base or Peaking 184
Start-Up Techniques 184
Performance Standards 184
ASME PTC 19.1: Test Uncertainty 185
ASME PTC 19.3: Part 3: Temperature Measurement Instruments and Apparatus 185
ASME PTC 19.5: Flow Measurement, Published 2004 186
PTC 19.10: Flue and Exhaust Gas Analyses, Part 10 187
ASME PTC 19.11: Steam and Water Sampling, Conditioning, and Analysis in the Power Cycle 187
ASME PTC 19.23: Guidance Manual for Model Testing, Published 1980 188
ASME PTC 46: Performance Test Code on Overall Plant Performance, Published January 1, 1996 188
Object and Scope 188
Performance Test Code on Gas Turbines 190
ASME PTC 22, Published 2006 190
ASME Measurement of Exhaust Emissions from Stationary Gas Turbine Engines B133.9, Published 1994 190
ASME PTC 36 Measurement of Industrial Sound (ASME B133.8), Published 2004 191
Mechanical Parameters 191
ASME B 133.2 Basic Gas Turbines, Published 1977 (Reaffirmed: 1997) 192
ASME B133.3 Procurement Standard for Gas Turbine Auxiliary Equipment, Published 1981 (Reaffirmed 1994) 192
ASME B133.4 Gas Turbine Control and Protection Systems, Published 1978 (Reaffirmed: 1997) 192

ASME B133.5 Procurement Standard for Gas Turbine Electrical Equipment, Published 1978 (Reaffirmed: 1994) **193**
ASME B 133.7M Gas Turbine Fuels, Published 1985 (Reaffirmed: 1992) **193**
ASME B133.8 Gas Turbine Installation Sound Emissions, Published 1977 (Reaffirmed: 1989) **193**
ASME B133.9 Measurement of Exhaust Emissions from Stationary Gas Turbine Engines, Published: 1994 **193**
API Std 616 Gas Turbines for the Petroleum, Chemical, and Gas Industry Services, Fourth Edition, August 1998 **194**
API Std 613 Special Purpose Gear Units for Petroleum, Chemical, and Gas Industry Services, Fourth Edition, June 1995 **194**
API Std 614 Lubrication, Shaft-Sealing, and Control-Oil Systems and Auxiliaries for Petroleum, Chemical, and Gas Industry Services, Fourth Edition, April 1999 **194**
API Std 618, Reciprocating Compressors for Petroleum, Chemical, and Gas Industry Services, Fourth Edition, June 1995 **195**
API Std 619, Rotary-Type Positive Displacement Compressors for Petroleum, Chemical, and Gas Industry Services, Third Edition, June 1997 **195**
ANSI/API Std 670 Vibration, Axial-Position, and Bearing-Temperature Monitoring Systems, Third Edition, November 1993 **195**
API Std 671, Special Purpose Couplings for Petroleum, Chemical, and Gas Industry Services, Third Edition, October 1998 **195**
API Std 677, General-Purpose Gear Units for Petroleum, Chemical, and Gas Industry Services, Second Edition, July 1997 (Reaffirmed: March 2000) **196**
Application of the Mechanical Standards to the Gas Turbine **196**
Gears **203**
Lubrication Systems **205**
Vibration Measurements **206**
Specifications **208**

5 Rotor Dynamics 215
Mathematical Analysis **215**
Undamped Free System **217**
Damped System **218**
Forced Vibrations **222**
Design Considerations **224**
Application to Rotating Machines **226**
Rigid Supports **226**
Flexible Supports **228**
Critical Speed Calculations for Rotor Bearing Systems **230**

Electromechanical Systems and Analogies 232
Forces Acting on a Rotor-Bearing System 233
Rotor-Bearing System Instabilities 236
Self-Excited Instabilities 239
Campbell Diagram 244
Bibliography 250

Part II Major Components 251

6 Centrifugal Compressors 253
Centrifugal Compressor Components 254
Inlet Guide Vanes 260
Impeller 262
Inducer 264
Centrifugal Section of an Impeller 267
Causes of Slip in an Impeller 269
Stodola Slip Factor 272
Stanitz Slip Factor 273
Diffusers 274
Scroll or Volute 275
Centrifugal Compressor Performance 278
Rotor Losses 279
Stator Losses 281
Compressor Surge 283
Effects of Gas Composition 289
External Causes and Effects of Surge 290
Surge Detection and Control 291
Process Centrifugal Compressors 292
Compressor Configuration 295
Impeller Fabrication 298
Bibliography 299

7 Axial-Flow Compressors 303
Introduction 303
Blade and Cascade Nomenclature 306
Elementary Airfoil Theory 309
Laminar-Flow Airfoils 311
Energy Increase 313
Velocity Triangles 313
Degree of Reaction 315
Radial Equilibrium 319
Diffusion Factor 320
The Incidence Rule 321
The Deviation Rule 323

Compressor Operation Characteristics **328**
Compressor Surge **328**
Compressor Choke **331**
Compressor Stall **331**
Individual Blade Stall **332**
Rotating Stall **332**
Stall Flutter **333**
Compressor Performance Parameters **337**
Performance Losses in an Axial-Flow Compressor **340**
New Developments in Axial-Flow Compressors **342**
Axial-Flow Compressor Research **344**
Cascade Tests **345**
Blade Profile **345**
Compressor Blade Material **351**
Acknowledgments **354**
Bibliography **355**

8 Radial-Inflow Turbines **357**
Hydraulic Radial-Inflow Turbines **357**
Radial-Inflow Turbines for Gas Applications **358**
Turbine Configurations **361**
Thermodynamic and Aerodynamic Theory **368**
Turbine Design Considerations **374**
Performance of a Radial-Inflow Turbine **376**
Losses in a Radial-Inflow Turbine **380**
Radial-Inflow Turbine Applications **381**
Bibliography **383**

9 Axial-Flow Turbines **385**
Turbine Geometry **385**
Thermodynamic and Aerodynamic Theory **387**
Utilization Factor **391**
Degree of Reaction **391**
Work Factor **392**
Velocity Diagrams **393**
Zero-Exit Swirl Diagram **393**
Impulse Diagram **394**
Symmetrical Diagram **394**
Impulse Turbine **394**
Turbine Blade Cooling Concepts **401**
Convection Cooling **405**
Impingement Cooling **405**
Film Cooling **405**
Transpiration Cooling **405**
Water/Steam Cooling **405**

Turbine Blade Cooling Design **406**
Convection and Impingement Cooling/Strut Insert Design **406**
Film and Convection Cooling Design **406**
Transpiration Cooling Design **408**
Multiple Small-Hole Design **408**
Water-Cooled Turbine Blades **410**
Steam-Cooled Turbine Blades **412**
Cooled-Turbine Aerodynamics **412**
Turbine Losses **420**
Bibliography **425**

10 Combustors **427**
Gas Turbine Combustors **427**
Typical Combustor Arrangements **429**
Can-Annular and Annular Combustors **429**
Silo-Type Combustors **431**
Combustion in Combustors **431**
The Diffusion-Type Combustor **432**
Air-Pollution Problems in a Diffusion Combustor **443**
Smoke **443**
Oxides of Nitrogen **443**
NO_x Prevention **445**
Diffusion Combustor Design **448**
The Diffusion Combustor **448**
Flame Stabilization **452**
Combustion and Dilution **452**
Film Cooling of the Liner **453**
Fuel Atomization and Ignition **453**
The Dry Low Emission Combustors **455**
Primary **467**
Lean–Lean **468**
Premix Transfer **468**
Piloted Premix **468**
Premix **469**
Tertiary Full-Speed No Load (FSNL) **469**
Silo-Type Combustors **477**
Operation of DLN/DLE Combustors **479**
Catalytic Combustion and Combustors **481**
Features of Catalytic Combustion **481**
Catalytic Combustor Design **483**
Preburner **484**
Main Fuel Injector **484**
Catalytic Reactor **484**
Transition Pieces **487**

Part III Materials, Fuel Technology, and Fuel Systems 491

11 Materials 493
General Metallurgical Behaviors in Gas Turbines **496**
Creep and Rupture **496**
Ductility and Fracture **497**
Cyclic Fatigue **498**
Thermal Fatigue **498**
Corrosion **499**
Gas Turbine Materials **503**
Turbine Wheel Alloys **505**
Compressor Blades **507**
Forgings and Non-destructive Testing **508**
Ceramics **508**
Coatings **509**
Shroud Coatings **513**
Future Coatings **513**
Bibliography **514**

12 Fuels 515
Fuel Specifications **519**
Fuel Properties **521**
Liquid Fuels **521**
Liquid Fuel Handling and Treatment **523**
Heavy Fuels **531**
Fuel Gas Handling and Treatment **535**
Equipment for Removal of Particulates and Liquids from Fuel Gas Systems **540**
Fuel Heating **542**
Cleaning of Turbine Components **543**
Hot Section Wash **544**
Compressor Washing **545**
Fuel Economics **546**
Operating Experience **548**
Heat Tracing of Piping Systems **549**
Types of Heat-Tracing Systems **550**
Stream Tracing Systems **550**
Electric Tracing **551**
Storage of Liquids **552**
Atmospheric Tanks **552**
Elevated Tanks **552**
Open Tanks **552**
Fixed Roof Tanks **552**
Floating Roof Tanks **552**
Pressure Tanks **553**
Bibliography **553**

Part IV Auxiliary Components and Accessories 555

13 Bearings and Seals 557
Bearings **557**
Rolling Bearings **557**
Journal Bearings **563**
Bearing Design Principles **565**
Tilting-Pad Journal Bearings **569**
Bearing Materials **572**
Bearing and Shaft Instabilities **573**
Thrust Bearings **573**
Factors Affecting Thrust-Bearing Design **577**
Thrust-Bearing Power Loss **578**
Seals **578**
Non-contacting Seals **579**
Labyrinth Seals **579**
Ring (Bushing) Seals **583**
Mechanical (Face) Seals **585**
Mechanical Seal Selection and Application **589**
Product **590**
Additional Product Considerations **592**
Seal Environment **592**
Seal Arrangement Considerations **593**
Equipment **593**
Secondary Packing **593**
Seal-Face Combinations **593**
Seal Gland Plate **593**
Main Seal Body **594**
Seal Systems **594**
Associated Oil System **595**
Dry Gas Seals **596**
Tandem Dry Gas Seals **599**
Tandem Dry Gas Seal with Labyrinth **599**
Double Gas Seals **600**
Operating Range of Dry Gas Seals **600**
Dry Gas Seal Materials **601**
Dry Gas Seal Systems **601**
Dry Gas Seal Degradation **601**
Bibliography **603**

14 Gears 605
Gear Types **607**
Factors Affecting Gear Design **608**
Pressure Angle **609**
Helix Angle **611**

Tooth Hardness 612
Scuffing 613
Gear Accuracy 613
Types of Bearings 614
Service Factor 614
Gear Housings 615
Lubrication 615
Manufacturing Processes 616
Hobbing 616
Hobbing and Shaving 616
Hobbing and Lapping 618
Grinding 618
Gear Rating 619
Gear Noise 619
Installation and Initial Operation 620
Gear Failures 622
Acknowledgement 624
Bibliography 625

Part V Installation, Operation, and Maintenance 627

15 Lubrication 629
Basic Oil System 629
Lubrication Oil System 629
Seal Oil System 634
Lubrication Management Program 636
Lubricant Selection 637
Oil Contamination 637
Filter Selection 638
Cleaning and Flushing 640
Oil Sampling and Testing 641
Oil Analysis Tests 641
Test Profiles 646
Gearboxes 646
Clean Oil Systems 647
Coupling Lubrication 648
Bibliography 649

16 Spectrum Analysis 651
Vibration Measurement 656
Displacement Transducers 657
Velocity Transducers 657
Acceleration Transducers 658
Dynamic Pressure Transducers 658

Taping Data 659
Interpretation of Vibration Spectra 660
Subsynchronous Vibration Analysis Using RTA 664
Synchronous and Harmonic Spectra 668
Bibliography 672

17 Balancing 675
Rotor Imbalance 675
Balancing Procedures 680
Orbital Balancing 681
Modal Balancing 682
Multiplane Balancing (Influence Coefficient Method) 683
Application of Balancing Techniques 686
User's Guide for Multiplane Balancing 688
Bibliography 690

18 Couplings and Alignment 693
Gear Couplings 695
Oil-Filled Couplings 698
Grease-Packed Couplings 699
Continuously Lubricated Couplings 699
Gear Coupling Failure Modes 700
Metal Diaphragm Couplings 701
Metal Disc Couplings 704
Turbomachinery Uprates 705
Curvic Couplings 709
Shaft Alignment 710
The Shaft Alignment Procedure 711
Bibliography 718

19 Control Systems and Instrumentation 721
Control Systems 721
Start-up Sequence 728
Condition Monitoring Systems 730
Requirements for an Effective Diagnostic System 732
Monitoring Software 733
Implementation of a Condition Monitoring System 735
Plant Power Optimization 736
Online Optimization Process 737
Life Cycle Costs 739
Diagnostic System Components and Functions 741
Data Inputs 741
Instrumentation Requirements 741
Typical Instrumentation (Minimum Requirements for Each Machine) 742
Desirable Instrumentation (Optional) 742

Criteria for the Collection of Aerothermal Data **742**
Pressure Drop in Filter System **745**
Temperature and Pressure Measurement for Compressors and Turbines **745**
Temperature Measurement **746**
Thermocouples **746**
Resistive Thermal Detectors **747**
Pyrometers **747**
Pressure Measurement **748**
Vibration Measurement **748**
Vibration Instrumentation Selection **750**
Selection of Systems for Analyses of Vibration Data **750**
Auxiliary System Monitoring **751**
Fuel System **751**
Torque Measurement **752**
Baseline for Machinery **752**
Data Trending **754**
The Gas Turbine **756**
Identification of Losses **759**
Compressor Aerothermal Characteristics and Compressor Surge **759**
Failure Diagnostics **760**
Compressor Analysis **760**
Combustor Analysis **761**
Turbine Analysis **762**
Turbine Efficiency **764**
Mechanical Problem Diagnostics **765**
Data Retrieval **767**
Summary **767**
Bibliography **768**

20 Gas Turbine Performance Test **769**
Introduction **769**
Performance Codes **770**
Flow Straighteners **771**
Pressure Measurement **771**
Temperature Measurement **774**
Flow Measurement **775**
Gas Turbine Test **777**
Gas Turbine **778**
Air Inlet Filter Module **779**
Compressor Module **779**
Combustor Module **780**
Expander Module **781**
Life Cycle Consideration of Various Critical Hot Section Components **782**
Performance Curves **782**

Performance Computations **782**
General Governing Equations **783**
Gas Turbine Performance Calculation **786**
Gas Turbine Performance Calculations **792**
Correction Factors for Gas Turbines **793**
Vibration Measurement **796**
Rotor Dynamics **796**
Vibration Measurements **796**
Emission Measurements **797**
Emissions **797**
Plant Losses **800**
Bibliography **802**

21 Maintenance Techniques **803**
Philosophy of Maintenance **803**
Maximization of Equipment Efficiency and Effectiveness **805**
Organization Structures for a Performance-Based Total Productive Maintenance Program **807**
Implementation of a Performance-Based Total Productive Maintenance **808**
Maintenance Department Requirements **810**
Training of Personnel **810**
I. Type of Personnel **810**
II. Types of Training **811**
Tools and Shop Equipment **814**
Spare Parts Inventory **814**
Condition and Life Assessment **815**
Availability and Reliability **815**
Redesign for Higher Machinery Reliability **817**
Gas Turbine Start-up **819**
Redesign for Higher Machinery Reliability **821**
Advanced Gas Turbines **821**
Axial-Flow Compressor **822**
Dry Low NO_x Combustors **823**
Axial-Flow Turbine **826**
Maintenance Scheduling **827**
Maintenance Communications **829**
Inspection **831**
Long-Term Service Agreements **833**
Borescope Inspection **835**
Maintenance of Gas Turbine Components **841**
Compressors **843**
Compressor Cleaning **850**
Compressor Water Wash **851**
Different Wash Systems **853**

On-Line Wash Cleaning System **853**
Off-Line Crank Wash Cleaning System **853**
On-Line and Off-Line Water Wash Fluids **856**
Off-Line Crank Wash Procedure **857**
Combustors **858**
Turbines **861**
Rejuvenation of Used Turbine Blades **866**
Rotor Dynamic System Characteristics **869**
Bearing Maintenance **870**
Clearance Checks **877**
Thrust-Bearing Failure **877**
Coupling Maintenance **880**
Repair and Rehabilitation of Turbomachinery Foundations **880**
Installation Defects **881**
Increasing Mass and Rigidity **882**
Bibliography **883**

22 Case Histories **885**
Axial-Flow Compressors **886**
Combustion Systems **897**
Transition Piece **902**
Axial-Flow Turbines **902**

Appendix: Equivalent Units **923**
Index **929**

Copyrighted Materials
Copyright © 2012 Elsevier Retrieved from www.knovel.com

Part I

Design: Theory and Practice

1 An Overview of Gas Turbines

The gas turbine is a power plant that produces a great amount of energy depending on its size and weight. The gas turbine has found increasing service in the past 60 years in the power industry among both utilities and merchant plants as well as the petrochemical industry throughout the world. Its compactness, low weight, and multiple fuel application make it a natural power plant for offshore platforms. Today there are gas turbines that run on natural gas, diesel fuel, naphtha, methane, crude, low-BTU gases, vaporized fuel oils, and biomass gases.

The last 20 years have seen a large growth in gas turbine technology. The growth is spearheaded by the growth of materials technology, new coatings, new cooling schemes, and the growth of combined-cycle power plants. This, with the conjunction of increase in compressor pressure ratio from 7:1 to as high as 45:1, has increased simple-cycle gas turbine thermal efficiency from about 15% to 45%.

Table 1-1 gives an economic comparison of various generation technologies from the initial cost of such systems to the operating costs of these systems. Because distributed generation is very site specific, the cost will vary and the justification of installation of these types of systems will also vary. Sites for distributed generation vary from large metropolitan areas to the slopes of the Himalayan mountain range. The economics of power generation depends on the fuel cost, running efficiencies, maintenance cost, and initial cost, in that order. Site selection depends on environmental concerns such as emissions, noise, fuel availability, size, and weight.

Gas Turbine Cycle in the Combined Cycle or Cogeneration Mode

The utilization of gas turbine exhaust gases, for steam generation or the heating of other heat transfer mediums, or the use of cooling or heating buildings or parts of cities is not a new concept and is currently being exploited to its full potential.

The fossil power plants of the 1990s and into the early part of the new millennium were the combined-cycle power plants, with the gas turbine being the center piece of the plant. It was estimated that, between 1997 and 2006, there was an addition of 147.7 GW of power. These plants have replaced the large steam turbine plants, which were the main fossil power plants through the 1980s. The combined-cycle power plant is not new in concept, since some have been in operation since the mid-1950s. These plants came into their own with the new high-capacity and high-efficiency gas turbines.

Gas Turbine Engineering Handbook, Fourth Edition. DOI: 10.1016/B978-0-12-383842-1.00001-9
Copyright © 2012 Elsevier Inc. All rights reserved.

Table 1-1 Economic Comparison of Various Generation Technologies*

Technology Comparison	Diesel Engine	Gas Engine	Simple Cycle Gas Turbine	Micro Turbine	Fuel Cell	Solar Energy Photovoltic Cell	Wind	Biomass	River Hydro
Product rollout	Available	Available	Available	Available	Available	Available	Available	Available	Available
Size range (kW)	20–100,000+	50–7,000+	500–450,000+	30–200	50–1,000+	1+	Up to 5,000	Up to 5,000	20–3,000+
Efficiency (%)	36–43%	28–42%	21–45%	25–30%	35–54%	NA	45–55%	25–35%	60–70%
Gen. set cost ($/kW)	125–400	250–600	300–600	800–1,200	1,500–3,000	NA	—	NA	NA
Turnkey cost No-heat recovery ($/kW)	200–500	600–1,000	400–850	1,200–2,400	2,500–5,000	5,000–10,000	700–1,300	800–1,500	750–1,200
Heat recovery added cost ($/kW)	75–100	75–100	150–300	100–250	1,900–3,500	NA	NA	150–300	NA
O&M cost ($/kW h)	0.007–0.015	0.005–0.012	0.003–0.008	0.006–0.010	0.005–0.010	0.001–0.004	0.007–0.012	0.006–0.011	0.005–0.010

*The above information is based on data obtained from several sources such as manufacturers and technical magazines.

The new market place of energy conversion will have many new and novel concepts in combined-cycle power plants. Figure 1-1 shows the heat rates of these plants, present and future, and Figure 1-2 shows the efficiencies of the same plants. The plants referenced are the simple-cycle gas turbine (SCGT) with firing temperatures of 2400 °F (1315 °C), recuperative gas turbine (RGT), the steam turbine (ST) Plant, the combined-cycle power plant (CCPP), and the advanced combined-cycle power plants (ACCPPs), such as combined-cycle power plants using advanced gas turbine cycles, and finally the hybrid power plants (HPP).

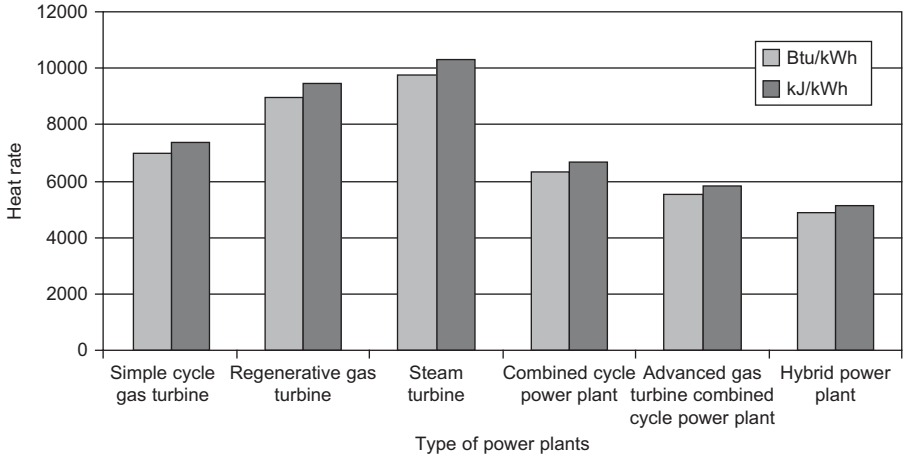


Figure 1-1 Heat rate of typical power plants.

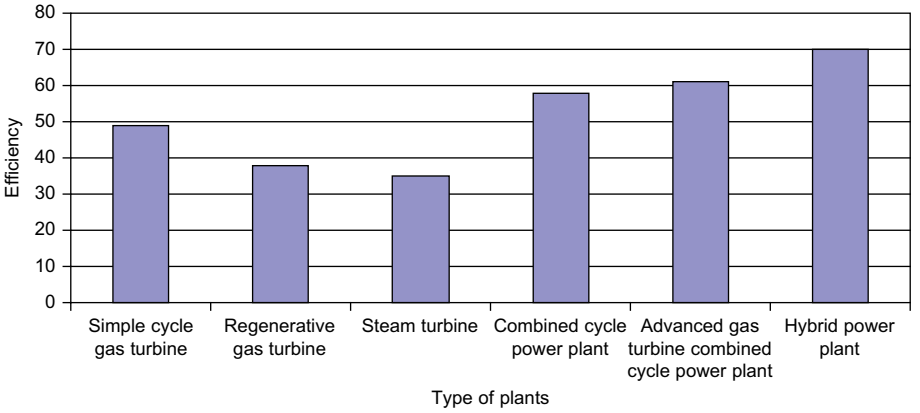


Figure 1-2 Efficiency.

Table 1-2 depicts an analysis of the competitive standing of the various types of power plants, their capital cost, heat rate, operation and maintenance costs, availability, reliability, and time for planning. By examining the capital cost and installation time of these new power plants, it is obvious that the gas turbine is the best choice for peaking power. Steam turbine plants are about 50% higher in initial costs of $800–$1000/kW than combined-cycle plants, which are about $400–$900/kW. Nuclear power plants are the most expensive plants. The high initial costs and the long time in construction make such a plant unrealistic for a deregulated utility.

Efficiency and heat rate are interchangeable, as they represent the efficient conversion of fuel to energy. The following relationship gives the easy conversion from heat rate to efficiency.

$$\text{Efficiency} = 3412.2/\text{BTU/kWh} = 2544.4/\text{BTU/HPh} = 3600/\text{kJ/kWh}$$

In the area of performance, the steam turbine power plants have an efficiency of about 35% when compared with combined-cycle power plants, which have an efficiency of about 55%. Newer gas turbine technology will make combined-cycle efficiencies range between 60% and 65%. As a rule of thumb, a 1% increase in the efficiency could mean that 3.3% more capital can be invested. However, one must be careful that the increase in the efficiency does not lead to a decrease in the availability. From 1996 to 2000, we have seen a growth in the efficiency of about 10% and a loss in the availability of about 10%. This trend must be turned around since many analyses show that a 1% drop in the availability needs about 2–3% increase in the efficiency to offset that loss. The larger gas turbines, just due to their size, take more time to undergo any of the regular inspections, such as combustor, hot gas path, and major overall inspections, thus reducing the availability of these turbines.

The time taken to install a steam plant from conception to production is about 42–60 months whereas it was about 22–36 months for combined-cycle power plants. The actual construction time is about 18 months, whereas obtaining environmental permits in many cases take 12 months and engineering takes 6–12 months. The time taken for bringing the plant online affects the economics of the plant, the longer the capital is employed without return the more it accumulates interest, insurance, and taxes.

It is obvious from this that as long as natural gas or diesel fuel is available, the choice of combined-cycle power plants is obvious.

Gas Turbine Performance

In 1791, John Barber, an Englishman, was the first to patent a design that used the thermodynamic cycle of the modem gas turbine. Figure 1-3 shows the sketch on which he based his patent. His design contained the basics of the modem gas turbine; it had a compressor, a combustion chamber, and a turbine. The main difference between his design and the modern one was that the turbine was equipped with a chain-driven reciprocating type of compressor. He intended its use for jet propulsion.

Many people consider Frank Whittle as the father of the modern-day gas turbine. The Whittle gas turbine was built in January 1930 and had a thrust of 1,000 lbf and an efficiency of 14%. The air was compressed in a centrifugal compressor and was then

Table 1-2 Economic and Operation Characteristics of Plant*

Type of Plant	Capital Cost ($/kW)	Heat Rate BTU/kWh (kJ/kWh)	Net Efficiency	Variable Operation and Maintenance ($/MWh)	Fixed Operation and Maintenance ($/MWh)	Availability (%)	Reliability (%)	Time from Planning to Completion (Months)
SCGT (2500 °F/1371 °C) Natural gas fired	300–350	7582–8000	45	5.8	0.23	88–95	97–99	10–12
SCGT oil fired	400–500	8322–8229	41	6.2	0.25	90–96	95–98	12–16
SCGT crude fired	500–600	10,662–11,250	32	13.5	0.25	75–80	90–95	12–16
Regenerative gas turbine natural gas fired	375–575	6824–7200	50	6	0.25	86–93	96–98	12–16
Combined-cycle gas turbine	600–900	6203–6545	55	4	0.35	86–93	95–98	22–24
Advanced gas turbine CCPP	800–1,000	5249–5538	65	4.5	0.4	84–90	94–96	28–30
Combined-cycle coal gasification	1,200–1,400	6950–7332	49	7	1.45	75–85	90–95	30–36
Combined-cycle fluidized bed	1,200–1,400	7300–7701	47	7	1.45	75–85	90–95	30–36
Nuclear power	1,800–200	10,000–10,550	34	8	2.28	80–89	92–98	48–60
Steam plant coal fired	800–1,000	9749–10285	35	3	1.43	82–89	94–97	36–42
Diesel generator-diesel fired	400–500	7582–8000	45	6.2	4.7	90–95	96–98	12–16
Diesel generator-power plant oil fired	600–700	8124–8570	42	7.2	4.7	85–90	92–95	16–18
Gas engine generator power plant	650–750	7300–7701	47	5.2	4.7	92–96	96–98	12–16

*The above information is based on data obtained from several sources such as manufacturers, technical magazines, as well as data obtained by the author.

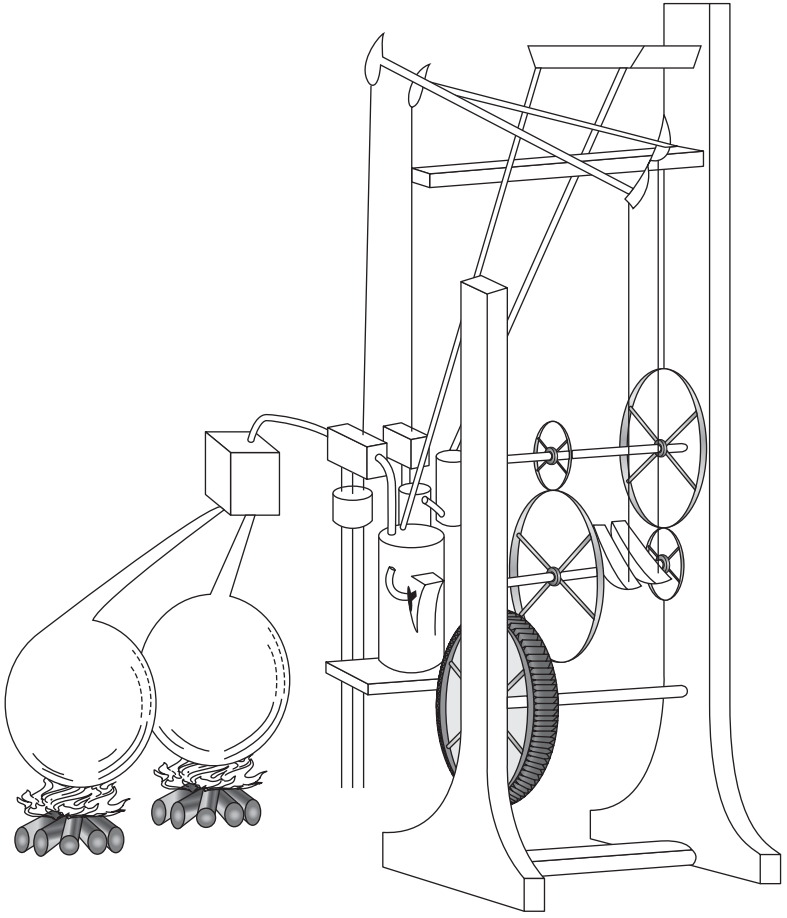


Figure 1-3 Barber's British Patent – 1791.

expanded through a radial-inflow turbine. Figure 1-4 is a photograph of the Whittle turbine and Figure 1-5 is its schematic diagram. In 1903, General Electric developed a turbocharger, and in 1941, it modified the Whittle engine for America's first aero-engine. In 1945, Westinghouse developed the first gas turbine based solely on US design; the turbine included an axial-flow compressor, a turbine, and an annular combustor.

The aerospace engines have been leaders in most of the technology in the gas turbine. The design criteria for these engines were high reliability, high performance, with many starts and flexible operation throughout the flight envelope. The engine life of about 3,500 hours between major overhauls was considered good. The performance of the aerospace engine has always been rated primarily on its thrust/weight ratio. Increase in engine thrust/weight ratio is achieved by developing the blades of high aspect ratio in the compressor as well as optimizing the pressure ratio and firing temperature of the turbine for maximum work output per unit flow.

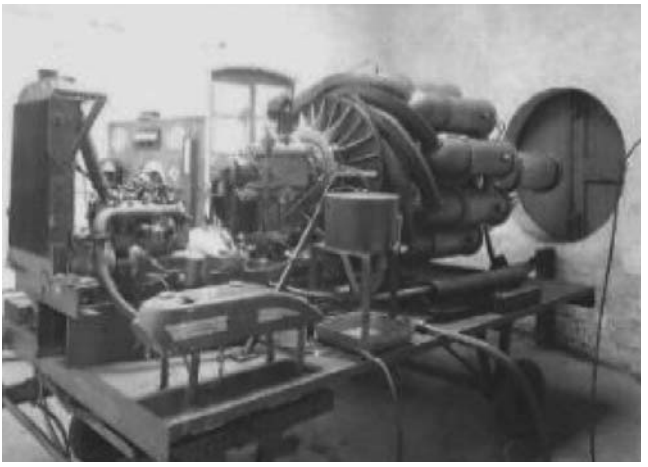


Figure 1-4 Whittle turbine.

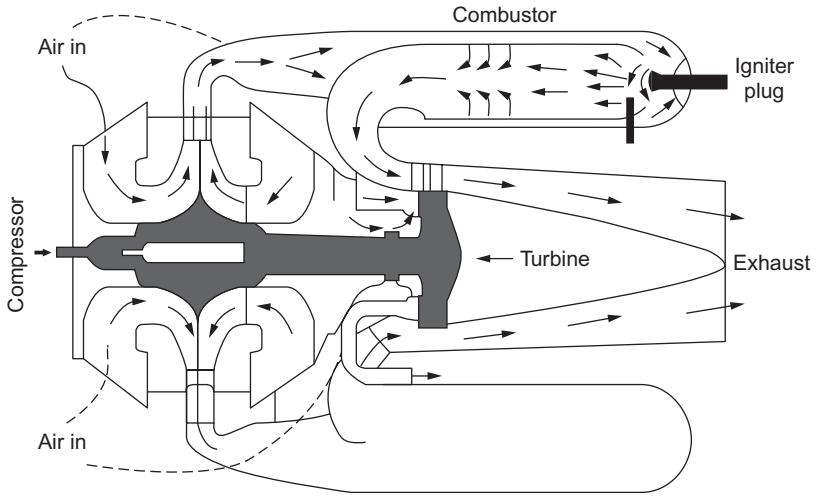


Figure 1-5 Schematic of Whittle turbine.

The industrial gas turbine has always emphasized long life and this conservative approach has resulted in the industrial gas turbine in many aspects giving up high performance for rugged operation. The industrial gas turbine has been conservative in the pressure ratio and the firing temperatures. This has all changed in the last 10 years; spurred on by the introduction of the "aeroderivative gas turbine," the industrial gas turbine has dramatically improved its performance in all operational aspects. This has resulted in a dramatic reduction of the performance gap between these two types of gas turbines. The gas turbine to date in the combined-cycle mode is fast replacing the steam turbine as the base load provider of electrical power throughout the world. This is even true in Europe and the United States of America where the large steam turbines

were the only type of base load power in the fossil energy sector. The gas turbine from the 1960s to the late 1980s was used only as peaking power in those countries; it was used as base load mainly in the "developing countries" where the need of power was increasing rapidly and that the waiting period of three to six years for a steam plant was unacceptable.

Figures 1-6 and 1-7 show the growth of the pressure ratio and firing temperature, respectively. The growth of these is parallel to each other, as both growths are necessary to achieve the optimum thermal efficiency.

The increase in pressure ratio increases the gas turbine thermal efficiency when accompanied by the increase in turbine's firing temperature. Figure 1-8 shows the effect on the overall cycle efficiency of the increasing pressure ratio and firing temperature. The increase in the pressure ratio increases the overall efficiency at a

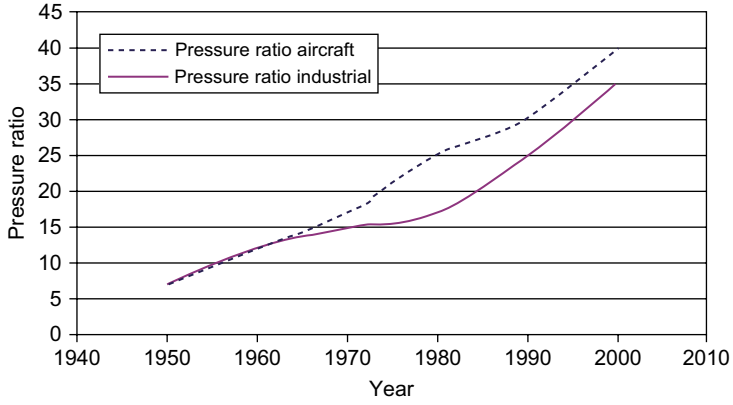


Figure 1-6 Engine pressure ratio development.

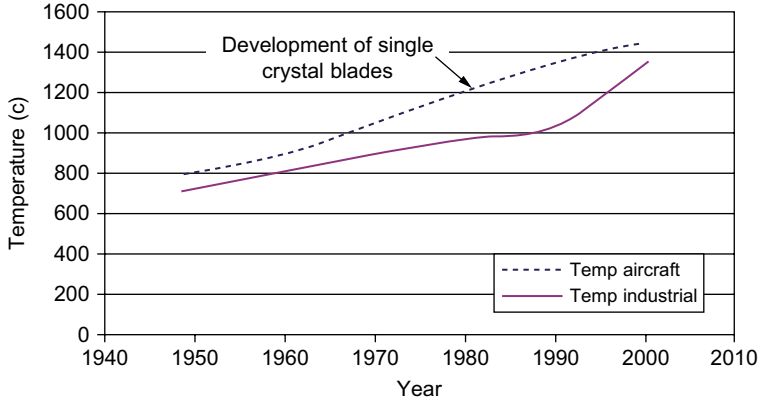


Figure 1-7 Trend in improvement in firing temperature.

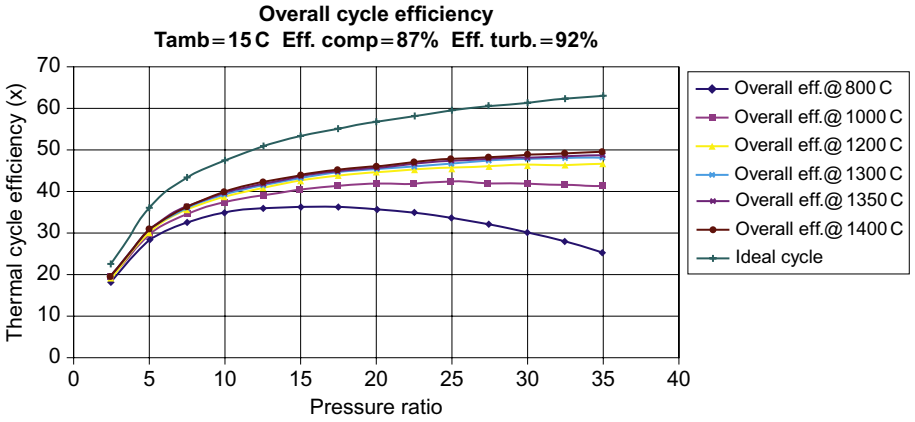


Figure 1-8 Overall cycle efficiency.

given temperature; however, increasing the pressure ratio beyond a certain value at any given firing temperature can actually result in lowering the overall cycle efficiency.

In the past, the gas turbine was perceived as a relatively inefficient power source when compared with other power sources. Its efficiencies were as low as 15% in the early 1950s; however, today its efficiencies are in the range of 45–50%, which translates to a heat rate of 7582 BTU/kW h (8000 kJ/kW h) to 6824 BTU/kW h (7199 kJ/kW h). The limiting factor for most gas turbines has been the turbine inlet temperature. With new schemes of cooling, using steam or conditioned air, and breakthroughs in blade metallurgy, higher turbine temperatures have been achieved. The new gas turbines have fired inlet temperatures as high as 2600 °F (1427 °C) and pressure ratios of 40:1 with the efficiencies of 45% and above.

Gas Turbine Design Considerations

The gas turbine is the best suited prime mover when the needs at hand such as capital cost, time from planning to completion, maintenance costs, and fuel costs are considered. The gas turbine has the lowest maintenance and capital costs among major prime movers. It also has the fastest completion time to full operation among other plants. Its disadvantage was its high heat rate but this has been addressed and the new turbines are among the most efficient types of prime movers. The combination of plant cycles further increases the efficiencies to the low 60% region.

The design of any gas turbine must meet essential criteria based on operational considerations. Chief among these criteria are as follows:

1. High efficiency
2. High reliability and thus high availability
3. Ease of service
4. Ease of installation and commission

5. Conformance with environmental standards
6. Incorporation of auxiliary and control systems that have a high degree of reliability
7. Flexibility to meet various service and fuel needs

A look at each of these criteria will enable the user to get a better understanding of the requirements.

The two factors that mostly affect the high turbine efficiencies are pressure ratios and the firing temperature. The axial-flow compressor, which produces the high-pressure gas in the turbine, has seen a dramatic change as the gas turbine pressure ratio has increased from 7:1 to 45:1 in some of the aero gas turbines used today. The increase in the pressure ratio increases the gas turbine thermal efficiency when accompanied with the increase in turbine's firing temperature. The increase in the pressure ratio increases the overall efficiency at a given temperature; however, increasing the pressure ratio beyond a certain value at any given firing temperature can actually result in lowering the overall cycle efficiency. It should also be noted that the very high-pressure ratios tend to reduce the operating range of the turbine compressor. This causes the turbine compressor to be much more intolerant to dirt build-up in the inlet air filter and on the compressor blades, and it creates large drops in cycle efficiency and performance. In some cases, it can lead to compressor surge, which in turn can lead to a flameout, or even serious damage and failure of the compressor blades, and the radial and thrust bearings of the gas turbine.

The effect of firing temperature is very predominant; for every 100 °F (55.5 °C) increase in the temperature, the work output increases approximately 10% and gives about a 0.5–1% increase in the efficiency. Higher pressure ratios and turbine inlet temperatures improve the efficiencies on the simple-cycle gas turbine. Figure 1-9 shows a simple-cycle gas turbine performance map as a function of pressure ratio and turbine inlet temperature.

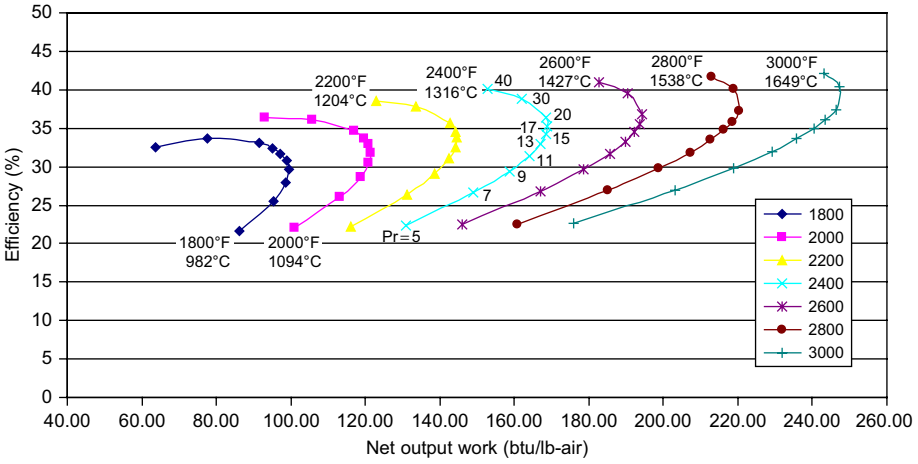


Figure 1-9 The performance map of a simple-cycle gas turbine.

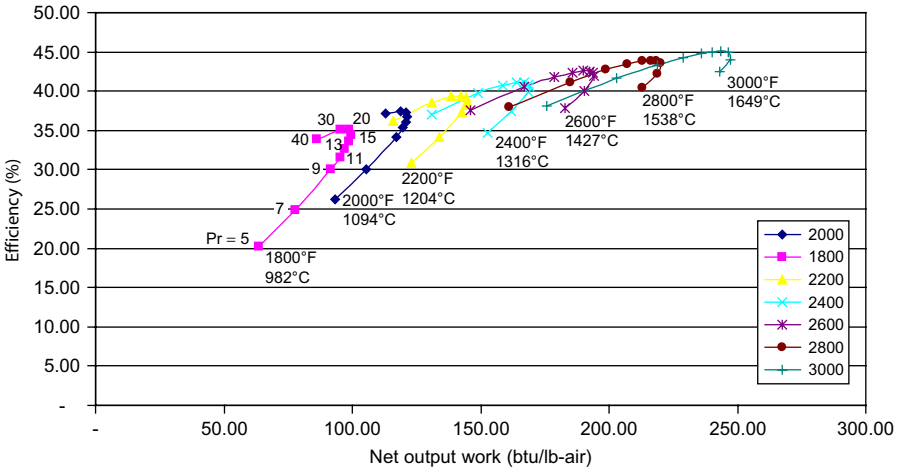


Figure 1-10 The performance map of a regenerative gas turbine cycle.

Another way to achieve higher efficiencies is to use the exhaust gases to heat the air leaving the compressor, thus reducing the amount of fuel required to reach the temperature that required to operate the turbine. This is achieved by the use of regenerators or recuperators, which heat the compressor exit air by the exhaust gases from the turbine exit. Regenerators or recuperators are usually used in small- to intermediate-sized gas turbines. Figure 1-10 shows the effects of pressure ratio and temperatures on efficiencies and work for a regenerative or recuperative cycle. Comparing Figure 1-10 with Figure 1-9 shows that increasing the pressure ratio lowers the efficiency in a regenerative or recuperative cycle. The effect of pressure ratio for this cycle is opposite to that experienced in the simple cycle. Regenerators or recuperators can increase efficiency as much as 15–20% of today's hot section operating temperatures. The use of a regenerator or a recuperator is that they are mostly used in gas turbines with outputs less than 10 MW. In these gas turbines, the airflow is small not requiring a large regenerator or recuperator and the firing temperature is low thus the pressure ratio is usually less than 10:1. The optimum pressure ratio, as seen in Figure 1-10, is about 20:1 for a regenerative system and 40:1 for the simple cycle at today's higher turbine inlet temperatures that are starting to approach 3000 °F (1649 °C).

High availability and reliability are the most important parameters in the design of a gas turbine. The availability of a power plant is the percentage of time the plant is available to generate power in any given period. The reliability of the plant is the percentage of time between planed overhauls. The following are the basic definitions of availability and reliability; expanded definitions of these terms are given in Chapter 21.

The availability of a power plant is defined as

$$A = \frac{P - S - F}{P}, \tag{1-1}$$

where

P = period of time (in hours), usually this is assumed as one year, which amounts to 8,760 hours;

S = scheduled outage hours for planned maintenance; and

F = forced outage hours or unplanned outage due to repair.

The reliability of a power plant is defined as:

$$R = \frac{P - F}{P}. \tag{1-2}$$

Availability and reliability have a very major impact on the plant's economy. Reliability is essential in that when the power is needed it must be there. When the power is not available, it must be generated or purchased and can be very costly to the operation of a plant. Planned outages are scheduled for non-peak periods. Peak periods are when the majority of the income is generated; as usually, there are various tiers of pricing depending on the demand. Many power purchase agreements have clauses, which contain capacity payments, thus making plant availability critical in the economics of the plant.

Reliability of a plant depends on many parameters, such as the type of fuel, the preventive maintenance programs, the operating mode, the control systems, and the firing temperatures.

To achieve a high availability and reliability factor, the designer must keep in mind many factors. Some of the more important considerations which govern the design are: blade and shaft stresses, blade loadings, material integrity, auxiliary systems, and control systems. The high temperatures required for high efficiencies have a disastrous effect on turbine blade life. Proper cooling must be provided to achieve blade metal temperatures between 1000 °F (537 °C) and 1300 °F (704 °C), below the levels of the onset of hot corrosion. Thus, the right type of cooling systems with proper blade coatings and materials are needed to ensure the high reliability of a turbine.

Serviceability is an important part of any design, because fast turnarounds result in high availability to a turbine and reduce maintenance and operations costs. Service can be accomplished by providing proper checks such as monitoring of exhaust temperature, shaft vibration, and surge. Moreover, the designer should incorporate borescope ports for fast visual checks of hot parts in the system. Split casings for fast disassembly, field balancing ports for easy access to the balance planes, and combustor cans that can be easily disassembled without removing the entire hot section, are some of the many ways that afford ease of service.

Ease of installation and commissioning is another reason for gas turbine use. A gas turbine unit can be tested and packaged at the factory. Use of a unit should be carefully planned so as to cause as few start cycles as possible. Frequent start-ups and shutdowns at commissioning greatly reduce the life of a unit.

Environmental considerations are critical in the design of any system. The system's impact on the environment must be within legal limits and thus must be addressed by the designer carefully. Combustors are the most critical component, and great care

must be taken to design them to provide low smoke and low NO_x output. The high temperatures result in increasing the NO_x emissions from the gas turbines. This resulted in initially attacking the NO_x problem by injecting water or steam into the combustor. The next stage was the development of dry low NO_x combustors. The development of new dry low NO_x combustors has been a very critical component in reducing the NO_x output, as the gas turbine's firing temperature is increased. The new low NO_x combustors increase the number of fuel nozzle and the complexity of the control algorithms.

Lowering the inlet velocities and providing proper inlet silencers can reduce air noise. Considerable work by NASA on compressor casings has greatly reduced noise.

Auxiliary systems and control systems must be designed carefully, since they are often responsible for the downtime in many units. Lubrication systems, one of the critical auxiliary systems, must be designed with a backup system and should be as close to failure-proof design as possible. The advanced gas turbines are all digitally controlled and incorporate online condition monitoring to some extent. The addition of new online monitoring requires new instrumentation. Control systems provide acceleration-time and temperature-time controls for start-ups as well as control various antisurge valves. At operating speeds, they must regulate fuel supply and monitor vibrations, temperatures, and pressures throughout the entire range.

Flexibility of service and fuels are the criteria that enhance a turbine system, but they are not necessary for every application. The energy shortage makes it closer to its operating point and thus it operate at higher efficiencies. This flexibility may entail a two-shaft design incorporating a power turbine, which is separate and not connected to the gasifier unit. Multiple fuel applications are now in greater demand, especially where there may be a shortage of various fuels at different times of the year.

Categories of Gas Turbines

The simple-cycle gas Turbine is classified into the following six broad groups:

1. *Frame type heavy-duty gas turbines*. The frame units are the large power generation units ranging from 3 to 480 MW in a simple-cycle configuration, with efficiencies ranging from 30% to 48%.
2. *Aircraft-derivative gas turbines*. Aeroderivatives, as the name indicates, are power generation units that have origin in the aerospace industry as the prime mover of aircraft. These units have been adapted to the electrical generation industry by removing the bypass fans and adding a power turbine at their exhaust. The power of these units ranges from about 2.5 to 50 MW. The efficiencies of these units can range from 35% to 45%.
3. *Industrial-type gas turbines*. These turbines vary in range from about 2.5 to 15 MW. These are used extensively in many petrochemical plants for compressor drive trains. The efficiencies of these units are in the low 30s.
4. *Small gas turbines*. These gas turbines are in the range from about 0.5 to 2.5 MW. They often have centrifugal compressors and radial-inflow turbines. The efficiencies of the simple-cycle applications vary from 15% to 25%.
5. *Microturbines*. These turbines are in the range from 20 to 350 kW. The growth of these turbines has been dramatic from the late 1990s, as there is an upsurge in the distributed generation market.

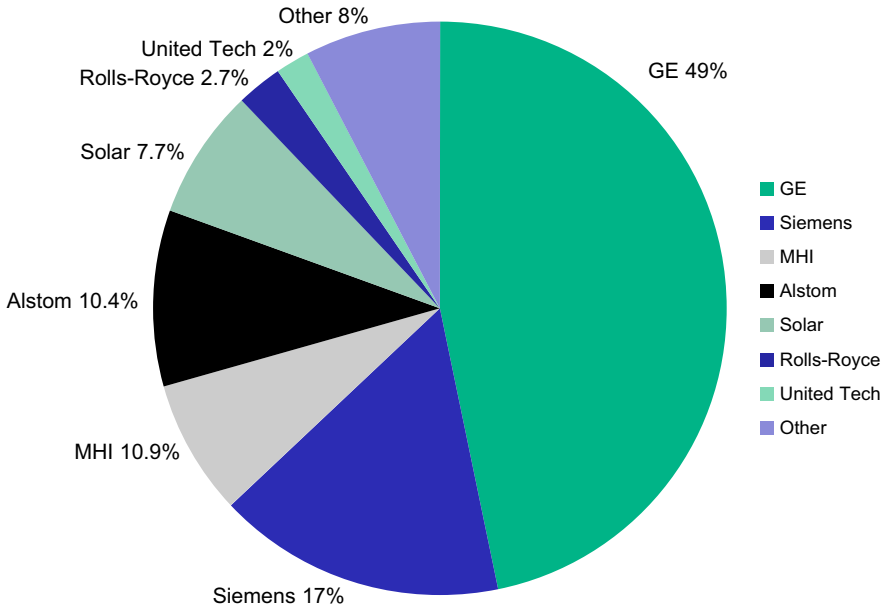


Figure 1-11 Distribution of gas turbine sales.

6. *Vehicular gas turbines*. These turbines have ranged from 300 to 1,500 HP. The first vehicular turbine was built in 1954 by Chrysler Corporation and followed by the Ford Motor Company's truck engine. The only vehicular turbine that has been very successful has been the gas turbine used in US Army Abrams Tank.

Figure 1-11 shows the distribution by manufacturers, total dollars of a $60-billion market, and the types of gas turbines that are sold throughout the world based on the data as given in the *Turbomachinery 2010 Handbook*. In this figure, GE is by far the largest supplier having about 49% of the market. Figure 1-12 shows the distribution by manufacturers and the number of turbines manufactured by each manufacturer; this figure shows that Solar Turbines Inc. holds the first place followed by GE.

Frame Type Heavy-Duty Gas Turbines

These gas turbines were designed shortly after World War II and introduced to the market in the early 1950s. The early heavy-duty gas turbine design was largely an extension of steam turbine design. Restrictions of weight and space were not important factors for these ground-based units, and so the design characteristics included heavy-wall casings split on horizontal centerlines, sleeve bearings, large-diameter combustors, thick airfoil sections for blades and stators, and large frontal areas. The overall pressure ratio of these units varied from 5:1 for the earlier units to 35:1 for the units in present-day service. Turbine inlet temperatures have been increased and run as high as

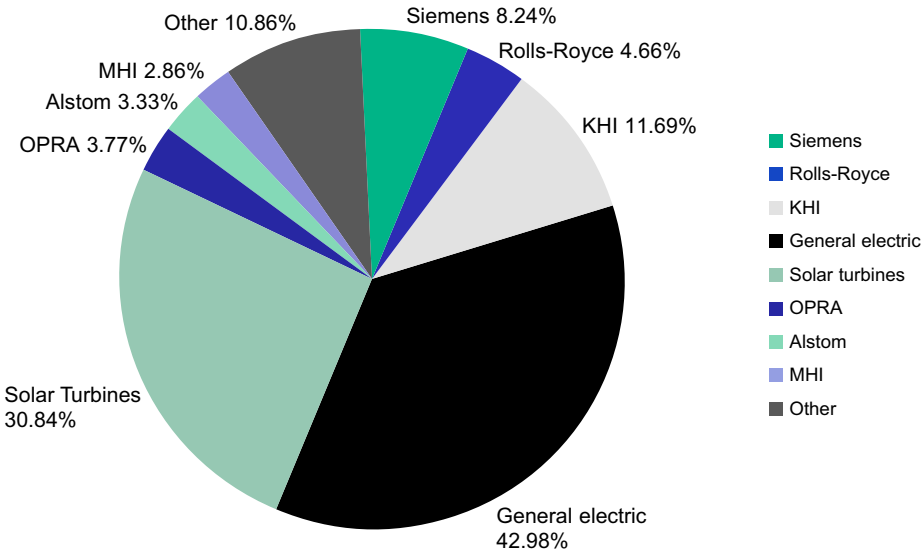


Figure 1-12 Gas turbine electrical power generation unit production, percent market share by headquarters 2010–2019.

2732 °F (1500 °C) on some of these units, which makes the gas turbine one of the most efficient prime movers on the market today reaching efficiencies in the high forties and above 60% in a combined-cycle mode. Projected temperatures approach 3000 °F (1649 °C) and, if achieved, would make the gas turbine even more efficient unit. The Advanced Gas Turbine Programs sponsored by the US Department of Energy have these high temperatures as one of its goals. To achieve these high temperatures, steam cooling is being used in some of the latest designs to achieve the goals of maintaining blade metal temperatures below 1300 °F (704 °C) and preventing hot corrosion problems.

The industrial heavy-duty gas turbines employ axial-flow compressors and turbines. The industrial turbine consists of a 15- to 25-stage axial-flow compressor; with multiple can-annular combustors each connected to the other by crossover tubes or single large annular combustors with multiple nozzles. The crossover tubes in can-annular combustors help propagate the flames from one combustor can to all the other chambers and also assures an equalization of the pressure between each combustor chamber. The earlier industrial European designs had single-stage side or silo-type combustors. The new European designs do not use the side- or silo-type combustor in most of their newer designs, they have can-annular or annular combustors since side- or silo-type combustors had a tendency to distort the casing.

The large frontal areas of the frame units reduce the inlet velocities, thus reducing air noise. The pressure rise in each compressor stage is reduced, creating a large, stable operating zone.

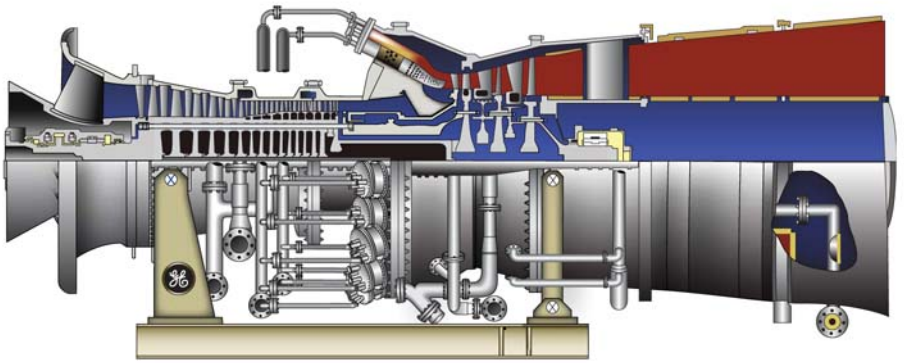
The auxiliary modules used on most of these units have gone through considerable hours of testing and are heavy-duty pumps and motors.

The advantages of the heavy-duty gas turbines are their long life, high availability, and slightly higher overall efficiencies. The noise level from this type of turbine is considerably less than an aircraft-type turbine. The heavy-duty gas turbine's largest customers are the electrical utilities and independent power producers. Since the 1990s industrial turbines have been the bulwarks of most combined-cycle power plants.

The latest frame type units introduced are 480-MW units using steam cooling in the combined-cycle mode, enabling the firing temperatures to reach 2600 °F (1427 °C). This enables the combined-cycle mode to reach an efficiency of more than 60%. Some of the newer gas turbines on the market are discussed below.

GE has the major market share of the frame-type gas turbine. Figure 1-13 is a cross-sectional representation of the GE industrial-type gas turbine. Frame 9 FA, a 50-cycle turbine, is rated at 256 MW with an efficiency of 37% and has a 17-stage axial-flow compressor with a pressure ratio of 16.6:1, with 14 can-annular combustors and a three-stage axial-flow turbine. The Frame 9 FA gas turbine has a sister turbine, the Frame 7 FA, which is a 60-cycle turbine producing 183 MW.

Figure 1-14 is the photograph of the new GE-developed advanced combined-cycle gas turbine technology that they have named the H System™– it is a combined-cycle system capable of breaking the 60% efficiency barrier and it integrates the gas turbine, steam turbine, and heat recovery steam generator into a seamless system, optimizing each component's performance. Figure 1-15 is a drawing of the GE H gas turbine showing a 17-stage axial-flow turbine, and this turbine employs a can-annular lean pre-mix dry low NO_x (DLN) combustor system. Fourteen combustion chambers are used on the 9 H, and twelve combustion chambers are used on the 7 H and a four-stage turbine section. The H system delivers higher efficiency (60%) and output



GT18029
MS9001F single-shaft gas turbine
FA-226.5 MW (simple-cycle), 50 Hz
FA-348.5 MW (combined-cycle), 50 Hz
Cross-section illustration

Figure 1-13 GE industrial-type gas turbine.

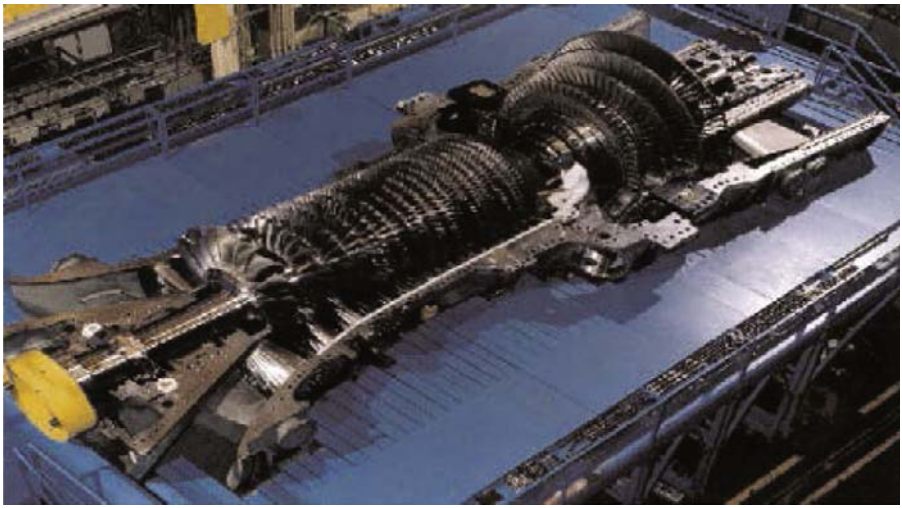


Figure 1-14 GE H system^{TM} gas turbine.

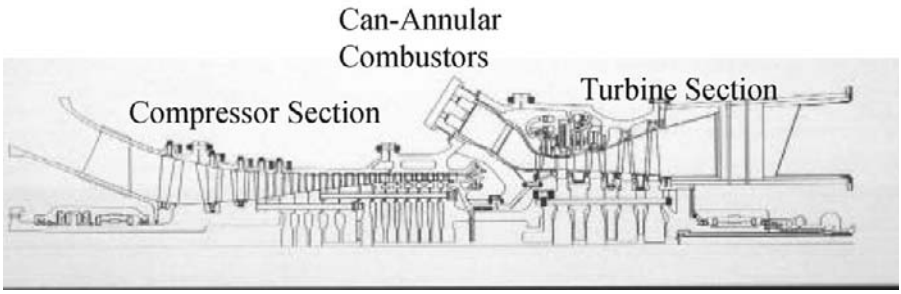


Figure 1-15 GE H gas turbine.

(480 MW) to reduce the cost of electricity of this gas-fired power generation system. Because fuel represents the largest individual expense of running a power plant, an efficiency increase of even a single percentage point can substantially reduce operating costs over the life of a typical gas-fired and combined-cycle plant in the 400–500 MW range.

The GE H gas turbine uses a closed-loop steam cooling system, which allows the turbine to fire at a higher temperature for increased performance. It is this closed-loop steam cooling that enables the H System to achieve 60% combined-cycle fuel efficiency, while maintaining strict adherence to environmental standards.

GE has also developed a new high-efficiency turbine in a simple-cycle gas turbine application. Figure 1-16 is an orthogonal drawing of the GE LMS 100 turbine designed with a high-efficiency core engine. The LMS 100 features a heavy-duty and low-pressure compressor derived from GE Power Systems' MS 6001 FA heavy-duty gas turbine compressor; its core, which includes the high-pressure compressor, combustor,

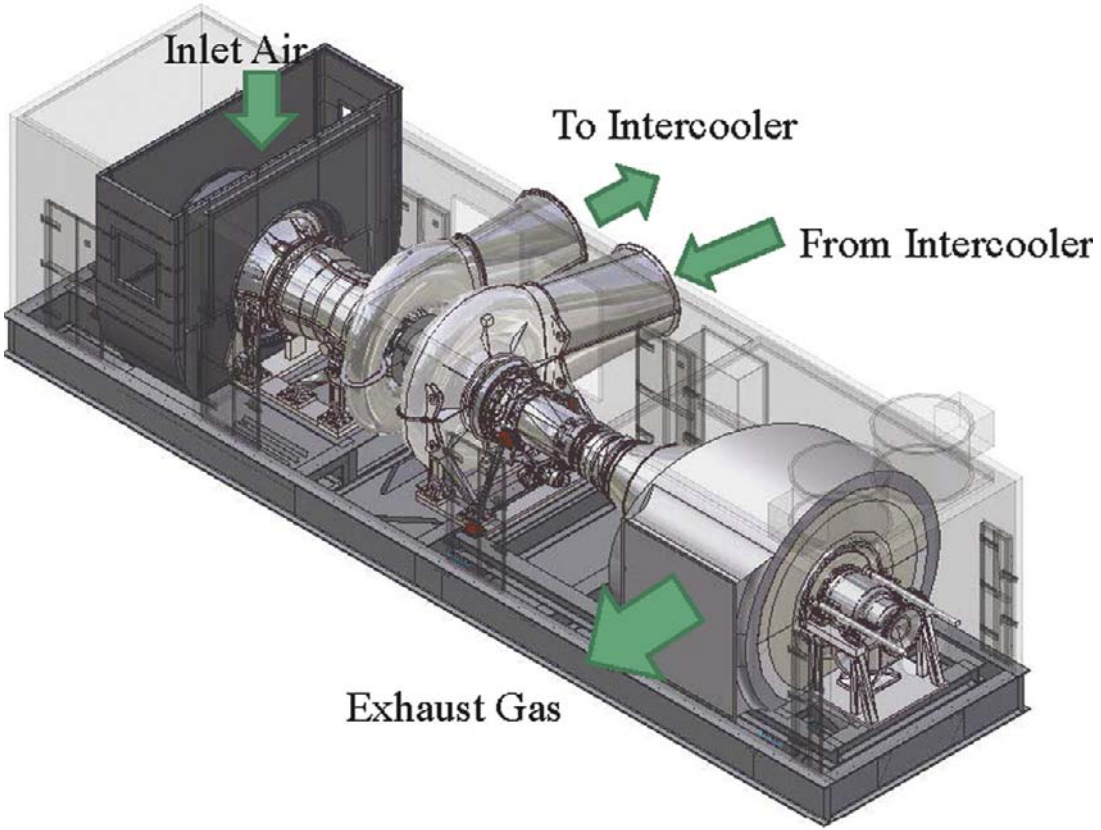


Figure 1-16 GE LMS 100 turbine.

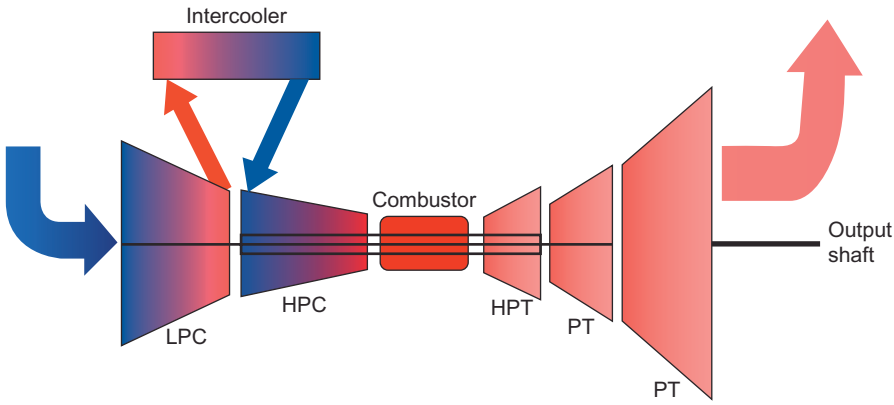


Figure 1-17 ABB turbine.

and high-pressure turbine, is derived from GE Aircraft Engines' CF6-80C2▫ and CF6-80E1▫. The design of the new two-stage intermediate-pressure turbine and new five-stage power turbine is based on the latest aero-derivative gas turbine technology. The exhaust and aft shaft for hot-end drive are designed using heavy-duty gas turbine practices. The compressed air from the low-pressure compressor (LPC) is cooled in either an air-to-air or air-to-water heat exchanger (intercooler) and ducted to the high-pressure compressor (HPC). This is the first gas turbine with an in-line intercooled compressor section. The old ABB turbines designed in 1950 had a similar design in that two axial-flow compressors had an intercooler between the two compressor stages as shown in Figure 1-17, which is a schematic representation of the system. The cooled flow means less work for the HPC, increased overall efficiency, and power output. The cooler LPC exit temperature air, used for turbine cooling, allows higher firing temperatures, resulting in increased power output and overall efficiency. The LMS 100 is a combination of two technologies, as shown in Figure 1-18, Frame and Aero technologies. A new two-stage intermediate-pressure turbine drives the first six stages of the Frame 6 compressor by the use of a coaxial shaft and the five-stage power turbine is based on the latest aeroderivative gas turbine technology and drives the generator on the hot side of the turbine. The exhaust and the aft shaft for hot-end drive are designed using heavy-duty gas turbine practices.

MS900 1H/MS700 1H Combined-Cycle Performance

	Net Plant Output (MW)	Heat Rate (BTU/kW h)	Heat Rate (kJ/kW h)	Net Plant Efficiency (%)	GT Number and Type
50 Hz S109H	480	5690	6000	60	1 × MS9001H
60 Hz S107H	480	5690	6000	60	1 × MS7001H

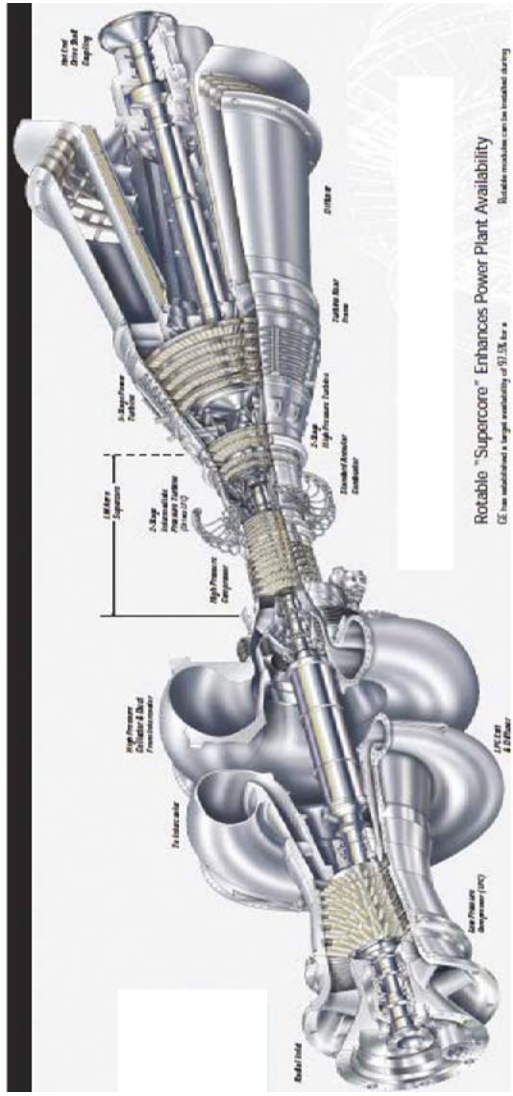


Figure 1-18 The LMS 100.

Early European turbines had a silo-type combustor as seen in the schematic drawing shown in Figure 1-19, which is a Siemens/KWU gas turbine vintage of the 1960s. These types of combustors were common on European turbines of the 1950s–1980s as also seen in Figures 1-20 and 1-21 which are photographs taken during an overhaul of a BBC/Alstom GT 11N2 gas turbine with the silo combustors. The new European turbines have gone toward the annular combustors as shown in Figure 1-22, which is a cross-sectional representation of the Siemens V94.2 annular combustor-type gas turbine. This turbine consists of a 16-stage axial-flow compressor followed by an annular combustor and a four-stage reaction type axial-flow turbine, which drives both the axial-flow compressor and the generator. Figure 1-23 is a design drawing of the same Siemens V94.2 gas turbine.

Siemens with their purchase of Westinghouse Gas Turbines is now the second major supplier of the frame type turbines. The Westinghouse turbines (W256/SGT-900 and W501 F/SGT6-5000 F) were designed using can-annular turbine technology common in the US-designed turbines, while the Siemens (V84 and V94) turbines were designed with annular combustor gas turbines common in European designs.

Figure 1-24 is the Siemens W501 F gas turbine with the can-annular gas turbine. The W501 F has a 16-stage axial-flow compressor, which produces a 17:1 pressure ratio that results in a pressure at the compressor exit of 250 psia. The combustion system comprises of a dry low NO_x (DLN) combustion system consisting of 16 can-annular-type combustors arranged in a circular array around the turbine rotor shaft. The turbine section has a four-stage reaction gas turbine, which produces 208 MW with an efficiency of 38.1%. Figures 1-25 and 1-26 are the W501 G gas turbine, which uses steam cooling for the combustor and transition pieces and the first-stage turbine nozzle vanes. The turbine produces 280 MW of power at an efficiency of 38.5%. This turbine has a 16-stage axial-flow compressor with a 19.2 pressure ratio and a 16 can-annular DLN combustor and a four-stage turbine. The can-annular combustor unlike other can-annular systems does not have crossover tubes; they have an igniter in each combustor. Siemens, in their new gas turbine primarily based on the Westinghouse turbine design, has decided to not continue with the concept of steam cooling. This could be due to many problems experienced in the W501 G gas turbines due to steam leakages.

Mitsubishi started in the gas turbine business as a licensee of Westinghouse Turbines and in the 1990s developed the 501 F gas turbine together. The compressor was designed by Mitsubishi and the hot section was originally designed by Westinghouse. These units are now sold individually after Siemens purchased Westinghouse and the cooperative venture was dissolved. The Westinghouse's W501 G and Mitsubishi's M501 G and M501 J gas turbines were developed separately by both parties since the end of their collaboration. The Mitsubishi's 501 F consists of a 16-stage axial-flow compressor with a 17:1 pressure ratio followed by a 14 can-annular combustors and a four-stage turbine section, whereas the Mitsubishi's M501 G shown in Figure 1-27 has a 15-stage compressor with a pressure ratio of 20:1, 14 can-annular combustors, and four-stage reaction turbines producing 267 MW of power at an efficiency of 39%. Mitsubishi's latest addition to the gas turbine field the M501 J as shown in Figure 1-28 has been developed with a firing temperature of 2912 °F (1600 °C). The M501 J has

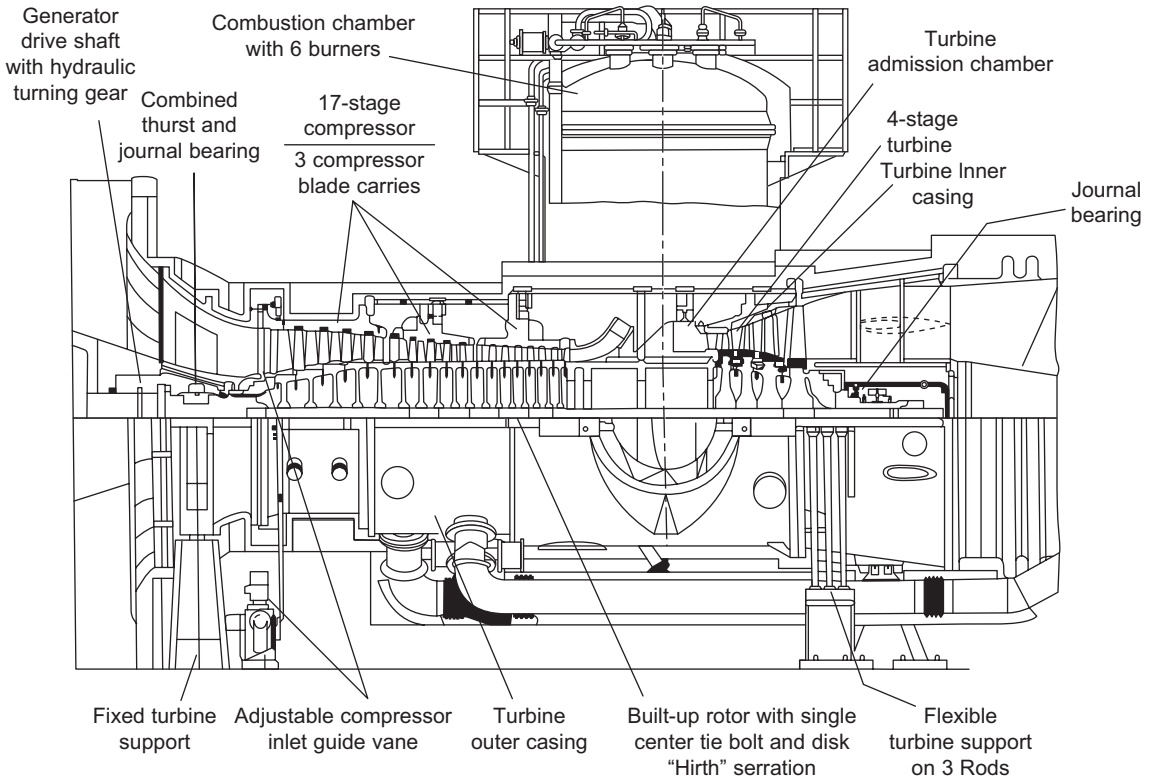


Figure 1-19 Longitudinal section of the Siemens/KWU gas turbine.



Figure 1-20 BBC/Alstom GT 11N2 being overhauled.

a 15-stage compressor, with the IGV and the first three stages having variable vanes and developing a pressure ratio of 23:1, followed by 14-can annular-type combustors. Figure 1-29 shows the M501 J rotor. The turbine section is a four-stage reaction turbine with the first three stages with thermal barrier coating (TBC) and air-cooled turbine blades for all four stages. The first two blades are un-shrouded and the last two stages are shrouded. The major differences in the J turbine as compared with the G turbine are in the turbine section, where the last two stages of the turbine blades are shrouded rather than the last stage only and all blade rows are cooled as compared with the last blade row un-cooled.

Alstom's GT24/26 gas turbines were introduced in 1995 – GT24 for the 60-Hz market and the GT26 for the 50-Hz market. Figure 1-30 is a cross section of the GT24/26 gas turbine. In combined-cycle applications, the efficiency for these turbines is in the 55–57% range. The GT24/26 fleet has now accumulated over 3,650,000 fired operating hours with more than 64,000 starts under various operating conditions, be it base load, intermediate, cycling, or daily start–stop. The turbines are unique in their design, as they have two in-line combustors thus taking advantage of the reheat gas turbine cycle as seen in the schematic diagram of the cycle in Figure 1-31 (see Chapter 2 for reheat gas turbine cycles). Brown Boveri the predecessor of Alstom are the only manufacturer in the world to have chosen to introduce the sequential combustion path, having installed its first sequential combustion unit in Switzerland in 1948. The

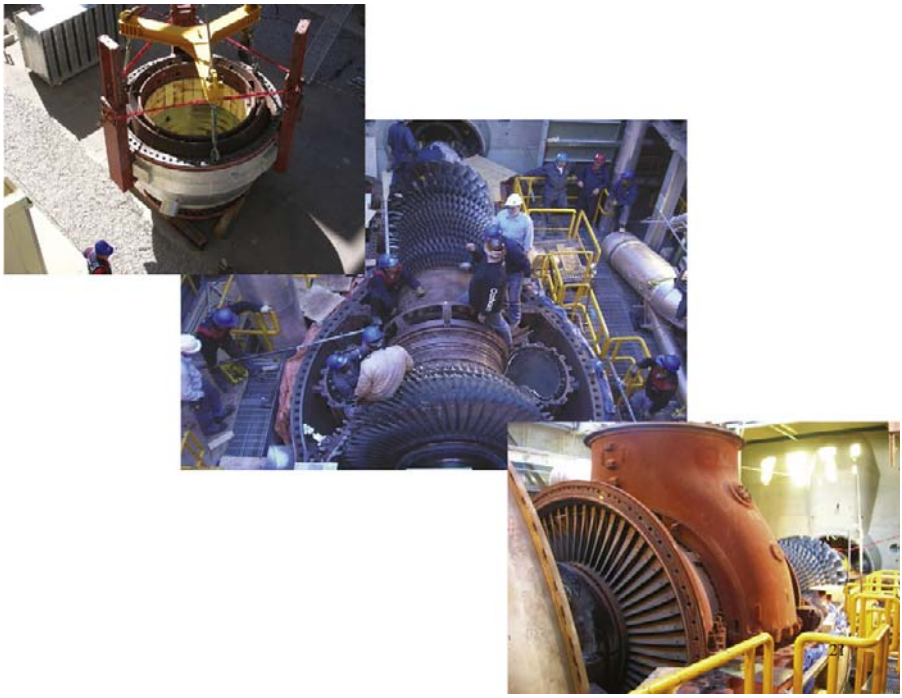


Figure 1-21 BBC/Alstom GT 11N2 being overhauled.

turbine compressor consists of 22 stages, the first 16 stages are the low pressure compressor at which point about 25% of the flow is diverted while about 75% of the flow is channeled to the last six stages of the compressor, the compressor produces a pressure ratio of more than 30. Figure 1-32 is a block diagram showing the characteristics of Alstom GT24/26 gas turbines. The compressor design employs controlled diffusion airfoil (CDA) blading (Chapter 7), thus allowing each compressor stage to be individually optimized according to specific requirements and boundary layer conditions. This leads to higher overall compressor efficiency, while retaining a high surge margin. The first three stages of the compressor have variable guide vanes that maintain at start-up and part load compressor efficiencies high. The entire gas turbine shaft, which consists of 22 stages of compression, a single-stage HP turbine, and four stages of a low-pressure turbine, is a one piece design with forged discs welded together. Figure 1-33 (a) shows the single shaft with the forged disks welded together. The first 16 rows of compressor blades and the five rows of turbine blades are anchored in fir tree slots as shown in Figure 1-33 (b). This welding technique advanced by Brown Boveri has been applied since 1929 to all GT and ST rotors. Figure 1-33 (c) shows such a rotor in a special jig manufactured by the Brown Boveri and now Alstom turbines that rotates the rotor in a vertical position while welding it and cooling the rotor to prevent any warping of the rotor.

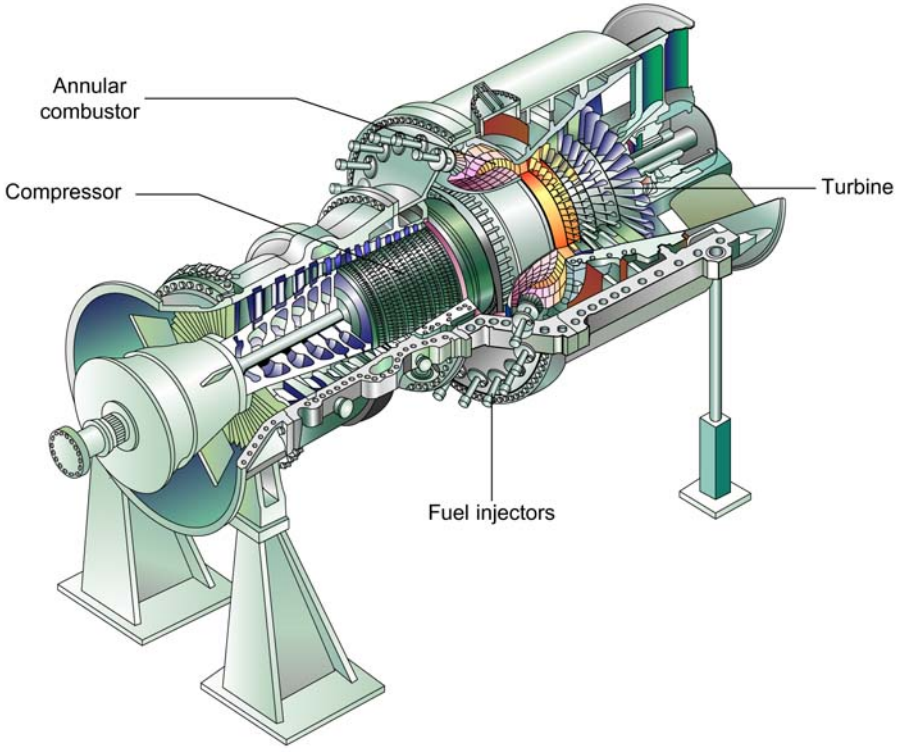
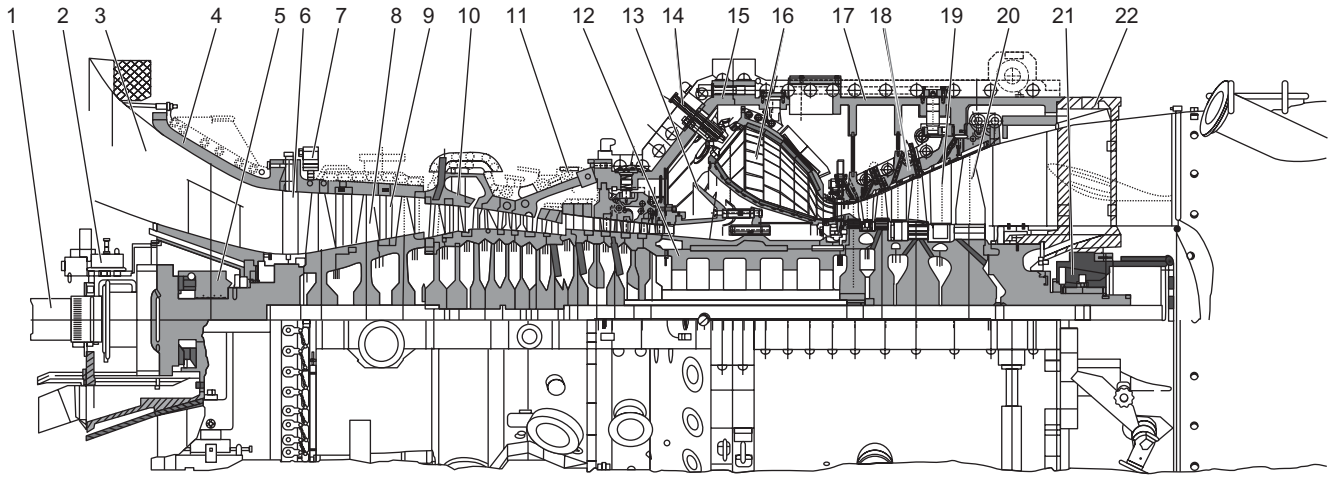


Figure 1-22 Siemen's V94.2.

The GT24/26 has low environmental emissions achieved using sequential combustion technology burning the fuel in two dry low NO_x combustors. It achieves this with low firing temperatures and with burners that are robust enough to cope with the wide fuel gas compositions that are seen in the market. Sequential combustion breaks the link between higher efficiency and higher inlet temperature. In sequential combustion, the process is characterized by splitting the combustion process into two stages separated by an expansion to an intermediate-pressure level. In this so-called "reheat" process, energy is added part way through the expansion process, resulting in high gas turbine efficiency and high power density.

The sequential combustion principle, applied to the large and heavy-duty GT26 gas turbine model, distinguishes it from conventional machines. In effect, sequential combustion can be visualized as a gas turbine comprising two combustor-turbines in series, where the exhaust gases from the first turbine feed the combustor of the second. The sequential combustors are known as the EnVironmental (EV) burner technology and the second burner is called the SEV burners. The EV burner gives the benefit of dry low NO_x combustion for operation with different natural gases, with the option to run with liquid fuel as an alternative. The burner is shaped like two half cones slightly offset laterally to form two inlet slots of constant width running the component's full



No	Component	No	Component	No	Component	No	Component
1	Intermediate shaft	6	Adjustable guide vanes	11	Bleed Port 2	16	Annular combustor
2	Hydraulic	7	System adjustor	12	Internal cylinder	17	Exterior casing No. 3
3	Inlet air passage	8	Compressor blades	13	Compressor diffuser exit	18	Diffuser turbine
4	Compressor and bearing case	9	Diffuser vanes	14	Fuel injector	19	Turbine nozzles
5	Radial and axial bearing	10	Bleed Port 1	15	Exterior casing No. 2	20	Radial bearing
						21	Exit casting

Figure 1-23 Siemen's V94.2 gas turbine.

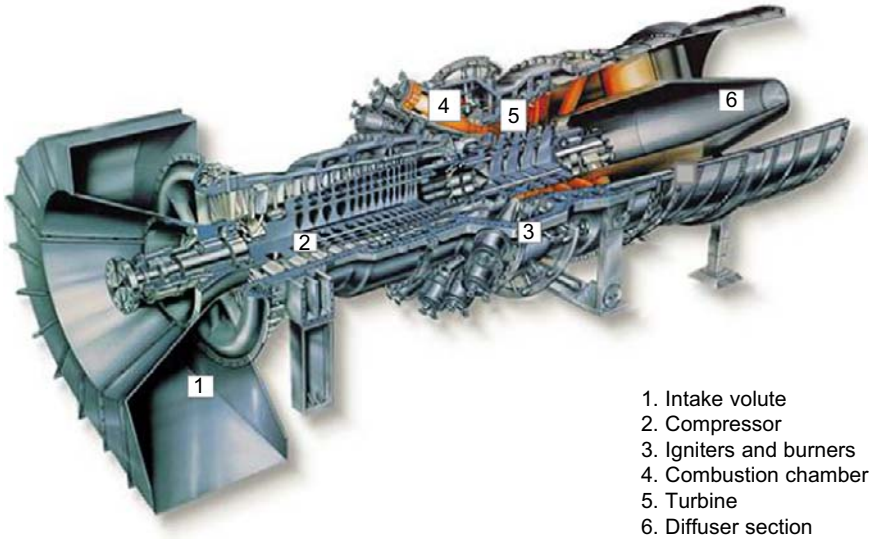


Figure 1-24 Siemen's W501 F gas turbine.

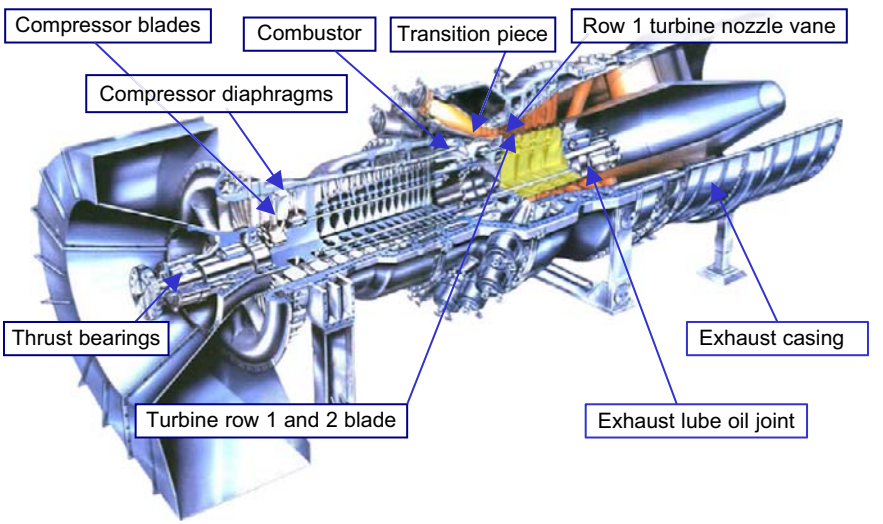


Figure 1-25 Siemen's W501 G gas turbine.

length. Combustion air enters the cone through these slots and fuel is injected through a series of fine holes in their edges. With this arrangement, fuel and air spiral into a vortex form and are intensively mixed.

The GT24/26 uses two fully annular combustion chambers that distribute the circumferential temperature evenly, while avoiding problem zones such as cross-firing

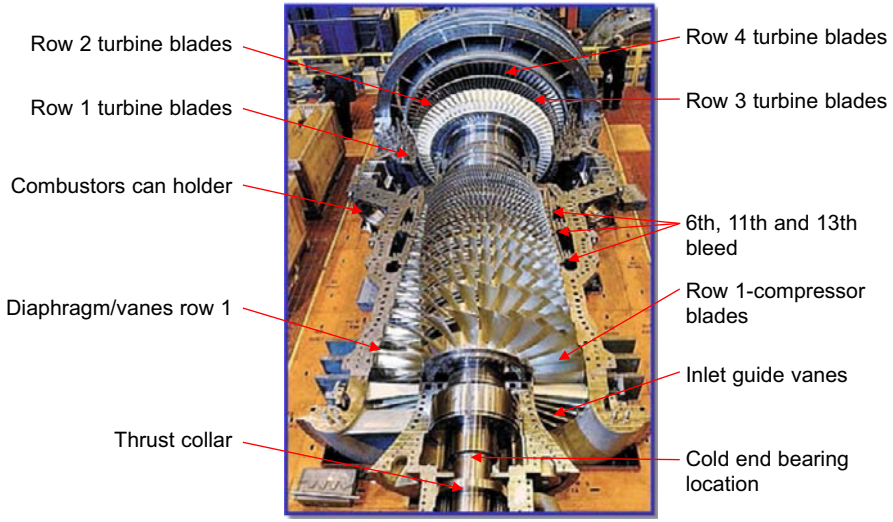


Figure 1-26 Siemen's W501 G gas turbine.

tubes or transition pieces. The sequential combustion concept results in a gas turbine exhibiting high power density and, therefore, affording smaller blade dimensions.

Air from the compressor cools the high-pressure turbine stage and the first three low-pressure turbine stages utilizing a combination of film and convection cooling techniques. Cooling air for the hot gas path components is taken from four extraction points along the compressor. Air from two of these secondary air flows is used directly, while the two other streams are cooled by heat exchangers (once through coolers) before entering the hot gas path components. The heat rejected is recovered in the water-steam cycle, which maximizes the performance of the GT26 in combined-cycle applications. In simple-cycle applications, the cooling is achieved by quenching water, which is introduced directly into the secondary air stream.

Aircraft-Derivative Gas Turbines

Aero-derivatives are used in electrical power generation due to their ability to start-up, shut down, and handle load changes more quickly than industrial machines. They are also used in the marine industry to reduce weight. The General Electric LM2500, General Electric LM6000, Rolls-Royce RB211, Rolls-Royce Avon, and the Pratt & Whitney FT-8 are common models of this type of machine.

Aero-derivative gas turbines consist of two basic components: an aircraft-derivative gas generator and a free-power turbine (Figure 1-34). The gas generator serves as a producer of gas energy; its job is to produce high-temperature gases at high pressure. The gas generator is derived from an aircraft engine modified to burn industrial fuels. Design innovations are usually incorporated to ensure the required long-life characteristics in the ground-based environment. In case of fan jet designs, the fan is removed and a couple of stages of compression are added in front of the existing

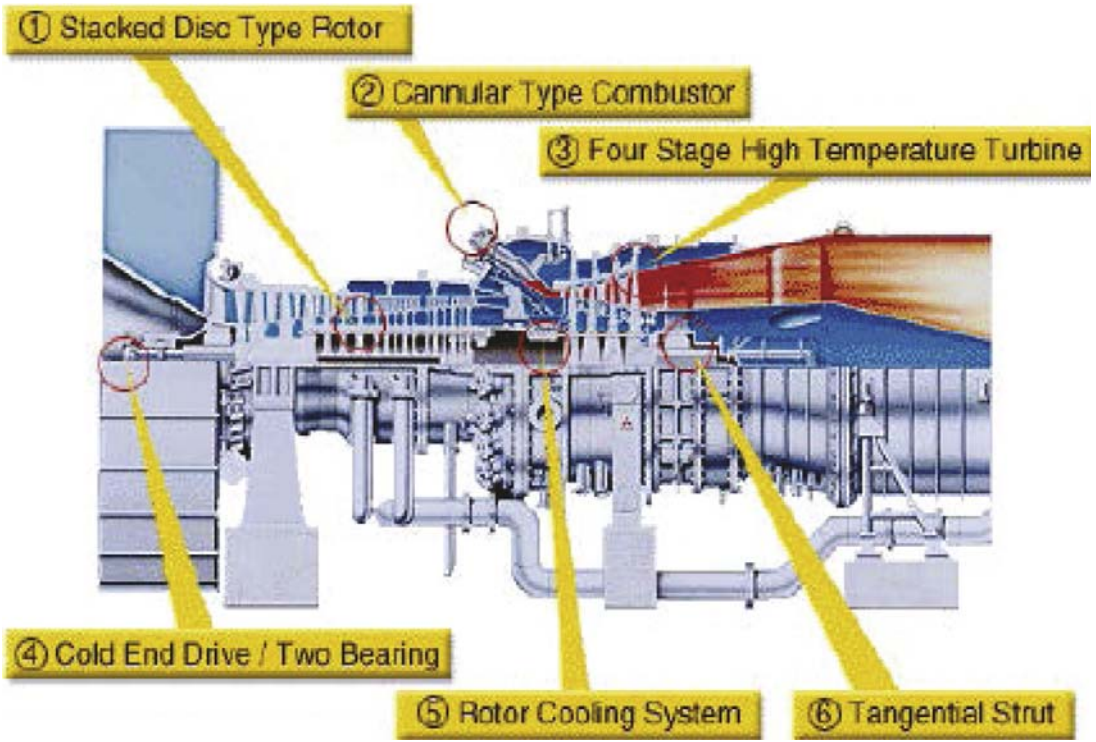


Figure 1-27 Mitsubishi's M501 G.

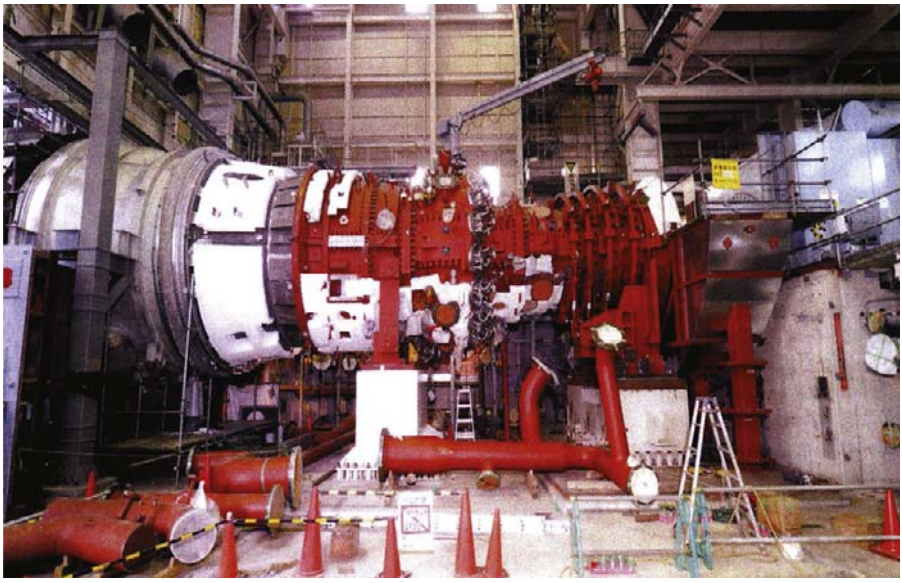


Figure 1-28 Mitsubishi's M501 J.



Figure 1-29 Mitsubishi's M501 J rotor.

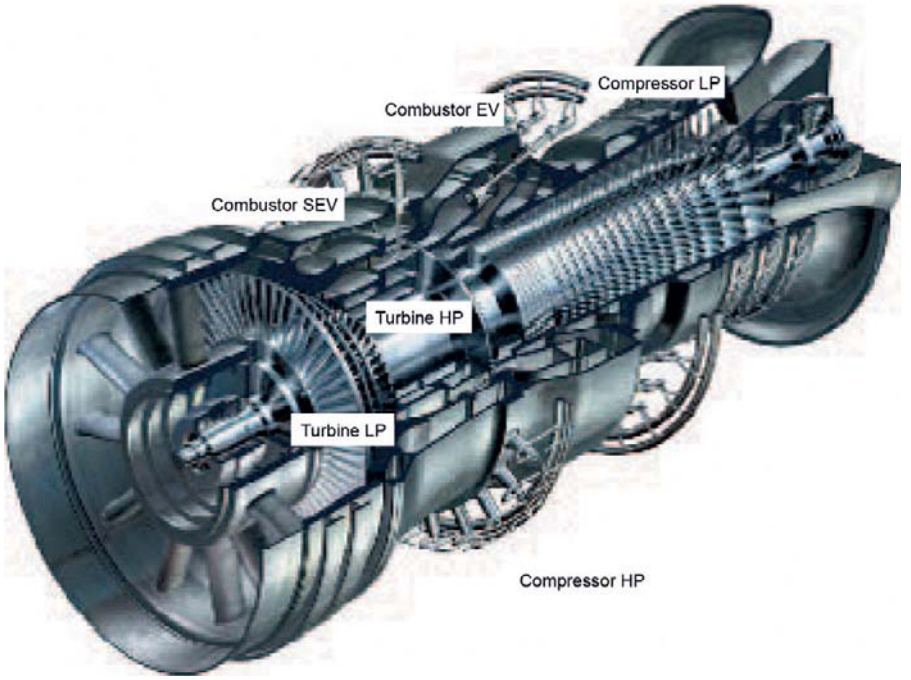


Figure 1-30 Alstom's GT24/26 gas turbine.

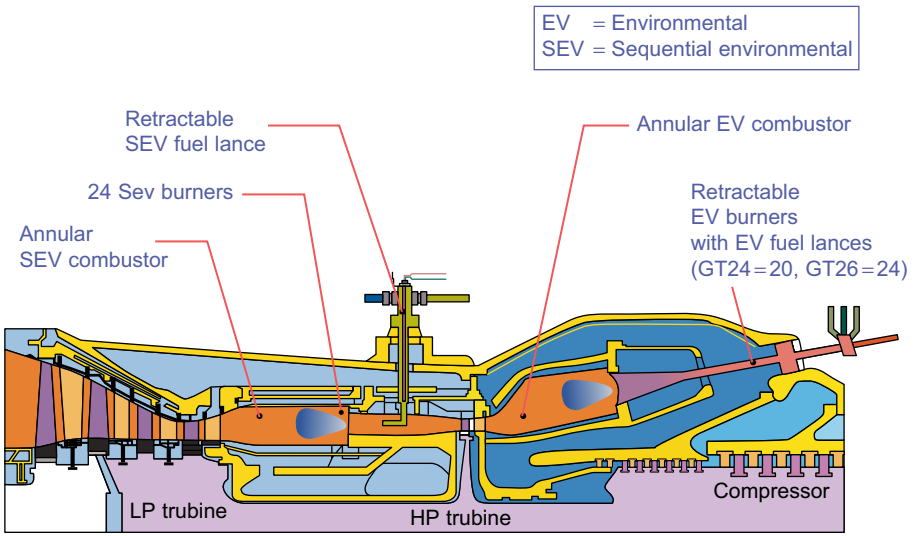


Figure 1-31 The reheat gas turbine cycle.

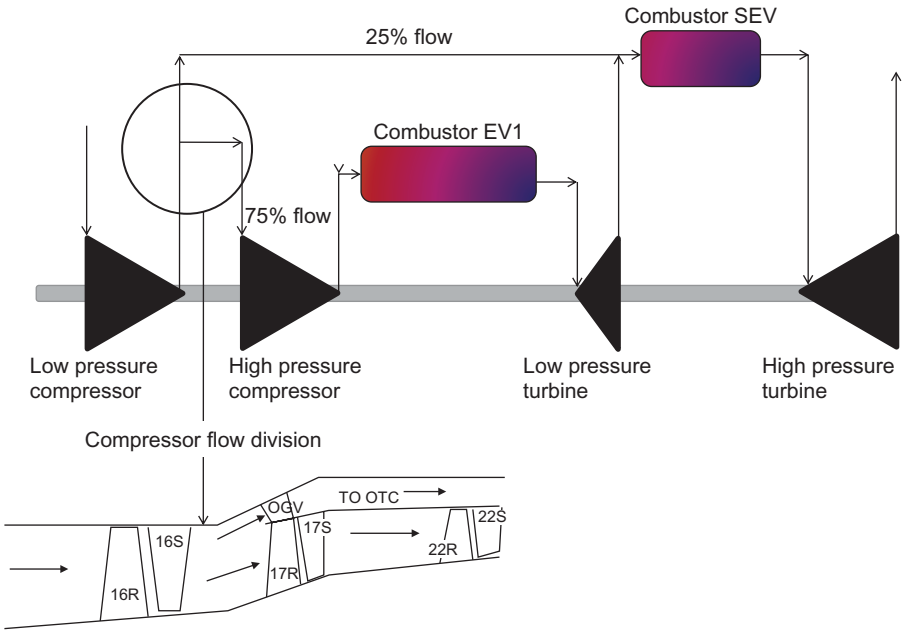


Figure 1-32 The Alstom GT24/26 gas turbine.

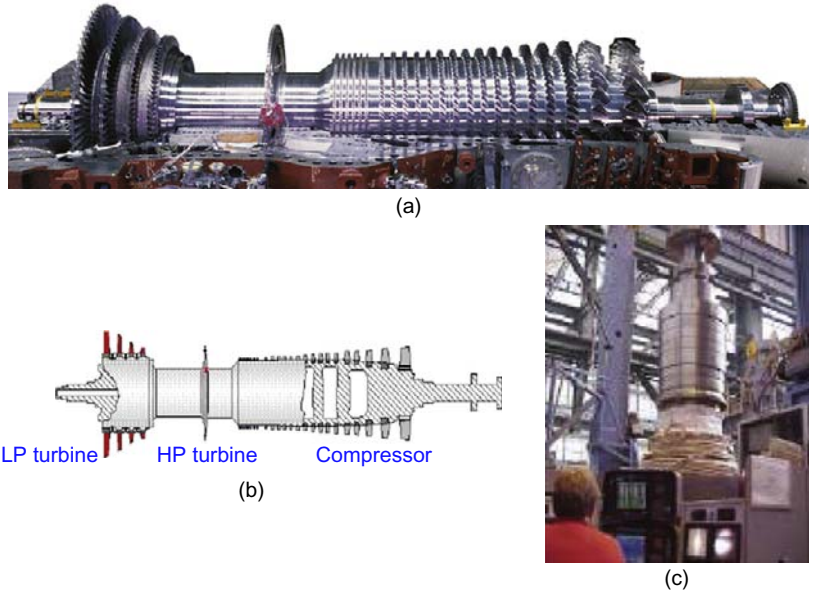


Figure 1-33 (a) One piece forged discs welded together; (b) The first 16 compressor stages and all turbine blades are anchored in fir tree slots; (c) A rotor in a special jig welding.

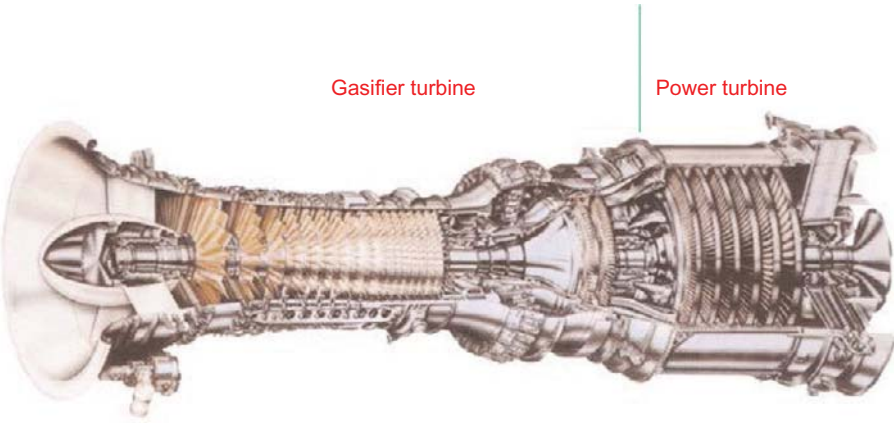


Figure 1-34 Free-power turbine.

low-pressure compressor. These additional stages are usually known as stage 00 and stage 0 thus keeping the stage numbering of the rest of the compressor stages the same as they were in the aircraft mode. The axial-flow compressor in most cases is divided into two sections – a low-pressure compressor followed by a high-pressure compressor. In those cases, there are usually a high-pressure turbine and a low-pressure turbine, which drive the corresponding sections of the compressor. The shafts are usually concentric thus the speeds of the high-pressure and low-pressure sections can be optimized. In these cases, the power turbine is separate and is not mechanically coupled; the only connection is via an aerodynamic coupling. The turbines have three shafts; the power turbine shaft is the drive shaft, all operate at independent speeds. The gas generator serves to raise combustion gas products to conditions of around 45–75 psi (3–5 Bar) and temperatures of 1300–1700 °F (704–927 °C) at the exhaust flange, that is entry to the power turbine. Figure 1-35 shows a cross section of the GE LM 6000 aero-derivative engine; it is most widely used in power production with an output of 48 MW and an efficiency of 41% in the simple-cycle gas turbine mode. In its sprint mode, water is injected between the low- and high-pressure compressor sections as shown in Figure 1-36. In this engine, there are two compressor sections – a low-pressure and a high-pressure compressor sections – and three turbine sections – a high-pressure gas turbine section, which drives the high-pressure compressor, a low-pressure turbine, which drives through a coaxial shaft the low-pressure compressor section, and finally a power turbine, which drives the driven equipment such as generators, compressors, and pumps. The LM 6000 with a once through steam generator (OTSG) is widely used in combined-cycle applications especially in small areas, as the foot print of an OTSG is much smaller than a regular heat recovery steam generator (HRSG), as shown in Figure 1-37.

The Rolls-Royce Aero-derivative Gas Turbines, the Avon and the RB-211, are widely used. The Rolls' Avon is used in compression gas pipelines stations, and the RB 211-HB3 with an output of about 42.4 MW and an efficiency of 39.3% is used

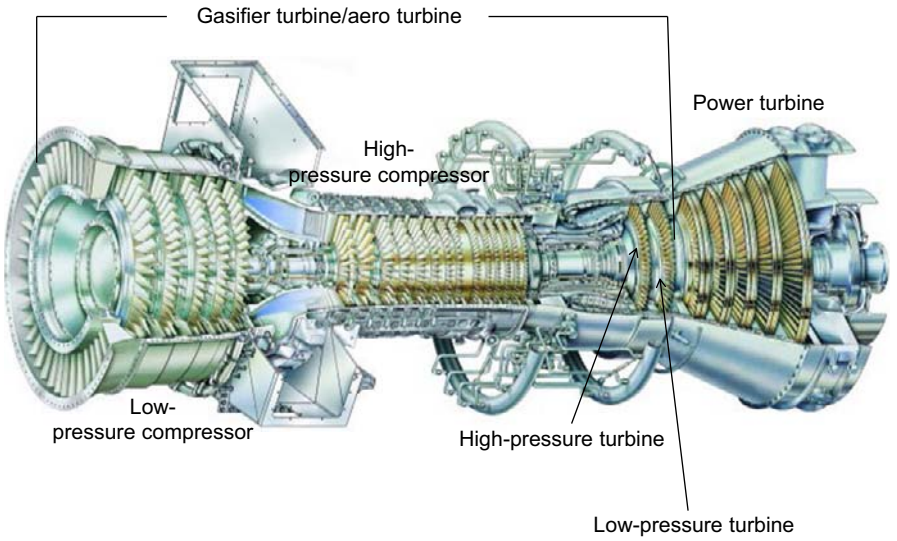


Figure 1-35 The GE LM 6,000 engine.

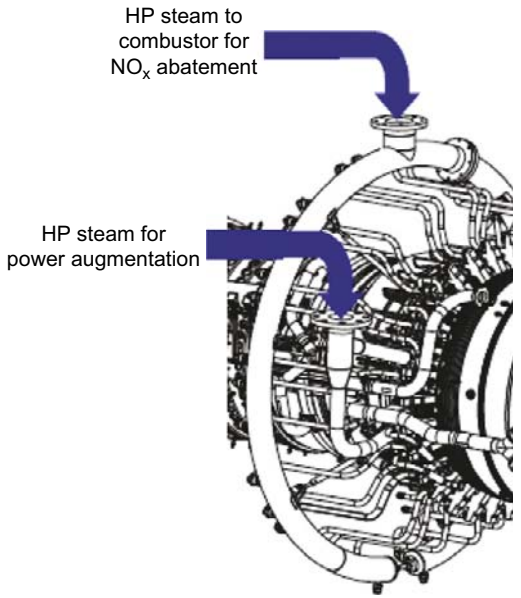


Figure 1-36 The GE LM 6,000 compressor section.

in power generation. Figure 1-38 is a cross-section of the RB 211. The RB 211 has a two-stage power turbine as shown in Figure 1-39. These types of power turbines are built by many compressor manufacturers such as Dresser-Rand and Cooper-Bessemer



Figure 1-37 Heat recovery steam generator.

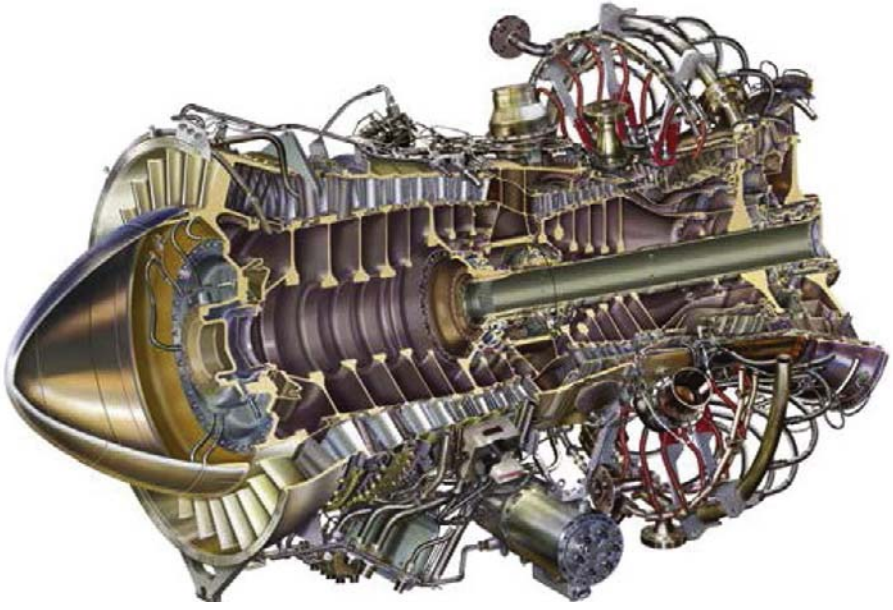


Figure 1-38 The RB 211.



Figure 1-39 A two-stage power turbine.

(now Cameron Industries) to power their compressors and also for power production.

The FT8 aero-derivative gas turbine made by Pratt & Whitney is in the 25-MW class and is used in industrial and municipal power supplies. The FT8 TwinPac unit offers 52 MW of electrical power from a two-engine single-generator configuration. The twin pack is a unit driving a single generator from both the ends. The FT8 gas turbine is based on aero-engine technology from Pratt & Whitney, adapted for industrial use as seen in Figure 1-40. The gas turbine is characterized by a compact and modular design. The PowerPac and the TwinPac offer two different variants of the FT8 gas turbine for power generation purposes. To drive compressors MechPac, the power turbine developed by MAN Diesel & Turbo is used. This has a rated speed of 5,500 rpm. Pollutant emissions are reduced by means of dry-low-NO_x-Brennkammer or by injecting water into the fuel chamber of the turbine. Typical applications include pipeline compressor units and gas treatment plant compressors.

Both the power and the petrochemical industries use the aircraft-type turbine. The power industry uses these units in a combined-cycle mode for power generation

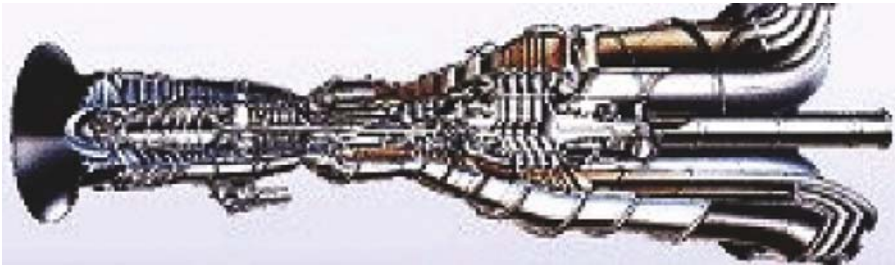


Figure 1-40 The FT8 gas turbine.

especially in remote areas where the power requirements are less than 100 MW. The petrochemical industry uses these types of turbines on offshore platforms especially for gas reinjection and as power plants for these offshore platforms, mostly due to their compactness and the ability to be easily replaced and then sent out to be repaired. The aero-derivative gas turbine is also used widely by gas transmission companies and petrochemical plants, especially for many variable speed mechanical drives. These turbines are also used as main drives for destroyers and cruise ships. The benefits of the aeroderivative gas turbines are as follows:

1. *Favorable installation cost.* The equipment involved is of a size and weight that it can be packaged and tested as a complete unit within the manufacturer's plant. Generally, the package will include either a generator or a driven pipeline compressor and all auxiliaries and control panels specified by the user. Immediate installation at the job site is facilitated by factory matching and debugging.
2. *Adaptation to remote control.* Users strive to reduce operating costs by automation of their systems. Nowadays, many new offshore and pipeline applications are designed for the remote unattended operation of the compression equipment. Jet gas turbine equipment lends itself to automatic control, as auxiliary systems are not complex, water cooling is not required (cooling by oil-to-air exchanges), and the starting device (gas expansion motor) requires little energy and is reliable. Safety devices and instrumentation adapt readily for the purposes of remote control and monitoring the performance of equipment.
3. *Maintenance concept.* The offsite maintenance plan fits in well with these systems where minimum operating personnel and unattended stations are the objectives. Technicians conduct minor running adjustments and perform instrument calibrations. Otherwise, the aero-derivative gas turbine runs without inspection until monitoring equipment indicates distress or sudden performance change. This plan calls for the removal of the gasifier section (the aero-engine) and sending it back to the factory for repair while another unit is installed. The power turbine does not usually have problems since its inlet temperature is much lower. Downtime due to the removal and replacement of the gasifier turbine is about eight hours.

Industrial-Type Gas Turbines

Industrial-type gas turbines are medium-range gas turbines and are usually rated between 5 and 20 MW. These units are similar in design to the large heavy-duty gas

turbines; their casing is thicker than the aero-derivative casing but thinner than the industrial gas turbines. They usually are split-shaft designs that are efficient in part-load operations. Efficiency is achieved by letting the gasifier section (the section that produces the hot gas) operate at maximum efficiency while the power turbine operates over a great range of speeds, especially in compressor drive service. The compressor is usually a 10- to 16-stage subsonic axial compressor, which produces a pressure ratio from about 5:1 to 15:1. Most American designs use annular combustors (about 5–10 combustor cans mounted in a circular ring) or annular-type combustors. Many European designs use side combustors and have lower turbine inlet temperatures compared with their American counterparts. Figure 1-41 shows an industrial-type gas turbine manufactured by Solar Turbines Inc., a Caterpillar Company Solar Turbines, is the largest manufacturer of industrial gas turbines by unit production as shown in Figure 1-12. Solar turbines range from the Solar Saturn 1.2 MW with an efficiency of 24.3% and a heat rate of 14,023 BTU/kW h (16,000 kJ/kW h) to the Titan, which is rated at 21.745 MW, at an efficiency of 40% and a heat rate of 9695 BTU/kW h (10,230 kJ/kW h).

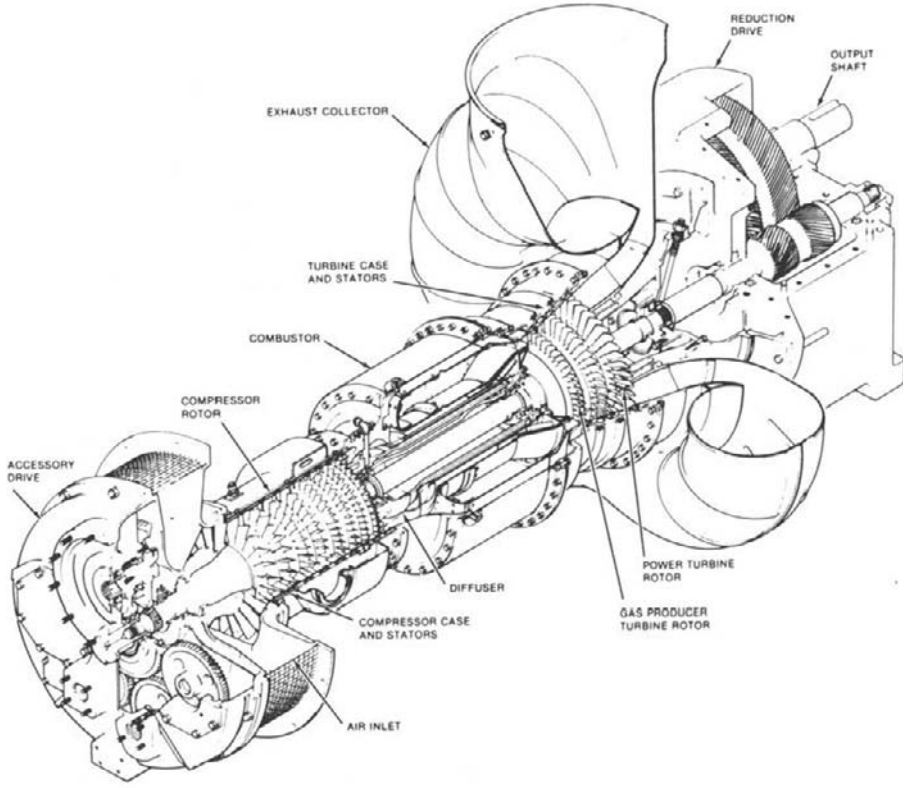


Figure 1-41 An industrial-type gas turbine from Solar Turbines Inc.

The gasifier turbine is usually a two- to three-stage axial turbine with an air-cooled first-stage nozzle and blade. The power turbine is usually a single- or two-stage axial-flow turbine that in many cases is not physically coupled with the gasifier turbine and the compressor of the gasifier section. The medium-range turbines are used on offshore platforms and are finding increasing use in petrochemical plants. The straight simple-cycle turbine is low in efficiency, but by using regenerators to consume exhaust gases, these efficiencies can be greatly improved. In process plants, this exhaust gas is used to produce steam. The combined-cycle (air-steam) cogeneration plant has very high efficiencies and is the trend of the future.

These gas turbines have, in many cases, regenerators or recuperators (Chapter 2 – Recuperative/Regenerator Brayton Cycle) to enhance their efficiency. Figure 1-42 shows an RGT design, by Solar Turbines, known as the Mercury, which has an efficiency of 41% and a heat rate of 8863 BTU/kW h (9351 kJ/kW h). Solar Turbines uses the term recuperator to describe its heat exchanger, which transfers energy between the exhaust hot gases and the cooler compressed air leaving the turbine. The recuperator in the solar turbine is a cross-flow heat exchanger made of Alloy 625. Figure 1-43 shows the flow path of the air as it enters the turbine and is then compressed to a pressure ratio of 9.9:1 in a 10-stage axial-flow compressor; the air then goes through the

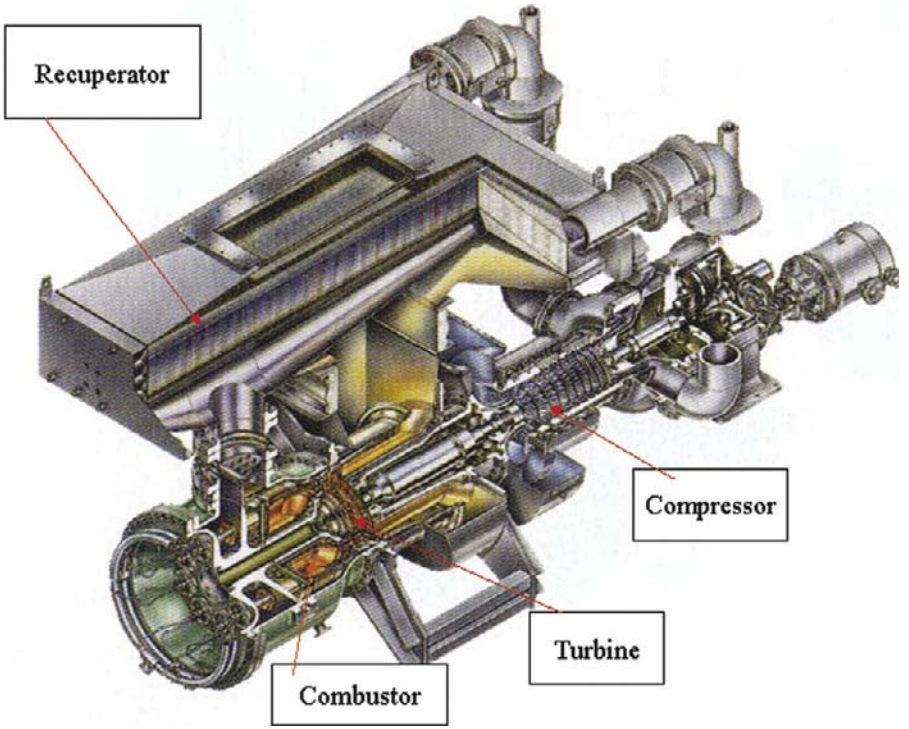


Figure 1-42 An RGT design, by Solar Turbines Inc.

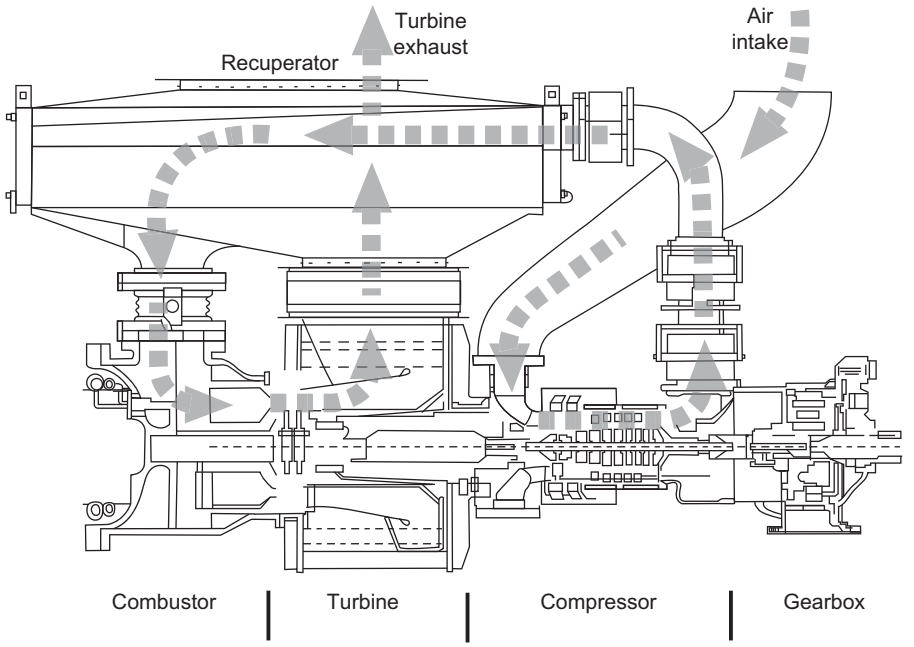


Figure 1-43 Air flow path.

recuperator where it is heated and then enters the annular combustor where it is fired to a temperature of about 2200 °F (1204 °C). The gas from the combustor is expanded through a two-stage axial-flow turbine. The exhaust gas from the turbine goes through the recuperator and heats the compressed air leaving the compressor.

Small Gas Turbines

Many small gas turbines that produce an output of less than 5 MW are designed similarly to the larger turbines already discussed; however, there are many designs that incorporate centrifugal compressors or combinations of centrifugal and axial compressors as well as radial-inflow turbines. A small turbine will often consist of a single-stage centrifugal compressor producing a pressure ratio as high as 8:1, a single-side combustor where temperatures of about 1800 °F (982 °C) are reached, and radial-inflow turbines. Figure 1-44 shows a schematic diagram of such a typical turbine.

Air is induced through an inlet duct to the centrifugal compressor, which rotates at high speed and imparts energy to the air. On leaving the impeller, air with increased pressure and velocity passes through a high-efficiency diffuser, which converts the velocity energy to static pressure. The compressed air, contained in a pressure casing, flows at low speed to the combustion chamber, which is a side combustor. A portion of the air enters the combustor head, mixes with the fuel, and burns continuously.

Next Page

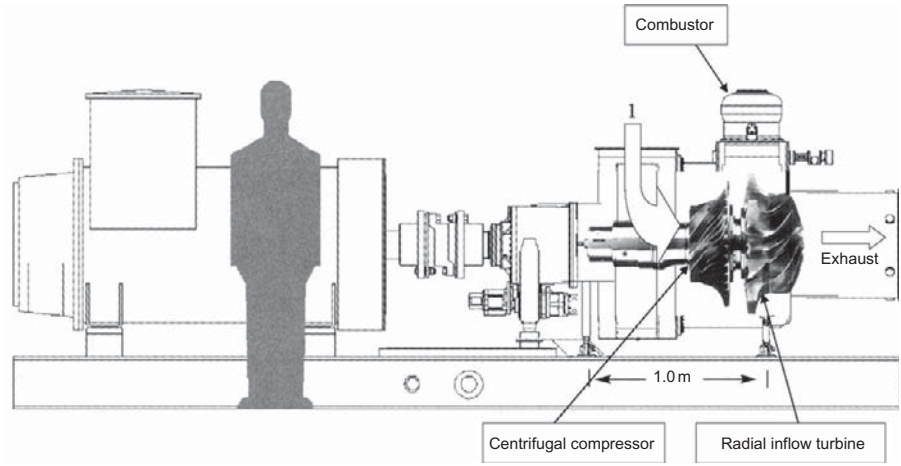


Figure 1-44 A radial-inflow turbine.

The remainder of the air enters through the wall of the combustor and mixes with the hot gases. Good fuel atomization and controlled mixing ensure an even temperature distribution in the hot gases, which pass through the volute to enter the radial-inflow turbine nozzles. High acceleration and expansion of the gases through the nozzle guide vane passages and turbine combine to impart rotational energy, which is used to drive the external load and auxiliaries on the cool side of the turbine. The efficiency of a small turbine is usually much lower than a larger unit because of the limitation of the turbine inlet temperature and the lower component efficiencies. Turbine inlet temperature is limited because the turbine blades are not cooled. Radial-flow compressors and impellers inherently have lower efficiencies than their axial counterparts. These units are rugged and their simplicity in design assures many hours of trouble-free operation. A way to improve the lower overall cycle efficiencies, 18–23%, is to use the waste heat from the turbine unit. High thermal efficiencies (30–35%) can be obtained, since nearly all the heat not converted into mechanical energy is available in the exhaust and most of this energy can be converted into useful work. These units when placed in a combined heat power (CHP) application can reach efficiencies, of the total process, as high as 60–70%.

The OPRA Turbine operates at a pressure ratio of 6.7:1 and produces 1910 kW of power at an efficiency of 26.9% and a heat rate of 12,732 BTU/kW h (13,433 kJ/kW h). The Dresser-Rand KG2-3E is a similar type turbine shown in Figure 1-45 and which used to be a Kongsberg gas turbine manufactured in Norway and has one-stage centrifugal compressor with a pressure ratio of 4.7 and single-stage radial-inflow turbine to produce a power of 1895 kW at an efficiency of 16.7% and a heat rate of 21,542 BTU/kW h (22,729 kJ/kW h). It is used for standby power with a 99.3% starting reliability.

The small Kawasaki gas turbines use centrifugal compressors and, in many cases, two centrifugal compressors are used as shown in Figure 1-46, but they use several

Copyrighted Materials
Copyright © 2012 Elsevier Retrieved from www.knovel.com

Part I

Design: Theory and Practice

1 An Overview of Gas Turbines

The gas turbine is a power plant that produces a great amount of energy depending on its size and weight. The gas turbine has found increasing service in the past 60 years in the power industry among both utilities and merchant plants as well as the petrochemical industry throughout the world. Its compactness, low weight, and multiple fuel application make it a natural power plant for offshore platforms. Today there are gas turbines that run on natural gas, diesel fuel, naphtha, methane, crude, low-BTU gases, vaporized fuel oils, and biomass gases.

The last 20 years have seen a large growth in gas turbine technology. The growth is spearheaded by the growth of materials technology, new coatings, new cooling schemes, and the growth of combined-cycle power plants. This, with the conjunction of increase in compressor pressure ratio from 7:1 to as high as 45:1, has increased simple-cycle gas turbine thermal efficiency from about 15% to 45%.

Table 1-1 gives an economic comparison of various generation technologies from the initial cost of such systems to the operating costs of these systems. Because distributed generation is very site specific, the cost will vary and the justification of installation of these types of systems will also vary. Sites for distributed generation vary from large metropolitan areas to the slopes of the Himalayan mountain range. The economics of power generation depends on the fuel cost, running efficiencies, maintenance cost, and initial cost, in that order. Site selection depends on environmental concerns such as emissions, noise, fuel availability, size, and weight.

Gas Turbine Cycle in the Combined Cycle or Cogeneration Mode

The utilization of gas turbine exhaust gases, for steam generation or the heating of other heat transfer mediums, or the use of cooling or heating buildings or parts of cities is not a new concept and is currently being exploited to its full potential.

The fossil power plants of the 1990s and into the early part of the new millennium were the combined-cycle power plants, with the gas turbine being the center piece of the plant. It was estimated that, between 1997 and 2006, there was an addition of 147.7 GW of power. These plants have replaced the large steam turbine plants, which were the main fossil power plants through the 1980s. The combined-cycle power plant is not new in concept, since some have been in operation since the mid-1950s. These plants came into their own with the new high-capacity and high-efficiency gas turbines.

Gas Turbine Engineering Handbook, Fourth Edition. DOI: 10.1016/B978-0-12-383842-1.00001-9
Copyright © 2012 Elsevier Inc. All rights reserved.

Table 1-1 Economic Comparison of Various Generation Technologies*

Technology Comparison	Diesel Engine	Gas Engine	Simple Cycle Gas Turbine	Micro Turbine	Fuel Cell	Solar Energy Photovoltic Cell	Wind	Biomass	River Hydro
Product rollout	Available	Available	Available	Available	Available	Available	Available	Available	Available
Size range (kW)	20–100,000+	50–7,000+	500–450,000+	30–200	50–1,000+	1+	Up to 5,000	Up to 5,000	20–3,000+
Efficiency (%)	36–43%	28–42%	21–45%	25–30%	35–54%	NA	45–55%	25–35%	60–70%
Gen. set cost ($/kW)	125–400	250–600	300–600	800–1,200	1,500–3,000	NA	—	NA	NA
Turnkey cost No-heat recovery ($/kW)	200–500	600–1,000	400–850	1,200–2,400	2,500–5,000	5,000–10,000	700–1,300	800–1,500	750–1,200
Heat recovery added cost ($/kW)	75–100	75–100	150–300	100–250	1,900–3,500	NA	NA	150–300	NA
O&M cost ($/kW h)	0.007–0.015	0.005–0.012	0.003–0.008	0.006–0.010	0.005–0.010	0.001–0.004	0.007–0.012	0.006–0.011	0.005–0.010

*The above information is based on data obtained from several sources such as manufacturers and technical magazines.

The new market place of energy conversion will have many new and novel concepts in combined-cycle power plants. Figure 1-1 shows the heat rates of these plants, present and future, and Figure 1-2 shows the efficiencies of the same plants. The plants referenced are the simple-cycle gas turbine (SCGT) with firing temperatures of 2400 °F (1315 °C), recuperative gas turbine (RGT), the steam turbine (ST) Plant, the combined-cycle power plant (CCPP), and the advanced combined-cycle power plants (ACCPPs), such as combined-cycle power plants using advanced gas turbine cycles, and finally the hybrid power plants (HPP).

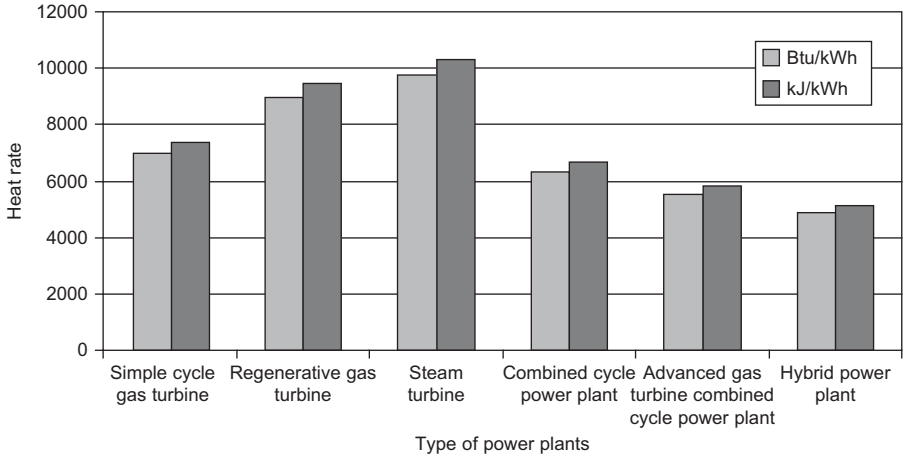


Figure 1-1 Heat rate of typical power plants.

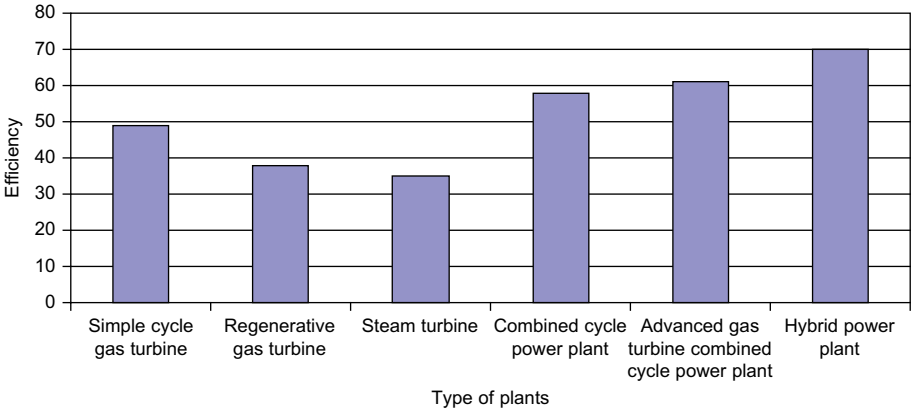


Figure 1-2 Efficiency.

Table 1-2 depicts an analysis of the competitive standing of the various types of power plants, their capital cost, heat rate, operation and maintenance costs, availability, reliability, and time for planning. By examining the capital cost and installation time of these new power plants, it is obvious that the gas turbine is the best choice for peaking power. Steam turbine plants are about 50% higher in initial costs of $800–$1000/kW than combined-cycle plants, which are about $400–$900/kW. Nuclear power plants are the most expensive plants. The high initial costs and the long time in construction make such a plant unrealistic for a deregulated utility.

Efficiency and heat rate are interchangeable, as they represent the efficient conversion of fuel to energy. The following relationship gives the easy conversion from heat rate to efficiency.

$$\text{Efficiency} = 3412.2/\text{BTU/kWh} = 2544.4/\text{BTU/HPh} = 3600/\text{kJ/kWh}$$

In the area of performance, the steam turbine power plants have an efficiency of about 35% when compared with combined-cycle power plants, which have an efficiency of about 55%. Newer gas turbine technology will make combined-cycle efficiencies range between 60% and 65%. As a rule of thumb, a 1% increase in the efficiency could mean that 3.3% more capital can be invested. However, one must be careful that the increase in the efficiency does not lead to a decrease in the availability. From 1996 to 2000, we have seen a growth in the efficiency of about 10% and a loss in the availability of about 10%. This trend must be turned around since many analyses show that a 1% drop in the availability needs about 2–3% increase in the efficiency to offset that loss. The larger gas turbines, just due to their size, take more time to undergo any of the regular inspections, such as combustor, hot gas path, and major overall inspections, thus reducing the availability of these turbines.

The time taken to install a steam plant from conception to production is about 42–60 months whereas it was about 22–36 months for combined-cycle power plants. The actual construction time is about 18 months, whereas obtaining environmental permits in many cases take 12 months and engineering takes 6–12 months. The time taken for bringing the plant online affects the economics of the plant, the longer the capital is employed without return the more it accumulates interest, insurance, and taxes.

It is obvious from this that as long as natural gas or diesel fuel is available, the choice of combined-cycle power plants is obvious.

Gas Turbine Performance

In 1791, John Barber, an Englishman, was the first to patent a design that used the thermodynamic cycle of the modem gas turbine. Figure 1-3 shows the sketch on which he based his patent. His design contained the basics of the modem gas turbine; it had a compressor, a combustion chamber, and a turbine. The main difference between his design and the modern one was that the turbine was equipped with a chain-driven reciprocating type of compressor. He intended its use for jet propulsion.

Many people consider Frank Whittle as the father of the modern-day gas turbine. The Whittle gas turbine was built in January 1930 and had a thrust of 1,000 lbf and an efficiency of 14%. The air was compressed in a centrifugal compressor and was then

Table 1-2 Economic and Operation Characteristics of Plant*

Type of Plant	Capital Cost ($/kW)	Heat Rate BTU/kWh (kJ/kWh)	Net Efficiency	Variable Operation and Maintenance ($/MWh)	Fixed Operation and Maintenance ($/MWh)	Availability (%)	Reliability (%)	Time from Planning to Completion (Months)
SCGT (2500 °F/1371 °C) Natural gas fired	300–350	7582–8000	45	5.8	0.23	88–95	97–99	10–12
SCGT oil fired	400–500	8322–8229	41	6.2	0.25	90–96	95–98	12–16
SCGT crude fired	500–600	10,662–11,250	32	13.5	0.25	75–80	90–95	12–16
Regenerative gas turbine natural gas fired	375–575	6824–7200	50	6	0.25	86–93	96–98	12–16
Combined-cycle gas turbine	600–900	6203–6545	55	4	0.35	86–93	95–98	22–24
Advanced gas turbine CCPP	800–1,000	5249–5538	65	4.5	0.4	84–90	94–96	28–30
Combined-cycle coal gasification	1,200–1,400	6950–7332	49	7	1.45	75–85	90–95	30–36
Combined-cycle fluidized bed	1,200–1,400	7300–7701	47	7	1.45	75–85	90–95	30–36
Nuclear power	1,800–200	10,000–10,550	34	8	2.28	80–89	92–98	48–60
Steam plant coal fired	800–1,000	9749–10285	35	3	1.43	82–89	94–97	36–42
Diesel generator-diesel fired	400–500	7582–8000	45	6.2	4.7	90–95	96–98	12–16
Diesel generator-power plant oil fired	600–700	8124–8570	42	7.2	4.7	85–90	92–95	16–18
Gas engine generator power plant	650–750	7300–7701	47	5.2	4.7	92–96	96–98	12–16

*The above information is based on data obtained from several sources such as manufacturers, technical magazines, as well as data obtained by the author.

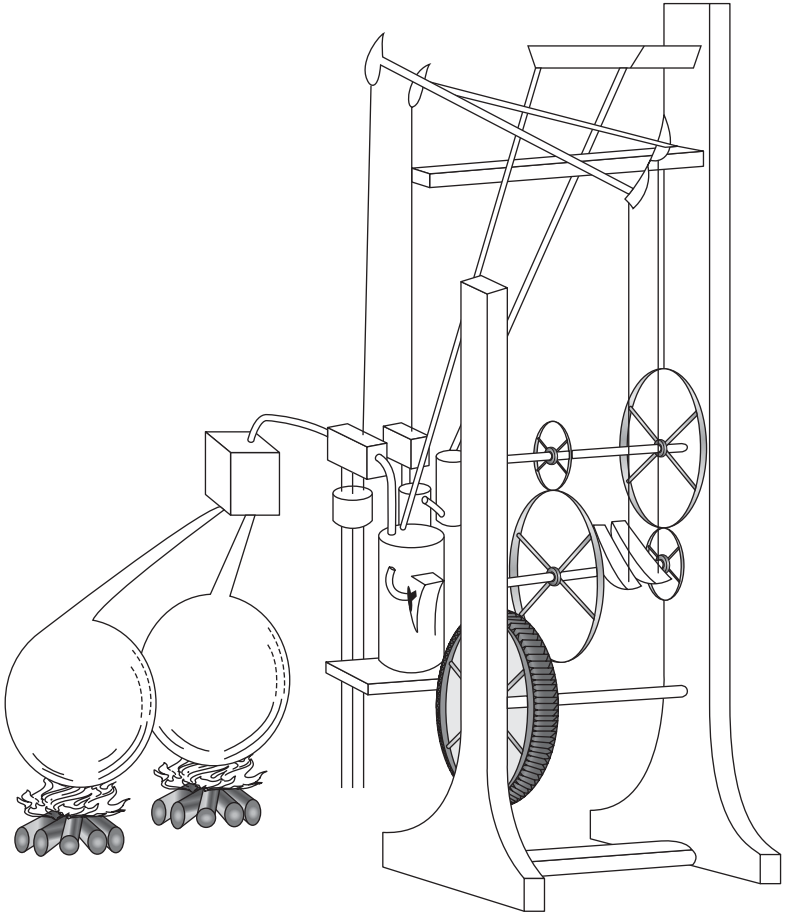


Figure 1-3 Barber's British Patent – 1791.

expanded through a radial-inflow turbine. Figure 1-4 is a photograph of the Whittle turbine and Figure 1-5 is its schematic diagram. In 1903, General Electric developed a turbocharger, and in 1941, it modified the Whittle engine for America's first aero-engine. In 1945, Westinghouse developed the first gas turbine based solely on US design; the turbine included an axial-flow compressor, a turbine, and an annular combustor.

The aerospace engines have been leaders in most of the technology in the gas turbine. The design criteria for these engines were high reliability, high performance, with many starts and flexible operation throughout the flight envelope. The engine life of about 3,500 hours between major overhauls was considered good. The performance of the aerospace engine has always been rated primarily on its thrust/weight ratio. Increase in engine thrust/weight ratio is achieved by developing the blades of high aspect ratio in the compressor as well as optimizing the pressure ratio and firing temperature of the turbine for maximum work output per unit flow.

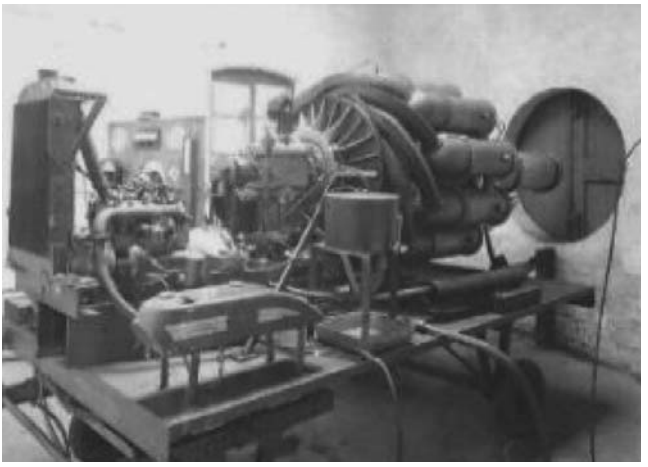


Figure 1-4 Whittle turbine.

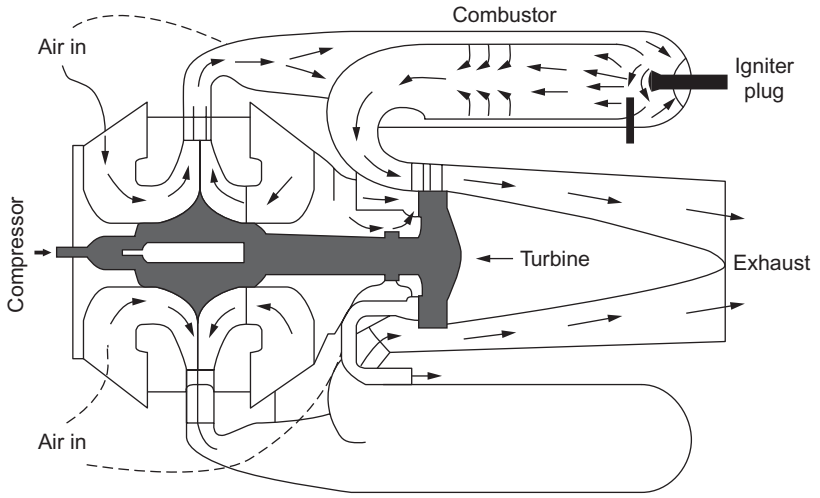


Figure 1-5 Schematic of Whittle turbine.

The industrial gas turbine has always emphasized long life and this conservative approach has resulted in the industrial gas turbine in many aspects giving up high performance for rugged operation. The industrial gas turbine has been conservative in the pressure ratio and the firing temperatures. This has all changed in the last 10 years; spurred on by the introduction of the "aeroderivative gas turbine," the industrial gas turbine has dramatically improved its performance in all operational aspects. This has resulted in a dramatic reduction of the performance gap between these two types of gas turbines. The gas turbine to date in the combined-cycle mode is fast replacing the steam turbine as the base load provider of electrical power throughout the world. This is even true in Europe and the United States of America where the large steam turbines

were the only type of base load power in the fossil energy sector. The gas turbine from the 1960s to the late 1980s was used only as peaking power in those countries; it was used as base load mainly in the "developing countries" where the need of power was increasing rapidly and that the waiting period of three to six years for a steam plant was unacceptable.

Figures 1-6 and 1-7 show the growth of the pressure ratio and firing temperature, respectively. The growth of these is parallel to each other, as both growths are necessary to achieve the optimum thermal efficiency.

The increase in pressure ratio increases the gas turbine thermal efficiency when accompanied by the increase in turbine's firing temperature. Figure 1-8 shows the effect on the overall cycle efficiency of the increasing pressure ratio and firing temperature. The increase in the pressure ratio increases the overall efficiency at a

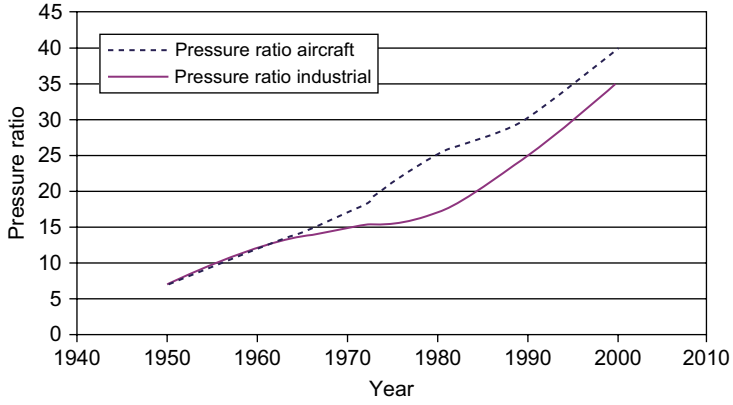


Figure 1-6 Engine pressure ratio development.

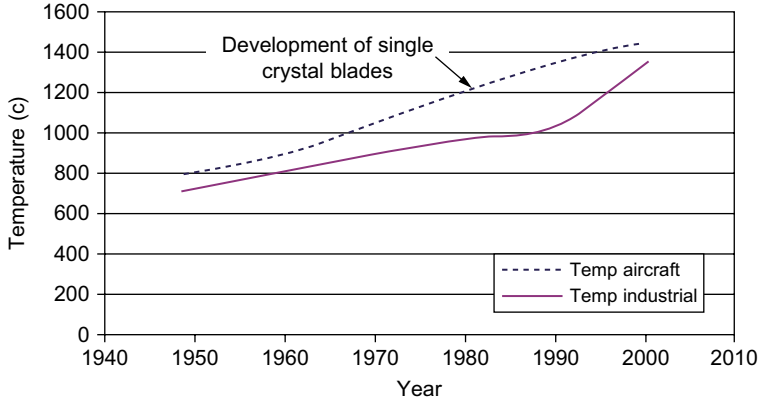


Figure 1-7 Trend in improvement in firing temperature.

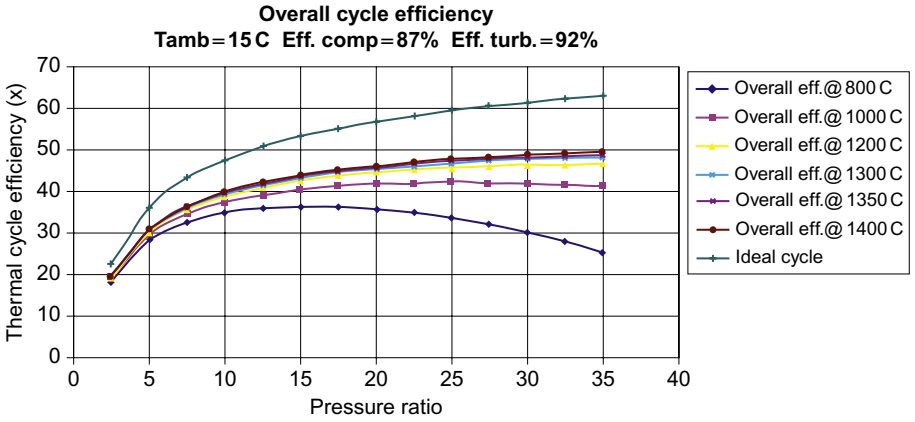


Figure 1-8 Overall cycle efficiency.

given temperature; however, increasing the pressure ratio beyond a certain value at any given firing temperature can actually result in lowering the overall cycle efficiency.

In the past, the gas turbine was perceived as a relatively inefficient power source when compared with other power sources. Its efficiencies were as low as 15% in the early 1950s; however, today its efficiencies are in the range of 45–50%, which translates to a heat rate of 7582 BTU/kW h (8000 kJ/kW h) to 6824 BTU/kW h (7199 kJ/kW h). The limiting factor for most gas turbines has been the turbine inlet temperature. With new schemes of cooling, using steam or conditioned air, and breakthroughs in blade metallurgy, higher turbine temperatures have been achieved. The new gas turbines have fired inlet temperatures as high as 2600 °F (1427 °C) and pressure ratios of 40:1 with the efficiencies of 45% and above.

Gas Turbine Design Considerations

The gas turbine is the best suited prime mover when the needs at hand such as capital cost, time from planning to completion, maintenance costs, and fuel costs are considered. The gas turbine has the lowest maintenance and capital costs among major prime movers. It also has the fastest completion time to full operation among other plants. Its disadvantage was its high heat rate but this has been addressed and the new turbines are among the most efficient types of prime movers. The combination of plant cycles further increases the efficiencies to the low 60% region.

The design of any gas turbine must meet essential criteria based on operational considerations. Chief among these criteria are as follows:

1. High efficiency
2. High reliability and thus high availability
3. Ease of service
4. Ease of installation and commission

5. Conformance with environmental standards
6. Incorporation of auxiliary and control systems that have a high degree of reliability
7. Flexibility to meet various service and fuel needs

A look at each of these criteria will enable the user to get a better understanding of the requirements.

The two factors that mostly affect the high turbine efficiencies are pressure ratios and the firing temperature. The axial-flow compressor, which produces the high-pressure gas in the turbine, has seen a dramatic change as the gas turbine pressure ratio has increased from 7:1 to 45:1 in some of the aero gas turbines used today. The increase in the pressure ratio increases the gas turbine thermal efficiency when accompanied with the increase in turbine's firing temperature. The increase in the pressure ratio increases the overall efficiency at a given temperature; however, increasing the pressure ratio beyond a certain value at any given firing temperature can actually result in lowering the overall cycle efficiency. It should also be noted that the very high-pressure ratios tend to reduce the operating range of the turbine compressor. This causes the turbine compressor to be much more intolerant to dirt build-up in the inlet air filter and on the compressor blades, and it creates large drops in cycle efficiency and performance. In some cases, it can lead to compressor surge, which in turn can lead to a flameout, or even serious damage and failure of the compressor blades, and the radial and thrust bearings of the gas turbine.

The effect of firing temperature is very predominant; for every 100 °F (55.5 °C) increase in the temperature, the work output increases approximately 10% and gives about a 0.5–1% increase in the efficiency. Higher pressure ratios and turbine inlet temperatures improve the efficiencies on the simple-cycle gas turbine. Figure 1-9 shows a simple-cycle gas turbine performance map as a function of pressure ratio and turbine inlet temperature.

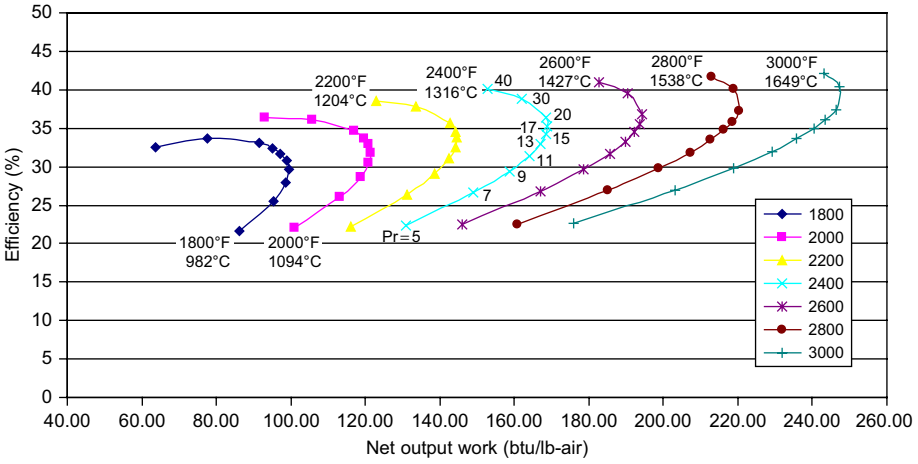


Figure 1-9 The performance map of a simple-cycle gas turbine.

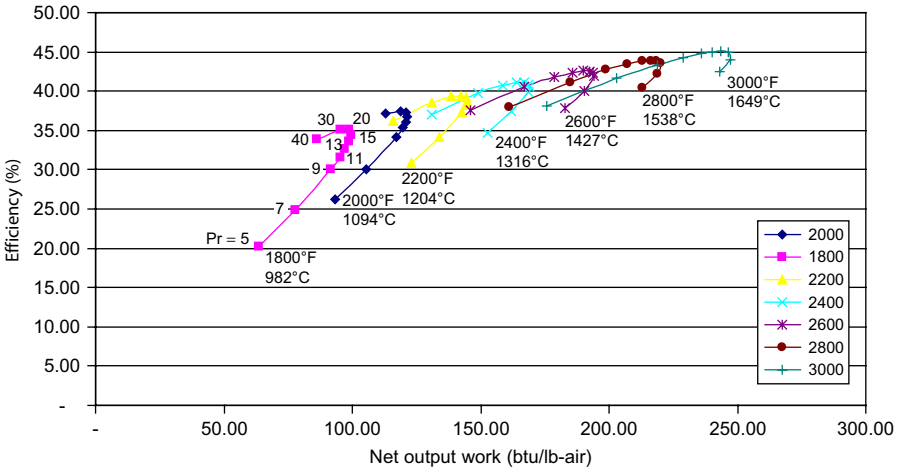


Figure 1-10 The performance map of a regenerative gas turbine cycle.

Another way to achieve higher efficiencies is to use the exhaust gases to heat the air leaving the compressor, thus reducing the amount of fuel required to reach the temperature that required to operate the turbine. This is achieved by the use of regenerators or recuperators, which heat the compressor exit air by the exhaust gases from the turbine exit. Regenerators or recuperators are usually used in small- to intermediate-sized gas turbines. Figure 1-10 shows the effects of pressure ratio and temperatures on efficiencies and work for a regenerative or recuperative cycle. Comparing Figure 1-10 with Figure 1-9 shows that increasing the pressure ratio lowers the efficiency in a regenerative or recuperative cycle. The effect of pressure ratio for this cycle is opposite to that experienced in the simple cycle. Regenerators or recuperators can increase efficiency as much as 15–20% of today's hot section operating temperatures. The use of a regenerator or a recuperator is that they are mostly used in gas turbines with outputs less than 10 MW. In these gas turbines, the airflow is small not requiring a large regenerator or recuperator and the firing temperature is low thus the pressure ratio is usually less than 10:1. The optimum pressure ratio, as seen in Figure 1-10, is about 20:1 for a regenerative system and 40:1 for the simple cycle at today's higher turbine inlet temperatures that are starting to approach 3000 °F (1649 °C).

High availability and reliability are the most important parameters in the design of a gas turbine. The availability of a power plant is the percentage of time the plant is available to generate power in any given period. The reliability of the plant is the percentage of time between planed overhauls. The following are the basic definitions of availability and reliability; expanded definitions of these terms are given in Chapter 21.

The availability of a power plant is defined as

$$A = \frac{P - S - F}{P}, \tag{1-1}$$

where

P = period of time (in hours), usually this is assumed as one year, which amounts to 8,760 hours;

S = scheduled outage hours for planned maintenance; and

F = forced outage hours or unplanned outage due to repair.

The reliability of a power plant is defined as:

$$R = \frac{P - F}{P}. \tag{1-2}$$

Availability and reliability have a very major impact on the plant's economy. Reliability is essential in that when the power is needed it must be there. When the power is not available, it must be generated or purchased and can be very costly to the operation of a plant. Planned outages are scheduled for non-peak periods. Peak periods are when the majority of the income is generated; as usually, there are various tiers of pricing depending on the demand. Many power purchase agreements have clauses, which contain capacity payments, thus making plant availability critical in the economics of the plant.

Reliability of a plant depends on many parameters, such as the type of fuel, the preventive maintenance programs, the operating mode, the control systems, and the firing temperatures.

To achieve a high availability and reliability factor, the designer must keep in mind many factors. Some of the more important considerations which govern the design are: blade and shaft stresses, blade loadings, material integrity, auxiliary systems, and control systems. The high temperatures required for high efficiencies have a disastrous effect on turbine blade life. Proper cooling must be provided to achieve blade metal temperatures between 1000 °F (537 °C) and 1300 °F (704 °C), below the levels of the onset of hot corrosion. Thus, the right type of cooling systems with proper blade coatings and materials are needed to ensure the high reliability of a turbine.

Serviceability is an important part of any design, because fast turnarounds result in high availability to a turbine and reduce maintenance and operations costs. Service can be accomplished by providing proper checks such as monitoring of exhaust temperature, shaft vibration, and surge. Moreover, the designer should incorporate borescope ports for fast visual checks of hot parts in the system. Split casings for fast disassembly, field balancing ports for easy access to the balance planes, and combustor cans that can be easily disassembled without removing the entire hot section, are some of the many ways that afford ease of service.

Ease of installation and commissioning is another reason for gas turbine use. A gas turbine unit can be tested and packaged at the factory. Use of a unit should be carefully planned so as to cause as few start cycles as possible. Frequent start-ups and shutdowns at commissioning greatly reduce the life of a unit.

Environmental considerations are critical in the design of any system. The system's impact on the environment must be within legal limits and thus must be addressed by the designer carefully. Combustors are the most critical component, and great care

must be taken to design them to provide low smoke and low NO_x output. The high temperatures result in increasing the NO_x emissions from the gas turbines. This resulted in initially attacking the NO_x problem by injecting water or steam into the combustor. The next stage was the development of dry low NO_x combustors. The development of new dry low NO_x combustors has been a very critical component in reducing the NO_x output, as the gas turbine's firing temperature is increased. The new low NO_x combustors increase the number of fuel nozzle and the complexity of the control algorithms.

Lowering the inlet velocities and providing proper inlet silencers can reduce air noise. Considerable work by NASA on compressor casings has greatly reduced noise.

Auxiliary systems and control systems must be designed carefully, since they are often responsible for the downtime in many units. Lubrication systems, one of the critical auxiliary systems, must be designed with a backup system and should be as close to failure-proof design as possible. The advanced gas turbines are all digitally controlled and incorporate online condition monitoring to some extent. The addition of new online monitoring requires new instrumentation. Control systems provide acceleration-time and temperature-time controls for start-ups as well as control various antisurge valves. At operating speeds, they must regulate fuel supply and monitor vibrations, temperatures, and pressures throughout the entire range.

Flexibility of service and fuels are the criteria that enhance a turbine system, but they are not necessary for every application. The energy shortage makes it closer to its operating point and thus it operate at higher efficiencies. This flexibility may entail a two-shaft design incorporating a power turbine, which is separate and not connected to the gasifier unit. Multiple fuel applications are now in greater demand, especially where there may be a shortage of various fuels at different times of the year.

Categories of Gas Turbines

The simple-cycle gas Turbine is classified into the following six broad groups:

1. *Frame type heavy-duty gas turbines*. The frame units are the large power generation units ranging from 3 to 480 MW in a simple-cycle configuration, with efficiencies ranging from 30% to 48%.
2. *Aircraft-derivative gas turbines*. Aeroderivatives, as the name indicates, are power generation units that have origin in the aerospace industry as the prime mover of aircraft. These units have been adapted to the electrical generation industry by removing the bypass fans and adding a power turbine at their exhaust. The power of these units ranges from about 2.5 to 50 MW. The efficiencies of these units can range from 35% to 45%.
3. *Industrial-type gas turbines*. These turbines vary in range from about 2.5 to 15 MW. These are used extensively in many petrochemical plants for compressor drive trains. The efficiencies of these units are in the low 30s.
4. *Small gas turbines*. These gas turbines are in the range from about 0.5 to 2.5 MW. They often have centrifugal compressors and radial-inflow turbines. The efficiencies of the simple-cycle applications vary from 15% to 25%.
5. *Microturbines*. These turbines are in the range from 20 to 350 kW. The growth of these turbines has been dramatic from the late 1990s, as there is an upsurge in the distributed generation market.

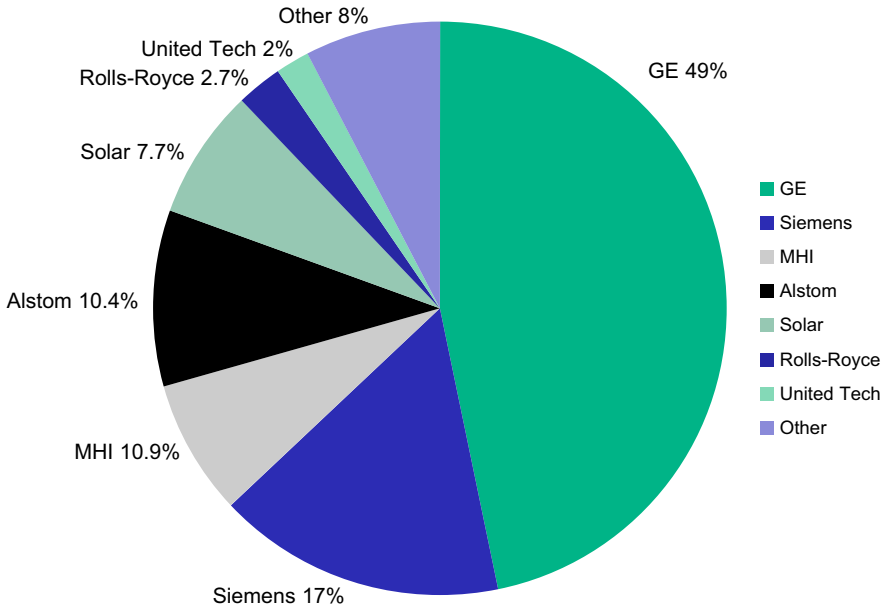


Figure 1-11 Distribution of gas turbine sales.

6. *Vehicular gas turbines*. These turbines have ranged from 300 to 1,500 HP. The first vehicular turbine was built in 1954 by Chrysler Corporation and followed by the Ford Motor Company's truck engine. The only vehicular turbine that has been very successful has been the gas turbine used in US Army Abrams Tank.

Figure 1-11 shows the distribution by manufacturers, total dollars of a $60-billion market, and the types of gas turbines that are sold throughout the world based on the data as given in the *Turbomachinery 2010 Handbook*. In this figure, GE is by far the largest supplier having about 49% of the market. Figure 1-12 shows the distribution by manufacturers and the number of turbines manufactured by each manufacturer; this figure shows that Solar Turbines Inc. holds the first place followed by GE.

Frame Type Heavy-Duty Gas Turbines

These gas turbines were designed shortly after World War II and introduced to the market in the early 1950s. The early heavy-duty gas turbine design was largely an extension of steam turbine design. Restrictions of weight and space were not important factors for these ground-based units, and so the design characteristics included heavy-wall casings split on horizontal centerlines, sleeve bearings, large-diameter combustors, thick airfoil sections for blades and stators, and large frontal areas. The overall pressure ratio of these units varied from 5:1 for the earlier units to 35:1 for the units in present-day service. Turbine inlet temperatures have been increased and run as high as

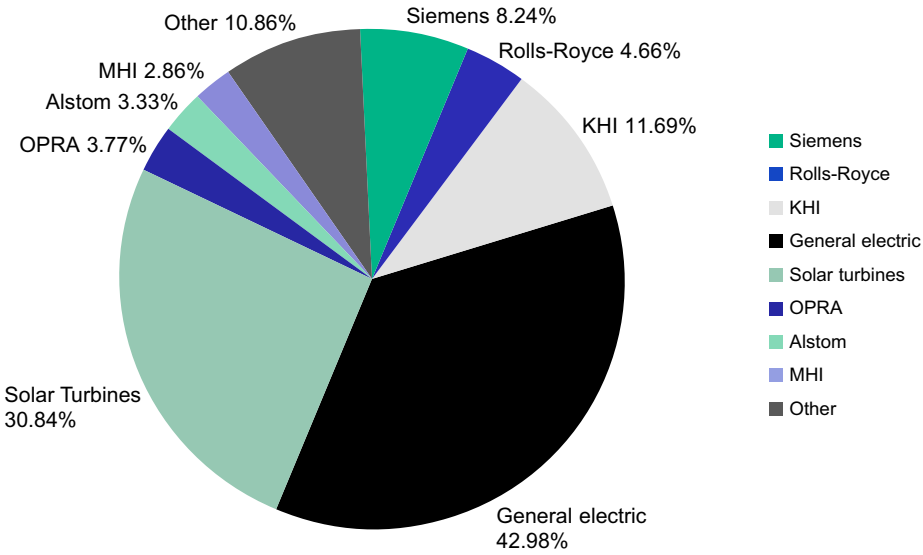


Figure 1-12 Gas turbine electrical power generation unit production, percent market share by headquarters 2010–2019.

2732 °F (1500 °C) on some of these units, which makes the gas turbine one of the most efficient prime movers on the market today reaching efficiencies in the high forties and above 60% in a combined-cycle mode. Projected temperatures approach 3000 °F (1649 °C) and, if achieved, would make the gas turbine even more efficient unit. The Advanced Gas Turbine Programs sponsored by the US Department of Energy have these high temperatures as one of its goals. To achieve these high temperatures, steam cooling is being used in some of the latest designs to achieve the goals of maintaining blade metal temperatures below 1300 °F (704 °C) and preventing hot corrosion problems.

The industrial heavy-duty gas turbines employ axial-flow compressors and turbines. The industrial turbine consists of a 15- to 25-stage axial-flow compressor; with multiple can-annular combustors each connected to the other by crossover tubes or single large annular combustors with multiple nozzles. The crossover tubes in can-annular combustors help propagate the flames from one combustor can to all the other chambers and also assures an equalization of the pressure between each combustor chamber. The earlier industrial European designs had single-stage side or silo-type combustors. The new European designs do not use the side- or silo-type combustor in most of their newer designs, they have can-annular or annular combustors since side- or silo-type combustors had a tendency to distort the casing.

The large frontal areas of the frame units reduce the inlet velocities, thus reducing air noise. The pressure rise in each compressor stage is reduced, creating a large, stable operating zone.

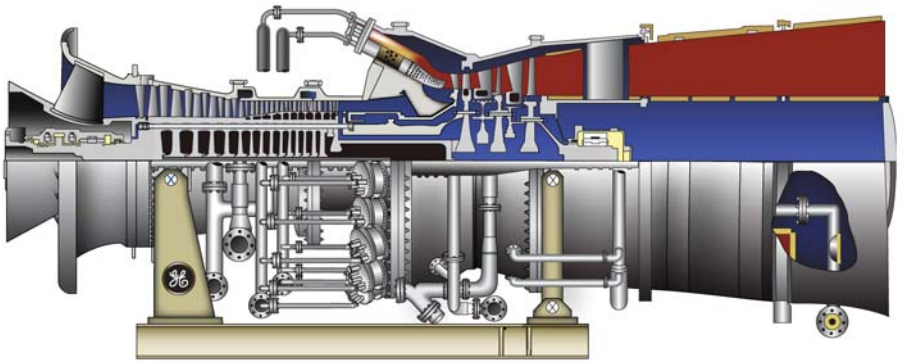
The auxiliary modules used on most of these units have gone through considerable hours of testing and are heavy-duty pumps and motors.

The advantages of the heavy-duty gas turbines are their long life, high availability, and slightly higher overall efficiencies. The noise level from this type of turbine is considerably less than an aircraft-type turbine. The heavy-duty gas turbine's largest customers are the electrical utilities and independent power producers. Since the 1990s industrial turbines have been the bulwarks of most combined-cycle power plants.

The latest frame type units introduced are 480-MW units using steam cooling in the combined-cycle mode, enabling the firing temperatures to reach 2600 °F (1427 °C). This enables the combined-cycle mode to reach an efficiency of more than 60%. Some of the newer gas turbines on the market are discussed below.

GE has the major market share of the frame-type gas turbine. Figure 1-13 is a cross-sectional representation of the GE industrial-type gas turbine. Frame 9 FA, a 50-cycle turbine, is rated at 256 MW with an efficiency of 37% and has a 17-stage axial-flow compressor with a pressure ratio of 16.6:1, with 14 can-annular combustors and a three-stage axial-flow turbine. The Frame 9 FA gas turbine has a sister turbine, the Frame 7 FA, which is a 60-cycle turbine producing 183 MW.

Figure 1-14 is the photograph of the new GE-developed advanced combined-cycle gas turbine technology that they have named the H System™– it is a combined-cycle system capable of breaking the 60% efficiency barrier and it integrates the gas turbine, steam turbine, and heat recovery steam generator into a seamless system, optimizing each component's performance. Figure 1-15 is a drawing of the GE H gas turbine showing a 17-stage axial-flow turbine, and this turbine employs a can-annular lean pre-mix dry low NO_x (DLN) combustor system. Fourteen combustion chambers are used on the 9 H, and twelve combustion chambers are used on the 7 H and a four-stage turbine section. The H system delivers higher efficiency (60%) and output



GT18029
MS9001F single-shaft gas turbine
FA-226.5 MW (simple-cycle), 50 Hz
FA-348.5 MW (combined-cycle), 50 Hz
Cross-section illustration

Figure 1-13 GE industrial-type gas turbine.

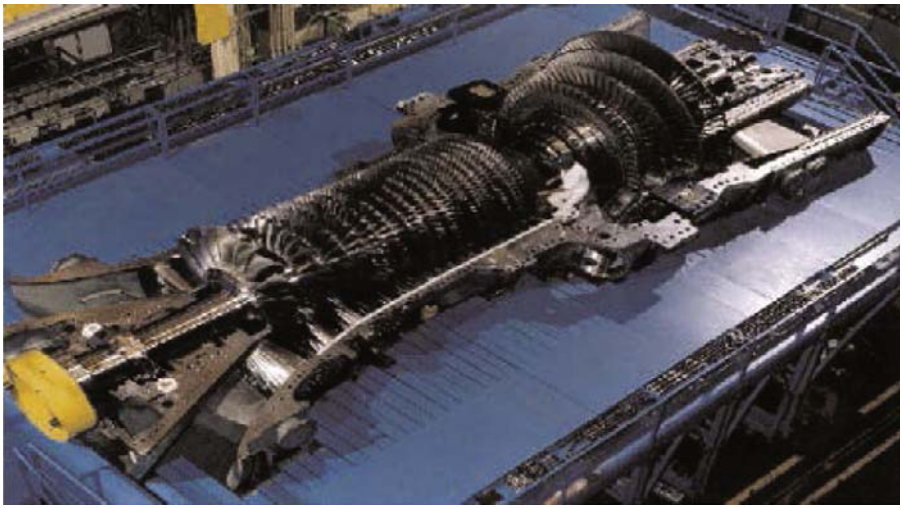


Figure 1-14 GE H system^{TM} gas turbine.

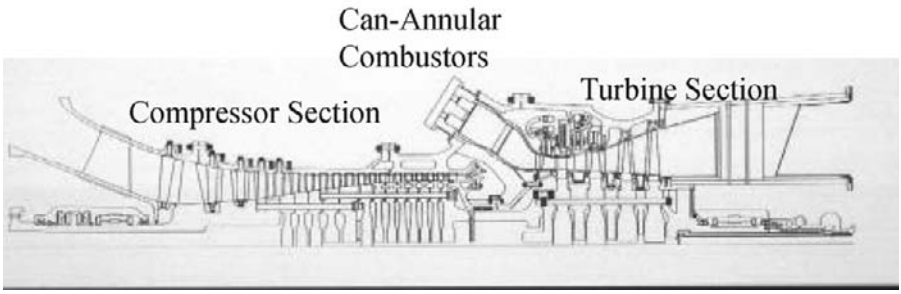


Figure 1-15 GE H gas turbine.

(480 MW) to reduce the cost of electricity of this gas-fired power generation system. Because fuel represents the largest individual expense of running a power plant, an efficiency increase of even a single percentage point can substantially reduce operating costs over the life of a typical gas-fired and combined-cycle plant in the 400–500 MW range.

The GE H gas turbine uses a closed-loop steam cooling system, which allows the turbine to fire at a higher temperature for increased performance. It is this closed-loop steam cooling that enables the H System to achieve 60% combined-cycle fuel efficiency, while maintaining strict adherence to environmental standards.

GE has also developed a new high-efficiency turbine in a simple-cycle gas turbine application. Figure 1-16 is an orthogonal drawing of the GE LMS 100 turbine designed with a high-efficiency core engine. The LMS 100 features a heavy-duty and low-pressure compressor derived from GE Power Systems' MS 6001 FA heavy-duty gas turbine compressor; its core, which includes the high-pressure compressor, combustor,

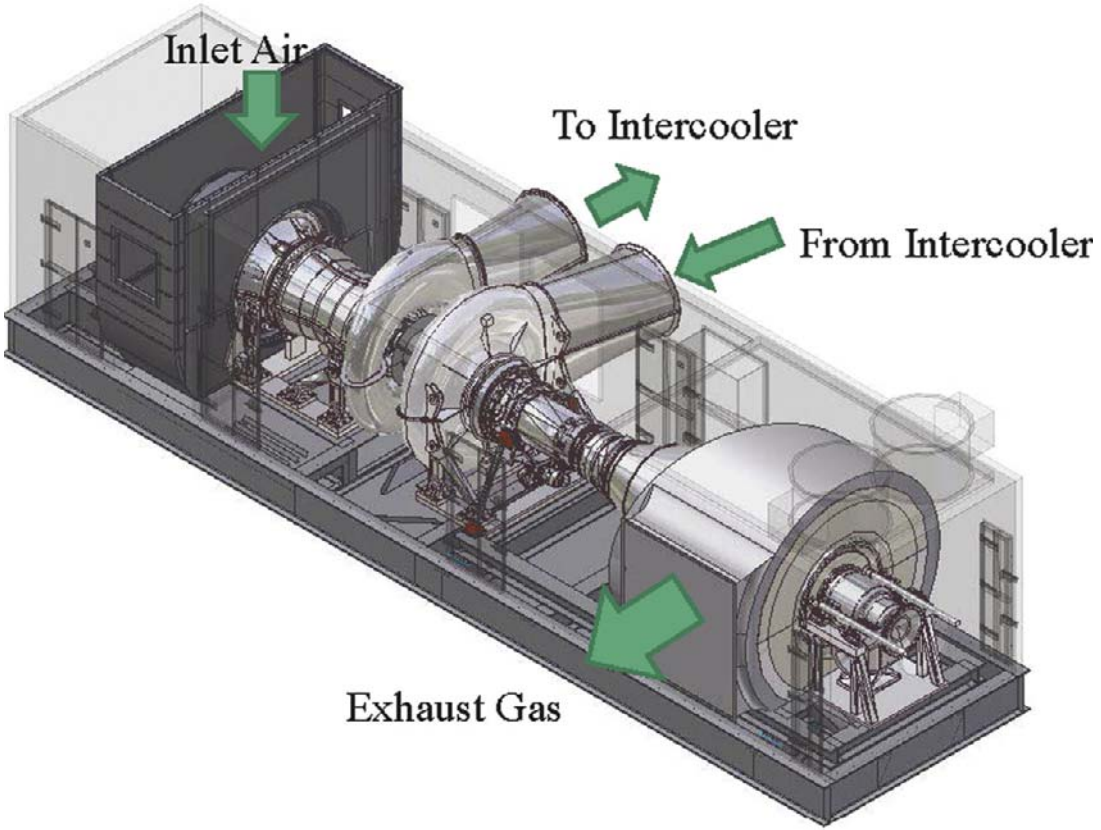


Figure 1-16 GE LMS 100 turbine.

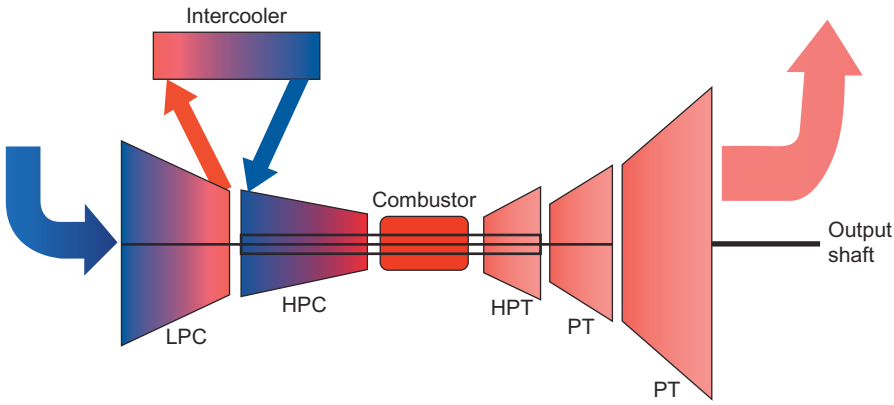


Figure 1-17 ABB turbine.

and high-pressure turbine, is derived from GE Aircraft Engines' CF6-80C2▫ and CF6-80E1▫. The design of the new two-stage intermediate-pressure turbine and new five-stage power turbine is based on the latest aero-derivative gas turbine technology. The exhaust and aft shaft for hot-end drive are designed using heavy-duty gas turbine practices. The compressed air from the low-pressure compressor (LPC) is cooled in either an air-to-air or air-to-water heat exchanger (intercooler) and ducted to the high-pressure compressor (HPC). This is the first gas turbine with an in-line intercooled compressor section. The old ABB turbines designed in 1950 had a similar design in that two axial-flow compressors had an intercooler between the two compressor stages as shown in Figure 1-17, which is a schematic representation of the system. The cooled flow means less work for the HPC, increased overall efficiency, and power output. The cooler LPC exit temperature air, used for turbine cooling, allows higher firing temperatures, resulting in increased power output and overall efficiency. The LMS 100 is a combination of two technologies, as shown in Figure 1-18, Frame and Aero technologies. A new two-stage intermediate-pressure turbine drives the first six stages of the Frame 6 compressor by the use of a coaxial shaft and the five-stage power turbine is based on the latest aeroderivative gas turbine technology and drives the generator on the hot side of the turbine. The exhaust and the aft shaft for hot-end drive are designed using heavy-duty gas turbine practices.

MS900 1H/MS700 1H Combined-Cycle Performance

	Net Plant Output (MW)	Heat Rate (BTU/kW h)	Heat Rate (kJ/kW h)	Net Plant Efficiency (%)	GT Number and Type
50 Hz S109H	480	5690	6000	60	1 × MS9001H
60 Hz S107H	480	5690	6000	60	1 × MS7001H

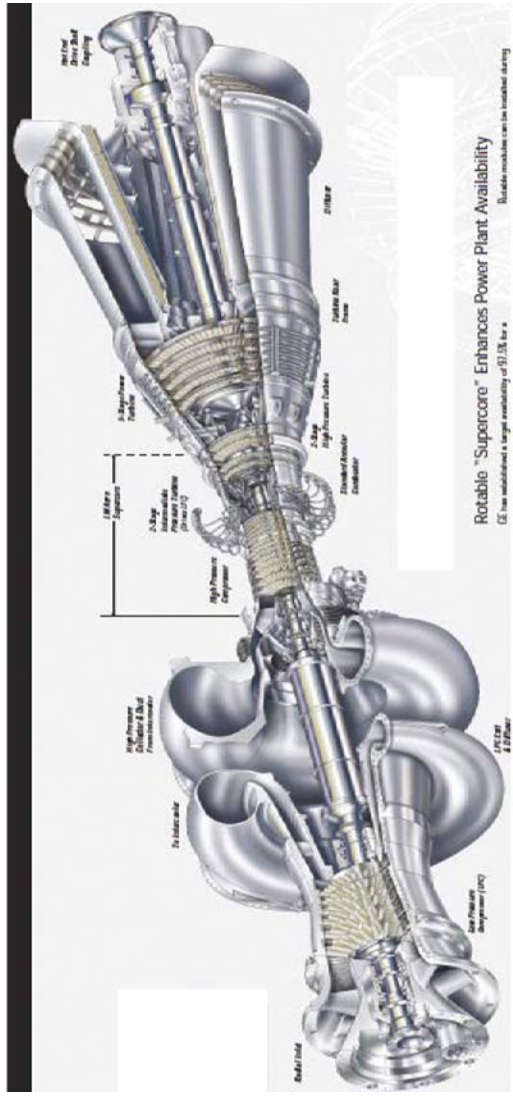


Figure 1-18 The LMS 100.

Early European turbines had a silo-type combustor as seen in the schematic drawing shown in Figure 1-19, which is a Siemens/KWU gas turbine vintage of the 1960s. These types of combustors were common on European turbines of the 1950s–1980s as also seen in Figures 1-20 and 1-21 which are photographs taken during an overhaul of a BBC/Alstom GT 11N2 gas turbine with the silo combustors. The new European turbines have gone toward the annular combustors as shown in Figure 1-22, which is a cross-sectional representation of the Siemens V94.2 annular combustor-type gas turbine. This turbine consists of a 16-stage axial-flow compressor followed by an annular combustor and a four-stage reaction type axial-flow turbine, which drives both the axial-flow compressor and the generator. Figure 1-23 is a design drawing of the same Siemens V94.2 gas turbine.

Siemens with their purchase of Westinghouse Gas Turbines is now the second major supplier of the frame type turbines. The Westinghouse turbines (W256/SGT-900 and W501 F/SGT6-5000 F) were designed using can-annular turbine technology common in the US-designed turbines, while the Siemens (V84 and V94) turbines were designed with annular combustor gas turbines common in European designs.

Figure 1-24 is the Siemens W501 F gas turbine with the can-annular gas turbine. The W501 F has a 16-stage axial-flow compressor, which produces a 17:1 pressure ratio that results in a pressure at the compressor exit of 250 psia. The combustion system comprises of a dry low NO_x (DLN) combustion system consisting of 16 can-annular-type combustors arranged in a circular array around the turbine rotor shaft. The turbine section has a four-stage reaction gas turbine, which produces 208 MW with an efficiency of 38.1%. Figures 1-25 and 1-26 are the W501 G gas turbine, which uses steam cooling for the combustor and transition pieces and the first-stage turbine nozzle vanes. The turbine produces 280 MW of power at an efficiency of 38.5%. This turbine has a 16-stage axial-flow compressor with a 19.2 pressure ratio and a 16 can-annular DLN combustor and a four-stage turbine. The can-annular combustor unlike other can-annular systems does not have crossover tubes; they have an igniter in each combustor. Siemens, in their new gas turbine primarily based on the Westinghouse turbine design, has decided to not continue with the concept of steam cooling. This could be due to many problems experienced in the W501 G gas turbines due to steam leakages.

Mitsubishi started in the gas turbine business as a licensee of Westinghouse Turbines and in the 1990s developed the 501 F gas turbine together. The compressor was designed by Mitsubishi and the hot section was originally designed by Westinghouse. These units are now sold individually after Siemens purchased Westinghouse and the cooperative venture was dissolved. The Westinghouse's W501 G and Mitsubishi's M501 G and M501 J gas turbines were developed separately by both parties since the end of their collaboration. The Mitsubishi's 501 F consists of a 16-stage axial-flow compressor with a 17:1 pressure ratio followed by a 14 can-annular combustors and a four-stage turbine section, whereas the Mitsubishi's M501 G shown in Figure 1-27 has a 15-stage compressor with a pressure ratio of 20:1, 14 can-annular combustors, and four-stage reaction turbines producing 267 MW of power at an efficiency of 39%. Mitsubishi's latest addition to the gas turbine field the M501 J as shown in Figure 1-28 has been developed with a firing temperature of 2912 °F (1600 °C). The M501 J has

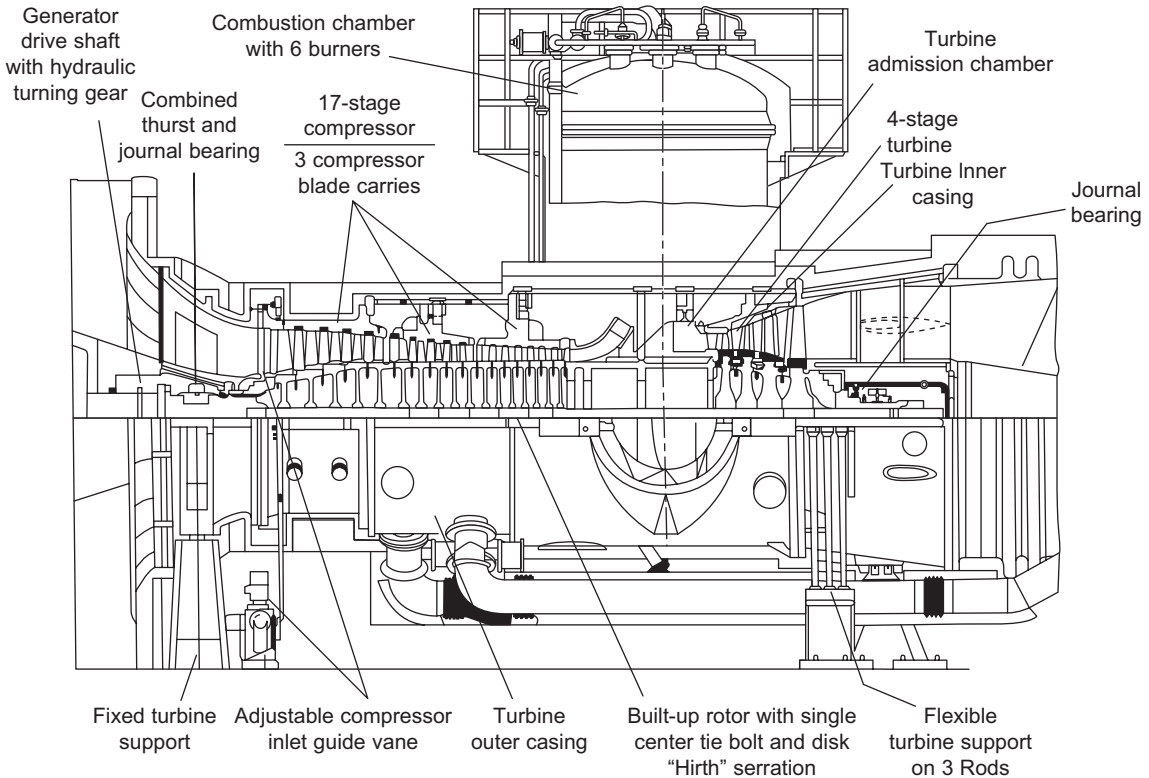


Figure 1-19 Longitudinal section of the Siemens/KWU gas turbine.



Figure 1-20 BBC/Alstom GT 11N2 being overhauled.

a 15-stage compressor, with the IGV and the first three stages having variable vanes and developing a pressure ratio of 23:1, followed by 14-can annular-type combustors. Figure 1-29 shows the M501 J rotor. The turbine section is a four-stage reaction turbine with the first three stages with thermal barrier coating (TBC) and air-cooled turbine blades for all four stages. The first two blades are un-shrouded and the last two stages are shrouded. The major differences in the J turbine as compared with the G turbine are in the turbine section, where the last two stages of the turbine blades are shrouded rather than the last stage only and all blade rows are cooled as compared with the last blade row un-cooled.

Alstom's GT24/26 gas turbines were introduced in 1995 – GT24 for the 60-Hz market and the GT26 for the 50-Hz market. Figure 1-30 is a cross section of the GT24/26 gas turbine. In combined-cycle applications, the efficiency for these turbines is in the 55–57% range. The GT24/26 fleet has now accumulated over 3,650,000 fired operating hours with more than 64,000 starts under various operating conditions, be it base load, intermediate, cycling, or daily start–stop. The turbines are unique in their design, as they have two in-line combustors thus taking advantage of the reheat gas turbine cycle as seen in the schematic diagram of the cycle in Figure 1-31 (see Chapter 2 for reheat gas turbine cycles). Brown Boveri the predecessor of Alstom are the only manufacturer in the world to have chosen to introduce the sequential combustion path, having installed its first sequential combustion unit in Switzerland in 1948. The

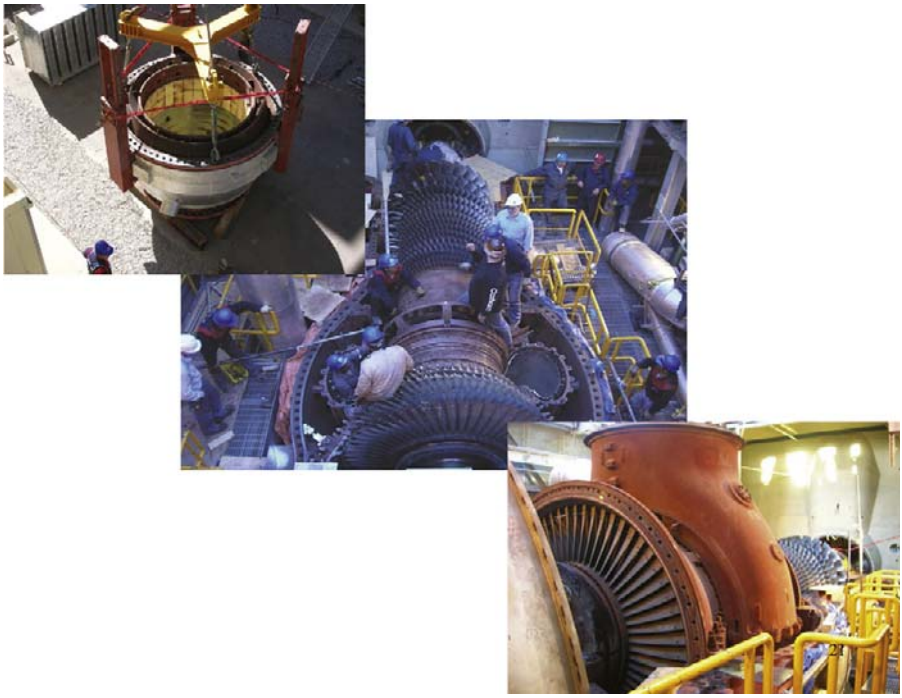


Figure 1-21 BBC/Alstom GT 11N2 being overhauled.

turbine compressor consists of 22 stages, the first 16 stages are the low pressure compressor at which point about 25% of the flow is diverted while about 75% of the flow is channeled to the last six stages of the compressor, the compressor produces a pressure ratio of more than 30. Figure 1-32 is a block diagram showing the characteristics of Alstom GT24/26 gas turbines. The compressor design employs controlled diffusion airfoil (CDA) blading (Chapter 7), thus allowing each compressor stage to be individually optimized according to specific requirements and boundary layer conditions. This leads to higher overall compressor efficiency, while retaining a high surge margin. The first three stages of the compressor have variable guide vanes that maintain at start-up and part load compressor efficiencies high. The entire gas turbine shaft, which consists of 22 stages of compression, a single-stage HP turbine, and four stages of a low-pressure turbine, is a one piece design with forged discs welded together. Figure 1-33 (a) shows the single shaft with the forged disks welded together. The first 16 rows of compressor blades and the five rows of turbine blades are anchored in fir tree slots as shown in Figure 1-33 (b). This welding technique advanced by Brown Boveri has been applied since 1929 to all GT and ST rotors. Figure 1-33 (c) shows such a rotor in a special jig manufactured by the Brown Boveri and now Alstom turbines that rotates the rotor in a vertical position while welding it and cooling the rotor to prevent any warping of the rotor.

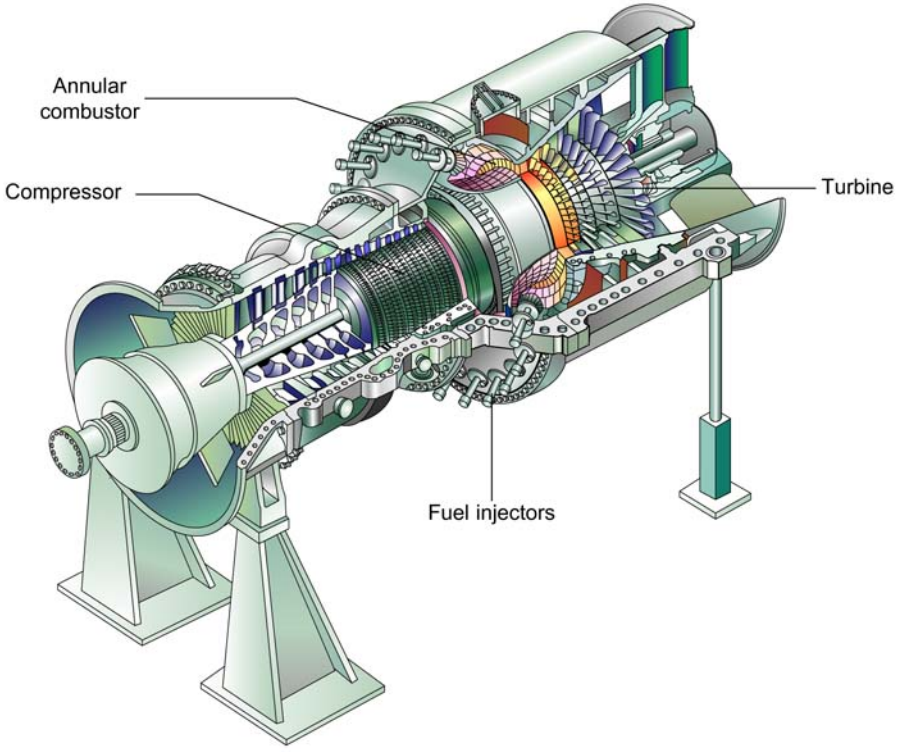
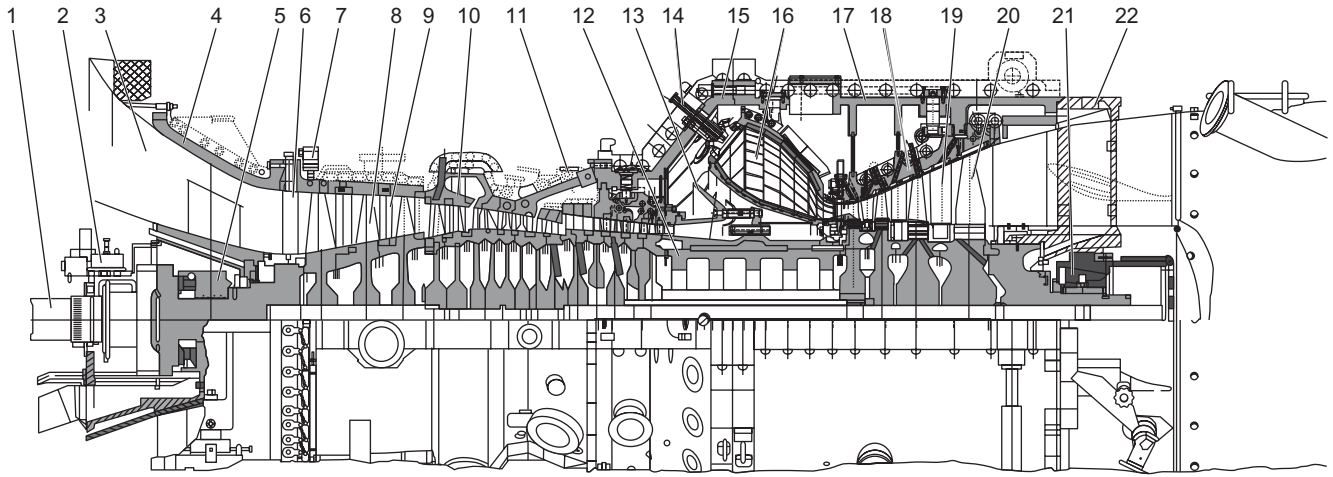


Figure 1-22 Siemen's V94.2.

The GT24/26 has low environmental emissions achieved using sequential combustion technology burning the fuel in two dry low NO_x combustors. It achieves this with low firing temperatures and with burners that are robust enough to cope with the wide fuel gas compositions that are seen in the market. Sequential combustion breaks the link between higher efficiency and higher inlet temperature. In sequential combustion, the process is characterized by splitting the combustion process into two stages separated by an expansion to an intermediate-pressure level. In this so-called "reheat" process, energy is added part way through the expansion process, resulting in high gas turbine efficiency and high power density.

The sequential combustion principle, applied to the large and heavy-duty GT26 gas turbine model, distinguishes it from conventional machines. In effect, sequential combustion can be visualized as a gas turbine comprising two combustor-turbines in series, where the exhaust gases from the first turbine feed the combustor of the second. The sequential combustors are known as the EnVironmental (EV) burner technology and the second burner is called the SEV burners. The EV burner gives the benefit of dry low NO_x combustion for operation with different natural gases, with the option to run with liquid fuel as an alternative. The burner is shaped like two half cones slightly offset laterally to form two inlet slots of constant width running the component's full



No	Component	No	Component	No	Component	No	Component
1	Intermediate shaft	6	Adjustable guide vanes	11	Bleed Port 2	16	Annular combustor
2	Hydraulic	7	System adjustor	12	Internal cylinder	17	Exterior casing No. 3
3	Inlet air passage	8	Compressor blades	13	Compressor diffuser exit	18	Diffuser turbine
4	Compressor and bearing case	9	Diffuser vanes	14	Fuel injector	19	Turbine nozzles
5	Radial and axial bearing	10	Bleed Port 1	15	Exterior casing No. 2	20	Radial bearing
						21	Exit casting

Figure 1-23 Siemen's V94.2 gas turbine.

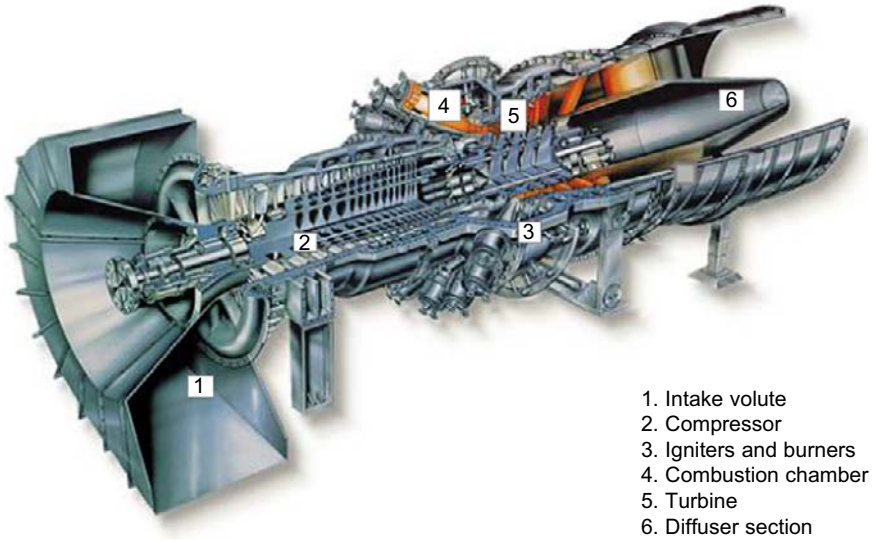


Figure 1-24 Siemen's W501 F gas turbine.

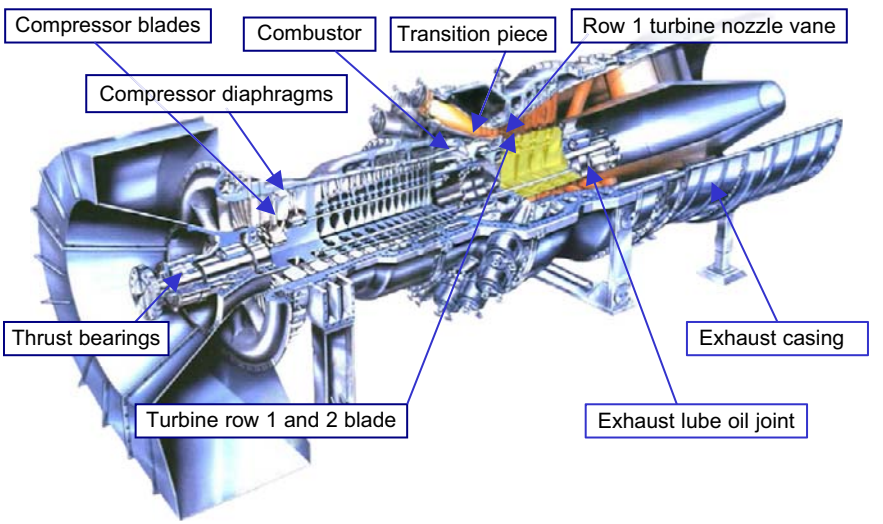


Figure 1-25 Siemen's W501 G gas turbine.

length. Combustion air enters the cone through these slots and fuel is injected through a series of fine holes in their edges. With this arrangement, fuel and air spiral into a vortex form and are intensively mixed.

The GT24/26 uses two fully annular combustion chambers that distribute the circumferential temperature evenly, while avoiding problem zones such as cross-firing

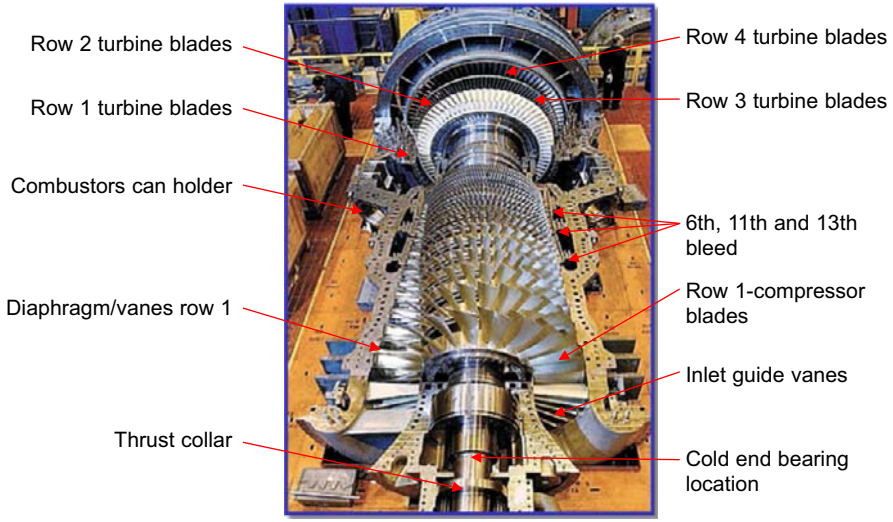


Figure 1-26 Siemen's W501 G gas turbine.

tubes or transition pieces. The sequential combustion concept results in a gas turbine exhibiting high power density and, therefore, affording smaller blade dimensions.

Air from the compressor cools the high-pressure turbine stage and the first three low-pressure turbine stages utilizing a combination of film and convection cooling techniques. Cooling air for the hot gas path components is taken from four extraction points along the compressor. Air from two of these secondary air flows is used directly, while the two other streams are cooled by heat exchangers (once through coolers) before entering the hot gas path components. The heat rejected is recovered in the water-steam cycle, which maximizes the performance of the GT26 in combined-cycle applications. In simple-cycle applications, the cooling is achieved by quenching water, which is introduced directly into the secondary air stream.

Aircraft-Derivative Gas Turbines

Aero-derivatives are used in electrical power generation due to their ability to start-up, shut down, and handle load changes more quickly than industrial machines. They are also used in the marine industry to reduce weight. The General Electric LM2500, General Electric LM6000, Rolls-Royce RB211, Rolls-Royce Avon, and the Pratt & Whitney FT-8 are common models of this type of machine.

Aero-derivative gas turbines consist of two basic components: an aircraft-derivative gas generator and a free-power turbine (Figure 1-34). The gas generator serves as a producer of gas energy; its job is to produce high-temperature gases at high pressure. The gas generator is derived from an aircraft engine modified to burn industrial fuels. Design innovations are usually incorporated to ensure the required long-life characteristics in the ground-based environment. In case of fan jet designs, the fan is removed and a couple of stages of compression are added in front of the existing

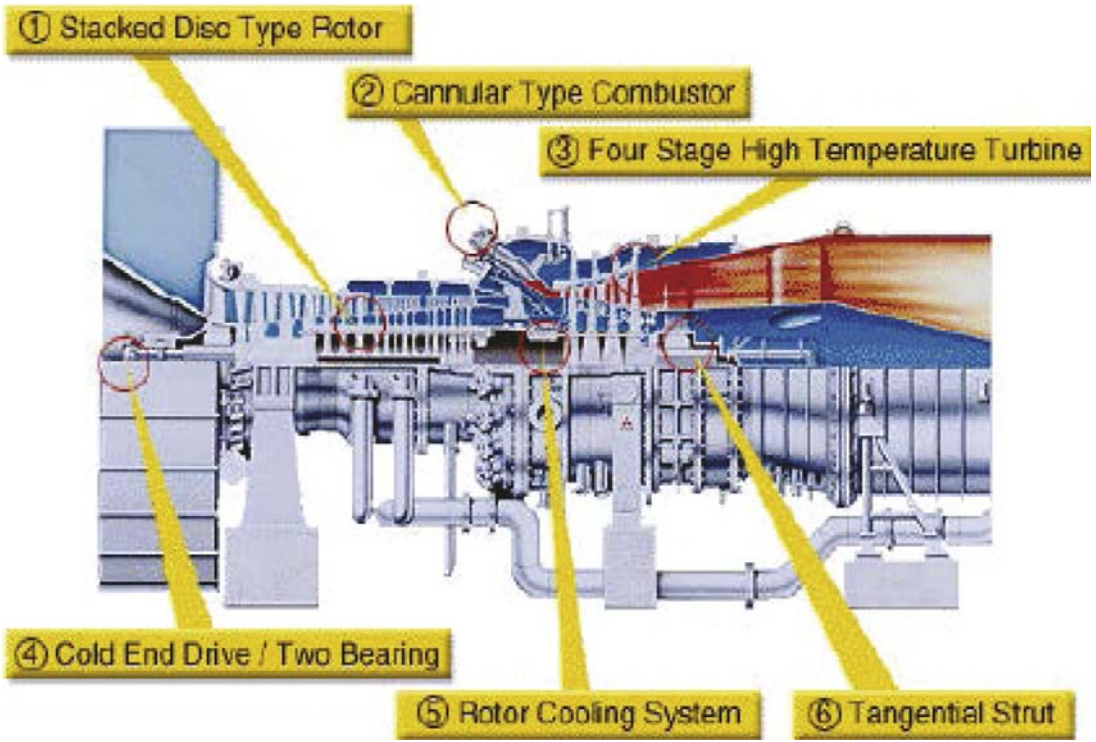


Figure 1-27 Mitsubishi's M501 G.

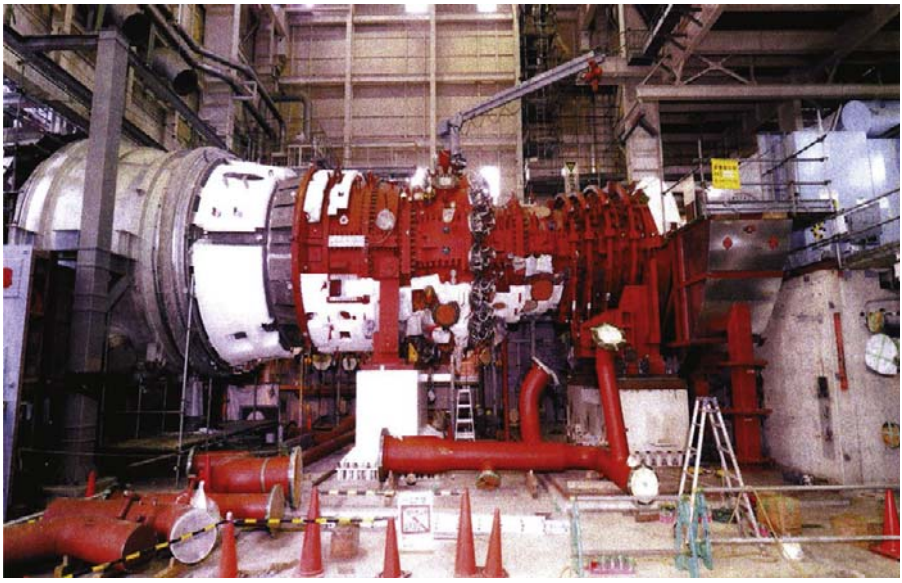


Figure 1-28 Mitsubishi's M501 J.



Figure 1-29 Mitsubishi's M501 J rotor.

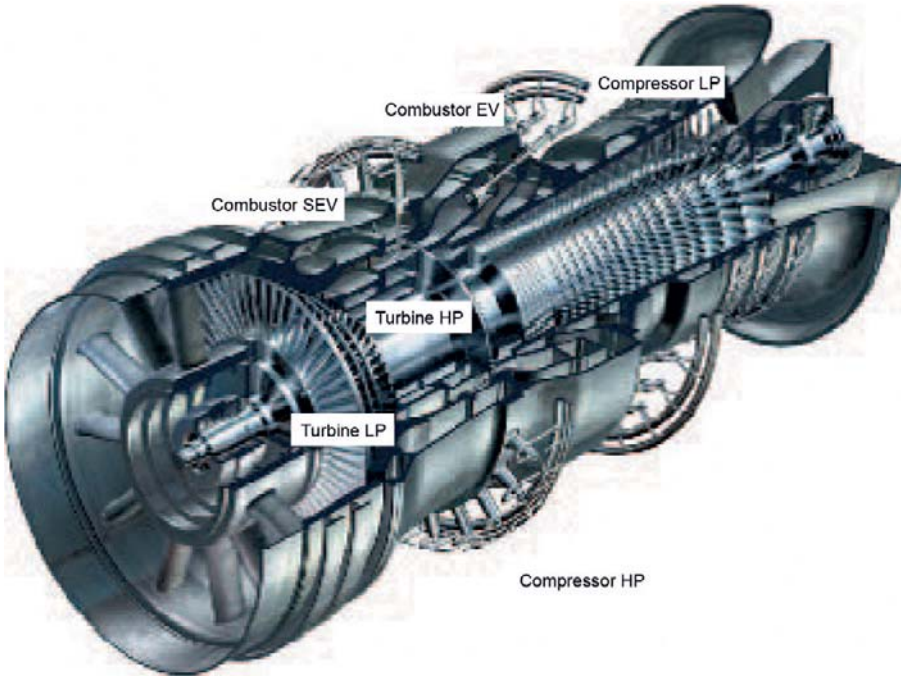


Figure 1-30 Alstom's GT24/26 gas turbine.

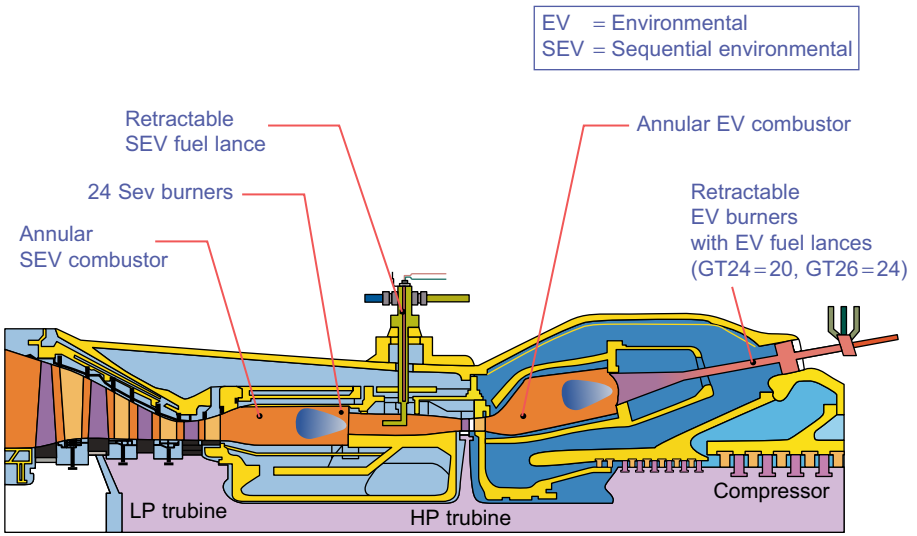


Figure 1-31 The reheat gas turbine cycle.

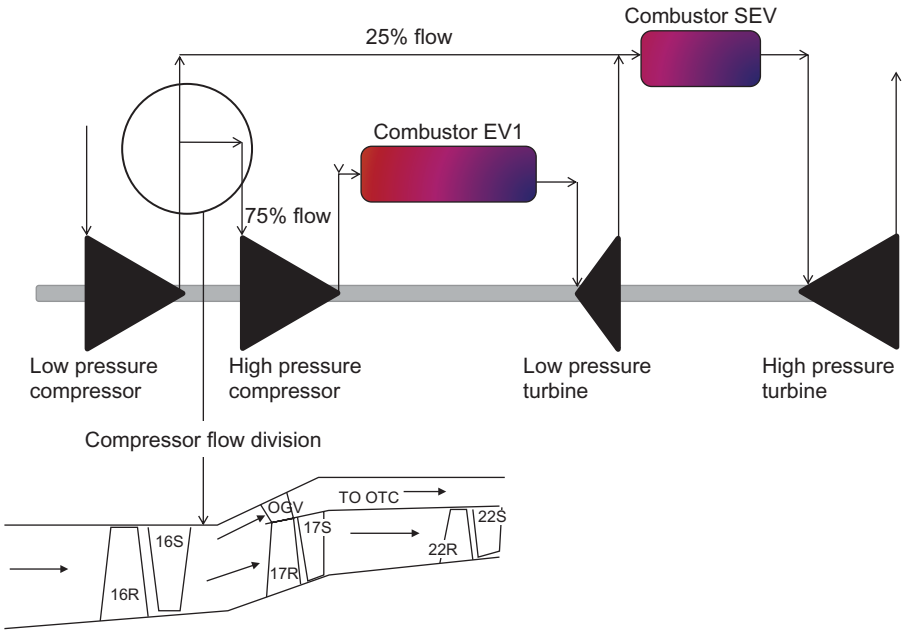


Figure 1-32 The Alstom GT24/26 gas turbine.

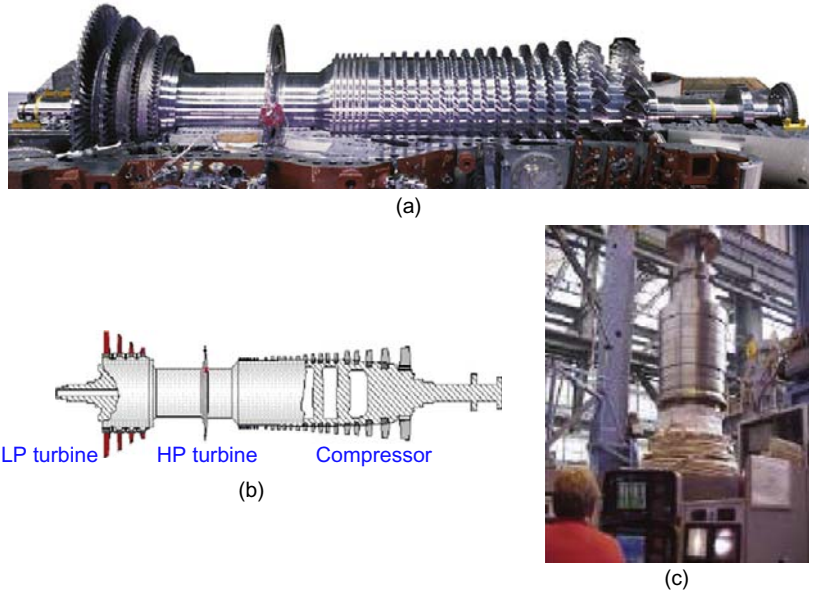


Figure 1-33 (a) One piece forged discs welded together; (b) The first 16 compressor stages and all turbine blades are anchored in fir tree slots; (c) A rotor in a special jig welding.

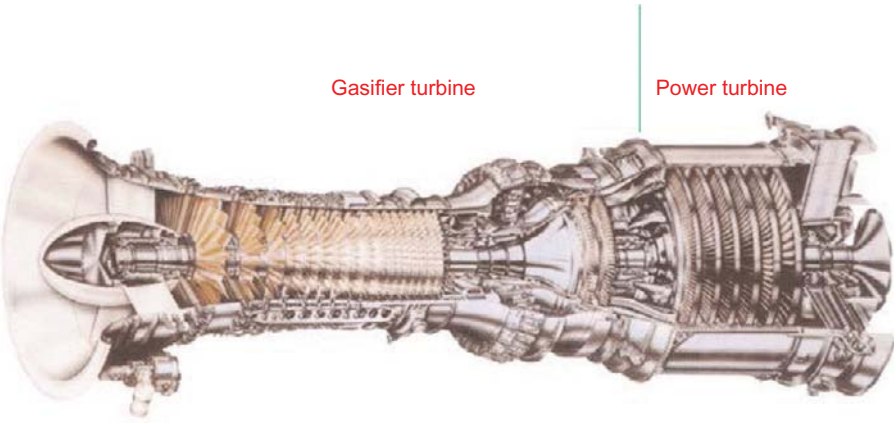


Figure 1-34 Free-power turbine.

low-pressure compressor. These additional stages are usually known as stage 00 and stage 0 thus keeping the stage numbering of the rest of the compressor stages the same as they were in the aircraft mode. The axial-flow compressor in most cases is divided into two sections – a low-pressure compressor followed by a high-pressure compressor. In those cases, there are usually a high-pressure turbine and a low-pressure turbine, which drive the corresponding sections of the compressor. The shafts are usually concentric thus the speeds of the high-pressure and low-pressure sections can be optimized. In these cases, the power turbine is separate and is not mechanically coupled; the only connection is via an aerodynamic coupling. The turbines have three shafts; the power turbine shaft is the drive shaft, all operate at independent speeds. The gas generator serves to raise combustion gas products to conditions of around 45–75 psi (3–5 Bar) and temperatures of 1300–1700 °F (704–927 °C) at the exhaust flange, that is entry to the power turbine. Figure 1-35 shows a cross section of the GE LM 6000 aero-derivative engine; it is most widely used in power production with an output of 48 MW and an efficiency of 41% in the simple-cycle gas turbine mode. In its sprint mode, water is injected between the low- and high-pressure compressor sections as shown in Figure 1-36. In this engine, there are two compressor sections – a low-pressure and a high-pressure compressor sections – and three turbine sections – a high-pressure gas turbine section, which drives the high-pressure compressor, a low-pressure turbine, which drives through a coaxial shaft the low-pressure compressor section, and finally a power turbine, which drives the driven equipment such as generators, compressors, and pumps. The LM 6000 with a once through steam generator (OTSG) is widely used in combined-cycle applications especially in small areas, as the foot print of an OTSG is much smaller than a regular heat recovery steam generator (HRSG), as shown in Figure 1-37.

The Rolls-Royce Aero-derivative Gas Turbines, the Avon and the RB-211, are widely used. The Rolls' Avon is used in compression gas pipelines stations, and the RB 211-HB3 with an output of about 42.4 MW and an efficiency of 39.3% is used

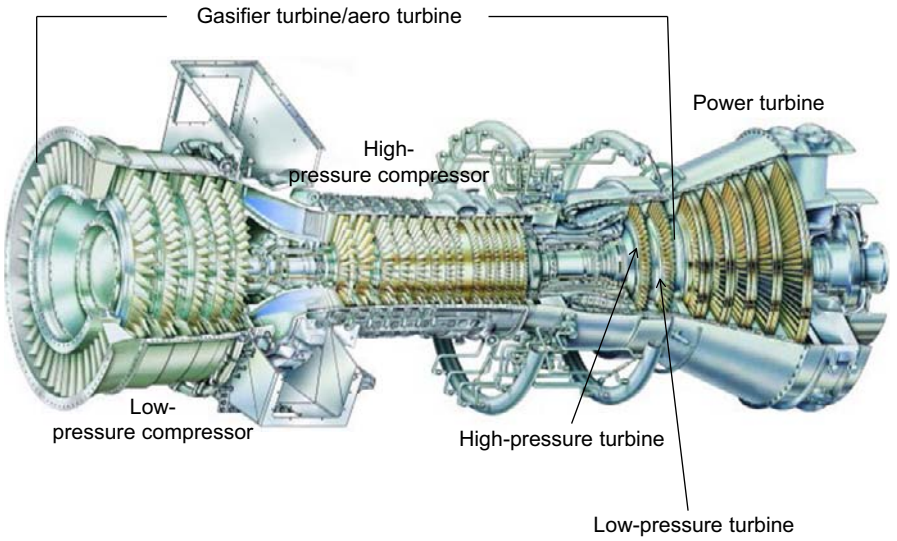


Figure 1-35 The GE LM 6,000 engine.

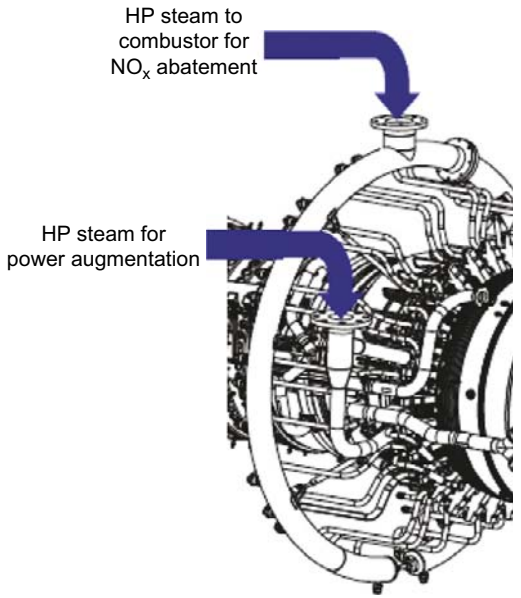


Figure 1-36 The GE LM 6,000 compressor section.

in power generation. Figure 1-38 is a cross-section of the RB 211. The RB 211 has a two-stage power turbine as shown in Figure 1-39. These types of power turbines are built by many compressor manufacturers such as Dresser-Rand and Cooper-Bessemer



Figure 1-37 Heat recovery steam generator.

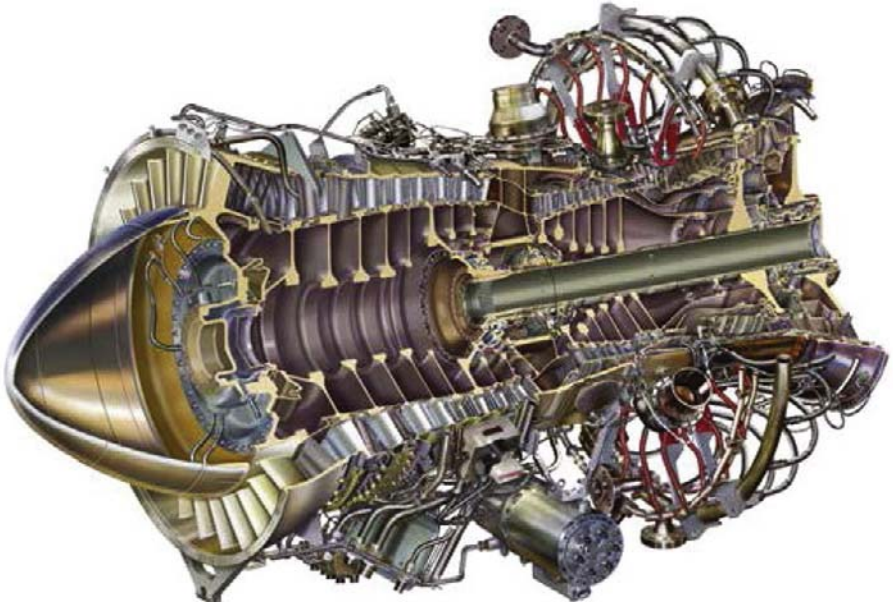


Figure 1-38 The RB 211.



Figure 1-39 A two-stage power turbine.

(now Cameron Industries) to power their compressors and also for power production.

The FT8 aero-derivative gas turbine made by Pratt & Whitney is in the 25-MW class and is used in industrial and municipal power supplies. The FT8 TwinPac unit offers 52 MW of electrical power from a two-engine single-generator configuration. The twin pack is a unit driving a single generator from both the ends. The FT8 gas turbine is based on aero-engine technology from Pratt & Whitney, adapted for industrial use as seen in Figure 1-40. The gas turbine is characterized by a compact and modular design. The PowerPac and the TwinPac offer two different variants of the FT8 gas turbine for power generation purposes. To drive compressors MechPac, the power turbine developed by MAN Diesel & Turbo is used. This has a rated speed of 5,500 rpm. Pollutant emissions are reduced by means of dry-low-NO_x-Brennkammer or by injecting water into the fuel chamber of the turbine. Typical applications include pipeline compressor units and gas treatment plant compressors.

Both the power and the petrochemical industries use the aircraft-type turbine. The power industry uses these units in a combined-cycle mode for power generation

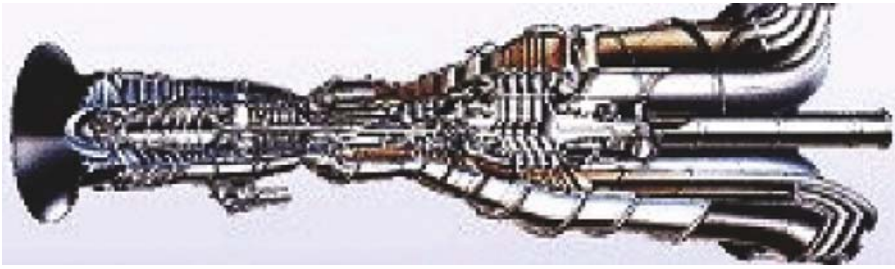


Figure 1-40 The FT8 gas turbine.

especially in remote areas where the power requirements are less than 100 MW. The petrochemical industry uses these types of turbines on offshore platforms especially for gas reinjection and as power plants for these offshore platforms, mostly due to their compactness and the ability to be easily replaced and then sent out to be repaired. The aero-derivative gas turbine is also used widely by gas transmission companies and petrochemical plants, especially for many variable speed mechanical drives. These turbines are also used as main drives for destroyers and cruise ships. The benefits of the aeroderivative gas turbines are as follows:

1. *Favorable installation cost.* The equipment involved is of a size and weight that it can be packaged and tested as a complete unit within the manufacturer's plant. Generally, the package will include either a generator or a driven pipeline compressor and all auxiliaries and control panels specified by the user. Immediate installation at the job site is facilitated by factory matching and debugging.
2. *Adaptation to remote control.* Users strive to reduce operating costs by automation of their systems. Nowadays, many new offshore and pipeline applications are designed for the remote unattended operation of the compression equipment. Jet gas turbine equipment lends itself to automatic control, as auxiliary systems are not complex, water cooling is not required (cooling by oil-to-air exchanges), and the starting device (gas expansion motor) requires little energy and is reliable. Safety devices and instrumentation adapt readily for the purposes of remote control and monitoring the performance of equipment.
3. *Maintenance concept.* The offsite maintenance plan fits in well with these systems where minimum operating personnel and unattended stations are the objectives. Technicians conduct minor running adjustments and perform instrument calibrations. Otherwise, the aero-derivative gas turbine runs without inspection until monitoring equipment indicates distress or sudden performance change. This plan calls for the removal of the gasifier section (the aero-engine) and sending it back to the factory for repair while another unit is installed. The power turbine does not usually have problems since its inlet temperature is much lower. Downtime due to the removal and replacement of the gasifier turbine is about eight hours.

Industrial-Type Gas Turbines

Industrial-type gas turbines are medium-range gas turbines and are usually rated between 5 and 20 MW. These units are similar in design to the large heavy-duty gas

turbines; their casing is thicker than the aero-derivative casing but thinner than the industrial gas turbines. They usually are split-shaft designs that are efficient in part-load operations. Efficiency is achieved by letting the gasifier section (the section that produces the hot gas) operate at maximum efficiency while the power turbine operates over a great range of speeds, especially in compressor drive service. The compressor is usually a 10- to 16-stage subsonic axial compressor, which produces a pressure ratio from about 5:1 to 15:1. Most American designs use annular combustors (about 5–10 combustor cans mounted in a circular ring) or annular-type combustors. Many European designs use side combustors and have lower turbine inlet temperatures compared with their American counterparts. Figure 1-41 shows an industrial-type gas turbine manufactured by Solar Turbines Inc., a Caterpillar Company Solar Turbines, is the largest manufacturer of industrial gas turbines by unit production as shown in Figure 1-12. Solar turbines range from the Solar Saturn 1.2 MW with an efficiency of 24.3% and a heat rate of 14,023 BTU/kW h (16,000 kJ/kW h) to the Titan, which is rated at 21.745 MW, at an efficiency of 40% and a heat rate of 9695 BTU/kW h (10,230 kJ/kW h).

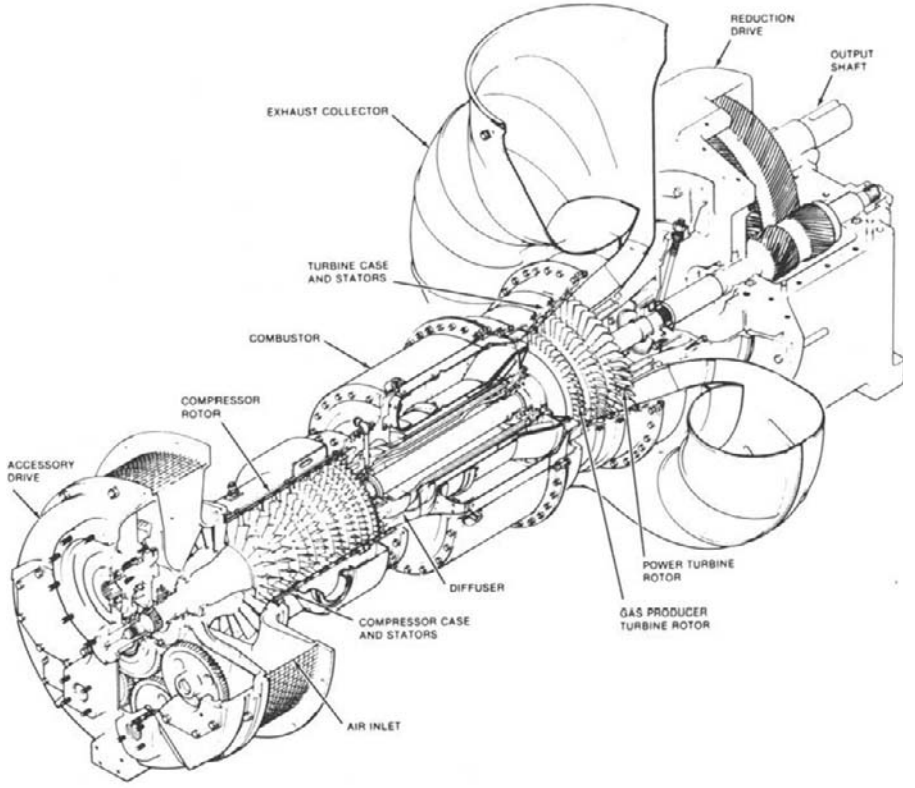


Figure 1-41 An industrial-type gas turbine from Solar Turbines Inc.

The gasifier turbine is usually a two- to three-stage axial turbine with an air-cooled first-stage nozzle and blade. The power turbine is usually a single- or two-stage axial-flow turbine that in many cases is not physically coupled with the gasifier turbine and the compressor of the gasifier section. The medium-range turbines are used on offshore platforms and are finding increasing use in petrochemical plants. The straight simple-cycle turbine is low in efficiency, but by using regenerators to consume exhaust gases, these efficiencies can be greatly improved. In process plants, this exhaust gas is used to produce steam. The combined-cycle (air-steam) cogeneration plant has very high efficiencies and is the trend of the future.

These gas turbines have, in many cases, regenerators or recuperators (Chapter 2 – Recuperative/Regenerator Brayton Cycle) to enhance their efficiency. Figure 1-42 shows an RGT design, by Solar Turbines, known as the Mercury, which has an efficiency of 41% and a heat rate of 8863 BTU/kW h (9351 kJ/kW h). Solar Turbines uses the term recuperator to describe its heat exchanger, which transfers energy between the exhaust hot gases and the cooler compressed air leaving the turbine. The recuperator in the solar turbine is a cross-flow heat exchanger made of Alloy 625. Figure 1-43 shows the flow path of the air as it enters the turbine and is then compressed to a pressure ratio of 9.9:1 in a 10-stage axial-flow compressor; the air then goes through the

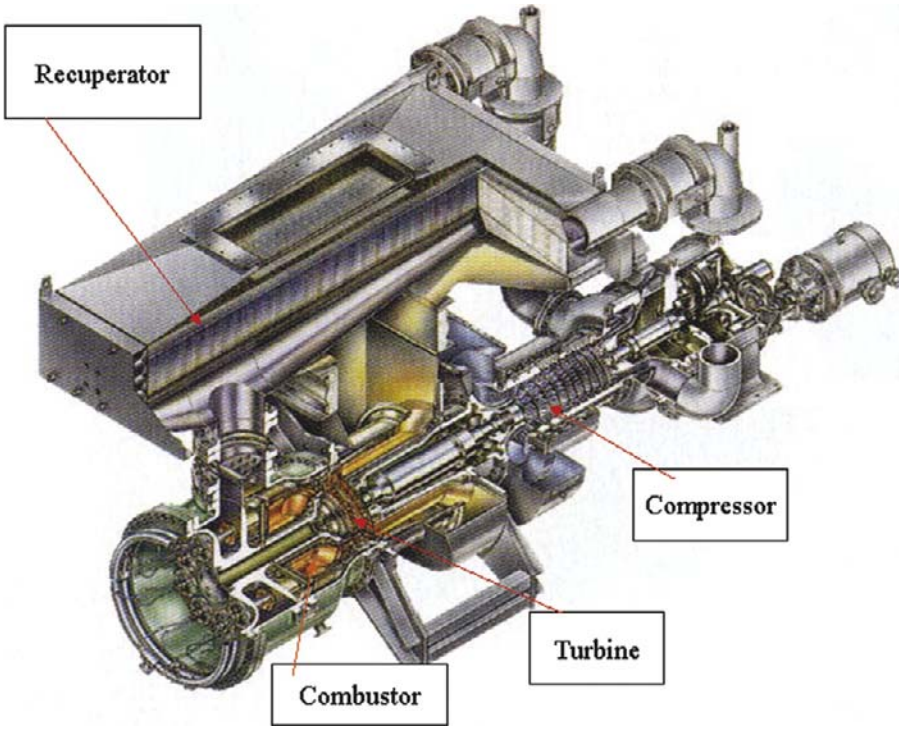


Figure 1-42 An RGT design, by Solar Turbines Inc.

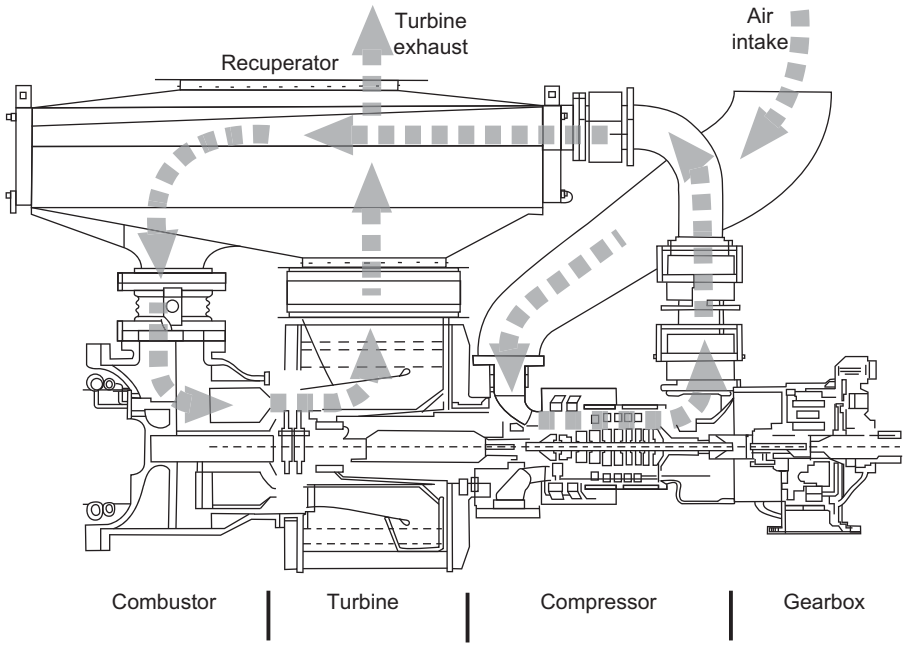


Figure 1-43 Air flow path.

recuperator where it is heated and then enters the annular combustor where it is fired to a temperature of about 2200 °F (1204 °C). The gas from the combustor is expanded through a two-stage axial-flow turbine. The exhaust gas from the turbine goes through the recuperator and heats the compressed air leaving the compressor.

Small Gas Turbines

Many small gas turbines that produce an output of less than 5 MW are designed similarly to the larger turbines already discussed; however, there are many designs that incorporate centrifugal compressors or combinations of centrifugal and axial compressors as well as radial-inflow turbines. A small turbine will often consist of a single-stage centrifugal compressor producing a pressure ratio as high as 8:1, a single-side combustor where temperatures of about 1800 °F (982 °C) are reached, and radial-inflow turbines. Figure 1-44 shows a schematic diagram of such a typical turbine.

Air is induced through an inlet duct to the centrifugal compressor, which rotates at high speed and imparts energy to the air. On leaving the impeller, air with increased pressure and velocity passes through a high-efficiency diffuser, which converts the velocity energy to static pressure. The compressed air, contained in a pressure casing, flows at low speed to the combustion chamber, which is a side combustor. A portion of the air enters the combustor head, mixes with the fuel, and burns continuously.

Next Page

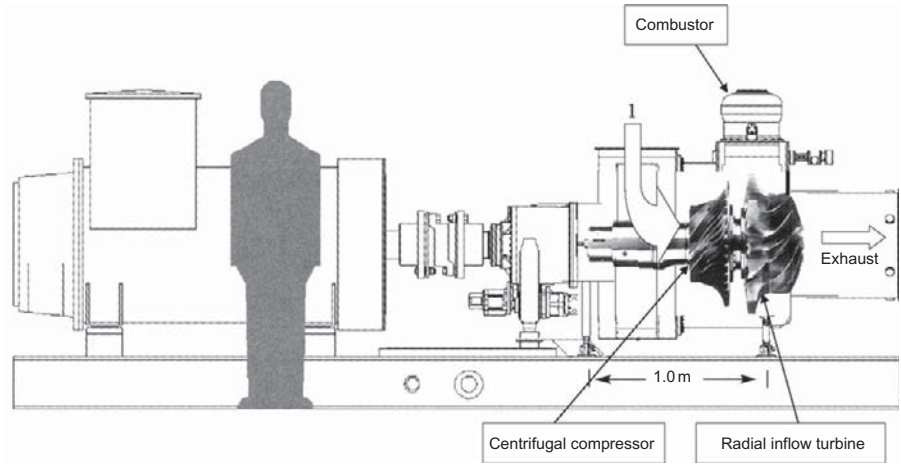


Figure 1-44 A radial-inflow turbine.

The remainder of the air enters through the wall of the combustor and mixes with the hot gases. Good fuel atomization and controlled mixing ensure an even temperature distribution in the hot gases, which pass through the volute to enter the radial-inflow turbine nozzles. High acceleration and expansion of the gases through the nozzle guide vane passages and turbine combine to impart rotational energy, which is used to drive the external load and auxiliaries on the cool side of the turbine. The efficiency of a small turbine is usually much lower than a larger unit because of the limitation of the turbine inlet temperature and the lower component efficiencies. Turbine inlet temperature is limited because the turbine blades are not cooled. Radial-flow compressors and impellers inherently have lower efficiencies than their axial counterparts. These units are rugged and their simplicity in design assures many hours of trouble-free operation. A way to improve the lower overall cycle efficiencies, 18–23%, is to use the waste heat from the turbine unit. High thermal efficiencies (30–35%) can be obtained, since nearly all the heat not converted into mechanical energy is available in the exhaust and most of this energy can be converted into useful work. These units when placed in a combined heat power (CHP) application can reach efficiencies, of the total process, as high as 60–70%.

The OPRA Turbine operates at a pressure ratio of 6.7:1 and produces 1910 kW of power at an efficiency of 26.9% and a heat rate of 12,732 BTU/kW h (13,433 kJ/kW h). The Dresser-Rand KG2-3E is a similar type turbine shown in Figure 1-45 and which used to be a Kongsberg gas turbine manufactured in Norway and has one-stage centrifugal compressor with a pressure ratio of 4.7 and single-stage radial-inflow turbine to produce a power of 1895 kW at an efficiency of 16.7% and a heat rate of 21,542 BTU/kW h (22,729 kJ/kW h). It is used for standby power with a 99.3% starting reliability.

The small Kawasaki gas turbines use centrifugal compressors and, in many cases, two centrifugal compressors are used as shown in Figure 1-46, but they use several

Copyrighted Materials
Copyright © 2012 Elsevier Retrieved from www.knovel.com

2 Theoretical and Actual Cycle Analyses

The analysis presented here is an outline of the air-standard Brayton cycle and its various modifications. These modifications are evaluated to examine the effects they have on the basic cycle. One of the most important is the augmentation of power in a gas turbine; this is treated in a special section in this chapter.

The Brayton Cycle

The Brayton cycle in its ideal form consists of two isobaric (constant pressure) processes and two isentropic (constant entropy) processes. The two isobaric processes consist of the combustor system of the gas turbine and the gas side of the HRSG. The two isentropic processes that are also adiabatic (thermodynamic process in which no heat is transferred to or from the working fluid) represent the compression (compressor) and the expansion (turbine expander) processes in the gas turbine. Figure 2-1 shows the ideal Brayton cycle.

A simplified application of the first law of thermodynamics to the air-standard Brayton cycle in Figure 2-1 (assuming no changes in kinetic and potential energies) has the following relationships:

Work of compressor:

$$W_c = \dot{m}_a(h_2 - h_1) \tag{2-1}$$

Work of turbine:

$$W_t = (\dot{m}_a + \dot{m}_f)(h_3 - h_4) \tag{2-2}$$

Total output work:

$$W_{\text{cyc}} = W_t - W_c \tag{2-3}$$

Heat added to system:

$$Q_{2,3} = \dot{m}_f x \,\text{LHV}_{\text{fuel}} = (\dot{m}_a + \dot{m}_f)(h_3) - \dot{m}_a h_2 \tag{2-4}$$

Gas Turbine Engineering Handbook, Fourth Edition. DOI: 10.1016/B978-0-12-383842-1.00002-0
Copyright © 2012 Elsevier Inc. All rights reserved.

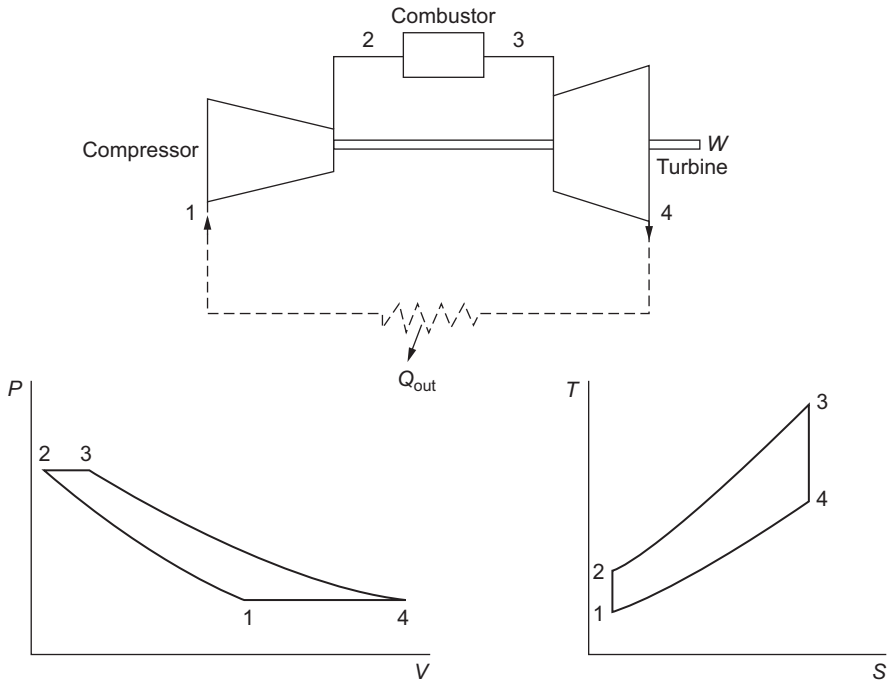


Figure 2-1 The air-standard Brayton cycle.

Thus, the overall adiabatic thermal cycle efficiency is:

$$\eta_{\text{cyc}} = \frac{W_{\text{cyc}}}{Q_{2,3}} \tag{2-5}$$

Increasing the pressure ratio and the turbine firing temperature increases the Brayton cycle's adiabatic thermal efficiency. This relationship of overall adiabatic thermal cycle efficiency is based on certain simplification assumptions such as: (1) $\dot{m}_a >> \dot{m}_f$, (2) the gas is calorically and thermally perfect, which means that the specific heat at constant pressure ($c_{p,}$) and the specific heat at constant volume (c_v) are constant thus the specific heat ratio γ remains constant throughout the cycle, (3) the pressure ratio (r_p) in both the compressor and the turbine are the same, and (4) all components operate at 100% efficiency. With these assumptions, the effect on the ideal adiabatic thermal cycle efficiency as a function of pressure ratio for the ideal Brayton cycle operating between the ambient temperature and the firing temperature is given by the following relationship:

$$\eta_{\text{ideal}} = \left(1 - \frac{1}{r_p^{\frac{\gamma-1}{\gamma}}}\right) \tag{2-6}$$

where r_p is the pressure ratio and γ is the ratio of the specific heats. The above equation tends to go to very high numbers, as the pressure ratio is increased.

Assuming that the pressure ratio is the same in both the compressor and the turbine; the following relationships hold using the pressure ratio in the compressor:

$$\eta_{\text{ideal}} = 1 - \frac{T_1}{T_2} \tag{2-7}$$

and using the pressure ratio in the turbine:

$$\eta_{\text{ideal}} = 1 - \frac{T_4}{T_3} \tag{2-8}$$

In the case of the actual cycle, the effect of the turbine compressor (η_c) and the efficiencies of expander (η_t) must also be taken into account, to obtain the overall adiabatic thermal cycle efficiency between the firing temperature T_f and the ambient temperature T_{amb} of the turbine. This relationship is given in the following equation:

$$\eta_{\text{cycle}} = \left(\frac{\eta_t T_f - \frac{T_{\text{amb}} r_p^{\left(\frac{\gamma-1}{\gamma}\right)}}{\eta_c}}{T_f - T_{\text{amb}} - T_{\text{amb}} \left(\frac{r_p^{\left(\frac{\gamma-1}{\gamma}\right)} - 1}{\eta_c} \right)} \right) \left(1 - \frac{1}{r_p^{\left(\frac{\gamma-1}{\gamma}\right)}} \right) \tag{2-9}$$

Figure 2-2 shows the effect on the overall adiabatic thermal cycle efficiency of the increasing pressure ratio and the firing temperature. The increase in the pressure ratio increases the overall efficiency at a given firing temperature; however, increasing the pressure ratio beyond a certain value at any given firing temperature can actually result in lowering the overall cycle efficiency. It should also be noted that the very high-pressure ratios tend to reduce the operating range of the turbine compressor. This causes the turbine compressor to be much more intolerant to dirt build up in the inlet air filter and on the compressor blades and creates large drops in the efficiency and

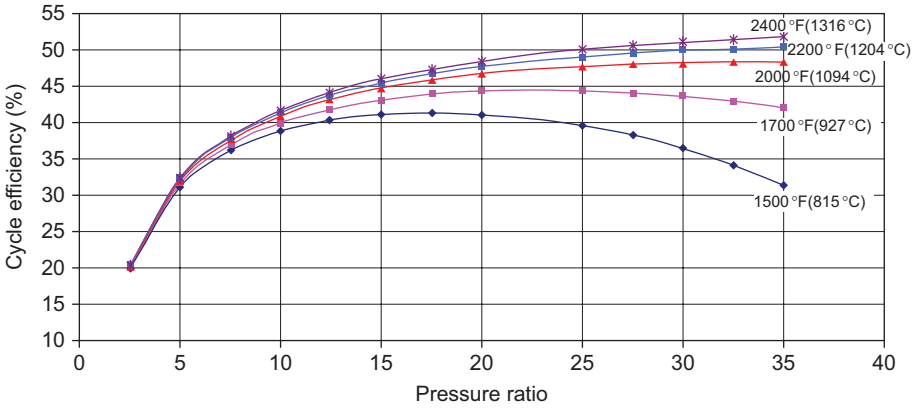


Figure 2-2 Overall cycle efficiency as a function of the firing temperature and pressure ratio. Based on a compressor efficiency of 87% and a turbine efficiency of 92%

performance of the adiabatic thermal cycle. In some cases, it can lead to compressor surge, which in turn can lead to a flameout or even serious damage and failure of the compressor blades and the radial and thrust bearings of the gas turbine.

To obtain a more accurate relationship between the overall adiabatic thermal cycle's efficiency and the inlet turbine temperatures, overall pressure ratios, and output work, consider the following relationships. For the maximum overall adiabatic thermal cycle efficiency, the following equation gives the optimum pressure ratio for fixed inlet temperatures and efficiencies of the compressor and turbine:

$$(r_p)_{\text{ecopt}} = \left\{ \frac{1}{T_1 T_3 \eta_t - T_1 T_3 + T_1^2} \left[T_1 T_3 \eta_t - \sqrt{(T_1 T_3 \eta_t)^2 - (T_1 T_3 \eta_t - T_1 T_3 + T_1^2)(T_3^2 \eta_c \eta_t - T_1 T_3 \eta_c \eta_t + T_1 T_3 \eta_t)} \right] \right\}^{\frac{\gamma}{\gamma - 1}} \tag{2-10}$$

The above equation for no losses in the compressor and turbine ($\eta_c = \eta_t = 1$) reduces to:

$$(r_p)_{\text{eopt}} = \left(\frac{T_1 T_3}{T_1^2} \right)^{\frac{\gamma}{\gamma - 1}} \tag{2-11}$$

The optimum pressure ratio for maximum output work for a turbine taking into account the adiabatic thermal efficiencies of the compressor and the turbine expander section can be expressed by the following relationship:

$$r_{p_{\text{wopt}}} = \left[\left(\frac{T_3 \eta_c \eta_t}{2T_1} \right) + \frac{1}{2} \right]^{\frac{\gamma}{\gamma - 1}} \tag{2-12}$$

Figure 2-3 shows the optimum pressure ratio for maximum adiabatic thermal efficiency or work per pounds (kilogram) of air. The optimum pressure ratio based on work occurs at a lower pressure ratio than the point of maximum adiabatic thermal efficiency at the same firing temperature.

Thus, a cursory inspection of the adiabatic thermal efficiency indicates that the overall adiabatic thermal efficiency of a cycle can be improved by increasing the pressure ratio or by increasing the turbine inlet temperature and the work per pounds (kilogram) of air can be increased by increasing the pressure ratio, by increasing the turbine inlet temperature, or by decreasing the inlet temperature.

Regeneration Effect

In a simple gas turbine cycle, the turbine exit temperature is nearly always appreciably higher than the temperature of the air leaving the compressor. Obviously, the fuel requirement can be reduced by the use of a regenerator in which the hot turbine exhaust

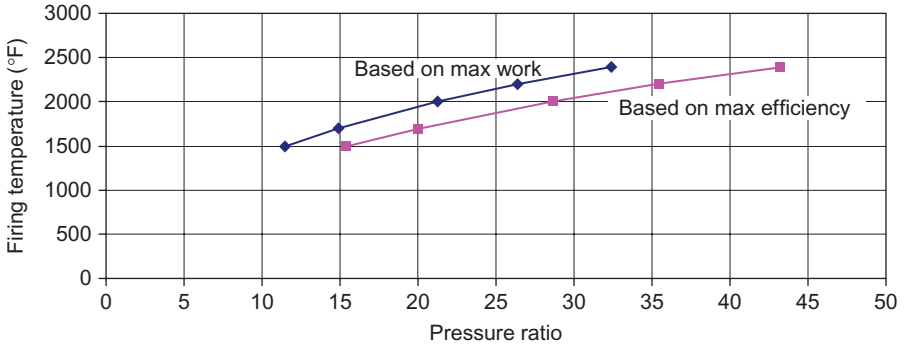


Figure 2-3 Pressure ratio based on maximum efficiency or work at various firing temperatures. Based on a compressor efficiency of 87% and a turbine efficiency of 92%.

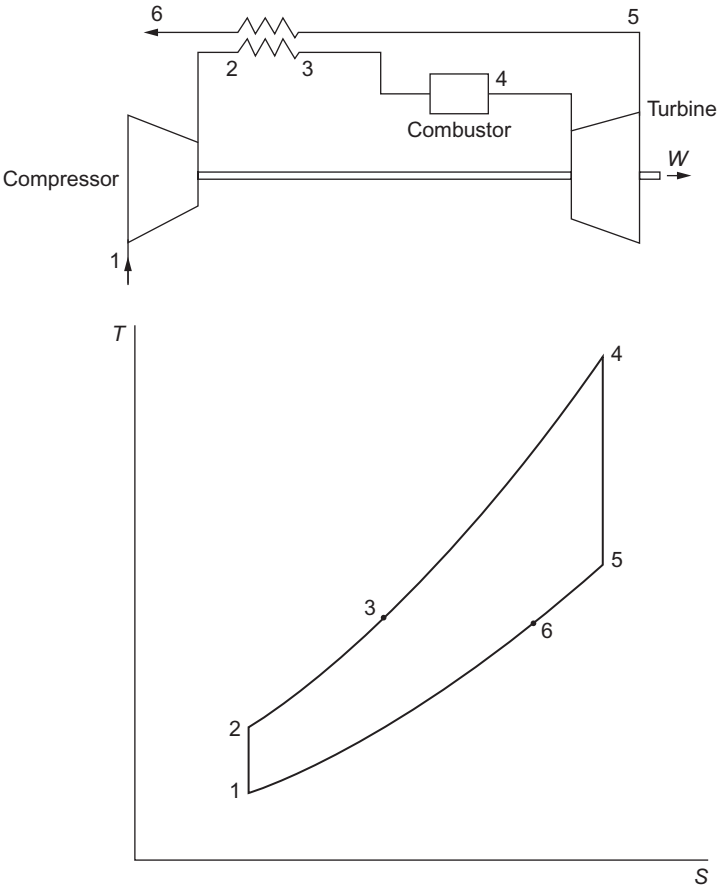


Figure 2-4 The regenerative gas turbine cycle.

gas preheats the air between the compressor and the combustion chamber. Figure 2-4 shows a schematic diagram of the regenerative cycle and its performance in the *T*–*S* diagram. In an ideal case, the flow through the regenerator is at constant pressure. The regenerator effectiveness (ε) is given by the following relationship:

$$\varepsilon_{\text{reg}} = \frac{T_3 - T_2}{T_5 - T_2} \tag{2-13}$$

Thus, the overall adiabatic thermal cycle efficiency for this system can be written as:

$$\eta_{\text{RCYC}} = \frac{(T_4 - T_5) - (T_2 - T_1)}{(T_4 - T_3)} \tag{2-14}$$

Increasing the effectiveness of a regenerator calls for more heat-transfer surface area, which increases the cost, the pressure drop, and the space requirements of the unit.

Figure 2-5 shows the improvement in cycle adiabatic thermal efficiency because of heat recovery with respect to a simple open-cycle gas turbine of 4.33:1 ratio pressure and 1200 °F inlet temperature. Cycle adiabatic thermal efficiency drops with an increasing pressure drop in the regenerator.

There are two types of heat exchangers, namely regenerative and recuperative. The term "regenerative heat exchanger" is used for a system in which the heat transfer between the two streams is affected by the exposure of a third medium alternately to the two flows. The heat flows successively in and out of the third medium, which undergoes a cyclic temperature. These types of heat exchangers are widely used where compactness is essential. The automotive regenerators consisted of a large circular

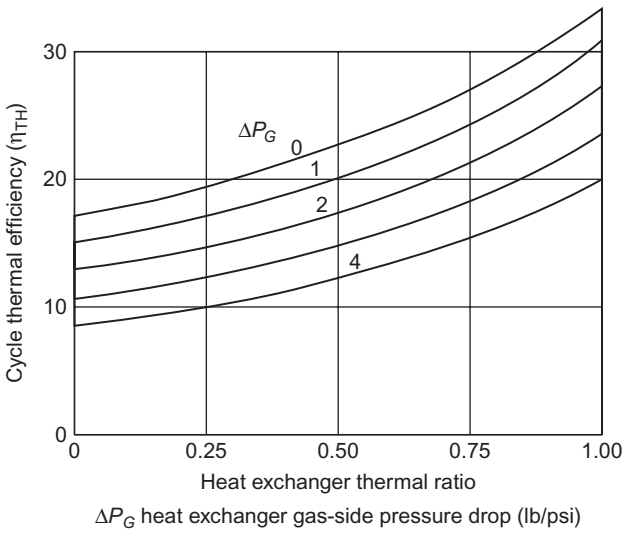


Figure 2-5 Variation of a gas turbine cycle efficiency with heat exchanger performance.

drum with honeycombed ceramic passages. The drum was rotated at a very low rpm (10–15 rpm). The drum surface was divided into two halves by an air seal. The hot air would pass through one-half of the circular drum heating the honeycombed passages the air would encounter, and then the cooler air would pass through the same passages and as the drum was rotated, it would be heated.

In a recuperative heat exchanger, each element of heat-transferring surface has a constant temperature and, by arranging the gas paths in contraflow, the temperature distribution in the matrix in the direction of flow is that giving optimum performance for the given heat-transfer conditions. This optimum temperature distribution can be achieved ideally in a contra-flow regenerator and approached very closely in a cross-flow regenerator.

The matrix permitting the maximum flow per unit area will yield the smaller regenerator for a given thermal and pressure drop performance. A material with a high heat capacity per unit volume is preferred, since this property of the material will increase the switching time and tend to reduce carry-over losses. Another desirable property of the arrangement is low thermal conductivity in the direction of the gas flow. All leakages within the regenerator must be avoided. A leakage of 3% reduces the regenerator effectiveness from 80% to 71%.

Increasing the Work Output of the Simple-Cycle Gas Turbine

The way to enhance the power output of a gas turbine can be achieved by intercooling and reheating.

Intercooling and Reheating Effects

The net work of a gas turbine cycle is given by:

$$W_{\text{cyc}} = W_t - W_c \tag{2-15}$$

and can be increased either by decreasing the work of the compressor or by increasing the work of turbine; these are the purposes of intercooling and reheating, respectively.

Multi-staging of compressors is sometimes used to allow for cooling between the stages to reduce the total work input. Figure 2-6 shows a polytropic compression process 1–*a* on the *P*–*V* plane. If there is no change in the kinetic energy, the work done is represented by the area 1–*a*–*j*–*k*–1. A constant temperature line is shown as 1–*x*. If the polytropic compression from State one to two is divided into two parts, 1–*c* and *d*–*e*, with constant pressure cooling to $T_d = T_1$ between them, the work done is represented by area 1–*c*–*d*–*e*–*I*–*k*–1. The area *c*–*a*–*e*–*d*–*c* represents the work saved by means of the two-stage compression with intercooling to the initial temperature. The optimum pressure for intercooling for specified values P_1 and P_2 is:

$$P_{\text{OPT}} = \sqrt{P_1 P_2} \tag{2-16}$$

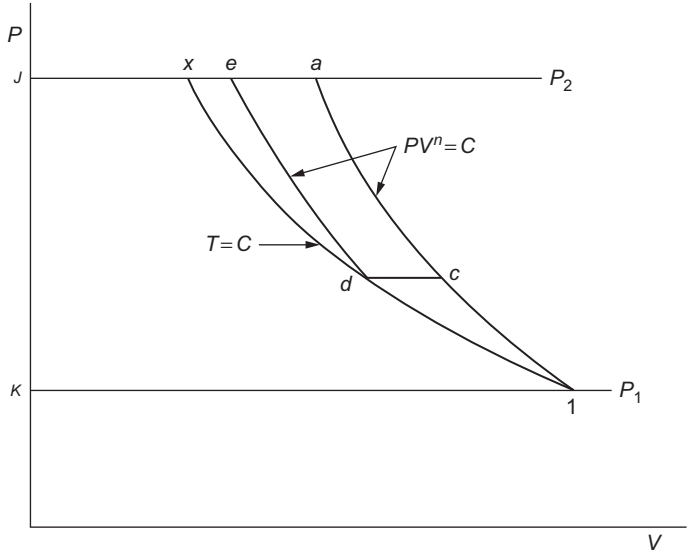


Figure 2-6 Multistages compression with inter-cooling.

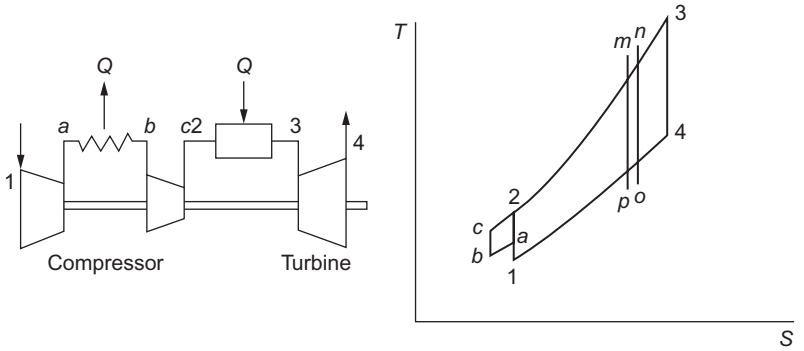


Figure 2-7 The inter-cooled gas turbine cycle.

Therefore, if a simple gas turbine cycle is modified with the compression accomplished in two or more adiabatic processes with intercooling between them, the net work of the cycle is increased with no change in the turbine work.

The thermal efficiency of an ideal simple cycle is decreased by the addition of an intercooler. Figure 2-7 shows the schematic diagram of such a cycle. The ideal simple gas turbine cycle is 1–2–3–4–1 and the cycle with the intercooling added is 1–*a*–*b*–*c*–2–3–4–1. Both the cycles in their ideal form are reversible and can be simulated by a number of Carnot cycles. Thus, if the simple gas turbine cycle 1–2–3–4–1 is divided into a number of cycles such as *m*–*n*–*o*–*p*–*m*, these little cycles approach the Carnot

cycle, as their number increases. The adiabatic thermal efficiency of such a Carnot cycle is given by the relationship:

$$\eta_{\text{CARNOT}} = 1 - \frac{T_m}{T_p} \tag{2-17}$$

Note that if the specific heats are constant then:

$$\frac{T_3}{T_4} = \frac{T_m}{T_p} = \frac{T_2}{T_1} = \left(\frac{P_2}{P_1}\right)^{\frac{\gamma-1}{\gamma}} \tag{2-18}$$

All the Carnot cycles making up the simple gas turbine cycle have the same adiabatic thermal efficiency. Likewise, all the Carnot cycles into which the cycle *a*–*b*–*c*–2–*a* might similarly be divided have a common value of adiabatic thermal efficiency lower than the Carnot cycles that comprise cycle 1–2–3–4–1. Thus, the addition of an intercooler, which adds *a*–*b*–*c*–2–*a* to the simple cycle, lowers the adiabatic thermal efficiency of the cycle.

The addition of an intercooler to a regenerative gas turbine cycle increases the cycle's adiabatic thermal efficiency and output work because a larger portion of the heat required for the process *c*3 in Figure 2-7 can be obtained from the hot turbine exhaust gas passing through the regenerator instead of from burning additional fuel.

The reheat cycle increases the turbine work, and consequently the net work of the cycle can be increased without changing the compressor work or the turbine inlet temperature by dividing the turbine expansion into two or more parts with constant pressure heating before each expansion. This cycle modification is known as reheating as seen in Figure 2-8. By reasoning similar to that used in connection with inter-cooling, it can be seen that the adiabatic thermal efficiency of a simple cycle is lowered by the

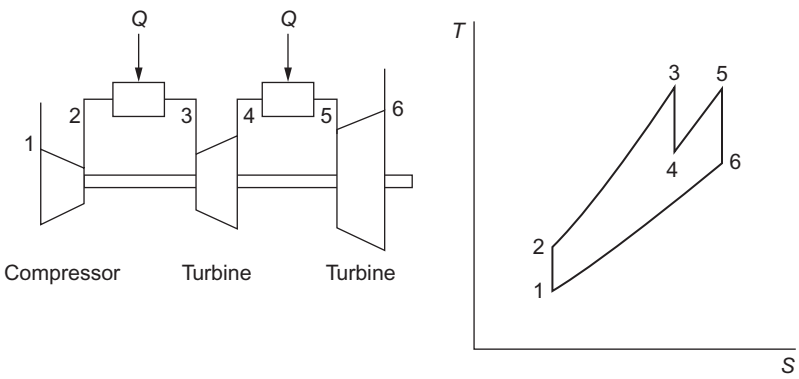


Figure 2-8 Reheat cycle and *T*–*S* diagram.

addition of reheating, while the work output is increased. However, a combination of regenerator and reheater can increase the adiabatic thermal efficiency.

Actual Cycle Analysis

The previous section dealt with the concepts of the various cycles. Work output and adiabatic thermal efficiency of all actual cycles are considerably less than those of the corresponding ideal cycles because of the effect of compressor and combustor, turbine efficiencies, and pressure losses in the system.

The Simple Cycle

The simple cycle is the most common type of cycle being used in gas turbines in the field today. The actual open simple cycle as shown in Figure 2-9 indicates the inefficiency of the compressor and turbine and the loss in pressure through the burner. Assuming that the compressor adiabatic thermal efficiency is η_c and the turbine adiabatic thermal efficiency is η_1, the actual compressor work and the actual turbine work is given by:

$$W_{\text{ca}} = \frac{\dot{m}_a(h_2 - h_1)}{\eta_c} \tag{2-19}$$

$$W_{\text{ta}} = (\dot{m}_a + \dot{m}_f)(h_{3a} - h_4)\eta_t \tag{2-20}$$

Thus, the actual total output work is:

$$W_{\text{act}} = W_{\text{ta}} - W_{\text{ca}} \tag{2-21}$$

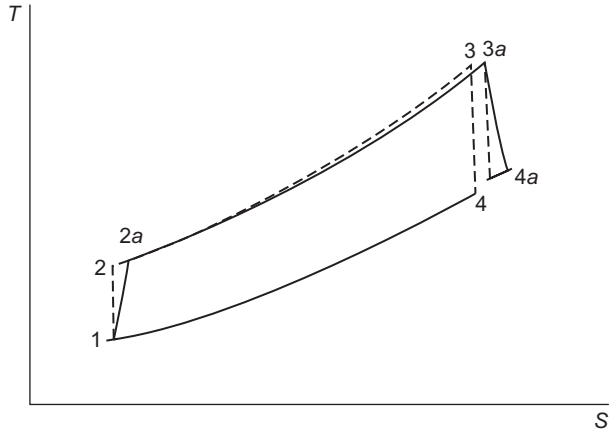


Figure 2-9 *T–S* diagram of the actual open simple cycle.

The actual fuel required to raise the temperature from $2a$ to $3a$ is:

$$\dot{m}_f = \frac{h_{3a} - h_{2a}}{(\text{LHV})\eta_b} \tag{2-22}$$

Thus, the overall adiabatic thermal cycle adiabatic thermal efficiency can be calculated from the following equation:

$$\eta_c = \frac{W_{\text{act}}}{\dot{m}_f(\text{LHV})} \tag{2-23}$$

Analysis of this cycle indicates that an increase in inlet temperature to the turbine causes an increase in the adiabatic thermal cycle efficiency. The optimum pressure ratio for maximum efficiency varies with the turbine inlet temperature from an optimum of about 15.5:1 at a temperature of 1500 °F (816 °C) to about 43:1 at a temperature of about 2400 °F (1316 °C). The pressure ratio for maximum work, however, varies from about 11.5:1 to about 35:1 for the same respective temperatures.

Thus, from Figure 2-10, it is obvious that for maximum performance, a pressure ratio of 30:1 at a temperature of 2800 °F (1537 °C) is optimal. The use of an axial-flow compressor requires 16–24 stages with a pressure ratio of 1.15–1.25:1 per stage. A 22-stage compressor producing a 30:1 pressure ratio is a relatively conservative design. If the pressure ratio was increased to 1.252:1 per stage, the number of stages would be about 16. The latter pressure ratio has been achieved with high efficiencies. This reduction in number of stages means a greater reduction in the overall cost. The increases in turbine temperatures give a greater increase in efficiency and power, so temperatures in the 2,400 °F (1316 °C) range at the turbine inlet are becoming the state-of-the-art.

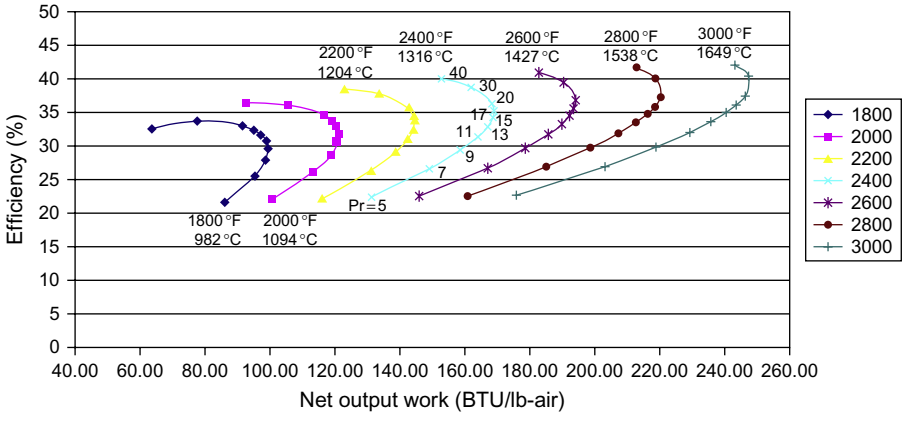


Figure 2-10 The performance map of a simple-cycle gas turbine.

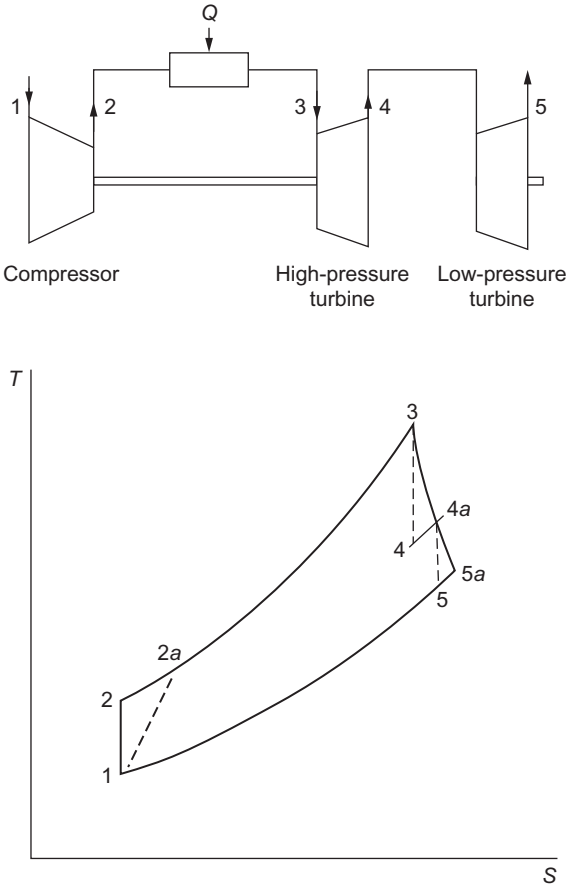


Figure 2-11 The split-shaft gas turbine cycle.

The Split-Shaft Simple Cycle

The split-shaft simple cycle is mainly used for high torque and large load variant. Figure 2-11 is a schematic diagram of the two-shaft simple cycle. The first turbine drives the compressor and the second turbine is used as a power source. If one assumes that the number of stages in a split-shaft simple cycle is more than that in a simple shaft cycle then the adiabatic thermal efficiency of the split-shaft cycle is slightly higher at design loads because of the reheat factor, as shown in Figure 2-12. However, if the number of stages is the same then there is no change in the overall adiabatic thermal efficiency. From the *H*–*S* diagram, one can find some relationships between turbines. Since the job of the HP turbine is to drive the compressor, the equations to use are as follows:

$$h_{4a} = h_3 - W_{\text{ca}} \tag{2-24}$$

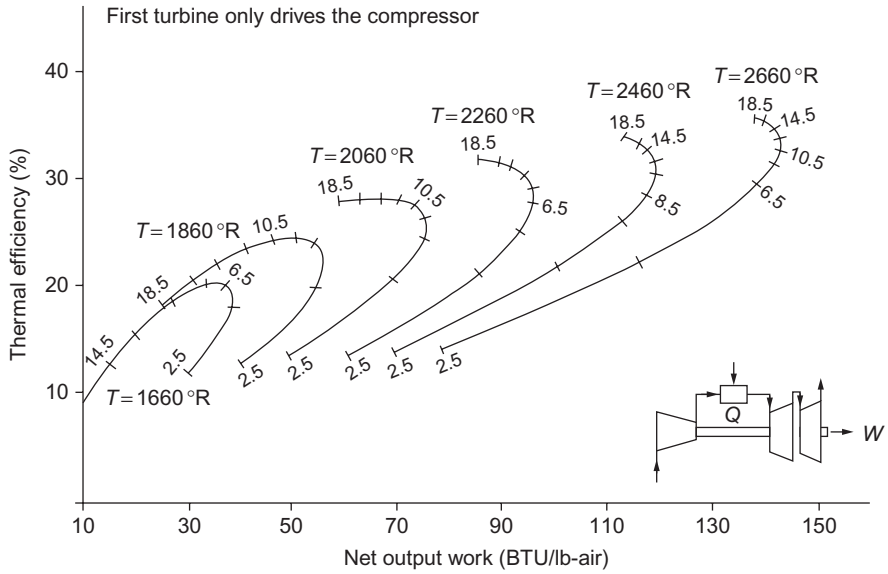


Figure 2-12 Performance map showing the effect of pressure ratio and turbine inlet temperature on a split-shaft cycle.

$$h_4 = h_3 - \left(\frac{W_{\text{ca}}}{\eta_{\text{t}}}\right) \tag{2-25}$$

Thus, the output work can be represented by the relationship:

$$W_a = (\dot{m}_a + \dot{m}_f)\,(h_{4a} - h_5)\,\eta_t \tag{2-26}$$

In the split-shaft cycle, the first shaft supports the compressor and the turbine that drives it, while the second shaft supports the free turbine that drives the load. The two shafts can operate at entirely different speeds. The advantage of the split-shaft gas turbine is its high torque at low speed. A free-power turbine gives a very high torque at low rpm. Very high torque at low rpm is convenient for automotive use, but with constant full-power operation, it is of little or no value. Its use is usually limited to variable mechanical-drive applications.

The Regenerative Cycle

The regenerative cycle is becoming prominent in these days of tight fuel reserves and high fuel costs. The amount of fuel needed can be reduced by the use of a regenerator in which the hot turbine exhaust gas is used to preheat the air between the compressor and the combustion chamber. From Figure 2-4 and the definition of a regenerator, the temperature at the exit of the regenerator is given by the following relationship:

$$T_3 = T_{2a} + \eta_{\text{reg}}\,(T_5 - T_{2a}), \tag{2-27}$$

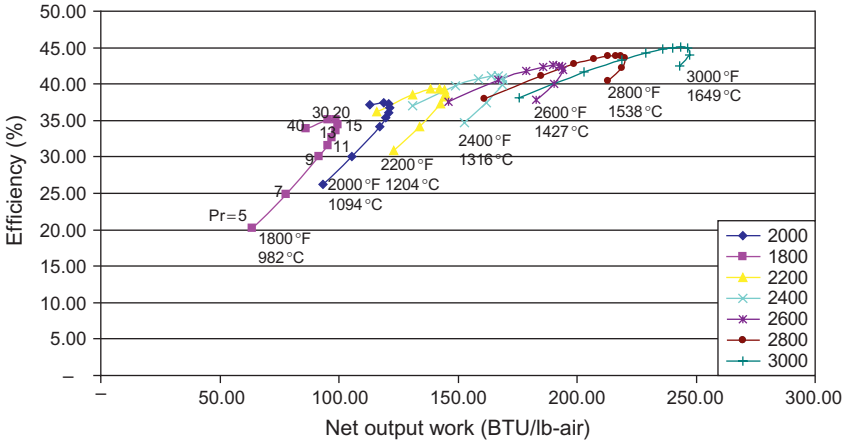


Figure 2-13 The performance map of a regenerative gas turbine cycle.

where T_{2a} is the actual temperature at the compressor exit. The regenerator increases the temperature of the air entering the burner, thus reducing the fuel-to-air ratio and increasing the adiabatic thermal efficiency.

For a regenerator assumed to have an effectiveness of 80%, the adiabatic thermal efficiency of the regenerative cycle is about 40% higher than its counterpart in the simple cycle, as shown in Figure 2-13. The work output per pound of air is about the same or slightly less than that experienced with the simple cycle. The point of maximum adiabatic thermal efficiency in the regenerative cycle occurs at a lower pressure ratio than that of the simple cycle, *but the optimum pressure ratio for the maximum work is the same in the two cycles*. Thus, when companies are designing gas turbines, the choice of pressure ratio should be such that maximum benefit from both cycles can be obtained, since most offer a regeneration option. It is not correct to say that a regenerator at off-optimum would not be effective, but a proper analysis should be made before a large expense is incurred.

The split-shaft regenerative turbine is very similar to the split-shaft cycle. The advantage of this turbine is the same as that mentioned before; namely, high torque at low rpm. The cycle efficiencies are also about the same. Figure 2-14 indicates the performance that may be expected from such a cycle.

The Inter-cooled Simple Cycle

A simple cycle with inter-cooler can reduce total compressor work and improve net output work. Figure 2-7 shows the simple cycle with inter-cooling between compressors. The assumptions made in evaluating this cycle are as follows: (1) compressor interstage temperature equals inlet temperature, (2) compressor efficiencies are the same, and (3) pressure ratios in both compressors are the same and equal to: $\sqrt{(P_2/P_1)}$.

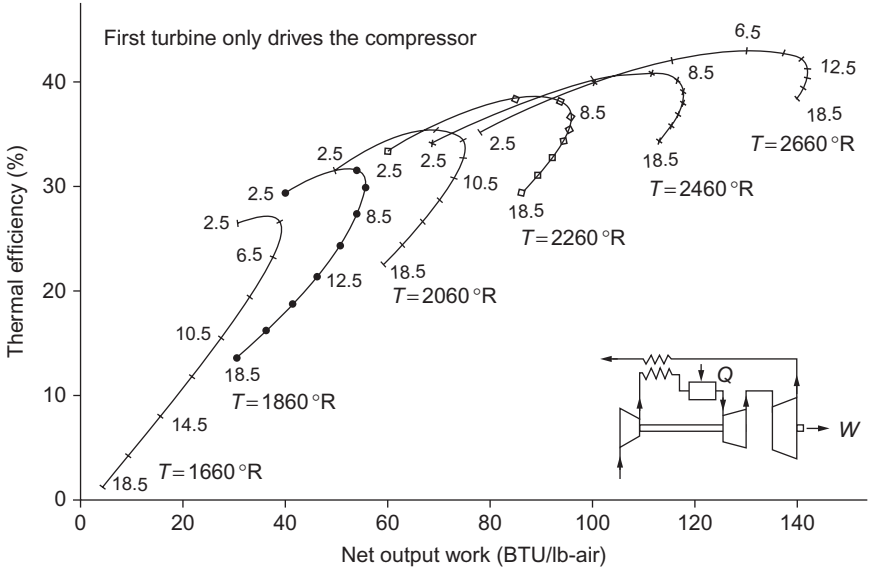


Figure 2-14 Performance map showing the effect of pressure ratio and turbine inlet temperature on a regenerative split-shaft cycle.

The inter-cooled simple cycle reduces the power consumed by the compressor. A reduction in consumed power is accomplished by cooling the inlet temperature in the second or other following stages of the compressor to the same as the ambient air and maintaining the same overall pressure ratio. The compressor work can then be represented by the following relationship:

$$W_c = (h_a - h_1) + (h_c - h_1) \tag{2-28}$$

This cycle produces an increase of 30% in work output, but the overall adiabatic thermal efficiency is slightly decreased as shown in Figure 2-15. An intercooling regenerative cycle can increase the power output and the adiabatic thermal efficiency. This combination provides an increase in efficiency of about 12% and an increase in power output of about 30%, as indicated in Figure 2-16. Maximum adiabatic thermal efficiency, however, occurs at lower pressure ratios, as compared with the simple or reheat cycles.

The Reheat Cycle

The regenerative cycles improve the adiabatic thermal efficiency of the split-shaft cycle, but do not provide any added work per pound of air flow. To achieve this latter goal, the concept of the reheat cycle must be utilized. The reheat cycle, as shown in Figure 2-8, consists of a two-stage turbine with a combustion chamber before each stage. The assumptions made in this chapter are that the HP turbine's only job is to drive the compressor and that the gas leaving this turbine is then reheated to the same

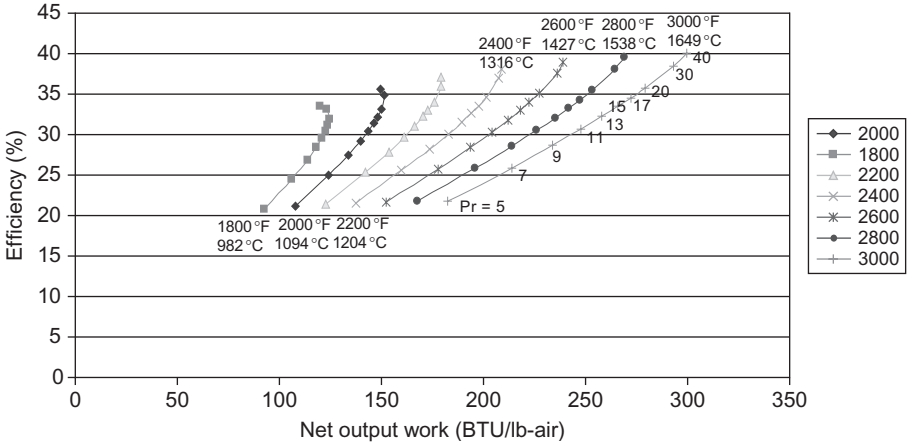


Figure 2-15 The performance map of an inter-cooled gas turbine cycle.

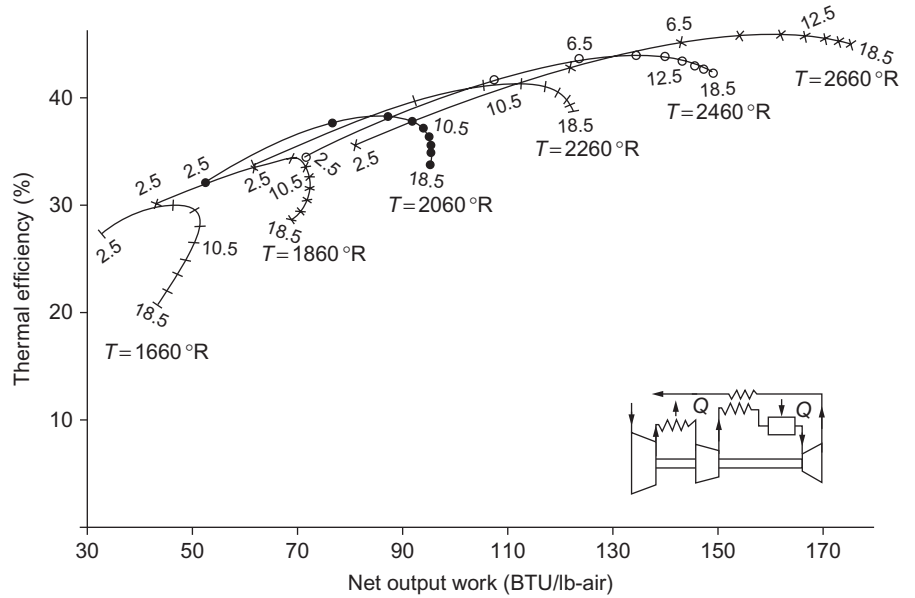


Figure 2-16 Performance map showing the effect of pressure ratio and turbine inlet temperature on an inter-cooled regenerative cycle.

temperature as in the first combustor before entering the low-pressure (LP) or low-power turbine. This reheat cycle has an adiabatic thermal efficiency that is less than that encountered in a simple cycle, but produces about 35% more shaft output power, as shown in Figure 2-17.

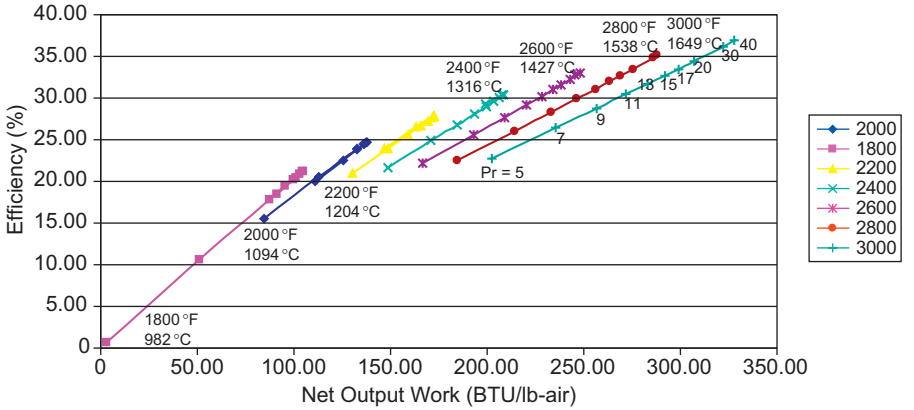


Figure 2-17 The performance of a reheat gas turbine cycle.

The Inter-cooled Regenerative Reheat Cycle

The Carnot cycle is the optimum cycle and all cycles incline toward this optimum. Maximum adiabatic thermal efficiency is achieved by approaching the isothermal compression and expansion of the Carnot cycle, or by inter-cooling in compression and reheating in the expansion process. Figure 2-18 shows the inter-cooled regenerative reheat cycle, which approaches this optimum cycle in a practical fashion.

This cycle achieves the maximum adiabatic thermal efficiency and work output of any of the cycles described to this point. With the insertion of an inter-cooler in the compressor, the pressure ratio for maximum adiabatic thermal efficiency moves to a much higher ratio, as indicated in Figure 2-19.

The Steam Injection Cycle

Steam injection has been used in reciprocating engines and gas turbines for a number of years. This cycle may be an answer to the present concern with pollution and higher adiabatic thermal efficiency. Corrosion problems are the major hurdle in such a system. The concept is simple and straightforward: water is injected into the compressor discharge air and increases the mass flow rate through the turbine, as shown in Figure 2-20. The steam being injected downstream from the compressor does not increase the work required to drive the compressor.

The steam used in this process is generated by the turbine exhaust gas. Typically, water at 14.7 psia (1 Bar) and 80 °F (26.7 °C) enters the pump and regenerator, where it is brought up to 60 psia (4 Bar) above the compressor discharge and the same temperature as the compressor discharged air. The steam is injected after the compressor but far upstream of the burner to create a proper mixture that helps to reduce the primary zone temperature in the combustor and the NO_x output. The enthalpy of State 3 (h_3) is the mixture enthalpy of air and steam. The following relationship describes the

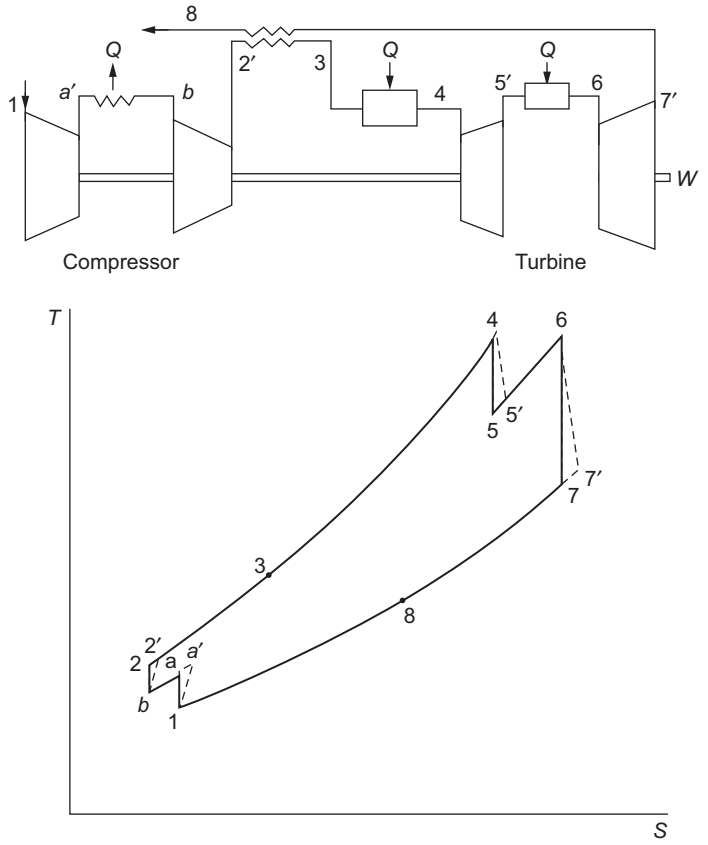


Figure 2-18 The inter-cooled, regenerative, reheat, split-shaft gas turbine cycle.

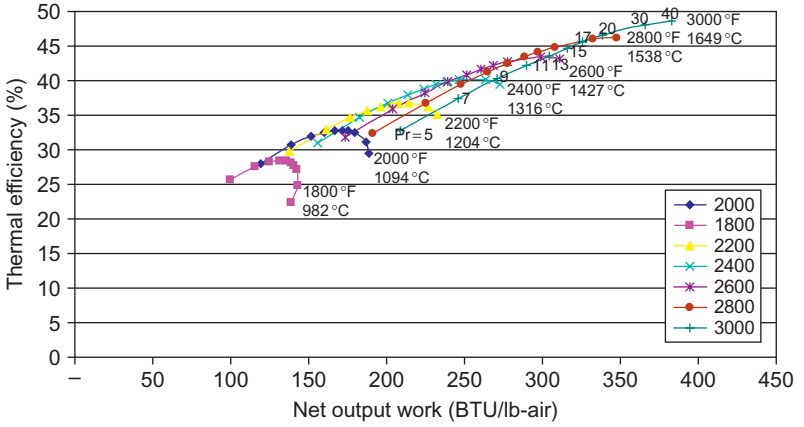


Figure 2-19 The performance of an inter-cooled, regenerative, reheat cycle.

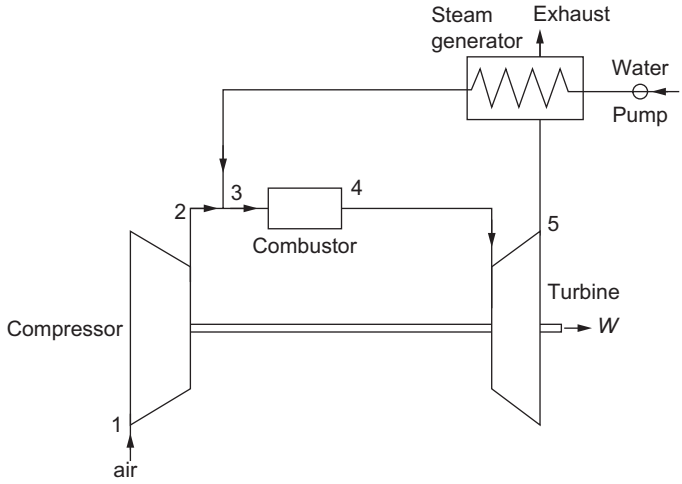


Figure 2-20 The steam injection cycle.

flow at that point:

$$h_3 = \left(\frac{\dot{m}_a h_{2a} + \dot{m}_s h_{3a}}{\dot{m}_a + \dot{m}_s} \right) \tag{2-29}$$

The enthalpy entering the turbine is given by the following relationship:

$$h_4 = \left(\frac{(\dot{m}_a + \dot{m}_f) h_{4a} + \dot{m}_s h_{4s}}{\dot{m}_a + \dot{m}_f + \dot{m}_s} \right) \tag{2-30}$$

with the amount of fuel needed to be added to this cycle as:

$$\dot{m}_f = \frac{h_4 - h_3}{\eta_b (\text{LHV})} \tag{2-31}$$

The enthalpy leaving the turbine is:

$$h_5 = \left(\frac{(\dot{m}_a + \dot{m}_f) h_{5a} + \dot{m}_s h_{5s}}{\dot{m}_a + \dot{m}_f + \dot{m}_s} \right) \tag{2-32}$$

Thus, the total work by the turbine is given by:

$$W_t = (\dot{m}_a + \dot{m}_s + \dot{m}_f)(h_4 - h_5)\eta_t \tag{2-33}$$

And the overall cycle adiabatic thermal efficiency is:

$$\eta_{\text{cyc}} = \frac{W_t - W_c}{\dot{m}_f (\text{LHV})} \tag{2-34}$$

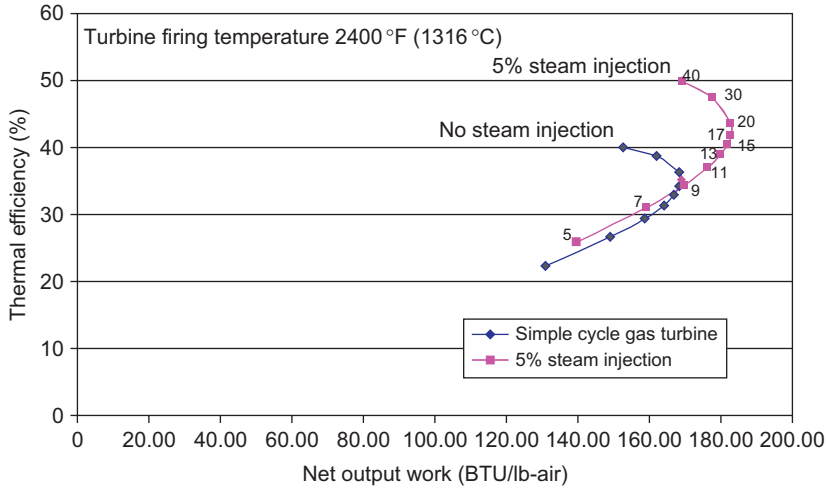


Figure 2-21 Comparison between 5% steam injection and simple-cycle gas turbine.

The cycle leads to an increase in output work and an increase in overall adiabatic thermal efficiency.

Figure 2-21 shows the effect of 5% by weight of steam injection at a turbine inlet temperature of 2400 °F (1316 °C) on the system. With about 5% injection at 2400 °F (1316 °C) and a pressure ratio of 17:1, an 8.3% increase in work output is noted with an increase of about 19% in cycle adiabatic thermal efficiency over that experienced in the simple cycle. The assumption here is that steam is injected at a pressure of about 60 psi (4 Bar) above the air from the compressor discharge and that all the steam is created by heat from the turbine exhaust. Calculations indicate that there is more than enough waste heat to achieve these goals.

Figure 2-22 shows the effect of 5% steam injection at different temperatures and pressures. Steam injection for power augmentation has been used for many years and is a very good option for plant renewable. The great advantage of this cycle is the low production level of nitrogen oxides. This low level is accomplished by the steam being injected in the compressor discharge diffuser wall, well upstream from the combustor, creating a uniform mixture of steam and air throughout the region. The uniform mixture reduces the oxygen content of the fuel-to-air mixture and increases its heat capacity, which in turn reduces the temperature of the combustion zone and the NO_x formed. Field tests show that the amount of steam equivalent to the fuel flow by weight will reduce the amount of NO_x emissions to levels of about 25 ppm, which is an acceptable level in many parts of the world. The location of the water injector is crucial for the proper operation of this system and cycle.

The attractiveness of this system is that major changes are not needed to add this feature to an existing system. The new gas turbines that use dry low NO_x/emission (DLN/DLE) combustors are being used to meet the US Environmental Protection Agency (EPA) target of about 9 ppm. Many states in the United States also require

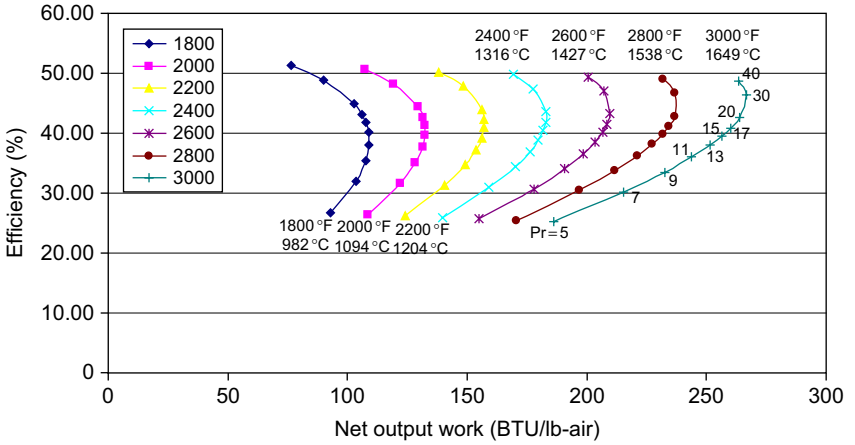


Figure 2-22 The performance map of a steam-injected gas turbine.

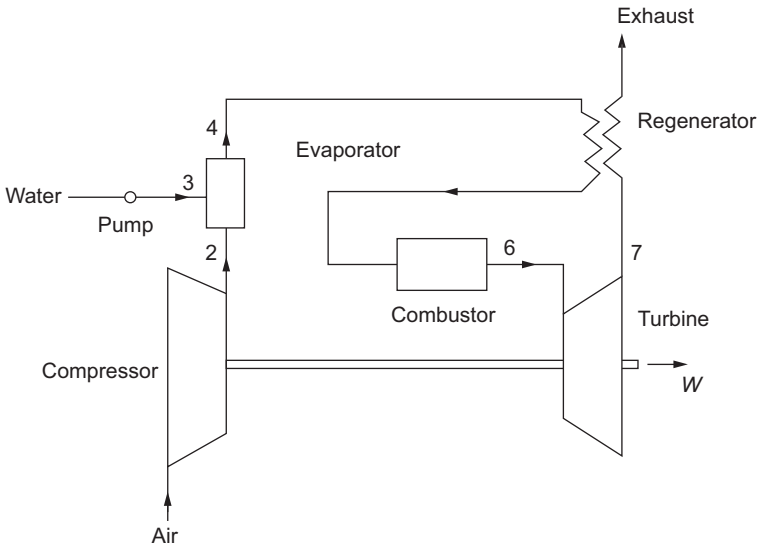


Figure 2-23 The evaporative regenerative cycle.

all the best known techniques available to be used; therefore, the new gas turbines use DLN/DLE combustors plus catalytic convertors.

The Evaporative Regenerative Cycle

This cycle, as shown in Figure 2-23, is a regenerative cycle with water injection. Theoretically, it has the advantages of both the steam injection and regenerative systems

reduction of NO_x emissions and higher adiabatic thermal efficiency. The work output of this system is about the same as that achieved in the steam injection cycle, but the adiabatic thermal efficiency of the system is much higher.

A high-pressure evaporator is placed between the compressor and the regenerator to add water vapor into the air steam, and in this process, it reduces the temperature of this mixed stream. The mixture then enters the regenerator at a lower temperature, increasing the temperature differential across the regenerator. Increasing the temperature differential reduces the temperature of the exhaust gases considerably, so that these exhaust gases, otherwise lost, are an indirect source of heat used to evaporate the water. Both the air and the evaporated water pass through the regenerator, combustion chamber, and turbine. The water enters at 80 °F (26.7 °C) and 14.7 psia (1 Bar) through a pump into the evaporator, where it is discharged as steam at the same temperature as the compressor discharged air and at a pressure of 60 psia (4 Bar) above the compressor discharge. It is then injected into the air stream in a fine mist where it is fully mixed. The governing equations are the same as in the previous cycle for the turbine section, but the heat added is altered because of the regenerator. The following equations govern this change in heat addition. From the first law of thermodynamics, the mixture temperature (T_4) is given by the following relationship:

$$T_4 = \frac{\dot{m}_a c_{pa} T_2 + \dot{m}_s c_{pw}(T_s - T_3) - \dot{m}_s h_{fg}}{\dot{m}_a c_{pa} + \dot{m}_s c_{ps}} \tag{2-35}$$

The enthalpy of the gas leaving the regenerator is given by the relationship:

$$h_5 = h_4 + \eta_{\text{reg}}\,(h_7 - h_4) \tag{2-36}$$

Similar to the regenerative cycle, the evaporative regenerative cycle has higher efficiencies at lower pressure ratios. Figures 2-24 and 2-25 show the performance of the system at various rates of steam injection and turbine inlet temperatures. Similar to the steam injection cycle, the steam is injected at 60 psi (4 Bar) higher than the air leaving the compressor. Corrosion in the regenerator is a problem in this system. When not completely clean, regenerators tend to develop hot spots that can lead to fires. This problem can be overcome with proper regenerator designs. This NO_x emission level is low and meets EPA standards.

The Brayton–Rankine Cycle

The combination of the gas turbine with the steam turbine is an attractive proposal, especially for electric utilities and process industries where steam is being used. In this cycle, as shown in Figure 2-26, the hot gases from the turbine exhaust are used in a supplementary fired boiler to produce super-heated steam at high temperatures for a steam turbine.

The computations of the gas turbine are the same as shown for the simple cycle. The steam turbine calculations are as follows:

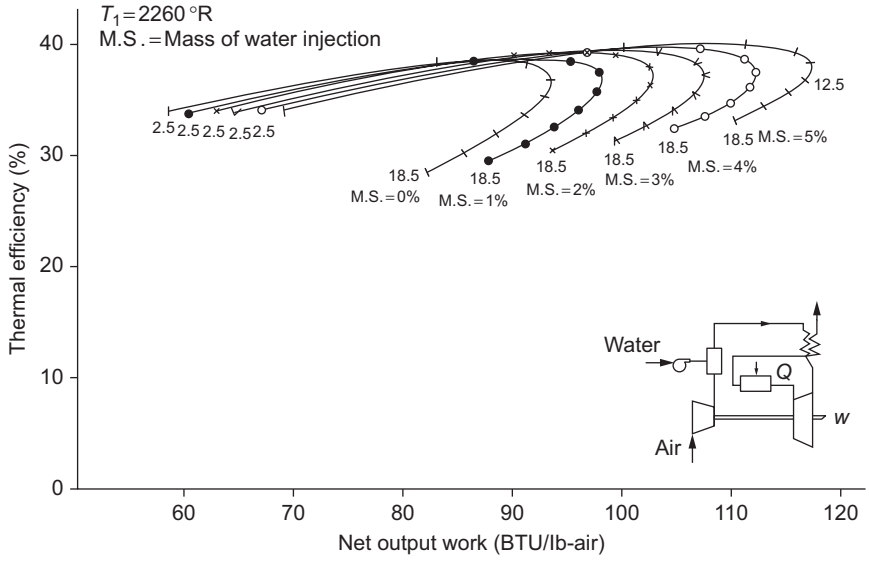


Figure 2-24 Performance map showing the effect of pressure ratio and steam flow rate on an evaporative regenerative cycle.

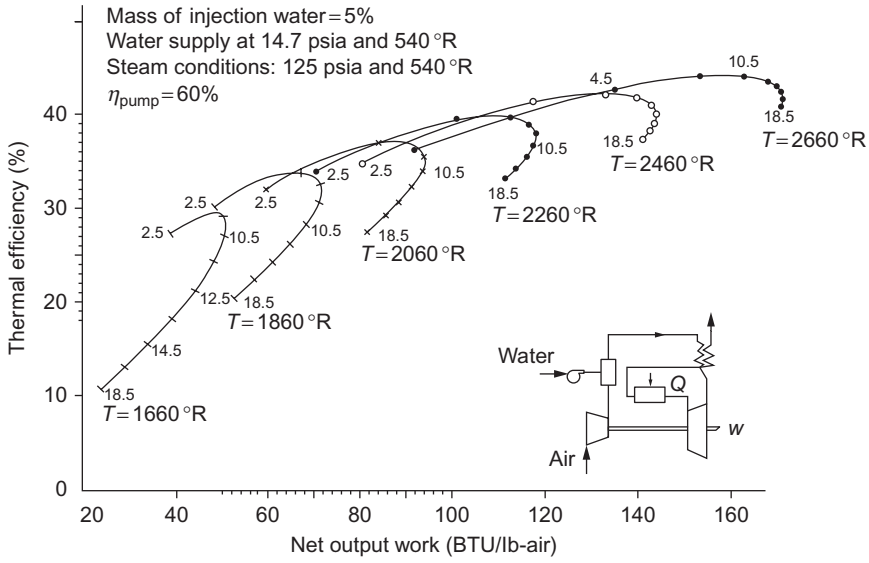


Figure 2-25 Performance map showing the effect of pressure ratio and steam flow rate on a fixed steam rate evaporative regenerative cycle.

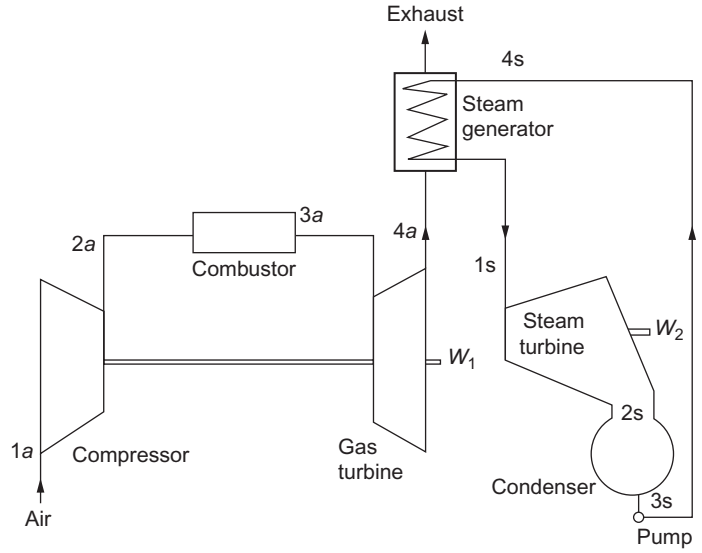


Figure 2-26 The Brayton–Rankine combined cycle.

Steam generator heat:

$$ {}_4Q_1 = h_{1S} - h_{4S} \tag{2-37} $$

Turbine work:

$$ W_{tS} = \dot{m}_s (h_{1S} - h_{2S}) \tag{2-38} $$

Pump work:

$$ W_p = \frac{\dot{m}_s (h_{4S} - H_{3S})}{h_p} \tag{2-39} $$

The combined-cycle work is equal to the sum of the net gas turbine work and the steam turbine work. About one-third to one-half of the design output is available as energy in the exhaust gases. The exhaust gas from the turbine is used to provide heat to the recovery boiler. Thus, this heat must be credited to the overall cycle. The following equations show the overall cycle work and adiabatic thermal efficiency:

Overall cycle work

$$ W_{cyc} = W_{ta} + W_{ts} - W_c - W_p \tag{2-40} $$

Overall cycle adiabatic thermal efficiency:

$$ \eta = \frac{W_{cyc}}{\dot{m}_f (\text{LHV})} \tag{2-41} $$

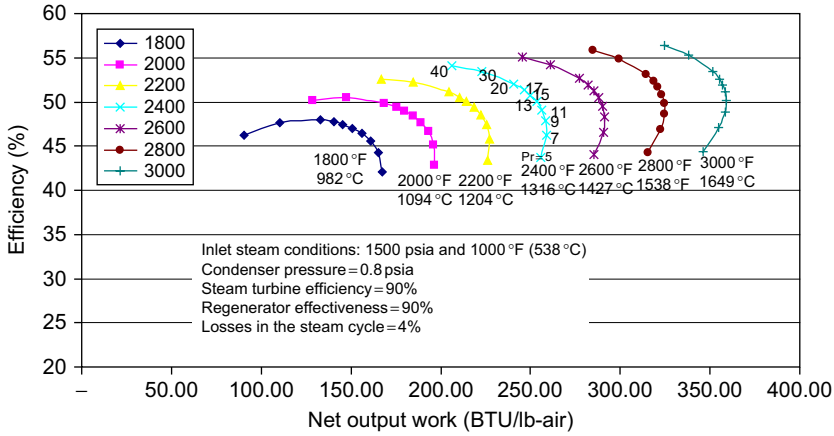


Figure 2-27 The performance map of a typical combined-cycle power plant.

This system, as can be seen from Figure 2-27, indicates that the net work is about the same as one would expect in a steam injection cycle, but the efficiencies are much higher. The disadvantages of this system are its high initial cost. However, just as in the steam injection cycle, the NO_x content of its exhaust remains the same and is dependent on the gas turbine used. This system is being used widely because of its high adiabatic thermal efficiency.

Summation of Cycle Analysis

Figures 2-28 and 2-29 give a good comparison of the effect of the various cycles on the output work and adiabatic thermal efficiency. The curves are drawn for a turbine inlet temperature of 2400 °F (1316 °C), which is a temperature presently being used by manufacturers. The output work of the regenerative cycle is very similar to the output work of the simple cycle, and the output work of the regenerative reheat cycle is very similar to that of the reheat cycle. The most work per pound of air can be expected from the inter-cooling regenerative reheat cycle.

The most effective cycle is the Brayton–Rankine cycle. This cycle has tremendous potential in power plants and in the process industries where steam turbines are in use in many areas. The initial cost of this system is high; however, in most cases, where steam turbines are being used, this initial cost can be greatly reduced.

Regenerative cycles are popular because of the high cost of fuel. Care should be observed not to indiscriminately attach regenerators to existing units. The regenerator is most efficient at low-pressure ratios. Cleansing turbines with abrasive agents may prove a problem in regenerative units, since the cleansers can get lodged in the regenerator and cause hot spots.

Water injection or steam injection systems are being used extensively to augment power. Corrosion problems in the compressor diffuser and combustor have not been

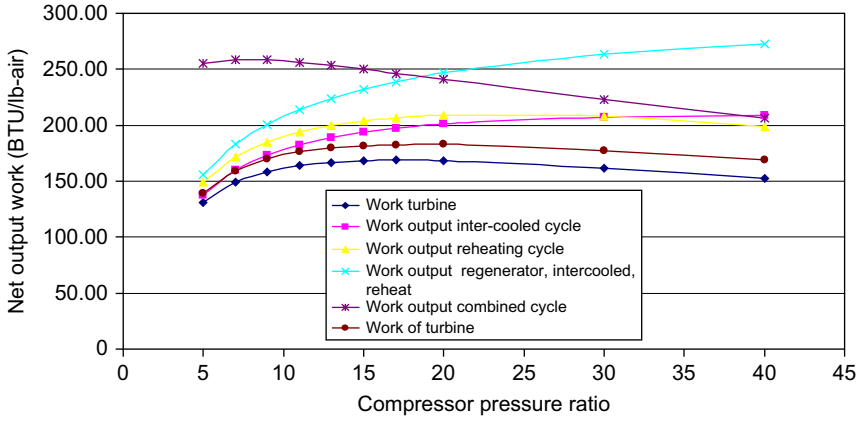


Figure 2-28 Comparison of net work output of various cycles at temperature 2400 °F (1315 °C).

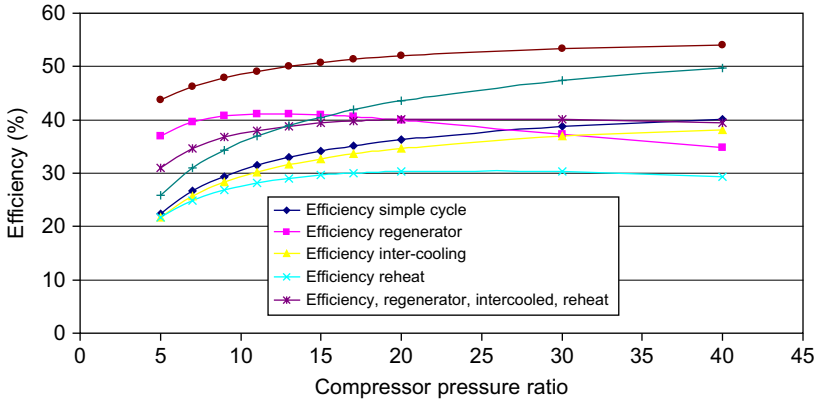


Figure 2-29 Comparison of thermal efficiency of various cycles at temperature 2400 °F (1315 °C).

found to be major problems. The increase in work and adiabatic thermal efficiency with a reduction in NO_x makes the process very attractive. Split-shaft cycles are attractive for use in variable-speed mechanical drives. The off-design characteristics of such an engine are high efficiency and high torque at low speeds.

A General Overview of Combined-Cycle Plants

There are many concepts of the combined cycle; these cycles range from the simple single pressure cycle in which the steam for the turbine is generated at only one pressure, to the triple pressure cycles, where the steam generated for the steam turbine is at three different levels. The energy flow diagram in Figure 2-30 shows the distribution

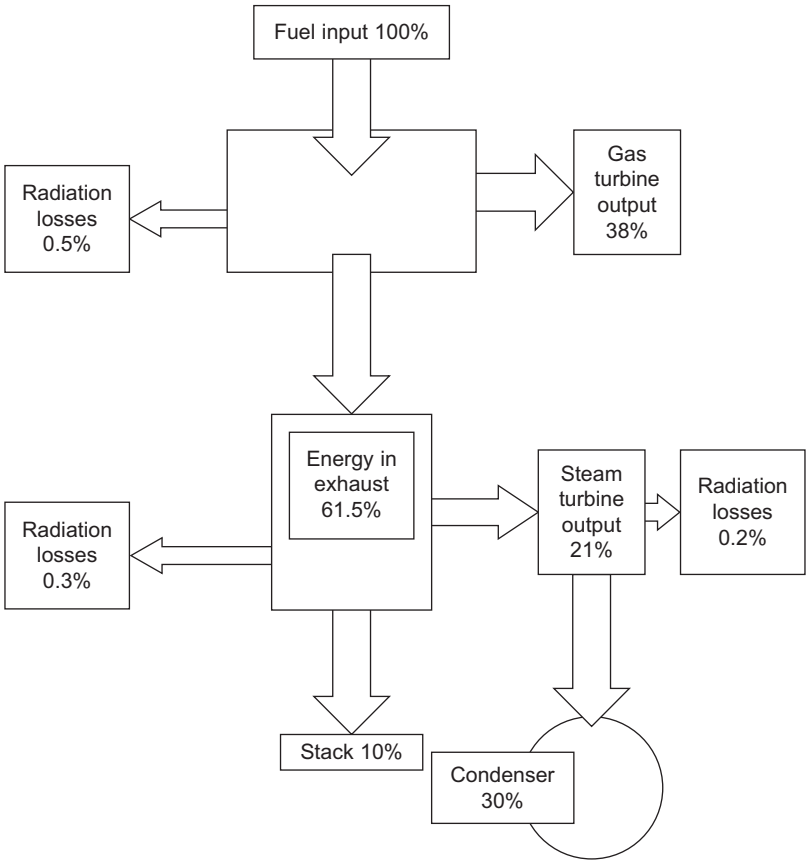


Figure 2-30 Energy distribution in a combined-cycle power plant.

of the entering energy into its useful component and the energy losses that are associated with the condenser and the stack losses. This distribution will vary somewhat with different cycles as the stack losses are decreased with more efficient multilevel pressure HRSGs.

The distribution in the energy produced by the power generation sections as a function of the total energy produced is shown in Figure 2-31. This diagram shows the load characteristics of each of the major prime-movers changes drastically with off-design operation. The gas turbine at design conditions supplies 60% of the total energy delivered and the steam turbine delivers 40% of the energy, whereas at off-design conditions (below 50% of the design energy), the gas turbine delivers 40% of the energy while the steam turbine also delivers 40% of the energy.

To fully understand the various cycles, it is important to define a few major parameters of the combined cycle. In most combined-cycle applications, the gas turbine is the topping cycle and the steam turbine is the bottoming cycle. The major components that make up a combined cycle are the gas turbine, the HRSG, and the steam turbine

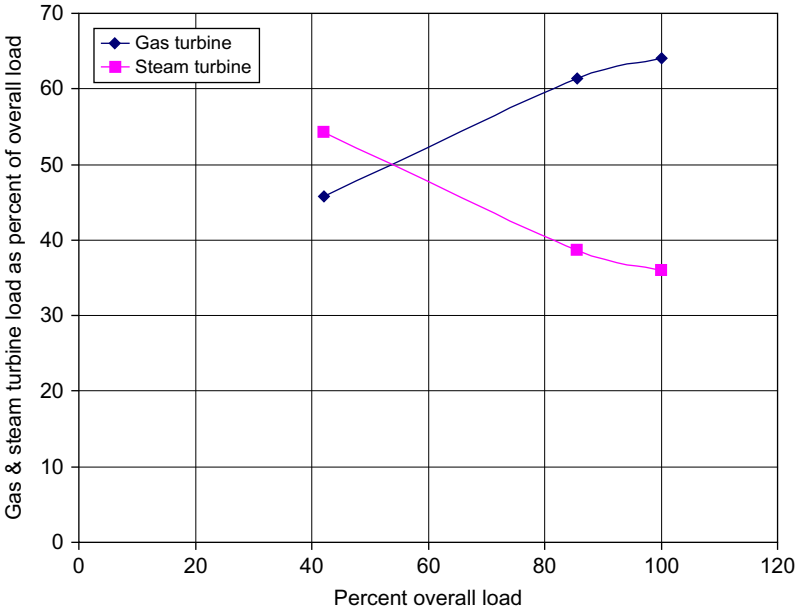


Figure 2-31 Load sharing between prime movers over the entire operating range of a combined-cycle power plant.

as shown in Figure 2-32, which shows a typical combined-cycle power plant with a single-pressure HRSG. Thermal efficiencies of the combined cycles can reach as high as 60%. In the typical combination, the gas turbine produces about 60% of the power and the steam turbine produces about 40%. The thermal efficiencies of the individual unit of the gas turbine and the steam turbine are between 30% and 40%. The steam turbine utilizes the energy in the exhaust gas of the gas turbine as its input energy. The energy transferred to the heat recovery steam generator (HRSG) by the gas turbine is usually equivalent to about the rated output of the gas turbine at design conditions. At off-design conditions, the inlet guide vanes (IGV) are used to regulate the air so as to maintain a high temperature to the HRSG.

The heat recovery steam generator (HRSG) is where the energy from the gas turbine is transferred to the water to produce steam. There are many different configurations of the HRSG units. Most HRSG units are divided into the same amount of sections as the steam turbine, as seen in Figure 2-33. In most cases, each section of the HRSG has a preheater or an economizer, an evaporator, and then one or two stages of super-heaters. The steam entering the steam turbine is super-heated.

The condensate entering the HRSG goes through a deaerator where the gases from the water or steam are removed. This is important because high oxygen content can cause corrosion of the piping and the components that would come in contact with the water/steam medium. An oxygen content of about 7–10 parts per billion (ppb) is recommended. The condensate is sprayed into the top of the deaerator, which is normally placed on the top of the feed-water tank. Deaeration takes place when the

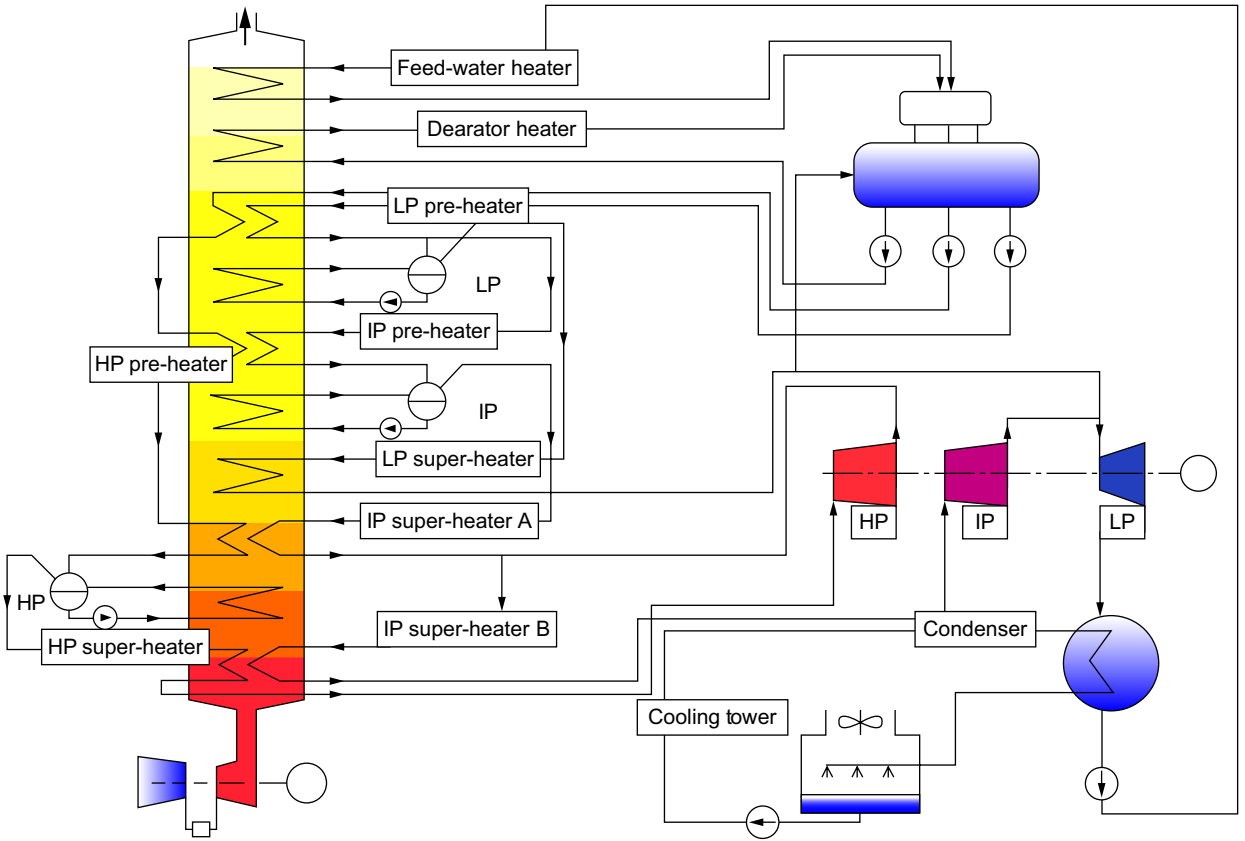


Figure 2-32 A typical large combined-cycle power plant HRSG.

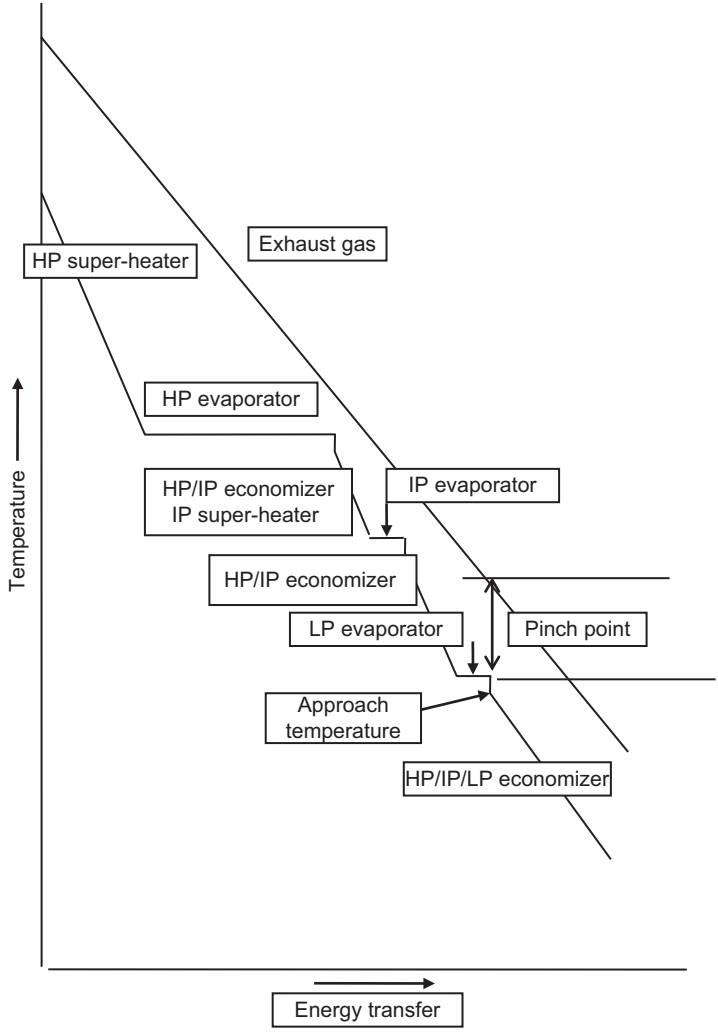


Figure 2-33 Energy/temperature diagram of the triple-pressure HRSG.

water is sprayed and then heated, thus releasing the gases that are absorbed in the water/steam medium. Deaeration must be done on a continuous basis because air is introduced into the system at the pump seals and piping flanges since they are under vacuum.

Deaeration can be either vacuum or over pressure deaeration. Most systems use vacuum deaeration because all the feed-water heating can be done in the feed-water tank and there is no need for additional heat exchangers. The heating steam in the vacuum deaeration process is a lower quality steam thus leaving the steam in the steam

cycle for expansion work through the steam turbine; this increases the output of the steam turbine and, therefore, the efficiency of the combined cycle. In the case of the overpressure deaeration, the gases can be exhausted directly to atmosphere independently of the condenser evacuation system.

Deaeration also takes place in the condenser. The process is similar to that in the deaerator, the turbine exhaust steam condenses and collects in the condenser hot well while the incondensable hot gases are extracted by means of evacuation equipment. A steam cushion separates the air and water such that re-absorption of the air cannot take place. Condenser deaeration can be as effective as the one in a deaerator. This could lead to not utilizing a separate deaerator/feed-water tank and the condensate being fed directly into the HRSG from the condenser. The amount of make-up water added to the system is a factor since make-up water is fully saturated with oxygen. If the amount of make-up water is less than 25% of the steam turbine exhaust flow, condenser deaeration may be employed but in cases where there is steam extraction for process use and, therefore, the make-up water is large, a separate deaerator is needed.

The economizer in the system is used to heat the water close to its saturation point. If they are not carefully designed, economizers can generate steam thus blocking the flow. To prevent this from occurring, the feed-water at the outlet is slightly sub-cooled. The difference between the saturation temperature and the water temperature at the economizer exit is known as the approach temperature. The approach temperature is kept as small as possible between 10 and 20 °F (5.5–11 °C). To prevent steaming in the evaporator, it is also useful to install a feed-water control valve downstream of the economizer, which keeps the pressure high and steaming is prevented. Proper routing of the tubes to the drum also prevents blockage if it occurs in the economizer.

Another important parameter is the temperature difference between the evaporator outlet temperature on the steam side and on the exhaust gas side. This difference is known as the pinch point. Ideally, the lower the pinch point, the more the heat recovered, but this calls for more surface area and, consequently, increases the back pressure and cost. In addition, excessively low pinch points can mean inadequate steam production if the exhaust gas is low in energy (low mass flow or low exhaust gas temperature). General guidelines call for a pinch point of 15–40 °F (8–22 °C). The final choice is obviously based on economic considerations.

The steam turbines in most of the large power plants are at a minimum divided into two major sections; the high-pressure (HP) and the low-pressure (LP) sections. In some plants, the high-pressure section is further divided into a high-pressure section and an intermediate-pressure (IP) section. The heat recovery steam generator (HRSG) is also divided into various sections corresponding to the steam turbine. The performance of LP steam turbine is further dictated by the condenser backpressure, which is a function of the cooling and the fouling.

The efficiency of the steam section in many of these plants varies from 30% to 40%. To ensure that the steam turbine is operating in an efficient mode, the gas turbine's exhaust temperature is maintained over a wide range of operating conditions. This enables the HRSG to maintain a high degree of effectiveness over this wide range of operation.

In a combined-cycle plant, high steam pressures do not necessarily convert into a high adiabatic thermal efficiency for a combined-cycle power plant. Expanding the steam at higher steam pressure causes an increase in the moisture content at the exit of the steam turbine. The increase in moisture content creates major erosion and corrosion problems in the later stages of the turbine. A limit is set at about 10% (90% steam quality) moisture content.

The advantages for a high steam pressure are that the mass flow of the steam is reduced and that the turbine output is also reduced. The lower steam flow reduces the size of the exhaust steam section of the turbine thus reducing the size of the exhaust stage blades. The smaller steam flow also reduces the size of the condenser and the amount of water required for cooling. It also reduces the size of the steam piping and the valve dimensions. These all account for lower costs especially for power plants that use the expensive and high energy-consuming air-cooled condensers.

Increasing the steam temperature at a given steam pressure lowers the steam output of the steam turbine slightly. This occurs because of two contradictory effects; first, the increase in enthalpy drop, which increases the output and second, the decrease in flow, which causes a loss in steam turbine output. The second effect is more predominant, which accounts for the lower steam turbine amount. Lowering the temperature of the steam also increases the moisture content.

Understanding the design characteristics of the dual or triple pressure HRSG and its corresponding steam turbine sections (HP, IP, and LP turbines) is important. Increasing the pressure of any section will increase the work output of the section for the same mass flow. However, at higher pressure, the mass flow of the steam generated is reduced. This effect is most significant for the LP turbine. The pressure in the LP evaporator should not be below about 45 psia (3.1 Bar), because the enthalpy drop in the LP steam turbine becomes very small, and the volume flow of the steam becomes very large; thus the size of the LP section becomes large, with long expensive blading. Increase in the steam temperature brings substantial improvement to the output. In the dual or triple pressure cycle, more energy is made available to the LP section if the amount of steam to the HP section is raised.

There is a very small increase in the overall cycle adiabatic thermal efficiency between a dual pressure cycle and a triple pressure cycle. To maximize their adiabatic thermal efficiency, these cycles are operated at high temperatures and extracting most heat from the system thus creating relatively low stack temperatures. This means that in most cases they must be only operated with natural gas as the fuel, as this fuel contains a very low to no sulfur content. Users have found that in the presence of even low levels of sulfur, such as when firing diesel fuel (No. 2 fuel oil) stack temperatures must be kept above 300 °F (149 °C) to avoid acid gas corrosion. The increase in adiabatic thermal efficiency between the dual and triple pressure cycles is due to the steam being generated at the IP level than at the LP level. The HP flow is slightly less than in the dual pressure cycle because the IP super-heater is at a higher level than the LP super-heater, thus removing energy from the HP section of the HRSG. In a triple-pressure cycle, the HP and IP sections must be increased together. Moisture at the steam turbine LP section exhaust plays a governing role. At the inlet pressure of about 1,500 psia (103.4 Bar), the optimum pressure of the IP



Figure 2-34 One of the world's largest combined cycle and heat power plants, producing 1875 MW of power and 800 tons of steam to a nearby chemical plant.

section is about 250 psia (17.2 Bar). The maximum steam turbine output is clearly definable with the LP steam turbine. The effect of the LP also affects the HRSG surface area, as the surface area increases with the decrease in LP steam pressure, because less heat exchange increases at the low temperature end of the HRSG. Figure 2-33 is the energy/temperature diagram of the triple pressure HRSG. The IP and LP flows are much smaller than the HP steam turbine flow. The ratio is in the neighborhood of 25:1.

The combined-cycle plants are becoming very important in the United States due to the resurgence of natural gas as the source of fuel for major power plants and their high adiabatic thermal efficiency of about 56%. Fracking shale gas is going to increase the quantity of gas making the combined-cycle plants more attractive, as gas prices fall. Figure 2-33 is a photograph of the world's largest combined-cycle gas turbine (CCGT) and combined heat and power plant. The plant produces 1875 MW power and up to 800 tons of process steam per hour for an adjacent chemical complex.

Power is provided from two combined-cycle power complexes of four heavy industrial gas turbines with maximum steam injection, driving generators rated at 154 MW at International Standard Organization's (ISO) conditions; which feed into four heat recovery steam generators (HRSGs) with supplementary firing. The steam from each set of four HRSGs feed into a steam turbines (ST)-driven generators that produce approximately 300 MW of electrical power each. A 60-MW gas turbine provides the plant with a black start capability.

Compressed Air Energy Storage Cycle

The compressed air energy storage (CAES) cycle is used as a peaking system that uses off-peak power to compress air into a large solution-mined underground cavern and withdraws the air to generate power during periods of high system power demand. Figure 2-35 is a schematic diagram of such a typical plant being operated

by Alabama Electric Cooperative Inc., with the plant heat and mass balance diagram, with generation-mode parameters at rated load and compression-mode parameters at average cavern conditions.

The compressor train is driven by the motor/generator, which has a pair of clutches that enable it to act as a motor when the compressed air is being generated for storage in the cavern and declutches it from the expander train and connects it to the compressor train. The compressor train consists of a three-section compressor; each section has an inter-cooler to cool the compressed air before it enters the other section thus reducing the overall compressor power requirements.

The power train consists of HP and LP expanders arranged in series, which drive the motor/generator, which in this mode is declutched from the compressor train and is connected by clutch to the HP and LP expander trains. The HP expander receives air from the cavern that is regeneratively heated in a recuperator utilizing exhaust gas from the LP expander, and then further combusted in combustors before entering the HP expander. The expanded air from the HP expander exhaust is reheated in combustors before entering the LP expander. Can-type combustors of similar design are employed in both the HP and LP expanders. The HP expander, which produces about 25% of the power, utilizes two combustors while the LP expander, which produces about 75% of the power, has eight combustors. The plant is designed to operate with either natural gas or No. two distillate oil fuels and operates over a range of 10–110 MW.

The generator is operated as a motor during the compression mode. The system is designed to operate on a weekly cycle, which includes power generation five days/one week, with cavern recharging during weekday nights and weekends.

Power Augmentation

The augmentation of power in a gas turbine is achieved by many different techniques. In this section, we are looking at techniques that could be achieved on existing gas turbines. Thus, techniques such as additional combustors are not considered as being practical on an existing turbine. In other words, the concentration in this section is on practical solutions. Practical power augmentation can be divided into two main categories. They range from the cooling of the inlet to injection of steam or water into the turbine.

Inlet Cooling

- Evaporative methods – either conventional evaporative coolers or direct water fogging.
- Refrigerated inlet cooling systems – utilizing absorption or mechanical refrigeration.
- Combination of evaporative and refrigerated inlet systems – the use of evaporative cooler to assist the chiller system to attain lower temperatures of the inlet air.
- Thermal energy storage systems – these are intermittent use systems where the cold air is produced off-peak and then used to chill the inlet air during the hot hours of the day.

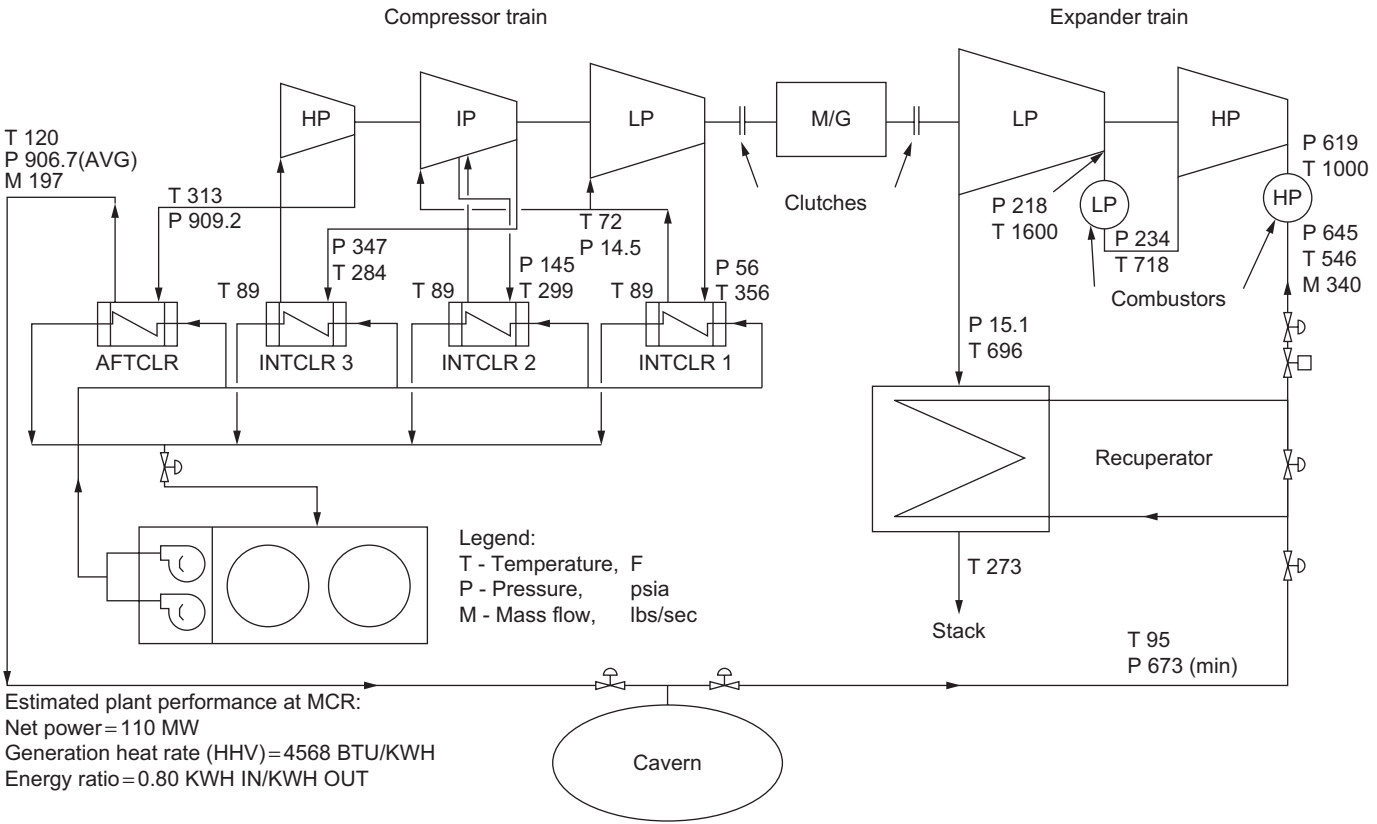


Figure 2-35 Schematic of a compressed air energy storage plant. ASME Technical Paper 2000-GT-0595.

Injection of Compressed Air, Steam, or Water

- Injection of humidified and heated compressed air – compressed air from a separate compressor is heated and humidified to about 60% relative humidity by the use of an HRSG and then injected into the compressor discharge.
- Steam injection – injection of the steam, obtained from the use of a low-pressure single-stage heat recovery steam generator (HRSG), at the compressor discharge and/or injection in the combustor.
- Water injection – mid-compressor flashing is used to cool the compressed air and add mass flow to the system.

Inlet Cooling Techniques

Evaporative Cooling of the Turbine

Traditional evaporative coolers that use media for evaporation of the water have been widely used in the gas turbine industry over the years, especially in hot climates with low humidity areas. The low capital cost, installation cost, and operating cost make it attractive for many turbine-operating scenarios. Evaporation coolers consist of water being sprayed over the media blocks, which are made of fibrous corrugated material. The airflow through these media blocks, evaporates the water, and as water evaporates, it consumes about 1,059 BTU (1,117 kJ) (latent heat of vaporization) at 60 °F (15 °C). This results in the reduction of the air temperature entering the compressor from that of the ambient air temperature. This technique is very effective in low-humidity regions.

The work required to drive the turbine compressor is reduced by lowering the compressor inlet temperature; thus increasing the output work of the turbine. Figure 2-36 is a schematic representation of the evaporative gas turbine and its effect on the Brayton cycle. The volumetric flow of most turbines is constant and, therefore, by increasing the mass flow, power increases in an inverse proportion to the temperature of the inlet air. The psychometric chart shows that the cooling is limited especially in highly humid conditions. It is a very low cost option and can be installed very easily. This technique does not, however, increase the adiabatic thermal efficiency of the turbine. The turbine inlet temperature is lowered by about 18 °F (10 °C), if the outside temperature is around 90 °F (32 °C). The cost of an evaporative cooling system is about $50/kW.

Direct inlet fogging is a type of evaporative cooling method, where demineralized water is converted into a fog by means of high-pressure nozzles operating at 1,000–3,000 psi (67–200 Bar). This fog then provides cooling when it evaporates in the air inlet duct of the gas turbine. The air can attain 100% relative humidity at the compressor inlet and, thereby, gives the lowest temperature possible without refrigeration (the web bulb temperature). Direct high-pressure inlet fogging can also be used to create a compressor inter-cooling effect by allowing excess fog into the compressor, thus boosting the power output further.

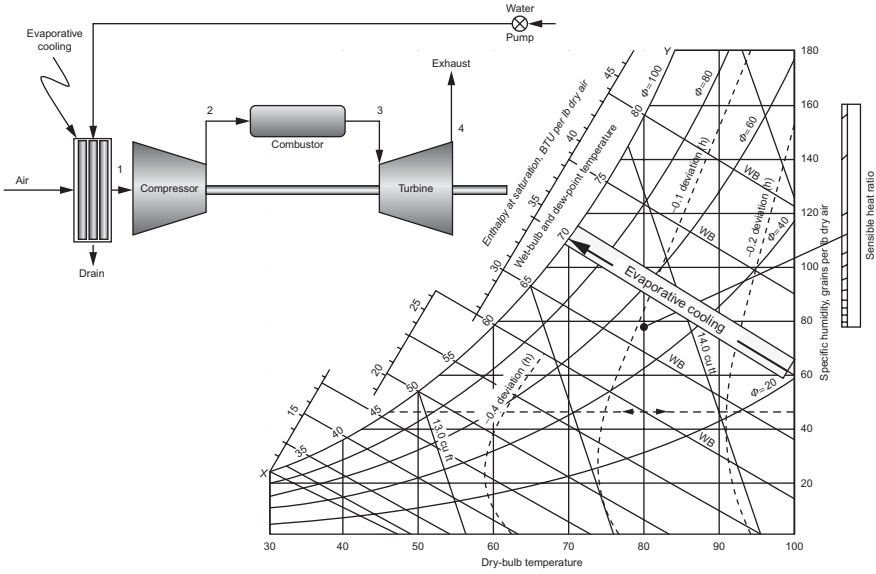


Figure 2-36 Schematic of evaporative cooling in a gas turbine.

Refrigerated Inlets for the Gas Turbines

The refrigerated inlets are more effective than the previous evaporative cooling systems, as they can lower the temperatures by about 45–55 °F (25–30 °C). Two techniques for refrigerating the inlet of a gas turbine are vapor compression (mechanical refrigeration) and absorption refrigeration.

Mechanical Refrigeration

In a mechanical refrigeration system, the refrigerant vapor is compressed by means of a centrifugal, screw, or reciprocating compressor. Figure 2-37 is a schematic diagram of a mechanical refrigeration intake for a gas turbine. The psychometric chart included shows that refrigeration provides considerable cooling and is very well suited for hot humid climates.

Centrifugal compressors are typically used for large systems in excess of 1,000 tons (12.4×10^6 BTU/13.082×10^6 kJ) and would be driven by an electric motor. Mechanical refrigeration has significantly high auxiliary power consumption for the compressor driver and pumps required for the cooling water circuit. After compression, the vapor passes through a condenser where it gets condensed. The condensed vapor is then expanded in an expansion valve and provides a cooling effect. The evaporator chills cooling water that is circulated to the gas turbine inlet chilling coils in the air stream.

Chlorofluorocarbon (CFC)-based chillers are now available and can provide a large tonnage for a relatively smaller plot space and can provide cooler temperature than

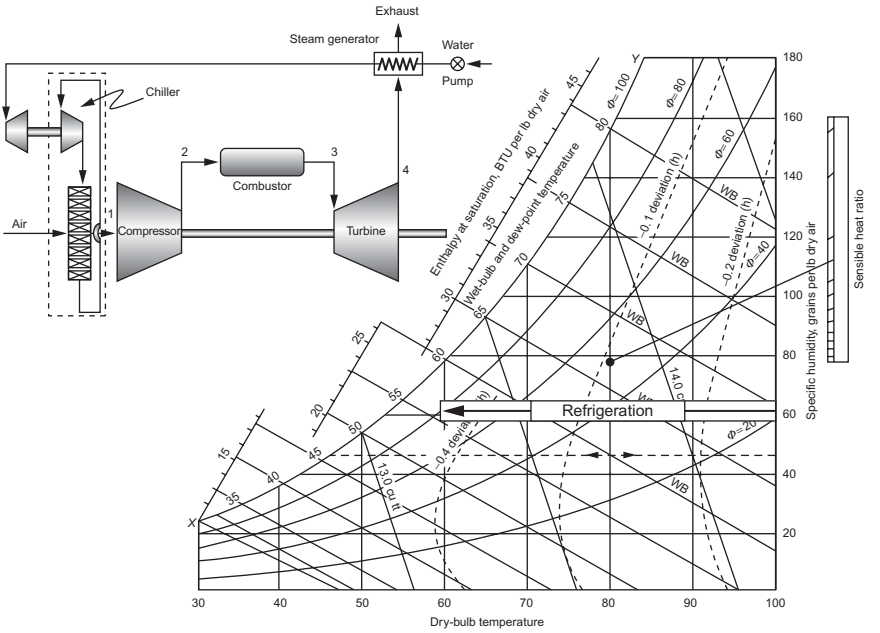


Figure 2-37 Mechanical refrigerated inlet system used to cool the inlet air of the gas turbine.

the lithium–bromide (Li–Br) absorption-based cooling systems. The drawbacks of mechanical chillers are high capital and high operation and maintenance (O&M) costs, high power consumption, and poor part load performance.

Direct expansion is also possible wherein the refrigerant is used to chill the incoming air directly without the chilled water circuit. Ammonia, which is an excellent refrigerant, is used in this sort of application. Special alarm systems would have to be utilized to detect the loss of the refrigerant into the combustion air and to shut down and evacuate the refrigeration system.

Absorption Cooling Systems

Absorption systems typically employ lithium–bromide (Li–Br) and water, with the Li–Br being the absorber and the water acting as the refrigerant. Such systems can cool the inlet air to 50 °F (10 °C). Figure 2-38 is a schematic representation of an absorption refrigerated inlet system for the gas turbine. The cooling shown on the psychometric chart is identical to the one for the mechanical system. The heat for the absorption chiller can be provided by gas, steam, or gas turbine exhaust. Absorption systems can be designed to be either single or double effect. A single effect system will have a coefficient of performance (COP) of 0.7–0.9 and a double effect unit will have a COP of 1.15. Part load performance of absorption systems is relatively good and adiabatic thermal efficiency does not drop off at part load like it does with mechanical

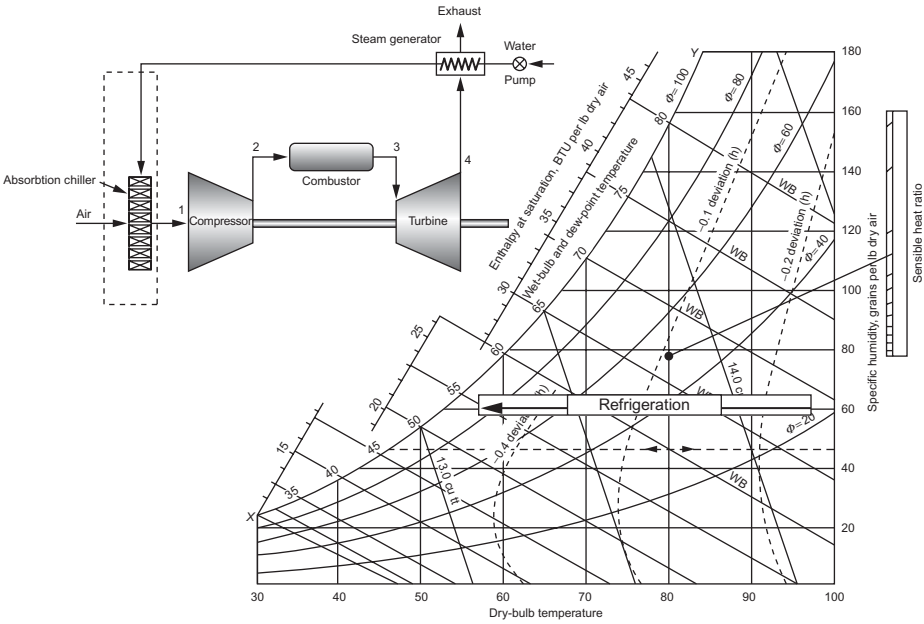


Figure 2-38 Absorption refrigerated inlet cooling system.

refrigeration systems. The costs of these systems are much higher than the evaporative cooling system; however, refrigerated inlet cooling systems in hot humid climates are more effective due to the very high humidity.

Combination of Evaporative and Refrigerated Inlet Systems

Depending on the specifics of the project, location, climatic conditions, engine type, and economic factors, a hybrid system utilizing a combination of the above technologies may be the best. The possibility of using fogging systems ahead of the mechanical inlet refrigeration system should be considered as shown in Figure 2-39. This may not always be intuitive, since evaporative cooling is an adiabatic process that occurs at constant enthalpy. When water is evaporated into an air stream, any reduction in sensible heat is accompanied by an increase in the latent heat of the air stream (the heat in the air stream being used to effect a phase change in the water from liquid to the vapor phase). If fog is applied in front of a chilling coil, the temperature will be decreased when the fog evaporates, but since the chiller coil will have to work harder to remove the evaporated water from the air steam, the result would yield no thermodynamic advantage.

To maximize the effect, the chiller must be designed in such a manner that, in combination with evaporative cooling, the maximum reduction in temperature is achieved. This can be done by designing a slightly undersized chiller that is not capable of

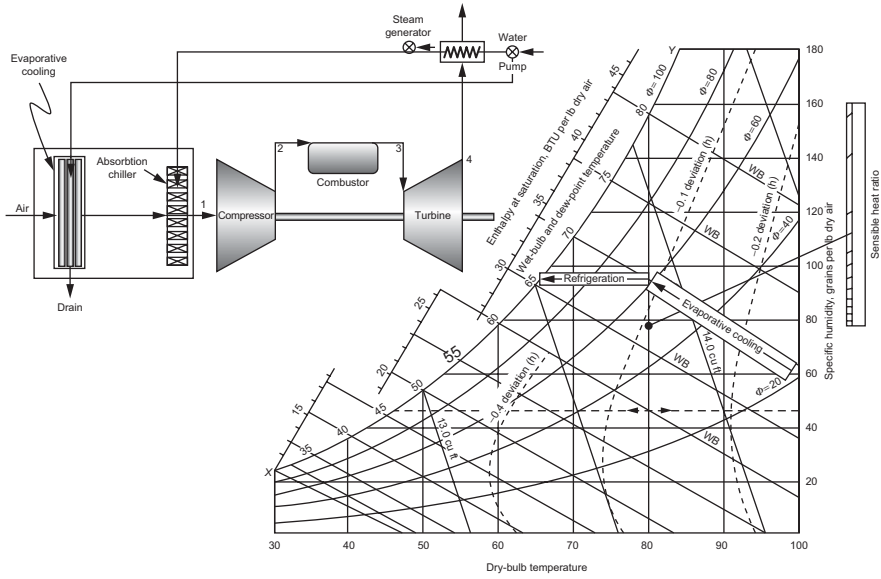


Figure 2-39 Evaporative and refrigerated inlet systems.

bringing the air temperature down to the ambient dew point temperature, but in conjunction with evaporative cooling, the same effect can be achieved, thus taking the advantage of evaporative cooling to reduce the load of refrigeration.

Thermal Energy Storage Systems

These systems are usually designed to operate the refrigeration system at off-peak hours and then use the refrigerated media at peak hours. The refrigerated media in most cases is ice and the gas turbine air is then passed through the media, which lowers its inlet temperature as seen in Figure 2-40. The size of the refrigeration system is greatly reduced, as it can operate for 8–10 hours at off-peak conditions to make the ice, which is then stored, and air passed through it at peak operating hours that may only be for about four–six hours.

The cost for such a system is about $90–110/kW. Moreover, they have been successfully employed for gas turbines producing 100–200 MW.

Injection of Compressed Air, Steam, or Water for Increasing Power

Mid-Compressor Flashing of Water

In this system, the water is injected into the mid-stages of the compressor to cool the air and approach an isothermal compression process as shown in Figure 2-41. The water

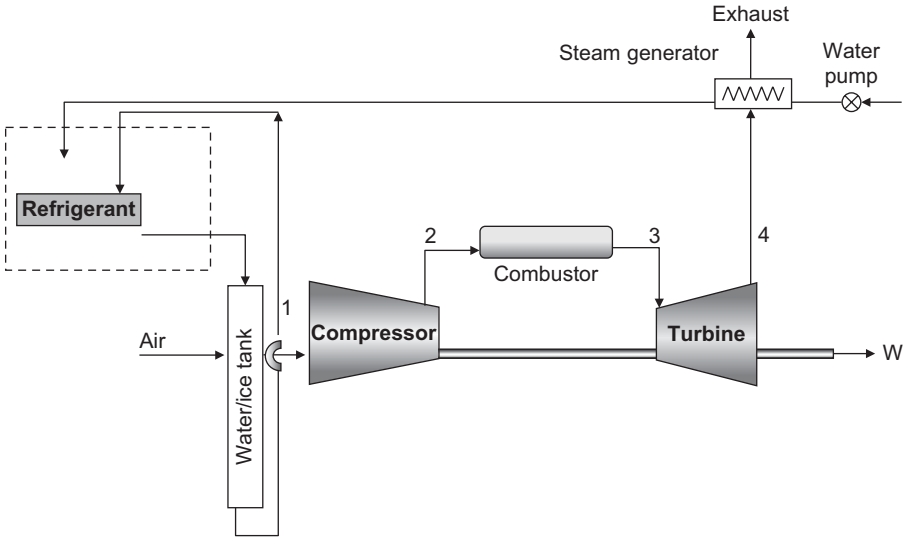


Figure 2-40 Thermal storage inlet system.

injected is usually mechanically atomized, so that very fine droplets are entered into the air. The water is evaporated, as it comes in contact with the high-pressure and -temperature air stream. As water evaporates, it consumes about 1,058 BTU (1,117 kJ, latent heat of vaporization) at the higher pressure and temperature resulting in lowering the temperature of the air stream entering the next stage. This lowers the work required to drive the compressor.

The inter-cooling of the compressed air has been very successfully applied to high-pressure engines. This system can be combined with any of the previously described systems.

Injection of Humidified and Heated Compressed Air

Compressed air from a separate compressor is heated and humidified to about 60% relative humidity by the use of an HRSG and then injected into the compressor discharge. Figure 2-42 is a simplified schematic diagram of a compressed air injection plant, which consists of the following major components:

1. A commercial combustion turbine with the provision to inject, at any point upstream of the combustor, the externally supplied humidified and pre-heated supplementary compressed air. Engineering and mechanical aspects of the air injection for the compressed air injection plant concepts are similar to the steam injection for the power augmentation, which has accumulated significant operating experience.
2. A supplementary compressor (consisting of commercial off-the-shelf compressor or standard compressor modules) to provide the supplementary airflow up-stream of combustors.
3. A saturation column for the supplementary air humidification and pre-heating.

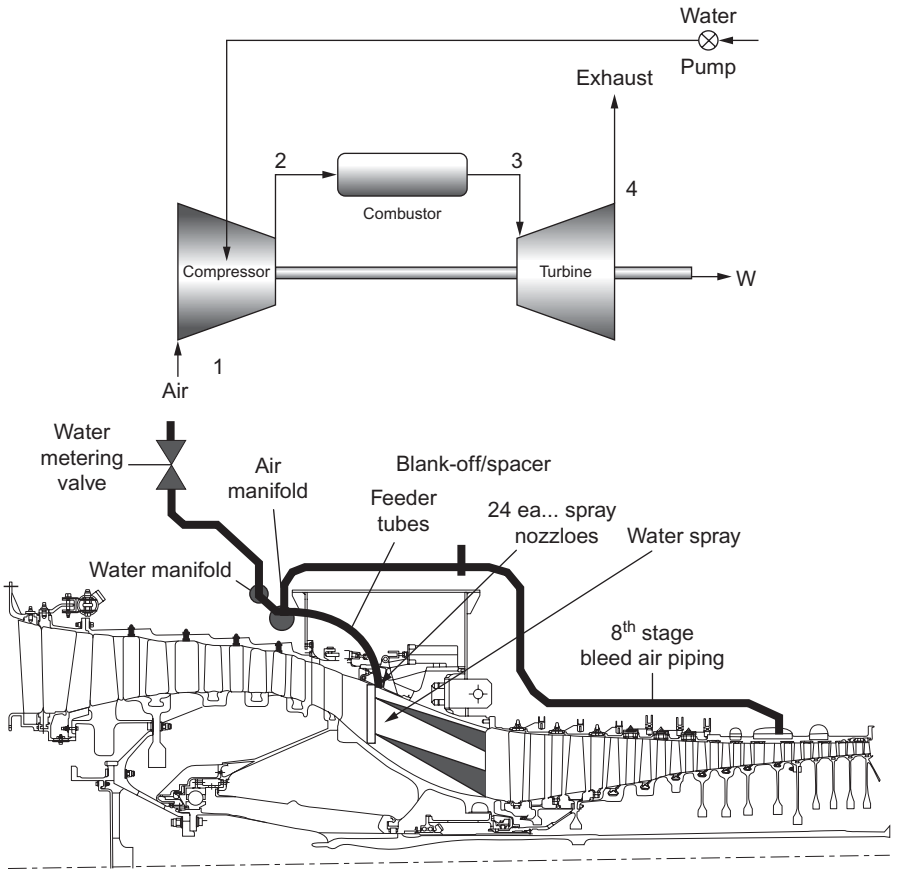


Figure 2-41 Mid compressor cooling showing a schematic as well as an actual application in a GE LM 6000 engine. Courtesy GE Power Systems.

4. Heat recovery water heater and the saturated air preheater.
5. Balance-of-plant equipment and systems including interconnecting piping, valves, controls, and so on.

Injection of Water or Steam at the Gas Turbine Compressor Exit

Steam injection or water injection has been often used to augment the power generated from the turbine as shown in Figure 2-43. Steam can be generated from the exhaust gases of the gas turbine. The HRSG for such a unit is very elementary, as the pressures are low. This technique augments power and also increases the turbine adiabatic thermal efficiency. The amount of steam is limited to about 12% of the airflow, which can result in a power increase of about 25%. The limits of the generator may restrict the amount of power, which can be added. The cost for such systems runs around $100/kW.

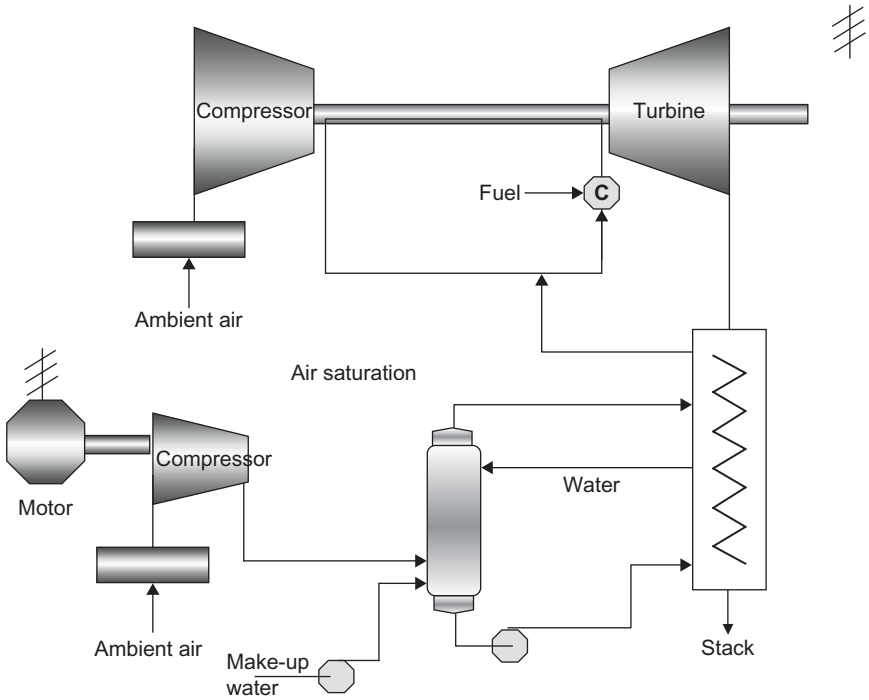


Figure 2-42 Heated and humidified compressed air injection system for power augmentation of a gas turbine.

Injection of Steam in the Combustor of the Gas Turbines Utilizing Present Dual Fuel Nozzles

Steam injection in the combustor has been commonly used for NO_x control as shown in Figure 2-44. The amount of steam, which can be added, is limited due to combustion concerns. This is limited to about 2–3% of the airflow. This would provide an additional 3–5% of the rated power. The dual fuel nozzles on many of the industrial turbines could easily be retrofitted to achieve the goal of steam injection. The steam would be produced using an HRSG. Multiple turbines could also be tied into one HRSG.

Combination of Evaporative Cooling and Steam Injection

The combination of the above techniques must also be investigated, as none of these techniques is exclusive of the other techniques and can be easily used in conjunction with each other. Figure 2-45 is a schematic representation of combining the inlet evaporative cooling with injection of steam in both the compressor exit and the combustor. In this system, the power is augmented benefiting from the cooling of the air and then augmented further by the addition of the steam.

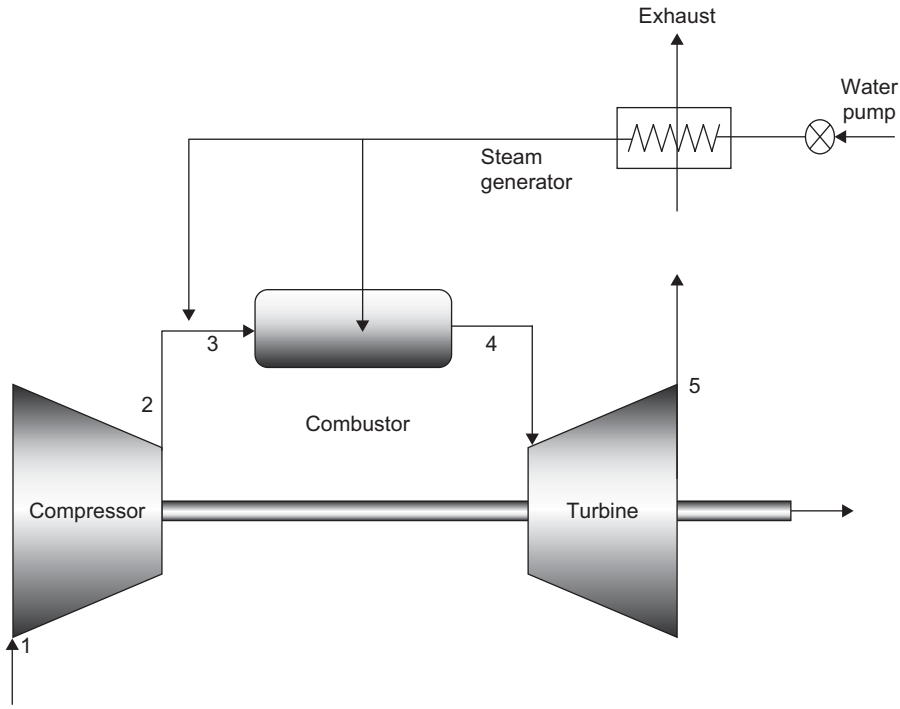


Figure 2-43 Steam injection at exit of compressor and in the combustor of the gas turbine.

Summation of the Power Augmentation Systems

The analysis of the different cycles examined here, which range from the simplest cycle such as evaporative cooling, to the more complex cycles such as the humidified and heated compressed air cycle, is rated to their effectiveness and to their cost is shown in Table 2-1. The cycles examined here have been used in actual operation of major power plants, thus there are no cycles evaluated which are only conceptual in nature. The results show addition from 3% to 21% in power and the increase in adiabatic thermal efficiency from 0.4% to 24%.

The cooling of the inlet air using an evaporative cycle, the simplest of the cycles, and which can be put into operation with the least outlay in capital are not very useful in operation in high humidity areas. The system would cost between $300,000 and $500,000 per turbine thus amounting to a cost of $135/kW.

Refrigerated inlet cooling is much more effective in humid areas and can add about 12.8% to the power output of the simple-cycle gas turbine. The cost outlay of such a system is among the costliest per kilowatt of the cycles evaluated. The concept here would be to have a single heat recovery steam generator (HRSG) supply enough steam to provide cooling for three turbines. The steam would be used to power a steam turbine, which would then operate a refrigeration compressor or use the steam to provide

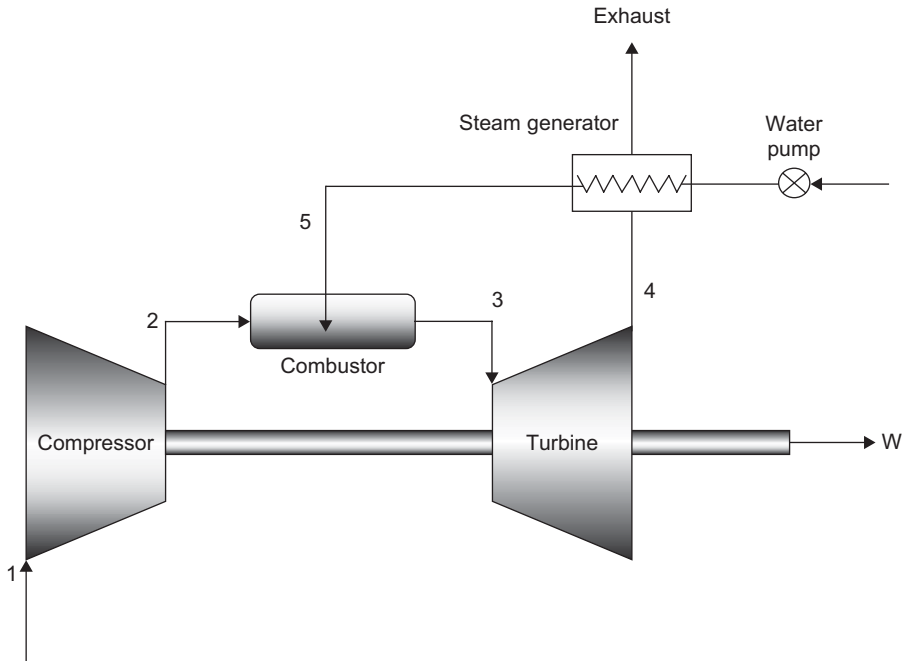


Figure 2-44 Steam injection in the gas turbine combustor.

absorption cooling for the three turbines. The concept was to reduce the turbine inlet temperature by about 30–50 °F (17–27 °C). The refrigeration unit could also be supplanted by the use of an ice storage system whose effect would be the same on the performance of the turbine except for the fact that it would operate for about eight hours in a day and the other 16 hours would be used to produce the ice used for cooling the air. In this manner, the refrigeration system could be much smaller than the system required for refrigeration of the inlet air 24 hours a day.

The cooling of the inter-stage compressor air by injecting water is also another very effective way for getting more power from the gas turbine. The problem in most units is that there is no convenient place to inject the water. The gas turbines would require substantial modification to install such a system. Care must be taken that any modification would not affect the integrity of the system. This type of a system is very effective in units where there is a low and HP compressor, providing a very convenient place to inject the water. This type of compressor is mostly available in aero-derivative units.

The concept of injecting humidified and heated compressed air just after the gas turbine compressor is another very interesting way to increase power and adiabatic thermal efficiency. In this system, compressed air is added to the compressed discharge air. The compressed air is about 5% of the main gas turbine air and this air after it has been compressed using an external compressor is then injected into an air saturation

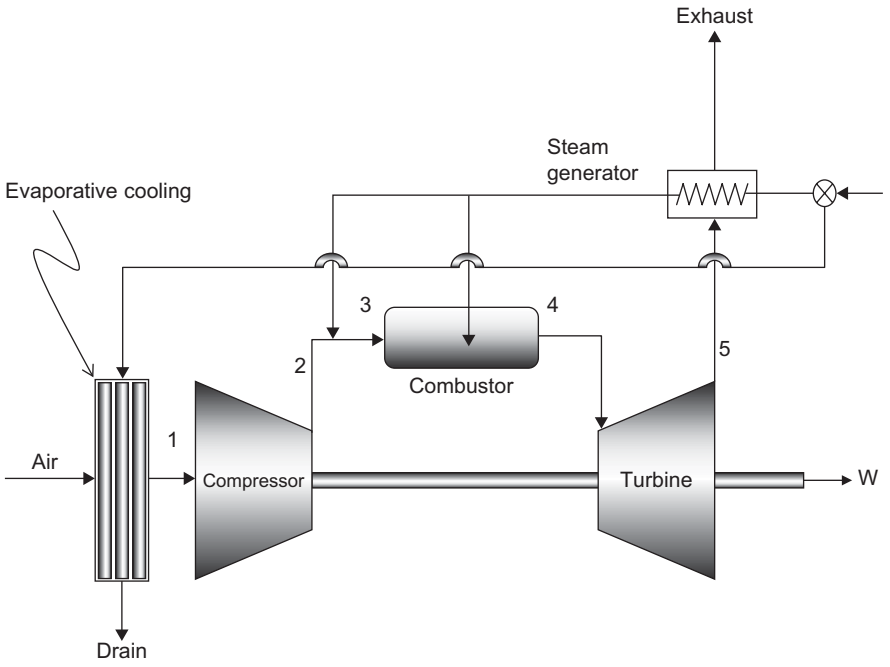


Figure 2-45 Evaporative cooling and steam injection in a gas turbine.

device where steam obtained from the HRSG unit is then injected into the device to saturate the air with water and the saturated air is then further heated in the HRSG before it is injected into the compressor discharge of the gas turbine.

The injection of steam in the compressor discharge has been utilized over the years and has been found to be very effective. The amount of steam to be injected can vary from 5% to 15%. The injection of steam created from properly treated water does not affect the life of the hot section of the turbines. This is based on a large number of units where steam injection has been used. Steam injection with an evaporative cooling inlet system would be best suited for hot humid areas; this application is based on the adiabatic thermal efficiency and the cost as shown in Figure 2-46.

The additional costs for incorporating the systems are also shown in Figure 2-46. The cost per kilowatt for the steam injection and the heated and humidified compressed air injection system is about the same. This is due to the fact that though the initial cost to install the compressed air system, for a turbine of about 100 MW, is about $3.7 million as compared with about $1.7 million for a steam injection system; the power generated by the heated and humidified compressed air injection system is much higher.

The rate of return on the steam injection system is higher than the compressed air injection system. This is due to the fact that though the adiabatic thermal efficiency of the steam injection system and the compressed air injection system is about the same,

Table 2-1 Evaluation of Various Techniques to Enhance the Operation of the Simple-Cycle Gas Turbine

Types of Process	Increase in Power (MW)	Percentage Increase in Power (%)	Percentage Increase in Adiabatic Thermal Efficiency %	Heat Rate (kJ/kW h)	Cost US$ Millions	Cost/kW (US$/kW)	Fuel Savings per Year US$	Increase in Sales Revenue per Year US($)	Total Earnings (US$)
Evaporative cooling	3.69	3.32	0.39	10,891	0.5	135.67	515,264	396,755	912,019
Refrigeration inlet cooling	12.77	11.51	2.5	10,672	2.5	195.74	605,075	1,379,901	1,984,977
Ice storage cooling	12.77	11.51	2.5	10,672	1.5	117.44	201,692	459,967	661,659
Interstage compressor cooling	17.41	15.69	14.19	9,576	2.5	143.56	3,743,308	2,291,365	6,034,672
Heated and humidified compressed air injection	23.44	21.12	21.23	9,020	3.7	157.84	5,597,388	3,368,355	8,965,744
Steam injection	10.11	9.11	22.13	8,954	1.7	168.19	5,220,193	1,466,792	6,686,985
Evaporative cooling and steam injection	13.97	12.59	24.02	8,817	2.1	150.34	5,770,444	2,068,616	7,839,060

Based on gas turbine operating at power = 110 MW, inlet temperature = 32 °C, efficiency = 32.92, and heat rate = 10,935 kJ/kW h.

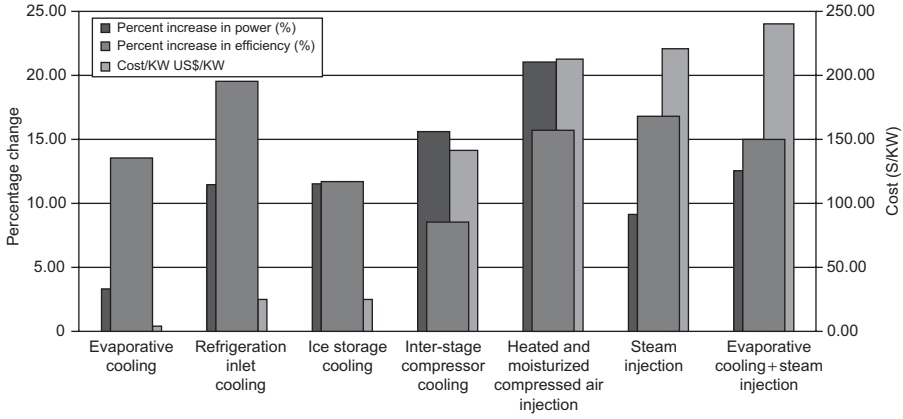


Figure 2-46 Comparison of various cycles based on percent change in power and efficiency and cost $/KW.

the initial cost of the steam injected system being over 50% lower than the compressed air injection system accounts for the difference.

The calculations for fuel gas savings have been based on an international price of fuel, at about US$2.64 per million kJ. The plant availability was taken at 97%, which is the availability throughout industry for most frame type plants. The cost of sale of new power was based on the average price of US$0.04/kW h.

Some of the major restrictions in putting these cycles on existing units can be described as follows:

1. *Generator Power Output Capacity*. The generator, as a general rule of thumb, is oversized by about 20% above the turbine-rated load. The changes have to be limited to that region by limiting the steam or compressed air injection.
2. *Turbine Firing Temperature*. The turbine firing temperature, the temperature of the gas measured at the inlet of the first-stage nozzles, is limited to the design firing temperatures, as the increase in firing temperatures would greatly reduce the life of the turbine hot section.
3. *Injection Pressure*. The injection pressure must be between 75 and 100 psia (5 and 7 Bar) above the compressor discharge pressure. In the case of the heated and humidified compressed air injected system, the air must be saturated.
4. *Nozzle Area of the First Turbine Stage (Expander Stage)*. This is a very critical parameter and limits the total airflow into the turbine section, thus this limits the amount of steam injection or the amount of the heated and humidified compressed air injection.
5. *Surge Control*. The injection systems will all require major modifications to the control system to prevent injection until the units have reached full load and stabilized operation. During shutdown, the system must first shutoff the injection system. These changes are very necessary to prevent the units from surging.
6. *NO_x Emissions*. The amount of NO_x emissions is very critical in most regions where gas turbines are being utilized for power generation. The present cap is about 22 ppm; the aim is to go down to as low as 9 ppm. The techniques offered here all are NO_x emission friendly, in that they do not increase the present levels of NO_x, in fact in the case of the injection systems,

both steam and heated and humidified compressed air will lower the NO_x emissions, making the plant even more environmentally friendly, especially in this critical location.

7. *Control Systems*. The costs in all these systems have taken into account modifications of the control systems. The control systems in most of these cases will have to be new to take into account the injection of steam and the heated and humidified compressed air, the HRSG, and all its associated equipments such as pumps.

Bibliography

Boyce, M.P., Meher-Homji, C.B., and Lakshminarasimha, A.N., "Gas Turbine and Combined Cycle Technologies for Power and Efficiency Enhancement in Power Plants," ASME 94-GT-435.

Boyce, M.P., "Turbo-Machinery for the Next Millennium," Russia Gas Turbo-Technology Publication, September–October 2000.

Boyce, M.P., "Advanced Cycles for Combined Cycle Power Plants," Russia Gas Turbo Technology Publication, November–December 2000.

Boyce, M.P., *Handbook for Cogeneration and Combined Cycle Power Plants*, 2nd edition, ASME Press, 2010.

Chodkiewicz, R., Porochnicki, J., and Potapczyk, A., "Electric Power and Nitric Acid Coproduction-A New Concept in Reducing The Energy Costs," Powergen Europe '98, Milan, Italy, 1998, Vol. 3, pp. 611–625.

Chodkiewicz, R., "A Recuperated Gas Turbine Incorporating External Heat Sources in the Combined Gas-Steam Cycle," ASME Paper No. 2000-GT-0593.

Cyrus, B., Meher-Homji, T.R., and Mee III, "Gas Turbine Power Augmentation by Fogging of Inlet Air," 28th Turbomachinery 28 Symposium Proceedings, 1999, p. 93.

Copyrighted Materials
Copyright © 2012 Elsevier Retrieved from www.knovel.com

3 Compressor and Turbine Performance Characteristics

This chapter examines the overall performance characteristics of compressors and turbines. This material is presented here to familiarize the reader with the behavior of these machines classified under the broad term "turbomachinery." Pumps and compressors are used to produce pressure and turbines produce power. These machines have some common characteristics. The main element is a rotor with blades or vanes, and the path of the fluid in the rotor may be axial, radial, or a combination of both.

There are three methods of studying the elements of turbomachinery operation. First, by examining forces and velocity diagrams, it is possible to discover some general relationships between capacity, pressure, speed, and power. Second, comprehensive experimentation can be undertaken to study relationships between different variables. Third, without considering the actual mechanics, one can use dimensional analysis to derive a set of factors whose grouping can shed light on overall behavior. The analysis presented in this chapter shows the typical performance diagrams one can expect from turbomachines. Off-design performance is also important in understanding trends and operating curves.

Aerothermodynamics of Turbomachinery

The motion of gas can be studied in two different ways: (1) the motion of each gas particle can be studied to determine its position, velocity, acceleration, and state variation with time and (2) each particle can be studied to determine its variation in velocity, acceleration, and the state of various particles at every location in space and time. In studying the movement of each fluid particle, we are studying *Lagrangian motion*; and in studying the spatial system, we are studying *Eulerian motion*. This book examines the *Eulerian motion* of the flow. The flow will be considered and fully described if the magnitude, direction, and thermodynamic properties of the gas at every point in space are determined.

To understand the flow in turbomachines, an understanding of the basic relationships of pressure, temperature, and type of flow must be acquired. Ideal flow in turbomachines exists when there is no transfer of heat between the gas and its surroundings, and the entropy of the gas remains unchanged. This type of flow is characterized as

Gas Turbine Engineering Handbook, Fourth Edition. DOI: 10.1016/B978-0-12-383842-1.00003-2
Copyright © 2012 Elsevier Inc. All rights reserved.

a reversible adiabatic flow. To describe this flow, the total and static conditions of pressure, temperature, and the concept of an ideal gas must be understood.

Ideal Gas

Gas properties are given in terms of its basic properties such as pressure and temperature. The general equation of state describing an ideal gas can be stated as:

$$\frac{P}{\rho^n} = \text{constant} \tag{3-1}$$

where

P = pressure
ρ = density
n = constant, which describes the type of process between two points and the value varies from 0 to $l\infty$.

Thus, to fully understand the properties, one needs to define the basic properties of pressure and temperature and the type of processes from one point to the other. Fluid systems (can be either gas or liquid), pressure, and temperature measurements are extremely complex. Fluid pressure can be defined as the measure of force per unit area exerted by a fluid, acting perpendicularly to any surface it contacts (a fluid can be either a gas or a liquid). In the English system, pressure is usually expressed in pounds per square inch (psi) or pounds per square foot, which is equivalent to one pound force ($1lb_f$) per square inch or square foot. The standard SI unit for pressure measurement is the Pascal (Pa) that is equivalent to one Newton per square meter (N/m^2) or the kilopascal (kPa), where 1 kPa = 1,000 Pa.

Pressure can be expressed in many different units including in terms of a height of a column of liquid. Table 3-1 lists commonly used units of pressure measurement and the conversion between the units in turbomachinery.

Pressure measurements can be divided into many categories: absolute pressure, gage pressure, dynamic pressure, and so on. Absolute pressure refers to the absolute value of the force per unit area exerted on a surface by a fluid. Therefore, the absolute pressure is the difference between the pressure at a given point in a fluid and the

Table 3-1 Commonly used Pressure Units in Turbomachinery

	psi	**kPa**	**in. H_2O**	**mm Hg**	**mBar**
1 psi	1.000	6.89473	27.6807	51.7148	68.9473
1 atm	14.6960	101.325	406.795	760.000	1,013.25
1 kPa	0.145038	1.000	4.01475	7.50062	10.000
1 in. H_2O	0.0361	0.249081	1.000	1.86826	2.49081
1 mm H_2O	0.0014223	0.009806	0.03937	0.07355	9.8×10^{-8}
1 mm Hg	0.0193368	0.133322	0.535257	1.000	1.33322
1 mBar	0.0145038	0.1000	0.401475	0.750062	1.000

absolute zero of pressure or a perfect vacuum. Gage pressure is the measurement of the difference between the absolute pressure and the local atmospheric pressure as shown in Figure 3-1. Local atmospheric pressure can vary depending on ambient temperature, altitude, and local weather conditions.

Figure 3-2 illustrates a dynamic system with a fluid flowing through a pipe or a duct. In this example, a static pressure tap is located in the duct wall. Static pressure is the pressure of the moving fluid. The static pressure of a gas is the same in all directions and is a scalar point function. It can be measured by drilling a hole in the pipe and keeping the probe flush with the pipe wall.

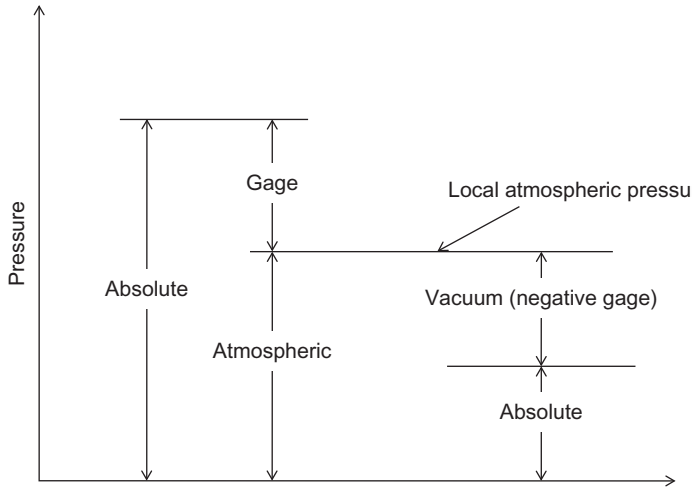


Figure 3-1 Relationships between absolute and local atmospheric pressures.

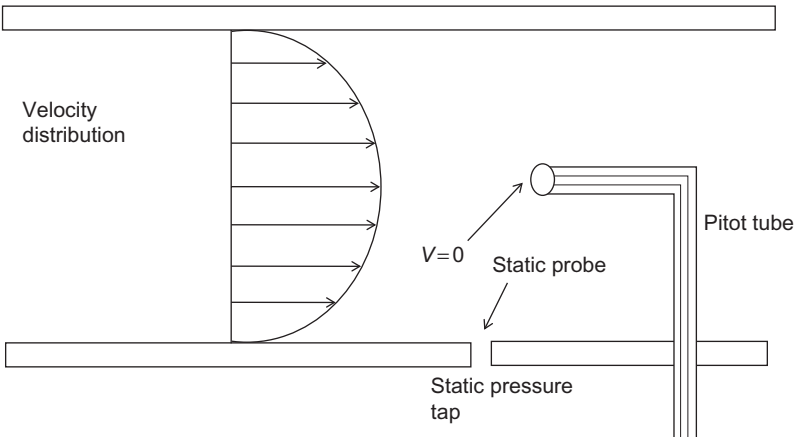


Figure 3-2 Static and total pressure measurements within a dynamic fluid system.

Total or stagnation pressure is the pressure of the gas brought to rest in a reversible adiabatic manner and is usually represented by P_o or P_t. The process that describes a reversible adiabatic process is known as an isentropic process. The difference between total and stagnation conditions is that a total process is reversible and adiabatic, whereas a stagnation process is not reversible or adiabatic; however, in the measurement area, the difference is small and thus most of the textbooks use stagnation and total conditions for pressure interchangeably. In this chapter, we will also do the same; thus, $P_o = P_t$, and $T_o = T_t$.

Total pressure can be measured by a Pitot tube placed in the flow steam. The gas is brought to rest at the probe tip in an adiabatic manner. In this chapter, the differences between total or stagnation conditions are not considered, and the terms total and stagnation conditions are used interchangeably. The relationship between total and static pressures is given as follows:

$$P_o = P_t = P_S + \frac{\rho V^2}{2g_c} \tag{3-2}$$

where $\rho V^2/2g_c$ is the dynamic pressure head that denotes the velocity of the moving gas.

Changes in total pressure in a system can only be affected by work or energy being introduced into a system (increase in pressure-compressor) or work or energy being extracted (decrease in pressure-turbine) from a system.

The tube inserted into the flow is called a Pitot tube, and it is inserted parallel to the flow with the tube opening directly into the flow. It is recommended that the static pressure tap be aligned in the same plane with the total pressure tap. The Pitot tube measures the total pressure at a point in the system, and the duct diameter should be at least 30 times higher than the Pitot tube's diameter. The total pressure measured at this point is referred often as the stagnation pressure (in most texts, stagnation and total pressure are used interchangeably). The stagnation pressure is the value obtained when a flowing fluid is decelerated to zero velocity in an isentropic (frictionless) adiabatic process. This process converts all the energy from the flowing fluid into a pressure that can be measured. The stagnation or total pressure is the static pressure plus the dynamic pressure. It is very difficult to accurately measure dynamic pressures. When dynamic pressure measurement is desired, the total and static pressures are measured and then subtracted to obtain the dynamic pressure. The dynamic pressure is a vector quantity, which depends on both magnitude and direction for the total flow measured, and can be used to determine the fluid velocities and flow rates in dynamic systems.

The total pressure measurement probe must be aligned directly with the flow, with the tube opening directly into the flow. Although the static pressure is independent of direction, the dynamic pressure is a vector quantity, which depends on both magnitude and direction for the total measured value. If the Pitot tube is misaligned with the flow, the accuracy of the total pressure will be affected. Figure 3-3 shows the various types of pressure probes. Figure 3-3 (a) shows a static pressure probe in which the static pressure taps are perpendicular to the flow. Figure 3-3 (b) is a total pressure probe, and for the probe to read accurately, the tube must be aligned parallel to the flow field

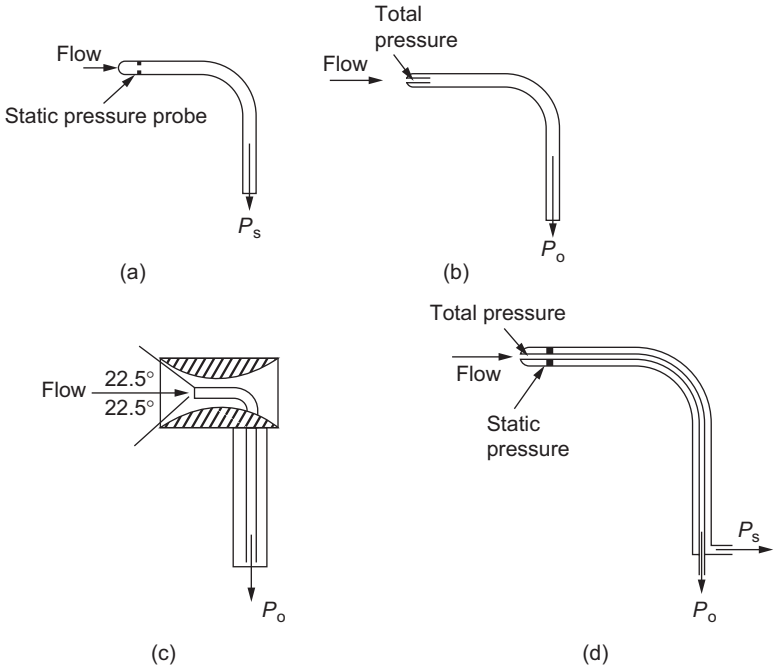


Figure 3-3 Various types of pressure probes (a) Static pressure probe (P_s). (b) Total pressure Pitot probe (P_o). (c) Kiel total pressure probe accurately measures the flow up to 22.5° from the flow stream. (d) Combination static pressure and total pressure Pitot tube (Pitot-static tube).

with the tube opening pointing directly into the flow. Figure 3-3 (c) is a Kiel probe that has a shield around the probe allowing the flow to be turbulent and upto angles of 22.5° from the horizontal for accurate total pressure readings. Figure 3-3 (d) is a Pitot-static tube where both the total and the static pressures are measured, and the difference in the measurements is the dynamic velocity.

The location of the pressure taps and probes, static and total, must also be selected carefully. Any location in the system in which the flow field may be disturbed should be avoided, both upstream and downstream. These locations include any obstruction or change, such as valves, elbows, flow splits, pumps, and fans. To increase the accuracy of pressure measurement in a dynamic system, allow at least 10 pipe/duct diameters downstream of any change or obstruction and at least two pipe/duct diameters upstream (see details given in Chapter 20).

Temperatures in a fluid flow are also very similar behavior to the pressure in which we have static and total temperatures. Like total pressure, changes in total temperature can only occur if work or energy is introduced into the system (increase in total temperature-compressor) or work or energy is removed from the system (decrease in total temperature-turbine).

Total temperature is the temperature rise in the gas if its velocity is brought to rest in a reversible adiabatic manner. Total temperature can be measured by the insertion

of a thermocouple, RTD, or thermometer in the fluid steam where the fluid is brought to rest at the probe tip. Total or stagnation temperature is the temperature of the gas brought to rest in a reversible adiabatic manner and is usually represented by T_o or T_t. The relationship between the total and static temperatures can be given as follows:

$$T_o = T_t = T_s + \frac{V^2}{2c_p g_c} \tag{3-3}$$

Static temperature is the temperature of the flowing gas. This temperature rises because of the random motion of the fluid molecules. The static temperature can only be measured by a measurement at rest relative to the moving gas. Therefore, the measurement of the static temperature is a difficult, if not impossible, task. However, it can be calculated from the measurements of total temperature and total and static pressure measurements.

$$T_s = \frac{T_t}{\left(\frac{P_t}{P_s}\right)^{\frac{\gamma-1}{\gamma}}} \tag{3-4}$$

where γ = ratio of specific heats = specific heat at constant pressure/specific heat at constant volume (c_p/c_v).

The three dominant temperature measurement devices used in automatic control are thermocouples, resistive thermal detectors (RTDs), and pyrometers; these devices are applicable over different temperature regimes.

The common temperature scales (Fahrenheit and Celsius) are based on the freezing and boiling points of water. The boiling point of water is 212 °F and 100 °C at low pressure. In the gas and energy equations, absolute temperatures are used; they are degrees Rankine (°R) and degrees Kelvin (°K) equations.

$$^\circ\text{R} = 459.67 + ^\circ\text{F}$$
$$^\circ\text{K} = 273.15 + ^\circ\text{C}$$

Dry- and Wet-bulb Temperatures

Steam in air at any relative humidity less than 100% must exist in a super-heated condition. The saturation temperature corresponding to the actual partial pressure of the steam in air is called the dew point. This term arose from the fact that when air at less than 100% relative humidity is cooled to the temperature at which it becomes saturated, the air has reached the minimum temperature to which it can be cooled without precipitation of the moisture (dew). Dew point can also be defined as that temperature at which the weight of steam associated with a certain weight of dry air is adequate to saturate the weight of air.

The dry-bulb temperature of air is the temperature that is indicated by an ordinary thermometer. When an air temperature is stated without any modifying term, it is always taken to be the dry-bulb temperature. In contrast to dry-bulb or air temperature,

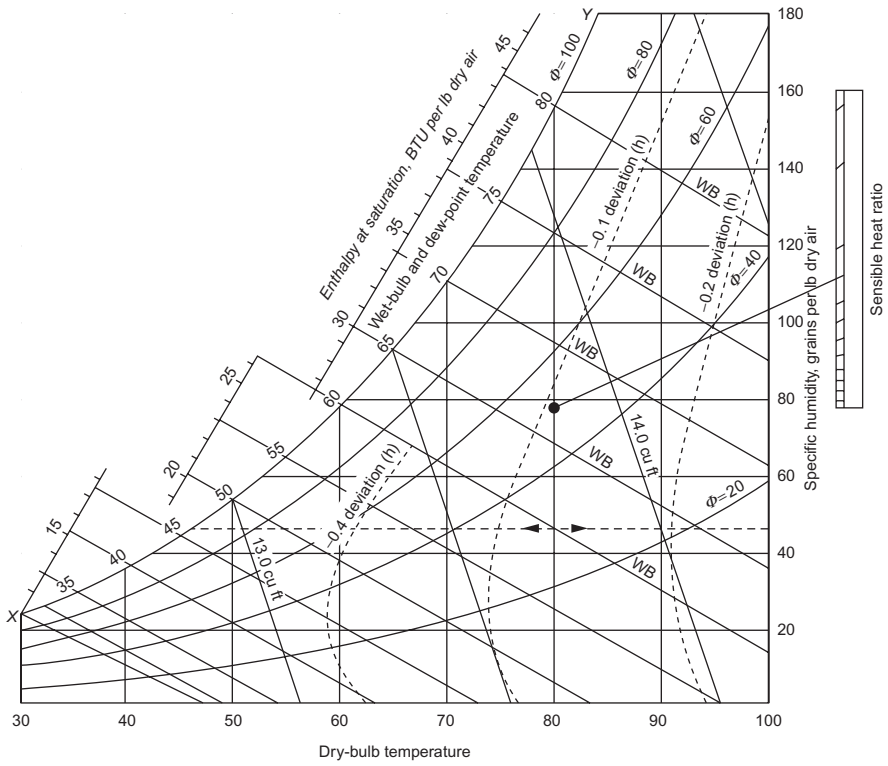


Figure 3-4 Psychrometric chart showing the relationship between dry and wet bulb temperatures and the specific humidity.

the term "wet-bulb temperature of the air," or simply wet-bulb temperature, is used. When a thermometer, with its bulb covered by a wick wetted with water, is moved through air unsaturated with water vapor, the water evaporates in proportion to the capacity of the air to absorb the evaporated moisture, and the temperature indicated by the thermometer drops below the dry-bulb or air temperature. The equilibrium temperature finally reached by the thermometer is known as the wet-bulb temperature. The purpose in measuring both the dry- and wet-bulb temperatures of the air is to find from the readings, by calculation or by use of a so-called psychrometric chart, the exact humidity characteristics of the air. Figure 3-4 is a psychrometric chart that can be used to find the relative and specific humidity of the air for a given dry- and wet-bulb temperatures.

Instruments for measuring wet- and dry-bulb temperatures are known as psychrometers. A sling psychrometer consists of two thermometers mounted side by side on a holder, with provision for whirling the whole device through the air. The dry-bulb thermometer is bare and the wet bulb is covered by a wick that is kept wetted with clean water. After being whirled a sufficient amount of time, the wet-bulb thermometer reaches its equilibrium point, and both the wet-bulb and dry-bulb thermometers are

then quickly read. Rapid relative movement of the air past the wet-bulb thermometer is necessary to get dependable readings.

Sensors reading directly the humidity are now available on the market. They are based on a thermoset capacitive polymer and use a three-layer capacitance construction. This consists of parallel plates with porous platinum electrodes, all mounted on a silicon substrate. The electrodes are coated with a dielectric polymer that absorbs, or desorbs, water vapor from the environment with changes in humidity. The resulting change in dielectric constant causes a variance in capacitance and impedance that relates to changes in relative humidity.

Temperature Measurement Devices

Temperature is measured in a number of different ways. Some of the most used techniques for temperature measurement which can be classified as follows:

1. *Thermal expansion of a gas (gas thermometer).* At constant volume, the pressure P of an ideal gas is directly proportional to its absolute temperature T. According to Boyle's gas law modified for a constant volume:

$$\frac{PV}{RT} = \frac{P_1 V_1}{RT_1} \tag{3-5}$$

Thus, $P = T(P_1/T_1)$
where

P_1 and T_1 = known quantities
R = gas constant (1545/mole weight of gas)

2. *Thermal expansion of a liquid or solid (mercury thermometer, bimetallic element).* Substances tend to expand with temperature. Thus, a change in temperature $T_2 - T_1$ causes a change in length $L_2 - L_1$, or a change in the volume $V_2 - V_1$, according to the following relationships:

$$L_2 - L_1 = \beta_1 (T_2 - T_1) L_1 \tag{3-6}$$

or

$$V_2 - V_1 = \beta_3 (T_2 - T_1) V_1 \tag{3-7}$$

where

β_1 = linear coefficients of thermal expansion ($1/^\circ$F, $1/^\circ$C)
β_3 = volumetric coefficients of thermal expansion

For a number of solids and fluids, β_1 and β_3 are reasonably constant over a limited temperature range. For solids, $\beta_3 = 3\beta_1$. The most common element used in a thermometer is mercury whose volumetric coefficient of thermal expansion at room temperature is approximately $0.00010\,^\circ\mathrm{F}^{-1}$ ($0.00018\,^\circ\mathrm{C}^{-1}$).

3. *Thermocouples.* Temperature measurements using thermocouples are based on the discovery by Seebeck in 1821 that when an electric current flowing in a continuous circuit of two dissimilar metals are brought into intimate contact, a voltage is developed, which depends on the temperature of the junction and the particular metals used. If two such junctions are connected in series with a voltage-measuring device, the measured voltage will be very

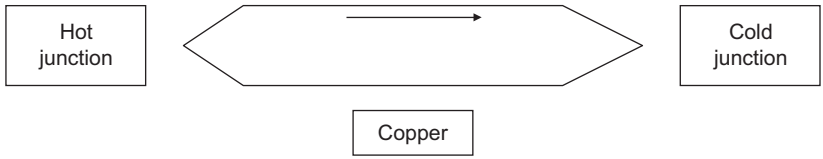


Figure 3-5 Schematic representation of a simple thermocouple.

nearly proportional to the temperature difference of the two junctions. The thermocouple may be represented diagrammatically as shown in Figure 3-5. Iron and copper are the two metals, and T_1 and T_2 are the temperatures of the junctions. Let T_1 be the reference junction (cold junction) and T_2 the measuring junction (hot junction). The thermoelectric current i flows from the iron across the cold junction. In this case, iron would be referred as thermoelectrically positive to copper. The thermal electromotive force (emf) is a measure of the difference in temperature between T_2 and T_1. The emf produced in this way are very small, only a small fraction of a volt in the most favorable combination. In control systems, the reference junction is usually located at the emf-measuring device. The reference junction may be held at constant temperature, such as in an ice bath or a thermostated oven, or it may be at ambient temperature but electrically compensated (cold junction–compensated circuit), so that it appears to be held at a constant temperature as shown in Figure 3-5.

4. *Resistance Temperature Detectors (RTDs)*. Resistance thermometers are constructed in a number of forms and offer greater accuracy and stability in some cases than thermocouples. While thermocouples use the Seebeck effect to generate a voltage, resistance thermometers use electrical resistance and require a power source to operate. The resistance ideally varies linearly with temperature.

Resistance temperature detectors (RTDs) are wire wound and thin film devices that measure temperature because of the physical principle of the positive temperature coefficient of electrical resistance of metals. The hotter they become, the larger or higher the value of their electrical resistance. RTDs using platinum are known variously as PRTs and PRT100s. Due to their nearly linear response over a wide range of temperatures and with a response time of a fraction of a second, they are the most popular RTD types available on the market. These RTDs are among the most precise temperature sensors available with resolution and measurement uncertainties of $\pm 0.1\,^{\circ}\mathrm{C}$ or better possible in special designs.

Commercial resistance temperature detectors (RTDs) using copper, nickel, and platinum conductors are in use and are characterized by a polynomial resistance–temperature relationship, such as:

$$T = A + BR_t + CR_0\frac{2}{T} + D\dot{R}_0\frac{3}{T} + ER_0\frac{4}{T} \tag{3-8}$$

where

R_t = resistance at prevailing temperature T in $^{\circ}\mathrm{C}$
$A,\ B,\ C,\ D,$ and E = range and material-dependent coefficients
R_0 = base resistance at $0\,^{\circ}\mathrm{C}$ used in the identification of the sensor.

RTDs Versus Thermocouples

The two most common ways of measuring industrial temperatures are with resistance temperature detectors (RTDs) and thermocouples. Choice between them is usually determined by four factors.

- *Temperature requirements*. *If process temperatures are between* −328 °F and 932 °F (−200 °C to 500 °C), an industrial RTD is the preferred option. Thermocouples have a range of 292–4208 °F (−180 °C to 2320 °C), so for temperatures above 932 °F (500 °C), they are the only contact temperature measurement device.
- *Time-response requirements*. If the process requires a very fast response to temperature changes – fractions of a second as opposed to seconds (e.g., 2.5–10 s) – then a thermocouple is the best choice. Time-response is measured by immersing the sensor in water moving at 3 ft/s (1 m/s) with a 63.2% step change.
- *Size requirements*. A standard RTD sheath is 0.1250–0.250 in. (3.175–6.35 mm) in diameter; sheath diameters for thermocouples can be less than 0.063 in. (1.6 mm).
- *Accuracy and stability requirements*.

If a tolerance of 3.6 °F (2 °C) is acceptable and the highest level of repeatability is not required, a thermocouple will serve. RTDs are capable of higher accuracy and can maintain stability for many years, whereas thermocouples can drift within the first few hours of use.

Optical and Radiation Pyrometers

The optical pyrometers are used for detecting high temperature measurements of various metals. These temperatures could range from 500 °F to 5000 °F (260–2760 °C). Optical pyrometers work on the basic principle of using the human eye to match the brightness of the hot object with the brightness of a calibrated lamp filament inside the instrument. The optical system contains filters that restrict the wavelength sensitivity of the devices to a narrow wavelength band around 0.65–0.66 μm (the red region of the visible spectrum). Other filters reduce the intensity so that one instrument can have a relatively wide temperature range capability. Modern radiation pyrometers provide the capability to measure within and below the range of the optical pyrometer with equal or better measurement precision plus faster time response, precise emissivity correction capability, better calibration stability, enhanced ruggedness, and relatively modest cost.

Pyrometers have been used in rotating machinery to determine the value of the blade metal temperatures, and when tied to a keyphasor (a device used to record the speed of the rotating element), individual blade temperatures can be recorded. This has been a very useful tool to ensure that a blade is not running hot due to lack of cooling or uneven flame temperatures.

The accuracy of the pyrometers depends on the following factors:

1. The emissivity of the surface targeted. Most of the temperature-estimation methods for pyrometers assume that the object is either a gray body or has known emissivity values. Proper selection of the pyrometer and accurate emissivity values can provide a high level of accuracy.
2. Ability of the pyrometer to focus on the target.

3. Absorption of the radiation between the target and the instrument. The medium through which the thermal radiation passes is not always transparent. It is recommended that a closed tube purged between the target and the instrument be used.

Viscosity

A perfect fluid can be defined as a fluid that is non-viscous and non-conducting. Fluid flow, compressible or incompressible, can be classified by the ratio of the inertial forces to the viscous forces. This ratio is represented by the Reynolds number (N_{Re}). At a low Reynolds number, the flow is considered to be laminar, and at high Reynolds numbers, the flow is considered to be turbulent. The limiting types of flow are the inertialess flow, sometimes called a Stokes flow, and the inviscid flow that occurs at an infinitely large Reynolds number. Reynolds numbers (dimensionless) for flow in a pipe is given as:

$$\mathrm{N_{Re}} = \frac{pVD}{\mu}$$

where

$\rho =$ the density of the fluid
$V =$ the velocity of the fluid
$D =$ the diameter or some characteristic measurement
$\mu =$ the viscosity of the fluid

while

$\nu = \mu/\rho,$ the kinematic viscosity.

In fluid motion where the frictional forces interact with inertia forces, it is important to consider the ratio of the viscosity (μ). Table 3-2 gives the kinematic viscosity for several fluids. A flow is considered to be adiabatic when there is no transfer of heat between the fluid and its surroundings. An isentropic flow is one in which the entropy of each fluid element remains constant. To fully understand the mechanics of flow, the following definitions explain the behavior of various types of fluids in both their static and flowing states. Table 3-2 gives the values of viscosity and kinematic viscosity at various temperatures.

Ideal Gas Laws

Ideal gas obeys the equation of state $PV = MRT$ or $P/\rho = MRT$, where P denotes the total pressure, V the volume, ρ the density, M the mass, T the total temperature of the gas, and R the gas constant per unit mass independent of pressure and temperature. All values of temperatures must be in absolute temperatures such as °R or °K. In most cases, the ideal gas laws are sufficient to describe the flow within 5% of actual conditions. When the perfect gas laws do not apply, the gas compressibility factor Z can be introduced:

$$Z(P,\ T) = \frac{PV}{RT} \tag{3-9}$$

Table 3-2 Density, Viscosity, and Kinematic Viscosity of Water and Air in Terms of Temperature

Temperature		Water			Air at a Pressure of 760 mm Hg (14.696 lbf/in.^{2})		
°C	°F	Density, ρ (lbf s^2/ft^4)	Viscosity, $\mu \times 10$ (lbf s/ft^2)	Kinematic Viscosity, $\nu \times 10^6$ (ft^2/s)	Density, ρ (lbf s^2/ft^4)	Viscosity, $\mu \times 10$ (lbf s/ft^2)	Kinematic Viscosity, $\nu \times 10^6$ (ft^2/s)
−20	−4	–	–	–	0.00270	0.326	122
−10	14	–	–	–	0.00261	0.338	130
0	32	1.939	37.5	19.4	0.00251	0.350	140
10	50	1.939	27.2	14.0	0.00242	0.362	150
20	68	1.935	21.1	10.9	0.00234	0.375	160
40	104	1.924	13.68	7.11	0.00217	0.399	183
60	140	1.907	9.89	5.19	0.00205	0.424	207
80	176	1.886	7.45	3.96	0.00192	0.449	234
100	212	1.861	5.92	3.19	0.00183	0.477	264

Figure 3-6 shows a schematic of the compressibility chart and Figure 3-7 is a detailed compressibility chart for a simple fluid

$$P_r = \frac{P}{P_c} \quad \text{and} \quad T_r = \frac{T}{T_c} \tag{3-10}$$

P_c and T_c are the pressure and temperature of the gas at the critical point.

Compressibility Effect

The effect of compressibility is important in high Mach number machines such as gas turbines. Mach number is the ratio of velocity to the acoustic speed of a gas at a given temperature $M \equiv V/a$. Acoustic speed (a) is defined as the ratio change in pressure of the gas with respect to its density if the entropy is held constant:

$$a^2 \equiv \left(\frac{\partial P}{\partial \rho}\right)_{s=c} \tag{3-11}$$

With incompressible fluids, the value of the acoustic speed tends toward infinity. For isentropic flow, the equation of state for a perfect gas can be written as follows:

$$\frac{P}{\rho^\gamma} = \text{constant}$$

Therefore

$$\ln P - \gamma \ln \rho = \text{constant} \tag{3-12}$$

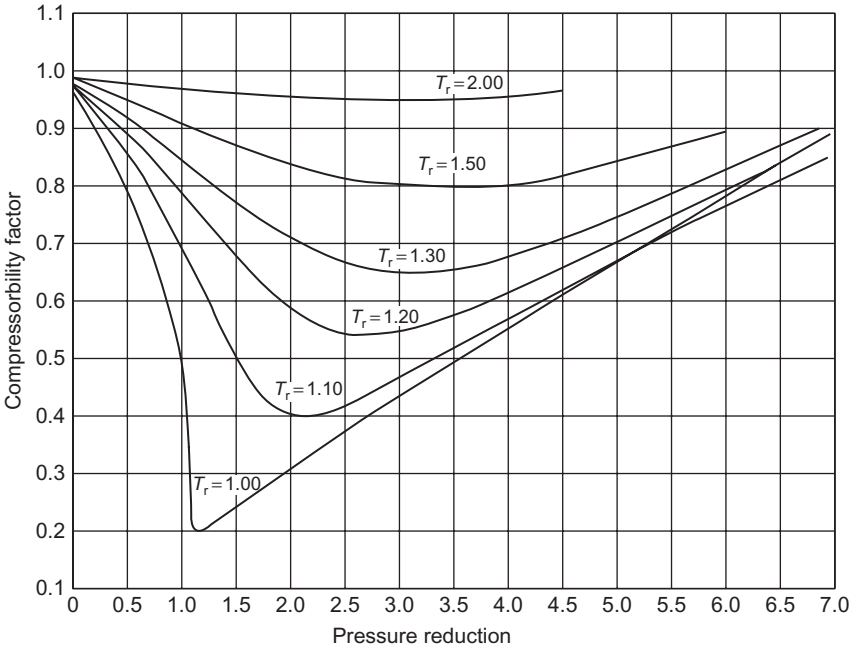


Figure 3-6 Generalized compressibility factor for a simple fluid.

Differentiating the above equation, the following relationship is obtained:

$$\frac{dP}{P} - \gamma \frac{d\rho}{\rho} = 0 \tag{3-13}$$

For an isentropic flow, the acoustic speed can be written as follows:

$$a^2 = \frac{dP}{d\rho}$$

Therefore,

$$a^2 = \frac{\gamma P}{\rho} \tag{3-14}$$

Substituting the general equation of state and the definition of the acoustic velocity, the following equation is obtained:

$$a^2 = \gamma g_c R T_s \tag{3-15}$$

where T_s (static temperature) is the temperature of the moving gas steam.

Since the static temperature cannot be measured, the value of static temperature must be computed using the measurements of static pressure, total pressure, and temperature. The value of static temperature is shown in Equation (3-16).

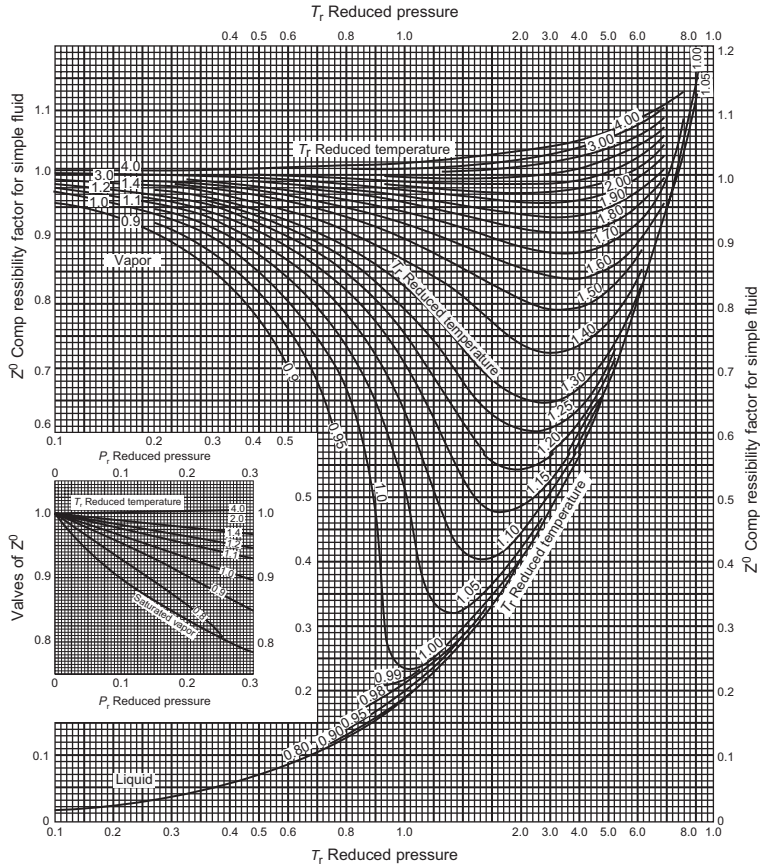


Figure 3-7 Generalized compressibility factor for a simple fluid. Source: Pitzer, K.S., et al., J.A.C.S. 77, 3427–3440 (1955). Adapted with permission from Journal of the American Chemical Society © 1955 American Chemical Society.

The relationship between static temperature and total temperature can also be given by the following relationship:

$$\frac{T_t}{T_s} = 1 + \frac{V^2}{2g_c c_p T_s} \tag{3-16}$$

where the specific heat c_p at constant volume can be written as follows:

$$c_p = \frac{\gamma R}{\gamma - 1} \tag{3-17}$$

where γ for an isentropic adiabatic process is the ratio of the specific heats of the gas:

$$\gamma = \frac{c_p}{c_v} \tag{3-18}$$

Combining Equations (3-12) and (3-13) gives the following relationship:

$$\frac{T_t}{T_s} = 1 + \frac{\gamma - 1}{2} M^2 \tag{3-19}$$

The relationship between the total and static conditions is isentropic; therefore:

$$\frac{T_t}{T_s} = \left(\frac{P_t}{P_s}\right)^{\frac{\gamma-1}{\gamma}} \tag{3-20}$$

and the relationship between total pressure and static pressure can be written as follows:

$$\frac{P_t}{P_s} = \left(1 + \frac{\gamma - 1}{2} M^2\right)^{\frac{\gamma}{\gamma-1}} \tag{3-21}$$

By measuring the total and static pressure and using Equation (3-16), the Mach number can be calculated. Using Equation (3-14), the static temperature can be computed, since the total temperature can be measured. Finally, using the definition of Mach number, the velocity of the gas steam can be calculated.

Aerothermal Equations

The gas stream can be defined by three basic aerothermal equations: (1) continuity, (2) momentum, and (3) energy.

Continuity Equation

The continuity equation is a mathematical formulation of the law of conservation of mass of a gas, which is a continuum. The law of conservation of mass states that the mass of a volume moving with the fluid remains unchanged:

$$\dot{m} = \rho A V$$

where

$\dot{m}$ = mass flow rate
ρ = fluid density
A = cross-sectional area
V = gas velocity

The previous equation can be written in the differential form:

$$\frac{\mathrm{d}A}{A} + \frac{\mathrm{d}V}{V} + \frac{\mathrm{d}\rho}{\rho} = 0 \tag{3-22}$$

Momentum Equation

The momentum equation is a mathematical formulation of the law of conservation of momentum. It states that the rate of change in linear momentum of a volume moving with a fluid is equal to the surface forces and the body forces acting on a fluid. Figure 3-8 shows the velocity components in a generalized turbomachine. The velocity vectors as shown are resolved into three mutually perpendicular components: the axial component (V_a), the tangential component (V_θ), and the radial component (V_m).

By examining each of these velocities, the following characteristics can be noted: the change in the magnitude of the axial velocity gives rise to an axial force, which is taken up by a thrust bearing; the change in radial velocity gives rise to a radial force, which is taken up by the journal bearing. The tangential component is the only component that causes a force, which corresponds to a change in angular momentum; the other two velocity components have no effect on this force, except for what bearing friction may arise.

By applying the conservation of momentum principle, the change in angular momentum obtained by the change in the tangential velocity is equal to the summation of all the forces applied on the rotor. This summation is the net torque of the rotor. A certain mass of fluid enters the turbomachine with an initial velocity V_{θ_1} at a radius r_1 and leaves with a tangential velocity V_{θ_2} at a radius r_2. Assuming that the mass flow rate through the turbomachine remains unchanged, the torque exerted by the changes

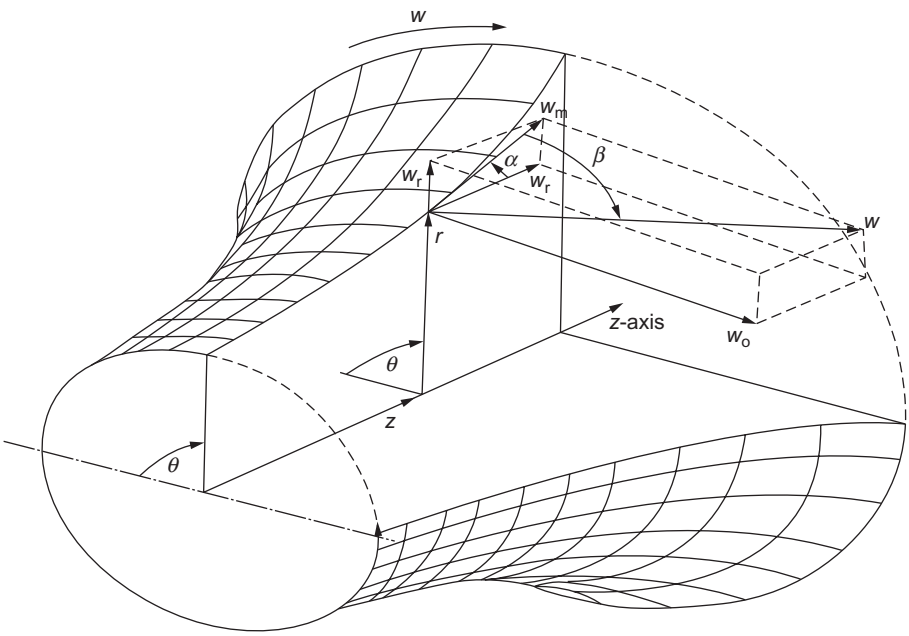


Figure 3-8 Velocity vectors in compressor rotor flow.

in angular velocity can be written as follows:

$$\tau = \frac{\dot{m}}{g_c}\left(r_1 V_{\theta_1} - r_2 V_{\theta_2}\right) \tag{3-23}$$

The rate of change of energy transfer (ft-lb$_f$/s) is the product of the torque and the angular velocity (ω):

$$\tau\omega = \frac{\dot{m}}{g_c}\left(r_1 \omega V_{\theta_1} - r_2 \omega V_{\theta_2}\right) \tag{3-24}$$

Thus, the total energy transfer can be written as follows:

$$E = \frac{\dot{m}}{g_c}\left(U_1 V_{\theta_1} - U_2 V_{\theta_2}\right) \tag{3-25}$$

where U_1 and U_2 are the linear velocity of the rotor at the respective radii. The previous relation per unit mass flow can be written in terms of the total enthalpy (H):

$$H = \frac{1}{g_c}\left(U_1 V_{\theta_1} - U_2 V_{\theta_2}\right) \tag{3-26}$$

where H is the energy transfer per unit mass flow (ft-lb$_f$/lb$_m$) or fluid pressure. Equation (3-26) is known as the Euler turbine equation.

The equation of motion as given in terms of angular momentum can be transformed into other forms that are more convenient to understand some of the basic design components. To understand the flow in a turbomachine, the concepts of absolute and relative velocities must be grasped. *Absolute velocity* (V) is the gas velocity with respect to a stationary coordinate system. *Relative velocity* (W) is the velocity relative to the rotor. In turbomachinery, the air entering the rotor will have a relative velocity component parallel to the rotor blade and an absolute velocity component parallel to the stationary blades. Mathematically, this relationship is written as follows:

$$\vec{V} = \vec{W} \rightarrow \vec{U} \tag{3-27}$$

where the absolute velocity (V) is the algebraic addition of the relative velocity (W) and the linear rotor velocity (U). The absolute velocity can be resolved into its components, the radial or meridional velocity (V_m) and the tangential component V_θ. From Figure 3-9, the following relationships are obtained:

$$\begin{aligned} V_1^2 &= V_{\theta_1}^2 + V_{m_1}^2 \\ V_2^2 &= V_{\theta_2}^2 + V_{m_2}^2 \\ W_1^2 &= \left(U_1 - V_{\theta_1}\right)^2 + V_{m_1}^2 \\ W_2^2 &= \left(U_2 - V_{\theta_2}\right)^2 + V_{m_2}^2 \end{aligned} \tag{3-28}$$

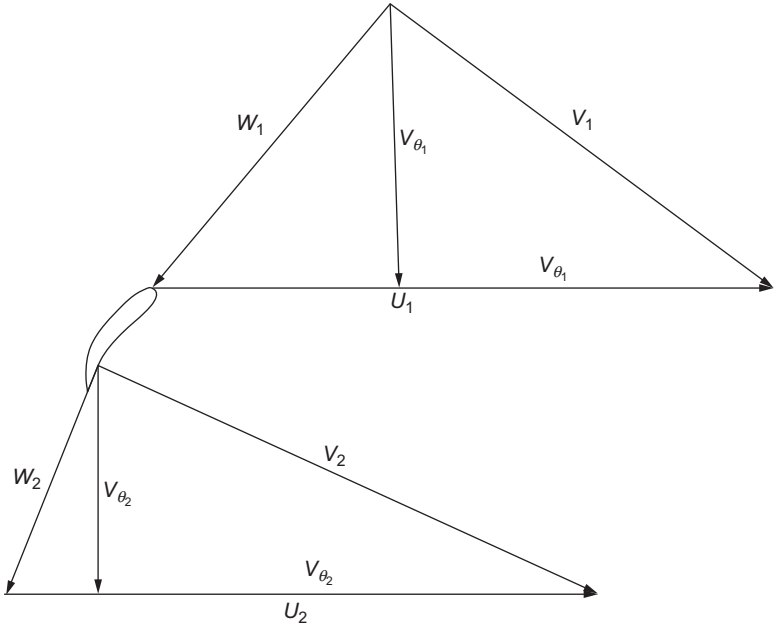


Figure 3-9 Velocity triangles for an axial-flow compressor.

By placing these relationships into Equation (3-26), the *Euler turbine equation*, the following relationship is obtained for the total enthalpy:

$$H_o = \frac{1}{2g_c}\left[\left(V_1^2 - V_2^2\right) + \left(U_1^2 - U_2^2\right) + \left(W_2^2 - W_1^2\right)\right] \tag{3-29}$$

Energy Equation

The energy equation is the mathematical formulation of the law of conservation of energy. It states that the rate at which energy enters the volume of a moving fluid is equal to the rate at which work is done on the surroundings by the fluid within the volume and the rate at which energy increases within the moving fluid. The energy in a moving fluid is composed of internal, flow, kinetic, and potential energies:

$$\varepsilon_1 + \frac{P_1}{\rho_1} + \frac{V_1^2}{2g_c} + Z_1 + {}_1Q_2 = \varepsilon_2 + \frac{P_2}{\rho_2} + \frac{V_2^2}{2g_c} + Z_2 + {}_1(\text{work})_2 \tag{3-30}$$

where

$\varepsilon =$ internal energy
$P/\rho =$ flow energy
$\varepsilon_1 + \frac{P_1}{\rho_1} =$ enthalpy (h_1)

$\frac{V_1^2}{2g_c}$ = kinetic energy

$h_1 + \frac{V_1^2}{2g_c} = H_t = H_0$ = total enthalpy

Z = potential energy

For isentropic flow, the energy equation can be written as follows, noting that the addition of internal and flow energies can be written as the enthalpy (h) of the fluid:

$$_1(\text{Work})_2 = (h_1 - h_2) + \left(\frac{V_1^2}{2g_c} - \frac{V_2^2}{2g_c}\right) + (Z_1 - Z_2) \tag{3-31}$$

Combining the energy and momentum equations provides the following relationships:

$$(h_1 - h_2) + \left(\frac{V_1^2}{2g_c} - \frac{V_2^2}{2g_c}\right) + (Z_1 - Z_2) = \frac{1}{g_c}\left[U_1 V_{\theta_2}\right]. \tag{3-32}$$

Assuming that there is no change in potential energies, the equation can be written as follows:

$$\left(h_1 + \frac{V_1^2}{2g_c}\right) - \left(h_2 + \frac{V_2^2}{2g_c}\right) = H_{1t} - H_{2t} = H_{01} - H_{02} = \frac{1}{g_c}\left[U_1 V_{\theta_1} - U_2 V_{\theta_2}\right] \tag{3-33}$$

Assuming that the gas is thermally and calorifically perfect, the equation can be written as follows:

$$T_{1t} - T_{2t} = \frac{1}{c_p g_c}\left[U_1 V_{\theta_2} - U_2 V_{\theta_2}\right] \tag{3-34}$$

For isentropic flow:

$$\frac{T_{2t}}{T_{1t}} = \left(\frac{P_{2t}}{P_{1t}}\right)^{\frac{\gamma-1}{\gamma}} \tag{3-35}$$

By combining Equations (3-30) and (3-31):

$$T_{1t}\left[1 - \left(\frac{P_{2t}}{P_{1t}}\right)^{\frac{\gamma-1}{\gamma}}\right] = \frac{1}{c_p g_c}\left[U_1 V_{\theta_1} - U_2 V_{\theta_2}\right] \tag{3-36}$$

Efficiencies

There are many types of efficiencies used in turbomachinery. Figure 3-10 is a chart showing the various efficiencies that must be considered in the design of a gas turbine

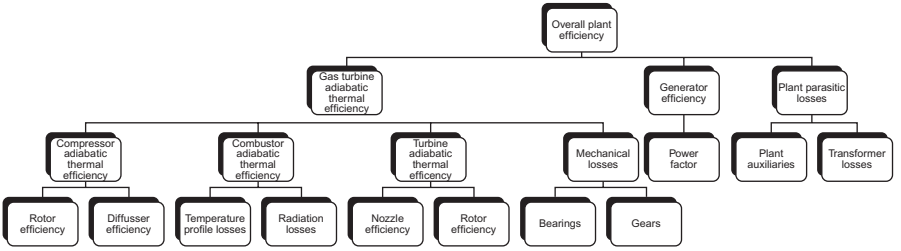


Figure 3-10 Efficiencies needed for a Gas Turbine Power Plant.

power plant. The overall plant efficiency consists of the gas turbine, the generator, and the various parasitic losses such as plant auxiliaries and transformer losses. It is an efficiency that is based on the ratio of the output power to the energy input into the entire plant system.

In gas turbines, we have the overall-cycle adiabatic thermal efficiency. This is the efficiency of the overall cycle and takes into account all component efficiencies, such as the compressor efficiency, the combustor efficiency, and the turbine efficiency in the composition of the cycle, that is, the exit total pressure and the total temperature of the compressor, the combustor, and the turbine are affected by the losses in these three components. Therefore, the losses affect the overall thermal efficiency to a certain degree, but it is the cycle between the two thermal sinks that governs the efficiency. It must be remembered that the most efficient cycle between any two thermal sinks is the Carnot cycle. The gas turbine follows the Brayton cycle and the steam turbine follows the Rankine cycle; each of these cycles have been defined in depth in Chapter 2. Thus, even if the compressor, combustor, and turbine losses were neglected (assuming that each component was operating at their 100% thermal efficiency), the overall thermal efficiency of the gas turbine depends mainly on the cycle thermal efficiency and would be less than the Carnot cycle. A common mistake in the field by engineers is the multiplication of the three component efficiencies to give the total overall efficiency, a value that has not even a remote connection to the actual thermal efficiency of the gas turbine.

The gas turbine adiabatic thermal efficiency is mainly dependent on the difference between the two thermal sinks: the inlet temperature and the firing temperature and the pressure ratio in the compressor. The cycle thermal efficiencies in gas turbines have increased from about 13% to 45% from 1960 to 2011, the firing temperatures increased from 1500 °F (816 °C) to 2600 °F (1427 °C), and the pressure ratio increased from 7:1 to 35:1 for commercial gas turbines.

Adiabatic Thermal Efficiency

The adiabatic thermal efficiency of the entire gas turbine (Brayton cycle) as depicted in Figure 3-11 is given by the total energy input to the net energy output of the cycle. All the values are based on total values of pressure, temperature, and enthalpy.

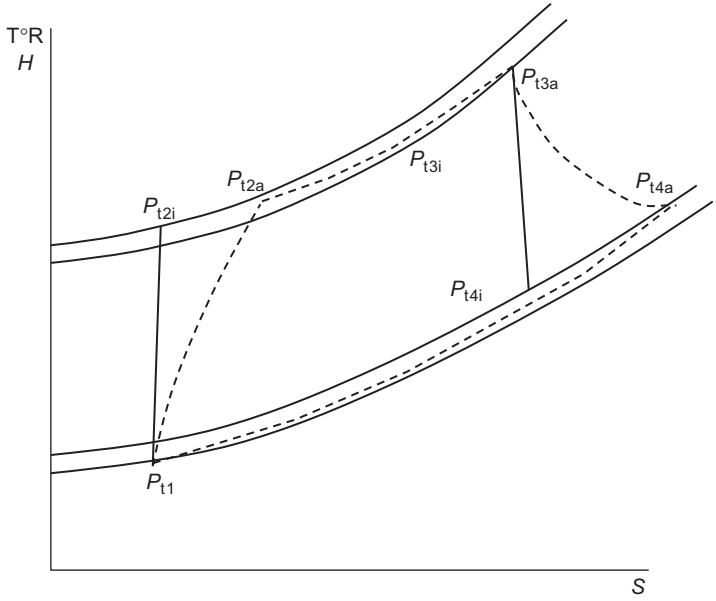


Figure 3-11 Gas turbine cycle (Brayton cycle).

The net energy output (W_{net}) is the turbine work ($H_{\text{t3a}} - H_{\text{t4a}}$) minus the compressor work ($H_{\text{t2a}} - H_{\text{t1a}}$) as shown in Equation (3-37):

$$W_{\text{net}} = \{(H_{\text{t3a}} - H_{\text{t4a}}) - (H_{\text{t2a}} - H_{\text{t1a}})\} \tag{3-37}$$

The net energy input (E_{input}) is the energy inputted into the turbine due to the combustion of the fuel in the combustor:

$$E_{\text{input}} = \left(\dot{m}_f \times \eta_{\text{comb}} \times \text{LHV}_{\text{fuel}}\right) = (H_{\text{t2a}} - H_{\text{t2a}}) \tag{3-38}$$

where

$\dot{m}_f$ = the mass flow of the fuel
LHV_{fuel} = the lower heating value of the fuel

Thus, the overall thermal efficiency of the gas turbine cycle ($\eta_{\text{cycle thermal}}$) is given by the ratio of the net energy output to the energy input to the turbine.

$$\eta_{\text{cycle thermal}} = \frac{\{(H_{\text{t3a}} - H_{\text{t4}a}) - (H_{\text{t2a}} - H_{t1\text{a}})\}}{(H_{\text{t3a}} - H_{\text{t2a}})} \tag{3-39}$$

The thermal efficiencies of the compressor and the turbine section are also represented by the total values of temperature, pressure, and enthalpy.

The work in a compressor or turbine under ideal conditions occurs at constant entropy as also shown in Figure 3-9. The actual work done is indicated by the dotted line. The isentropic efficiency of the compressor can be written in terms of the total changes in enthalpy:

$$\eta_{\mathrm{ad}_c} = \frac{\text{Isentropic work}}{\text{Acutual work}} = \frac{(H_{\mathrm{t2i}} - H_{1\mathrm{t}})\, id}{(H_{\mathrm{t2a}} - H_{1\mathrm{t}})\, \text{act}} \tag{3-40}$$

This equation can be rewritten for a thermally and calorifically perfect gas in terms of total pressure and temperature as follows:

$$\eta_{\mathrm{ad}_c} = \frac{\left[\left(\frac{P_{\mathrm{t2}}}{P_{\mathrm{t1}}}\right)^{\frac{\gamma-1}{\gamma}} - 1\right]}{\left[\frac{T_{\mathrm{t2a}}}{T_{\mathrm{t1}}-1}\right]} \tag{3-41}$$

The process between 1 and 2_a can be defined by the following equation of state:

$$\frac{P}{\rho^n} = \text{constant} \tag{3-42}$$

where n defines a process from point 1 to point 2a. The adiabatic efficiency can then be represented by:

$$\eta_{\mathrm{ad}_c} = \frac{\left[\left(\frac{P_{\mathrm{t2}}}{P_{\mathrm{t1}}}\right)^{\frac{\gamma-1}{\gamma}} - 1\right]}{\left[\left(\frac{P_{\mathrm{t2}}}{P_{t1}}\right)^{\frac{n-1}{n}} - 1\right]} \tag{3-43}$$

The isentropic efficiency of the turbine can be written in terms of the total enthalpy change:

$$\eta_{\mathrm{ad}_t} = \frac{\text{Actual work}}{\text{Isentropic work}} = \frac{H_{\mathrm{t3a}} - H_{\mathrm{t4a}}}{H_{\mathrm{t3a}} - H_{\mathrm{t4}}} \tag{3-44}$$

This equation can be rewritten for a thermally and calorically perfect gas in terms of total pressure and temperature:

$$\eta_{\mathrm{ad}_t} = \frac{\left[1 - \frac{T_{\mathrm{t4a}}}{T_{\mathrm{t3a}}}\right]}{1 - \left(\frac{P_{\mathrm{t4}}}{P_{\mathrm{t3a}}}\right)^{\frac{\gamma-1}{\gamma}}} \tag{3-45}$$

Polytropic Efficiency

Polytropic efficiency is another concept of efficiency often used in compressor evaluation. It is often referred as small stage or infinitesimal stage efficiency. It is the true aerodynamic efficiency exclusive of the pressure-ratio effect. The efficiency is the same as if the fluid is incompressible and identical with the hydraulic efficiency:

$$\eta_{\text{pc}} = \frac{\left[1 + \frac{dP_{\text{t2}}}{P_{t1}}\right]^{\frac{\gamma-1}{\gamma}} - 1}{\left[1 + \frac{dP_{\text{t2}}}{P_{t1}}\right]^{\frac{n-1}{n}} - 1} \tag{3-46}$$

which can be expanded using a Taylor expansion series and assuming that:

$$\frac{dP_{\text{t2}}}{P_{t1}} \ll 1$$

The expansion of the numerator is:

$$\left[1 + \frac{dP_{\text{t2}}}{P_{t1}}\right]^{\frac{\gamma-1}{\gamma}} = \left[1 + \frac{\gamma-1}{\gamma}\right]\left(\frac{dP_{\text{t2}}}{P_{t1}}\right) + \left[\frac{\gamma-1}{\gamma}\right]\left(\frac{dP_{\text{t2}}}{P_{t1}}\right)^2 + \left[\frac{\gamma-1}{\gamma}\right]\left(\frac{dP_{\text{t2}}}{P_{t1}}\right)^3 + \cdots$$

The expansion of the denominator is:

$$\left[1 + \frac{dP_{\text{t2}}}{P_{t1}}\right]^{\frac{n-1}{n}} = \left[1 + \frac{n-1}{n}\right]\left(\frac{dP_{\text{t2}}}{P_{t1}}\right) + \left[\frac{n-1}{n}\right]\left(\frac{dP_{\text{t2}}}{P_{t1}}\right)^2 + \left[\frac{n-1}{n}\right]\left(\frac{dP_{\text{t2}}}{P_{t1}}\right)^3 + \cdots$$

Neglecting second and above order terms, since $\mathrm{d}P_{\text{t2}}/P_{t1} \ll 1$, the following relationship is obtained:

$$\eta_{\text{pc}} = \frac{1 + \frac{\gamma-1}{\gamma} - 1}{1 + \frac{n-1}{n} - 1} \tag{3-47}$$

which can be written as:

$$\eta_{\text{pc}} = \frac{\frac{\gamma-1}{\gamma}}{\frac{n-1}{n}} \tag{3-48}$$

From this relationship, it is obvious that polytropic efficiency is the limiting value of the isentropic efficiency as the pressure increase approaches zero, and the value

of the polytropic efficiency is higher than the corresponding adiabatic efficiency. Figure 3-12 shows the relationship between adiabatic and polytropic efficiencies as the pressure ratio across the compressor increases. Figure 3-13 shows the relationship across the turbine.

Another characteristic of polytropic efficiency is that the polytropic efficiency of a multistage unit is equal to the stage efficiency if each stage has the same efficiency.

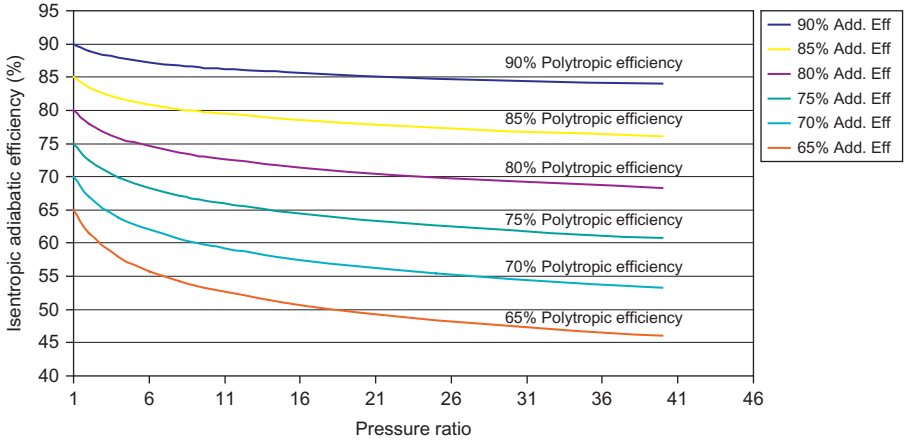


Figure 3-12 Compressor adiabatic and polytropic efficiency relationship for air.

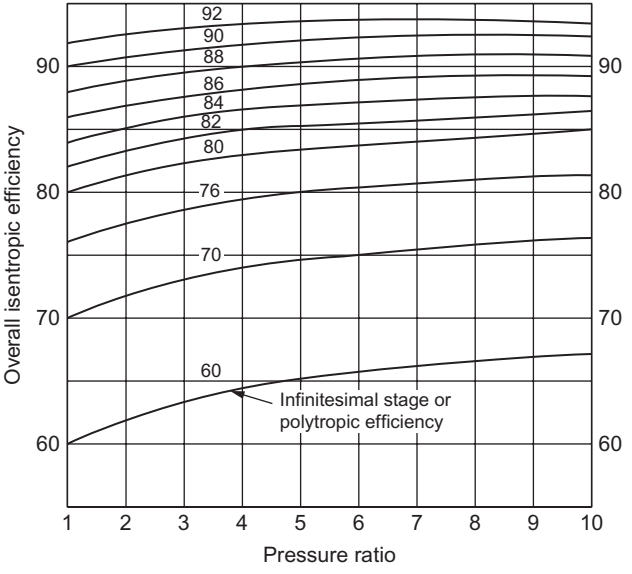


Figure 3-13 Overall and polytropic efficiency expansion.

Dimensional Analysis

Turbomachines can be compared with each other by *dimensional analysis*. This analysis gives various types of geometrically similar parameters. Dimensional analysis is a procedure where variables representing a physical situation are reduced into groups that are dimensionless. These dimensionless groups can then be used to compare performance of various types of machines with each other. Dimensional analysis as used in turbomachines can be employed to (1) compare data from various types of machines – it is a useful technique in the development of blade passages and blade profiles; (2) to select various types of units based on maximum efficiency and pressure head required; and (3) to predict a prototype performance from tests conducted on a smaller scale model or at lower speeds.

Dimensional analysis leads to various dimensionless parameters that are based on the dimension mass (M), length (L), and time (T). Based on these elements, one can obtain various independent parameters such as density (ρ), viscosity (μ), speed (N), diameter (D), and velocity (V). The independent parameters lead to forming various dimensionless groups that are used in fluid mechanics of turbomachines. Reynolds number is the ratio of the intertia forces to the viscous forces:

$$\mathrm{Re} = \frac{\rho V D}{\mu} \tag{3-49}$$

where

ρ = the density of the gas
V = the velocity
D = the diameter of the impeller
μ = the viscosity of the gas

The specific speed compares the head and flow rates in geometrically similar machines at various speeds:

$$N_\mathrm{s} = \frac{N\sqrt{Q}}{H^{3/4}} \tag{3-50}$$

where

H = the adiabatic head
Q = the volume rate
N = the speed

For turbines, it is given as:

$$N_\mathrm{s} = \frac{N\sqrt{P}}{H^{5/4}}$$

where P is the power in horsepower.

The specific diameter compares head and flow rates in geometrically similar machines at various diameters:

$$D_s = \frac{DH^{1/4}}{\sqrt{Q}}$$

The flow coefficient is the capacity of the flow rate expressed in dimensionless form:

$$\phi = \frac{Q}{ND^3} \tag{3-51}$$

The pressure coefficient is the pressure or pressure rise expressed in dimens ionless form:

$$\psi = \frac{H}{N^2D^2} \tag{3-52}$$

The previous equations are some of the major dimensionless parameters. For the flow to remain dynamically similar, all the parameters must remain constant; however, constancy is not possible in a practical sense, so one must make choices.

In selecting turbomachines, the choice of specific speed and diameter determines the most suitable compressor (Figure 3-14) and turbine (Figure 3-15). It is obvious from Figure 3-14 that high head and low flow require a positive displacement unit,

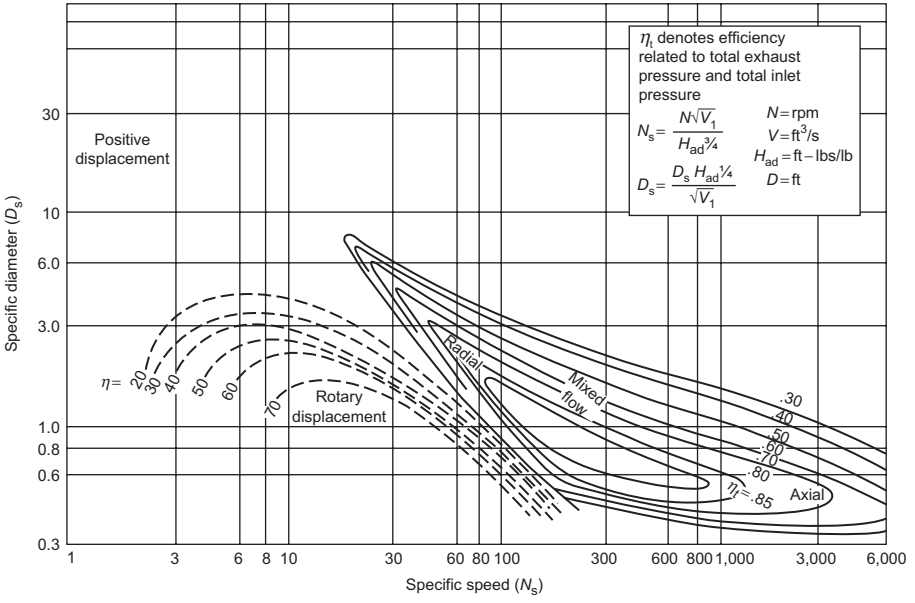


Figure 3-14 Compressor map.

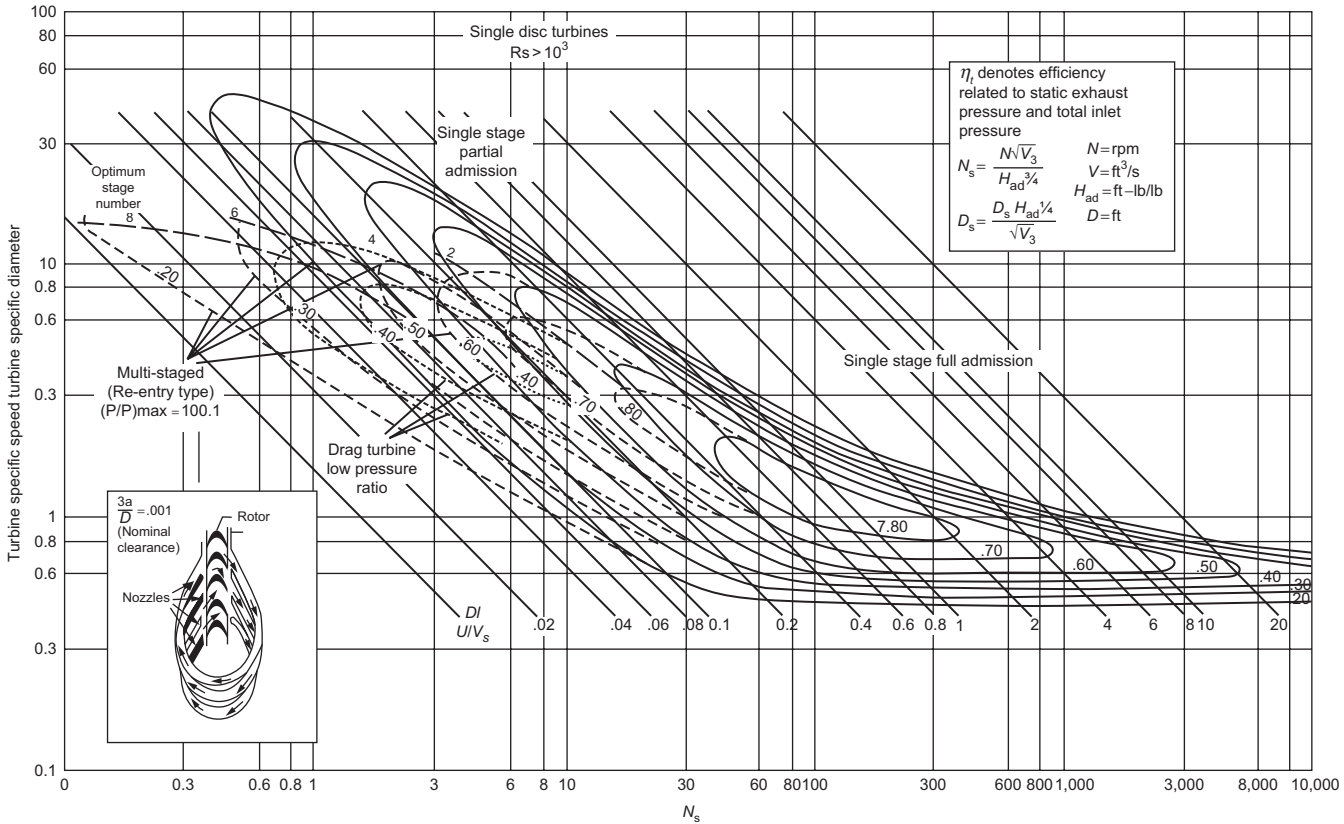


Figure 3-15 Turbine map (Balje, 1964).

medium head and medium flow require a centrifugal unit, and high flow and low head require an axial-flow unit. Figure 3-14 also shows the efficiency of the various types of compressors. This comparison can be made with the different compressors. Although results from Figures 3-14 and 3-15 may vary with actual machines, the results do give a good indication of the type of turbomachine required for the head at the highest efficiency.

Flow coefficients and pressure coefficients can be used to determine various off-design characteristics. The Reynolds number affects the flow calculations for skin friction and velocity distribution.

When using dimensional analysis in computing or predicting performance based on tests performed on smaller scale units, it is not physically possible to keep all parameters constant. The variation of the final results will depend on the scale-up factor and the difference in the fluid medium. It is important in any type of dimensionless study to understand the limit of the parameters and that the geometrical scale-up of similar parameters must remain constant. Many scale-ups have developed major problems because stress, vibration, and other dynamic factors were not considered.

Compressor Performance Characteristics

Compressor performance can be represented in various ways. The commonly accepted practice is to plot the speed lines as a function of the pressure delivered and the flow. Figure 3-16 is a performance map for a centrifugal compressor. The constant speed lines shown in Figure 3-16 are constant aerodynamic speed lines, not constant mechanical speed lines.

The actual mass flow rates and speeds are corrected by factors ($\sqrt{\theta}/\delta$) and ($1/\sqrt{\theta}$), respectively, reflecting variations in inlet temperature and pressure. The surge line joins different speed lines where the compressor's operation becomes unstable. A compressor is in surge when the main flow through a compressor reverses the direction of flow, during which the back (exit) pressure drops and the main flow assumes its proper direction. This process is followed by a rise in back pressure, causing the main flow to reverse again. If allowed to persist, this unsteady process may result in irreparable damage to the machine. Lines of constant adiabatic efficiency (sometimes called efficiency islands) are also plotted on the compressor map. A condition known as "choke" indicates the maximum mass flow rate possible through a compressor at operating speed (Figure 3-16). Flow rate cannot be increased, since at this point it is beyond Mach one at the minimum area of the compressor, or a phenomenon known as "stone walling" occurs, causing a rapid drop in efficiency and pressure ratio.

Figure 3-17 shows a similar performance map for an axial-flow compressor. Note the smaller operational flow range for the axial-flow compressor compared with the centrifugal compressor. Figure 3-18 shows a typical compressor map presented from a slightly different viewpoint. On this map, the constant aerodynamic speed lines are functions of the power and flow rate. Constant pressure lines and efficiency islands are also shown on the same map.

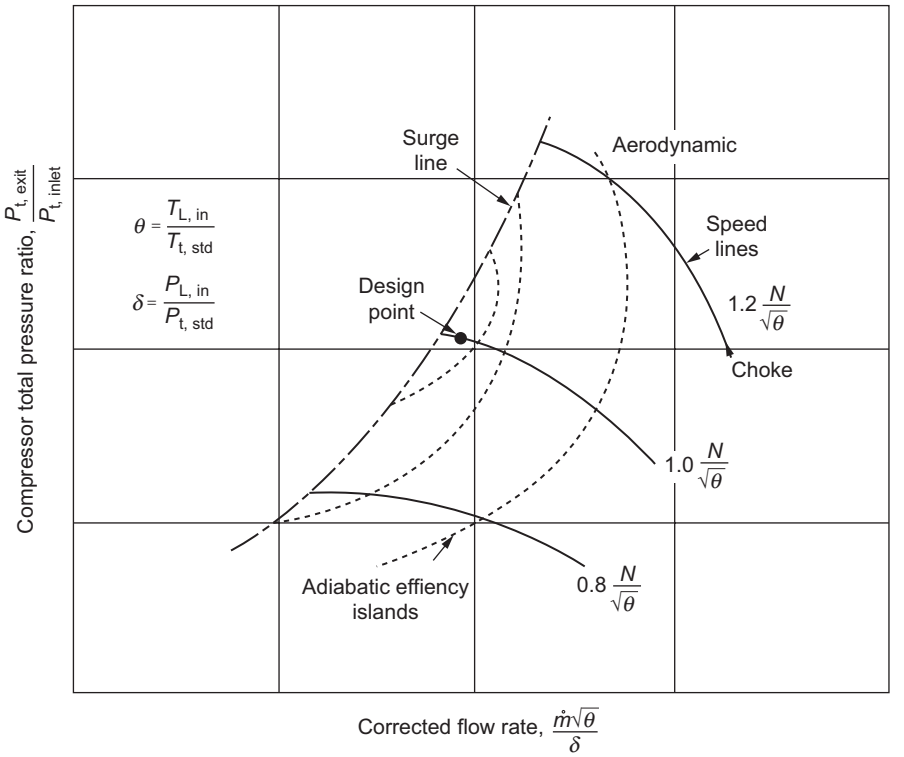


Figure 3-16 Typical centrifugal compressor performance characteristics.

Turbine Performance Characteristics

The two types of turbines – axial flow and radial inflow – can be divided further into impulse- or reaction-type units. Impulse turbines take their entire enthalpy drop through the nozzles, whereas the reaction turbine takes a partial drop through both the nozzles and the impeller blades.

The two conditions that vary the most in a turbine are the inlet pressure and temperature. Two diagrams are needed to show their characteristics. Figure 3-19 is a performance map that shows the effect of turbine inlet temperature and pressure while power is dependent on the efficiency of the unit, the flow rate, and the available energy (turbine inlet temperature). The effect of efficiency with speed is shown in Figure 3-20. Figure 3-20 also shows the difference between an impulse and a 50% reaction turbine. An impulse turbine is a zero-reaction turbine.

Gas Turbine Performance Computation

The following is a sample computation of the techniques used to determine the performance of a gas turbine. A test was run on a G.E. Frame 5 simple-cycle single-shaft

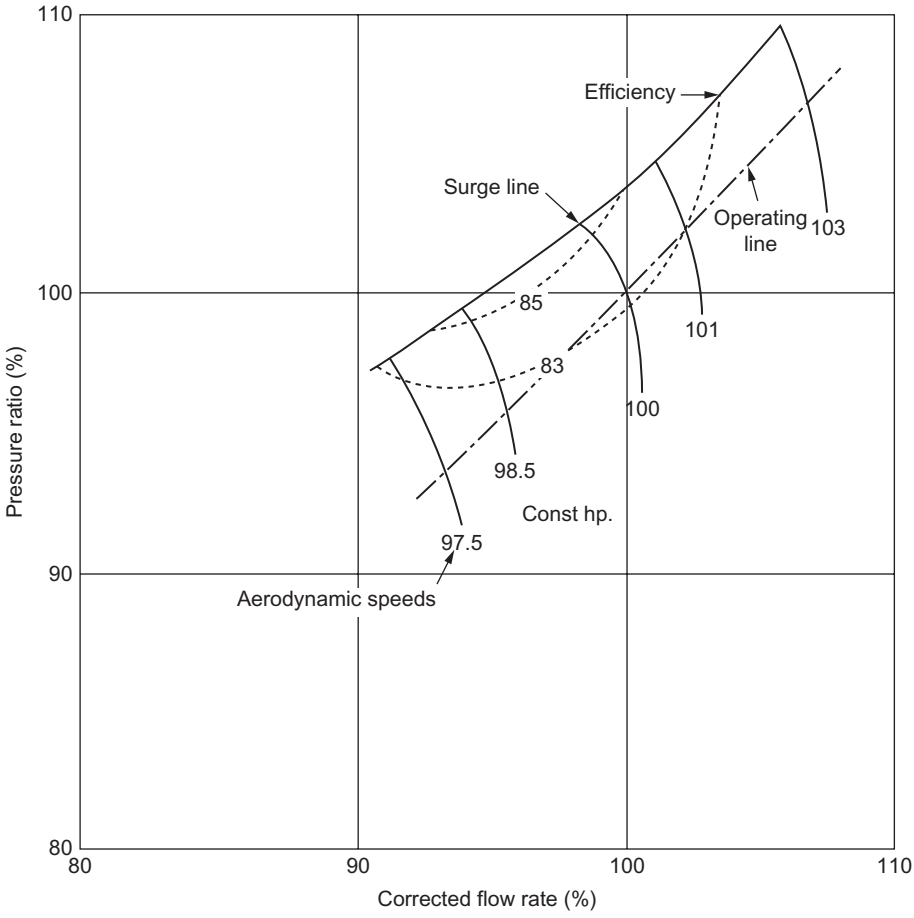


Figure 3-17 Typical flow map for an axial-flow compressor.

unit as shown in Figure 3-21. The exhaust energy from this unit was recovered in a heat recovery boiler, which with supplementary gas firing delivered 175,000 lbs/h (79,545 kg/h) of steam at 665 psia (44.8 Bar) and 750 °F (398 °C). It has a small steam turbine that acts as a starter unit. Figure 3-22 is a schematic representation of the system. The gas turbine was operated from about 25% load to full load. Full load was determined when the turbine's automatic controls took over. These controls are actuated by the exhaust temperature.

Figure 3-23 shows the effect of efficiency as a function of the load for both the compressor and the turbine. Part-load turbine efficiencies are affected more than compressor efficiencies. The discrepancy results from the compressor operating at a relatively constant inlet temperature, pressure, and pressure ratio, while the turbine inlet temperature is greatly varied as shown in Figure 3-24. However, the turbine pressure ratio remains relatively constant. The temperatures shown in Figure 3-24 are low compared

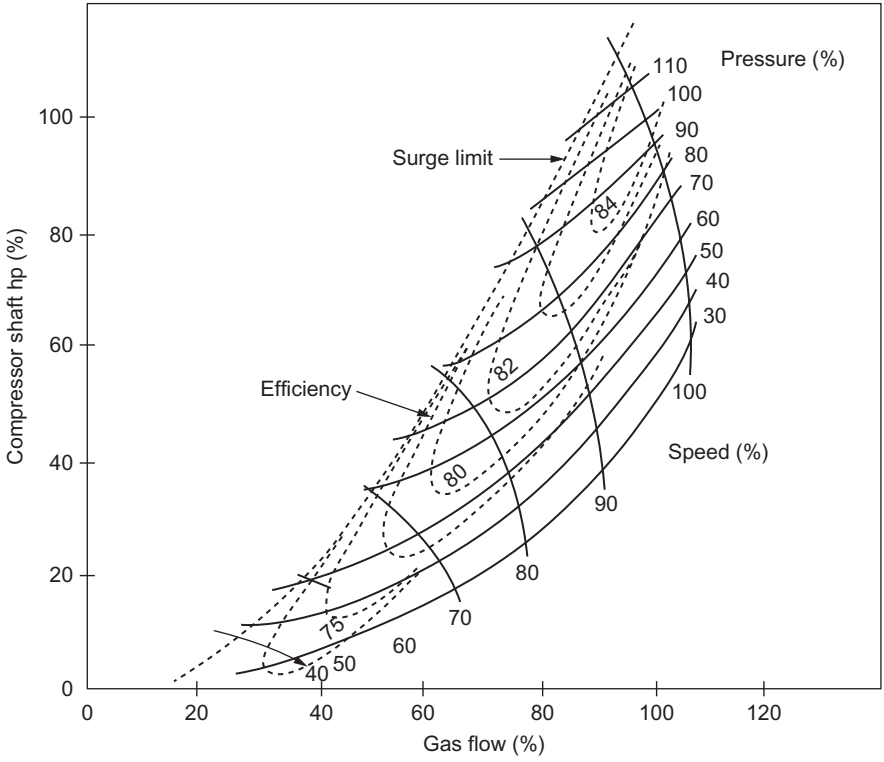


Figure 3-18 Typical compressor map where speed lines are a function of horsepower and flow rate.

with today's advanced gas turbines as the pressure ratio in the turbine illustrated here as a pressure ratio of about 7:1, compared with today's pressure ratios that are between 17:1 and 35:1, giving a computed inlet turbine temperature between 2300 °F (1260 °C) and 2800 °F (1538 °C). The back pressure on the turbine was measured at a relatively constant value of 30.25 in. Hg abs (1.02 Bar). This value creates about a 9-in. H_2O (228 mm H_2O) back pressure on the turbine. The efficiency of the compressor is based on the following equation:

$$\eta_{\text{ad}_c} = \frac{\left[\left(\frac{P_{\text{t2}}}{P_{\text{t1}}}\right)^{\frac{\gamma-1}{\gamma}} - 1\right]}{[T_{\text{t2a}} - T_{t1}]} \tag{3-53}$$

where

T_{t1} = inlet total temperature
P_{t2} = pressure at compressor outlet
P_{t1} = pressure at compressor inlet

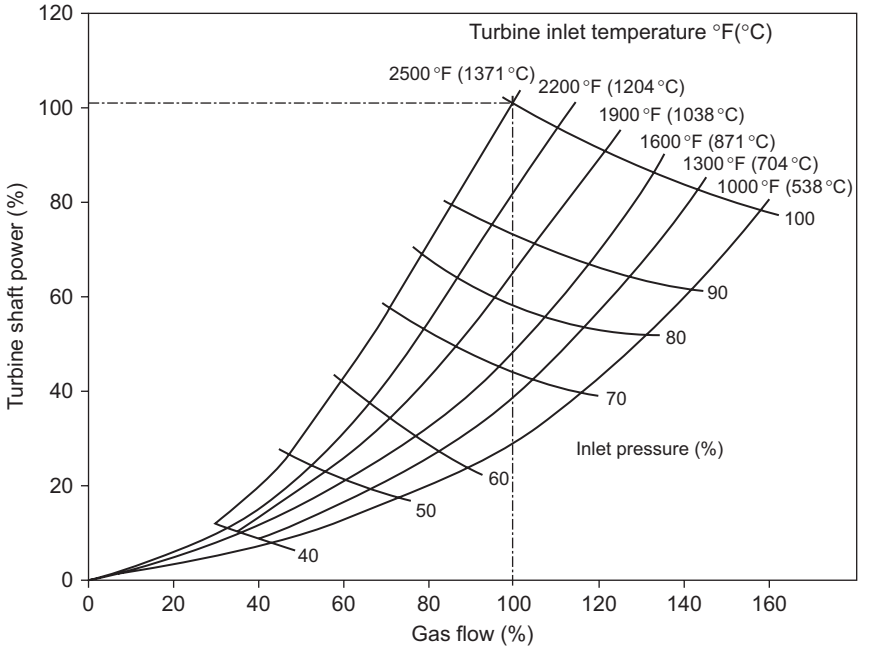


Figure 3-19 Typical centrifugal compressor performance map.

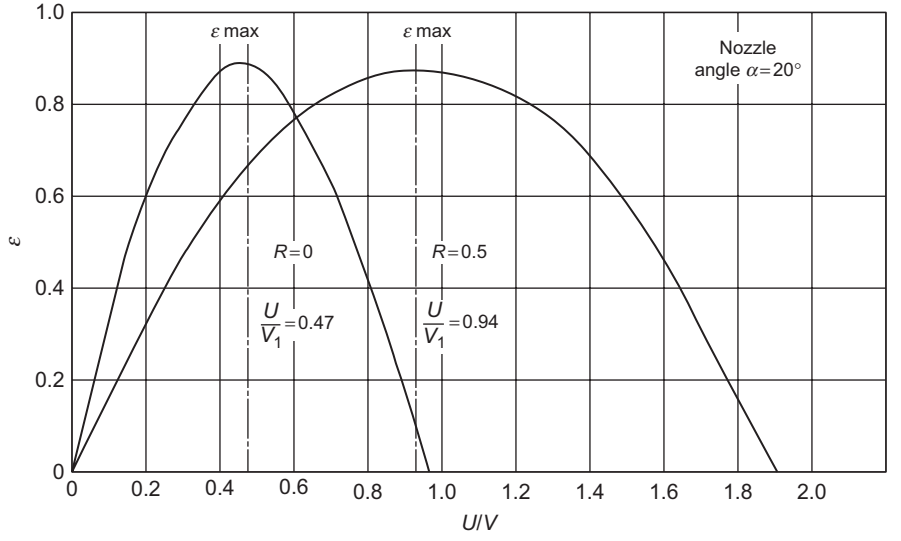


Figure 3-20 Variation of utilization factor with U/V_1 for $R = 0$ and $R = 0.5$ (from Principles of Turbomachinery by Dennis G. Shepherd, © 1956, Macmillan Publishing Co., Inc.).

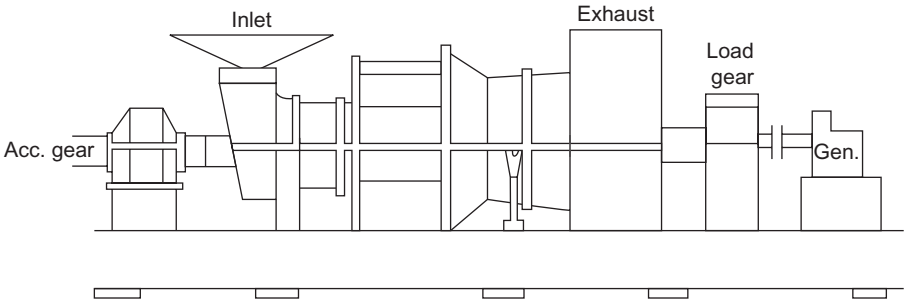


Figure 3-21 Typical industrial gas turbine.

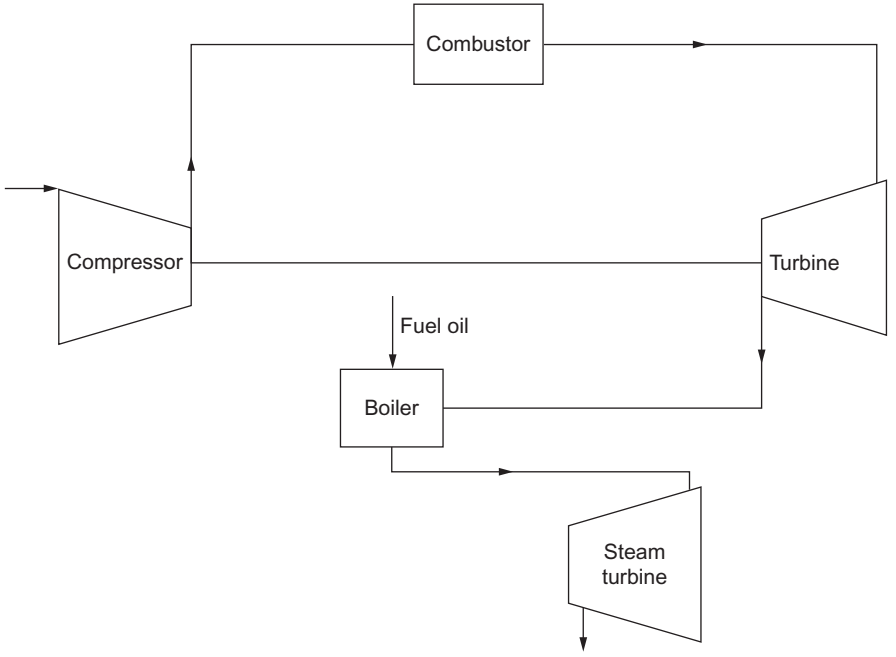


Figure 3-22 Schematic representation of a combined cycle gas turbine.

T_{t2a} = actual total temperature leaving the compressor
γ = specific heat ratio; average value between inlet and outlet temperatures was used

The turbine efficiency calculation is more complex. The first part is the calculation of the turbine inlet temperature (T_{t3a}). The calculation is based on the following equation:

$$T_{t3a} = \frac{\dot{m}_a c_{p2} T_{t2a} + \eta_b \dot{m}_f LHV_{\text{natural gas}}}{c_{p3}\left(\dot{m}_f + \dot{m}_a\right)} \tag{3-54}$$

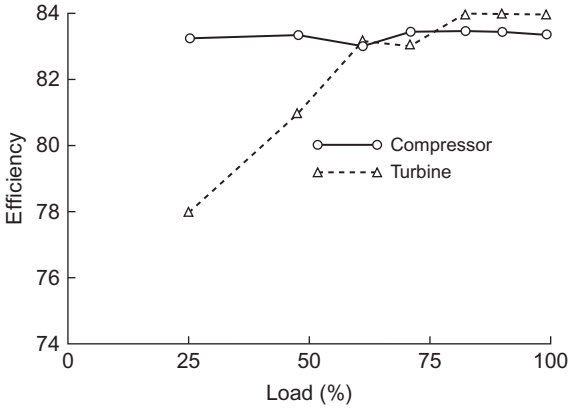


Figure 3-23 Compressor and turbine efficiencies as a function of load.

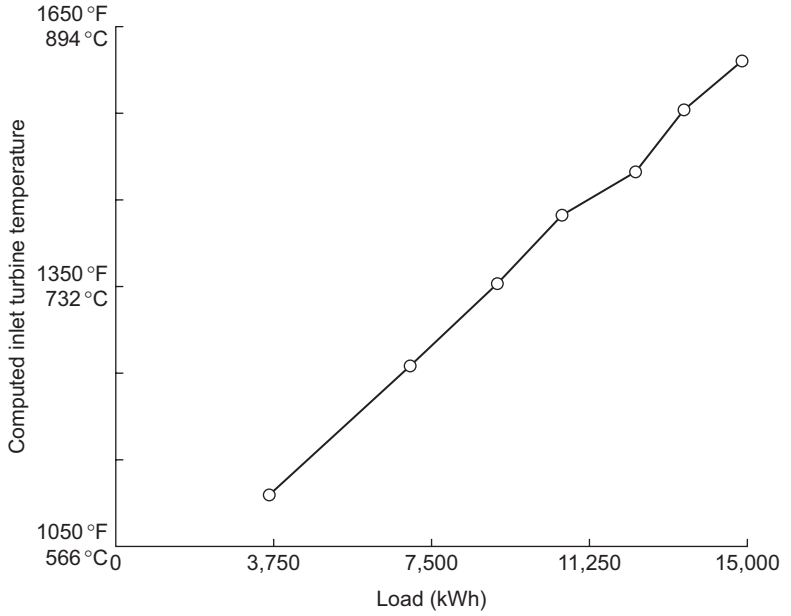


Figure 3-24 Turbine inlet temperature as a function of turbine load.

where

T_{t2a} = temperature at the outlet of the compressor
c_{p2} = specific heat at constant pressure at compressor exit
c_{p3} = specific heat at constant pressure at turbine inlet
$\dot{m}_f$ = mass flow rate for the fuel
$\dot{m}_a$ = mass flow rate of the air

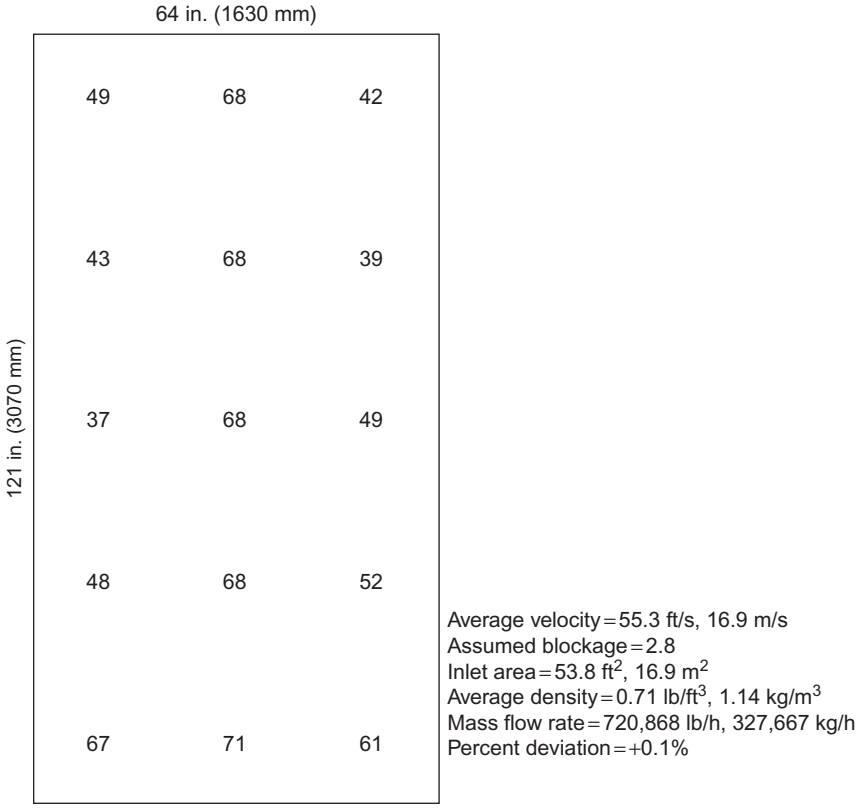


Figure 3-25 Typical inlet velocity profile for an industrial gas turbine.

η_b = combustion efficiency
LHV = lower heating value of the natural gas supplied (950 BTU/ft^3 [35,426 kJ/m^3] and specific gravity 0.557)

The mass flow value of the air was obtained by measuring the flow at the inlet of the gas turbine using an ion-gun velocimeter. Figure 3-25 shows the values obtained across the inlet. These values give an average flow rate of 720,868 lbs/h (327,667 kg/h). This flow rate is within experimental accuracy. The temperature drop in the turbine is computed by subtracting the actual measured exit temperature from the turbine inlet temperature:

$$\Delta T_{\text{tact}} = T_{\text{t3a}} - T_{\text{t4(measured)}} \tag{3-55}$$

The temperature drop in the turbine (ΔT_{tact}) can also be based on an energy balance and is given by the following equation:

$$\Delta T_{\text{tact}} = \frac{\frac{W_{\text{load}}}{\eta_{\text{gen}}} + W_{\text{comp}}}{\left(\dot{m}_f + \dot{m}_a\right) c\text{p}_{\text{tavg}}} = \tag{3-56}$$

where

W_{load} = generator output in kilowatts
η_{gen} = generator efficiency
$c\text{p}_{\text{tavg}}$ = turbine average specific heat
$W_{\text{comp}} = \dot{m}_a c_{\text{pcavg}} (T_{\text{t2a}} - T_{t1})$
c_{Pcavg} = compressor average specific heat
ΔT_{tact} = temperature drop in turbine

The temperature drop calculated in this manner was compared with the drop calculated by subtracting the measured average exhaust temperature reading from the inlet temperature as obtained by the previous equation. The difference between these two methods was about 20 °F (11 °C) at the high-temperature exit. The second method gives a smaller drop, indicating that the temperature recorded is lower than the actual temperature. This result is expected, since the thermocouples are placed a distance downstream from the turbine blades and are not measuring the actual gas exhaust temperature. This comment is not a criticism of the control package, since that operates on a base exhaust temperature.

The turbine efficiency can now be calculated with the use of the following relationship:

$$\eta_t = \frac{\Delta T_{\text{tact}}}{T_{\text{t3}} \left\{ \left[1 - \frac{1}{\left(\frac{P_{\text{t3}}}{P_{\text{t4}}}\right)^{\frac{\gamma-1}{\gamma}}} \right] \right\}} \tag{3-57}$$

where the value of γ was an average value in the turbine.

The gas turbine is coupled with a steam recovery boiler. The exhaust gas from the turbine is used to supplement fire the boiler. The thermal efficiency of the gas turbine alone was calculated by using the following relationship:

$$\eta_{\text{ad}} = \frac{W_{\text{load}} K}{(\text{LHV}) Q} \tag{3-58}$$

where

$K = 3{,}412$ BTU/kW h (3,600 kJ/kW/h)
LHV = heating value, BTU/ft^3(kJ/cum^3)
Q = volume flow rate of fuel to turbine, ft$^3/h$(cum^3/h)

The overall system efficiency is based on the following equation:

$$\eta_{\text{sad}} = \frac{W_{\text{load}} K + \dot{m}_{\text{sb}} (h_s - h_{\text{fw}})}{(\text{LHV}) Q + (\text{LHV}) Q_{\text{fb}}} \tag{3-59}$$

where

$\dot{m}_{sb}$ = mass flow of steam from recovery boiler
h_s = enthalpy of the superheated steam
h_{fw} = enthalpy of the feed-water
Q_{fb} = volume flow rate of fuel to boiler

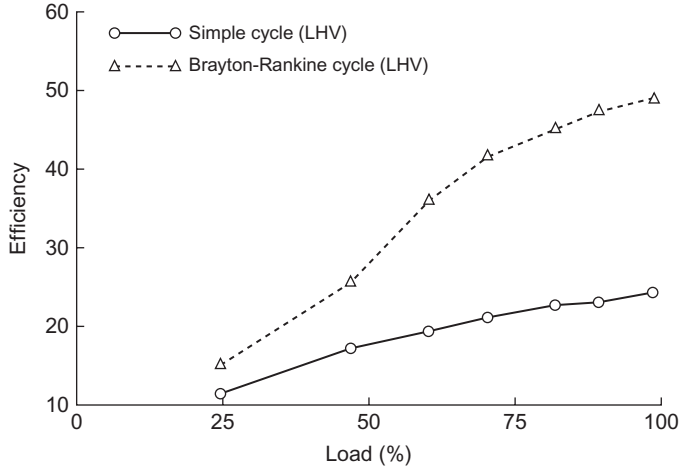


Figure 3-26 Combined- and simple-cycle efficiencies as a function of gas turbine load.

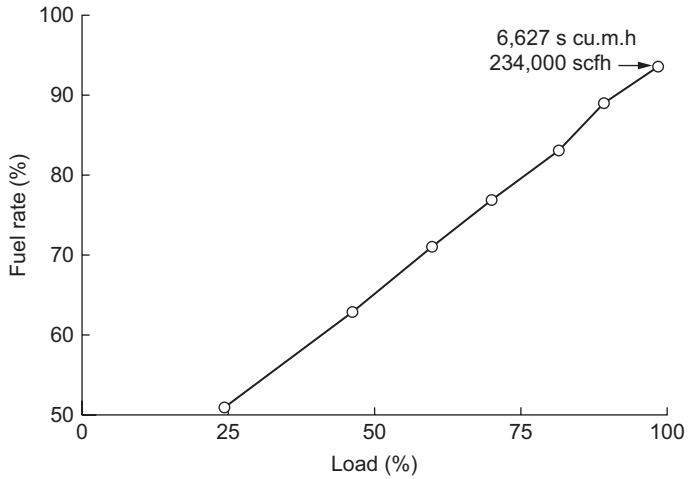


Figure 3-27 Fuel consumption as a function of gas turbine load.

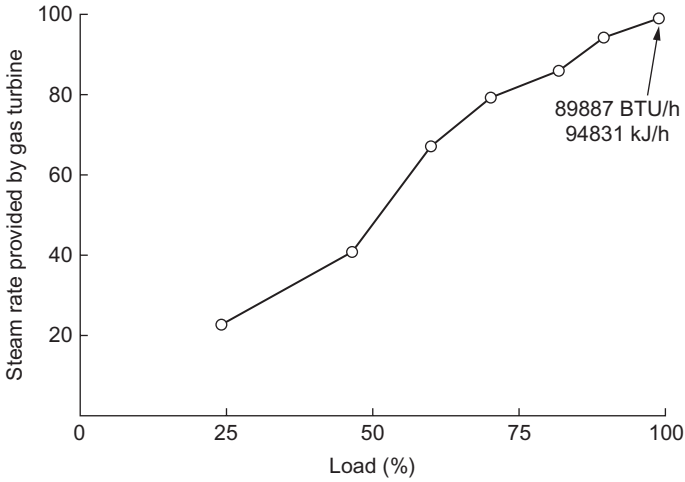


Figure 3-28 Steam generated by exhaust gases of gas turbine as a function of gas turbine load.

Figure 3-26 shows the thermal efficiency of the gas turbine and the Brayton–Rankine cycle (gas turbine exhaust being used in the boiler) based on the *LHV* of the gas. This figure shows that below 50% of the rated load, the combination cycle is not effective. At full load, it is obvious that one can reap the benefits from a combination cycle. Figure 3-27 shows the fuel consumption as a function of the load, and Figure 3-28 shows the amount of steam generated by the recovery boiler.

Bibliography

Balje, O.E., "A Study of Reynolds Number Effects in Turbomachinery," Journal of Engineering for Power, ASME Trans., Vol. 86, Series A, 1964, p. 227.

Shepherd, D.G., "Principles of Turbomachinery," Macmillan Publishing Co., Inc., New York, 1956.

Copyrighted Materials
Copyright © 2012 Elsevier Retrieved from www.knovel.com

4 Performance and Mechanical Standards

The gas turbine is a complex machine, and its performance and reliability are governed by many standards. The American Society of Mechanical Engineers (ASME) performance test codes have been written to ensure that tests are conducted in a manner that guarantees that all turbines are tested under the same set of rules and conditions to ensure that the test results can be compared in a judicious manner. The reliability of the turbines depends on the mechanical codes that govern the design of many gas turbines. The mechanical standards and codes have been written by both ASME and the American Petroleum Institute.

Major Variables for a Gas Turbine Application

The major variables that affect the gas turbines are the following factors:

1. Type of application
2. Plant location and site configuration
3. Plant size and efficiency
4. Type of fuel
5. Enclosures
6. Plant operation mode: base or peaking
7. Start-up techniques

Each of the above points are discussed in the following sections.

Type of Application

The gas turbine is used in many applications, and in most parts, the application determines the type of gas turbine that is best suited. The three major types of applications are aircraft propulsion, power generation, and mechanical drives.

Aircraft Propulsion

The aircraft propulsion gas turbines can be subdivided into two major categories: the jet propulsion and turboprop engines. The jet engine consists of a gasifier section and a propulsive thrust section as shown in Figure 4-1. The gasifier section of the turbine produces high-pressure and -temperature gas for the power turbine. This comprises a

Gas Turbine Engineering Handbook, Fourth Edition. DOI: 10.1016/B978-0-12-383842-1.00004-4
Copyright © 2012 Elsevier Inc. All rights reserved.

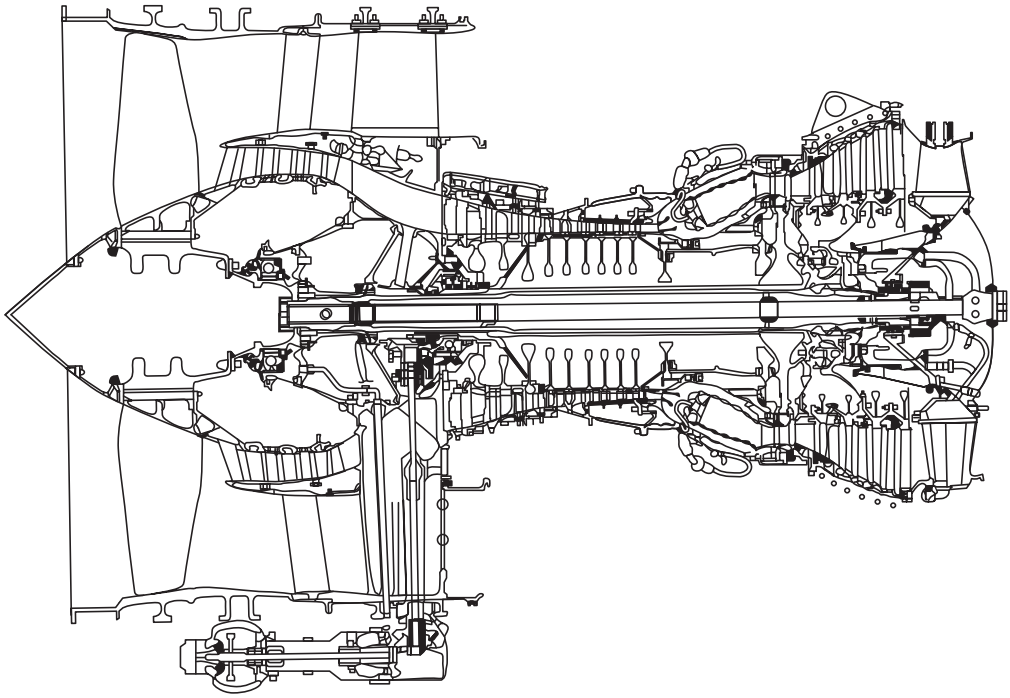


Figure 4-1 A schematic representation of a fan jet engine with a bypass fan.

compressor section and a turbine section. The sole job of the gasifier turbine section is to drive the gas turbine compressor. This section has one or two shafts. The two-shaft gasifier section usually exists in the new high-pressure type gas turbine, where the compressor produces a very high pressure ratio, and has two different sections. Each section comprises many stages. The two different compressor sections consist of the low-pressure compressor section, followed by a high-pressure section. Each section may have between 10 and 15 stages. The jet engine has a nozzle following the gasifier turbine, which produces the thrust for the engine. In the newer jet turbines, the compressor also has a fan section ahead of the turbine, and a large amount of the air from the fan section bypasses the rest of the compressor and produces thrust. The thrust from the fan amounts to more than the thrust from the exhaust.

The jet engine has lead the field of gas turbines in firing temperatures. Pressure ratio of 40:1 with firing temperatures reaching 2500 °F (1371 °C) is now the mode of operation of these engines.

The turboprop engine has a power turbine instead of the nozzle as shown in Figure 4-2. This power turbine drives the propeller. The unit shown is schematically a two-shaft unit; it enables the speed of the propeller to be better controlled, as the gasifier turbine can then operate at a nearly constant speed. Similar engines are used in helicopter drive applications, and many have axial-flow compressors combined with a centrifugal compressor as the last stage as shown in Figure 4-2.

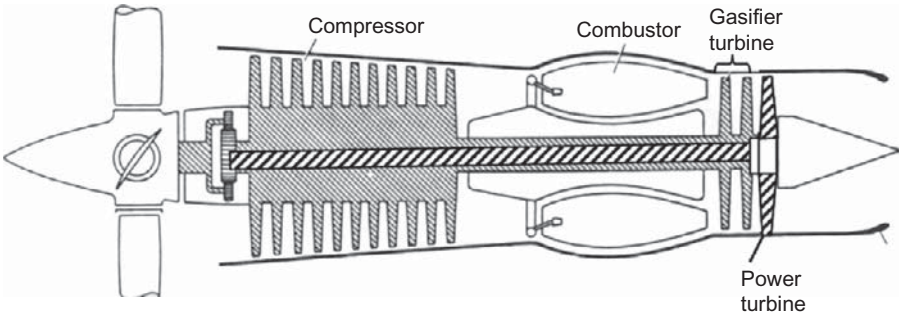


Figure 4-2 A schematic representation of a turboprop engine.

Mechanical Drives

Mechanical drive gas turbines are widely used to drive pumps and compressors. Their application is widely used in offshore and petrochemical industrial complexes. These turbines must be operated at various speeds and thus usually have a gasifier section and a power section. These units in most cases are aeroderivative turbines, which were originally designed for aircraft application. There are some smaller frame-type units, which have been converted to mechanical drive units with a gasifier and power turbine.

Power Generation

The power generation turbines can be further divided into three categories:

- Small standby power turbines (<2 MW): the smaller size of these turbines in many cases has centrifugal compressors driven by radial-inflow turbines, the larger units in this range are usually axial-flow compressors sometimes combined with a centrifugal compressor as the last stage, which are operated by axial turbines.
- Medium-sized gas turbines (between 5 and 50 MW): these turbines are a combination of aeroderivative and frame-type turbines. These gas turbines have axial-flow compressors and axial-flow turbines.
- Large power turbines (>50–480 MW): these are frame-type turbines. The new large turbines operate at very high firing temperatures, about 2400 °F (1315 °C) with cooling provided by steam, at pressure ratios approaching 35:1.

Plant Location and Site Configuration

The location of the plant is the principal determination of the type of plant best configured to meet its needs. Aeroderivatives are used on offshore platforms. Industrial turbines are mostly used in petrochemical applications, and the frame-type units are used for large power production.

Other important parameters that govern the selection and location of the plant are distance from transmission lines, location from fuel ports or pipe lines, and type of

fuel availability. Site configuration is generally not a constraint. Periodically, sites are encountered where one plant configuration or another is best suited.

Plant Type

The determination to have an aeroderivative- or a frame-type gas turbine is based on the plant location. In most cases, if the plant is located offshore on a platform then the aeroderivative-type gas turbine is required. On the other hand, in most onshore applications, if the size of the plant exceeds 100 MW then the frame-type gas turbine is best suited. In smaller plants (between 2 and 20 MW) the industrial-type small turbines best suit the application, and in larger plants (between 20 and 100 MW) both aeroderivative or frame types can be applied. Aeroderivatives have lower maintenance and high heat-recovery capabilities. In many cases, the type of fuel and service facilities may be the determinant. Natural gas or diesel No. 2 would be suited for aeroderivative gas turbines, but heavy fuels would be required for frame-type gas turbine.

Gas Turbine Size and Efficiency

The size of gas turbine is important in determining the cost of the plant. The larger the gas turbine, the lesser the initial cost per kilowatt. The aeroderivative turbines have traditionally been higher in efficiency; however, the new frame-type turbines have been closing the gap in efficiency. Figure 4-3 is a reference to plant pricing and efficiency based on ISO base load output rating at 59 °F (15 °C) and operated on natural gas for all sizes of gas turbines. Figure 4-4 shows typical gas turbine cost and efficiency as a function of gas turbine output for an industrial-type turbine. Industrial turbines range from microturbines of 20 kW at an installed cost of nearly $1,000/kW and an efficiency of about 15%–18% to turbines rated at about 10 MW at a cost of $500/kW and an efficiency of about 28%–32%. The efficiency in these figures is a simple-cycle gas turbine efficiency. These efficiencies can be increased by regeneration or other techniques detailed in Chapter 3. Figure 4-5 shows the aeroderivative-type turbines rated between 10 and 40 MW with an installed cost of $400/kW and an efficiency of about 40%. Figure 4-6 shows frame-type turbines that range from about 10 to 250 MW with an installed cost for the larger units at $350/kW and efficiencies of the newer units reaching 40%.

Type of Fuel

The type of fuel is one of the most important aspects that govern the selection of a gas turbine. Chapter 12 describes the type of fuels and their effect in detail. Natural gas would be the choice of most operators if natural gas was available since its effects on pollution are minimal and maintenance cost would also be the lowest. Table 4-1 shows how the maintenance cost would increase from natural gas to the heavy oils.

Aeroderivative gas turbines cannot operate on heavy fuels; thus, if heavy fuel was a criterion, then the frame-type turbines would have to be used. With heavy fuels, the

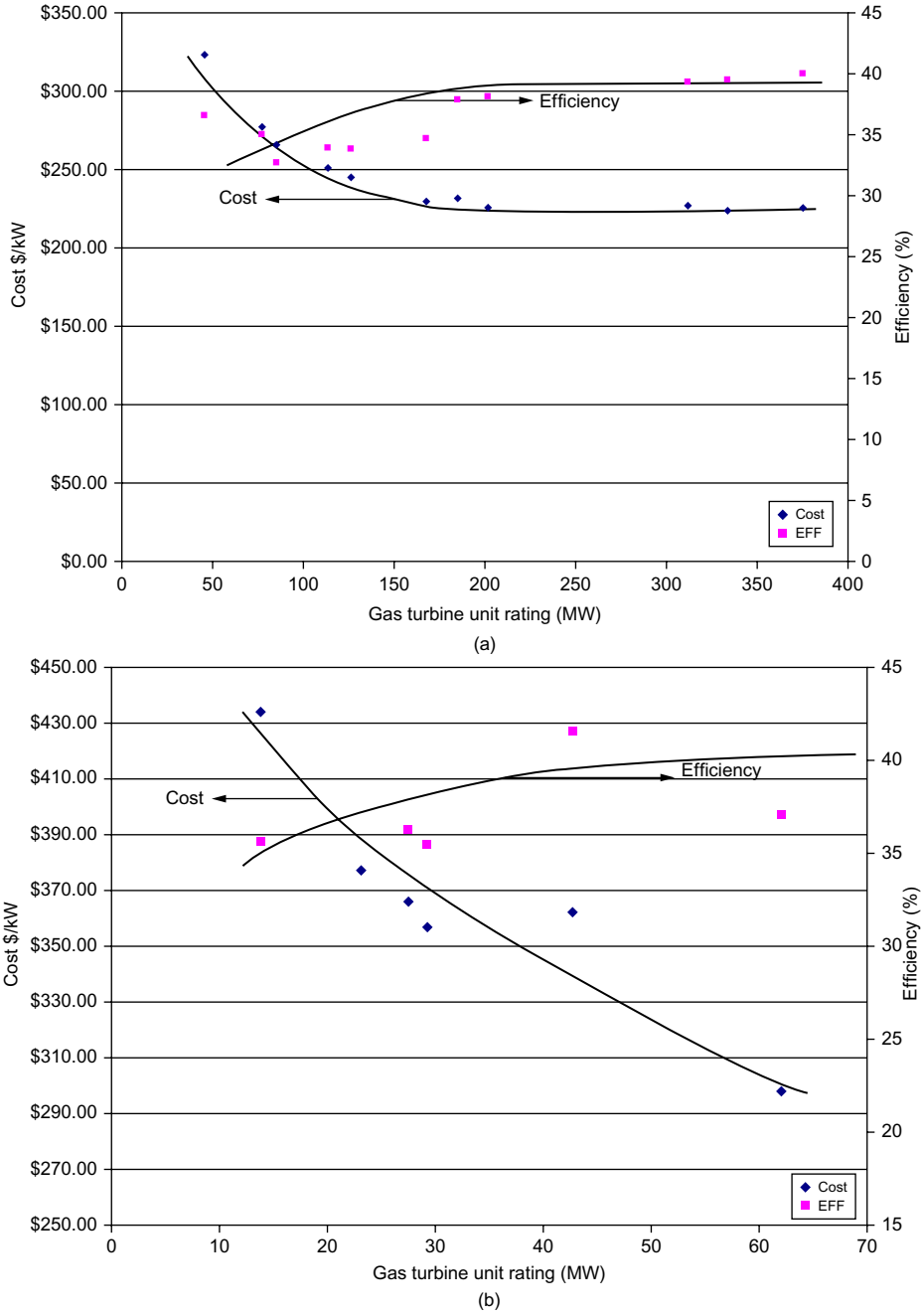


Figure 4-3 Installed cost and efficiency of all types of gas turbines.

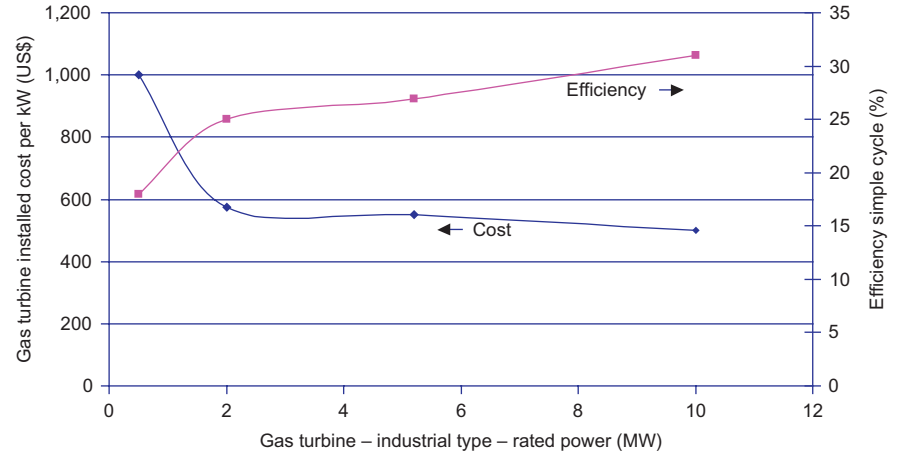


Figure 4-4 Installed cost and efficiency of industrial type turbines.

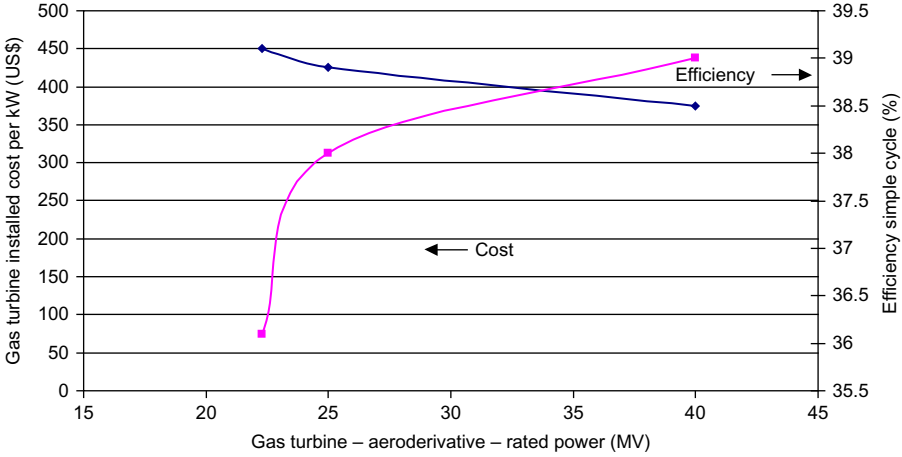


Figure 4-5 Installed cost and efficiency of aeroderivative-type turbines.

power delivered would be reduced after about a weeks of operation by about 10%. Online turbine wash is recommended for turbines with high vanadium content in their fuel, since magnesium salts have to be added to counteract vanadium. These salts cause the vanadium when combusted in the turbine to be turned to ashes. This ash settles on the turbine blades and reduces the cross-sectional area, thus reducing the turbine power.

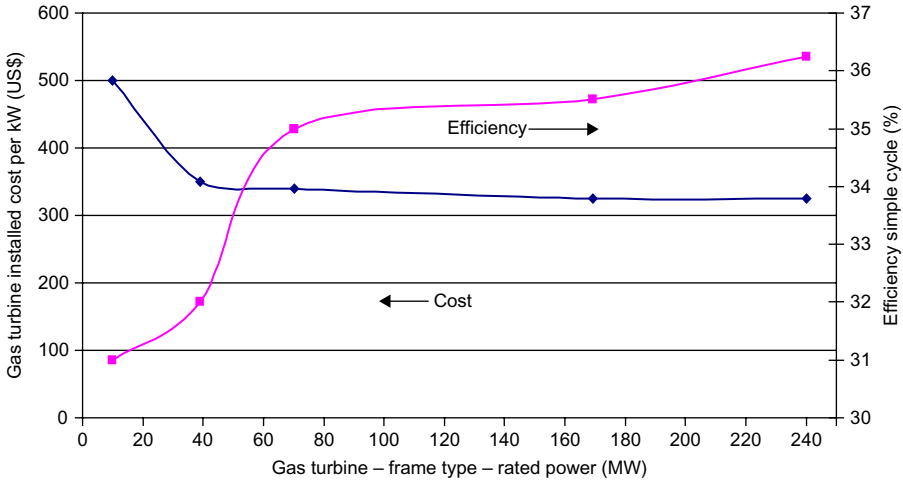


Figure 4-6 Installed cost and efficiency of frame-type turbines.

Table 4-1 Typical Gas Turbine Maintenance Cost based on Type of Fuel

Type of Fuel	Expected Actual Maintenance Cost	Relative Maintenance Cost Factor
Natural gas	0.35	1.0
No. 2 distillate oil	0.49	1.4
Typical crude oil	0.77	2.2
No. 6 residual oil	1.23	3.5

Enclosures

Gas turbines usually come packaged in their own enclosures. These enclosures are designed so that they limit the noise to 70 dB at a 100 ft (30 m) from the gas turbine. In the case of a combined-cycle power plant consisting of the gas turbine, heat-recovery steam generator (HRSG) and the steam turbine, this can be either inside or outside. Although open plants are less expensive than enclosed plants, some owners prefer to enclose their steam turbines in a building and use permanent cranes for maintenance; thus, leaving the gas turbine and the HRSG in the open environment. In severe climate areas, the entire plant is enclosed in a building. A single-shaft combined-cycle power plant with the generator in the middle requires a wider building to allow the generator to be moved to facilitate rotor removal and inspection. Plant arrangements that do not use axial or side exhaust steam turbines result in a taller building and higher building costs.

Plant Operation Mode: Base or Peaking

Gas turbines in the petrochemical industries are usually used under base load conditions powering compressors or pumps. In the power industry, the gas turbine has traditionally been used in peaking service, especially in the United States and Europe. In the developing world, the gas turbine has been used as a base-loaded plant since the 1960s. Since the 1990s, the gas turbine, being the prime mover in combined-cycle power plants, has been developed to operate at high pressures and temperatures, consequently high efficiencies have been achieved. Combined-cycle power plants are not, as were originally planned, base-loaded plants. It is common for the plant to be cycled from 40% to 100% load in a single day, every day of the year. This type of cycling affects the life of many of the hot section components in the gas turbine.

Start-Up Techniques

The start-up of a gas turbine is done by the use of electrical motors, diesel motors, and in plants where there is an independent source of steam, by a steam turbine. New turbines use the generator as a motor for start-up. After combustion occurs and the turbine reaches a certain speed, the motor declutches and becomes a generator. Use of a synchronous clutch between two rotating pieces of equipment is not new. It is very common in use with start-up equipment. In the case of single-shaft combined-cycle power plants, a synchronous clutch can be used to connect the steam turbine to the gas turbine. However, use of a clutch in transmitting over 100 MW of power is new and has not found unequivocal customer acceptance. Although use of a synchronous clutch leads to additional space requirements, additional capital and O&M costs, and potentially reduced availability, it does offer the tangible benefit of easy and fast plant start-up. A major drawback of a single-shaft combined-cycle power plant with a clutch is that the generator installation, maintenance, and power evacuation are more complex and costly because the generator is located in the middle.

Performance Standards

The purpose of the ASME performance test codes is to provide standard directions and rules for the conduct and report of tests of specific equipment and the measurement of related phenomena. These codes provide explicit test procedures with accuracies consistent with current engineering knowledge and practice. These codes are applicable to the determination of performance of specific equipment. They are suitable for incorporation as a part of commercial agreements to serve as a means to determine fulfillment of contract obligations. The parties to the test should agree to accept the code results as determined or, alternatively, agree to mutually acceptable limits of uncertainty established by prior agreement of the principal parties concerned.

The performance tests must be run as much as possible to meet the ASME performance codes. These codes are well written and fully delineate the tests required. Meetings should be held in advance with the vendors to decide which part of the code would not be valid and what assumptions and correction factors must be undertaken to

meet the various power and efficiency guarantees. The determination of special data or verification of particular guarantees, which are outside of the scope of the codes, should be made only after the written agreement of both parties to the test, especially regarding methods of measurement and computation, which should be completely described in the test report.

All ASME PTC standards depend on the ASME PTC 19 series of codes, which is made up of various subseries of codes on various instruments to measure pressure, temperature, and flow and to compute uncertainties in measurement. The scope of the work of Technical Committee No. 19 on Instruments and Apparatus is to describe the various types of instruments and methods of measurement likely to be prescribed in any of the ASME performance test codes. Details such as the limits and sources of error, method of calibration, precautions, and placement of probes will determine their range of application.

Only the methods of measurement and instruments, including instructions for their use, specified in the individual test codes are mandatory. Other methods of measurement and instruments, which may be treated in the supplements on Instruments and Apparatus, shall not be used unless agreeable to all the parties to the test.

In accordance with the established policy of the American Society of Mechanical Engineers concerning the inclusion of metric (International System [SI]) units in all ASME publications, this document includes an appendix of appropriate conversion factors, which will enable the user to utilize both the systems. These conversions are listed in the appendix as they first appear throughout the supplement. Extensive use was made of the *ASME Orientation and Guide for Use of Metric Units*, third edition and *The ASTM Metric Practice Guide E380-92*. These two publications should be referred to for additional material concerning conversions from the US system to SI units.

ASME PTC 19.1: Test Uncertainty

This standard specifies procedures for the evaluation of uncertainties in test parameters and methods and for propagation of those uncertainties into the uncertainty of a test result. Depending on the application, uncertainty sources may be classified either by the presumed effect (systematic or random) on the measurement or test result, or by the process in which they may be quantified (type A or B). The end result of an uncertainty analysis is a numerical estimate of the test uncertainty with an appropriate confidence level. This is the most important part of the test result as it determines the test accuracy.

ASME PTC 19.3: Part 3: Temperature Measurement Instruments and Apparatus

This supplement on Instruments and Apparatus, Part 3 on Temperature Measurement, replaces an earlier supplement published during the period from 1952 to 1961. Since

that time, the technology of temperature measurement has so changed and broadened that the earlier material has become obsolete. This necessitated a complete revision to the supplement resulting in the currently expanded and more comprehensive document.

This edition was approved by the Performance Test Codes Committee on 12 July, 1973. It was approved and adopted by the Council of the Society by action of the Board on Codes and Standards on 29 May, 1974.

ASME PTC 19.5: Flow Measurement, Published 2004

This performance test code supplement describes the techniques and methods of flow measurements required or recommended by the equipment performance test codes.

PTC 19.5 is issued as an addenda performance test code because of its breadth. Thus, the code will be kept up to date with every new development in flow metering as it is applicable to performance testing rather than on a 5- to10-year re-publication cycle. This is critical for a code for which technology may change very quickly. PTC 19.5-2004 offers a major advancement in the development of orifice coefficient of discharge equations based on fluid-dynamic theory. A new five-term equation was developed for orifice discharge coefficients that considers the non-dimensional geometric effects of the area ratio on flow in closed conduits, the boundary layer's effect on differential pressure measurement, and velocity profile effects as characterized by a linear perturbation in the velocity of approach factor. Hence, the Euler number is introduced into the equation for the discharge coefficient such that the discharge coefficient becomes a function of Reynolds number, area ratio, and Euler number. Prior to the 2004 edition of PTC 19.5, only the Reynolds number, diameter ratio, and tap loci were considered; and then only through a curve fitting to an equation driven almost entirely by statistics, rather than by fluid-dynamic theory.

It is shown that the calibration interpretation methodology introduced in PTC 19.5 for orifice metering and reviewed for other types of differential pressure metering reduces the uncertainty of calibrated differential pressure metering sections, even when used outside the calibration range.

All the contents are state of the art in whichever chapter it is referenced. Coverage includes the following:

- Differential pressure class meters including: the general equation for mass flow through a differential pressure class meter, basic physical concepts used in the derivation of the general equation for mass, theoretical flow rate – liquid, gas, or vapor – as the flowing fluid, discharge coefficient, C, and the expansion factor for gases, determining coefficient of discharge for differential pressure class meters; thermal expansion/contraction of pipe and primary elements, selection and recommended use of differential pressure class meters, procedure for sizing a differential pressure class meter, flow calculation procedure, and sample calculations including interpretation and extrapolation of laboratory calibration data using the new discharge coefficient formulation, pulsating flow measurement for orifices, nozzles, and turbine meters.
- Flow conditioning and meter installation requirements for differential pressure meters.

- Sonic flow nozzles and venturis clearly explain basic theoretical relationships: theoretical mass flow calculations, designs of sonic nozzles and venturi nozzles, coefficients of discharge, installation, pressure and temperature measurements.
- Flow measurement by velocity traverse covers traverse measurement stations, recommended installation requirements, calibration requirements for sensors, flow measurement procedures, and flow computation, including examples.
- Ultrasonic flow meters cover applications, flow meter descriptions, implementation, operational limits and error sources and their reduction. Examples are large (to 20 ft) pipe field calibrations, installation considerations, and meter factor determination and verification.
- Electromagnetic flow meters cover their construction, calibration, and proper application.
- Tracer methods – constant-rate injection method using non-radioactive chemicals covers the constant-rate injection method, selection of tracer chemicals, fluorometric analysis, procedures, and test setup. Also included are radioactive tracer techniques for measuring water flow rate covering the same aforementioned areas.
- Mechanical meters are fully explained with the newest calibration presentations and correlations of their performance under plant and field test conditions, which include positive displacement meters, turbine meters, turbine meter signal transducers and indicators, calibration, recommendations for use, piping installations, and the effects of disturbances.

PTC 19.10: Flue and Exhaust Gas Analyses, Part 10

Presented are descriptions of methods, apparatus, and calculations, which are used in conjunction with performance test codes to quantitatively determine the gaseous constituents of exhausts resulting from stationary combustion sources. The gases covered by this PTC supplement are oxygen, carbon dioxide, carbon monoxide, nitrogen, sulfur dioxide, sulfur trioxide, nitric oxide, nitrogen dioxide, hydrogen sulfide, and hydrocarbons. Stationary combustion sources include steam generators, gas turbines, internal combustion engines, incinerators, and so on. Many methods are available for measuring the constituents in flue and exhaust gases. This PTC supplement describes in detail the most commonly used instrumentation and analytical procedures used for flue and exhaust gas analyses. Included are instrumental methods as well as normal wet chemical methods. The instrumental methods include instruments used for noncontinuous or continuous sampling using extractive samples and in situ type instruments that require no sampling system.

ASME PTC 19.11: Steam and Water Sampling, Conditioning, and Analysis in the Power Cycle

The object of this code is to specify and discuss the methods and instrumentation for testing boiler makeup and feed-water, steam, and condensate in relation to performance testing as may be required in performance test codes in on-time acceptance testing and continuous performance monitoring. This code also provides guidance to power plant management, engineers, chemists, and operators in the design

and operation of sampling systems for monitoring cycle chemistry. The methods and equipment recommended herein may be useful for monitoring other influent and effluent streams of the power plant.

Contamination of the steam and water cycle must be at or less than the maximum specified for the performance test before a turbine, condenser, or deaerator performance test is made.

This supplement includes the following:

- Sample selection
- Sample collection and conditioning
- Sample analysis
- Data analysis

ASME PTC 19.23: Guidance Manual for Model Testing, Published 1980

This standard provides guidance for the design and application of models by those concerned with the extension or supplementation of prototype tests of equipment using ASME performance test codes. When there are test codes in existence covering specific equipment, the guiding principles, instruments, and methods of measurement from such codes shall be used with only such modifications as it becomes necessary by virtue of the fact that a model is being tested instead of a prototype. A model is a device, machine, structure, or system, which can be used to predict the behavior of an actual and similar device, machine, structure, or system, which is called the prototype. A physical model may be smaller than, the same size as, or larger than the prototype. PTC 19.23 consists of (a) general discussion of model testing, (b) example problems, and (c) theoretical background.

ASME PTC 46: Performance Test Code on Overall Plant Performance, Published January 1, 1996

Object and Scope

This code is written to establish the overall plant performance and applies to any plant size. Power plants, which produce secondary energy output such as cogeneration facilities, are included within the scope of this code. For cogeneration facilities, there is no requirement for a minimum percentage of the facility output to be in the form of electricity; however, the guiding principles, measurement methods, and calculation procedures are predicated on electricity being the primary output. It can be used to measure the performance of a plant in its normal operating condition, with all equipment in a clean and a fully functional condition. This code provides explicit methods and procedures for combined-cycle power plants and for most gas-, liquid-, and solid-fueled Rankine cycle plants. There is no intent to restrict the use of this code for other types of heat-cycle power plants, providing the explicit procedures can be met.

It does not, however, apply to simple-cycle gas turbine power plants (see ASME PTC 22 instead). The scope of this code begins for a gas turbine-based power generating unit when a heat-recovery steam generator is included within the test boundary.

To test a particular power plant or cogeneration facility, the following conditions must be met:

a. Means must be available to determine, through either direct or indirect measurements, all the heat inputs entering the test boundary and all the electrical power and secondary outputs leaving the test boundary.
b. Means must be available to determine, through either direct or indirect measurements, all the parameters to correct the results from the test to the base reference condition.
c. The test result uncertainties are expected to be less than or equal to the uncertainties given in Subsection 1.3 for the applicable plant type.
d. The working fluid for vapor cycles must be steam. This restriction is imposed only to the extent that other fluids may require measurements or measurement methods different from those provided by this code for steam cycles. In addition, this code does not provide specific references for the properties of working fluids other than steam.

Tests addressing other power plant performance-related issues are outside the scope of this code. These include the following:

Emissions tests. Testing to verify compliance with regulatory emissions levels (e.g., airborne gaseous and particulate, solid and wastewater, and noise) or required for calibration and certification of emission-monitoring systems.
Operational demonstration tests. The various standard power plant tests typically conducted during start-up, or periodically thereafter, to demonstrate specified operating capabilities (e.g., minimum load operation, automatic load control and load ramp rate, and fuel switching capability).
Reliability tests. Tests conducted over an extended period of days or weeks to demonstrate the capability of the power plant to produce a specified minimum output level or availability.

The measurement methods, calculations, and corrections to design conditions included herein may be of use in designing tests of this type; however, this code does not address this type of testing in terms of providing explicit testing procedures or acceptance criteria.

As a result, a test of a facility with a low proportion of electric output, may not be capable of meeting the expected test uncertainties of this code. This code provides explicit procedures for the determination of power plant thermal performance and electrical output. Test results provide a measure of the performance of a power plant or thermal island at a specified cycle configuration, operating disposition and/or fixed power level, and at a unique set of base reference conditions. Test results can then be used as defined by a contract for the basis of determination of fulfillment of contract guarantees. Test results can also be used by a plant owner, for either comparison to a design number or to trend performance changes over time of the overall plant. The results of a test conducted in accordance with this code will not provide a basis for comparing the thermo-economic effectiveness of different plant design.

Power plants comprised many equipment components. Test data required by this code may also provide limited performance information for some of this equipment; however, this code was not designed to facilitate simultaneous code level testing of

individual equipment. ASME PTCs, which address testing of major power plant equipment, provide a determination of the individual equipment isolated from the rest of the system.

PTC 46 has been designed to determine the performance of the entire heat cycle as an integrated system. When the performance of individual equipment operating within the constraints of their design-specified conditions are of interest, ASME PTCs developed for the testing of specific components should be used. Likewise, determining overall thermal performance by combining the results of ASME code tests conducted on each plant component is not an acceptable alternative to a PTC 46 test.

Performance Test Code on Gas Turbines

ASME PTC 22, Published 2006

Description

The object is to determine the thermal performance of the gas turbine when operating at test conditions, and correct these test results to specified reference conditions, or to standard or specified operating and control conditions. The code provides for the testing of gas turbines supplied with gaseous or liquid fuels (or solid fuels converted to liquid or gas prior to entrance to the gas turbine). Test of gas turbines with water or steam injection for emission control and/or power augmentation is included. The tests can be applied to gas turbines in combined-cycle power plants or with other heat-recovery systems.

This code provides explicit procedures for the determination of correct power output, corrected heat rate (efficiency), corrected exhaust flow, energy, and temperature. Tests may be designated to satisfy different goals, including absolute performance and comparative performance. It is the intent of the code to provide results with the highest level of accuracy consistent with the best engineering knowledge and practice in the gas turbine industry.

Meetings should be held with all parties concerned as to how the test will be conducted and an uncertainty analysis should be performed prior to the test. The overall test uncertainty will vary because of the differences in the scope of supply, fuels used, and driven equipment characteristics. The code establishes a limit for the uncertainty of each measurement required; the overall uncertainty is then calculated in accordance with the procedures. In planning the test, an uncertainty analysis defined in the code and by ASME PTC 19.1 must demonstrate that the proposed instrumentation and measurement techniques meet the requirements of the code.

ASME Measurement of Exhaust Emissions from Stationary Gas Turbine Engines B133.9, Published 1994

This standard provides guidance in the measurement of exhaust emissions for the emissions performance testing (source testing) of stationary gas turbines. Source testing is required to meet federal state and local environmental regulations. The

standard is not intended for use in continuous emissions monitoring although many of the online measurement methods defined may be used in both applications. This standard applies to engines that operate on natural gas and liquid distillate fuels. Much of this standard will also apply to engines operated on special fuels such as alcohol, coal gas, residual oil, or process gas or liquid. However, these methods may require modification or be supplemented to account for the measurement of exhaust components resulting from the use of a special fuel.

ASME PTC 36 Measurement of Industrial Sound (ASME B133.8), Published 2004

The scope of this code includes measurement procedures in a variety of acoustical environments, including outdoor settings influenced by background noise. Generally, sound pressure levels and/or sound power levels in prescribed frequency bands are used to quantify the sound emission of industrial equipment and facilities. Sound pressure level measurements or sound intensity measurements obtained using the procedures of this code may be used to calculate sound power level.

Mechanical Parameters

Some of the best standards from a mechanical point of view have been written by the American Petroleum Institute (API) and the American Society of Mechanical Engineers, as part of their mechanical equipment standards. The ASME and the API mechanical equipment standards are an aid in specifying and selecting equipment for general petrochemical use. The intent of these specifications is to facilitate the development of high-quality equipment with a high degree of safety and standardization. The user's problems and experience in the field are considered in writing these specifications. The task force which writes these specifications, consists of members from the user, the contractor, and the manufacturers. Thus, the task-force team brings together both experience and know-how.

The petroleum industry is one of the largest users of gas turbines as prime movers for drives of mechanical equipment and also for power generation equipment. Thus, the specifications written are well suited for this industry, and the tips of operation and maintenance apply for all industries. This section deals with some of the applicable API and ASME standards for the gas turbine and other various associated pieces.

It is not the intent of this section to detail the API or ASME standards, but to discuss some of the pertinent points of these standards and other available options. It is strongly recommended that the reader can obtain all mechanical equipment standards from ASME and API.

The purpose of the ASME B133 standards is to provide criteria for the preparation of gas turbine procurement specifications. These standards will also be useful for response to such specifications.

The B133 standards provide essential information for the procurement of gas turbine power plants. These standards apply to open-cycle, closed-cycle, and semiclosed-cycle gas turbines with conventional combustion systems for industrial, marine, and electric power applications. All auxiliaries needed for proper operation are covered. Not included are gas turbines applied to earth-moving machines, agricultural- and industrial-type tractors, automobiles, trucks, buses, and aeropropulsion units.

For gas turbines using unconventional or special heat sources (such as chemical processes for nuclear reactors or furnaces for supercharged boilers), these standards may be used as a basis; but appropriate modifications may be necessary.

The intent of the B133 standards is to cover the normal requirements of the majority of applications, recognizing that economic trade-offs and reliability implications may differ in some applications. The user may desire to add, delete, or modify the requirements in this standard to meet his/her specific needs, and he/she has the option of doing so in their own procurement specification.

ASME B 133.2 Basic Gas Turbines, Published 1977 (Reaffirmed: 1997)

This standard presents and describes features that are desirable for the user to specify in order to select a gas turbine that will yield satisfactory performance, availability, and reliability. The standard is limited to a consideration of the basic gas turbine, including the compressor, combustion system, and turbine.

ASME B133.3 Procurement Standard for Gas Turbine Auxiliary Equipment, Published 1981 (Reaffirmed 1994)

The aim of this standard is to provide guidance to facilitate the preparation of gas turbine procurement specifications for gas turbine auxiliary equipment. It is intended for use with gas turbines for industrial, marine, and electric power applications. The standard also covers auxiliary systems, such as lubrication, cooling, fuel (but not its control), atomizing, starting, heating–ventilating, fire protection, cleaning, inlet, exhaust, enclosures, couplings, gears, piping, mounting, painting, and water and steam injection.

ASME B133.4 Gas Turbine Control and Protection Systems, Published 1978 (Reaffirmed: 1997)

The intent of this standard is to cover the normal requirements of the majority of applications, recognizing that economic trade-offs and reliability implications may differ in some applications. The user may desire to add, delete, or modify the requirements in this standard to meet his/her specific needs, and he/she has the option of doing so in his own bid specification. The gas turbine control system shall include sequencing, control, protection, and operator information, which shall provide for an orderly and safe start-up of the gas turbine, control of proper loading, and an orderly shutdown procedure. It shall also include an emergency shutdown capability, which can be operated

automatically or manually by suitable failure detectors. Coordination between gas turbine control and driven equipment must be provided for start-up, operation, and shutdown.

ASME B133.5 Procurement Standard for Gas Turbine Electrical Equipment, Published 1978 (Reaffirmed: 1994)

This standard is no longer an American National Standard or an ASME-approved standard as of 27 July, 2007. It is available for historical reference only.

The purpose of this standard is to provide guidance to facilitate the preparation of gas turbine procurement specifications. It is intended for use with gas turbines for industrial, marine, and electric power applications. This standard covers auxiliary systems, such as lubrication, cooling, fuel (but not its control), atomizing, starting, heating–ventilating, fire protection, cleaning, inlet, exhaust, enclosures, couplings, gears, piping, mounting, painting, and water and steam injection.

The B133.5 standard applies mostly to gas turbine stations used for power generation. Appropriate sections, however, can be used where applicable for mechanical drive turbine stations. The size of station considered in the B133.5 standard includes all electric utility size units but not small power supplies of a semiportable nature.

ASME B 133.7M Gas Turbine Fuels, Published 1985 (Reaffirmed: 1992)

Gas turbines may be designed to burn either gaseous or liquid fuels, or both with or without changeover while under load. This standard covers both types of fuel. With many DLN combustors, there are major problems to change while under load.

ASME B133.8 Gas Turbine Installation Sound Emissions, Published 1977 (Reaffirmed: 1989)

This standard gives methods and procedures for specifying the sound emissions of gas turbine installations for industrial, pipeline, and utility applications. Included are practices for making field sound measurements and for reporting field data. This standard can be used by users and manufacturers to write specifications for procurement and to determine compliance with specification after installation. Information is included, for guidance, to determine expected community reaction to noise.

ASME B133.9 Measurement of Exhaust Emissions from Stationary Gas Turbine Engines, Published: 1994

This standard provides guidance in the measurement of exhaust emissions for the emissions performance testing (source testing) of stationary gas turbines. Source testing is required to meet federal, state, and local environmental regulations. The standard is not intended for use in continuous emissions monitoring although many of the online measurement methods defined may be used in both applications. This standard

applies to engines that operate on natural gas and liquid distillate fuels. Much of this standard will also apply to engines operated on special fuels such as alcohol, coal gas, residual oil, or process gas or liquid. However, these methods may require modification or be supplemented to account for the measurement of exhaust components resulting from the use of a special fuel.

API Std 616 Gas Turbines for the Petroleum, Chemical, and Gas Industry Services, Fourth Edition, August 1998

This standard covers the minimum requirements for open-, simple-, and regenerative-cycle combustion gas turbine units for services of mechanical drive, generator drive, or process gas generation. All auxiliary equipment required for starting and controlling gas turbine units and for turbine protection is either discussed directly in this standard or referred in this standard through references to other publications. Specifically, gas turbine units that are capable of continuous service firing gas or liquid fuel or both are covered by this standard. In conjunction with the API specifications, the following ASME codes also supply significant data in the proper selection of the gas turbine.

API Std 613 Special Purpose Gear Units for Petroleum, Chemical, and Gas Industry Services, Fourth Edition, June 1995

Gears, wherever used, can be a major source of problem and downtime. This standard specifies the minimum requirements for special purpose, enclosed, precision, single- and double-helical one- and two-stage speed increasers and reducers of parallel-shaft design for refinery services, primarily intended for gears that are in continuous service without installed spare equipment. These standards apply for gears used in the power industry.

API Std 614 Lubrication, Shaft-Sealing, and Control-Oil Systems and Auxiliaries for Petroleum, Chemical, and Gas Industry Services, Fourth Edition, April 1999

Lubrication, besides providing lubrication, also provides cooling for various components of the turbine. This standard covers the minimum requirements for lubrication systems, oil-type shaft-sealing systems, and control-oil systems for special purpose applications. Such systems may serve compressors, gears, pumps, and drivers. The standard includes the systems' components, along with the required controls and instrumentation. Data sheets and typical schematics of both system components and complete systems are also provided. This standard includes general requirements, special purpose oil systems, general purpose oil systems, and dry gas seal module systems. This standard is well written, and the tips detailed are good practices for all type of systems.

API Std 618, Reciprocating Compressors for Petroleum, Chemical, and Gas Industry Services, Fourth Edition, June 1995

This standard could be adapted to the fuel compressor for the natural gas to be brought up to the injection pressure required for the gas turbine. It covers the minimum requirements for reciprocating compressors and their drivers used in petroleum, chemical, and gas industry services for handling process air or gas with either lubricated or non-lubricated cylinders. Compressors covered by this standard are of moderate-to-low speed and in critical services. The non-lubricated cylinder types of compressors are used for injecting the fuel into gas turbines at the high pressure needed. It also covers related lubricating systems, controls, instrumentation, intercoolers, after-coolers, pulsation suppression devices, and other auxiliary equipment.

API Std 619, Rotary-Type Positive Displacement Compressors for Petroleum, Chemical, and Gas Industry Services, Third Edition, June 1997

Dry helical lobe rotary compressors non-lubricated cylinder types of compressors are used for injecting the fuel into gas turbines at the high pressure needed. The gas turbine application requires that the compressor be dry. This standard is primarily intended for compressors that are in special purpose applications and covers the minimum requirements for dry helical lobe rotary compressors used for vacuum or pressure or both in petroleum, chemical, and gas industry services. This edition also includes a new inspector's checklist and new schematics for general purpose and typical oil systems.

ANSI/API Std 670 Vibration, Axial-Position, and Bearing-Temperature Monitoring Systems, Third Edition, November 1993

This standard provides a purchase specification to facilitate the manufacture, procurement, installation, and testing of vibration, axial position, and bearing-temperature monitoring systems for petroleum, chemical, and gas industry services. It covers the minimum requirements for monitoring radial shaft vibration, casing vibration, shaft axial position, and bearing temperatures. It outlines a standardized monitoring system and covers requirements for hardware (sensors and instruments), installation, testing, and arrangement. Standard 678 has been incorporated into this edition of Standard 670. This is a well-documented standard, widely used in all industries.

API Std 671, Special Purpose Couplings for Petroleum, Chemical, and Gas Industry Services, Third Edition, October 1998

This standard covers the minimum requirements for special purpose couplings intended to transmit power between the rotating shafts of two pieces of refinery equipment. These couplings are designed to accommodate parallel offset, angular misalignment, and axial displacement of the shafts without imposing excessive mechanical loading on the coupled equipment.

API Std 677, General-Purpose Gear Units for Petroleum, Chemical, and Gas Industry Services, Second Edition, July 1997 (Reaffirmed: March 2000)

This standard covers the minimum requirements for general-purpose, enclosed single-, and multistage gear units incorporating parallel-shaft helical and right-angle spiral bevel gears for the petroleum, chemical, and gas industries. Gears manufactured according to this standard are limited to the following pitchline velocities: helical gears shall not exceed 12,000 ft/min (60 m/s) and spiral bevel gears shall not exceed 8,000 ft/min (40 m/s). This standard includes related lubricating systems, instrumentation, and other auxiliary equipment. This edition also included the new material related to gear inspection.

Application of the Mechanical Standards to the Gas Turbine

An examination of the above standards as they apply to the gas turbine and its auxiliaries is further explored in this section. The ASME B 133.2, *Basic Gas Turbines*, and the API Standard 616, *Gas Turbines for the Petroleum, Chemical, and Gas Industry Services*, are intended to cover the minimum specifications necessary to maintain a high degree of reliability in an open-cycle gas turbine for mechanical drive, generator drive, or hot-gas generation. This standard also covers the necessary auxiliary requirements directly or indirectly by referring to other listed standards.

It defines terms used in the industry and describes the basic design of the unit. It deals with the casing, rotors and shafts, wheels and blades, combustors, seals, bearings, critical speeds, pipe connections and auxiliary piping, mounting plates, weatherproofing, and acoustical treatment.

The specifications call preferably for a two-bearing construction. Two-bearing construction is desirable in single-shaft units, as a three-bearing configuration can cause considerable trouble, especially when the center bearing in the hot zone develops alignment problems. The preferable casing is a horizontally split unit with easy visual access to the compressor and turbine, permitting field balancing planes without removal of the major casing components. The stationary blades should be easily removable without removing the rotor.

A requirement of the standards is that the fundamental natural frequency of the blade should be at least two times the maximum continuous speed, and at least 10% away from the passing frequencies of any stationary parts. Experience has shown that the natural frequency should be at least four times the maximum continuous speed. Care should be exercised on units where there is a great change in the number of blades between stages.

A controversial requirement of the specifications is that rotating blades or labyrinths for shrouded rotating blades be designed for slight rubbing. A slight rubbing of the labyrinths is usually acceptable, but excessive rubbing can lead to major problems. New gas turbines use “squealer blades,” but some manufacturers suggest using ceramic tips, but whatever is used, great care should be exercised or blade failure and housing damage may occur.

Labyrinth seals should be used at all external points, and sealing pressures should be kept close to atmospheric pressure. The bearings can be either rolling element bearings, usually used in aeroderivative-type gas turbines, or hydrodynamic bearings used in the heavier frame-type gas turbines. In the case of hydrodynamics bearings, tilting pad bearings are recommended since they are less susceptible to oil whirl and can better handle misalignment problems.

Chapter 5 defines in detail the terms used in this section. A quick definition of these terms can be given as follows:

- Unbalance is caused by the uneven distribution of mass about the geometric axis of the system (Chapter 18).
- Critical speed is the speed of the turbine, which is equal to the system's natural frequency. A turbine operating below its first critical speed should be at least 20% above the operating speed range. The term commonly used for describing units operating below their first critical is that the unit has a "stiff shaft," while units operating above their first critical are said to have a "flexible shaft."

There are many exciting frequencies that need to be considered in a turbine. Some of the sources that provide excitation in a turbine system are as follows:

1. Rotor unbalance
2. Rotation is the turning of the rotor around its own axis, and whirling is the movement of the rotor center in a circular motion mechanisms such as:
   a. Oil whirl
   b. Coulomb whirl
   c. Aerodynamic cross-coupling whirl
   d. Hydrodynamic whirl
   d. Hysteretic whirl
3. Blade and vane passing frequencies are based on the number of blades or vanes times the rotational speed
4. Gear mesh frequencies are based on the number of gear teeth times the rotational speed
5. Misalignment is the alignment of the drive with the driven equipment after both units have reached their operating temperatures (Chapter 18)
6. Flow separation in boundary layer exciting blades
7. Ball/race frequencies in antifriction bearings usually used in aeroderivative-type gas turbines

Torsional criticals is the twisting of the shaft during rapid starts. It should be at least 10% away from the first or second harmonics of the rotating frequency. Torsional excitations can be excited by some of the following factors:

1. Start-up conditions, such as speed detents
2. Undersized shaft
3. Gear problems, such as unbalance and pitchline runout
4. Fuel pulsation, especially in low NO_x combustors

The maximum unbalance is not to exceed 2.0 mils (0.051 mm) on rotors with speeds below 4,000 rpm, 1.5 mils (0.04 mm) for speeds between 4,000 and 8,000 rpm, 1.0 mil (0.0254 mm) for speeds between 8,000 and 12,000 rpm, and 0.5 mils (0.0127 mm) for speeds above 12,000 rpm. These requirements are to be met in any plane and also

include shaft runout. The following relationship is specified by the API standard:

$$L_v = \sqrt{\frac{12{,}000}{N}} \tag{4-1}$$

where

L_v = vibration limit mils (thousandth of an inch) or millimeters (mils × 25.4)
N = operating speed (rpm)

The maximum unbalance per plane (journal) shall be given by the following relationships:

$$U_{max} = \frac{4W}{N} \tag{4-2}$$

where

U_{max} = residual unbalance ounce – inches (gram – millimeters)
W = journal static weight lbs (kilogram)

A computation of the force on the bearings should be calculated to determine whether or not the maximum unbalance is an excessive force.

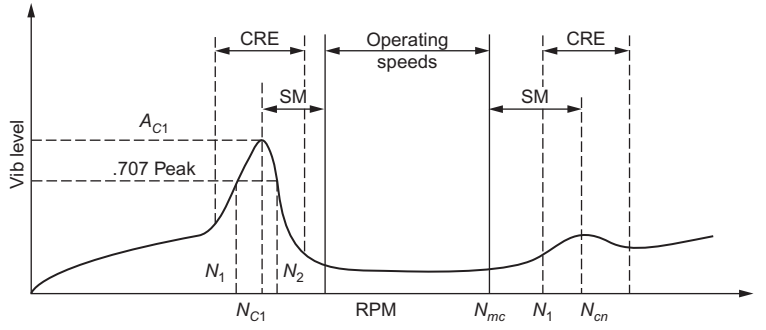
The concept of an amplification factor (AF) is introduced in the new API 616 standard. Amplification factor is defined as the ratio of the critical speed to the speed change at the root mean square of the critical amplitudes:

$$\text{AF} = \frac{N_{c1}}{(N_2 - N_1)} \tag{4-3}$$

Figure 4-7 is an amplitude–speed curve showing the location of the running speed to the critical speed and the amplitude increase near the critical speed. When the rotor amplification factor, as measured at the vibration probe, is greater than or equal to 2.5 that frequency is called critical and the corresponding shaft rotational frequency is called a critical speed. For the purposes of this standard, a critically damped system is one in which the amplification factor is less than 2.5.

Balancing requirement in the specifications require that the rotor with blades assembled must be dynamically balanced without the coupling, but with the half key, if any, in place. The specifications do not discuss whether this balancing is to be done at high or low speeds. The balancing conducted in most shops is at low speed. A high-speed balancing should be used on problem shafts, and any units, which operate above the second critical. Field balancing requirements should be specified.

The lubrication system for the turbine is designed to provide both lubrication and cooling. It is not unusual that in the case of many gas turbines, the maximum temperature reached in the bearing section is about 10–15 minutes after the unit has been



N_{C1} = Rotor first critical, center frequency, cycles per minute
N_{cn} = Critical speed, nth
N_+ = Trip speed
N_{mc} = Maximum continuous speed, 105%
N_1 = Initial (lesser) speed at .707 × peak amplitude (critical)
N_2 = Final (greater) speed at .707 × peak amplitude (critical)
$N_2 - N_1$ = Peak width at the "half-power" point

AF = Amplification factor $= \dfrac{N_{C1}}{N_2 - N_1}$
SM = Separation margin
CRE = Critical response envelope
N_{c1} = Amplitude @ N_{c1}
A_{cn} = Amplitude @ N_{cn}

Figure 4-7 Rotor response plot. (Figure 7 of Standard 617, *Centrifugal Compressors for General Refinery Services*, Fourth Edition, 1979, reprinted by courtesy of the American Petroleum Institute.)

shutdown. This means that the lubrication system should continue to operate for a minimum of 20 minutes after the turbine has been shutdown. This system closely follows the outline in API Standard 614, which is discussed in detail in Chapter 15. Separate lubrication systems for various sections of the turbine and driven equipment may be supplied. Many vendors and some manufacturers provide two separate lubrication systems: one for hot bearings in the gas turbines and the other for cool bearings of the driven compressor. These and other lubrication systems should be detailed in the specifications.

The inlet and exhaust systems in gas turbines are described. The inlet and exhaust systems consist of an inlet filter, silencers, ducting, and expansion joints. The design of these systems can be critical to the overall design of a gas turbine. Proper filtration is a must; otherwise, problems of blade contamination and erosion ensue. The standards are minimal for the specifications, calling for a coarse metal screen to prevent debris from entering, a rain or snow shield for protection from the elements, and a differential pressure alarm. Most manufacturers are now suggesting so-called high-efficiency filters that have two stages of filtration: an inertia stage, to remove particles above 5 μm, followed by one or more filter screens, self-cleaning filters, pad-type prefilters, or a combination of them, to remove particles below 5 μm. Differential pressure alarms are provided by manufacturers, but the trend among users has been to ignore them. It is suggested that more attention be paid to differential pressure than in the past, to assure high-efficiency operation.

Silencers are also minimally specified. Work in this area has progressed dramatically in the past few years with the NASA quiet engine program. There are some good silencers now available on the market, and inlets can be acoustically treated.

Starting equipment will vary, depending on the location of the unit. Starting drives include electric motors, steam turbines, diesel engines, expansion turbines, and hydraulic motors. The sizing of a starting unit will depend on whether the unit is a single- or a multiple-shaft turbine with a free-power turbine. The vendor is required to produce speed-torque curves of the turbine and driven equipment with the starting unit torque superimposed. In a free-power turbine design, the starting unit has to only overcome the torque to start the gas generator system. In a single-shaft turbine, the starting unit has to overcome the total torque. Turning gears are recommended in the specifications, especially on large units to avoid shaft bowing. They should always be turned on after the unit has been "brought down" and should be kept operational until the rotor is cooled.

The gears should meet API Standard 613. Gear units should be double-helical gears provided with thrust bearings. Load gears should be provided with a shaft extension to permit torsional vibration measurements. On high-speed gears, proper use of the lubricant as a coolant should be provided. Spraying oil as a coolant on the teeth and face of the units is recommended to prevent distortion. Chapter 14 details the design and operation characteristics of gears.

Couplings should be designed to take the necessary casing and shaft expansion. Expansion is one reason for the wide acceptance of dry flexible coupling. A flexible diaphragm coupling is more forgiving in angular alignment; however, a gear-type coupling is better for axial movement. Access for hot alignment checks must be provided. The couplings should be dynamically balanced independently of the rotor system. Chapter 18 deals with the various types of couplings and the alignment techniques for gas turbines.

Controls, instrumentation, and electrical systems in a gas turbine are defined. The outline in the standard is the minimum a user needs for safe operation of a unit. More details of the instrumentation and controls are given in Chapter 19.

The starting system can be manual, semiautomatic, or automatic, but in all cases, it should provide controlled acceleration to minimum governor speed and then, although not called for in the standards, to full speed. Units that do not have controlled acceleration to full speed have burned out first- and second-stage nozzles when combustion occurred in those areas instead of in the combustor. Purging the system of the fuel after a failed start is mandatory, even in the manual operation mode. Sufficient time for the purging of the system should be provided, so that the volume of the entire exhaust system has been displaced at least five times.

Alarms should be provided on a gas turbine. The standards call for alarms to be provided to indicate malfunction of oil and fuel pressure, high exhaust temperature, high differential pressure across the air filter, excessive vibration levels, low oil reservoir levels, high differential pressure across oil filters, and high oil drain temperatures from the gearings. Shutdown occurs with low oil pressure, high exhaust temperature, and combustor flameout. It is recommended that shutdown also occur with high thrust-bearing temperatures and with a temperature differential in the exhaust temperature.

Vibration detectors suggested in the standards are noncontacting probes. Presently, most manufacturers provide velocity transducers mounted on the casing, but these are inadequate. A combination of noncontacting probes and accelerometers are needed to ensure the smooth operation and diagnostic capabilities of the unit.

Fuel systems can cause many problems, and fuel nozzles are especially susceptible to trouble. A gaseous fuel system consists of fuel filters, regulators, and gauges. Fuel is injected at a pressure of about 60 psi (4 Bar) above the compressor discharge pressure for which a gas compression system is needed. Knockout drums or centrifuges are recommended and should be implemented to ensure that there are no liquid carry-overs in the gaseous system.

Liquid fuels require atomization and treatment to inhibit sodium and vanadium content. Liquid fuels can drastically reduce the life of a unit if not properly treated. A typical fuel system is shown in Figure 4-8. The effect of fuels on gas turbines and the details of types of fuel handling systems are given in Chapter 12.

Recommended materials are outlined in the standards. Some of the recommendations in the standard are carbon steel for base plates, heat-treated forged steel for compressor wheels, heat-treated forged alloy steel for turbine wheels, and forged steel for couplings. The growth of materials technology has been so rapid, especially in the area of high-temperature materials, which the standard does not deal with. Details of some of the materials technology of the high-temperature alloys and single-crystal blades are dealt in Chapters 9 and 11. However, the standards call for blading, which must have at least 8,000 trouble-free operating hours in similar operating conditions.

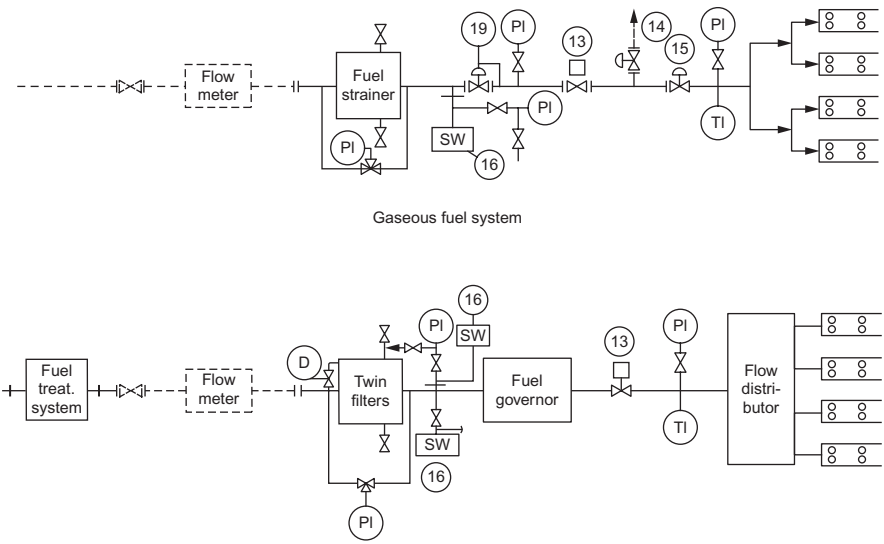


Figure 4-8 Fuel systems for gas turbines (figures C-2 and C-3 of Standard 616, *Combustion Gas Turbines for General Refinery Services*, First edition, 1968, reprinted by courtesy of the American Petroleum Institute).

The vendor is required to present Campbell (Chapter 5) and Goodman diagrams (Chapter 11) for the blading backed by demonstrated experience in the application of identical blades operating with the same source or frequency of excitation that is present in the unit. The Campbell diagram locates the speed at which various components are excited by the rotational speed of the turbine. The Goodman diagram shows the effect of alternating stresses on the life of the material in concern, such as a compressor or turbine blade. The vendor shall indicate on the Goodman diagrams the standard acceptance margins. Chapter 11 deals with the Goodman diagram for materials. All Campbell diagrams shall show the blade frequencies that have been corrected to reflect actual operating conditions. Whenever applicable, the diagrams for shrouded blades shall show frequencies above and below the blade lock-up speed and shall specify the speed at which blade lock-up occurs. Chapter 5 gives details of the Campbell diagram, and Chapter 16 deals with the types of signals emitted by the resonance of blades.

The tips of rotating blades and the labyrinths of shrouded rotating blades shall be designed to allow the unit to start-up at any time in accordance with the vendor's requirements. When the design permits rubbing during normal start-up, the component shall be designed to be rub tolerant and the vendor shall state in his/her proposal if rubbing is expected.

The blade natural frequencies shall not coincide with any source of excitation from 10% below minimum governed speed to 10% above maximum continuous speed. If this is not feasible, blade stress levels developed at any specified driven equipment operation shall be low enough to allow unrestricted operation for the minimum service life. Blades shall be designed to withstand operation at resonant frequencies during normal warm-up. Speeds below the operation range corresponding to such blade resonance should be clearly specified.

Excitation sources, which should be included in the Campbell diagrams, should include: fundamental and first harmonic passing frequencies of rotating and stationary blades upstream and downstream of each blade row, gas passage splitters, irregularities in vane and nozzle pitch at horizontal casing flanges, the first 10 rotor speed harmonics, meshing frequencies in gear units, and periodic impulses caused by the combustor arrangement.

The turbine undergoes three basic tests: hydrostatic, mechanical, and performance. Hydrostatic tests are to be conducted on pressure-containing parts with water at least one-and-a-half times the maximum operating pressure. The mechanical run tests are to be conducted for at least a period of four hours at maximum continuous speed. This test is usually done at no-load conditions. It checks out the bearing performance and vibration levels as well as overall mechanical operability. It is suggested that the user have a representative at this test to tape record as much of the data as possible. The data are helpful in further evaluation of the unit or can be used as baseline data. Performance tests should be conducted at maximum power with normal fuel composition. The tests should be conducted in accordance with ASME PTC-22, which is described in more detail in Chapter 20.

Gears

This standard API Standard 613 covers special purpose gears. They are defined as gears, which have either or both actual pinion speeds of more than 2,900 rpm and pitchline velocities of more than 5,000 ft/min (27 m/s). The standard applies to helical gears employed in speed-reducer or speed-increaser units.

The scope and terms used are well defined and includes a listing of standards and codes for reference. The purchaser is required to make decisions regarding gear-rated horsepower and rated input and output speeds.

This standard includes basic design information and is related to AGMA Standard 421. Specifications for cooling water systems as well as information about shaft assembly designation and shaft rotation are given. Gear-rated power is the maximum power capability of the driver. Normally, the horsepower rating for gear units between a driver and a driven unit would be 110% of the maximum power required by the driven unit or 110% of the maximum power of the driver, whichever is greater.

The tooth-pitting index or K factor is defined as:

$$K = \frac{W_t}{F \times d} \times \frac{(R+1)}{R} \tag{4-4}$$

where

W_t = transmitted tangential load, in pounds at the operating pitch diameter

$$W_t = \frac{12{,}600 \times \text{gear} - \text{rated horse poower}}{\text{Pinion rpm} \times d}$$

where

F = net face width, inches
d = pinion pitch diameter, inches
R = ratio (number teeth in gear divided by number teeth in pinion)

The allowable K factor is given by

$$\text{Allowable}\, K = \frac{\text{Material index number}}{\text{Service factor}} \tag{4-5}$$

Service factors and material index number tabulation are provided for various typical applications, allowing the determination of the K factor. Gear tooth size and geometry are selected so that bending stresses do not exceed certain limits. The bending stress number (S_t) is given by:

$$S_t = \frac{W_t \times P_{nd}}{F} \times \text{SF} \times \frac{1.8 \cos \phi}{J} \tag{4-6}$$

where

W_t = as defined in Equation (4-4)
P_{nd} = normal diametral pitch
F = net face width, inches
ϕ = helix angle
J = geometry factor (from AGMA 226)
SF = service factor

Design parameters on casings, joint supports, bolting methods, and some service and size criteria are included.

Critical speeds correspond to the natural frequencies of the gears and the rotor bearings support system. A determination of the critical speed is made by knowing the natural frequency of the system and the forcing function. Typical forcing functions are caused by rotor unbalance, oil filters, misalignment, and a synchronous whirl.

Gear elements must be multiplane and dynamically balanced. When keys are used in couplings, half-keys must be in place. The maximum allowable unbalanced force at maximum continuous speed should not exceed 10% of static weight load on the journal. The maximum allowable residual unbalance in the plane of each journal is calculated using the following relationship:

$$F = mrw^2. \tag{4-7}$$

since the force must not exceed 10% of the static journal load,

$$mr = \frac{0.1W}{\varpi^2} \tag{4-8}$$

Taking the correction constants, the equation can be written as:

$$\text{Maximumun balanced force} = \frac{56{,}347 \times \text{Journal static weight load}}{\text{rpm}^2}. \tag{4-9}$$

The double amplitude of unfiltered vibration in any plane measured on the shaft adjacent to each radial bearing is not to exceed 2.0 mils (0.05 mm) or the value given by:

$$\text{Amplitude} = \sqrt{\frac{12{,}000}{\text{rpm}}} \tag{4-10}$$

where rpm is the maximum continuous speed. It is more meaningful for gears to be instrumented using accelerometers. Design specifications for bearings, seals, and lubrication are also given.

Accessories such as couplings, coupling guards, mounting plates, piping, instrumentation, and controls are described. Inspection and testing procedures are detailed.

The purchaser is allowed to inspect the equipment during manufacture after notifying the vendor. All welds in rotating parts must receive 100% inspection. To conduct a mechanical run test, the unit must be operated at maximum continuous speed until the bearing and lube oil temperatures have stabilized. Then, the speed is increased to 110% of maximum continuous speed and run for four hours.

Lubrication Systems

This API Standard 614 covers the minimum requirements for lubrication systems, oil-type shaft-sealing systems, and related control systems for special purpose applications. The terms are fully defined, references are well documented, and basic design is described. Details of the lubrication system are presented in Chapter 15.

Lubrication systems should be designed to meet continuously all conditions for a nonstop operation of three years. Typical lubricants should be hydrocarbon oils with approximate viscosities of 150 SUS at 100 °F (37.8 °C). Oil reservoirs should be sealed to prevent the entrance of dirt and water and sloped at the bottom to facilitate drainage. The reservoir working capacity should be sufficient for at least a five minutes flow. A typical reservoir is shown in Figure 4-9. The oil system should include a main oil pump and a standby oil pump. Each pump must have its own driver sized according to API Standard 610. Pump capacities should be based on the systems' maximum usage plus a minimum of 15%. For seal oil systems, the pump capacity should be maximum capacity plus 20% or 10 gpm, whichever is greater. The standby oil pump should have an automatic start-up control to maintain safe operation if the main pump fails. Twin oil coolers should be provided, and each should be sized to accommodate the total cooling load. Full-flow twin oil filters should be furnished downstream of the coolers. Filtration should be 10 μm nominal. The pressure drop for clean filters should not exceed five psi (0.34 Bar) at 100 °F (37.8 °C) operating temperature during normal flow.

Overhead tanks, purifiers, and degasing drums are covered. All pipe welding is to be done according to Section IX of the ASME code, and all piping must be seamless carbon steel, minimum schedule of 80 for sizes 1½ in. (38.1 mm) and smaller, and a minimum schedule of 40 for pipe sizes two inches. (50.8 mm) or greater.

The lubrication control system should enable orderly start-up, stable operation, warning of abnormal conditions, and shutdown of main equipment in the event of impending damage. A list of required alarm and shutdown devices is provided. Figure 4-10 is a schematic representation of a seal lube and control-oil system. The purchaser has the right to inspect the work and test the sub-components if he/she informs the vendor in advance. Each cooler, filter, accumulator, and other pressure vessels should be hydrostatically tested at one and one-half times design pressure. Cooling water jackets and other water-handling components should be tested at one and one-half times design pressure. The test pressure should not be less than 115 psig (7.9 Bar). Tests should be maintained for durations of at least 30 minutes.

Operational tests should:

1. Detect and correct all leaks.
2. Determine relief pressures and check for proper operation of each relief valve.

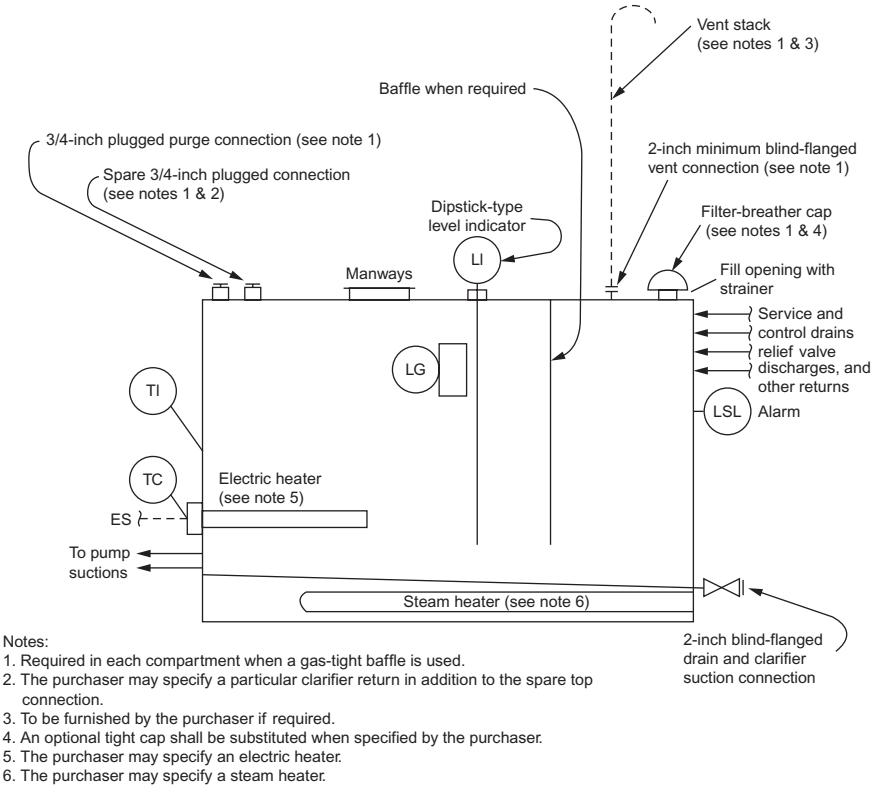
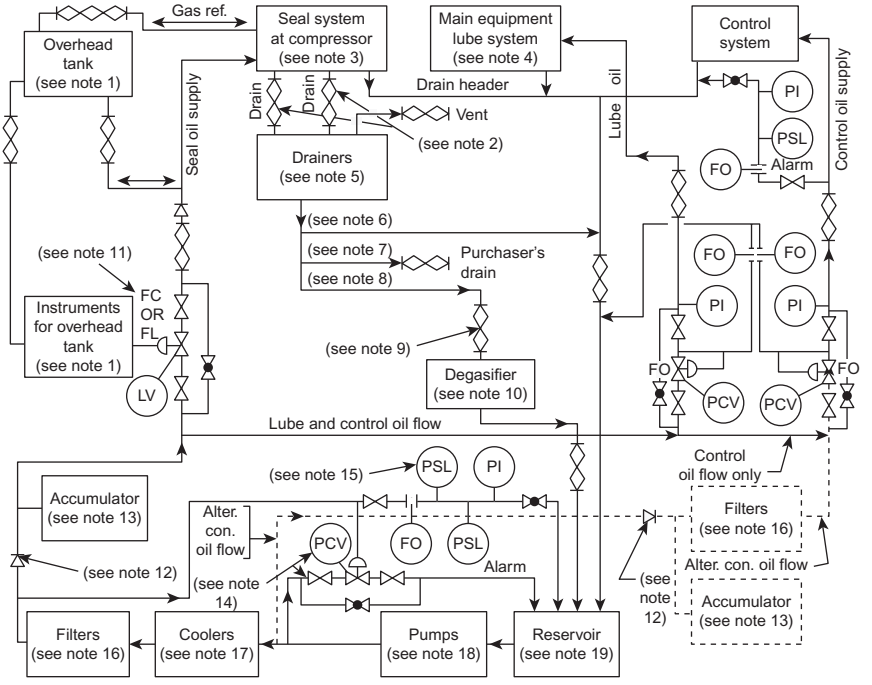


Figure 4-9 Standard oil reservoir (Figure A-2 of Standard 614, *Lubrication, Shaft-Sealing, and Control Oil Systems for Special-Purpose Applications*, First Edition, 1973, reprinted by courtesy of the American Petroleum Institute).

3. Accomplish a filter cooler changeover without causing start-up of the standby pump.
4. Demonstrate that the control valves have suitable capacity, response, and stability.
5. Demonstrate that the oil pressure control valve can control-oil pressure.

Vibration Measurements

The API Standard 670 covers the minimum requirements for non-contacting vibration in an axial-position monitoring system. The accuracy for the vibration channels should meet a linearity of ±5% of 200 mV/mil (0.001 in., 0.0254 mm) sensitivity over a minimum operating range of 80 mils (2.032 mm). For the axial position, the channel linearity must be ±5% of 200 mV/mil sensitivity and a ±1.0 mil of a straight line over a minimum operating range of 80 mils (2.032 mm). Temperature should not affect the linearity of the system by more than 5% over a temperature range of −30–350 °F (−34.4–176.7 °C) for the probe and extension cable. The oscillator demodulator is a signal conditioning device powered by −24 V of direct current. It sends a radio frequency signal to the probe and demodulates the probe output. It



This arrangement is valid only when the pressure of the seal oil supply is higher than the pressure of the control oil supply

Notes:
1. Overhead tank with instrumentation.
2. Connections by vendor when drainers are mounted on compressor baseplate.
3. Seal oil system at compressor only.
4. Lubrication system at main equipment only.
5. Float-controlled inner-seal drainers for transmitter-controlled inner-seal drainers.
6. Drain to reservoir.
7. Drain to purchaser's drains.
8. Drain to degassing drum.
9. Connections by vendor if degasifier is mounted on compressor baseplate.
10. Degassing drum.
11. The purchaser must specify the desired failure action for the LV.
12. Omit check valve if accumulator is not used.
13. Direct-contact-type accumulator or bladder-type accumulator when required.
14. Omit the bypass PCV circuit if centrifugal pumps are used.
15. Switch to start standby pump.
16. Single oil filter or twin oil filters.
17. Single oil cooler or twin oil coolers.
18. Primary pumps.
19. Oil reservoir.

Figure 4-10 Combined seal, lube, and control-oil system with an overhead tank (Figure A-32 of Standard 614, *Lubrication, Shaft-Sealing, and Control Oil Systems for Special-Purpose Applications*, First Edition, 1973, reprinted by courtesy of the American Petroleum Institute).

should maintain linearity over the temperature range of −30–150 °F (−34.4–65.6 °C). The monitors and power supply should maintain their linearity over a temperature range of −20–150 °F (−28.9–65.6 °C). The probes, cables, oscillator demodulators, and power supplies installed on a single train should be physically and electrically interchangeable.

The non-contacting vibration and axial-position monitoring system, consisting of probe, cables, connectors, oscillator demodulator, power supply, and monitors. The probe tip diameters should be 0.190–0.195 in. (4.8–4.95 mm) with body diameters of ¼ (6.35 mm) − 28 UNF – 2A threaded, or 0.3–0.312 in. (7.62–7.92 mm) with a body

diameter of 3/8 (9.52 mm) – 24 UNF – 24A threaded. The probe length is about one inch. long. Tests conducted on various manufacturer's probes indicate that the 0.3–312 in. (7.62–7.92 mm) probe has a better linearity in most cases. The integral probe cables have a cover of tetra-fluoroethylene, a flexible stainless steel armoring, which extends to within four inches of the connector. The overall physical length should be approximately 36 in. (914.4 mm) measured from probe tip to the end of the connector. The electrical length of the probe and integral cable should be six feet. The extension cables should be coaxial with electrical and physical lengths of 108 in. (2743.2 mm). The oscillator demodulator will operate with a standard supply voltage of −24 V dc and will be calibrated for a standard electrical length of 15 ft (5 m). This length corresponds to the probe integral cable and extension. Monitors should operate from a power supply of 117 V ±5% with the linearity requirements specified. False shutdown from power interruption will be prevented regardless of mode or duration. Power supply failure should actuate an alarm.

The radial transducers should be placed within three inches of the bearing, and there should be two radial transducers at each bearing. Care should be taken not to place the probe at the nodal points. The two probes should be mounted 90 °apart (±5 °) at a 45 °(±5 °) angle from each side of the vertical center. Viewed from the drive end of the machine train, the *x* probe will be on the right side of the vertical and the *y* probe will be on the left side of the vertical. Figures 4-11 and 4-12 show protection systems for a turbine and a gearbox, respectively.

The axial transducers should have one probe sensing the shaft itself within 12 inches (305 mm) of the active surface of the thrust collar with the other probe sensing the machined surface of the thrust collar. The probes should be mounted facing the opposite directions. Temperature probes embedded in the bearings are often more useful in preventing thrust-bearing failures than the proximity probe. This is because of expansion of the shaft casing and the probability that the probe is located far from the thrust collar.

When designing a system for thrust-bearing protection, it is necessary to monitor small changes in rotor axial movement equal to oil film thickness. Probe system accuracy and probe mounting must be carefully analyzed to minimize temperature drift. Drift from temperature changes can be unacceptably high.

A functional alternative to the use of proximity probes for bearing protection is bearing temperature, bearing temperature rise (bearing temperature − bearing oil temperature), and rate of change in bearing temperature. A matrix combining these functions can produce a positive indication of bearing distress.

A phase-angle transducer should also be supplied with each train. This transducer should record one event per revolution. When intervening gearboxes are used, a mark and phase-angle transducer should be provided for each different rotational speed.

Specifications

The previous API standards are guidelines to information regarding machine train applications. The more pertinent the information obtained during the evaluation of the proposal, the better the selection for the problem. The following list contains items

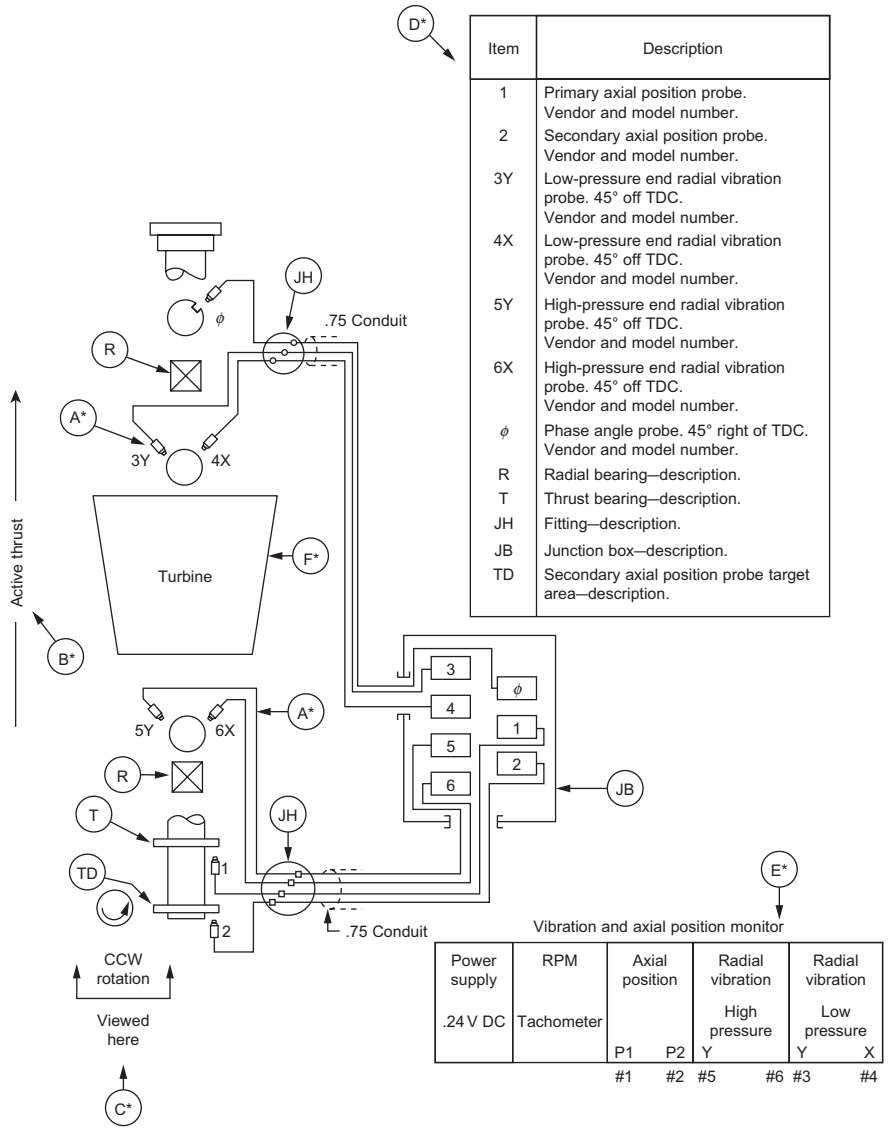
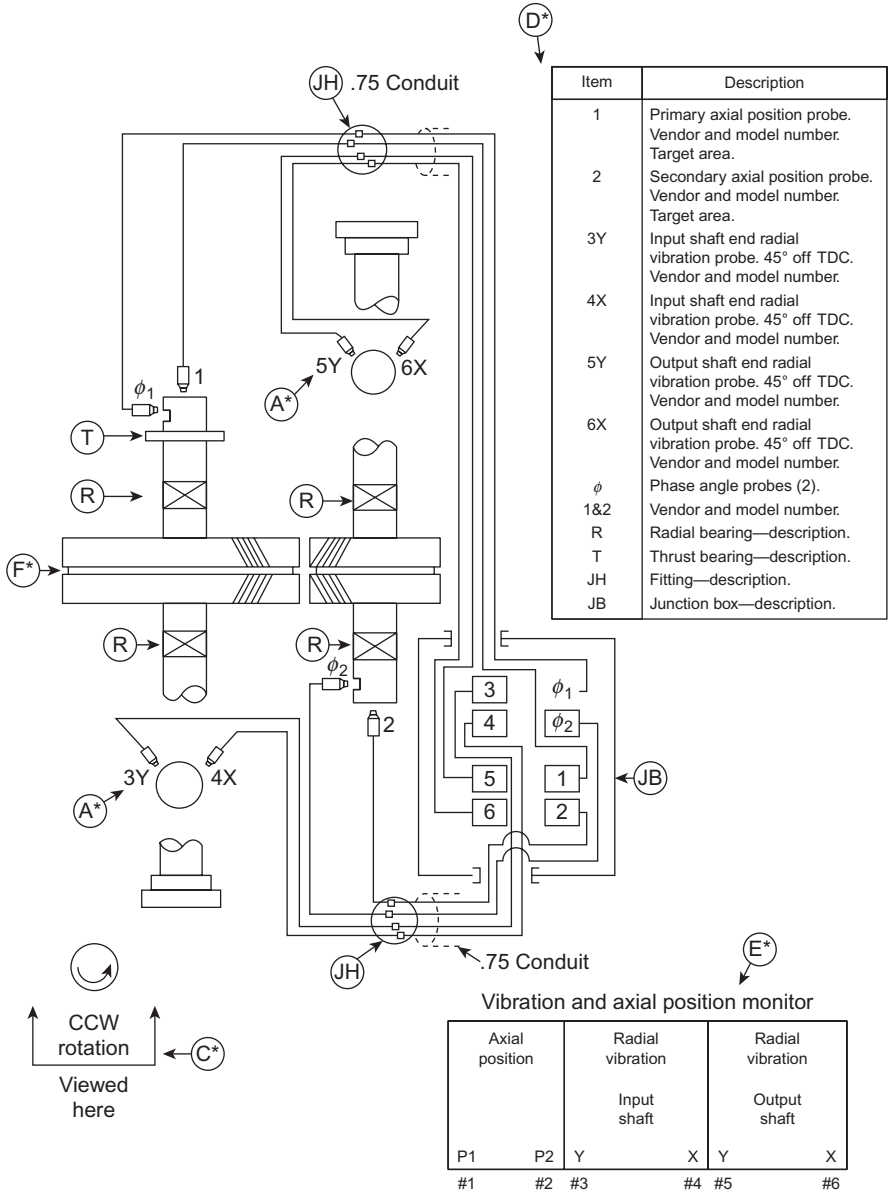


Figure 4-11 Typical protection system for a turbine (Figure C-1 of Standard 670, *Noncontacting Vibration and Axial-Position Monitoring Systems*, First Edition, 1976, reprinted by courtesy of the American Petroleum Institute).

the user should consider in his/her attempt to properly evaluate the bid. Some of these points are covered in the API standards.

Table 4-2 indicates the main points an engineer must consider in evaluating different gas turbine units. Table 4-3 lists the important points that must be supplied to the vendor, while the important points to consider in evaluating centrifugal compressors



Item	Description
1	Primary axial position probe. Vendor and model number. Target area.
2	Secondary axial position probe. Vendor and model number. Target area.
3Y	Input shaft end radial vibration probe. 45° off TDC. Vendor and model number.
4X	Input shaft end radial vibration probe. 45° off TDC. Vendor and model number.
5Y	Output shaft end radial vibration probe. 45° off TDC. Vendor and model number.
6X	Output shaft end radial vibration probe. 45° off TDC. Vendor and model number.
ϕ	Phase angle probes (2).
1&2	Vendor and model number.
R	Radial bearing—description.
T	Thrust bearing—description.
JH	Fitting—description.
JB	Junction box—description.

Figure 4-12 Typical protection system for a gearbox (Figure C-3 of Standard 670, *Noncontacting Vibration and Axial-Position Monitoring Systems*, First Edition, 1976, reprinted by courtesy of the American Petroleum Institute).

are listed in Table 4-4. These tables will enable the engineer to make a proper evaluation of each critical point and ensure that he/she is purchasing units of high reliability and efficiency.

Table 4-2 Point to Consider in a Gas Turbine

1. Types of turbine
   Aeroderivative
   Frame type
2. Type of fuel
3. Type of compressor
4. Number of stages and pressure ratio
5. Types of blades, blade attachment, and wheel attachment
6. Number of bearings
7. Type of bearings
8. Type of thrust bearings
9. Critical speed
10. Torsional criticals
11. Campbell diagrams
12. Balance planes
13. Balance pistons
14. Type of combustor
15. Wet and dry combustors
16. Types of fuel nozzles
17. Transition pieces
18. Type of turbine
19. Power transmission curvic coupling
20. Number of stages
21. Free-power turbine
22. Turbine inlet temperature
23. Fuel additives
24. Types of couplings
25. Alignment data
26. Exhaust diffuser
27. Performance map of turbine and compressor
28. Gearing
29. Drawings

Accessories

a. Lubrication systems
b. Intercoolers
c. Inlet filtration system
d. Control system
e. Protection system

Table 4-3 Vendor Requirements to Be Provided By the User for a Compressor Train

1. *The gas to be handled* (*each stream*)
   Composition by mol%, volume %, or weight %. To what extent does composition vary?

   Corrosive effects. Limits to discharge temperature, which may cause problems with the gas.
2. *Quantity to be handled for each stage*
   Stage quantity and unit of measurement.
   If by volume, show:
   a. Whether wet or dry.
   b. Pressure and temperature reference points.
3. *Inlet conditions for each stage*
   Barometer
   Pressure at compressor flange
   State whether gauge or absolute
   Temperature at compressor flange
   Relative humidity
   Ratio of specific heats
   Compressibility
4. *Discharge conditions*
   Pressure at compressor flange
   State whether gauge or absolute
   Compressibility
   State temperature reference
5. *Interstage conditions*
   Temperature difference between gas out of cooler and water into cooler
   Is there interstage removal or addition of gas?
   Between what pressures may this be done? Advise permissible range
   If gas is removed, treated, and returned between stages, advise pressure loss
   What quantity change is involved?
   If this changes gas composition, a resultant analysis (ratio of specific heats, relative humidity, and compressibility at specific interstage pressure and temperature) must be provided
6. *Variable conditions*
   State-expected variation in intake conditions – pressure, temperature, relative humidity, molecular weight, etc.
   State-expected variation in discharge pressure
   It is extremely important that changing conditions be related to each other.
   If relative humidity varies from 50% to 100% and inlet temperature varies from 0 °F to 100 °F, does 100% RH correspond with 100 °F?
   Variations in conditions are best shown in tabular form with all conditions included in each column

(*Continued*)

Table 4-3 (*Continued*)

7. *Flow diagram*
   Provide a schematic flow sheet showing controls involved
8. *Regulation*
   What is to be controlled – pressure, flow, or temperature?
   Advise permissible variation in controlled item
   Is regulation manual or automatic?
   If automatic, are operating devices and/or instruments to be included?
   How many control steps are desired on a reciprocator?
9. *Cooling water*
   Temperature: maximum and minimum
   Pressure at inlet and back pressure, if any
   Whether open or closed cooling system is desired
   Source of water
   Fresh, sale, or brackish
   Silty or corrosive
10. *Driver*
    Specify type of driver
    Electric motor: type, current conditions, power factor, enclosure, service factor, temperature rise, ambient temperature
    Steam: inlet and exhaust pressure, inlet temperature and quality, importance of minimum water rate
    Fuel gas: gas analysis, available pressure, low heating value of gas
    Geared: AGMA rating if special
11. *General*
    Acceptability of petroleum lubricants?
    Indoor or outdoor installation?
    Floor space, special shape? Provide a sketch
    Soil character
    List accessories desired and advise which are to be spared
    Pulsation dampeners or intake or discharge silencers to be supplied
12. *Specifications*
    Provide each bidder with three copies of any specification for the particular project
    Complete information enables all manufacturers to bid competitively on the same basis and assists the purchaser in evaluating bids

Table 4-4 Points to Consider in a Centrifugal Compressor

1. Number of stages
2. Pressure ratio and mass flow (per casing)
3. Type of gas seals (inner seal) and oil seals
4. Type of bearings (radial)
5. Bearing stiffness coefficients
6. Types of thrust bearings (tapered land, nonequalizing tilting pad, and Kingsbury)
7. Thrust float
8. Temperature for journal and thrust bearings (operating temperature)
9. Critical speed diagram (speed vs. bearing stiffness curve)
10. Type of impeller:
    a. Shroud or unshrouded
    b. Blading
    c. Attachment of blades to hub and shroud
11. Attachment of impellers to shaft:
    a. Shrink fit
    b. Key fit
    c. Other
12. Campbell diagrams of impellers:
    a. Number of blades (impellers)
    b. Number of blades (diffuser)
    c. Number of blades (guide vanes)
13. Balance piston
14. Balance planes (location):
    a. How is it balanced (detail)
15. Weight of toros (assembled):
    a. Split casing
    b. Barrel
16. Data on torsional vibration (bending criticals)
17. Alignment data
18. Type of coupling between tandems
19. Performance curves (separate casings):
    a. Surge margin
    b. Surge line
    c. Aerodynamic speed
    d. Efficiency
20. Intercooling type of cooler:
    a. Temperature drop
    b. Pressure drop
    c. Efficiency
21. Horsepower curves

Copyrighted Materials
Copyright © 2012 Elsevier Retrieved from www.knovel.com

5 Rotor Dynamics

The present trend in rotating equipment is toward increasing design speeds, which increases operational problems from vibration; hence the importance of vibration analysis. A thorough appreciation of vibration analysis will aid in the diagnoses of rotor dynamics problems.

This chapter is devoted to vibration theory fundamentals concerning undamped and damped freely oscillating systems. Application of vibration theory to solving rotor dynamics problems is then discussed. Next, critical speed analysis and balancing techniques are examined. The latter part of the chapter discusses important design criteria for rotating machinery, specifically bearing driver types, and design and selection procedures.

Mathematical Analysis

The study of vibrations was confined to musicians until classical mechanics had advanced sufficiently to allow an analysis of this complex phenomenon. Newtonian mechanics provides an approach which, conceptually, is easy to understand. Lagrangian mechanics provides a more sophisticated approach, but it is intuitively more difficult to conceive. Since this book uses some basic concepts, we will approach the subject using Newtonian mechanics.

Vibration systems fall into two major categories: forced and free. A free system vibrates under forces inherent in the system. This type of system will vibrate at one or more of its natural frequencies, which are properties of the elastic system. Forced vibration is vibration caused by external force being impressed on the system. This type of vibration takes place at the frequency of the exciting force, which is an arbitrary quantity independent of the natural frequencies of the system. When the frequency of the exciting force and the natural frequency coincide, a resonance condition is reached, and dangerously large amplitudes may result. All vibrating systems are subject to some form of damping due to energy dissipated by friction or other resistances.

The number of independent coordinates, which describe the system motion, are called the degrees of freedom of the system. A single degree of freedom system is one that requires a single independent coordinate to completely describe its vibration configuration. The classical spring mass system shown in Figure 5-1 is a single degree of freedom system.

Gas Turbine Engineering Handbook, Fourth Edition. DOI: 10.1016/B978-0-12-383842-1.00005-6
Copyright © 2012 Elsevier Inc. All rights reserved.

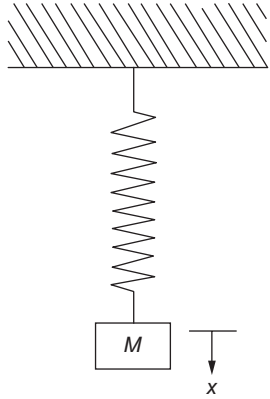


Figure 5-1 System with single degree of freedom.



Figure 5-2 System with infinite number of degrees of freedom.

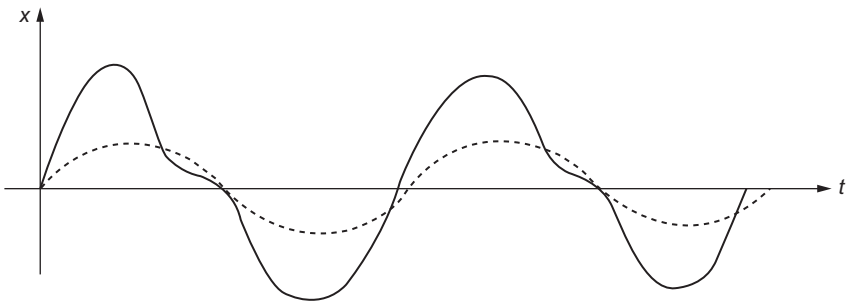


Figure 5-3 Periodic motion with harmonic components.

Systems with two or more degrees of freedom vibrate in a complex manner where frequency and amplitude have no definite relationship. Among the multitudes of unorderly motion, there are some very special types of orderly motion called principal modes of vibration.

During these principal modes of vibration, each point in the system follows a definite pattern of common frequency. A typical system with two or more degrees of vibration is shown in Figure 5-2. This system can be a string stretched between two points or a shaft between two supports. The dotted lines in Figure 5-2 show the various principal vibration modes.

Most types of motion due to vibration occur in periodic motion. Periodic motion repeats itself at equal time intervals. A typical periodic motion is shown in Figure 5-3. The simplest form of periodic motion is harmonic motion, which can be represented by

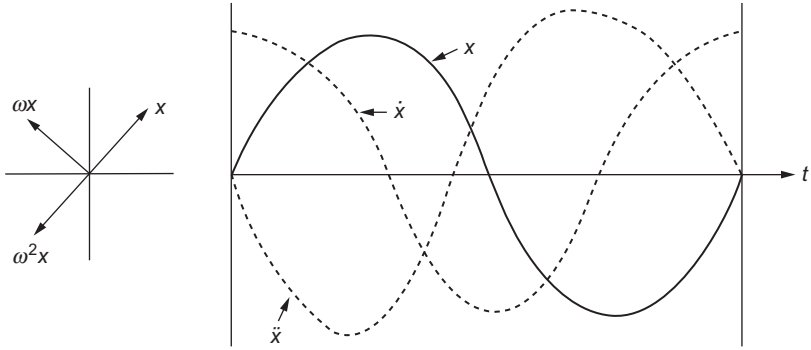


Figure 5-4 Harmonic motion of displacement, velocity, and acceleration.

sine or cosine functions. It is important to remember that harmonic motion is always periodic; however, periodic motion is not always harmonic. Harmonic motion of a system can be represented by the following relationship:

$$x = A\sin\omega t \tag{5-1}$$

Thus, one can determine the velocity and acceleration of that system by differentiating the equation with respect to t

$$\text{Velocity} = \frac{dx}{dt} = A\omega\cos\omega t = A\omega\sin\left(\omega t + \frac{\pi}{2}\right) \tag{5-2}$$

$$\text{Acceleration} = \frac{d^2x}{dt^2} = -A\omega^2\sin\omega t = A\omega^2\sin(\omega t + \pi) \tag{5-3}$$

The previous equations indicate that the velocity and acceleration are also harmonic and can be represented by vectors, which are 90° and 180° ahead of the displacement vectors. Figure 5-4 shows the various harmonic motions of displacement, velocity, and acceleration. The angles between the vectors are called phase angles; therefore, one can say that the velocity leads displacement by 90° and that the acceleration acts in a direction opposite to displacement, or that it leads displacement by 180°.

Undamped Free System

This system is the simplest of all vibration systems and consists of a mass suspended on a spring of negligible mass. Figure 5-5 shows this simple, single degree of freedom system. If the mass is displaced from its original equilibrium position and released, the unbalanced force, the restoring ($-Kx$) of the spring, and acceleration are related through Newton's second law. The resulting equation can be written as follows:

$$m\ddot{x} = -Kx \tag{5-4}$$

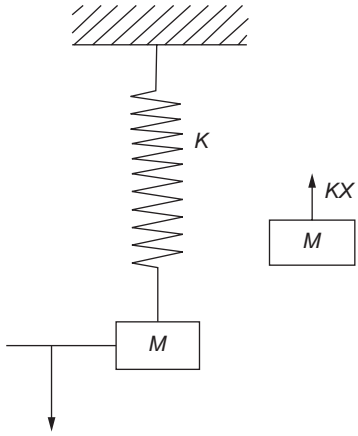


Figure 5-5 Single degree of freedom system (spring mass system).

This equation is called the motion equation for the system, and it can be rewritten as follows:

$$\ddot{x} + \frac{K}{m}x = 0 \tag{5-5}$$

Assuming that a harmonic function will satisfy the equation, let the solution be in the form:

$$x = C_1 \sin \omega t + C_2 \cos \omega t \tag{5-6}$$

Substituting Equation (5-6) into Equation (5-5), the following relationship is obtained:

$$\left(-\omega^2 + \frac{K}{M}\right)x = 0$$

which can be satisfied for any value of x if

$$\omega = \sqrt{\frac{K}{M}} \tag{5-7}$$

Thus, the system has a single natural frequency given by the relationship in Equation (5-7).

Damped System

Damping is the dissipation of energy. There are several types of damping – viscous damping, friction or coulomb damping, and solid damping. Viscous damping is

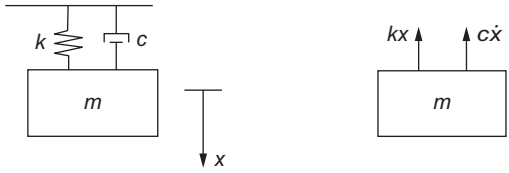


Figure 5-6 Free vibration with viscous damping.

encountered by bodies moving through a fluid. Friction damping usually arises from sliding on dry surfaces. Solid damping, often called structural damping, is due to internal friction within the material itself. An example of a free vibrating system with viscous damping is given here.

As shown in Figure 5-6, viscous damping force is proportional to velocity and is expressed by the following relationship:

$$F_{\text{damp}} = -c\dot{x}$$

where c is the coefficient of viscous damping.

The Newtonian approach gives the equation of motion as follows:

$$m\ddot{x} = -kx - c\dot{x} \tag{5-8}$$

or it can be written as

$$m\ddot{x} + c\dot{x} + kx = 0$$

The solution to this equation is found by using the trial solution:

$$x = c(e^{rt}) \tag{5-9}$$

which when substituted in Equation (5-8) yields the following characteristic equation:

$$\left(r^2 + \frac{c}{m}r + \frac{k}{m}\right)e^{rt} = 0 \tag{5-10}$$

This equation is satisfied for all values of t when:

$$r_{1,2} = \frac{-c}{2m} \pm \sqrt{\frac{c^2}{4m^2} - \frac{k}{m}} \tag{5-11}$$

from which the general solution is obtained as follows:

$$x = e^{\frac{-c}{2m}t}\left[C_1 e^{\sqrt{\frac{c^2}{4m^2} - \frac{k}{m}}(t)} + C_2 e^{-\sqrt{\frac{c^2}{4m^2} - \frac{k}{m}}(t)}\right] \tag{5-12}$$

The nature of the solution given by Equation (5-9) depends upon the nature of the roots, r_1 and r_2. The behavior of this damped system depends upon whether the root is real, imaginary, or zero. The critical damping coefficient c_c can now be defined as that which makes the radical zero. Thus:

$$\frac{c^2}{4m^2} = \frac{k}{m}$$

which can be written as:

$$\frac{c}{2m} = \sqrt{\frac{k}{m}} = \omega_n \tag{5-13}$$

One can therefore specify the amount of damping in any system by the damping factor:

$$\zeta = \frac{c}{c_c} \tag{5-14}$$

Overdamped System

If $c^2/4m^2 > k/m$, then the expression under the radical sign is positive and the roots are real. If the motion is plotted as a function of time, the curve in Figure 5-7 is obtained. This type of non-vibratory motion is referred to as aperiodic motion.

Critically Damped System

If $c^2/4m^2 = k/m$, then the expression under the radical sign is zero, and the roots r_1 and r_2 are equal. When the radical is zero and the roots are equal, the displacement decays the fastest from its initial value as seen in Figure (5-8). The motion in this case also is aperiodic.

This very special case is known as critical damping. The value of c for this case is given by:

$$\frac{c_{cr}^2}{4m^2} = \frac{k}{m}$$

$$c_{cr}^2 = 4m^2 \frac{k}{m} = 4mk$$

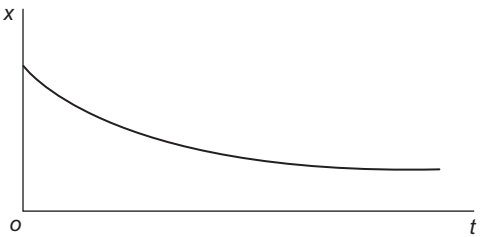


Figure 5-7 Overdamped decay.

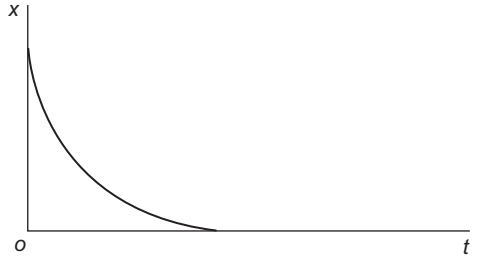


Figure 5-8 Critcal damping decay.

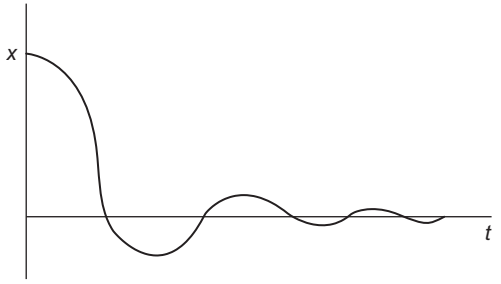


Figure 5-9 Underdamped decay.

Thus:

$$c_{cr} = \sqrt{4mk} = 2m\sqrt{\frac{k}{m}} = 2m\omega_n$$

Underdamped System

If $c^2/4m^2 < k/m$, then the roots r_1 and r_2 are imaginary, and the solution is an oscillating motion as shown in Figure 5-9. All the previous cases of motion are characteristic of different oscillating systems, although a specific case will depend upon the application. The underdamped system exhibits its own natural frequency of vibration. When $c^2/4m < k/m$, the roots r_1 and r_2 are imaginary and are given by:

$$r_{1,2} = \pm i\sqrt{\frac{k}{m} - \frac{c^2}{4m^2}} \tag{5-15}$$

Then the response becomes:

$$x = e^{-(c/2m)t}\left[C_1 e^{i\sqrt{\frac{k}{m}-\frac{c^2}{4m^2}}} + C_2 e^{-i\sqrt{\frac{k}{m}-\frac{c^2}{4m^2}}}\right]$$

which can be written as follows:

$$x = e^{-(c/2m)t}[A\cos\omega_d t + B\sin\omega_d t] \tag{5-16}$$

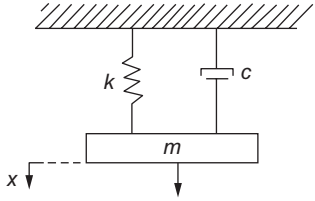


Figure 5-10 Forced vibration system.

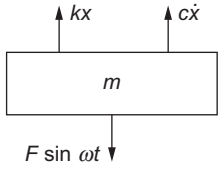


Figure 5-11 Free body diagram of mass (M).

Forced Vibrations

So far, the study of vibrating systems has been limited to free vibrations where there is no external input into the system. A free vibration system vibrates at its natural resonant frequency until the vibration dies down due to energy dissipation in the damping.

Now the influence of external excitation will be considered. In practice, dynamic systems are excited by external forces, which are themselves periodic in nature. Consider the system shown in Figure 5-10.

The externally applied periodic force has a frequency ω, which can vary independently of the system parameters. The motion equation for this system may be obtained by any of the previously stated methods. The Newtonian approach will be used here because of its conceptual simplicity. The freebody diagram of the mass m is shown in Figure 5-11.

The motion equation for the mass m is given by:

$$m\ddot{x} = F\sin\omega t - kx - c\dot{x} \tag{5-17}$$

and can be rewritten as:

$$m\ddot{x} + c\dot{x} + kx = F\sin\omega t$$

Assuming that the steady-state oscillation of this system is represented by the following relationship:

$$x = D\sin(\omega t - \theta) \tag{5-18}$$

where

$D =$ amplitude of the steady-state oscillation

$\theta =$ phase angle by which the motion lags the impressed force

The velocity and acceleration for the system are given by the following relationships:

$$v = \dot{x} = D\omega\cos(\omega t - \theta) = D\omega\sin\left(\omega t - \theta + \frac{\pi}{2}\right) \tag{5-19}$$

$$a = \ddot{x} = D\omega^2\sin(\omega t - \theta) = D\omega^2\sin\left(\omega t - \theta + \frac{\pi}{2}\right) \tag{5-20}$$

Substituting the previous relationships into motion Equation (5-17), the following relationship is obtained:

$$\begin{aligned} mD\omega^2\sin(\omega t - \theta) - cD\omega\sin\left(\omega t - \theta + \frac{\pi}{2}\right) \\ - D\sin(\omega t - \theta) + F\sin\omega t = 0 \end{aligned} \tag{5-21}$$

Inertia force + Damping force + Spring force + Impressed force = 0

From the previous equation, the displacement lags the impressed force by the phase angle θ, and the spring force acts opposite in direction to displacement. The damping force lags the displacement by 90° and is therefore in the opposite direction to the velocity. The inertia force is in phase with the displacement and acts in the opposite direction to the acceleration. This information is in agreement with the physical interpretation of harmonic motion. The vector diagram as seen in Figure 5-12 shows the various forces acting on the body, which is undergoing a forced vibration with viscous damping. Thus, from the vector diagram, it is possible to obtain the value of the phase angle and the amplitude of steady oscillation.

$$D = \frac{F}{\sqrt{(k - m\omega^2)^2 + c\omega^2}} \tag{5-22}$$

$$\tan\theta = \frac{c\omega}{k - m\omega^2} \tag{5-23}$$

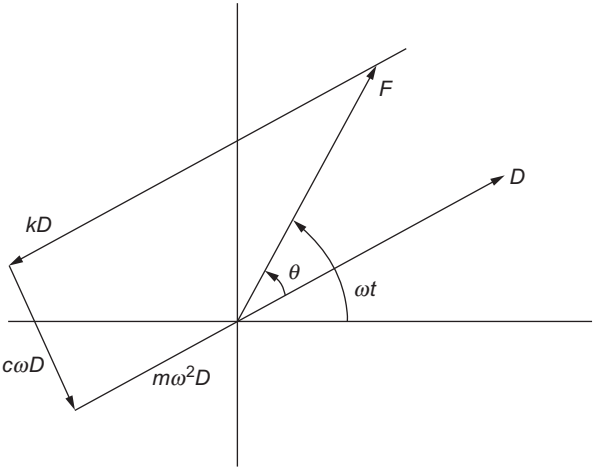


Figure 5-12 Vector diagram of forced vibration with viscous damping.

The non-dimensional form of D and θ can be written as

$$D = \frac{F/k}{\sqrt{\left(1 - \frac{\omega^2}{\omega_n^2}\right) + \left(2\zeta \frac{\omega}{\omega_n}\right)^2}} \tag{5-24}$$

$$\tan\theta = \frac{2\zeta \frac{\omega}{\omega_n}}{1 - \left(\frac{\omega}{\omega_n}\right)^2} \tag{5-25}$$

where:

$\omega_n = \sqrt{k/m}$ = natural frequency

$\zeta = \frac{c}{c_c}$ = damping factor

$c_c = 2m\omega_n$ = critical damping coefficient.

From these equations, the effect on the magnification factor $(D/F/k)$ and the phase angle (θ) is mainly a function of the frequency ratio ω/ω_n, and the damping factor ζ. Figures 5-13 (a) and 5-13 (b) show these relationships. The damping factor has great influence on the amplitude and phase angle in the region of resonance. For small values of $\omega/\omega_n \ll 1.0$, the inertia and damping force terms are small and result in a small phase angle. For a value of $\omega/\omega_n = 1.0$, the phase angle is 90°. The amplitude at resonance approaches infinity as the damping factor approaches zero. The phase angle undergoes nearly a 180° shift for light damping as it passes through the critical frequency ratio. For large values of $\omega/\omega_n \gg 1.0$, the phase angle approaches 180°, and the impressed force is expended mostly in overcoming the large inertia force.

Design Considerations

Design of rotating equipment for high-speed operation requires careful analysis. The discussion in the preceding section presents elementary analysis of such problems. Once a design is identified as having a problem, it is an altogether different matter to change this design to cure the problem. The following paragraphs discuss some observations and guidelines based on the analysis presented in the previous sections.

Natural Frequency

This parameter for a single degree of freedom is given by $\omega_n = \sqrt{k/m}$. Increasing the mass reduces ω_n, and increasing the spring constant k increases it. From a study of the damped system, the damped natural frequency $\omega_d = \omega_n\sqrt{1-\zeta^2}$ is lower than ω_n.

Unbalances

All rotating machinery is assumed to have an unbalance. Unbalance produces excitation at the rotational speed. The natural frequency of the system ω_n is also known as the critical shaft speed. From the study of the forced-damped system, the following

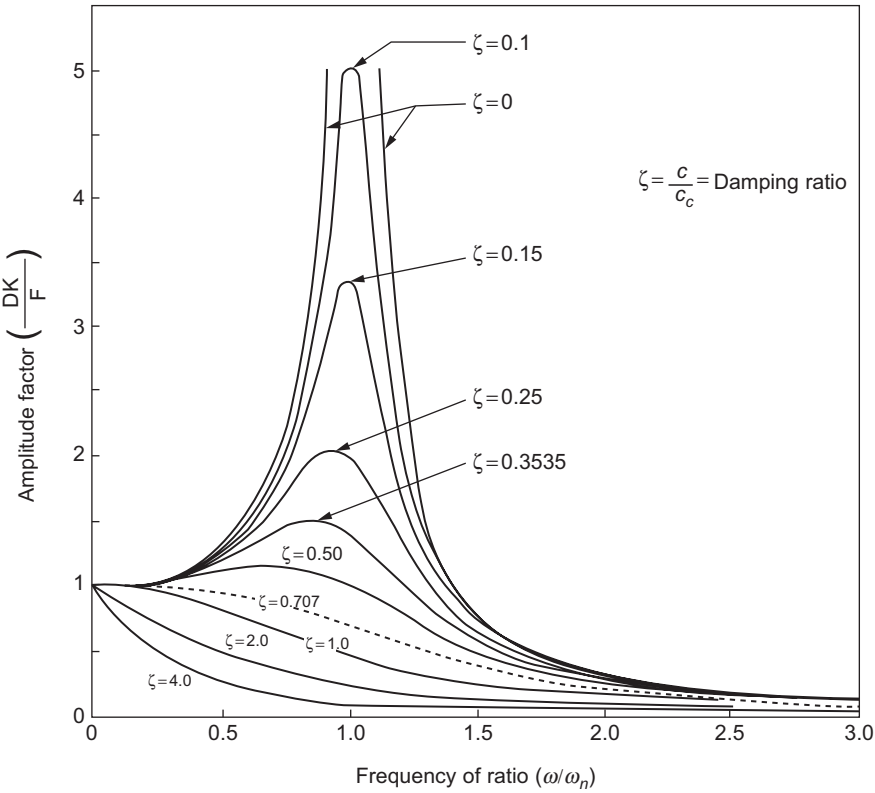


Figure 5-13 (a) Amplitude factor as a function of the frequency ratio r for various amounts of viscous damping.

conclusions can be drawn: (1) the amplitude ratio reaches its maximum values at $\omega_m = \omega_n\sqrt{1-2\zeta^2}$, and (2) the damped natural frequency ω_d does not enter the analysis of the forced-damped system. The more important parameter is ω_n, the natural frequency of the undamped system.

In the absence of damping the amplitude ratio becomes infinite at $\omega = \omega_n$. For this reason, the critical speed of a rotating machine should be kept away from its operating speed.

Small machinery involves small values of mass m and has large values of the spring constant k (bearing stiffness). This design permits a class of machines, which are small in size and of low speed in operation, to operate in a range below their critical speeds. This range is known as subcritical operation, and it is highly desirable if it can be attained economically.

The design of large rotating machinery – centrifugal compressors, gas and steam turbines, and large electrical generators – poses a different problem. The mass of the rotor is usually large, and there is a practical upper limit to the shaft size that can be used. Also, these machines operate at high speeds.

This situation is resolved by designing a system with a very low critical speed in which the machine is operated above the critical speed. This is known as supercritical

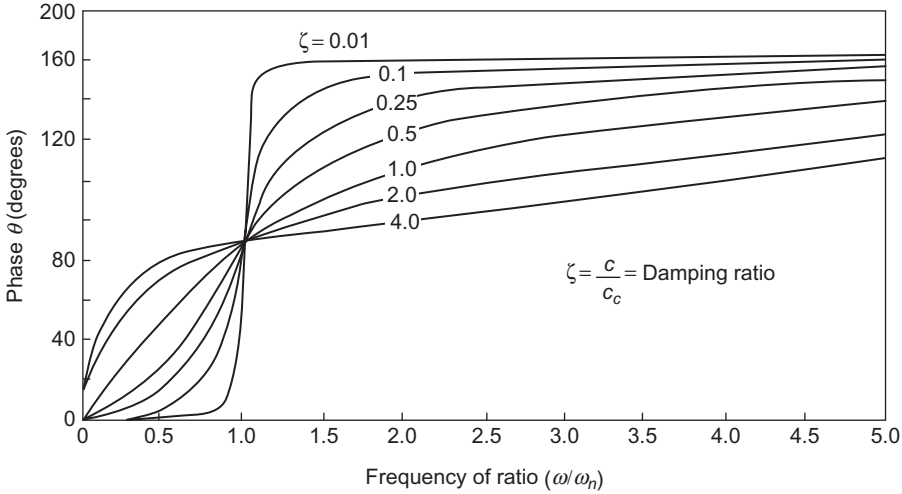


Figure 5-13 (b) Phase angle as a function of the frequency ratio for various amounts of viscous damping.

operation. The main problem is that during start-up and shut down, the machine must pass through its critical speed. To avoid dangerously large amplitudes during these passes, adequate damping must be located in the bearings and foundations.

The natural structural frequencies of most large systems are also in the low-frequency range, and care must be exercised to avoid resonant couplings between the structure and the foundation. The excitation in rotating machinery comes from rotating unbalanced masses. These unbalances result from four factors:

1. An uneven distribution of mass about the geometric axis of the system. This distribution causes the center of mass to be different from the center of rotation.
2. A deflection of the shaft due to the weight of the rotor, causing further distance between the center of mass and the center of rotation. Additional discrepancies can occur if the shaft has a bend or a bow in it.
3. Static eccentricities are amplified due to rotation of the shaft about its geometric center.
4. If supported by journal bearings, the shaft may describe an orbit so that the axis of rotation itself rotates about the geometric center of the bearings.

These unbalance forces increase as a function of ω^2, making the design and operation of high-speed machinery a complex and exacting task. Balancing is the only method available to tame these excitation forces.

Application to Rotating Machines

Rigid Supports

The simplest model of a rotating machine consists of a large disc mounted on a flexible shaft with the ends mounted in rigid supports. The rigid supports constrain a rotating

machine from any lateral movement, but allow free angular movement. A flexible shaft operates above its first critical. Figures 5-14 (a) and 5-14 (b) show such a shaft. The mass center of the disc "e" is displaced from the shaft centerline or geometric center of the disc due to manufacturing and material imperfections. When this disc is rotated at a rotational velocity ω, the mass causes it to be displaced so that the center of the disc describes an orbit of radius δ_r, from the center of the bearing centerline. If the shaft flexibility is represented by the radial stiffness (K_r), it will create a restoring force on the disc of $K_r\delta_r$ that will balance the centrifugal force equal to $m\omega^2(\delta_r + e)$. Equating the two forces obtains:

$$K_r\delta = m\omega^2(\delta_r + e)$$

therefore

$$\delta_r = \frac{m\omega^2 e}{K_r - m\omega^2} = \frac{(\omega/\omega_n)^2 e}{1 - (\omega/\omega_n)^2} \tag{5-26}$$

where $\omega_n = K_r/m$, the natural frequency of the lateral vibration of the shaft and disc at zero speed.

The previous equation shows that when $\omega < \omega_n$, δ_r is positive. Thus, when operating below the critical speed, the system rotates with the center of mass on the outside of the geometric center. Operating above the critical speed ($\omega < \omega_n$), the shaft deflection δ_r tends to infinity. Actually, this vibration is damped by outside forces. For very high speeds ($\omega >> \omega_n$), the amplitude δ_r equals $-e$, meaning that the disc rotates about its center of gravity.

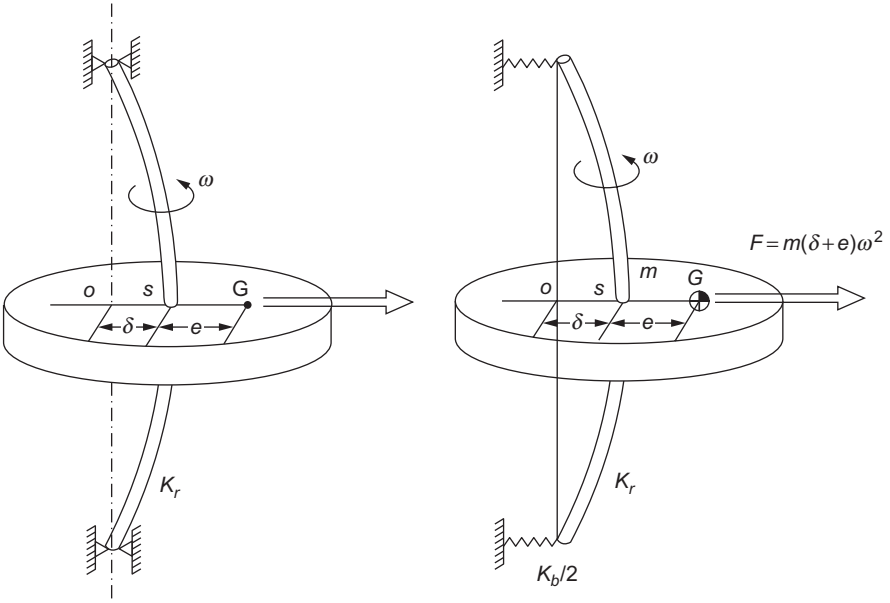


Figure 5-14 (a) Rigid supports. (b) Flexible supports.

Flexible Supports

The previous section discussed the flexible shaft with rigid bearings. In the real world, the bearings are not rigid but possess some flexibility. If the flexibility of the system is given by K_b, then each support has a stiffness of $K_b/2$. In such a system, the flexibility of the entire lateral system can be calculated by the following relationship:

$$\frac{1}{K_t} = \frac{1}{K_r} + \frac{1}{K_b} = \frac{K_b + K_r}{K_r K_b} \tag{5-27}$$

$$K_r = \frac{K_r K_b}{K_b + K_r}$$

therefore, the natural frequency

$$\begin{aligned} \omega_{nt} &= \sqrt{\frac{K_t}{m}} = \sqrt{\frac{K_r K_b}{K_b + K_r} \Big/ m} \\ &= \sqrt{\frac{K_r}{m}} \times \sqrt{\frac{K_b}{K_b + K_r}} \\ &= \omega_n \sqrt{\frac{K_b}{K_b + K_r}} \end{aligned} \tag{5-28}$$

It can be observed from the previous expression that when $K_b \ll K_r$ (very rigid support), then $\omega_{nt} = \omega_n$ or the natural frequency of the rigid system. For a system with a finite stiffness at the supports, or $K_b \square K_r$, then ω_n is less than ω_{nt}. Hence, flexibility causes the natural frequency of the system to be lowered. Plotting the natural frequency as a function of bearing stiffness on a log scale provides a graph as shown in Figure 5-15.

When $K_b \ll K_r$, then $\omega_{nt} = \omega_n K_b / K_r$. Therefore, ω_{nt} is proportional to the square root of K_b, or $\log \omega_n t$ is proportional to one-half $\log K_b$. Thus, this relationship is shown by a straight line with a slope of 0.5 in Figure 5-15. When $K_b \gg K_r$, the total effective natural frequency is equal to the natural rigid-body frequency. The actual curve lies below these two straight lines as shown in Figure 5-15.

The critical speed map shown in Figure 5-15 can be extended to include the second, third, and higher critical speeds. Such an extended critical speed map can be very useful in determining the dynamic region in which a given system is operating. One can obtain the locations of a system's critical speeds by superimposing the actual support versus the speed curve on the critical speed map. The intersection points of the two sets of curves define the locations of the system's critical speeds.

When the previously described intersections lie along the straight line on the critical speed map with a slope of 0.5, the critical speed is bearing controlled. This condition is often referred to as a "rigid-body critical."

When the intersection points lie below the 0.5 slope line, the system is said to have a "bending critical speed." It is important to identify these points, since they indicate the increasing importance of bending stiffness over support stiffness.

Figure 5-16 (a) and 5-16 (b) show vibration modes of a uniform shaft supported at its ends by flexible supports. Figure 5-16 (a) shows rigid supports and a flexible rotor. Figure 5-16 (b) shows flexible supports and rigid rotors.

To summarize the importance of the critical speed concept, one should bear in mind that it allows an identification of the operation region of the rotor-bearing system, probable mode shapes, and approximate locations of peak amplitudes.

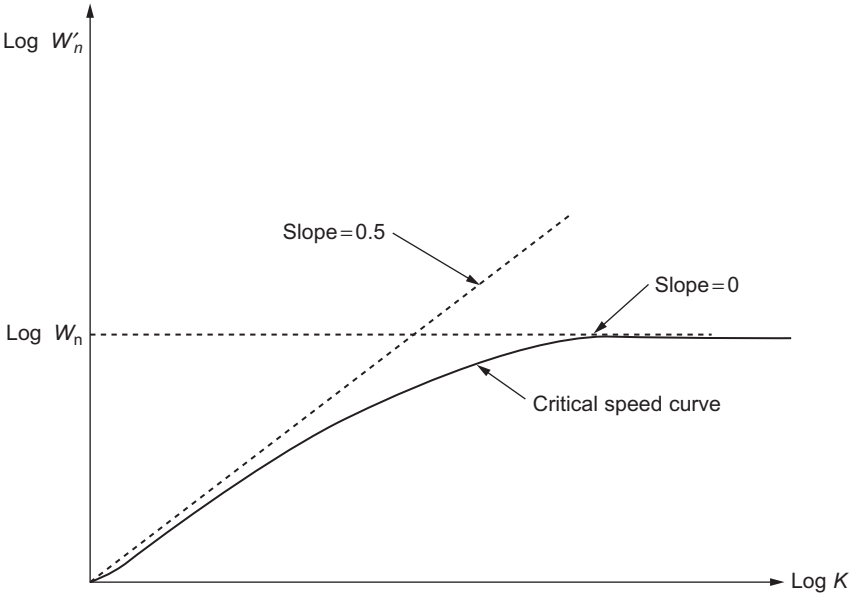


Figure 5-15 Critical speed map.

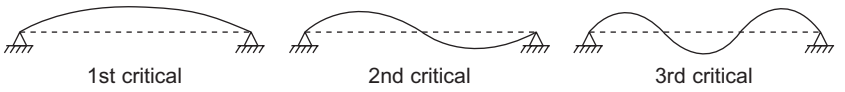


Figure 5-16 (a) Rigid supports and a flexible rotor.

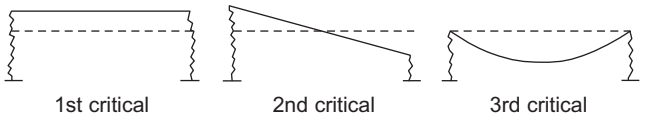


Figure 5-16 (b) Flexible supports and rigid rotors.

Critical Speed Calculations for Rotor Bearing Systems

Methods for calculating undamped and damped critical speeds that closely follow the works of Prohl and Lund, respectively, are listed herein. Computer programs can be developed that use the equations shown in this section to provide estimations of the critical speeds of a given rotor for a range of bearing stiffness and damping parameters.

The method of calculating critical speeds as suggested by Prohl and Lund has several advantages. By this method, any number of orders of critical frequencies may be calculated, and the rotor configuration is not limited in the number of diameter changes or in the number of discs attached. In addition, shaft supports may be assumed rigid or may have any values of damping or stiffness. The gyroscopic effect associated with the moment of attached disc inertia may also be taken into account. Perhaps the greatest advantage of the technique, however, is the relative simplicity with which all the capabilities are performed.

The rotor is first divided into a number of station points, including the ends of the shafting, points at which diameter changes occur, points at which discs are attached, and bearing locations. The shafting connecting the station points is modeled as massless sections which retain the flexural stiffness associated with the section's length, diameter, and modulus of elasticity. The mass of each section is divided in half and lumped at each end of the section where it is added to any mass provided by attached discs or couplings.

The critical-speed calculation of a rotating shaft proceeds with equations to relate loads and deflections from station $n-1$ to station n. The shaft shear V can be computed using the following relationship:

$$V_n = V_{n-1} + M_{n-1}\omega^2 Y_{n-1} \tag{5-29}$$

and the bending moment

$$M_n = M_{n-1} + V_n Z_n$$

The angular displacement can be computed using the following relationship:

$$\theta_n = \beta_n \left[\frac{M_{n-1}}{2} + \frac{M_n}{2} \right] + \theta_{n-1} \tag{5-30}$$

where $\beta =$ flexibility constant.

The vertical linear displacement is:

$$Y_n = \beta_n \left[\frac{M_{n-1}}{3} + \frac{M_n}{6} \right] Z_n + \theta_{n-1} Z_n + Y_{n-1} \tag{5-31}$$

When crossing a flexible bearing at station n from the left side to the right side, the following relationships hold:

$$K_{xx} Y_n = -[(V_n)_{\text{Right}} - (V_n)_{\text{Left}}] \tag{5-32}$$

$$K_{\theta\theta} \theta_n = [(M_n)_{\text{Right}} - (M_n)_{\text{Left}}] \tag{5-33}$$

$$(\theta_n)_{\text{Right}} = (\theta_n)_{\text{Left}} \tag{5-34}$$

$$(Y_n)_{\text{Right}} = (Y_n)_{\text{Left}} \tag{5-35}$$

The initial boundary conditions are $V_1 = M_1 = 0$ for a free end and, to assign initial values for Y_1 and θ_1, the calculation proceeds in two parts with the assumptions given as:

Pass 1	$Y_1 = 1.0$	$\theta_1 = 0.0$
Pass 2	$Y_1 = 0.0$	$\theta_1 = 1.0$

For each part, the calculation starts at the free end and, using Equations (5-29) through (5-35), proceeds from station to station until the other end is reached. The values for the shear and moment at the far end are dependent on the initial values by the relationship:

$$\begin{aligned} V_n &= V_{n'\text{Pass}1} Y_1 + V_{n'\text{Pass}2} \theta_1 \\ M_n &= M_{n'\text{Pass}1} Y_1 + M_{n'\text{Pass}2} \theta_1 \end{aligned} \tag{5-36}$$

The critical speed is the speed at which both $V_n = M_n = 0$, which requires iterating the assumed rotational speed until this condition is observed.

If structural damping is to be considered, then a revised set of relationships must be used. For a system allowing vertical and horizontal shaft motion, the change in shear and moment across a station is given by:

$$\begin{bmatrix} -V'_x \\ -V'_y \\ -M'_x \\ -M'_y \end{bmatrix}_n = \begin{bmatrix} -V_x \\ -V_y \\ -M_x \\ -M_y \end{bmatrix}_n + \begin{bmatrix} s^2 mX \\ s^2 my \\ s^2 J_T \theta + s\omega J_P \phi \\ s^2 J_T \phi + s\omega J_P \theta \end{bmatrix}_n + (K + sB)_n \begin{bmatrix} X \\ Y \\ \phi \\ \theta \end{bmatrix}_n \tag{5-37}$$

The calculation of parameters between stations utilizes the following relationships:

$$X_{n+1} = X_n + Z_n \theta_n + C_1 [Z_n^2 (V'_{xn} - \epsilon M'_{yn})/2 + C_2 (V'_{yn} - \epsilon V'_{xn})]$$

$$Y_{n+1} = Y_n + Z_n \phi_n + C_1 [Z_n^2 (M'_{yn} - \epsilon M'_{xn})/2 + C_2 (V'_{yn} - \epsilon M'_{xn})]$$

$$\theta_{n+1} = \theta_n + C_1 [Z_n (M'_{xn} - \epsilon M'_{yn})/2 + Z_n^2 (V'_{xn} - \epsilon V'_{xn})/2]$$

$$\phi_{n+1} = \phi_n + C_1 [Z_n (M'_{yn} - \epsilon M'_{xn}) + Z_n^2 (V'_{yn} - \epsilon V'_{xn})/2]$$

$$M_{x,n+1} = M'_{xn} + Z_n V'_{xn}$$

$$M_{y,n+1} = M'_{yn} + Z_n V'_{yn}$$

$$V_{x,n+1} = V'_{xn}$$

$$V_{y,n+1} = V'_{yn}$$

where

$$C_1 = 1/(EI)_n\sqrt{1+\epsilon^2}$$
$$C_2 = \frac{Z_n^2}{6} - \frac{(Z\,EI)_n}{(\alpha\,GA)_n} \tag{5-38}$$

where

E = Young's modulus of elasticity
I = sectional moment of inertia
G = shear modulus
ϵ = logarithmic decrement of internal shaft damping divided by shaft vertical position
α = cross-sectional shape factor ($\alpha = .75$ for circular cross section)

Electromechanical Systems and Analogies

Where physical systems are so complex that mathematical solutions are not possible, experimental techniques based on various analogies may be one type of solution. Electrical systems that are analogous to mechanical systems are usually the easiest, cheapest, and fastest solution to the problem. The analogy between systems is a mathematical one based on the similarity of the differential equations. Thomson has given an excellent treatise on this subject in his book on vibration. Some of the highlights are given here.

A forced-damped system is shown in Figure 5-17. This system has a mass M, which is suspended on a spring K with a spring constant and a dash pot to produce damping. The viscous damping coefficient is c.

$$M\frac{dv}{dt} + cv + K\int_0^t v\,dt = f(t) \tag{5-39}$$

A force-voltage system can be designed to represent this mechanical system as shown in Figure 5-18.

The equation representing this system when $e(t)$ is the voltage and represents the force, while inductance (L), capacitance C, and resistance R represent the mass, spring constant, and the viscous damping, respectively, can be written as follows:

$$L\frac{di}{dt} + Ri + \frac{1}{C}\int_0^t i\,dt = e(t) \tag{5-40}$$

A force-current analogy can also be obtained where the mass is represented by capacitance, the spring constant by the inductance, and the resistance by the conductance as shown in Figure 5-19. The system can be represented by the following relationship:

$$C\frac{de}{dt} + Ge + \frac{1}{L}\int_0^t e\,dt = i(t) \tag{5-41}$$

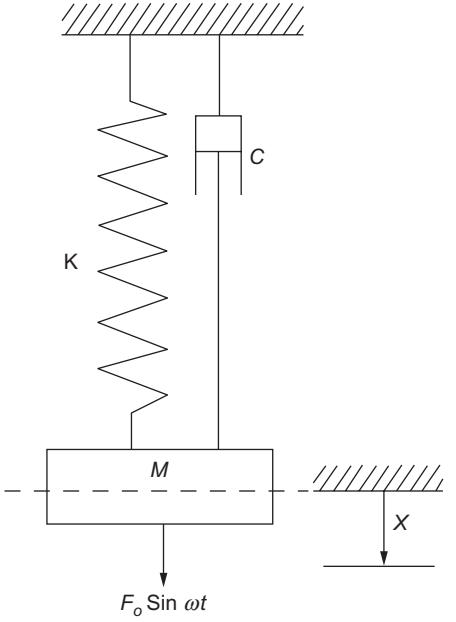


Figure 5-17 Forced vibration with viscous damping.

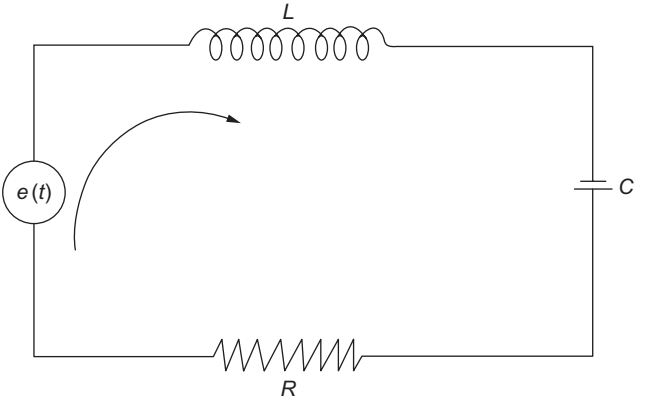


Figure 5-18 A force-voltage system.

Comparing all these equations shows that the mathematical relationships are all similar. These equations convey the analogous values. For convenience, Table 5-1 also shows these relationships.

Forces Acting on a Rotor-Bearing System

There are many types of forces that act on a rotor-bearing system. The forces can be classified into three categories: (1) casing and foundation forces, (2) forces generated

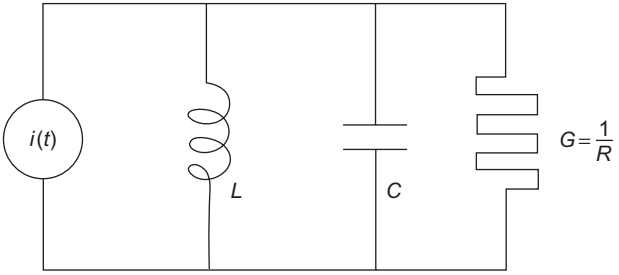


Figure 5-19 Force-current analogy.

Table 5-1 Electromechanical System Analogies

Mechanical Parameters	Electrical Parameters	
	Force-Voltage Analogy	**Force-Current Analogy**
Force (F)	Voltage e	Current i
Velocity $\dot{x}$ or v	Current i	Voltage e
Displacement $x = \int_0^t v dt$	Charge $q = \int_0^t i dt$	
Mass M	Inductance L	Capacitance C
Dashpot c Coefficient	Resistance R	Conductance G
Spring Constant k	Capacitance C	Inductance L

by rotor motion, and (3) forces applied to a rotor. Table 5-2 by Reiger is an excellent compilation of these forces.

Forces Transmitted to Casing and Foundations

These forces can be due to foundation instability, other nearby unbalanced machinery, piping strains, rotation in gravitational or magnetic fields, or excitation of casing or foundation natural frequencies. These forces can be constant or variable with impulse loadings. The effect of these forces on the rotor-bearing system can be great. Piping strains can cause major misalignment problems and unwanted forces on the bearings. Operation of reciprocating machinery in the same area can cause foundation forces and unduly excite the rotor of a turbomachine.

Forces Generated by Rotor Motion

These forces can be classified into two categories: (1) forces due to mechanical and material properties, and (2) forces caused by various loadings of the system. The forces from mechanical and material properties are unbalanced and are caused by a lack of homogeneity in materials, rotor bow, and elastic hysteresis of the rotor. The forces

Table 5-2 Forces Acting on Rotor-Bearing Systems

Source of Force	Description	Application
1. Forces transmitted to foundations, casing, or bearing pedestals.	Constant, unidirectional force	Constant linear acceleration.
	Constant force, rotational	Rotation in gravitational or magnetic field.
	Variable, unidirectional	Impressed cyclic ground or foundation-motion.
	Impulsive forces	Air blast, explosion, or earthquake.
	Random forces	Nearby unbalanced machinery. Blows, impact.
2. Forces generated by rotor motion.	Rotating unbalance: residual, or bent shaft.	Present in all rotating machinery.
	Coriolis forces	Motion around curve of varying radius.
		Space applications.
		Rotary-coordinated analyses.
	Elastic hysteresis of rotor	Property of rotor material, which appears when rotor is cyclically deformed in bending, torsionally or axially.
	Coulomb friction	Construction damping arising from relative motion between shrinkfitted assemblies.
		Dry-friction bearing whirl.
	Fluid friction	Viscous shear of bearings.
		Fluid entrainment in turbomachinery. Windage.
	Hydrodynamic forces, static	Bearing load capacity.
		Volute pressure forces.
	Hydrodynamic forces, dynamic	Bearing stiffness and damping properties.
	Dissimilar elastic beam stiffness reaction forces	Rotors with differing rotor lateral stiffnesses. Slotted rotors, electrical machinery, keyway.
		Abrupt speed change conditions.

(*Continued*)

Table 5-2 (*Continued*)

Source of Force	Description	Application
	Gyroscopic moments	Significant in high-speed flexible rotors with discs.
3. Applied to rotor	Drive torque	Accelerating or constant-speed operation.
	Cyclic forces	Internal combustion engine torque and force components.
	Oscillating torques	Misaligned couplings. Propellers. Fans. Internal combustion engine drive.
	Transient torques	Gears with indexing or positioning errors.
	Heavy applied rotor force	Drive gear forces. Misaligned 3-or-more rotor-bearing assembly
	Gravity	Nonvertical machines. Nonspatial applications.
	Magnetic field: stationary or rotating	Rotating electrical machinery.
	Axial forces	Turbomachine balance piston, cyclic forces from propeller, or fan. Self-excited bearing forces. Pneumatic hammer.

caused by loadings of the system are viscous and hydrodynamic forces in the rotor-bearing system, and various blade loading forces, which vary in the operational range of the unit.

Forces Applied to a Rotor

Rotor-applied forces can be due to drive torques, couplings, gears, misalignment, and axial forces from piston and thrust unbalance. They can be destructive, and they often result in the total destruction of a machine.

Rotor-Bearing System Instabilities

Instabilities in rotor-bearing systems may be the result of different forcing mechanisms. Ehrich, Gunter, Alford, and others have done considerable work to identify these instabilities. One can divide these instabilities into two general yet distinctly

Table 5-3 Characteristics of Forced and Self-Excited Vibration

	Forced or Resonant Vibration	**Self-Excited or Instability Vibration**
Frequency/rpm relationship	$N_F = N_{rpm}$ or N or rational fraction	Constant and relatively independent of rotating speed.
Amplitude/rpm relationship	Peak in narrow bands of rpm	Blossoming at onset and continue to increase with increasing rpm.
Influence of damping	Additional damping Reduce amplitude No change in rpm at which it occurs	Additional damping may defer to a higher rpm. Will not materially affect amplitude.
System geometry	Lack of axial sym. External forces	Independent of symmetry. Small deflection to an axisymmetric system. Amplitude will self-propagate.
Vibration frequency	At or near shaft critical or natural frequency	Same.
Avoidance	1. Critical freq. above running speed	1. Operating rpm below onset.
	2. Axisymmetric	2. Eliminates instability.
	3. Damping	Introduce damping.

different categories: (1) the forced OR resonant instability dependent on outside mechanisms in frequency of oscillations; and (2) the self-excited instabilities that are independent of outside stimuli and independent of the frequency. Table 5-3 is the characterization of the two categories of vibration stimuli.

Forced (Resonant) Vibration

In forced vibration the usual driving frequency in rotating machinery is the shaft speed or multiples of this speed. This speed becomes critical when the frequency of excitation is equal to one of the natural frequencies of the system. In forced vibration, the system is a function of the frequencies. These frequencies can also be multiples of rotor speed excited by frequencies other than the speed frequency such as blade passing frequencies, gear mesh frequencies, and other component frequencies. Figure 5-20 shows that for forced vibration, the critical frequency remains constant at any shaft speed. The critical speeds occur at one-half, one, and two times the rotor speed. The effect of damping in forced vibration reduces the amplitude, but it does not affect the frequency at which this phenomenon occurs.

Typical forced vibration stimuli are as follows:

1. *Unbalance.* This stimulus is caused by material imperfections and tolerances, amongst other things. The mass center of gravity is different from the geometric case, leading to a centrifugal force acting on the system.

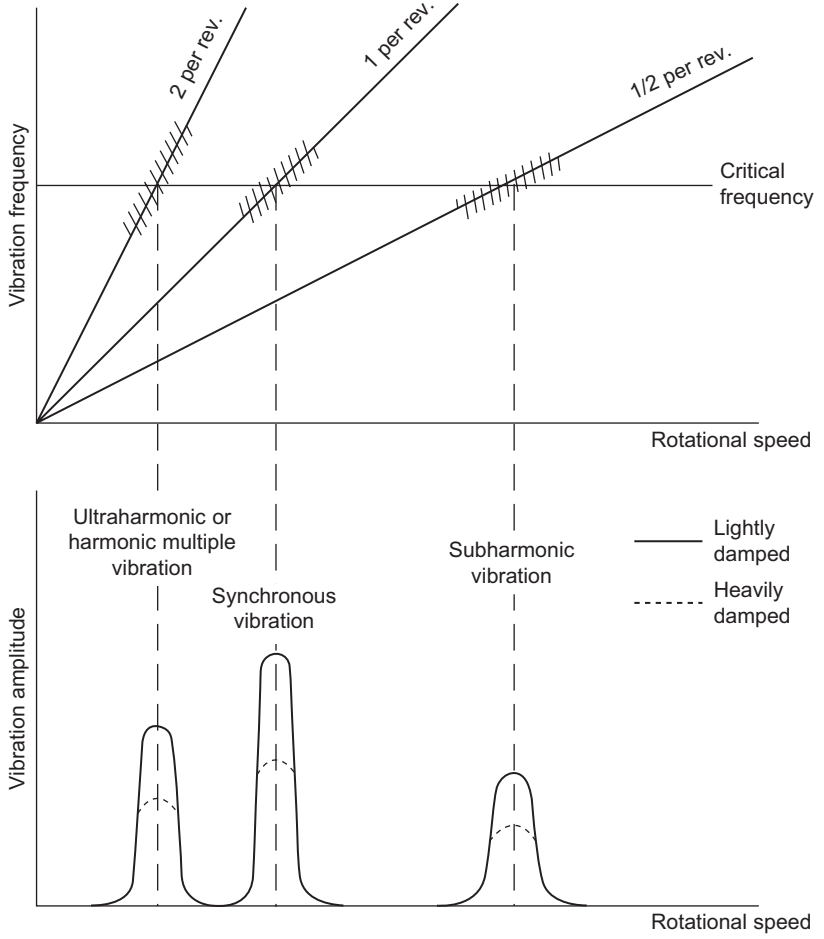


Figure 5-20 Characteristic of forced vibration or resonance in rotating machinery (Ehrich, F.F., "Identification and Avoidance of Instabilities and Self-Excited Vibrations in Rotating Machinery," Adopted from ASME Paper 72-DE-21, General Electric Co., Aircraft Engine Group, Group Engineering Division, 11 May, 1972).

2. *Asymmetric flexibility.* The sag in a rotor shaft will cause a periodic excitation force twice every revolution.
3. *Shaft misalignment.* This stimulus occurs when the rotor centerline and the bearing support line are not true. Misalignment may also be caused by an external piece such as the driver to a centrifugal compressor. Flexible couplings and better alignment techniques are used to reduce the large reaction forces.

Periodic Loading

This type of loading is caused by external forces that are applied to the rotor by gears, couplings, and fluid pressure, which are transmitted through the blade loading.

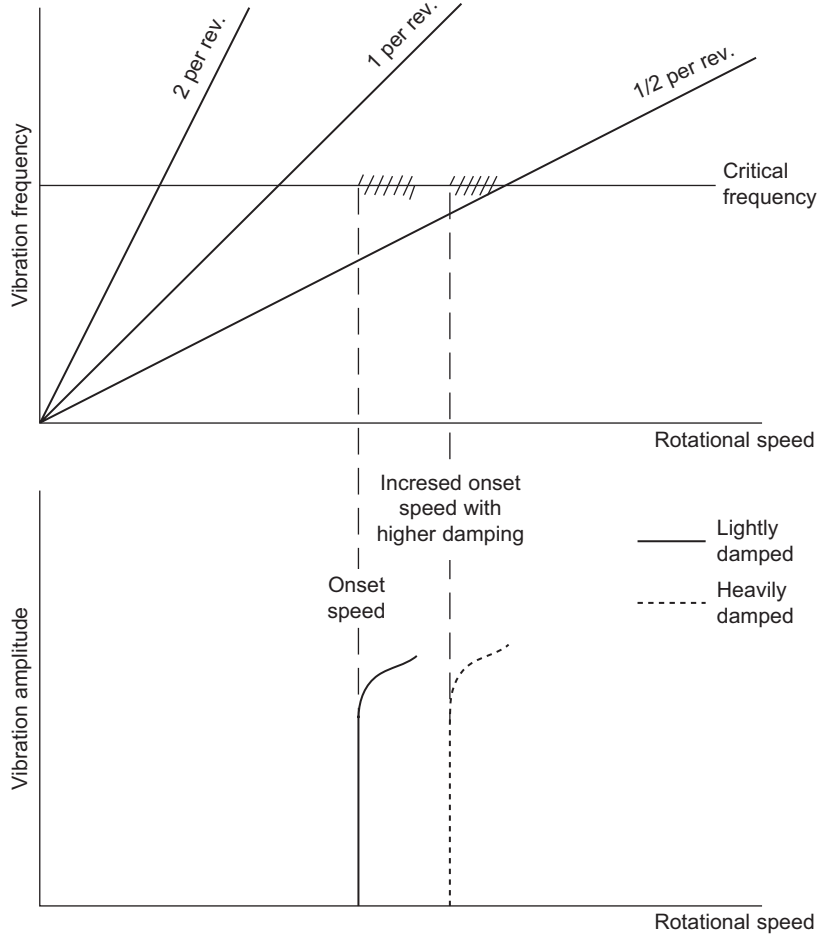


Figure 5-21 Characteristic of instabilities or self-excited vibration in rotating machinery (Ehrich, F.F., "Identification and Avoidance of Instabilities and Self-Excited Vibrations in Rotating Machinery," Adopted from ASME Paper 72-DE-21, General Electric Co., Aircraft Engine Group, Group Engineering Division, May 11, 1972).

Self-Excited Instabilities

The self-excited instabilities are characterized by mechanisms, which whirl at their own critical frequency independent of external stimuli. These types of self-excited vibrations can be destructive, since they induce alternating stress that leads to fatigue failures in rotating equipment. The whirling motion, which characterizes this type of instability, generates a tangential force normal to the radial deflection of the shaft, and a magnitude proportional to that deflection. The type of instabilities, which fall under this category, are usually called whirling or whipping. At the rotational speed where such a force is started, it will overcome the external stabilizing damping force and induce a whirling motion of ever-increasing amplitude. Figure 5-21 shows the onset

speed. The onset speed does not coincide with any particular rotation frequency. Also, damping results from a shift of this frequency, not in the lowering of the amplitude as in forced vibration. Important examples of such instabilities include hysteretic whirl, dry-friction whip, oil whip, aerodynamic whirl, and whirl due to fluid trapped in the rotor. In a self-excited system, friction or fluid energy dissipations generate the destabilizing force.

Hysteretic Whirl

This type of whirl occurs in flexible rotors and results from shrink fits. When a radial deflection is imposed on a shaft, a neutral-strain axis is induced normal to the direction of flexure. From first-order considerations, the neutral-stress axis is coincident with the neutral-strain axis, and a restoring force is developed perpendicular to the neutral-stress axis. The restoring force is then parallel to and opposing the induced force. In actuality, internal friction exists in the shaft, which causes a phase shift in the stress. The result is that the neutral-strain axis and neutral-stress axis are displaced so that the resultant force is not parallel to the deflection. The tangential force normal to the deflection causes whirl instability. As whirl begins, the centrifugal force increases, causing greater deflections – which result in greater stresses and still greater whirl forces. This type of increasing whirl motion may eventually be destructive as seen in Figure 5-22 (a).

Some initial impulse unbalance is often required to start the whirl motion. Newkirk has suggested that the effect is caused by interfaces of joints in a rotor (shrink fits) rather than defects in rotor material. This type of whirl phenomenon occurs only at rotational speeds above the first critical. The phenomenon may disappear and then reappear at a higher speed. Some success has been achieved in reducing this type of whirl by reducing the number of separate parts, restricting the shrink fits, and providing some lockup of assembled elements.

Dry-Friction Whirl

This type of whirl is experienced when the surface of a rotating shaft comes into contact with an unlubricated stationary guide. The effect takes place because of an unlubricated journal, contact in radial clearance of labyrinth seals, and loss of clearance in hydrodynamic bearings.

Figure 5-22 (b) shows this phenomenon. When contact is made between the surface and the rotating shaft, the coulomb friction will induce a tangential force on the rotor. This friction force is approximately proportional to the radial component of the contact force, creating a condition for instability. The whirl direction is counter to the shaft direction.

Oil Whirl

This instability begins when fluid entrained in the space between the shaft and bearing surfaces begins to circulate with an average velocity of one-half of the shaft surface speed. Figure 5-23 (a) shows the mechanism of oil whirl. The pressures developed in the oil are not symmetric about the rotor. Because of viscous losses of the fluid

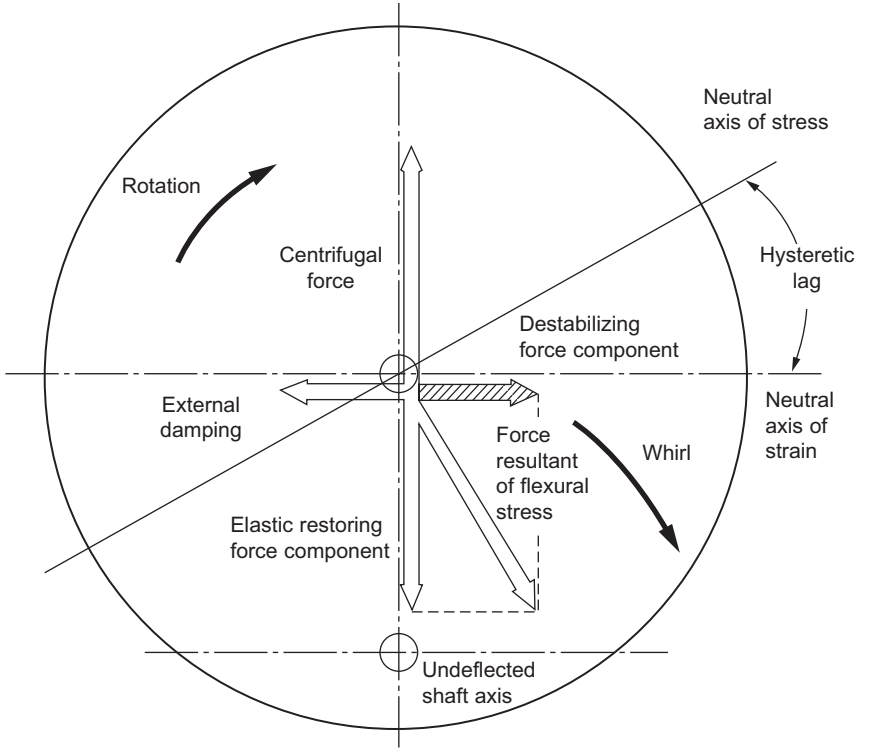


Figure 5-22 (a) Hysteretic whirl (Ehrich, F.F., "Identification and Avoidance of Instabilities and Self-Excited Vibrations in Rotating Machinery," Adopted from ASME Paper 72-DE-21, General Electric Co., Aircraft Engine Group, Group Engineering Division, May 11, 1972).

circulating through the small clearance, higher pressure exists on the upstream side of the flow than on the downstream side. Again, a tangential force results. A whirl motion exists when the tangential force exceeds any inherent damping. It has been shown that the shafting must rotate at approximately twice the critical speed for whirl motion to occur. Thus, the ratio of frequency to rpm is close to 0.5 for oil whirl. This phenomenon is not restricted to the bearing, but it also can occur in the seals.

The most obvious way to prevent oil whirl is to restrict the maximum rotor speed to less than twice its critical. Sometimes oil whirl can be reduced or eliminated by changing the viscosity of the oil or by controlling the oil temperature. Bearing designs that incorporate grooves or tilting pads are also effective in inhibiting oil-whirl instability.

Aerodynamic Whirl

Although the mechanism is not clearly understood, it has been shown that aerodynamic components, such as compressor wheels and turbine wheels, can create cross-coupled forces due to the wheel motion. Figure 5-23 (b) is one representation of how such forces may be induced.

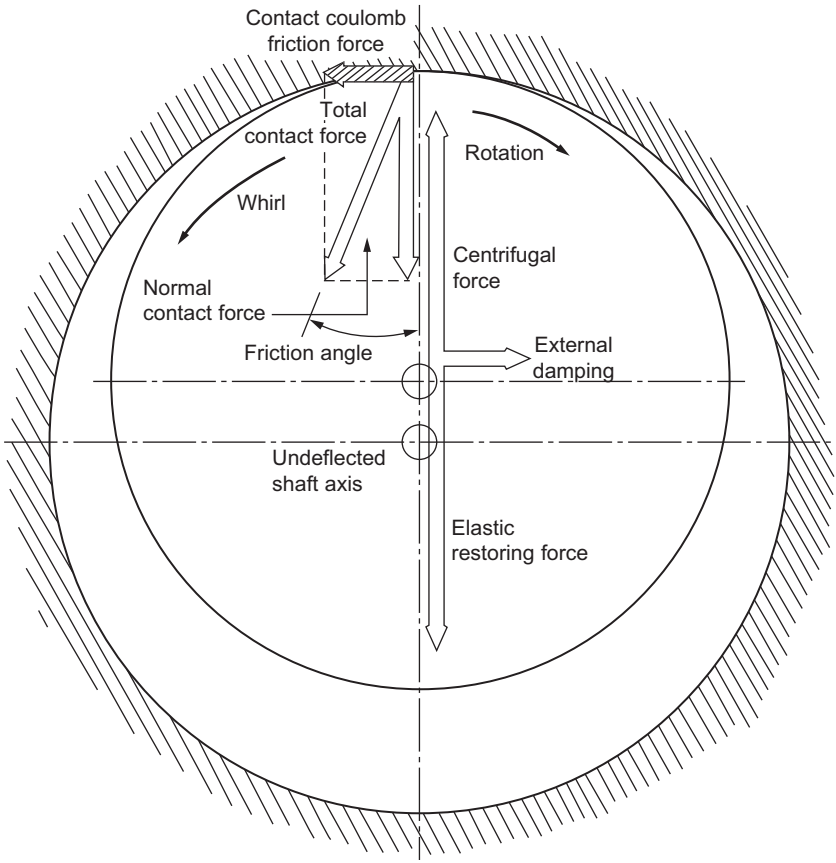


Figure 5-22 (b) Dry friction whirl (Ehrich, F.F., "Identification and Avoidance of Instabilities and Self-Excited Vibrations in Rotating Machinery," Adopted from ASME Paper 72-DE-21, General Electric Co., Aircraft Engine Group, Group Engineering Division, May 11, 1972).

The acceleration or deceleration of the process fluid imparts a net tangential force on the blading. If the clearance between the wheel and housing varies circumferentially, a variation of the tangential forces on the blading may also be expected, resulting in a net destabilizing force as shown in Figure 5-23 (b). The resultant force from the cross-coupling of angular motion and radial forces may destabilize the rotor and cause a whirl motion.

The aerodynamic cross-coupling effect has been quantified into equivalent stiffness. For instance, in axial-flow machines:

$$K_{xy} = -K_{yx} = \frac{\beta T}{D_P H} \tag{5-42}$$

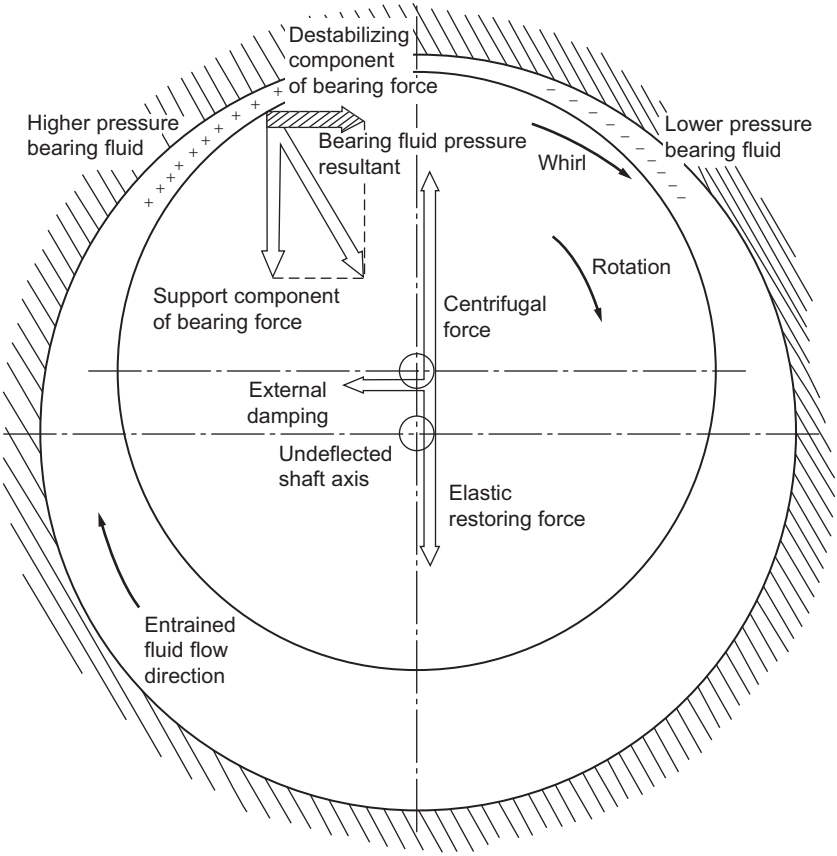


Figure 5-23 (a) Oil whirl (Ehrich, F.F., "Identification and Avoidance of Instabilities and Self-Excited Vibrations in Rotating Machinery," Adopted from ASME Paper 72-DE-21, General Electric Co., Aircraft Engine Group, Group Engineering Division, May 11, 1972).

where

β = efficiency slope versus displacement over blade-height curve
T = stage torque
D_P = average pitch diameter
H = average blade height

The stiffness that results from the previous quantification may be used in a critical-speed program in much the same manner as bearing coefficients.

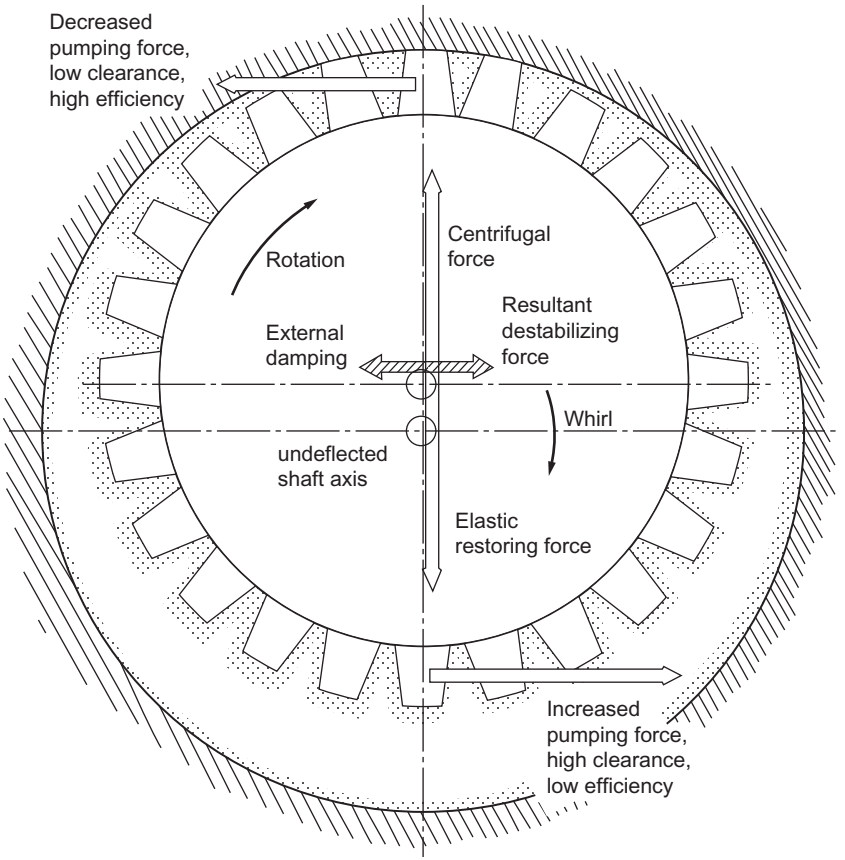


Figure 5-23 (b) Aerodynamic cross-coupling (Ehrich, F.F., "Identification and Avoidance of Instabilities and Self-Excited Vibrations in Rotating Machinery," Adopted from ASME Paper 72-DE-21, General Electric Co., Aircraft Engine Group, Group Engineering Division, May 11, 1972).

Whirl from Fluid Trapped in the Rotor

This type of whirl occurs when liquids are inadvertently trapped in an internal rotor cavity. The mechanism of this instability is shown in Figure 5-24. The fluid does not flow in a radial direction but flows in a tangential direction. The onset of instability occurs between the first and second critical speeds. Table 5-4 is a handy summary for both avoidance and diagnosis of self-excitation and instabilities in rotating shafts.

Campbell Diagram

The Campbell diagram is an overall or bird's-eye view of regional vibration excitation that can occur on an operating system. The Campbell diagram can be generated

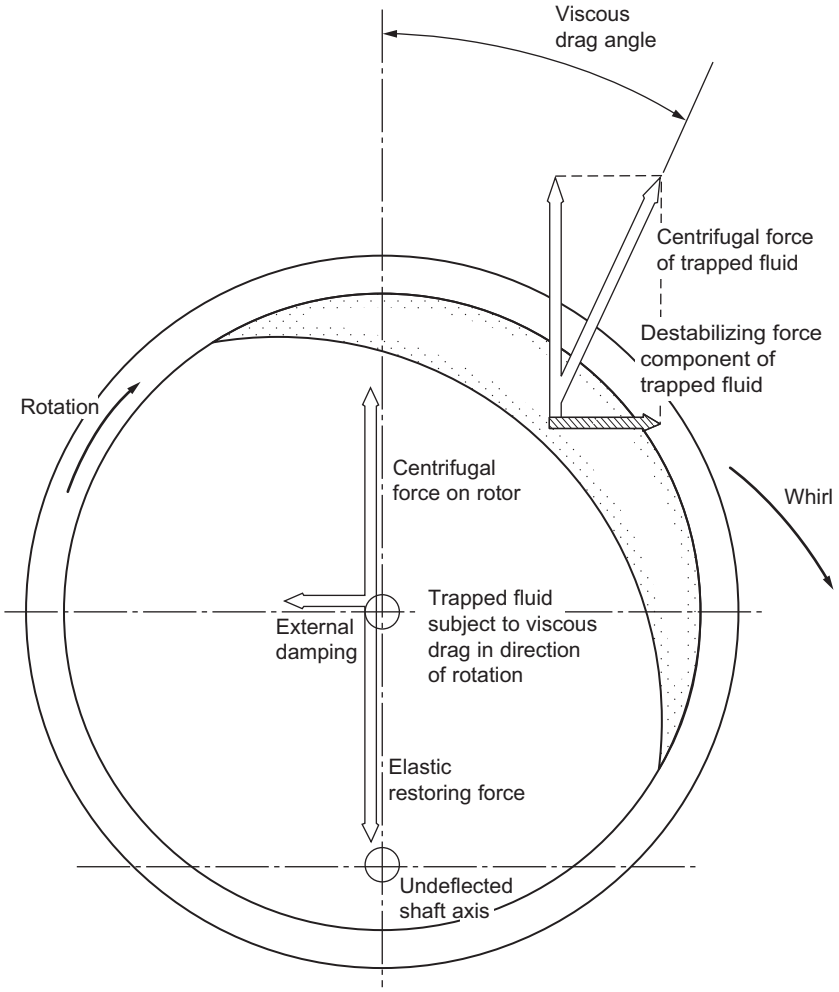


Figure 5-24 Whirl from fluid trapped in the rotor (Ehrich, F.F., "Identification and Avoidance of Instabilities and Self-Excited Vibrations in Rotating Machinery," Adopted from ASME Paper 72-DE-21, General Electric Co., Aircraft Engine Group, Group Engineering Division, May 11, 1972).

from machine design criteria or from machine operating data. A typical Campbell diagram plot is shown in Figure 5-25. Engine rotational speed is along the *X* axis. The system frequency is along the *Y* axis. The fan lines are engine-order lines: one-half engine order, one times engine order, two times engine order, three times engine order, four times engine order, five times engine order, 10 times engine order, and so on. This form of design study is necessary, especially when designing an axial compressor to determine if a natural blade frequency is excited by a running frequency, its harmonics, or sub-harmonics. For example, take the second-stage blade of

Table 5-4 Characteristics of Rotor Instabilities

Type of Instability	Onset	Frequency Response	Caused by
Forced vibration			
Unbalance	Any speed	$N_f = N$	Nonhomogeneous material
Shaft misalignment	Any speed	$N_f = 2N$	Driver and driven equipment misaligned
Self-excited vibration			
Hysteretic whirl	$N > N_1$	$N_f \approx N_1$ $N_f = .5N$	Shrink fits and built-up parts
Hydrodynamic whirl (Oil whirl)	$N > 2N_1$	$N_f \leq .5N$	Fluid film bearings and seals
Aerodynamic whirl	$N > N_1$	$N_f = N_1$	Compressor or turbine, tip clearance effects, balance pistons
Dry-friction whirl	Any speed	$N_{f1} = -nN$	Shaft in contact with stationary guide
Entrained fluid	$N1 < N < 2N$	$N_f = N_1$ $.5N < Nf < N$	Liquid or steam entrapped in rotor

a hypothetical compressor. Its first flexural natural frequency is calculated and found to be 200 Hz. From the Campbell diagram figure, it is apparent that a forcing frequency of 12,000 rpm produced by operating the compressor at 12,000 rpm will excite the 200-Hz first flexural frequency of the blade (200 Hz $\times$ 60 = 12,000 rpm). Also, there are five inlet guide vanes ahead of the second-stage blade row. Operating the compressor at 2,400 rpm will excite the 200-Hz natural frequency of the blade (200 Hz $\times$ 60 = 5 $\times$ 2,400 rpm).

Following a calculation of the blade natural frequency and a Campbell diagram study of possible excitation sources, it is usual practice to check for the natural frequency band spread by testing the blades on a shaker table. This natural frequency band spread plotted on the Campbell diagram now indicates that operating the compressor between 11,700 rpm and 12,600 rpm should be prohibited. When there are several blade rows on the compressor and several sources of excitation, the designer can be confronted with the difficult task of designing the blade and guide vane rows to meet structural and aerodynamic criteria. Natural blade frequency will be affected by rotational and aerodynamic loading, and it needs to be factored in. In most axial compressors there are specific operational speed ranges, which are restricted to avoid blade failure from fatigue.

To ensure that blade stress levels are within the fatigue life requirements of the compressor, it is usual practice to strain-gauge the blading on one or two prototype

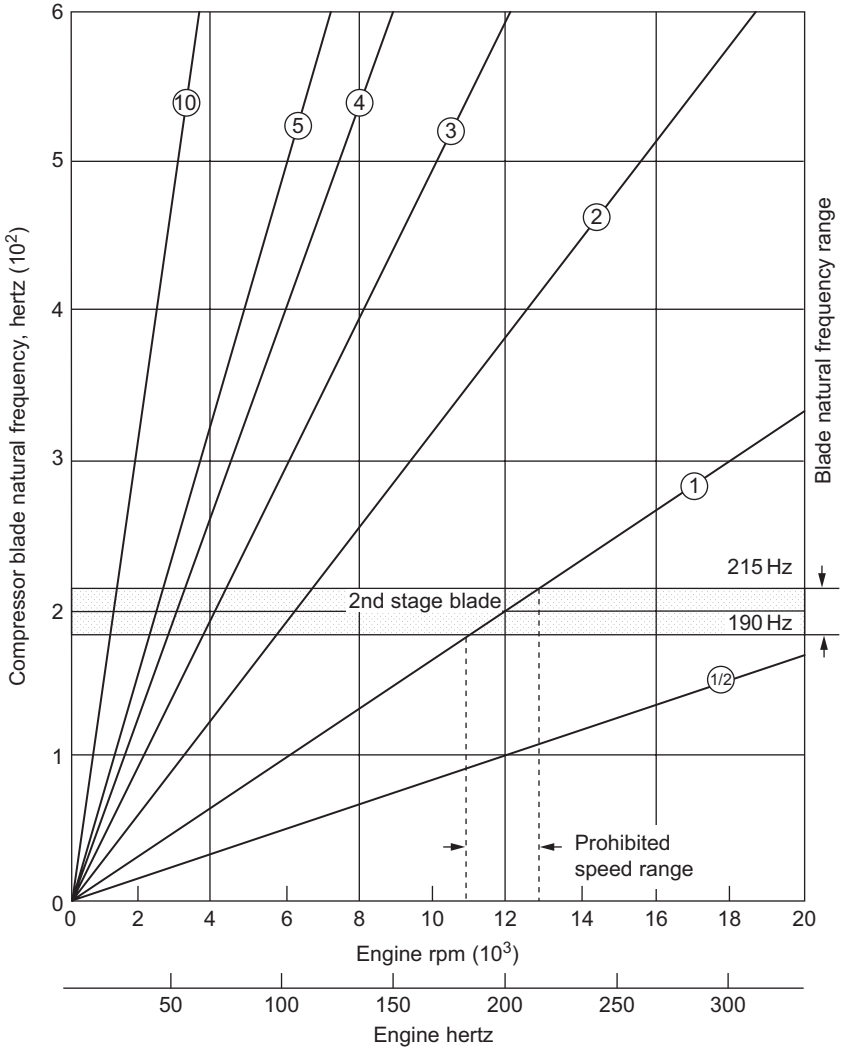


Figure 5-25 Campbell diagram.

machines, measure the stress levels, and generate a Campbell diagram showing the plotted test data. To measure data, an impeller can also be mounted on a shaker table with a variable frequency output (0–10,000 Hz). Accelerometers can be mounted at various positions on the impeller to obtain the frequency responses in conjunction with a spectrum analyzer (Figure 5-26).

Initially, tests are run to identify the major critical frequencies of the impeller. Mode shapes are then determined visually at each of the critical frequencies. To obtain these mode visualizations, salt is sprinkled evenly on the disc surface. The shaker is maintained at a particular frequency, at which value a given critical frequency is excited

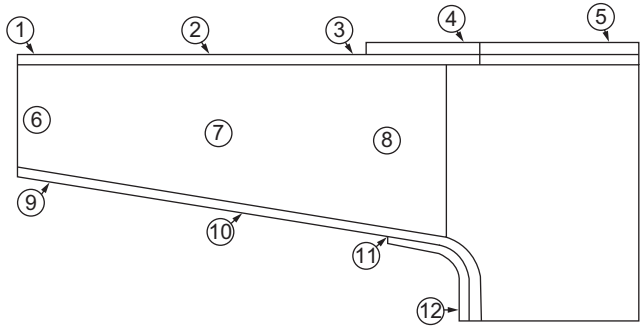


Figure 5-26 Accelerometer locations on impeller tested.

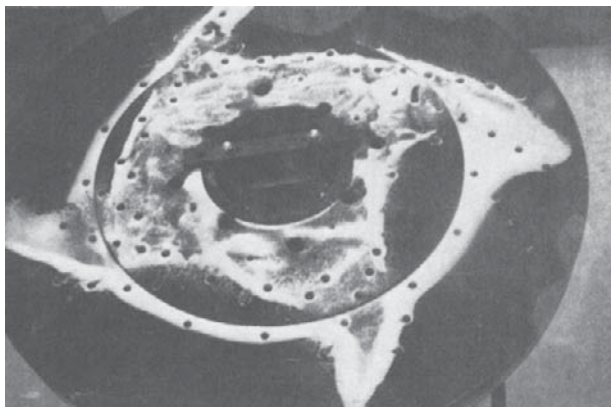


Figure 5-27 Impeller showing nodal points.

for a certain length of time so that the salt particles display the mode shape. The salt accumulates in the nodal regions. Photographs are taken at lower values of these critical frequencies. Photography allows a qualitative identification of the appropriate mode shapes corresponding to each frequency. Figure 5-27 shows an impeller with the mode shapes.

The next step in the testing procedure is to record accelerometer readings at various disc, blade, and shroud locations at lower critical frequencies. The objective of this test is to quantitatively identify the high and low excitation regions. For this test, a six- or five-blade region is considered sufficiently large to be representative of the entire impeller. The results of these tests are plotted on a Campbell diagram, as shown for one such impeller in Figure 5-28.

Lines of excitation frequencies are then drawn vertically on the Campbell diagram, and a line corresponding to the design speed is drawn horizontally. Where the lines of excitation frequencies and multiples of running speed intersect near the line of design rpm, a problem area may exist. If, for instance, an impeller has 20 blades, a design

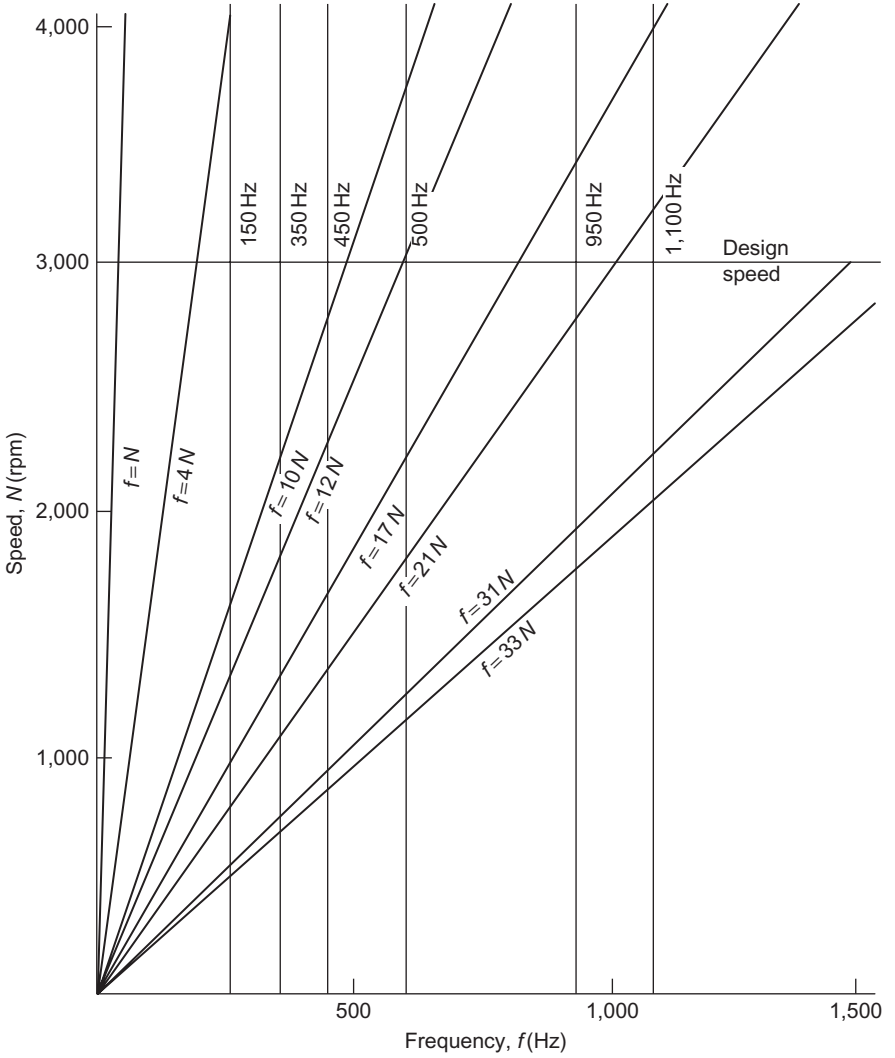


Figure 5-28 Campbell diagram of tested impeller.

speed of 3,000 rpm (50 Hz), and a critical frequency of 1,000 Hz, the impeller is very likely to be severely excited, since the critical is exactly 20*N*. On a Campbell diagram the previous example will correspond to an exact intersect of the running speed line, 1,000 Hz frequency line, and the line of slope 20*N*.

A shrouded impeller was tested containing 12 blades and a design speed of 3,000 rpm. The 12-bladed impeller's first excitation mode occurred at a frequency of 150 Hz, resulting in a single-umbrella mode occurring at the contact point between the two back shrouds. At 350 Hz a coupled mode existed. At these two frequencies it is the back shroud that is the exciting force. At 450 Hz a two-diameter mode existed.

This mode is characterized by four nodal radial lines and in many instances can be the most troublesome mode. This mode is excited by the front shroud and the impeller eye. A double-umbrella mode occurred at 600 Hz. At the last two frequencies, the blade eye experienced high excitation. The Campbell diagram (Figure 5-28) showed that at design speed this frequency coincided with the 12*N* line. This coincidence is undesirable, since the number of blades is 12 and may be the exciting force needed to cause a problem. At 950 Hz, a three-diameter mode existed, and at 1100 Hz a four-diameter mode existed. At 1100 Hz the blade-tip frequency is the predominant forcing function. This impeller seemed to be in trouble at 600 Hz, since this frequency coincided with the number of blades. To remove this problem, it was recommended that either the number of blades should be increased to 15 or the blades should be made out of a thicker stock. This type of analysis is useful mostly in the design stages so that problems may be prevented. An analysis may also be helpful in the field. If a problem exists, the machine can be run at a different speed to avert a catastrophe.

Bibliography

Alford, J.S., "Protecting Turbomachinery from Self-Excited Rotor Whirl," Journal of Engineering for Power, ASME Transactions, October, 1965, pp. 333–344.

Ehrich, F.F., "Identification and Avoidance of Instabilities and Self-Excited Vibrations in Rotating Machinery," Adopted from ASME Paper 72-De-21, General Electric Co., Aircraft Engine Group, Group Engineering Division, 11 May, 1972.

Gunter, E.J., Jr., "Rotor Bearing Stability," Proceedings of the 1st Turbomachinery Symposium, Texas A&M University, October, 1972, pp. 119–141.

Lund, J.W., "Stability and Damped Critical Speeds of a Flexible Rotor in Fluid-Film Bearings," ASME No. 73-DET-103.

Newkirk, B.L., "Shaft Whipping," *General Electric Review*, Vol. 27, (1924), p. 169.

Nicholas John, C., and Moll Randall, W., "Shifting Critical Speeds Out of the Operating Range by Changing from Tilting Pad to Sleeve Bearings," Proceedings of the 22nd Turbomachinery Symposium, Texas A&M University, p. 25, 1993.

Prohl, M.A., "General Method of Calculating Critical Speeds of Flexible Rotors," Trans. ASME, *J. Appl. Mech.*, Vol. 12, No. 3, September 1945, pp. A142–A148.

Reiger, D., "The Whirling of Shafts," *Engineer*, London, Vol. 158, 1934, pp. 216–228.

Thomson, W.T., *Mechanical Vibrations*, 2nd edition, Prentice-Hall, Inc., Englewood Cliffs, NJ, 1961.

Copyrighted Materials
Copyright © 2012 Elsevier Retrieved from www.knovel.com

Part II

Major Components

6 Centrifugal Compressors

Centrifugal compressors are used in small gas turbines and are the driven units in most gas turbine compressor trains. They are an integral part of the petrochemical industry, finding extensive use because of their smooth operation, large tolerance of process fluctuations, and their higher reliability compared to other types of compressors. Centrifugal compressors range in size from pressure ratios of 1:3 per stage to as high as 12:1 on experimental models. Discussion here will be limited to pressure ratios below 3.5:1, since this type is prevalent in the petrochemical industry. The proper selection of a compressor is a complex and important decision. The successful operation of many plants depends on smooth and efficient compressor operations. To ensure the best selection and proper maintenance of a centrifugal compressor, the engineer must have a knowledge of many engineering disciplines.

In a typical centrifugal compressor the fluid is forced through the impeller by rapidly rotating impeller blades. The velocity of the fluid is converted to pressure, partially in the impeller and partially in the stationary diffusers. Most of the velocity leaving the impeller is converted into pressure energy in the diffuser as shown in Figure 6-1. It is normal practice to design the compressor so that half the pressure rise takes place in the impeller and the other half in the diffuser. The diffuser consists essentially of vanes, which are tangential to the impeller. These vane passages diverge to convert the velocity head into pressure energy. The inner edges of the vanes are in line with the direction of the resultant airflow from the impeller as shown in Figure 6-2.

Centrifugal compressors, in general, are used for higher-pressure ratios and lower-flow rates compared to lower-stage pressure ratios and higher-flow rates in axial compressors. Figure 6-3 is a map for centrifugal compressors that shows the effect of specific speed (N_s) and specific diameter (D_s) on their efficiency. The most efficient region for centrifugal compressor operation is in a specific speed range between $60 < N_s > 1{,}500$. Specific speeds of more than 3,000 usually require an axial-flow-type compressor. In a centrifugal compressor the angular momentum of the gas flowing through the impeller is increased partly because the impeller's outlet diameter is significantly greater than its inlet diameter. The major difference between axial and centrifugal compressors is the variance in the diameters of the inlet and the outlet. The flow leaving the centrifugal compressor is usually perpendicular to the axis of rotation.

Gas Turbine Engineering Handbook, Fourth Edition. DOI: 10.1016/B978-0-12-383842-1.00006-8
Copyright © 2012 Elsevier Inc. All rights reserved.

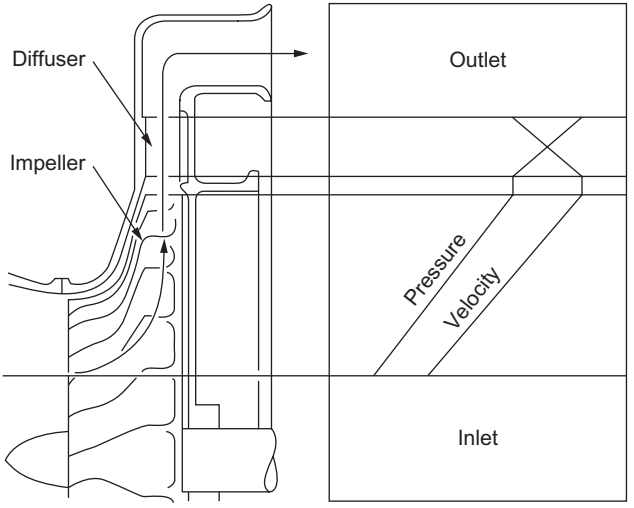


Figure 6-1 Pressure and velocity through a centrifugal compressor.

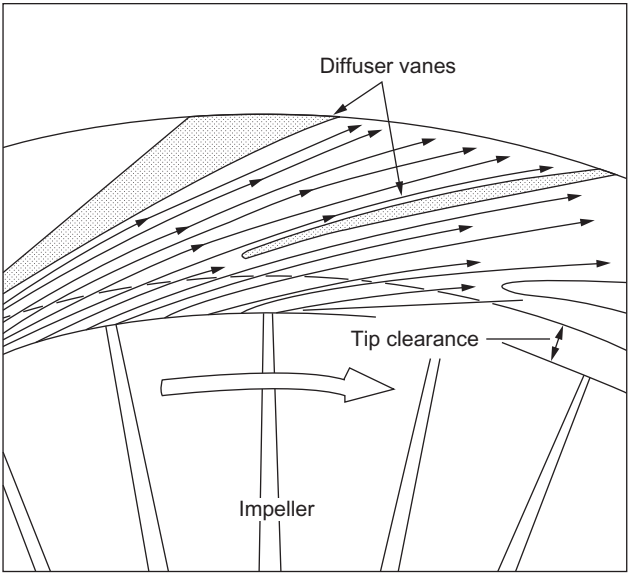


Figure 6-2 Flow entering a vaned diffuser.

Centrifugal Compressor Components

The terminology used to define the components of a centrifugal compressor is shown in Figure 6-4. A centrifugal compressor is composed of inlet guide vanes, an inducer, an impeller, a diffuser, and a scroll. The inlet guide vanes (IGVs) are used in only a

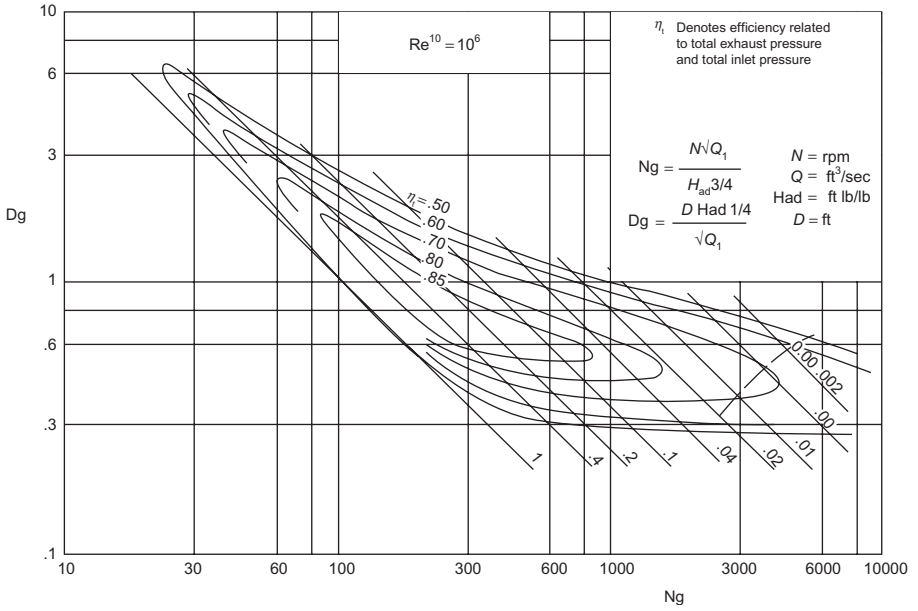


Figure 6-3 Centrifugal compressor map. Balje, O.E., "A Study of Reynolds Number Effects in Turbomachinery," *Journal of Engineering for Power*, ASME Trans., Vol. 86, Series A, p. 227.

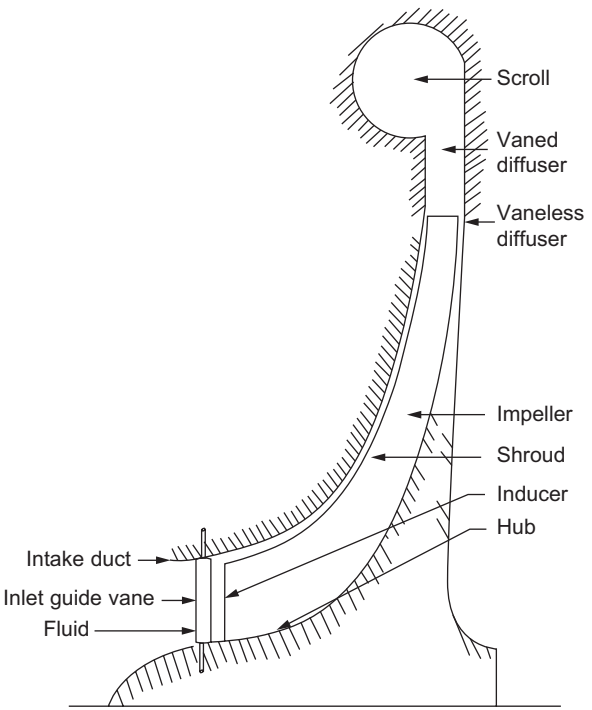


Figure 6-4 Schematic of a centrifugal compressor.

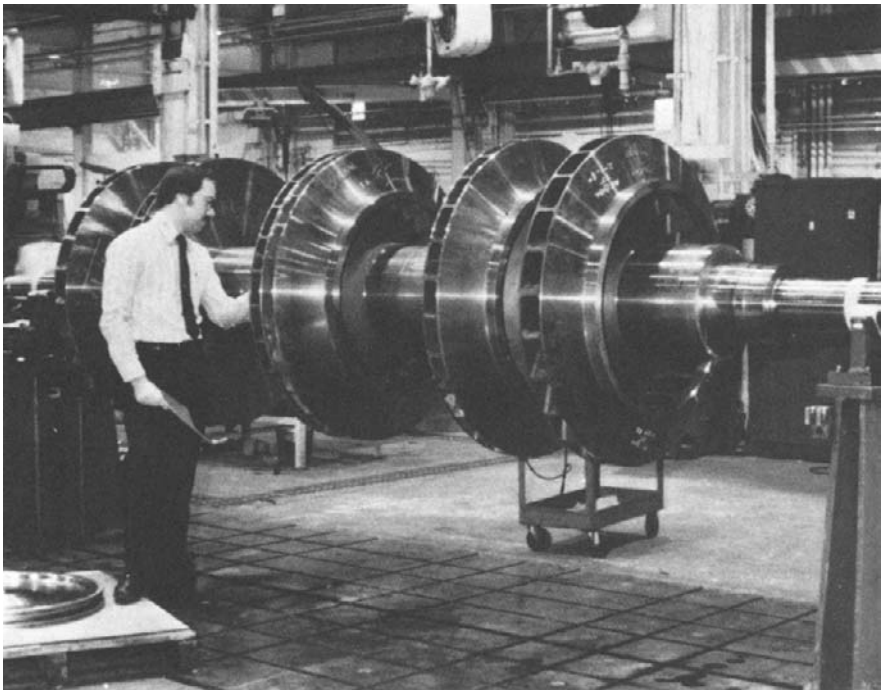


Figure 6-5 Closed impeller (courtesy Elliott Company, Jeannette, PA).

high-pressure ratio transonic compressor. Centrifugal compressor impellers are either shrouded or un-shrouded as seen in Figures 6-5 and 6-6.

The fluid comes into the compressor through an intake duct and is given pre-whirl by the IGVs. It then flows into an inducer without any incidence angle, and its flow direction is changed from axial to radial. The fluid is given energy at this stage by the rotor as it goes through the impeller while compressing. It is then discharged into a diffuser, where the kinetic energy is converted into static pressure. The flow enters the scroll from which the compressor discharge is taken. Figure 6-1 shows the variations in pressure and velocity through a compressor.

There are two kinds of energy inducer systems: a single-entry inducer and a double-entry inducer as shown in Figure 6-7.

A double-entry inducer system halves the inlet flow so that a smaller inducer-tip diameter can be used, reducing the inducer-tip Mach number; however, the design is difficult to integrate into many configurations.

There are three impeller vane types, as shown in Figure 6-8. These are defined according to the exit blade angles. Impellers with exit blade angle $\beta_2 = 90^\circ$ are radial vanes. Impellers with $\beta_2 < 90^\circ$ are backward-curved or backward-swept vanes, and for $\beta_2 > 90^\circ$, the vanes are forward-curved or forward-swept. They have different characteristics of theoretical head-flow relationship to each other, as shown in Figure 6-9. Although in Figure 6-9 the forward-curved head is the largest, in actual

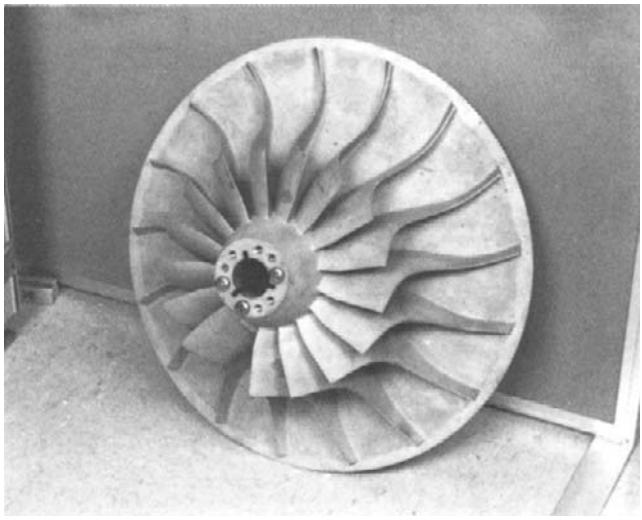


Figure 6-6 Open-faced impeller.

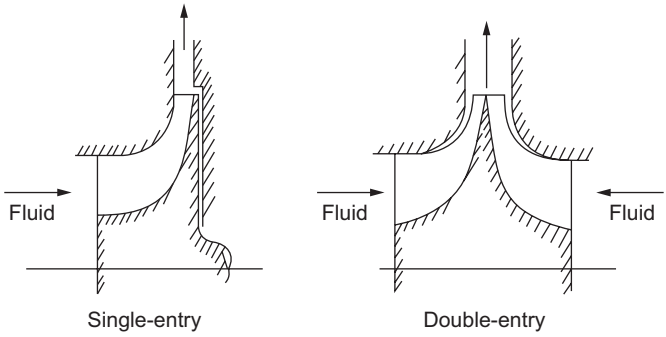


Figure 6-7 Types of entry-inducer systems.

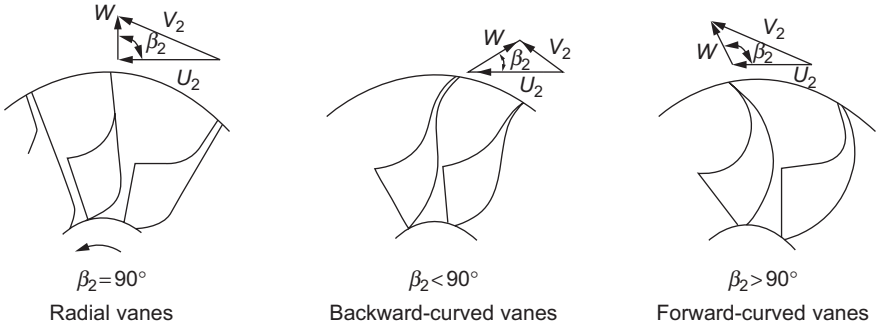


Figure 6-8 Various types of impeller blading.

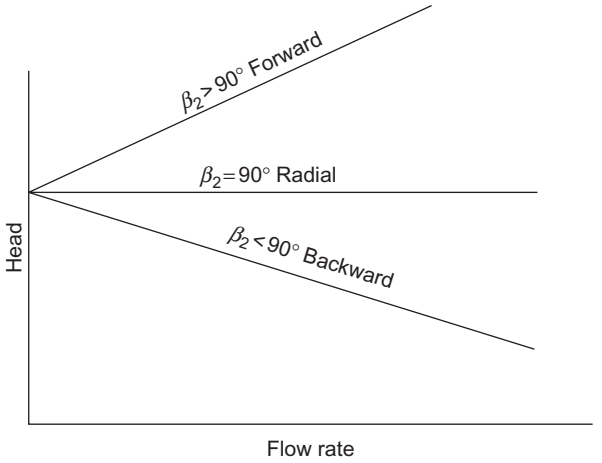


Figure 6-9 Head flow-rate characteristics for various outlet blade angles.

Table 6-1 The Advantages and Disadvantages of Various Impellers

Types of Impellers	Advantages	Disadvantages
Radial vanes	1. Reasonable compromise between low-energy transfer and high absolute outlet velocity 2. No complex bending stress 3. Easy manufacturing	1. Surge margin is relatively narrow
Backward-curved vanes	1. Low-outlet kinetic energy = low-diffuser inlet Mach number 2. Surge margin is wide	1. Low-energy transfer 2. Complex bending stress 3. Hard manufacturing
Forward-curved vanes	1. High-energy transfer	1. High-outlet kinetic energy = high-diffuser inlet Mach number 2. Surge margin is less than radial vanes 3. Complex bending stress 4. Hard manufacturing

practice the head characteristics of all the impellers are similar to the backward-curved impeller. Table 6-1 shows the advantages and disadvantages of various impellers.

The Euler equation, assuming simple one-dimensional flow theory, is the theoretical amount of work imparted to each pound of fluid as it passes through the impeller, and it is given by:

$$H = \frac{1}{g_c}[U_1 V_{\theta 1} - U_2 V_{\theta 2}] \tag{6-1}$$

where

H = work per lb of fluid
U_2 = impeller peripheral velocity
U_1 = inducer velocity at the mean radial station
$V_{\theta 2}$ = absolute tangential fluid velocity at impeller exit
$V_{\theta 1}$ = absolute tangential air velocity at inducer inlet

For the axial inlet:

$$V_{\theta 1} = 0$$

then

$$H = -\frac{1}{g_c}(U_2 V_{\theta 2}) \tag{6-2}$$

Supposing constant rotational speeds, no slip, and an axial inlet, the velocity triangles are as shown in Figure 6-10. For the radial vane, the absolute tangential fluid velocity at the impeller exit is constant – even if the flow rate is increased or decreased.

Therefore:

$$H \approx U_2 V''_{\theta 2} \approx U_2 V_{\theta 2} \approx U_2 V'_{\theta 2} \tag{6-3}$$

flow decrease — flow increase

For backward-curved vanes, the absolute tangential fluid velocity at the impeller exit increases with the reduction of flow rates and decreases with the increase in flow

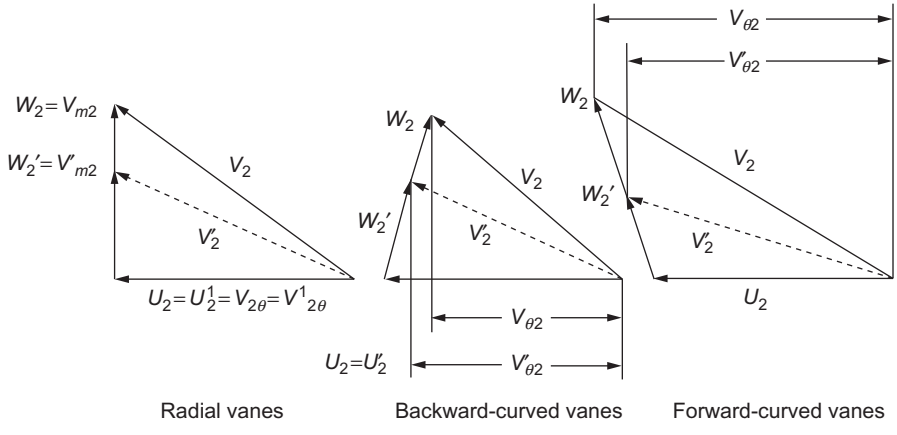


Figure 6-10 Velocity triangles.

rate as shown in the following equation:

$$H \approx \underset{\substack{\text{flow}\\ \text{decrease}}}{-U_2 V''_{\theta 2}} > -U_2 V_{\theta 2} < \underset{\substack{\text{flow}\\ \text{increase}}}{-U_2 V'_{\theta 2}} \tag{6-4}$$

For forward-curved vanes, the absolute tangential fluid velocity at the impeller exit decreases with the reduction of flow rates and increases with the decrease in flow rates as shown in the following equation:

$$H \approx \underset{\substack{\text{flow}\\ \text{decrease}}}{-U_2 V'_{\theta}} < U_2 V_{\theta 2} > \underset{\substack{\text{flow}\\ \text{increase}}}{U_2 V'_{\theta}} \tag{6-5}$$

Inlet Guide Vanes

The inlet guide vanes give circumferential velocity to the fluid at the inducer inlet. This function is called pre-whirl. Figure 6-11 shows inducer inlet velocity diagrams with and without IGVs.

IGVs are installed directly in front of the inducer or, where an axial entry is not possible, located radially in an intake duct.

A positive vane angle produces pre-whirl in the direction of the impeller rotation, and a negative vane angle produces pre-whirl in the opposite direction. The disadvantage of positive pre-whirl is that a positive inlet whirl velocity reduces the energy transfer. Since $V_{\theta 1}$ is positive according to the Euler equation:

$$H = \frac{1}{g_c}[U_1 V_{\theta 1} - U_2 V_{\theta 2}] \tag{6-6}$$

non-pre-whirl (without IGVs axial entry), $V_{\theta 1}$ is equal to zero. Then the Euler work is:

$$H = -U_2 V_{\theta 2}.$$

With positive pre-whirl, the first term of the Euler equation remains $H = U_1 V_{\theta 1} - U_2 V_{\theta 2}$. Therefore, Euler work is reduced by the use of positive pre-whirl. On the other hand, negative pre-whirl increases the energy transfer by the amount $U_1 V_{\theta 1}$. This results in a larger pressure head being produced in the case of the negative pre-whirl for the same impeller diameter and speed.

The positive pre-whirl decreases the relative Mach number at the inducer inlet. However, negative pre-whirl increases it. A relative Mach number is defined by:

$$M_{\text{rel}} = \frac{W_1}{a_1} \tag{6-7}$$

where

M_{rel} = relative Mach number
W_1 = relative velocity at an inducer inlet
a_1 = sonic velocity at inducer inlet conditions

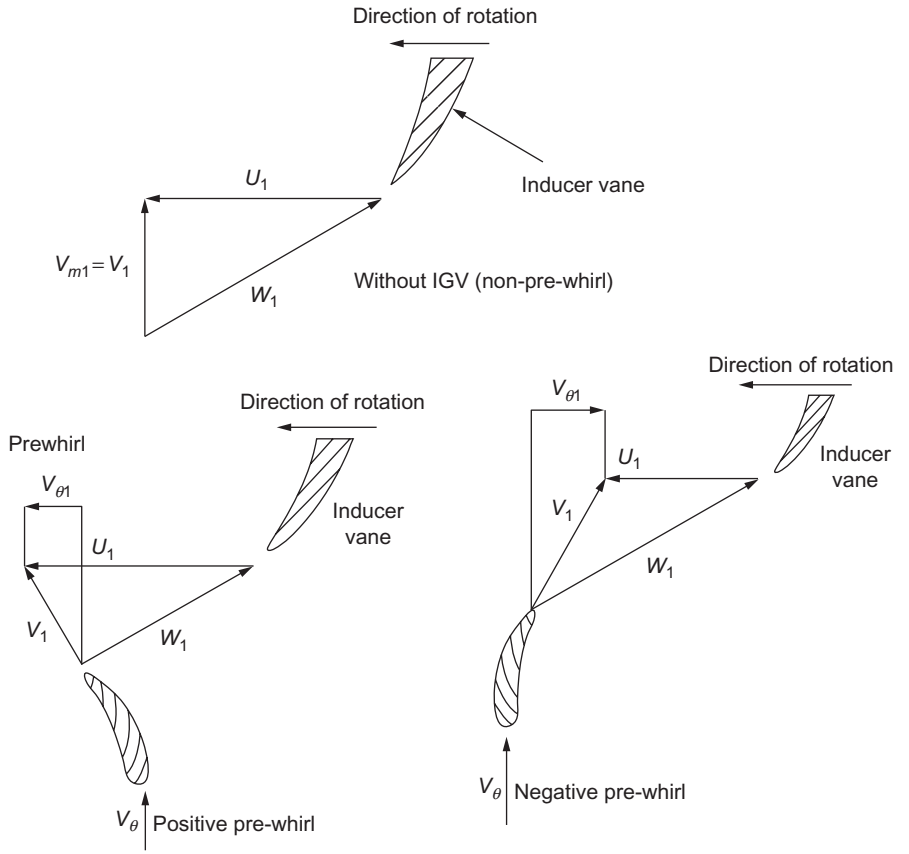


Figure 6-11 Inducer inlet velocity diagrams.

The purpose of installing the IGVs is to decrease the relative Mach number at the inducer-tip (impeller eye) inlet because the highest relative velocity at the inducer inlet is at the tip section. When the relative velocity is close to the sonic velocity or greater than it, a shock wave takes place in the inducer section. A shock wave produces shock loss and chokes the inducer. Figure 6-12 shows the effect of inlet pre-whirl on compressor efficiency.

There are three kinds of pre-whirl:

1. *Free-vortex pre-whirl.* This type is represented by $r_1 V_{\theta 1} =$ constant with respect to the inducer inlet radius. This pre-whirl distribution is shown in Figure 6-13. $V_{\theta 1}$ is at a minimum at the inducer inlet shroud radius. Therefore, it is not effective in decreasing the relative Mach number in this manner.
2. *Forced-vortex pre-whirl.* This type is shown as $V_{\theta 1}/r_1 =$ constant. This pre-whirl distribution is also shown in Figure 6-14. $V_{\theta 1}$ is at a maximum at the inducer inlet shroud radius, contributing to a decrease in the inlet relative Mach number.
3. *Control-vortex pre-whirl.* This type is represented by $V_{\theta 1} = AR_1 + B/r_1$, where A and B are constants. This equation shows the first type with $A = 0, B \neq 0$, and the second type with $B = 0, A \neq 0$.

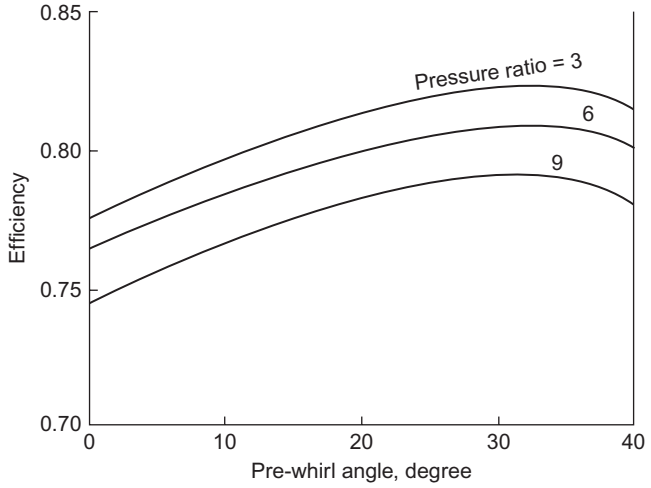


Figure 6-12 Estimate effect of inlet pre-whirl. (Rodgers, C., and Shapiro, L., "Design Considerations for High-Pressure-Ratio Centrifugal Compressors," ASME Paper No.: 73-GT-31, 1972.)

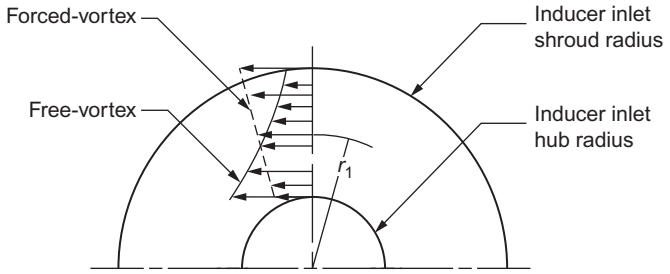


Figure 6-13 Pre-whirl distribution patterns.

Euler work distributions at an impeller exit, with respect to the impeller width, are shown in Figure 6-14. From Figure 6-14, the pre-whirl distribution should be made not only from the relative Mach number at the inducer inlet shroud radius, but also from Euler work distribution at the impeller exit. Uniform impeller exit flow conditions, considering the impeller losses, are important factors in obtaining good compressor performance.

Impeller

An impeller in a centrifugal compressor imparts energy to a fluid. The impeller consists of two basic components: (1) an inducer like an axial-flow rotor, and (2) the radial blades where energy is imparted by centrifugal force. Flow enters the impeller in the axial direction and leaves in the radial direction. The velocity variations from hub to shroud resulting from these changes in flow directions complicate the design

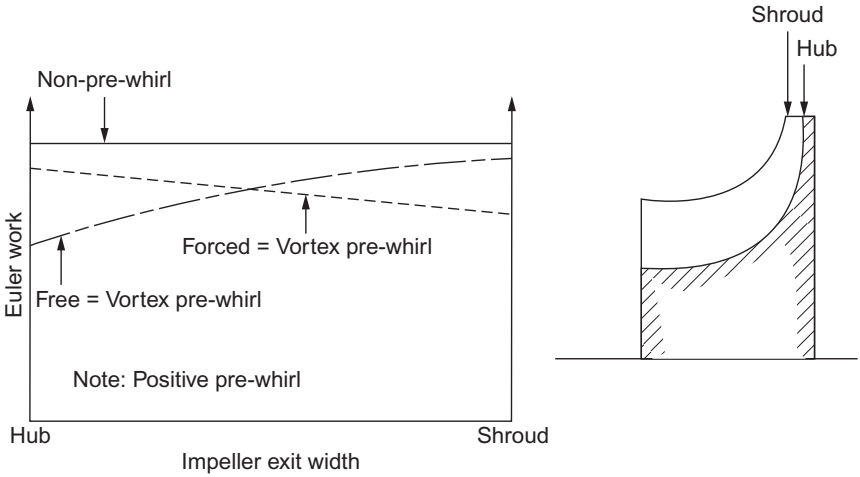


Figure 6-14 Euler work distribution at an impeller exit.

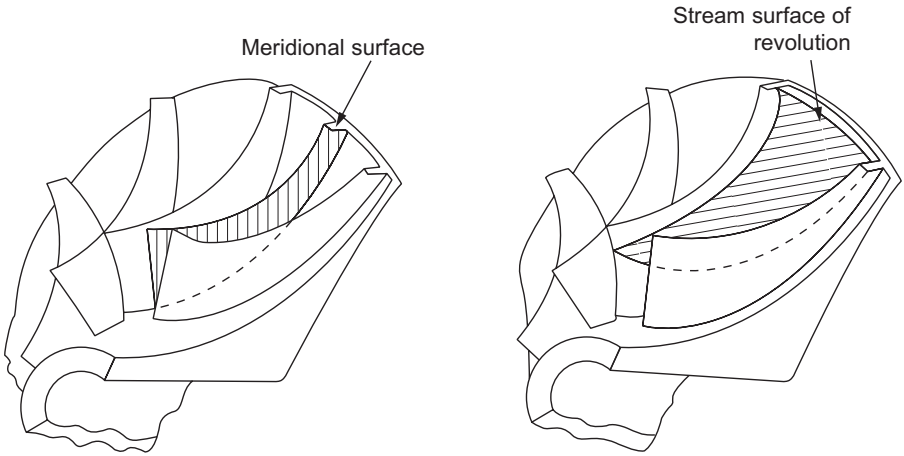


Figure 6-15 Two-dimensional surface for a flow analysis.

procedure for centrifugal compressors. C.H. Wu has presented the three-dimensional theory in an impeller, but it is difficult to solve for the flow in an impeller using the previous theory without certain simplified conditions. Others have dealt with it as a quasi-three-dimensional solution. It is composed of two solutions, one in the meridional surface (hub-to-shroud), and the other in the stream surface of revolution (blade-to-blade). These surfaces are illustrated in Figure 6-15.

By the application of the previous method using a numerical solution to the complex flow equations, it is possible to achieve impeller efficiencies of more than 90%. The actual flow phenomenon in an impeller is more complicated than the one

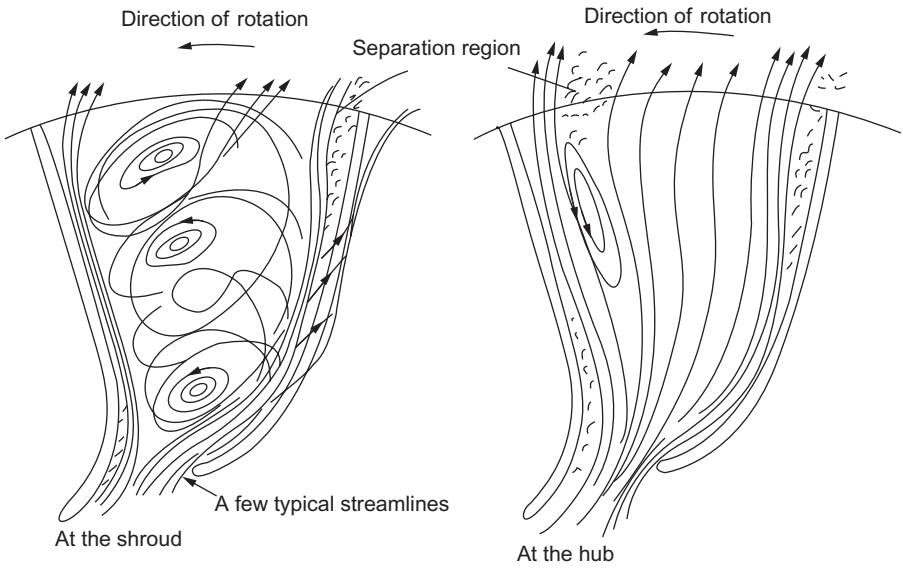


Figure 6-16 Flow map of impeller plane.

calculated. One example of this complicated flow is shown in Figure 6-16. The stream lines observed in Figure 6-16 do not cross, but are actually in different planes observed near the shroud. Figure 6-17 shows the flow in the meridional plane with separation regions at the inducer section and at the exit.

Experimental studies of the flow within impeller passages have shown that the distribution of velocities on the blade surfaces are different from the distributions predicted theoretically. It is likely that the discrepancies between theoretical and experimental results are due to secondary flows from pressure losses and boundary-layer separation in the blade passages. High-performance impellers should be designed, when possible, with the aid of theoretical methods for determining the velocity distributions on the blade surfaces.

Examples of the theoretical velocity distributions in the impeller blades of a centrifugal compressor are shown in Figure 6-18. The blades should be designed to eliminate large decelerations or accelerations of flow in the impeller that lead to high losses and separation of the flow. Potential flow solutions predict the flow well in regions away from the blades where boundary-layer effects are negligible. In a centrifugal impeller the viscous shearing forces create a boundary layer with reduced kinetic energy. If the kinetic energy is reduced below a certain limit, the flow in this layer becomes stagnant, then it reverses.

Inducer

The function of an inducer is to increase the fluid's angular momentum without increasing its radius of rotation. In an inducer section the blades bend toward the

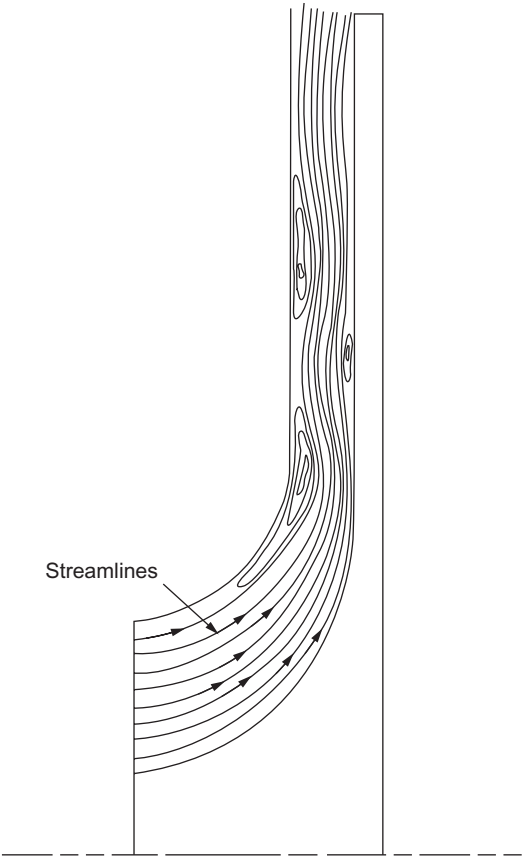


Figure 6-17 Flow map as seen in meridional plane.

direction of rotation as shown in Figure 6-19. The inducer is an axial rotor and changes the flow direction from the inlet flow angle to the axial direction. It has the largest relative velocity in the impeller and, if not properly designed, can lead to choking conditions at its throat as shown in Figure 6-19.

There are three forms of inducer camber lines in the axial direction. These are circular arc, parabolic arc, and elliptical arc. Circular arc camber lines are used in compressors with low pressure ratios, while the elliptical arc produces good performance at high pressure ratios where the flow has transonic Mach numbers.

Because of choking conditions in the inducer, many compressors incorporate a splitter-blade design. The flow pattern in such an inducer section is shown in Figure 6-20 (a). This flow pattern indicates a separation on the suction side of the splitter blade. Other designs include tandem inducers. In tandem inducers the inducer section is slightly rotated as shown in Figure 6-20 (b). This modification gives additional kinetic energy to the boundary, which is otherwise likely to separate.

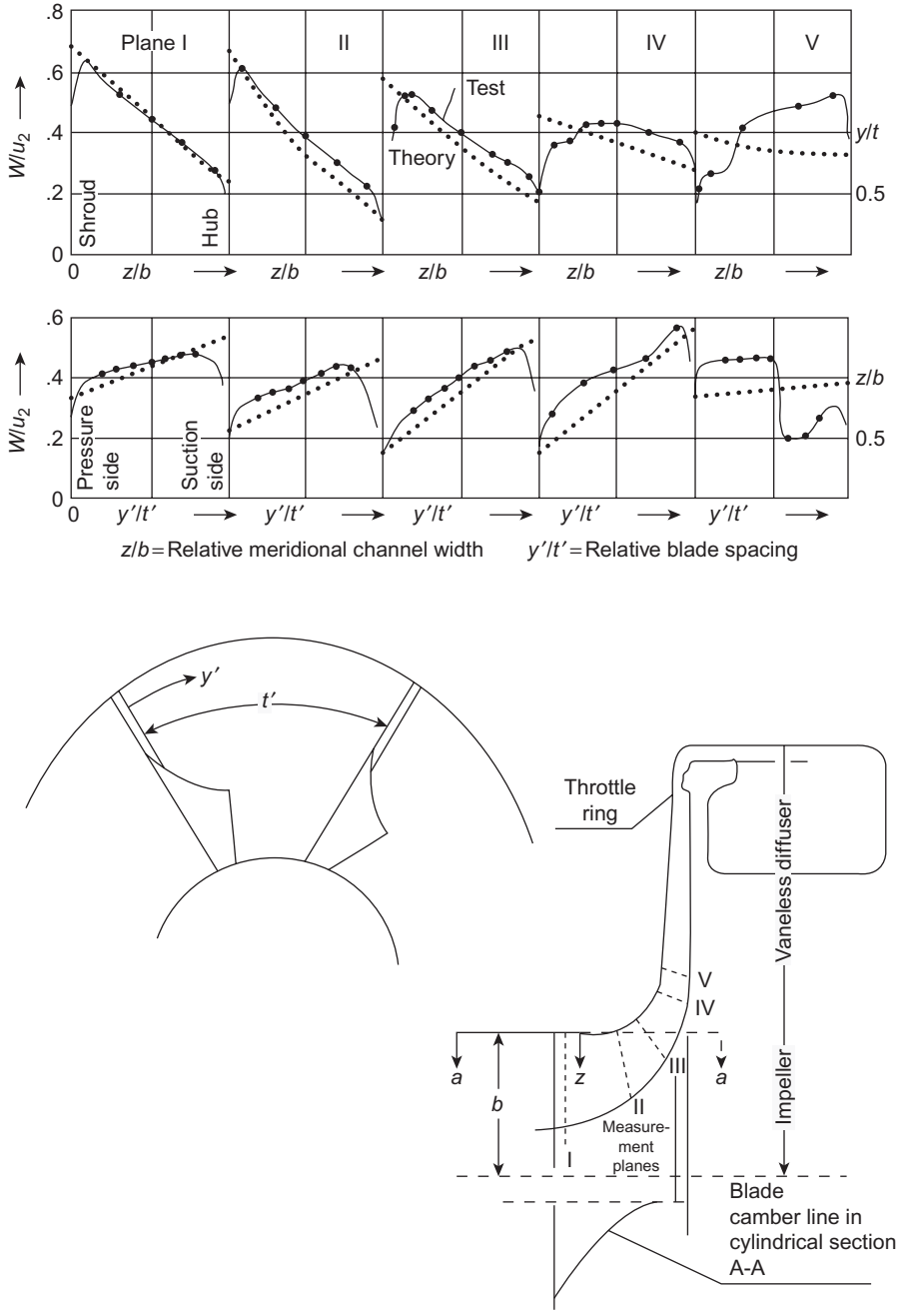


Figure 6-18 Velocity profiles through a centrifugal compressor.

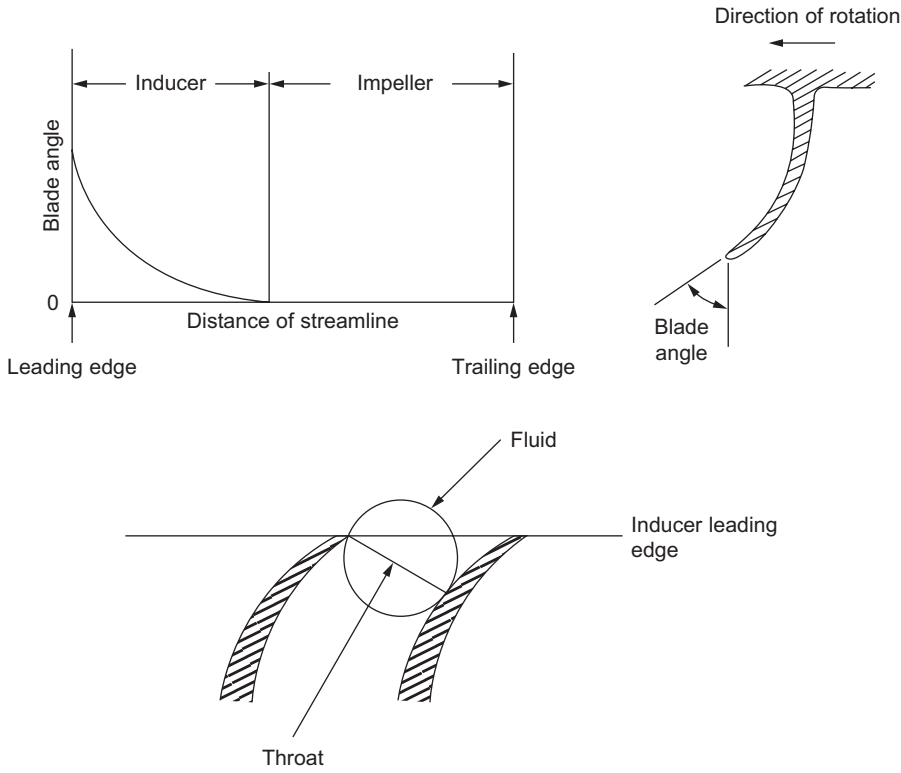


Figure 6-19 Inducer centrifugal compressor.

Centrifugal Section of an Impeller

The flow in this section of the impeller enters from the inducer section and leaves the impeller in the radial direction. The flow in this section is not completely guided by the blades, and hence the effective fluid outlet angle does not equal the blade outlet angle.

To account for flow deviation (which is similar to the effect accounted for by the deviation angle in axial-flow machines), the slip factor is used:

$$\mu = \frac{V_{\theta 2}}{V_{\theta 2\infty}} \tag{6-8}$$

where $V_{\theta 2}$ is the tangential component of the absolute exit velocity with a finite number of blades, and $V_{\theta 2\infty}$ is the tangential component of the absolute exit velocity, if the impeller were to have an infinite number of blades (no slipping back of the relative velocity at outlet).

With radial blades at the exit:

$$\mu = \frac{V_{\theta 2}}{U_2} \tag{6-9}$$

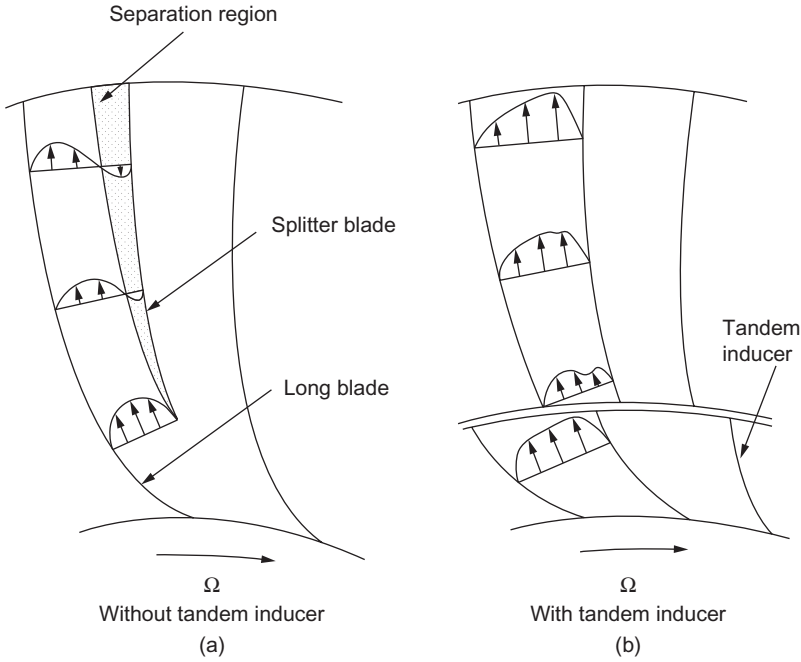


Figure 6-20 Impeller channel flow.

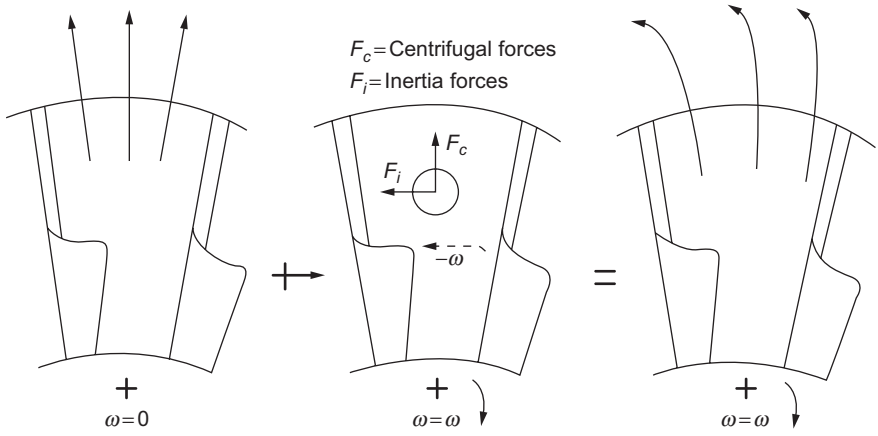


Figure 6-21 Forces and flow characteristics in a centrifugal compressor.

Flow in a rotating impeller channel (blade passage) will be a vector sum of flow with the impeller stationary and the flow due to rotation of the impeller as seen in Figure 6-21.

In a stationary impeller, the flow is expected to follow the blade shape and exit tangentially to it. A high adverse pressure gradient along the blade passage and subsequent flow separation are not considered to be general possibilities.

Inertia and centrifugal forces cause the fluid elements to move closer to and along the leading surface of the blade toward the exit. Once out of the blade passage, where there is no positive impelling action present, these fluid elements slow down.

Causes of Slip in an Impeller

The definite cause of the slip phenomenon that occurs within an impeller is not known. However, some general reasons can be used to explain why the flow is changed.

Coriolis Circulation

Because of the pressure gradient between the walls of two adjacent blades, the Coriolis forces, the centrifugal forces, and the fluid all follow the Helmholtz vorticity law. The combined gradient that results causes a fluid movement from one wall to the other and vice versa. This movement sets up circulation within the passage as seen in Figure 6-22. Because of this circulation, a velocity gradient results at the impeller exit with a net change in the exit angle.

Boundary-Layer Development

The boundary layer that develops within an impeller passage causes the flowing fluid to experience a smaller exit area as shown in Figure 6-23. This smaller exit is due to small flow (if any) within the boundary layer. For the fluid to exit this smaller area, its velocity must increase. This increase gives a higher relative exit velocity. Since

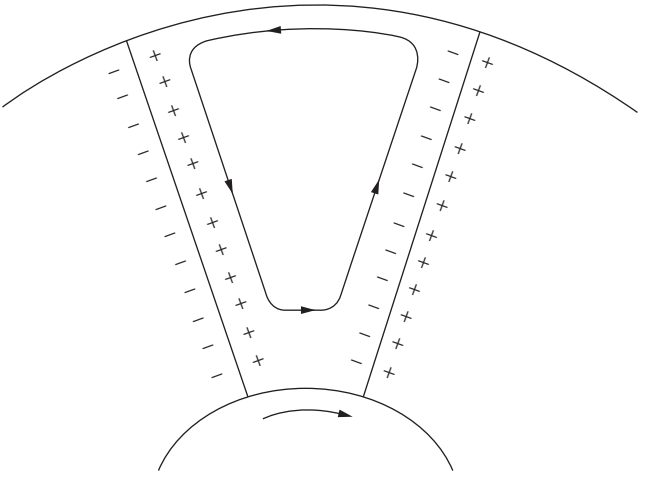


Figure 6-22 Coriolis circulation.

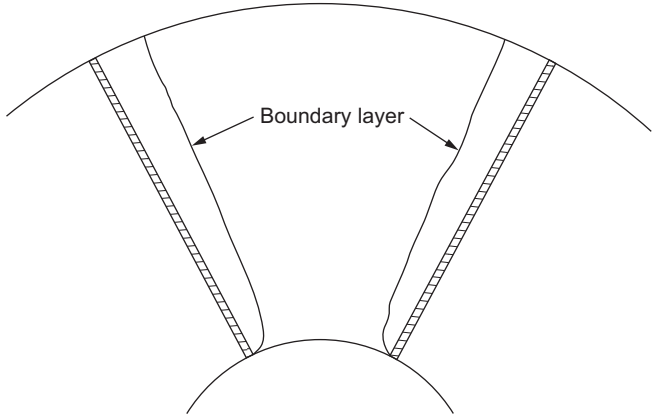


Figure 6-23 Boundary-layer development.

the meridional velocity remains constant, the increase in relative velocity must be accompanied by a decrease in absolute velocity.

Although it is not a new approach, boundary-layer control is being used more than ever before. It has been used with success on airfoil designs when it has delayed separation, thus giving a larger usable angle of attack. Control of the flow over an airfoil has been accomplished in two ways: by using slots through the airfoil and by injecting a stream of fast-moving air.

Separation regions are also encountered in the centrifugal impeller as shown previously. Applying the same concept (separation causes a loss in efficiency and power) reduces and delays their formation. Diverting the slow-moving fluid away lets the separation regions be occupied by a faster stream of fluid, which reduces boundary-layer build-up and thus decreases separation.

To control the boundary layer in the centrifugal impeller, slots in the impeller blading at the point of separation are used. To realize the full capability of this system, these slots should be directional and converging in a cross-sectional area from the pressure to the suction sides as seen in Figure 6-24. The fluid diverted by these slots increases in velocity and attaches itself to the suction sides of the blades. This results in moving the separation region closer to the tip of the impeller, thus reducing slip and losses encountered by the formation of large boundary-layer regions. The slots must be located at the point of flow separation from the blades. Experimental results indicate: improvement in the pressure ratio, efficiency, and surge characteristics of the impeller as seen in Figure 6-24.

Leakage

Fluid flow from one side of a blade to the other side is referred to as leakage. Leakage reduces the energy transfer from impeller to fluid and decreases the exit velocity angle.

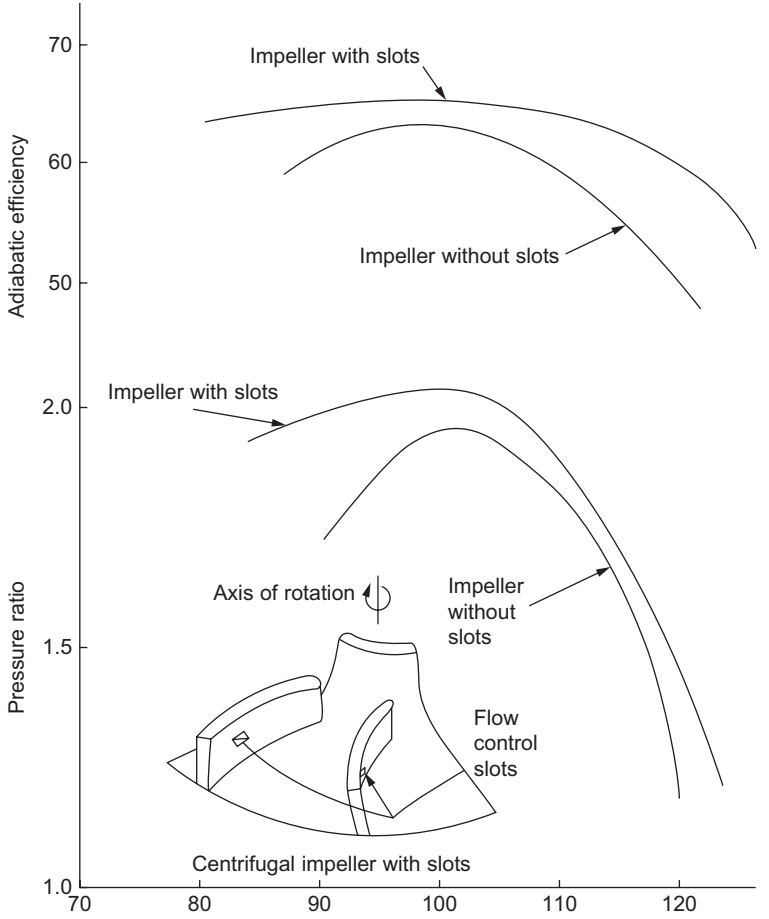


Figure 6-24 Percent design flow – laminar flow control in a centrifugal compressor.

Number of Vanes

The greater the number of vanes, the lower the vane loading, and the closer the fluid follows the vanes. With higher vane loadings, the flow tends to group up on the pressure surfaces and introduces a velocity gradient at the exit.

Vane Thickness

Because of manufacturing problems and physical necessity, impeller vanes are thick. When fluid exits the impeller, the vanes no longer contain the flow, and the velocity is immediately slowed. Because it is the meridional velocity that decreases, both the relative and absolute velocities decrease, changing the exit angle of the fluid.

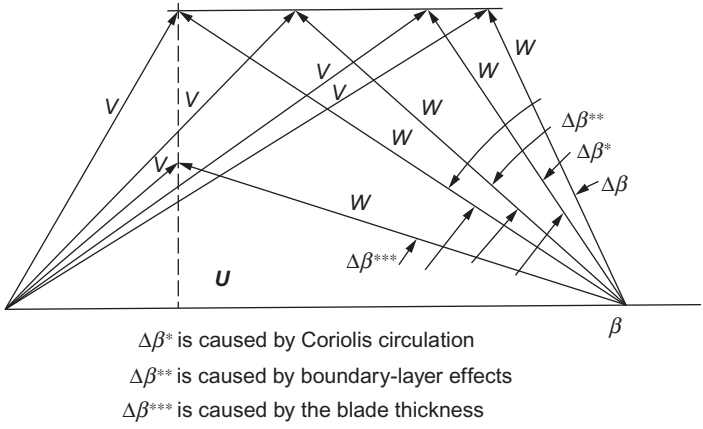


Figure 6-25 Effect on exit velocity triangles by various parameters.

A backward-curved impeller blade combines all these effects. The exit velocity triangle for this impeller with the different slip phenomenon changes is shown in Figure 6-25. This triangle shows that actual operating conditions are far removed from the projected design condition.

Several empirical equations have been derived for the slip factor (see Figure 6-26). These empirical equations are limited. Two of the more common slip factors are presented here.

Stodola Slip Factor

The second Helmholtz law states that the vorticity of a frictionless fluid does not change with time. Hence, if the flow at the inlet to an impeller is irrotational, the absolute flow must remain irrotational throughout the impeller. As the impeller has an angular velocity ω, the fluid must have an angular velocity $-\omega$ relative to the impeller. This fluid motion is called the relative eddy. If there were no flow through the impeller, the fluid in the impeller channels would rotate with an angular velocity equal and opposite to the impeller's angular velocity.

To approximate the flow, Stodola's theory assumes that the slip is due to the relative eddy. The relative eddy is considered as a rotation of a cylinder of fluid at the end of the blade passage at an angular velocity of $-\omega$ about its own axis. The Stodola slip factor is given by:

$$\mu = 1 - \frac{\pi}{Z}\left[1 - \frac{\sin\beta_2}{\dfrac{V_{m2}\cot\beta_2}{U_2}}\right] \tag{6-10}$$

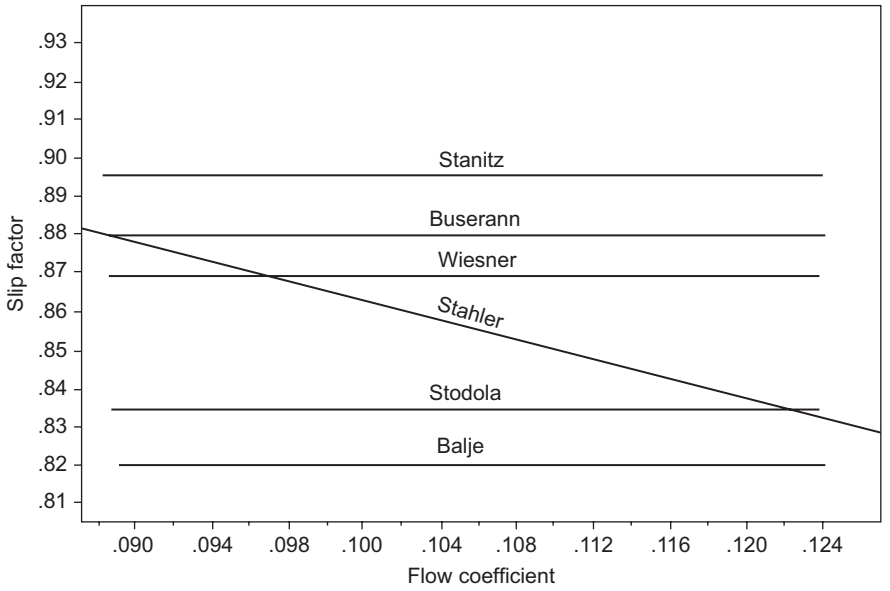


Figure 6-26 Various slip factors as a function of the coefficient.

where

$\beta_2 =$ the blade angle
$Z =$ the number of blades
$V_{m2} =$ the meridional velocity
$U_2 =$ blade tip speed

Calculations using this equation have been found to be lower than experimental values.

Stanitz Slip Factor

Stanitz calculated blade-to-blade solutions for eight impellers and concluded that for the range of conditions covered by the solutions, U is a function of the number of blades (Z), and the blade exit angle (β_2) is approximately the same whether the flow is compressible or incompressible:

$$\mu = 1 - \frac{0.63\pi}{Z}\left[1 - \frac{1}{\frac{W_{m2}}{U_2}\cot\beta_2}\right] \tag{6-11}$$

Stanitz's solutions were for $\pi/4 < \beta_2 < \pi/2$. This equation compares well with experimental results for radial or near-radial blades.

Diffusers

Diffusing passages have always played a vital role in obtaining good performance from turbomachines. Their role is to recover the maximum possible kinetic energy leaving the impeller with a minimum loss in total pressure. The efficiency of centrifugal compressor components has been steadily improved by advancing their performance. However, significant further improvement in efficiency will be gained only by improving the pressure recovery characteristics of the diffusing elements of these machines, since these elements have the lowest efficiency.

The performance characteristics of a diffuser are complicated functions of diffuser geometry, inlet flow conditions, and exit flow conditions. Figure 6-27 shows typical diffusers classified by their geometry. The selection of an optimum channel diffuser for a particular task is difficult, since it must be chosen from an almost infinite number of cross-sectional shapes and wall configurations. In radial and mixed-flow compressors the requirement of high performance and compactness leads to the use of vaned diffusers as shown in Figure 6-28. Figure 6-28 also shows the flow regime of a vane-island diffuser.

Matching the flow between the impeller and the diffuser is complex because the flow path changes from a rotating system into a stationary one. This complex, unsteady flow is strongly affected by the jet-wake of the flow leaving the impeller, as seen in Figure 6-29. The three-dimensional boundary layers, the secondary flows in the vaneless region, and the flow separation at the blades also affect the overall flow in the diffuser.

The flow in the diffuser is usually assumed to be of a steady nature to obtain the overall geometric configuration of the diffuser. In a channel-type diffuser the viscous shearing forces create a boundary layer with reduced kinetic energy. If the kinetic energy is reduced below a certain limit, the flow in this layer becomes stagnant and then reverses. This flow reversal causes separation in a diffuser passage, which results in eddy losses, mixing losses, and changed-flow angles. Separation should be avoided or delayed to improve compressor performance.

The high-pressure-ratio centrifugal compressor has a narrow yet stable operating range. This operating range is due to the close proximity of the surge and choke flow limits. The word "surge" is widely used to express unstable operation of a compressor. Surge is the flow breakdown period during unstable operation. The unsteady flow phenomena during the onset of surge in a high-pressure-ratio centrifugal compressor causes the mass flow throughout the compressor to oscillate during supposedly "stable" operations. The throat pressure in the diffuser increases during the precursor period up to collector pressure P_{col} at the beginning of surge. All pressure traces (except plenum pressure) suddenly drop at the surge point. The sudden change of pressure can be explained by the measured occurrence of backflow from the collector through the impeller during the period between the two sudden changes.

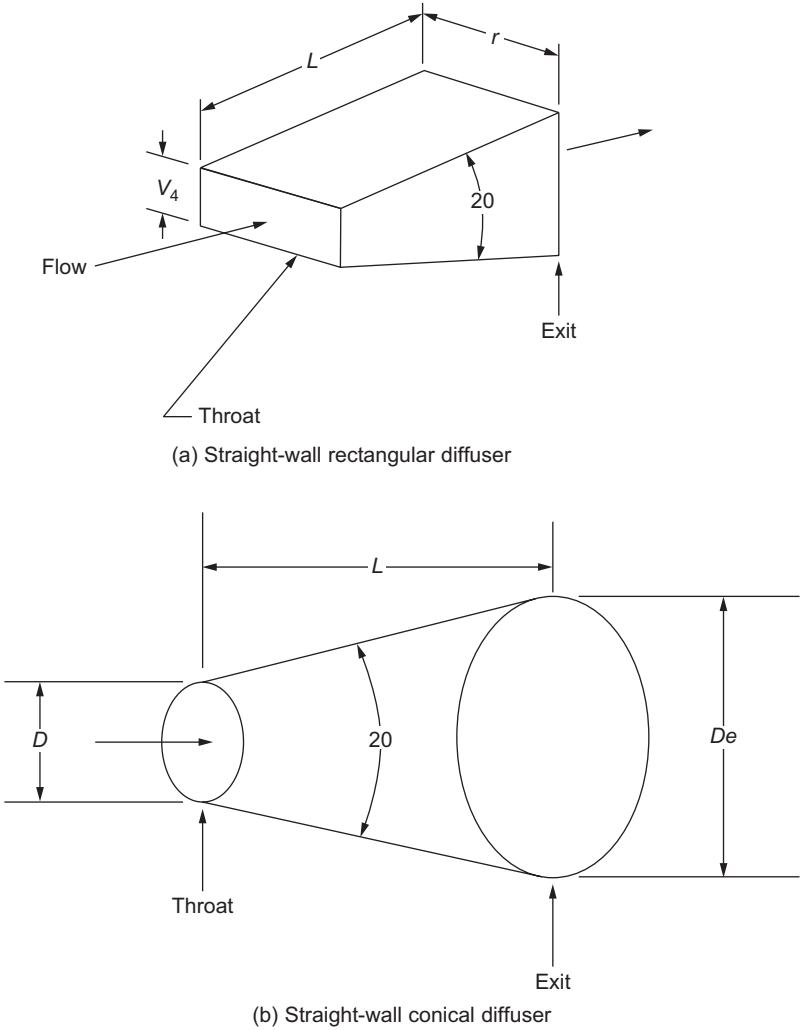


Figure 6-27 Geometric classification of diffusers.

Scroll or Volute

The purpose of the volute is to collect the fluid leaving the impeller or diffuser, and deliver it to the compressor outlet pipe. The volute has an important effect on the overall efficiency of the compressor. Volute design embraces two schools of thought. First, the angular momentum of the flow in the volute is constant, neglecting any friction effects. The tangential velocity $V_{5\theta}$ is the velocity at any radius in the volute. The following equation shows the relationship if the angular momentum is held

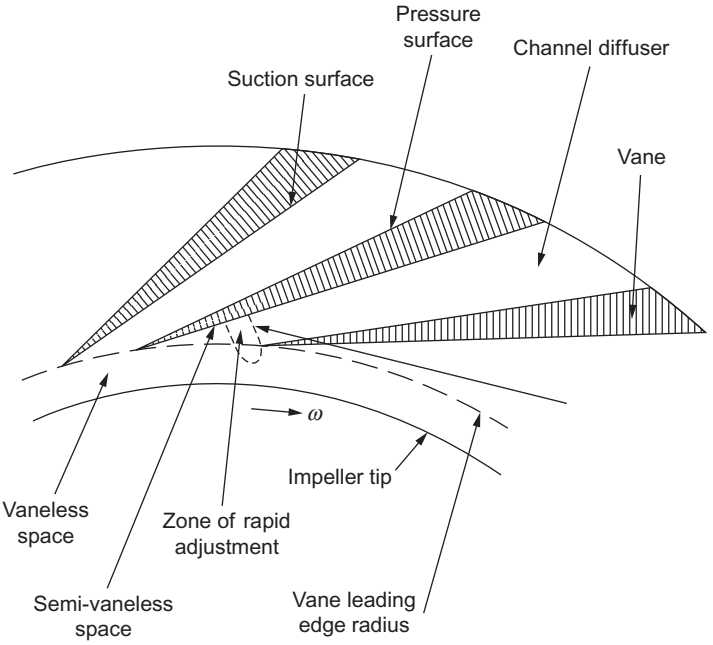


Figure 6-28 Flow regions of the vaned diffuser.

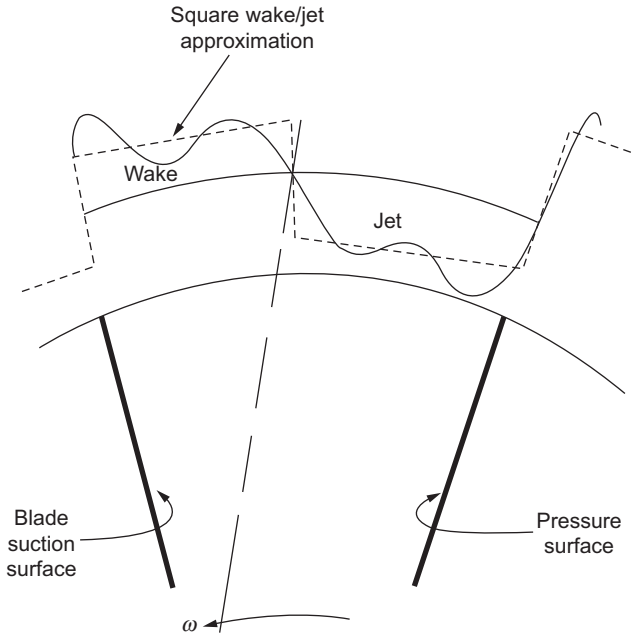


Figure 6-29 Jet-wake flow distribution from an impeller.

constant:

$$V_{5\theta} r = \text{constant} = K \tag{6-12}$$

Assuming no leakage past the tongue and a constant pressure around the impeller periphery, the relationship of flow at any section Q_θ to the overall flow in the impeller Q is given by:

$$Q_\theta = \frac{\theta}{2\pi} Q \tag{6-13}$$

Thus, the area distribution at any section θ can be given by the following relationship:

$$A_\theta = Qr \times \frac{\theta}{2\pi} \times \frac{L}{K} \tag{6-14}$$

where

r = radius to the center of gravity
L = volume width

Second, design the volute by assuming that the pressure and velocity are independent of θ. The area distribution in the volute is given by:

$$A_\theta = K \frac{Q}{V_{5\theta}} \frac{\theta}{2\pi} \tag{6-15}$$

To define the volute section at a given θ, the shape and area of the section must be decided. Flow patterns in various types of volute are shown in Figure 6-30. The flow in the asymmetrical volute has a single-vortex instead of the double-vortex in the symmetrical volute. Where the impeller is discharging directly into the volute, it is better to have the volute width larger than the impeller width. This enlargement results in the flow from the impeller being bounded by the vortex generated from the gap between the impeller and the casing.

At flows different from design conditions, there exists a circumferential pressure gradient at the impeller tip and in the volute at a given radius. At low flows, the pressure rises with the peripheral distance from the volute tongue. At high flows, the pressure falls with distance from the tongue. This condition results because near the tongue the flow is guided by the outer wall of the passage. The circumferential pressure gradients reduce efficiency away from the design point. Non-uniform pressure at the impeller discharge results in unsteady flows in the impeller passage, causing flow reversal and separation in the impeller.

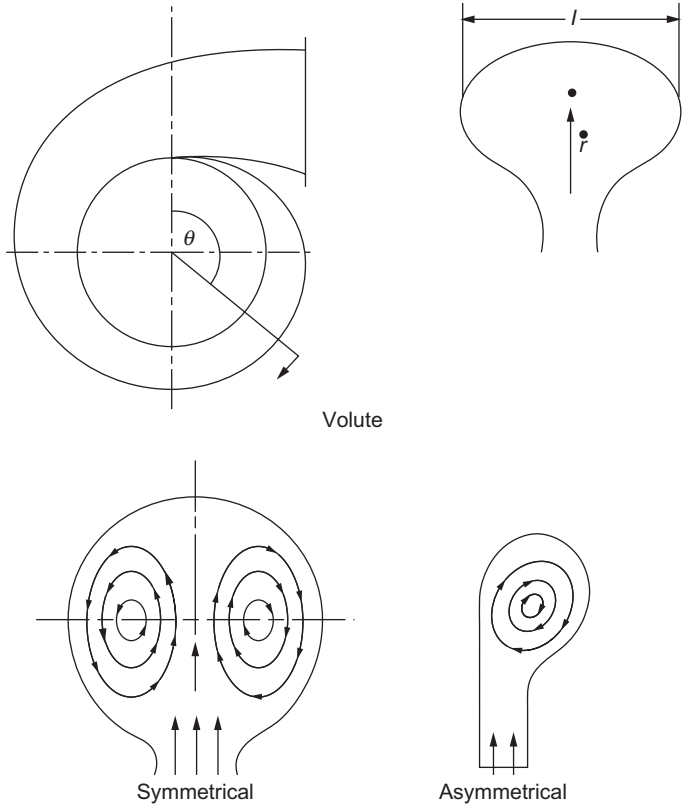


Figure 6-30 Flow patterns in volute.

Centrifugal Compressor Performance

Calculating the performance of a centrifugal compressor in both design and off-design conditions requires a knowledge of various losses encountered in a centrifugal compressor.

The accurate calculation and proper evaluation of losses within a centrifugal compressor is as important as the calculation of the blade-loading parameters. If the proper parameters are not controlled, efficiency decreases. The evaluation of various losses is a combination of experimental results and theory. The losses are divided into two groups: (1) losses encountered in the rotor, and (2) losses encountered in the stator.

A loss is usually expressed as a loss of heat or enthalpy. A convenient way to express them is in a non-dimensional manner with reference to the exit blade speed. The theoretical total head available (q_{tot}) is equal to the head available from the energy equation:

$$q_{\text{th}} = \frac{1}{U_2^2}(U_2 V_{\theta 2} - U_1 V_{\theta 1}) \tag{6-16}$$

plus the head, which is lost because of disc friction (Δq_{df}) and resulting from any recirculation (Δq_{rc}) of the air back into the rotor from the diffuser:

$$q_{\mathrm{tot}} = q_{\mathrm{th}} + \Delta q_{\mathrm{df}} + \Delta q_{\mathrm{rc}} \tag{6-17}$$

The adiabatic head that is actually available at the rotor discharge is equal to the theoretical head minus the heat from the shock in the rotor (Δq_{sh}), the inducer loss (Δq_{in}), the blade loadings (Δq_{bl}), the clearance between the rotor and the shroud (Δq_c), and the viscous losses encountered in the flow passage (Δq_{sf}):

$$q_{\mathrm{ia}} = q_{\mathrm{th}} - \Delta q_{\mathrm{in}} - \Delta q_{\mathrm{sh}} - \Delta q_{\mathrm{bl}} - \Delta q_c - \Delta q_{\mathrm{sf}} \tag{6-18}$$

Therefore, the adiabatic efficiency in the impeller is:

$$\eta_{\mathrm{imp}} = \frac{q_{\mathrm{ia}}}{q_{\mathrm{tot}}} \tag{6-19}$$

The calculation of the overall stage efficiency must also include losses encountered in the diffuser. Thus, the overall actual adiabatic head attained will be the actual adiabatic head of the impeller minus the head losses encountered in the diffuser from wake caused by the impeller blade (Δq_w), the loss of part of the kinetic head at the exit of the diffuser (Δq_{ed}), and the loss of head from frictional forces (Δq_{osf}) encountered in the vaned or vaneless diffuser space:

$$q_{\mathrm{oa}} = q_{\mathrm{ia}} - \Delta q_w - \Delta q_{\mathrm{ed}} - \Delta q_{\mathrm{osf}} \tag{6-20}$$

The overall adiabatic efficiency in an impeller is given by the following relationship:

$$\eta_{\mathrm{ov}} = \frac{q_{\mathrm{oa}}}{q_{\mathrm{tot}}} \tag{6-21}$$

The individual losses can now be computed. These losses are broken up into two categories: (1) losses in the rotor, and (2) losses in the diffuser.

Rotor Losses

Rotor losses are divided into the following categories:

Shock in Rotor Losses

This loss is due to shock occurring at the rotor inlet. The inlet of the rotor blades should be wedge-like to sustain a weak oblique shock, and then gradually expanded to the blade thickness to avoid another shock. If the blades are blunt, a bow shock will result, causing the flow to detach from the blade wall and the loss to be higher.

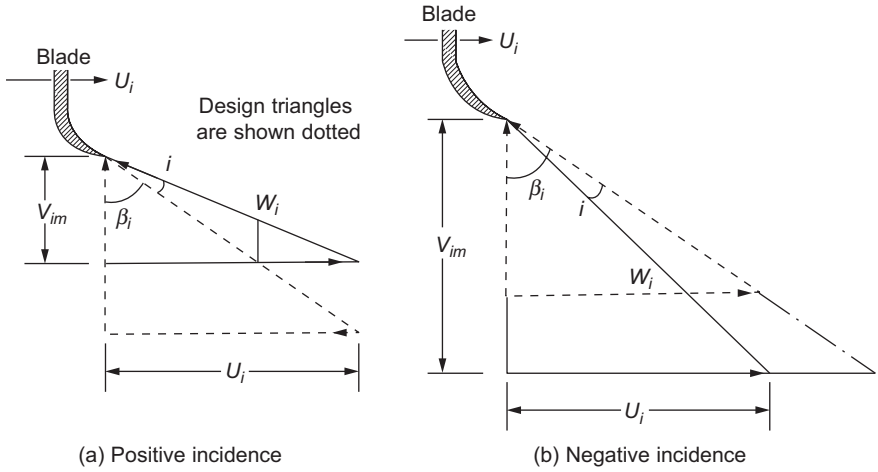


Figure 6-31 Inlet velocity triangle at nonzero incidents.

Incidence Loss

At off-design conditions, flow enters the inducer at an incidence angle that is either positive or negative, as shown in Figure 6-31. A positive incidence angle causes a reduction in flow. Fluid approaching a blade at an incidence angle suffers an instantaneous change of velocity at the blade inlet to comply with the blade inlet angle. Separation of the blade can create a loss associated with this phenomenon.

Disc Friction Loss

This loss results from frictional torque on the back surface of the rotor as seen in Figure 6-32. This loss is the same for a given size disc whether it is used for a radial-inflow compressor or a radial-inflow turbine. Losses in the seals, bearings, and gear box are also lumped in with this loss, and the entire loss can be called an external loss. Unless the gap is of the magnitude of the boundary layer, the effect of the gap size is negligible. The disc friction in a housing is less than that on a free disc due to the existence of a "core," which rotates at half the angular velocity.

Diffusion-Blading Loss

This loss develops because of negative velocity gradients in the boundary layer. Deceleration of the flow increases the boundary layer and gives rise to separation of the flow. The adverse pressure gradient that a compressor normally works against increases the chances of separation and causes significant loss.

Clearance Loss

When a fluid particle has a translatory motion relative to a non-inertial rotating coordinate system, it experiences the Coriolis force. A pressure difference exists between

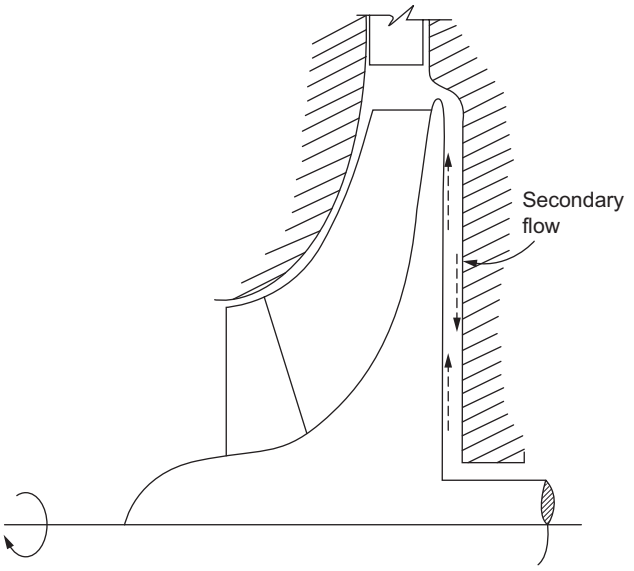


Figure 6-32 Secondary flow at the back of an impeller.

the driving and trailing faces of an impeller blade caused by Coriolis acceleration. The shortest and least resistant path for the fluid to flow and neutralize this pressure differential is provided by the clearance between the rotating impeller and the stationary casing. With shrouded impellers, such a leakage from the pressure side to the suction side of an impeller blade is not possible. Instead, the existence of a pressure gradient in the clearance between the casing and the impeller shrouds, predominant along the direction shown in Figure 6-33, accounts for the clearance loss. Tip seals at the impeller eye can reduce this loss considerably.

This loss may be quite substantial. The leaking flow undergoes a large expansion and contraction caused by temperature variation across the clearance gap that affects both the leaking flow and the stream into which it discharges.

Skin Friction Loss

Skin friction loss is the loss from the shear forces on the impeller wall caused by turbulent friction. This loss is determined by considering the flow as an equivalent circular cross section with a hydraulic diameter. The loss is then computed based on well-known pipe flow pressure loss equations.

Stator Losses

Recirculating Loss

This loss occurs because of backflow into the impeller exit of a compressor and is a direct function of the air exit angle. As the flow through the compressor decreases,

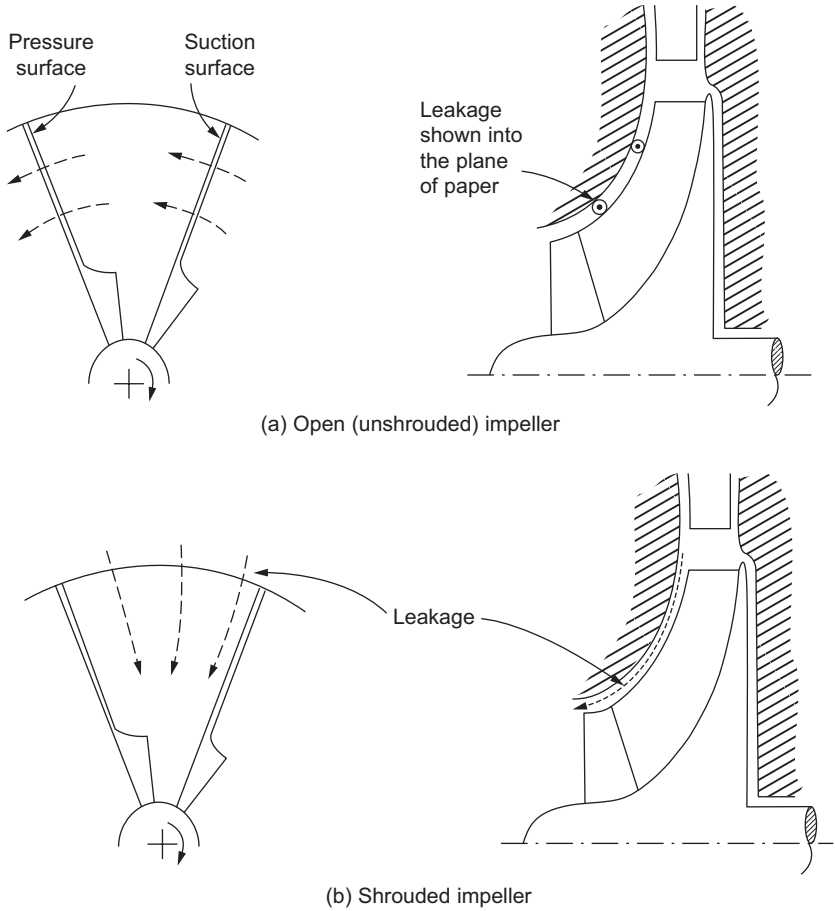


Figure 6-33 Leakage affecting clearance loss.

there is an increase in the absolute flow angle at the exit of the impeller as seen in Figure 6-34. Part of the fluid is recirculated from the diffuser to the impeller, and its energy is returned to the impeller.

Wake-Mixing Loss

This loss is from the impeller blades, and it causes a wake in the vaneless space behind the rotor. It is minimized in a diffuser, which is symmetric around the axis of rotation.

Vaneless Diffuser Loss

This loss is experienced in the vaneless diffuser and results from friction and the absolute flow angle.

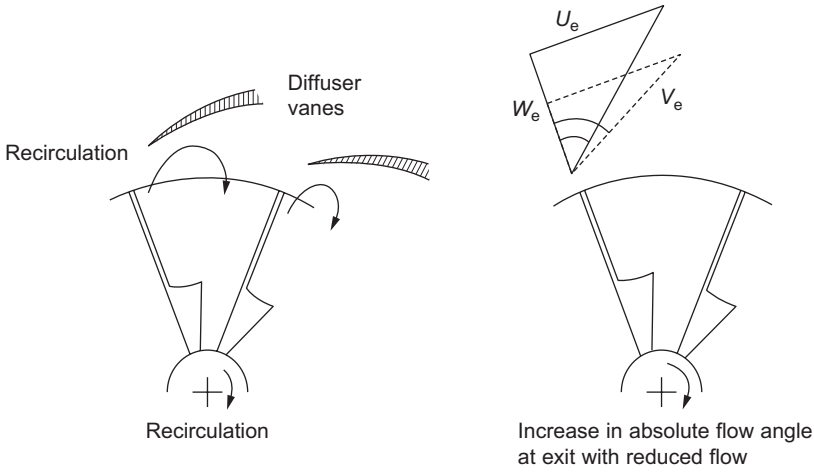


Figure 6-34 Recirculating loss.

Vaned Diffuser Loss

Vaned diffuser losses are based on conical diffuser test results. They are a function of the impeller blade loading and the vaneless space radius ratio. They also take into account the blade incidence angle and skin friction from the vanes.

Exit Loss

The exit loss assumes that one-half of the kinetic energy leaving the vaned diffuser is lost.

Losses are complex phenomena and as discussed here are a function of many factors, including inlet conditions, pressure ratios, blade angles, and flow. Figure 6-35 shows the losses distributed in a typical centrifugal stage of pressure ratio below 2:1 with backward-curved blades. This figure is only a guideline.

Compressor Surge

A plot showing the variation of total pressure ratio across a compressor as a function of the mass flow rate through it at various speeds is known as a performance map. Figure 6-36 shows such a plot.

The actual mass flow rates and speeds are corrected by factors $(\sqrt{\theta}/\delta)$ and $(1/\sqrt{\theta})$, respectively, to account for variation in the inlet conditions of temperature and pressure. The surge line joins the different speed lines where the compressor's operation becomes unstable. A compressor is in "surge" when the main flow through the compressor reverses its direction and flows from the exit to the inlet for short time intervals. If allowed to persist, this unsteady process may result in irreparable damage to the machine. Lines of constant adiabatic efficiency (sometimes called efficiency

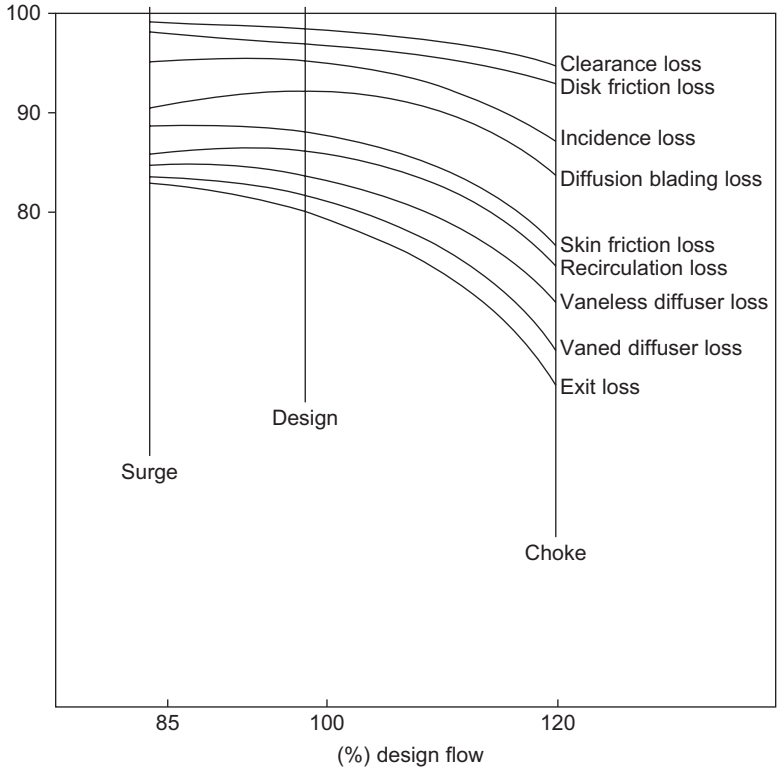


Figure 6-35 Losses in a centrifugal compressor.

islands) are also plotted on the compressor map. A condition known as "choke" or "stone walling" is indicated on the map, showing the maximum mass flow rate possible through the compressor at that operating speed.

Compressor surge is a phenomenon of considerable interest, yet it is not fully understood. It is a form of unstable operation and should be avoided in both design and operation. Surge has been traditionally defined as the lower limit of stable operation in a compressor and involves the reversal of flow. This reversal of flow occurs because of some kind of aerodynamic instability within the system. Usually a part of the compressor is the cause of the aerodynamic instability, although it is possible that the system arrangement could be capable of augmenting this instability. Figure 6-36 shows a typical performance map for a centrifugal compressor with efficiency islands and constant aerodynamic speed lines. The total pressure ratio can be seen to change with flow and speed. Compressors are usually operated at a working line separated by some safety margin from the surge line.

Surge is often symptomized by excessive vibration and an audible sound; however, there have been cases in which surge problems that were not audible have caused failures. Extensive investigations have been conducted on surge. Poor quantitative universality of aerodynamic loading capacities of different diffusers and impellers and an

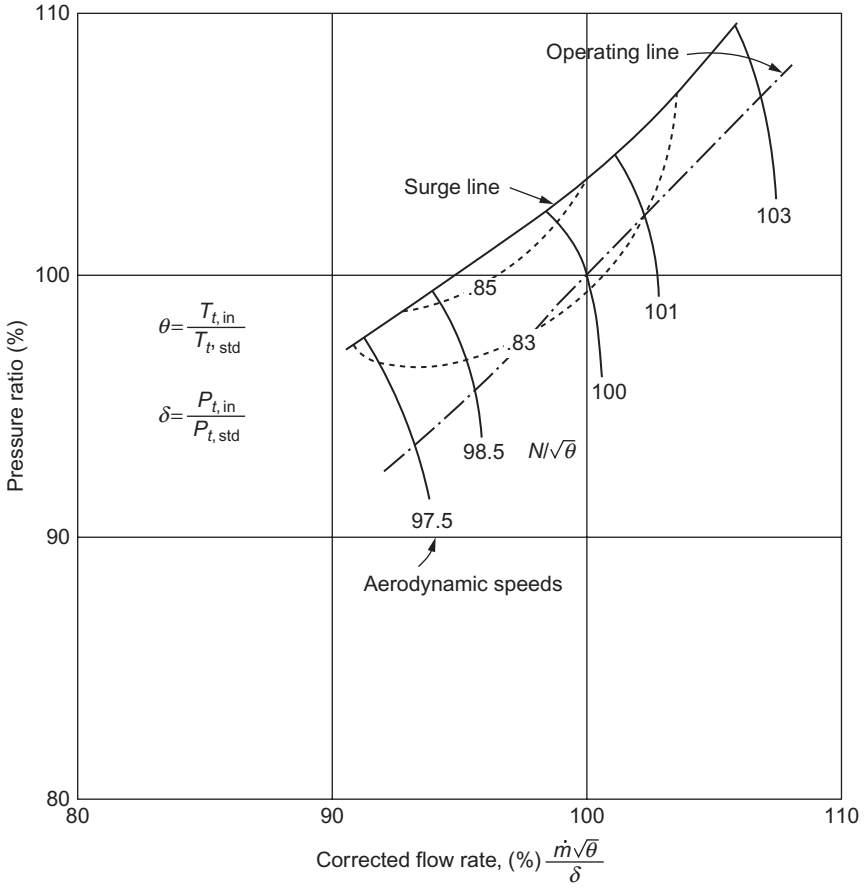


Figure 6-36 Typical compressor performance map.

inexact knowledge of boundary-layer behavior make the exact prediction of flow in turbomachines at the design stage difficult. However, it is quite evident that the underlying cause of surge is aerodynamic stall. The stall may occur in either the impeller or the diffuser.

When the impeller seems to be the cause of surge, the inducer section is where the flow separation begins. A decrease in the mass flow rate, an increase in the rotational speed of the impeller, or both, can cause the compressor to surge.

Surge can be initiated in the diffuser by flow separation occurring at the diffuser entrance. A diffuser usually consists of a vaneless space with the pre-diffuser section before the throat containing the initial portion of the vanes in a vaned diffuser. The vaneless space accepts the velocity generated by the centrifugal impeller and diffuses the flow so that it enters the vaned diffuser passage at a lower velocity, avoiding any shock losses and resultant separation of the flow. When the vaneless diffuser stalls, the flow will not enter the throat. A separation occurs, causing the flow to finally reverse

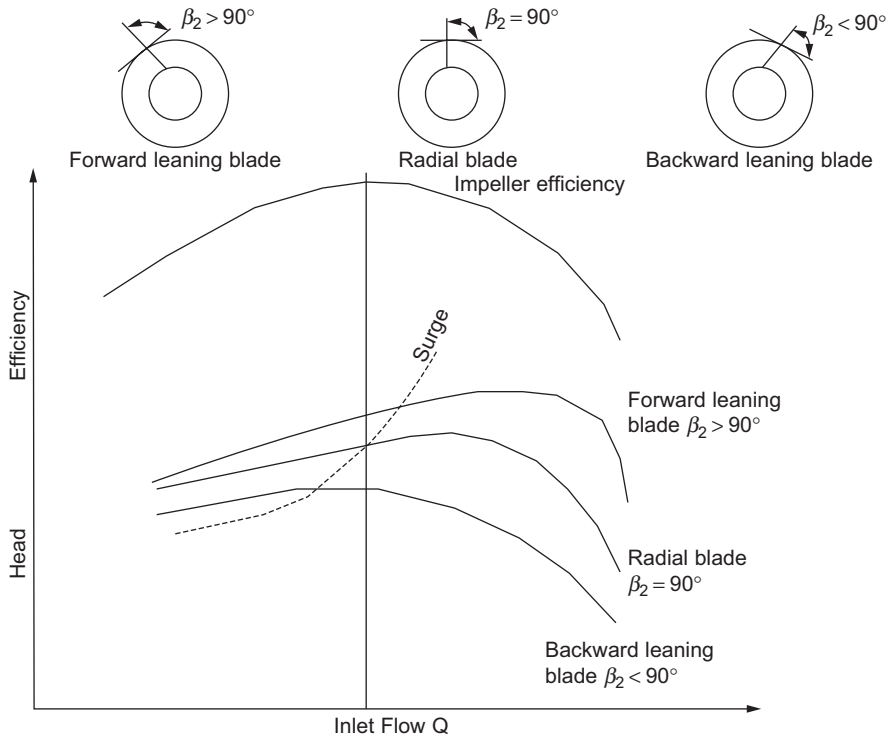


Figure 6-37 Effect of blade angle on stability.

and surge the compressor. Stalling of the vaneless diffuser can be accomplished in two ways – by increasing impeller speed or decreasing the flow rate.

Whether surge is caused by a decrease in flow velocity or an increase in rotational speeds, either the inducer or vaneless diffuser can stall. Which stalls first is difficult to determine, but considerable testing has shown that for a low-pressure-ratio compressor, the surge initiates in the diffuser section. For units with single-stage pressure ratios above 3:1, surge is probably initiated in the inducer.

Most centrifugal compressors have, for the most part, impellers with backward-leaning impeller blades. Figure 6-37 depicts the effects of impeller blade angle on the stable range and shows the variance in steepness of the slope of the head-flow curve.

The three curves are based on the same speed and show actual head. The relationship of an ideal or theoretical head to the inlet flow for different blade angles would be represented by straight lines. For backward-leaning blades, the slope of the line would be negative. The line for radial blades would be horizontal. Forward-leaning blades would have a positively sloped line. For the average petrochemical process plant application, the compressor industry commonly uses a backward-leaning blade with an angle (β_2) of between about 55–75°(or backward leaning angle of 15–35°), because it provides a wider stable range and a steeper slope in the operating range.

This impeller design has proven to be about the best compromise between pressure delivered, efficiency, and stability. Forward-leaning blades are not commonly used in compressor design, since the high exit velocities lead to large diffuser losses. A plant air compressor operating at steady conditions from day to day would not require a wide stable range, but a machine in a processing plant can be the victim of many variables and upsets, so more stability is highly desirable. Actually, the lower curve in Figure 6-37 appears to have a more gentle slope than either the middle or upper curve. This comparison is true in the overall sense, but it must be remembered that the normal operating range lies between 100% flow (Q) and flow at surge, plus a safety margin of, usually, about 10%. The right-hand tail ends of all three curves are not in the operating range. The machine must operate with a suitable margin to the left of where these curves begin their steep descent or tail-off, and in the resultant operating range, the curve for backward-leaning blades is steeper. This steeper curve is desirable for control purposes. Such a curve produces a meaningful change in pressure drop across the orifice for a small change in flow. The blade angle by itself does not tell the overall performance story. The geometry of other components of a stage will contribute significant effects also.

Most centrifugal compressors in service in petroleum or petrochemical processing plants use vaneless diffusers. A vaneless diffuser is generally a simple flow channel with parallel walls and does not have any elements inside to guide the flow.

When the inlet flow to the impeller is reduced while the speed is held constant, there is a decrease in the relative velocity leaving the impeller and the air angle associated with it. As the air angle decreases, the length of the flow path spiral increases. The effect is shown in Figure 6-38.

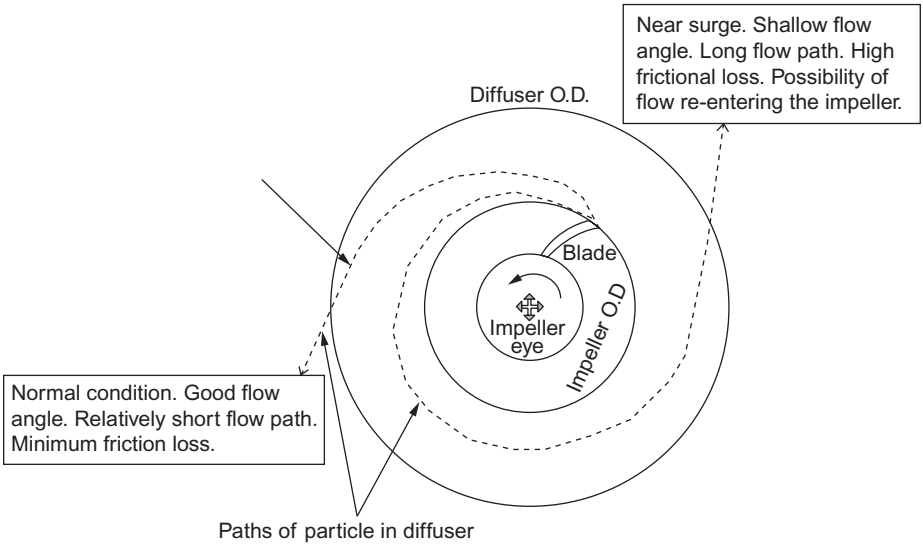


Figure 6-38 Flow trajectory in a vaneless diffuser.

If the flow path is extended enough, the flow momentum at the diffuser walls is excessively dissipated by friction and stall. With this greater loss, the diffuser becomes less efficient and converts a proportionately smaller part of the velocity head to pressure. As this condition progresses, the stage will eventually stall. This could lead to a surge.

Vaned diffusers are used to force the flow to take a shorter, more efficient path through the diffuser. There are many styles of vaned diffusers, with major differences in the types of vanes, vane angles and contouring, and vane spacing. Commonly used vaned diffusers employ wedge-shaped vanes (vane islands) or thin-curved vanes. In high head stages, there can be two to four stages of diffusion. These usually consist of vaneless spaces to decelerate the flow, followed by two or three levels of vaned blades in order to prevent build-up of boundary layer, which causes separation and surging of the compressor. Figure 6-38 indicates the flow pattern in a vaned diffuser. The vaned diffuser can increase the efficiency of a stage by two to four percentage points, but the price for the efficiency gain is generally a narrower operating span on the head-flow curve with respect to both surge and stonewall. Figure 6-39 also shows the effect of off-design flows.

Excessive positive incidence at the leading edge of the diffuser vane occurs when the exit flow is too small at reduced flow, and this condition brings on a stall.

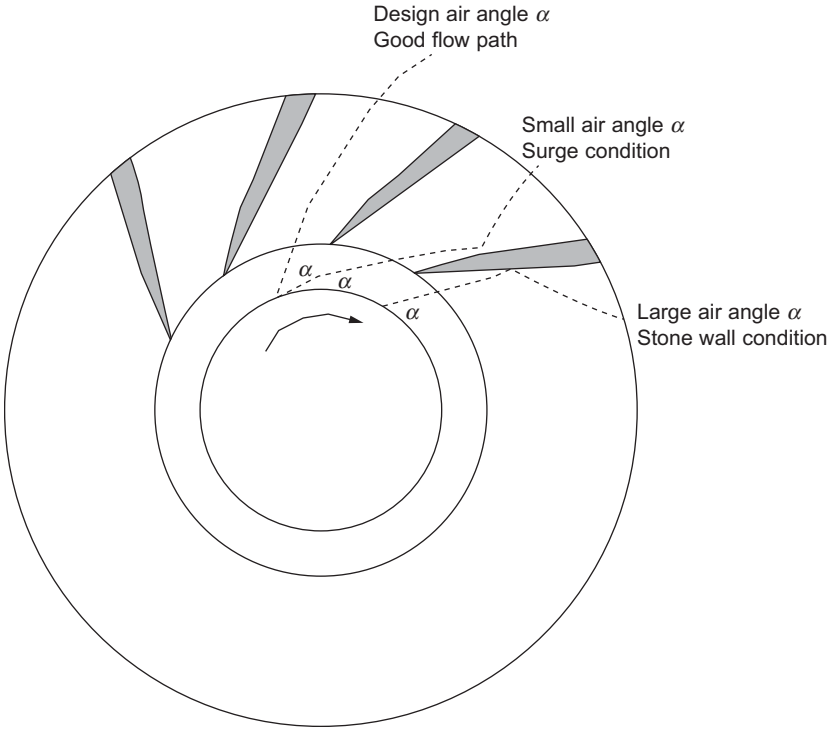


Figure 6-39 Vaned diffuser.

Conversely, as the flow increases beyond the rated point, excessive negative incidence can cause stonewall. Despite its narrowing effect on the usable operating range on the characteristic curve, the vaned diffuser has its application in situations where efficiency is of utmost importance. Although seldom used, movable diffuser vanes or vane islands can be used to alleviate the shock losses at off-design conditions. However, as the adjusting mechanisms required are quite complicated, they generally are applied to only single-stage machines.

It should be noted that the illustrations of the flow paths in Figure 6-37 through 6-39 are somewhat simplistic. Each flow path is indicated by a single streamline. The actual flow field is far more complex, with flow separation and recalculation present. Nevertheless, these figures should help with a practical understanding of the effects of changes in velocity triangles.

Stationary guide vanes direct the flow to the eye of the impeller in an orderly fashion. Depending upon the head requirements of an individual stage, these vanes may direct the flow in the same direction as the rotation or tip speed of the wheel, an action known as positive pre-swirl. This is usually done to reduce the relative Mach number entering the inducer, in order to prevent shock losses. This, however, reduces the head delivered but improves the operating margin. The opposite action is known as counter-rotation or negative pre-swirl. This increases the head delivered but also increases the inlet relative Mach number. Negative pre-swirl is rarely used, since it also decreases the operating range. Sometimes the guide vanes are set at zero degrees of swirl; these vanes are called radial guide vanes. Movable inlet guide vanes are occasionally employed on single-stage machines, or on the first stage of multi-stage compressors driven by electric motors at a constant speed. The guide vane angle can be manually or automatically adjusted while the unit is on stream to accommodate off-design operating requirements. Because of the mechanical complexity of the adjusting mechanism and physical dimensional limitations, the variable feature can only be applied to the first wheel in almost all machine designs. Hence, the effect of changing vane angle is diluted in the stages downstream of the first. Although the flow to the entire machine is successfully adjusted by moving the first stage vanes, the remaining stages must pump the adjusted flow at a fixed guide vane angle.

Incidentally, a butterfly throttle valve in the suction line to the machine will produce nearly the same effects as moving the first stage guide vanes. However, throttling is not as efficient as moving the guide vanes, so that in many cases, the added cost of the movable vane mechanism can be justified by power savings.

Effects of Gas Composition

Figure 6-40 shows the performance of an individual stage at a given speed for three levels of gas molecular weight.

The heavy gas class includes gases such as propane, propylene, and standardized refrigerant mixtures. Air, natural gases, and nitrogen are typical of the medium class. Hydrogen-rich gases found in hydrocarbon processing plants are representative of the light class.

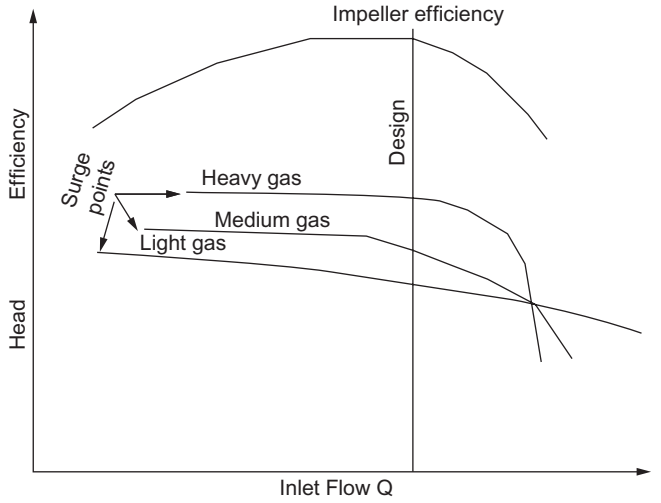


Figure 6-40 Effect of gas composition.

The following observations can be made with respect to the curve for heavy gas:

1. The flow at surge is higher.
2. The stage produces slightly more head than that corresponding to medium gas.
3. The right-hand side of the curve turns downward (approaches stonewall) more rapidly.
4. The curve is flatter in the operating stage.

It is the last point (4) that often presents a problem to the designer of the anti-surge control system. It should be noted that the flatness gets worse as stages are added in series. Since the RTS is small, there is a large change in flow corresponding to a small change in Head. The control system, therefore, must be more responsive. It should be obvious that curves for lighter gases have a more desirable shape.

External Causes and Effects of Surge

The following are some of the usual causes of surge that are not related to machine design:

1. Restriction in suction or discharge of a system.
2. Process changes in pressure, temperature, or gas composition.
3. Internal plugging of the flow passages of the compressor (fouling).
4. Inadvertent loss of speed.
5. Instrument or control valve malfunction.
6. Malfunction of hardware such as variable inlet guide vanes.
7. Operator error.
8. Maldistribution of load in parallel operation of two or more compressors.
9. Improper assembly of a compressor, such as a mispositioned rotor.

The effects of surge can range from a simple lack of performance to serious damage to the machine or to the connected system. Internal damage to labyrinths, diagrams,

the thrust bearing, and the rotor can be experienced. There has been a reported case of a bent rotor caused by violent surge. Surge often excites lateral shaft vibration and could produce torsional damage to such items as couplings and gears. Externally, devastating piping vibration can occur, causing structural damage, shaft misalignment, and failure of fittings and instruments.

The effects of the size and configuration of the connected system, as well as different operating conditions, on the intensity of surge can be astonishing. For example, a compressor system in a test set-up at the factory may exhibit only a mild reaction to surge. At the installation, however, the same compressor with a different connected system may react in a tumultuous manner. Surge can often be recognized by check valve hammering, piping vibration, noise, wriggling of pressure gauges or an ammeter on the driver, or lateral and/or axial vibration of the compressor shaft. Mild cases of surge are sometimes difficult to discern.

Surge Detection and Control

Surge-detection devices may be divided into two groups: (1) static devices, and (2) dynamic devices. To date, static surge-detection devices have been widely used; more research needs to be done before dynamic detection devices are generally used. A dynamic device will probably meet the requirements and hopes of many engineers for a control device that can anticipate stall and surge, and prevent it. Obviously, detection devices must be linked to a control device that can prevent the unstable operation of a compressor.

Static surge-detection devices attempt to avoid stall and surge by the measurement of compressor conditions and ensure that a pre-decided value is not exceeded. When conditions meet or exceed the limit, control action is taken. A typical pressure-oriented anti-surge control system is shown in Figure 6-41. The pressure transmitter monitors the pressure and controls a device, which opens a blowoff valve.

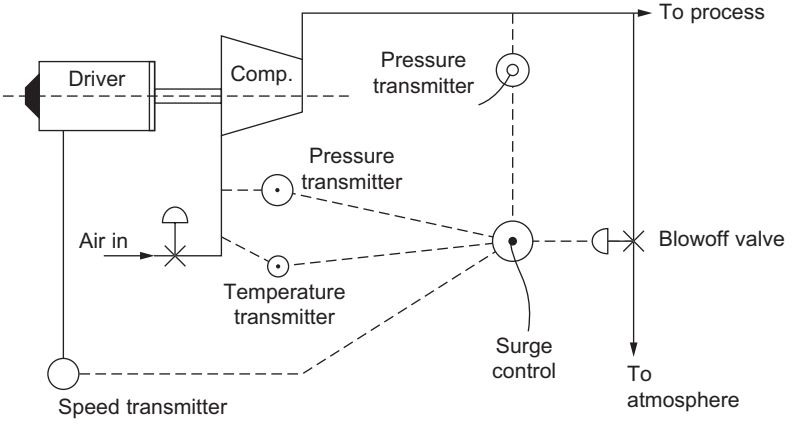


Figure 6-41 Pressure-oriented anti-surge control system.

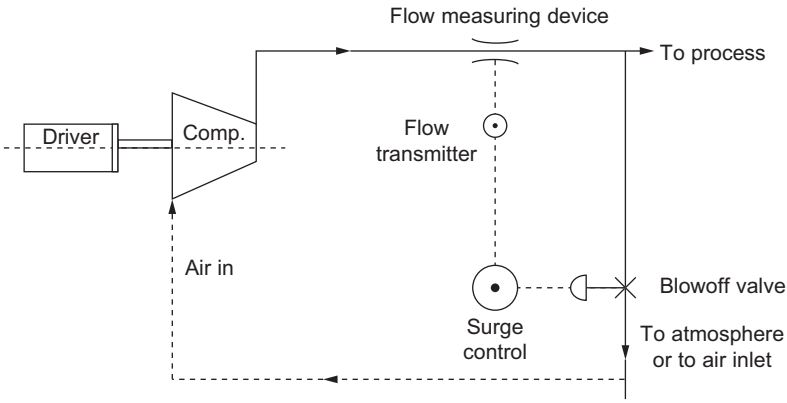


Figure 6-42 Flow-oriented anti-surge control system.

A temperature-sensing device corrects the readings of flow and speed for the effect of temperature. A typical flow-oriented device is also shown in Figure 6-42.

In all static surge-detection devices, the actual phenomenon of flow reversal (surge) is not directly monitored. What is monitored are other conditions related to surge. Control limits are set from past experience and a study of compressor characteristics.

Dynamic surge-detection and control methods are under study. They attempt to detect the *start* of a reversal of flow before it reaches the critical situation of surge. This procedure uses a boundary-layer probe.

The author has a patent for a dynamic surge-detection system, using a boundary-layer probe, presently undergoing field tests. This system consists of specially mounted probes in the compressor to detect boundary-layer flow reversal, as shown in Figure 6-43. The concept assumes that the boundary layer will reverse before the entire unit is in surge. Since the system is measuring the actual onset of surge by monitoring the flow reversal, it is not dependent on the molecular weight of the gas and is not affected by the movement of the surge line.

The use of pressure transducers and casing accelerometers in the exit piping has been instrumental in detecting compressor surge. It has been found that, as the unit approaches surge, the blade passing frequency (number of blades times rpm) and its second and third harmonic become excited. In a limited number of tests it has been noted that when the second harmonic of the blade passing frequency reaches the same order of magnitude as the blade passing frequency, the unit is very close to surge.

Process Centrifugal Compressors

These compressors have impellers with a very low pressure ratio (1.1–1.3) and thus large surge-to-choke margins. Figure 6-44 shows a cross section of a typical multistage centrifugal compressor used in the process industries.

The common method of classifying process-type centrifugal compressors driven by gas turbines is based on the number of impellers and the casing design. Table 6-2

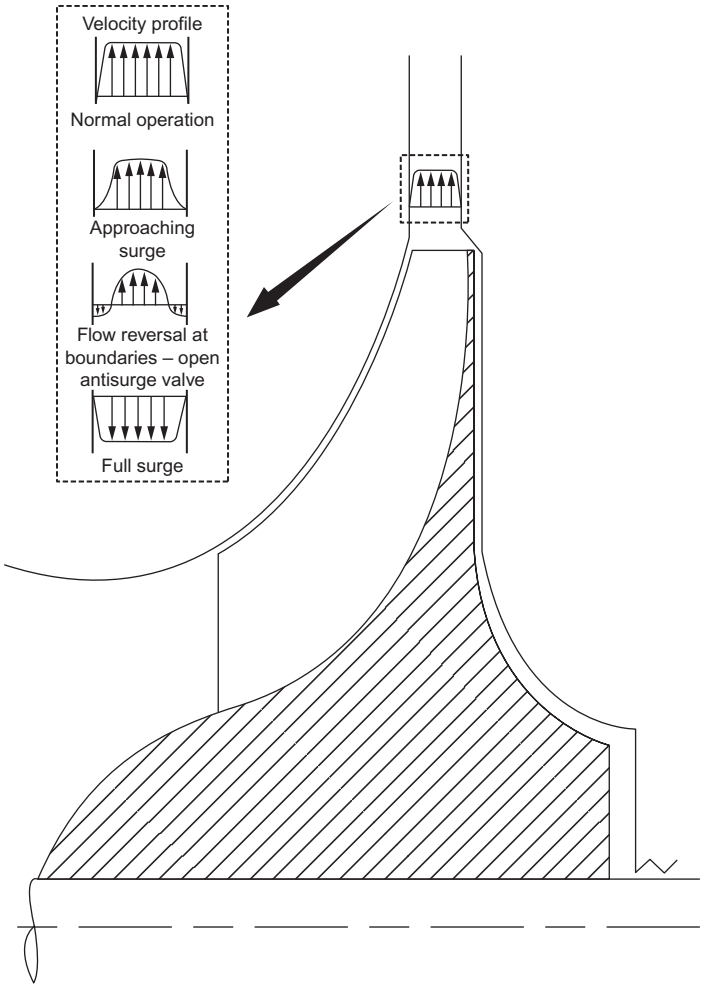


Figure 6-43 Boundary-layer surge prediction technique.

shows three types of centrifugal compressors. For each type of compressor, approximate maximum ratings of pressure, capacity, and brake horsepower are also shown. Sectionalized casing types have impellers, which are usually mounted on the extended motor shaft, and similar sections are bolted together to obtain the desired number of stages. The casing material is either steel or cast iron. These machines require minimum supervision and maintenance, and are quite economic in their operating range. The sectionalized casing design is used extensively in supplying air for combustion in ovens and furnaces.

The horizontally split types have casings split horizontally at the midsection and the top. The bottom halves are bolted and doweled together as shown in Figure 6-45.

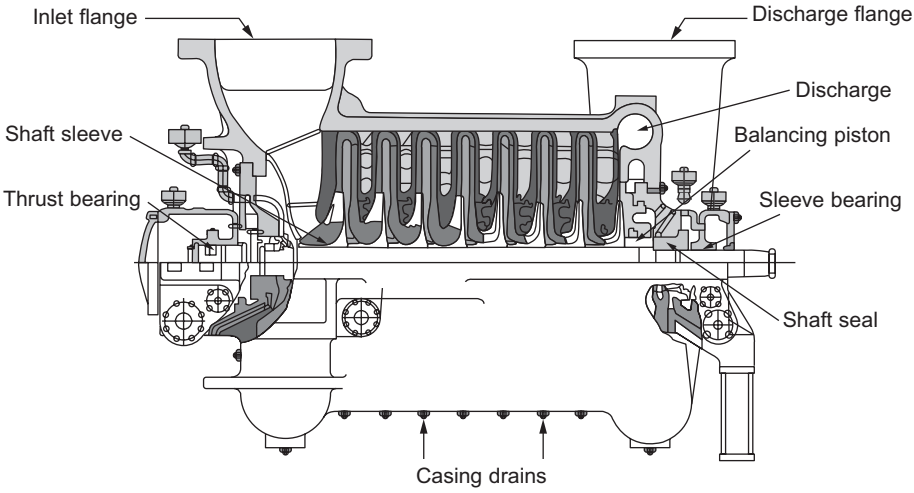


Figure 6-44 Cross section of a typical multi-stage centrifugal compressor (courtesy Elliott Company, Jeannette, PA).

Table 6-2 Industrial Centrifugal Compressor Classification Based on Casing Design

	Approximate Maximum Ratings		
Casing Type	**Approximate Pressure psig (Bar)**	**Approximate Inlet Capacity cfm (cmm)**	**Approximate Power Horsepower (kW)**
1. Sectionalized			
Usually multi-stage	10 (0.7)	20,000 (566)	600 (447)
2. Horizontally split			
Single-stage (double-suction)	15 (1.03)	650,000 (18,406)	10,000 (7,457)
Multi-stage	1,000 (69)	200,000 (5,663)	35,000 (26,100)
3. Vertically split			
Single-stage (single-suction)			
Overhung	30 (2.07)	250,000 (7,079)	10,000 (7,457)
Pipeline	1,200 (82)	25,000 (708)	20,000 (14,914)
Multi-stage	More than 5,500 (379)	20,000 (566)	15,000 (11,185)

This design type is preferred for large multi-stage units. The internal parts such as shaft, impellers, bearings, and seals are readily accessible for inspection and repairs by removing the top half. The casing material is cast iron or cast steel.

There are various types of barrel or centrifugal compressors. Low-pressure types with overhung impellers are used for combustion processes, ventilation, and conveying applications. Multi-stage barrel casings are used for high-pressures in which the horizontally split joint is inadequate. Figure 6-46 shows the barrel compressor in the

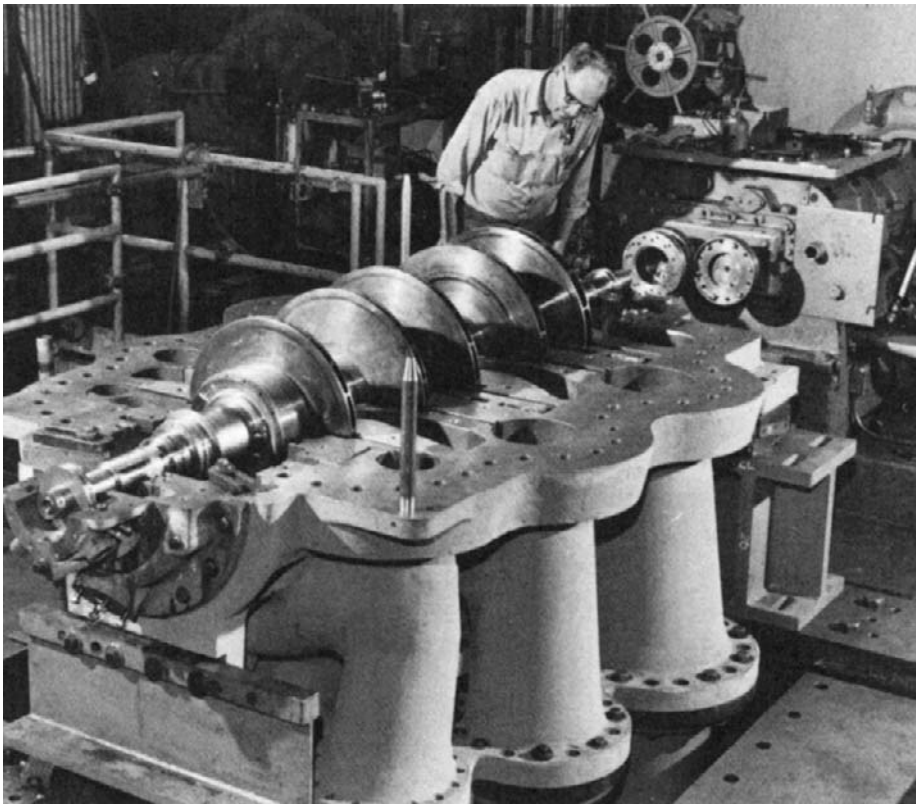


Figure 6-45 Horizontally split centrifugal compressor with shrouded rotors (courtesy of Elliott Company).

background and the inner bundle from the compressor in front. Once the casing is removed from the barrel, it is horizontally split.

Compressor Configuration

To properly design a centrifugal compressor, one must know the operating conditions – the type of gas, its pressure, temperature, and molecular weight. One must also know the corrosive properties of the gas so that proper metallurgical selection can be made. Gas fluctuations due to process instabilities must be pinpointed so that the compressor can operate without surging.

Centrifugal compressors for industrial applications have relatively low pressure ratios per stage. This condition is necessary so that the compressors can have a wide operating range while stress levels are kept at a minimum. Because of the low pressure ratios for each stage, a single machine may have a number of stages in one "barrel" to achieve the desired overall pressure ratio. Figure 6-47 shows some of the many

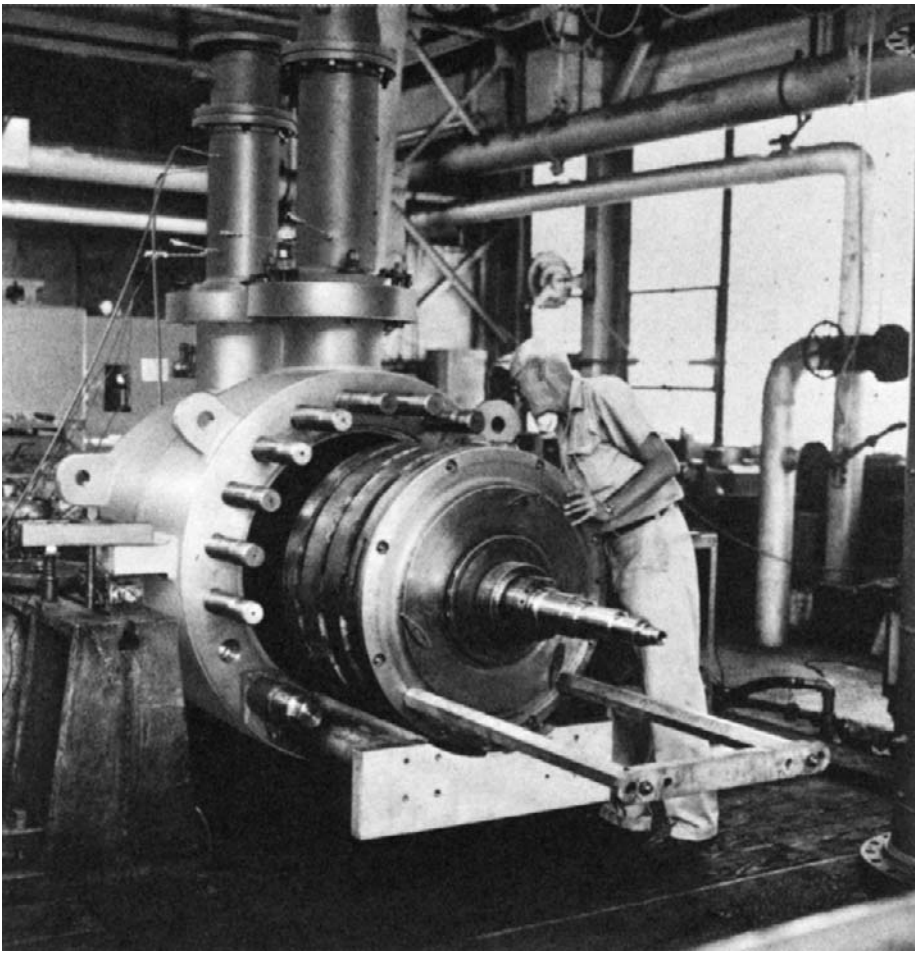


Figure 6-46 Barrel-type compressor (courtesy Elliott Company, Jeannette, PA).

configurations. Some factors to be considered when selecting a configuration to meet plant needs are:

1. Inter-cooling between stages can considerably reduce the power consumed.
2. Back-to-back impellers allow for a balanced rotor thrust and minimize overloading of the thrust bearings.
3. Cold inlet or hot discharge at the middle of the case reduces oil-seal and lubrication problems.
4. Single inlet or single discharge reduces external piping problems.
5. Balance planes that are easily accessible in the field can appreciably reduce field-balancing time.
6. Balance piston with no external leakage will greatly reduce wear on the thrust bearings.

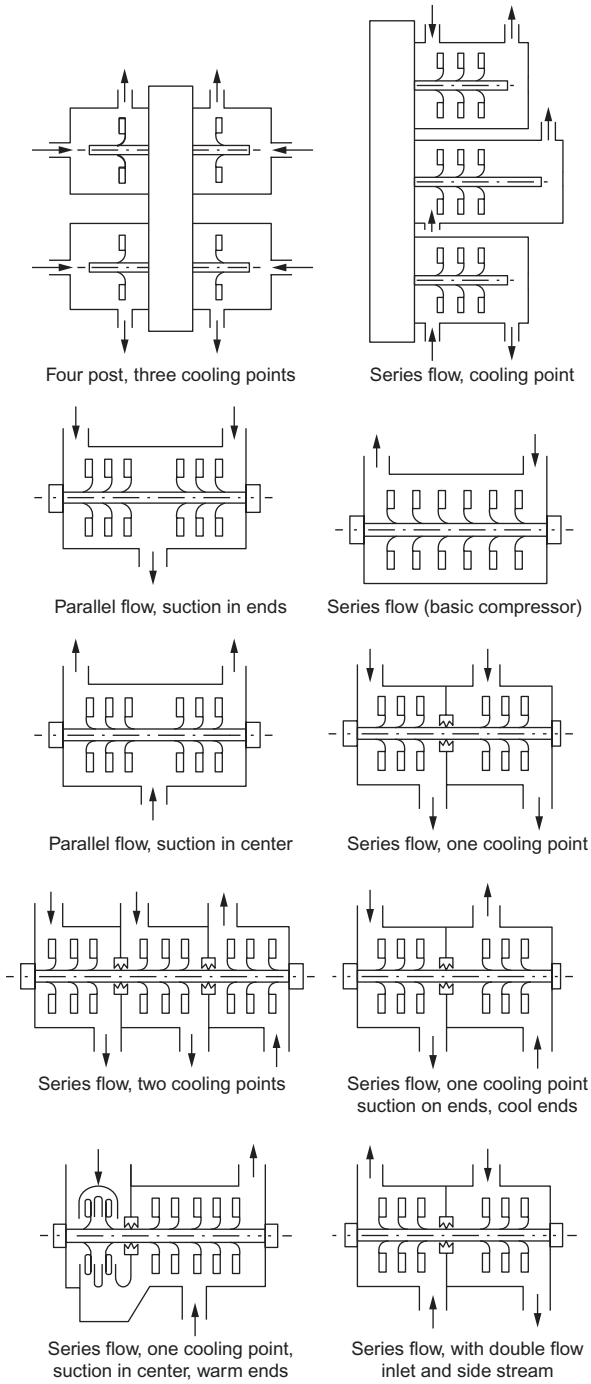


Figure 6-47 Various configurations of centrifugal compressors.

7. Hot and cold sections of the case that are adjacent to each other will reduce thermal gradients and thus reduce case distortion.
8. Horizontally split casings are easier to open for inspection than vertically split ones, reducing maintenance time.
9. Overhung rotors present an easier alignment problem because shaft-end alignment is necessary only at the coupling between the compressor and driver.
10. Smaller, high-pressure compressors that do the same job will reduce foundation problems but will have a greatly reduced operational range.

Impeller Fabrication

Centrifugal-compressor impellers are either shrouded or unshrouded. Open, shrouded impellers that are mainly used in single-stage applications are made by investment casting techniques or by three-dimensional milling. Such impellers are used, in most cases, for the high pressure ratio stages. The shrouded impeller is commonly used in the process compressor because of its low pressure ratio stages. The low tip stresses in this application make it a feasible design. Figure 6-48 shows several fabrication techniques. The most common type of construction is seen in (a) and (b) where the blades are fillet-welded to the hub and shroud. In (b) the welds are full penetration. The disadvantage in this type of construction is the obstruction of the aerodynamic passage. In (c), the blades are partially machined with the covers and then butt-welded

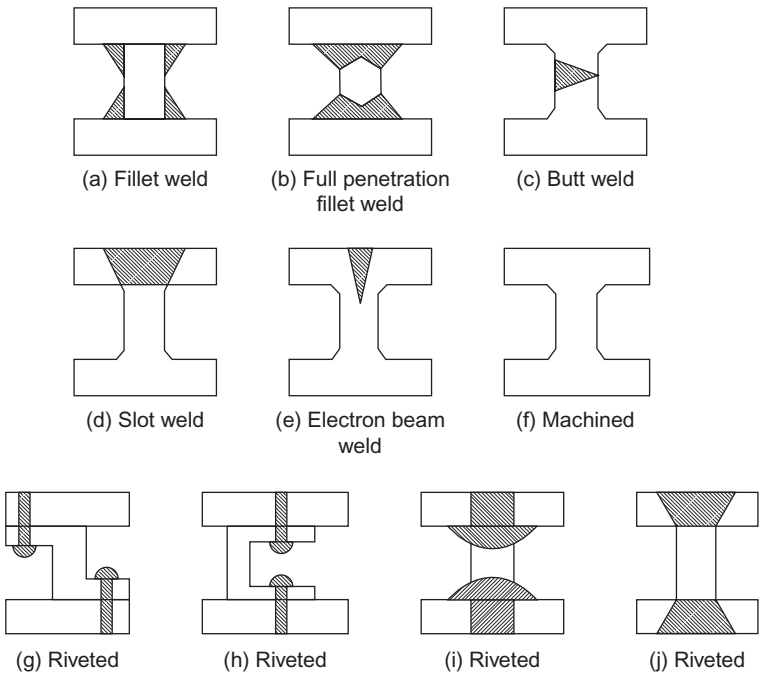


Figure 6-48 Several fabrication techniques for centrifugal impellers.

down the middle. For backward lean-angled blades, this technique has not been very successful, and there has been difficulty in achieving a smooth contour around the leading edge.

(d) illustrates a slot-welding technique and is used where blade-passage height is too small (or the backward lean-angle too high) to permit conventional fillet welding. In (e), an electron-beam technique is still in its infancy, and work needs to be done to perfect it. Its major disadvantage is that electron-beam welds should preferably be stressed in tension but, for the configuration of (e), they are in shear. The configurations of (g) through (j) use rivets. Where the rivet heads protrude into the passage, aerodynamic performance is reduced.

Materials for fabricating these impellers are usually low-alloy steels, such as AISI 4140 or AISI 4340. AISI 4140 is satisfactory for most applications; AISI 4340 is used for larger impellers requiring higher strengths. For corrosive gases, AISI 410 stainless steel (about 12% chromium) is used. Monel K-500 is employed in halogen gas atmospheres and oxygen compressors because of its resistance to sparking. Titanium impellers have been applied to chlorine service. Aluminum-alloy impellers have been used in great numbers, especially at lower temperatures (below 300 °F). With new developments in aluminum alloys, this range is increasing. Aluminum and titanium are sometimes selected because of their low density. This low density can cause a shift in the critical speed of the rotor, which may be advantageous.

Bibliography

Anderson, R.J., Ritter, W.K., and Dildine, D.M., "An Investigation of the Effect of Blade Curvature on Centrifugal Impeller Performance," NACA TN-1313, 1947.

Balje, O.E., "Loss and Flow-Path Studies on Centrifugal Compressors, Parts I and II," ASME Paper Nos 70-GT-1 2-A and 70-GT-1 2-B, June 1970.

Balje, O.E., "A Study of Reynolds Number Effects in Turbomachinery," *Journal of Engineering for Power*, ASME Trans., Vol. 86, Series A, 1964, p. 227.

Bammert, K., and Rautenberg, M., "On the Energy Transfer in Centrifugal Compressors," ASME Paper No. 74-GT-121, 1974.

Boyce, M.P., "A Practical Three-Dimensional Flow Visualization Approach to the Complex Flow Characteristics in a Centrifugal Impeller," ASME Paper No. 66-GT-83, June 1983.

Boyce, M.P., "How to Achieve On-Line Availability of Centrifugal Compressors," *Chemical Weekly*, June 1978, pp. 115–127.

Boyce, M.P., "New Developments in Compressor Aerodynamics," Proceedings of the 1st Turbomachinery Symposium, Texas A&M, October 1972.

Boyce, M.P., "Principles of Operation and Performance Estimation of Centrifugal Compressors," Proceedings of the 22nd Turbomachinery Symposium, Dallas, Texas, September 1993, pp. 161–178.

Boyce, M.P., "Rerating of Centrifugal Compressors-Part I," *Diesel and Gas Turbine Worldwide*, October 1988, pp. 46–50.

Boyce, M.P. "Rerating of Centrifugal Compressors-Part II," *Diesel and Gas Turbine Worldwide*, January–February 1989, pp. 8–20.

Boyce, M.P., and Bale, Y.S., "A New Method for the Calculation of Blade Loadings in Radial-Flow Compressors," ASME Paper No. 71-GT-60, June 1971.

Boyce, M.P., and Bale, Y.S., "Diffusion Loss in a Mixed-Flow Compressor," Intersociety Energy Conversion Engineering Conference, San Diego, Paper No. 729061, September 1972.

Boyce, M.P., and Desai, A.R., "Clearance Loss in a Centrifugal Impeller," Proceedings Of the 8th Intersociety Energy Conversion Engineering Conference, Paper No. 739126, August 1973, p. 638.

Boyce, M.P., and Nishida, A., "Investigation of Flow in Centrifugal Impeller with Tandem Inducer," JSME Paper, Tokyo, Japan, May 1977.

Centrifugal Impeller Performance," NACA TN-1313, 1947.

Coppage, J.E. et al., "Study of Supersonic Radial Compressors for Refrigeration and Pressurization Systems," WADC Technical Report 55-257, Astia Document No. AD110467, 1956.

Dallenback, F., "The Aerodynamic Design and Performance of Centrifugal and Mixed-Flow Compressors," SAE International Congress, January 1961.

Dawes, W., "A Simulation of the Unsteady Interaction of a Centrifugal Impeller with its Vaned Diffuser: Flows Analysis," *ASME Journal of Turbo-machinery*, Vol. 117, 1995, pp. 213–222.

Deniz, S., Greitzer, E. and Cumpsty, N., 1998, "Effects of Inlet Flow Field Conditions on the Performance of Centrifugal Compressor Diffusers Part 2: Straight-Channel Diffuser," ASME Paper No. 98-GT-474.

Domercq, O., and Thomas, R., 1997, "Unsteady Flow Investigation in a Transonic Centrifugal Compressor Stage," AIAA Paper No. 97-2877.

Eckhardt, D., "Instantaneous Measurements in the Jet-Wake Discharge Flow of a Centrifugal Compressor Impeller," ASME Paper No. 74-GT-90.

Filipenco, V., Deniz, S., Johnston, J., Greitzer, E. and Cumpsty, N., 1998, "Effects of Inlet Flow Field Conditions on the Performance of Centrifugal Compressor Diffusers Part 1: Discrete Passage Diffuser," ASME Paper No. 98-GT-473.

Johnston, R., and Dean, R., 1966, "Losses in Vaneless Diffusers of Centrifugal Compressors and Pumps," *ASME Journal of Basic Engineering*, Vol. 88, pp. 49–60.

Katsanis, T., "Use of Arbitrary Quasi-Orthogonals for Calculations Flow Distribution in the Meridional Plane of a Turbomachine," NASA TND-2546, 1964.

Klassen, H.A., "Effect of Inducer Inlet and Diffuser Throat Areas on Performance of a Low-Pressure Ratio Sweptback Centrifugal Compressor," NASA TM X-3148, Lewis Research Center, January 1975.

Owczarek, J.A., *Fundamentals of Gas Dynamics*, International Textbook Company, Scranton, Pennsylvania, 1968, pp. 165–197.

Phillips, M., 1997, "Role of Flow Alignment and Inlet Blockage on Vaned Diffuser Performance," Report No. 229, Gas Turbine Laboratory, Massachusetts Institute of Technology.

Rodgers, C., "Influence of Impeller and Diffuser Characteristic and Matching on Radial Compressor Performance," SAE Preprint 268B, January 1961.

Rodgers, C., 1982, "The Performance of Centrifugal Compressor Channel Diffusers," ASME Paper No. 82-GT-10.

Rodgers, C., and Sapiro, L., "Design Considerations for High-Pressure-Ratio Centrifugal Compressors," ASME Paper No. 73-GT-31, 1972.

Schlichting, H., *Boundary Layer Theory*, 4th edition, McGraw-Hill Book Co., New York, 1962, pp. 547–550.

Senoo, Y., and Nakase, Y., "An Analysis of Flow Through a Mixed Flow Impeller," ASME Paper No. 71-GT-2 1972.

Senoo, Y., and Nakase, Y., "A Blade Theory of an Impeller with an Arbitrary Surface of Revolution," ASME Paper No. 71-GT-17, 1972.

Shouman, A.R., and Anderson J.R., "The Use of Compressor-Inlet pre-whirl for the Control of Small Gas Turbines," *Journal of Engineering for Power*, Trans ASME, Vol. 86, Series A, 1964, pp. 136–140.

Stahler, A.F., "The Slip Factor of a Radial Bladed Centrifugal Compressor," ASME Paper No. 64-GTP-1.

Stanitz, J.D., "Two-Dimensional Compressible Flow in Conical Mixed-Flow Compressors," NACA TN-1744, 1948.

Stanitz, J.D., and Prian, V.D., "A Rapid Approximate Method for Determining Velocity Distribution on Impeller Blades of Centrifugal Compressors," NACA TN-2421, 1951.

Stodola, A., *Steam and Gas Turbines*, McGraw-Hill Book Co., New York, 1927.

Wiesner, F.J., "A Review of Slip Factors for Centrifugal Impellers," *Journal of Engineering for Power*, ASME Trans., October 1967, p. 558.

Woodhouse, H., "Inlet Conditions of Centrifugal Compressors for Aircraft Engine Superchargers and Gas Turbines," *J. Inst. Aeron, Sc*., Vol. 15, 1948, p. 403.

Wu, C.H., "A General Theory of Three-Dimensional Flow in Subsonic and Supersonic Turbomachines of Axial, Radial, and Mixed-Flow Type," NACA TN-2604, 1952.

Copyrighted Materials
Copyright © 2012 Elsevier Retrieved from www.knovel.com

Part II

Major Components

6 Centrifugal Compressors

Centrifugal compressors are used in small gas turbines and are the driven units in most gas turbine compressor trains. They are an integral part of the petrochemical industry, finding extensive use because of their smooth operation, large tolerance of process fluctuations, and their higher reliability compared to other types of compressors. Centrifugal compressors range in size from pressure ratios of 1:3 per stage to as high as 12:1 on experimental models. Discussion here will be limited to pressure ratios below 3.5:1, since this type is prevalent in the petrochemical industry. The proper selection of a compressor is a complex and important decision. The successful operation of many plants depends on smooth and efficient compressor operations. To ensure the best selection and proper maintenance of a centrifugal compressor, the engineer must have a knowledge of many engineering disciplines.

In a typical centrifugal compressor the fluid is forced through the impeller by rapidly rotating impeller blades. The velocity of the fluid is converted to pressure, partially in the impeller and partially in the stationary diffusers. Most of the velocity leaving the impeller is converted into pressure energy in the diffuser as shown in Figure 6-1. It is normal practice to design the compressor so that half the pressure rise takes place in the impeller and the other half in the diffuser. The diffuser consists essentially of vanes, which are tangential to the impeller. These vane passages diverge to convert the velocity head into pressure energy. The inner edges of the vanes are in line with the direction of the resultant airflow from the impeller as shown in Figure 6-2.

Centrifugal compressors, in general, are used for higher-pressure ratios and lower-flow rates compared to lower-stage pressure ratios and higher-flow rates in axial compressors. Figure 6-3 is a map for centrifugal compressors that shows the effect of specific speed (N_s) and specific diameter (D_s) on their efficiency. The most efficient region for centrifugal compressor operation is in a specific speed range between $60 < N_s > 1{,}500$. Specific speeds of more than 3,000 usually require an axial-flow-type compressor. In a centrifugal compressor the angular momentum of the gas flowing through the impeller is increased partly because the impeller's outlet diameter is significantly greater than its inlet diameter. The major difference between axial and centrifugal compressors is the variance in the diameters of the inlet and the outlet. The flow leaving the centrifugal compressor is usually perpendicular to the axis of rotation.

Gas Turbine Engineering Handbook, Fourth Edition. DOI: 10.1016/B978-0-12-383842-1.00006-8
Copyright © 2012 Elsevier Inc. All rights reserved.

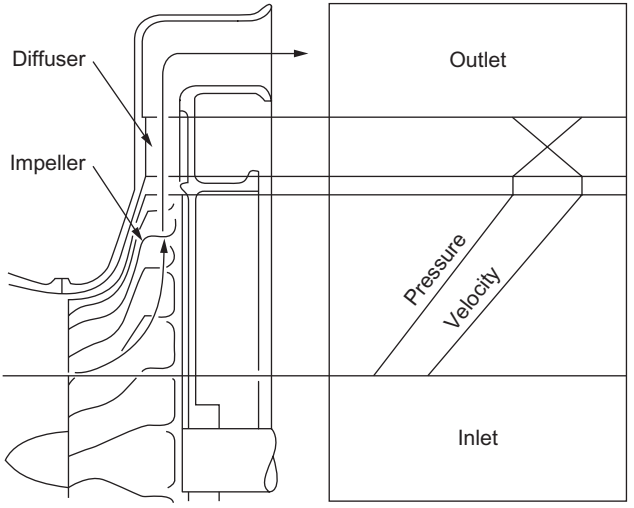


Figure 6-1 Pressure and velocity through a centrifugal compressor.

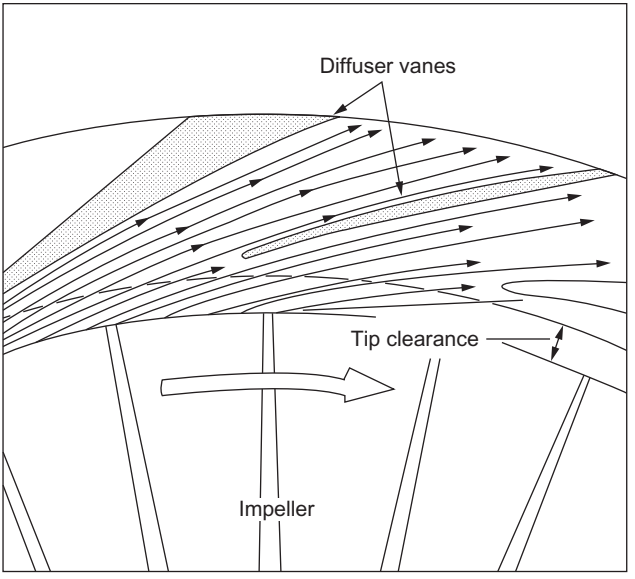


Figure 6-2 Flow entering a vaned diffuser.

Centrifugal Compressor Components

The terminology used to define the components of a centrifugal compressor is shown in Figure 6-4. A centrifugal compressor is composed of inlet guide vanes, an inducer, an impeller, a diffuser, and a scroll. The inlet guide vanes (IGVs) are used in only a

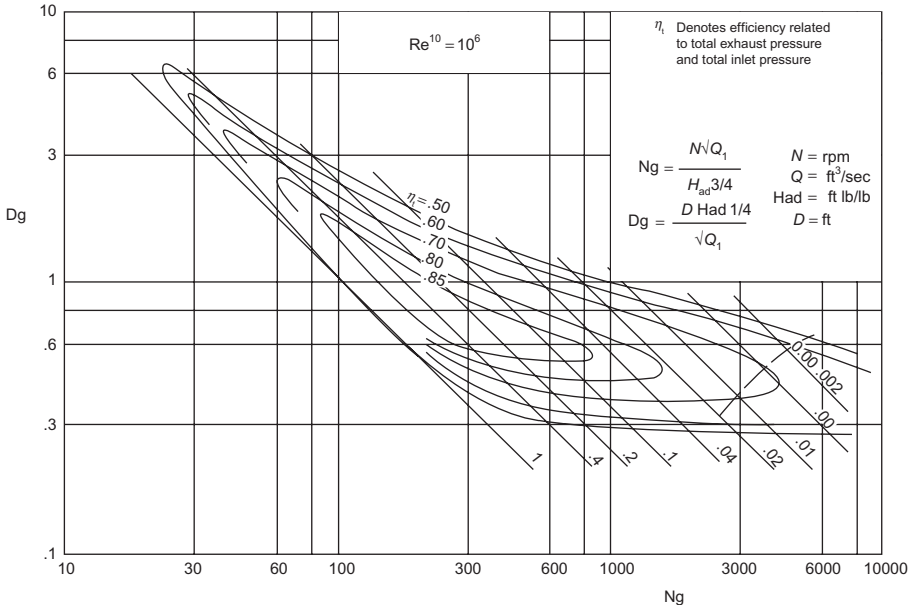


Figure 6-3 Centrifugal compressor map. Balje, O.E., "A Study of Reynolds Number Effects in Turbomachinery," *Journal of Engineering for Power*, ASME Trans., Vol. 86, Series A, p. 227.

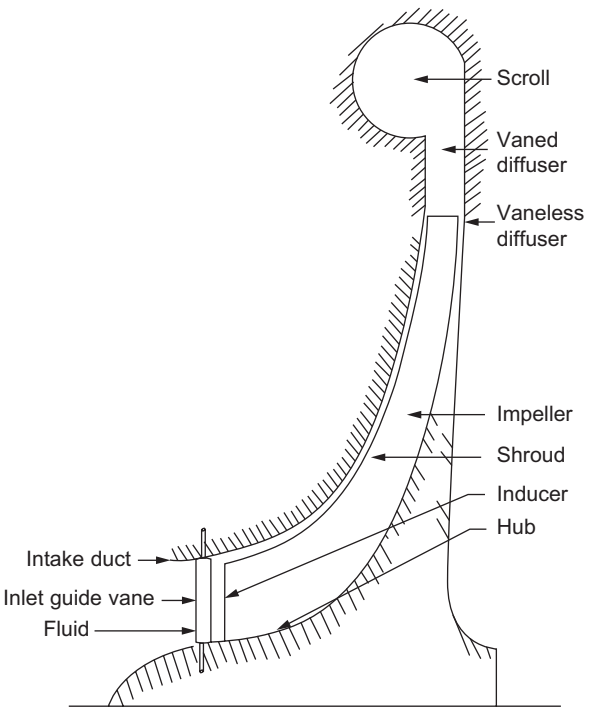


Figure 6-4 Schematic of a centrifugal compressor.

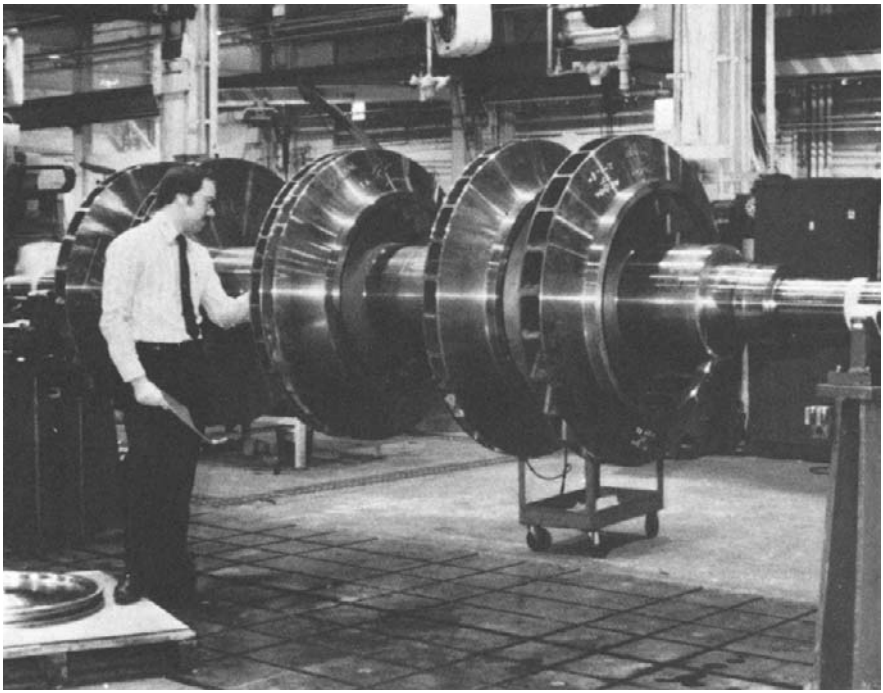


Figure 6-5 Closed impeller (courtesy Elliott Company, Jeannette, PA).

high-pressure ratio transonic compressor. Centrifugal compressor impellers are either shrouded or un-shrouded as seen in Figures 6-5 and 6-6.

The fluid comes into the compressor through an intake duct and is given pre-whirl by the IGVs. It then flows into an inducer without any incidence angle, and its flow direction is changed from axial to radial. The fluid is given energy at this stage by the rotor as it goes through the impeller while compressing. It is then discharged into a diffuser, where the kinetic energy is converted into static pressure. The flow enters the scroll from which the compressor discharge is taken. Figure 6-1 shows the variations in pressure and velocity through a compressor.

There are two kinds of energy inducer systems: a single-entry inducer and a double-entry inducer as shown in Figure 6-7.

A double-entry inducer system halves the inlet flow so that a smaller inducer-tip diameter can be used, reducing the inducer-tip Mach number; however, the design is difficult to integrate into many configurations.

There are three impeller vane types, as shown in Figure 6-8. These are defined according to the exit blade angles. Impellers with exit blade angle $\beta_2 = 90^\circ$ are radial vanes. Impellers with $\beta_2 < 90^\circ$ are backward-curved or backward-swept vanes, and for $\beta_2 > 90^\circ$, the vanes are forward-curved or forward-swept. They have different characteristics of theoretical head-flow relationship to each other, as shown in Figure 6-9. Although in Figure 6-9 the forward-curved head is the largest, in actual

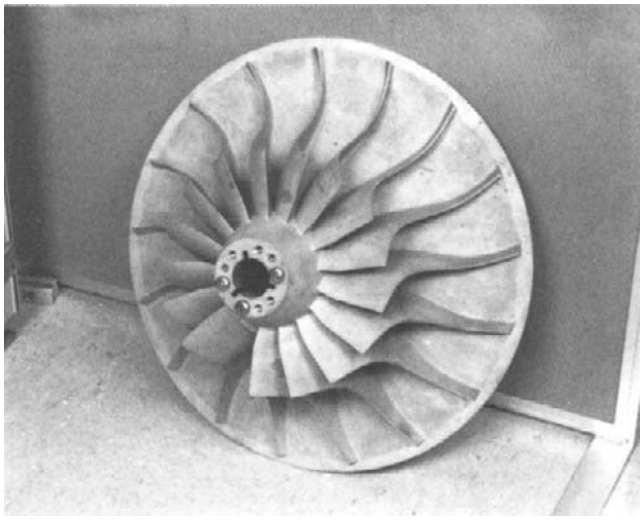


Figure 6-6 Open-faced impeller.

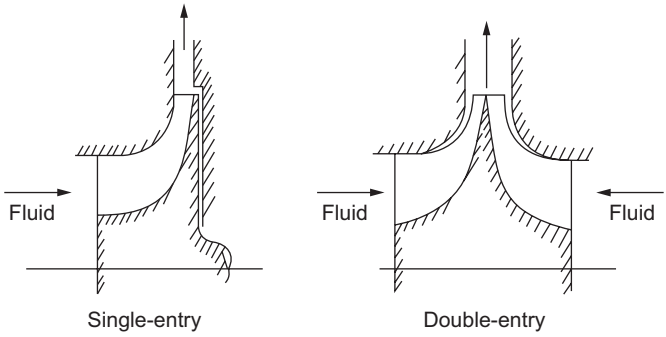


Figure 6-7 Types of entry-inducer systems.

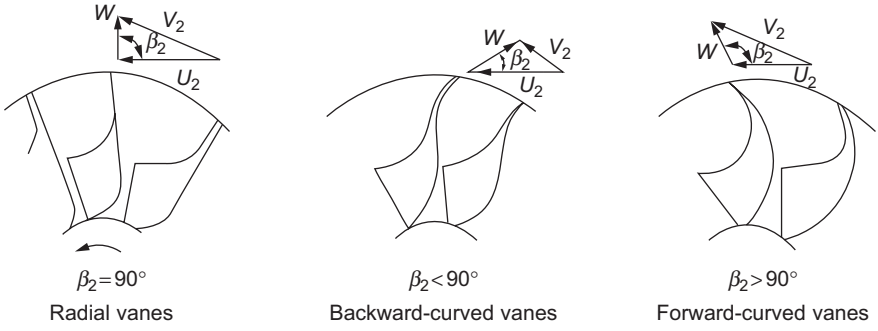


Figure 6-8 Various types of impeller blading.

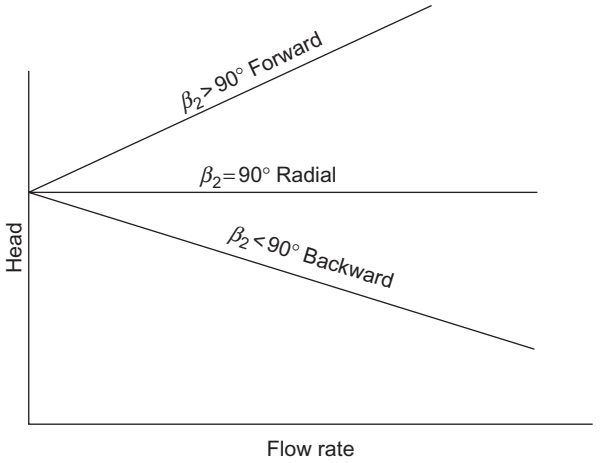


Figure 6-9 Head flow-rate characteristics for various outlet blade angles.

Table 6-1 The Advantages and Disadvantages of Various Impellers

Types of Impellers	Advantages	Disadvantages
Radial vanes	1. Reasonable compromise between low-energy transfer and high absolute outlet velocity 2. No complex bending stress 3. Easy manufacturing	1. Surge margin is relatively narrow
Backward-curved vanes	1. Low-outlet kinetic energy = low-diffuser inlet Mach number 2. Surge margin is wide	1. Low-energy transfer 2. Complex bending stress 3. Hard manufacturing
Forward-curved vanes	1. High-energy transfer	1. High-outlet kinetic energy = high-diffuser inlet Mach number 2. Surge margin is less than radial vanes 3. Complex bending stress 4. Hard manufacturing

practice the head characteristics of all the impellers are similar to the backward-curved impeller. Table 6-1 shows the advantages and disadvantages of various impellers.

The Euler equation, assuming simple one-dimensional flow theory, is the theoretical amount of work imparted to each pound of fluid as it passes through the impeller, and it is given by:

$$H = \frac{1}{g_c}[U_1 V_{\theta 1} - U_2 V_{\theta 2}] \tag{6-1}$$

where

H = work per lb of fluid
U_2 = impeller peripheral velocity
U_1 = inducer velocity at the mean radial station
$V_{\theta 2}$ = absolute tangential fluid velocity at impeller exit
$V_{\theta 1}$ = absolute tangential air velocity at inducer inlet

For the axial inlet:

$$V_{\theta 1} = 0$$

then

$$H = -\frac{1}{g_c}(U_2 V_{\theta 2}) \tag{6-2}$$

Supposing constant rotational speeds, no slip, and an axial inlet, the velocity triangles are as shown in Figure 6-10. For the radial vane, the absolute tangential fluid velocity at the impeller exit is constant – even if the flow rate is increased or decreased.

Therefore:

$$H \approx U_2 V''_{\theta 2} \approx U_2 V_{\theta 2} \approx U_2 V'_{\theta 2} \tag{6-3}$$

flow decrease — flow increase

For backward-curved vanes, the absolute tangential fluid velocity at the impeller exit increases with the reduction of flow rates and decreases with the increase in flow

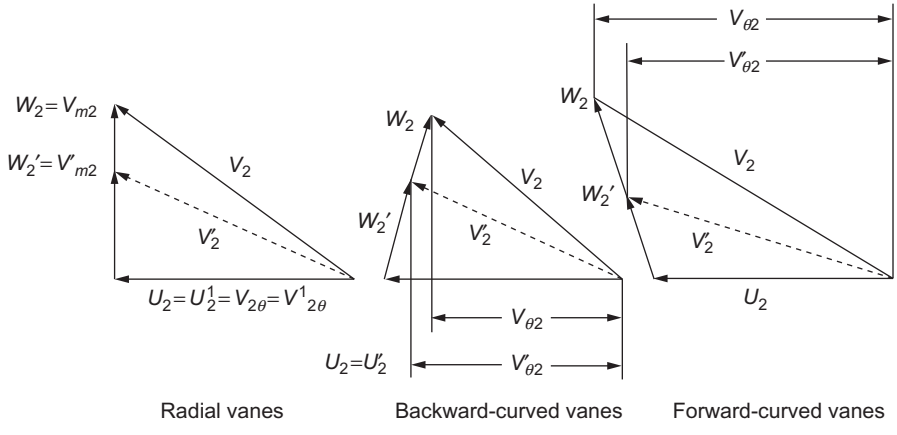


Figure 6-10 Velocity triangles.

rate as shown in the following equation:

$$H \approx \underset{\substack{\text{flow}\\ \text{decrease}}}{-U_2 V''_{\theta 2}} > -U_2 V_{\theta 2} < \underset{\substack{\text{flow}\\ \text{increase}}}{-U_2 V'_{\theta 2}} \tag{6-4}$$

For forward-curved vanes, the absolute tangential fluid velocity at the impeller exit decreases with the reduction of flow rates and increases with the decrease in flow rates as shown in the following equation:

$$H \approx \underset{\substack{\text{flow}\\ \text{decrease}}}{-U_2 V'_{\theta}} < U_2 V_{\theta 2} > \underset{\substack{\text{flow}\\ \text{increase}}}{U_2 V'_{\theta}} \tag{6-5}$$

Inlet Guide Vanes

The inlet guide vanes give circumferential velocity to the fluid at the inducer inlet. This function is called pre-whirl. Figure 6-11 shows inducer inlet velocity diagrams with and without IGVs.

IGVs are installed directly in front of the inducer or, where an axial entry is not possible, located radially in an intake duct.

A positive vane angle produces pre-whirl in the direction of the impeller rotation, and a negative vane angle produces pre-whirl in the opposite direction. The disadvantage of positive pre-whirl is that a positive inlet whirl velocity reduces the energy transfer. Since $V_{\theta 1}$ is positive according to the Euler equation:

$$H = \frac{1}{g_c}[U_1 V_{\theta 1} - U_2 V_{\theta 2}] \tag{6-6}$$

non-pre-whirl (without IGVs axial entry), $V_{\theta 1}$ is equal to zero. Then the Euler work is:

$$H = -U_2 V_{\theta 2}.$$

With positive pre-whirl, the first term of the Euler equation remains $H = U_1 V_{\theta 1} - U_2 V_{\theta 2}$. Therefore, Euler work is reduced by the use of positive pre-whirl. On the other hand, negative pre-whirl increases the energy transfer by the amount $U_1 V_{\theta 1}$. This results in a larger pressure head being produced in the case of the negative pre-whirl for the same impeller diameter and speed.

The positive pre-whirl decreases the relative Mach number at the inducer inlet. However, negative pre-whirl increases it. A relative Mach number is defined by:

$$M_{\text{rel}} = \frac{W_1}{a_1} \tag{6-7}$$

where

M_{rel} = relative Mach number
W_1 = relative velocity at an inducer inlet
a_1 = sonic velocity at inducer inlet conditions

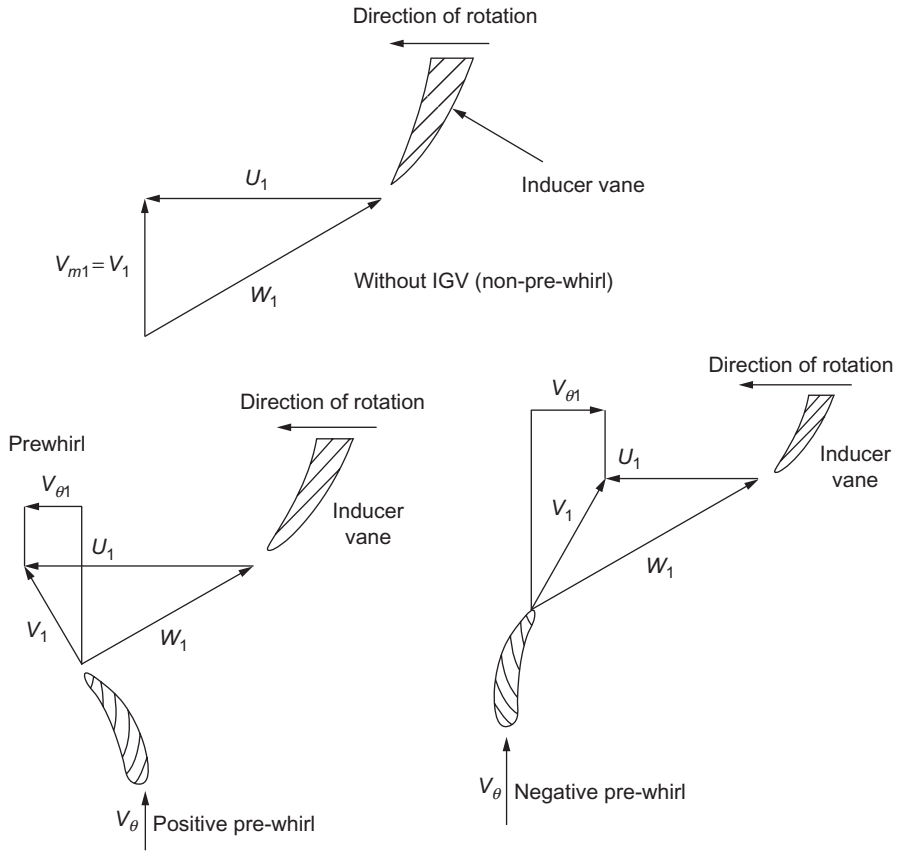


Figure 6-11 Inducer inlet velocity diagrams.

The purpose of installing the IGVs is to decrease the relative Mach number at the inducer-tip (impeller eye) inlet because the highest relative velocity at the inducer inlet is at the tip section. When the relative velocity is close to the sonic velocity or greater than it, a shock wave takes place in the inducer section. A shock wave produces shock loss and chokes the inducer. Figure 6-12 shows the effect of inlet pre-whirl on compressor efficiency.

There are three kinds of pre-whirl:

1. *Free-vortex pre-whirl.* This type is represented by $r_1 V_{\theta 1} =$ constant with respect to the inducer inlet radius. This pre-whirl distribution is shown in Figure 6-13. $V_{\theta 1}$ is at a minimum at the inducer inlet shroud radius. Therefore, it is not effective in decreasing the relative Mach number in this manner.
2. *Forced-vortex pre-whirl.* This type is shown as $V_{\theta 1}/r_1 =$ constant. This pre-whirl distribution is also shown in Figure 6-14. $V_{\theta 1}$ is at a maximum at the inducer inlet shroud radius, contributing to a decrease in the inlet relative Mach number.
3. *Control-vortex pre-whirl.* This type is represented by $V_{\theta 1} = AR_1 + B/r_1$, where A and B are constants. This equation shows the first type with $A = 0, B \neq 0$, and the second type with $B = 0, A \neq 0$.

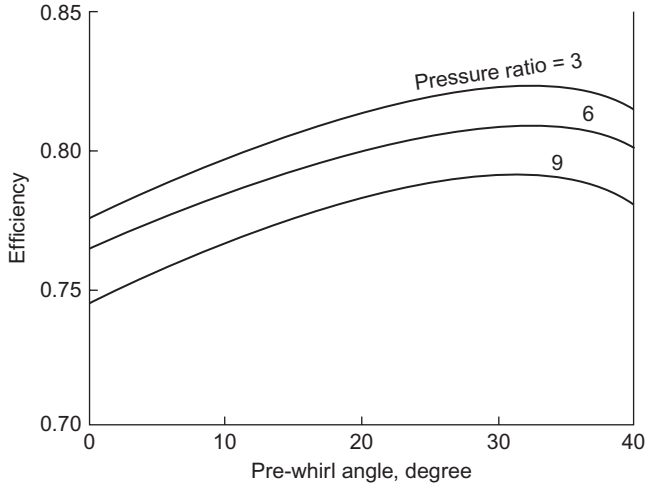


Figure 6-12 Estimate effect of inlet pre-whirl. (Rodgers, C., and Shapiro, L., "Design Considerations for High-Pressure-Ratio Centrifugal Compressors," ASME Paper No.: 73-GT-31, 1972.)

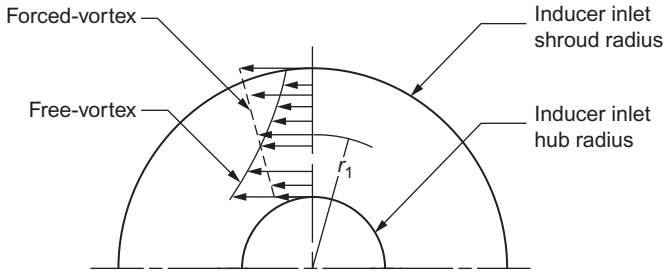


Figure 6-13 Pre-whirl distribution patterns.

Euler work distributions at an impeller exit, with respect to the impeller width, are shown in Figure 6-14. From Figure 6-14, the pre-whirl distribution should be made not only from the relative Mach number at the inducer inlet shroud radius, but also from Euler work distribution at the impeller exit. Uniform impeller exit flow conditions, considering the impeller losses, are important factors in obtaining good compressor performance.

Impeller

An impeller in a centrifugal compressor imparts energy to a fluid. The impeller consists of two basic components: (1) an inducer like an axial-flow rotor, and (2) the radial blades where energy is imparted by centrifugal force. Flow enters the impeller in the axial direction and leaves in the radial direction. The velocity variations from hub to shroud resulting from these changes in flow directions complicate the design

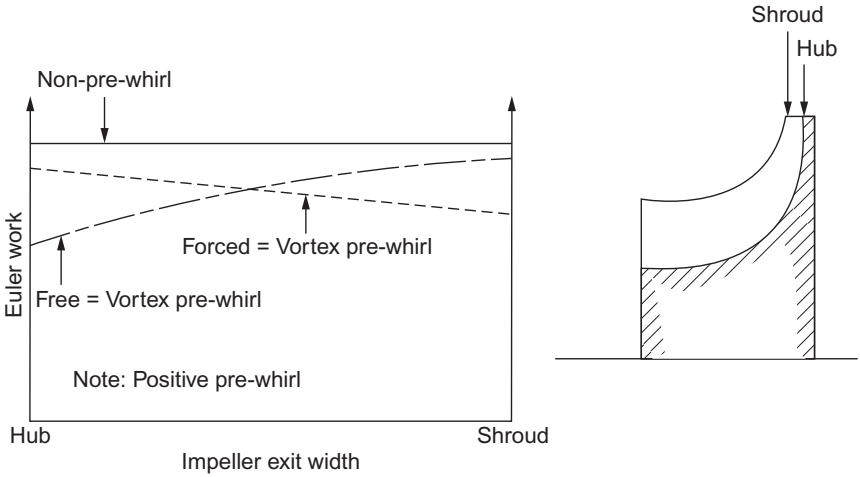


Figure 6-14 Euler work distribution at an impeller exit.

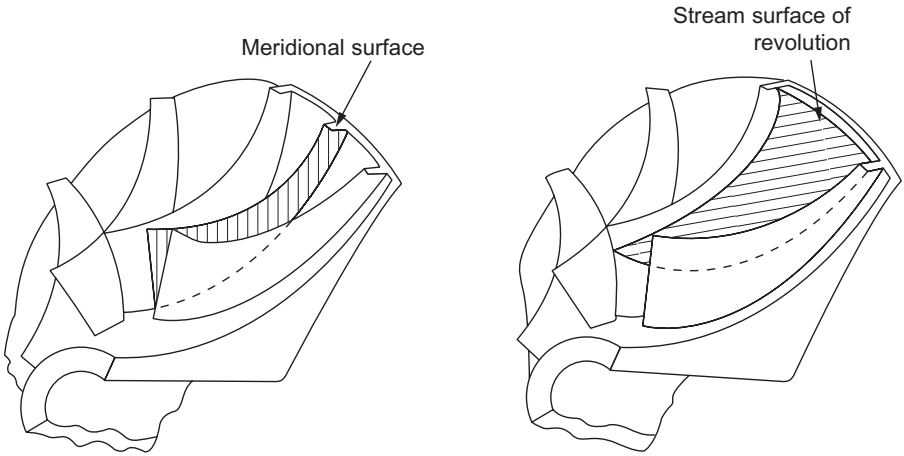


Figure 6-15 Two-dimensional surface for a flow analysis.

procedure for centrifugal compressors. C.H. Wu has presented the three-dimensional theory in an impeller, but it is difficult to solve for the flow in an impeller using the previous theory without certain simplified conditions. Others have dealt with it as a quasi-three-dimensional solution. It is composed of two solutions, one in the meridional surface (hub-to-shroud), and the other in the stream surface of revolution (blade-to-blade). These surfaces are illustrated in Figure 6-15.

By the application of the previous method using a numerical solution to the complex flow equations, it is possible to achieve impeller efficiencies of more than 90%. The actual flow phenomenon in an impeller is more complicated than the one

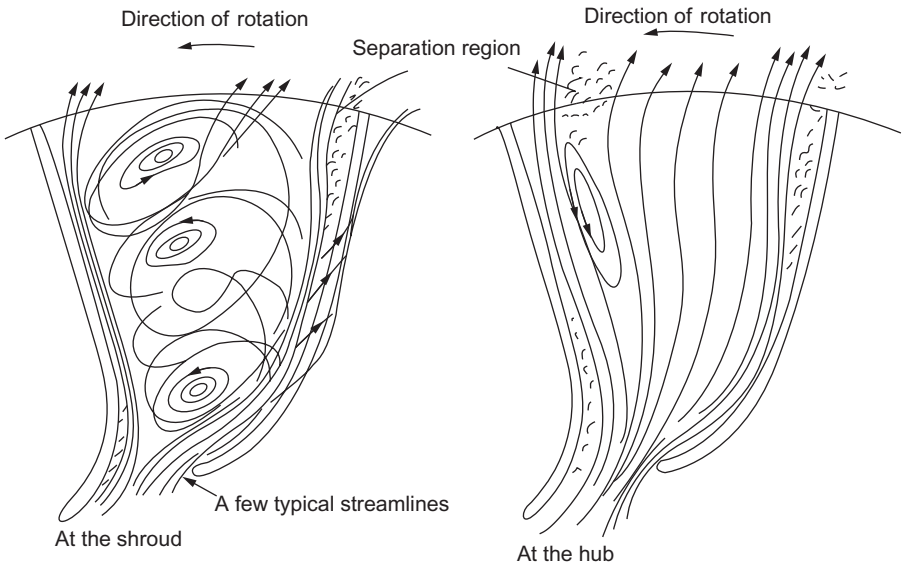


Figure 6-16 Flow map of impeller plane.

calculated. One example of this complicated flow is shown in Figure 6-16. The stream lines observed in Figure 6-16 do not cross, but are actually in different planes observed near the shroud. Figure 6-17 shows the flow in the meridional plane with separation regions at the inducer section and at the exit.

Experimental studies of the flow within impeller passages have shown that the distribution of velocities on the blade surfaces are different from the distributions predicted theoretically. It is likely that the discrepancies between theoretical and experimental results are due to secondary flows from pressure losses and boundary-layer separation in the blade passages. High-performance impellers should be designed, when possible, with the aid of theoretical methods for determining the velocity distributions on the blade surfaces.

Examples of the theoretical velocity distributions in the impeller blades of a centrifugal compressor are shown in Figure 6-18. The blades should be designed to eliminate large decelerations or accelerations of flow in the impeller that lead to high losses and separation of the flow. Potential flow solutions predict the flow well in regions away from the blades where boundary-layer effects are negligible. In a centrifugal impeller the viscous shearing forces create a boundary layer with reduced kinetic energy. If the kinetic energy is reduced below a certain limit, the flow in this layer becomes stagnant, then it reverses.

Inducer

The function of an inducer is to increase the fluid's angular momentum without increasing its radius of rotation. In an inducer section the blades bend toward the

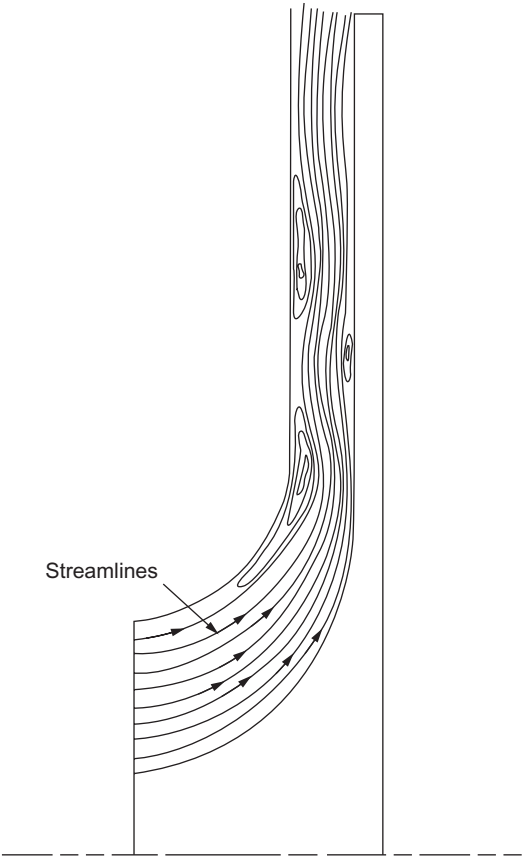


Figure 6-17 Flow map as seen in meridional plane.

direction of rotation as shown in Figure 6-19. The inducer is an axial rotor and changes the flow direction from the inlet flow angle to the axial direction. It has the largest relative velocity in the impeller and, if not properly designed, can lead to choking conditions at its throat as shown in Figure 6-19.

There are three forms of inducer camber lines in the axial direction. These are circular arc, parabolic arc, and elliptical arc. Circular arc camber lines are used in compressors with low pressure ratios, while the elliptical arc produces good performance at high pressure ratios where the flow has transonic Mach numbers.

Because of choking conditions in the inducer, many compressors incorporate a splitter-blade design. The flow pattern in such an inducer section is shown in Figure 6-20 (a). This flow pattern indicates a separation on the suction side of the splitter blade. Other designs include tandem inducers. In tandem inducers the inducer section is slightly rotated as shown in Figure 6-20 (b). This modification gives additional kinetic energy to the boundary, which is otherwise likely to separate.

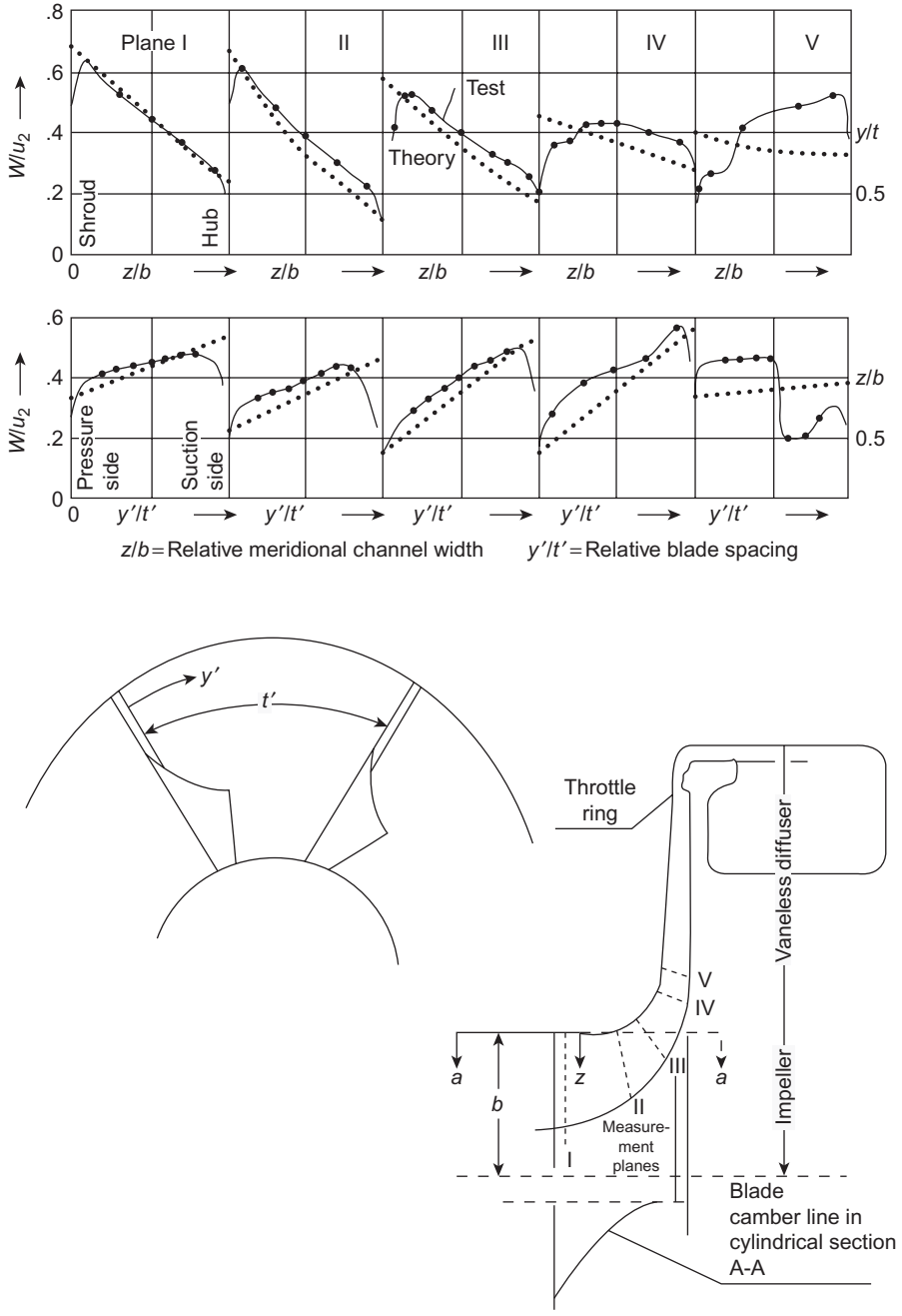


Figure 6-18 Velocity profiles through a centrifugal compressor.

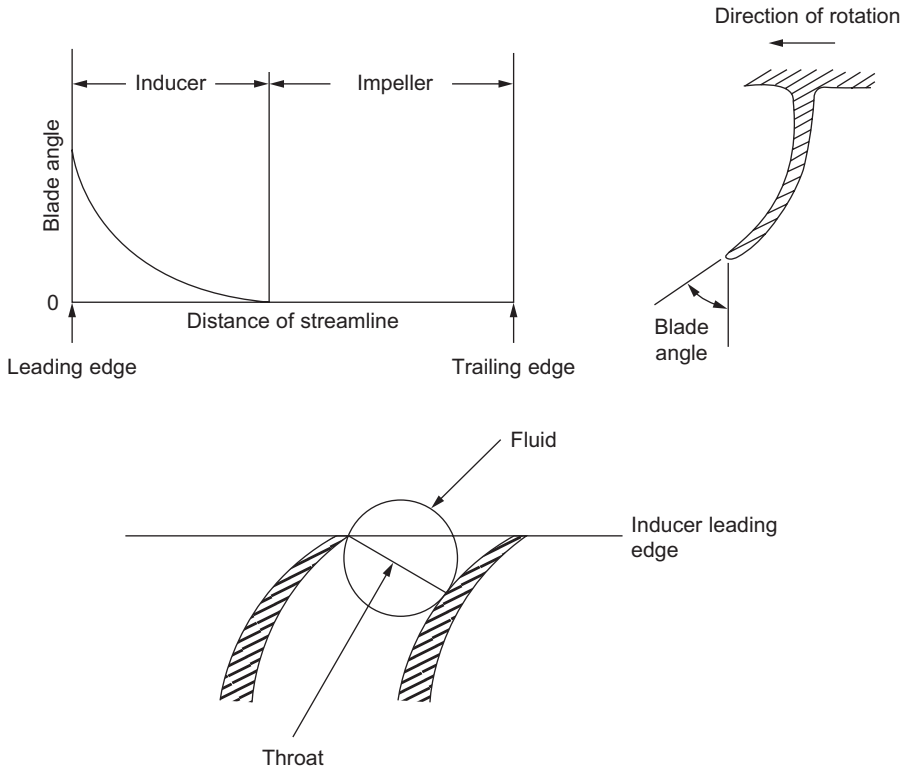


Figure 6-19 Inducer centrifugal compressor.

Centrifugal Section of an Impeller

The flow in this section of the impeller enters from the inducer section and leaves the impeller in the radial direction. The flow in this section is not completely guided by the blades, and hence the effective fluid outlet angle does not equal the blade outlet angle.

To account for flow deviation (which is similar to the effect accounted for by the deviation angle in axial-flow machines), the slip factor is used:

$$\mu = \frac{V_{\theta 2}}{V_{\theta 2\infty}} \tag{6-8}$$

where $V_{\theta 2}$ is the tangential component of the absolute exit velocity with a finite number of blades, and $V_{\theta 2\infty}$ is the tangential component of the absolute exit velocity, if the impeller were to have an infinite number of blades (no slipping back of the relative velocity at outlet).

With radial blades at the exit:

$$\mu = \frac{V_{\theta 2}}{U_2} \tag{6-9}$$

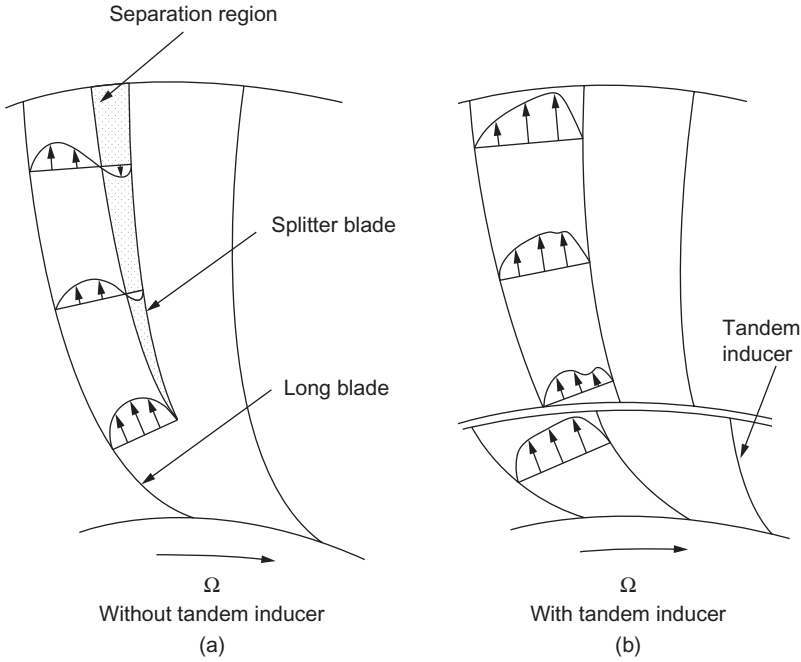


Figure 6-20 Impeller channel flow.

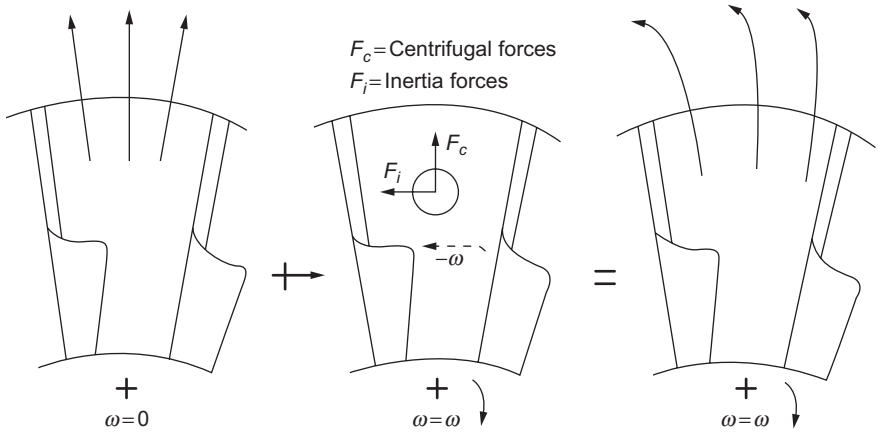


Figure 6-21 Forces and flow characteristics in a centrifugal compressor.

Flow in a rotating impeller channel (blade passage) will be a vector sum of flow with the impeller stationary and the flow due to rotation of the impeller as seen in Figure 6-21.

In a stationary impeller, the flow is expected to follow the blade shape and exit tangentially to it. A high adverse pressure gradient along the blade passage and subsequent flow separation are not considered to be general possibilities.

Inertia and centrifugal forces cause the fluid elements to move closer to and along the leading surface of the blade toward the exit. Once out of the blade passage, where there is no positive impelling action present, these fluid elements slow down.

Causes of Slip in an Impeller

The definite cause of the slip phenomenon that occurs within an impeller is not known. However, some general reasons can be used to explain why the flow is changed.

Coriolis Circulation

Because of the pressure gradient between the walls of two adjacent blades, the Coriolis forces, the centrifugal forces, and the fluid all follow the Helmholtz vorticity law. The combined gradient that results causes a fluid movement from one wall to the other and vice versa. This movement sets up circulation within the passage as seen in Figure 6-22. Because of this circulation, a velocity gradient results at the impeller exit with a net change in the exit angle.

Boundary-Layer Development

The boundary layer that develops within an impeller passage causes the flowing fluid to experience a smaller exit area as shown in Figure 6-23. This smaller exit is due to small flow (if any) within the boundary layer. For the fluid to exit this smaller area, its velocity must increase. This increase gives a higher relative exit velocity. Since

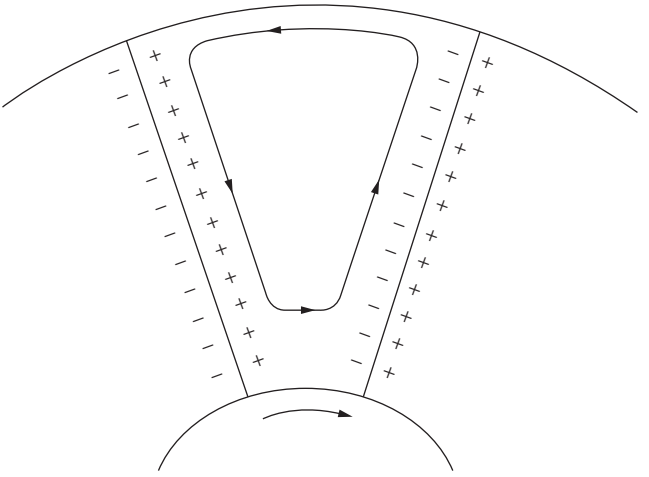


Figure 6-22 Coriolis circulation.

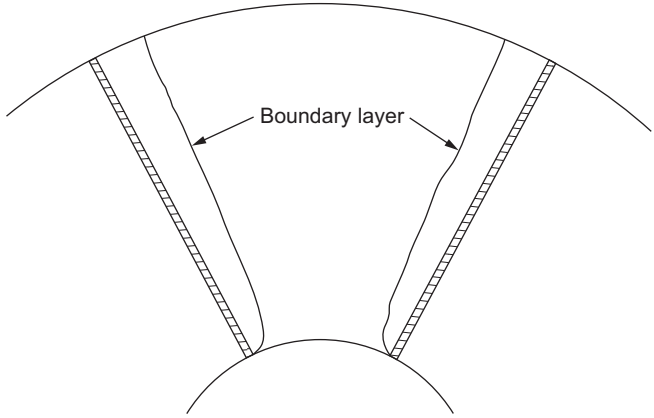


Figure 6-23 Boundary-layer development.

the meridional velocity remains constant, the increase in relative velocity must be accompanied by a decrease in absolute velocity.

Although it is not a new approach, boundary-layer control is being used more than ever before. It has been used with success on airfoil designs when it has delayed separation, thus giving a larger usable angle of attack. Control of the flow over an airfoil has been accomplished in two ways: by using slots through the airfoil and by injecting a stream of fast-moving air.

Separation regions are also encountered in the centrifugal impeller as shown previously. Applying the same concept (separation causes a loss in efficiency and power) reduces and delays their formation. Diverting the slow-moving fluid away lets the separation regions be occupied by a faster stream of fluid, which reduces boundary-layer build-up and thus decreases separation.

To control the boundary layer in the centrifugal impeller, slots in the impeller blading at the point of separation are used. To realize the full capability of this system, these slots should be directional and converging in a cross-sectional area from the pressure to the suction sides as seen in Figure 6-24. The fluid diverted by these slots increases in velocity and attaches itself to the suction sides of the blades. This results in moving the separation region closer to the tip of the impeller, thus reducing slip and losses encountered by the formation of large boundary-layer regions. The slots must be located at the point of flow separation from the blades. Experimental results indicate: improvement in the pressure ratio, efficiency, and surge characteristics of the impeller as seen in Figure 6-24.

Leakage

Fluid flow from one side of a blade to the other side is referred to as leakage. Leakage reduces the energy transfer from impeller to fluid and decreases the exit velocity angle.

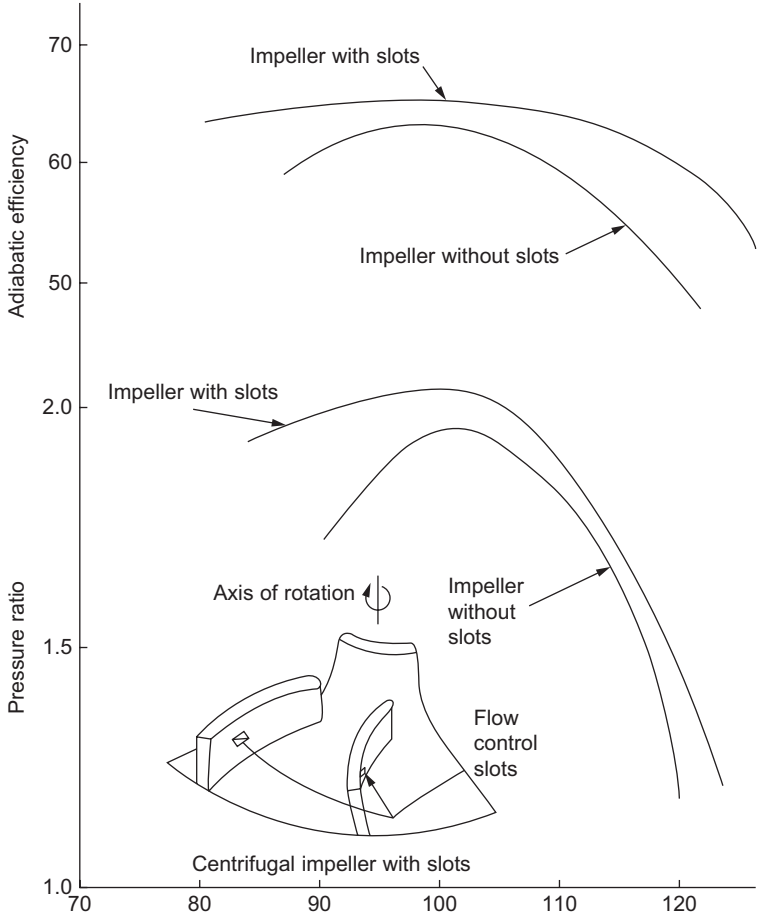


Figure 6-24 Percent design flow – laminar flow control in a centrifugal compressor.

Number of Vanes

The greater the number of vanes, the lower the vane loading, and the closer the fluid follows the vanes. With higher vane loadings, the flow tends to group up on the pressure surfaces and introduces a velocity gradient at the exit.

Vane Thickness

Because of manufacturing problems and physical necessity, impeller vanes are thick. When fluid exits the impeller, the vanes no longer contain the flow, and the velocity is immediately slowed. Because it is the meridional velocity that decreases, both the relative and absolute velocities decrease, changing the exit angle of the fluid.

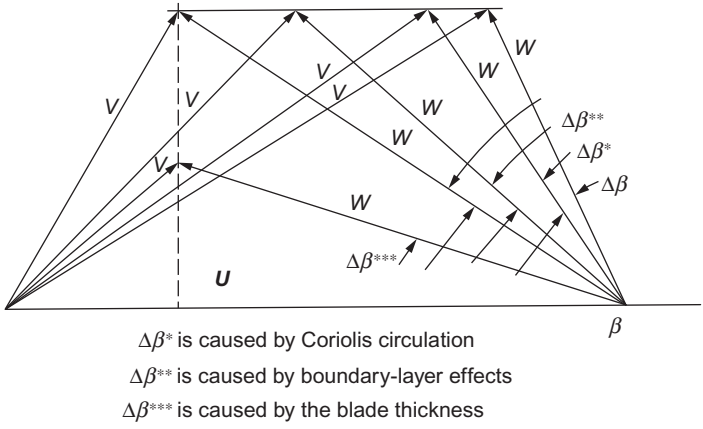


Figure 6-25 Effect on exit velocity triangles by various parameters.

A backward-curved impeller blade combines all these effects. The exit velocity triangle for this impeller with the different slip phenomenon changes is shown in Figure 6-25. This triangle shows that actual operating conditions are far removed from the projected design condition.

Several empirical equations have been derived for the slip factor (see Figure 6-26). These empirical equations are limited. Two of the more common slip factors are presented here.

Stodola Slip Factor

The second Helmholtz law states that the vorticity of a frictionless fluid does not change with time. Hence, if the flow at the inlet to an impeller is irrotational, the absolute flow must remain irrotational throughout the impeller. As the impeller has an angular velocity ω, the fluid must have an angular velocity $-\omega$ relative to the impeller. This fluid motion is called the relative eddy. If there were no flow through the impeller, the fluid in the impeller channels would rotate with an angular velocity equal and opposite to the impeller's angular velocity.

To approximate the flow, Stodola's theory assumes that the slip is due to the relative eddy. The relative eddy is considered as a rotation of a cylinder of fluid at the end of the blade passage at an angular velocity of $-\omega$ about its own axis. The Stodola slip factor is given by:

$$\mu = 1 - \frac{\pi}{Z}\left[1 - \frac{\sin\beta_2}{\dfrac{V_{m2}\cot\beta_2}{U_2}}\right] \tag{6-10}$$

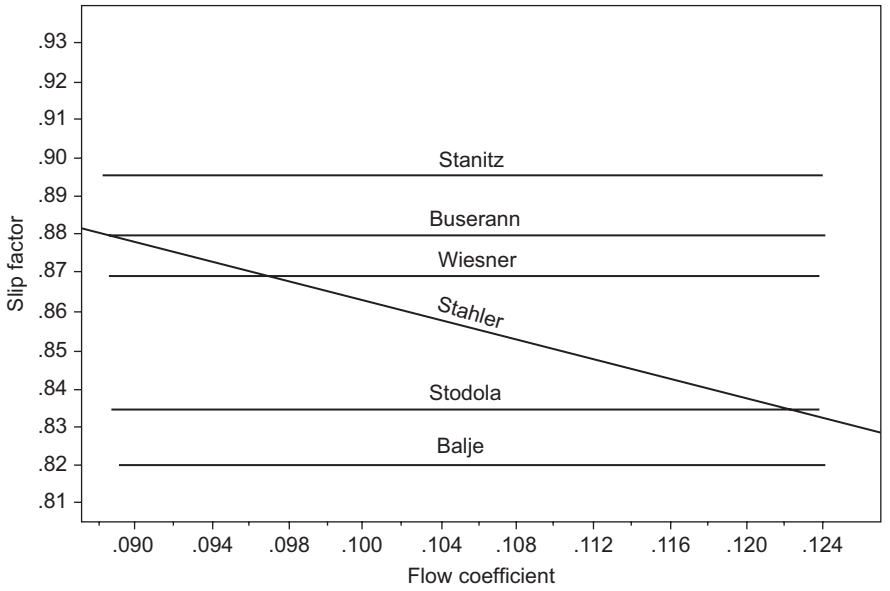


Figure 6-26 Various slip factors as a function of the coefficient.

where

$\beta_2 =$ the blade angle
$Z =$ the number of blades
$V_{m2} =$ the meridional velocity
$U_2 =$ blade tip speed

Calculations using this equation have been found to be lower than experimental values.

Stanitz Slip Factor

Stanitz calculated blade-to-blade solutions for eight impellers and concluded that for the range of conditions covered by the solutions, U is a function of the number of blades (Z), and the blade exit angle (β_2) is approximately the same whether the flow is compressible or incompressible:

$$\mu = 1 - \frac{0.63\pi}{Z}\left[1 - \frac{1}{\frac{W_{m2}}{U_2}\cot\beta_2}\right] \tag{6-11}$$

Stanitz's solutions were for $\pi/4 < \beta_2 < \pi/2$. This equation compares well with experimental results for radial or near-radial blades.

Diffusers

Diffusing passages have always played a vital role in obtaining good performance from turbomachines. Their role is to recover the maximum possible kinetic energy leaving the impeller with a minimum loss in total pressure. The efficiency of centrifugal compressor components has been steadily improved by advancing their performance. However, significant further improvement in efficiency will be gained only by improving the pressure recovery characteristics of the diffusing elements of these machines, since these elements have the lowest efficiency.

The performance characteristics of a diffuser are complicated functions of diffuser geometry, inlet flow conditions, and exit flow conditions. Figure 6-27 shows typical diffusers classified by their geometry. The selection of an optimum channel diffuser for a particular task is difficult, since it must be chosen from an almost infinite number of cross-sectional shapes and wall configurations. In radial and mixed-flow compressors the requirement of high performance and compactness leads to the use of vaned diffusers as shown in Figure 6-28. Figure 6-28 also shows the flow regime of a vane-island diffuser.

Matching the flow between the impeller and the diffuser is complex because the flow path changes from a rotating system into a stationary one. This complex, unsteady flow is strongly affected by the jet-wake of the flow leaving the impeller, as seen in Figure 6-29. The three-dimensional boundary layers, the secondary flows in the vaneless region, and the flow separation at the blades also affect the overall flow in the diffuser.

The flow in the diffuser is usually assumed to be of a steady nature to obtain the overall geometric configuration of the diffuser. In a channel-type diffuser the viscous shearing forces create a boundary layer with reduced kinetic energy. If the kinetic energy is reduced below a certain limit, the flow in this layer becomes stagnant and then reverses. This flow reversal causes separation in a diffuser passage, which results in eddy losses, mixing losses, and changed-flow angles. Separation should be avoided or delayed to improve compressor performance.

The high-pressure-ratio centrifugal compressor has a narrow yet stable operating range. This operating range is due to the close proximity of the surge and choke flow limits. The word "surge" is widely used to express unstable operation of a compressor. Surge is the flow breakdown period during unstable operation. The unsteady flow phenomena during the onset of surge in a high-pressure-ratio centrifugal compressor causes the mass flow throughout the compressor to oscillate during supposedly "stable" operations. The throat pressure in the diffuser increases during the precursor period up to collector pressure P_{col} at the beginning of surge. All pressure traces (except plenum pressure) suddenly drop at the surge point. The sudden change of pressure can be explained by the measured occurrence of backflow from the collector through the impeller during the period between the two sudden changes.

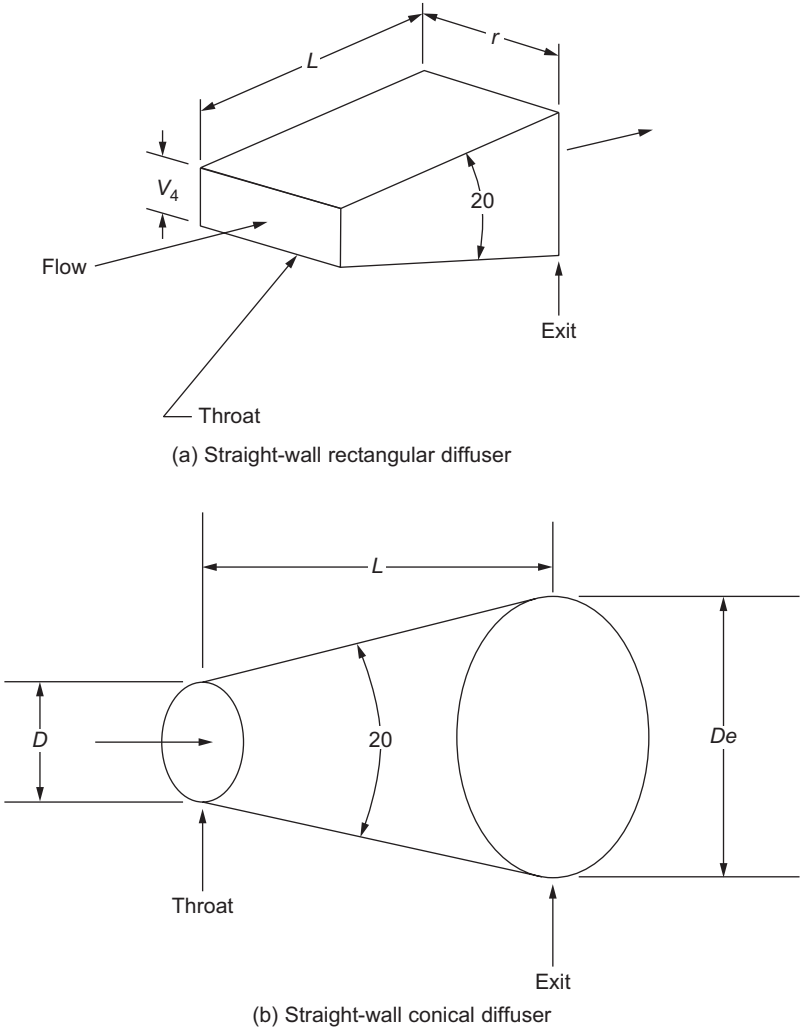


Figure 6-27 Geometric classification of diffusers.

Scroll or Volute

The purpose of the volute is to collect the fluid leaving the impeller or diffuser, and deliver it to the compressor outlet pipe. The volute has an important effect on the overall efficiency of the compressor. Volute design embraces two schools of thought. First, the angular momentum of the flow in the volute is constant, neglecting any friction effects. The tangential velocity $V_{5\theta}$ is the velocity at any radius in the volute. The following equation shows the relationship if the angular momentum is held

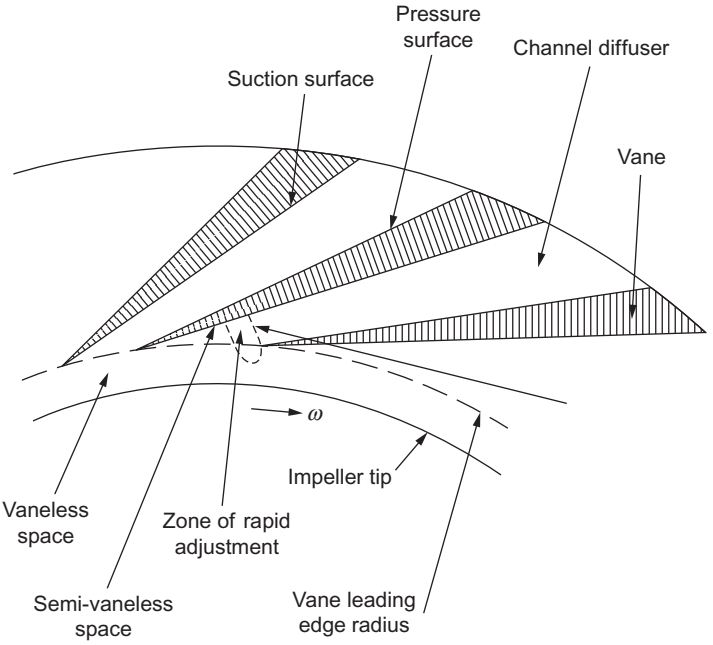


Figure 6-28 Flow regions of the vaned diffuser.

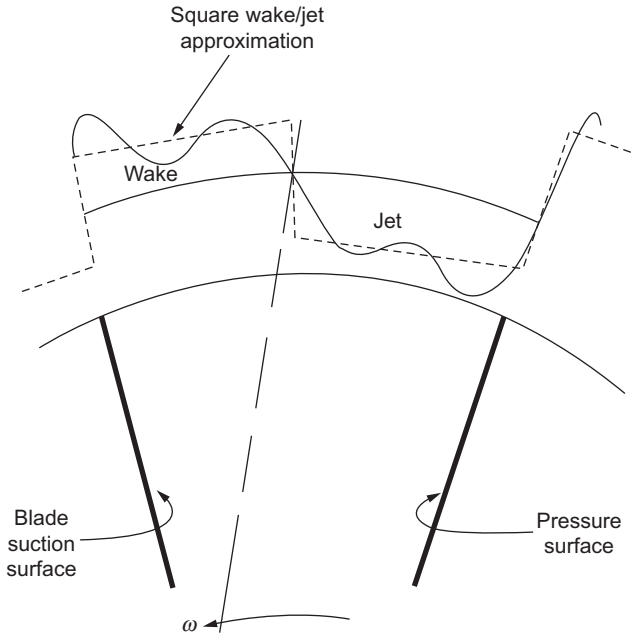


Figure 6-29 Jet-wake flow distribution from an impeller.

constant:

$$V_{5\theta} r = \text{constant} = K \tag{6-12}$$

Assuming no leakage past the tongue and a constant pressure around the impeller periphery, the relationship of flow at any section Q_θ to the overall flow in the impeller Q is given by:

$$Q_\theta = \frac{\theta}{2\pi} Q \tag{6-13}$$

Thus, the area distribution at any section θ can be given by the following relationship:

$$A_\theta = Qr \times \frac{\theta}{2\pi} \times \frac{L}{K} \tag{6-14}$$

where

r = radius to the center of gravity
L = volume width

Second, design the volute by assuming that the pressure and velocity are independent of θ. The area distribution in the volute is given by:

$$A_\theta = K \frac{Q}{V_{5\theta}} \frac{\theta}{2\pi} \tag{6-15}$$

To define the volute section at a given θ, the shape and area of the section must be decided. Flow patterns in various types of volute are shown in Figure 6-30. The flow in the asymmetrical volute has a single-vortex instead of the double-vortex in the symmetrical volute. Where the impeller is discharging directly into the volute, it is better to have the volute width larger than the impeller width. This enlargement results in the flow from the impeller being bounded by the vortex generated from the gap between the impeller and the casing.

At flows different from design conditions, there exists a circumferential pressure gradient at the impeller tip and in the volute at a given radius. At low flows, the pressure rises with the peripheral distance from the volute tongue. At high flows, the pressure falls with distance from the tongue. This condition results because near the tongue the flow is guided by the outer wall of the passage. The circumferential pressure gradients reduce efficiency away from the design point. Non-uniform pressure at the impeller discharge results in unsteady flows in the impeller passage, causing flow reversal and separation in the impeller.

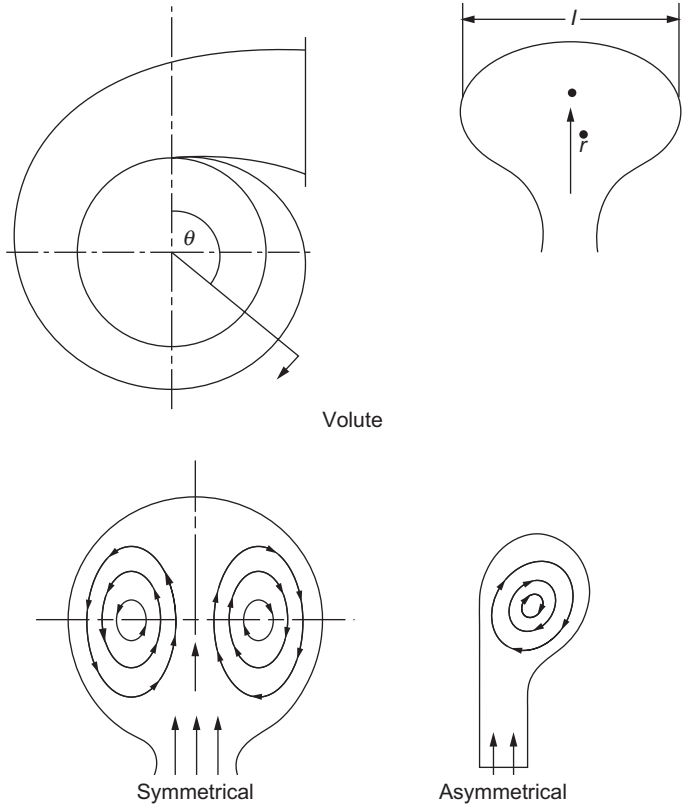


Figure 6-30 Flow patterns in volute.

Centrifugal Compressor Performance

Calculating the performance of a centrifugal compressor in both design and off-design conditions requires a knowledge of various losses encountered in a centrifugal compressor.

The accurate calculation and proper evaluation of losses within a centrifugal compressor is as important as the calculation of the blade-loading parameters. If the proper parameters are not controlled, efficiency decreases. The evaluation of various losses is a combination of experimental results and theory. The losses are divided into two groups: (1) losses encountered in the rotor, and (2) losses encountered in the stator.

A loss is usually expressed as a loss of heat or enthalpy. A convenient way to express them is in a non-dimensional manner with reference to the exit blade speed. The theoretical total head available (q_{tot}) is equal to the head available from the energy equation:

$$q_{\text{th}} = \frac{1}{U_2^2}(U_2 V_{\theta 2} - U_1 V_{\theta 1}) \tag{6-16}$$

plus the head, which is lost because of disc friction (Δq_{df}) and resulting from any recirculation (Δq_{rc}) of the air back into the rotor from the diffuser:

$$q_{\mathrm{tot}} = q_{\mathrm{th}} + \Delta q_{\mathrm{df}} + \Delta q_{\mathrm{rc}} \tag{6-17}$$

The adiabatic head that is actually available at the rotor discharge is equal to the theoretical head minus the heat from the shock in the rotor (Δq_{sh}), the inducer loss (Δq_{in}), the blade loadings (Δq_{bl}), the clearance between the rotor and the shroud (Δq_c), and the viscous losses encountered in the flow passage (Δq_{sf}):

$$q_{\mathrm{ia}} = q_{\mathrm{th}} - \Delta q_{\mathrm{in}} - \Delta q_{\mathrm{sh}} - \Delta q_{\mathrm{bl}} - \Delta q_c - \Delta q_{\mathrm{sf}} \tag{6-18}$$

Therefore, the adiabatic efficiency in the impeller is:

$$\eta_{\mathrm{imp}} = \frac{q_{\mathrm{ia}}}{q_{\mathrm{tot}}} \tag{6-19}$$

The calculation of the overall stage efficiency must also include losses encountered in the diffuser. Thus, the overall actual adiabatic head attained will be the actual adiabatic head of the impeller minus the head losses encountered in the diffuser from wake caused by the impeller blade (Δq_w), the loss of part of the kinetic head at the exit of the diffuser (Δq_{ed}), and the loss of head from frictional forces (Δq_{osf}) encountered in the vaned or vaneless diffuser space:

$$q_{\mathrm{oa}} = q_{\mathrm{ia}} - \Delta q_w - \Delta q_{\mathrm{ed}} - \Delta q_{\mathrm{osf}} \tag{6-20}$$

The overall adiabatic efficiency in an impeller is given by the following relationship:

$$\eta_{\mathrm{ov}} = \frac{q_{\mathrm{oa}}}{q_{\mathrm{tot}}} \tag{6-21}$$

The individual losses can now be computed. These losses are broken up into two categories: (1) losses in the rotor, and (2) losses in the diffuser.

Rotor Losses

Rotor losses are divided into the following categories:

Shock in Rotor Losses

This loss is due to shock occurring at the rotor inlet. The inlet of the rotor blades should be wedge-like to sustain a weak oblique shock, and then gradually expanded to the blade thickness to avoid another shock. If the blades are blunt, a bow shock will result, causing the flow to detach from the blade wall and the loss to be higher.

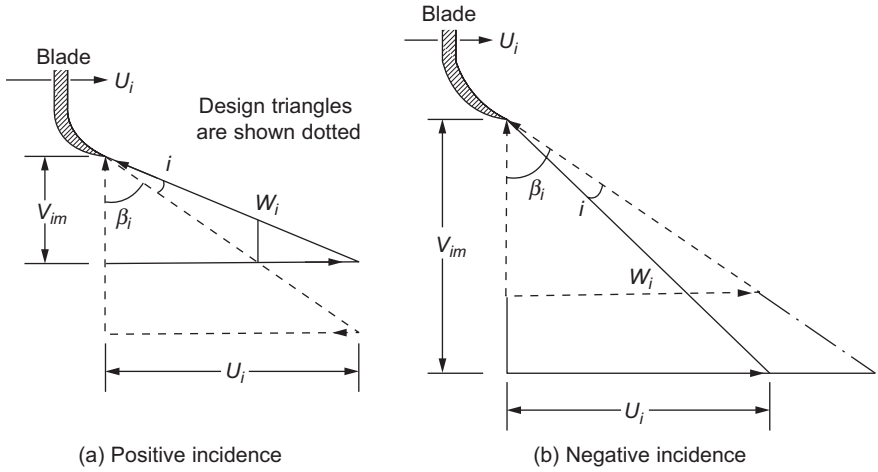


Figure 6-31 Inlet velocity triangle at nonzero incidents.

Incidence Loss

At off-design conditions, flow enters the inducer at an incidence angle that is either positive or negative, as shown in Figure 6-31. A positive incidence angle causes a reduction in flow. Fluid approaching a blade at an incidence angle suffers an instantaneous change of velocity at the blade inlet to comply with the blade inlet angle. Separation of the blade can create a loss associated with this phenomenon.

Disc Friction Loss

This loss results from frictional torque on the back surface of the rotor as seen in Figure 6-32. This loss is the same for a given size disc whether it is used for a radial-inflow compressor or a radial-inflow turbine. Losses in the seals, bearings, and gear box are also lumped in with this loss, and the entire loss can be called an external loss. Unless the gap is of the magnitude of the boundary layer, the effect of the gap size is negligible. The disc friction in a housing is less than that on a free disc due to the existence of a "core," which rotates at half the angular velocity.

Diffusion-Blading Loss

This loss develops because of negative velocity gradients in the boundary layer. Deceleration of the flow increases the boundary layer and gives rise to separation of the flow. The adverse pressure gradient that a compressor normally works against increases the chances of separation and causes significant loss.

Clearance Loss

When a fluid particle has a translatory motion relative to a non-inertial rotating coordinate system, it experiences the Coriolis force. A pressure difference exists between

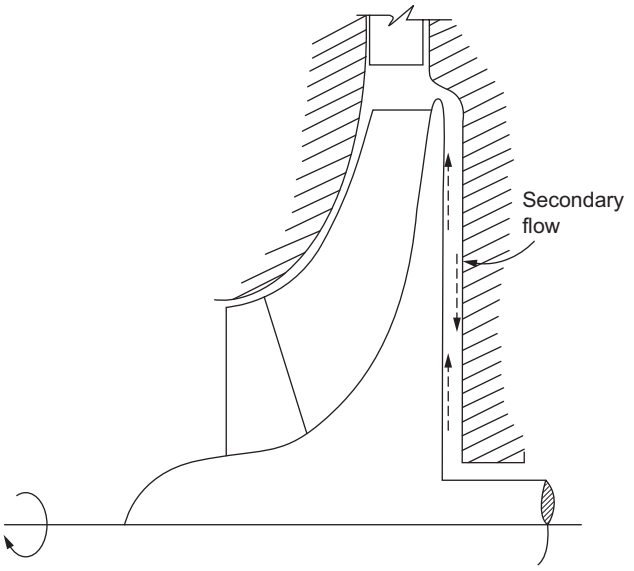


Figure 6-32 Secondary flow at the back of an impeller.

the driving and trailing faces of an impeller blade caused by Coriolis acceleration. The shortest and least resistant path for the fluid to flow and neutralize this pressure differential is provided by the clearance between the rotating impeller and the stationary casing. With shrouded impellers, such a leakage from the pressure side to the suction side of an impeller blade is not possible. Instead, the existence of a pressure gradient in the clearance between the casing and the impeller shrouds, predominant along the direction shown in Figure 6-33, accounts for the clearance loss. Tip seals at the impeller eye can reduce this loss considerably.

This loss may be quite substantial. The leaking flow undergoes a large expansion and contraction caused by temperature variation across the clearance gap that affects both the leaking flow and the stream into which it discharges.

Skin Friction Loss

Skin friction loss is the loss from the shear forces on the impeller wall caused by turbulent friction. This loss is determined by considering the flow as an equivalent circular cross section with a hydraulic diameter. The loss is then computed based on well-known pipe flow pressure loss equations.

Stator Losses

Recirculating Loss

This loss occurs because of backflow into the impeller exit of a compressor and is a direct function of the air exit angle. As the flow through the compressor decreases,

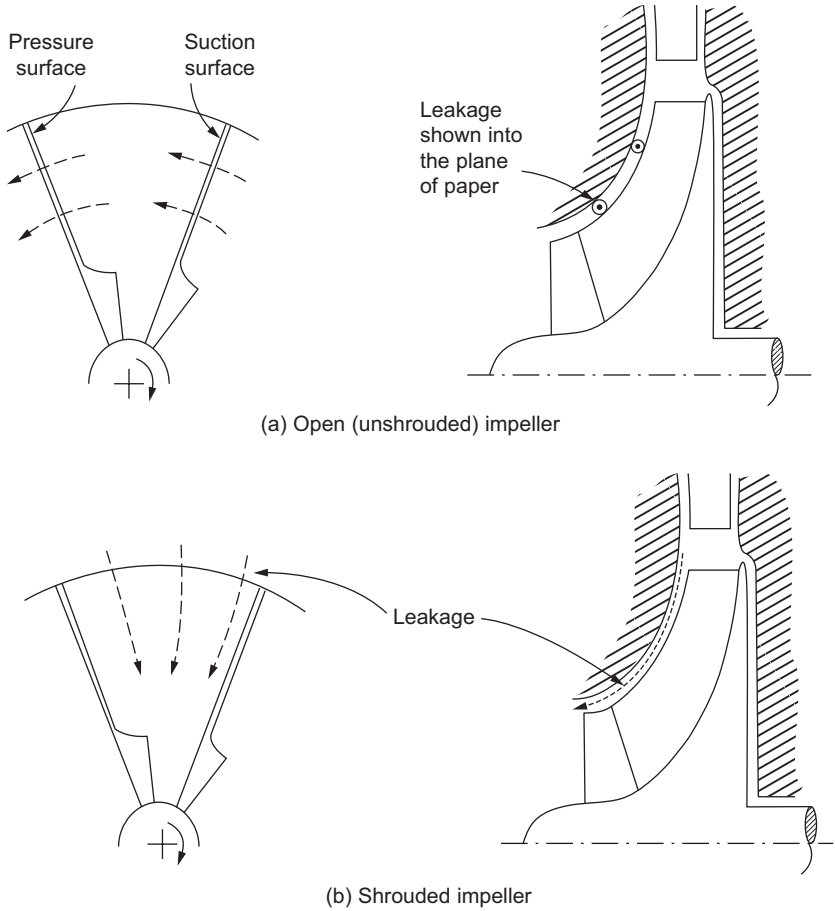


Figure 6-33 Leakage affecting clearance loss.

there is an increase in the absolute flow angle at the exit of the impeller as seen in Figure 6-34. Part of the fluid is recirculated from the diffuser to the impeller, and its energy is returned to the impeller.

Wake-Mixing Loss

This loss is from the impeller blades, and it causes a wake in the vaneless space behind the rotor. It is minimized in a diffuser, which is symmetric around the axis of rotation.

Vaneless Diffuser Loss

This loss is experienced in the vaneless diffuser and results from friction and the absolute flow angle.

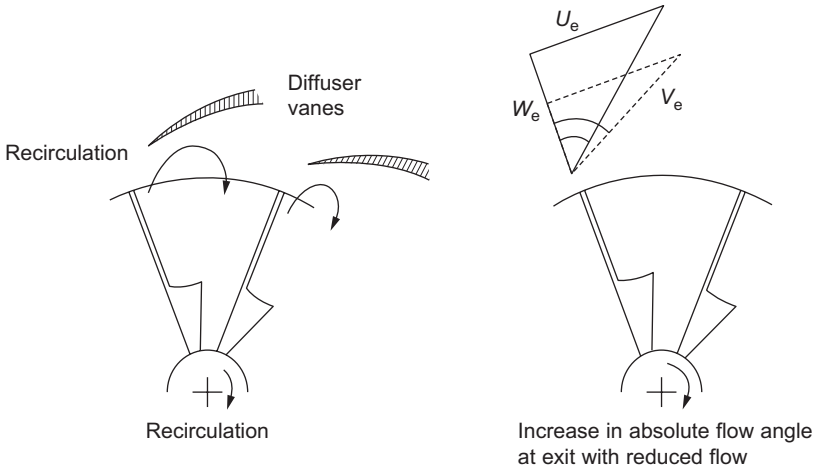


Figure 6-34 Recirculating loss.

Vaned Diffuser Loss

Vaned diffuser losses are based on conical diffuser test results. They are a function of the impeller blade loading and the vaneless space radius ratio. They also take into account the blade incidence angle and skin friction from the vanes.

Exit Loss

The exit loss assumes that one-half of the kinetic energy leaving the vaned diffuser is lost.

Losses are complex phenomena and as discussed here are a function of many factors, including inlet conditions, pressure ratios, blade angles, and flow. Figure 6-35 shows the losses distributed in a typical centrifugal stage of pressure ratio below 2:1 with backward-curved blades. This figure is only a guideline.

Compressor Surge

A plot showing the variation of total pressure ratio across a compressor as a function of the mass flow rate through it at various speeds is known as a performance map. Figure 6-36 shows such a plot.

The actual mass flow rates and speeds are corrected by factors $(\sqrt{\theta}/\delta)$ and $(1/\sqrt{\theta})$, respectively, to account for variation in the inlet conditions of temperature and pressure. The surge line joins the different speed lines where the compressor's operation becomes unstable. A compressor is in "surge" when the main flow through the compressor reverses its direction and flows from the exit to the inlet for short time intervals. If allowed to persist, this unsteady process may result in irreparable damage to the machine. Lines of constant adiabatic efficiency (sometimes called efficiency

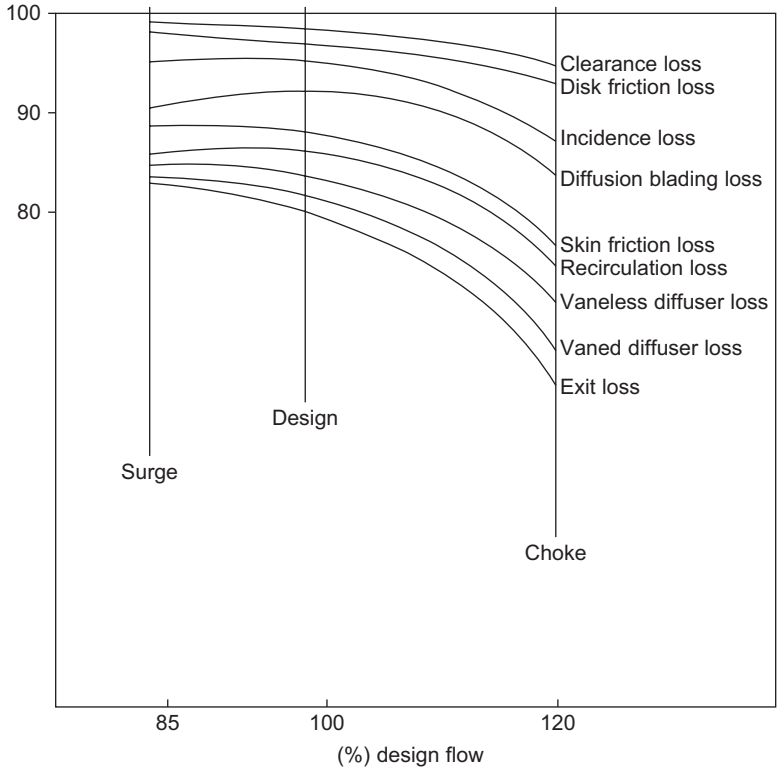


Figure 6-35 Losses in a centrifugal compressor.

islands) are also plotted on the compressor map. A condition known as "choke" or "stone walling" is indicated on the map, showing the maximum mass flow rate possible through the compressor at that operating speed.

Compressor surge is a phenomenon of considerable interest, yet it is not fully understood. It is a form of unstable operation and should be avoided in both design and operation. Surge has been traditionally defined as the lower limit of stable operation in a compressor and involves the reversal of flow. This reversal of flow occurs because of some kind of aerodynamic instability within the system. Usually a part of the compressor is the cause of the aerodynamic instability, although it is possible that the system arrangement could be capable of augmenting this instability. Figure 6-36 shows a typical performance map for a centrifugal compressor with efficiency islands and constant aerodynamic speed lines. The total pressure ratio can be seen to change with flow and speed. Compressors are usually operated at a working line separated by some safety margin from the surge line.

Surge is often symptomized by excessive vibration and an audible sound; however, there have been cases in which surge problems that were not audible have caused failures. Extensive investigations have been conducted on surge. Poor quantitative universality of aerodynamic loading capacities of different diffusers and impellers and an

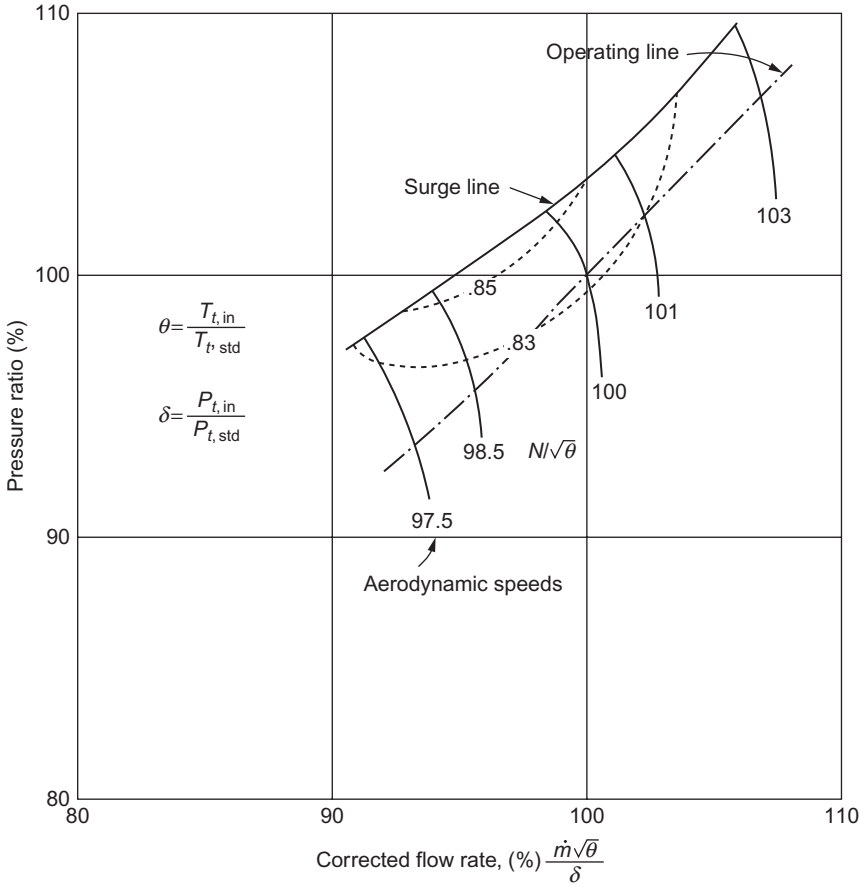


Figure 6-36 Typical compressor performance map.

inexact knowledge of boundary-layer behavior make the exact prediction of flow in turbomachines at the design stage difficult. However, it is quite evident that the underlying cause of surge is aerodynamic stall. The stall may occur in either the impeller or the diffuser.

When the impeller seems to be the cause of surge, the inducer section is where the flow separation begins. A decrease in the mass flow rate, an increase in the rotational speed of the impeller, or both, can cause the compressor to surge.

Surge can be initiated in the diffuser by flow separation occurring at the diffuser entrance. A diffuser usually consists of a vaneless space with the pre-diffuser section before the throat containing the initial portion of the vanes in a vaned diffuser. The vaneless space accepts the velocity generated by the centrifugal impeller and diffuses the flow so that it enters the vaned diffuser passage at a lower velocity, avoiding any shock losses and resultant separation of the flow. When the vaneless diffuser stalls, the flow will not enter the throat. A separation occurs, causing the flow to finally reverse

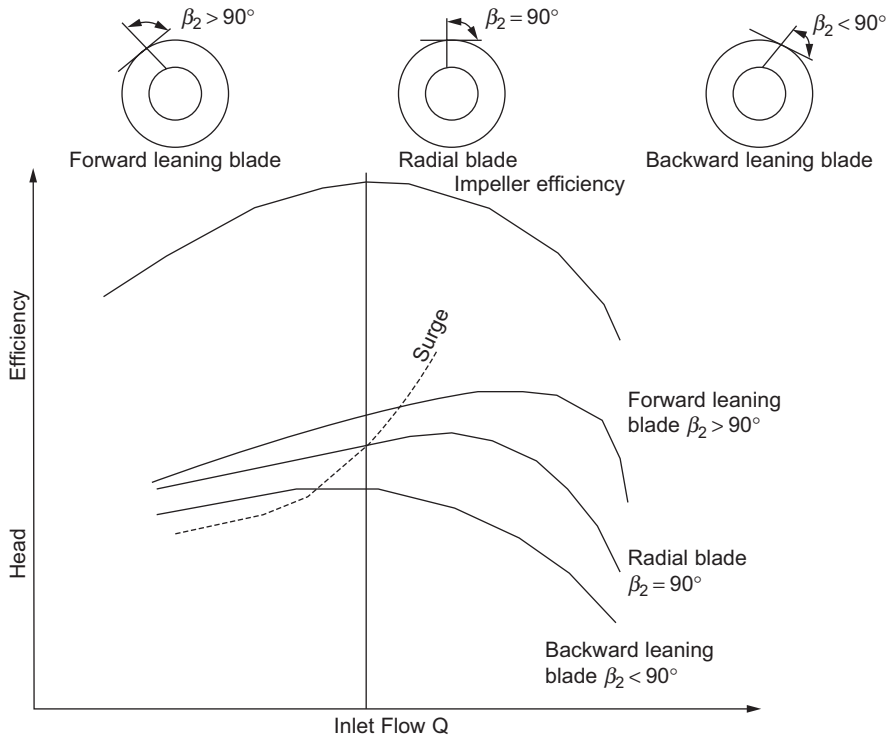


Figure 6-37 Effect of blade angle on stability.

and surge the compressor. Stalling of the vaneless diffuser can be accomplished in two ways – by increasing impeller speed or decreasing the flow rate.

Whether surge is caused by a decrease in flow velocity or an increase in rotational speeds, either the inducer or vaneless diffuser can stall. Which stalls first is difficult to determine, but considerable testing has shown that for a low-pressure-ratio compressor, the surge initiates in the diffuser section. For units with single-stage pressure ratios above 3:1, surge is probably initiated in the inducer.

Most centrifugal compressors have, for the most part, impellers with backward-leaning impeller blades. Figure 6-37 depicts the effects of impeller blade angle on the stable range and shows the variance in steepness of the slope of the head-flow curve.

The three curves are based on the same speed and show actual head. The relationship of an ideal or theoretical head to the inlet flow for different blade angles would be represented by straight lines. For backward-leaning blades, the slope of the line would be negative. The line for radial blades would be horizontal. Forward-leaning blades would have a positively sloped line. For the average petrochemical process plant application, the compressor industry commonly uses a backward-leaning blade with an angle (β_2) of between about 55–75°(or backward leaning angle of 15–35°), because it provides a wider stable range and a steeper slope in the operating range.

This impeller design has proven to be about the best compromise between pressure delivered, efficiency, and stability. Forward-leaning blades are not commonly used in compressor design, since the high exit velocities lead to large diffuser losses. A plant air compressor operating at steady conditions from day to day would not require a wide stable range, but a machine in a processing plant can be the victim of many variables and upsets, so more stability is highly desirable. Actually, the lower curve in Figure 6-37 appears to have a more gentle slope than either the middle or upper curve. This comparison is true in the overall sense, but it must be remembered that the normal operating range lies between 100% flow (Q) and flow at surge, plus a safety margin of, usually, about 10%. The right-hand tail ends of all three curves are not in the operating range. The machine must operate with a suitable margin to the left of where these curves begin their steep descent or tail-off, and in the resultant operating range, the curve for backward-leaning blades is steeper. This steeper curve is desirable for control purposes. Such a curve produces a meaningful change in pressure drop across the orifice for a small change in flow. The blade angle by itself does not tell the overall performance story. The geometry of other components of a stage will contribute significant effects also.

Most centrifugal compressors in service in petroleum or petrochemical processing plants use vaneless diffusers. A vaneless diffuser is generally a simple flow channel with parallel walls and does not have any elements inside to guide the flow.

When the inlet flow to the impeller is reduced while the speed is held constant, there is a decrease in the relative velocity leaving the impeller and the air angle associated with it. As the air angle decreases, the length of the flow path spiral increases. The effect is shown in Figure 6-38.

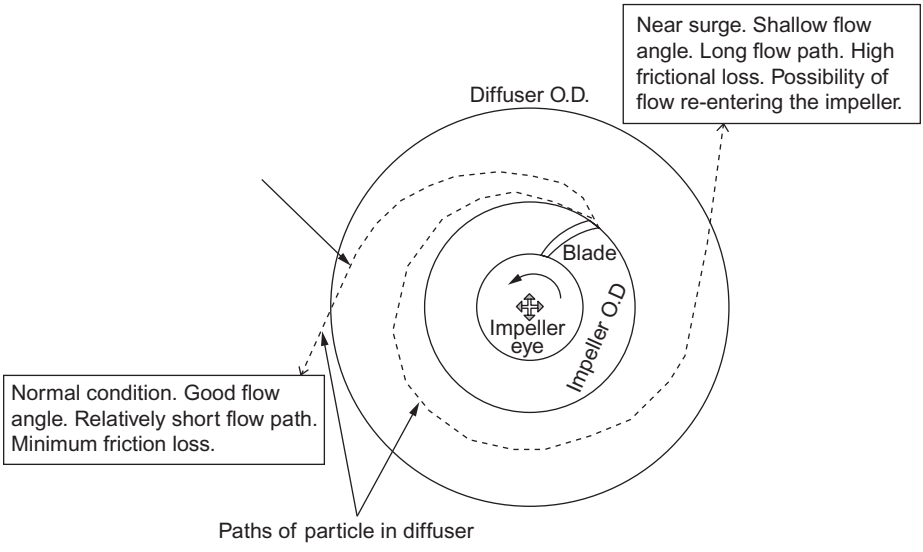


Figure 6-38 Flow trajectory in a vaneless diffuser.

If the flow path is extended enough, the flow momentum at the diffuser walls is excessively dissipated by friction and stall. With this greater loss, the diffuser becomes less efficient and converts a proportionately smaller part of the velocity head to pressure. As this condition progresses, the stage will eventually stall. This could lead to a surge.

Vaned diffusers are used to force the flow to take a shorter, more efficient path through the diffuser. There are many styles of vaned diffusers, with major differences in the types of vanes, vane angles and contouring, and vane spacing. Commonly used vaned diffusers employ wedge-shaped vanes (vane islands) or thin-curved vanes. In high head stages, there can be two to four stages of diffusion. These usually consist of vaneless spaces to decelerate the flow, followed by two or three levels of vaned blades in order to prevent build-up of boundary layer, which causes separation and surging of the compressor. Figure 6-38 indicates the flow pattern in a vaned diffuser. The vaned diffuser can increase the efficiency of a stage by two to four percentage points, but the price for the efficiency gain is generally a narrower operating span on the head-flow curve with respect to both surge and stonewall. Figure 6-39 also shows the effect of off-design flows.

Excessive positive incidence at the leading edge of the diffuser vane occurs when the exit flow is too small at reduced flow, and this condition brings on a stall.

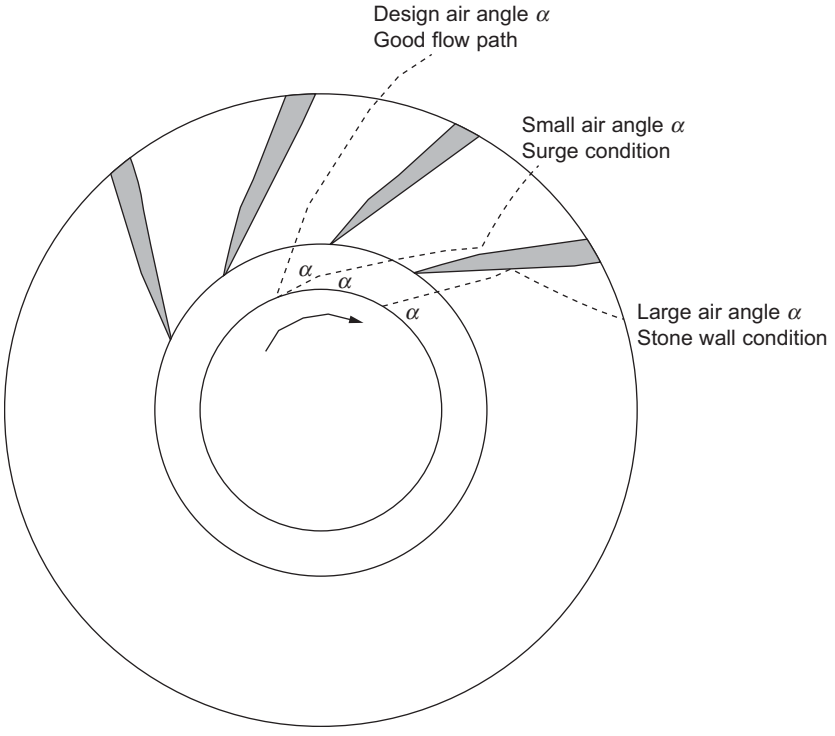


Figure 6-39 Vaned diffuser.

Conversely, as the flow increases beyond the rated point, excessive negative incidence can cause stonewall. Despite its narrowing effect on the usable operating range on the characteristic curve, the vaned diffuser has its application in situations where efficiency is of utmost importance. Although seldom used, movable diffuser vanes or vane islands can be used to alleviate the shock losses at off-design conditions. However, as the adjusting mechanisms required are quite complicated, they generally are applied to only single-stage machines.

It should be noted that the illustrations of the flow paths in Figure 6-37 through 6-39 are somewhat simplistic. Each flow path is indicated by a single streamline. The actual flow field is far more complex, with flow separation and recalculation present. Nevertheless, these figures should help with a practical understanding of the effects of changes in velocity triangles.

Stationary guide vanes direct the flow to the eye of the impeller in an orderly fashion. Depending upon the head requirements of an individual stage, these vanes may direct the flow in the same direction as the rotation or tip speed of the wheel, an action known as positive pre-swirl. This is usually done to reduce the relative Mach number entering the inducer, in order to prevent shock losses. This, however, reduces the head delivered but improves the operating margin. The opposite action is known as counter-rotation or negative pre-swirl. This increases the head delivered but also increases the inlet relative Mach number. Negative pre-swirl is rarely used, since it also decreases the operating range. Sometimes the guide vanes are set at zero degrees of swirl; these vanes are called radial guide vanes. Movable inlet guide vanes are occasionally employed on single-stage machines, or on the first stage of multi-stage compressors driven by electric motors at a constant speed. The guide vane angle can be manually or automatically adjusted while the unit is on stream to accommodate off-design operating requirements. Because of the mechanical complexity of the adjusting mechanism and physical dimensional limitations, the variable feature can only be applied to the first wheel in almost all machine designs. Hence, the effect of changing vane angle is diluted in the stages downstream of the first. Although the flow to the entire machine is successfully adjusted by moving the first stage vanes, the remaining stages must pump the adjusted flow at a fixed guide vane angle.

Incidentally, a butterfly throttle valve in the suction line to the machine will produce nearly the same effects as moving the first stage guide vanes. However, throttling is not as efficient as moving the guide vanes, so that in many cases, the added cost of the movable vane mechanism can be justified by power savings.

Effects of Gas Composition

Figure 6-40 shows the performance of an individual stage at a given speed for three levels of gas molecular weight.

The heavy gas class includes gases such as propane, propylene, and standardized refrigerant mixtures. Air, natural gases, and nitrogen are typical of the medium class. Hydrogen-rich gases found in hydrocarbon processing plants are representative of the light class.

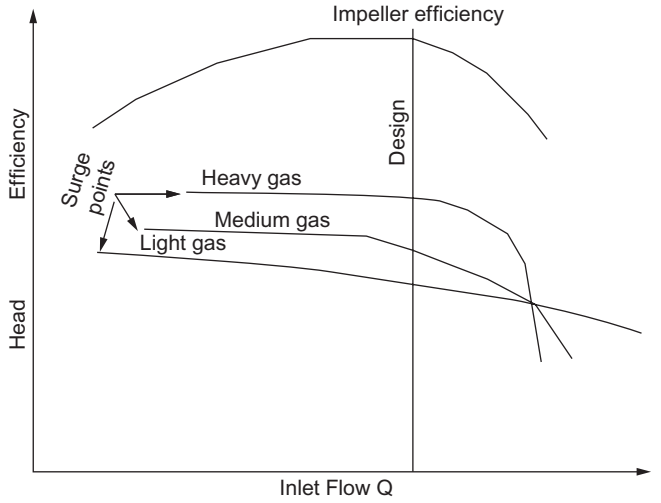


Figure 6-40 Effect of gas composition.

The following observations can be made with respect to the curve for heavy gas:

1. The flow at surge is higher.
2. The stage produces slightly more head than that corresponding to medium gas.
3. The right-hand side of the curve turns downward (approaches stonewall) more rapidly.
4. The curve is flatter in the operating stage.

It is the last point (4) that often presents a problem to the designer of the anti-surge control system. It should be noted that the flatness gets worse as stages are added in series. Since the RTS is small, there is a large change in flow corresponding to a small change in Head. The control system, therefore, must be more responsive. It should be obvious that curves for lighter gases have a more desirable shape.

External Causes and Effects of Surge

The following are some of the usual causes of surge that are not related to machine design:

1. Restriction in suction or discharge of a system.
2. Process changes in pressure, temperature, or gas composition.
3. Internal plugging of the flow passages of the compressor (fouling).
4. Inadvertent loss of speed.
5. Instrument or control valve malfunction.
6. Malfunction of hardware such as variable inlet guide vanes.
7. Operator error.
8. Maldistribution of load in parallel operation of two or more compressors.
9. Improper assembly of a compressor, such as a mispositioned rotor.

The effects of surge can range from a simple lack of performance to serious damage to the machine or to the connected system. Internal damage to labyrinths, diagrams,

the thrust bearing, and the rotor can be experienced. There has been a reported case of a bent rotor caused by violent surge. Surge often excites lateral shaft vibration and could produce torsional damage to such items as couplings and gears. Externally, devastating piping vibration can occur, causing structural damage, shaft misalignment, and failure of fittings and instruments.

The effects of the size and configuration of the connected system, as well as different operating conditions, on the intensity of surge can be astonishing. For example, a compressor system in a test set-up at the factory may exhibit only a mild reaction to surge. At the installation, however, the same compressor with a different connected system may react in a tumultuous manner. Surge can often be recognized by check valve hammering, piping vibration, noise, wriggling of pressure gauges or an ammeter on the driver, or lateral and/or axial vibration of the compressor shaft. Mild cases of surge are sometimes difficult to discern.

Surge Detection and Control

Surge-detection devices may be divided into two groups: (1) static devices, and (2) dynamic devices. To date, static surge-detection devices have been widely used; more research needs to be done before dynamic detection devices are generally used. A dynamic device will probably meet the requirements and hopes of many engineers for a control device that can anticipate stall and surge, and prevent it. Obviously, detection devices must be linked to a control device that can prevent the unstable operation of a compressor.

Static surge-detection devices attempt to avoid stall and surge by the measurement of compressor conditions and ensure that a pre-decided value is not exceeded. When conditions meet or exceed the limit, control action is taken. A typical pressure-oriented anti-surge control system is shown in Figure 6-41. The pressure transmitter monitors the pressure and controls a device, which opens a blowoff valve.

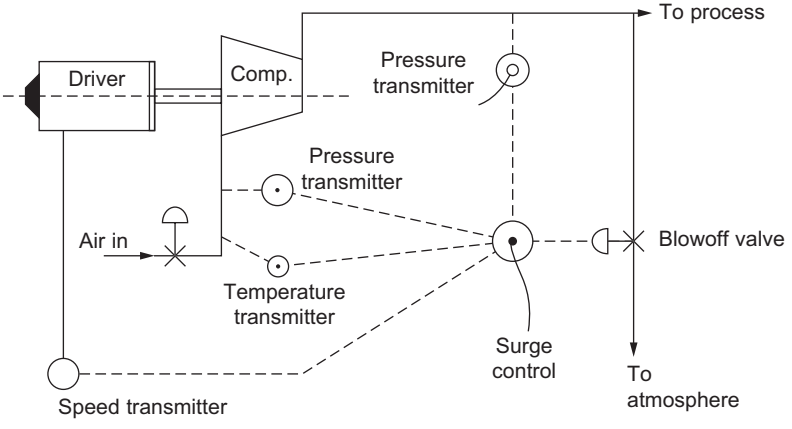


Figure 6-41 Pressure-oriented anti-surge control system.

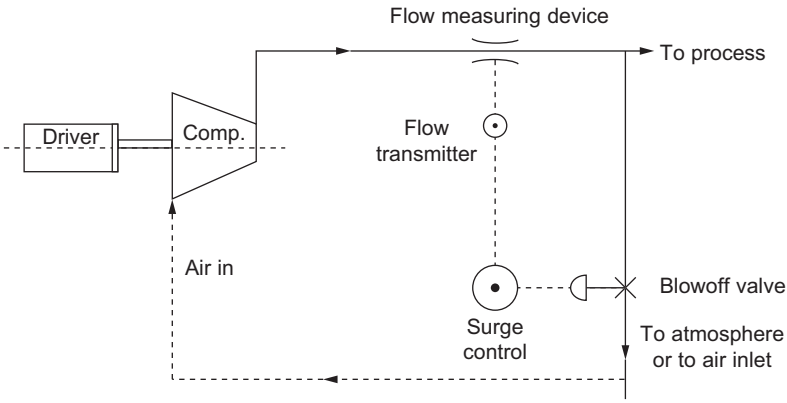


Figure 6-42 Flow-oriented anti-surge control system.

A temperature-sensing device corrects the readings of flow and speed for the effect of temperature. A typical flow-oriented device is also shown in Figure 6-42.

In all static surge-detection devices, the actual phenomenon of flow reversal (surge) is not directly monitored. What is monitored are other conditions related to surge. Control limits are set from past experience and a study of compressor characteristics.

Dynamic surge-detection and control methods are under study. They attempt to detect the *start* of a reversal of flow before it reaches the critical situation of surge. This procedure uses a boundary-layer probe.

The author has a patent for a dynamic surge-detection system, using a boundary-layer probe, presently undergoing field tests. This system consists of specially mounted probes in the compressor to detect boundary-layer flow reversal, as shown in Figure 6-43. The concept assumes that the boundary layer will reverse before the entire unit is in surge. Since the system is measuring the actual onset of surge by monitoring the flow reversal, it is not dependent on the molecular weight of the gas and is not affected by the movement of the surge line.

The use of pressure transducers and casing accelerometers in the exit piping has been instrumental in detecting compressor surge. It has been found that, as the unit approaches surge, the blade passing frequency (number of blades times rpm) and its second and third harmonic become excited. In a limited number of tests it has been noted that when the second harmonic of the blade passing frequency reaches the same order of magnitude as the blade passing frequency, the unit is very close to surge.

Process Centrifugal Compressors

These compressors have impellers with a very low pressure ratio (1.1–1.3) and thus large surge-to-choke margins. Figure 6-44 shows a cross section of a typical multistage centrifugal compressor used in the process industries.

The common method of classifying process-type centrifugal compressors driven by gas turbines is based on the number of impellers and the casing design. Table 6-2

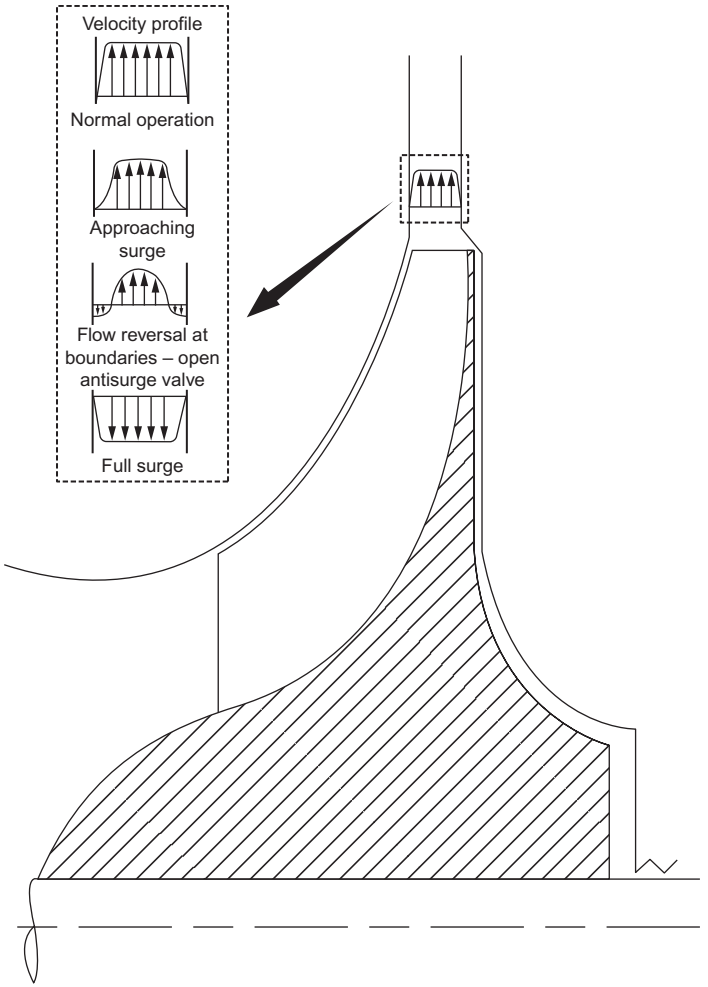


Figure 6-43 Boundary-layer surge prediction technique.

shows three types of centrifugal compressors. For each type of compressor, approximate maximum ratings of pressure, capacity, and brake horsepower are also shown. Sectionalized casing types have impellers, which are usually mounted on the extended motor shaft, and similar sections are bolted together to obtain the desired number of stages. The casing material is either steel or cast iron. These machines require minimum supervision and maintenance, and are quite economic in their operating range. The sectionalized casing design is used extensively in supplying air for combustion in ovens and furnaces.

The horizontally split types have casings split horizontally at the midsection and the top. The bottom halves are bolted and doweled together as shown in Figure 6-45.

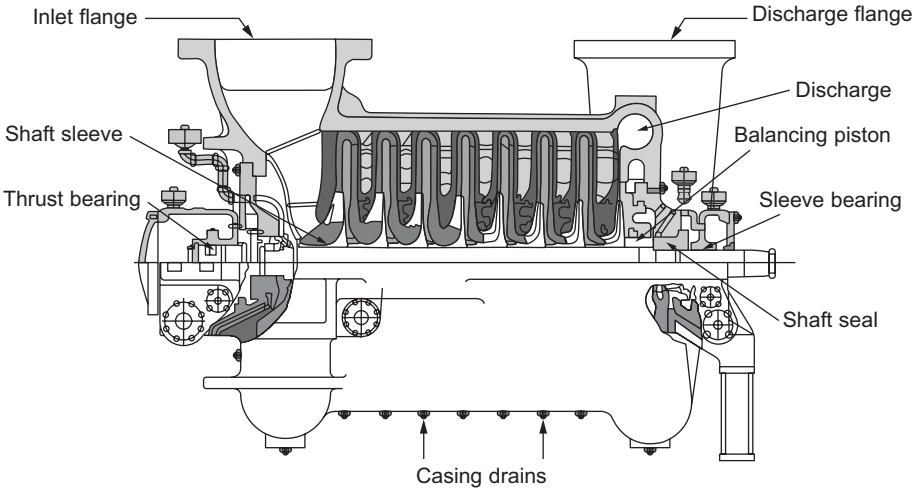


Figure 6-44 Cross section of a typical multi-stage centrifugal compressor (courtesy Elliott Company, Jeannette, PA).

Table 6-2 Industrial Centrifugal Compressor Classification Based on Casing Design

	Approximate Maximum Ratings		
Casing Type	**Approximate Pressure psig (Bar)**	**Approximate Inlet Capacity cfm (cmm)**	**Approximate Power Horsepower (kW)**
1. Sectionalized			
Usually multi-stage	10 (0.7)	20,000 (566)	600 (447)
2. Horizontally split			
Single-stage (double-suction)	15 (1.03)	650,000 (18,406)	10,000 (7,457)
Multi-stage	1,000 (69)	200,000 (5,663)	35,000 (26,100)
3. Vertically split			
Single-stage (single-suction)			
Overhung	30 (2.07)	250,000 (7,079)	10,000 (7,457)
Pipeline	1,200 (82)	25,000 (708)	20,000 (14,914)
Multi-stage	More than 5,500 (379)	20,000 (566)	15,000 (11,185)

This design type is preferred for large multi-stage units. The internal parts such as shaft, impellers, bearings, and seals are readily accessible for inspection and repairs by removing the top half. The casing material is cast iron or cast steel.

There are various types of barrel or centrifugal compressors. Low-pressure types with overhung impellers are used for combustion processes, ventilation, and conveying applications. Multi-stage barrel casings are used for high-pressures in which the horizontally split joint is inadequate. Figure 6-46 shows the barrel compressor in the

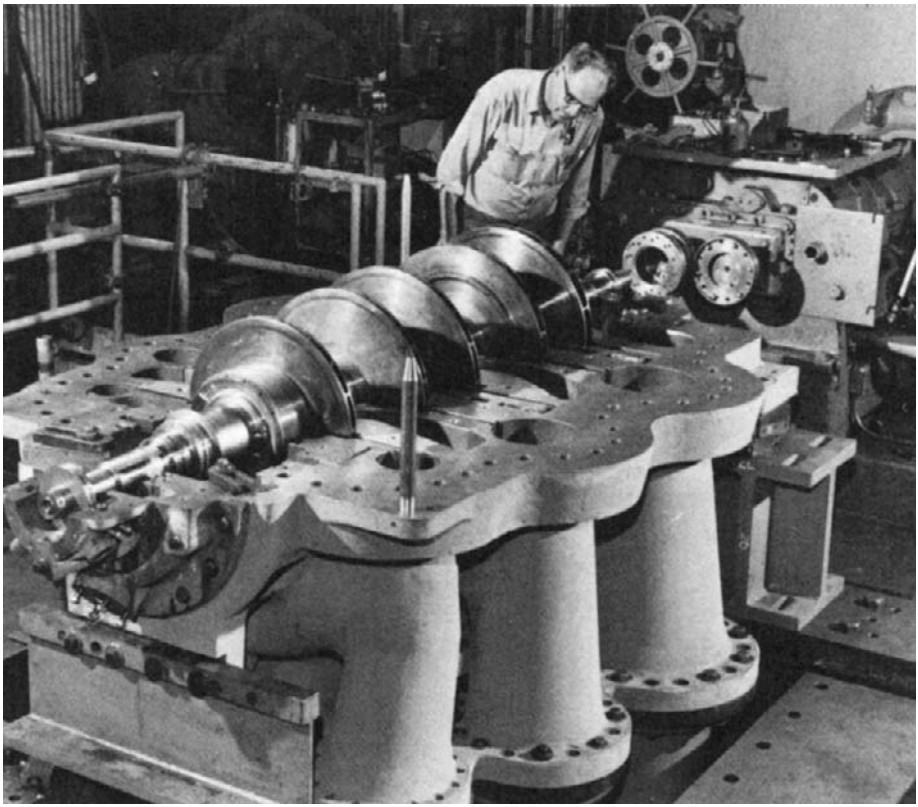


Figure 6-45 Horizontally split centrifugal compressor with shrouded rotors (courtesy of Elliott Company).

background and the inner bundle from the compressor in front. Once the casing is removed from the barrel, it is horizontally split.

Compressor Configuration

To properly design a centrifugal compressor, one must know the operating conditions – the type of gas, its pressure, temperature, and molecular weight. One must also know the corrosive properties of the gas so that proper metallurgical selection can be made. Gas fluctuations due to process instabilities must be pinpointed so that the compressor can operate without surging.

Centrifugal compressors for industrial applications have relatively low pressure ratios per stage. This condition is necessary so that the compressors can have a wide operating range while stress levels are kept at a minimum. Because of the low pressure ratios for each stage, a single machine may have a number of stages in one "barrel" to achieve the desired overall pressure ratio. Figure 6-47 shows some of the many

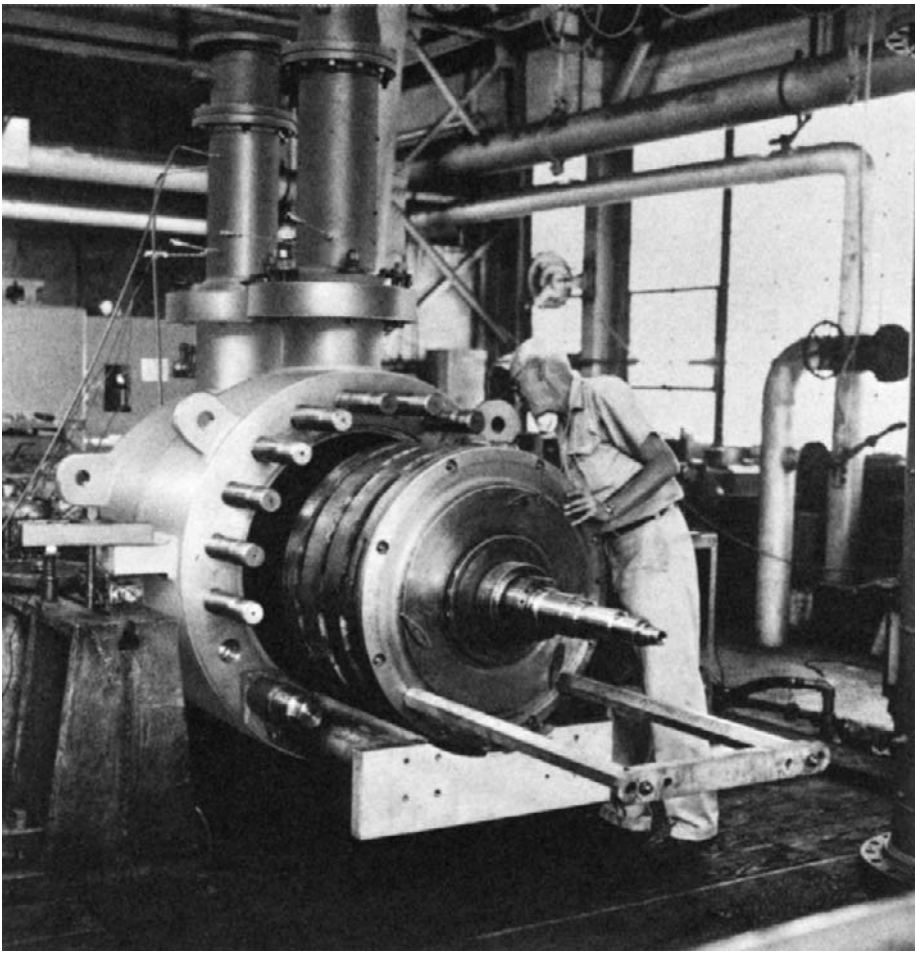


Figure 6-46 Barrel-type compressor (courtesy Elliott Company, Jeannette, PA).

configurations. Some factors to be considered when selecting a configuration to meet plant needs are:

1. Inter-cooling between stages can considerably reduce the power consumed.
2. Back-to-back impellers allow for a balanced rotor thrust and minimize overloading of the thrust bearings.
3. Cold inlet or hot discharge at the middle of the case reduces oil-seal and lubrication problems.
4. Single inlet or single discharge reduces external piping problems.
5. Balance planes that are easily accessible in the field can appreciably reduce field-balancing time.
6. Balance piston with no external leakage will greatly reduce wear on the thrust bearings.

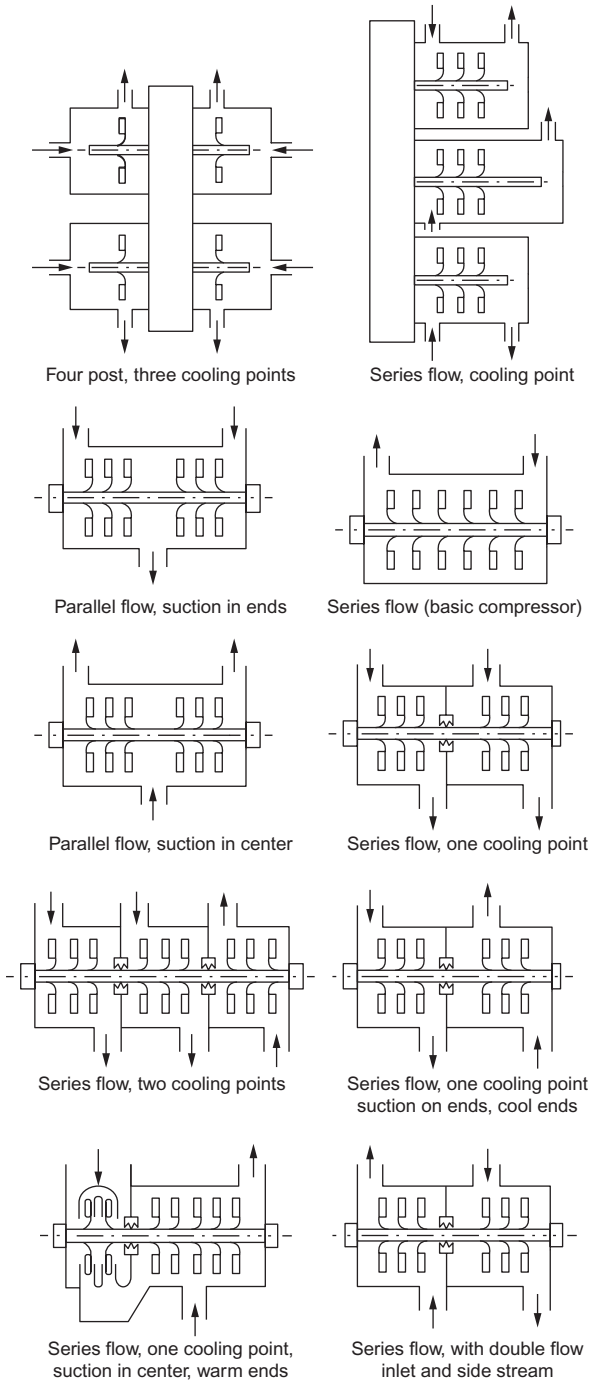


Figure 6-47 Various configurations of centrifugal compressors.

7. Hot and cold sections of the case that are adjacent to each other will reduce thermal gradients and thus reduce case distortion.
8. Horizontally split casings are easier to open for inspection than vertically split ones, reducing maintenance time.
9. Overhung rotors present an easier alignment problem because shaft-end alignment is necessary only at the coupling between the compressor and driver.
10. Smaller, high-pressure compressors that do the same job will reduce foundation problems but will have a greatly reduced operational range.

Impeller Fabrication

Centrifugal-compressor impellers are either shrouded or unshrouded. Open, shrouded impellers that are mainly used in single-stage applications are made by investment casting techniques or by three-dimensional milling. Such impellers are used, in most cases, for the high pressure ratio stages. The shrouded impeller is commonly used in the process compressor because of its low pressure ratio stages. The low tip stresses in this application make it a feasible design. Figure 6-48 shows several fabrication techniques. The most common type of construction is seen in (a) and (b) where the blades are fillet-welded to the hub and shroud. In (b) the welds are full penetration. The disadvantage in this type of construction is the obstruction of the aerodynamic passage. In (c), the blades are partially machined with the covers and then butt-welded

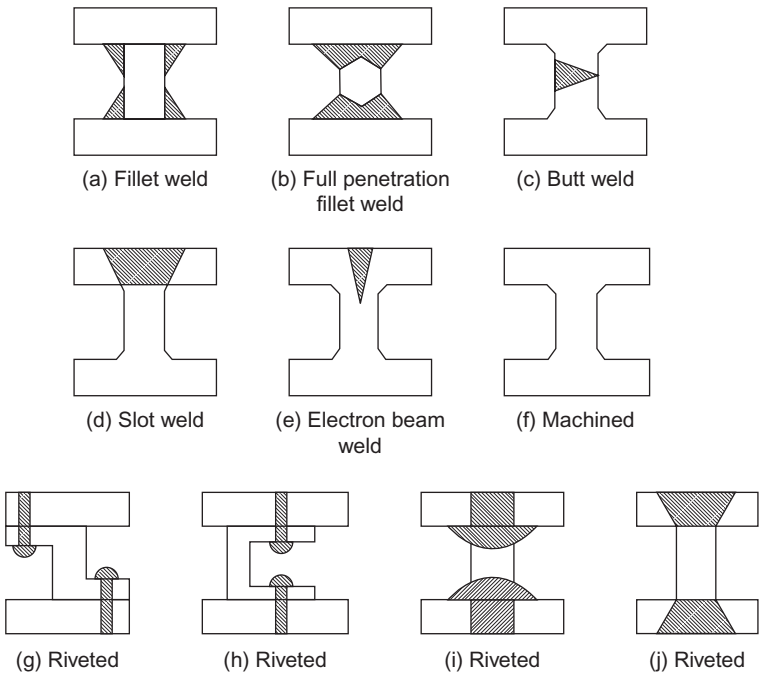


Figure 6-48 Several fabrication techniques for centrifugal impellers.

down the middle. For backward lean-angled blades, this technique has not been very successful, and there has been difficulty in achieving a smooth contour around the leading edge.

(d) illustrates a slot-welding technique and is used where blade-passage height is too small (or the backward lean-angle too high) to permit conventional fillet welding. In (e), an electron-beam technique is still in its infancy, and work needs to be done to perfect it. Its major disadvantage is that electron-beam welds should preferably be stressed in tension but, for the configuration of (e), they are in shear. The configurations of (g) through (j) use rivets. Where the rivet heads protrude into the passage, aerodynamic performance is reduced.

Materials for fabricating these impellers are usually low-alloy steels, such as AISI 4140 or AISI 4340. AISI 4140 is satisfactory for most applications; AISI 4340 is used for larger impellers requiring higher strengths. For corrosive gases, AISI 410 stainless steel (about 12% chromium) is used. Monel K-500 is employed in halogen gas atmospheres and oxygen compressors because of its resistance to sparking. Titanium impellers have been applied to chlorine service. Aluminum-alloy impellers have been used in great numbers, especially at lower temperatures (below 300 °F). With new developments in aluminum alloys, this range is increasing. Aluminum and titanium are sometimes selected because of their low density. This low density can cause a shift in the critical speed of the rotor, which may be advantageous.

Bibliography

Anderson, R.J., Ritter, W.K., and Dildine, D.M., "An Investigation of the Effect of Blade Curvature on Centrifugal Impeller Performance," NACA TN-1313, 1947.

Balje, O.E., "Loss and Flow-Path Studies on Centrifugal Compressors, Parts I and II," ASME Paper Nos 70-GT-1 2-A and 70-GT-1 2-B, June 1970.

Balje, O.E., "A Study of Reynolds Number Effects in Turbomachinery," *Journal of Engineering for Power*, ASME Trans., Vol. 86, Series A, 1964, p. 227.

Bammert, K., and Rautenberg, M., "On the Energy Transfer in Centrifugal Compressors," ASME Paper No. 74-GT-121, 1974.

Boyce, M.P., "A Practical Three-Dimensional Flow Visualization Approach to the Complex Flow Characteristics in a Centrifugal Impeller," ASME Paper No. 66-GT-83, June 1983.

Boyce, M.P., "How to Achieve On-Line Availability of Centrifugal Compressors," *Chemical Weekly*, June 1978, pp. 115–127.

Boyce, M.P., "New Developments in Compressor Aerodynamics," Proceedings of the 1st Turbomachinery Symposium, Texas A&M, October 1972.

Boyce, M.P., "Principles of Operation and Performance Estimation of Centrifugal Compressors," Proceedings of the 22nd Turbomachinery Symposium, Dallas, Texas, September 1993, pp. 161–178.

Boyce, M.P., "Rerating of Centrifugal Compressors-Part I," *Diesel and Gas Turbine Worldwide*, October 1988, pp. 46–50.

Boyce, M.P. "Rerating of Centrifugal Compressors-Part II," *Diesel and Gas Turbine Worldwide*, January–February 1989, pp. 8–20.

Boyce, M.P., and Bale, Y.S., "A New Method for the Calculation of Blade Loadings in Radial-Flow Compressors," ASME Paper No. 71-GT-60, June 1971.

Boyce, M.P., and Bale, Y.S., "Diffusion Loss in a Mixed-Flow Compressor," Intersociety Energy Conversion Engineering Conference, San Diego, Paper No. 729061, September 1972.

Boyce, M.P., and Desai, A.R., "Clearance Loss in a Centrifugal Impeller," Proceedings Of the 8th Intersociety Energy Conversion Engineering Conference, Paper No. 739126, August 1973, p. 638.

Boyce, M.P., and Nishida, A., "Investigation of Flow in Centrifugal Impeller with Tandem Inducer," JSME Paper, Tokyo, Japan, May 1977.

Centrifugal Impeller Performance," NACA TN-1313, 1947.

Coppage, J.E. et al., "Study of Supersonic Radial Compressors for Refrigeration and Pressurization Systems," WADC Technical Report 55-257, Astia Document No. AD110467, 1956.

Dallenback, F., "The Aerodynamic Design and Performance of Centrifugal and Mixed-Flow Compressors," SAE International Congress, January 1961.

Dawes, W., "A Simulation of the Unsteady Interaction of a Centrifugal Impeller with its Vaned Diffuser: Flows Analysis," *ASME Journal of Turbo-machinery*, Vol. 117, 1995, pp. 213–222.

Deniz, S., Greitzer, E. and Cumpsty, N., 1998, "Effects of Inlet Flow Field Conditions on the Performance of Centrifugal Compressor Diffusers Part 2: Straight-Channel Diffuser," ASME Paper No. 98-GT-474.

Domercq, O., and Thomas, R., 1997, "Unsteady Flow Investigation in a Transonic Centrifugal Compressor Stage," AIAA Paper No. 97-2877.

Eckhardt, D., "Instantaneous Measurements in the Jet-Wake Discharge Flow of a Centrifugal Compressor Impeller," ASME Paper No. 74-GT-90.

Filipenco, V., Deniz, S., Johnston, J., Greitzer, E. and Cumpsty, N., 1998, "Effects of Inlet Flow Field Conditions on the Performance of Centrifugal Compressor Diffusers Part 1: Discrete Passage Diffuser," ASME Paper No. 98-GT-473.

Johnston, R., and Dean, R., 1966, "Losses in Vaneless Diffusers of Centrifugal Compressors and Pumps," *ASME Journal of Basic Engineering*, Vol. 88, pp. 49–60.

Katsanis, T., "Use of Arbitrary Quasi-Orthogonals for Calculations Flow Distribution in the Meridional Plane of a Turbomachine," NASA TND-2546, 1964.

Klassen, H.A., "Effect of Inducer Inlet and Diffuser Throat Areas on Performance of a Low-Pressure Ratio Sweptback Centrifugal Compressor," NASA TM X-3148, Lewis Research Center, January 1975.

Owczarek, J.A., *Fundamentals of Gas Dynamics*, International Textbook Company, Scranton, Pennsylvania, 1968, pp. 165–197.

Phillips, M., 1997, "Role of Flow Alignment and Inlet Blockage on Vaned Diffuser Performance," Report No. 229, Gas Turbine Laboratory, Massachusetts Institute of Technology.

Rodgers, C., "Influence of Impeller and Diffuser Characteristic and Matching on Radial Compressor Performance," SAE Preprint 268B, January 1961.

Rodgers, C., 1982, "The Performance of Centrifugal Compressor Channel Diffusers," ASME Paper No. 82-GT-10.

Rodgers, C., and Sapiro, L., "Design Considerations for High-Pressure-Ratio Centrifugal Compressors," ASME Paper No. 73-GT-31, 1972.

Schlichting, H., *Boundary Layer Theory*, 4th edition, McGraw-Hill Book Co., New York, 1962, pp. 547–550.

Senoo, Y., and Nakase, Y., "An Analysis of Flow Through a Mixed Flow Impeller," ASME Paper No. 71-GT-2 1972.

Senoo, Y., and Nakase, Y., "A Blade Theory of an Impeller with an Arbitrary Surface of Revolution," ASME Paper No. 71-GT-17, 1972.

Shouman, A.R., and Anderson J.R., "The Use of Compressor-Inlet pre-whirl for the Control of Small Gas Turbines," *Journal of Engineering for Power*, Trans ASME, Vol. 86, Series A, 1964, pp. 136–140.

Stahler, A.F., "The Slip Factor of a Radial Bladed Centrifugal Compressor," ASME Paper No. 64-GTP-1.

Stanitz, J.D., "Two-Dimensional Compressible Flow in Conical Mixed-Flow Compressors," NACA TN-1744, 1948.

Stanitz, J.D., and Prian, V.D., "A Rapid Approximate Method for Determining Velocity Distribution on Impeller Blades of Centrifugal Compressors," NACA TN-2421, 1951.

Stodola, A., *Steam and Gas Turbines*, McGraw-Hill Book Co., New York, 1927.

Wiesner, F.J., "A Review of Slip Factors for Centrifugal Impellers," *Journal of Engineering for Power*, ASME Trans., October 1967, p. 558.

Woodhouse, H., "Inlet Conditions of Centrifugal Compressors for Aircraft Engine Superchargers and Gas Turbines," *J. Inst. Aeron, Sc*., Vol. 15, 1948, p. 403.

Wu, C.H., "A General Theory of Three-Dimensional Flow in Subsonic and Supersonic Turbomachines of Axial, Radial, and Mixed-Flow Type," NACA TN-2604, 1952.

Copyrighted Materials
Copyright © 2012 Elsevier Retrieved from www.knovel.com

7 Axial-Flow Compressors

Introduction

The compressors in most gas turbine applications, especially units over 5 MW, use axial-flow compressors. An axial-flow compressor is one in which the flow enters the compressor in an axial direction (parallel with the axis of rotation), and exits from the gas turbine also in an axial direction. The axial-flow compressor compresses its working fluid by first accelerating the fluid and then diffusing it to obtain a pressure increase. The fluid is accelerated by a row of rotating airfoils (blades) called the rotor, and then diffused in a row of stationary blades (the stator). The diffusion in the stator converts the velocity increase gained in the rotor to a pressure increase. A compressor consists of several stages. A combination of a rotor followed by a stator make up a stage in a compressor. An additional row of pitch variable blades, known as Inlet Guide Vanes (IGV), are frequently used at the compressor inlet to ensue that air enters the first-stage rotors at the desired flow angle. These vanes are also pitch variable, and thus can be adjusted to the varying flow requirements of the engine. In addition to the stators, another diffuser at the exit of the compressor consisting of another set of vanes, often known as the Exit Guide Vanes (EGV), further diffuses the fluid and controls its velocity entering the combustors.

In an axial-flow compressor, air passes from one stage to the next, each stage raising the pressure slightly. By producing low-pressure increases on the order of 1.1:1 to 1.4:1, very high efficiencies can be obtained as seen in Table 7-1. The use of multiple stages permits overall pressure increases of up to 40:1 in some aerospace applications, and a pressure ratio of 30:1 in some industrial applications.

The last 20 years has seen a large growth in gas turbine technology. The growth is spearheaded by the increase in compressor pressure ratio, advanced combustion techniques, the growth of materials technology, new coatings, and new cooling schemes. The increase in gas turbine efficiency is dependent on two basic parameters:

- Increase in pressure ratio
- Increase in firing temperature

It also should be remembered that the gas turbine axial-flow compressor consumes between 55–65% of the power produced by the turbine section of the gas turbine.

The aerospace engines have been the leaders in most of the technology in the gas turbine. The design criteria for these engines was high reliability, high performance,

Gas Turbine Engineering Handbook, Fourth Edition. DOI: 10.1016/B978-0-12-383842-1.00007-X
Copyright © 2012 Elsevier Inc. All rights reserved.

Table 7-1 Axial Flow Compressor Characteristics

Type of Application	Type of Flow	Inlet Relative Velocity Mach Number	Pressure Ratio per Stage	Efficiency per Stage
Industrial	Subsonic	0.4–0.8	1.05–1.2	88–92%
Aerospace	Transonic	0.7–1.1	1.15–1.6	80–85%
Research	Supersonic	1.05–2.5	1.8–2.2	75–85%

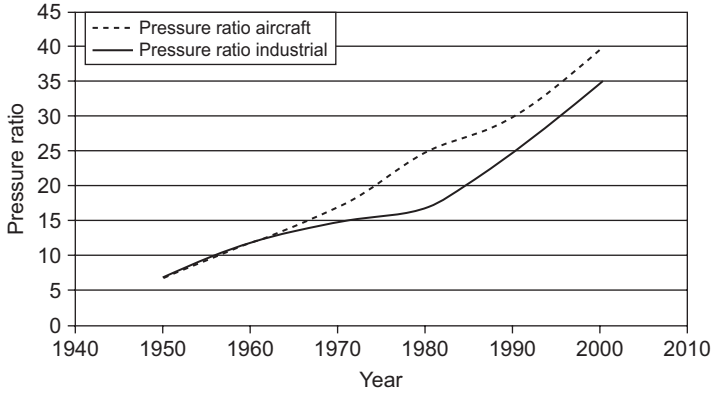


Figure 7-1 Development of pressure ratio over the past 50 years.

with many starts and flexible operation throughout the flight envelope. The engine life of about 3,500 hours between major overhauls was considered good. The aerospace engine performance has always been rated primarily on its thrust/weight ratio. Increase in engine thrust/weight ratio is achieved by the development of high aspect ratio blades in the compressor as well as optimizing the pressure ratio and firing temperature of the turbine for maximum work output per unit flow.

The industrial gas turbine has always emphasized long life, and this conservative approach has resulted in the industrial gas turbine in many aspects giving up high performance for rugged operation. The industrial gas turbine has been conservative in the pressure ratio and the firing temperatures. This has all changed in the last 10 years; spurred on by the introduction of the aero-derivative gas turbine the industrial gas turbine has improved its performance dramatically in all operational aspects. This has resulted in dramatically reducing the performance gap between these two types of gas turbines.

Figure 7-1 indicates the growth of the pressure ratio in a gas turbine over the past 50 years. The growth of both the pressure ratio and firing temperature parallel each other, as both growths are necessary to achieving the increase in thermal efficiency in gas turbines. The axial-flow compressor in most advanced gas turbines is a multistage compressor consisting of 17 to 22 stages with an exceedingly high pressure ratio. It is not uncommon to have pressure ratios in industrial gas turbines in the 17 to 20:1 range, with some units having pressure ratios in the 30:1 range. Figure 7-2 shows a multistage high-pressure axial-flow compressor rotor. The low-pressure increase per stage also

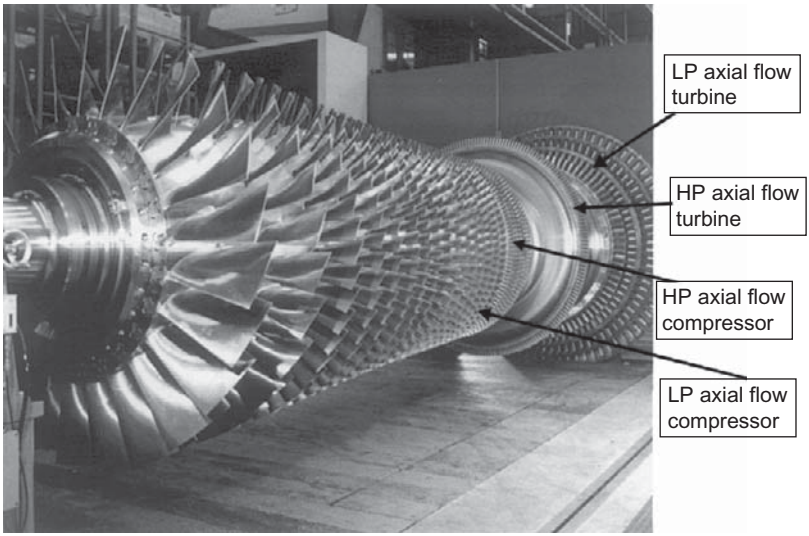


Figure 7-2 Axial-flow compressor rotor.



Figure 7-3 Axial-flow compressor stators located in the casing.

simplifies calculations in the preliminary design of the compressor by justifying the air as incompressible in its flow through the stage.

Figure 7-3, shows the stators, the stationary blades that are in between each rotor blade and cause the flow to be diffused (increase in the static pressure, reduction of the

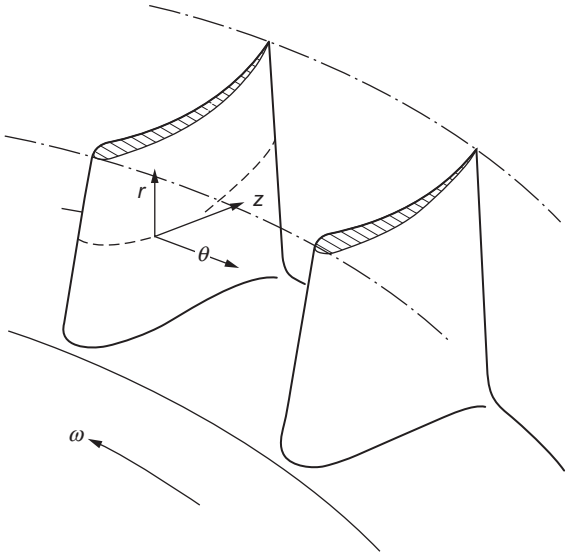


Figure 7-4 Coordinate system for axial-flow compressor.

absolute velocity). The early stages of the stators in Figure 7-3 are adjustable, as can be noted by their circular base. The adjustable stators allow the stator to be positioned to the correct flow angle leaving the blades as the air mass flow varies with load and inlet temperature.

As with other types of rotating machinery, an axial compressor can be described as a cylindrical coordinate system. The z axis is along the axis of rotation, which is along the running length of the compressor shaft; the radius r is measured outward from the shaft; and the angle of rotation θ is the angle turned by the blades in Figure 7-4. This coordinate system will be used throughout this discussion of axial-flow compressors.

Figure 7-5 shows the pressure, velocity, and total temperature (enthalpy) variation for flow through several stages of an axial compressor. As indicated in Figure 7-3, the length of the blades and the annulus area (the area between the shaft and shroud) decreases throughout the length of the compressor. This reduction in flow area compensates for the increase in fluid density as it is compressed, permitting a constant axial velocity. In most preliminary calculations used in the design of a compressor, the average blade height is used as the blade height for the stage.

Blade and Cascade Nomenclature

Since airfoils are employed in accelerating and diffusing the air in a compressor, much of the theory and research concerning the flow in axial compressors is based on studies of isolated airfoils. The nomenclature and methods of describing compressor blade shapes are almost identical to that of aircraft wings. Research in axial compressors

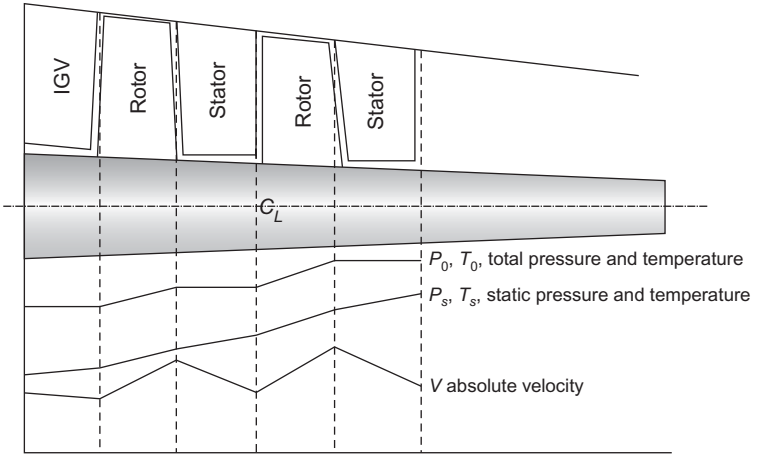


Figure 7-5 Variation of temperature (enthalpy), velocity, and pressure through an axial-flow compressor.

involves the intereffect of one blade on the other, thus several blades are placed in a row to simulate a compressor rotor or stator. Such a row is called a *cascade.* When discussing blades, all angles that describe the blade and its orientation are measured with respect to the shaft (z axis) of the compressor.

The airfoils are curved, convex on one side and concave on the other, with the rotor rotating toward the concave side. The concave side is called the pressure side of the blade, and the convex side is called the suction side of the blade. The chordline of an airfoil is a straight line drawn from the leading edge to the trailing edge of the airfoil, and the chord is the length of the chordline as seen in Figure 7-6. The camberline is a line drawn halfway between the two surfaces, and the distance between the camberline and the chordline is the camber of the blade. The camber angle θ is the turning angle of the camberline. The blade shape is described by specifying the ratio of the chord to the camber at some particular length on the chordline, measured from the leading edge. The aspect ratio AR is the ratio of the blade length to the chord length. The term "hub-to-tip ratio" is used frequently instead of aspect ratio. The aspect ratio becomes important when three-dimensional flow characteristics are discussed. The aspect ratio is established when the mass flow characteristics are discussed. The aspect ratio is established when the mass flow and axial velocity have been determined.

The pitch S_b of a cascade is the distance between blades, usually measured between the camberlines at the leading or trailing edges of the blades. The ratio of the chord length to the pitch is the solidity σ of the cascade. The solidity measures the relative interference effects of one blade with another. If the solidity is on the order of 0.5 to 0.7, the single or isolated airfoil test data, from which there are a profusion of shapes to choose, can be applied with considerable accuracy. The same methods can be applied up to a solidity of about 1.0 but with reduced accuracy. When the solidity is on the order of 1.0 to 1.5, cascade data are necessary. For solidity in excess of 1.5, the channel theory can be employed. The majority of present designs are in the cascade region.

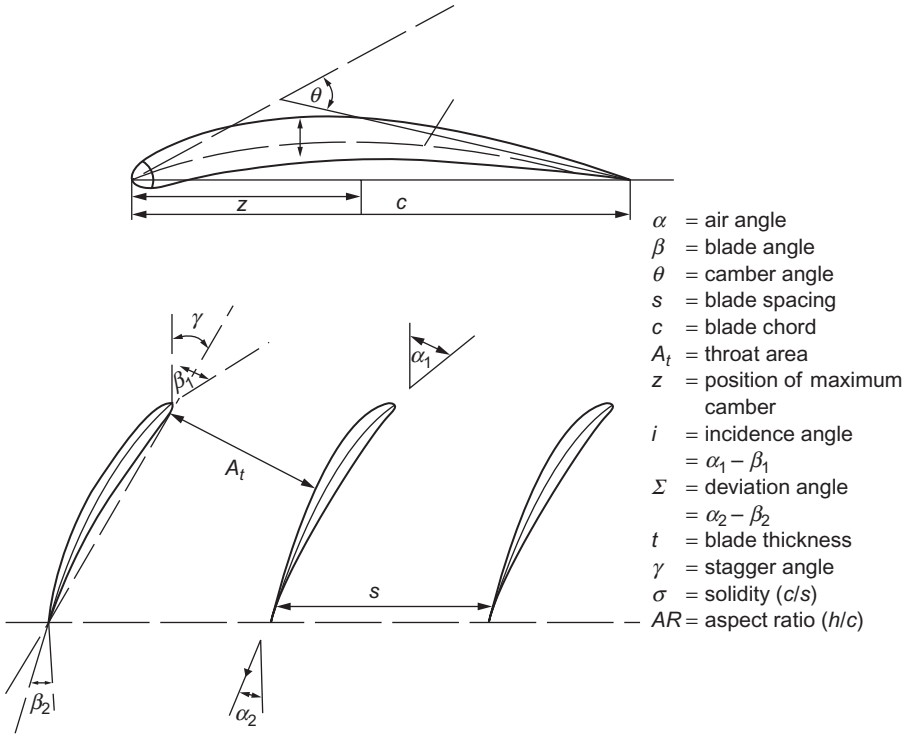


Figure 7-6 Blade profile nomenclature.

The blade inlet angle β_1 is the angle formed by a line drawn tangent to the forward end of the camberline and the axis of the compressor. The blade outlet angle β_2 is the angle of a line drawn tangent to the rear of the camberline. Subtracting β_2 from β_1 gives the blade camber angle. The angle that the chordline makes with the axis of the compressor is γ, the setting or stagger angle of the blade. High-aspect ratio blades often are pretwisted so that at full operational speed the centrifugal forces acting on the blades will untwist the blades to the designed aerodynamic angle. The pretwist angle at the tip for blades with *AR* ratios of about four is between two and four degrees.

The air inlet angle α_1, the angle at which incoming air approaches the blade, is different from β_1. The difference between these two angles is the incidence angle i. The angle of attack α is the angle between the inlet air direction and the blade chord. As the air is turned by the blade, it offers resistance to turning and leaves the blade at an angle greater than β_2. The angle at which the air does leave the blade is the air outlet angle α_2. The difference between β_2 and α_2 is the deviation angle δ. The air turning angle is the difference between α_1 and α_2 and is sometimes called the deflection angle.

The original work by NACA and NASA is the basis on which most modern axial-flow compressors are designed. Under NACA, a large number of blade profiles were

tested. The test data on these blade profiles is published. The cascade data conducted by NACA is the most extensive work of its kind. In most commercial axial-flow compressors in gas turbines built before 1990 NACA 65 series blades are used. These blades are usually specified by notation similar to the following: 65-(18) 10. This notation means that the blade has a lift coefficient of 1.8, a profile shape 65, and a thickness/chord ratio of 10%. The lift coefficient can be directly related to the blade camber angle by the following relationship for 65 series blades:

$$\Theta \approx 25 C_L \tag{7-1}$$

The new advanced compressor rotors have fewer blades with higher loadings, and the blades are thinner, larger, and are designed using advanced radial equilibrium theory, which create three-dimensional and controlled diffusion-shaped airfoils (3D/CDA), with smaller clearances and higher loading per stage.

Elementary Airfoil Theory

When a single airfoil is parallel to the velocity of a flowing gas, the air flows over the airfoil as shown in Figure 7-7 (a). The air divides around the body, separates at the leading edge, and joins again at the trailing edge of the body. The main stream itself suffers no permanent deflection from the presence of the airfoil. Forces are applied to

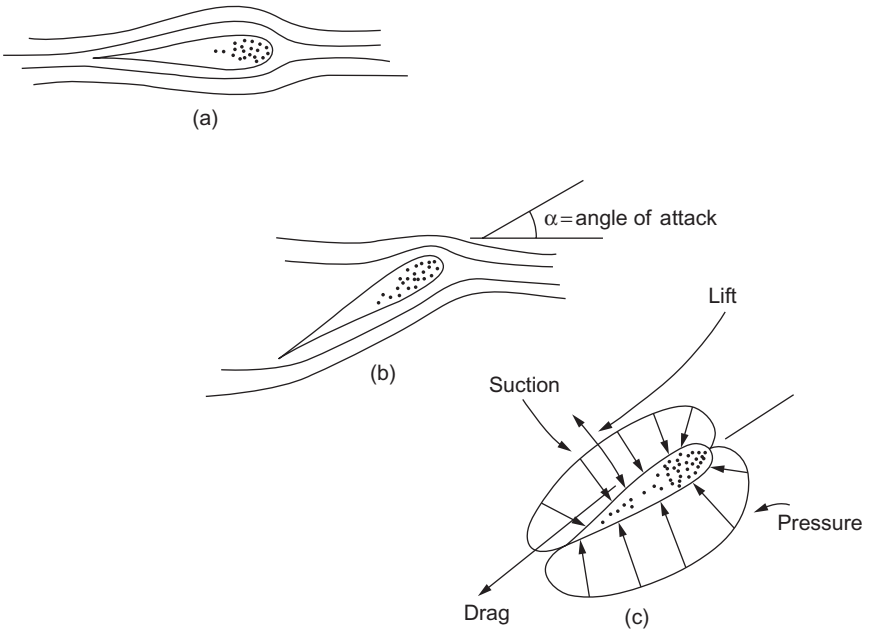


Figure 7-7 Flow around an airfoil at various angles of attack.

the foil by the local distribution of the steam and the friction of the fluid on the surface. If the airfoil is well designed, the flow is streamlined with little or no turbulence.

If the airfoil is set at the angle of attack to the air stream (as in Figure 7-7 (b)), a greater disturbance is created by its presence, and the streamline pattern will change. The air undergoes a local deflection, though at some distance ahead of and behind the body the flow is still parallel and uniform. The upstream disturbance is minor compared to the downstream disturbance. The local deflection of the air stream can, by Newton's laws, be created only if the blade exerts a force on the air; thus, the reaction of the air must produce an equal and opposite force on the airfoil. The presence of the airfoil has changed the local pressure distribution and, by the Bernoulli equation, the local velocities. Examination of the streamlines about the body shows that over the top of the airfoil, the lines approach each other, indicating an increase of velocity and a reduction in static pressure. On the underside of the airfoil, the action separates the streamlines, resulting in a static pressure increase.

Measurement of the pressure at various points on the surface of the airfoil will reveal a pressure distribution as shown in Figure 7-7 (c). The vectorial sum of these pressures will produce some resultant force acting on the blade. This resultant force can be resolved into a lift component L at right angles to the undisturbed air stream, and a drag component D, moving the airfoil in the direction of flow motion. This resultant force is assumed to act through a definite point located in the airfoil so that the behavior will be the same as if all the individual components were acting simultaneously.

By experimentation, it is possible to measure the lift and drag forces for all values of airflow velocity, angles of incidence, and various airfoil shapes. Thus, for any one airfoil the acting forces can be represented as shown in Figure 7-8 (a). Using such observed values, it is possible to define relations between the forces:

$$D = C_D A \rho V^2/2 \tag{7-2}$$

$$\mathrm{L} = C_L A \rho V^2/2 \tag{7-3}$$

where

L = lift force
D = drag force
C_L = lift coefficient
C_D = drag coefficient
A = surface area
ρ = fluid density
V = fluid velocity

Two coefficients have been defined, C_L and C_D, relating velocity, density, area, and lift or drag forces. These coefficients can be calculated from wind-tunnel tests and plotted as shown in Figure 7-8 (b) versus the angle of attack for any desired section. These curves can then be employed in all future predictions involving this particular foil shape.

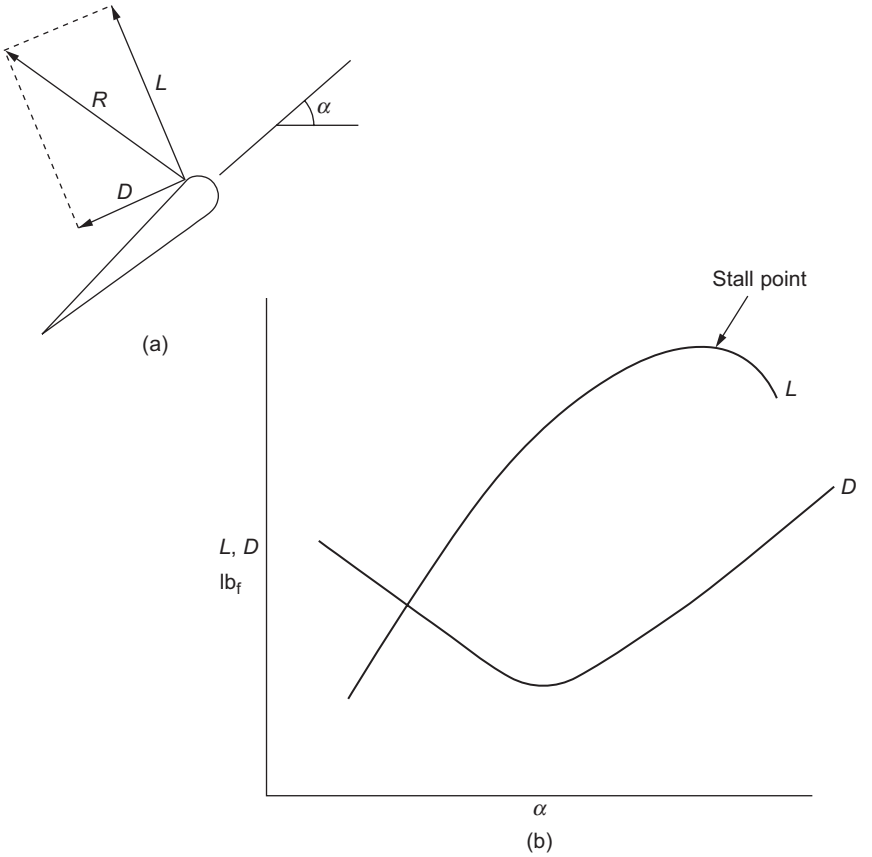


Figure 7-8 Characteristics of the lift and drag forces on an airfoil.

Examination of Figure 7-8 reveals that there is an angle of attack that produces the highest lift force and lift coefficient. If this angle is exceeded, the airfoil "stalls" and the drag force increases rapidly. As this maximum angle is approached, a great percentage of the energy available is lost in overcoming friction, and a reduction in efficiency occurs. Thus, there is a point, usually before the maximum lift coefficient is reached, at which the most economical operation occurs as measured by effective lift for a given energy supply.

Laminar-Flow Airfoils

Just before and during World War II, much attention was given to laminar-flow airfoils. These airfoils are designed so that the lowest pressure on the surface occurs as far back as possible. The reason for this design is that the stability of the laminar boundary layer increases when the external flow is accelerated (in the flow with a pressure

drop), and the stability decreases when the flow is directed against increasing pressure. A considerable reduction in skin friction is obtained by extending the laminar region in this way, provided that the surface is sufficiently smooth.

A disadvantage of this type of airfoil is that the transition from laminar to turbulent flow moves forward suddenly at small angles of attack. This sudden movement results in a narrow low-drag bucket, which means that the drag at moderate-to-large attack angles is much greater than an ordinary airfoil for the same attack angle as seen in Figure 7-9. This phenomenon can be attributed to the minimum pressure point moving forward; therefore, the point of transition between laminar and turbulent flow is also advanced toward the nose as shown in Figure 7-10. The more an airfoil is surrounded by turbulent airflow, the greater its skin friction.

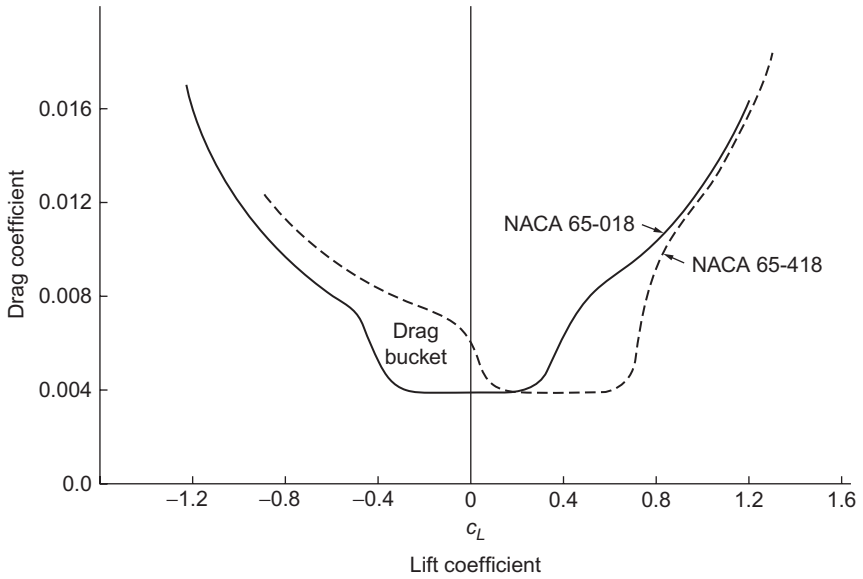


Figure 7-9 NACA measurements of drag coefficients for two laminar airfoils.

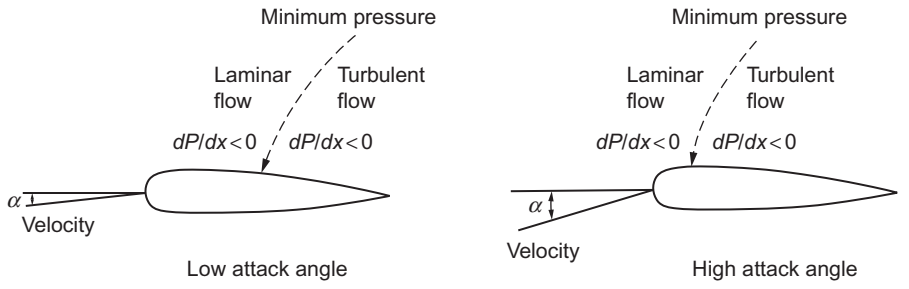


Figure 7-10 Laminar flow airfoils.

Energy Increase

In an axial-flow compressor air passes from one stage to the next with each stage raising the pressure and temperature slightly. By producing low-pressure increases on the order of 1.1:1 to 1.4:1, very high efficiencies can be obtained. The use of multiple stages permits overall pressure increases up to 40:1. Figure 7-5 shows the pressure, velocity, and total temperature (enthalpy) variation for flow through several stages of an axial-flow compressor. It is important to note here that the changes in the total conditions for pressure, temperature, and enthalpy occur only in the rotating component where energy is inputted to the system. As seen also in Figure 7-5, the length of the blades and the annulus area, which is the area between the shaft and shroud, decreases throughout the length of the compressor. This reduction in flow area compensates for the increase in fluid density as it is compressed, permitting a constant axial velocity. In most preliminary calculations used in the design of a compressor, the average blade height is used as the blade height for the stage.

The rule of thumb for a multiple stage gas turbine compressor would be that the energy rise per stage would be constant, rather than the commonly held perception that the pressure rise per stage is constant. The energy rise per stage can be written as:

$$\Delta H = \frac{[H_2 - H_1]}{N_S} \tag{7-4}$$

where

$H_1,\ H_2 =$ Total inlet and exit enthalpy BTU/$\text{lb}_{\text{m (kJ/kg)}}$

$N_s =$ number of stages

Assuming that the gas is thermally and calorically perfect (c_p and γ are constant) Equation 7-1 can be rewritten as:

$$\Delta T_{stage} = \frac{T_{in}\left[\left(\frac{P_2}{P_1}\right)^{\frac{\gamma-1}{\gamma}} - 1\right]}{N_s} \tag{7-5}$$

where

$T_{in} =$ Total inlet temperature (°F, °C)

$P_1,\ P_2 =$ Total inlet and exit pressure (psia, Bar)

$\gamma =$ Ratio of specific heats ($\gamma = 1.4$ @ 60°F (15°F))

Velocity Triangles

As started earlier, an axial-flow compressor operates on the principle of putting work into the incoming air by acceleration and diffusion. Air enters the rotor as shown in Figure 7-11 with an absolute velocity (V) and an angle α_1, which combines vectorally

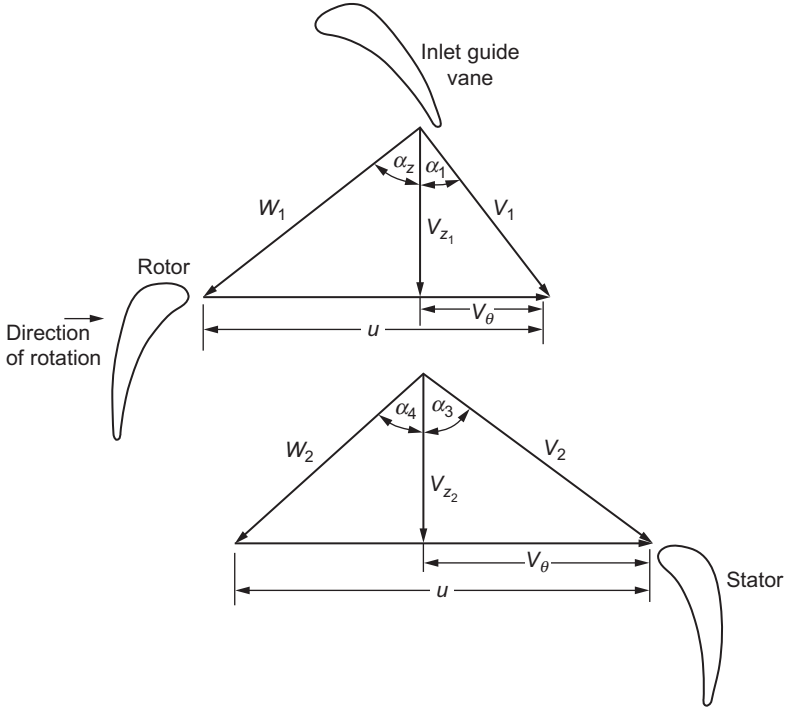


Figure 7-11 Typical velocity triangles for an axial-flow compressor.

with the tangential velocity of the blade (U) to produce the resultant relative velocity W_1 at an angle α_2. Air flowing through the passages formed by the rotor blades is given a relative velocity W_2 at an angle α_4, which is less than α_2 because of the camber of the blades. Note that W_2 is less than W_1, resulting from an increase in the passage width as the blades become thinner toward the trailing edges. Therefore, some diffusion will take place in the rotor section of the stage. The combination of the relative exit velocity and blade velocity produce an absolute velocity V_2 at the exit of the rotor. The air then passes through the stator, where it is turned through an angle so that the air is directed into the rotor of the next stage with a minimum incidence angle. The air entering the rotor has an axial component at an absolute velocity V_{Z1} and a tangential component $V_{\theta 1}$.

Applying the Euler turbine equation:

$$H = \frac{1}{g_c}[U_1 V_{\theta 1} - U_2 V_{\theta 2}] \tag{7-6}$$

and assuming that the blade speeds at the inlet and exit of the compressor are the same, and noting the relationships:

$$V_{\theta 1} = V_{z1} \tan \alpha_1 \tag{7-7}$$

$$V_{\theta 2} = V_{z2} \tan \alpha_3 \tag{7-8}$$

Equation (7-1) can be written:

$$H = \frac{U_1}{g_c}\left(V_{z1}\tan\,\alpha_2 - V_{z2}\tan\,\alpha_3\right) \tag{7-9}$$

Assuming that the axial component (V_Z) remains unchanged:

$$H = \frac{UV_z}{g_c}\left(\tan\,\alpha_1 - \tan\,\alpha_3\right) \tag{7-10}$$

The previous relationship is in terms of the absolute inlet and outlet velocities. By rewriting the previous equation in terms of the blade angles or the relative air angles, the following relationship is obtained:

$$U_1 - U_2 = V_{Z1}\tan\,\alpha_1 = V_{Z1}\tan\,\alpha_2 = V_{Z2}\tan\,\alpha_3 + V_{Z2}\tan\,\alpha_4$$

therefore:

$$H = \frac{UV_z}{g_c}\left(\tan\,\alpha_2 - \tan\,\alpha_4\right) \tag{7-11}$$

The previous relationship can be written to calculate the pressure rise in the stage:

$$c_p T_{in}\left[\left(\frac{P_2}{P_1}\right)^{\frac{\gamma-1}{\gamma}} - 1\right] = \frac{UV_2}{g_c}\left(\tan\,\alpha_2 - \tan\,\alpha_4\right) \tag{7-12}$$

which can be rewritten

$$\frac{P_2}{P_1} = \left\{\frac{UV_z}{g_c c_p T_{in}}\left[\tan\,\alpha_2 - \tan\,\alpha_4\right] + 1\right\}^{\frac{\gamma}{\gamma+1}} \tag{7-13}$$

The velocity triangles can be joined together in several different ways to help visualize the changes in velocity. One of the methods is to simply join these triangles into a connected series. The two triangles can also be joined and superimposed using the sides formed by either the axial velocity, which is assumed to remain constant as shown in Figure 7-12 (a), or the blade speed as a common side, assuming that the inlet and exit blade speed are the same as shown in Figure 7-12 (b).

Degree of Reaction

The degree of reaction in an axial-flow compressor is defined as the ratio of the change of static head in the rotor to the head generated in the stage:

$$R = \frac{H_{rotor}}{H_{stage}} \tag{7-14}$$

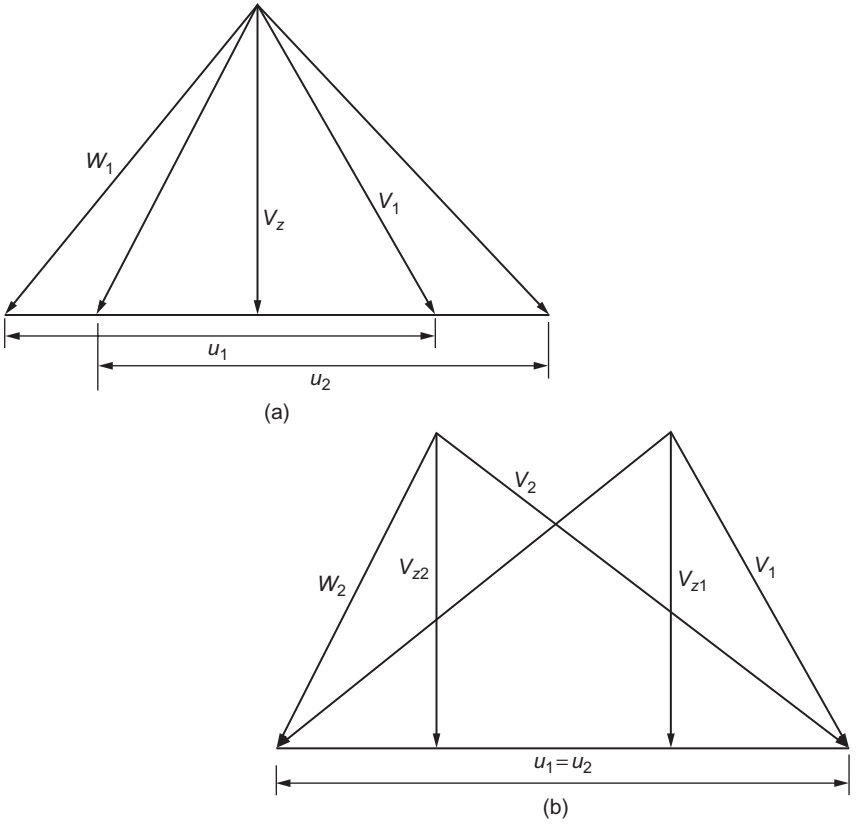


Figure 7-12 Velocity triangles.

The change in static head in the rotor is equal to the change in relative kinetic energy:

$$H_r = \frac{1}{2g_c}\left({W_1}^2 - {W_2}^2\right) \tag{7-15}$$

and

$${W_1}^2 = {V_{z1}}^2 + (V_{z1}\tan\,\alpha_2)^2 \tag{7-16}$$

$${W_2}^2 = {V_{z2}}^2 + (V_{z2}\tan\,\alpha_4)^2 \tag{7-17}$$

therefore

$$H_r = \frac{V_z^2}{2g_c}\left(\tan\,^2\alpha_2 - \tan\,^2\alpha_4\right)$$

Thus, the reaction of the stage can be written:

$$R = \frac{V_z}{2U} \frac{\tan^2 \alpha_2 - \tan^2 \alpha_4}{\tan \alpha_2 - \tan \alpha_4} \tag{7-18}$$

Simplifying the previous equation:

$$R = \frac{V_z}{2U} (\tan \alpha_2 + \tan \alpha_4) \tag{7-19}$$

In the symmetrical axial-flow stage the blades and their orientation in the rotor and stator are reflected images of each other. Thus, in a symmetrical axial-flow stage where $V_1 = W_2$ and $V_2 = W_1$ as seen in Figure 7-13, the head delivered in velocity as given by the Euler turbine equation can be expressed as:

$$H = \frac{1}{2g_c} \left[\left({U_1}^2 - {U_2}^2 \right) + \left({V_1}^2 - {V_2}^2 \right) + \left({W_2}^2 - {W_1}^2 \right) \right] \tag{7-20}$$

$$H = \frac{1}{2g_c} \left({W_2}^2 - {W_1}^2 \right) \tag{7-21}$$

The reaction for a symmetrical stage is 50%.

The 50% reaction stage is widely used, since an adverse pressure rise on either the rotor or stator blade surfaces is minimized for a given stage pressure rise. When designing a compressor with this type of blading, the first stage must be preceded by inlet guide vanes to provide pre-whirl and the correct velocity entrance angle to the first-stage rotor. With a high tangential velocity component maintained by each

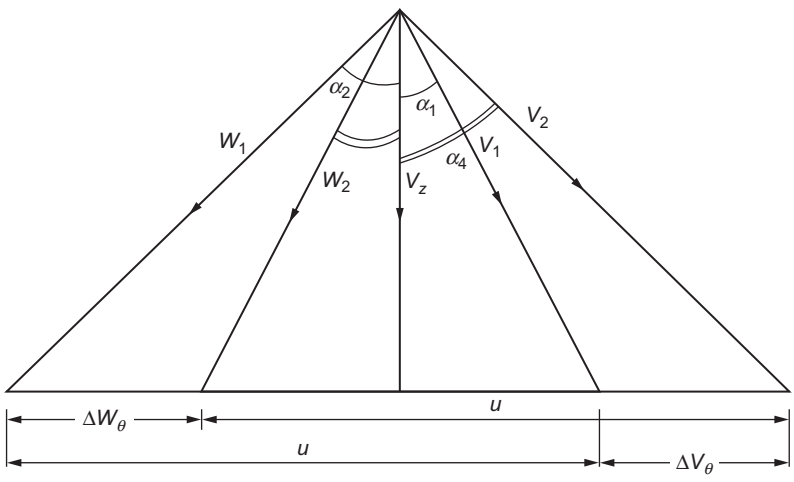


Figure 7-13 Symmetrical velocity triangle for 50% reaction stage.

succeeding stationary row, the magnitude of W_1 is decreased. Thus, higher blade speeds and axial-velocity components are possible without exceeding the limiting value of 0.70 to 0.75 for the inlet Mach number. Higher blade speeds result in compressors of smaller diameter and less weight.

Another advantage of the symmetrical stage comes from the equality of static pressure rises in the stationary and moving blades, resulting in a maximum static pressure rise for the stage. Therefore, a given pressure ratio can be achieved with a minimum number of stages, a factor in the lightness of this type of compressor. The serious disadvantage of the symmetrical stage is the high exit loss resulting from the high axial-velocity component. However, the advantages are of such importance in aircraft applications that the symmetrical compressor is normally used. In stationary applications the symmetrical compressor is not normally used; where weight and frontal area are of lesser importance, one of the other stage types is used.

The term *asymmetrical stage* is applied to stages with reaction other than 50%. The axial-inflow stage is a special case of an asymmetrical stage where the entering absolute velocity is in the axial direction. The moving blades impart whirl to the velocity of the leaving flow, which is removed by the following stator. From this whirl and the velocity diagram as seen in Figure 7-14, the major part of the stage pressure rise occurs in the moving row of blades with the degree of reaction varying from 60% to 90%. The stage is designed for constant energy transfer and axial velocity at all radii so that the vortex flow condition is maintained in the space between blade rows.

The advantage of a stage with greater than 50% reaction is the low exit loss resulting from lower axial velocity and blade speeds. Because of the small static pressure rise in the stationary blades, certain simplifications can be introduced such as constant-section stationary blades and the elimination of interstage seals. Higher actual efficiencies have been achieved in this stage type than with the symmetrical stage, primarily because of the reduced exit loss. The disadvantages result from a low static pressure rise in the stationary blades that necessitates a greater number of stages to achieve a given pressure ratio and create a heavy compressor. The lower axial velocities and blade speed, necessary to keep within inlet Mach number limitations, result in large diameters. In stationary applications where the increased weight and frontal area are not of great importance, this type is used frequently to take advantage of the higher efficiency.

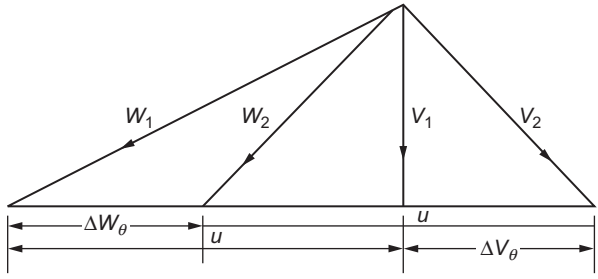


Figure 7-14 Axial-entry stage velocity diagram.

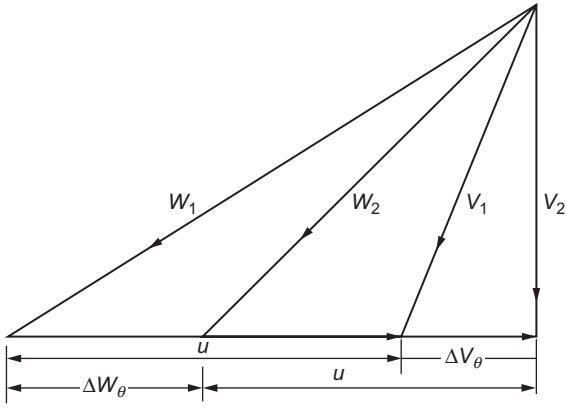


Figure 7-15 Axial-outflow stage velocity diagram.

The axial-outflow stage diagram in Figure 7-15 shows another special case of the asymmetrical stage with reaction greater than 50%. With this type of design, the absolute exit velocity is in an axial direction, and all the static pressure rise occurs in the rotor. A static pressure decrease occurs in the stator so that the degree of reaction is in excess of 100%. The advantages of this stage type are low axial velocity and blade speeds, resulting in the lowest possible exit loss. This design produces a heavy machine of many stages and of large diameter. To keep within the allowable limit of the inlet Mach number, extremely low values must be accepted for the blade velocity and axial velocity. The axial-outflow stage is capable of the highest actual efficiency because of the extremely low exit loss and the beneficial effects of designing for free vortex flow. This compressor type is particularly well suited for closed-cycle plants where smaller quantities of air are introduced to the compressor at an elevated static pressure.

Although a reaction of less than 50% is possible, such a design results in high inlet Mach numbers to the stator row, causing high losses. The maximum total divergence of the stators should be limited to approximately 20° to avoid excessive turbulence. Combining the high inlet for the limiting divergence angles produces a long stator, thereby producing a longer compressor.

Radial Equilibrium

The flow in an axial-flow compressor is defined by the continuity, momentum, and energy equations. A complete solution to these equations is not possible because of the complexity of the flow in an axial-flow compressor. Considerable work has been done on the effects of radial flow in an axial-flow compressor. The first simplification used considers the flow axisymmetrically. This simplification implies that the flow at each radial and axial station within the blade row can be represented by an average circumferential condition. Another simplification considers the radial component

of the velocity as much smaller than the axial component velocity, so it can be neglected.

For the low-pressure compressor with a low-aspect ratio, and where the effect of streamline curvature is not significant, the simple radial equilibrium change of the radial velocity component along the axial direction is zero ($\partial V_{rad}/\partial_Z = 0$) and the change of entropy in the radial direction is zero negligible (a s/$\partial r = 0$). The meridional velocity (V_m) is equal to the axial velocity (V_Z), since the effect of steamline curvature is not significant. The radial gradient of the static pressure can be given:

$$\frac{\partial P}{\partial r} = \rho \frac{V_\theta^2}{r} \tag{7-22}$$

Using the simple radial equilibrium equation, the computation of the axial velocity distribution can be calculated. The accuracy of the techniques depends on how linear $V_{\theta/r}^2$ is with the radius.

The assumption is valid for low-performance compressors, but it does not hold well for the high-aspect ratio, highly loaded stages where the effects of streamline curvature become significant. The radial acceleration of the meridional velocity and the pressure gradient in the radial direction must be considered. The radial gradient of static pressure for the highly curved streamline can be written:

$$\frac{\partial P}{\partial r} = \rho \left(\frac{V_\theta^2}{r} \pm \frac{V_m^2 \cos \in}{r_c} \right) \tag{7-23}$$

where $\in$ is the angle of the streamline curvature with respect to the axial direction and r_c is the radius of curvature.

To determine the radius of curvature and the streamline slope accurately, the configuration of the streamline through the blade row must be known. The streamline configuration is a function of the annular passage area, the camber and thickness distribution of the blade, and the flow angles at the inlet and outlet of the blade. Since there is no simple way to calculate the effects of all the parameters, the techniques used to evaluate these radial accelerations are empirical. By using iterative solutions, a relationship can be obtained. The effect of high-radial acceleration with high-aspect ratios can be negated by tapering the tip of the compressor inward so that the hub curvature is reduced.

Diffusion Factor

The diffusion factor first defined by Lieblien is a blade-loading criterion:

$$D = \left(1 - \frac{W_2}{W_1}\right) + \frac{V_{\theta 1} - V_{\theta 2}}{2\sigma W_1} \tag{7-24}$$

The diffusion factor should be less than 0.4 for the rotor tip and less than 0.6 for the rotor hub and the stator. The distribution of the diffusion factor throughout the

compressor is not properly defined. However, the efficiency is less in the later stages due to distortions of the radial velocity distributions in the blade rows. Experimental results indicate that even though efficiency is less in the later stages, as long as the diffusion loading limits are not exceeded, the stage efficiencies remain relatively high.

The Incidence Rule

For low-speed airfoil design, the region of low-loss operation is generally flat, and it is difficult to establish the precise value of the incidence angle that corresponds to the minimum loss as seen in Figure 7-16. Since the curves are generally symmetrical, the minimum loss location was established at the middle of the low-loss range. The range is defined as the change in incidence angle corresponding to a rise in the loss coefficient equal to the minimum value.

The following method for calculation of the incidence angle is applicable to cambered airfoils. Work by NASA on the various cascades is the basis for the technique. The incidence angle is a function of the blade camber, which is an indirect function of the air-turning angle:

$$i = ki_0 + m\varsigma + \delta_m \tag{7-25}$$

where i_0 is the incidence angle for zero camber, and m is the slow of the incidence angle variation with the air-turning angle (ξ). The zero-camber incidence angle is defined as a function of inlet air angle and solidity as seen in Figure 7-17 and the value of m is given as a function of the inlet air angle and the solidity as seen in Figure 7-18.

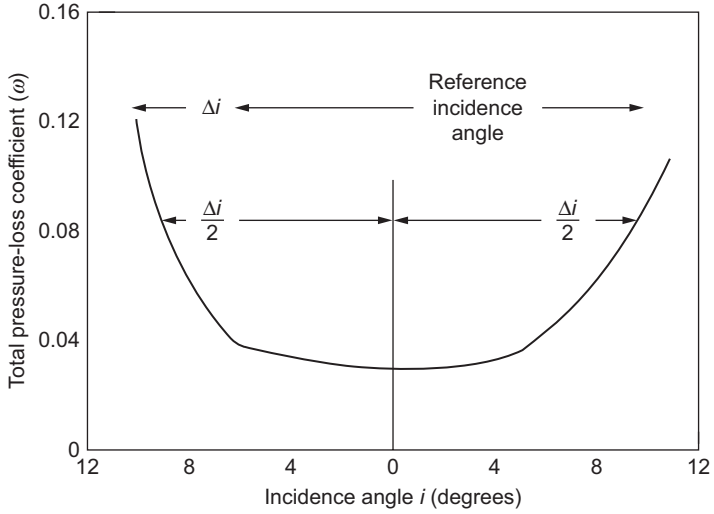


Figure 7-16 Loss as a function of incidence angle.

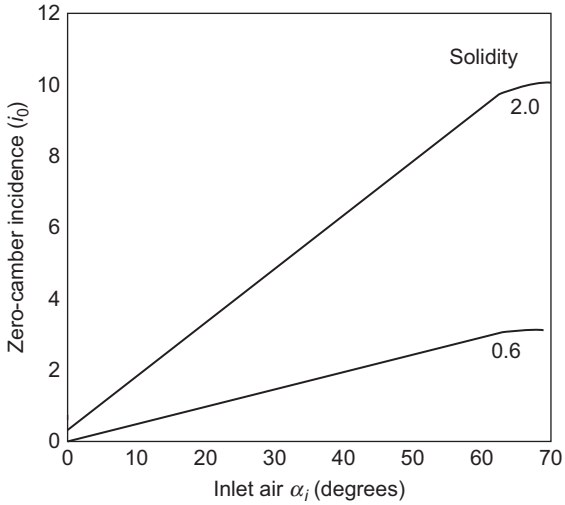


Figure 7-17 Incidence angle for zero-camber airfoil.

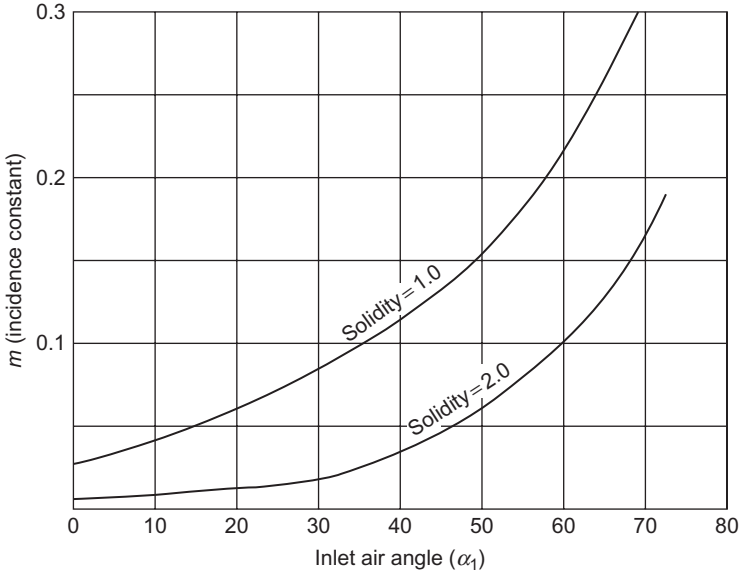


Figure 7-18 Slope of incidence angle variation with air angle.

The incidence angle i_0 is for a 10% blade thickness. For blades of other than 10% thickness, a correction factor K is used, which is obtained from Figure 7-19.

The incidence angle now must be corrected for the Mach number effect (δ_m). The effect of the Mach number on incidence angle is shown in Figure 7-20. The incidence angle is not affected until a Mach number of 0.7 is reached.

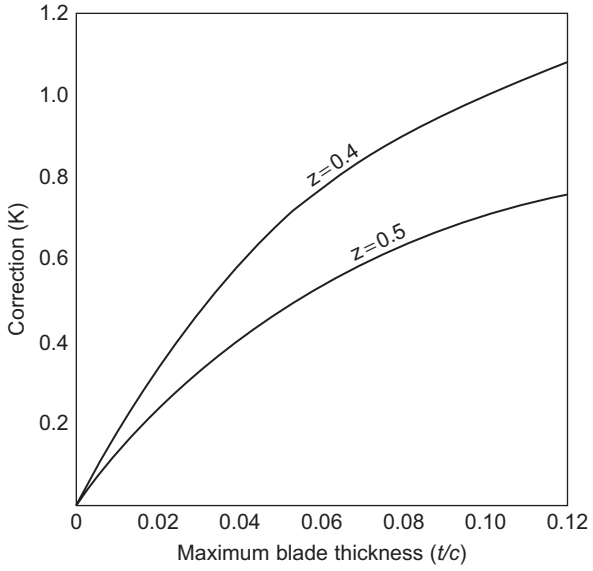


Figure 7-19 Correction factor for blade thickness and incidence angle calculation.

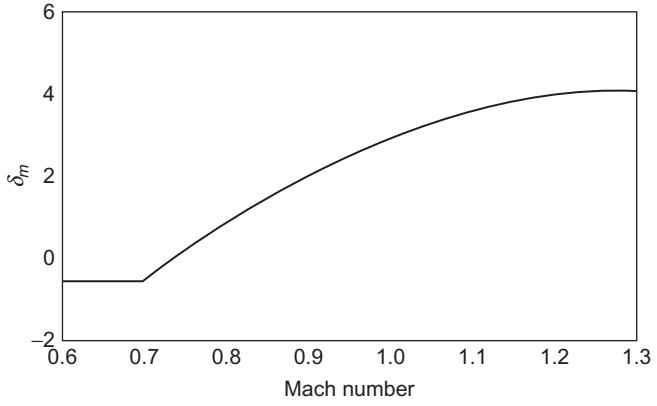


Figure 7-20 Mach-number correction for incidence angle.

The incidence angle is now fully defined. Thus, when the inlet and outlet air angles and the inlet Mach number are known, the inlet blade angle can be computed in this manner.

The Deviation Rule

Carter's rule, which shows that the deviation angle is directly a function of the camber angle and is inversely proportional to the solidity $\left(\delta = m\theta\sqrt{1/\sigma}\right)$ has been modified[10]

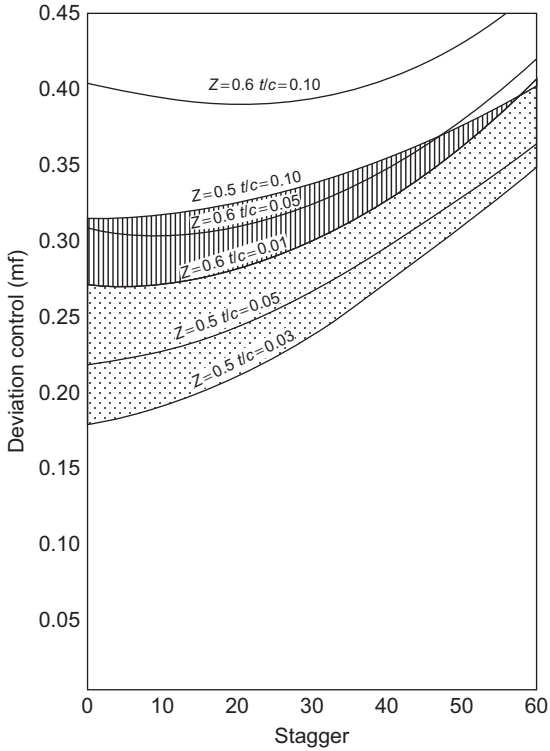


Figure 7-21 Position of maximum thickness effect on deviation.

to take into account the effect of stagger, solidity, Mach number, and blade shape as shown in the following relationship:

$$\delta_f = m_f \theta \sqrt{1/\sigma} + 12.15 t/c\,(1 - \theta/8.0) + 3.33\,(M_1 - 0.75) \tag{7-26}$$

where m_f is a function of the stagger angle, maximum thickness, and the position of maximum thickness as seen in Figure 7-21. The second term of the equation should be used only for camber angles $0 < \theta > 8$. The third term must be used only when the Mach number is between $0.75 < \mathrm{M} > 1.3$.

The use of NACA cascade data for calculating the exit air angle is also widely used. Mellor has replotted some of the low-speed NACA 65 series cascade data in convenient graphs of inlet air angle against exit air angle for blade sections of given lift and solidity set at various staggers. Figure 7-22 shows the NACA 65 series of airfoils.

The 65 series blades are specified by an airfoil notation similar to 65-(18)10. This specification means that an airfoil has the profile shape 65 with a camber line corresponding to a life coefficient $(C_L) = 1.8$ and approximate thickness of 10% of the

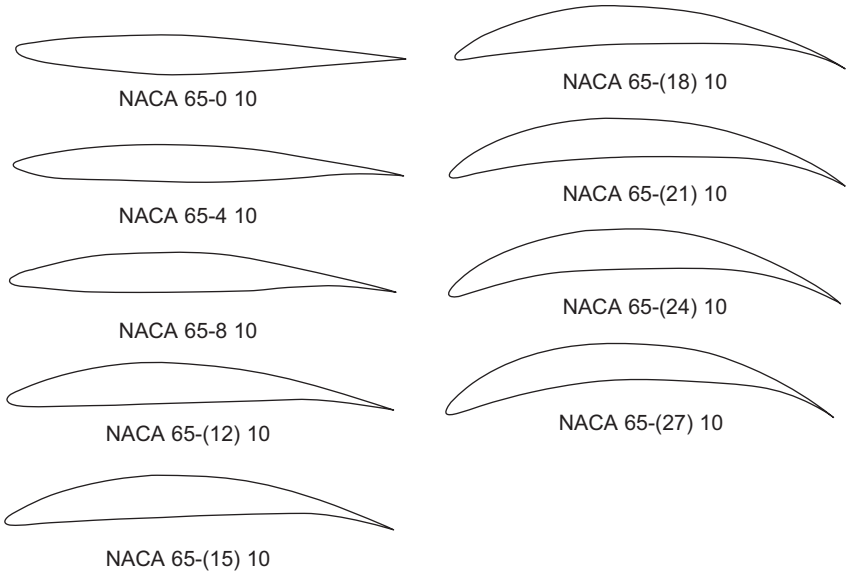


Figure 7-22 The NACA 65 series of cascade airfoils.

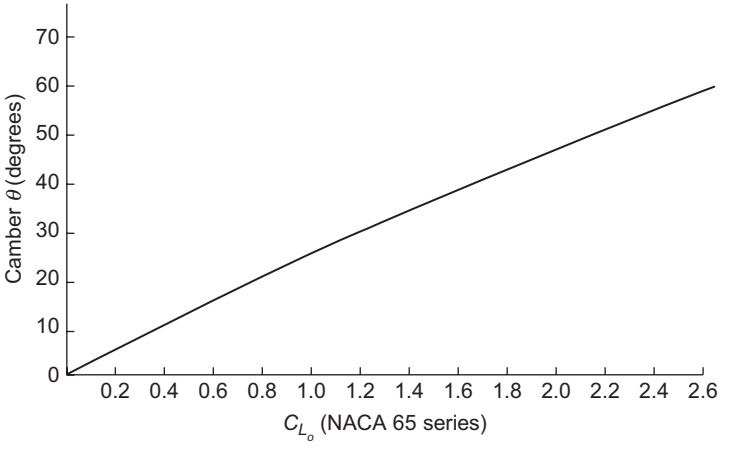


Figure 7-23 Approximate relation between camber (θ) and C_{L0} of NACA 65 series.

chord length. The relationship between the camber angle and the lift coefficient for the 65 series blades is shown in Figure 7-23.

The low-speed cascade data have been replotted by Mellor in the form of graphs of α_2 against α_1 for blade sections of given camber and space-chord ratio but set at varying stagger γ, and tested at varying incidence ($i = \alpha_i - \beta_1$) or angle of attack ($\alpha_1 - \gamma$) as seen in Figure 7-24. The range on each block of results is indicated with

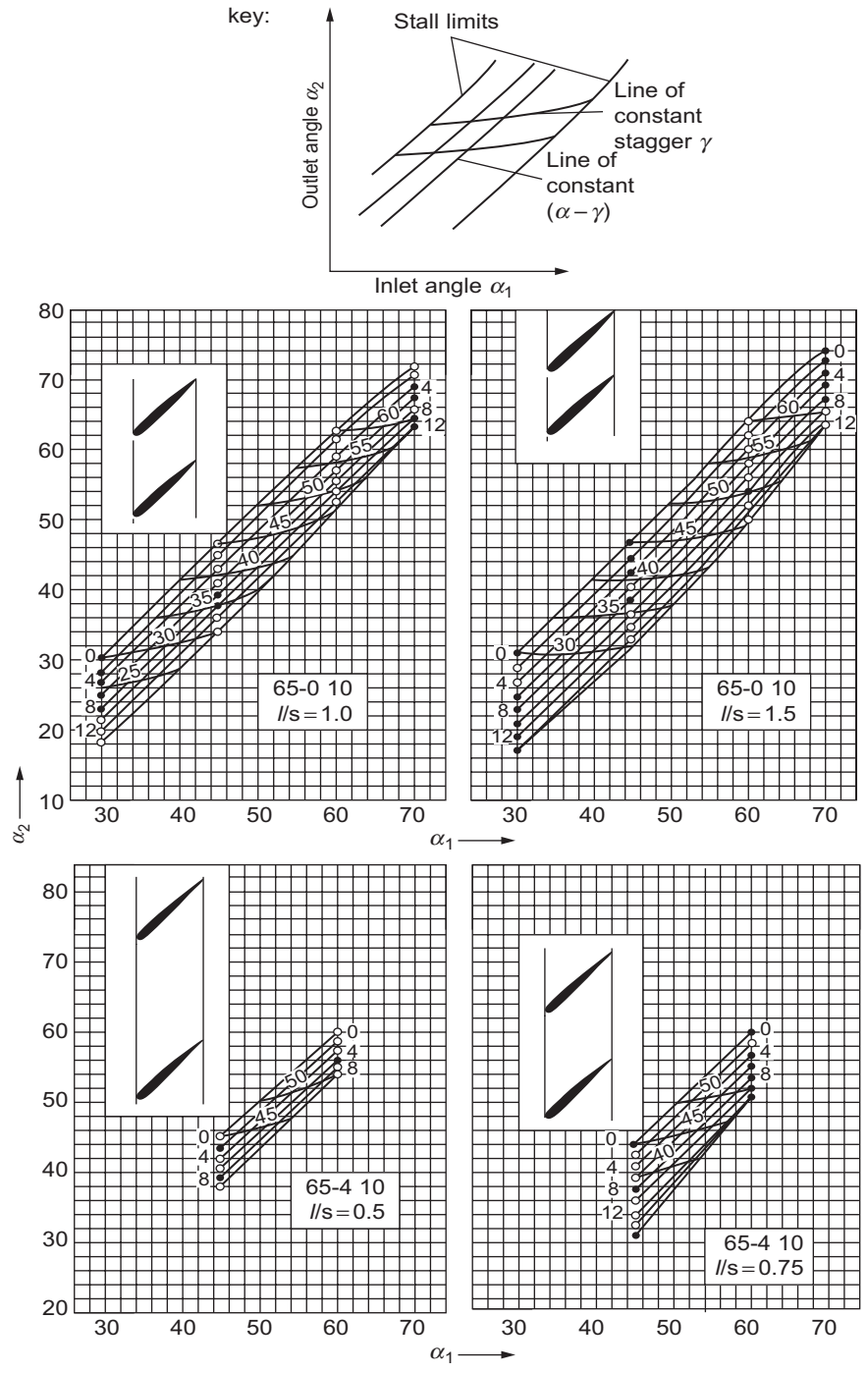


Figure 7-24 The NACA 65 series cascade data (courtesy of G. Mellor, Massachusetts Institute of Technology, Gas Turbine Laboratory Publication).

heavy black lines, which show the attack angle at which the drag coefficient increases by 50% over the mean unstalled drag coefficient.

NACA has given "design points" for each cascade tested. Each design point is chosen on the basis of the smoothest pressure distribution observed on the blade surfaces: if the pressure distribution is smooth at one particular incidence at low speed, it is probable that the section will operate efficiently at a higher Mach number at the same incidence, and that this same incidence should be selected as a design point.

Although such a definition appears somewhat arbitrary at first, the plots of such design points against solidity and camber give consistent curves. These design points are re-plotted in Figure 7-25, showing the angle of attack $(\alpha_1 - \gamma)$ plotted against space-chord ratio and the camber is independent of the stagger.

If the designer has complete freedom to choose space-chord ratio, camber, and stagger, then a design point choice may be made by trial and error from the plots of Figures 7-24 and 7-25. For example, if an outlet angle (α_2) of 15 is required from an inlet angle of 35, a reference to the curves of the figures will show that a space-chord ratio of 1.0, camber 1.2, and stagger 23 will give a cascade operating at its design point. There are a limited variety of cascades of different space-chord ratios, but one cascade that will operate at *design point* at the specified air angles. For example, if the space-chord ratio were required to be 1.0 in the previous example, then the only cascade that will produce design point operation is that of camber 1.2, stagger 23.

Such a design procedure may not always be followed, for the designer may choose to design the stage to operate closer to the positive stalling limit or closer to the negative stalling (choking) limit at design operating conditions to obtain more flexibility at off-design conditions.

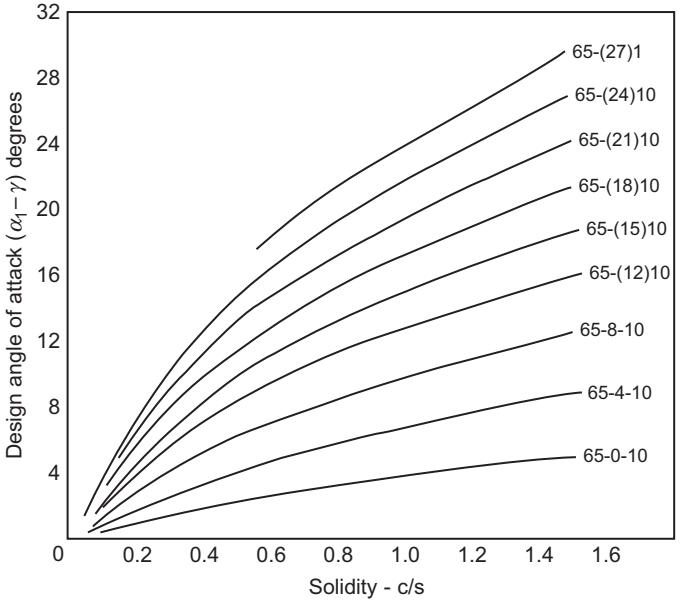


Figure 7-25 Design angles of attack $(\alpha_1 - \gamma)$ for NACA 65 series.

Compressor Operation Characteristics

A compressor operates over a large range of flow and speed delivering a stable head/pressure ratio. During start-up the compressor must be designed to operate in a stable condition at low rotational speeds. There is an unstable limit of operation known as *surging*, and it is shown on the performance map as the surge line. The surge point in a compressor occurs when the compressor back pressure is high and the compressor cannot pump against this high head, causing the flow to separate and reverse its direction. Surge is a reversal of flow and is a complete breakdown of the continuous steady flow through the whole compressor. It results in mechanical damage to the compressor due to the large fluctuations of flow, which results in changes in direction of the thrust forces on the rotor, creating damage to the blades and the thrust bearings. The phenomenon of surging should not be confused with the stalling of a compressor stage. Stalling is the breakaway of the flow from the suction side of the blade aerofoil, thus causing an aerodynamic stall. A multistage compressor may operate stably in the un-surged region with one or more of the stages stalled, and the rest of the stages un-stalled.

Compressor Surge

Compressor surge is a phenomenon of considerable interest; yet it is not fully understood. It is a form of unstable operation and should be avoided. It is a phenomenon that, unfortunately, occurs frequently, sometimes with damaging results. Surge has been traditionally defined as the lower limit of stable operation in a compressor, and it involves the reversal of flow. This reversal of flow occurs because of some kind of aerodynamic instability within the system. Usually, a part of the compressor is the cause of the aerodynamic instability, although it is possible for the system arrangement to be capable of augmenting this instability. Compressors usually are operated at a working line, separated by some safety margin from the surge line. Extensive investigations have been conducted on surge. Poor quantitative universality or aerodynamic loading capacities of different blades and stators, and an inexact knowledge of boundary-layer behavior make the exact prediction of flow in the compressor at the off-design stage difficult.

A decrease in the mass flow rate, an increase in the rotational speed of the impeller, or both can cause the compressor to surge. Whether surge is caused by a decrease in flow velocity or an increase in rotational speeds, the blades or the stators can stall. Note that operating at higher efficiency implies operation closer to surge. It should be noted here that total pressure increases occur only in the rotational part of the compressor, the blades. To make the curve general, the concept of aerodynamic speeds and corrected mass flow rates has been used in the performance maps in this chapter.

The surge line slope on multistage compressors can range from a simple single parabolic relationship to a complex curve containing several break-points or even "notches." The complexity of the surge line shape depends on whether or not the flow limiting stage changes with operating speed from one compression stage to another; in

particular, very closely matched stage combinations frequently exhibit complex surge lines. In the case of compressors with variable inlet guide vanes, the surge line tends to bend more at higher flows than with units that are speed controlled.

Usually surge is linked with excessive vibration and an audible sound; yet, there have been cases where surge not accompanied by audible sound has caused failures. Usually, operation in surge and, often, near surge is accompanied by several indications, including general and pulsating noise level increases, axial shaft position changes, discharge temperature excursions, compressor differential pressure fluctuations, and lateral vibration amplitude increases. Frequently, with high-pressure compressors, operation in the incipient surge range is accompanied by the emergence of a low frequency, asynchronous vibration signal that can reach predominant amplitudes, as well as excitation of various harmonics of blade passing frequencies. Extended operation in surge causes thrust and journal bearing failures. Failures of blades and stators are also experienced due to axial movement of the shaft causing contact of blades and stators. Due to the large flow instabilities experienced, severe aerodynamic stimulation at one of the blade natural response frequencies is caused, leading to blade failure.

The performance map of axial-flow compressors displays the variation of total pressure ratio across a compressor, as a function of corrected mass flow (usually expressed as percent of design value), at a series of constant corrected speed lines (N_c). The axial-flow compressor adiabatic efficiency (η_c) is shown as islands on the performance map, and can also be depicted versus corrected mass flow, which is shown for a representative multistage compressor in Figure 7-26.

On a given corrected speed line, as the corrected mass flow is reduced the pressure ratio (usually) increases until it reaches a limiting value on the surge line. For an operating point at or near the surge line the orderly flow (i.e., nearly axi-symmetric) in the compressor tends to break down (flow becomes asymmetric with rotating stall) and can become violently unsteady. Thus the surge line is a locus of unstable compressor operating points and is to be avoided. To cope with this instability, the surge margin (*SM*) is defined as:

$$SM = \frac{(PR_{surge} - PR_{working})}{PR_{working}} \tag{7-27}$$

In Equation 7-27, $PR_{surge/working}$ denotes the pressure ratio on the surge/working line at the same corrected mass flow rate; thus the corrected speed would be higher for operating points on the surge line. For operation on the constant corrected speed line an alternative definition for surge margin in terms of corrected mass flow on the working line and on surge line at the same corrected speed would be preferable. For stable operation of a multistage compressor a surge margin is specified.

Compressors are designed to operate at a condition referred to as the design point. At the design point the various stages mounted on the same shaft are matched aerodynamically; that is, the inlet flow to each stage is such that the stage is at the design point, and this occurs for only one combination of corrected speed and mass flow (for this reason the design point is also known as match point). Although the design

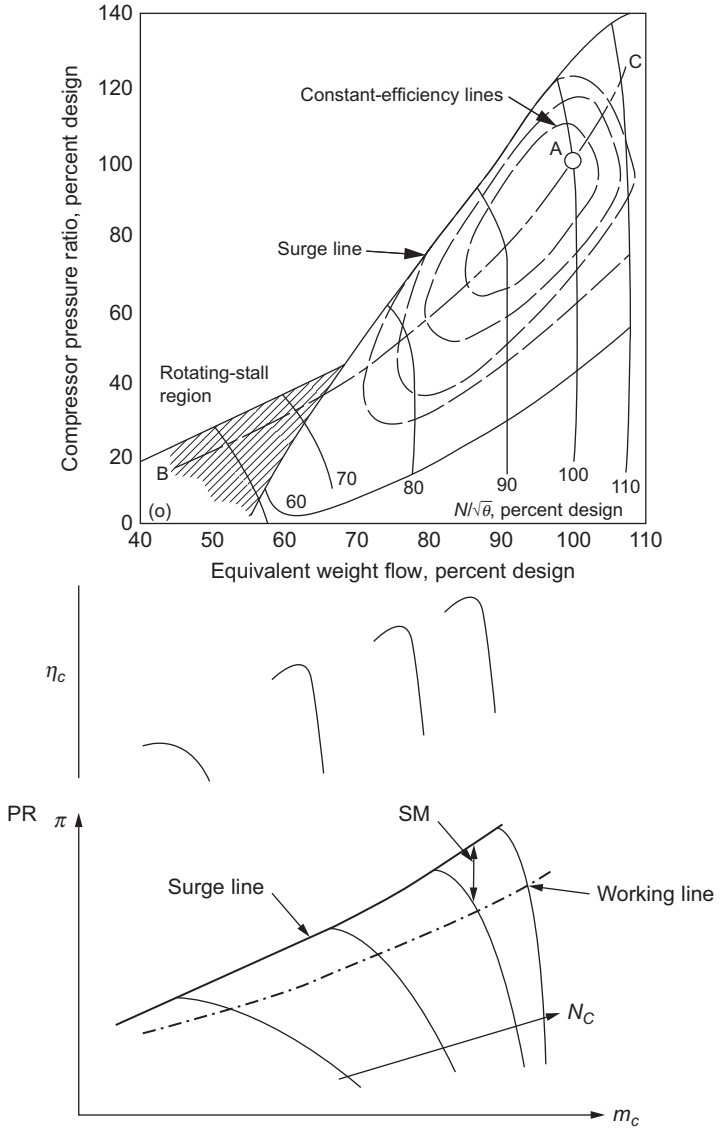


Figure 7-26 Multistage axial compressor maps.

point is one at which the compressor will operate most of the time, there are situations of low-speed operation during the starting of gas turbines where the compressor also must provide adequate pressure rise and efficiency. For compressor operations at a corrected speed or at the same speed, the corrected mass flow will be different from those at design. Difficulties arise due to the requirements of matching the inlet flow to one stage to the outlet flow from those of upstream. As an illustration, consider changes

along constant corrected speed line. The effect of reduction in mass flow relative to the working line results in a higher pressure rise and therefore a greater increase in density in the first stage than was predicted at design. The greater increase in density means the second stage has an even lower value of flow coefficient than the first stage, with an even greater increase in density. The effect is cumulative, so that the last stage approaches stall, whereas the front stage is only slightly altered. Conversely, increasing the mass flow relative to working line would result in a lower pressure rise and therefore a smaller increase in density. The smaller increase in density means the second stage has an even higher value of flow coefficient than the first stage, with an even smaller increase in density. The consequence is that the last stage approaches stalling at negative incidence with low efficiency performance. Similarly, we can also show that reducing the rotational speed along the working line through the design point can lead to stalling of front stages and wind-milling of rear stages. Methods for coping with low-speed difficulties include use of compressor air bleed at intermediate stage, use of variable geometry compressor, and use of multispool compressors or a combinations of these.

Compressor Choke

The compressor choke point is when the flow in the compressor reaches Mach 1 at the blade throat, a point where no more flow can pass through the compressor. This phenomenon often is known in the industry as *stone walling*. The more stages, the higher the pressure ratio, the smaller the operational margin between surge and choke regions of the compressor, as shown in Figure 7-27.

Compressor Stall

There are three distinct stall phenomena. Rotating stall and individual blade stall are aerodynamic phenomena. Stall flutter is an aeroelastic phenomenon.

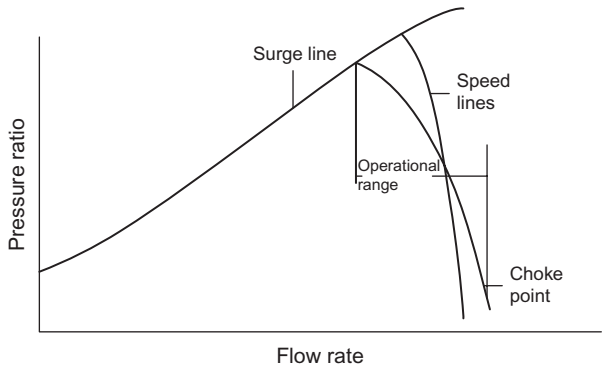


Figure 7-27 A high-pressure multistage axial-flow compressor map.

Individual Blade Stall

This type of stall occurs when all the blades around the compressor annulus stall simultaneously without the occurrence of a stall propagation mechanism. The circumstances under which individual blade stall is established are unknown at present. It appears that the stalling of a blade row generally manifests itself in some type of propagating stall and that individual blade stall is an exception.

Rotating Stall

Rotating, or propagating stall, was first observed by Whittle and his team on the inducer vanes of a centrifugal compressor. Rotating stall (propagating stall) consists of large stall zones covering several blade passages and propagates in the direction of the rotation and at some fraction of rotor speed. The number of stall zones and the propagating rates vary considerably. Rotating stall is the most prevalent type of stall phenomenon.

The propagation mechanism can be described by considering the blade row to be a cascade of blades as shown in Figure 7-28. A flow perturbation causes blade two to

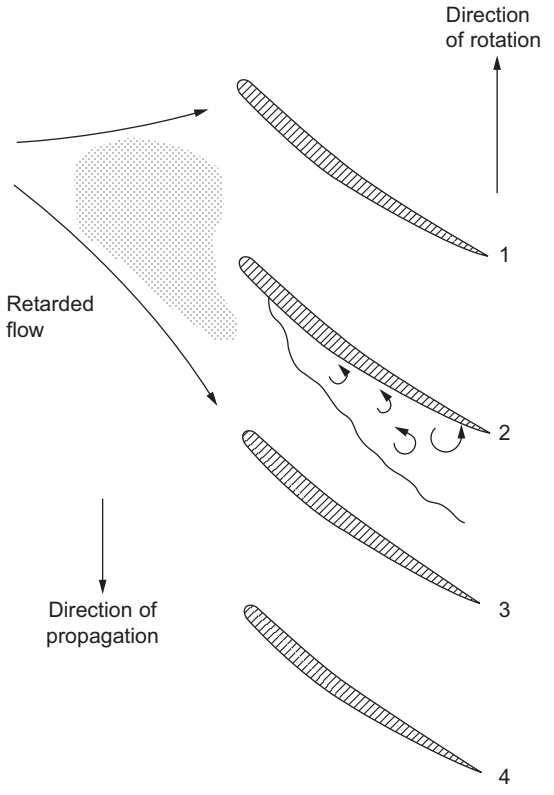


Figure 7-28 Propagating stall in a blade cascade.

reach a stalled condition before the other blades. This stalled blade does not produce a sufficient pressure rise to maintain the flow around it, and an effective flow blockage or a zone of reduced flow develops. This retarded flow diverts the flow around it so that the angle of attack increases on blade three and decreases on blade one. In this way a stall cell may move along the cascade in the direction of the lift on the blades. The stall propagates downward relative to the blade row at a rate about half the rotational speed; the diverted flow stalls the blades below the retarded-flow zone and unstalls the blades above it. The retarded flow or stall zone moves from the pressure side to the suction side of each blade in the opposite direction of rotor rotation. The stall zone may cover several blade passages. The relative speed of propagation has been observed from compressor tests to be less than the rotor speed. Observed from an absolute frame of reference, the stall zones appear to be moving in the direction of rotor rotation. The radial extent of the stall zone may vary from just the tip to the whole blade length. Table 7-2 (a), and 7-2 (b) show the characteristics of rotating stall for single and multistage axial-flow compressors.

Stall Flutter

This phenomenon is caused by self-excitation of the blade and is an aeroelastic phenomenon. It must be distinguished from classic flutter, since classic flutter is a coupled torsional-flexural vibration that occurs when the free-stream velocity over a wing or airfoil section reaches a certain critical velocity. Stall flutter, on the other hand, is a phenomenon that occurs due to the stalling of the flow around a blade.

Blade stall causes Karman vortices in the airfoil wake. Whenever the frequency of these vortices coincides with the natural frequency of the airfoil, flutter will occur. Stall flutter is a major cause of compressor blade failure.

Several types of flutter have been identified and these are indicated as various flutter boundaries on the operating map of a high-speed (transonic) compressor in Figure 7-29. Besides $\dot{m}_c$ and N_c, additional non-dimensional parameters have to be introduced to adequately characterize the flutter boundaries. One such parameter is the reduced frequency that is given by the ratio of blade chord to the wavelength of the unsteady disturbance induced by the blade motion. Often the inverse of reduced frequency, reduced velocity is used instead. More recently Khalak (2002) proposed and developed a framework for flutter operability assessment in which a set of four non-dimensional parameters are used to characterize the flutter boundary. These parameters are the corrected mass flow, the corrected speed, the compressible reduced frequency $\left(\frac{c\omega_0}{\sqrt{\gamma RT}}\right)$ (where c denotes blade chord length, ω_0 the modal frequency), and the combined mass-damping parameter (ratio of mechanical damping to blade mass). In analogy with the surge margin, a flutter margin FM is specified in Equation 7-28:

$$FM = \frac{(PR_{flutter} - PR_{working})}{PR_{working}} \tag{7-28}$$

$PR_{flutter}$ is the pressure ratio on the flutter boundary at the same corrected mass flow corresponding to that for $PR_{working}$ on the working line. For operation on the constant

Table 7-2 (a) Summary of Rotating Stall Data

Single-Stage Compressors

Type of Velocity Diagram	Hub-tip Radius Ratio	Number of Stall Zones	Propagation Rate, Stall Speed, abs/Rotor Speed	Weight-flow Fluctuation during stall, $\Delta\left[\frac{\rho V}{(\rho V)_{avg}}\right]$	Radial Extent of Stall Zone	Type of Stall
Symmetrical	0.50	3	0.420	1.39	Partial	Progressive
		4	0.475	2.14		
		5	0.523	1.66		
	0.90	1	0.305	1.2	Total	Abrupt
	0.80	8	0.87	0.76	Partial	Progressive
		1	0.36	1.30	Total	Abrupt
	0.76	7	0.25	2.14	Partial	Progressive
		8	0.25	1.10		
		5	0.25	1.10		
		3	0.23	2.02		
		4	0.48	1.47		
		3	0.48	2.02		
		2	0.49	1.71	Total	
	0.72	6, 8	0.245	0.71 = 1.33		
Free Vortex	0.60	1	0.48	0.60	Partial	Progressive
		2	0.36	0.60	Partial	Progressive
		1	0.10	0.68	Total	Abrupt
Solid Body	0.60	1	0.45	0.60	Partial	Progressive
		1	0.12	0.65	Total	Abrupt
Transonic Vortex	0.50	3	0.816	—	Partial	Progressive
		2	0.634	—	Total	Progressive
		1	0.565	—	Total	Abrupt
	0.40	2	—	—	Partial	Progressive

corrected speed line it would be preferable to define the flutter margin in terms of corrected mass flow on the working line and on the flutter boundary at the same corrected speed.

An example of a typical failure due to flutter in an axial-flow compressor fifth stage is discussed in this section. There were three blade failures of the fifth stage blade all within three to ten hours of operation. The cause of the failure had to be determined. A dynamic pressure transducer with a voltage output was used to obtain the frequency spectra. In the first four stages of the compressor no outstanding

Table 7-2 (b) Summary of Rotating Stall Data

Multistage Compressors						
Type of Velocity Diagram	**Hub to Tip Ratio**	**Number of Stall Zones**	**Propagation Rate, Stall Speed, abs/Rotor Speed**	**Radial Extent of Stall Zone**	**Periodicity**	**Type of Stall**
Symmetrical	0.5	3 4 5 6 7	0.57	Partial	Steady	Progressive[1]
Symmetrical	0.9	4 5 6	0.55	Partial	Intermittent	Progressive
Symmetrical	0.80	1	0.48	Partial	Steady	Progressive
Symmetrical	0.76	1 2 3 4	0.57	Partial	Steady	Progressive
Symmetrical	0.72	1 2 3 4 5	0.57	Partial	Intermittent	Progressive
Free Vortex	0.60	1	0.47	Total	Steady	Abrupt[2]
Solid Body	0.60	1	0.43	Total	Steady	Abrupt
Transonic Vortex	0.50	1	0.53	Total	Steady	Abrupt

1. "Progressive" stall is a smooth continuous change in the performance pressure characteristics in the stall region.
2. "Abrupt" stall is a discontinuous change in the performance pressure characteristics in the stall region.

vibration amplitudes were recorded. A signal was noted at $48N$ (N being the running speed), but the amplitude was not high, and it did not fluctuate. A measurement at the low-pressure bleed chamber taken from the fourth stage showed similar characteristics. The compressor high-pressure bleed chamber occurs after the eighth stage. A measurement at this chamber showed a high, fluctuating $48N$ signal. As there are 48 blades on the fifth-stage wheel, a problem in the fifth stage was suspected. However, above the fifth stage are blade rows of $86N$ ($2 \times 48N$), so further analysis was needed. It was found that the measurement at the high-pressure bleed chamber showed only very small $86N$ amplitude compared to the high amplitude of the $48N$ frequency. Since blade rows of 86 blades were closer to the high-pressure bleed chamber, the expected high signal should have been $86N$ compared to $48N$ under normal operating

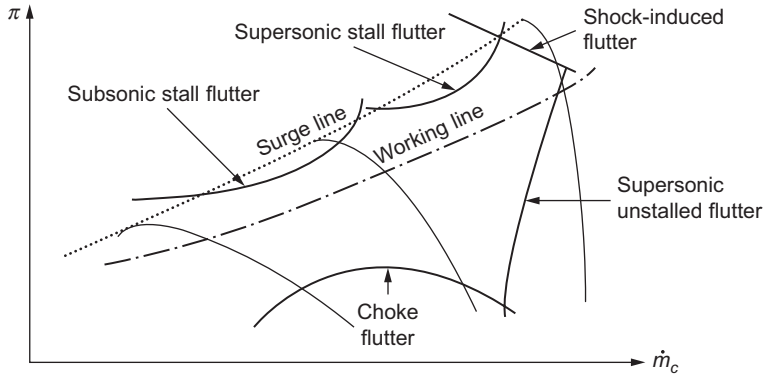


Figure 7-29 Flutter regions on the operating map of a transonic compressor (after Mikolajczak et al., 1975).

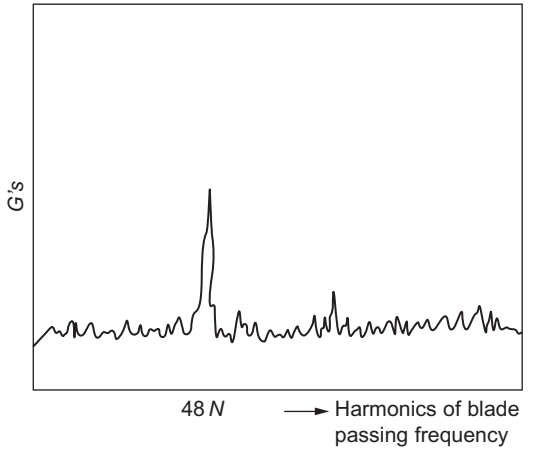


Figure 7-30 High-pressure bleed chamber – 4,100 rpm.

conditions. This high amplitude of 48*N* indicated that it was the fifth stage that caused the high, fluctuating signal; thus, a stall condition in that section was probable.

Figures 7-30 through 7-33 show the spectrum at speeds of 4,100; 5,400; 8,000; and 9,400 rpm, respectively. At 9,400 rpm, the second and third harmonics of 48*N* were also very predominant.

Next, the fifth-stage pressure was measured. Once again, high amplitude at 48*N* was found. However, a predominant reading was also observed at 1,200 Hz frequencies. Figures 7-34 and 7-35 show the largest amplitudes at speeds of 5,800 and 6,800 rpm, respectively.

At the compressor exit, predominate frequencies of 48*N* existed up to speeds of 6,800 rpm. At 8,400 rpm, the 48*N* and 86*N* frequencies were of about equal magnitudes – the only signal where the 48*N* and 86*N* frequencies were the same. The

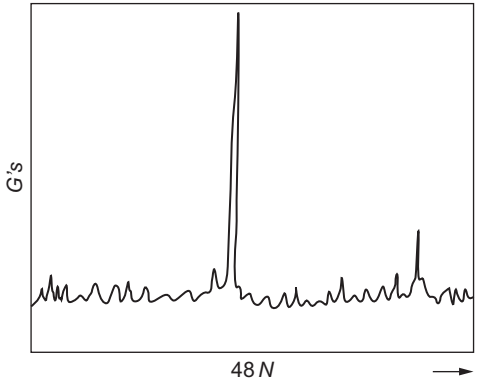


Figure 7-31 High-pressure bleed chamber – 5,400 rpm.

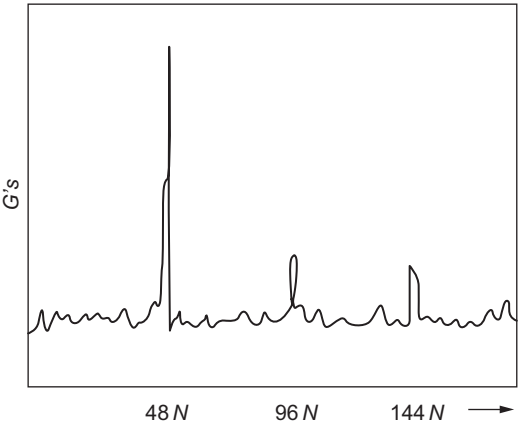


Figure 7-32 High-pressure bleed chamber – 8,000 rpm.

pressure was measured from a static port in the chamber. All other pressures were measured from the shroud, thus indicating the phenomena occurred at the blade tip. Since the problem was isolated to the fifth stage, the conclusion was that the stall occurred at the fifth-stage rotor tip. The solution to the problem was the redesign of the fifth-stage blade with a modified angle so that it would not be as subject to stall flutter.

Compressor Performance Parameters

For a gas compressor, the functional dependence of compressor exit total/stagnation pressure P_{texit} and the adiabatic compressor efficiency η_c can be expressed as a function () of the following parameters:

$$(P_{texit,}\eta_c) = f(\dot{m}, P_{tin}, T_{tin}, N, \nu, R, \gamma, \text{design}, D) \tag{7-29}$$

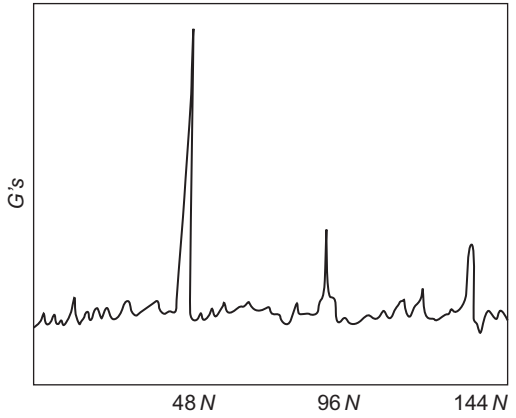


Figure 7-33 High-pressure bleed chamber – 9,400 rpm.

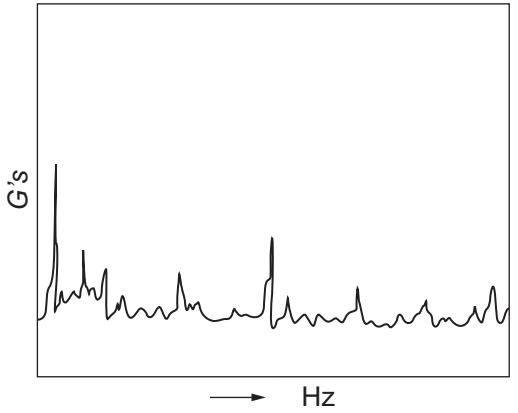


Figure 7-34 Fifth-stage bleed pressure – 5,800 rpm.

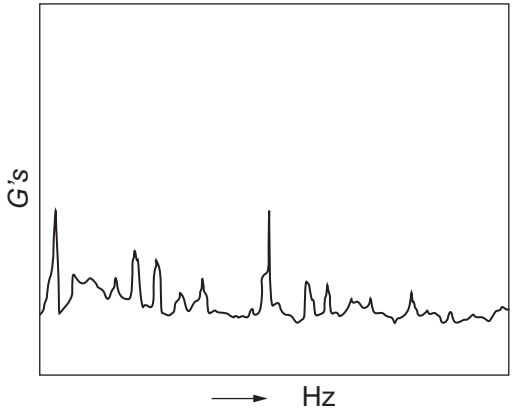


Figure 7-35 Fifth-stage bleed pressure – 6,800 rpm.

The gas properties of relevance to the compression process are characterized by the kinematic viscosity ν, specific heat ratio γ, and the gas constant R. The geometry dependence of the machine is set by the design and its characteristic size D such as the tip diameter of the compressor. Use of dimensional analysis reduces the complexity of Equation 7-29 (noting that γ and design can be regarded as nondimensional) to yield:

$$\frac{P_{texit}}{P_{tin}}, \eta_c = f\left(\frac{\dot{m}\sqrt{RT_{tin}}}{P_{tin}D^2}, \frac{ND}{\sqrt{\gamma RT_{tin}}}, \frac{ND^2}{\nu}, \gamma\right) \tag{7-30}$$

For a given compressor and for inlet conditions for which γ does not vary, Equation 7-30 reduces to:

$$\frac{P_{texit}}{P_{tin}}, \eta_c = f\left(\frac{\dot{m}\sqrt{T_{tin}}}{P_{tin}}, \frac{N}{\sqrt{T_{tin}}}, \frac{ND^2}{\nu}\right) \tag{7-31}$$

At high enough Reynolds number ($>3 \times 105$), changes in this number have little effect on compressor performance so that $\left(\frac{P_{texit}}{P_{tin}}, \eta_c\right)$ can be correlated in terms of:

$$\left(\frac{\dot{m}\sqrt{T_{tin}}}{P_{tin}}, \frac{N}{\sqrt{T_{tin}}}\right); \text{that is,}$$

$$\frac{P_{texit}}{P_{tin}}, \eta_c = f\left(\frac{\dot{m}\sqrt{T_{tin}}}{P_{tin}}, \frac{N}{\sqrt{T_{tin}}}\right) \tag{7-32 (a)}$$

As no functional dependence is implied if the non-dimensional variables on the RHS are scaled by a constant, we can thus choose to replace them by the corrected mass: flow rate $\dot{m}_c = \left(\frac{\dot{m}\sqrt{\theta}}{\delta}\right)$ and corrected speed $N_c = \left(\frac{N}{\sqrt{\theta}}\right)$ so that

$$\frac{P_{texit}}{P_{tin}}, \eta_c = f\left(\frac{\dot{m}\sqrt{\theta}}{\delta}, \frac{N}{\sqrt{\theta}}\right) = f(\dot{m}_c, N_c) \tag{7-32 (b)}$$

In equation 7-32 (b), $\theta = \frac{T_{tin}}{T_{ref}}$ and $\delta = \frac{P_{tin}}{P_{ref}}$, where the reference temperature T_{ref} and the reference pressure P_{ref} are taken to be the sea-level value for the standard atmosphere, 59.6 °F (15 °C) and 14.7 psi (101 kN/m^2), respectively. The advantage of using these corrected variables is that their numerical magnitude is similar to the actual value so that its significance is not obscured.

We can also use the Euler Turbine Equation 7-8 for a compressor stage:

$$c_p(\mathrm{T}_{texit} - T_{tin}) = \omega\left[(rV_\theta)_2 - (rV_\theta)_1\right] \tag{7-33}$$

to elucidate the functional dependence and to deduce why the performance characteristics look the way they are on a compressor map. Assuming isentropic flow (i.e, no

loss) then the stagnation pressure ratio across the (ideal) stage is given by:

$$PR_s = \frac{P_{textit}}{P_{tin}} = \left\{1 + \left[\frac{(\omega r_2)^2}{c_p T_{tin}}\right]\left[1 - \left(\frac{V_{z2}}{\omega r_2}\right)\left(\tan\,\beta_{exit} + \frac{V_{z1} r_1}{V_{z2} r_2}\tan\,\alpha_{exit}\right)\right]\right\}^{\frac{\gamma}{\gamma-1}} \tag{7-34}$$

In Equation 7-33 and 7-34 subscripts 1 and 2 refer to variables evaluated at rotor inlet and rotor exit respectively, V_θ denotes tangential velocity, V_z the axial velocity, ω the angular velocity of rotor, α_{exit} the absolute flow angle at stator exit, β_{exit} the relative flow angle at rotor exit, and r the radius. Upon introducing the corrected variables into Equation 7-34 we have:

$$PR_s = \left\{1 + k_0 N_c^2 - k_1 N_c \dot{m}_c G(M_1)\left(\tan\,\alpha_{exit} + \tan\,\beta_{exit}\right)\right\}^{\frac{\gamma}{\gamma-1}} \tag{7-35}$$

where $G(M_1)$ has a weak dependence on the incoming Mach number $M_1, k_0 \propto r^2$, and $k_1 \propto r$. For a given compressor stage $(\tan\,\alpha_{exit} + \tan\,\beta_{exit})$ is fixed and neglecting the variation in $G(M_1)$ we have $PR_s = PR_s(\dot{m}_c, N_c)$. The general dependence of PR_s on $\dot{m}_c$ and N_c is shown in Figure 7-36 as a series of dashed lines of constant corrected speed for the ideal stage; Equation 7-35 can be used to obtain the trend in the variation of the ideal stage characteristic with $\dot{m}_c$ and N_c. The solid lines (of constant corrected speed) in Figure 7-36 are the $PR_s vs \dot{m}_c$ curves with stagnation pressure losses taken into account. The flow angle varies as the corrected mass flow rate changes along a given corrected speed line. The point of minimum difference between the dash (ideal) and the solid (actual) curve corresponds to a corrected mass flow that yields an angle of incidence for minimum loss; moving away from this point along a constant corrected speed line amounts to changing the incidence angle (increasing the angle of incidence for decreasing $\dot{m}_c$ or decreasing the angle of incidence for increasing $\dot{m}_c$) so as to lead to higher loss. This is reflected in the increasing difference between the two curves (ideal versus actual) at corrected mass flow other than that corresponding to minimum loss. We thus deduce from these arguments that the actual pressure rise (and the efficiency) can also be characterized in terms of $\dot{m}_c$ and N_c. The pressure ratio of a complete compressor consisting of many stages can be obtained by taking the products of the stage performance.

Performance Losses in an Axial-Flow Compressor

The calculation of the performance of an axial-flow compressor at both design and off-design conditions requires the knowledge of the various types of losses encountered in an axial-flow compressor.

The accurate calculation and proper evaluation of the losses within the axial-flow compressor are as important as the calculation of the blade-loading parameter, since unless the proper parameters are controlled, the efficiency drops. The evaluation of the various losses is a combination of experimental results and theory. The losses are

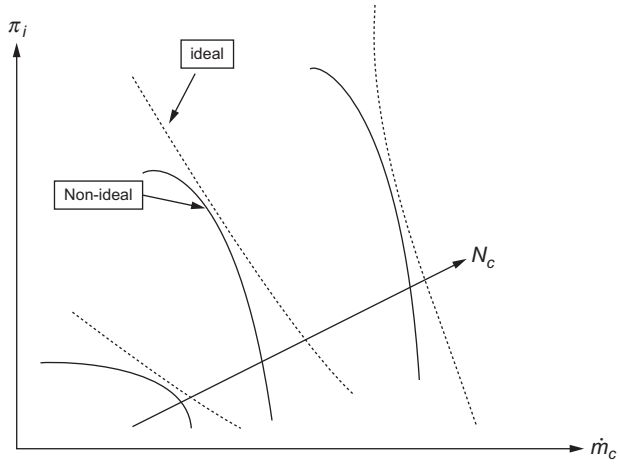


Figure 7-36 Performance map of compressor stage.

divided into two groups: (1) losses encountered in the rotor, and (2) losses encountered in the stator. The losses are usually expressed as a loss of heat and enthalpy.

A convenient way to express the losses is in a nondimensional manner with reference to the blade speed. The theoretical total head available (q_{tot}) is equal to the head available from the energy equation ($q_{th} = q_{tot}$) plus the head which is loss from disc friction:

$$q_{tot} = q_{th} + q_{df} \tag{7-36}$$

The adiabatic head that is actually available at the rotor discharge is equal to the theoretical head minus the heat losses from the shock in the rotor, the incidence loss, the blade loadings and profile losses, the clearance between the rotor and the shroud, and the secondary losses encountered in the flow passage:

$$q_{ia} = q_{th} - q_{in} - q_{sh} - q_{bl} - q_c - q_{sf} \tag{7-37}$$

Therefore, the adiabatic efficiency in the impeller is:

$$\eta imp = \frac{q_{ia}}{q_{tot}} \tag{7-38}$$

The calculation of the overall stage efficiency must also include the losses encountered in the stator. Thus, the overall actual adiabatic head attained would be the actual adiabatic head of the impeller minus the head losses encountered in the stator from the wake caused by the impeller blade, the loss of part of the kinetic head at the exit of the stator, and the loss of head from the frictional forces encountered in the stator

$$q_{oa} = q_{ia} - q_w - q_{ex} - q_{osf} \tag{7-39}$$

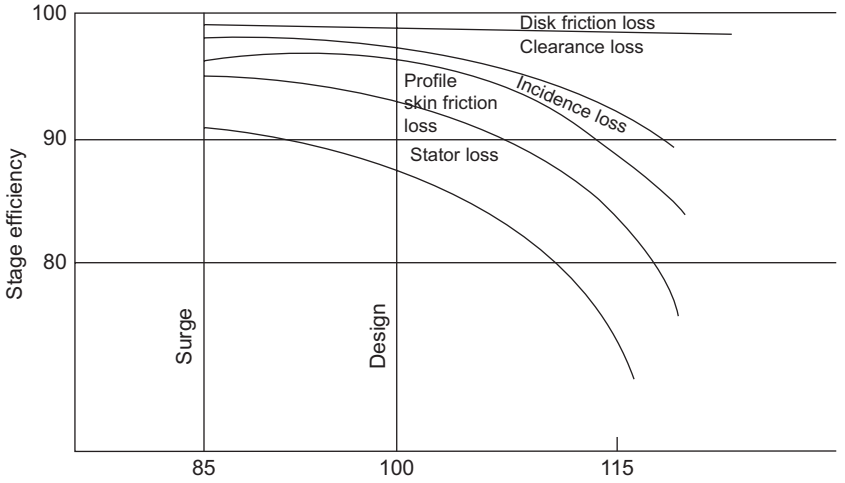


Figure 7-37 Losses in an axial-flow compressor stage.

Therefore, the adiabatic efficiency in the stage:

$$\eta stage = \frac{q_{oa}}{q_{tot}} \tag{7-40}$$

The losses as mentioned earlier can be further described:

1. *Disc friction loss.* This loss is from skin friction on the discs that house the blades of the compressors. This loss varies with different types of discs.
2. *Incidence loss.* This loss is caused by the angle of the air and the blade angle not being coincident. The loss is minimum to about an angle of $\pm 4^{\circ}$, after which the loss increases rapidly.
3. *Blade loading and profile loss.* This loss is due to the negative velocity gradients in the boundary layer, which gives rise to flow separation.
4. *Skin friction loss.* This loss is from skin friction on the blade surfaces and on the annular walls.
5. *Clearance loss.* This loss is due to the clearance between the blade tips and the casing.
6. *Wake loss.* This loss is from the wake produced at the exit of the rotary.
7. *Stator profile and skin friction loss.* This loss is from skin friction and the attack angle of the flow entering the stator.
8. *Exit loss.* This loss is due to the kinetic energy head leaving the stator.

Figure 7-37 shows the various losses as a function of flow. Note that the compressor is more efficient as the flow nears surge conditions.

New Developments in Axial-Flow Compressors

The new advanced compressor rotors have fewer blades with higher loadings, and the blades are thinner, larger, and are designed using advanced radial equilibrium theory,

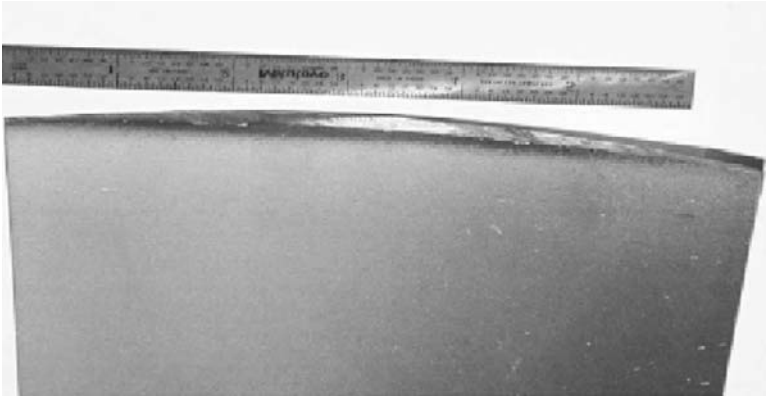


Figure 7-38 Compressor blade with tip rub.

which creates three-dimensional and controlled diffusion shaped airfoils (3D/CDA), with smaller clearances and higher loading per stage.

There are also trends toward water injection at the inlet or between compressor sections that will likely affect airfoil erosion life. The smaller clearances (20–50 mils) and high pressure ratios tend to increase the probability of encountering rubs. These tip rubs usually occur near the bleed flow sections of the turbines where there are inner diameter changes, and the compressor casing could be out of round. Figure 7-38 shows one such blade that encountered tip rub.

The advanced compressor blades also usually have squealer sections on the blade tips, which are designed to wear in a safe manner if the blades are in contact with the casing. Figure 7-39 is one such blade. These rubs, if severe, can lead to tip fractures and overall destruction of the downstream blades and diffuser vanes due to domestic object damage (DOD).

The very high temperature at the exit of the compressor, which in some cases exceeds 1000 °F (537.78 °C), causes a very hot compression section, which also requires the cooling of the bleed flows before they can be used for cooling the turbine section. This requires large heat exchangers, and in some combined cycle plants steam is used to cool the compressed air. This also limits the down time between start-ups of the turbines. Design margins are set by Finite Element Modeling (FEM) at the element level, which results in lower safety margins than previous designs. The costs of these larger, thinner, less-rub tolerant, and more twisted-shape airfoils are usually higher. When several of the major characteristics of advanced gas turbines are examined from a risk viewpoint (i.e., probability and consequences of failure), there are no characteristics that reduce the probability of failure and/or decrease the consequence of failure.

Table 7-3 indicates the changes in the compressor blades that are now prevalent on advanced gas turbines. The first column represents previous gas turbine designs, the second column represents new gas turbine designs, and the last column indicates the change in risk (↑represents higher) for the design differences. Most of the comparisons are self-explanatory.

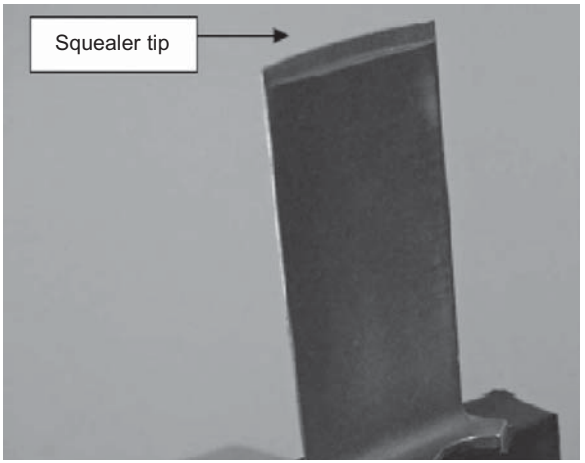


Figure 7-39 Axial-flow compressor rotor blade with squealer tip.

Table 7-3 State of Gas Turbine Technology Compressors

Previous Designs	New Designs	Risk
• 2D double circular arc or NACA 65 profiles	• 3D or Controlled Diffusion Airfoil (CDA) profiles	↑
• Large number of airfoils	• Reduced airfoil count	↑
• Repeating stages/shorter chords	• Stages unique/longer chords	↑
• Low/modest aspect ratios	• High aspect ratios	↑
• Large clearances	• Smaller clearances	↑
• Low/modest pressure ratios (R_c)	• Much higher pressure ratios (R_c)	↑
• Low/modest blade loading per stage	• High blade loading per stage	↑
• Wider operating margin	• Narrow operating margin	↑
• Thicker leading edges	• Thinner leading edges	↑
• Dry operation	• Wet operation	↑
• Bulk safety margins	• Safety margins by FEM	↑
• Lower costs	• Higher costs	↑

Axial-Flow Compressor Research

Considerable research is being carried out on improving the performance of axial-flow compressors. This research is being carried out in many different aspects of the axial-flow compressor:

1. Effects of aspect ratio (AR) on blade loading, blade excitation, and the pre-twist blade angles (centrifugal forces on the blade). Increase in blade loading was carried out by increasing the aspect ratio of the blade. Blade aspect ratios were increased to (AR) = 9. At these high aspect ratios the blades had to be designed with mid-span shrouds and tip shrouds.

This decreases the efficiency of the stage; however, without the shrouds the pre-twist blade angle had to be increased to about 12°, and the blade excitation resulted in blade failure. Presently most blade designs are limited to an $(AR) = 4$.

2. Increasing the operational range (surge – choke) at a given compressor speed by developing new blade profiles to reduce blade stall in compressors.

Cascade Tests

The data on blades in an axial-flow compressor are from various types of cascades, since theoretical solutions are very complex, and their accuracy is in question because of the many assumptions required to solve the equations. The most thorough and systematic cascade testing has been conducted by NACA staff at the Lewis Research Center. The bulk of the cascade testing was carried out at low Mach numbers and at low turbulence levels.

The NACA 65 blade profiles were tested in a systematic manner by Herrig, Emergy, and Erwin. The cascade tests were carried out in a cascade wind tunnel with boundary-layer suction at the end walls. Tip effects were studied in a specially designed water cascade tunnel with relative motion between wall and blades.

Cascade tests are useful in determining all aspects of secondary flow. For better visualization, tests have been conducted in water cascades. The flow patterns are studied by injecting globules of dibutyl phatalate and kerosene in a mixture equal to the density of water. The mixture is useful in tracing secondary flow, since it does not coagulate.

An impeller designed for air can be tested using water if the dimensionless parameters, Reynolds number (R_e), and specific speed (N_s) are held constant:

$$R_e = \frac{\rho_{air} V_{air} D}{\mu_{air}} = \frac{\rho_{water} V_{water} D}{\mu_{water}} \tag{7-41}$$

$$N_s = \frac{Q_{air}}{N_{air} D^3} = \frac{Q_{water}}{N_{water} D^3} \tag{7-42}$$

where

ρ = medium density
V = velocity
D = impeller diameter
μ = viscosity
N = speed

Using this assumption, we can apply this flow visualization method to any working medium.

One designed apparatus consists of two large tanks on two different levels. The lower tank is constructed entirely out of Plexiglas and receives a constant flow from the upper tank. The flow entering the lower tank comes through a large, rectangular opening that houses a number of screens so that no turbulence is created by water entering the lower tank. The center of the lower tank can be fitted with various boxes for the various flow visualization problems to be studied. This modular design enables a rapid interchanging of models and works on more than one concept at a time.

Blade Profile

To study the effect of laminar flow, the blades were slotted as shown in Figure 7-40. For the blade treatment cascade rig experiment, a Plexiglas cascade was designed and built.

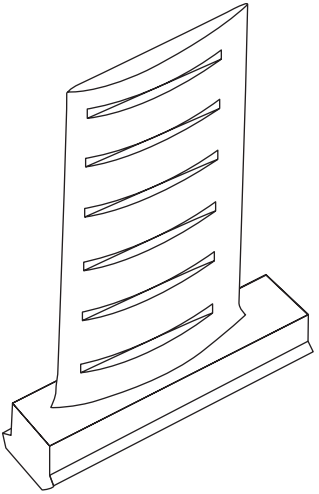


Figure 7-40 Perspective of compressor blade with treatment.

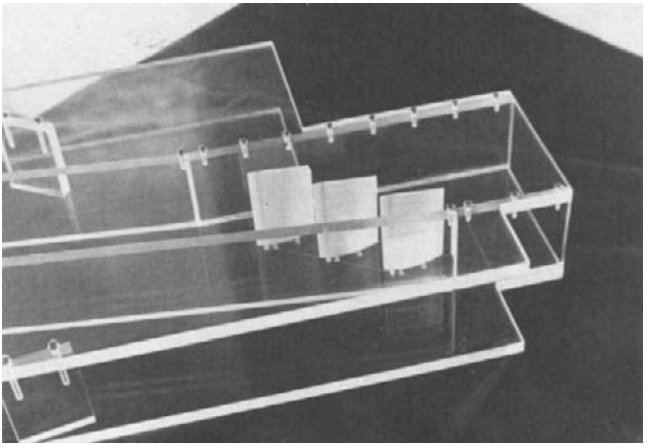


Figure 7-41 Cascade model in axial-flow test tank.

Figure 7-41 shows the cascade. This cascade was then placed in the bottom tank and maintained at a constant head. Figure 7-42 shows the entire setup, and Figure 7-43 shows the cascade flow. Note the large extent of the laminar-flow regions on the treated center blades as compared to the untreated blades.

3. Reduction of flow leakage at the compressor tips.

The effect of casing treatment in axial-flow compressors was studied in a water cascade tunnel. In this study the same Reynolds number and specific speeds were maintained as those experienced in an actual axial-flow compressor.

In an actual compressor the blade and the passage are rotating with respect to the stationary shroud. It would be difficult for a stationary observer to obtain data on the rotating

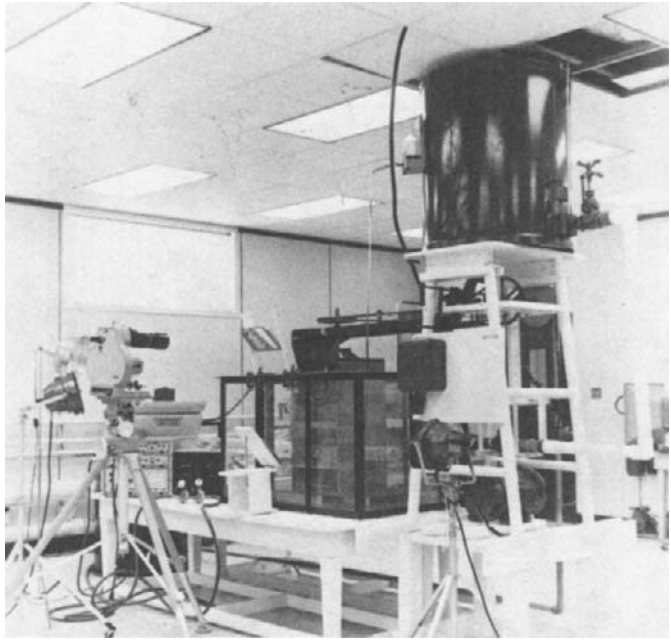


Figure 7-42 Apparatus for testing axial-flow cascade model.

blade passage. However, if that observer were rotating with the blade passage, data would be easier to acquire. This was accomplished by holding the blade passage stationary with respect to the observer and rotating the shroud. Furthermore, since casing treatment affects the region around the blade tip, it was sufficient to study only the upper portion of the blade passage. These were the criteria in the design of the apparatus.

The modeling of the blade passage required provisions for controlling the flow in and out of the passage. This control was accomplished by placing the blades, which partially form the blade passage, within a Plexiglas tube. The tube had to be of sufficient diameter to accommodate the required flow through the passage without tube wall effect distorting the flow as it entered or left the blade passage. This allowance was accomplished by using a tube three times the diameter of the blade pitch. The entrance to the blades was designed so that the flow entering the blades was a fully developed turbulent flow. The flow in the passage between the blade tip and the rotating shroud was laminar. This laminar flow was expected in the narrow passage.

A number of blade shapes could have been chosen; therefore, it was necessary to pick one shape for this study, which would be the most representative for casing treatment considerations. Since casing treatment is most effective from an acoustic standpoint in the initial stages of compression, the maximum point of camber was chosen toward the rear of the blade ($Z = .6$ chord). This type of blade profile is most commonly used for transonic flow and is usually in the initial stages of compression.

The rotating shroud must be in close proximity to the blade tips within the tube. To get this proximity, a shaft-mounted Plexiglas disc was suspended from above the blades. The Plexiglas disc was machined as shown in Figure 7-44. The Plexiglas tube was slotted so

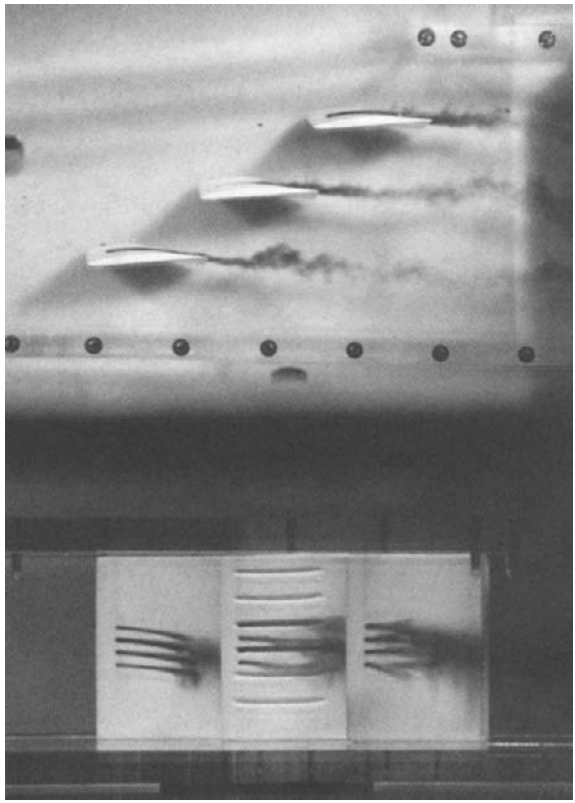


Figure 7-43 Treatments on center cascade blade.

that the disc could be centered on the centerline of the tube and its stepped section lowered through the two slots in the tube. Clearances between the slot edges and the disc were minimized. One slot was cut directly above the blade passage emplacement. The other slot was sealed off to prevent leakage. As the disc was lowered into close proximity to the blade tips, the blade passage was completed. The clearance between disc and blade was kept at 0.035 of an inch. The disc, when spun from above, acted as the rotating shroud.

There are only two basic casing treatment designs other than a blank design – which corresponds to no casing treatment at all. The first type of casing treatment consists of radial grooves. A radial groove is a casing treatment design in which the groove is essentially parallel to the chordline of the blade. The second basic type is the circumferential groove. This type of casing treatment has its grooves perpendicular to the blade chordline. Figure 7-45 is a photograph of two discs showing the two types of casing treatment used. The third disc used is a blank, representing the present type of casing. The results indicate that the radial casing treatment is most effective in reducing leakage and also in increasing the surge-to-stall margin. Figure 7-46 shows the leakage at the tips for the various casing treatments. Figure 7-47 shows the velocity patterns observed by the use of various casing treatments. Note that for the treatment along the chord (radial), the flow is maximum at the tip. This flow maximum at the tip indicates that the chance of rotor tip stall is greatly reduced.

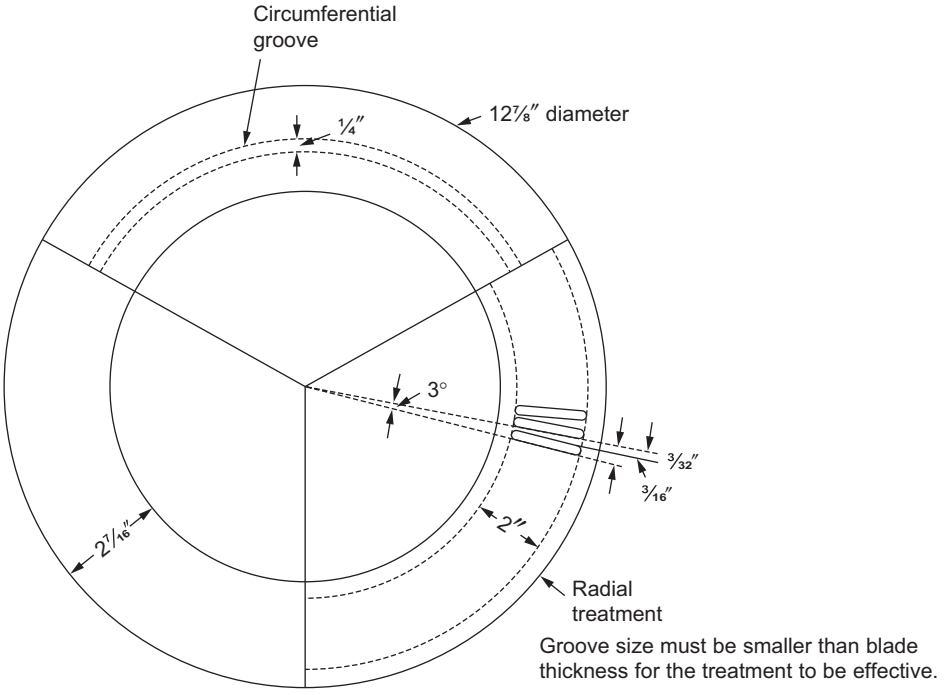


Figure 7-44 Details of the various casing treatments. Each treatment was on a separate disc.

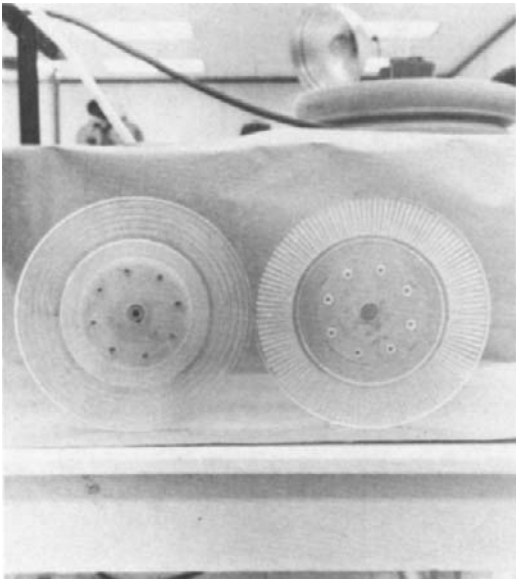


Figure 7-45 Two discs with casing treatment.

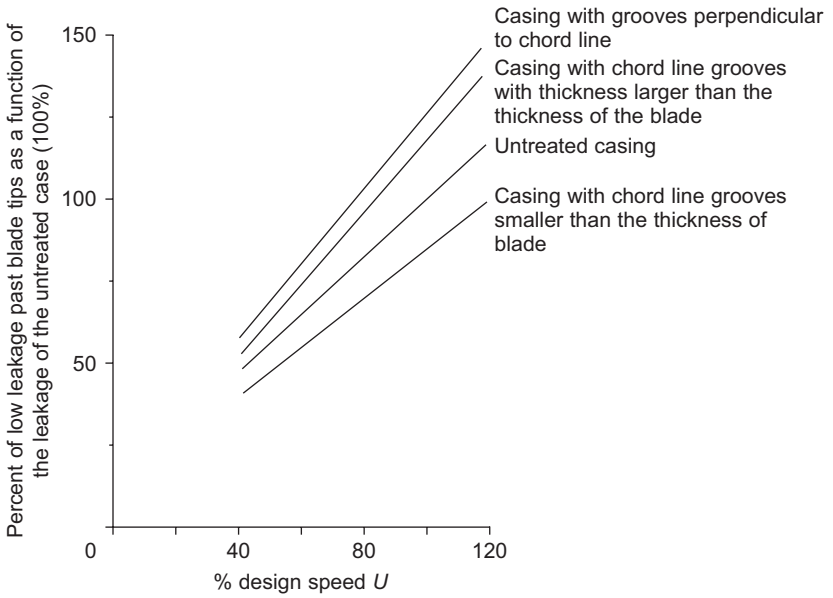


Figure 7-46 Mass flow leakage at tips for various casing treatments.

4. Enhancement of Numerical Solutions of the Navier-Stokes Equation (viscous compressible flow).

   The solution of the full Navier Stokes equation requires very enhanced numerical techniques. The old solutions used inviscous flow and quasi-three-dimensional flow solutions. There are many new enhanced numerical programs underway to solve the equation in its entity.

5. Supersonic Blade Profiles for higher pressure ratio per stage (>2.1).

   Transonic blades have been designed with the point of maximum thickness at about 0.6 of blade chord from the leading edge of the blade. Supersonic blade design has problems with standing shock waves which can occur as the flow enters the stators. The losses with the diffusion process are very high and thus design changes are being experimented on so that the flow entering the diffuser is easily swallowed, and so that if any shock waves exist they are oblique shocks with minimal losses. Cascade testing is being conducted on various profiles to ensure that the stage losses are minimized.

6. Compressor inter-stage cooling by water injection between stages.

   In this system the water is injected into the mid-stages of the compressor to cool the air and approach an isothermal compression process as shown in Figure 7-48. The water injected is usually mechanically atomized so that very fine droplets are entered into the air. The water is evaporated as it comes in contact with the high pressure and temperature air stream. As water evaporates, it consumes about 1,058 BTU (1,117 kJ) (latent heat of vaporization) at the higher pressure and temperature resulting in lowering the temperature of the air stream entering the next stage. This lowers the work required to drive the compressor. The inter-cooling of the compressed air has been very successfully applied to high-pressure ratio engines.

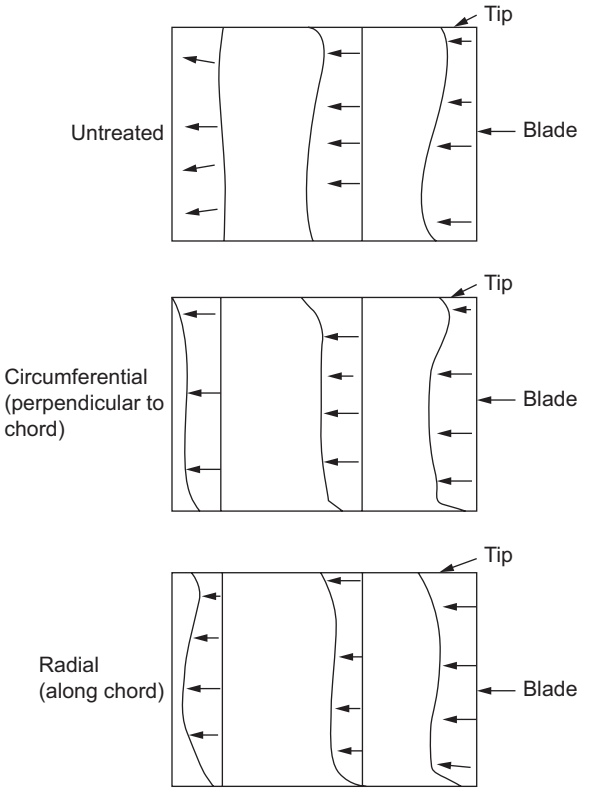


Figure 7-47 Velocity patterns observed in the side view of the blade passage for various casing treatments.

Compressor Blade Material

Compressor blading is made by forging, extrusion, or machining. All production blades, until the advent of the new Advanced Gas Turbines, have been made from stainless steels, Type 403 or 403 Cb both having about 12 Cr. This family of alloys has properties which include good ductility at high strength levels, uniform properties, and good strength at temperatures up to about 900 °F (482 °C). Due to the fact that the new axial flow compressors have pressure ratios of 30:1 to 40:1 and exit temperatures between 1000–1150 °F (538–621 °C), new compressor blade material, a precipitation hardened, martensitic stainless steel such as 15-5 PH nominal, was introduced into production for advanced and uprated machines,as shown in Table 7-4. This material provides increased tensile strength without sacrificing stress corrosion resistance. Substantial increases in the high-cycle fatigue and corrosion fatigue strength are also achieved with this material, compared with the Type 403 stainless steel with 12Cr. Superior corrosion resistance is also achieved due to the metal's higher concentration of chromium and molybdenum content. Compressor corrosion results from

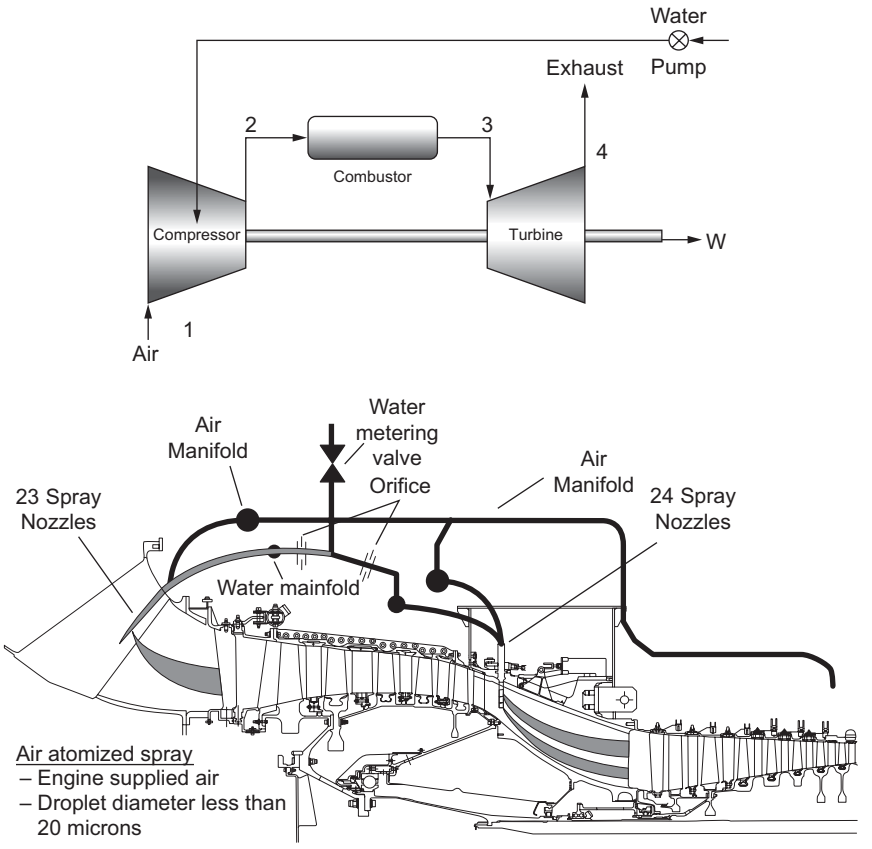


Figure 7-48 Mid-Compressor Cooling showing a schematic as well as an actual application in a GE LM 6000 Engine (courtesy GE Power Systems).

moisture containing salts and acids collecting on the blading. During operation, moisture can be present because of rain, use of evaporative coolers, fogging systems, or compressor water washes, or condensation resulting from humid air being accelerated at the compressor inlet. Moisture may be present in the compressor during operation up to between stage five and stage eight, where it usually becomes warm enough to prevent condensation. When the turbine is not in operation, the compressor can still become wet if metal temperatures are below the local dew point; this can happen to units stored in humid environments. The chemistry of this moisture deposit especially the salt in the air, depositing on the blading determines the severity of the corrosion phenomenon.

The high temperature blade alloy is normally produced byvacuum-arc remelting to reduce inclusions, and is advertised to have a balanced chemistry that minimizes the formation of delta-ferrite. Inclusions and the delta-ferrite would provide planes of weakness in that part. It is not uncommon for the mill to supply forging stock that has

Table 7-4 Compressor Blade Material

Compressor Blade Type	Max.Temp	Components Percent													
		C	S	Mn	P	Si	Cr	Mo	Ni	Cu	Al	Cb	Mg	O	Fe
AISI 403	900 °F	.11					12						–	–	Bal
AISI 403+Cb	900 °F	.15	–	–	–	–	12	–	–	–	–	0.2	–	–	Bal
Martensitic high temperature stainless steel	1250 °F	.08	–	.14	–	.4	15.6	.08	3.8–6.5	2.9	.9	–	–	–	Bal
15–5 PH, nominal		<.07	<.03	<1.0	<0.04–	<1.0	14–15.5	–	3.5–5.5	3.2	.9	.15–.45	–	–	Bal

first been given a 1900 °F heat treatment, just for better forgeability. The forged blanks are then usually reheat-treated at 1900 °F, followed by hardening treatments between 1100 °F and 1150 °F depending on the properties sought. There is a general correlation between hardness and strength (tensile/fatigue). A hardness of RC 32 suggests that the tensile strength is around 150,000 psi and that the hardening temperature used during manufacture was somewhere around 1100 °F to 1150 °F.

Coating of the compressor blades is now very common. Compressor blades suffer a great amount of corrosion pitting from impurities in the air stream. This corrosion pitting has lead to blade failures. Compressor blades in many cases have over 100,000 hours but due to pitting can be reduced considerably to between 20,000–60,000 hours. It has been a very common practice for over 30 years to coat at least the first five to eight stages depending on the compressor design. The first stages are considered to be the "wet stages" due to the fact that many units now use on-line water washes, as well as have evaporative cooling and fogging for power augmentation.

Coating for these blades is usually consistent of a duplex type coating, which must be at least three mils in thickness. This coatings, as in on most typical coatings, have a sacrificial undercoating which is placed on the base metal and ceramic coating. Ni-Cd coating is also used in selected applications, and later for new coating usually consisting a of an aluminum slurry coating which has a protective ceramic top layer that provides improved erosion resistance. This type of coating as compared to a conventional aluminum slurry coating is better in corrosion protection and substantially better in erosion resistance. This type of coating also improves the performance of the gas turbine by reducing the amount of power consumed by the compressor. Tests conducted show a reduction of 2%–3% in the power consumed by the compressor which pays back additional cost of coating in four to six months of operation.

The aspect ratio of axial flow compressors including the IGV vary from about $AR=4$, to an aspect ratio of about $AR=0.5$. All IGV's and the first five to eight stages of rotating and stationary airfoils in the compressor are made from Martensitic High Temperature Stainless Steel; or 15-5 PH nominal blade material. The next stages are usually coated AISI 403 or 403 Cb.

Acknowledgments

The author would like to express his sincere thanks to Dr. Choon Sooi Tan and Dr. Yifang Gong for their contributions to the sections on Stall Flutter and Compressor Performance Parameters. Dr. Tan is a senior research engineer, and Dr. Gong is a research engineer at the MIT Gas Turbine Laboratory.

Dr. Tan is a leading authority on unsteady and three-dimensional flow in multistage Turbomachinery and is an author of 38 publications and a co-author of the book entitled "Internal Flow: Concepts and Applications," Cambridge University Press, 2004.

Dr. Gong is an authority on compressor aerodynamics and instability in compressor/compression systems; he is presently working on the design and development of a gas turbine power plant using supercritical CO_2 as the working fluid.

Bibliography

Boyce, M.P., "Fluid Flow Phenomena in Dusty Air," (Thesis), University of Oklahoma Graduate College, 1969, p. 18.

Boyce M.P., Schiller, R.N., and Desai, A.R., "Study of Casing Treatment Effects in Axial-Flow Compressors," ASME Paper No. 74-GT-89, 1974.

Boyce, M.P., "Secondary Flows in Axial-Flow Compressors with Treated Blades," AGARD-CCP-214 pp. 5-1 to 5-13, 1977.

Boyce, M.P., "Transonic Axial-Flow Compressor." ASME Paper No. 67-GT-47, 1967.

Caltech Lecture Notes on Jet Propulsion JP121 Graduate Course (Instructor: Zukoski E.E.).

Carter, A.D.S., "The Low-Speed Performance of Related Aerofoils in Cascade," Rep. R.55, British NGTE, September, 1949.

Cumpsty, N.A., 1989, *Compressor Aerodynamics*, Longman Group UK Ltd., London, England.

Cumpsty, N.A., 1998, *Jet Propulsion*, Cambridge University Press, Cambridge, England.

Giamati, C.C., and Finger, H.B., "Design Velocity Distribution in Meridional Plane," NASA SP 36, Chapter VIII, 1965, p. 255.

Graham, R.W., and Guentert, E.C., "Compressor Stall and Blade Vibration," NASA SP 365, 1956, Chapter XI, p. 311.

Hatch, J.E., Giamati, C.C., and Jackson, R.J., "Application of Radial Equilibrium Condition to Axial-Flow Turbomachine Design Including Consideration of Change of Enthropy with Radius Downstream of Blade Row," NACA RM E54A20, 1954.

Herrig, L.J., Emery, J.C., and Erwin, J.R., "Systematic Two Dimensional Cascade Tests of NACA 65 Series Compressor Blades at Low Speed," NACA R.M. E 55H11, 1955.

Hill, P.G., Peterson, C.R., 1992, *Mechanics and Thermodynamics of Propulsion*, Second Edition, Addison-Wesley Publishing Company, Reading, MA.

Holmquist, L.O., and Rannie, W.D., "An Approximate Method of Calculating Three-Dimensional Flow in Axial Turbomachines" (Paper) Meeting Inst. Aero. Sci., New York, 24-28 January, 1955.

Kerrebrock, J.L., 1992, *Aircraft Engines and Gas Turbines*, MIT Press, Cambridge, MA.

Khalak, A., 2002, "A Framework for Futter Clearance of Aeroengine Blades," *Journal of Engineering for Gas Turbine and Power*, Vol 124, No. 4. Also ASME 2001-GT-0270, ASME Turbo Expo 2001, New Orleans, LA, 2001.

Lieblein, S., Schwenk, F.C., and Broderick, R.L., "Diffusion Factor for Estimating Losses and Limiting Blade Loading in Axial-Flow Compressor Blade Elements," NACA RM #53001, 1953.

Mellor, G., "The Aerodynamic Performance of Axial Compressor Cascades with Applications to Machine Design," (Sc. D. Thesis), M.I.T. Gas Turbine Lab, M.I.T. Rep. No. 38, 1957.

Mikolajczak, A.A., Arnoldi, R.A., Snyder, L.E., Stargardter, H., 1975, "Advances in Fan and Compressor Blade Flutter Analysis and Prediction," *Journal of Aircraft* 12.

Stewart, W.L., "Investigation of Compressible Flow Mixing Losses Obtained Downstream of a Blade Row," NACA RM E54120, 1954.

Copyrighted Materials
Copyright © 2012 Elsevier Retrieved from www.knovel.com

8 Radial-Inflow Turbines

Hydraulic Radial-Inflow Turbines

Radial-flow turbines have been used for a long time. The early turbines were radial-outflow turbines such as the Hero's turbine and the Ljungström-type outward flow radial turbine as shown in Figure 8-1. The Hero's turbine type is used as water sprinklers on lawns to wet them. A unique feature of the Ljungström turbine is that it does not have any stationary blade rows. The two rows of blades comprising each of the stages rotate in opposite directions, so that they can both be regarded as rotors.

The radial-inflow turbine has been used for many years. It first appeared as a practical power-producing unit in the hydraulic turbine field. The *Francis turbine* is the most common water turbine designed by James B. Francis in Lowell Massachusetts. It is an inward-flow reaction turbine that combines radial and axial-flow concepts. The inward-flow radial turbine covers tremendous ranges of power, rates of mass flow, and rotational speeds from very large Francis turbines used in hydroelectric power generation and developing hundreds of megawatts down to tiny closed cycle gas turbines for space power generation of a few kilowatts.

Francis turbines are the most common water turbine in use today. They operate in a head range of 10–650 m and are primarily used for electrical power production. The power output ranges from 10 to 750 MW, with the exception of mini-river hydros. A casement is needed to contain the water flow. The turbine is located between the high-pressure water source and the low-pressure water exit, usually at the base of a dam. The inlet is spiral shaped. Guide vanes direct the water tangentially to the turbine wheel, known as a *runner*. This radial-flow acts on the runner's vanes, causing the runner to spin. The guide vanes (or wicket gate) may be adjustable to allow efficient turbine operation for a range of water flow conditions. Figure 8-2 is a schematic representation of a Francis turbine with a parts list. Runner diameters are between 1 and 10 m. The speed range of the turbine is from 83 to 1,000 rpm. Medium- and large-sized Francis turbines are most often arranged with a vertical shaft. The vertical shaft may also be used for small-size turbines, but normally they have a horizontal shaft.

Figure 8-3 shows one of the Francis turbine's scroll and runner turbines used at the Coulee Dam. Figure 8-4 is a runner used in one of the 26 turbines at the Three Gorges Dam that spans the Yangtze River. It is the largest power station in terms of installed capacity of 18,200 MW and was completed 30 October, 2008.

Gas Turbine Engineering Handbook, Fourth Edition. DOI: 10.1016/B978-0-12-383842-1.00008-1
Copyright © 2012 Elsevier Inc. All rights reserved.

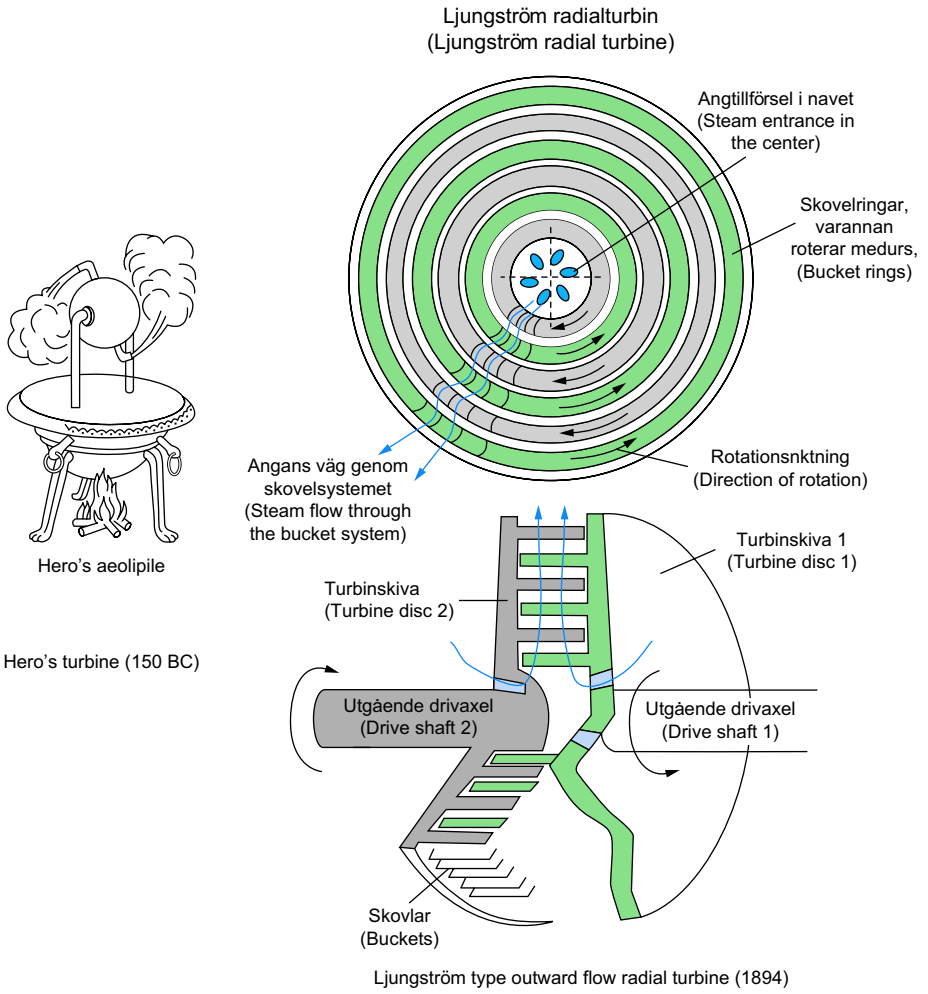
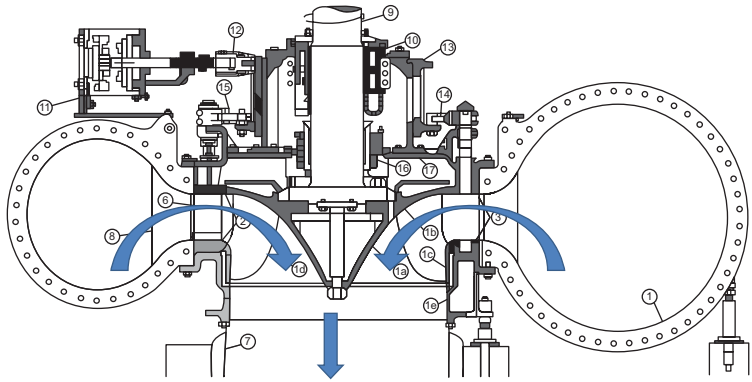


Figure 8-1 Early radial-outflow turbines.

Radial-Inflow Turbines for Gas Applications

The radial-inflow turbine for gas turbine application is basically a centrifugal compressor with reversed flow and opposite rotation, the radial-flow turbine was the first used in jet engine flight in the late 1930s. It was considered the natural combination for centrifugal compressor used in the same engine. Designers thought it easier to match the thrust from the two rotors and that the turbine would have a higher efficiency than a compressor for the same rotor because of the accelerating nature of the flow.

The performance of the radial-inflow turbine is now being investigated with more interest by the transportation and chemical industries. In transportation, this turbine is used in turbochargers for both spark ignition and diesel engines; in aviation, the



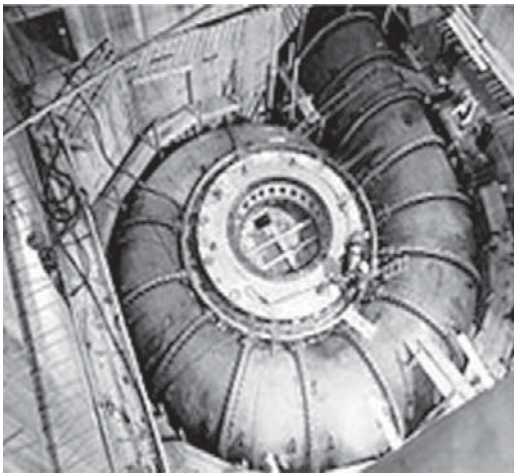
Parts list for Francis and Kaplan turbine drawings			
1	Turbine runner	7	Draft tube
1a	Runner cone	8	Discharge ring
1b	Runner crown (Francis)	9	Turbine shaft
1c	Runner band (Francis)	10	Turbine guide bearing
1d	Runner bucket (Francis)	11	Wicket gate servomotors
1e	Runner hub (Kaplan)	12	Servomotor connecting rod
1f	Runner blade (Kaplan)	13	Wicket gate operating ring or shift ring
2	Wearing rings or seal rings (Francis)	14	Wicket gate link
3	Facing plates or curb plates	15	Wicket gate arm
4	Spiral case or scroll case	16	Packing box or stuffing box (Mechnaical Seals)
5	Stary vane	17	Head cover
6	Wicket gate	18	Runner blade servomotor (Kaplan)

Figure 8-2 A cross section of a typical Francis turbine.

radial-inflow turbine is used as an expander in environmental control systems; and in the petrochemical industry, it is used in expander designs, gas liquefaction expanders, and other cryogenic systems. Radial-flow turbines are also used in various small gas turbines to power helicopters and as standby generating units.

The radial-inflow turbine is a rugged turbine often used as the hot gas expander of gases in a refinery. It is designed to run under severe gas conditions and continuously, year after year, in extreme conditions with the primary objective of reliability and ease of operation. Refinery gas often has particulates in the gas stream, and even after they have been removed the gas is still full of micron-size particles. Recovering energy from process pressure drops makes economic sense. Special expanders are used in combined cycle plants where the inlet gas pressure has to be lowered before it can be injected into the gas turbine. Waste heat, pressure let down, and hydrocarbon compression are only few of the many applications, and multiple expanders are used for applications in the excess of 15 MW.

The radial-inflow turbine's greatest advantage is that the work produced by a single stage is equivalent to that of two or more stages in an axial turbine. This phenomenon



Francis inlet scroll



Francis runner

Figure 8-3 The Francis turbine used in the Grand Coulee Dam.



Three Gorges dam (18,200 MW)



A typical runner for one of the 26 turbines

Figure 8-4 The Francis turbine used at the Three Gorges Dam in China.

occurs because a radial-flow turbine usually has a higher tip speed than an axial turbine. Since the power output is a function of the square of the tip speed ($P \propto U^2$) for a given flow rate, the work is greater than that in a single-stage axial-flow turbine.

The radial-inflow turbine has another advantage: its cost is much lower than that of a single- or multistage axial-flow turbine. The radial-inflow turbine has lower turbine efficiency than the axial-flow turbine; however, lower initial costs may be an incentive to choose a radial-inflow turbine (5,6).

The radial-inflow turbine is especially attractive when the Reynolds number ($\mathrm{Re} = \rho UD/\mu$) becomes low enough ($\mathrm{R} = 10^5 - 10^6$) that the efficiency of the axial-flow turbine is lesser than that of a radial-inflow turbine, as shown in Figure 8-5.

The effect of specific speed ($N_s = N\sqrt{Q}/H^{0.75}$) and specific diameter ($D_s = DH^{0.25}/\sqrt{Q}$) on the efficiency of a turbine is shown in Figure 8-6. Radial-inflow turbines are more efficient at a Reynolds number between 10^5 and 10^6 and specific speeds below $N_s = 10$.

Turbine Configurations

The radial-inflow turbine has many components similar to those of a centrifugal compressor. However, their names and functions differ. There are two types of

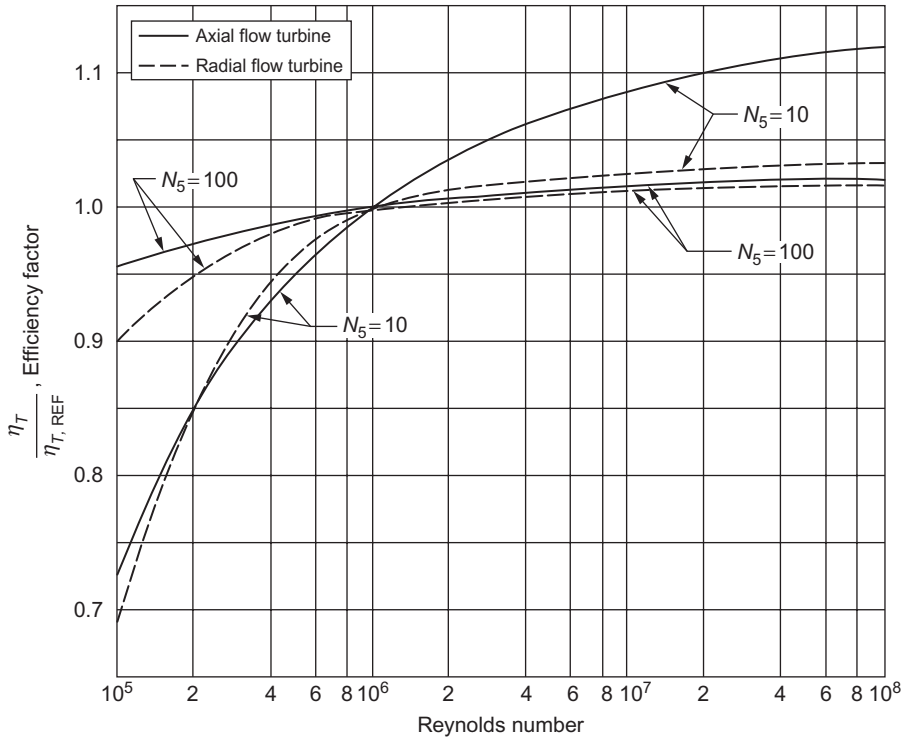


Figure 8-5 Influence of Reynolds number on turbine stage efficiency.

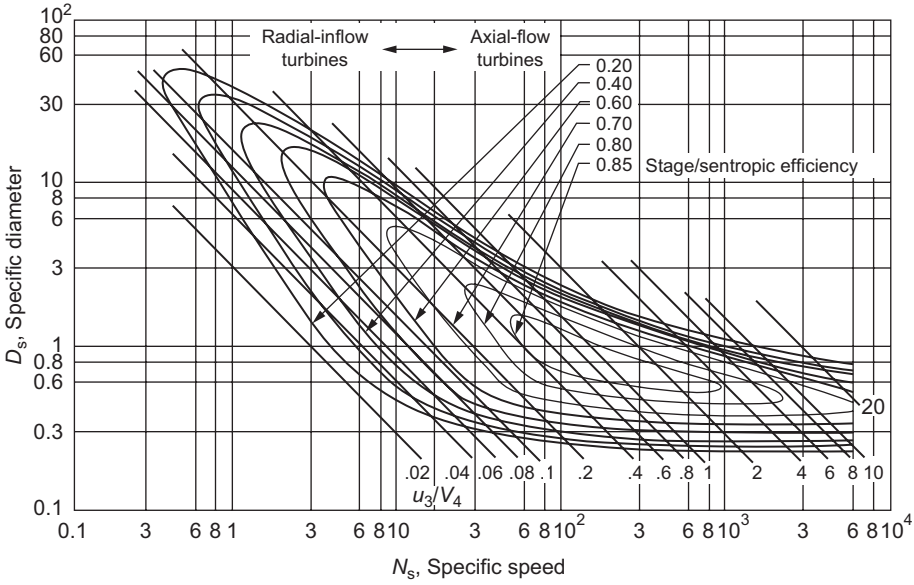


Figure 8-6 N_s versus D_s diagram for a turbine stage. Efficiency is on a total-to-total basis; that is, it is related to inlet and exit stagnation conditions. Diagram values are suitable for machine Reynolds number Re $> 10^6$ (Balje, 1964).

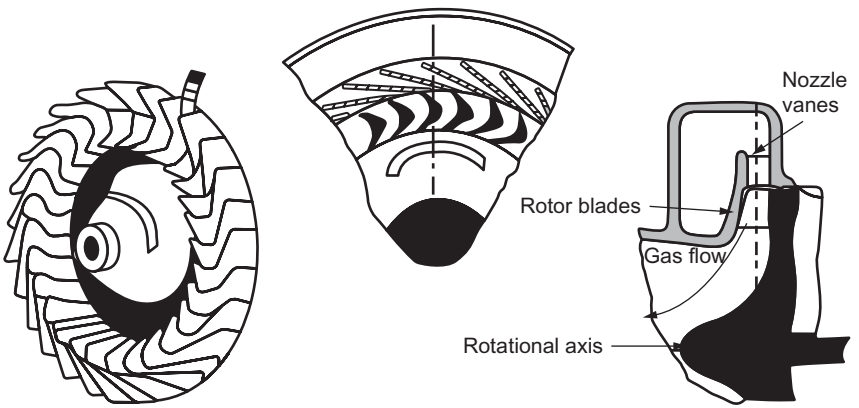


Figure 8-7 Cantilever-type radial-inflow turbine.

radial-inflow turbines: the cantilever radial-inflow turbine and the mixed-flow radial-inflow turbine. Cantilever blades are often two-dimensional and use non-radial inlet angles. There is no acceleration of the flow through the rotor, which is equivalent to an impulse or a low-reaction turbine. The cantilever-type radial-inflow turbine is infrequently used because of low efficiency and production difficulties. This type of turbine also has rotor blade flutter problems.

The radial-inflow turbine can be the cantilever type as shown in Figure 8-7. Aerodynamically, the cantilever turbine is similar to an axial-impulse turbine and can even be designed by similar methods. Figure 8-8 shows the velocity triangles at rotor inlet and outlet. In this case, the relative velocities entering and leaving the turbine are about equal except for the loss due to blade friction. The fact that the flow is radially inward hardly alters the design procedure, because the blade radius ratio r_2/r_3 is close to unity. The absolute velocity leaving the turbine is axial to get minimal exit loss; thus, the tangential component of the absolute velocity is zero. From the velocity triangles in Figure 8-4, the tangential component of the absolute inlet velocity is $2U_2$. Thus, the output for this turbine would be approximately equal to $2[U_2]^2$.

The mixed-flow radial-inflow turbine and the radial-inflow turbine have slight differences at the blade inlet as shown in Figure 8-9. The radial-inflow turbine has a full 90° change from the inlet to the exit as the blades are in a radial position. In the mixed-flow impeller, the blade inlet is at a 45° angle with the axis. The mixed-flow

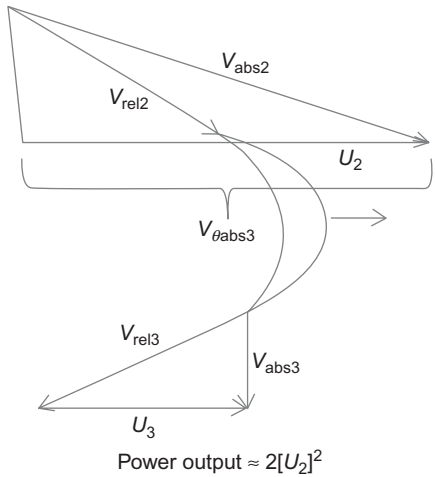


Figure 8-8 Velocity triangles for a cantilever-type radial-inflow turbine.

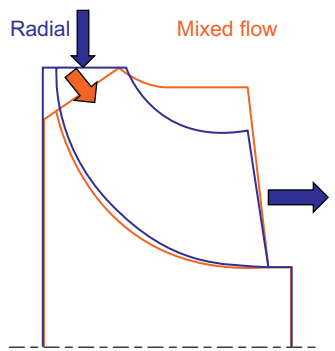


Figure 8-9 Meridional cross section of radial- and mixed-flow impellers.

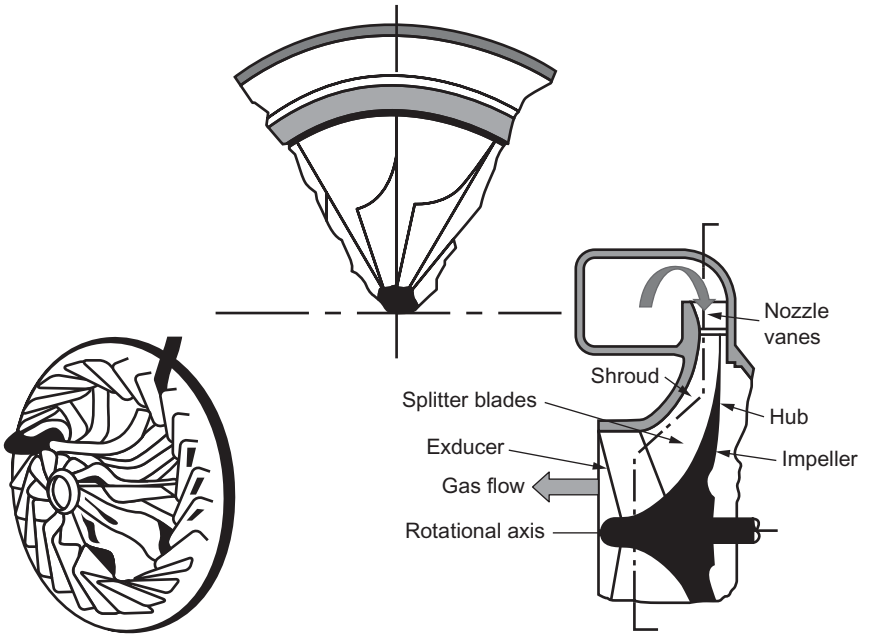


Figure 8-10 Nomenclature of radial- and mixed-inflow type turbine.

impeller has an advantage in the moment of inertia over the radial turbine. Both the designs are widely used. Figure 8-10 shows the components of a mixed- and radial-inflow turbine. The scroll or collector receives the flow from a single duct. The scroll usually has a decreasing cross-sectional area around the circumference. In some designs, the scrolls are used as vaneless nozzles. The nozzle vanes are omitted for economy to avoid erosion in turbines where fluid or solid particles are trapped in the air flow. Frictional flow losses in vaneless designs are greater than that in vaned nozzle designs because of the non-uniformity of the flow and the greater distance the accelerating air flow must travel. Vaneless nozzle configurations are used extensively in turbochargers in which efficiency is not important, since in most engines the amount of energy in the exhaust gases far exceeds the energy needs of the turbocharger.

The mixed-flow and the radial-flow type of turbine have higher structural strength as compared with the cantilever turbine, and hence the axial-outflow (90°) mixed-flow radial-inflow turbine is the preferred type. The blades at the inlet of the impeller are generally radial blades (blade angle = 0), a fact dictated by the material strength and often high gas temperature. The rotor vanes are subject to high stress levels caused by the centrifugal force field, together with a pulsating and often unsteady gas flow at high temperatures. Despite possible performance gains, the use of non-radial (or backward swept) vanes is generally avoided, mainly because of the additional stresses that arise due to bending. However, there are designs that have used swept-back vanes to increase the work output of the radial-inflow turbines.



Figure 8-11 Different types of radial turbine scallops.

There are also many designs that have scalloped hubs at the inlet of the impeller to ensure that there is no failure of the hub material at the inlet due to the very high temperatures, as shown in Figure 8-11. Scallops in radial turbines cause a reduction in peak efficiency of between 2% and 4%. The geometric difference between the high and low efficiency reductions was a relatively minor reduction in the scallop step. Heavy scalloping, as shown in Figure 8-12, is used in many turbocharger designs. It reduces the moment of inertia reduction by nearly 45%, which is a big advantage for stop and start applications. The impeller efficiency is reduced by only about 6%, which does not affect the engine performance since there is usually considerable waste heat in the engine exhaust. It also allows materials to be used, which due to the material properties cannot take very high temperature, and therefore are less costly. Other techniques of cooling can be accomplished by providing cooling air from a supplementary source to the impellers back surface and the radial inlet impeller blade tips as shown in Figure 8-13. Here, the cooling air is impinged on the rotor and vane tips.

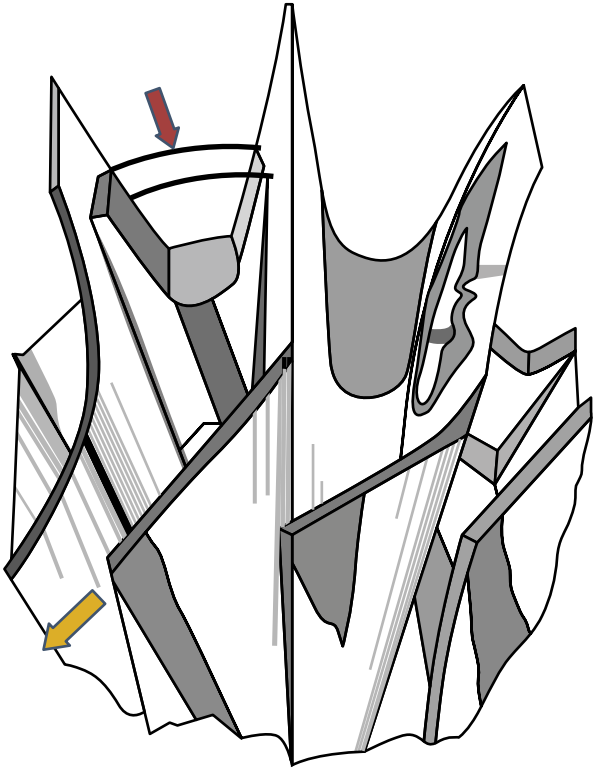


Figure 8-12 Deep scallops used mainly in radial-inflow turbines in turbo chargers.

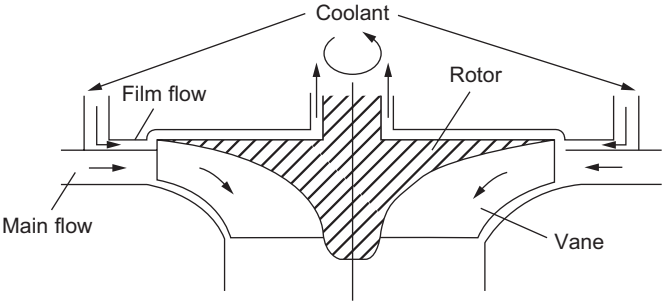


Figure 8-13 Radial impeller with coolant air flow on the back face of the impeller.

The nozzle blades in a vaned turbine design are usually fitted around the rotor to direct the flow inward with the desired whirl component in the inlet velocity. The flow is accelerated through these blades. In low-reaction turbines, the entire acceleration occurs in the nozzle vanes. Figure 8-14 is a diagram of a radial-inflow turbine with adjustable nozzle blades. The impeller wheel shown in this figure is a

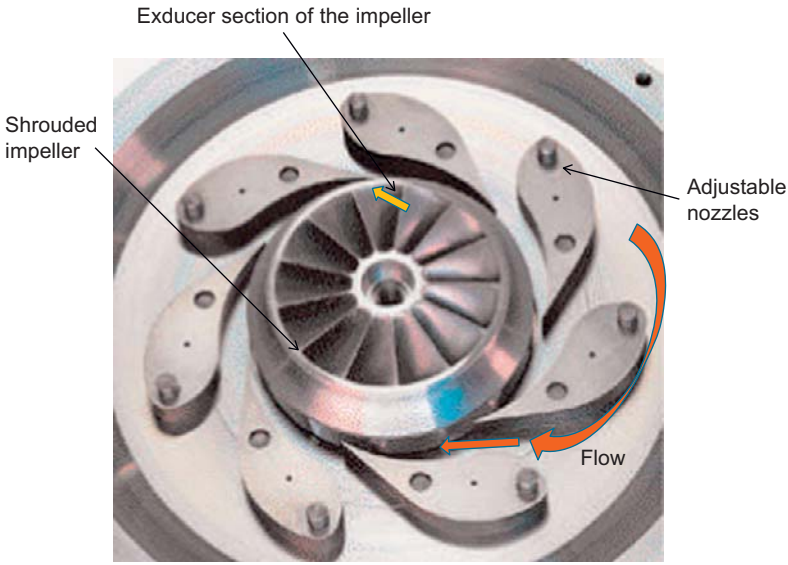


Figure 8-14 Diagram of a shrouded radial-inflow turbine with adjustable nozzle blades.

shrouded radial-inflow impeller. Variable area nozzles are used to control the flow capacity of radial turbines in hydraulic turbines, power recovery turbines, and cryogenic expanders. The widespread adoption of variable geometry turbines for diesel engine turbochargers has been the major factor in increasing the commercial use of this technology. Variable area is commonly, but not exclusively, achieved by pivoting the nozzle vanes about an axis disposed in the span-wise direction. The ability to move the nozzle vanes in this way requires a clearance gap between the vanes and the stationary sidewalls. Such a gap allows fluid to leak from the blade passage, and this leakage causes a loss of efficiency for the turbine. To limit the loss, it is important to minimize the clearance gap, but at the same time, a certain space is required in order to ensure reliable operation of the variable nozzle vanes. This is particularly challenging in a hot gas environment, such as a turbocharger, where the thermal growth of the housing in operation, and fouling due to soot particles, can be significant.

The rotor or impeller of the radial-inflow turbine consists of a hub, blades, and in some cases, a shroud. Figure 8-15 is a sketch of an open-face radial-inflow impeller with splitter vanes and fixed nozzles. This impeller has splitter blades to guide the flow better. The splitter blades start at the entrance of the impeller and end at the start of the exducer. The hub is the solid axi-symmetrical portion of the rotor. It defines the inner boundary of the flow passage and is sometimes called the disc. The blades are integral to the hub and exert a normal force on the flow stream. The exit section of the blading is called an exducer and it is constructed separately like an inducer in a centrifugal compressor. The exducer is curved to remove some of the tangential velocity force at the outlet.

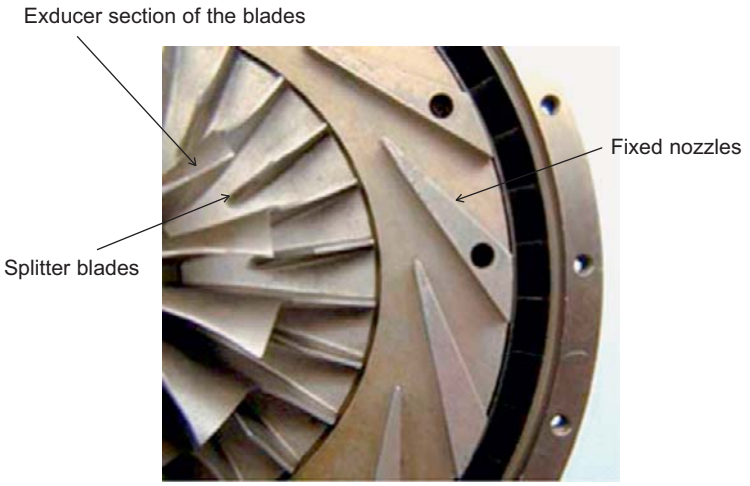


Figure 8-15 An open-faced radial-inflow impeller with splitter vanes.

The outlet diffuser is used to convert the high absolute velocity leaving the exducer into static pressure. If this conversion is not done, the efficiency of the unit will be low. This conversion of the flow to a static head must be done carefully, since the low-energy boundary layers cannot tolerate great adverse pressure gradients.

Thermodynamic and Aerodynamic Theory

The general principles of energy transfer in a radial-inflow turbine are similar to those already outlined in Chapter 3. These are governed by the following basic equations:

1. Equation of state
2. Conservation of energy
3. Momentum equation
4. Energy equation

The momentum equation is transformed to the cylindrical coordinate system (r–θ–z), and Figure 8-16 shows the velocity vectors in turbine rotor flow. The Euler turbine equation previously derived in Chapter 3 using the relationships of the above named equations holds for flow in any turbomachine. Figure 8-17 shows the nomenclature and relates the numerical flow positions that match the following equations in this section:

$$H = \frac{1}{g_c}(U_3 V_{\theta 3} - U_4 V_{\theta 4}) \tag{8-1}$$

where

U = blade speed

V_θ = tangential component of the absolute velocity

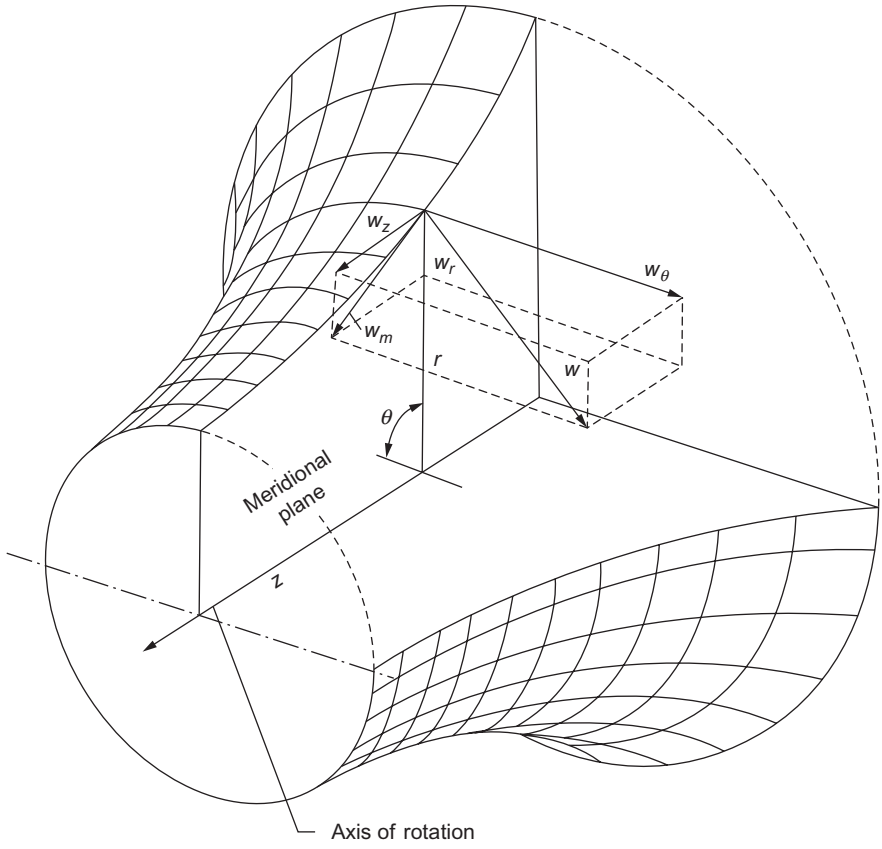


Figure 8-16 Velocity vectors in turbine rotor flow.

subscripts three and four represent the conditions at the inlet and exit of the impeller, respectively

It may be written in terms of the absolute and relative velocities:

$$H = \frac{1}{2g_c}\left[\left(U_3 - U_4^2\right) + \left(V_3^2 - V_4^2\right) + \left(W_4^2 - W_3^2\right)\right] \tag{8-2}$$

where

U = blade speed
V = absolute velocity
W = relative velocity
subscripts three and four represent the conditions at the inlet and exit of the impeller, respectively

For a positive power output, this indicates that power is being transmitted, the blade tip speed and whirl velocity combination at the inlet must be greater than that at the

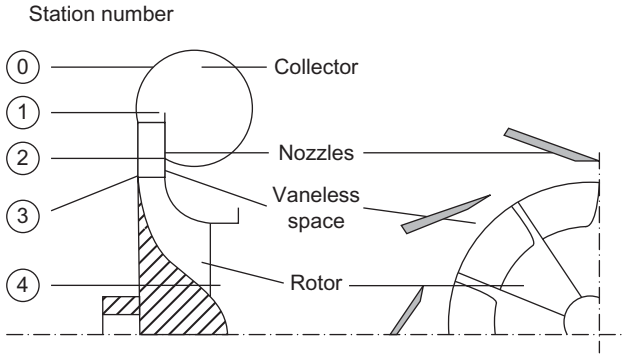


Figure 8-17 Nomenclature and numerical positions for components of a radial-inflow turbine.

exit. From Equation 8-2, the flow must be radially inward, so that centrifugal effects may be used. The velocity exiting from a turbine is considered to be unrecoverable; therefore, the utilization factor is defined as the ratio of the total head to the total head plus the absolute exit velocity:

$$\epsilon = \frac{H}{H + \left(\frac{1}{2} V_4{}^2\right)} \tag{8-3}$$

where

H = total adiabatic head

V_4 = absolute velocity of the gas at the exit

The relative proportions of energy transfers obtained by a change of static and dynamic pressure are used to classify turbomachinery. The parameter used to describe this relationship is called the degree of reaction. In this case, reaction is energy transfer by means of a change in static pressure in a rotor to the total energy transfer in the rotor.

$$R = \frac{\frac{1}{2g}\left[\left(U_3{}^2 - U_4{}^2\right) + \left(W_4{}^2 - W_3{}^2\right)\right]}{H} \tag{8-4}$$

The overall efficiency of a radial-inflow turbine is a function of efficiencies from various components such as the nozzle and rotor. A typical turbine expansion enthalpy/entropy diagram is shown in Figure 8-18. The total enthalpy remains constant throughout the nozzle, since neither work nor heat is transferred to or from the fluid. The total enthalpy changes within the rotor. Downstream of the rotor, the total enthalpy remains constant. Total pressure decrease in the nozzle and outlet diffuser is only from frictional losses. In an ideal nozzle or diffuser, the total pressure drop is zero. Isentropic efficiency (η_{is}) is defined as the ratio of the actual work to the

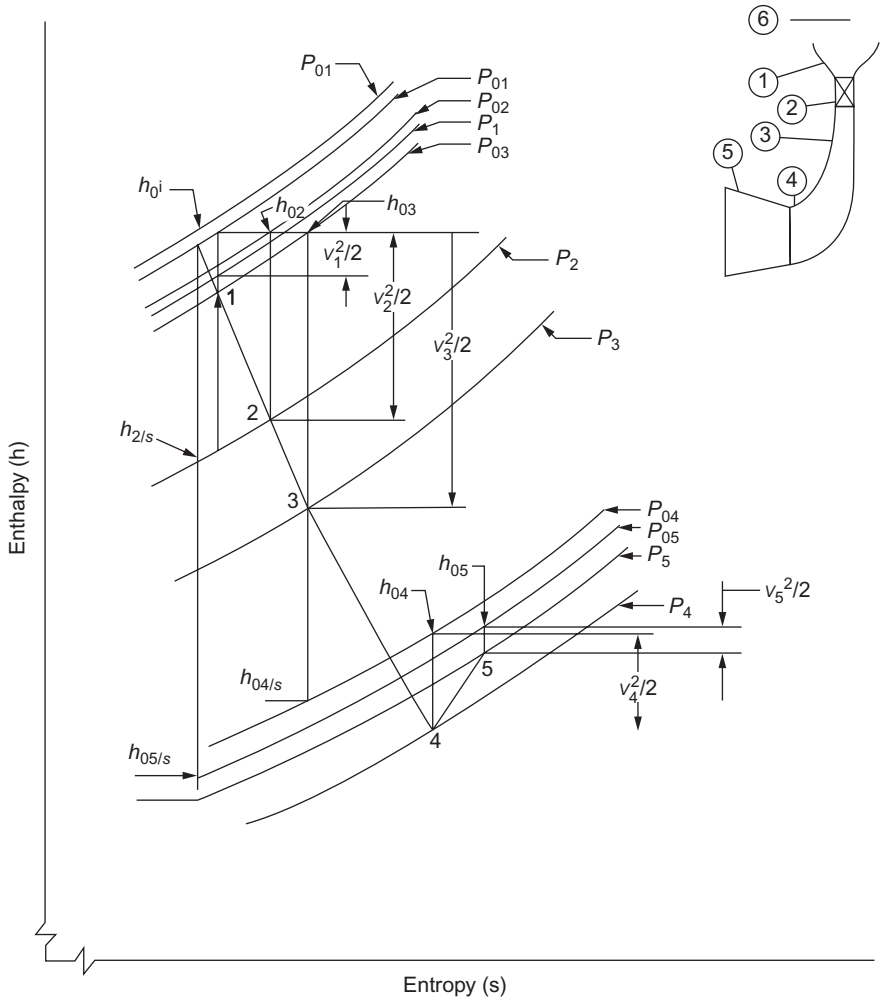


Figure 8-18 Enthalpy–entropy for a radial-inflow single stage.

isentropic enthalpy decrease, which is the expansion from the inlet total pressure to the outlet total pressure:

$$\eta_{\text{is}} = \frac{h_{0i} - h_{05}}{h_{0i} - h_{05_{\text{is}}}} \tag{8-5}$$

where

$h_0 =$ total enthalpy

subscripts represent the conditions at the points shown in the Figures 8-17 and 8-18.

The nozzle efficiency can be calculated as shown in the following relationship:

$$\eta_{\text{noz}} = \frac{h_{0i} - h_2}{h_{0i} - h_{2\text{is}}} \tag{8-6}$$

where

h_0 = total enthalpy

subscripts represent the conditions at the points shown in Figures 8-17 and 8-18.

The rotor efficiency can be defined as shown in the following relationship:

$$\eta_{\text{rotor}} = \frac{h_{0i} - h_4}{h_{0i} - h_{4\text{is}}} \tag{8-7}$$

where

h_0 = total enthalpy

subscripts represent the conditions at the points shown in Figures 8-17 and 8-18.

Similar to the concept of small-stage efficiency in a compressor, the polytropic efficiency in a turbine is the small-stage efficiency in a turbine. The isentropic efficiency can be written in terms of the total pressure as follows:

$$\eta_{\text{is}} = \frac{1 - \left(\frac{P_{05}}{P_{0i}}\right)^{\frac{n-1}{n}}}{1 - \left(\frac{P_{05}}{P_{0i}}\right)^{\frac{\gamma-1}{\gamma}}} \tag{8-8}$$

where

P_0 = total pressure

n = polytropic exponent

γ = isentropic exponent = ratio of specific heats = c_p/c_v

subscripts represent the conditions at the points shown in Figures 8-17 and 8-18.

The equation of state P/ρ^n = constant, represents the polytropic process for any particular expansion process. When $n = \gamma$, the process is an ideal isentropic process. The polytropic efficiency can be written as follows:

$$\begin{aligned} \eta_{\text{poly}} &= \frac{dh_{0\text{act}}}{dh_{0\text{isen}}} \\ &= \frac{1 - \left[1 - \frac{n-1}{n}\left(\frac{\Delta P_0}{P_{0i}}\right), \ldots,\right]}{1 - \left[1 - \frac{\gamma-1}{\gamma}\left(\frac{\Delta P_{0i}}{P_{0i}}\right), \ldots,\right]} \\ &= \left(\frac{n-1}{n}\right) \Big/ \left(\frac{\gamma-1}{\gamma}\right) \end{aligned} \tag{8-9}$$

The polytropic efficiency in a turbine can be related to the isentropic efficiency and obtained by combining the previous two equations:

$$\eta_{is} = \frac{1 - \left(\frac{P_{05}}{P_{0i}}\right)^{\eta_{poly}\frac{\gamma-1}{\gamma}}}{1 - \left(\frac{P_{05}}{P_{0i}}\right)^{\frac{\gamma-1}{\gamma}}} \tag{8-10}$$

$$\eta_{poly} = \frac{\ln\left[1 - \eta_{is} + \eta_{is}\left(\frac{P_{05}}{P_{0i}}\right)^{\frac{\gamma-1}{\gamma}}\right]}{\left(\frac{\gamma-1}{\gamma}\right)\ln\left(\frac{P_{05}}{P_{0i}}\right)} \tag{8-11}$$

The relationship between the two efficiencies is plotted in Figure 8-19. The multistage turbine on an enthalpy/entropy diagram is shown in Figure 8-20. Examining

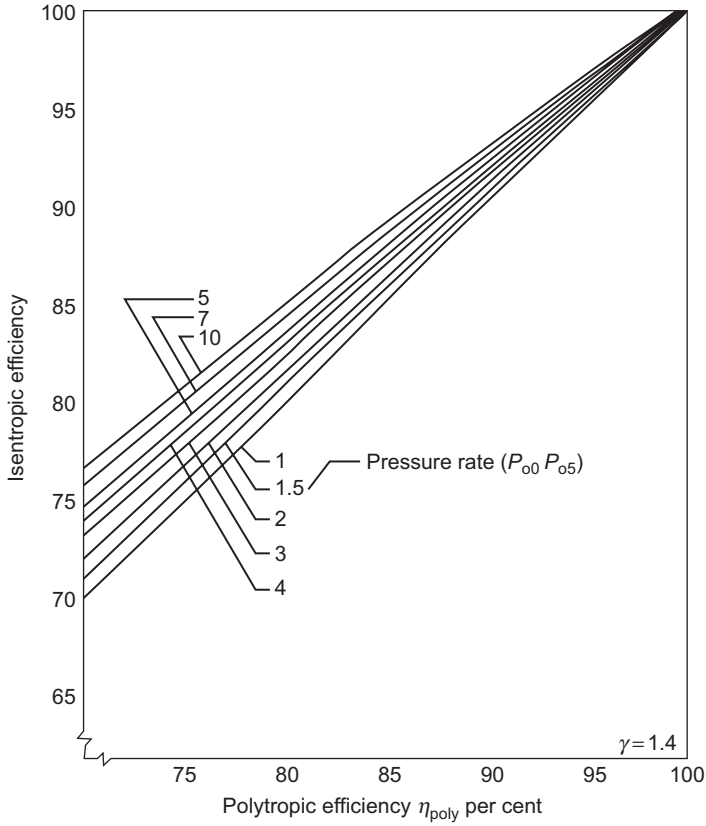


Figure 8-19 Relationship between polytropic and isentropic efficiency during expansion.

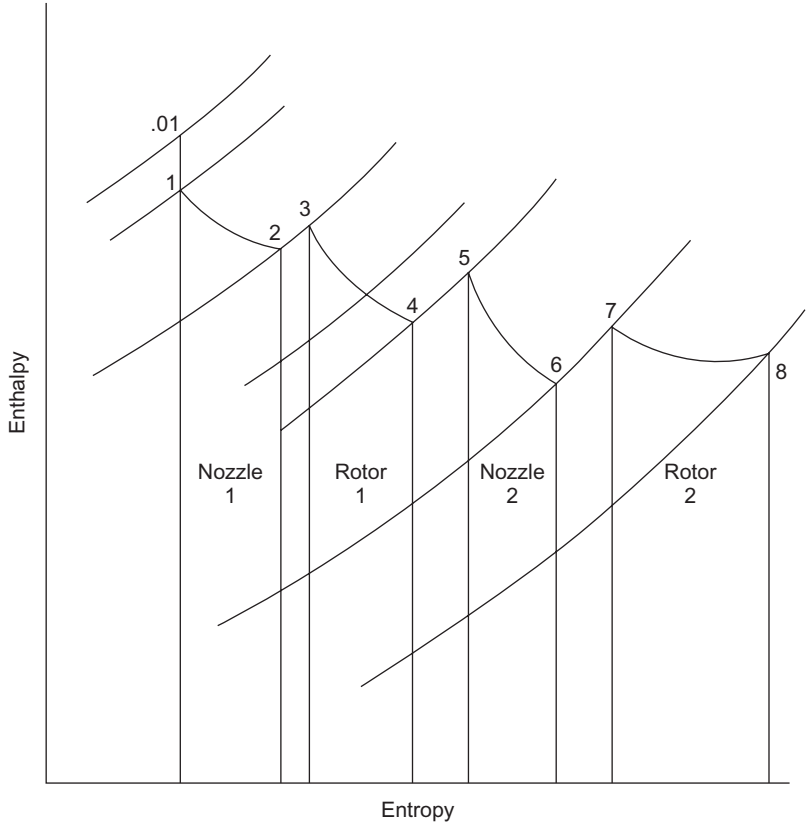


Figure 8-20 Enthalpy–entropy diagram for a multistage turbine.

the characteristic of the multistage unit, the isentropic enthalpy decrease of the incremental stages as compared to the isentropic enthalpy decrease of a single whole stage (which encompasses the multistages) is defined as the reheat factor. Since the pressure lines diverge as entropy increases, the sum of the small-stage isentropic decreases is somewhat greater than the overall isentropic decrease for the same pressure. Hence, the reheat factor is greater than unity, and the turbine's isentropic efficiency is greater than the polytropic efficiency of the turbine. The reheat factor is a ratio of the isentropic efficiency to the polytropic efficiency:

$$R_f = \frac{\eta_{\text{isen}}}{\eta_{\text{poly}}} \tag{8-12}$$

Turbine Design Considerations

To design a radial-inflow turbine of the highest efficiency, the exit velocity leaving the turbine must be axial. If the exit velocity is axial, the Euler turbine equation

reduces to:

$$H = U_3 V_{\theta 3} \tag{8-13}$$

since the tangential component $V_{\theta 4} = 0$ for the axial outlet velocity.

The flow entering the rotor of a radial-inflow turbine must have a certain incidence angle corresponding to the "slip flow" in a centrifugal impeller and not to zero incidence. By relating this concept to the radial-inflow turbine, the following relationship can be obtained for the ratio of whirl velocity to blade tip speed:

$$\frac{V_{\theta 3}}{U_3} = \left[1 - \frac{\pi}{2N_{\text{blades}}} \frac{D_3}{D_3 - D_4}\right] \tag{8-14}$$

This ratio is usually in the neighborhood of 0.8. A ratio of D_3/D_4 for radial-inflow rotors is around 2.2, and N_{blades} is the number of blades.

With the aid of the previous relationships, a velocity diagram for the flow entering a radial-inflow turbine can be drawn as shown in Figure 8-21.

The variation in stage efficiency can be shown as a function of the tip speed ratio. The tip speed ratio is a function of the blade speed and the theoretical spouting velocity if the entire enthalpy drop takes place in the nozzle as given by the following equation:

$$\phi = \frac{U}{V_\circ} \tag{8-15}$$

Figure 8-22 shows the efficiency variation with the tip speed ratio. This curve also shows the runaway speed. Runaway speed is achieved when turbine torque falls to

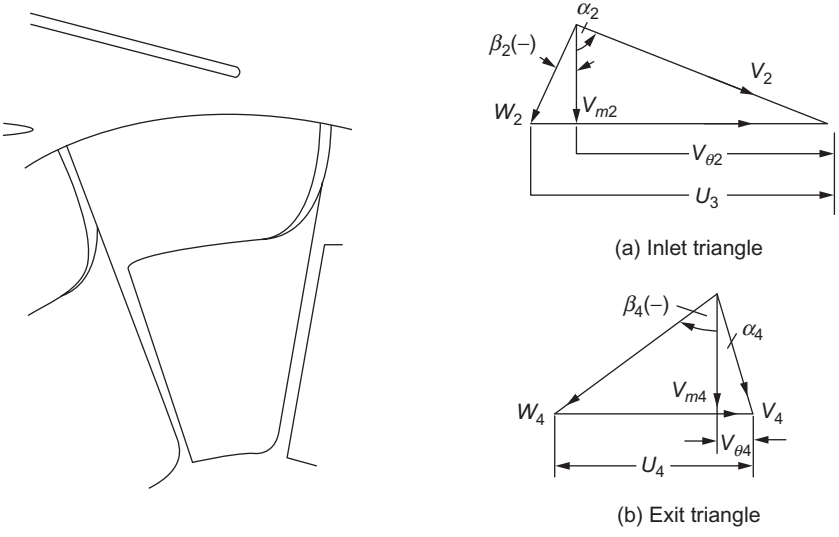


Figure 8-21 Velocity triangles for a radial-inflow turbine.

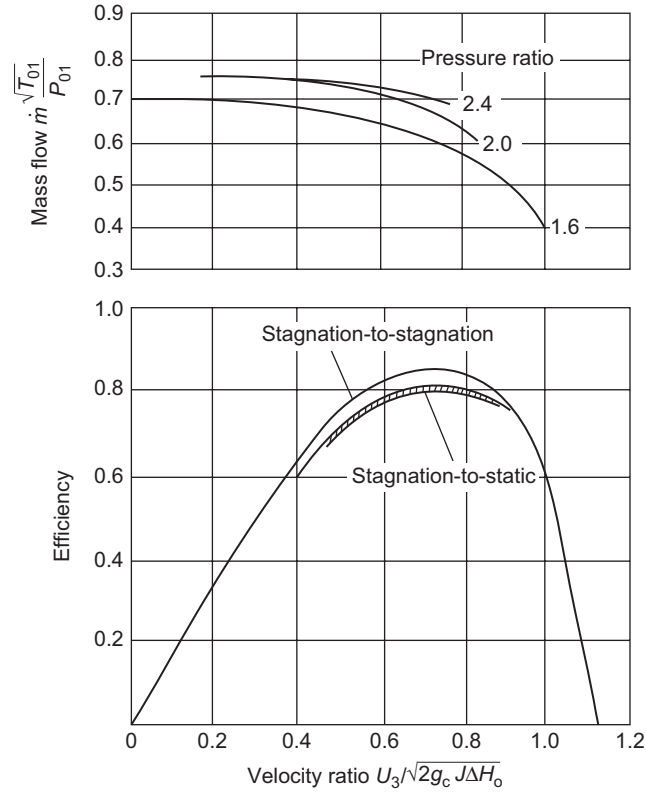


Figure 8-22 An example of a radial-inflow turbine characteristic (courtesy Institution of Mechanical Engineers).

zero at blade speeds higher than the design speed. If failure occurs above the tip speed, the rotor can be defined as a fail-safe rotor design.

The inlet area at the blade tip can be calculated using the continuity equation:

$$A_3 = \pi D_3 b_3 - \eta_B t_3 b_3 = \frac{\dot{m}}{\rho V_3 \cos\beta_3} \tag{8-16}$$

where b_3 is the blade height and t_3 the blade thickness.

At the exit of the turbine, the absolute exit velocity is axial. Since the blade speed varies at the exit from hub to shroud, a series of blade diagrams are obtained as shown in Figure 8-23.

Performance of a Radial-Inflow Turbine

A turbine is designed for a single operating condition called the design point. In many applications, the turbine is required to operate at conditions other than the design point. The turbine work output can be varied by adjusting the rotational speed, pressure ratio,

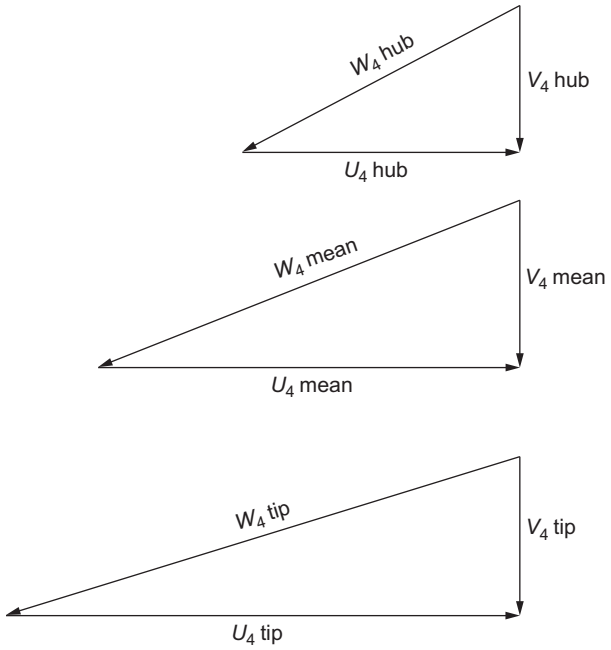
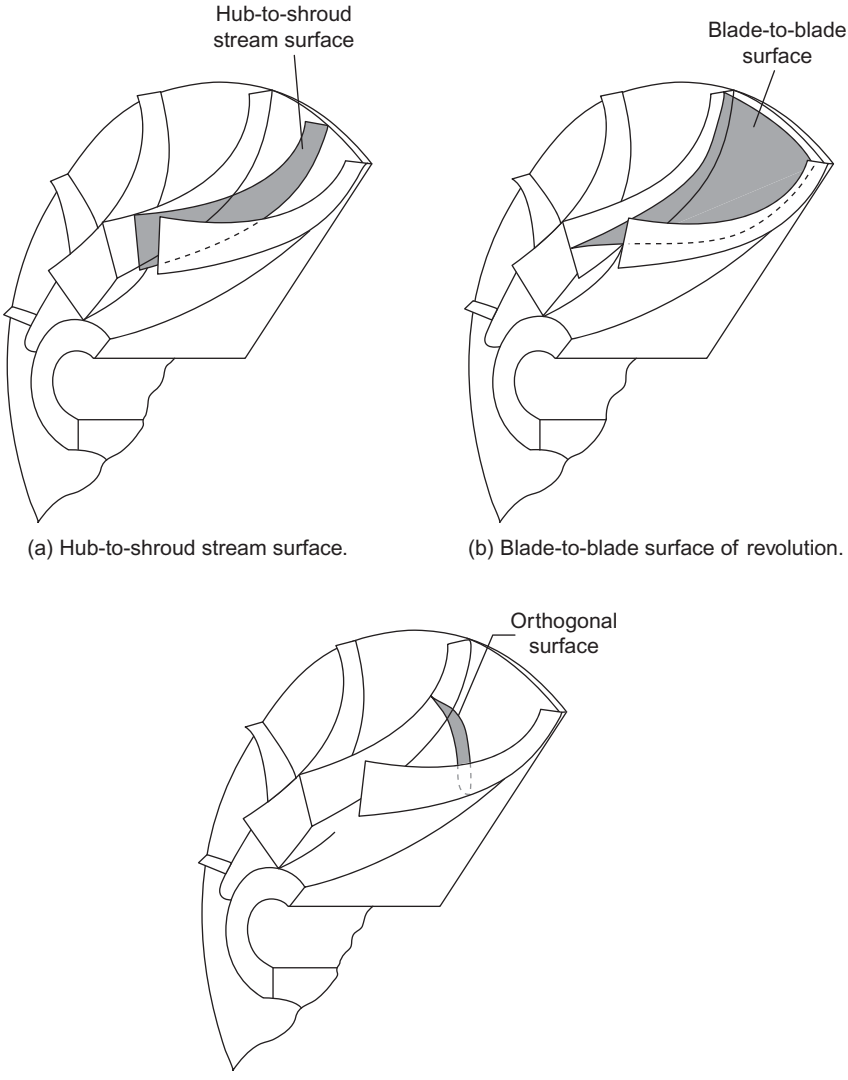


Figure 8-23 Exit velocity diagrams for a radial-inflow turbine.

and turbine inlet temperature. Under these different running conditions, the turbine is operating at off-design conditions.

To predict turbine characteristics, it is necessary to compute flow characteristics throughout the turbine. To perform this computation, the flow must be analyzed inside the blade passage. First, the three-dimensional flow is simplified to two-dimensional flow to provide solutions in the meridional, blade–blade, and orthogonal surfaces of blade passages. This analysis is done by first examining the flow in the meridional plane, sometimes called the hub-to-shroud plane as shown in Figure 8-24 (a). A solution is then obtained for the flow in the blade-to-blade plane as shown in Figure 8-24 (b), as it flows through the orthogonal surface as shown in Figure 8-24 (c). Once this solution is obtained, the flows in the two planes can be combined to give the final quasi-three-dimensional flow. The velocity distribution in the meridional plane varies between the hub and shroud as shown in Figure 8-25. The velocity distribution between the suction and pressure surfaces also varies. The velocity between the suction and pressure surfaces varies because the blades are working on the fluid and, as a result, there must be a pressure difference across the blade. The form of velocity distribution on the rotor blades at the hub and shroud and also between the pressure and suction sides is shown in Figure 8-26.

The boundary layer along the blade surfaces must be well energized so that no separation of the flow occurs. Figure 8-27 shows a schematic diagram of the flow in a radial-inflow impeller. Off-design work indicates that radial-inflow turbine efficiency is not affected by changes in flow and pressure ratio to the extent of an axial-flow turbine.



(a) Hub-to-shroud stream surface.

(b) Blade-to-blade surface of revolution.

(c) Orthogonal surface across flow passage.

Figure 8-24 Two dimensional surfaces for flow analysis in a radial-inflow turbine.

In a radial-inflow turbine, the problems of erosion and exducer blade vibration are prominent. The size of the particles being entrained decreases with the square root of the turbine wheel diameter. Inlet filtration is suggested for expanders in the petrochemical industry. The filter usually has to be an inertia type to remove most of the larger particles. The exducer fatigue problem is serious in a radial turbine, although it varies with blade loading. The exducer should be designed such that it has a natural frequency four times above the blade passing frequency.

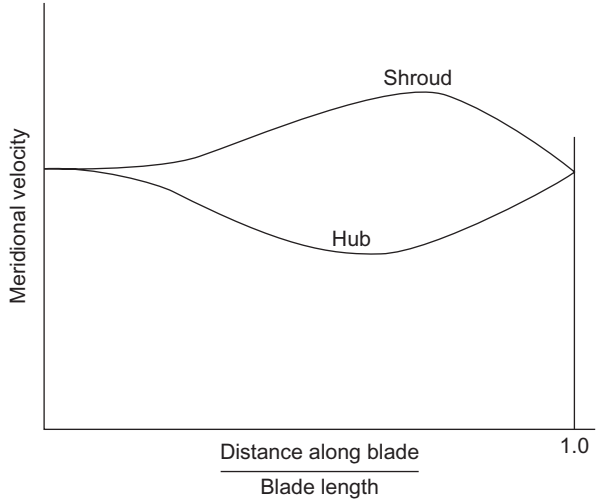


Figure 8-25 Meridional velocity distribution from hub to should along the blade length.

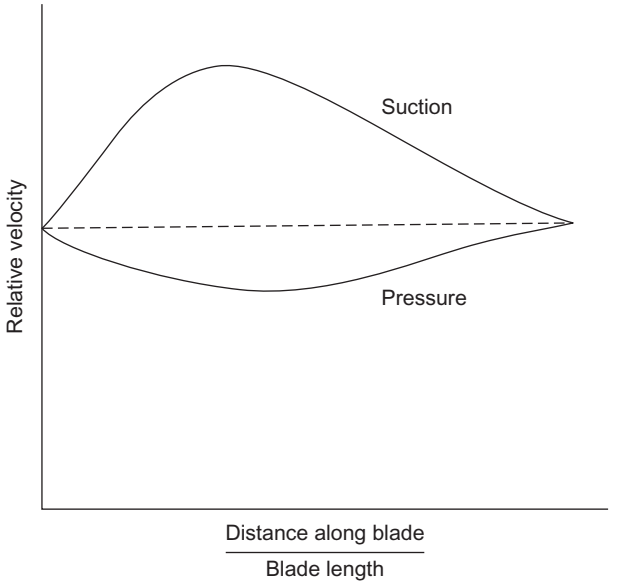


Figure 8-26 Relative velocity distribution of suction and pressure side along the blade length.

Noise problems in a radial-inflow turbine come from the following four sources:

1. Pressure fluctuations
2. Turbulence in boundary layers
3. Rotor wakes
4. External noise

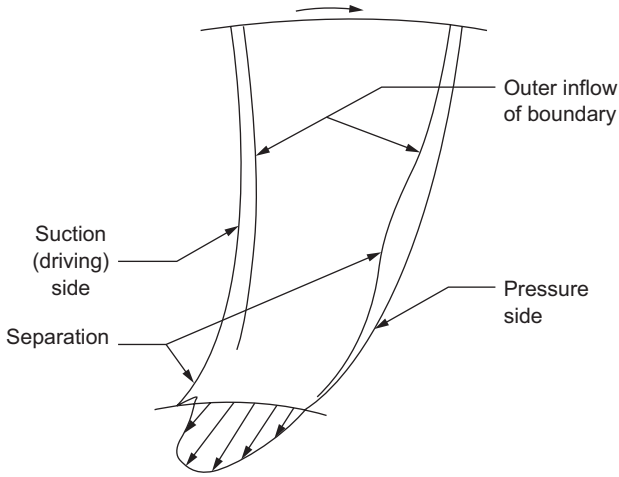


Figure 8-27 Boundary-layer formation in a radial-inflow impeller.

Severe noise can be generated by pressure fluctuations. This noise is created by the passage of the rotor blades through the varying velocity fields produced by the nozzles. The noise generated by turbulent flow in boundary layers occurs on most internal surfaces. However, this noise source is negligible. Noise generated from rotor flow is due to the wakes generated downstream in the diffuser. The noise generated by the rotor exducer is considerable. The noise consists of high-frequency components and is proportional to the eighth power of the relative velocity between the wake and the free stream. Outside noise sources are many, but the gear box is the primary source. Intense noise is generated by pressure fluctuations that result from tooth interactions in gearboxes. Other noises may result from out-of-balance conditions and vibratory effects on mechanical components and casings.

Losses in a Radial-Inflow Turbine

Losses in a radial-inflow turbine are similar to those in a centrifugal impeller, as outlined in Chapter 6. The losses can be divided into following major categories:

1. *Blade loading or diffusion loss.* This loss is due to the type of loading in an impeller. The increase in momentum loss comes from the rapid increase in boundary-layer growth when the velocity close to the wall is reduced. This loss varies from around 7% at a high-flow setting to about 12% at a low-flow setting.
2. *Frictional loss.* Frictional loss is due to wall shear forces. This loss varies from about 1% to 2% as the flow varies from a low-flow to a high-flow setting.
3. *Secondary loss.* This loss is caused by the movement of the boundary layers in a direction different from the main stream. This loss is small in a well-designed machine and is usually less than 1%.
4. *Clearance loss.* This loss is caused by flow passing between the stationary shroud and the rotor blades and is a function of the blade height and clearance. The clearance is usually

fixed by tolerances and, for smaller blade heights, the loss is usually a greater percentage. This loss varies between 1% and 2%.

5. *Heat loss.* This loss is due to heat lost to the walls from cooling.
6. *Incidence loss.* This loss is minimal at design conditions but will increase with off-design operation. These losses vary from about ½% to 1½%.
7. *Exit loss*. The fluid leaving a radial-inflow turbine constitutes a loss of about one-quarter of the total exit head. This loss varies from about 2% to 5%.

The external losses are from disc friction, the seal, the bearings, and the gears. The disc friction loss is about ½%. The seal, bearings, and gear losses vary from about 5% to 9%. In most radial-inflow turbines, tilting pad bearings are used for journal bearings. These bearings offer rotor stability and excellent stiffness and damping characteristics.

Radial-Inflow Turbine Applications

The most common radial-inflow turbine applications are turbochargers for internal combustion engines, natural gas, diesel, and gasoline powered units. The advantage of a turbocharger is that it compresses the air, thus letting the engine squeeze more air into a cylinder, and more air means that more fuel can be added. Therefore, you get

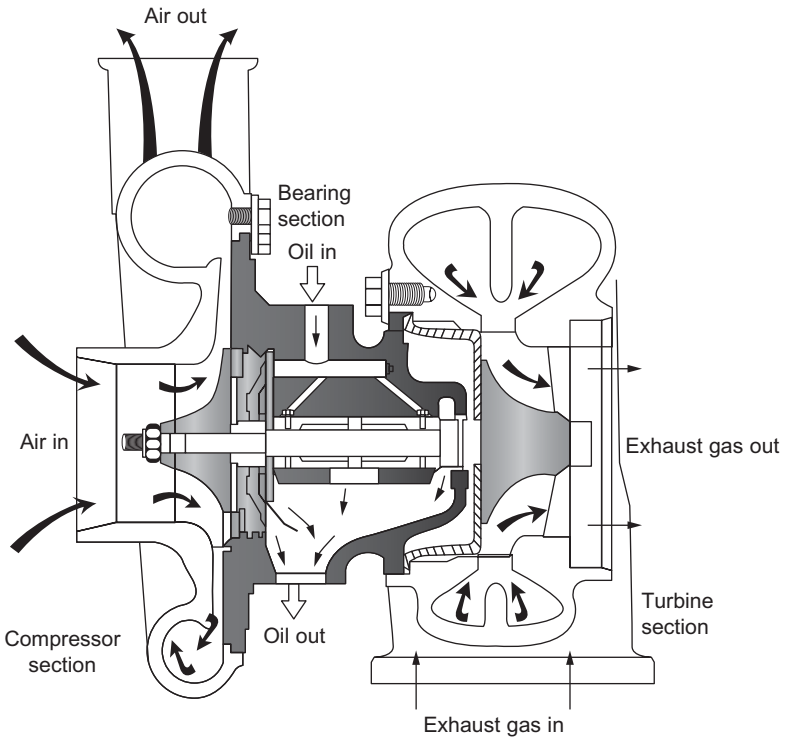


Figure 8-28 A typical cross section of a turbocharger.

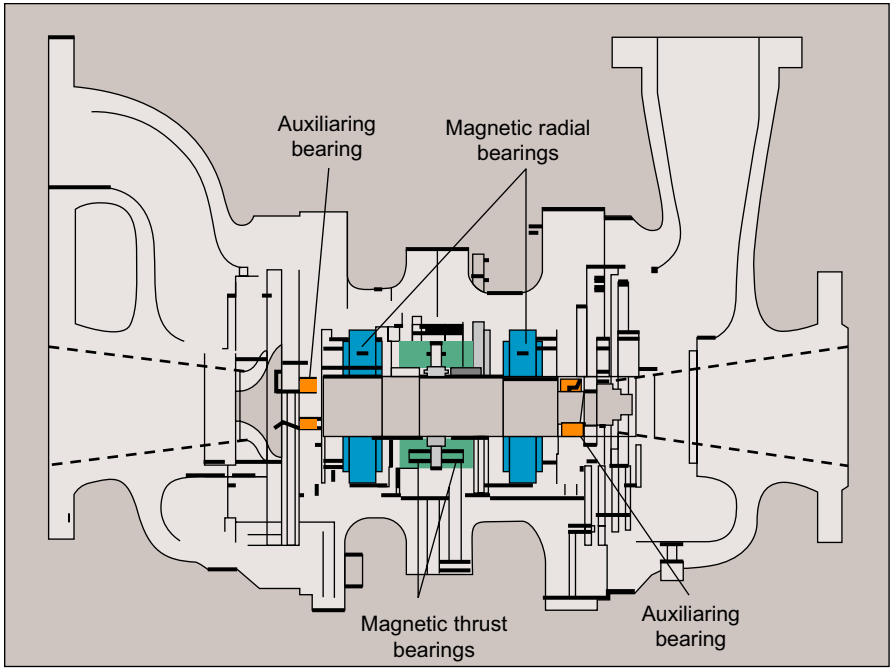


Figure 8-29 Turboexpander with magnetic bearings. (Courtesy GE Oil and Gas.)

more power from each explosion in each cylinder. A turbocharged engine produces more power overall than the same engine without turbocharging. This can significantly improve the power-to-weight ratio for the engine. Figure 8-28 is a cross section of a turbocharger. The turbocharger consists of a centrifugal compressor and a radial-inflow turbine. The air is sucked into the compressor from the air filters and is compressed and then injected into the engine cylinders. The exhaust gases from the cylinders are injected into the radial-inflow turbine that drives the compressor. The turbine in the turbocharger spins at speeds of up to 150,000 rpm. This is about 30 times faster than most car engines. And since it is hooked up to the exhaust, the temperatures in the turbine are also very high.

Figure 8-27 also shows the two-ring collector that receives air from the two exhaust manifolds commonly used on these engines to collect all the gases from the cylinders.

Applications of turbo expanders in the chemical industry abound in the petrochemical and chemical industries. Turbo expanders using radial-inflow turbines have a much higher ruggedness than turbo expanders using axial-flow turbines. They are less susceptible of small micron-size particles found in many gas streams in this industry. Turbo expanders are very widely used as sources of refrigeration in industrial processes such as the extraction of ethane and natural gas liquids from natural gas and also in the liquefaction of gases, such as oxygen, nitrogen, helium.

GE's Rotoflow Division has produced turbo expanders with active magnetic bearings; this offers an alternative to conventional oil-bearing systems. Magnetic bearings require no lubrication, thus eliminating the risk of contamination from oil. It simplifies

the system as it does not require any oil system components, such as pumps, filters, and coolers. In an expander/compressor with magnetic bearings, the rotor assembly is supported by active magnetic radial bearings as shown in Figure 8-29. Thrust handling capabilities of turbo expanders with active magnetic bearings are enhanced by an automatic thrust control system, which controls the position of the rotor by adjusting current to the electromagnets in response to signals from shaft position sensors. Sensors are combined to automatically cancel rotation signal harmonics or elliptical or triangular deformation on the rotor surface.

Turbo expanders have also been used in generating power from hot gases from fluid catalytic reactors. The flue gas from regenerators is sent through swirl tubes to remove the catalyst fines, this removes 70% to 90% of the residual catalyst fines. Because of the residual fines in the gas, the gas is expanded in a radial-inflow turbine due to its ruggedness. Axial-flow turbines would have problems with these fines.

Bibliography

Abidat, M.I., Chen, H., Baines, N.C., and Firth, M.R., "Design of a Highly Loaded Mixed Flow Turbine," Proceedings of the Institution of Mechanical Engineers Part A, Journal of Power and Energy, 206: 95–107, 1992.

Arcoumanis, C., Martinez-Botas, R.F., Nouri, J.M., and Su, C.C., "Performance and Exit Flow Characteristics of Mixed Flow Turbines," International Journal of Rotating Machinery, 3(4): 277–293, 1997.

Baines, N.A., Hajilouy-Benisi, A., and Yeo, J.H., "The Pulse Flow Performance and Modeling of Radial Inflow Turbines," IMechE, Paper No. a405/017, 1994.

Balje, O.E., "A Contribution to the Problem of Designing Radial Turbo-machines," Transactions of ASME, Vol. 74: p. 451, 1952.

Balje, O.E., "A Study of Reynolds Number Effects in Turbomachinery," Journal of Engineering for Power, ASME Trans., Vol. 86, Series A, p. 227, 1964.

Benisek, E., "Experimental and Analytical Investigation for the Flow Field of a Turbocharger Turbine," IMechE, Paper No. 0554/027/98, 1998.

Benson, R.S., "A Review of Methods for Assessing Loss Coefficients in Radial Gas Turbines," International Journal of Mechanical Sciences, 12: 905–932, 1970.

Karamanis, N. Martinez-Botas, R.F., Su, C.C., "Mixed Flow Turbines: Inlet and Exit flow under steady and pulsating conditions," ASME 2000-GT-470.

Cox, G., Wu, J., and Finnigan, B., "A study on the Flow around the Scallops of Mixed-Flow Turbine and its effect on Efficiency," ASME 2007 GT2007-27330.

Knoernschild, E.M., "The Radial Turbine for Low Specific Speeds and Low Velocity Factors," Journal of Engineering for Power, Transaction of the ASME, Serial A, 83: 1–8, 1961.

Rodgers, C., "Efficiency and Performance Characteristics of Radial Turbines," SAE Paper 660754, October, 1966.

Shepherd, D.G., Principles of Turbomachinery, New York, The Macmillan Company, 1956.

Vavra, M.H., "Radial Turbines," Pt 4., AGARD-VKI Lecture Series on Flow in Turbines (Series No. 6), March, 1968.

Vincent, E.T., "Theory and Design of Gas Turbines and Jet Engines," New York, McGraw-Hill, 1950.

Wallace, F.J., and Pasha, S.G.A., "Design, Construction and Testing of a Mixed-Flow Turbine." The Second International JSME Symposium Fluid, 1972.

Copyrighted Materials
Copyright © 2012 Elsevier Retrieved from www.knovel.com

9 Axial-Flow Turbines

Axial-flow turbines are the most widely employed turbines using a compressible fluid. Axial-flow turbines power most gas turbine units – except the smaller horsepower turbines – and they are more efficient than radial-inflow turbines in most operational ranges. The axial-flow turbine is also used in steam turbine design; however, there are some significant differences between the axial-flow turbine design for a gas turbine and a steam turbine.

The development of steam turbine preceded the gas turbine by many years. Thus, the axial-flow turbine used in gas turbines is an outgrowth of steam turbine technology. In recent years, the trend in high turbine inlet temperatures in gas turbines has required various cooling schemes. These schemes are described in detail in this chapter with attention to both cooling effectiveness and aerodynamic effects. The development of steam turbine has resulted in the design of two turbine types: the impulse turbine and the reaction turbine. The reaction turbine in most steam turbine designs has a 50% reaction level that has been found to be very efficient. This reaction level varies considerably in gas turbines and from hub to tip in a single-blade design.

Axial-flow turbines are now designed with a high work factor (ratio of stage work to square of blade speed) to obtain lower fuel consumption and reduce the noise from the turbine. Lower fuel consumption and lower noise require the design of higher bypass ratio engines. A high bypass ratio engine requires many turbine stages to drive the high-flow, low-speed fan. Work is being conducted to develop high-work, low-speed turbine stages that have high efficiencies.

Turbine Geometry

The axial-flow turbine, similar to its counterpart, the axial-flow compressor, has flow that enters and leaves in the axial direction. There are two types of axial turbines: (1) impulse type and (2) reaction type. The impulse turbine has its entire enthalpy drop between the nozzle; therefore, it has a very high velocity entering the rotor. The reaction turbine divides the enthalpy drop between the nozzle and the rotor. Figure 9-1 is a schematic of an axial-flow turbine, also depicting the distribution of the pressure, temperature, and the absolute velocity.

Most axial-flow turbines consist of more than one stage; the front stages are usually impulse (zero reaction) and the later stages have about 50% reaction. The impulse

Gas Turbine Engineering Handbook, Fourth Edition. DOI: 10.1016/B978-0-12-383842-1.00009-3
Copyright © 2012 Elsevier Inc. All rights reserved.

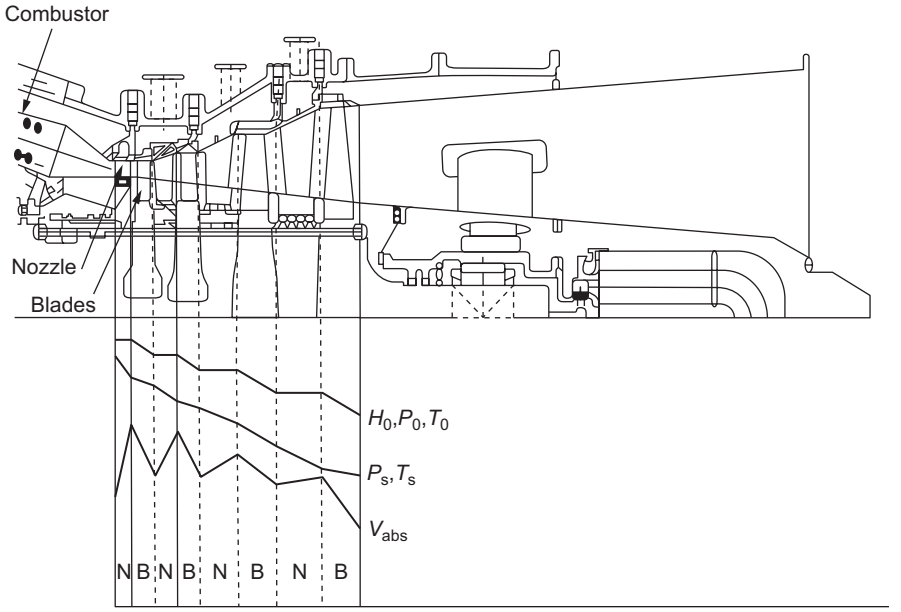


Figure 9-1 Schematic of an axial-flow turbine flow characteristics.

stages produce about twice the output of a comparable 50% reaction stage, whereas the efficiency of an impulse stage is less than that of a 50% reaction stage.

The high temperatures that are now available in the turbine section are due to improvements in the metallurgy of the blades in the turbines. The development of directionally solidified blades as well as the new single-crystal blades, with the new coatings and the new cooling schemes, is responsible for the increase in firing temperatures. The high-pressure ratio in the compressor also causes the cooling air used in the first stages of the turbine to be very hot. The temperatures leaving the gas turbine compressor can reach as high as 1200 °F (649 °C). Thus, the present cooling schemes which require cooling of the compressor air and the cooling passages are in many cases also coated to prevent corrosion of the cooling passages. The cooling schemes are limited in the amount of air they can use, before there is a negating effect on the overall thermal efficiency due to an increase in the amount of air used in cooling. The rule of thumb in this area is that if you need more than 8% of the air for cooling, you are losing the advantage from the increase in the firing temperature.

The new gas turbines being designed for the new millennium, are investigating the use of steam as a cooling agent for the first and second stages of the turbines. Steam cooling is possible in the new combined-cycle power plants, which is the base of most of the new high-performance gas turbines. Steam, as a part of the cooling of the first-stage nozzles, cools the nozzle vanes and the energy transferred to the steam actually heats the steam that is usually taken from the exit of the high-pressure (HP) section of the turbine, before it enters the intermediate-pressure (IP) stage and thus increases the power generated by the IP section and the low-pressure (LP) section

causing an increase in the overall cycle power and efficiency. Steam cooling for turbine nozzle vanes is not a new concept; for example, it was the basis of the cooling schemes proposed by the team of United Technology and Stal-Laval in their conceptual study for the US Department Study on the High Turbine Temperature Technology Program, which was investigating the possibilities of firing temperatures reaching 3000 °F (1649 °C), in the early 1980s. The extra power obtained by the use of steam is the cheapest MW/$ available.

Steam injection used for NO_x control is injected into the combustion chamber with the fuel injection; the steam introduced for power enhancement is mixed with the air leaving the compressor and entering the combustor. The injection of about 5% of steam by weight of air amounts to about 12% more power. The pressure of the injected steam must be at least 40 Bar above the compressor discharge. The way steam is injected must be done very carefully so as to avoid compressor surge. These are not new concepts and have been used and demonstrated in the past.

Thermodynamic and Aerodynamic Theory

There are three state points within a turbine that are important when analyzing the flow. They are located at the nozzle entrance, the rotor entrance, and the rotor exit. Fluid velocity is an important variable governing the flow and energy transfer within a turbine. The absolute velocity (V) is the fluid velocity relative to some stationary point and is usually parallel to the stationary vanes. Absolute velocity is important when analyzing the flow across a stationary blade such as a nozzle. When considering the flow across a rotating element or rotor blade, the relative velocity (W) is important and is usually parallel to the rotating velocity. Vectorially, the relative velocity is defined as:

$$\vec{W} = \vec{V} - \vec{U} \tag{9-1}$$

where $\vec{U}$ is the tangential velocity of the blade.

Examination of the effect of Reynolds number and its efficiency on an axial-flow turbine is shown in Figure 9-2; the axial-flow turbine is especially attractive when the Reynolds number ($\mathrm{Re} = \rho UD/\mu$) is high indicating high flow ($\mathrm{Re} = 10^6 - 0^8$), which is also accompanied by high efficiency. The axial-flow efficiency, which in today's new advanced turbine, reaches about 92%, which is much higher than that of a radial-inflow turbine.

Examining the Balje diagram for turbines as shown in Figure 9-3, the effects of specific speed ($N_s = N\sqrt{\mathrm{Q}}/H^{0.75}$) and specific diameters ($D_s = DH^{0.25}/\sqrt{\mathrm{Q}}$) on the efficiency of an axial-flow turbine can be clearly noted. Axial-flow turbines are most efficient at a Reynolds number between 10^5 and 10^6 and specific speeds between $N_s = 10^2$ and $N_s = 10^4$. This indicates that an axial-flow turbine should be used for high flow and low rise in pressure ratio. The other advantage of the axial-flow turbine is its low sleek profile as compared to a high frontal area of a radial-inflow turbine.

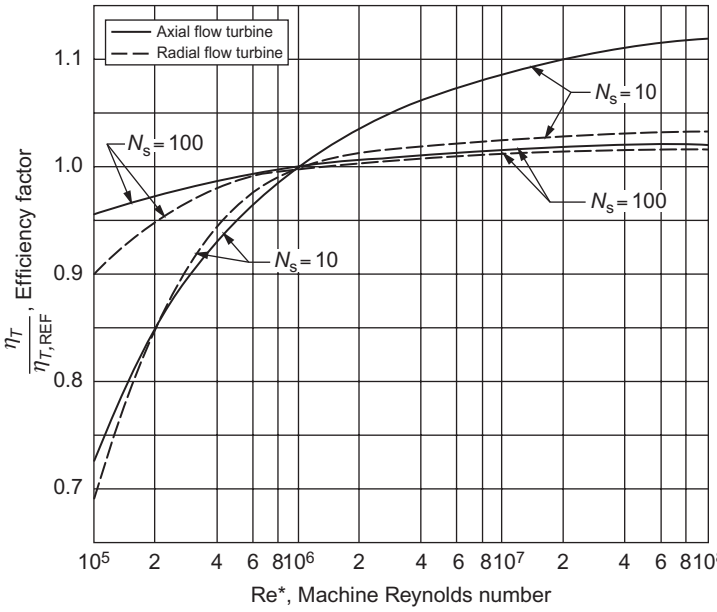


Figure 9-2 Influence of Reynolds number on turbine-stage efficiency.

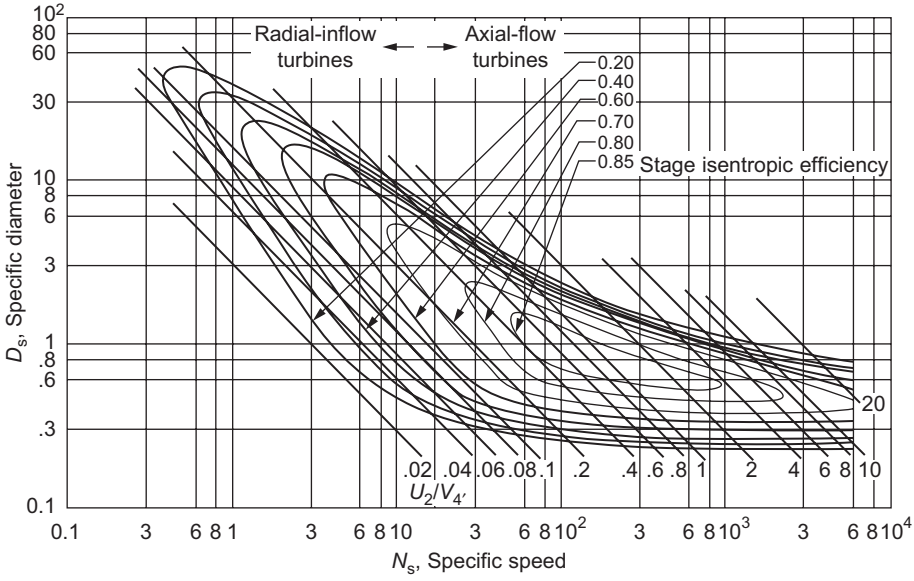


Figure 9-3 N_s–D_s diagram for a turbine stage. Efficiency is on a total-to-total basis; that is, it is related to inlet and exit stagnation conditions. Diagram values are suitable for machine Reynolds number $\mathrm{Re} > 10^6$ (Balje, 1964).

The general principles of energy transfer in an axial-flow turbine are similar to those already outlined in Chapter 3. These are governed by the following basic equations:

1. Equation of State
2. Conservation of Energy
3. Momentum Equation
4. Energy Equation

The momentum equation is transformed to the cylindrical coordinate system (r–θ–z) and Figure 9-4 shows the velocity vectors in turbine rotor flow. The Euler turbine equation previously derived in Chapter 3 using the above-mentioned equations holds for flow in any turbomachine.

Figure 9-5 shows the nomenclature and relates the numerical flow positions that match the equations that are following in this section. It is important to note here that the nomenclatures differ from book to book and from country to country. Some of the most common nomenclatures used in various texts on axial-flow turbines are as follows:

Absolute velocity $= V = V_{\text{abs}} = C$

Tangential component of the absolute velocity $= V_\theta = V_{\theta\text{abs}} = C_\theta$

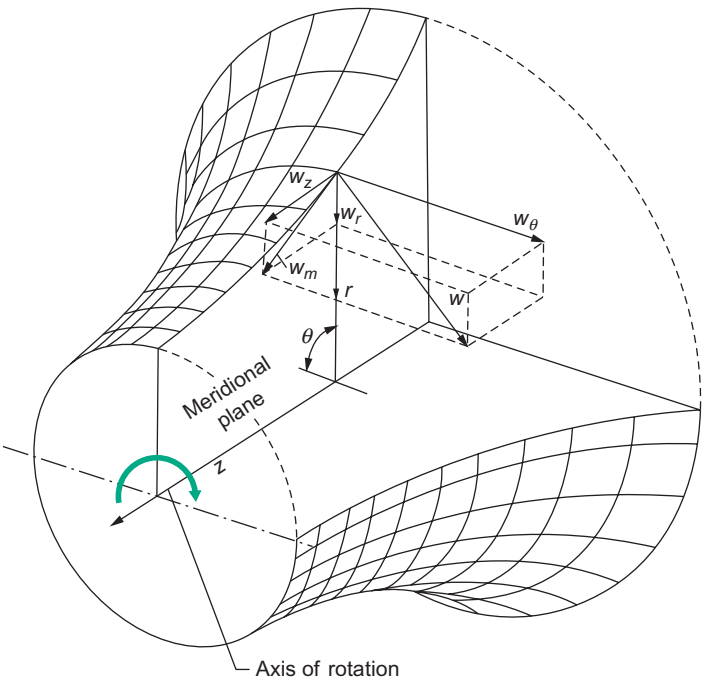


Figure 9-4 Flow relative velocity vectors in the turbine rotor.

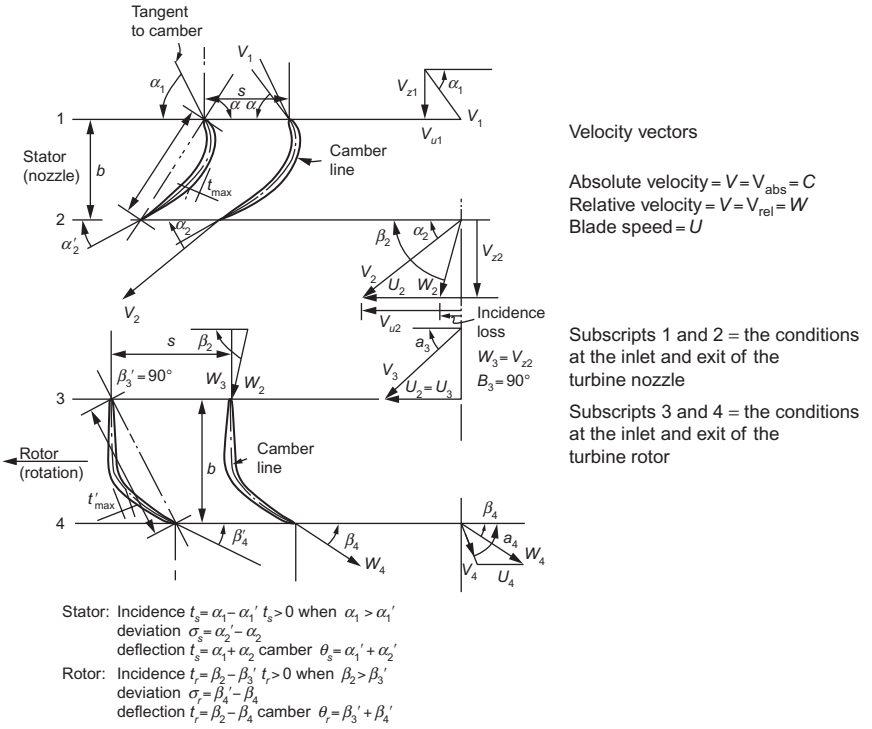


Figure 9-5 Nomenclature and numerical positions for components of an axial-flow turbine.

Relative velocity $= \vec{W} = \vec{V}_{\text{rel}} = \vec{V} - \vec{U}$

Blade speed $= U$

This relationship is shown in Figure 9-5. The subscript z used in this figure denotes the axial velocity and θ denotes the tangential component.

Two angles are defined in Figure 9-5. The first angle is the air angle α, which is defined with respect to the tangential direction. The air angle α represents the direction of the flow leaving the nozzle. In the rotor, the air angle α represents the angle of the absolute velocity leaving the rotor. The blade angle β is the angle the relative velocity makes with the tangential direction. It is the angle of the rotor blade under ideal conditions (no incidence angle).

The Euler turbine equation previously defined holds for flow in any turbomachine in an axial-flow turbine it can be written as:

$$H = \frac{1}{g_c}\left(U_3 V_{\theta_3} - U_4 V_{\theta_4}\right) \tag{9-2}$$

where

$U =$ Blade speed

$V_\theta =$ Tangential component of the absolute velocity

It may be written in terms of the absolute and relative velocities:

$$H_{\mathrm{O}} = \frac{1}{2g_{\mathrm{c}}}\left[\left(V_3^2 - V_4^2\right) + \left(U_3^2 - U_4^2\right) + \left(W_3^2 - W_4^2\right)\right] \tag{9-3}$$

where

U = Blade speed
V = Absolute velocity
W = Relative velocity
subscripts 3 and 4 = the conditions at the inlet and exit of the rotor blades, respectively.

For a positive power output, this indicates that power is being transmitted, the blade tip speed and whirl velocity combination at the inlet must be greater than that at the exit as in Equation (9-2).

Utilization Factor

In a turbine, not all energy supplied can be converted into useful work – even with an ideal fluid. There must be some kinetic energy at the exit that is discharged due to the exit velocity. Thus, the utilization factor is defined as the ratio of ideal work to the energy supplied:

$$E = \frac{H_{\mathrm{id}}}{H_{\mathrm{id}} + \dfrac{V_4^2}{2\mathrm{g}}} \tag{9-4}$$

and it can be written in terms of the velocity for a single rotor with constant radius:

$$E = \frac{\left(V_3^2 - V_4^2\right) + \left(W_4^2 - W_3^2\right)}{V_3^2 + \left(W_4^2 - W_3^2\right)} \tag{9-5}$$

Degree of Reaction

The degree of reaction in an axial-flow turbine is the ratio of change in the static enthalpy to the change in total enthalpy:

$$R = \frac{h_1 - h_4}{h_{01} - h_{04}} \tag{9-6}$$

A rotor with a constant radius and an axial velocity constant throughout can be written as:

$$R = \frac{\left(W_4^2 - W_3^2\right)}{\left(V_3^2 - V_4^2\right) + \left(W_4^2 - W_3^2\right)} \tag{9-7}$$

From the previous relationship, it is obvious that for a zero-reaction turbine (impulse turbine) the relative exit velocity is equal to the relative inlet velocity. Most

turbines have a degree of reaction between zero and one; negative reaction turbines have much lower efficiencies and are not usually used.

Work Factor

In addition to the degree of reaction and the utilization factor, another parameter used to determine the blade loading is the work factor:

$$\Gamma \equiv \frac{\Delta h_\theta}{U^2} \tag{9-8}$$

and it can be written for a constant radius turbine:

$$\Gamma = \frac{V_{\theta 3} - V_{\theta 4}}{U} \tag{9-9}$$

The previous equation can be further modified for the maximum utilization factor where the absolute exit velocity is axial and no exit swirl exists:

$$\Gamma = \frac{V_{\theta 3}}{U} \tag{9-10}$$

The value of the work factor for an impulse turbine (zero reaction) with a maximum utilization factor is two. In a 50% reaction turbine with a maximum utilization factor, the work factor is one.

In recent years, the trend has been toward high work factor turbines. The high work factor indicates that the blade loading in the turbine is high. The trend in many fan engines is toward a high bypass ratio for lower fuel consumption and lower noise levels. As the bypass ratio increases, the relative diameter of the direct-drive fan turbine decreases, resulting in lower blade tip speeds. Lower blade tip speeds mean that with conventional work factors, the number of turbine stages increases. Considerable research is being conducted to develop turbines with high work factors, high blade loadings, and high efficiencies. Figure 9-6 shows the effect of turbine stage work and

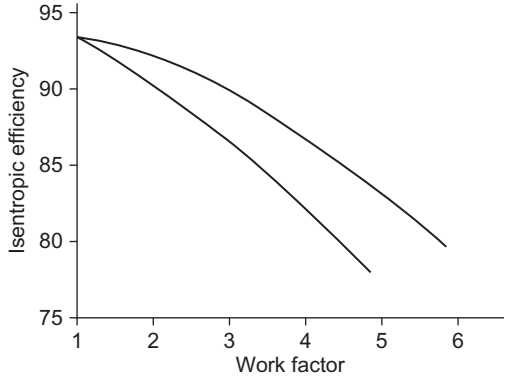


Figure 9-6 Effect of stage work on efficiency.

efficiency. This diagram indicates that efficiency drops considerably as the work factor increases. There is little information on turbines with work factors over two.

Velocity Diagrams

An examination of various velocity diagrams for different degrees of reaction is shown in Figure 9-7. These types of blade arrangements with varying degrees of reaction are all possible although not practical.

Examining the utilization factor, the discharge velocity ($V_4^2/2$), represents the kinetic energy loss or the unused energy part. For maximum utilization, the exit velocity should be at a minimum and, by examining the velocity diagrams, this minimum is achieved when the exit velocity is axial. This type of a velocity diagram is considered to have zero-exit swirl. Figure 9-8 shows the various velocity diagrams as a function of the work factor and the turbine type. This diagram shows that zero-exit swirl can exist for any type of turbine.

Zero-Exit Swirl Diagram

In many cases, the tangential angle of the exit velocity ($V_{\theta 4}$) represents a loss in efficiency. A blade designed for zero-exit swirl ($V_{\theta 4} = 0$) minimizes the exit loss. If the work parameter is less than two, this type of diagram produces the highest static efficiency. In addition, the total efficiency is approximately the same as in the other types of diagrams. If $r > 2.0$, stage reaction is usually negative, a condition best avoided.

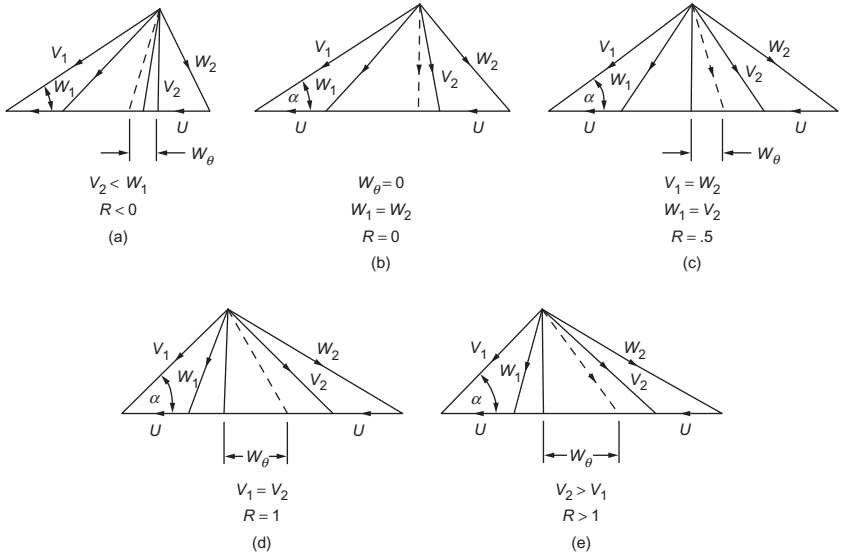


Figure 9-7 Turbine velocity triangles showing the effect of various degrees of reaction.

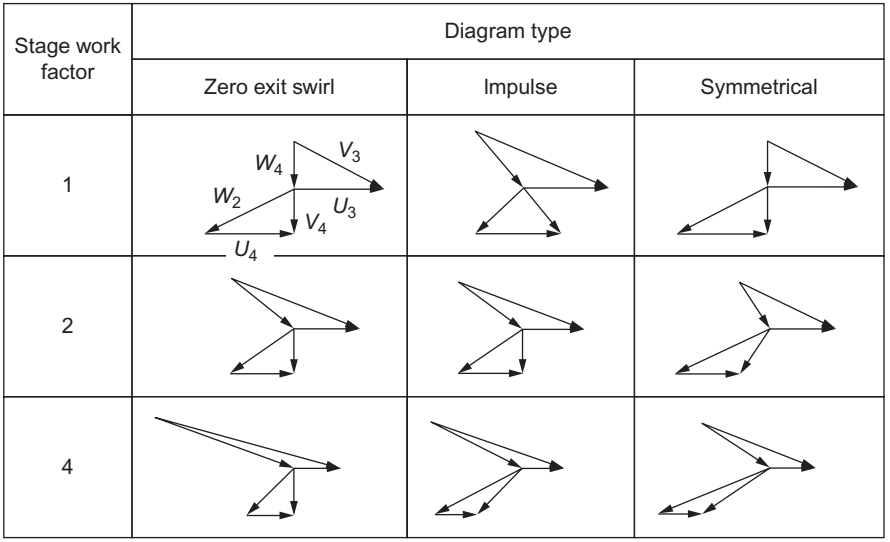


Figure 9-8 Effect of diagram type and stage work factor on velocity diagram shape.

Impulse Diagram

For the impulse rotor, the reaction is zero; therefore, the relative velocity of the gas is constant, or $W_3 = W_4$. If the work factor is less than two, the exit swirl is positive, which reduces the stage work. For this reason, an impulse diagram should be used only if the work factor is two or greater. This type of diagram is a good choice for the last stage because for $r > 2.0$, an impulse rotor has the highest static efficiency.

Symmetrical Diagram

The symmetrical-type diagram is constructed so that the entrance and exit diagrams have the same shape: $V_3 = W_4$ and $V_4 = W_3$. This equality means that the reaction is:

$$R = 0.5 \tag{9-11}$$

If the work factor $r = 1.0$, then the exit swirl is zero. As the work factor increases, the exit swirl increases. Since the reaction of 0.5 leads to a high total efficiency, this design is useful if the exit swirl is not counted as a loss as in the initial and intermediate stages.

Impulse Turbine

The impulse turbine is the simplest type of turbine. It consists of a group of nozzles followed by a row of blades. The gas is expanded in the nozzle, converting the high

thermal energy into kinetic energy. This conversion can be represented by the following relationship:

$$V_3 = \sqrt{2\Delta h_0} \tag{9-12}$$

The high-velocity gas impinges on the blade where a large portion of the kinetic energy of the moving gas stream is converted into turbine shaft work.

Figure 9-9 shows a diagram of a single-stage impulse turbine. The static pressure decreases in the nozzle with a corresponding increase in the absolute velocity. The absolute velocity is then reduced in the rotor; however, the static pressure and the relative velocity remain constant. To get the maximum energy transfer, the blades must rotate at about one-half the velocity of the gas jet velocity. Two or more rows of moving blades are sometimes used in conjunction with one nozzle to obtain wheels with low blade tip speeds and stresses. In-between the moving rows of blades are guide vanes that redirect the gas from one row of moving blades to another as shown in Figure 9-10. This type of turbine is sometimes called a Curtis turbine.

Another impulse turbine is the pressure compound or Ratteau turbine. In this turbine, the work is broken down into various stages. Each stage consists of a nozzle and blade row where the kinetic energy of the jet is absorbed into the turbine rotor as

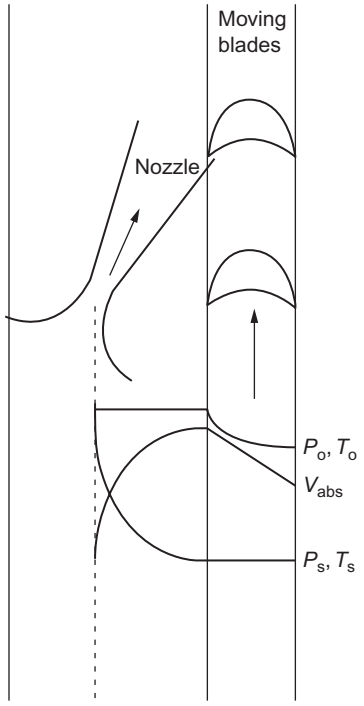


Figure 9-9 Schematic of an impulse turbine showing the variation of the thermodynamic and fluid mechanic properties.

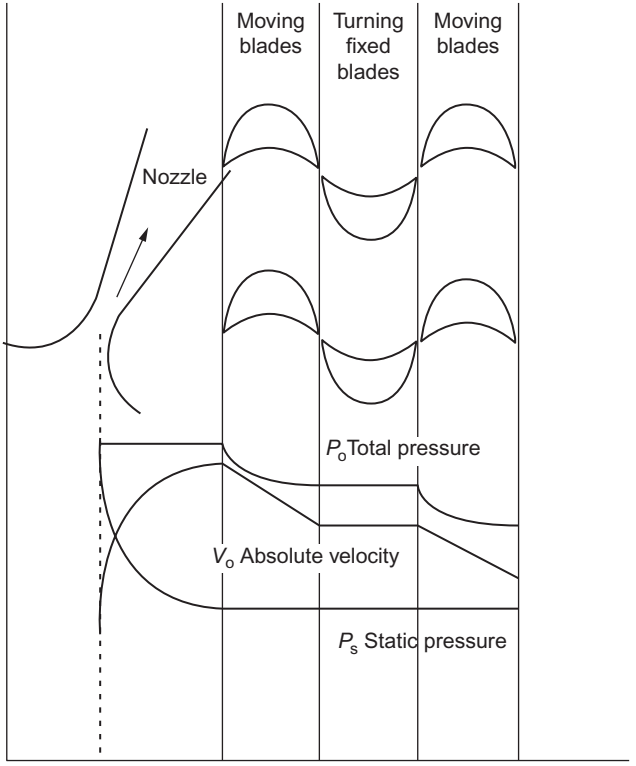


Figure 9-10 Pressure and velocity distributions in a Curtis-type impulse turbine.

useful work. The air that leaves the moving blades enters the next set of nozzles where the enthalpy decreases further, and the velocity is increased and then absorbed in an associated row of moving blades.

Figure 9-11 shows the Ratteau turbine. The total pressure and temperature remain unchanged in the nozzles, except for minor frictional losses.

By definition, the impulse turbine has a degree of reaction equal to zero. This degree of reaction means that the entire enthalpy drop is taken in the nozzle and the exit velocity from the nozzle is very high. Since there is no change in enthalpy in the rotor, the relative velocity entering the rotor equals the relative velocity exiting from the rotor blade. For the maximum utilization factor, the absolute exit velocity must be axial as shown in Figure 9-12. The air angle α for maximum utilization is:

$$\cos\alpha_3 = \frac{2U}{V_3} \tag{9-13}$$

The air angle α is usually small, between 12 °and 25 °. The limit on this angle is placed by the throughflow velocity, $V_1 \sin \alpha$. If the limit is too small, the angle

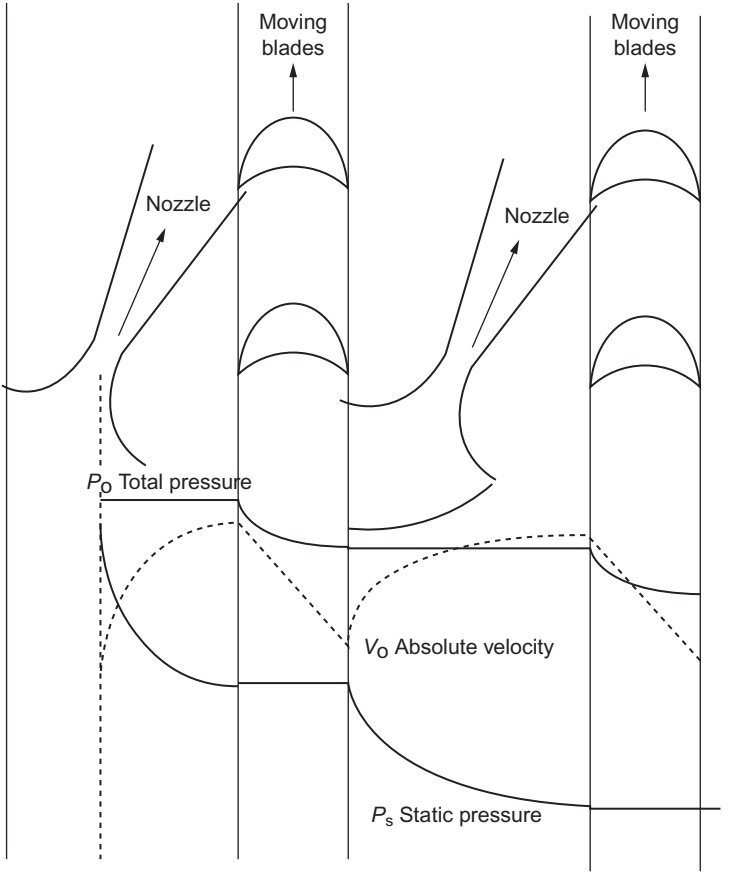


Figure 9-11 Pressure and velocity distributions in a Ratteau-type impulse turbine.

will require a longer blade length. The flow factor, which is a ratio of the blade speed to the inlet velocity, is a useful parameter to compare with the utilization factor (Figure 9-12).

The optimum value of U/V_3 is a criterion indicating the maximum energy transfer to the shaft work. It also represents the departure from the optimum design value of cos α, causing a loss of energy transfer. The losses will increase at off-design conditions because of the incorrect attack angle of the gas with respect to the rotor blade. The maximum efficiency of the stage will still occur at or near the value of: $U/V_3 = \cos \alpha_3/2$.

The power developed by the flow in an impulse turbine is given by the Euler equation:

$$P = \dot{m}U(V_{\theta 3} - V_{\theta 4}) = U(V_{\theta 3} - v_{\theta 4}) \tag{9-14}$$

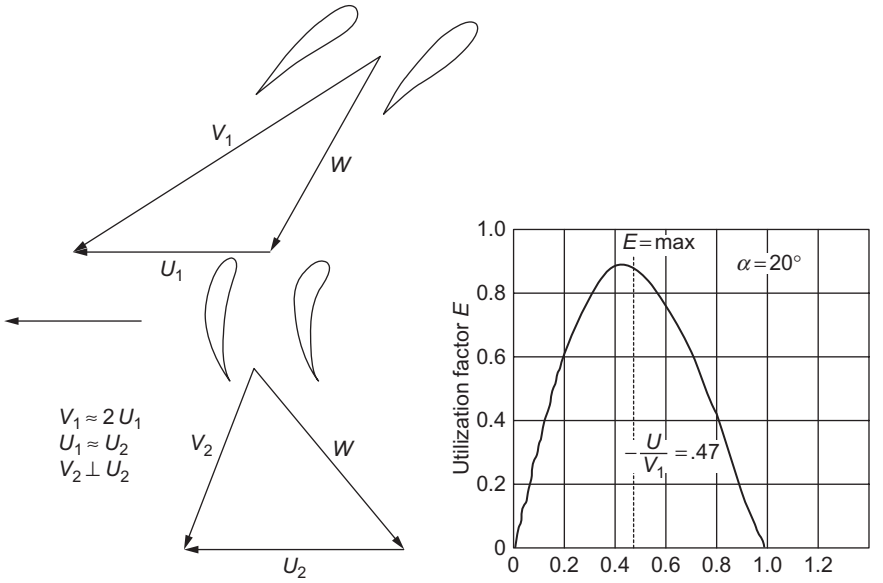


Figure 9-12 Effect of velocity and air angle on utilization factor.

This equation, rewritten in terms of the absolute velocity and the nozzle angle α for maximum utilization, can be shown as:

$$P = \dot{m}U(V_{\theta 3}\cos\alpha_3) \tag{9-15}$$

The relative velocity W remains unchanged in a pure impulse turbine, except for frictional and turbulence effects. This loss varies from about 20% for very high-velocity turbines (3,000 ft/s) to about 8% for low-velocity turbines (500 ft/s). Since the blade speed ratio is equal to $(\cos\alpha)/2$ for maximum utilization, the energy transferred in an impulse turbine can be written as:

$$P = \dot{m}U(V_{\theta 3} - V_{\theta 4}) = U(V_{\theta 3} - V_{\theta 4}) \tag{9-16}$$

The axial-flow reaction turbine is the most widely used turbine. In a reaction turbine both the nozzles and blades act as expanding nozzles. Therefore, the static pressure decreases in both the fixed and the moving blades. The fixed blades act as nozzles and direct the flow to the moving blades at a velocity slightly higher than the velocity of the moving blades. In the reaction turbine, the velocities are usually much lower and the relative velocities of the entering blade are nearly axial. Figure 9-13 shows a schematic view of a reaction turbine.

In most designs, the reaction of the turbine varies from hub to shroud. The impulse turbine is a reaction turbine with a degree of reaction of zero ($R = 0$). The utilization factor for a fixed nozzle angle will increase as the reaction approaches 100%. For

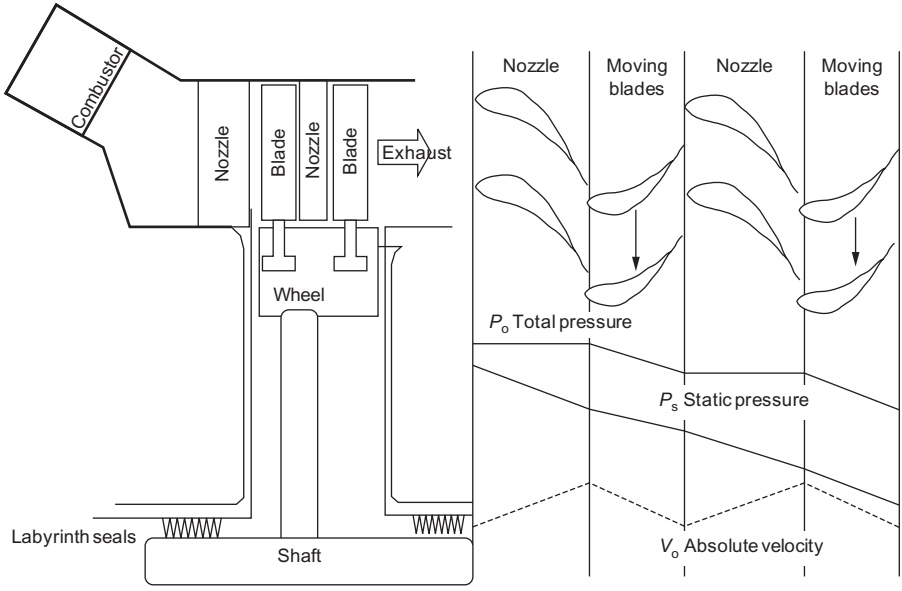


Figure 9-13 Schematic of a reaction-type turbine showing the distribution of the thermodynamic and fluid mechanic properties.

$R = 1$, the utilization factor does not reach unity but reaches some maximum finite value. The 100% reaction turbine is not practical because of the high rotor speed necessary for a good utilization factor. For a degree of reaction less than zero, the rotor has a diffusing action. Diffusing action in the rotor is undesirable, since it leads to flow losses.

The 50% reaction turbine has been used widely and has special significance. The velocity diagram for a 50% reaction is symmetrical and, for the maximum utilization factor, the exit velocity (V_4) must be axial. Figure 9-14 shows a velocity diagram of a 50% reaction turbine and the effect on the utilization factor. From the diagram $W_3 = V_4$; the angles of both the stationary and rotating blades are identical. Therefore, for maximum utilization:

$$\frac{U}{V_3} = \cos\alpha \tag{9-17}$$

The 50% reaction turbine has the highest efficiency of all the various types of turbines. Equation (9-17) shows that the effect on efficiency is relatively small for a wide range of blade speed ratios (0.6–1.3).

The power developed by the flow in a reaction turbine is also given by the general Euler equation. This equation can be modified for maximum utilization:

$$P = \dot{m}U(V_3 \cos\alpha_3) \tag{9-18}$$

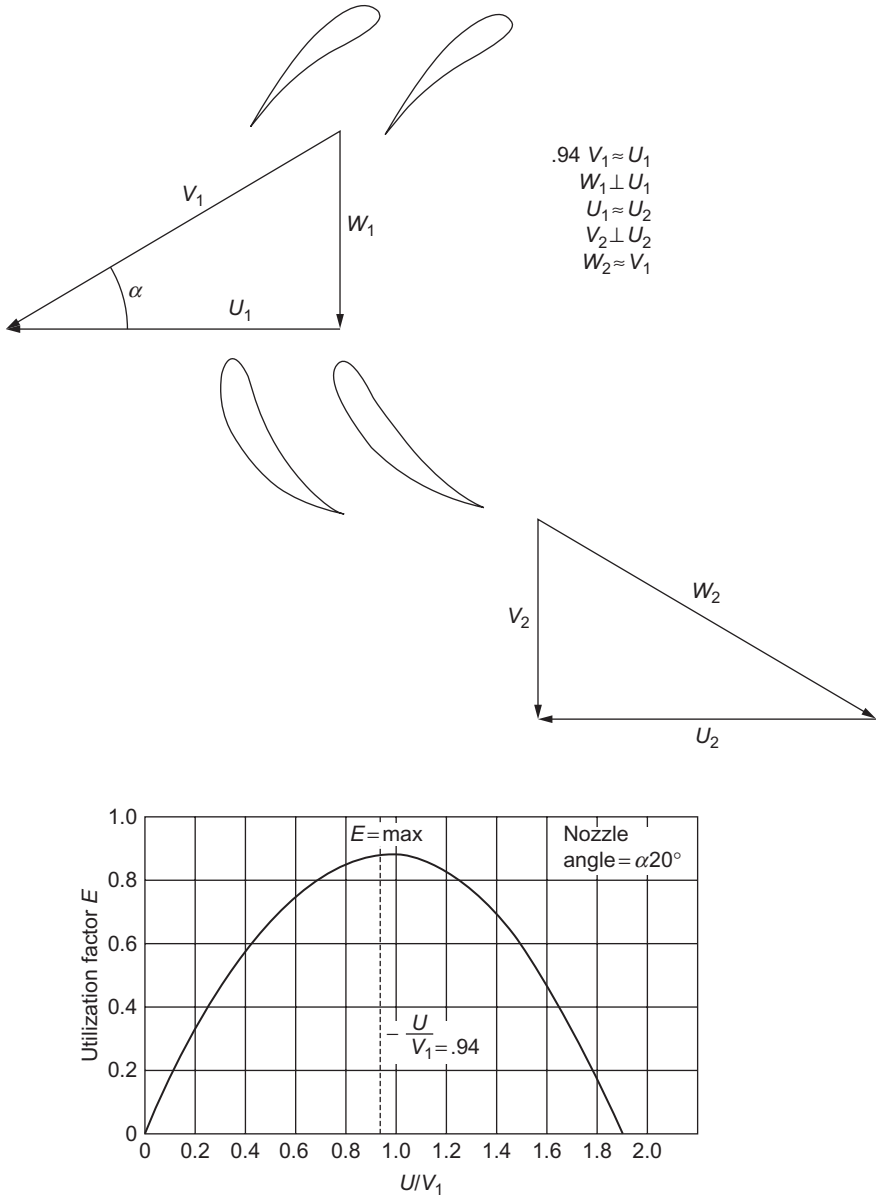


Figure 9-14 The effect of exit velocity and air angle on the utilization factor.

For a 50% reaction turbine, Equation (9-18) reduces to:

$$P = \dot{m}U(U) = \dot{m}U^2 \tag{9-19}$$

The work produced in an impulse turbine with a single-stage running at the same blade speed is twice that of a reaction turbine. Hence, the cost of a reaction turbine

for the same amount of work is much higher, since it requires more stages. It is a common practice to design multistage turbines with impulse stages in the first few stages to maximize the pressure decrease and to follow it with 50% reaction turbines. The reaction turbine has a higher efficiency due to blade suction effects. This type of combination leads to an excellent compromise, since otherwise an all-impulse turbine would have a very low efficiency and an all-reaction turbine would have an excessive number of stages.

Turbine Blade Cooling Concepts

The turbine inlet temperatures of gas turbines have increased considerably over the past years and will continue to do so. This trend has been made possible by advancement in materials and technology and the use of advanced turbine blade cooling techniques. The development of new materials as well as cooling schemes has seen the rapid growth of the turbine firing temperature leading to high turbine efficiencies. The Stage one blade must withstand the most severe combination of temperature, stress, and environment; it is generally the limiting component in the machine. Figure 9-15 shows the trend of firing temperature and blade alloy capability.

Since 1950, turbine bucket material temperature capability has advanced approximately 850 °F (472 °C), approximately 20 °F (10 °C) per year. The importance of this increase can be appreciated by noting that an increase of 100 °F (56 °C) in turbine firing temperature can provide a corresponding increase of 8–13% in output and 2–4% improvement in simple-cycle efficiency. Advances in alloys and processing, while expensive and time-consuming, provide significant incentives through increased power density and improved efficiency. The cooling air is bled from the compressor and is directed to the stator, the rotor, and other parts of the turbine rotor and casing to provide adequate cooling. The effect of the coolant on the aerodynamics depends on the type of cooling involved, the temperature of the coolant compared with the mainstream temperature, the location and direction of coolant injection, and the amount of coolant. A number of such factors are being studied experimentally in annular and two-dimensional cascades.

In high-temperature gas turbines cooling systems need to be designed for turbine blades, vanes, endwalls, shroud, and other components to meet metal temperature limits. The concepts underlie the following five basic air-cooling schemes (Figure 9-16):

1. Convection cooling
2. Impingement cooling
3. Film cooling
4. Transpiration cooling
5. Water/steam cooling

Since 1995, gas turbines have seen a great rise in firing temperatures, which in turn requires a large improvement in material and cooling technologies. The temperatures of turbine inlet, by 2015, will approach 3000 °F (1650 °C) at maximum power for the latest large commercial turbofan engines, resulting in high fuel efficiency and thrust levels approaching 100,000 lbs (445 KN.). In commercial industrial

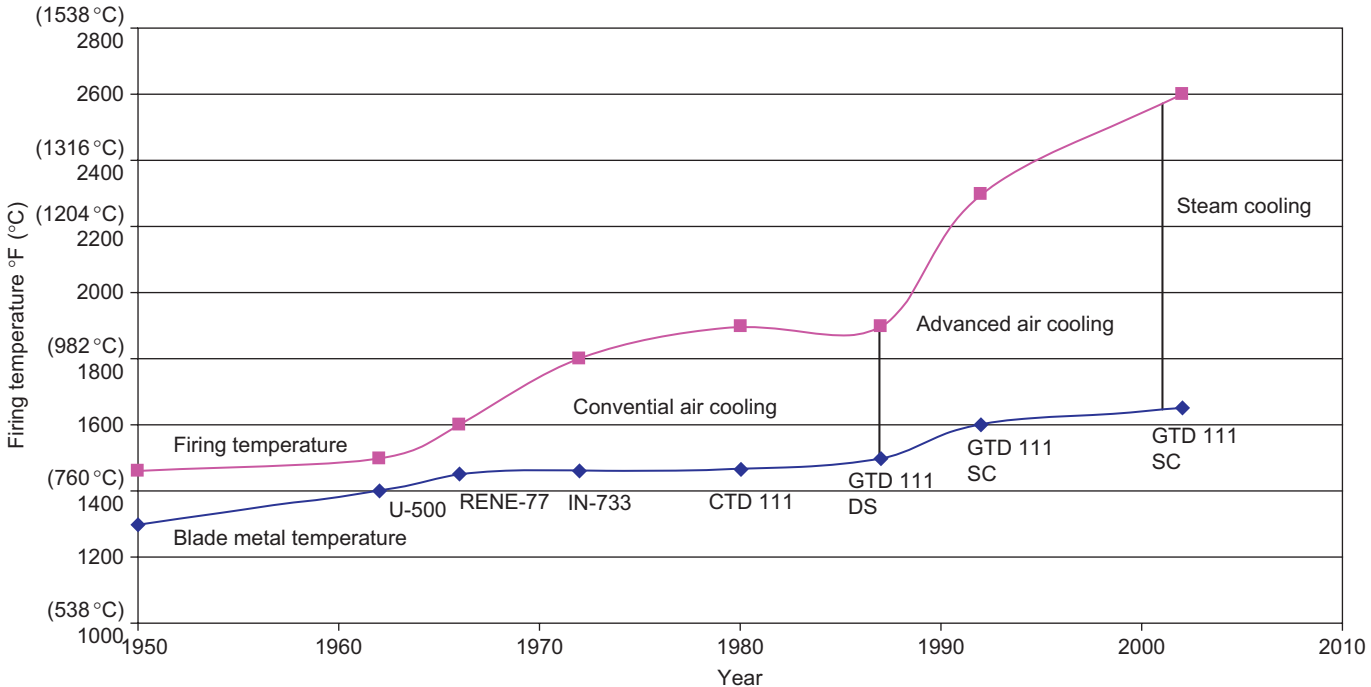


Figure 9-15 Firing temperature increase with blade material improvement.

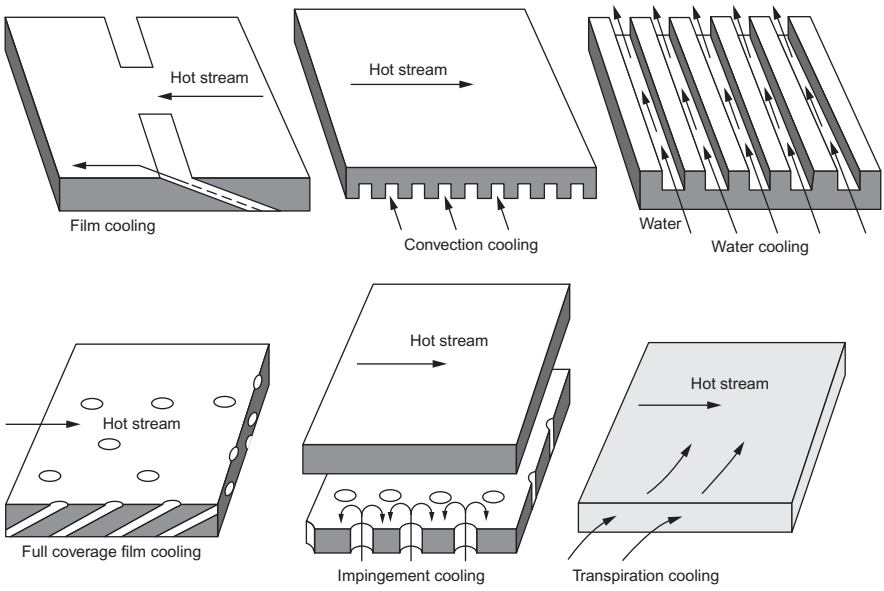


Figure 9-16 Various suggested cooling schemes.

engines, the temperature rise follows closely the aeroengines and engine size range up to 450 MW (GE Frame 7 and 9 H and the Mitsubishi J series). High reliability and durability must be intrinsically designed into turbine engines to meet operating economic targets. These applications are demanding, turbine airfoils with high reliability up to 25,000 hours, with greater than 50% of the time spent at maximum power. This level of performance has been brought about by a combination of the following:

1. Advances in air-cooling for turbine blades and vanes.
2. Design technology for stresses and airflow.
3. Single crystal (SC) and directionally solidified (DS) casting process improvements.
4. Development and use of rhenium (Re $< 6\%$) in nickel-based superalloys with advanced coatings, including full-airfoil ceramic thermal barrier coatings (TBCs).

There has been great strides in cooling of turbine blades and vanes, from cooling with air and steam to development of new blade structures. The new advanced gas turbine blades operating at very high temperatures are designed to eliminate both transverse and linear grain boundaries, thus becoming SC blades. Most nozzle and blade castings are made by using the conventional equiaxed investment casting process. In this process, the molten metal is poured into a ceramic mold in a vacuum, to prevent the highly reactive elements in the super alloys from reacting with the oxygen and nitrogen in the air. With proper control of metal and mold thermal conditions, the molten metal solidifies from the surface to the center of the mold, creating an equiaxed structure. Directional solidification (DS) is also being employed to produce advanced technology nozzles and blades. This was first used in aircraft engines more than 25 years ago and was adapted for the use in large airfoils in the early 1990s. By exercising careful control over temperature gradients, a planar solidification front is developed in the

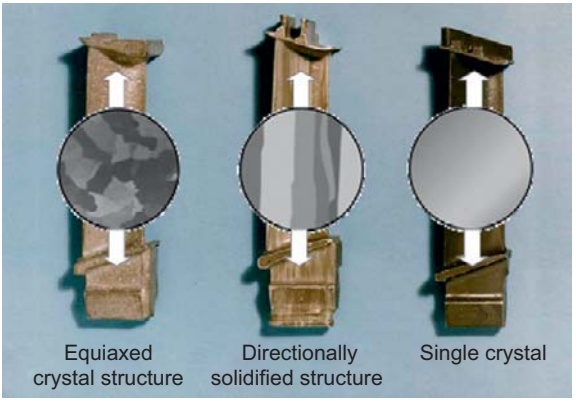


Figure 9-17 Three major types of materials for gas turbine blades.

blade and the part is solidified by moving this planar front longitudinally through the entire length of the part. The result is a blade with an oriented grain structure that runs parallel to the major axis of the part and contains no transverse grain boundaries, as in ordinary blades. Figure 9-17 shows the grain structure of the blades from the equiaxed blades to the directionally solidified blades and the single-crystal blades. The elimination of these transverse grain boundaries confers additional creep and rupture strength on the alloy, and the orientation of the grain structure provides a favorable modulus of elasticity in the longitudinal direction to enhance fatigue life. The use of directionally solidified blades results in a substantial increase in the creep life or substantial increase in tolerable stress for a fixed life. This advantage is due to the elimination of transverse grain boundaries from the bucket, the traditional weak link in the microstructure. In addition to improved creep life, the directionally solidified blades possess more than 10 times the strain control or thermal fatigue when compared with equiaxed blades. The impact strength of the DS blades is also superior to that of equiaxed, showing an advantage of more than 33%.

Single-crystal blades have been used in gas turbines since the late 1990s. These blades offer additional creep and fatigue benefits through the further elimination of grain boundaries. In single-crystal material, all grain boundaries are eliminated from the material structure and a single crystal with controlled orientation is produced in an airfoil shape. By eliminating the grain boundaries and the associated grain boundary strengthening additives, a substantial increase in the melting point of the alloy can be achieved, thus providing a corresponding increase in high-temperature strength. The transverse creep and fatigue strengths are increased when compared with equiaxed or DS structures. The advantage of single-crystal alloys compared with equiaxed and DS alloys in low-cycle fatigue (LCF) life is increased by about 10%.

The addition of rhenium (Re) to cast airfoil superalloys not only improves creep and thermomechanical fatigue strengths but also improves environmental properties including coating performance. A range of critical properties of these alloys is being reviewed in relation to turbine component performance and life. The addition of Re dramatically slows down diffusion in these alloys at high operating temperatures.

Industrial turbines are now commencing to use this aero developed turbine technology in both small and large frame units in addition to aero-derivative industrial engines.

Until the late 1960s, convection cooling was the primary means of cooling gas turbine blades; some film cooling was occasionally employed in critical regions. Film cooling in the 1980s and 1990s was used extensively. In 2001, steam cooling was introduced in the production of frame-type engines used in combined-cycle applications. The new turbines have very high-pressure ratios and this leads to compressor air leaving at very high temperatures, which affects their cooling capacity.

Convection Cooling

This form of cooling is achieved by designing the cooling air to flow inside the turbine blade or vane and remove heat through the walls. Usually, the air flow is radial, making multiple passes through a serpentine passage from the hub to the blade tip. Convection cooling is the most widely used cooling concept in contemporary gas turbines.

Impingement Cooling

In this high-intensity form of convection cooling, the cooling air is blasted on the inner surface of the airfoil by high-velocity air jets, permitting an increased amount of heat to be transferred to the cooling air from the metal surface. This cooling method can be restricted to desired sections of the airfoil to maintain even temperatures over the entire surface. For instance, the leading edge of a blade needs to be cooled more than the midchord section or trailing edge, so the gas is impinged.

Film Cooling

This type of cooling is achieved by allowing the working air to form an insulating layer between the hot gas stream and the walls of the blade. This film of cooling air protects an airfoil in the same way combustor liners are protected from hot gases at very high temperatures.

Transpiration Cooling

Cooling by this method requires the coolant flow to pass through the porous wall of the blade material. The heat transfer takes place directly between the coolant and the hot gas. Transpiration cooling is effective at very high temperatures, since it covers the entire blade with coolant flow.

Water/Steam Cooling

Water is passed through a number of tubes embedded in the blade. The water is emitted from the blade tips as steam to provide excellent cooling. This method keeps blade metal temperatures below 1000 °F (537.8 °C).

Steam is passed through a number of tubes embedded in the nozzle or blades of the turbine. In many cases, the steam is bled from after the HP steam turbine of a

combined-cycle power plant and returned after cooling the gas turbine blades, where the steam gets heated in the process to the IP steam turbine. This is a very effective cooling scheme and it keeps the blade metal temperature below 1250 °F (649 °C).

Turbine Blade Cooling Design

The incorporation of blade cooling concepts into actual blade designs is very important. There are five different blade cooling designs.

Convection and Impingement Cooling/Strut Insert Design

The strut insert design shown in Figure 9-18 has a mid-chord section that is convection-cooled through horizontal fins and a leading edge that is impingement cooled. The coolant is discharged through a split trailing edge. The air flows up the central cavity formed by the strut insert and through holes at the leading edge of the insert to impingement cool the blade leading edge. The air then circulates through horizontal fins between the shell and strut, and discharges through slots in the trailing edge. The temperature distribution for this design is shown in Figure 9-19.

The stresses in the strut insert are higher than those in the shell and the stresses on the pressure side of the shell are higher than those on the suction side. Considerably more creep strain takes place toward the trailing edge than the leading edge. The creep strain distribution at the hub section is unbalanced. This unbalance can be improved by a more uniform wall temperature distribution.

Film and Convection Cooling Design

This type of blade design is shown in Figure 9-20. The mid-chord region is convection cooled and the leading edges are both convection and film cooled. The cooling air is injected through the blade base into the two central and one leading edge cavities. The air then circulates up and down a series of vertical passages.

At the leading edge, the air passes through a series of small holes in the wall of the adjacent vertical passages and then impinges on the inside surface of the leading edge and passes through film cooling holes. The trailing edge is convection-cooled by air discharging through slots. The temperature distribution for film and convection cooling design is shown in Figure 9-21. From the cooling distribution diagram, the hottest section can be seen to be the trailing edge. The web, which is the most highly stressed blade part, is also the coolest part of the blade.

A similar cooling scheme with some modifications is used in some of the latest gas turbine designs. The firing temperature of GE FA units is about 2350 °F (1288 °C), which is the highest in the power generation industry. To accommodate this increased firing temperature, the FA employs advanced cooling techniques developed by GE Aircraft Engines. The first- and second-stage blades as well as all three-nozzle stages are air cooled. The first-stage blade is convectively cooled by means of an advanced aircraft-derived serpentine arrangement as shown in Figure 9-22.

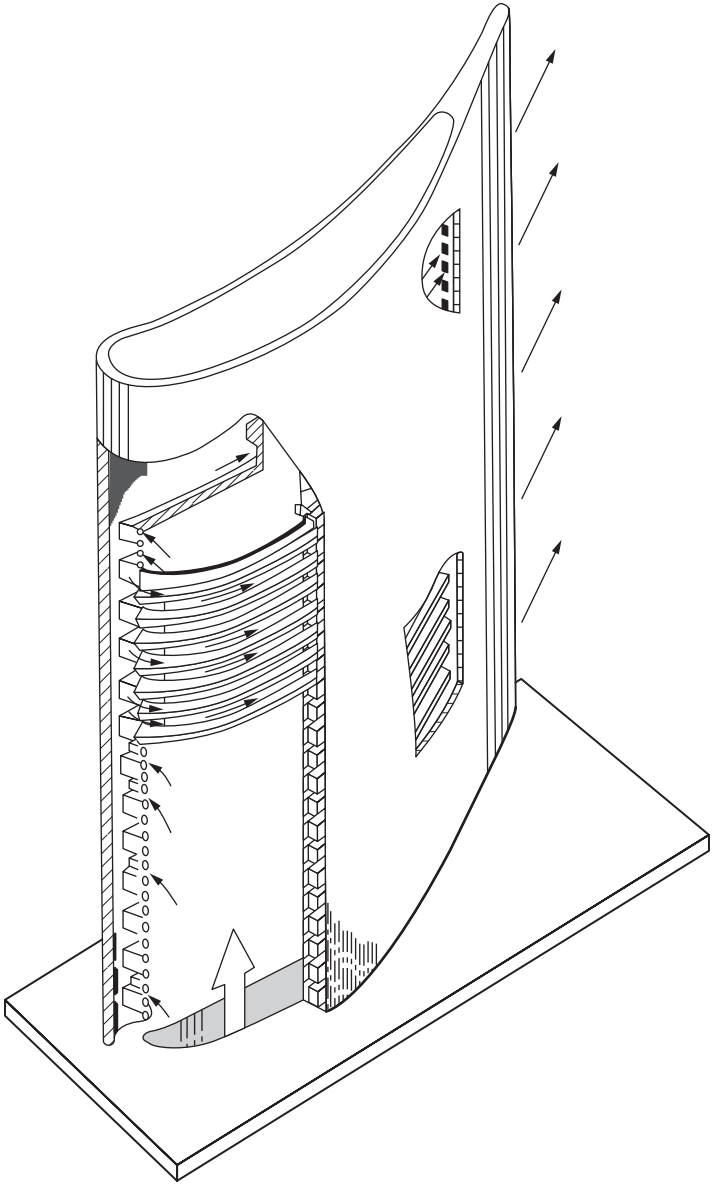


Figure 9-18 Strut insert blade.

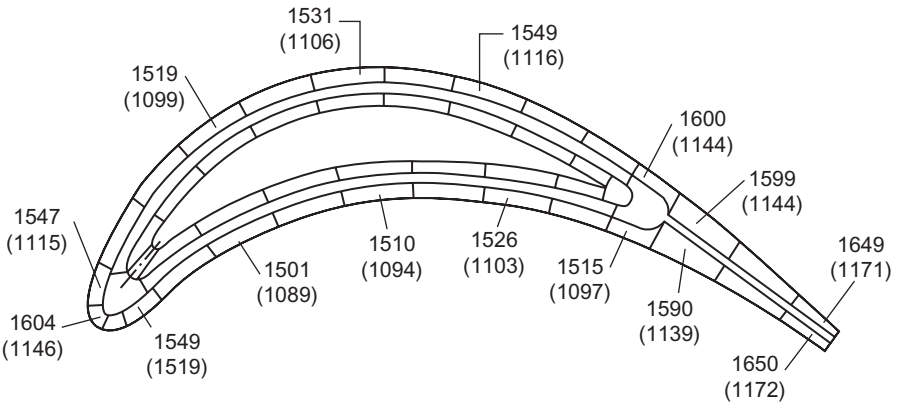


Figure 9-19 Temperature distribution for strut insert design, °F (cooled).

Cooling air exits through axial airways located on the bucket's trailing edge and tip, and also through leading edge and sidewalls for film cooling.

Transpiration Cooling Design

This design has a strut-supported porous shell (Figure 9-23). The shell attached to the strut is of wire from porous material. Cooling air flows up the central plenum of the strut, which is hollow with various-size metered holes on the strut surface. The metered air then passes through the porous shell. The shell material is cooled by a combination of convection and film cooling. This process is effective due to the infinite number of pores on the blade surface. The temperature distribution is shown in Figure 9-24.

The trailing edge of the strut develops the highest creep strain. This strain occurs despite the sharp stress relaxation at the trailing edge projection. The creep strain in the strut is well balanced. Transpiration cooling requires a material of porous mesh resistant to oxidation at a temperature of 1600 °F (871.1 °C) or more.

Otherwise, the superior creep properties of this design are insignificant. Since oxidation will close the pores, causing uneven cooling and high thermal stresses, the possibility of blade failure exists. The reason for superior creep property is a relatively low strut temperature 1400 °F average (760.0 °C), which more than compensates for the high level of centrifugal stress required to support the porous shell.

Multiple Small-Hole Design

With this particular design, primary cooling is achieved by film cooling with cold air injected through small holes over the airfoil surface (Figure 9-25). The temperature distribution is shown in Figure 9-26.

These holes are considerably larger than holes formed with porous mesh for transpiration cooling. In addition, because of their larger size, they are less susceptible to

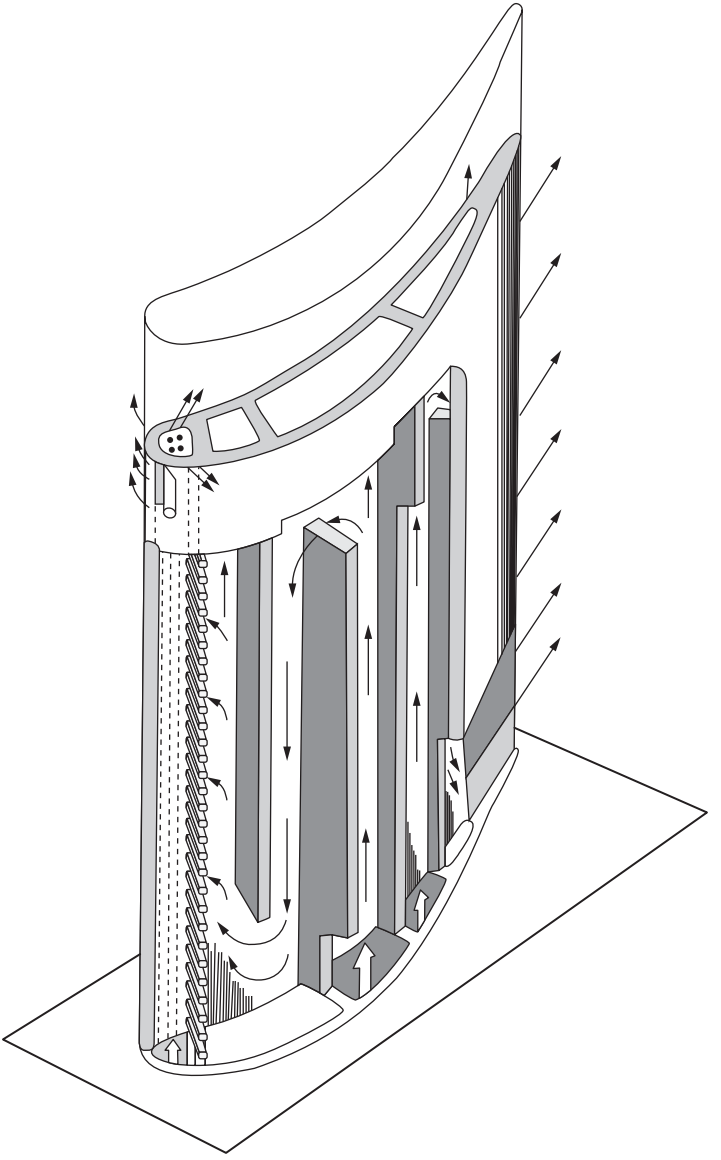


Figure 9-20 Film and convection-cooled blade.

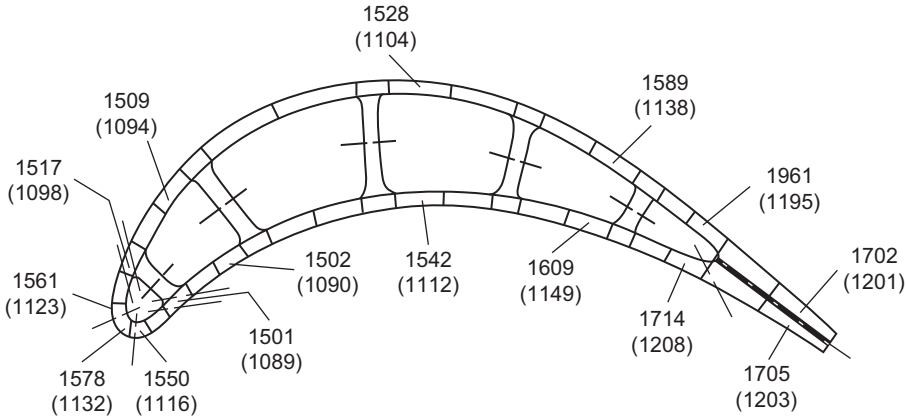


Figure 9-21 Temperature distribution for film convection-cooled design, °F (cooled).

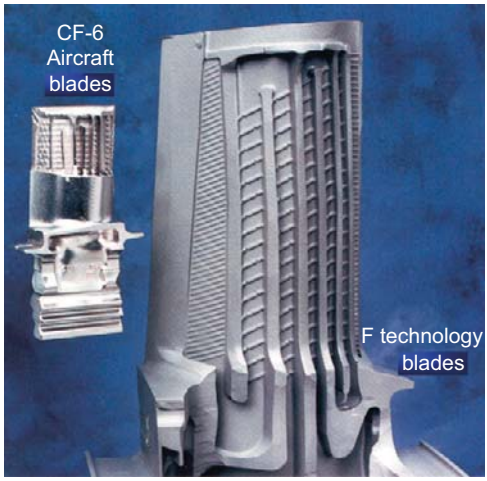


Figure 9-22 Internal of the frame FA blades, showing cooling passage (courtesy: GE Power Systems).

clogging by oxidation. In this design, the shell is supported by cross ribs and is capable of supporting itself without a strut under engine operating conditions. This design has the highest creep life next to a transpiration-cooled design and it has the best strain distribution between leading and trailing edges. It is the closest to optimum.

Water-Cooled Turbine Blades

This design has a number of tubes embedded inside the turbine blade to provide channels for the water (Figure 9-27). In most cases, these tubes are constructed from copper

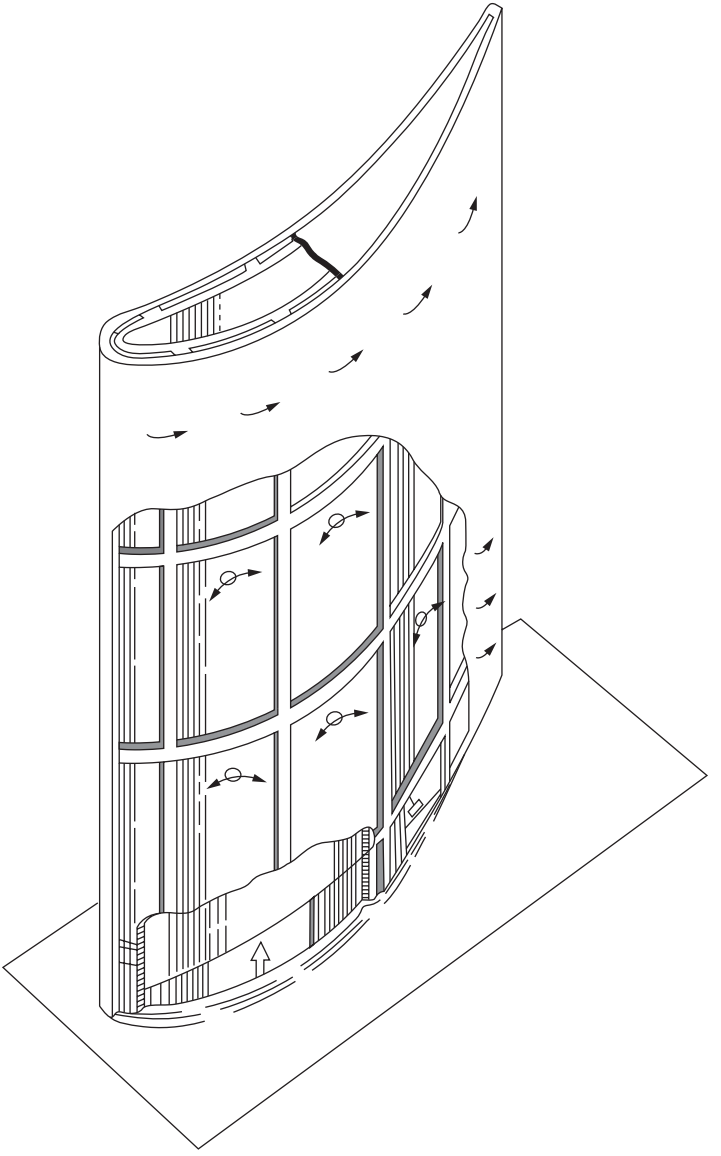


Figure 9-23 Transpiration-cooled blade.

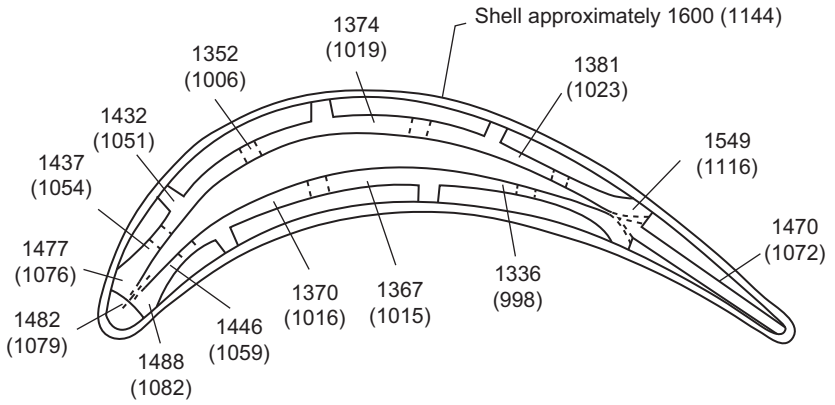


Figure 9-24 Temperature distribution for transpiration-cooled design, °F (cooled).

for good heat-transfer conditions. The water, which is converted to steam by the time it reaches the blade tips, is then injected into the flow stream. These blades are presently in the experimental stage. They hold great promise for the turbine of the future in which turbine inlet temperatures of 3000 °F (1648.8 °C) are possible. This type of cooling should keep blade metal temperatures below 1000 °F (537.8 °C), so that there will be no hot-corrosion problems.

Steam-Cooled Turbine Blades

This design has a number of tubes embedded inside the turbine blade to provide channels for steam. In most cases these tubes are made of copper for good heat-transfer conditions. Steam injection is becoming the prime source of cooling for gas turbines in a combined-cycle application. The steam, which is extracted from the exit of the HP turbine, is sent through the nozzle blades, where the steam is heated and the blade metal temperature decreased. The steam is then injected into the flow stream entering the IP steam turbine. This increases the overall efficiency of the combined cycle.

In the case of the rotating blades, the steam, after it is used in the cooling of the blades, is returned through a series of specially designed slip rings to the steam flow entering the IP steam turbine. Steam cooling in combined-cycle power plants holds great promise for the turbines of the future in which turbine inlet temperatures of 3000 °F (1649 °C) are possible. This type of cooling should keep blade metal temperatures below 1200 °F (649 °C) so that hot-corrosion problems will be minimized. It will also help to increase the efficiency of the total combined-cycle power plant by between 1% and 3%. An evaluation of the six different blade designs is shown in Table 9-1.

Cooled-Turbine Aerodynamics

The injection of coolant air in the turbine rotor or stator causes a slight decrease in turbine efficiency; however, the higher turbine inlet temperature usually makes up for

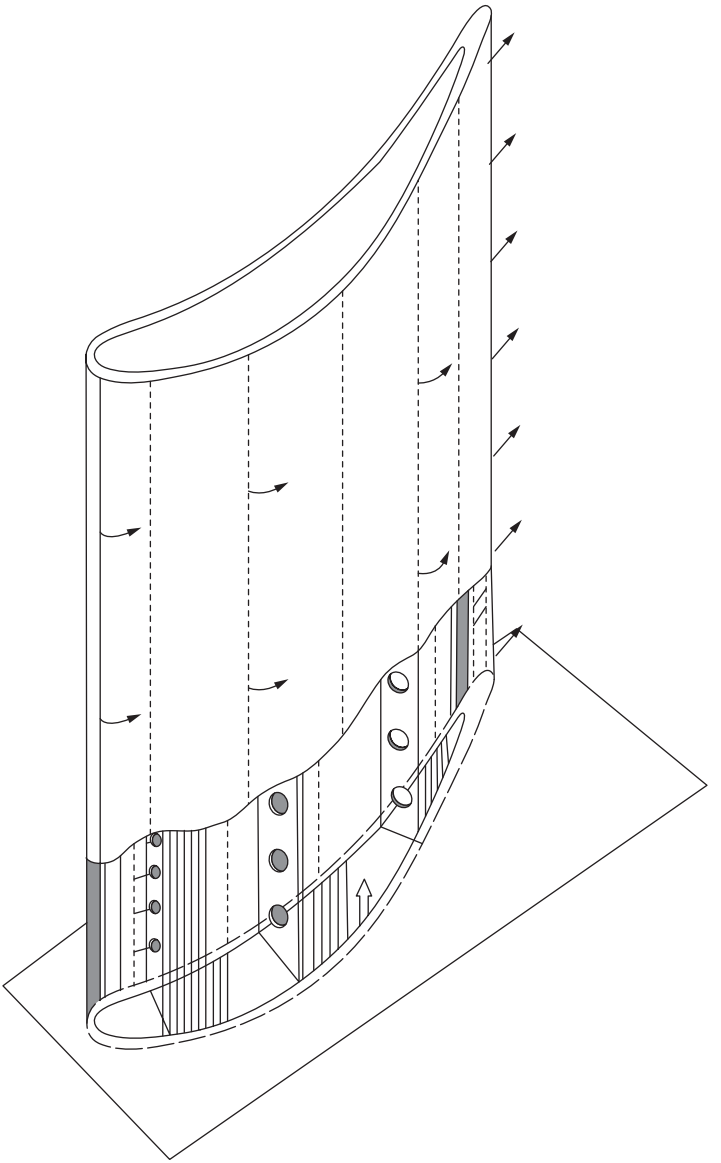


Figure 9-25 Multiple small-hole transpiration-cooled blade.

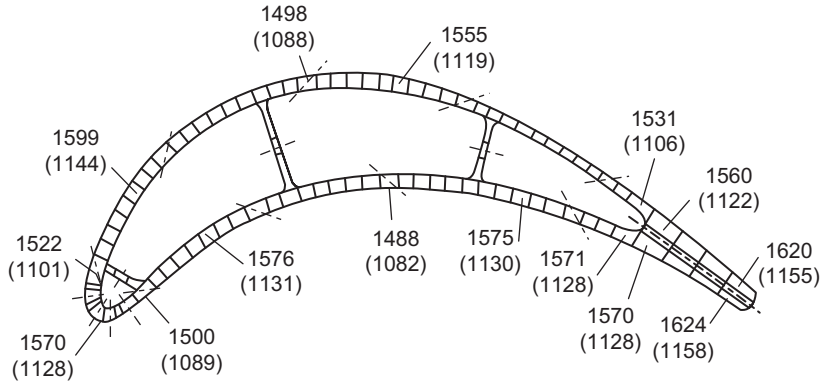


Figure 9-26 Temperature distribution for a multiple small-hole design, °F (cooled).

the loss of the turbine component efficiency, giving an overall increase in cycle efficiency. Tests by NASA on three different types of cooled stator blades were conducted on a specially built 30-in. turbine cold-air test facility. The outer shell profile of all the three blade types was the same, as shown in Figure 9-28.

Total pressure surveys were made downstream of the stators in both the radial and the circumferential directions to determine the effect of coolant on stator losses. The wake traces for the stator with discrete holes and the stator with trailing edge slots show that there is a considerable difference in total pressure loss patterns as a function of the type of cooling and the amount of cooling air supplied. As the coolant flow for the porous blades increases, the disturbance to the flow pattern and the wake thickness increases. Consequently, the losses increase. In a blade with trailing edge slots, the loss initially starts to increase with coolant flow as the wake thickens. However, as the coolant flow is increased, it tends to energize the wake and reduce losses. For a higher coolant flow, the coolant pressures must be higher, resulting in an energization of the flow.

By comparing the various cooling techniques, it becomes obvious that a blade with trailing edge slots is thermodynamically the most efficient, as shown in Figure 9-29. The porous stator blades decrease the stage efficiency considerably. This efficiency indicates losses in the turbine but does not take into account cooling effectiveness. As indicated earlier, the porous blades are more effective for cooling.

The advanced gas turbines use large quantities of air as is apparent from new cross sections of the nozzle vanes and the turbine blades shown schematically in Figure 9-30. Figure 9-31 shows the top of the first-stage nozzle vane shroud of a high-temperature gas turbine; note the three large cooling air inserts and the number of small cooling holes at the nozzle vane shroud.

The new advanced gas turbines also require that the turbine nozzle vanes require cooling on the nozzle vane shrouds and also on the turbine nozzle vane platforms, as shown in Figures 9-32 and 9-33, respectively. Both figures show that the nozzle vane body is close to a transpiration-cooled nozzle vane system. These figures clearly show that these nozzle vanes require a total encapsulated cooling

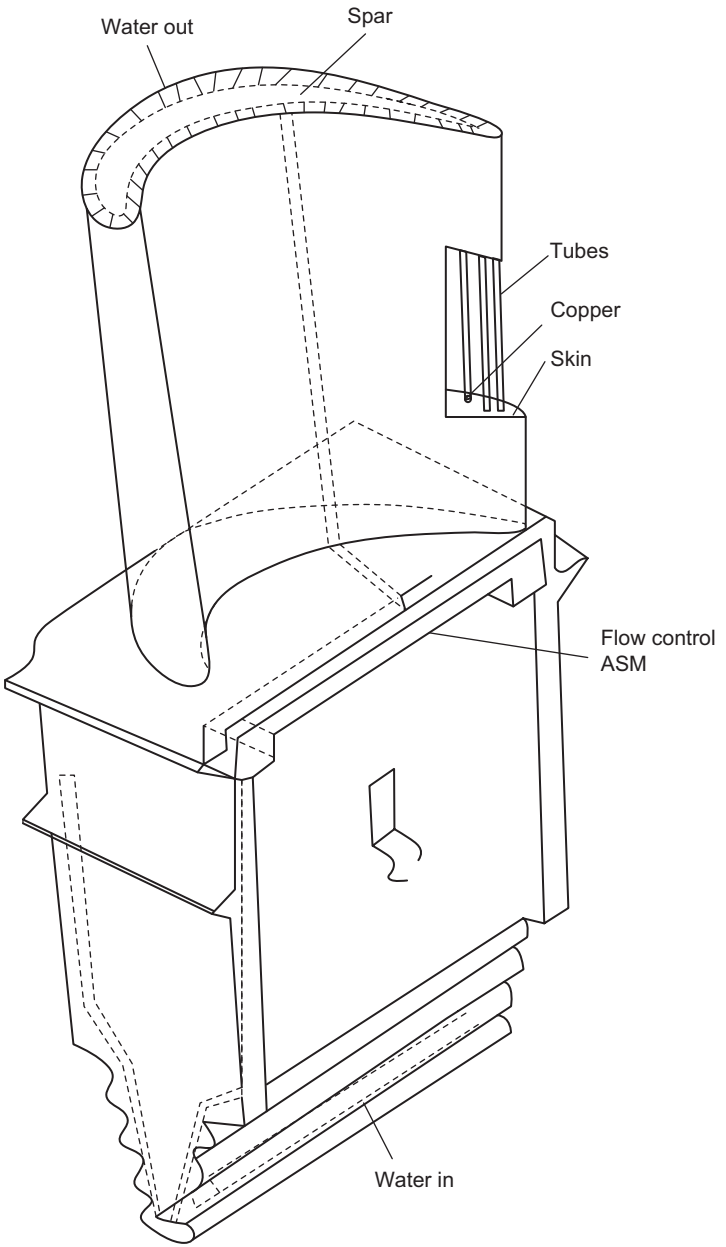


Figure 9-27 Water-cooled turbine blade (courtesy: General Electric Company).

Table 9-1 Summary of Creep Life Experiments

Blade Cooling Design	Time to 1% Creep Strain (hrs)	
	Based on Initial Conditions	**Based on Average Conditions**
Strut design	2430	47,900
Film convection	186	46,700
Transpiration	2530	Infinite
Multiple small-hole	4800	33,500
Water cooled	150	Infinite
Steam cooled	150	35,000

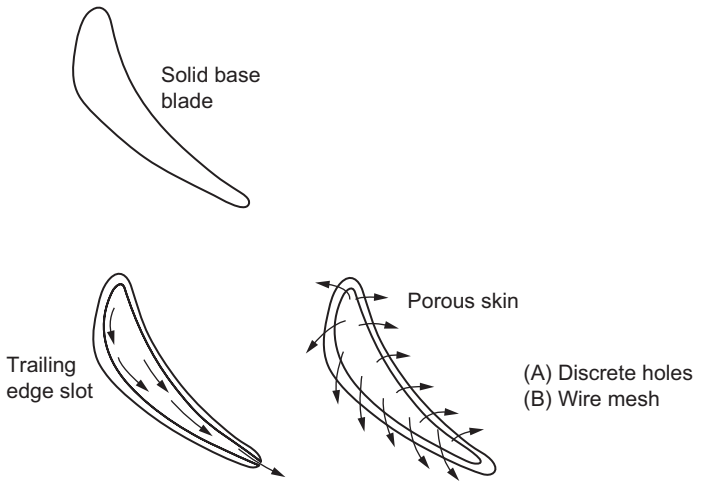


Figure 9-28 Cooled turbine blade types.

unlike the vanes and blades of turbines that had firing temperatures around 2100 °F (1149 °C).

First-stage turbine blades also require cooling at various positions along the blade airfoil body, as well as on the leading and trailing edges of the blades, blade tips, and also the blade platforms. Figure 9-34 shows a first-stage turbine blade with a shower headtype cooling at the leading edge of the blade, cooling holes in rows throughout the blade span airfoil section, and also cooling holes along the trailing edge. The advanced technology turbine blades have a thermal barrier coating (TBC) to further protect the blade. The blades are coated by a coating layer of 15–25 mil thickness which reduces the metal temperature of the blades by 8–16 °F reduction per mil of coating.

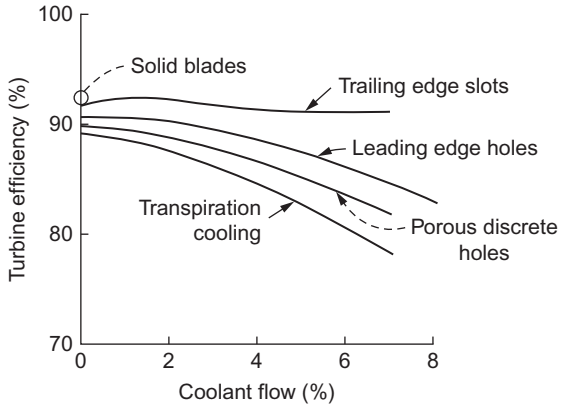


Figure 9-29 The effect of various types of cooling on turbine efficiency.

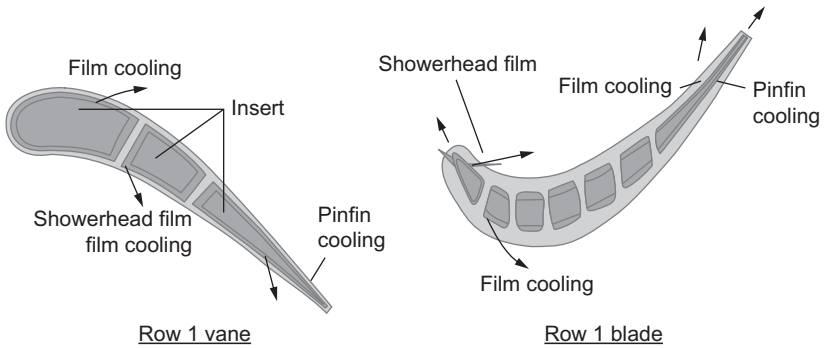


Figure 9-30 Vane and blade cooling diagrams.

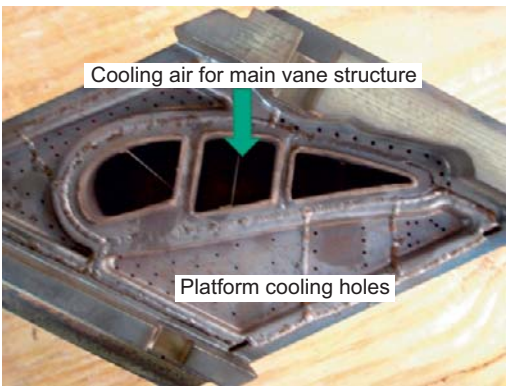


Figure 9-31 Entrance of cooling air at the top surface shroud of the nozzle vane.

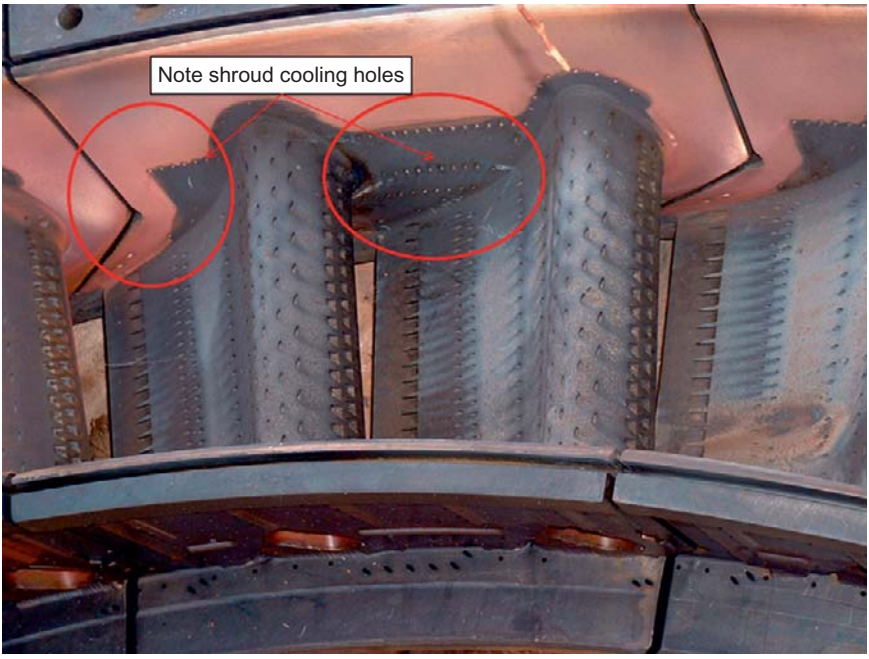


Figure 9-32 First-stage nozzle vane of an advanced gas turbine (note shroud section cooling).

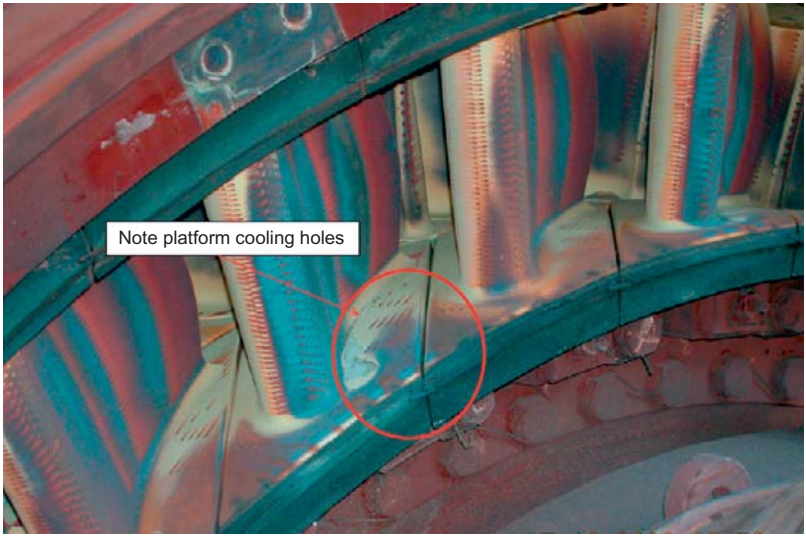


Figure 9-33 First-stage nozzle vane of an advanced gas turbine (note platform section cooling).

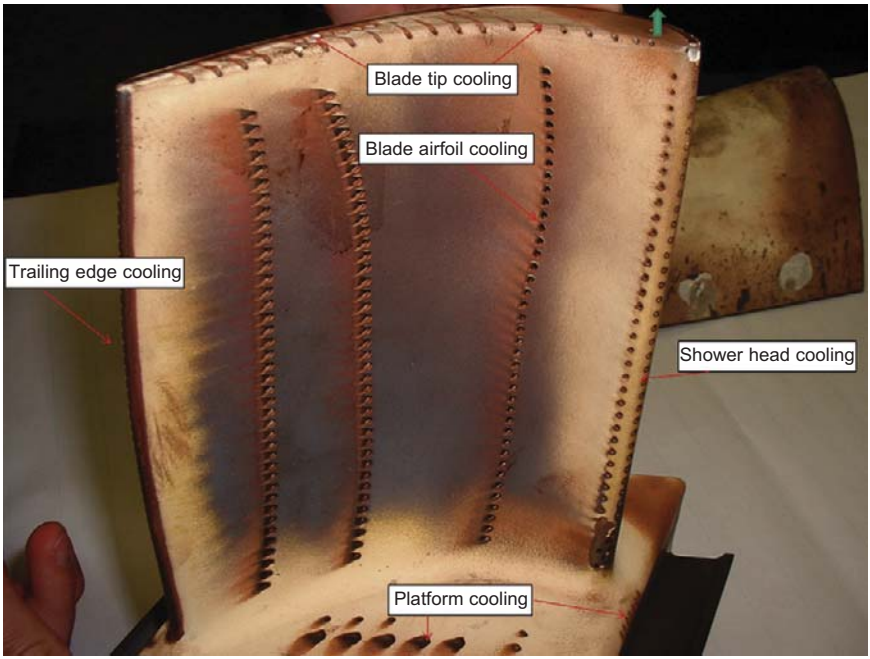


Figure 9-34 First-stage blade of a typical hightemperature first-stage blade.

Usually, the second-stage blades in the new advanced gas turbines also have air cooling and a TBC to further protect the blades. The temperatures entering the second-stage nozzles are considerably less than that of the gas entering the first-stage nozzles. The temperatures entering the second-stage nozzles and entering the second-stage blades are still high enough to require cooling of the vanes and blades. As seen in Figure 9-35 (a) the leading edge and the trailing edge require cooling as well as the platform of the nozzle vanes. Figure 9-35 (b) shows the turbine blades and the cooling at the leading and trailing edges. There is also blade cooling in the airfoil section. The nozzle temperatures in the second stage vary between a fourstage turbine and a three-stage turbine designs The first-stage turbines in most designs have an impulse turbine where the entire enthalpy drop is taken in the first-stage nozzle vanes.

The third- and fourth-stage turbine nozzles and blades are usually not cooled. These blades are long and therefore are shrouded blades as shown in Figure 9-36, which shows a typical set of shrouded blades, to avoid blade resonance that could lead to blade failure. The shrouds as shown in Figure 9-36 are interlocked with each other at the tip. It is important to examine the interlock of these blades and if it is found that the two interlocks are not well connected the blade may have stretched radially; this could lead to blade failures. Figure 9-37 shows a typical fir tree-type holder machined into the rotor disk and often blade disks are joined together via curvic couplings.

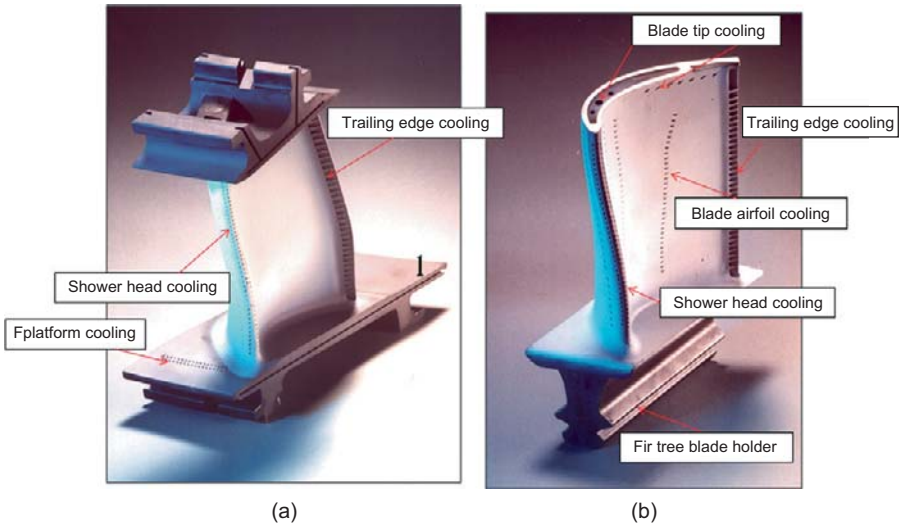


Figure 9-35 Second-stage nozzle vanes and blades.



Figure 9-36 A typical set of tips-hrouded blades.

To ensure proper clearance between the turbine shroud casing and the rotor blade tips the casing is lined by tip-shrouded blocks/rings, which control the gap between the blade tips and the casing. These shroud blocks prevent excessive heat reaching the turbine cover. The shroud blocks that cover the first-stage rotor tips need to be cooled, as the casing at that point is exceedingly hot. The shroud blocks cover and protect the casing from being distorted by the heat. In Figure 9-38, the tip shrouded the blocks from excessive rubbing. Many shroud blocks have a coat of TBC to protect them from the temperature of hot gases in the rotor.

Turbine Losses

The primary cause of efficiency losses in an axial-flow turbine is the build-up of boundary layer on the blade and end walls. The losses associated with a boundary layer

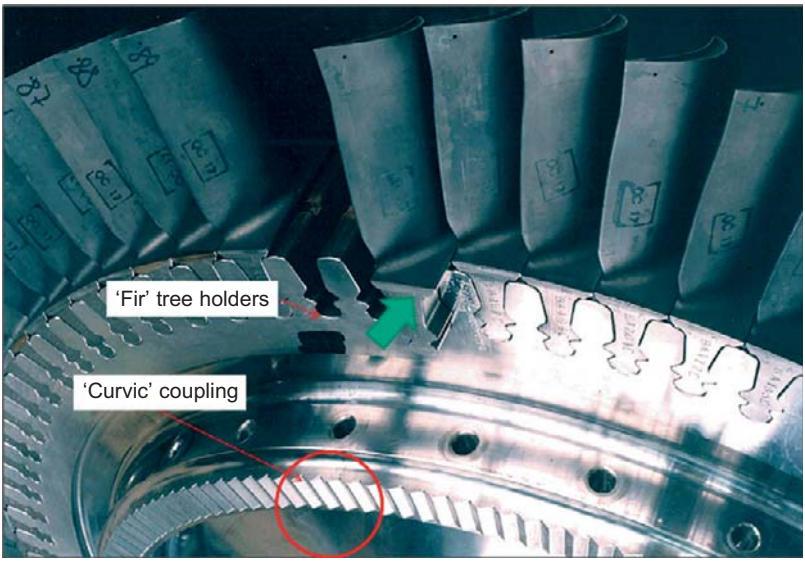


Figure 9-37 Rotor disk showing the fir tree holders and the curvic coupling.

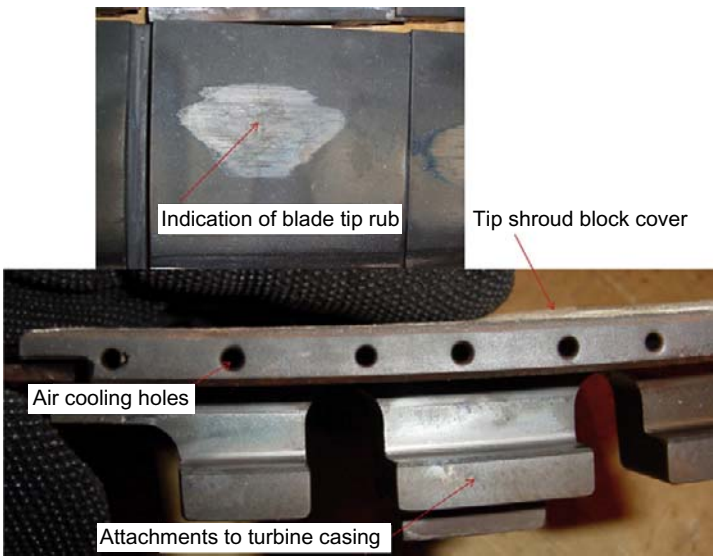


Figure 9-38 Tip-shrouded blocks/rings.

are viscous losses, mixing losses, and trailing edge losses. To calculate these losses, the growth of the boundary layer on a blade must be known, so that the thickness of displacement and momentum can be computed. A typical distribution of thickness of the displacement and the momentum is shown in Figure 9-39. The profile loss from this type of boundary-layer build-up is due to a loss of stagnation pressure, which in

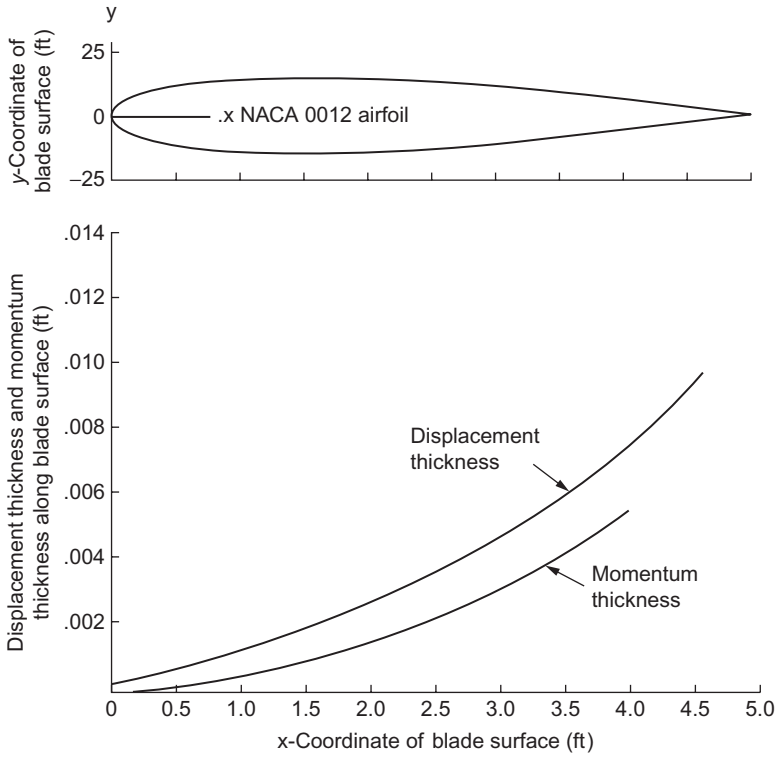


Figure 9-39 Growth of displacement and momentum thickness on an airfoil.

turn is caused by a loss of momentum in the viscous fluid. The blade shape and the pressure gradient to which the flow is subjected are major factors in this type of loss. The endwall losses are also due to a loss of momentum and, although they are also dependent on the profile and pressure gradient, the profile shape and pressure gradient are considerably different. End-wall losses are often combined with secondary losses, since adjacent blade profiles cause a pressure gradient from the pressure surface to the suction surface. The blade loading is thus produced by the different pressures on the opposite side of the same blade. The pressure gradient across the blade passage induces flow from the higher- to the lower-pressure regions. This secondary flow causes losses and results in vorticity in the exit flow.

Tip clearance loss occurs when the blade tip is mechanically free of the shroud casing and the pressure gradient across the blade thickness induces flow leakage through the clearance space. This flow across the tip causes turbulence, a pressure drop, and interferes with the main stream flow. All these effects contribute to tip clearance loss. Another loss is caused by flow incidence when the gas angle and the blade angle of the flow do not coincide, resulting in a disruption of the flow at the blade leading edge. Disc friction loss occurs in an axial-flow compressor because of the close clearances between the casing and the rotor disc. The entrapped fluid causes a viscous power

Table 9-2 Turbine Loss Values in the Overall Stage

Loss Mechanics	Loss (%)
Profile	2–4
Endwall	1½–4
Secondary flow	1–2
Rotor incidence	1–3
Tip clearance	1½–3
Wheel disc	1–2

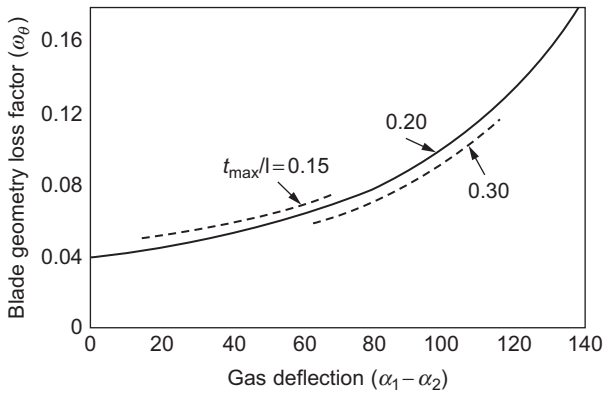


Figure 9-40 Blade geometry loss.

dissipation when the fluid is dragged by the rotor. Table 9-2 shows the approximate value of these losses in the overall stage.

A simple but effective technique for calculating the loss in an axial-flow turbine has been developed. In the loss computation, the blade geometry, the spacing between the blades, the aspect ratio, the thickness ratio, and the effect of the Reynolds number are taken into account. These factors cause the deflection between the incoming and leaving air flows. Figure 9-40 shows the blade geometry loss due to the gas deflection. However, those factors not taken into account are the stagger angle, the trailing edge thickness, and the effects of Mach number.

Neglecting Mach number effects causes a problem in the highly loaded stages. The optimum solidity ($\sigma = c/s$) of the blades is computed from:

$$\sigma = 2.5(\cot\alpha_2 + \cot\alpha_1)\sin^2\alpha_2 \tag{9-20}$$

The loss coefficient can now be computed:

$$\omega = \left(\frac{10^5}{\mathrm{Re}}\right)^{1/4}\left[(1+\omega_\theta)(0.975 + 0.075/\mathrm{AR}) - 1\right]\omega_\mathrm{i} \tag{9-21}$$

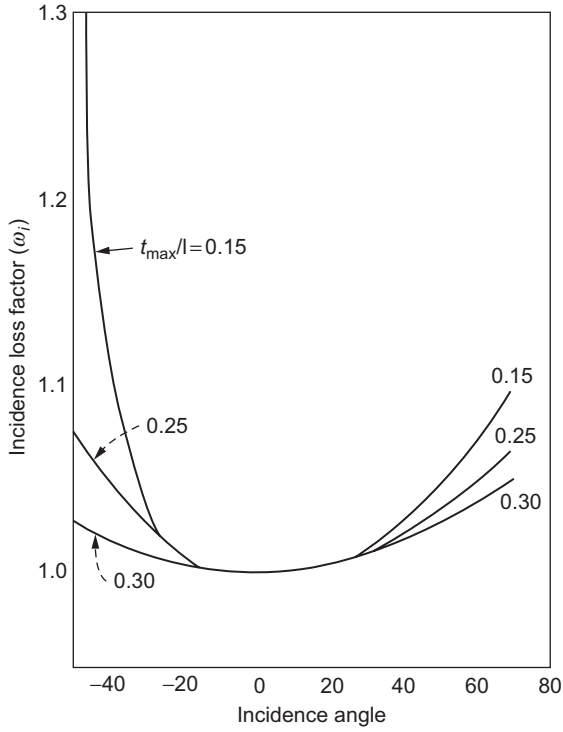


Figure 9-41 Incidence angle loss.

where

$\text{AR} = \text{aspect ratio } (h/c)$

$\omega_\theta =$ the loss from blade geometry seen in Figure 9-40

$\omega_\text{i} =$ the loss due to the incidence angle seen in Figure 9-41

$$\text{Re} = \frac{V_3 Dn}{v_3}$$

where

$$Dn = \frac{2\text{AR}\,\text{s}\sin\alpha_2}{\sigma \sin\alpha_2 + \text{AR}}$$

The change in enthalpy is given by:

$$h_{2a} = h_{2s} + \omega V_3^2/2 \tag{9-22}$$

This loss is now to be re-computed for the rotor.

The off-design characteristics of a turbine are as important to define as the design-point characteristics. Figure 9-42 shows the effect of the speed-to-pressure ratio on

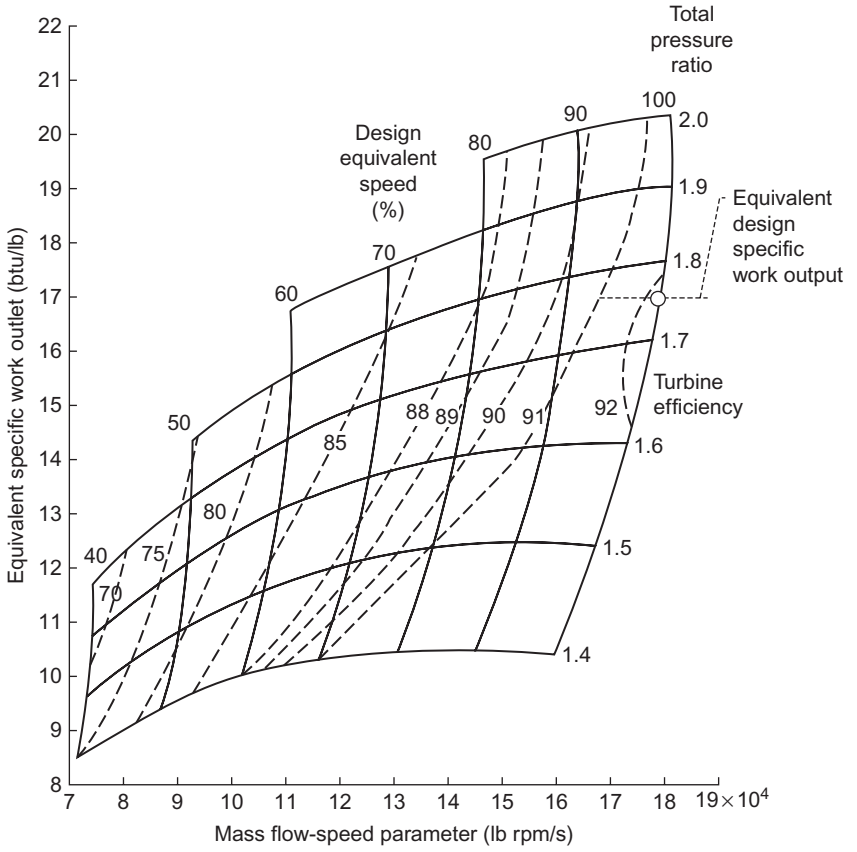


Figure 9-42 Turbine performance map.

the work output. It is obvious from these diagrams that turbine inlet temperature and pressure ratio are the two factors that affect the turbine output most significantly. To obtain these off-design performance characteristics, it is necessary to study the effect of various dimensionless parameters, such as pressure and temperature coefficients, as a function of the flow coefficient. Other techniques used to study flow phenomena and distribution of the flow through the blade are also used for determining off-design conditions.

Bibliography

Balje, O.E., "A Study of Reynolds Number Effects in Turbomachinery," Journal of Engineering for Power, ASME Trans., Vol. 86, Series A, 1964, p. 227.

Copyrighted Materials
Copyright © 2012 Elsevier Retrieved from www.knovel.com

10 Combustors

Gas Turbine Combustors

Heat input to the gas turbine Brayton cycle is provided by a combustor. The combustor accepts air from the compressor and delivers it, at an elevated temperature, to the turbine (ideally with no pressure loss). Thus, the combustor is a direct-fired air heater in which fuel is burned almost stoichiometrically with about 8–30% of the compressor discharge air depending on the lower heating value of the fuel from a high heating value of about 1,050 BTU/lbm (2,443 kJ/kg) to 300 BTU/lbm (698 kJ/kg), respectively. Combustion products are then mixed with the remaining air to arrive at a suitable turbine inlet temperature.

All gas turbine combustors perform the same function; they increase the temperature of the high-pressure gas. Combustor-inlet temperature depends on engine pressure ratio, load and engine type, and whether or not the turbine is regenerative or non-regenerative especially at the low-pressure ratios. Regenerative gas turbines have a lower pressure ratio of between 8:1 and 12:1, compared with the new industrial gas turbines whose pressure ratios are between 17:1 and 35:1, which means that the combustor-inlet temperatures range from 1005 °F (541 °C) to 1139 °F (614 °C) for lower pressure rate regenerative gas turbines and 1266 °F (686 °C) to 1574 °F (857 °C) for higher pressure ratio gas turbines. Combustor-exit temperatures range from 1700 °F (927 °C) to 2900 °F (1593 °C). The new aircraft engines have pressure ratios, which are in excess of 45:1, which have combustor-inlet temperatures of about 1697 °F (541 °C) to 1139 °F (925 °C) and exit temperature of about 2990 °F (1593 °C).

Combustor performance is measured by efficiency, the pressure decrease encountered in the combustor, and the evenness of the outlet temperature profile. Combustion efficiency is a measure of combustion completeness. Combustion completeness affects fuel consumption directly, since the heating value of any unburned fuel is not used to increase the turbine inlet temperature. Normal combustion temperatures range from 3400 °F (1871 °C) to 3500 °F (1927 °C). At this temperature, the volume of nitric oxide in the combustion gas is about 0.01%. If the combustion temperature is lowered, the amount of nitric oxide is substantially reduced.

The use of natural gas and the use of the new dry low NO_x combustors have reduced NO_x levels below 10 ppm. Since September 1979, when regulations required that NO_x emissions be limited to 75 ppmvd (parts per million by volume, dry), thousands of heavy- and medium-duty gas turbines have accumulated millions of operating hours

Gas Turbine Engineering Handbook, Fourth Edition. DOI: 10.1016/B978-0-12-383842-1.00010-X
Copyright © 2012 Elsevier Inc. All rights reserved.

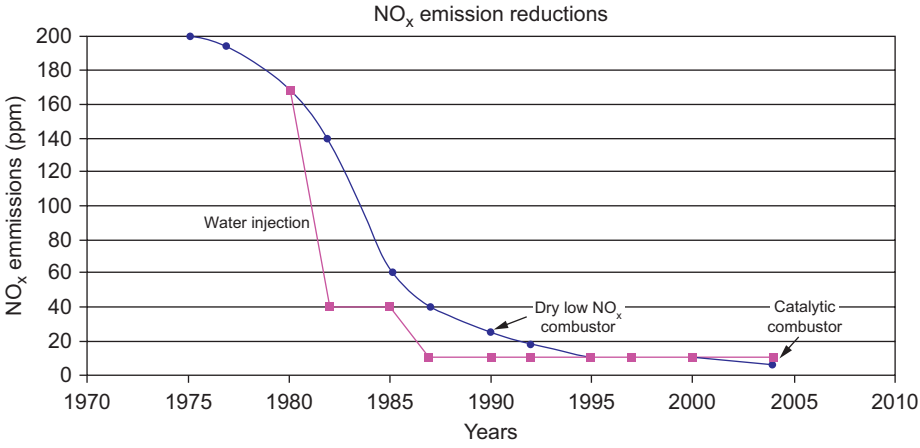


Figure 10-1 Control of gas turbine NO_x emissions over the years.

using either steam or water-injection to meet required NO_x emissions levels, sometimes producing levels even lower than required. Figure 10-1 shows the reduction of NO_x in the past 30 years. The amount of water required to accomplish this is approximately 0.5–0.75% of the fuel flow. However, there is a 1.8% heat rate penalty associated with using water to control NO_x emissions for oil-fired simple-cycle gas turbines. Output increases by approximately 3%, making water (or steam) injection for power augmentation economically attractive in some circumstances (such as peaking applications).

Single-nozzle combustors that use water or steam injection are limited in their ability to reduce NO_x levels below 42 ppmvd on gas fuel and 65 ppmvd on oil fuel. Since October 1987, multi-nozzle combustors using separate fuel and water/steam injection nozzles (see Figure 10-26) have achieved 25 ppmvd NO_x (at 15% O_2) on gas fuel and 42 ppmvd on oil. The use of steam injection (wet combustors) in the diffusion combustors, and then in the1990s, the dry low emission/NO_x combustors have greatly reduced the NO_x output. Most new turbines have progressed to dry low emission or dry low NO_x (DLE/DLN) combustors from the wet diffusion combustors, which were injected by steam in the primary zone of the combustor. The diffusion combustors have a single nozzle while most DLE combustors have multiple fuel nozzles for each can. New units under development have goals, which would reduce NO_x levels below nine ppm and values of as low as two ppm can be attainable in the future. Catalytic converters have also been used in conjunction with both types of combustors to further reduce the NO_x emissions.

Fuel rates vary with load, and fuel atomizers may be required for flow ranges as great as 100:1, as well as heavier fuels, and in DLE/DLN combustors the flow requires staging. However, the variation in the fuel-to-air ratio between idle and full-load conditions usually does not vary by more than a factor of three. During transient conditions, fuel-to-air ratios vary. At light off and during acceleration, a much higher fuel-to-air ratio is needed because of the higher temperature rise. On deceleration, the

conditions may be appreciably leaner. Thus, a combustor that can operate over a wide range of mixtures without the danger of blowouts simplifies the control system.

New research in combustors such as catalytic combustors has great promise. Catalytic combustors are already being used in some engines under the US Department of Energy's (DOE) Advanced Gas Turbine Program and have obtained very encouraging results, showing nearly zero levels of NO_x, and the ability of the catalyst to last about 5,000–8,000 hours.

Typical Combustor Arrangements

There are different methods to arrange combustors on a gas turbine. Designs fall into three main categories:

1. Can-annular
2. Annular
3. Silo-type combustor.

Can-Annular and Annular Combustors

Most American large gas turbines have can-annular combustors. Figure 10-2 shows a set of can-annular combustors on a frame-type gas turbine; there are 10–16 such cans in an annular arrangement on a single gas turbine. The can-annular combustors are easy to maintain, as each can be removed easily and worked on independently. In most can-annular designs, each can is connected with the can next to it through a "cross-over tube" as shown in Figure 10-3. The cross-over tubes are used to equalize the pressure in each can; they are also used during start-up to allow the flame to travel from the two igniter cans to all the other cans. This ensures start-up reliability. Can-annular combustors can be of the straight-through or reverse-flow design and have single fuel nozzles in the diffusion combustors, while in the DLE/DLN combustors each combustor can have three to eight nozzles and one pilot nozzle in the center. If can-annular cans are used in aircraft, the straight-through design is used, while a reverse-flow design may be used on industrial engines.

The annular designs are used on European frame-type gas turbines. Figure 10-4 is a typical frame-type annular combustor used in large gas turbines. Annular combustors are especially popular in new aircraft designs; however, the can-annular design is still used because of the developmental difficulties associated with annular designs. Annular combustor popularity increases with higher temperatures or low-BTU gases, since the amount of cooling air required is much less than in can-annular designs due to a much smaller surface area. The amount of cooling air required becomes an important consideration in low-BTU gas applications, since most of the air is used up in the primary zone and little is left for film cooling. Annular combustors are almost always straight-through flow designs.

The development of a can-annular design requires experiments with only one can, whereas the annular combustor must be treated as a unit and requires much more hardware and a large amount of compressor flow.

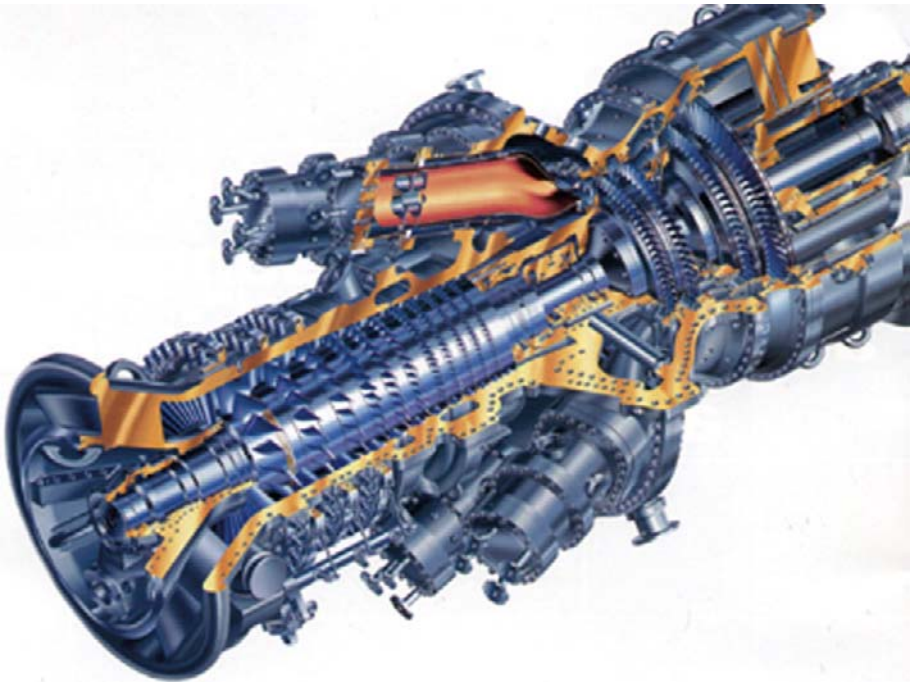


Figure 10-2 A typical diffusion combustor can with straight-through flow.

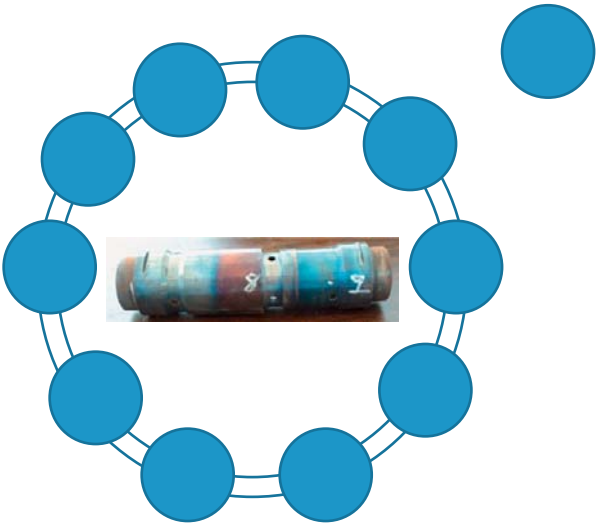


Figure 10-3 Can-annular combustors with cross-over tubes connecting each adjacent combustor.

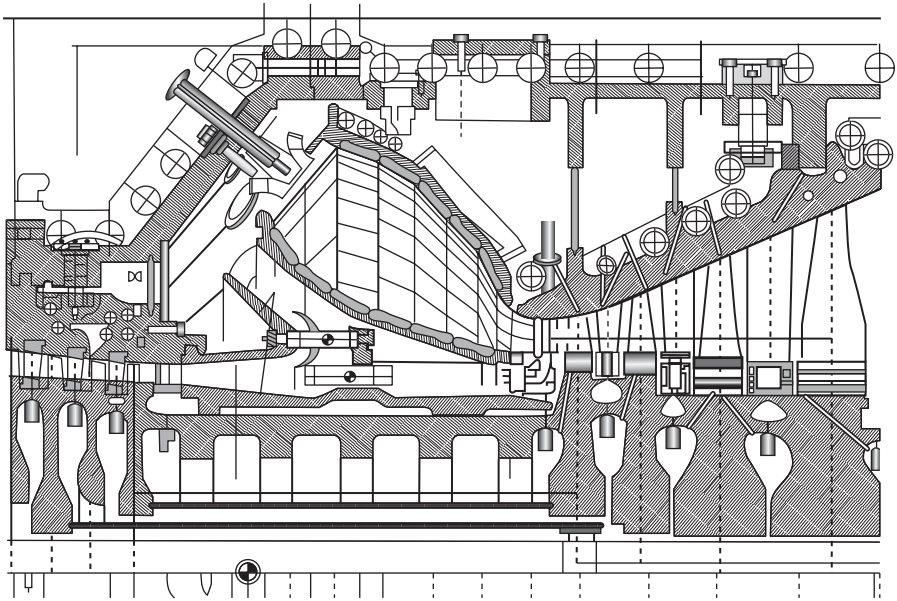


Figure 10-4 A typical industrial-type DLE/DLN annular combustor (Courtesy: Siemens Corp.).

Silo-Type Combustors

Silo-type combustors and side combustors are found on large industrial turbines, especially of European design. Figure 10-5 shows a large frame-type gas turbine with two silo-type side combustors. Smaller side combustors and some small vehicular gas turbines have a combustor as shown in Figure 10-6. They offer the advantages of simplicity of design, ease of maintenance, and long-life due to low heat-release rates. These combustors may be of the "straight-through" or "reverse-flow" design. In the reverse-flow design, air enters the annulus between the combustor can and its housing, usually via a hot-gas pipe, to the turbine. Reverse-flow designs have minimal length.

Combustion in Combustors

There are two types of combustion in combustors:

1. Diffusion combustion
2. Dry low NO_x (DLN) or dry low emission (DLE) combustion.

Gas turbine combustors have seen considerable change in their designs. The original diffusion-type combustors were changed to wet combustors by adding water or steam in the combustion zone to restrict the amounts of NO_x produced. Most new turbines have progressed to dry low emission/NO_x combustors from the wet diffusion combustors, which were injected by steam in the primary zone of the combustor. Diffusion combustors have a single nozzle while most DLE combustors have multiple fuel nozzles per can.

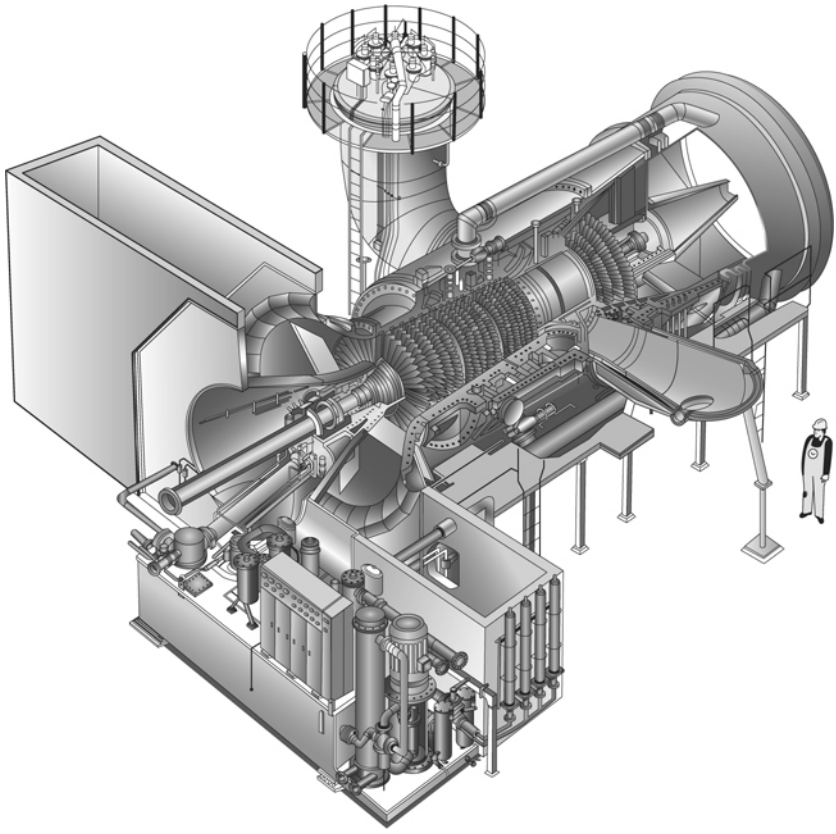


Figure 10-5 Silo-type combustor.

The Diffusion-Type Combustor

This is the most common combustor on the market but it is being displaced by the more complex DLN/DLE combustors.

The gas turbine diffusion combustor uses very little of its air (10%) in the combustion process due to the high BTU content of the gas. The rest of the air is used for cooling and mixing. New combustors are also circulating steam through the combustor liners for cooling purpose. The air from the compressor must be diffused before it enters the combustor. The velocity of the air leaving the compressor is about 400–600 ft/s (122–183 m/s) and the velocity in the combustor must be maintained below 50 ft/s (15.2 m/s). Even at these low velocities, care must be taken to avoid the flame being carried on downstream.

The combustor is a direct-fired air heater in which fuel is burned almost stoichiometrically with one-third or less of the compressor discharge air. Combustion products are then mixed with the remaining air to arrive at a suitable turbine inlet temperature. Despite the many design differences in combustors, all gas turbine combustion

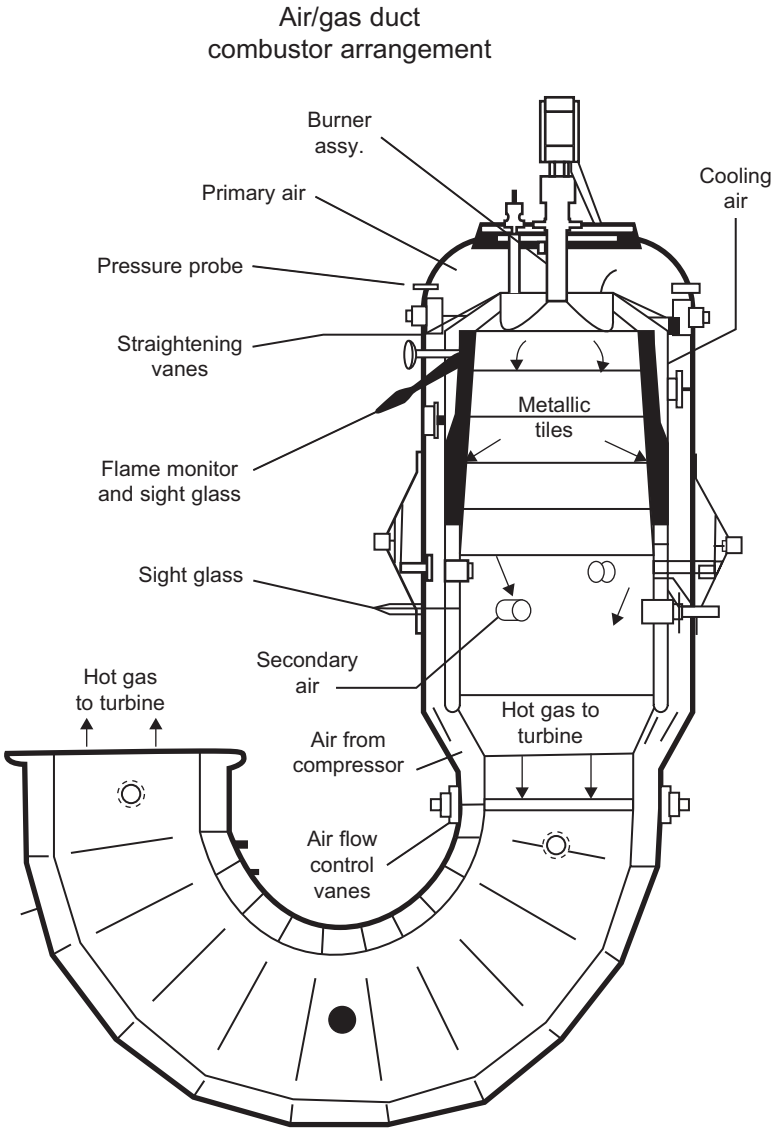


Figure 10-6 A typical single can side combustor.

chambers have three features: (1) a recirculation zone, (2) a burning zone (with a recirculation zone that extends to the dilution region), and (3) a dilution zone, as shown in Figure 10-7. The air entering a combustor is divided, so that the flow is distributed among three major regions: (1) primary zone, (2) dilution zone, and (3) annular space between the liner and casing.

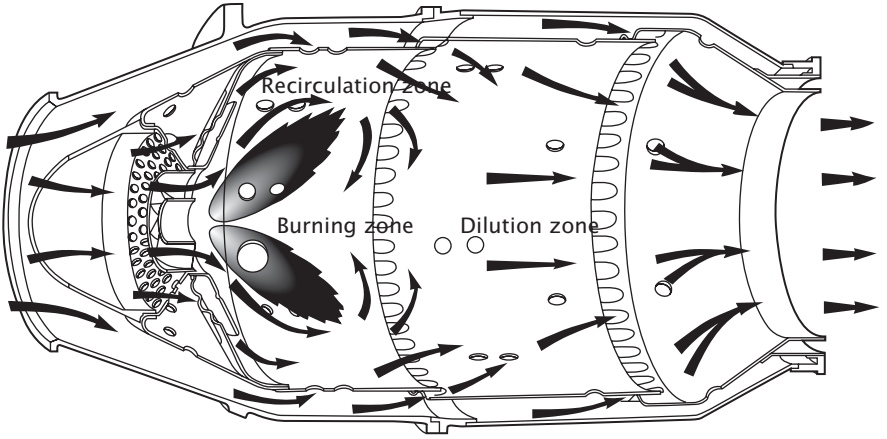


Figure 10-7 A typical diffusion combustor can with straight-through flow.

The combustion in a combustor takes place in the primary zone. Combustion of natural gas is a chemical reaction that occurs between carbon, or hydrogen, and oxygen. Heat is given off as the reaction takes place. The products of combustion are carbon dioxide and water. The reaction is stoichiometric, which means that the proportions of the reactants are such that there are exactly enough oxidizer molecules to bring about a complete reaction to stable molecular forms in the products. The air enters the combustor in a straight-through flow or reverse flow. Most aero-engines have straight-through flow-type combustors. Most of the large frame-type units have reverse flow. The function of the recirculation zone is to evaporate, partly burn, and prepare the fuel for rapid combustion within the remainder of the burning zone. Ideally, at the end of the burning zone, all fuel should be burnt, so that the function of the dilution zone is solely to mix the hot gas with the dilution air. The mixture leaving the chamber should have a temperature and velocity distribution acceptable to the guide vanes and turbine. Generally, the addition of dilution air is so abrupt that if combustion is not complete at the end of the burning zone, chilling occurs that prevents completion. However, there is evidence with some chambers that if the burning zone is run over-rich, some combustion does occur within the dilution region. Figure 10-8 shows the distribution of the air in the various regions of the diffusion-type combustor. The theoretical or reference velocity is the flow of combustor-inlet air through an area equal to the maximum cross section of the combustor casing. The flow velocity is 25 fps (7.6 mps) in a reverse-flow combustor and is between 80 fps (24.4 mps) and 135 fps (41.1 mps) in a straight-through flow turbojet combustor. Figure 10-9 shows a typical diffusion-type combustor used in the frame-type gas turbines. There may be 6–16 of these types of combustors placed in an annular configuration. Note that the main flow from the compressor in many of these combustors goes up between the combustor can and the liner and flows into the combustor liner at various points; thus, it is known as a reverse-flow combustor. Only about 18% of the flow enters the can at the top through the swirler where it combusts with the fuel. The rest of the flow enters the

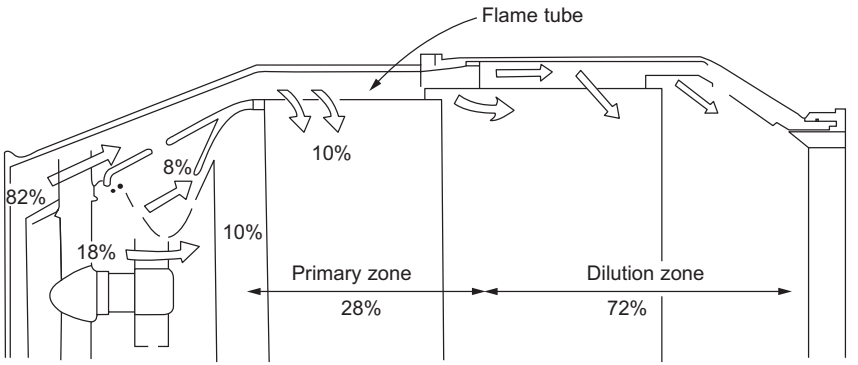


Figure 10-8 Air distribution in a typical diffusion combustor.

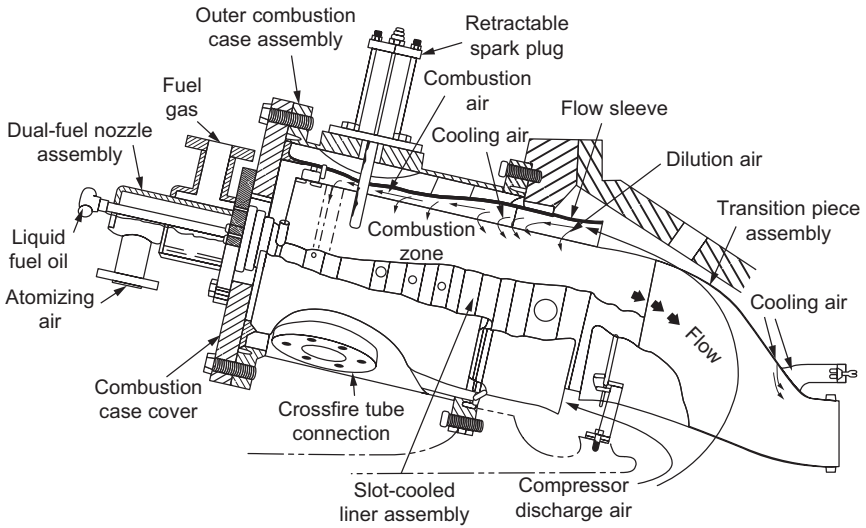


Figure 10-9 A typical reverse-flow diffusion can-annular combustor.

liner through a series of small holes around the liner diameter thus keeping the liner and the can cooled.

As mentioned in the introduction of this chapter, the combustor-inlet temperature depends on engine pressure ratio, load and engine type, and whether or not the turbine is regenerative or non-regenerative especially at the low-pressure ratios.

Combustor performance is measured by efficiency, the pressure decrease encountered in the combustor, and the evenness of the outlet temperature profile. Combustion efficiency is a measure of combustion completeness. Combustion completeness affects fuel consumption directly, since the heating value of any unburned fuel is not used to increase the turbine inlet temperature. To calculate combustion efficiency, the actual heat increase of the gas is ratioed to the theoretical heat input of the fuel

(lower heating value):

$$\eta_{\text{comb}} = \frac{\Delta h_{\text{actual}}}{\Delta h_{\text{theoretical}}} = \frac{(\dot{m}_{\text{a}} + \dot{m}_{\text{f}})\, h_3 - \dot{m}_{\text{a}} h_2}{\dot{m}_{\text{f}} \text{LHV}} \tag{10-1}$$

where

h_2 = enthalpy leaving the compressor section
h_3 = enthalpy entering the turbine section
$\dot{m}_{\text{a}}$ = mass of air flow
$\dot{m}_{\text{f}}$ = mass of fuel flow
LHV = lower heating value of the fuel

The loss of pressure in a combustor is a major problem, since it affects both the fuel consumption on a unit MW basis and power output. A pressure loss occurs in a combustor because of diffusion, friction, and momentum. Total pressure loss is usually in the range of 2–4% of static pressure (compressor outlet pressure). The efficiency of the engine will be reduced by an equal percentage. The result is increased fuel consumption and lower power output that affects the size and weight of the engine.

The uniformity of the combustor outlet profile affects the useful level of the turbine inlet temperature, since the average gas temperature is limited by the peak gas temperature. The profile factor is the ratio between the maximum exit temperature and the average exit temperature. Figure 10-10 is a temperature profile measured at the exit of the gas turbine at different loads; this is a very important parameter for determining the health of the gas turbine. In this map, we see a relatively smooth profile. Exhaust temperature spread readings are based on the exhaust gas readings at the exit of the turbine. In this turbine, there were 16 probes used in the control system, and the turbine settings for shutdown for gas turbines operating on natural gas usually are set at about 100 °F (56 °C) between the maximum and minimum temperatures at any given time at the exit. Temperature differences between adjacent probes should not exceed 40–50 °F (22–28 °C) for turbines operating on natural gas. The temperature readings at the exit of the turbine represent conditions occurring between 30 ° and 40 ° upstream and against the direction of rotation.

The uniformity of the combustor outlet profile affects the useful level of turbine inlet temperature, since the average gas temperature is limited by the peak gas temperature. This uniformity assures adequate turbine nozzle vane life, which depends on operating temperature. The average inlet temperature to the turbine affects both fuel consumption and power output. A large combustor outlet gradient will work to reduce average gas temperature and consequently reduce power output and efficiency. The traverse number is defined as the peak gas temperature minus mean gas temperature divided by mean temperature rise in nozzle design. Thus, the traverse number must have a lower value between 0.05 and 0.15 in the turbine nozzle vanes.

Equally important are the factors that affect satisfactory operation and life of the combustor. To achieve satisfactory operation, the flame must be self-sustaining and combustion must be stable over a range of fuel-to-air ratios to avoid ignition loss during transient operation. Moderate metal temperatures are necessary to assure long

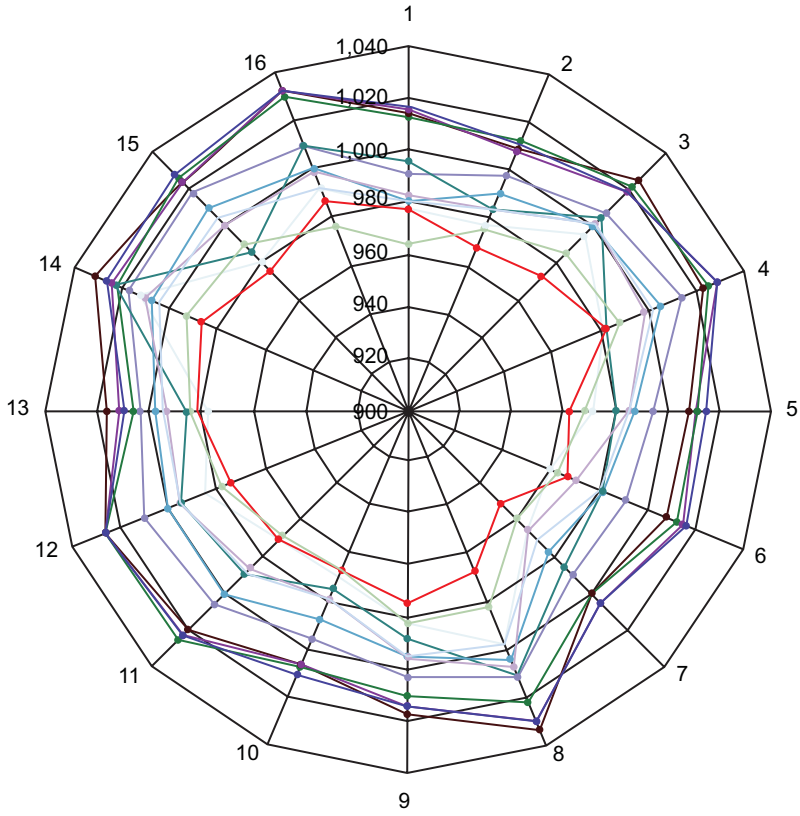


Figure 10-10 Exit temperature profile of a typical gas turbine taken at various load settings.

life. In addition, steep temperature gradients, which warp and crack the combustion liner, must be avoided. Carbon deposits can distort the liner and alter the flow patterns to cause pressure losses. Smoke is environmentally objectionable as well as a fouler of heat exchangers. Minimum carbon deposits and smoke emissions also help assure satisfactory operations.

The combustion in a combustor takes place in the primary zone. Combustion of natural gas is a chemical reaction that occurs between the hydrocarbons and oxygen. Heat is given off as the reaction takes place. The products of combustion are carbon dioxide and water. The reaction is stoichiometric, which means that the proportions of the reactants are such that there are exactly enough oxidizer molecules to bring about a complete reaction to stable molecular forms in the products. The ratio of the oxygen content at stoichiometric conditions and actual conditions is called the equivalence ratio:

$$\Phi = \frac{\text{Oxygen/Fuel at stoichiometric condition}}{\text{Oxygen/Fuel at actual condition}} \tag{10-2}$$

Normal stoichiometric combustion temperatures range from 3400 °F (1871 °C) to 3500 °F (1927 °C). At this temperature, the volume of nitric oxide in the combustion gas is about 0.01%. If the combustion temperature is lowered, the amount of nitric oxide is substantially reduced. To fully understand the combustion process, one must be familiar with the various combustion terms that define the combustion process in a diffusion combustor.

Diffusion Combustor Design Considerations

Some of the major parameters that define a diffusion combustor design are discussed in the following sections.

Cross-Sectional Area

The combustor cross section can be determined by dividing the volumetric flow at the combustor inlet by a reference velocity, which has been selected as being appropriate for the particular turbine conditions based on the proven performance in a similar engine. Another basis for selecting a combustor cross section comes from correlations of thermal loading per unit cross section. Thermal loading is proportional to the primary-zone air flow because fuel/air mixtures are near stoichiometric in all combustors.

Length

Combustor length must be sufficient to provide for flame stabilization, combustion, and mixing with dilution air. The typical value of the length-to-diameter ratio for liners ranges from three to six. Ratios for casing range from two to four.

Reference Velocity

The theoretical velocity for flow of combustor-inlet air through an area is equal to the maximum cross section of the combustor casing [25 fps (8 mps) in a reverse-flow combustor and 80–135 fps (24–41 mps) in a straight-through flow turbojet combustor].

Profile Factor

It is defined as the ratio between the maximum exit temperature and the average exit temperature.

Temperature factor, also known as the traverse number, can be defined as:

1. The peak gas temperature minus mean gas temperature divided by mean temperature rise in the nozzle design.
2. The difference between the highest and the average radial temperatures.

Stoichiometric Proportions

Constituent proportions of the reactants are such that there are exactly enough oxidizer molecules to bring about a complete reaction to stable molecular forms in the products.

Equivalence Ratio

It is the ratio of the oxygen content at stoichiometric and actual conditions:

$$\Phi = \frac{\text{Oxygen/Fuel at stoichiometric condition}}{\text{Oxygen/Fuel at actual condition}}$$

Lower Heating Value

The lower heating value of the gas is one in which the H_2O in the products has not condensed. The lower heating value is equal to the higher heating value minus the latent heat of the condensed water vapor.

Pressure Drop

A pressure loss occurs in a combustor because of diffusion, friction, and momentum. The pressure drop value is 2–10% of the static pressure (compressor outlet pressure). The efficiency of the engine will be reduced by an equal percentage. The minimum practical pressure drop – excluding diffuser loss – is about 14 times higher than the reference velocity pressure. Higher values are frequently used. Some values for this pressure loss are as follows: 100 fps (30 mps), 4%; 80 fps (24 mps), 2.5%; 70 fps (21 mps), 2%; and 50 fps (15 mps), 1%.

Wobbe Number

Wobbe number is an indicator of the characteristics and stability of the combustion process. Increasing the Wobbe number can cause the flame to burn closer to the liner, and decreasing the Wobbe number can cause pulsations in the combustor.

Volumetric Heat-Release Rate

The heat-release rate is proportional to the fuel-to-air ratio and the combustor pressure, and it is a function of combustor capacity. Actual space required for combustion, as chemical limits are approached, varies with pressure to the 1.8 power.

Liner Holes

Liner area to casing area and liner hold area to casing area are important to the performance of combustors. For example, the pressure loss coefficient has a minimum value in the range of 0.6 of the liner area-to-casing area ratio with a temperature ratio of 4:1.

In practice, it has been found that the diameter of holes in the primary zone should be no larger than 0.1 of the liner diameter. Tubular lines with about 10 rings of eight holes each give good efficiency. As discussed before, swirl vanes with holes yield better combustor performance. In the dilution zone, sizing of the holes can be used to provide a desired temperature profile.

Combustion Liners

Three major changes have occurred since the original AISI 309 stainless louver-cooled liners. The first change was the adoption of better materials such as Hastelloy

X/RA333 in the 1960s and Nimonic 75 and the adoption of the slot-cooled liner in the early 1970s. This slot-cooled design offers considerably more liner cooling effectiveness and, from a materials standpoint, presents a new area of processing challenges. Fabrication and repair of liners is primarily by a combination of brazing and welding. On the other hand, earlier liners were made using a welded construction with mechanically formed louvers.

For resistance against fatigue, Nimonic 75 has been used with Nimonic 80 and Nimonic 90. Nimonic 75 is an 80–20 nickel–chromium alloy stiffened with a small amount of titanium carbide. Nimonic 75 has excellent oxidation and corrosion resistance at elevated temperatures, a reasonable creep strength, and good fatigue resistance. In addition, it is easy to press, draw, and mold. As firing temperatures have increased in the newer gas turbine models, HA-188, a Cr, Ni-based alloy, has recently been employed in the latter section of some combustion liners for improved creep rupture strength.

Second, in addition to the base material changes, many of today's combustors also have thermal barrier coatings (TBCs), which have an insulation layer of the total thickness 0.015–0.025 inches (0.4–0.6 mm) and are based on ZrO_2–Y_2O_3 and can reduce metal temperatures by 90–270 °F (50–150 °C).

TBCs consist of two different materials applied to the hot side of the component: a bond coat applied to the surface of the part and an insulating oxide applied over the bond coat. The characteristics of TBCs are that the insulation is porous and they have two layers. The first layer is a bond coat of NICrAlY and the second is a top coat of YTTRIA-stabilized zirconia.

The advantages of the TBCs are the reduction of metal temperatures of cooled components, by about 8–14 °F (4–9 °C) per mil (25.4 μm) of the coating, the microstructure, and a coated liner. The primary benefit of the TBCs is to provide an insulating layer that reduces the underlying base material temperature and mitigates the effects of hot streaking or uneven gas temperature distributions. These coatings are now standard on most high-performance gas turbines and have demonstrated excellent performance in production machines.

The third major change was the introduction of steam cooling of the liners. This concept, especially in combined-cycle application, has great potential.

Reliability of Combustors

The heat from combustion, pressure fluctuation, and vibration in the compressor may cause cracks in the liner and nozzle. In addition, there are corrosion and distortion problems. The edges of the holes in the liner are of great concern because the holes act as stress concentrators for any mechanical vibrations and, on rapid temperature fluctuations, high-temperature gradients are formed in the region of the hole edge, giving rise to a corresponding thermal fatigue.

It is necessary to modify the edge of the hole in various ways to reduce these stress concentrations. Some methods of modification are priming, plunging, and standard radiusing and polishing. In the dry low NO_x combustors, especially in the lean premix

chambers, pressure fluctuations can set up very high vibrations, which lead to major failures.

Combustion Process

In its simplest form, combustion is a process in which some material or fuel is burned. Whether it is striking a match or firing a jet engine, the principles involved are the same and the products of combustion are similar.

Combustion of natural gas is a chemical reaction that occurs between carbon, or hydrogen, and oxygen. Heat is given off as the reaction takes place. The products of combustion are carbon dioxide and water. The reaction is as follows:

$$\begin{aligned} &CH_4 + 4O \rightarrow CO_2 + 2H_2O + \text{Heat} \\ &(\text{Methane} + \text{Oxygen}) \qquad (\text{Carbondioxide} + \text{Water} + \text{Heat}) \end{aligned} \tag{10-3}$$

Four parts of oxygen are required to burn one part of methane. The products of combustion are one part of carbon dioxide and two parts of water. One cubic foot of methane will produce one cubic foot of carbon dioxide gas.

Oxygen used for combustion occurs in the atmosphere. The chemical composition of air is approximately 21% oxygen and 79% nitrogen, or one part of oxygen to four parts of nitrogen. In other words, for each cubic foot of oxygen contained in the air, there are about 4 ft^3 of nitrogen.

Oxygen and nitrogen molecules each contain two atoms of oxygen or nitrogen. Noting that one part, or molecule, of methane requires four parts of oxygen for complete combustion, and since the oxygen molecule contains two atoms, or two parts, the volumetric ratio of methane and oxygen is as follows:

$$CH_4 + 2(O_2 + 4N_2) \rightarrow 2H_2O + CO_2 + 8N_2 + \text{Heat} \tag{10-4}$$

The preceding equation is the true chemical equation for the combustion process. One cubic foot of methane actually requires 2 ft^3 of oxygen for combustion. Since the oxygen is contained in air, which also has nitrogen, the combustion reaction can be written as follows:

$$\begin{aligned} &1CH_4 + 2(O_2 + 4N_2) \rightarrow 1CO_2 + 8N_2 + 2H_2O + \text{Heat} \\ &(\text{Methane} + \text{Air}) \qquad (\text{Carbondioxide} + \text{Nitrogen} + \text{Water} + \text{Heat}) \end{aligned} \tag{10-5}$$

One cubic foot (0.03 m^3) of methane requires 10 ft^3 (0.28 m^3) of air, 2 ft^3 (0.06 m^3) of oxygen, and 8 cubic feet (0.23 cubic meter) of nitrogen for combustion. The products are carbon dioxide, nitrogen, and water. The combustion product of 1 ft^3 of methane yields a total of 9 ft^3 of carbon dioxide gas. In addition, the gas burned contains some ethane, propane, and other hydrocarbons. The yield of inert combustion gas from burning a cubic foot of methane will be 9.33 ft^3 (0.26 m^3). If the combustion process created only the reactions shown in the previous discussion, no provision would

be necessary for control. Unfortunately, other reactions occur in which undesirable products are formed.

The chemical reaction that occurs in the formation of nitric acid during the combustion process is as follows:

$$2N + 5O + H_2O \rightarrow \underset{\text{(Nitirc Oxide)}}{2NO} + 3O + H_2O \rightarrow \underset{\text{(Nitirc Oxide)}}{2HNO_3} \tag{10-6}$$

The water required in the previous reaction comes from the water of combustion. The intermediate reaction shown previously (nitric acid formation) does not occur during the combustion process, but occurs after the nitric oxide is further oxidized to nitrogen dioxide (NO_2) and cooled. Consequently, it is necessary to control the formation of nitric oxide during the combustion process to prevent its ultimate conversion to nitric acid. The formation of nitric oxide during combustion can be retarded by reducing the temperature at which combustion occurs. Normal combustion temperatures range from 3400 to 3500 °F (1871–1927 °C). At this temperature, the volume of nitric oxide in the combustion gas is about 0.01%. If the combustion temperature is lowered, the amount of nitric oxide is substantially reduced. By maintaining a temperature below 2800 °F (1538 °C) at the burner, the nitric oxide volume will be below the maximum limit of 20 parts per million (0.002%). This minimum is attained by injecting a noncombustible gas (flue gas) around the burner to cool the combustion zone.

Sulfuric acid is another common by-product of combustion. Its reaction is as follows:

$$H_2S + 4O \rightarrow \underset{\text{Sulfur Oxide}}{SO_2} + H_2O \rightarrow \underset{\text{Sulfuric acid}}{H_2SO_4}$$

The formation of sulfuric acid cannot be economically retarded in the combustion process. The best method of eliminating sulfuric acid as a combustion product is to remove sulfur from the incoming fuel gas. Two separate sweetening processes are used to remove all sulfur from the fuel gas that will be burned.

The amount of oxygen in the combustion gas is regulated by controlling the ratio of air to fuel in the primary section. As previously mentioned, the ideal volumetric ratio of air to methane is 10:1. If less than 10 volumes of air are used with one volume of methane, the combustion gas will contain carbon monoxide. The reaction is as follows:

$$1CH_4 + 1.5(O_2 + 4N_2) \rightarrow 2H_2O + 1CO + 6N_2 + \text{Heat} \tag{10-7}$$

In gas turbines, there is plenty of air, so that the carbon monoxide is very low but can be significant from an environmental emissions standpoint.

Velocity is used as a criterion in combustor design, especially with respect to flame stabilization. The importance of air velocity in the primary zone is known. A transition zone is often included before the primary zone, so that the high-velocity air from the compressor is diffused to a lower velocity and higher pressure and distributed around the combustion liner. The secondary, or dilution air should only be added after the primary reaction has reached completion. Dilution air is added gradually so as not to

quench the reaction in "conventional" combustors. Flame tubes should be designed to produce a desirable outlet profile and to last a long time in the combustor environment. Adequate life is assured by film cooling the liner.

The air enters the annular space between the liner and casing and is admitted into the space within the liner through holes and slots because of the pressure difference. The design of these holes and slots divides the liner into distinct zones for flame stabilization, combustion, and dilution, and it provides film cooling for the liner.

The liner experiences a high temperature because of heat radiated by the flame and combustion. To improve the life of the liner, it is necessary to lower the temperature of the liner and use a material which has a high resistance to thermal stress and fatigue. The air-cooling method reduces the temperature both inside and outside the surface of the liner. This reduction is accomplished by fastening a metal ring inside the liner to leave a definite annular clearance. Air is admitted into this clearance space through rows of small holes in the liner and is directed by metal rings as a film of cooling air along the liner inside.

Air-Pollution Problems in a Diffusion Combustor

Smoke

In general, it has been found that much visible smoke is formed in small, local fuel-rich regions. The general approach to eliminate smoke is to develop leaner primary zones with an equivalence ratio between 0.9 and 1.5. Another supplementary way to eliminate smoke is to supply relatively small quantities of air to those exact, local, and over-rich zones.

Un-burnt hydrocarbons and carbon monoxide are only produced in incomplete combustion typical of idle conditions. It appears probable that idling efficiency can be improved by detailed design to provide better atomization in the case of liquid fuels and higher local temperatures.

Oxides of Nitrogen

The main oxides of nitrogen produced in combustion are NO, with the remaining 10% as NO_2. These products are of great concern because of their role of creating harmful particulate matter, ground-level ozone, and acid rain in the atmosphere, especially at full-load conditions. The formation mechanism of NO can be explained as follows:

1. Fixation of atmospheric oxygen and nitrogen at high-flame temperature.
2. Attack of carbon or hydrocarbon radicals of fuel on nitrogen molecules, resulting in NO formation.
3. Oxidation of the chemically bound nitrogen in fuel.

In 1977, the Environmental Protection Agency (EPA) in the United States issued proposed rules that limited the emissions of new, modified, and reconstructed gas turbines to:

- 75 volumetric parts per million (vppm) NO_x at 15% oxygen (dry basis).

- 150 vppm SO_x at 15% oxygen (dry basis), controlled by limiting fuel sulfur content to less than 0.8 wt%.

These standards applied to simple- and regenerative-cycle gas turbines and to the gas turbine portion of combined-cycle steam/electric generating systems. The 15% oxygen level was specified to prevent the NO_x ppm level being achieved by dilution of the exhaust with air.

In 1977, it was recognized that there were a number of ways to control oxides of nitrogen:

1. Use of a rich primary zone in which little NO formed, followed by rapid dilution in the secondary zone.
2. Use of a very lean primary zone to minimize peak flame temperature by dilution.
3. Use of water or steam admitted with the fuel for cooling the small zone downstream from the fuel nozzle.
4. Use of inert exhaust gas recirculated into the reaction zone.
5. Catalytic clean-up of NO_x and CO from the gas turbine exhaust.
6. Design of the combustor to limit the formation of pollutants in the burning zone by utilizing "lean-premixed" combustion technology. Work on the DLE combustor and the first DLN system was tested in 1980.

"Wet" control combustors were the preferred method in the 1980s and most of 1990s, since "dry" controls and catalytic cleanup were both at very early stages of development. Catalytic converters were used in the 1980s and are still being widely used; however, the cost of rejuvenating the catalyst is very high.

There has been a gradual tightening of the NO_x limits over the years from 75 ppm to 25 ppm, and the new gas turbine goals are as low as two ppm.

Advances in combustion technology now make it possible to control the levels of NO_x production at source, removing the need for "wet" controls. This of course opened up the market for the gas turbine to operate in areas with limited supplies of suitable quality water, for example, deserts or marine platforms.

Although water injection is still used, "dry" control combustion technology has become the preferred method for the major players in the industrial power generation market. DLN (dry low NO_x) was the first acronym to be coined, but with the requirement to control NO_x without increasing carbon monoxide and un-burned hydrocarbons, this has now become DLEs (dry low emissions).

Nitrogen oxides ($NO_x = NO + NO_2$) must be divided into two classes according to their mechanism of formation. Nitrogen oxides formed from the oxidation of the free nitrogen in the combustion air or fuel are called "thermal NO_x." They are mainly a function of the stoichiometric adiabatic flame temperature of the fuel, which is the temperature reached by burning a theoretically correct mixture of fuel and air in an insulated vessel. The following is the relationship between combustor operating conditions and thermal NO_x production:

- NO_x increases strongly with fuel-to-air ratio or with firing temperature.
- NO_x increases exponentially with combustor-inlet air temperature.
- NO_x increases with the square root of the combustor-inlet pressure.
- NO_x increases with increasing residence time in the flame zone.

- NO_x decreases exponentially with increasing water or steam injection or increasing specific humidity.

Emissions that are due to oxidation of organically bound nitrogen in the fuel – fuel-bound nitrogen (FBN) – are called "organic NO_x." Only few parts per million of the available free nitrogen (almost all from air) are oxidized to form nitrogen oxide, but the oxidation of FBN to NO_x is very efficient. For conventional combustion systems, the efficiency of conversion of FBN into nitrogen oxide is 100% at low FBN contents. At higher levels of FBN, the conversion efficiency decreases. Organic NO_x formation is less well understood than thermal NO_x formation. It is important to note that the reduction of flame temperatures to abate thermal NO_x has little effect on organic NO_x. For liquid fuels, water and steam injection actually increases organic NO_x yields. Organic NO_x formation is also affected by turbine firing temperature. The contribution of organic NO_x is important only for fuels that contain significant amounts of FBN such as crude or residual oils.

The majority of the NO_x produced in the combustion chamber is "thermal NO_x." This mechanism is called thermal, since the breakup of the strong N_2 triple bond needs a high activation energy. It is produced by a series of chemical reactions between the nitrogen (N_2) and the oxygen (O_2) in the air that occur at the elevated temperatures and pressures in gas turbine combustors. The reaction rates are highly temperature dependent, and the NO_x production rate becomes significant above flame temperatures of about 3300 °F (1815 °C). The mechanism on thermal NO_x production was first postulated by Zeldovich, and Figure 10-11 shows the flame temperature of distillate fuel as a function of the equivalence ratio, and that the thermal NO_x production rises very rapidly as the stoichiometric flame temperature is reached. Away from this point, thermal NO_x production decreases rapidly. This theory has provided the mechanism of thermal NO_x control in a diffusion flame combustor, thus the primary way to control thermal NO_x is to reduce the flame temperature. Equivalence ratio as defined earlier in this chapter is a measure of fuel-to-air ratio in the combustor normalized by stoichiometric fuel-to-air ratio. At the equivalence ratio of unity, the stoichiometric conditions are reached. The flame temperature is highest at this point. At equivalence ratios less than one, a "lean" combustor exists. At the values greater than one, the combustor is "rich." Gas turbine combustors are designed to operate in the lean region.

Figure 10-12 shows, schematically, flame temperatures and, therefore, NO_x production zones inside a conventional diffusion combustor. This design deliberately burned all the fuel in a series of zones going from fuel rich to fuel lean to provide good stability and combustion efficiency over the entire power range.

The great dependence of NO_x formation on temperature reveals the direct effect of water or steam injection on NO_x reduction. Recent research showed an 85% reduction of NO_x by steam or water injection with optimizing combustor aerodynamics.

NO_x Prevention

Emissions from turbines are a function of temperature and thus a function of the fuel to air (F/A) ratio. Figure 10-13 shows that as the temperature is increased, the amount of NO_x emissions is increased, whereas the amount of CO and the un-burnt hydrocarbons

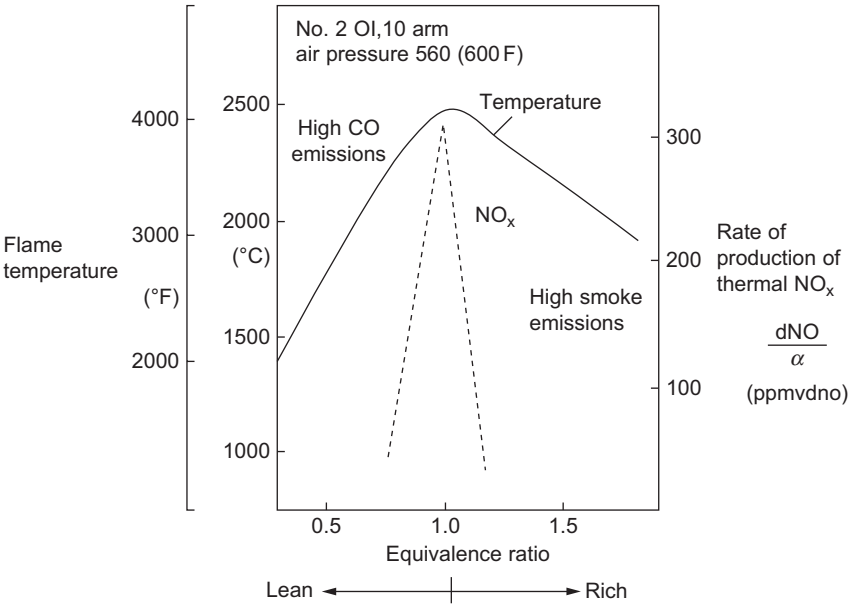


Figure 10-11 NO_x production rate.

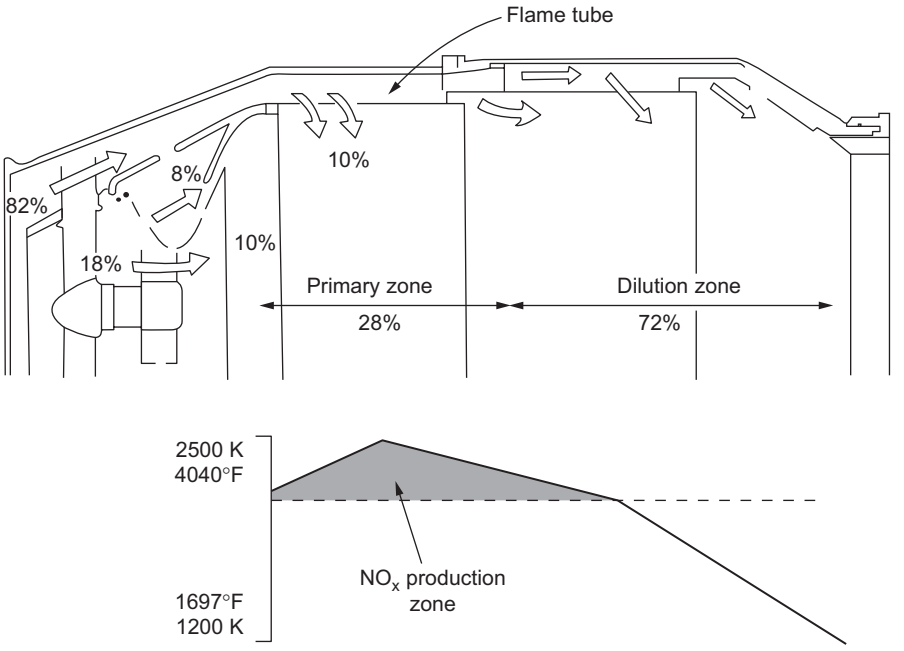


Figure 10-12 Flame temperatures in various zones in a combustor.

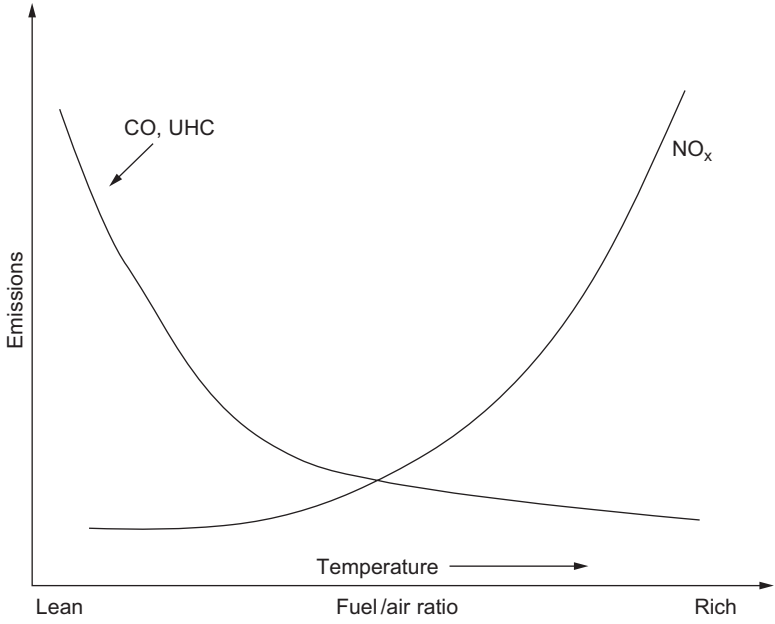


Figure 10-13 Effect on emissions with fuel-to-air ratio (temperature) increase.

are decreased. The principal mechanism for NO_x formation is the oxidation of nitrogen in air when exposed to high temperatures in the combustion process, the amount of NO_x is thus dependent on the temperature of the combustion gases and also, to a lesser amount, on the time the nitrogen is exposed to these high temperatures.

The challenge in these designs is to lower the NO_x without degradation in unit stability. In the combustion of fuels that do not contain nitrogen compounds, NO_x compounds (primarily NO) are formed by two main mechanisms: thermal mechanism and the prompt mechanism. In the thermal mechanism, NO is formed by the oxidation of molecular nitrogen through the following reactions known as the Zeldovich mechanism:

$$O + N_2 \leftrightarrow NO + N \tag{10-8}$$

$$N + O_2 \leftrightarrow NO + O \tag{10-9}$$

$$N + OH \leftrightarrow NO + H \tag{10-10}$$

Since thermal NO formation requires very large activation energy, the formation of NO_x in gas turbine combustion is only significant at high-flame temperatures. In a first-order approximation, the NO_x formation rate is described by the following relationship:

$$\frac{dNO}{dt} \propto \exp\left(T_{\text{flame}}\right) \tag{10-11}$$

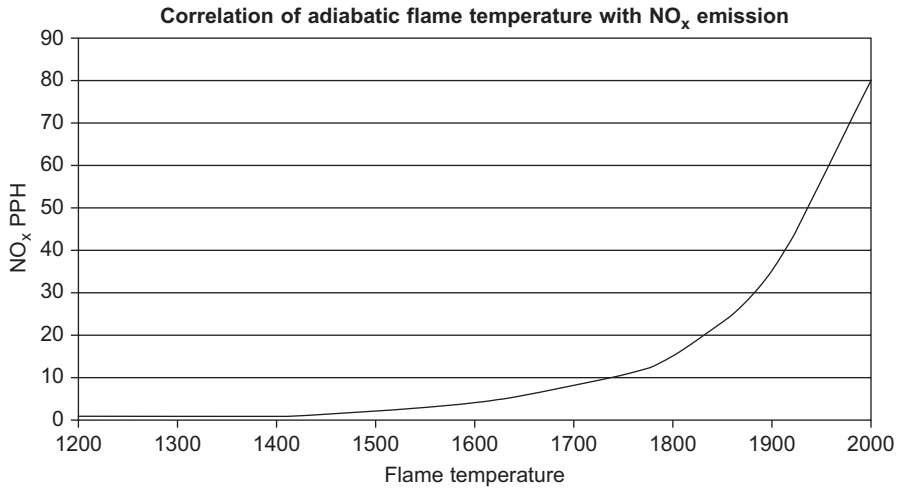


Figure 10-14 Correlation between adiabatic flame temperature and NO_x emission.

As can be seen from the above relationship, NO_x is primarily formed through high-temperature reaction between nitrogen (N) and oxygen (O_2) from the air.

Hydrocarbon radicals, predominantly through the reaction, initiate the prompt mechanism.

$$CH + N_2 \rightarrow HCN + N \tag{10-12}$$

The HCN and N are converted rapidly to NO by reaction with oxygen and hydrogen atoms in the flame.

The prompt mechanism predominates at low temperatures under fuel-rich conditions, whereas the thermal mechanism becomes important at temperatures above 2732 °F (1500 °C). Due to the onset of the thermal mechanism, the formation of NO_x in the combustion of fuel/air mixtures increases rapidly with temperature above 2732 °F (1500 °C) and also increases with residence time in the combustor.

The important parameters in the reduction of NO_x are the temperature of the flame, the nitrogen and oxygen content, and the residence time of the gases in the combustor. Figure 10-14 is a correlation between the adiabatic flame temperature and the emission of NO_x. Reduction of any and all these parameters will reduce the amount of NO_x emitted from the turbine.

Diffusion Combustor Design

The Diffusion Combustor

The simplest combustor is a straight-walled duct connecting the compressor and turbine as shown in Figure 10-15. Actually, this arrangement is impractical because of the excessive pressure loss resulting from combustion at high velocities. The fundamental pressure loss from combustion is proportional to the air velocity squared. Since

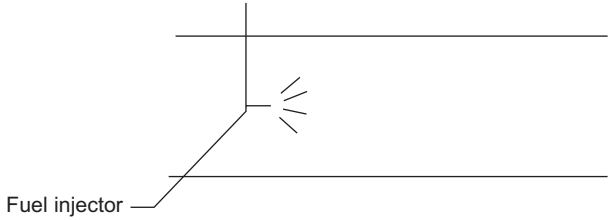


Figure 10-15 Simple straight-walled duct combustor

compressor discharge velocities can be on the order of 500 ft/s (152.4 m/s), the combustion pressure loss can be up to one quarter of the pressure rise produced by the compressor. For this reason, air entering the combustor is first diffused to lower the velocity. Still, up to half the combustor pressure loss can be caused by this diffusion.

Even with a diffuser, velocities are still too high to permit stable combustion. With flame speeds of a few fps (ft/sec), a steady flame cannot be produced by simple injection into an airstream with a velocity of one to two orders of magnitude greater. Even if ignited initially, the flame will be carried downstream and cannot be sustained without continuous ignition. A baffle of some type needs to be added to create a region of low velocity and flow reversal for flame stabilization as shown in Figure 10-16. The baffle creates an eddy region in the flow continually drowning in gases to be burned, mixing them, and completing the combustion reaction. It is this steady circulation that stabilizes the flame and provides continuous ignition. The problem in combustion then becomes one of the producing only enough turbulences for mixing and burning, and avoiding an excess, which results in increased pressure loss.

It is desirable to be able to analyze the controlling features of a stabilizing system, so that a good combustion efficiency with respect to pressure loss is attained. Since combustor design involves the formation of turbulent zones with complicated fluid flow and chemical reaction effects, combustor designers must resort to empiricism. A simple bluff body, such as a baffle placed in the flow stream, is the simplest case of flame stabilization. Although the basic flow pattern in each combustor primary zone is similar (fuel and air mixed, ignited by recirculating flame, and burned in a highly turbulent region), there are various ways to create flame stability in the primary zone. However, they are more complicated and difficult to analyze than the simple baffle. Figures 10-17 and 10-18 show two such designs. In one, a strong vortex is created by swirl vanes around the fuel nozzle. Another flow pattern is formed when combustor air is admitted through rings of radial jets. Jet impingement at the combustor axis results in upstream flow forming a torroidal recirculation zone that stabilizes the flame.

Velocity is an important factor in primary-zone design. A fixed velocity value in the combustor creates a limited range of mixture strength for which the flame is stable. In addition, different flame stabilizing arrangements (baffles, jets, or swirl vanes) exhibit different ranges of burnable mixtures at a given velocity. Figure 10-19 is a general stability diagram that shows how the range of burnable mixtures decreases as velocity increases. Changing baffle size will affect the range of burnable limits as well as the pressure loss. To accommodate a wide operating range of fuel-to-air ratios,

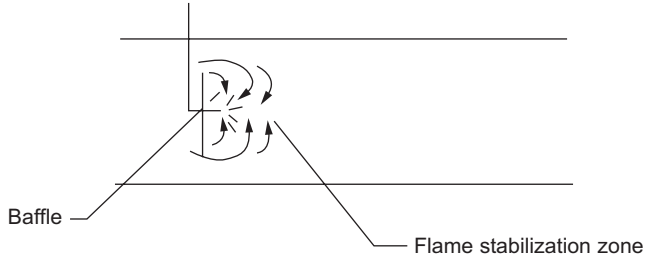


Figure 10-16 Baffle added to straight-walled duct to create flame stabilization zone.

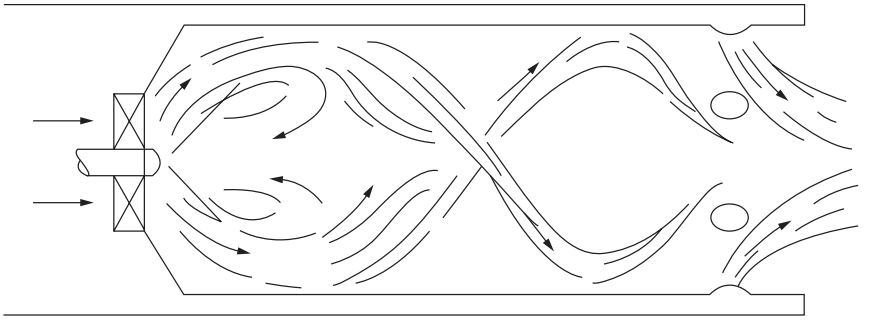


Figure 10-17 Flame stabilization region created by swirl vanes.

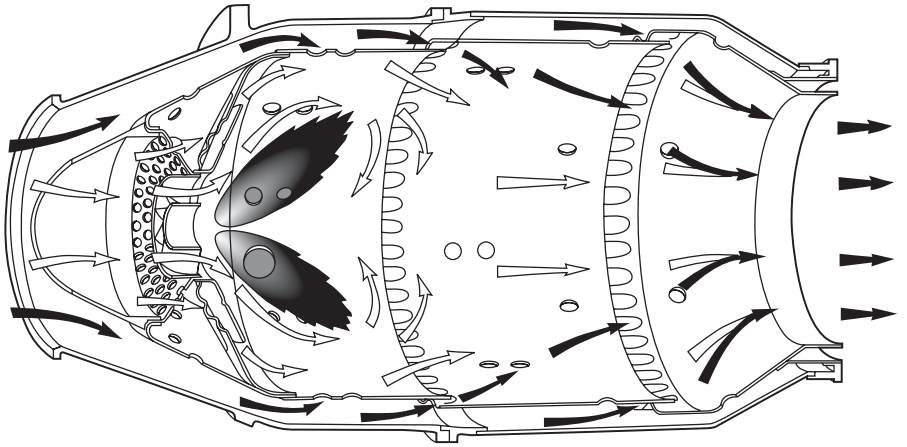


Figure 10-18 Flame stabilization created by impinging jets and general airflow pattern (© Rolls-Royce Limited).

the combustor is designed to operate well below the blowout velocity. Gas turbine compressors operate with nearly constant air velocities at all loads. This constant air velocity results from the compressor operating at a constant speed, and in the cases

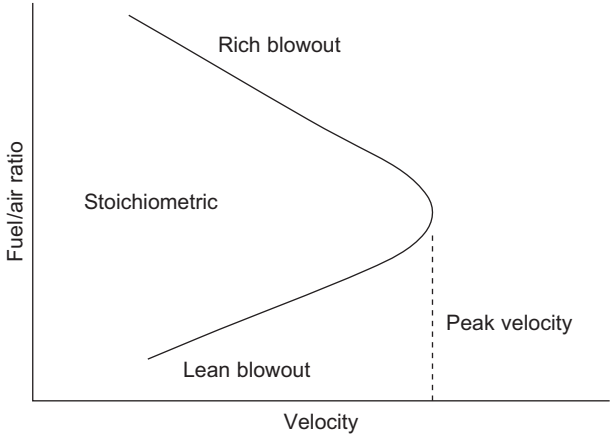


Figure 10-19 Range of burnable fuel-to-air ratios versus combustor gas velocity.

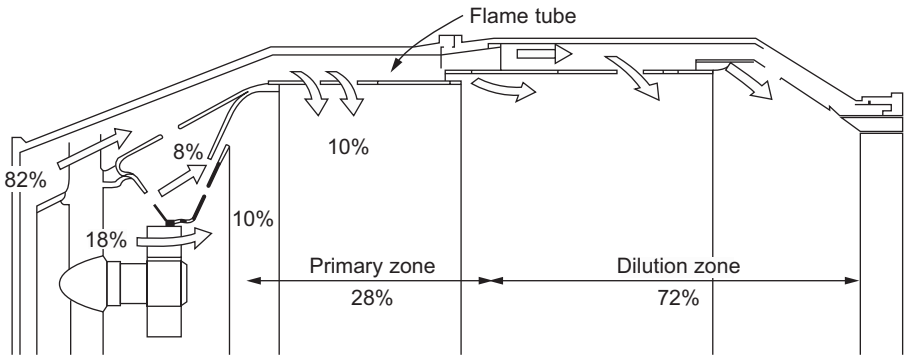


Figure 10-20 Addition of flame tube distributes flow between primary and dilution zones.

where the mass flow varies as a function of the load, the static pressure varies similarly; the volumetric air flow is nearly constant. Therefore, velocity can be used as a criterion in combustor design, especially with respect to flame stabilization.

The importance of air velocity in the primary zone is known. In the primary zone, fuel-to-air ratios are about 60:1; the remaining air must be added somewhere. The secondary, or dilution, air should only be added after the primary reaction has reached completion. Dilution air should be added gradually so as not to quench the reaction. The addition of a flame tube as a basic combustor component accomplishes this, as shown in Figure 10-20. Flame tubes should be designed to produce a desirable outlet profile and to last a long time in the combustor environment. Adequate life is assured by film cooling of the liner.

Figure 10-21 is a schematic of a can-annular combustor. At the left is a transition zone in which high-velocity air from the compressor is diffused to a lower velocity and higher pressure, and distributed around the combustion liner. The air enters the annular space between the liner and casing and is admitted into the space within the

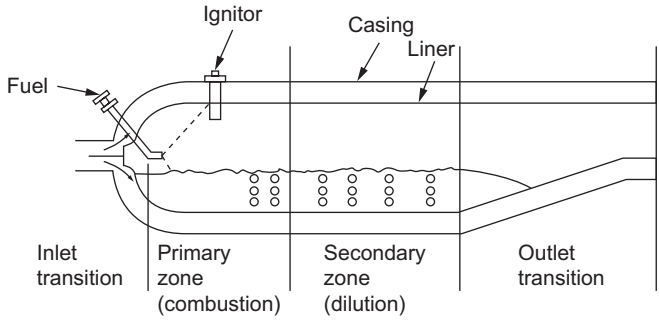


Figure 10-21 Schematic of a can-annular combustor.

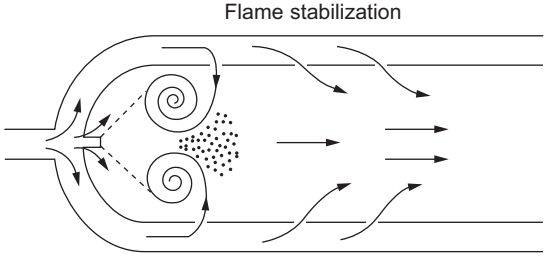


Figure 10-22 Flow pattern by swirl vanes and radial jets.

liner through holes and slots because of the pressure difference. The design of these holes and slots divides the liner into distinct zones for flame stabilization, combustion, dilution, and it provides film cooling of the liner.

Flame Stabilization

With the aid of swirl vanes surrounding the fuel nozzle, strong vortex flow occurs in the combustion air in the combustion region. Figure 10-22 shows a suitable distribution of axial and rotational momentum. A low-pressure region is created at the combustor axis, which causes recirculation of the flame toward the fuel nozzle. At the same time, radial holes around the liner supply air to the center of the vortex, making the flame grow to some extent. Jet angles and penetration from the holes are such that jet impingement along the combustor axis results in upstream flow. The upstream flow forms a torroidal recirculation zone, which stabilizes the flame.

Combustion and Dilution

With torroidal air flow, combustors will operate without visible smoke when properly developed for a primary-zone equivalence ratio below 1.5. Visible smoke is an air-pollution problem.

After combustion, the rich burning mixture leaves the combustion zone and flows between the rows of air jets entering the liner. Each jet entrains air and burning fuel and carries it toward the combustor axis, forming torroidal recirculation patterns around each jet that result in intensive turbulence and mixing throughout the combustor. This combustion product is diluted with air entering through holes on the liner to make the temperature appropriate for blade material and to have enough volume flow in the dilution zone. Air is jet penetrated mainly because of converging clearances and creates high local pressure.

Film Cooling of the Liner

The liner experiences a high temperature because of heat radiated by the flame and combustion. To improve the life of the liner, it is necessary to lower the temperature of the liner and use a material that has a high resistance to thermal stress and fatigue. The air film cooling method reduces the temperature both inside and outside the surface of the liner. This reduction is accomplished by fastening a metal ring inside the liner to leave a definite annular clearance. Air is admitted into this clearance space through rows of small holes in the liner and is directed by the metal rings as a film of cooling air along the liner inside. Figure 10-23 (a) shows how the flow is induced by the static pressure drop across the liner surface. In high air mass flow combustors, this pressure drop may be too small to be effective. It may be necessary to use the total pressure difference in high air mass flow combustors. This type of arrangement is shown in Figure 10-23 (b).

Figure 10-24 (a) is a photograph of a typical diffusion combustor liner (GE Frame Type). Figure 10-24 (a) shows the outside of the combustor liner, note the rows of small holes through which the air enters the liner, and Figure 10-24 (b) shows how it flows along the inner liner surface. Figure 10-24 (a) shows where the crossover tubes connect adjacent liners. The dilution holes are holes through which larger airflows enter the dilution zone of the liner.

Fuel Atomization and Ignition

In most gas turbines, liquid fuel is atomized and injected into the combustors in the form of a fine spray. A typical low-pressure fuel-atomization nozzle is shown in Figure 10-25. The fuel spray entrains air because of the momentum and drag of fuel

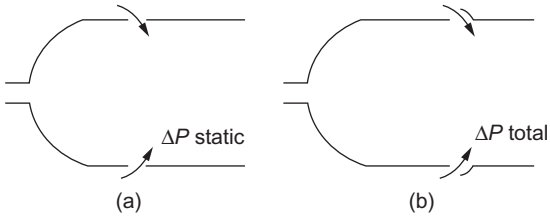
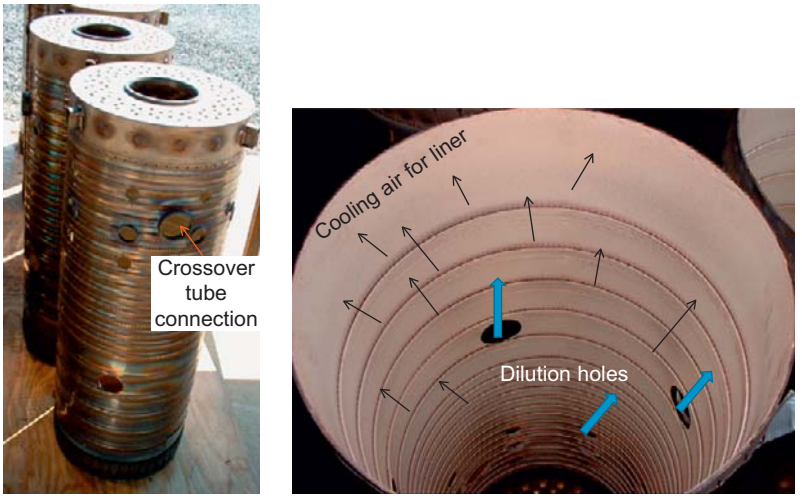


Figure 10-23 Film cooling of a combustor liner.



(a) Combustor liner outer surface

(b) Combustor liner inner surface

Figure 10-24 Diffusion combustor liners (GE frame type).

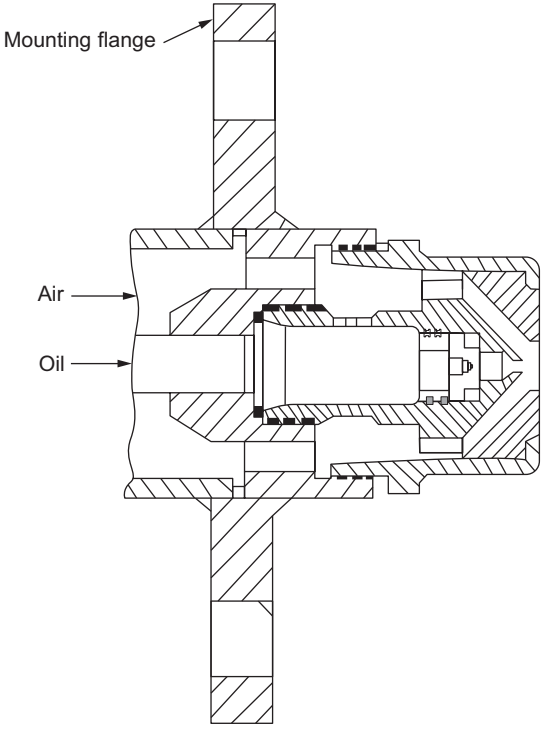


Figure 10-25 Low-pressure air atomizer.

droplets; however, this process produces a low-pressure region inside the spray cone that causes it to converge downstream of the nozzle. This low-pressure region is counteracted by upstream axial flow of combustion products, preventing convergence in the combustion chamber.

In a simple pressure-atomizing fuel nozzle, the flow rate varies as the square root of the pressure. Aircraft turbines operating over a wide range of altitudes and power levels require atomizers that have a capacity range of about 100:1 with a moderate range of fuel pressures. This wide range can be provided with dual-orifice nozzles, spill-control nozzles, variable-area nozzles, or air-atomizing nozzles.

The dual-orifice nozzle consists of two concentric simplex fuel nozzles. The outer nozzle has 2–10 times the flow capacity of the inner nozzle. Ignition is usually obtained from an igniter interfaced with a high-energy capacitive discharge ignition system.

Water injection is an extremely effective means for reducing NO_x formation; however, the combustor designer must observe certain cautions when using this reduction technique. To maximize the effectiveness of the water used, fuel nozzles have been designed with additional passages to inject water into the combustor head end. The water is thus effectively mixed with the incoming combustion air and reaches the flame zone at its hottest point. Steam injection for NO_x reduction follows essentially the same path into the combustor head end as water. However, steam is not as effective as water in reducing thermal NO_x. The high latent heat of water acts as a strong thermal sink in reducing the flame temperature. In general, for a given NO_x reduction, approximately 1.6 times as much steam as water on a mass basis is required for control. There are practical limits to the amount of water or steam that can be injected into the combustor before serious problems occur.

For NO_x control, a typical water spray nozzles directing the water injection spray toward the fuel nozzle tip swirler has been effective in controlling the NO_x emissions; the water spray has a tendency to impinge on the nozzle tip swirler and on the liner cap/cowl assembly. Resulting thermal strain usually leads to cracks, which limits the combustion inspections to 8,000 hours or less. Figure 10-26 shows a typical fuel nozzle with a ring of water injection system.

In multiple combustion installations, all combustors are interconnected by tubes located near the upstream ring of perforations. Ignitors are provided in only some of the combustors. When one combustor lights, the sudden increase in pressure loss forces flame through the interconnecting tubes to the adjacent combustors, immediately lighting the other combustors. An ignitor plug is shown in Figure 10-27. This plug is a surface discharge plug, thus energy does not have to jump an air gap. The plug end is covered by a semi-conductive material and is formed by a pellet, permitting an electrical leakage from the central high-tension electrode to the body. The discharge takes the form of a high-intensity flash from the electrode to the body.

The Dry Low Emission Combustors

There are three principal methods for controlling gas turbine emissions:

1. Injection of a diluent such as water or steam into the burning zone of a conventional (diffusion flame) combustor as seen in the earlier section of this chapter.

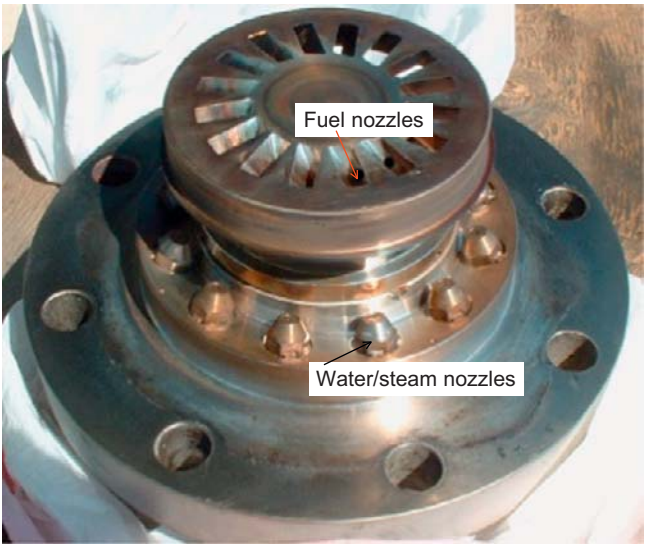


Figure 10-26 A typical fuel nozzle showing both water and fuel nozzles for a typical wet diffusion combustor used for NO_x reduction ($NO_x \approx 25$ ppm).

2. Catalytic cleanup of NO_x and CO from the gas turbine exhaust.
3. Design of the combustor to limit the formation of pollutants in the burning zone by utilizing "lean-premixed" combustion technology.

Frequent combustion inspections and decreased hardware life are undesirable side effects that can result from the use of diluents injection to reduce NO_x emissions from combustion turbines. For applications that require NO_x emissions between 42 and 25 ppmvd and to avoid the significant cycle efficiency penalties incurred when water or steam injection is used for NO_x control, one of the other two principal methods of NO_x control mentioned above must be used.

The flame stability is inherently greater in conventional diffusion-type combustion over a wider range of fuel-to-air ratio. On the other hand, the NO_x emissions are much greater compared with premix DLN combustion. Fundamentally, stable combustion in DLN combustion systems requires more accurate control of fuel and air (i.e., fuel-to-air ratio) quantities in the combustion chamber at all load levels. Many factors can upset the combustor flame stability such as changes in fuel composition, calorific content (LHV), grid frequency, ambient conditions, operating load transients, and even operator-influenced conditions during transient operations. In DLN combustors, the interaction of turbulent flow and chemistry is indispensable.

The DLE approach is to burn most (at least 75%) of the fuel at cool and fuel-lean conditions to avoid any significant production of NO_x. The principal features of such a combustion system is the premixing of the fuel and air before the mixture enters the combustion chamber and leanness of the mixture strength in order to lower the

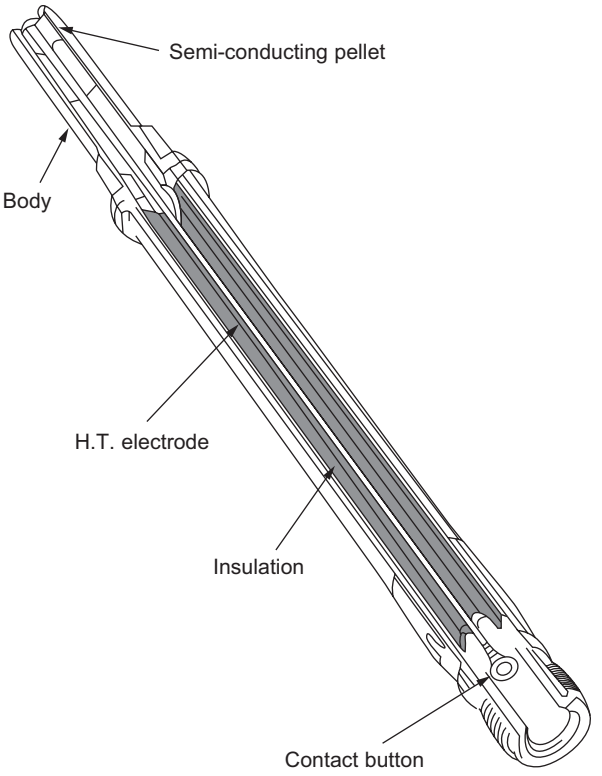


Figure 10-27 An ignitor plug (© Rolls-Royce Limited).

flame temperature and reduce NO_x emission. This action brings the full-load operating point down on the flame temperature and closer to the lean limit curve as shown in Figure 10-28. Controlling CO emissions thus can be difficult and rapid engine off-loads bring the problem of avoiding flame extinction, which, if it occurs, cannot be safely reestablished without bringing the engine to rest and going through the restart procedure.

The DLE combustors have two or more fuel circuits. The main fuel, approximately 97% of the total, is injected into the air stream immediately downstream of the swirler at the inlet to the premixing chamber. The pilot fuel is injected directly into the combustion chamber with little if any premixing. Figure 10-29 shows a schematic comparison of a typical dry low emission/NO_x combustor and a conventional combustor. In both cases, a swirler is used to create the required flow conditions in the combustion chamber to stabilize the flame. The DLE fuel injector is much larger because it contains the fuel/air premixing chamber and the quantity of air being mixed is large, approximately 50–60% of the combustion air flow.

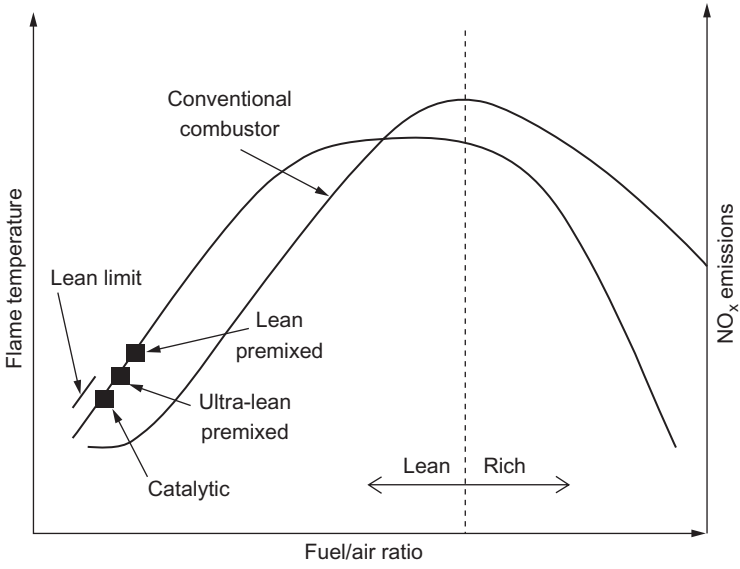


Figure 10-28 Effect of fuel-to-air ratio on flame temperature and NO_x emissions.

The NO_x formation and combustion performance are shown schematically for a typical premixed low-NO_x burner in Figure 10-30. With the flame temperature being much closer to the lean limit than in a conventional combustion system, some action has to be taken when the engine load is reduced to prevent flameout. If no action were taken flameout would occur since the mixture strength would become too lean to burn. A small proportion of the fuel is always burned richer to provide a stable "piloting" zone, while the remainder is burned lean. In both cases, a swirler is used to create the required flow conditions in the combustion chamber to stabilize the flame.

One method is to close the compressor inlet guide vanes progressively as the load is lowered. This reduces the engine airflow and hence reduces the change in mixture strength that occurs in the combustion chamber. This method, on a single-shaft engine, generally provides sufficient control to allow low-emission operation to be maintained down to 50% engine load. Another method is to deliberately dump air overboard prior to or directly from the combustion section of the engine. This reduces the airflow and also increases the fuel flow required (for any given load) and hence the combustion fuel-to-air ratio can be held approximately constant at the full-load value. The latter method causes the part load thermal efficiency of the engine to fall off by as much as 20%.

Even with these air management systems, the lack of combustion stability range can be encountered particularly when the load is rapidly reduced.

If the combustor does not feature variable geometry, then it is necessary to turn on the fuel in stages as the engine power is increased. The expected operating range of the engine will determine the number of stages, but typically at least two or three stages

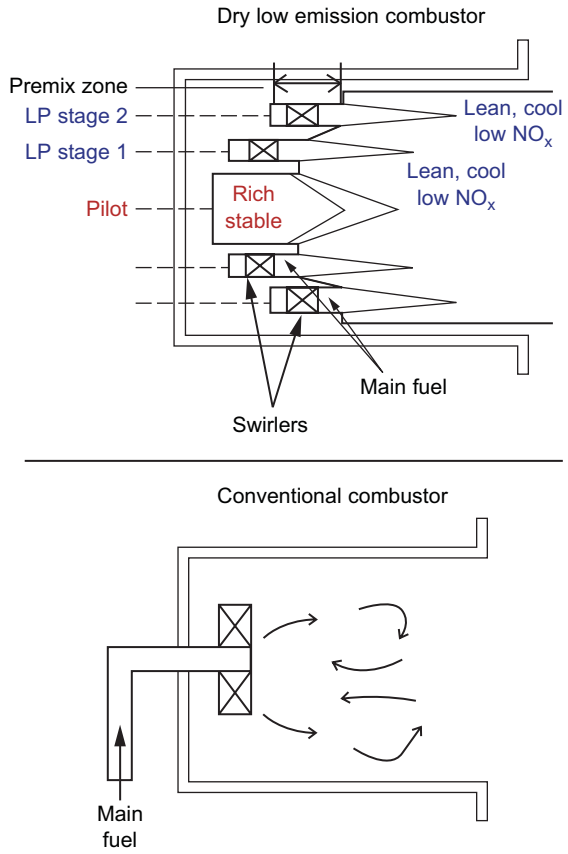


Figure 10-29 A schematic comparison of a typical dry low emission NO_x combustor and a conventional diffusion combustor.

are used as shown in Figure 10-31. Some units have very complex staging as the units are started or operated at off-design conditions.

The following are the major design challenges associated with very lean combustors:

- First, care must be taken to ensure that the flame is stable at the design operating point.
- Second, a turndown capability is necessary since a gas turbine must ignite, accelerate, and operate over the entire load range.
- The above challenges are driven by the need to operate the combustor at low flame temperatures to achieve very low emissions.
- The combustor operating point at full load is just above the flame blowout point, which is the point at which a premixed fuel/air mixture is unable to self-sustain.
- At lower loads, as fuel flow to the combustors decreases, the flame temperature will approach the blowout point and at some point the flame will become either unstable or blow out.

This behavior in a DLE combustor is in direct contrast to that of a diffusion flame combustor. In a diffusion combustor, the fuel is injected unmixed and burns

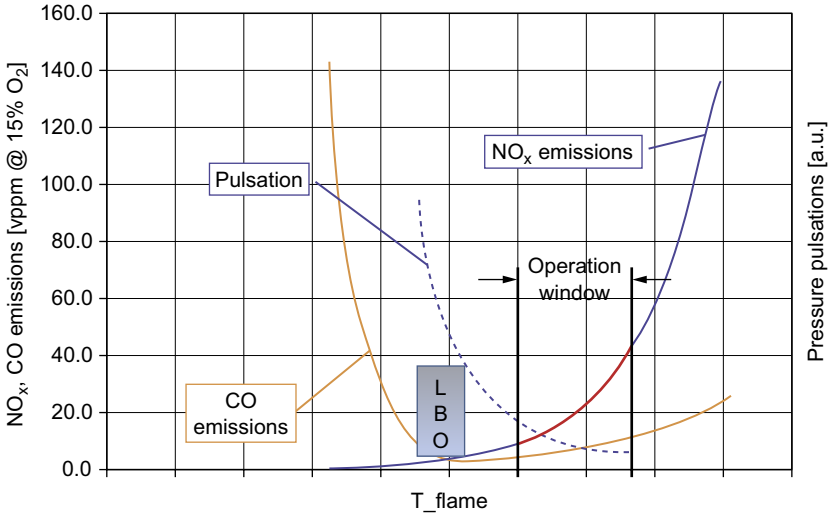


Figure 10-30 General emission performance of a lean premix burner.

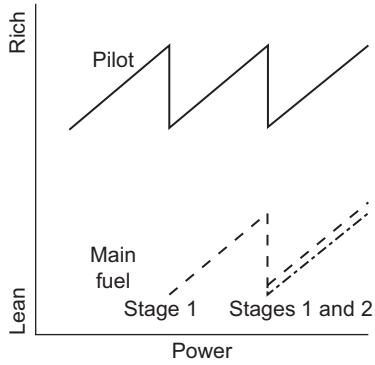


Figure 10-31 The staging of dry low emissions combustor, as the turbine is brought to full power.

at maximum flame temperature using only a portion of the available air. This gives the following characteristics in a diffusion combustor:

- High NO_x emissions.
- Very good flame stability, because the flame burns at the same temperature independent of fuel flow.

In response to these challenges, combustion system designers use staged combustors, so that a portion of the flame zone air can mix with the fuel at lower loads or during start-up. The two types of staged combustors are fuel- and air-staged combustors. Figure 10-31 is a schematic of the staged combustors. In its simplest and most

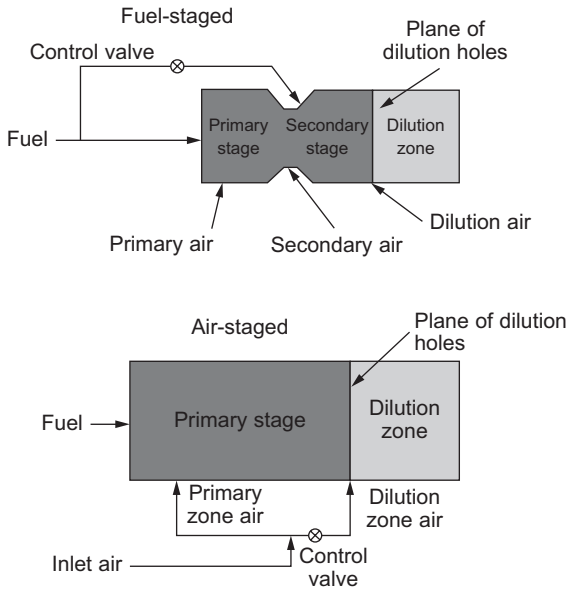


Figure 10-32 Conceptual drawings of fuel- and air-staged combustors.

common configuration, a fuel-staged combustor has two flame zone; each receives a constant fraction of the combustor airflow. Fuel flow is divided between the two zones, so that at each machine operating condition, the amount of fuel fed to a stage matches the amount of air available. An air-staged combustor uses a mechanism for diverting a fraction of the airflow from the flame zone to the dilution zone at low load to increase turndown. These methods can be combined, but both work to achieve the same objective, to maintain a stable flame temperature just above the blowout point as seen in Figure 10-32.

DLN/DLE combustors have many more fuel nozzles in each can-annular combustor can or annular combustor than a diffusion-type combustor, so that a lean mixture of fuel can be injected. A simple two-stage premixed combustor, as shown in Figure 10-33, includes four major components:

1. fuel injection system
2. liner
3. venturi
4. cap/center body assembly.

These components form two stages in the combustor. In the premixed mode, the first stage thoroughly mixes the fuel and air and delivers a uniform, lean, and unburned fuel/air mixture to the second stage. If required, both the primary and secondary fuel nozzles can be dual-fuel nozzles, thus allowing automatic transfer from gas to oil throughout the load range. This in some cases has been problematic leading to flashback-type problems. When burning either natural gas or distillate oil, the system can

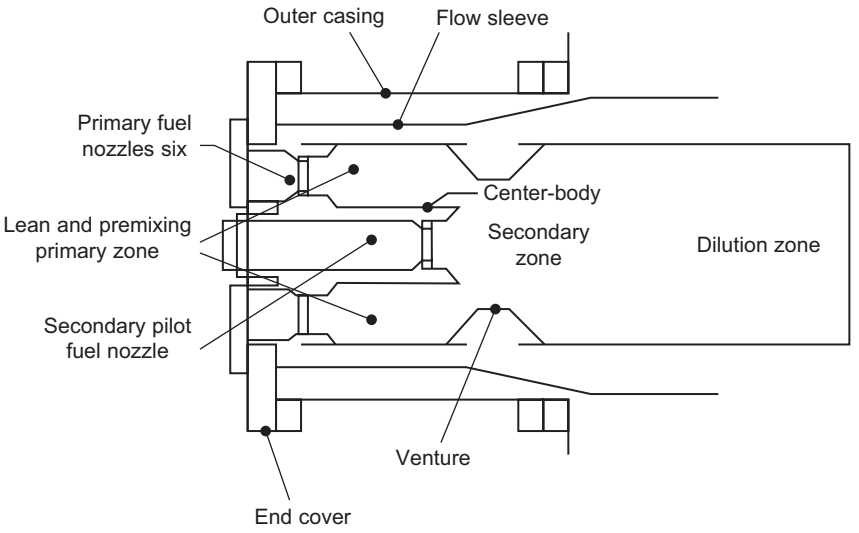


Figure 10-33 A typical premixed combustor (courtesy: GE).

operate to full load in the lean–lean mode. This allows wet abatement of NO_x on oil fuel and power augmentation with water on gas.

This system uses five primary fuel nozzles for smaller machines and six primary fuel nozzles for larger machines. A well-stabilized diffusion flame is essential that burns efficiently at ignition and during part-load operation. In addition, the multi-nozzle fuel injection system provides a satisfactory spatial distribution of fuel flow entering the first-stage mixer. The primary fuel–air mixing section is bound by the combustor first-stage wall, the cap/center body, and the forward cone of the venturi. This volume serves as a combustion zone when the combustor operates in the primary and lean–lean modes. Since ignition occurs in this stage, crossfire tubes are installed to propagate flame and to balance pressures between adjacent chambers. Film slots on the liner walls provide cooling, as they do in a standard combustor.

This type of combustion system operates in four distinct staged modes, as shown in Figure 10-34 during premixed fuel operation:

1. Primary operation ignition to 20% load.
   Fuel to the primary nozzles only. Flame is in the primary stage only. This mode of operation is used to ignite, accelerate, and operate the machine over low to mid loads, up to a preselected combustion reference temperature.
2. Lean–lean operation 20–50% load.
   Fuel to both the primary and secondary nozzles. Flame is in both the primary and secondary stages. This mode of operation is used for intermediate loads between two preselected combustion reference temperatures.
3. Secondary-stage burning transient during transfer to full load.
   Fuel to the secondary nozzle only. Flame is in the secondary zone only. This mode is a transition state between lean–lean and premix modes. This mode is necessary to extinguish the flame in the primary zone, before fuel is reintroduced into what becomes the primary premixing zone.

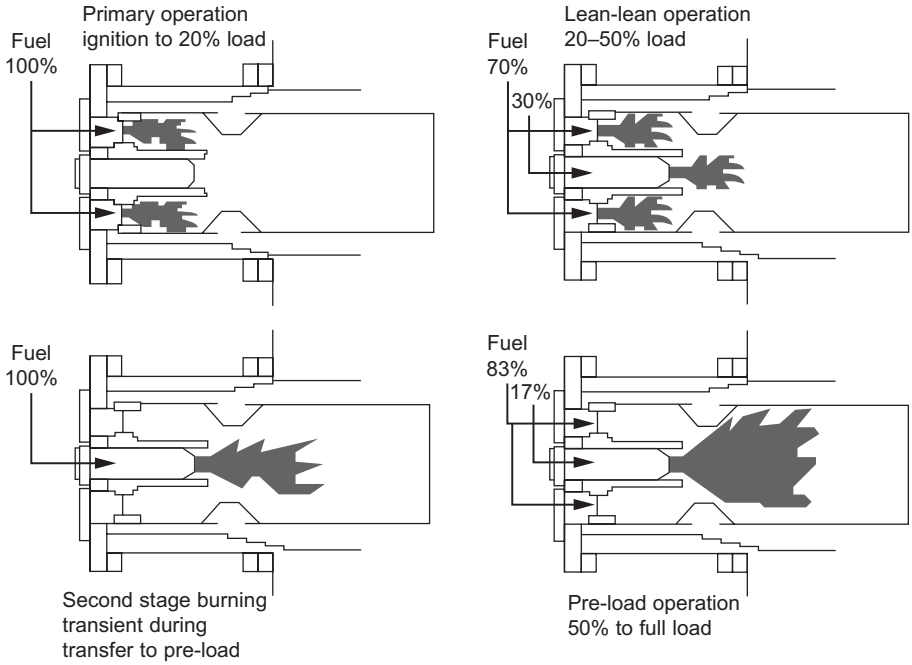


Figure 10-34 Fuel-staged dry low NO_x operating modes.

4. Preload operation 50% to full load.
Fuel to both primary and secondary nozzles. Flame is in the secondary stage only. This mode of operation is achieved at and near the combustion reference temperature design point. Optimum emissions are generated in premix mode.

Figure 10-35 is a schematic of a single combustor can that houses a set of fuel nozzles and a center pilot nozzle (GE DLN-type can-annular combustor). Each can-annular combustor has a set of three to eight fuel nozzles, plus a pilot nozzle in the center, for each individual can on a single gas turbine. There are 8–16 such cans in an annular arrangement on a single gas turbine, generally each connected to the other with cross-over tubes. The premixer assembly shown in Figure 10-36 is designed to hold the six fuel nozzles as shown in Figure 10-37. The fuel nozzles shown in Figure 10-37 fit into the premixer chamber and are flush with the chamber surface. This is a set of DLN fuel nozzles with a center pilot nozzle. The premixer and fuel nozzle assembly are located in the premixer chamber as schematically shown in the top half of the combustor can in Figure 10-35.

The fuel nozzles are mounted on the end cover, as shown in Figure 10-38 and schematically shown in Figure 10-39, the diffusion passages of four of the fuel nozzles are fed from a common manifold, called the primary, which is built into the end cover. The premixed passages of the same four nozzles are fed from another internal manifold called the secondary. The premixed passages of the remaining nozzle are supplied by the tertiary fuel system; the diffusion passage of that nozzle is always

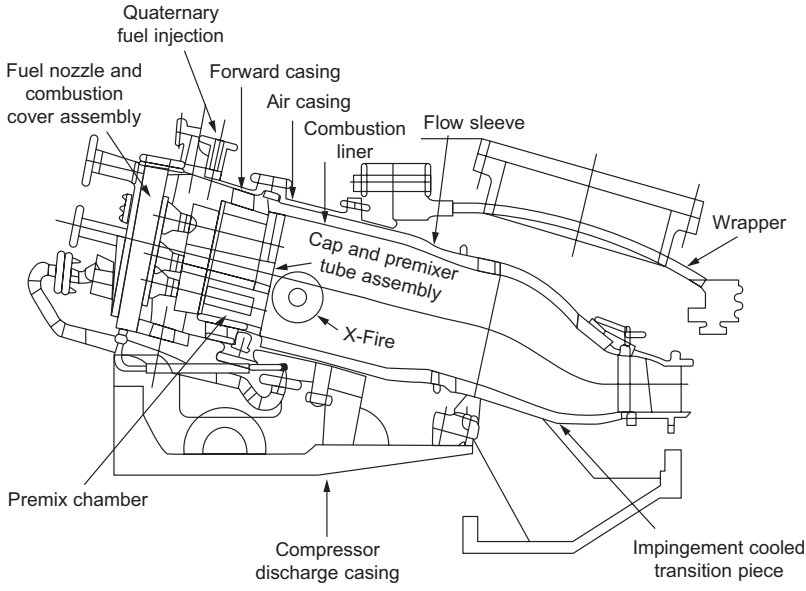


Figure 10-35 A schematic of a single can from a can-annular gas turbine combustion system (Courtesy: GE Gas Turbines).



Figure 10-36 A premix chamber in a DLE combustor.

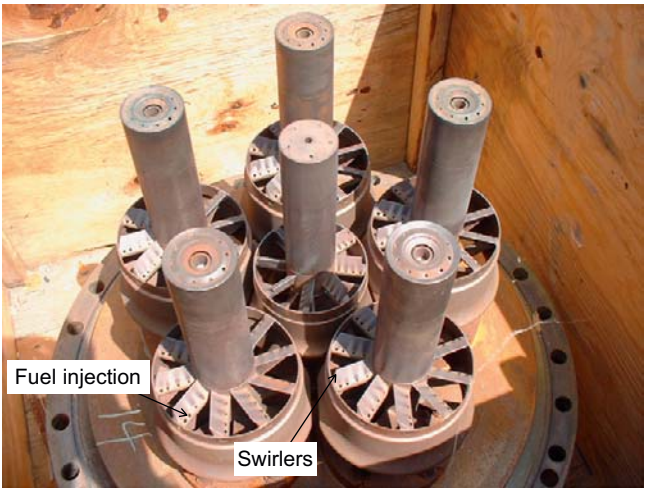


Figure 10-37 A typical set of five fuel nozzles and center pilot nozzle for a single DLE combustor can (GE DLN Combustors).

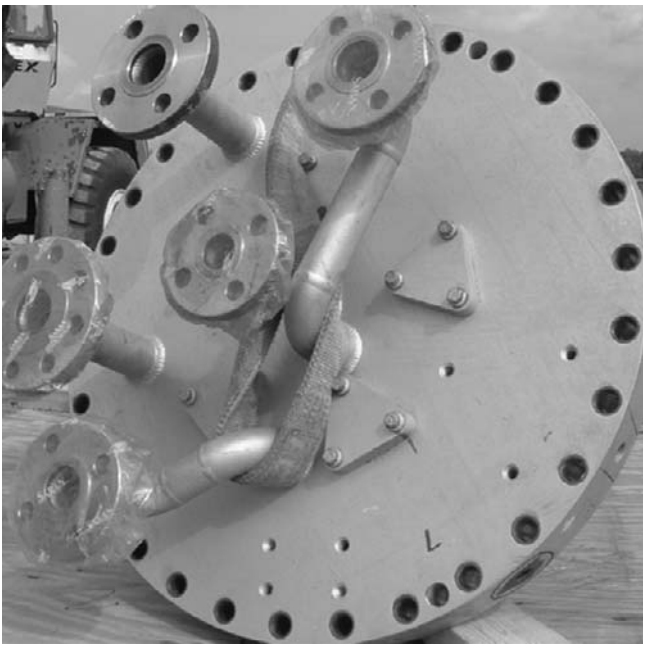


Figure 10-38 DLN fuel nozzles mounted on the cover of the combustor.

purged with compressor discharge air and passes no fuel. The following are the definitions of the four functional categories of the fuel (these terms may be defined by various manufacturers differently, the following are the GE definitions):

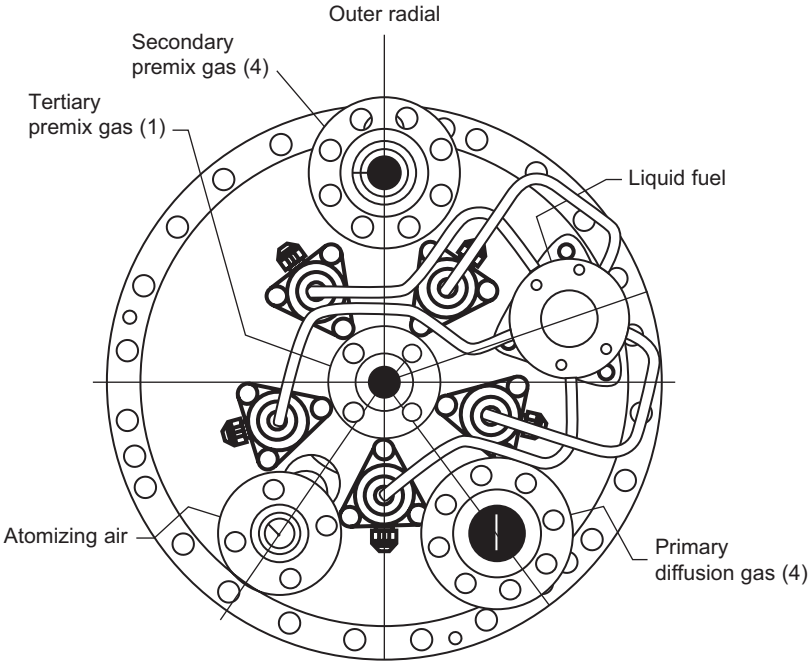


Figure 10-39 Schematic of DLN fuel nozzles mounted on the cover of the combustor.

- *Primary fuel* – fuel gas entering through the diffusion gas holes in the swirler assembly of each of the outboard four fuel nozzles.
- *Secondary fuel* – premix fuel gas entering through the gas metering holes in the fuel gas injector spokes of each of the outboard four fuel nozzles.
- *Tertiary fuel* – premix fuel gas delivered by the metering holes in the fuel gas injector spokes of the inboard fuel nozzle.
- *The quaternary system* – injects a small amount of fuel into the airstream just up-stream from the fuel nozzle swirlers.

Figure 10-40 is a schematic of a typical cross section of a secondary single-fuel nozzle shown in Figure 10-37. The nozzle has passages for diffusion gas, premixed gas, oil, and water. The six-fuel nozzle design is the advanced DLN-2 combustor by GE, which was designed to lower NO_x output to as low as nine ppm. The center nozzle allowed to extend its turndown well beyond the older design. By fueling the center nozzle separately from the outer nozzles, the fuel-to-air ratio can be modulated relative to the outer nozzles leading to approximately 200 °F of turndown from baseload with 9 ppm NOx. Turning the fuel down in the center burner does not result in any additional CO generation. The design calls for three premixed manifolds staging fuel to the six burners and a fourth premixed manifold for injecting quaternary fuel for dynamics abatement. Figure 10-41 is a schematic of the first three premixed manifolds, designated PM1, PM2, and PM3, are configured such that any number (1–6) of burners can be operated at any time. The PM1 manifold fuels the center nozzle, the PM2 manifold fuels the two outer nozzles located at the cross-fire tubes, and the PM3 manifold fuels

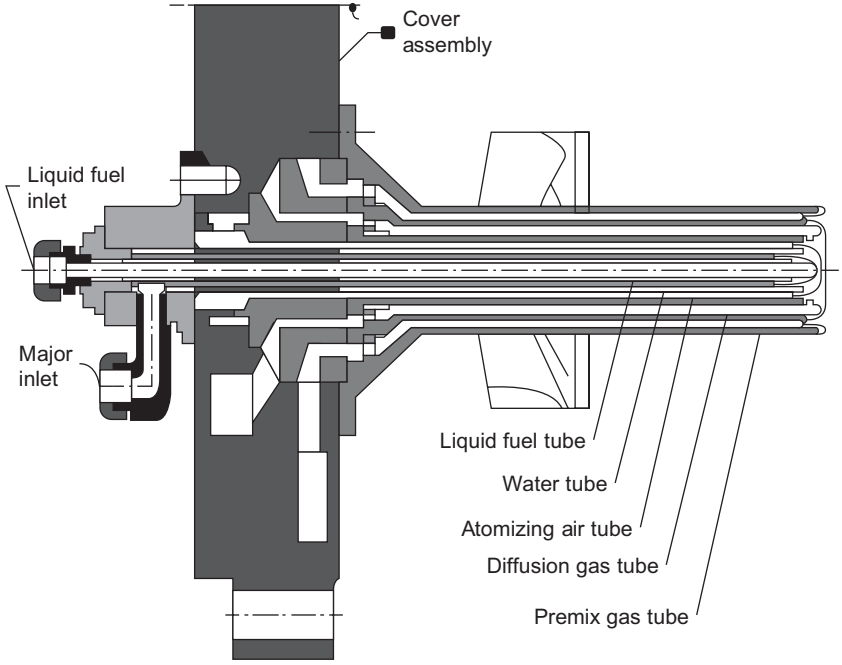


Figure 10-40 A cross section of a DLN fuel nozzle.

the remaining three outer nozzles. The five outer nozzles are identical to those used for the DLN2, while the center nozzle is similar but with simplified geometry to fit within the available space.

Each GE DLN combustor system has a single burning zone formed by the combustor liner and the face of the cap. In low-emission operation, 90% of the gas fuel is injected through radial gas injection spokes in the premixer and combustion air is mixed with the fuel in tubes surrounding each of the five fuel nozzles. The premixer tubes are part of the cap assembly as shown in Figures 10-38 and 10-39. The fuel and air are thoroughly mixed, flow out of the six tubes at high velocity and enter the burning zone, where lean, low-NO_x combustion occurs. The vortex breakdown from the swirling flow exiting the premixers, along with the sudden expansion in the liner, is a mechanism for flame stabilization. Six nozzle/premixer tube assemblies are located on the head end of the combustor. A quaternary fuel manifold is located on the circumference of the combustion casing to bring the remaining fuel flow to casing injection pegs located radially around the casing. This combustion system can operate in several different modes.

Primary

Fuel only to the primary side of the four fuel nozzles, diffusion flame. Primary mode is used from ignition to 81% corrected speed.

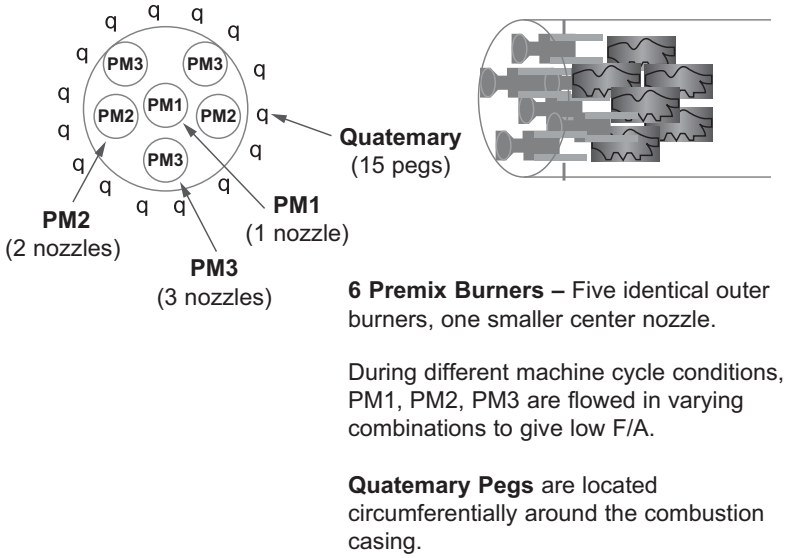


Figure 10-41 Fuel nozzles installed on the combustion chamber end cover and the connections for the primary, secondary, and tertiary fuel systems.

Lean–Lean

Fuel to the primary (diffusion) fuel nozzles and single tertiary (premixing) fuel nozzle. This mode is used from 81% corrected speed to a pre-selected combustion reference temperature. The percentage of primary fuel flow is modulated throughout the range of operation as a function of combustion reference temperature. If necessary, lean–lean mode can be operated throughout the entire load range of the turbine. Selecting "lean–lean base on" locks out premix operation and enables the machine to be taken to base load in lean–lean.

Premix Transfer

Transition state between lean–lean and premix modes. Throughout this mode, the primary and secondary gas control valves modulate to their final position for the next mode. The premix splitter valve is also modulated to hold a constant tertiary flow split.

Piloted Premix

Fuel is directed to the primary, secondary, and tertiary fuel nozzles. This mode exists while operating with temperature control off as an intermediate mode between lean–lean and premix modes. This mode also exists as a default mode out of premix mode and, in the event that premix operating is not desired, piloted premix can be selected

and operated to baseload. Primary, secondary, and tertiary fuel splits are constant during this mode of operation.

Premix

Fuel is directed to the secondary, tertiary, and quaternary fuel passages and premixed flame exists in the combustor. The minimum load for premixed operation is set by the combustion reference temperature and IGV position. It typically ranges from 50% with inlet bleed heat on to 65% with inlet bleed heat off. Mode transition, from premix to piloted premix or piloted premix to premix, can occur whenever the combustion reference temperature is greater than 2200 °F/1204 °C. Optimum emissions are generated in premix mode.

Tertiary Full-Speed No Load (FSNL)

It is initiated upon a breaker open event from any load >12.5%. Fuel is directed to the tertiary nozzle only and the unit operates in secondary FSNL mode for a minimum of 20 s, then transfers to lean–lean mode. Figure 10-41 illustrates the fuel flow scheduling associated with DLN-2 operation. Fuel staging depends on combustion reference temperature and IGV temperature control operation mode.

The MHI DLN can-annular combustion system, as shown in Figure 10-42, consists of a pilot nozzle and eight main fuel nozzles in each combustion chamber. The primary function of the pilot nozzle is to produce a stable diffusion flame that can maintain high flammability in the premixed flame. An air bypass valve is installed downstream at the transition piece for maintaining almost constant fuel-to-air ratio at the combustion chamber. The air bypass valves of all combustion chambers of the gas turbine

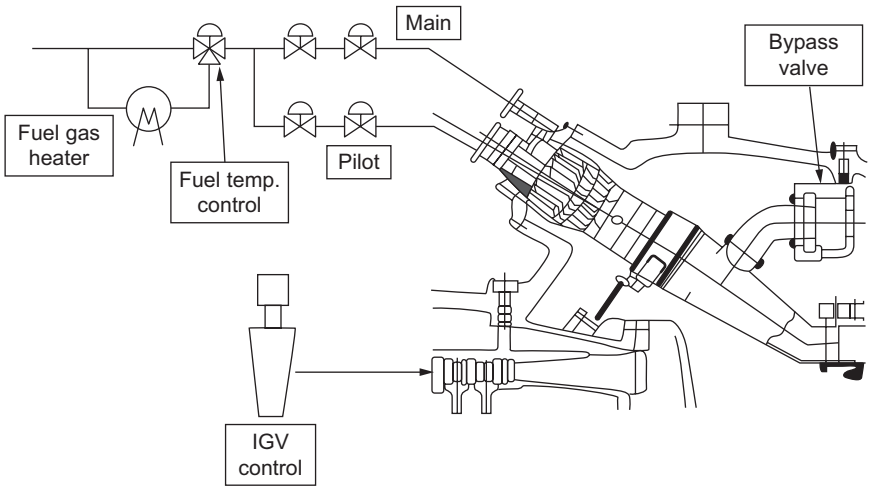


Figure 10-42 A premix can-annular DLN combustor for an MHI-F series gas turbines with controls.

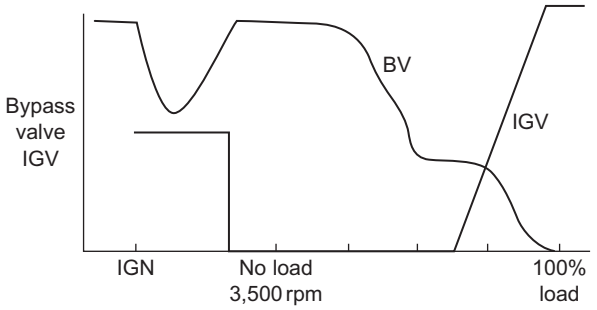


Figure 10-43 Control diagram between the inlet guide vanes and the bleed valve on each combustor system.

are actuated by a hydraulic piston, which is an integral part of a common linkage in the gas turbine. The bypass valve modulates during transient conditions, ignition, acceleration, and partial load operation and it moves toward the close position with increasing load. The air bypass valve is also used to prevent flame-out, combustion oscillations, and flash-backs that can be induced by changes in the GT total airflow resulting from IGV position changes. The MHI DLN combustion system does not require fuel staging for maintaining the fuel-to-air ratio, as is the case of the previous combustor design systems outlined in this chapter. Figure 10-43 shows a typical interaction between the IGV position and the bypass valve opening to maintain a constant fuel-to-air ratio. The overall combustion control is quite simple; fuel to each combustor is supplied through one single pilot port and one single main fuel port. The pilot and main ports of all combustion chambers are connected to one pilot and one main manifold, respectively. The fuel flow to each manifold is controlled by the pilot and main control valves. In addition to controlling the fuel-to-air ratio as described above, the DLN system manipulates the pilot-to-main fuel ratio for emissions and combustion stability control. The pilot-to-main fuel ratio is set higher at ignition, acceleration, and lower load, and it is progressively reduced with increasing load conditions in order to reduce NO_x emission. Figure 10-44 shows a set of eight fuel nozzles, plus a pilot nozzle, for a single can of MHI/Westinghouse frame-type gas turbine, which is housed in a combustor can as shown in Figure 10-45.

Figures 10-46 shows an annular combustor with flow entering from a ring of 24 fuel and air nozzles in an annular DLE combustor of a Siemens large frame-type gas turbines V84.3 and V94.3 and exiting into the first-stage nozzle vanes. This ring of combustor nozzles ensures a continuous ring flame with a reasonably uniform temperature profile. Note the ceramic tiles that line the annular combustor; the tiles replaced the rectangular metal plates, which were held down by bolts. These bolts were air-cooled to prevent the elongation of the bolt causing the plates to be rooted out by air getting behind the metal plates causing major damage to the turbine blades. The metal plates with the metal screws were still maintained in the last row of plates as ceramic could not be molded to the shape required. Figure 10-47 is a schematic of the fuel injector used in the turbine and Figure 10-48 is a photograph of the same fuel air

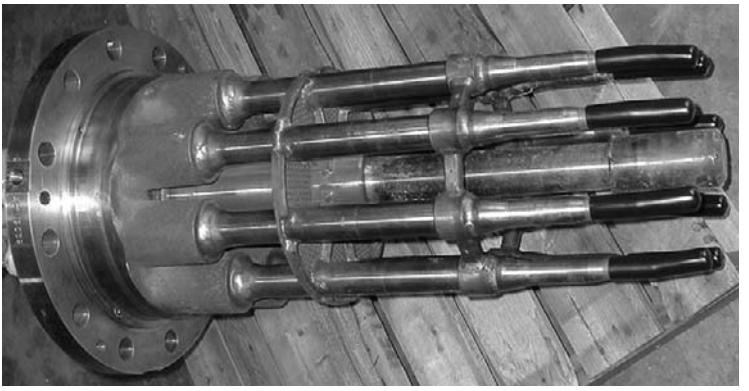


Figure 10-44 A typical set of eight fuel nozzles, plus a center pilot nozzle for a single DLE combustor can (Mitsubishi/Westinghouse DLN Combustors).

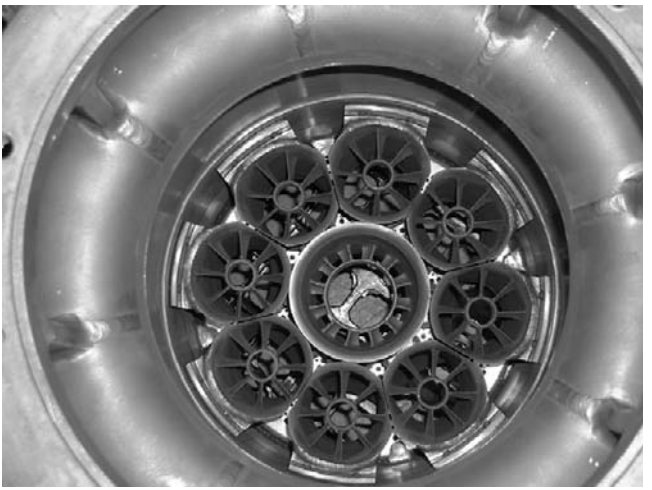


Figure 10-45 A typical MHI/Westinghouse liner that houses the eight fuel nozzles and the center pilot nozzle.

nozzle injector. Figure 10-49 shows a close-up of each of the fuel nozzles used with swirling vanes in the Siemens annular combustor.

The Alstom annular DLN combustion chambers used in GT 13, 24, and 26 like all the DLN combustors discussed previously must address the same problems:

- Flame stability.
- Homogenization of flame temperature distribution in the combustor.
- Combustion control.

Figure 10-50 is a schematic of a DLN combustor designed by Alstom, which is cooled by a combination of convective and film cooling. The combustor as shown in

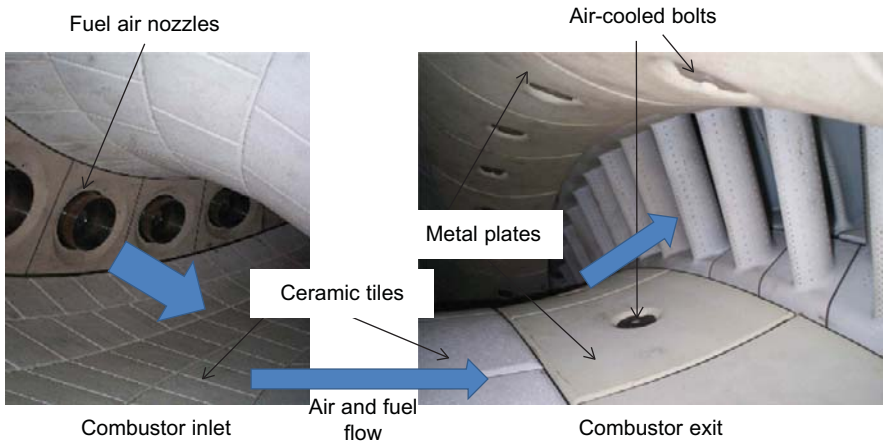


Figure 10-46 A DLN annular combustor (Siemens V94.3 Gas Turbine).

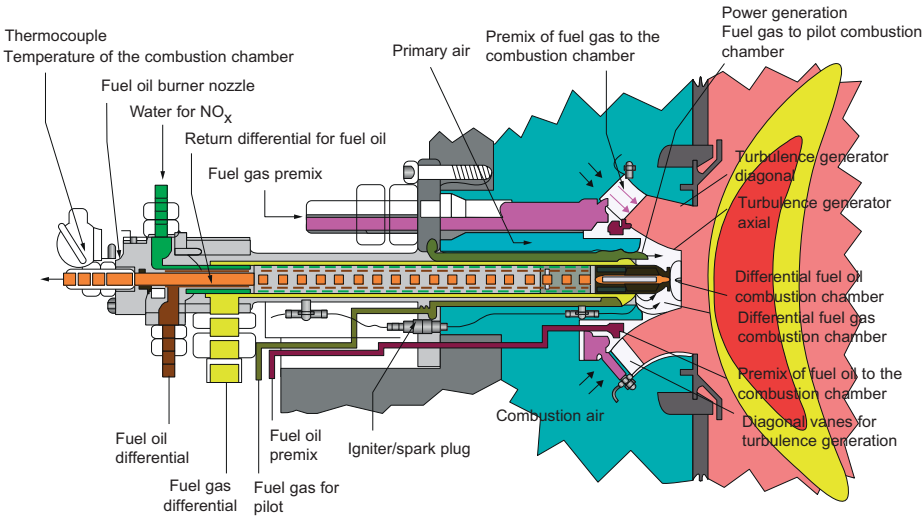


Figure 10-47 Fuel injector for Siemens combustor (courtesy: Siemens Corporation).

Figure 10-51 incorporates 72 EV burners (EV stands for EnVironmental), and the EV burner is a lean premix burner for dual-fuel (oil and natural gas) operation. It basically consists of two half cones that are radially shifted apart to give way to two air inlet slots with constant slot width as shown in Figure 10-52. Gaseous fuel is injected into the air through a number of holes along the inlet slots and mixes with the air. Since the radial distance of the air inlet slots with respect to the centerline increases in downstream direction, the swirl strength increases toward the end of the burner. A vortex breakdown occurs in the burner center when the swirling flow expands into the combustion chamber. The recirculation of hot combustion products in the vortex

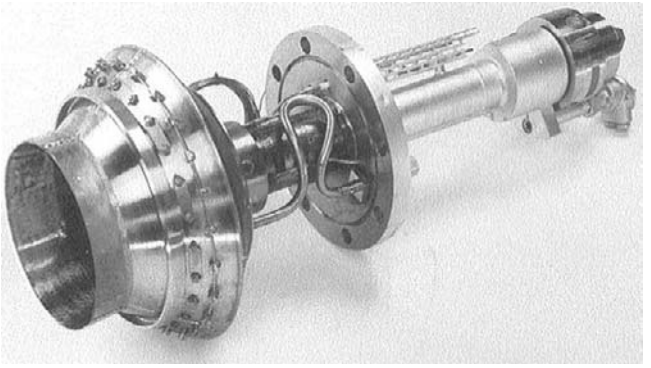


Figure 10-48 Photograph of a Siemens fuel injector.

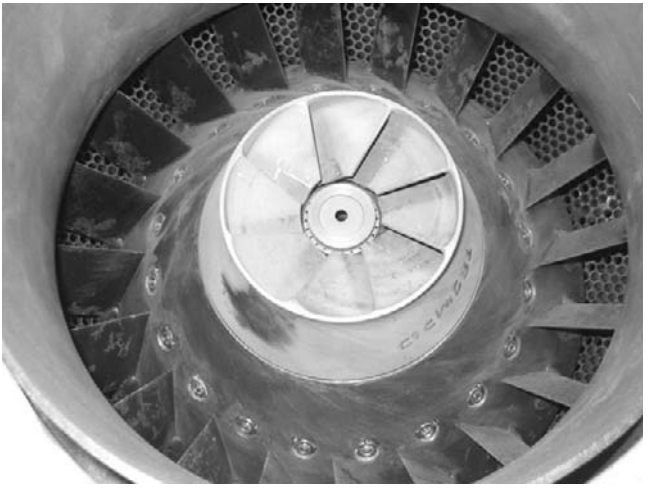


Figure 10-49 Close-up of the fuel injector (note the swirler vanes for the fuel and the air).

breakdown stabilizes the flame in free space. The high-velocity airflow inside the burner cone protects the metal surfaces from the flame. Liquid fuel can be injected in the center of the burner. This fuel is evaporated and mixed with the air inside the burner. The swirling motion promotes the fine scale mixing of fuel and air, which is a prerequisite to achieve low NO_x emissions.

Since dry low NO_x combustion systems are operated in lean-premixed mode, the flame temperature being much closer to the lean limit than in a conventional combustion system, some action has to be taken when the engine load is reduced to prevent flame-out. If no action was taken, flame-out would occur since the mixture strength would become too lean to burn. In order to provide stable combustion at part load, burner staging is applied during premix operation down to 60% relative load. Burner

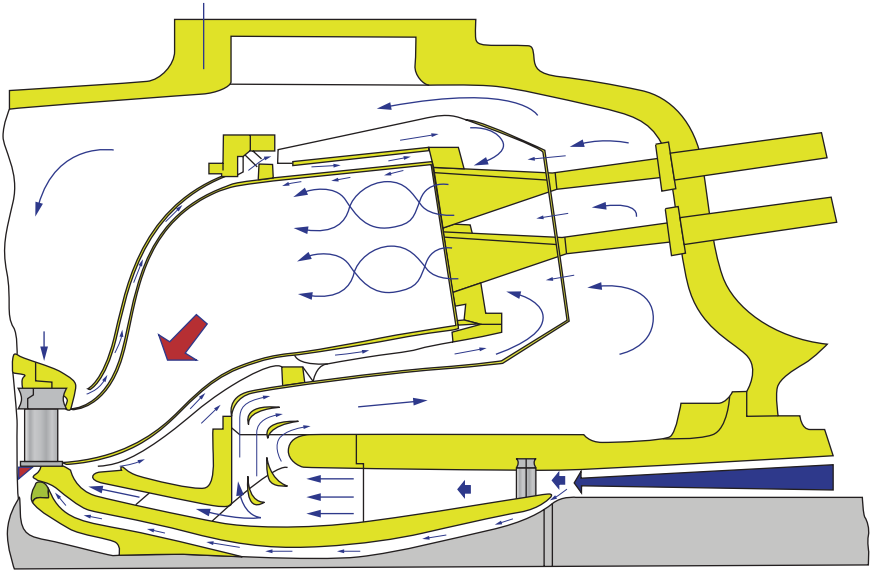


Figure 10-50 Schematic of a dry low emission NO_x combustor (courtesy: Alstom Turbines).

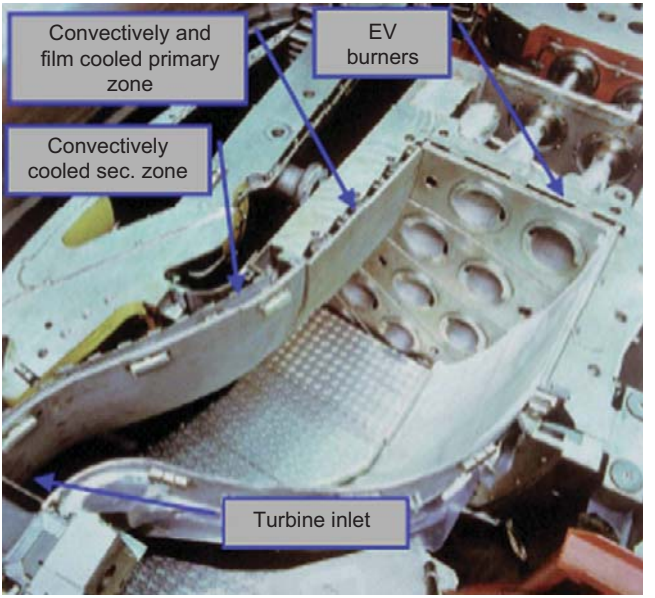
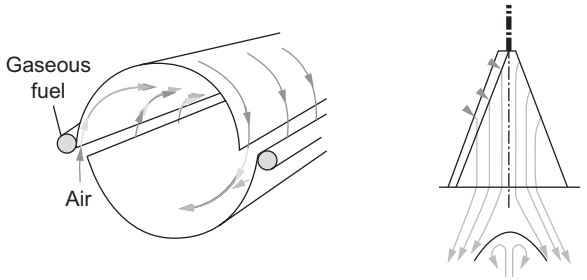


Figure 10-51 Annular dry low NO_x combustor for a frame-type gas turbine (courtesy: Alstom Turbines).



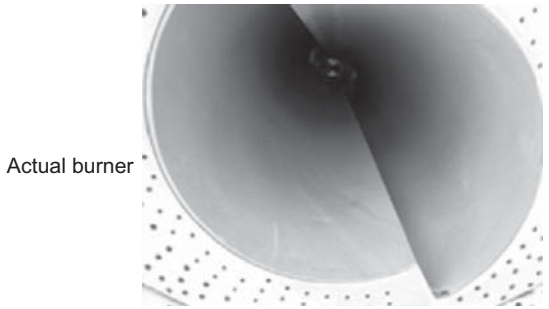


Figure 10-52 Basic principle of the EV lean premix burner with vortex breakdown flame stabilization (courtesy: Alstom Turbines).

staging is achieved, as shown in Figure 10-53, by splitting the premix gas fuel system into two groups:

1. A rich main burner group, which is operated in a fuel-rich and stable mode. This group includes three-fourth of the total number of burners (54 burners).
2. A lean-staged burner group, which can be operated below the flame stability limit and is used to control the gas turbine load at part load. This group includes the remaining one-fourth of burners (18 burners).

The design of the combustor provides sufficient mixing and residence time between the two burner groups to oxidize the fuel of the staged burners in the hot combustion gases of the main burner group. Since the staged burner group includes one-fourth of the total number of burners, the staging ratio (SR) can vary between 0% and 25%, where homogeneous operation of the two burner groups is reached.

The design point of the combustor, which is the firing temperature at full load, is chosen in a way that even at full load the homogenous point is not reached. This means that the staged group is always operated below the stability limit and, therefore, hardly contributes to the NO_x emissions of the gas turbine. Since the main NO_x formation occurs in the flames of the stable main burner group, it is essential that these burners have an almost homogenous individual flame temperature.

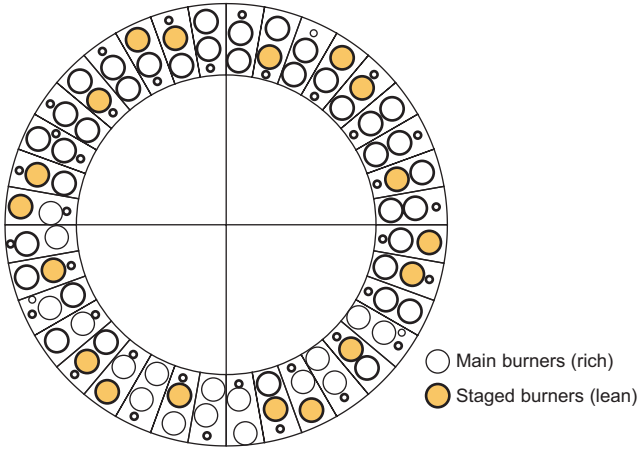


Figure 10-53 A schematic of the staging of the main fuel burners.

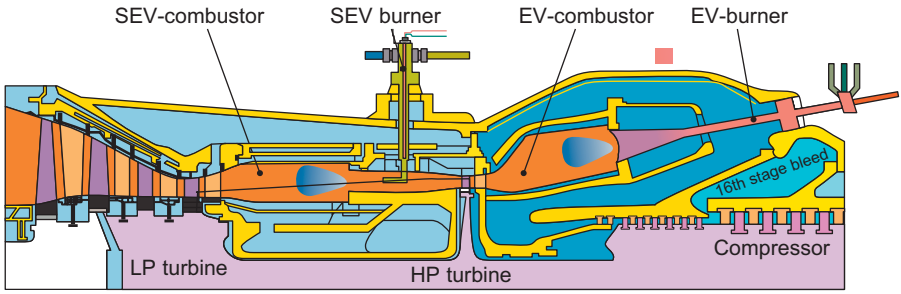


Figure 10-54 Schematic of the GT 24/26 arrangement of the two in-line combustor system.

The Alstom GT 24/26, a schematic of which is shown in Figure 10-54, is the only gas turbine with two sequential online combustors on the market. This design makes the GT 24/26 a reheat gas turbine. The GT 24/26 has a 22-stage compressor and has a bleed off of about 20–25% of the air bled out at the end of the 16th compressor stage. The remainder of the flow goes through the first EV combustor where it is heated and then sent through the HP turbine. The gas leaving the HP turbine is mixed with air bled from the 16th stage and the combined air flow goes through the second EV combustor. This compressed air bled-off is mixed with the remaining flow, after single-stage HP turbine, and the mixture of gases is then refired in the second EV (SEV) combustor. This is possible since there is lot of oxygen in the gas. The EV and SEV combustors both fire the gas to about 2600 °F (1427 °C).

DLN combustors are also used in aircraft gas turbines. Figure 10-55 shows a schematic of an actual dry low emission annular NO_x combustor in an aero-engine.

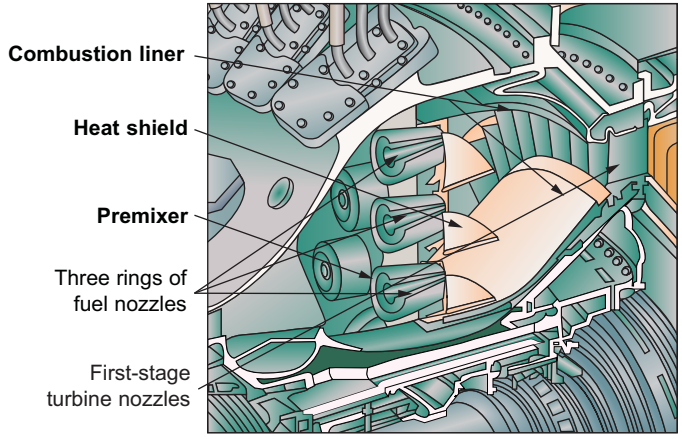


Figure 10-55 Annular DLE combustor for an aero-engine. Note the three concentric rings of fuel nozzles.



Figure 10-56 Top-half of a silo-type gas turbine.

Note the three concentric rings of swirlers and fuel nozzles, which are used in staging the combustion as indicated in the previous sections in this chapter.

Silo-Type Combustors

The DLN silo-type combustors, which are mostly used in European combustors, have similar problems that many of DLN annular combustors have. The Alston annular



Figure 10-57 A look into a silo-type combustor.

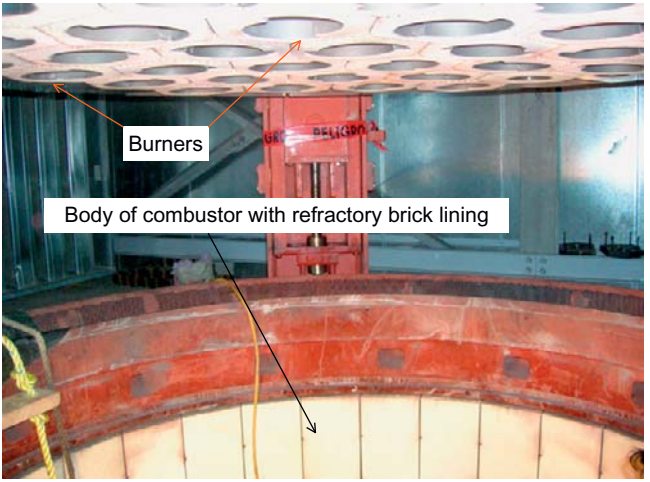


Figure 10-58 A silo-type combustor with the top of the combustor raised, which houses the burners.

DLN combustor is very similar to the annular DLN silo-type combustor. Figure 10-56 is a photograph of the GT 11 gas turbine's top part of the casing with the silo-type combustor with its cover removed. Figure 10-57 looks down the silo combustor and one can note the bricks that cover the silo section of the combustor. In Figure 10-58, the top cover of the combustor, which has the burners in it, has been raised and the burners can be seen in the top cover. The burners are similar to the ones shown in Figure 10-52.

Operation of DLN/DLE Combustors

Gas turbines often experience problems with these DLN/DLE combustors; some of the common problems experienced are:

- Auto-ignition and flash-back.
- Combustion instability.

These problems can result in sudden loss of power because a fault is sensed by the engine control system and the engine is shutdown.

Autoignition is the spontaneous self-ignition of a combustible mixture. For a given fuel mixture, at a particular temperature and pressure, there is a finite time before self-ignition occurs. Diesel engines (knocking) rely on it to work, but spark-ignition engines must avoid it.

DLN/DLE combustors have premix modules on the head of the combustor to mix the fuel uniformly with air. To avoid autoignition, the residence time of the fuel in the premix tube must be less than the autoignition delay time of the fuel. If autoignition does occur in the premix module then it is probable that the resulting damage will require repair and/or replacement of parts before the engine is run again at full load.

Some operators are experiencing engine shutdowns because of autoignition problems. The response of the engine suppliers to rectify the situation has not been encouraging, but the operators feel that the reduced reliability cannot be accepted as the "norm."

If autoignitions occur then the design does not have sufficient safety margin between the autoignition delay time for the fuel and the residence time of the fuel in the premix duct. Autoignition delay times for fuels do exist, but a literature search will reveal that there is considerable variability for a given fuel. Reasons for autoignition could be classified as follows:

- Long fuel autoignition delay time assumed.
- Variations in fuel composition reducing autoignition delay time.
- Fuel residence time incorrectly calculated.
- Autoignition triggered "early" by ingestion of combustible particles.

Flashback into a premix duct occurs when the local flame speed is faster than the velocity of the fuel/air mixture leaving the duct.

Flashback usually happens during unexpected engine transients, e.g. compressor surge. The resultant change of air velocity would almost certainly result in flashback. Unfortunately, as soon as the flame-front approaches the exit of the premix duct, the flame-front pressure drop will cause a reduction in the velocity of the mixture through the duct. This amplifies the effect of the original disturbance, thus prolonging the occurrence of the flashback.

Advanced cooling techniques could be offered to provide some degree of protection during a flashback event caused by engine surge. Flame detection systems coupled with fast-acting fuel control valves could also be designed to minimize the impact of a flashback. The new combustors also have steam cooling provided.

High-pressure burners for gas turbines use premixing to enable combustion of lean mixtures. The stoichiometric mixture of air and fuel varies between 1.4 and 3.0 for gas turbines. The flames become unstable when the mixture exceeds a factor of 3.0, and below 1.4 the flame is too hot and NO_x emissions will rise rapidly. The new combustors are, therefore, shortened to reduce the time the gasses are in the combustor. The number of nozzles is increased to give better atomization and better mixing of the gases in the combustor. The number of nozzles in most cases increases by a factor of 5–10, which does lead to a more complex control system. The trend now is to an evolution toward the can-annular burners. For example, a frame-type turbine had one combustion chamber with one burner; however, a new similar turbine has 12 can-annular combustors and 72 burners.

Combustion instability only used to be a problem with conventional combustors at very low engine powers. The phenomenon was called "rumble." It was associated with the fuel-lean zones of a combustor, where the conditions for burning are less attractive. The complex 3D flow structure that exists in a combustor will always have some zones that are susceptible to oscillatory burning. In a conventional combustor, the heat release from these "oscillating" zones was only a significant percentage of the total combustor heat release at low power conditions.

With DLN/DLE combustors, the aim is to burn most of the fuel very lean to avoid the high-combustion temperature zones that produce NO_x. Therefore, these lean zones that are prone to oscillatory burning are now present from idle to 100% power. Resonance can occur (usually) within the combustor. The pressure amplitude at any given resonant frequency can rapidly build up and cause failure of the combustor. The modes of oscillation can be axial, radial, circumferential, or all the three at the same time. The use of a dynamic pressure transducer in the combustor section, especially in the low NO_x combustors, ensures that each combustor can is burning evenly. This is achieved by controlling the flow in each combustor can till the spectrums obtained from each combustor can match. This technique has been used and found to be very effective and ensures combustor stability.

The calculation of the fuel residence time in the combustor or the premixing tube is not easy. The mixing of the fuel and the air to produce a uniform fuel-to-air ratio at the exit of the mixing tube is often achieved by the interaction of flows. These flows are composed of swirl, shear layers, and vortex. CFD modeling of the mixing tube aerodynamics is required to ensure the success of the mixing process and to establish that there is a sufficient safety margin for auto-ignition.

By limiting the flame temperature to a maximum of 2650 °F (1454 °C), single-digit NO_x emissions can be achieved. To operate at a maximum flame temperature of 2650 °F (1454 °C), which is up to 250 °F (139 °C) lower than the LP system previously described, requires premixing of 60–70% of the air flow with the fuel prior to admittance into the combustion chamber. With such a high amount of the available combustion air flow required for flame temperature control, insufficient air remains to be allocated solely for cooling the chamber wall or diluting the hot gases down to the turbine inlet temperature. Consequently, some of the air available has to do double duty, being used for both cooling and dilution. In engines using high turbine inlet temperatures, 2400–2600 °F (1316–1427 °C), although dilution is hardly necessary there

is not enough air left over to cool the chamber walls. In this case, the air used in the combustion process itself has to do double duty and be used to cool the chamber walls before entering the injectors for premixing with the fuel. This double-duty requirement means that film or effusion cooling cannot be used for the major portion of the chamber walls. Some units are looking into steam cooling. Walls are also coated with thermal barrier coating (TBC), which has a low thermal conductivity and hence insulates the metal. This is a ceramic material that is plasma sprayed on during combustion chamber manufacture. The temperature drop across the TBC, typically by 300 °F (149 °C), means the combustion gases are in contact with a surface that is operating at approximately 2000 °F (1094 °C), which also helps to prevent the quenching of the CO oxidation.

Catalytic Combustion and Combustors

Catalytic combustion is a process in which a combustible compound and oxygen react on the surface of a catalyst, leading to complete oxidation of the compound. This process takes place without a flame and at much lower temperatures than those associated with conventional flame combustion. Due partly to the lower operating temperature, catalytic combustion produces lower emissions of nitrogen oxides (NO_x) than conventional combustion. Catalytic combustion is now widely used to remove pollutants from exhaust gases and there is growing interest in applications in power generation, particularly in gas turbine combustors.

In catalytic combustion of a fuel/air mixture, the fuel reacts on the surface of the catalyst by a heterogeneous mechanism. The catalyst can stabilize the combustion of ultra-lean fuel/air mixtures with adiabatic combustion temperatures below 1500 °C. Thus, the gas temperature will remain below 1500 °C and very little thermal NO_x will be formed, as can be seen in Figure 10-14. However, the observed reduction in NO_x in catalytic combustors is much greater than that expected from the lower combustion temperature. The reaction on the catalytic surface apparently produces no NO_x directly, although some NO_x may be produced by homogeneous reactions in the gas phase initiated by the catalyst.

Features of Catalytic Combustion

Surface Temperatures

At low temperatures, the oxidation reactions on the catalyst are kinetically controlled, and the catalyst activity is an important parameter. As the temperature increases, the build-up of heat on the catalyst surface due to the exothermic surface reactions produces ignition and the catalyst surface temperature jumps rapidly to the adiabatic flame temperature of the fuel/air mixture on ignition. Figure 10-59 shows a schematic of the temperature profiles for catalyst and bulk gas in a traditional catalytic combustor. At the adiabatic flame temperature, oxidation reactions on the catalyst are very rapid and the overall steady state reaction rate is determined by the rate of mass transfer of fuel to the catalytic surface. The bulk gas temperature rises along the reactor because of

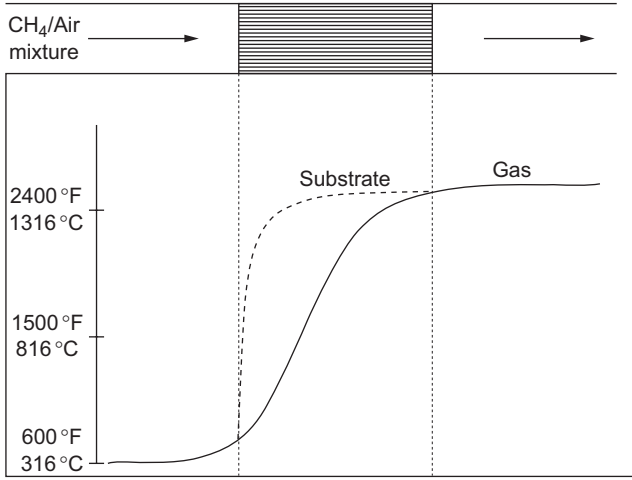


Figure 10-59 Schematic temperature profiles for catalyst (substrate) and bulk gas in a traditional catalytic combustor.

heat transfer from the hot catalyst substrate and eventually approaches the catalyst surface temperature.

As the catalyst surface temperature is equal to the adiabatic flame temperature after ignition, it is independent of the overall conversion in the combustion reaction. It follows that the catalyst surface temperature cannot be reduced simply by limiting the conversion (by using a short reactor or a monolith with large cells, for example). Therefore, unless some other means of limiting the catalyst surface temperature is used, the catalyst materials must be able to withstand the adiabatic flame temperature of the fuel/air mixture during the combustion reaction. For the present generation of gas turbines, this temperature will be equal to the required turbine inlet temperature of 1300 °C, which presents severe problems for existing combustion catalysts.

Catalytica Combustion Systems Inc., a corporation based in California, has developed a new approach to catalytic combustion, and Tanaka Kikinzoku Kogyo K.K. combines catalytic and homogeneous combustions in a multistage process. In this approach, shown schematically in Figure 10-60, the full fuel/air mixture required to obtain the desired combustor outlet temperature is reacted over a catalyst. However, a self-regulating chemical process limits the temperature rise over the catalyst. Therefore, the catalyst temperature at the inlet stage remains low and the catalyst can maintain very high activity over long periods of time. Because of the high catalyst activity at the inlet stage, ignition temperatures are low enough to allow operation at, or close to, the compressor discharge temperature, which minimizes the use of a pre-burner. The outlet stage brings the partially combusted gases to the temperature required to attain homogeneous combustion. Because the outlet stage operates at a higher catalyst temperature, the stable catalyst in this stage will have a lower activity than the inlet stage catalyst. However, as the gas temperature in this stage is higher, the lower

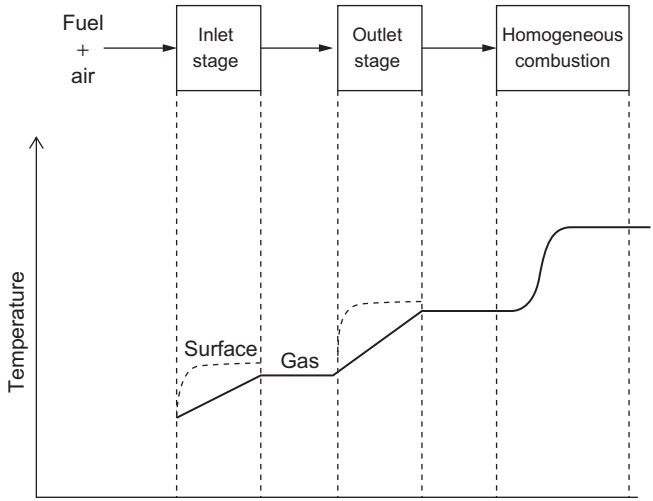


Figure 10-60 Schematic temperature profiles for catalytic combustion system in which the wall temperature is limited and complete combustion occurs after the catalyst.

activity is adequate. In the final stage, homogeneous gas phase reactions complete the combustion of the fuel and bring the gases to the required combustor outlet temperature.

The temperature rise in the inlet stage is limited by taking advantage of the unique properties of palladium combustion catalysts. Under combustion conditions, palladium can be in the form of either the oxide or the metal. Palladium oxide is a highly active combustion catalyst, whereas palladium metal is much less active. Palladium oxide is formed under oxidizing conditions at temperatures higher than 400 °F (200 °C), but decomposes to the metal at temperatures between 1436 °F (780 °C) and 1690 °F (920 °C), depending on the pressure. Therefore, when the catalyst temperature reaches about 1472 °F (800 °C) the catalytic activity will suddenly fall off due to the formation of the less active palladium metal, preventing any further rise in temperature. The catalyst essentially acts as a kind of chemical thermostat that controls its own temperature.

Catalytic Combustor Design

Testing at full scale has been done in a catalytic combustor system developed by GE for its MS9001E gas turbine. The MS9001E combustor operates with a full-load firing temperature of 2020 °F (1105 °C) and a combustor exit temperature of about 2170 °F (1190 °C). The key components of the test stand at the GE Power Generation Engineering Laboratories in Schenectady, New York, are shown in Figure 10-61.

There are three major sub-assemblies in the overall catalytic combustion system: the pre-burner, the main fuel injector, and the catalytic reactor.

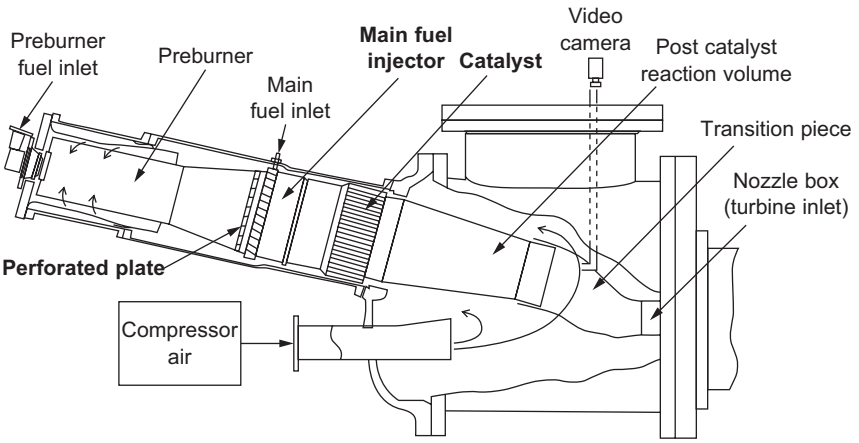


Figure 10-61 Schematic of a full scale catalytic combustor (courtesy: GE Power Systems and Catalytica Combustion Systems Inc.).

Preburner

The preburner carries the machine load at operating points where the conditions in the catalytic reactor are outside of the catalyst operating window. Most often, these are the low load points where the fuel required for turbine operation is insufficient for the catalyst to generate the necessary minimum exit gas temperature. As the turbine load is increased, progressively more fuel is directed through the main injector and progressively less goes to the pre-burner. Ultimately, the pre-burner receives only enough fuel to maintain the catalyst above its minimum inlet temperature.

Main Fuel Injector

This unit is designed to deliver a fuel/air mixture to the catalyst that is uniform in composition, temperature, and velocity. A multi-venturi tube (MVT) fuel injection system was developed by GE specifically for this purpose. It consists of 93 individual venturi tubes arrayed across the flow path, with four fuel injection orifices at the throat of each venturi.

Catalytic Reactor

The role of the catalyst was described earlier; it must burn enough of the incoming fuel to generate an outlet gas temperature high enough to initiate rapid homogeneous combustion just past the catalyst exit.

The catalytic combustor has great potential in the application of gas turbines in new combined-cycle power plants, as the NO_x emissions in high attainment areas will have to be below two ppm.

Selective Catalytic Reactor

The DLE combustors in many countries especially in the United States require the addition of a selective catalyst reactor to reduce further the NO_x emissions. Selective catalytic reduction (SCR) converts NO and NO_2 in the gas turbine exhaust stream to molecular nitrogen and oxygen by reacting the NO_x with ammonia in the presence of a catalyst. Conventional SCR technology requires that the temperature of the exhaust stream remain in a narrow range (550–750 °F or 288–399 °C) and is restricted to applications with a heat recovery system installed in the exhaust. Most of the SCR systems are part of an HRSG system in a combined-cycle power plant. The SCR is installed at a location in the HRSG where the exhaust gas temperature has decreased to the above temperature range. New high-temperature SCR technology is being developed that may allow SCRs to be used for applications without heat recovery steam generators.

The main reason for it to be part of an HRSG system is the fact that to get acceptable life from the catalyst the temperature of the gas must be reduced from the gas turbine exit temperature of about 1050 °F (566 °C) to about 750 °F (399 °C). HRSGs are furnished and installed with a complete SCR system to control concentrations of NO_x generated by the gas turbine. SCR is a means of converting nitrogen oxides, also referred to as NO_x with the aid of a catalyst to diatomic N_2 and water (H_2O). A gaseous reductant, typically anhydrous or aqueous ammonia, is added to the stream of exhaust gas and is absorbed onto a catalyst.

The NO_x reduction reaction takes place as the gases pass through the catalyst chamber. Before entering the catalyst chamber, the ammonia is injected and mixed with the gases. The stoichiometric reaction using either anhydrous or aqueous ammonia for a selective catalytic reduction process is as follows:

$$4NO + 4NH_3 + O_2 \rightarrow 4N_2 + 6H_2O$$
$$2NO_2 + 4NH_3 + O_2 \rightarrow 3N_2 + 6H_2O$$
$$NO + NO_2 + 2NH_3 \rightarrow 2N_2 + 3H_2O$$

With several secondary reactions:

$$2SO_2 + O_2 \rightarrow 2SO_3$$
$$2NH_3 + SO_3 + H_2O \rightarrow (NH_4)_2\,SO_4$$
$$NH_3 + SO_3 + H_2O \rightarrow NH_4HSO_4$$

The optimal reaction temperature for the gas ranges between 700 and 860 °F (370–460 °C) but it can operate from 450 to 830 °F (227–447 °C) with longer residence time. The minimum effective temperature depends on the various fuels, gas constituents, and catalyst geometry

SCR catalysts are manufactured from various ceramic materials, such as titanium oxide, used as a carrier and active catalytic components, they are usually either oxides

of base metals such as vanadium and tungsten. Base metals catalysts, such as vanadium and tungsten, lack high thermal durability, but are less expensive and operate very well at the temperature ranges most commonly seen in industrial and utility HRSG applications.

The two most common designs of SCR catalyst geometry used today are honeycomb and plate. The honeycomb form usually is an extruded ceramic applied homogeneously throughout the ceramic carrier or coated on the substrate. Like the various types of catalysts, their configuration also has advantages and disadvantages. Plate-type catalysts have lower pressure drops and are less susceptible to plugging and fouling than the honeycomb types, but plate configurations are much larger and more expensive. Honeycomb configurations are smaller than plate types, but have higher pressure drops and plug much more easily.

A common problem with all SCR systems is the release of unreacted ammonia. This is called ammonia slip. Slip can occur when catalyst temperatures are not in the optimal range for the reaction or when too much ammonia is injected into the process. An additional oxidation catalyst called a slip catalyst is typically fitted downstream of an SCR system to reduce such slip. Ammonia slip should be limited to five ppm or less. These systems require about 20% aqueous ammonia to the SCR reactor. Care must be taken in the design of the HRSG to ensure an equal gas and ammonia distribution over the catalyst.

The ammonia injection grid is located upstream of the SCR reactor chamber in a zone where gas or surface temperatures do not exceed 800 °F (427 °C). Figure 10-62 shows the location of the ammonia grid and the catalyst in a typical HRSG. The injection grid is designed and arranged to ensure uniform mixing of the ammonia and the exhaust gas stream. Re-circulated gas is used as the dilution and vaporization medium.

Most SCR systems are guaranteed to provide the emission reductions specified without requiring rejuvenation, maintenance, addition, or replacement of the catalyst for five calendar years or 40,000 hours of operation.

The SCR system is considered an integral part of the HRSG. Design, fabrication, inspection, testing, and installation of the SCR equipment, therefore, are in accordance with the requirements of the HRSG.

The SCR location of the catalyst modules should be optimized with respect to temperature, and required outlet NO_x system shall include consideration of sliding pressure operation of the HRSG, with optimization of the concentration.

The outer casing shall have provisions for test connections before and after the SCR system to determine the performance of the catalyst. The SCR system must be considered as an integral part of the HRSG system. The catalyst chamber is located in a temperature zone of the HRSG where the catalyst will be most effective at all loads and ambient temperatures.

Access shall be provided for the removal of catalyst coupons and to allow cleaning of the catalyst during periodic maintenance intervals. The internal structure of the HRSG casing is designed to allow complete access to the catalyst front face without the removal of internal structures.

Transition Pieces

Although technically not part of the combustor they are an important part of the combustion system. They connect the combustors round section to the rectangular sections of the first-stage nozzle. Less complicated than the liners, the transition pieces have probably been more challenging from a materials/processes standpoint. Therefore, new materials have tended to be first introduced on the transition piece. From a design standpoint, significant improvements have been made on advanced models through the use of heavier walls, single-piece aft ends, ribs, floating seal arrangements, and selective cooling. These design changes have been matched by material improvements. Early transition pieces were made from AISI 309 stainless steel. In the early 1960s, nickel base alloys Hastelloy-X and RA-333 were used in the more limiting parts. These alloys became standard for transition pieces by 1970. In the early 1980s, a new material, Nimonic 263, was introduced into service for transition pieces. This material is a precipitation-strengthened, nickel-base alloy with higher strength capability than Hastelloy-X. Since the early 1980s, thermal barrier coatings (TBCs) have

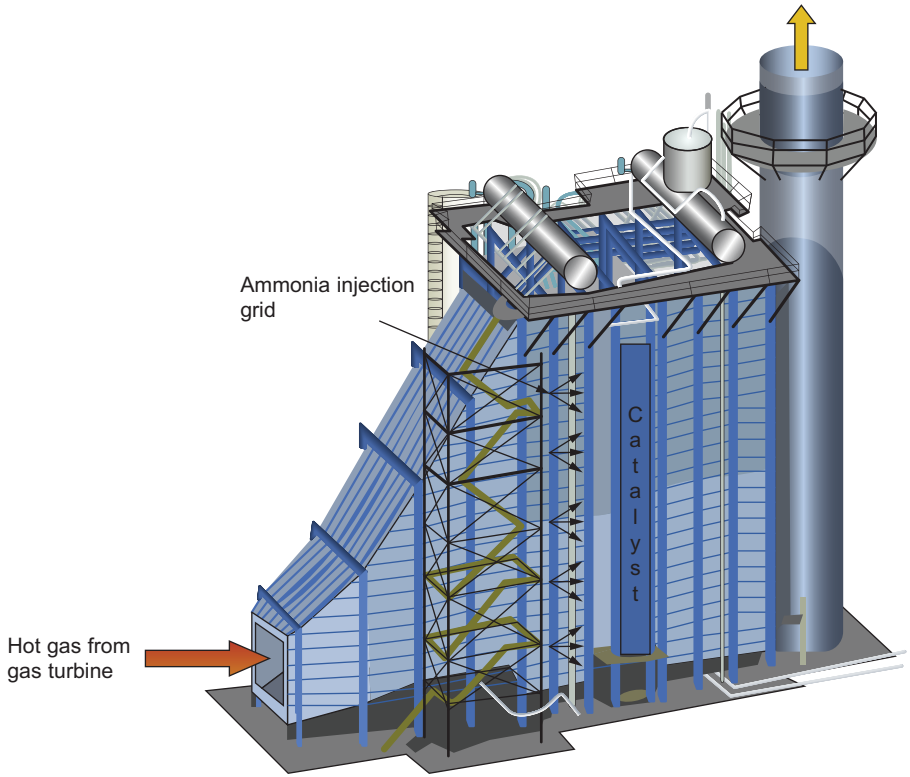


Figure 10-62 Location of SCR and ammonia grid in a typical HRSG.



Figure 10-63 Transition pieces for W501 D gas turbine.

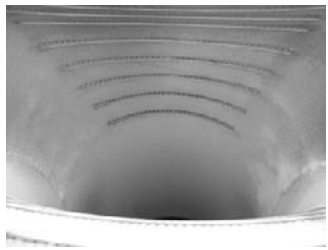


Figure 10-64 Internal cooling scheme for a W501 F gas turbine transition piece.

been applied to the transition pieces of the higher firing temperature gas turbine models and to uprated machines. Field experience over thousands of hours of service has demonstrated good durability for this coating on transition pieces.

Improvement has also been made to increase the wear resistance of some transition pieces in the aft end or picture frame area. Cobalt-base hard coatings applied by thermal spray have been tested in field machines and the best spray has been shown to improve the wear life of sealing components by more than four times.

Figures 10-63 and 10-64 are transition pieces for an older turbine the W501 D, which has a lower firing temperature. Note the cooling holes that bring in cooler air to line the inner surface with a blanket of cooling air. Figures 10-61 and 10-66 show a transition pieces for a newer gas turbine, the W 501 F gas turbine, which has a higher firing temperature. Note the cooling holes on the outer skin of the transition piece to ensure cooling. Figure 10-67 is a transition piece of GE Frame 7FA gas turbine. This

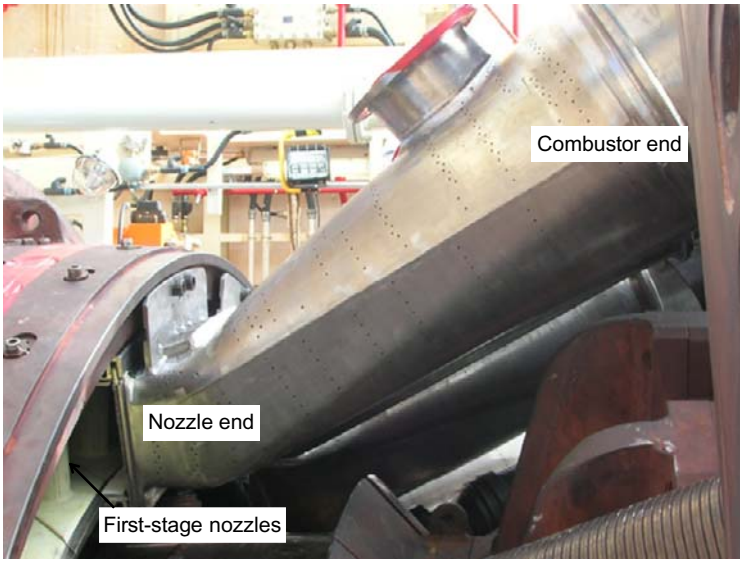


Figure 10-65 A transition piece for the W501F gas turbine joining the combustor to the sections of the first-stage nozzles.



Figure 10-66 A series of transition pieces joined to the combustor.

being a higher temperature gas turbine has a cooling jacket, which cools the metal and has inner cooling holes for the liner. Figure 10-68 is transition piece used with steam cooling. The steam is brought from the exit of the HP section of the steam turbine. This helps not only to cool the transition piece but also to heat the steam before it enters the intermediate section of the steam turbine. The transition piece has three layers and



Figure 10-67 Transition piece of a GE frame 7FA gas turbine.



Figure 10-68 Transition piece Siemens W501 FA gas turbine.

has cooling pipes in between the layers. Note the marks inside the liner where there has been some discoloration of the thermal barrier coating showing the layout of the cooling coils.

Copyrighted Materials
Copyright © 2012 Elsevier Retrieved from www.knovel.com

Part III

Materials, Fuel Technology, and Fuel Systems

11 Materials

Temperature limitations are the most crucial limiting factors to gas turbine efficiencies. Figures 11-1 (a) and 11-1 (b) show how the increased turbine inlet temperatures decrease both specific fuel and air consumption while increasing efficiency. Materials and alloys that can operate at high temperatures are very costly – both to buy and to work on. Figure 11-1 (c) shows relative raw material costs. Thus, the cooling of blades, nozzles, and combustor liners is an integral part of the total materials picture.

Since the design of turbomachinery is complex and the efficiency is directly related to material performance, the material selection is of prime importance. Gas and steam turbines exhibit similar problem areas, but these problem areas are of different magnitudes. Turbine components must operate under a variety of stress, temperature, and corrosion conditions. Compressor blades operate at a relatively low temperature

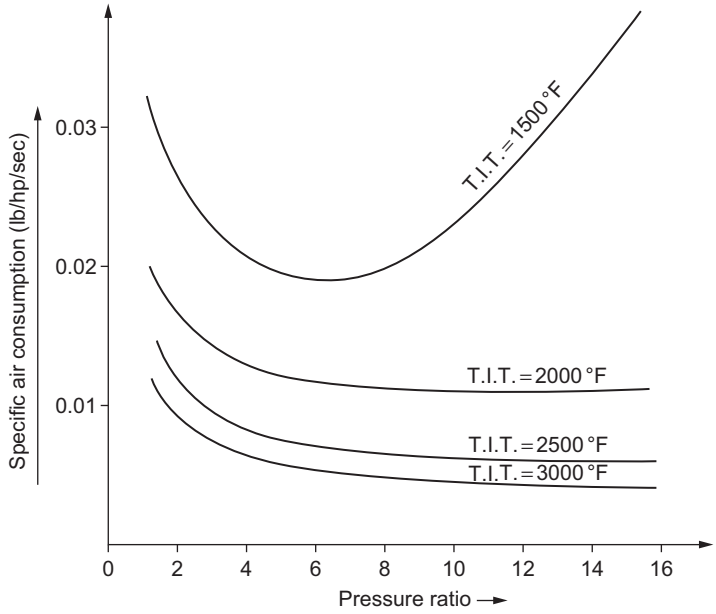


Figure 11-1 (a) Specific air versus pressure ratio and turbine inlet temperatures.

Gas Turbine Engineering Handbook, Fourth Edition. DOI: 10.1016/B978-0-12-383842-1.00011-1
Copyright © 2012 Elsevier Inc. All rights reserved.

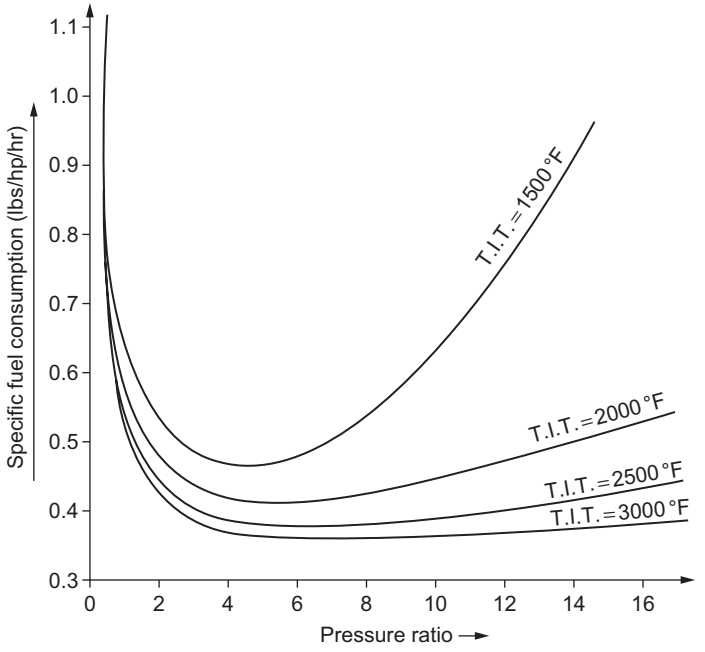


Figure 11-1 (b) Specific fuel consumption versus pressure ratio and turbine inlet temperature.

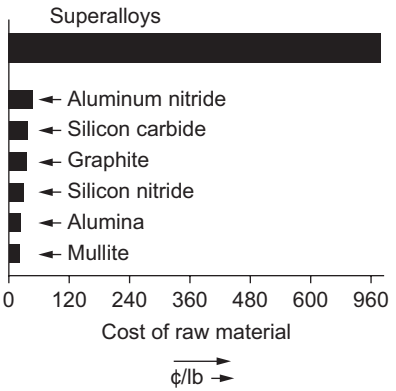


Figure 11-1 (c) A comparison of raw material costs.

but are highly stressed. The combustor operates at a relatively high temperature and low stress conditions. The turbine blades operate under extreme conditions of stress, temperature, and corrosion. These conditions are more extreme in gas turbine than in steam turbine applications. As a result, the selection of materials for individual components is based on varying criteria in both gas and steam turbines.

A design is only as efficient as the performance of the selected component materials. The combustor liner and turbine blades are the most critical components in existing high-performance and long-life gas turbines. The extreme conditions of stress, temperature, and corrosion make the gas turbine blade a material's challenge. Other turbine components present operational problem areas, but to a lesser degree. For this reason, gas turbine blade metallurgy will be discussed for solutions to problem areas. Definition of potential solutions will also relate to other turbine components.

The interaction of stress, temperature, and corrosion yields a complex mechanism that cannot be predicted by existing technology. The required material characteristics in a turbine blade for high performance and long life include limited creep, high-rupture strength, resistance to corrosion, good fatigue strength, low coefficient of thermal expansion, and high thermal conductivity to reduce thermal strains. The failure mechanism of a turbine blade is related primarily to creep and corrosion and secondarily to thermal fatigue. Satisfying these design criteria for turbine blades will ensure high performance, long life, and minimal maintenance.

The development of new materials as well as cooling schemes has seen the rapid growth of turbine firing temperatures leading to high turbine efficiencies. The fist-stage blade must withstand the most severe combination of temperature, stress, and environment; it is generally the limiting component in the machine. Figure 11-2 shows the trend of firing temperature and blade alloy capability.

Since 1950, the capability of turbine bucket material's temperature has advanced approximately 850 °F (472 °C), approximately 20 °F (10 °C) per year. The importance of this increase can be appreciated by noting that an increase of 100 °F (56 °C) in turbine firing temperature can provide a corresponding increase of 8–13% in output and a 2–4% improvement in simple-cycle efficiency. Advances in alloys and processing, while expensive and time consuming, provide significant incentives through increased power density and improved efficiency. Before discussing some of these materials in depth, it is important to understand the general behavior of metals.

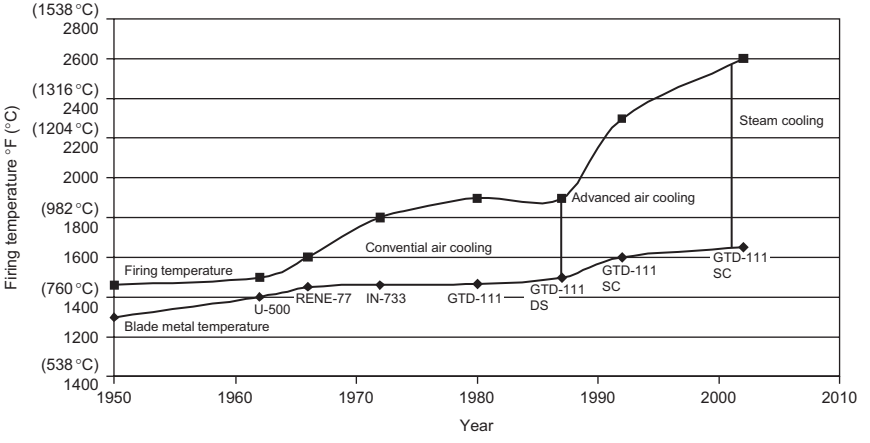


Figure 11-2 Firing temperature increase with blade material improvement.

General Metallurgical Behaviors in Gas Turbines

Creep and Rupture

The melting point of different metals varies considerably and their strengths at various temperatures are different. At low temperatures, all materials deform elastically, then plastically, and are time independent. However, at higher temperatures, deformation is noted under constant load conditions. This high-temperature and time-dependent behavior is called creep-rupture. Figure 11-3 shows a schematic of a creep curve with the various stages of creep. The initial or elastic strain is the first region that proceeds into a plastic strain region at a decreasing rate. Then, a nominally constant plastic strain rate is followed by an increasing strain rate to fracture.

The nature of this creep depends on the material, stress, temperature, and environment. Limited creep ($< 1\%$) is desired for turbine blade application. Cast superalloys fail with only a minimum elongation. These alloys fail in brittle fracture – even at elevated operating temperatures.

Stress-rupture data are often presented in a Larson–Miller curve, which indicates the performance of an alloy in a complete and compact graphical style. Although widely used to describe an alloy's stress-rupture characteristics over a wide temperature, life, and stress range, it is also useful in comparing the elevated temperature capabilities of many alloys. The Larson–Miller parameter is given as follows:

$$P_{\mathrm{LM}} = T(20 + \log t) \times 10^{-3} \tag{11-1}$$

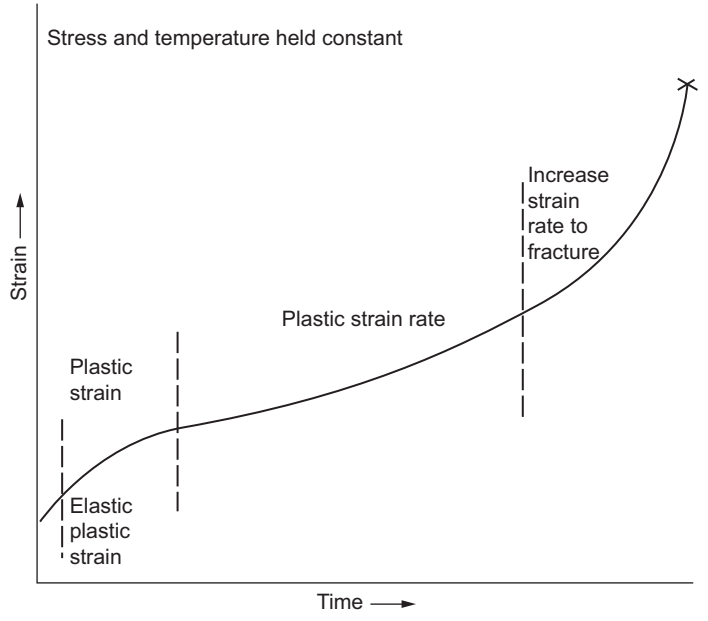


Figure 11-3 Time-dependent strain curve under constant load.

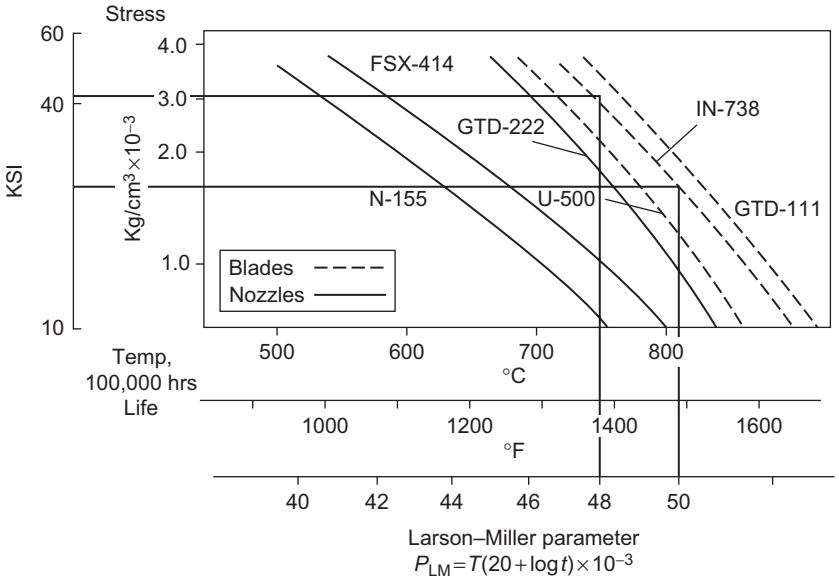


Figure 11-4 Larson–Miller parameter for various types of blades.

where

$$P_{\mathrm{LM}} = \text{Larson}-\text{Miller parameter}$$
$$T = \text{temperature}\,(^{\circ}\text{R})$$
$$t = \text{rupturetime}\,(\text{h})$$

The Larson–Miller parameters are plotted in Figure 11-4 for the specified turbine blade alloys. A comparison of A-286 and Udimet 700 alloy curves reveals the difference in capabilities. The operational life (in hours) of the alloys can be compared for similar stress and temperature conditions.

Ductility and Fracture

Ductility is commonly measured by elongation and reduction in area. In many cases, all three stages of creep shown in Figure 11-3 are not present. At high temperatures or stresses, very little primary creep is seen, while in the case of cast superalloys, failure occurs with just a small extension. This amount of extension is ductility. In a time-creep curve, there are two elongations of interest.

One elongation is from the plastic strain rate and the second elongation is the total elongation or the elongation at fracture. Ductility is erratic in its behavior and is not always repeatable – even under laboratory conditions. Ductility of a metal is affected by the grain size, the specimen shape, and the techniques used for manufacturing. A fracture that results from elongation can be of two types: brittle or ductile, depending on the alloy. A brittle fracture is intergranular with little or no elongation. A ductile

fracture is transgranular and typical of normal ductile tensile fracture. Turbine blade alloys tend to indicate low ductility at operating temperatures. As a result, surface notches are initiated by erosion or corrosion and then cracks are propagated rapidly.

Cyclic Fatigue

All materials would fail at a certain load if subjected to a large number of cycles. A very common type of failure that blades in turbines undergo is known as "high-cycle fatigue." This type of failure is caused when the blade is subjected to an unsteady load repeatedly. Most materials, under these alternating loads, would fail in about 10^7 cycles, assuming that the resonance frequency for a given blade is 10^3 Hz. This would tend to mean that the material would fail within 10^4 s, about 2.8 h, if the blade was subjected to an alternating force, which would excite the frequency of blade resonance. This type of failure would be depicted by a chevron type of markings on the failed surface, near the trailing edge of the blade. A Goodman diagram of the material is often used to determine the amount of alternating stress on the blades at different loadings. The Goodman diagram is shown in Figure 11-5. The Goodman diagram is particularly helpful in determining the effectiveness of a material or component that will be subjected to a cyclic stress superimposed upon a non-zero mean stress. The horizontal axis is the mean, stress, or ultimate strength of the material in pounds-force per square inch or megapascals and the vertical axis is the alternating stress, which is half the ultimate strength or mean stress multiplied by any correction or safety factors.

Thermal Fatigue

Thermal fatigue of turbine blades is a secondary failure mechanism. Temperature differentials developed during the starting and stopping of the turbine produce thermal

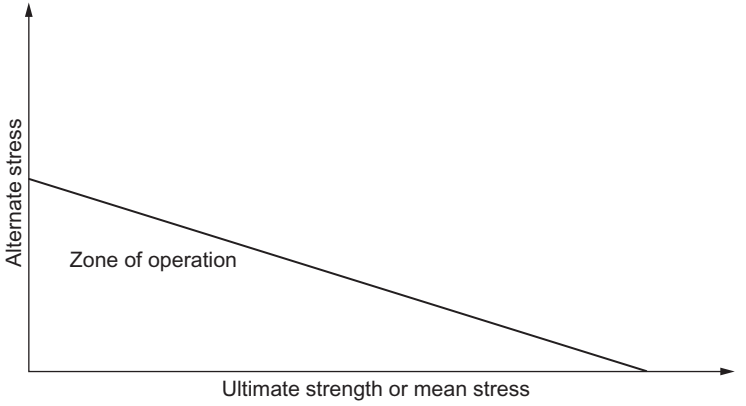


Figure 11-5 Goodman diagram.

stress. The cycling of these thermal stresses is thermal fatigue. Thermal fatigue is low cycle and similar to a creep-rupture failure. The analysis of thermal fatigue is essentially a problem in heat transfer and properties such as modulus of elasticity, coefficient of thermal expansion, and thermal conductivity.

The most important metallurgical factors are ductility and toughness. Highly ductile materials tend to be more resistant to thermal fatigue. They also seem more resistant to crack initiation and propagation.

Research programs are underway to demonstrate that brittle materials can be successfully utilized in demanding high-temperature structural applications.

From the previous work, it has been established that silicon nitride and silicon carbide, in their variety of forms and fabrications, are the two most likely candidates for the future ceramic engine. Both exhibit a suitable workability, the desired strength at high temperatures, and have the specific resistance, availability, and manufacturing ease to make them likely prospects for gas turbine components.

The operating schedule of a gas turbine produces a low-frequency thermal fatigue. The number of starts per hour of operating time directly affects the blade life. Table 11-1 shows that fewer starts per operating time increases turbine life.

Corrosion

The use of Ni-base superalloys as turbine blades in an actual end-use atmosphere produces deterioration of material properties. This deterioration can result from erosion or corrosion. Erosion results from hard particles impinging on the turbine blade and removing material from the blade surface. The particles may enter through the turbine inlet or can be loosened scale deposits from within the combustor.

Corrosion is described as hot corrosion and sulfidation processes. Hot corrosion is an accelerated oxidation of alloys caused by the deposition of Na_2SO_4. Oxidation results from the ingestion of salts in the engine and sulfur from the combustion of fuel. Sulfidation corrosion is considered a form of hot corrosion in which the residue contains alkaline sulfates. Corrosion causes the deterioration of blade materials and reduces component life.

Hot corrosion is a rapid form of attack that is generally associated with alkali metal contaminants, such as sodium and potassium, reacting with sulfur in the fuel to form molten sulfates. The presence of only a few parts per million (ppm) of such contaminants in the fuel, or the equivalent in the air, is sufficient to cause this corrosion. Sodium can be introduced in a number of ways, such as: salt water in liquid fuel, through the turbine air inlet at sites near salt water or other contaminated areas, or as contaminants in water/steam injections. Besides the alkali metals such as sodium and potassium, other chemical elements can influence or cause corrosion on bucketing. Notable in this connection is vanadium, primarily found in crude and residual oils.

There are now two distinct forms of hot corrosion recognized by the industry, although the end result is the same, which are high-temperature (Type 1) and low-temperature (Type 2) hot corrosion.

Table 11-1 Operation and Maintenance Life of an Industrial Turbine

Type of Application and Fuel	Starts/h	Firing Temperature below 1700 °F (927 °C)			Firing Temperature above 1700 °F (927 °C)		
		Comb. liners	First-stage nozzle	First-stage blades	Comb. liners	First-stage nozzle	First-stage blades
Base load		+	+	+			
Natural gas	1/1,000	30,000	60,000	100,000	15,000	25,000	35,000
Natural gas	1/10	7,500	42,000	72,000	3,750	20,000	25,000
Distillate oil	1/1,000	22,000	45,000	72,000	11,250	22,000	30,000
Distillate oil	1/10	6,000	35,000	48,000	3,000	13,500	18,000
Residual	1/1,000	3,500	20,000	28,000	2,500	10,000	15,000
Residual	1/10						
System peaking							
Normal max. load of short duration and daily starts							
Natural gas	1/10	7,500	34,000	60,000	5,000	15,000	24,000
Natural gas	1/5	3,800	28,000	40,000	3,000	12,500	18,000
Distillate	1/10	6,000	27,200	53,500	4,000	12,500	19,000
Distillate	1/5	3,000	22,400	32,000	2,500	10,000	16,000
Turbine peaking							
Operating above 50–100 °F (28–56 °C) Firing temperature							
Natural gas	1/5	2,000	12,000	20,000	2,000	12,500	18,000
Natural gas	1/1	400	9,000	15,000	400	10,000	15,000
Distillate	1/5	1,600	10,000	16,000	1,700	11,000	15,000
Distillate	1/1	400	7,300	12,000	400	8,500	12,000

High-temperature hot corrosion has been known since 1950s. It is an extremely rapid form of oxidation that takes place at temperatures between 1500 °F (816 °C) and 1700 °F (927 °C) in the presence of sodium sulfate (Na_2SO_4).

Sodium sulfate is generated in the combustion process as a result of the reaction among sodium, sulfur and oxygen. Sulfur is present as a natural contaminant in the fuel.

Low-temperature hot corrosion was recognized as a separate mechanism of corrosion attack in the mid-1970s. This attack can be very aggressive if the conditions are right. It takes place at temperatures in the 1100 °F (593 °C) to 1400 °F (760 °C) range and requires a significant partial pressure of SO_2. It is caused by low-melting eutectic compounds resulting from the combination of sodium sulfate and some of the alloy constituents such as nickel and cobalt. It is, in fact, somewhat analogous to the type of corrosion called fireside corrosion in coal-fired boilers.

The two types of hot corrosion cause different types of attack. High-temperature corrosion features intergranular attack, sulfide particles, and a denuded zone of base metal. Metal oxidation occurs when oxygen atoms combine with metal atoms to form oxide scales. The higher the temperature, the more rapid the process, which creates the potential for the failure of components if too much of the substrate material is consumed in the formation of these oxides.

Low-temperature corrosion characteristically shows no denuded zone, no intergranular attack, and a layered type of corrosion scale.

The lines of defense against both types of corrosion are similar. First, reduce the contaminants. Second, use materials that are as corrosion resistant as possible. Third, apply coatings to improve the corrosion resistance of the bucket alloy.

Hot corrosion includes two mechanisms:

1. *Accelerated Oxidation*

During initial stages – blade surface clean

$$Na_2SO_4 + Ni\,(\text{metal}) \rightarrow NiO\,(\text{porous})$$

2. *Catastrophic Oxidation*

Occurs with Mo, W, and V present – reduces NiO layer – increases oxidation rate

Reactions – Ni-Base Alloys

Protective oxide films

$$2Ni + O_2 \rightarrow 2NiO$$
$$4Cr + 3O_2 \rightarrow 2Cr_2O_3$$

Sulfate

$$2Na + S + 2O_2 \rightarrow Na_2SO_4$$
$$Na - \text{from NaCl (salt)}$$
$$S - \text{from fuel}$$

Other Oxides

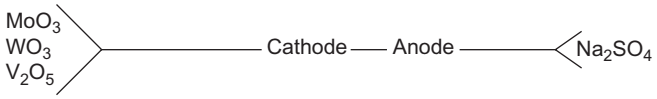
$$2Mo + 3O_2 \rightarrow 2MoO_3$$
$$2W + 3O_2 \rightarrow 2WO_3$$
$$4V + 5O_2 \rightarrow 2V_2O_5$$

The Ni-base alloy surface is exposed to an oxidizing gas, oxide nuclei and a continuous oxide film form (Ni) (Cr_2O_3, etc.). This oxide film is a protective layer. The metal ions diffuse to the surface of the oxide layer and combine with the molten Na_2SO_4 to destroy the protective layer. Ni_2S and Cr_2S_3 results (*sulfidation*):

$$NaCl\,(sea\,salt) \rightarrow Na + Cl$$
$$Na + S\,(fuel) + 2O_2 \rightarrow Na_2SO_4$$
$$Cl - grainboundaries - \textit{causes intergranular corrosion}$$

The extent of the corrosion depends on the amount of nickel and chromium in the alloy. The oxide films become porous and non-protective, which increases the oxidation rate (accelerated oxidation).

Catastrophic oxidation requires the presence of Na_2SO_4 and Mo, W, and/or V. Crude oils are high in V; ash will be 65% V_2O_5 or higher. V can be alloyed in metal. A galvanic cell is generated:



The galvanic corrosion deletes the protective oxide film and increases the oxidation rate. The corrosion problem includes: (1) erosion, (2) sulfidation, (3) intergranular corrosion, and (4) hot corrosion. The 20% Cr alloys increase oxidation resistance.

Sixteen percent Cr alloys (Inconel 600) are less resistant. Cr in alloys reduces grain boundary oxidation, while high Ni alloys tend to oxidize along grain boundaries. Age-hardened gas turbine blades of 10–20% Cr will corrode (sulfidation) at more than 1400 °F. Ni_2S forms in the grain boundary. The addition of cobalt to the alloy increases the temperature at which the attack occurs. To reduce corrosion, either increase the Cr amount or apply a coating (Al or Al + Cr).

A high-nickel alloy is used for increased strength at elevated temperatures and a chromium content in excess of 20% is desired for corrosion resistance. An optimum composition to satisfy the interaction of stress, temperature, and corrosion has not been developed. The rate of corrosion is directly related to alloy composition, stress level, and environment. The corrosive atmosphere contains chloride salts, vanadium, sulfides, and particulate matter. Other combustion products, such as NO_x, CO, and CO_2, also contribute to the corrosion mechanism. The atmosphere changes with the type of fuel used. Fuels, such as natural gas, diesel #2, naphtha, butane, propane, methane, and fossil fuels, will produce different combustion products that affect the corrosion mechanism in different ways.

Gas Turbine Materials

The composition of the new and conventional alloys throughout the turbine is shown in Table 11-2. This table describes materials used in the GE line of turbines but the materials are common to all brands of high-temperature turbine even though there may be some variations in the composition of the alloys. In the early years of turbine development, increases in the capability of temperature in blade alloy accounted for the majority of the firing temperature increase until air cooling was introduced, which decoupled firing temperature from the blade metal temperature. In addition, as the metal temperatures approached a temperature range of 1600 °F (870 °C), hot corrosion of blades became more life limiting than strength until the introduction of protective coatings. During the 1980s, emphasis turned toward two major areas: improved materials technology to achieve greater capability of blade alloy without sacrificing alloy corrosion resistance, and advanced and highly sophisticated air-cooling technology to achieve the firing temperature capability required for the new generation of gas turbines. The use of steam cooling to further increase combined-cycle efficiencies in combustors was introduced in the mid- to late 1990s. Steam cooling in blades and nozzles was introduced to commercial operation in 2002.

In the 1980s, IN-738 blades were widely used. IN-738 was the acknowledged corrosion standard for the industry. New alloys, such as GTD-111, were developed and patented by GE in the mid-1970s. GTD-111 possesses about a 35 °F (20 °C) improvement in rupture strength as compared with IN-738. GTD-111 is also superior to IN-738 in low-cycle fatigue strength.

The design of this alloy was unique in that it utilized phase stability and other predictive techniques to balance the levels of critical elements (Cr, Mo, Co, Al, W, and Ta), thereby maintaining the hot corrosion resistance of IN-738 at higher strength levels without compromising phase stability. Most nozzle and blade castings are made by using the conventional equiaxed investment casting process. In this process, the molten metal is poured into a ceramic mold in a vacuum, to prevent the highly reactive elements in the superalloys from reacting with the oxygen and nitrogen in the air. With proper control of metal and mold thermal conditions, the molten metal solidifies from the surface to the center of the mold, creating an equiaxed structure. Directional solidification (DS) is also being employed to produce advanced-technology nozzles and blades. First used in aircraft engines more than 25 years ago, it was adapted for the use in large airfoils in the early 1990s. By exercising careful control over temperature gradients, a planar solidification front is developed in the bade, and the part is solidified by moving this planar *front* longitudinally through the entire length of the part. The result is a blade with an oriented grain structure that runs parallel to the major axis of the part and contains no transverse grain boundaries, as in ordinary blades. The elimination of these transverse grain boundaries confers additional creep and rupture strengths on the alloy, and the orientation of the grain structure provides a favorable modulus of elasticity in the longitudinal direction to enhance fatigue life. The use of directionally solidified blades results in a substantial increase in the creep life or substantial increase in tolerable stress for a fixed life. This advantage is due to the elimination of transverse grain boundaries from

Table 11-2 High-Temperature Alloys (Courtesy: GE Power Systems)

Component	Cr	Ni	Co	Fe	W	Mo	Ti	Al	Cb	V	C	B	Ta
Turbine blades													
U-500	18.5	BAL	18.5	–	–	4	3	3	–	–	0.07	0.006	–
RENE-77 (U700)	15	BAL	17	–	–	5.3	3.35	4.25	–	–	0.07	0.02	–
IN-738	16	BAL	8.3	0.2	2.6	1.75	3.4	3.4	0.9	–	0.10	0.001	1.75
GTD-111	14	BAL	9.5	–	3.8	1.5	4.9	3.0	–	–	0.10	0.01	2.8
Turbine nozzles													
X40	25	10	BAL	1	8	–	–	–	–	–	0.50	0.01	–
X45	25	10	BAL	1	8	–	–	–	–	–	0.25	0.01	–
FSX414	28	10	BAL	1	7	–	–	–	–	–	0.25	0.01	–
N155	21	20	20	BAL	2.5	3	–	–	–	–	0.20	–	–
GTD-222	22.5	BAL	19	–	2.0	2.3	1.2	0.8	–	0.10	0.008	1.00	–
Combustors													
SS309	23	13	–	BAL	–	–	–	–	–	–	0.10	–	–
HAST X	22	BAL	1.5	1.9	0.7	9	–	–	–	–	0.07	0.005	–
N-263	20	BAL	20	0.4	–	6	2.1	0.4	–	–	0.06	–	–
HA-188	22	22	BAL	1.5	14.0	–	–	–	–	–	0.05	0.01	–
Turbine wheels													
Alloy 718	19	BAL	–	18.5	–	3.0	0.9	0.5	5.1	–	0.03	–	–
Alloy 706	16	BAL	–	37.0	–	–	1.8	–	2.9	–	0.03	–	–
Cr–Mo–V	1	0.5	–	BAL	–	1.25	–	–	–	0.25	0.30	–	–
A286	15	25	–	BAL	–	1.2	2	0.3	–	0.25	0.08	0.006	–
M152	12	2.5	–	BAL	–	1.7	–	–	–	0.3	0.12	–	–
Compressor blades													
AISI 403	12	–	–	BAL	–	–	–	–	–	–	0.11	–	–
AISI 403 + Cb	12	–	–	BAL	–	–	–	–	0.2	–	0.15	–	–
GTD-450	15.5	6.3	–	BAL	–	0.8	–	–	–	–	0.03	–	–

the bucket, the traditional weak link in the microstructure. In addition to improved creep life, the directionally solidified blades possess more than 10 times the strain control or thermal fatigue compared to equiaxed blades. The impact strength of the DS blades is also superior to that of equiaxed blades, showing an advantage of more than 33%.

In the late 1990s, single-crystal blades were introduced in gas turbines. These blades offer additional creep and fatigue benefits through the elimination of grain boundaries. In single-crystal material, all grain boundaries are eliminated from the material structure, and a single crystal with controlled orientation is produced in an airfoil shape. By eliminating all grain boundaries and the associated grain boundary strengthening additives, a substantial increase in the melting point of the alloy can be achieved, thus providing a corresponding increase in high-temperature strength. The transverse creep and fatigue strengths are increased compared with equiaxed or DS structures. The advantage of single-crystal alloys compared with equiaxed and DS alloys in low-cycle fatigue (LCF) life is increased by about 10%.

Blade life comparison is provided in the form of the stress required for rupture as a function of a parameter that relates time and temperature (the Larson–Miller parameter). The Larson–Miller parameter is a function of blade metal's temperature and the time the blade is exposed to those temperatures. Figure 11-4 shows the comparison of some of the alloys used in blade and nozzle applications. This parameter is one of the several important design parameters that must be satisfied to ensure the proper performance of the alloy in a blade application, especially for long service life. Creep life, HCF and LCF, thermal fatigue, tensile strength and ductility, impact strength, hot corrosion and oxidation resistance, producibility, coatability, and physical properties must also be considered.

Turbine Wheel Alloys

Alloy 718 Nickel-Based Alloy

This nickel-based and precipitation-hardened alloy is the newest being developed for the next generation of frame-type gas turbine machines. This alloy has been used for wheels in aircraft turbines for more than 20 years. Alloy 718 contains a high concentration of alloying elements and is, therefore, difficult to produce in the very large ingot sizes needed for the large frame-type turbine wheel and spacer forgings. This effort requires close cooperation between the manufacturer and its superalloy melters and large forging suppliers to conduct the solidification and forging flow studies that are necessary to bring a new wheel material for large wheels into production. This development effort has resulted in the production of the largest ingots ever made and forged into high-quality qualification turbine wheel and spacer forgings.

Alloy 706 Nickel-Based Alloy

This nickel-based and precipitation-hardened alloy is being used in large frame-type units by GE such as the frame 7FA, 9FA, 6FA, and 9EC turbine wheel and

spacer alloys and it offers a very significant increase in stress-rupture and tensile-yield strengths compared with the other wheel alloys. Figures 11-6 and 11-7 show the stress rupture and tensile yield strength of the various alloys. This alloy is similar to Alloy 718, but contains somewhat lower concentrations of alloying elements and is, therefore, easier to produce in the very large ingot sizes needed for large frame-type gas turbines.

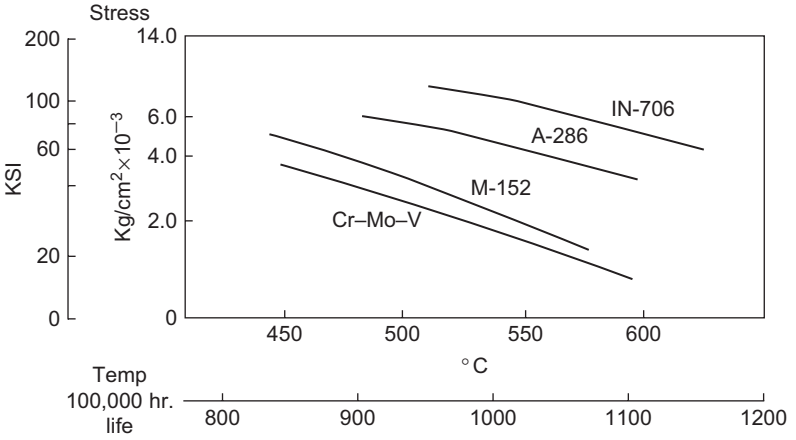


Figure 11-6 Turbine wheel alloys stress-rupture comparison.

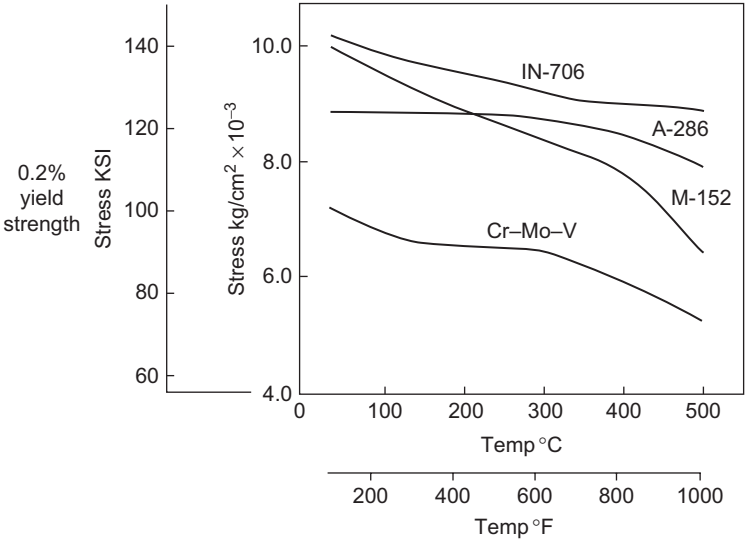


Figure 11-7 Turbine wheel alloys tensile strength comparison.

Cr–Mo–V Alloy

Turbine wheels and spacers of most GE single-shaft heavy-duty gas turbines are made of 1% Cr–1.25% Mo–0.25% V steel. This alloy is used in the quenched and tempered condition to enhance bore toughness. Stress-rupture strength of the dovetail region (periphery) is controlled by providing extra stock at the periphery to produce a slower cooling rate during quenching.

The stress-rupture properties of this alloy are shown in Figure 11-6.

12 Cr Alloys

This family of alloys has a combination of properties that make them especially valuable for turbine wheels. These properties include good ductility at high-strength levels, uniform properties throughout thick sections, and favorable strength at temperatures up to about 900 °F (482 °C).

M-152 alloy is a 2–3% nickel-containing member of the 12 Cr family of alloys. Initially, it was used as an upgrade in gas turbines as a replacement for A-286. It features outstanding fracture toughness, in addition to the properties common to other 12 Cr alloys. M-152 alloy is intermediate in rupture strength, between the Cr–Mo–V and A-286 alloys (Figure 11-6), and it has higher tensile strength than these alloys. These features, together with its favorable coefficient of expansion and good fracture toughness, make the alloy attractive for use in gas turbine applications.

A-286 Alloy

A-286 is an austenitic iron-base alloy that has been used for years in aircraft engine applications. Its use for industrial gas turbines started about 1965, when technological advances made the production of sound ingots sufficient in size to produce these wheels possible.

As knowledge of the capabilities of M-152 increased, the production of the wheels was switched from A-286 to M-152. A-286 is currently being introduced in turbines as a part of a composite aft shaft.

Compressor Blades

Compressor blading is variously made by forging, extrusion, or machining. All production blades, until recently, have been made from Type 403 or 403 Cb (both 12 Cr) stainless steels. During the 1980s, a new compressor blade material, GTD-450, a precipitation-hardened and martensitic stainless steel, was introduced into production for advanced and uprated machines, as shown in Table 11-2. This material provides increased tensile strength without sacrificing stress corrosion resistance. Substantial increases in the high-cycle fatigue and corrosion fatigue strength are also achieved with this material, compared with Type 403. Superior corrosion resistance is also achieved due to high concentrations of chromium and molybdenum. Compressor corrosion is usually caused by moisture and salt ingested by the turbine. Coating of compressor blades is also highly recommended.

Forgings and Non-destructive Testing

Most other rotor parts in gas turbines are individually forged. This includes compressor wheels, spacers, distance pieces, and stub shafts. All are made from quenched and tempered low-alloy steels (Cr–Mo–V or Ni–Cr–Mo–V) with the material and heat treatment optimized for the specific part. The intent is to achieve the best balance of strength, toughness with ductility, processing, and non-destructive evaluation capabilities, particularly when it is recognized that some of these parts may be exposed to operating temperatures as low as –60 °F (–51 °C).

It is recommended that parts are sonic and magnetic particle tested. Many last-stage compressor wheels are spun in a manner analogous to turbine wheels as a means of proof testing and imparting bore residual stresses. This last-stage compressor wheel is probably the next most critical rotor component after the turbine wheels, especially in the new very high pressure ratio compressors.

New non-destructive techniques to inspect turbine forgings to greater levels of sensitivity than ever before possible have been developed. These new ultrasonic inspection techniques are being applied to all the turbine forgings to ensure an even greater level of confidence in these high-strength forgings.

Additional development efforts continue to improve the current processing of other forgings by working with our suppliers on the further optimization of properties and forging quality. In-process non-destructive evaluation of all rotor components continues to be emphasized as a critical aspect in the production of quality forgings.

Ceramics

The day when turbines will operate at 2500–3000 °F (1371–1649 °C), yielding double the present horsepower at half the present engine size, may not be far off. This dream may turn into reality because of ceramics and unique cooling systems. Ceramics were, until recently, dismissed as being too brittle, hard to fabricate, and not suited to flight engines. However, the addition of aluminum to ceramics forms a compound that is more ductile.

Since 1945, the temperature limits of flight engine alloys have been steadily increasing about 20 °F (11 °C) per year. Transpiration and internally cooled metal blades have resulted in higher temperatures and more efficient operation. However, the direct correlation between efficiency and fabrication cost has resulted in a situation of diminishing returns for the superalloys. As more and more cooling air is needed for the superalloy components, the efficiency of the engine drops to a point where turbine inlet temperatures around 2300 °F (1260 °C) are the optimum and, at that point, they are uneconomic for automotive use.

Increasing efficiency with the use of 2500 °F (1371 °C) tolerant uncooled ceramic blades provides an improvement in fuel consumption of more than 20% from a 1800 °F (982 °C) turbine inlet temperature. This rate represents almost a 50% improvement in specific air consumption. This improvement implies that for the same size engine, power almost doubles, or conversely (and possibly more important to automakers), engine flow size could be cut into half and retain the same horsepower output.

Ceramics are quite tolerant of such contaminants as sodium and vanadium, which are present in low-cost fuels and highly corrosive to currently used nickel alloys. Ceramics are also up to 40% lighter than comparable high-temperature alloys – another advantage in application. However, the biggest advantage is material cost. Ceramics cost around 5% of the cost of superalloys.

Despite all the advantages of ceramics, they are brittle; unless this problem is overcome, the use of ceramics in gas turbines will not be practical.

Coatings

Blade coatings were originally developed by the aircraft engine industry for aircraft gas turbines. Metal temperatures in heavy-duty gas turbines are lower than those in aircraft engines. However, heavy-duty gas turbines are generally subjected to excessive contamination or accelerated attack known as hot corrosion.

Blade coatings are required to protect the blade from corrosion, oxidation, and mechanical property degradation. As superalloys have become more complex, it has been increasingly difficult to obtain both the higher strength levels that are required and a satisfactory level of corrosion and oxidation resistance without the use of coatings. Thus, the trend toward higher firing temperatures increases the need for coatings. The function of all coatings is to provide a surface reservoir of elements that will form very protective and adherent oxide layers, thus protecting the underlying base material from oxidation and corrosion attack and degradation.

Experience has shown that the lives of both uncoated and coated blades depend to a large degree on the amount of fuel and air contamination, as well as the operating temperature of the blade. The effect of sodium, a common contaminant, on bucket life at 1600 °F (871 °C) is shown in Figure 11-8. When sodium sulfate (Na_2SO_4) is present,

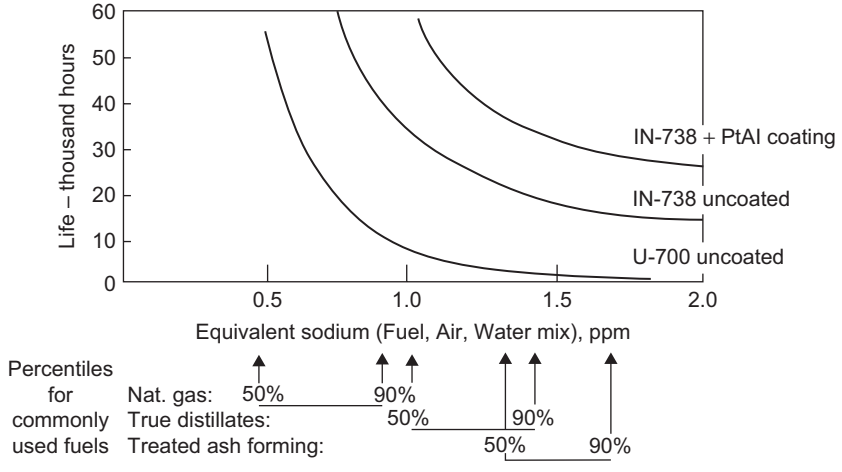


Figure 11-8 Effect of sodium corrosion on blade life.

hot corrosion is greatly accelerated. Sodium sulfate is a product of combustion. The presence of only a few parts per million (ppm) of sodium and sulfate is sufficient to cause extensive hot corrosion damage. Sulfur is present as a natural contaminant in the fuel. Sodium can be introduced as a natural contaminant in the fuel or in the atmosphere of sites located near salt water or contaminated areas.

The Pt–Al coating is a precious metal applied by uniformly electroplating a thin layer (0.00025 in) of platinum (Pt) onto the bucket at the airfoil surface, followed by pack-diffusion steps to deposit a layer of aluminum and chromium. The resulting coating has an outer skin of an extremely corrosion resistant, platinum–aluminum intermetallic composition. As shown in Figure 11-8, a test was conducted for comparative corrosion on coated and uncoated IN-738 blades. The blades were run side-by-side in the same machine under severe corrosive conditions. The two blades were removed for interim evaluation after 11,300 service hours (289 starts). The unit burnt sour natural gas containing about 3.5% ppm sulfur and was located in a region where the soil surrounding the site contains up to 3% sodium. The uncoated blade showed a 0.005-in corrosion attack over 50% of the airfoil concave face, with about 0.010-in penetration at the base of the airfoil. The examination of the coated blade revealed no visual evidence of attack, except for one small roughened spot on the leading edge about 1 in up from the platform, and a second spot in the middle of the convex side about 1 in down from the tip.

Metallographic examination of other areas revealed similar degrees of corrosion on the two blades. At no point on the coated blade had the corrosion penetrated to the base metal, although in the two areas on the coated blade about 0.002 in of the original 0.003-in coating had been oxidized.

Experience with uncoated IN-738 blades in this very hostile environment indicates that a blade life of about 25,000 hours can be attained. The coated blade life, based on this interim evaluation, should add an additional 20,000 hours of life.

Experience has shown that the lives of both uncoated and coated blades depend to a large degree on the amount of fuel and air contamination. This effect is shown in Figure 11-8, which illustrates the effect of sodium, a common contaminant, on blade life at 1600 °F (871 °C). The presence of increased levels of contaminants gives rise to an accelerated form of attack called hot corrosion.

Hot corrosion is distinctly different from the pure oxidation of an aircraft environment; hence, coatings for heavy-duty gas turbines have different capabilities compared with coatings for aircraft engines. In addition to hot corrosion, high-temperature oxidation and thermal fatigue resistance have become important criteria in the higher firing gas turbines, as shown in Figure 11-9. In today's advanced machines, oxidation is of concern not only for external blade surfaces, but also for internal passages such as cooling holes, due to the high temperature of the cooling air, which in turn is due to the high pressure ratio in the compressor. The main requirements of a coating are to protect blades against oxidation, corrosion, and cracking problems. Coatings are there to prevent the base metal from attack. Other benefits of coatings include thermal fatigue from cyclic operation, surface smoothness and erosion in compressor coatings, and heat flux loading when one is considering thermal barriers. A secondary consideration, but perhaps rather more relevant to thermal barriers, is their ability to tolerate damage from light impacts without spalling to an unacceptable extent because of the

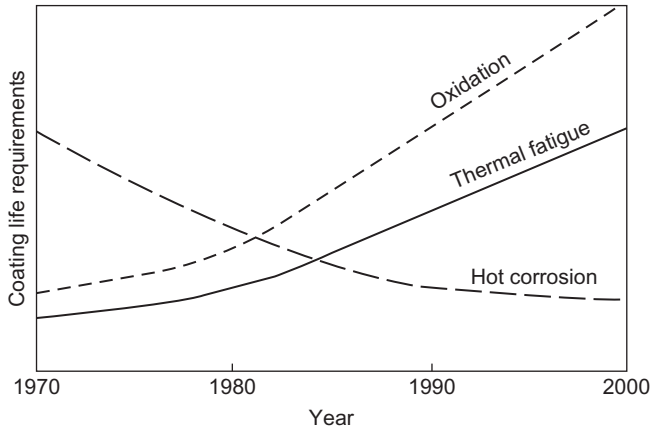


Figure 11-9 Blade coating requirements and coating evolution.

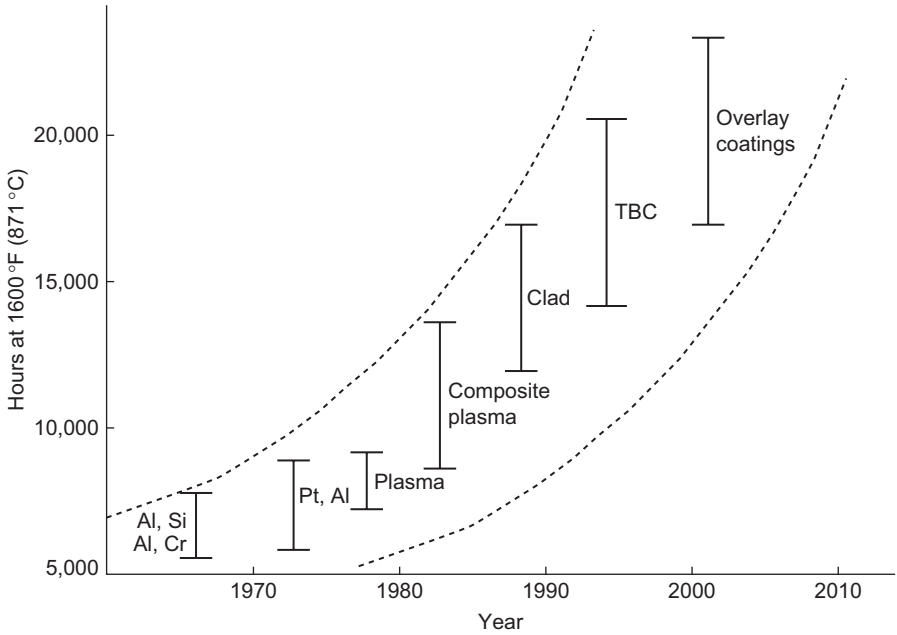


Figure 11-10 Developments of coatings.

resulting rise in the local metal temperatures. Coatings also extend life, provide protection by enduring the operational conditions, and protect the blades by being sacrificial, by allowing the coating to be restripped and recoated on the same base metal.

Past and future trends in the development of coatings are shown in Figure 11-10. Present-day coatings last 10–20 times longer than coatings used 10 years ago. Coated blades last up to twice as long as uncoated blades in the field.

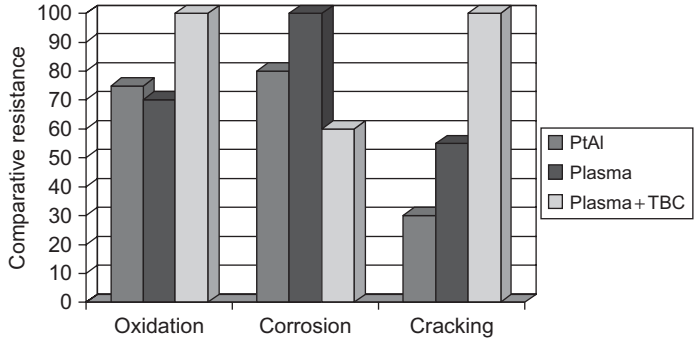


Figure 11-11 Comparative resistance in various types of coatings.

Figure 11-11 is a comparison between the various types of coatings and the comparative resistance in the areas of oxidation, corrosion, and cracking. To improve the oxidation protection, an increase in the aluminum content in the outer region of the coating matrix is needed. The higher aluminum content forms a more protective aluminum oxide layer that greatly improves the high-temperature oxidation resistance.

Life of coatings depends on composition, thickness, and the standard of evenness to which it has been deposited. Most of the new coatings are applied by vacuum plasma spray technique to ensure that the coating has been applied in a uniform and controlled manner. Coatings help extend the life of bladings by protecting them against oxidation, corrosion, cracking, thermal fatigue, temperature excursions, and foreign object damage (FOD). Oxidization is a prime consideration in a "clean fuel" regime, while corrosion is due to higher metal temperatures and is emphasized in not so clean a fuel.

For a given combination of loadings, coating life is governed by:

1. Composition of the coating that includes environmental and mechanical properties such as thermal fatigue.
2. Coating thickness that provides a greater protective reservoir if thicker. However, thicker coatings may have lower thermal fatigue resistance.
3. Standard of deposition such as thickness uniformity or defined thickness variation and coating defects.

There are three basic types of coatings: thermal barrier coatings, diffusion coatings, and plasma-sprayed coatings. The advancements in coating have also been essential in ensuring that the blade base metal is protected at these high temperatures. Coatings ensure that the life of the blades is extended and in many cases coatings are used as a sacrificial layer, which can be stripped and recoated. The general type of coatings is very little different from the coatings used 10–15 years ago. These include various types of diffusion coatings such as aluminide coatings originally developed nearly 40 years ago. The thickness required is between 25 and 75 μm thick. These coatings consisted of Ni/Co = about 30% Al. The new aluminide coatings with platinum (Pt) increase the oxidation resistance and also the corrosion resistance. Platinum increases the activity of aluminum in the coating, enabling a very protective and adherent Al_2O_3 scale to form on the surface.

Coatings developed some 30–35 years ago, commonly known as MCrAlY, have a wide range of composition tailored to the type of performance required and are Ni/Co based as shown in the following three common types of coatings:

1. Ni, 18% Cr, 12% Al, 0.3% Y.
2. Co, 29% Cr, 3% Al, 0.3% Y.
3. Co, 25% Ni, 20% Cr, 8% Al, 0.3% Y.

These coatings are usually 75–500 μm thick and sometimes have other minor element additions used to improve environmental resistance such as Pt, Hf, Ta, and Zr. Carefully chosen, these coatings can give very good performance.

The thermal barrier coatings have an insulation layer of 100–300 μm thick and are based on ZrO_2–Y_2O_3 and can reduce metal temperatures by 90–270 °F (50–150 °C). This type of coating is used in combustion cans, transition pieces, nozzle guide vanes, and also blade platforms.

The interesting point to note is that some of the major manufacturers are switching away from corrosion protection-biased coatings to coatings that are not only oxidation resistant but also oxidation resistant at higher metal temperatures. Thermal barrier coatings are being used on the first few stages in all the advanced technology units. The use of internal coatings is getting popular due to the high temperature of the compressor discharge, which results in oxidation of the internal surfaces. Most of these coatings are aluminide-type coatings. The choice is restricted due to access problems to slurry-based or gas-phase/chemical vapor deposition. Care must be taken in production otherwise internal passages may be blocked. The use of pyrometer technology on some of the advanced turbines has located blades with internal passages blocked causing these blades to operate at metal temperatures of 50–100 °F (28–56 °C) higher than the neighboring blades.

Shroud Coatings

New high-temperature gas turbines operate at considerably higher temperatures than previous heavy-duty gas turbines. Therefore, to provide a durable stationary shroud component, coatings are being used on the surface of this high-temperature and inner shroud component. The coating of shrouds was developed and has been used extensively in aircraft engines. This provides an extremely oxidation-resistant surface and a rub-tolerant coating if the blade tips rub against the stationary shroud. The coating also reduces leakage between the blades and the shroud thus reducing tip losses.

Future Coatings

The investigation of even more corrosion-resistant coating materials has been an area of intensive research and development for the past few years. The goals of this research are to further improve the oxidation-resistance and thermal fatigue resistance of high-temperature bucket coatings. In addition to these environmentally resistant coating development efforts, work is also underway to develop advanced TBCs for application to stationary and rotating gas path components. By careful process control,

the structure of these TBCs may be made more resistant to thermal fatigue and their lives greatly extended. The capabilities of new coatings are initially evaluated in the laboratory on specially designed rainbow rotor test rigs to determine their corrosion resistance and effect on mechanical properties.

Another area of research is the development of techniques to ensure that the application of the coatings is extremely even. The external deposition source can be electron beam vapor deposition, sputtering, plasma spray, cladding, or any number of other techniques. The technique for the application of overlay coatings, which appears to have the most promise, is high-velocity plasma. For this technique, powder particles of the desired coating composition are accelerated through a plasma field to velocities as high as three times the speed of sound. The impact of the powder onto the workpiece results in a much stronger bond between the coating and workpiece than can be achieved by using conventional subsonic plasma spray deposition. In addition, much higher coating densities can be achieved using the high-velocity plasma.

One company has developed and patented a "detonation gun" to be used for coating application. Basically, the gun detonates a metered mixture of oxygen, acetylene, and particles of the desired coating material and throws them at supersonic velocities at the workpiece surface. The workpiece itself remains at quite low temperatures, so its metallurgical properties are not modified.

Bibliography

Bernstein, H.L., "High Temperature Coatings for Industrial Gas Turbine Users," *Proceedings of the 28th Turbomachinery Symposium*, Texas A&M University, p. 179, 1999.

Bernstien, H.L., "Materials Issues for Users of Gas Turbines," *Proceedings of the 27th Texas A&M Turbomachinery Symposium*, 1998.

Lavoie, R. and McMordie, B.G., "Measuring Surface Finish of Compressor Airfoils Protected by Environmentally Resistant Coatings," *30th Annual Aerospace/Airline Plating and Metal Finishing Forum*, April 1994.

McMordie, B.G., "Impact of Smooth Coatings on the Efficiency of Modern Turbomachinery," *2000 Aerospace/Airline Plating & Metal Finishing Forum*, Cincinnati, Ohio, March 2000.

Schilke, P.W., "Advanced Gas Turbine Materials and Coatings," *39th GE Turbine State-of-the-Art Technology Seminar*, NY, August 1996.

Warnes, B.M. and Hampson, L.M., "Extending the Service Life of Gas Turbine Hardware," *ASME 2000-GT-559*, 2000.

Wood, M.I., "Developments in Blade Coatings: Extending the Life of Blades? Reducing Lifetime Costs?" CCGT Generation, March 1999, IIR Ltd.

Copyrighted Materials
Copyright © 2012 Elsevier Retrieved from www.knovel.com

Part III

Materials, Fuel Technology, and Fuel Systems

11 Materials

Temperature limitations are the most crucial limiting factors to gas turbine efficiencies. Figures 11-1 (a) and 11-1 (b) show how the increased turbine inlet temperatures decrease both specific fuel and air consumption while increasing efficiency. Materials and alloys that can operate at high temperatures are very costly – both to buy and to work on. Figure 11-1 (c) shows relative raw material costs. Thus, the cooling of blades, nozzles, and combustor liners is an integral part of the total materials picture.

Since the design of turbomachinery is complex and the efficiency is directly related to material performance, the material selection is of prime importance. Gas and steam turbines exhibit similar problem areas, but these problem areas are of different magnitudes. Turbine components must operate under a variety of stress, temperature, and corrosion conditions. Compressor blades operate at a relatively low temperature

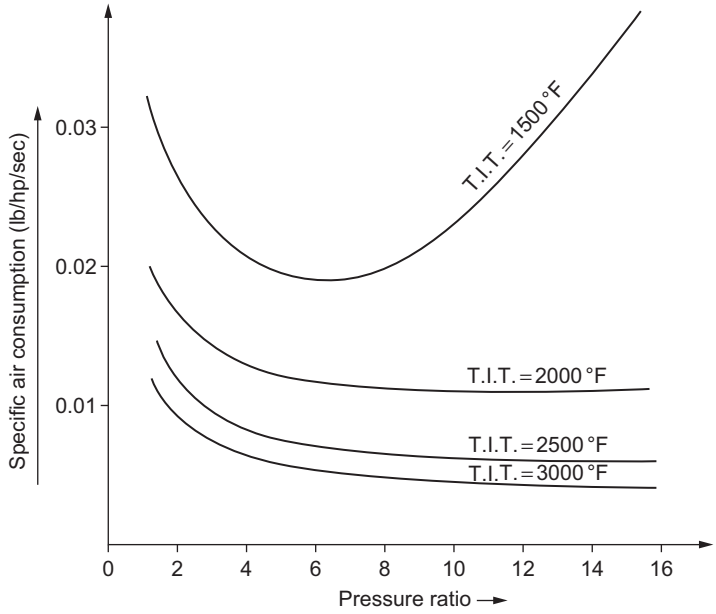


Figure 11-1 (a) Specific air versus pressure ratio and turbine inlet temperatures.

Gas Turbine Engineering Handbook, Fourth Edition. DOI: 10.1016/B978-0-12-383842-1.00011-1
Copyright © 2012 Elsevier Inc. All rights reserved.

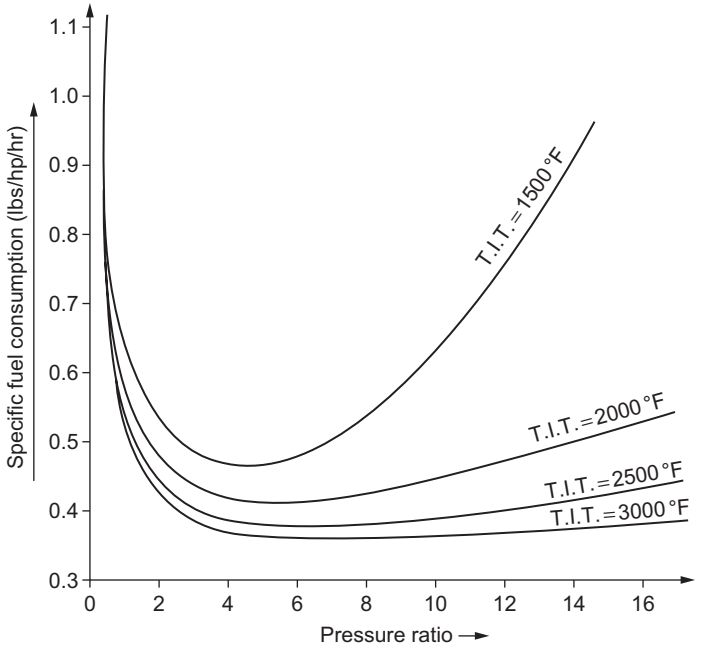


Figure 11-1 (b) Specific fuel consumption versus pressure ratio and turbine inlet temperature.

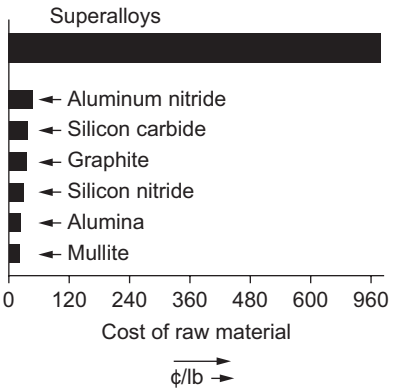


Figure 11-1 (c) A comparison of raw material costs.

but are highly stressed. The combustor operates at a relatively high temperature and low stress conditions. The turbine blades operate under extreme conditions of stress, temperature, and corrosion. These conditions are more extreme in gas turbine than in steam turbine applications. As a result, the selection of materials for individual components is based on varying criteria in both gas and steam turbines.

A design is only as efficient as the performance of the selected component materials. The combustor liner and turbine blades are the most critical components in existing high-performance and long-life gas turbines. The extreme conditions of stress, temperature, and corrosion make the gas turbine blade a material's challenge. Other turbine components present operational problem areas, but to a lesser degree. For this reason, gas turbine blade metallurgy will be discussed for solutions to problem areas. Definition of potential solutions will also relate to other turbine components.

The interaction of stress, temperature, and corrosion yields a complex mechanism that cannot be predicted by existing technology. The required material characteristics in a turbine blade for high performance and long life include limited creep, high-rupture strength, resistance to corrosion, good fatigue strength, low coefficient of thermal expansion, and high thermal conductivity to reduce thermal strains. The failure mechanism of a turbine blade is related primarily to creep and corrosion and secondarily to thermal fatigue. Satisfying these design criteria for turbine blades will ensure high performance, long life, and minimal maintenance.

The development of new materials as well as cooling schemes has seen the rapid growth of turbine firing temperatures leading to high turbine efficiencies. The fist-stage blade must withstand the most severe combination of temperature, stress, and environment; it is generally the limiting component in the machine. Figure 11-2 shows the trend of firing temperature and blade alloy capability.

Since 1950, the capability of turbine bucket material's temperature has advanced approximately 850 °F (472 °C), approximately 20 °F (10 °C) per year. The importance of this increase can be appreciated by noting that an increase of 100 °F (56 °C) in turbine firing temperature can provide a corresponding increase of 8–13% in output and a 2–4% improvement in simple-cycle efficiency. Advances in alloys and processing, while expensive and time consuming, provide significant incentives through increased power density and improved efficiency. Before discussing some of these materials in depth, it is important to understand the general behavior of metals.

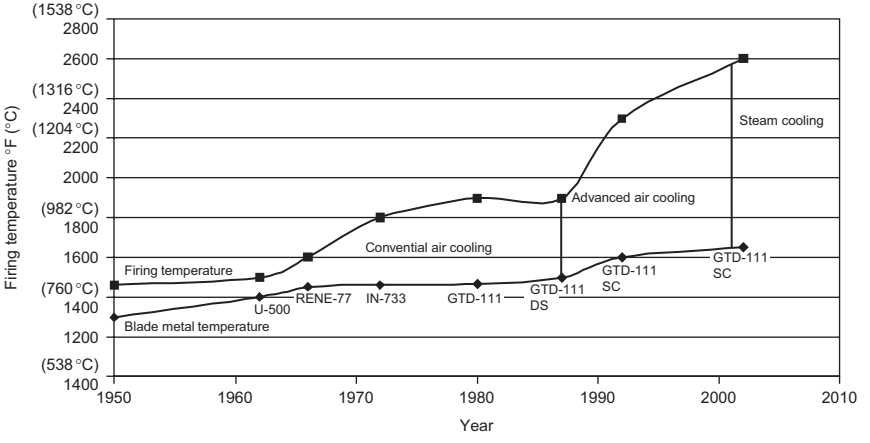


Figure 11-2 Firing temperature increase with blade material improvement.

General Metallurgical Behaviors in Gas Turbines

Creep and Rupture

The melting point of different metals varies considerably and their strengths at various temperatures are different. At low temperatures, all materials deform elastically, then plastically, and are time independent. However, at higher temperatures, deformation is noted under constant load conditions. This high-temperature and time-dependent behavior is called creep-rupture. Figure 11-3 shows a schematic of a creep curve with the various stages of creep. The initial or elastic strain is the first region that proceeds into a plastic strain region at a decreasing rate. Then, a nominally constant plastic strain rate is followed by an increasing strain rate to fracture.

The nature of this creep depends on the material, stress, temperature, and environment. Limited creep ($< 1\%$) is desired for turbine blade application. Cast superalloys fail with only a minimum elongation. These alloys fail in brittle fracture – even at elevated operating temperatures.

Stress-rupture data are often presented in a Larson–Miller curve, which indicates the performance of an alloy in a complete and compact graphical style. Although widely used to describe an alloy's stress-rupture characteristics over a wide temperature, life, and stress range, it is also useful in comparing the elevated temperature capabilities of many alloys. The Larson–Miller parameter is given as follows:

$$P_{\mathrm{LM}} = T(20 + \log t) \times 10^{-3} \tag{11-1}$$

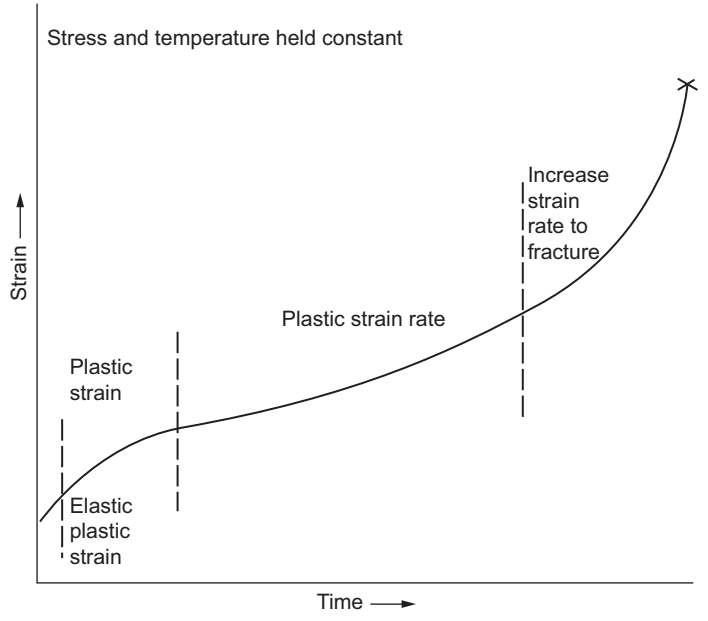


Figure 11-3 Time-dependent strain curve under constant load.

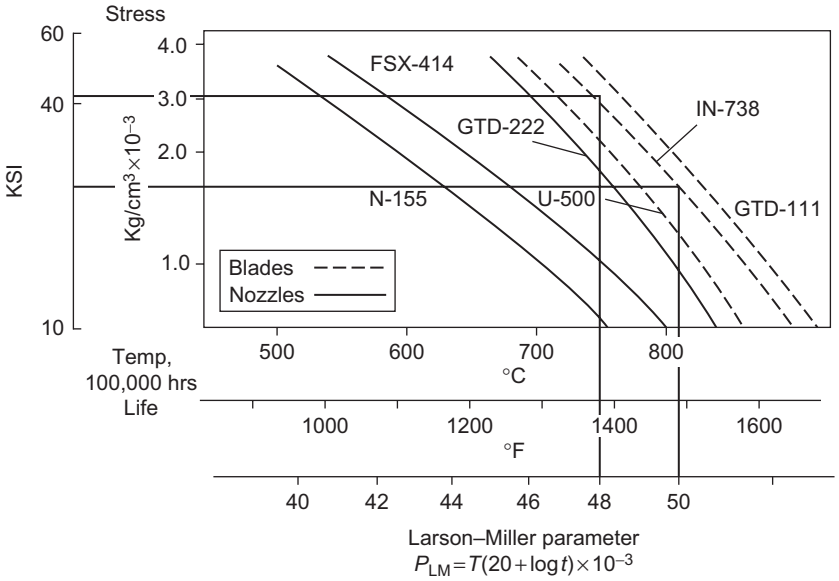


Figure 11-4 Larson–Miller parameter for various types of blades.

where

$$P_{\mathrm{LM}} = \text{Larson}-\text{Miller parameter}$$
$$T = \text{temperature}\,(^{\circ}\text{R})$$
$$t = \text{rupturetime}\,(\text{h})$$

The Larson–Miller parameters are plotted in Figure 11-4 for the specified turbine blade alloys. A comparison of A-286 and Udimet 700 alloy curves reveals the difference in capabilities. The operational life (in hours) of the alloys can be compared for similar stress and temperature conditions.

Ductility and Fracture

Ductility is commonly measured by elongation and reduction in area. In many cases, all three stages of creep shown in Figure 11-3 are not present. At high temperatures or stresses, very little primary creep is seen, while in the case of cast superalloys, failure occurs with just a small extension. This amount of extension is ductility. In a time-creep curve, there are two elongations of interest.

One elongation is from the plastic strain rate and the second elongation is the total elongation or the elongation at fracture. Ductility is erratic in its behavior and is not always repeatable – even under laboratory conditions. Ductility of a metal is affected by the grain size, the specimen shape, and the techniques used for manufacturing. A fracture that results from elongation can be of two types: brittle or ductile, depending on the alloy. A brittle fracture is intergranular with little or no elongation. A ductile

fracture is transgranular and typical of normal ductile tensile fracture. Turbine blade alloys tend to indicate low ductility at operating temperatures. As a result, surface notches are initiated by erosion or corrosion and then cracks are propagated rapidly.

Cyclic Fatigue

All materials would fail at a certain load if subjected to a large number of cycles. A very common type of failure that blades in turbines undergo is known as "high-cycle fatigue." This type of failure is caused when the blade is subjected to an unsteady load repeatedly. Most materials, under these alternating loads, would fail in about 10^7 cycles, assuming that the resonance frequency for a given blade is 10^3 Hz. This would tend to mean that the material would fail within 10^4 s, about 2.8 h, if the blade was subjected to an alternating force, which would excite the frequency of blade resonance. This type of failure would be depicted by a chevron type of markings on the failed surface, near the trailing edge of the blade. A Goodman diagram of the material is often used to determine the amount of alternating stress on the blades at different loadings. The Goodman diagram is shown in Figure 11-5. The Goodman diagram is particularly helpful in determining the effectiveness of a material or component that will be subjected to a cyclic stress superimposed upon a non-zero mean stress. The horizontal axis is the mean, stress, or ultimate strength of the material in pounds-force per square inch or megapascals and the vertical axis is the alternating stress, which is half the ultimate strength or mean stress multiplied by any correction or safety factors.

Thermal Fatigue

Thermal fatigue of turbine blades is a secondary failure mechanism. Temperature differentials developed during the starting and stopping of the turbine produce thermal

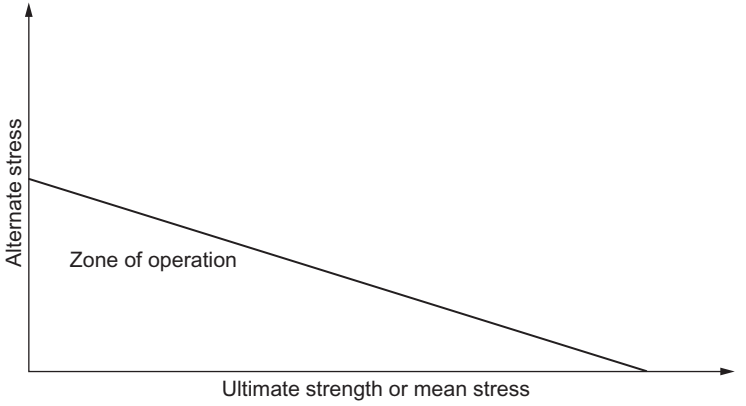


Figure 11-5 Goodman diagram.

stress. The cycling of these thermal stresses is thermal fatigue. Thermal fatigue is low cycle and similar to a creep-rupture failure. The analysis of thermal fatigue is essentially a problem in heat transfer and properties such as modulus of elasticity, coefficient of thermal expansion, and thermal conductivity.

The most important metallurgical factors are ductility and toughness. Highly ductile materials tend to be more resistant to thermal fatigue. They also seem more resistant to crack initiation and propagation.

Research programs are underway to demonstrate that brittle materials can be successfully utilized in demanding high-temperature structural applications.

From the previous work, it has been established that silicon nitride and silicon carbide, in their variety of forms and fabrications, are the two most likely candidates for the future ceramic engine. Both exhibit a suitable workability, the desired strength at high temperatures, and have the specific resistance, availability, and manufacturing ease to make them likely prospects for gas turbine components.

The operating schedule of a gas turbine produces a low-frequency thermal fatigue. The number of starts per hour of operating time directly affects the blade life. Table 11-1 shows that fewer starts per operating time increases turbine life.

Corrosion

The use of Ni-base superalloys as turbine blades in an actual end-use atmosphere produces deterioration of material properties. This deterioration can result from erosion or corrosion. Erosion results from hard particles impinging on the turbine blade and removing material from the blade surface. The particles may enter through the turbine inlet or can be loosened scale deposits from within the combustor.

Corrosion is described as hot corrosion and sulfidation processes. Hot corrosion is an accelerated oxidation of alloys caused by the deposition of Na_2SO_4. Oxidation results from the ingestion of salts in the engine and sulfur from the combustion of fuel. Sulfidation corrosion is considered a form of hot corrosion in which the residue contains alkaline sulfates. Corrosion causes the deterioration of blade materials and reduces component life.

Hot corrosion is a rapid form of attack that is generally associated with alkali metal contaminants, such as sodium and potassium, reacting with sulfur in the fuel to form molten sulfates. The presence of only a few parts per million (ppm) of such contaminants in the fuel, or the equivalent in the air, is sufficient to cause this corrosion. Sodium can be introduced in a number of ways, such as: salt water in liquid fuel, through the turbine air inlet at sites near salt water or other contaminated areas, or as contaminants in water/steam injections. Besides the alkali metals such as sodium and potassium, other chemical elements can influence or cause corrosion on bucketing. Notable in this connection is vanadium, primarily found in crude and residual oils.

There are now two distinct forms of hot corrosion recognized by the industry, although the end result is the same, which are high-temperature (Type 1) and low-temperature (Type 2) hot corrosion.

Table 11-1 Operation and Maintenance Life of an Industrial Turbine

Type of Application and Fuel	Starts/h	Firing Temperature below 1700 °F (927 °C)			Firing Temperature above 1700 °F (927 °C)		
		Comb. liners	First-stage nozzle	First-stage blades	Comb. liners	First-stage nozzle	First-stage blades
Base load		+	+	+			
Natural gas	1/1,000	30,000	60,000	100,000	15,000	25,000	35,000
Natural gas	1/10	7,500	42,000	72,000	3,750	20,000	25,000
Distillate oil	1/1,000	22,000	45,000	72,000	11,250	22,000	30,000
Distillate oil	1/10	6,000	35,000	48,000	3,000	13,500	18,000
Residual	1/1,000	3,500	20,000	28,000	2,500	10,000	15,000
Residual	1/10						
System peaking							
Normal max. load of short duration and daily starts							
Natural gas	1/10	7,500	34,000	60,000	5,000	15,000	24,000
Natural gas	1/5	3,800	28,000	40,000	3,000	12,500	18,000
Distillate	1/10	6,000	27,200	53,500	4,000	12,500	19,000
Distillate	1/5	3,000	22,400	32,000	2,500	10,000	16,000
Turbine peaking							
Operating above 50–100 °F (28–56 °C) Firing temperature							
Natural gas	1/5	2,000	12,000	20,000	2,000	12,500	18,000
Natural gas	1/1	400	9,000	15,000	400	10,000	15,000
Distillate	1/5	1,600	10,000	16,000	1,700	11,000	15,000
Distillate	1/1	400	7,300	12,000	400	8,500	12,000

High-temperature hot corrosion has been known since 1950s. It is an extremely rapid form of oxidation that takes place at temperatures between 1500 °F (816 °C) and 1700 °F (927 °C) in the presence of sodium sulfate (Na_2SO_4).

Sodium sulfate is generated in the combustion process as a result of the reaction among sodium, sulfur and oxygen. Sulfur is present as a natural contaminant in the fuel.

Low-temperature hot corrosion was recognized as a separate mechanism of corrosion attack in the mid-1970s. This attack can be very aggressive if the conditions are right. It takes place at temperatures in the 1100 °F (593 °C) to 1400 °F (760 °C) range and requires a significant partial pressure of SO_2. It is caused by low-melting eutectic compounds resulting from the combination of sodium sulfate and some of the alloy constituents such as nickel and cobalt. It is, in fact, somewhat analogous to the type of corrosion called fireside corrosion in coal-fired boilers.

The two types of hot corrosion cause different types of attack. High-temperature corrosion features intergranular attack, sulfide particles, and a denuded zone of base metal. Metal oxidation occurs when oxygen atoms combine with metal atoms to form oxide scales. The higher the temperature, the more rapid the process, which creates the potential for the failure of components if too much of the substrate material is consumed in the formation of these oxides.

Low-temperature corrosion characteristically shows no denuded zone, no intergranular attack, and a layered type of corrosion scale.

The lines of defense against both types of corrosion are similar. First, reduce the contaminants. Second, use materials that are as corrosion resistant as possible. Third, apply coatings to improve the corrosion resistance of the bucket alloy.

Hot corrosion includes two mechanisms:

1. *Accelerated Oxidation*

During initial stages – blade surface clean

$$Na_2SO_4 + Ni\,(\text{metal}) \rightarrow NiO\,(\text{porous})$$

2. *Catastrophic Oxidation*

Occurs with Mo, W, and V present – reduces NiO layer – increases oxidation rate

Reactions – Ni-Base Alloys

Protective oxide films

$$2Ni + O_2 \rightarrow 2NiO$$
$$4Cr + 3O_2 \rightarrow 2Cr_2O_3$$

Sulfate

$$2Na + S + 2O_2 \rightarrow Na_2SO_4$$
$$Na - \text{from NaCl (salt)}$$
$$S - \text{from fuel}$$

Other Oxides

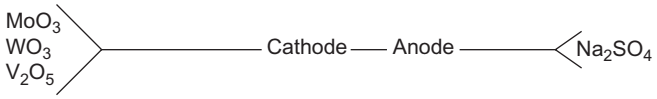
$$2Mo + 3O_2 \rightarrow 2MoO_3$$
$$2W + 3O_2 \rightarrow 2WO_3$$
$$4V + 5O_2 \rightarrow 2V_2O_5$$

The Ni-base alloy surface is exposed to an oxidizing gas, oxide nuclei and a continuous oxide film form (Ni) (Cr_2O_3, etc.). This oxide film is a protective layer. The metal ions diffuse to the surface of the oxide layer and combine with the molten Na_2SO_4 to destroy the protective layer. Ni_2S and Cr_2S_3 results (*sulfidation*):

$$NaCl\,(sea\,salt) \rightarrow Na + Cl$$
$$Na + S\,(fuel) + 2O_2 \rightarrow Na_2SO_4$$
$$Cl - grainboundaries - \textit{causes intergranular corrosion}$$

The extent of the corrosion depends on the amount of nickel and chromium in the alloy. The oxide films become porous and non-protective, which increases the oxidation rate (accelerated oxidation).

Catastrophic oxidation requires the presence of Na_2SO_4 and Mo, W, and/or V. Crude oils are high in V; ash will be 65% V_2O_5 or higher. V can be alloyed in metal. A galvanic cell is generated:



The galvanic corrosion deletes the protective oxide film and increases the oxidation rate. The corrosion problem includes: (1) erosion, (2) sulfidation, (3) intergranular corrosion, and (4) hot corrosion. The 20% Cr alloys increase oxidation resistance.

Sixteen percent Cr alloys (Inconel 600) are less resistant. Cr in alloys reduces grain boundary oxidation, while high Ni alloys tend to oxidize along grain boundaries. Age-hardened gas turbine blades of 10–20% Cr will corrode (sulfidation) at more than 1400 °F. Ni_2S forms in the grain boundary. The addition of cobalt to the alloy increases the temperature at which the attack occurs. To reduce corrosion, either increase the Cr amount or apply a coating (Al or Al + Cr).

A high-nickel alloy is used for increased strength at elevated temperatures and a chromium content in excess of 20% is desired for corrosion resistance. An optimum composition to satisfy the interaction of stress, temperature, and corrosion has not been developed. The rate of corrosion is directly related to alloy composition, stress level, and environment. The corrosive atmosphere contains chloride salts, vanadium, sulfides, and particulate matter. Other combustion products, such as NO_x, CO, and CO_2, also contribute to the corrosion mechanism. The atmosphere changes with the type of fuel used. Fuels, such as natural gas, diesel #2, naphtha, butane, propane, methane, and fossil fuels, will produce different combustion products that affect the corrosion mechanism in different ways.

Gas Turbine Materials

The composition of the new and conventional alloys throughout the turbine is shown in Table 11-2. This table describes materials used in the GE line of turbines but the materials are common to all brands of high-temperature turbine even though there may be some variations in the composition of the alloys. In the early years of turbine development, increases in the capability of temperature in blade alloy accounted for the majority of the firing temperature increase until air cooling was introduced, which decoupled firing temperature from the blade metal temperature. In addition, as the metal temperatures approached a temperature range of 1600 °F (870 °C), hot corrosion of blades became more life limiting than strength until the introduction of protective coatings. During the 1980s, emphasis turned toward two major areas: improved materials technology to achieve greater capability of blade alloy without sacrificing alloy corrosion resistance, and advanced and highly sophisticated air-cooling technology to achieve the firing temperature capability required for the new generation of gas turbines. The use of steam cooling to further increase combined-cycle efficiencies in combustors was introduced in the mid- to late 1990s. Steam cooling in blades and nozzles was introduced to commercial operation in 2002.

In the 1980s, IN-738 blades were widely used. IN-738 was the acknowledged corrosion standard for the industry. New alloys, such as GTD-111, were developed and patented by GE in the mid-1970s. GTD-111 possesses about a 35 °F (20 °C) improvement in rupture strength as compared with IN-738. GTD-111 is also superior to IN-738 in low-cycle fatigue strength.

The design of this alloy was unique in that it utilized phase stability and other predictive techniques to balance the levels of critical elements (Cr, Mo, Co, Al, W, and Ta), thereby maintaining the hot corrosion resistance of IN-738 at higher strength levels without compromising phase stability. Most nozzle and blade castings are made by using the conventional equiaxed investment casting process. In this process, the molten metal is poured into a ceramic mold in a vacuum, to prevent the highly reactive elements in the superalloys from reacting with the oxygen and nitrogen in the air. With proper control of metal and mold thermal conditions, the molten metal solidifies from the surface to the center of the mold, creating an equiaxed structure. Directional solidification (DS) is also being employed to produce advanced-technology nozzles and blades. First used in aircraft engines more than 25 years ago, it was adapted for the use in large airfoils in the early 1990s. By exercising careful control over temperature gradients, a planar solidification front is developed in the bade, and the part is solidified by moving this planar *front* longitudinally through the entire length of the part. The result is a blade with an oriented grain structure that runs parallel to the major axis of the part and contains no transverse grain boundaries, as in ordinary blades. The elimination of these transverse grain boundaries confers additional creep and rupture strengths on the alloy, and the orientation of the grain structure provides a favorable modulus of elasticity in the longitudinal direction to enhance fatigue life. The use of directionally solidified blades results in a substantial increase in the creep life or substantial increase in tolerable stress for a fixed life. This advantage is due to the elimination of transverse grain boundaries from

Table 11-2 High-Temperature Alloys (Courtesy: GE Power Systems)

Component	Cr	Ni	Co	Fe	W	Mo	Ti	Al	Cb	V	C	B	Ta
Turbine blades													
U-500	18.5	BAL	18.5	–	–	4	3	3	–	–	0.07	0.006	–
RENE-77 (U700)	15	BAL	17	–	–	5.3	3.35	4.25	–	–	0.07	0.02	–
IN-738	16	BAL	8.3	0.2	2.6	1.75	3.4	3.4	0.9	–	0.10	0.001	1.75
GTD-111	14	BAL	9.5	–	3.8	1.5	4.9	3.0	–	–	0.10	0.01	2.8
Turbine nozzles													
X40	25	10	BAL	1	8	–	–	–	–	–	0.50	0.01	–
X45	25	10	BAL	1	8	–	–	–	–	–	0.25	0.01	–
FSX414	28	10	BAL	1	7	–	–	–	–	–	0.25	0.01	–
N155	21	20	20	BAL	2.5	3	–	–	–	–	0.20	–	–
GTD-222	22.5	BAL	19	–	2.0	2.3	1.2	0.8	–	0.10	0.008	1.00	–
Combustors													
SS309	23	13	–	BAL	–	–	–	–	–	–	0.10	–	–
HAST X	22	BAL	1.5	1.9	0.7	9	–	–	–	–	0.07	0.005	–
N-263	20	BAL	20	0.4	–	6	2.1	0.4	–	–	0.06	–	–
HA-188	22	22	BAL	1.5	14.0	–	–	–	–	–	0.05	0.01	–
Turbine wheels													
Alloy 718	19	BAL	–	18.5	–	3.0	0.9	0.5	5.1	–	0.03	–	–
Alloy 706	16	BAL	–	37.0	–	–	1.8	–	2.9	–	0.03	–	–
Cr–Mo–V	1	0.5	–	BAL	–	1.25	–	–	–	0.25	0.30	–	–
A286	15	25	–	BAL	–	1.2	2	0.3	–	0.25	0.08	0.006	–
M152	12	2.5	–	BAL	–	1.7	–	–	–	0.3	0.12	–	–
Compressor blades													
AISI 403	12	–	–	BAL	–	–	–	–	–	–	0.11	–	–
AISI 403 + Cb	12	–	–	BAL	–	–	–	–	0.2	–	0.15	–	–
GTD-450	15.5	6.3	–	BAL	–	0.8	–	–	–	–	0.03	–	–

the bucket, the traditional weak link in the microstructure. In addition to improved creep life, the directionally solidified blades possess more than 10 times the strain control or thermal fatigue compared to equiaxed blades. The impact strength of the DS blades is also superior to that of equiaxed blades, showing an advantage of more than 33%.

In the late 1990s, single-crystal blades were introduced in gas turbines. These blades offer additional creep and fatigue benefits through the elimination of grain boundaries. In single-crystal material, all grain boundaries are eliminated from the material structure, and a single crystal with controlled orientation is produced in an airfoil shape. By eliminating all grain boundaries and the associated grain boundary strengthening additives, a substantial increase in the melting point of the alloy can be achieved, thus providing a corresponding increase in high-temperature strength. The transverse creep and fatigue strengths are increased compared with equiaxed or DS structures. The advantage of single-crystal alloys compared with equiaxed and DS alloys in low-cycle fatigue (LCF) life is increased by about 10%.

Blade life comparison is provided in the form of the stress required for rupture as a function of a parameter that relates time and temperature (the Larson–Miller parameter). The Larson–Miller parameter is a function of blade metal's temperature and the time the blade is exposed to those temperatures. Figure 11-4 shows the comparison of some of the alloys used in blade and nozzle applications. This parameter is one of the several important design parameters that must be satisfied to ensure the proper performance of the alloy in a blade application, especially for long service life. Creep life, HCF and LCF, thermal fatigue, tensile strength and ductility, impact strength, hot corrosion and oxidation resistance, producibility, coatability, and physical properties must also be considered.

Turbine Wheel Alloys

Alloy 718 Nickel-Based Alloy

This nickel-based and precipitation-hardened alloy is the newest being developed for the next generation of frame-type gas turbine machines. This alloy has been used for wheels in aircraft turbines for more than 20 years. Alloy 718 contains a high concentration of alloying elements and is, therefore, difficult to produce in the very large ingot sizes needed for the large frame-type turbine wheel and spacer forgings. This effort requires close cooperation between the manufacturer and its superalloy melters and large forging suppliers to conduct the solidification and forging flow studies that are necessary to bring a new wheel material for large wheels into production. This development effort has resulted in the production of the largest ingots ever made and forged into high-quality qualification turbine wheel and spacer forgings.

Alloy 706 Nickel-Based Alloy

This nickel-based and precipitation-hardened alloy is being used in large frame-type units by GE such as the frame 7FA, 9FA, 6FA, and 9EC turbine wheel and

spacer alloys and it offers a very significant increase in stress-rupture and tensile-yield strengths compared with the other wheel alloys. Figures 11-6 and 11-7 show the stress rupture and tensile yield strength of the various alloys. This alloy is similar to Alloy 718, but contains somewhat lower concentrations of alloying elements and is, therefore, easier to produce in the very large ingot sizes needed for large frame-type gas turbines.

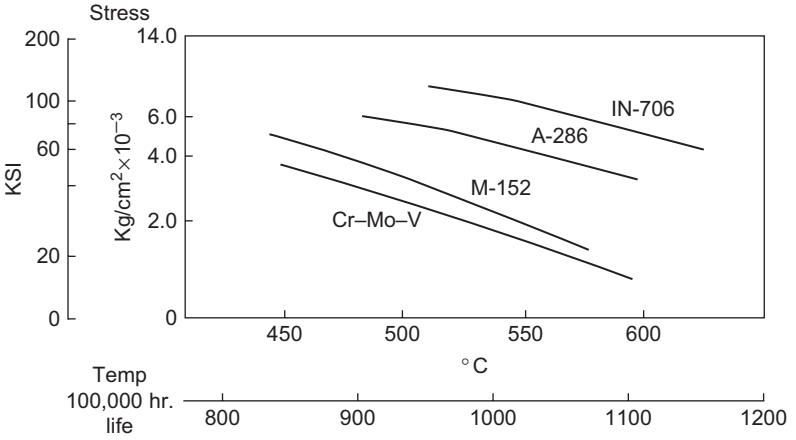


Figure 11-6 Turbine wheel alloys stress-rupture comparison.

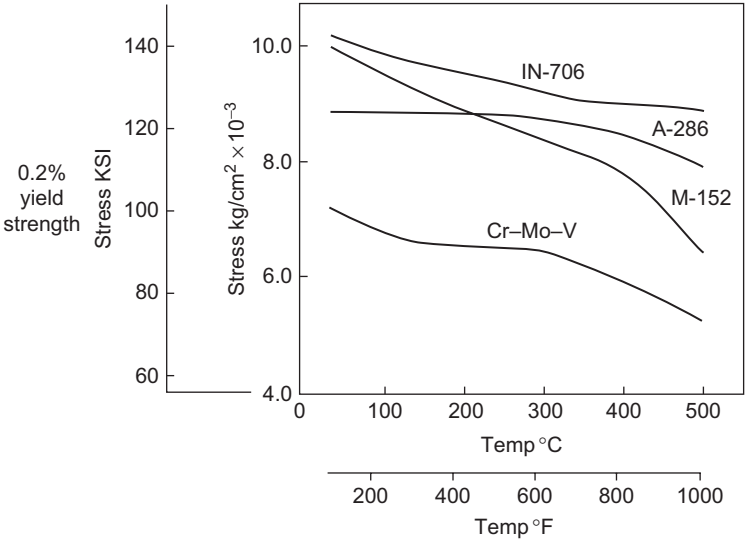


Figure 11-7 Turbine wheel alloys tensile strength comparison.

Cr–Mo–V Alloy

Turbine wheels and spacers of most GE single-shaft heavy-duty gas turbines are made of 1% Cr–1.25% Mo–0.25% V steel. This alloy is used in the quenched and tempered condition to enhance bore toughness. Stress-rupture strength of the dovetail region (periphery) is controlled by providing extra stock at the periphery to produce a slower cooling rate during quenching.

The stress-rupture properties of this alloy are shown in Figure 11-6.

12 Cr Alloys

This family of alloys has a combination of properties that make them especially valuable for turbine wheels. These properties include good ductility at high-strength levels, uniform properties throughout thick sections, and favorable strength at temperatures up to about 900 °F (482 °C).

M-152 alloy is a 2–3% nickel-containing member of the 12 Cr family of alloys. Initially, it was used as an upgrade in gas turbines as a replacement for A-286. It features outstanding fracture toughness, in addition to the properties common to other 12 Cr alloys. M-152 alloy is intermediate in rupture strength, between the Cr–Mo–V and A-286 alloys (Figure 11-6), and it has higher tensile strength than these alloys. These features, together with its favorable coefficient of expansion and good fracture toughness, make the alloy attractive for use in gas turbine applications.

A-286 Alloy

A-286 is an austenitic iron-base alloy that has been used for years in aircraft engine applications. Its use for industrial gas turbines started about 1965, when technological advances made the production of sound ingots sufficient in size to produce these wheels possible.

As knowledge of the capabilities of M-152 increased, the production of the wheels was switched from A-286 to M-152. A-286 is currently being introduced in turbines as a part of a composite aft shaft.

Compressor Blades

Compressor blading is variously made by forging, extrusion, or machining. All production blades, until recently, have been made from Type 403 or 403 Cb (both 12 Cr) stainless steels. During the 1980s, a new compressor blade material, GTD-450, a precipitation-hardened and martensitic stainless steel, was introduced into production for advanced and uprated machines, as shown in Table 11-2. This material provides increased tensile strength without sacrificing stress corrosion resistance. Substantial increases in the high-cycle fatigue and corrosion fatigue strength are also achieved with this material, compared with Type 403. Superior corrosion resistance is also achieved due to high concentrations of chromium and molybdenum. Compressor corrosion is usually caused by moisture and salt ingested by the turbine. Coating of compressor blades is also highly recommended.

Forgings and Non-destructive Testing

Most other rotor parts in gas turbines are individually forged. This includes compressor wheels, spacers, distance pieces, and stub shafts. All are made from quenched and tempered low-alloy steels (Cr–Mo–V or Ni–Cr–Mo–V) with the material and heat treatment optimized for the specific part. The intent is to achieve the best balance of strength, toughness with ductility, processing, and non-destructive evaluation capabilities, particularly when it is recognized that some of these parts may be exposed to operating temperatures as low as –60 °F (–51 °C).

It is recommended that parts are sonic and magnetic particle tested. Many last-stage compressor wheels are spun in a manner analogous to turbine wheels as a means of proof testing and imparting bore residual stresses. This last-stage compressor wheel is probably the next most critical rotor component after the turbine wheels, especially in the new very high pressure ratio compressors.

New non-destructive techniques to inspect turbine forgings to greater levels of sensitivity than ever before possible have been developed. These new ultrasonic inspection techniques are being applied to all the turbine forgings to ensure an even greater level of confidence in these high-strength forgings.

Additional development efforts continue to improve the current processing of other forgings by working with our suppliers on the further optimization of properties and forging quality. In-process non-destructive evaluation of all rotor components continues to be emphasized as a critical aspect in the production of quality forgings.

Ceramics

The day when turbines will operate at 2500–3000 °F (1371–1649 °C), yielding double the present horsepower at half the present engine size, may not be far off. This dream may turn into reality because of ceramics and unique cooling systems. Ceramics were, until recently, dismissed as being too brittle, hard to fabricate, and not suited to flight engines. However, the addition of aluminum to ceramics forms a compound that is more ductile.

Since 1945, the temperature limits of flight engine alloys have been steadily increasing about 20 °F (11 °C) per year. Transpiration and internally cooled metal blades have resulted in higher temperatures and more efficient operation. However, the direct correlation between efficiency and fabrication cost has resulted in a situation of diminishing returns for the superalloys. As more and more cooling air is needed for the superalloy components, the efficiency of the engine drops to a point where turbine inlet temperatures around 2300 °F (1260 °C) are the optimum and, at that point, they are uneconomic for automotive use.

Increasing efficiency with the use of 2500 °F (1371 °C) tolerant uncooled ceramic blades provides an improvement in fuel consumption of more than 20% from a 1800 °F (982 °C) turbine inlet temperature. This rate represents almost a 50% improvement in specific air consumption. This improvement implies that for the same size engine, power almost doubles, or conversely (and possibly more important to automakers), engine flow size could be cut into half and retain the same horsepower output.

Ceramics are quite tolerant of such contaminants as sodium and vanadium, which are present in low-cost fuels and highly corrosive to currently used nickel alloys. Ceramics are also up to 40% lighter than comparable high-temperature alloys – another advantage in application. However, the biggest advantage is material cost. Ceramics cost around 5% of the cost of superalloys.

Despite all the advantages of ceramics, they are brittle; unless this problem is overcome, the use of ceramics in gas turbines will not be practical.

Coatings

Blade coatings were originally developed by the aircraft engine industry for aircraft gas turbines. Metal temperatures in heavy-duty gas turbines are lower than those in aircraft engines. However, heavy-duty gas turbines are generally subjected to excessive contamination or accelerated attack known as hot corrosion.

Blade coatings are required to protect the blade from corrosion, oxidation, and mechanical property degradation. As superalloys have become more complex, it has been increasingly difficult to obtain both the higher strength levels that are required and a satisfactory level of corrosion and oxidation resistance without the use of coatings. Thus, the trend toward higher firing temperatures increases the need for coatings. The function of all coatings is to provide a surface reservoir of elements that will form very protective and adherent oxide layers, thus protecting the underlying base material from oxidation and corrosion attack and degradation.

Experience has shown that the lives of both uncoated and coated blades depend to a large degree on the amount of fuel and air contamination, as well as the operating temperature of the blade. The effect of sodium, a common contaminant, on bucket life at 1600 °F (871 °C) is shown in Figure 11-8. When sodium sulfate (Na_2SO_4) is present,

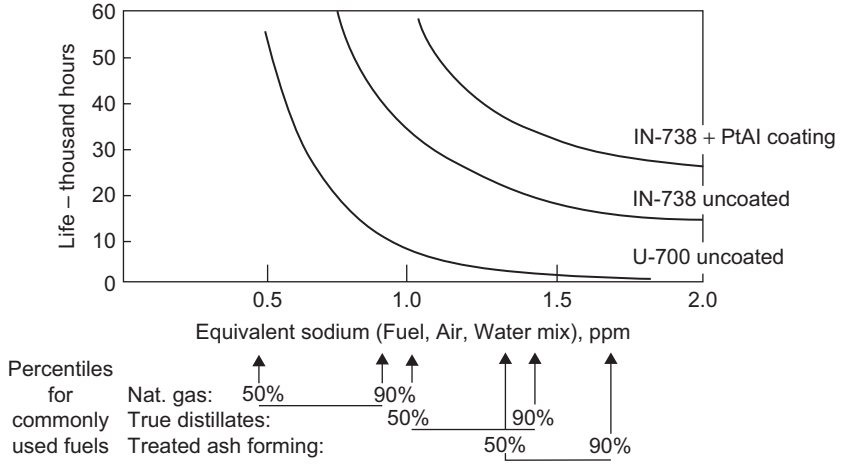


Figure 11-8 Effect of sodium corrosion on blade life.

hot corrosion is greatly accelerated. Sodium sulfate is a product of combustion. The presence of only a few parts per million (ppm) of sodium and sulfate is sufficient to cause extensive hot corrosion damage. Sulfur is present as a natural contaminant in the fuel. Sodium can be introduced as a natural contaminant in the fuel or in the atmosphere of sites located near salt water or contaminated areas.

The Pt–Al coating is a precious metal applied by uniformly electroplating a thin layer (0.00025 in) of platinum (Pt) onto the bucket at the airfoil surface, followed by pack-diffusion steps to deposit a layer of aluminum and chromium. The resulting coating has an outer skin of an extremely corrosion resistant, platinum–aluminum intermetallic composition. As shown in Figure 11-8, a test was conducted for comparative corrosion on coated and uncoated IN-738 blades. The blades were run side-by-side in the same machine under severe corrosive conditions. The two blades were removed for interim evaluation after 11,300 service hours (289 starts). The unit burnt sour natural gas containing about 3.5% ppm sulfur and was located in a region where the soil surrounding the site contains up to 3% sodium. The uncoated blade showed a 0.005-in corrosion attack over 50% of the airfoil concave face, with about 0.010-in penetration at the base of the airfoil. The examination of the coated blade revealed no visual evidence of attack, except for one small roughened spot on the leading edge about 1 in up from the platform, and a second spot in the middle of the convex side about 1 in down from the tip.

Metallographic examination of other areas revealed similar degrees of corrosion on the two blades. At no point on the coated blade had the corrosion penetrated to the base metal, although in the two areas on the coated blade about 0.002 in of the original 0.003-in coating had been oxidized.

Experience with uncoated IN-738 blades in this very hostile environment indicates that a blade life of about 25,000 hours can be attained. The coated blade life, based on this interim evaluation, should add an additional 20,000 hours of life.

Experience has shown that the lives of both uncoated and coated blades depend to a large degree on the amount of fuel and air contamination. This effect is shown in Figure 11-8, which illustrates the effect of sodium, a common contaminant, on blade life at 1600 °F (871 °C). The presence of increased levels of contaminants gives rise to an accelerated form of attack called hot corrosion.

Hot corrosion is distinctly different from the pure oxidation of an aircraft environment; hence, coatings for heavy-duty gas turbines have different capabilities compared with coatings for aircraft engines. In addition to hot corrosion, high-temperature oxidation and thermal fatigue resistance have become important criteria in the higher firing gas turbines, as shown in Figure 11-9. In today's advanced machines, oxidation is of concern not only for external blade surfaces, but also for internal passages such as cooling holes, due to the high temperature of the cooling air, which in turn is due to the high pressure ratio in the compressor. The main requirements of a coating are to protect blades against oxidation, corrosion, and cracking problems. Coatings are there to prevent the base metal from attack. Other benefits of coatings include thermal fatigue from cyclic operation, surface smoothness and erosion in compressor coatings, and heat flux loading when one is considering thermal barriers. A secondary consideration, but perhaps rather more relevant to thermal barriers, is their ability to tolerate damage from light impacts without spalling to an unacceptable extent because of the

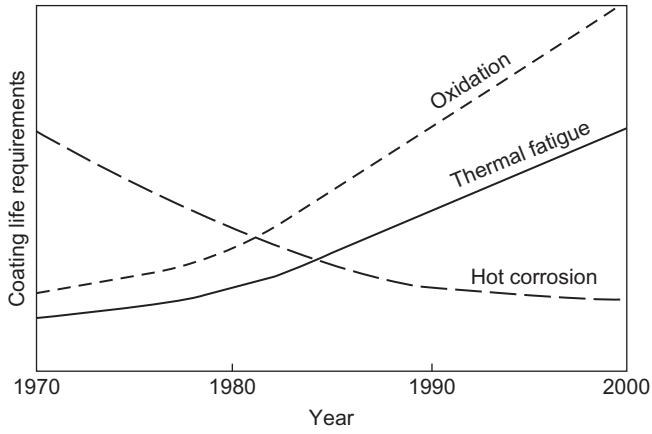


Figure 11-9 Blade coating requirements and coating evolution.

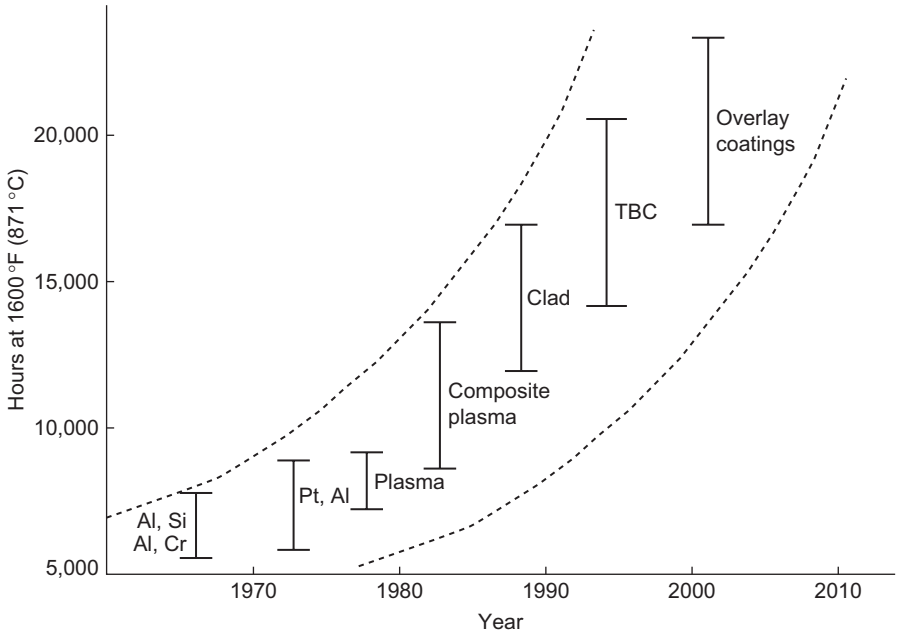


Figure 11-10 Developments of coatings.

resulting rise in the local metal temperatures. Coatings also extend life, provide protection by enduring the operational conditions, and protect the blades by being sacrificial, by allowing the coating to be restripped and recoated on the same base metal.

Past and future trends in the development of coatings are shown in Figure 11-10. Present-day coatings last 10–20 times longer than coatings used 10 years ago. Coated blades last up to twice as long as uncoated blades in the field.

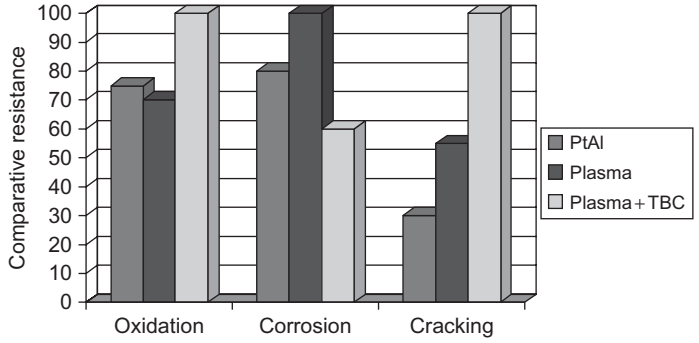


Figure 11-11 Comparative resistance in various types of coatings.

Figure 11-11 is a comparison between the various types of coatings and the comparative resistance in the areas of oxidation, corrosion, and cracking. To improve the oxidation protection, an increase in the aluminum content in the outer region of the coating matrix is needed. The higher aluminum content forms a more protective aluminum oxide layer that greatly improves the high-temperature oxidation resistance.

Life of coatings depends on composition, thickness, and the standard of evenness to which it has been deposited. Most of the new coatings are applied by vacuum plasma spray technique to ensure that the coating has been applied in a uniform and controlled manner. Coatings help extend the life of bladings by protecting them against oxidation, corrosion, cracking, thermal fatigue, temperature excursions, and foreign object damage (FOD). Oxidization is a prime consideration in a "clean fuel" regime, while corrosion is due to higher metal temperatures and is emphasized in not so clean a fuel.

For a given combination of loadings, coating life is governed by:

1. Composition of the coating that includes environmental and mechanical properties such as thermal fatigue.
2. Coating thickness that provides a greater protective reservoir if thicker. However, thicker coatings may have lower thermal fatigue resistance.
3. Standard of deposition such as thickness uniformity or defined thickness variation and coating defects.

There are three basic types of coatings: thermal barrier coatings, diffusion coatings, and plasma-sprayed coatings. The advancements in coating have also been essential in ensuring that the blade base metal is protected at these high temperatures. Coatings ensure that the life of the blades is extended and in many cases coatings are used as a sacrificial layer, which can be stripped and recoated. The general type of coatings is very little different from the coatings used 10–15 years ago. These include various types of diffusion coatings such as aluminide coatings originally developed nearly 40 years ago. The thickness required is between 25 and 75 μm thick. These coatings consisted of Ni/Co = about 30% Al. The new aluminide coatings with platinum (Pt) increase the oxidation resistance and also the corrosion resistance. Platinum increases the activity of aluminum in the coating, enabling a very protective and adherent Al_2O_3 scale to form on the surface.

Coatings developed some 30–35 years ago, commonly known as MCrAlY, have a wide range of composition tailored to the type of performance required and are Ni/Co based as shown in the following three common types of coatings:

1. Ni, 18% Cr, 12% Al, 0.3% Y.
2. Co, 29% Cr, 3% Al, 0.3% Y.
3. Co, 25% Ni, 20% Cr, 8% Al, 0.3% Y.

These coatings are usually 75–500 μm thick and sometimes have other minor element additions used to improve environmental resistance such as Pt, Hf, Ta, and Zr. Carefully chosen, these coatings can give very good performance.

The thermal barrier coatings have an insulation layer of 100–300 μm thick and are based on ZrO_2–Y_2O_3 and can reduce metal temperatures by 90–270 °F (50–150 °C). This type of coating is used in combustion cans, transition pieces, nozzle guide vanes, and also blade platforms.

The interesting point to note is that some of the major manufacturers are switching away from corrosion protection-biased coatings to coatings that are not only oxidation resistant but also oxidation resistant at higher metal temperatures. Thermal barrier coatings are being used on the first few stages in all the advanced technology units. The use of internal coatings is getting popular due to the high temperature of the compressor discharge, which results in oxidation of the internal surfaces. Most of these coatings are aluminide-type coatings. The choice is restricted due to access problems to slurry-based or gas-phase/chemical vapor deposition. Care must be taken in production otherwise internal passages may be blocked. The use of pyrometer technology on some of the advanced turbines has located blades with internal passages blocked causing these blades to operate at metal temperatures of 50–100 °F (28–56 °C) higher than the neighboring blades.

Shroud Coatings

New high-temperature gas turbines operate at considerably higher temperatures than previous heavy-duty gas turbines. Therefore, to provide a durable stationary shroud component, coatings are being used on the surface of this high-temperature and inner shroud component. The coating of shrouds was developed and has been used extensively in aircraft engines. This provides an extremely oxidation-resistant surface and a rub-tolerant coating if the blade tips rub against the stationary shroud. The coating also reduces leakage between the blades and the shroud thus reducing tip losses.

Future Coatings

The investigation of even more corrosion-resistant coating materials has been an area of intensive research and development for the past few years. The goals of this research are to further improve the oxidation-resistance and thermal fatigue resistance of high-temperature bucket coatings. In addition to these environmentally resistant coating development efforts, work is also underway to develop advanced TBCs for application to stationary and rotating gas path components. By careful process control,

the structure of these TBCs may be made more resistant to thermal fatigue and their lives greatly extended. The capabilities of new coatings are initially evaluated in the laboratory on specially designed rainbow rotor test rigs to determine their corrosion resistance and effect on mechanical properties.

Another area of research is the development of techniques to ensure that the application of the coatings is extremely even. The external deposition source can be electron beam vapor deposition, sputtering, plasma spray, cladding, or any number of other techniques. The technique for the application of overlay coatings, which appears to have the most promise, is high-velocity plasma. For this technique, powder particles of the desired coating composition are accelerated through a plasma field to velocities as high as three times the speed of sound. The impact of the powder onto the workpiece results in a much stronger bond between the coating and workpiece than can be achieved by using conventional subsonic plasma spray deposition. In addition, much higher coating densities can be achieved using the high-velocity plasma.

One company has developed and patented a "detonation gun" to be used for coating application. Basically, the gun detonates a metered mixture of oxygen, acetylene, and particles of the desired coating material and throws them at supersonic velocities at the workpiece surface. The workpiece itself remains at quite low temperatures, so its metallurgical properties are not modified.

Bibliography

Bernstein, H.L., "High Temperature Coatings for Industrial Gas Turbine Users," *Proceedings of the 28th Turbomachinery Symposium*, Texas A&M University, p. 179, 1999.

Bernstien, H.L., "Materials Issues for Users of Gas Turbines," *Proceedings of the 27th Texas A&M Turbomachinery Symposium*, 1998.

Lavoie, R. and McMordie, B.G., "Measuring Surface Finish of Compressor Airfoils Protected by Environmentally Resistant Coatings," *30th Annual Aerospace/Airline Plating and Metal Finishing Forum*, April 1994.

McMordie, B.G., "Impact of Smooth Coatings on the Efficiency of Modern Turbomachinery," *2000 Aerospace/Airline Plating & Metal Finishing Forum*, Cincinnati, Ohio, March 2000.

Schilke, P.W., "Advanced Gas Turbine Materials and Coatings," *39th GE Turbine State-of-the-Art Technology Seminar*, NY, August 1996.

Warnes, B.M. and Hampson, L.M., "Extending the Service Life of Gas Turbine Hardware," *ASME 2000-GT-559*, 2000.

Wood, M.I., "Developments in Blade Coatings: Extending the Life of Blades? Reducing Lifetime Costs?" CCGT Generation, March 1999, IIR Ltd.

Copyrighted Materials
Copyright © 2012 Elsevier Retrieved from www.knovel.com

12 Fuels

The gas turbine's major advantage has been its inherent fuel flexibility. Fuel candidates encompass the entire spectrum from gases to solids. Gaseous fuels traditionally include natural gas, process gas, low-Btu coal gas, and vaporized fuel oil gas. "Process gas" is a broad term used to describe gas formed by some industrial process. Process gases include refinery gas, producer gas, coke oven gas, and blast furnace gas among others. Natural gas is the fuel of choice and is usually the basis on which performance for a gas turbine is compared, since it is a clean fuel fostering longer machine life.

Vaporized fuel oil gas behaves very closely to natural gas because it provides high performance with a minimum reduction of component life. About 40% of the turbine power installed operates on liquid fuels. Liquid fuels can vary from light volatile naphtha through kerosene to the heavy viscous residuals. The classes of liquid fuels and their requirements are shown in Table 12-1.

The light distillates are equal to natural gas as a fuel, and 90% of installed units use either light distillates or natural gas fuels. Care must be taken in handling liquid fuels to avoid contamination, and the very light distillates like naphtha require special attention in designing their fuel systems because of their high volatility. Generally, a fuel tank of the floating head type with no area for vaporization is employed. The heavy true distillates like #2 distillate oil can be considered the standard fuel. The true distillate fuel is a good turbine fuel; however, because trace elements of vanadium, sodium, potassium, lead, and calcium are found in the fuel, the fuel has to be treated. The corrosive effect of sodium and vanadium is very detrimental to the life of a turbine.

Vanadium originates as a metallic compound in crude oil and is concentrated by the distillation process into heavy oil fractions. Sodium compounds are most often present in the form of salt water, which results from salty wells, transport over seawater, or mist ingestion in an ocean environment. Fuel treatments are costly and do not remove all traces of these metals. As long as the fuel oil properties fall within specific limits, no special treatment is required. Blends are residuals that have been mixed with lighter distillates to improve properties. The specific gravity and viscosity can be reduced by blending. About 1% of the total of installed machines can operate on blends.

A final fuels group contains high-ash crudes and residuals. These account for 5% of installed units. Residual fuel is the high-ash by-product of distillation. Low cost makes them attractive; however, special equipment must always be added to a fuel system before they can be utilized. Crude is attractive as a fuel, since in pumping applications it is burned straight from the pipeline. Table 12-2 shows data obtained

Gas Turbine Engineering Handbook, Fourth Edition. DOI: 10.1016/B978-0-12-383842-1.00012-3
Copyright © 2012 Elsevier Inc. All rights reserved.

Table 12-1 Comparison of Liquid Fuels for Gas Turbines

General Fuel Type	True Distillate & Naphthas	Blended Heavy Distillates & Low-Ash Crudes	Residuals & High-Ash Crude
Fuel pre-heat	No	Yes	Yes
Fuel atomization	Mech/LP air	HP/LP air	HP air
Desalting	No	Some	Yes
Fuel inhibition	Usually none	Limited	Always
Turbine washing	No	Yes, except distillate	Yes
Start-up fuel	With naphtha	Some fuels	Always
Base fuel cost	Highest	Intermediate	Lowest
Description	High-quality distillate essentially ash-free	Low-ash, limited contaminant levels	Low-volatility High-ash
Types of fuels included	True distillates (naphtha, kerosene, no. 2 diesel, no. 2 fuel oil, JP-4, JP-5)	High-quality crudes, slightly contaminated distillates Navy distillate	Residuals and low-grade crude No. 6 fuel, Bunker C)
ASTM designation	1-GT, 2-GT, 3-GT	3-GT	4-GT
Turbine inlet temperature	Highest	Intermediate	Lowest

Table 12-2 Operation and Maintenance Life of an Industrial Turbine

Type of Application and Fuel		Firing Temperature below 1700 °F (927 °C)			Firing Temperature above 1700 °F (927 °C)		
		Comb. Liners	1st Stage Nozzle	1st Stage Blades	Comb. Liners	1st Stage Nozzle	1st Stage Blades
BASE LOAD	Starts/hr	+	+	+			
Nat. gas	1/1000	30,000	60,000	100,000	15,000	25,000	35,000
Nat. gas	1/10	7,500	42,000	72,000	3,750	20,000	25,000
Distillate oil	1/1000	22,000	45,000	72,000	11,250	22,000	30,000
Distillate oil	1/10	6,000	35,000	48,000	3,000	13,500	18,000
Residual	1/1000	3,500	20,000	28,000	2,500	10,000	15,000
Residual	1/10						
SYSTEM PEAKING							
Normal max. load of short duration and daily starts							
Nat. gas	1/10	7,500	34,000	60,000	5,000	15,000	24,000
Nat. gas	1/5	3,800	28,000	40,000	3,000	12,500	18,000
Distillate	1/10	6,000	27,200	53,500	4,000	12,500	19,000
Distillate	1/5	3,000	22,400	32,000	2,500	10,000	16,000
TURBINE PEAKING							
Operating above 50 °F–100 °F (28–56 °C) Firing temperature							
Nat. gas	1/5	2,000	12,000	20,000	2,000	12,500	18,000
Nat. gas	1/1	400	9,000	15,000	400	10,000	15,000
Distillate	1/5	1,600	10,000	16,000	1,700	11,000	15,000
Distillate	1/1	400	7,300	12,000	400	8,500	12,000

from a number of users that indicate a considerable reduction in downtime, depending on the type of service and fuel used. This table also shows that natural gas is by far the best fuel. The effect of various fuels on the output work of the turbine can be seen in Figure 12-1. This figure shows that vaporized fuel oil gives a higher output. This high output results when steam is mixed with the hot fuel gas, which enters the combustor at (371 °C). Corrosion effects have not been detected with this fuel, since the steam is not allowed to condense in the turbine.

Assuming that natural gas is the base line fuel to obtain the same power using diesel fuel the gas turbine would have to be fired at a higher temperature, and for low Btu (400 Btu/cu ft, 14911 kJ/m^3) gases at the same firing temperature the turbine would produce more power due to the fact that the amount of fuel could be increased by threefold, thus increasing the overall mass flow through the turbine. The limitation in using low Btu gases is that it takes about 30% of the air for combustion as compared

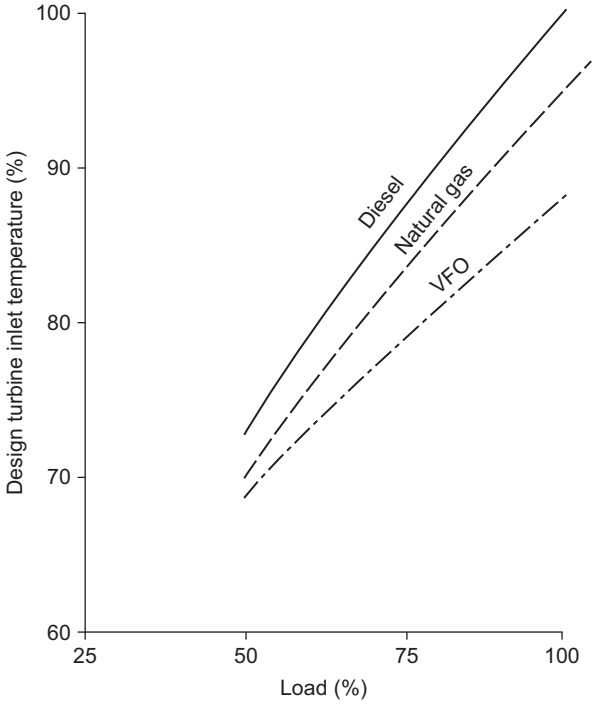


Figure 12-1 Effect of various fuels on turbine inlet temperature.

to 10% of the air for natural gas leaving much less air for cooling the combustor liners. Because of this, for low Btu gases, it is easier to modify annular combustor turbines, which have less of a combustor liner surface area than can-annular combustors. Another problem is that in some cases the extra flow can choke the turbine nozzles. For turbines used in combined cycle application there is a tendency to keep the same firing temperature at off-load conditions, but with the use of inlet guide vanes it is necessary to vary the airflow rate.

Presently, little success has been achieved in burning gases with a heating value lower than 200 Btu/ft^3 (7,456 kJ/m^3). To provide the same energy as natural gas, a 150 Btu/ft^3 (5,592 kJ/m^3) low-Btu gas must be utilized at the rate of seven times that of natural gas on a volumetric basis. Therefore, the mass flow rate to provide the same energy must be about 8–10 times that of natural gas. The flammability of low-Btu gases is very much dependent on the mixture of CH_4 and other inert gases. Figure 12-2 shows this effect by illustrating that a mixture of CH_4-CO_2 of less than 240 Btu/ft^3 (8,947 kJ/m^3) is inflammable, and a CH_4-N_2 mixture of less than about 150 Btu/ft^3 is less inflammable. Low-Btu gases near these values have greatly restricted flammability limits when compared to CH_4 in the air. Vaporized fuel oil gas is produced by mixing superheated steam with oil and then vaporizing the oil to provide a gas whose properties and heating value are close to natural gas.

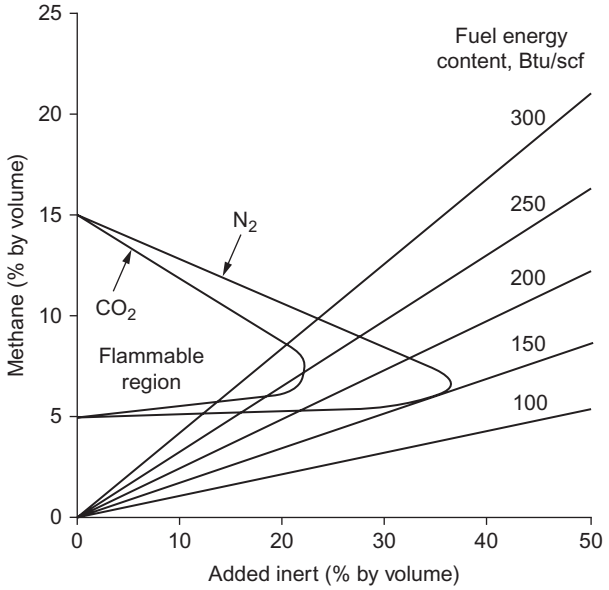


Figure 12-2 Flammable fuel mixtures of CH_4-N_2 and CH_4-CO_2 at one atm showing various energy levels.

Fuel Specifications

To decide which fuel to use, a host of factors must be considered. The object is to obtain high efficiency, minimum downtime, and the total economic picture. The following are some fuel requirements that are important in designing a combustion system and any necessary fuel treatment equipment:

1. Heating value
2. Cleanliness
3. Corrosivity
4. Deposition and fouling tendencies
5. Availability

The heating of a fuel affects the overall size of the fuel system. Generally, fuel heating is a more important concern in connection with gaseous fuels, since liquid fuels all come from petroleum crude and show narrow heating-value variations. Gaseous fuels, on the other hand, can vary from 1,100 Btu/ft^3 (41,000 kJ/m^3) for natural gas to (11,184 kJ/m^3) or below for process gas. The fuel system will of necessity have to be larger for the process gas, since more is required for the same temperature rise.

Cleanliness of the fuel must be monitored if the fuel is naturally "dirty" or can pick up contaminants during transportation. The nature of the contaminants depends on the particular fuel. The definition of cleanliness here concerns particulates that can be strained out and is not concerned with soluble contaminants. These contaminants can cause damage or fouling in the fuel system and result in poor combustion.

Corrosion by fuel usually occurs in the hot section of the engine, either in the combustor or the turbine blading. Corrosion is related to the amounts of certain heavy metals in the fuel. Fuel corrosivity can be greatly reduced by specific treatments discussed later in this chapter.

Deposition and fouling can occur in the fuel system and in the hot section of the turbine. Deposition rates depend on the amounts of certain compounds contained in the fuel. Some compounds that cause deposits can be removed by fuel treating.

Finally, fuel availability must be considered. If future reserves are unknown, or seasonal variations are expected, dual fuel capability must be considered.

Fuel requirements are defined by various fuel properties. By coincidence, the heating-value requirement is also a property and needs no further mention.

Cleanliness is a measure of the water and sediment and the particulate content. Water and sediment are found primarily in liquid fuels, while particulates are found in gaseous fuels. Particulates and sediments cause clogging of fuel filters. Water leads to oxidation in the fuel system and poor combustion. A fuel can be cleaned by filtration.

Carbon residue, pour point, and viscosity are important properties in relation to deposition and fouling. Carbon residue is found by burning a fuel sample and weighing the amount of carbon left. The carbon residue property shows the tendency of a fuel to deposit carbon on the fuel nozzles and combustion liner. Pour point is the lowest temperature at which a fuel can be poured by gravitational action. Viscosity is related to the pressure loss in the pipe flow. Both pour point and viscosity measure the tendency of a fuel to foul the fuel system. Sometimes, heating of the fuel system and piping is necessary to assure a proper flow.

The ash content of liquid fuels is important in connection with cleanliness, corrosion, and deposition characteristics of the fuel. Ash is the material remaining after combustion. Ash is present in two forms: (1) as solid particles corresponding to that material called sediment, and (2) as oil or water soluble traces of metallic elements. As mentioned earlier, sediment is a measure of cleanliness. The corrosivity of a fuel is related to the amount of various trace elements in the fuel ash. Certain high-ash fuels tend to be very corrosive. Finally, since ash is the fuel element remaining after combustion, the deposition rate is directly related to the ash content of the fuel.

Sulfur content must be controlled in units with exhaust recovery systems. If sulfur condenses in the exhaust stack, corrosion can result. In units without exhaust recovery there is no problem, since stack temperatures are considerably higher than the dew point. Sulfur can, however, promote hot-section corrosion in combustion with certain alkali metals such as sodium or potassium. This type of corrosion is sulfidation or hot corrosion and is controlled by limiting the intake of sulfur and alkali metals. Contaminants found in a gas depend on the particular gas. Common contaminants include tar, lamp black, coke, sand, and lube oil.

Table 12-3 is a summary of liquid fuel specifications set by manufacturers for efficient machine operations. The water and sediment limit is set at 1% by maximum volume to prevent fouling of the fuel system and obstruction of the fuel filters. Viscosity is limited to 20 centistokes at the fuel nozzles to prevent clogging of the fuel lines. Also, it is advisable that the pour point be 20 °F (11 °C) below the minimum ambient temperature. Failure to meet this specification can be corrected by heating the fuel lines. Carbon residue should be less than 1% by weight based on 100% of

Table 12-3 Liquid Fuel Specifications

Water and sediment	1.0% (V%) Max.
Viscosity	20 centistokes at fuel nozzle
Pour point	About 20° below min. ambient
Carbon residue	1.0% (wt) based on 100% of sample
Hydrogen	11.% (wt) minimum
Sulfur	1% (wt) maximum

Typical Ash Analysis and Specifications

Metal	Lead	Calcium	Sodium & Potassium	Vanadium
Spec. max. (ppm)	1	10	1	0.5 untreated
Naphtha	0–1	0–1	0–1	500 treated
Kerosene	0–1	0–1	0–1	0–1
Light distill.	0–1	0–1	0–1	0–1
Heavy distill. (true)	0–1	0–1	0–1	0–1
Heavy distill. (blend)	0–1	0–5	0–20	.1/80
Residual	0–1	0–20	0–100	5/400
Crude	0–1	0–20	0–122	.1/80

the sample. The hydrogen content is related to the smoking tendency of a fuel. Lower hydrogen-content fuels emit more smoke than the higher-hydrogen fuels. The sulfur standard is to protect those systems with exhaust heat recovery from corrosion.

The ash analysis receives special attention because of certain trace metals in the ash that cause corrosion. Elements of prime concern are vanadium, sodium, potassium, lead, and calcium. The first four are restricted because of their contribution to corrosion at elevated temperatures; however, all these elements may leave deposits on the blading.

Sodium and potassium are restricted because they react with sulfur at elevated temperatures to corrode metals by hot corrosion or sulfurization. The hot-corrision mechanism is not fully understood; however, it can be discussed in general terms. It is believed that the deposition of alkali sulfates (Na_2SO_4) on the blade reduces the protective oxide layer. Corrosion results from the continual forming and removing of the oxide layer. Also, oxidation of the blades occurs when liquid vanadium is deposited on the blade. Fortunately, lead is not encountered very often. Its presence is primarily from contamination by leaded fuel or as a result of some refinery practice. Presently, there is no fuel treatment to counteract the presence of lead.

Fuel Properties

Liquid Fuels

Important liquid fuel properties for a gas turbine are shown in Table 12-4. The flash point is the temperature at which vapors begin combustion. The flash point is the maximum temperature at which a fuel can be handled safely.

Table 12-4 Fuel Properties

	Diesel Fuel Burner Fuel				High-Ash Crude Heavy Residual	Typical Libyan Crude	Navy Distillate	Heavy Distillate	Low-Ash Crude
	Kerosene	**#2**	**Oil #2**	**JP-4**					
Flash point °F	130/160	118–220	150/200	<RT	175/265		186 °F	198	50/200
Pour point °F	−50	−55 to +10	−10/30		15/95	68	10 °F		15/110
Visc. CS @ 100 °F	1.4/2.2	2.48/2.67	2.0/4.0	.79	100/1,800	7.3	6.11	6.20	2/100
SSU		34.4					45.9		
Sulfur %	.01/.1	.169/.243	.1/.8	.047	.5/4	.15	1.01	1.075	.1/2.7
API gr.		38.1	35.0	53.2			30.5		
Sp. gr. @ 100 °F	.78/.83	.85	.82–.88	.7543@60 °F	.92/1.05	.84	.874	.8786	.80/.92
Water & ded.			0			.1%wt			
Heating value $\frac{\text{Btu}}{\text{lb}}$	19,300/ 19,700	18,330	19,000/19,600	18,700/ 18,820	18.300/18,900	18,250		18,239	19,000/ 19,400
Hydrogen %	12.8/14.5	12.83	12/13.2	14.75	10/12.5			12.40	12/13.2
Carbon residue 10% bottoms	.01/.1	.104	.03/.3			2/10			.3/3
Ash ppm	1/5	.001	0/20		100/1,000	36 ppm			20/200
Na + K ppm	01.5		0/1		1/350	2.2/4.5			0/50
V	0/.1		0/.1		5/400	0/1			0/15
Pb	0/.5		0/1		0/25				
Ca	0/1	0/2	0/2		0/50				

The pour point is an indication of the lowest temperature at which a fuel oil can be stored and still be capable of flowing under gravitational forces. Fuels with higher pour points are permissible where the piping has been heated. Water and sediment in the fuel lead to fouling of the fuel system and obstruction in fuel filters.

The carbon residue is a measure of the carbon compounds left in a fuel after the volatile components have vaporized. Two different carbon residue tests are used, one for light distillates, and one for heavier fuels. For the light fuels, 90% of the fuel is vaporized, and the carbon residue is found in the remaining 10%. For heavier fuels, since the carbon residue is large, 100% of the sample can be used. These tests give a rough approximation of the tendency to form carbon deposits in the combustion system. The metallic compounds present in the ash are related to the corrosion properties of the fuel.

Viscosity is a measure of the resistance to flow and is important in the design of fuel pumping systems.

Specific gravity is the weight of the fuel in relation to water. This property is important in the design of centrifugal fuel washing systems. Sulfur content is important in connection with emission concerns and in connection with the alkali metals present in the ash. Sulfur reacting with alkali metals forms compounds that corrode by a process labeled sulfidation.

Luminosity is the amount of chemical energy in the fuel that is released as thermal radiation.

Finally, the weight of a fuel, light or heavy, refers to volatility. The most volatile fuels vaporize easily and come out early in the distillation process. Heavy distillates will come out later in the process. What remains after distillation is referred to as residual. The ash content of residual fuels is high.

Catastrophic oxidation requires the presence of Na_2SO_4 and Mo, W, and/or V. Crude oils are high in V; ash will be 65% V_2O_5 or higher. The rate at which corrosion proceeds is related to temperature. At temperatures of more than 1500 °F, attack by sulfidation takes place rapidly. At lower temperatures with vanadium-rich fuels, oxidation catalyzed by vanadium pentoxide can exceed sulfidation. The effect of temperature on IN 718 corrosion by sodium and vanadium is shown in Figure 12-3. The corrosive threshold is generally accepted to be in the range of 1100–1200 °F (593–649 °C), and this cannot be considered a feasible firing temperature due to losses in efficiency and power output. Figure 12-4 shows the effect of sodium plus potassium and vanadium on life. Allowable limits for 100%, 50%, 20%, and 10% of normal life with uncontaminated fuel at standard firing temperatures are shown.

Liquid Fuel Handling and Treatment

Liquid fuels, in most cases, require special treatment. Liquid fuels as mentioned earlier have to be free of Sodium, and Vanadium. A corrosion-inhibiting fuel treatment has been developed for the use of lower-grade liquid fuels. Sodium, potassium, and calcium compounds are most often present in fuel in the form of seawater. These compounds result from salty wells and transportation over seawater, or they can be

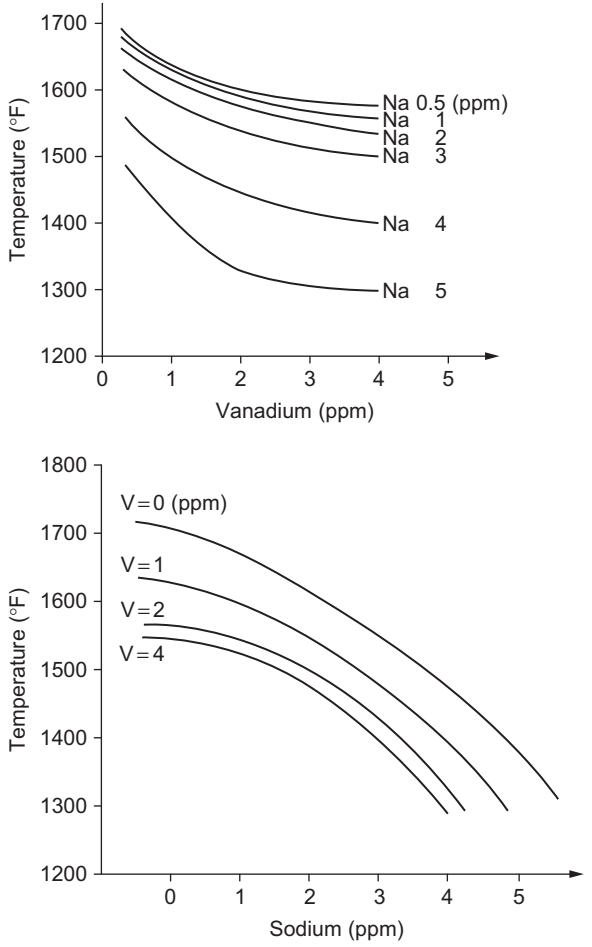


Figure 12-3 The effect of temperature on IN 718 corrosion by sodium and vanadium.

ingested by the compressor in mist form in ocean environments. Methods developed to remove the salt and reduce the sodium, potassium, and calcium rely on the water-solubility of these compounds. Removal of these compounds through their water-solubility is known as fuel washing. A prerequisite for the reduction of sodium content in crude fuel oil is that the oil is washable. A definition of washable fuel is:

- The fuel oil contains no chemically bound sodium
- The fuel oil does not form an emulsion that cannot be broken by the system, and furthermore permits a substantial water separation.

To prevent the formation of an emulsion during the fuel purification and to aid in the separation process an oil-conditioning agent (demulsifier) is added to the fuel. A "Demulsifier'' is a chemical agent used to prevent emulsion between water particles

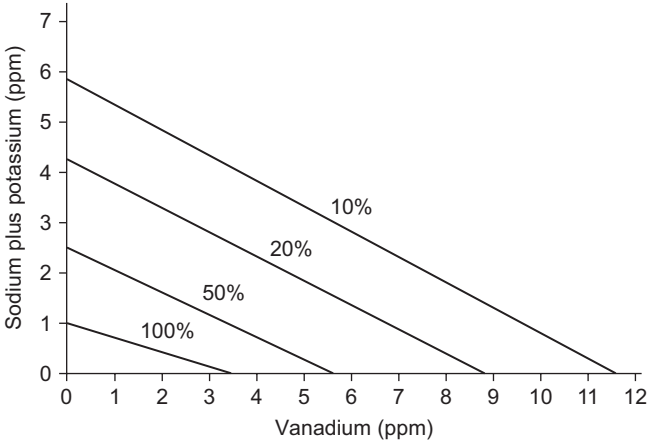


Figure 12-4 Effect of sodium, potassium, and vanadium on combustor life.

and oil in an effort to increase separation efficiency. This agent is injected at a rate of approximately 100–200 ppm, based on the sodium and water content and the viscosity of the fuel.

Water injection is sometimes necessary when the fuel to be centrifuged has very low quantities of free water or has a high salt content. The water soluble trace metals may not be removed by centrifuging if there is not enough free water for them to bind with. By injecting water up to 5.3 cu. ft/h (0.15 cu. m/h) maximum, the water soluble trace metals can be reduced to acceptable levels by centrifuging.

Fuel washing systems fall into four categories: centrifugal, DC electric, AC electric, and hybrids. The centrifugal fuel cleaning process consists of mixing 5–10% water with the oil plus an emulsion breaker to aid the separation of water and oil. Figure 12-5 shows a typical fuel treatment system. The untreated fuel oil is pumped using a centrifugal pump through a suction strainer, which removes any coarse solids from the fuel. The fuel flow is controlled by modulating the flow control valve in response to signals from the treated crude oil tank. A demulsifier is injected continuously into the oil ahead of the plate heat exchanger through a chemical metering pump in a static in-line mixer. The demulsifier is added to counteract the naturally occurring emulsifying species found in the oil and aid separation of the original water from the oil.

Normal processing temperature is 130 °F–140 °F (55 °C–60 °C) and the oil is brought up to this temperature in various stages. The oil is first pre-heated indirectly in the regenerative plate heat exchanger by the hot purified oil leaving the plant. Final heating is carried out by an electric heater. When processing temperature is reached the untreated crude oil is forwarded to the separation modules, which includes the centrifugal separators. Untreated crude oil is fed continuously through the shut-off valve and into the separator bowl where any water and solids are separated from the crude oil by the action of centrifugal force.

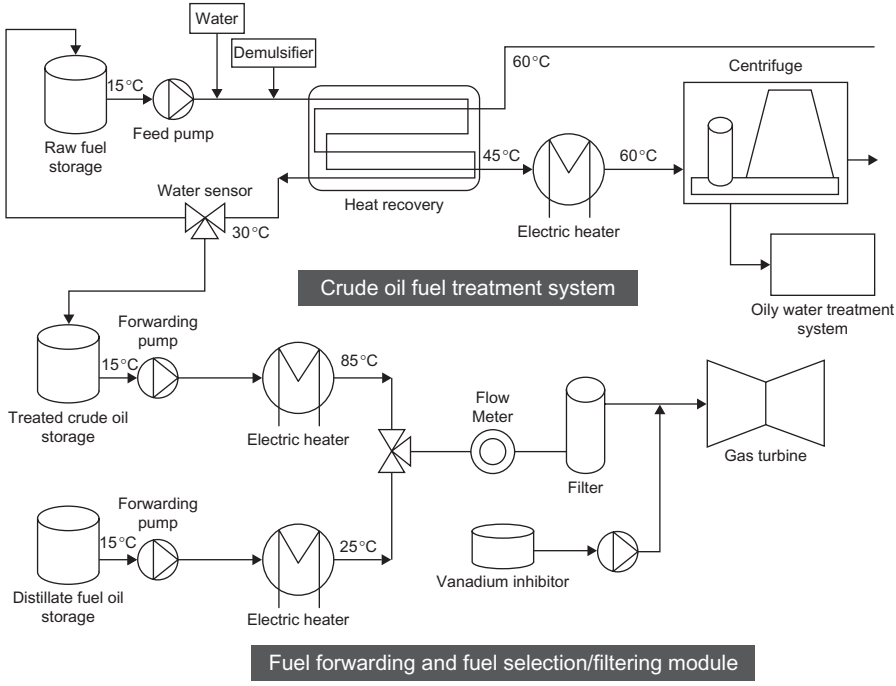


Figure 12-5 A typical fuel treament system.

Purified crude oil and separated water are discharged continuously through their own outlets and the solids accumulate at the periphery of the bowl. The solids are discharged periodically before they build up to a point where they would interfere with the separation process. The discharge cycle is initiated at the control panel by either a push button or automatically by the electronic program control system on completion of a set time cycle.

Water and sludge removed by the centrifugal separators collect in sludge tanks and are transferred to a central storage tank by a sludge pump.

An oil and water monitor in the purified crude oil discharge line checks the quality of the oil leaving the centrifugal separators and if there is any deviation from the set-point an alarm is set off. The system usually consists of a sensor and a monitoring unit. It is designed for the accurate determination of the quantity of water in the oil stream.

Treated fuel oil (Crude) is stored in a treated fuel day tank and maintained at a predetermined temperature below 170 °F (77 °C). Fuel oil is pumped to the GT valve skid under the control of the Turbine Control System.

The treated fuel will contain some oil soluble trace metals, particularly Vanadium, which is deleterious to the GT hot gas path components if not treated. The treated fuel will be further treated to inhibit Vanadium by injecting a 10% solution of Magnesium Sulfate ($MgSO_4$) at a predetermined ratio and thoroughly mixing it with the fuel upstream of the fuel valve skid. $MgSO_4$ will be pumped via positive displacement, using adjustable metering pumps, into the treated fuel piping ahead of a static in-line mixer.

Sludge from the fuel wash skid (containing solids, salt bearing reject wash water, and some oil) flows by gravity in a batch process to a dedicated sump where it is collected for further processing through the plant oily/water separator. Sludge is pumped from the sump to the oily/water separator where oil is separated from the influent and collected into storage drums. The oil collected is pumped in a batch process back to the raw crude oil tank. Oil free wastewater (water with no visible sheen) flows by gravity from the oily/water separator to the plant wastewater disposal system for discharge. Solids are removed in a manual batch process from the sump and the oily/water separator on an as-required basis for disposal off-site.

Free water must be decanted from the raw crude storage tank automatically (by others) and gravity flows to a wastewater sump (by others). It will be pumped from the sump (by others) to the oily/water separator to remove traces of oil to meet local water discharge criteria before being discharged to the local wastewater receptor.

Fuel chemistry must be continuously monitored through a batch sampling procedure to ensure that the turbine is not contaminated. Grab samples should be gathered from each storage tank periodically throughout the day and tested to determine the level of trace metals, salts, and concentrations of chemical additives. An Atomic Photo-spectrometer could be utilized to process the grab samples and determine trace metal content of the fuel and the effectiveness of the inhibitor chemicals.

The GT, when fired using heavy fuels, will usually start and stop on No. 2 Fuel Oil (LFO) to assure that the heavy fuel oil does not coke in the fuel nozzles upon shutdown and that the fuel delivery piping is up to operating temperature on start-up before introducing treated fuel oil. In the case of some light crudes such as the Saudi Crudes starting and stopping has been successful. However, in most cases it is recommended that start-up should be with diesel fuel. Typically the GT will operate approximately 30 minutes on LFO during start-up and a similar period of time on shutdown. The valve skid as shown in Figure 12-5 handles the transfer of both fuels as directed by the Turbine Control requirements. The valve skid is located in close proximity to the GT fuel inlet flange and contains the emergency shutoff valve and fuel management instrumentation and control sensors together with a duplex fuel filter. This fuel filter is upstream of the final fuel filter on the GT base skid and serves to assure no foreign particles in the fuel effect the operation of the GT combustion system.

Diesel fuel (LFO), used for starting and stopping the GT, is usually pumped from the LFO storage tank to the valve skid as required. If there are any suspicions that the fuel may have been contaminated with brackish water the diesel fuel should also be treated and the fuel should be sent to a centrifuge before it is injected into the gas turbine, so as to remove the sodium. The Turbine Control will determine the fuel to be delivered to the GT and select the appropriate valve positions. The crude oil treatment plant is controlled, monitored, and supervised from its own centralized control console, which is connected to the turbine control system.

In the case of Heavy Fuels where the specific gravity of the fuel is above .96 or viscosity exceeds 3,500 SSU @ 100 °F (37.8 °C), centrifugal separation is impractical, and the specific gravity of one of the components must be increased. Dissolving epsom salt in it can increase water weight. Fuel blending can decrease specific gravity of the fuel. Figure 12-6 shows the relation is linear, and the blend has a specific gravity, which is the average of the constituents. However, viscosity blending

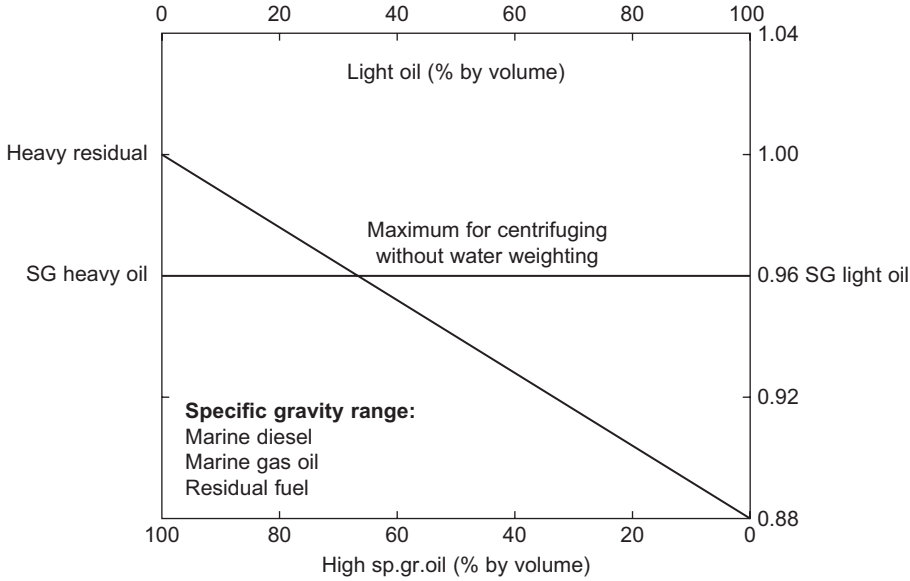


Figure 12-6 Fuel blending for specific gravity reduction. Specific gravity heavy oil = 1.0. Specific gravity light oil = .88.

is a logarithmic relation as shown in Figure 12-7. To reduce viscosity from 10,000 to 3,000 SSU, a 3:1 reduction requires a dilution of only 1:10. An added advantage of the centrifugal process is that sludge and particulates that can cause fuel system fouling are removed.

Electrostatic separators operate on a principle similar to centrifugal separation. The salt is first dissolved in the water, and the water is then separated. Electrostatic separators utilize an electric field to coalesce droplets of water for an increase in diameter and an associated increased settling rate. The DC separators are most efficient with light fuels of low conductivity, and AC separators are used with heavier, highly conductive fuels. Electrostatic separators are attractive because of safety considerations (no rotating machinery) and maintenance (few overhauls). However, sludge removal is more difficult. Water washing systems are summarized in Table 12-5.

Vanadium originates as a metallic compound in crude oil and is concentrated by the distillation process into the heavy-oil fractions. Blade oxidation occurs when liquid vanadium is deposited onto a blade and acts as a catalyst. Vanadium compounds are oil-soluble and are thus unaffected by fuel washing. Without additives, vanadium forms low-melting-temperature compounds, which deposit on a blade in a molten slag state that causes rapid corrosion. However, by the addition of a suitable compound (magnesium, for example), the melting point of the vanadates is increased sufficiently to prevent them from being in the liquid state under service conditions. Thus, slag deposition on the blades is avoided. Calcium was initially selected as the inhibiting agent, as tests indicated it was more effective at 1750 °F (954 °C). Subsequent tests showed magnesium gave better protection at 1650 °F (899 °C) and below. However,

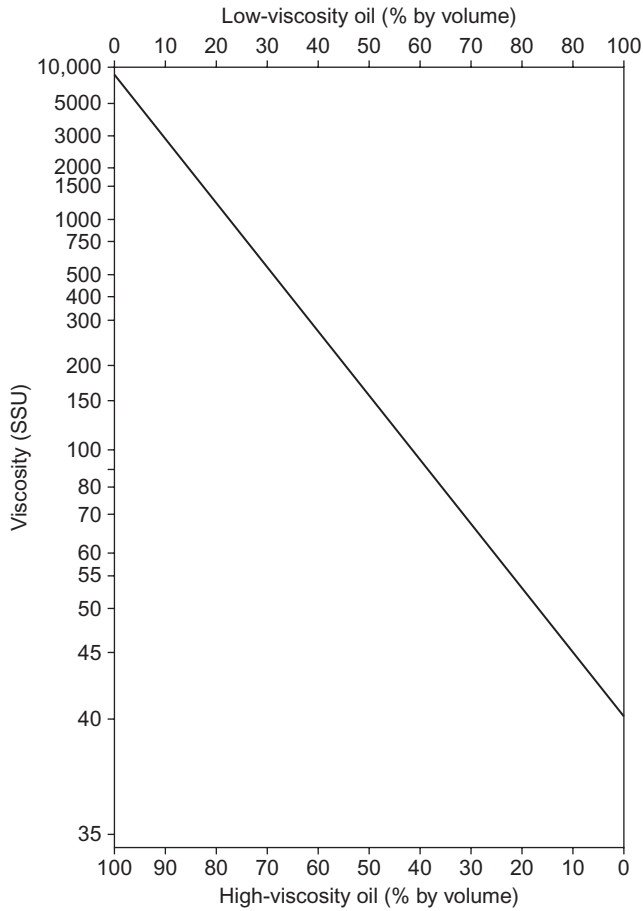


Figure 12-7 Fuel viscosity blending chart. High-viscosity oil = 10,000 SSU. Low viscosity oil = 40 SSU.

at temperatures of 1750 °F (954 °C) and over, magnesium no longer inhibits but rather *accelerates* corrosion. Magnesium also provides more friable deposits than calcium inhibitors. A magnesium/vanadium ratio of 3:1 reduces corrosion by a factor of six between temperatures of 1550 °F (843 °C) and 1400 °F (760 °C).

The particular magnesium compound selected for inhibition is dependent upon fuel characteristics. For low-vanadium concentrations (below 50 ppm), an oil-soluble compound such as magnesium sulfonate is added in the correct proportion to the vanadium present. The cost of oil-soluble inhibitors becomes prohibitive above concentrations of 50 ppm.

At higher concentrations of vanadium, magnesium sulfate or magnesium oxide is used as an inhibitor. Both are approximately equal in material cost, but magnesium sulfate has proven itself, while magnesium oxide is still under study. Magnesium sulfate

Table 12-5 Selection of Fuel Washing Systems

Fuel	Washing System
Distillate	Centrifugal or DC electrostatic desalter
Heavy distillates	Centrifugal or AC electrostatic desalter
Light-medium crudes	Centrifugal or AC electrostatic desalter
Light residual	Centrifugal or AC electrostatic desalter
Heavy crudes	Centrifugal desalter and hybrid systems
Heavy residuals	Centrifugal desalter and hybrid systems

requires by far the most capital cost, as it must be first dissolved, then adjusted to a known concentration. It is mixed with an oil and an emulsifying agent to form an emulsion to suspend in the fuel. Two different injection procedures are used. One method is to mix the solution with desalted fuel in a dispersion mixer just prior to the combustion chamber. The inhibited oil is burned quickly, usually within a minute of mixing, because the solution has a tendency to settle out. Also, the solution can be dispersed in the fuel prior to the service tanks. To avoid settling out of the solution, the tanks are re-circulated through distribution headers. Since a magnesium- to-vanadium ratio of 3:25 $\pm$ 0:25:1 is used in practice, the second dispersion method is the standard practice as the tanks can be certified "within specification" before burning. Adequate knowledge of contaminants is essential for successful inhibition.

An alternate approach to fuel washing is to utilize a vaporized fuel oil system (VFO). This technology was developed as a method for converting natural gas fuel systems to liquid fuel. The process involves mixing steam with the liquid fuel and then vaporizing the mixture. The vaporized mixture exhibits the same combustion properties as natural gas.

VFO works well in gas turbines. In a nine-month test program, the combustion properties of VFO were studied in a combustion test module. A gas turbine was also operated on VFO. The tests were conducted to study the combustion characteristics of VFO, the erosive and corrosive effects of VFO, and the operation of a gas turbine on VFO. The combustion tests were conducted on a combustion test module built from a GE Frame 5 combustion can and liner. The gas turbine tests were conducted on a Ford model 707 industrial gas turbine. Both the combustion module and gas turbine were used in the erosion and corrosion evaluation. The combustion tests showed the VFO to match natural gas in flame patterns, temperature profile, and flame color. The operation of the gas turbine revealed that the gas turbine not only operated well on VFO, but its performance was improved. The turbine inlet temperature was lower at a given output with VFO than with either natural gas or diesel fuel. This phenomenon is due to the increase in exhaust mass flow provided by the addition of steam in the diesel for the vaporization process. Following the tests, a thorough inspection was made of materials in the combustion module and on the gas turbine, which came into contact with the vaporized fuel or with the combustion gas. The inspection revealed no harmful effects on any of the components due to the use of VFO.

The VFO technology provides a means of converting natural gas systems to liquid fuel without requiring new fuel liners, nozzles, and control systems. However, VFO also offers a method of treating contaminated fuel. The VFO process vaporizes only a portion of the liquid fuel; the contaminants stay in the remaining liquid fuel. The remaining liquid can be utilized either as fuel or as feedstock for other processes. It has been found that if 90% of the fuel is vaporized, the remaining 10% provides the heat required for vaporization. The heat required to vaporize the liquid fuel is recovered in the gas turbine as heat added into the combustion can, so the process is very efficient. The only loss is the energy in the heated gases leaving the vaporizer exhaust.

The overall costs for a VFO unit can be lower than the costs of conventional liquid fuel treatment plants. The U.S. Department of Energy conducted a survey that showed that the costs of operating a liquid fuel treatment system over a 20-year period is approximately $0.50 MMBtu output. This cost includes the initial capital investment, maintenance, and operating costs. The initial cost of a VFO unit with an output of 800 MMBtu/hr (required for a 60 MW gas turbine) is approximately $1,150/MMBtu/hr output ($920,000 total). The operating costs of a VFO unit are very low, since the only power requirement is the electrical power needed to drive several small pumps. The energy required to vaporize the oil is obtained from burning the unvaporized oil. Any additional expense in operating a VFO system results from maintenance. Maintenance will be minimal with properly selected components.

Heavy Fuels

With heavy fuels, the ambient temperature and the fuel type must be considered. Even at warm environmental temperatures, the high viscosity of the residual could require fuel preheating or blending. If the unit is planned for operation in extremely cold regions, the heavier distillates could become too viscous. Fuel system requirements limit viscosity to 20 centistokes at the fuel nozzles.

The start-up and shutdown of the gas turbine for heavy fuels is conducted using distillate oil. The problems usually occur when there is an unplanned shutdown. In that case the turbine is shut down on the heavy fuel, and so does not have the opportunity to cleanse the fuel feed system at the turbine with distillate fuel. The heavy fuel, which is in the fuel feed system, solidifies and blocks the fuel system. This, in most cases, requires the total dismantling of the fuel system to cleanse it of the solidified fuel.

Fuel system fouling is related to the amount of water and sediment in the fuel. A by-product of fuel washing is the de-sludging of the fuel. Washing rids the fuel of those undesirable constituents that cause clogging, deposition, and corrosion in the fuel system. The last part of treatment is filtration just prior to entering the turbine. Washed fuel should have less than .025% bottom sediment and water.

The combustion of liquid fuel oil in a gas turbine requires an air atomization system. When liquid fuel oil is sprayed into the turbine combustion chambers, it forms large droplets as it leaves the fuel nozzles. The droplets will not burn completely in

the chambers and many could go out of the exhaust stack in this state. A low pressure atomizing air system is used to provide atomizing air through supplementary orifices in the fuel nozzle which directs the air to impinge upon the fuel jet discharging from each nozzle. This stream of atomizing air breaks the fuel jet up into a fine mist, permitting ignition and combustion with significantly increased efficiency and a decrease of combustion particles discharging through the exhaust into the atmosphere. It is necessary, therefore, that the air atomizing system be operative from the time of ignition firing through acceleration, and through operation of the turbine.

Atomizing air systems provide sufficient pressure in the air atomizing chamber of the fuel nozzle body to maintain the ratio of atomizing air pressure to compressor discharge pressure at approximately 1.4 or greater over the full operating range of the turbine.

In most cases the atomization air is bled off the compressor discharge of the gas turbine and then is sent through a shell tube heat exchanger, where it is cooled, with minimum pressure drop. The discharge air conditions leaving the Gas Turbine depend on the pressure ratio of the gas turbine compressor. The air leaving, in most cases, is at a pressure of about 150 psia–300 psia (10–20 bar) and a temperature of 750 °F–950 °F (400 °C–480 °C). This air bled from the gas turbine is cooled in a shell and tube cooler to about 250 °F (120 °C) so that the power required to compress that gas is significantly lowered. The compressor used to compress the bleed air is usually a centrifugal compressor, which is operated at the auxiliary gear box of the turbine or a stand-alone electric motor. This compressor usually operates at a very high speed, between 40,000–60,000 rpm. The compressor will deliver a flow of about 120–150% of the fuel flow and at a pressure ratio of about 1.4 to 1.7 of the compressor discharge pressure depending on the viscosity of the fuel. Since the output of the main atomizing air compressor, driven by the accessory gear, is low at turbine firing speed, a starting atomizing air compressor provides a similar pressure ratio during the firing and warm-up period of the starting cycle, and during a portion of the accelerating cycle.

Major system components include: the main atomizing air compressor, starting atomizing air compressor, and atomizing air heat exchanger. Figure 12-8 is a schematic diagram of the system. Air bled from the gas turbine compressor using the atomizing air extraction manifold of the compressor discharge casing passes through the air-to-water heat exchanger (pre-cooler) so as to reduce the temperature of the air. This would maintain a uniform air inlet temperature to the atomizing air compressor, and reduces the power. An alarm is suggested if the temperature of the air from the atomizing air pre-cooler entering the main atomizing air compressor is excessive. Improper control of the temperature will be due to failure of the sensor, the pre-cooler, or insufficient cooling water flow. Continued operation above 285 °F (140 °C) should not be permitted for any significant length of time since it may result in failure of the main atomizing air compressor or in insufficient atomizing air to provide proper combustion.

Compressor discharge air, now cleaned and cooled, reaches the main atomizing air compressor. This is a single-stage, flange mounted, centrifugal compressor driven by an inboard shaft of the turbine accessory gear. It contains a single impeller mounted on the pinion shaft of the integral input speed increasing gear box driven directly above

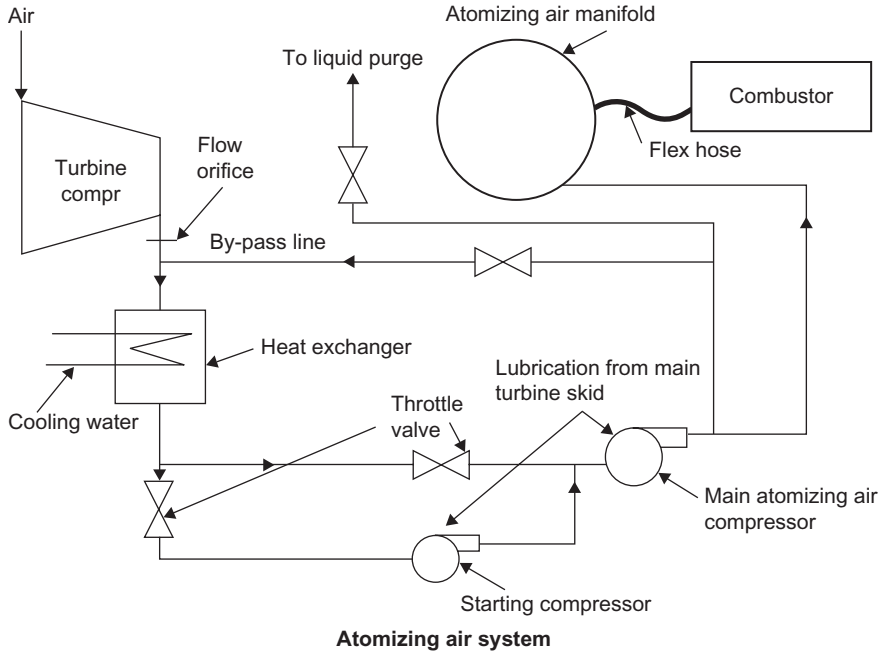


Figure 12-8 Atomization air system for liquid fuel oil systems.

the accessory gear. Output of the main compressor provides sufficient air for atomizing and combustion when the turbine is at approximately 70% speed.

The differential pressure switch, located in a bypass around the compressor, monitors the air pressure and annunciates an alarm if the pressure rise across the compressor should drop to a level inadequate for proper atomization of the fuel.

Air, now identified as atomizing air, leaves the compressor and is piped to the atomizing air manifold with "pigtail" piping providing equal pressure distribution of atomizing air to the individual fuel nozzles.

When the turbine is first fired, the accessory gear is not rotating at full speed and the main atomizing air compressor is not outputting sufficient air for proper fuel atomization. During this period, the starting (booster) atomizing air compressor, driven by an electric motor, is in operation supplying the necessary atomizing air. The starting atomizing air compressor at this time has a high pressure ratio and is discharging through the main atomizing air compressor which has a low pressure ratio. The main atomizing air compressor pressure ratio increases with increasing turbine speed, and at approximately 70% speed the slow demand of the main atomizing air compressor approximates the maximum flow capability of the starting atomizing air compressor. The check valve in the air input line to the main compressor begins to open, allowing air to be supplied to the main compressor simultaneously from both the main air line and the starting air compressor. The pressure ratio of the starting atomizing air

compressor decreases to one, and when the turbine becomes self-sustaining, the starting compressor is shut down at approximately 95% speed. Now all of the air being supplied to the main compressor is directly from the pre-cooler through the check valve, bypassing the starting air compressor completely.

When water washing the gas turbine's compressor section and turbine section, it is important to keep water out of the atomizing air system. To keep water out of the atomizing air system, the system inlet and discharge should be equipped with a vent valves and an isolation valve. The vent valves are used to avoid completely throttling or deadening the compressors and the drain valves to remove any leakage past the isolation valve.

During normal operation of the gas turbine, the vent and drain valves must be closed and the isolation valve must be open. Before initiating water wash the isolation valve must be closed to keep water out of the atomizing air system. The vent valve must be opened to allow air to pass through the atomizing air compressors.

Running the atomizing air compressors completely throttled or deadened may result in overheating and damage to the compressor.

At the conclusion of water wash, drain water from the atomizing air piping opening the low point drain valves. When the water has drained from the piping, the drain valves and vent valves must be closed.

Running the atomizing air compressors with water in the piping will result in damage to the atomizing air compressors.

Frequently, no visible smoke and no carbon deposition are design parameters. Smoke is an environmental concern, while excessive carbon can impair the fuel spray quality and cause higher liner temperatures due to the increased radiation emissivity of the carbon particles as compared to the surrounding gases. Smoke and carbon are a fuel-related property. The hydrogen saturation influences smoke and free carbon. The less-saturated fuels like benzene (C_6H_6) tend to be smokers; the better fuels like methane (CH_4) are saturated hydrocarbons. This effect is shown in Figure 12-9. Boiling temperature is a function of molecular weight. Heavier molecules tend to boil at a higher temperature. Since a less saturated molecule will weigh more (higher molecular weight), one can expect residuals and heavy distillates to be smokers. This expectation is founded in practice. The design solution pioneered by General Electric on its LM 2,500, which has an annular combustor as shown in Figure 12-10, was to increase flow and swirl through the dome surrounding the fuel injector. The increased flow helped to avoid rich pockets and promoted good mixing. The axial swirler achieved a no smoke condition and reduced liner temperature.

Special consideration must be afforded to the combustion chamber walls. Low-grade fuels tend to release a higher amount of their energy as thermal radiation instead of heat. This energy release, coupled with the large diameter of the single can and the formation of carbon deposits, can lead to an overheating problem on the liner. One vendor advocates the use of metallic tiles as combustor liners. The tiles hook into the wall in slots provided for them. The tiles have fine pitched fins cast on the back. The fins form a double wall structure by bridging the gap between the flame-tube wall and the tile. This annulus is fed by air, thus providing a strong cooling action. The standard sheet metal design was abandoned due to warpage.

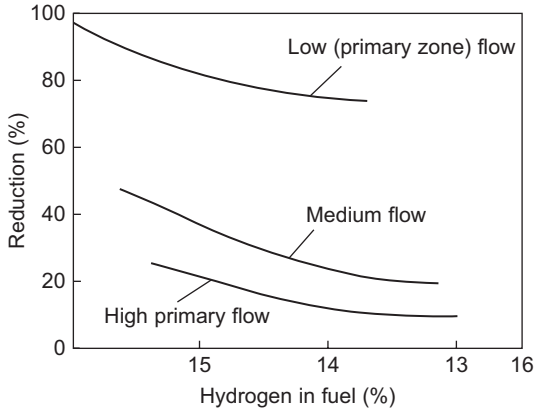


Figure 12-9 Effect of hydrogen saturation in primary flow on smoke.

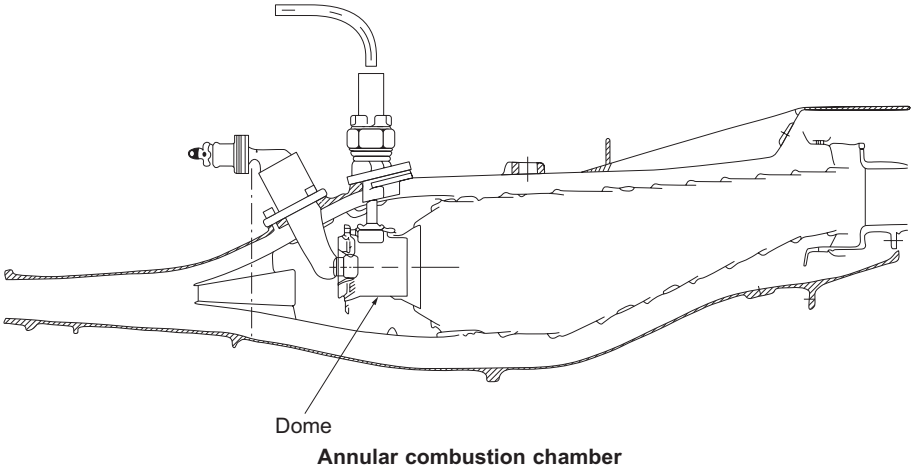


Figure 12-10 Cross section of an annular combustor showing high dome flow configuration (Courtesy of General Electric Company).

Fuel Gas Handling and Treatment

Natural gas is the desired fuel for gas turbines, but this fuel gas must be clean dry gas especially for advanced-technology gas turbines. This statement is very necessary because the Dry Low NO_x Combustors are very sensitive to any liquid carry-over into the combustor, which leads to failure due to flashback problems in these combustors. This requires the gas to be clean and heated to ensure the fuel gas would meet the requirements of the gas turbine OEM. The general degradation of gas quality in the United States makes it especially important to carefully monitor gas quality and to take corrective actions, in order to prevent damage to gas turbines (especially advanced gas turbines), which are very sensitive to any liquids in the fuel.

Gas fuel piped to any plant will contain different contaminants as a result of the production and transportation of the natural gas. Some of the most common contaminants found in the natural gas are:

- Hydrocarbon liquids
- Glycols from dehydration process
- Crude oil
- Lubricating oil from the pumping station along the pipeline
- Water and salt water
- Rust
- Construction debris such as portions of weld rods, weld slag, grinding particles, metal shavings, sand, and mud

Construction debris is common and despite gas line pigging and vigorous blowdowns, which are necessary and recommended, some contaminants will be found in the gas supply, especially during the early commissioning period. During this phase, extra precautions are taken by installing temporary "witch hat" fine mesh strainers at the inlet to the gas control module and selected sections of gas piping within the turbine enclosure.

Once satisfactory operation has been achieved and the temporary strainers no longer pick up debris and contaminants, they are removed. Installation of these strainers does not provide a substitute for a properly engineered gas clean-up system and frequent outages will be required to clean or replace the strainers if an adequate filtration system is not installed.

The removal of liquids, such as liquid hydrocarbons and water, is much more difficult, and thus requires more careful planning on the part of the manufacturer, engineering constructor, and the end user. Liquids in the gas stream can affect combustion by causing autoignition, and variations in the heating value. Liquids are formed from the condensable higher hydrocarbons found in natural gas, generally those higher than about pentane (C_5), as well as moisture from water vapor. Moisture is undesirable because it can combine with methane and other hydrocarbons to generate solids in the form of hydrates. Many factors influence liquid removal, such as droplet size and distribution, and are hard to quantify. If not carefully analyzed and accounted for by the engineering constructor, this could result in liquid hydrocarbons being admitted into the gas turbine fuel systems and then into the combustion chamber where they can cause a problem. Due to the design of Dry Low NO_x combustor, even extremely small amounts, if allowed to accumulate in downstream piping, can cause damage to the combustor. The Dry Low NO_x combustor requires very dry gas, a fact that should be known by all in the power generating industry, and thus great care must be taken to ensure that the fuel conditions of NO_x liquids should be met by proper design of the fuel handling system.

Variations in the heating value as a result of gas phase composition variation affect gas turbine emissions, output, and combustor stability. Changes greater than 10% require gas control hardware modifications, but are not a common problem.

Some local distribution companies use propane/air injection as a method for stabilizing variations in heating value. The quantity of air injected is well below that required to reach the rich flammability limit of the gas and poses no safety issues.

Variations in heating value could be an issue if gas is purchased from a variety of suppliers depending on the daily or weekly variations. In this situation, the user should ensure that the variations are within the values allowed by the gas turbine OEM. Many of the large power plants have on-line instruments that determine and monitor heating values for both the good of the turbine and in some cases the purchase of the fuel gas is based on the heating value rather than the volume of the gas.

Slugging of hydrocarbon liquids affects the energy delivered to the turbine and can result in significant control problems and potential damage to the fuel nozzles and combustor liners due to flashback problems. Carry-over of liquids to the turbine can result in uncontrolled heat release rates if sufficient quantities are present, resulting in possible damage to the hot gas path. Another problem is the exposure of small quantities of hydrocarbon liquids to compressor discharge air. Dry Low NO_x combustion systems require premixing of gas fuel and compressor discharge air in order to produce a uniform fuel/air mixture and to minimize locally fuel-rich NO_x-producing regions in the combustor. Auto Ignition Temperatures (AIT), the temperatures required for spontaneous combustion with no ignition source, for these liquids are in the 400 °F–550 °F (204 °C–288 °C) range and fall below compressor discharge temperature of 625 °F–825 °F (329 °C–451 °C range). Exposure to compressor discharge air above the AIT will result in instantaneous ignition of the liquid droplets, causing, in some cases, premature ignition of the premixed gases, often called flashback. Varnish-like deposits could also occur and hot spots can be noted on turbine nozzle vanes and blades from the impact of the liquid hydrocarbons on them. Because of the seriousness of the problem, gas specifications by OEMs do not allow any liquids in the gas fuel.

The fuel gas characteristics given in Table 12-6 state very clearly that there should be no liquids in the gas stream. Knowing fully well that no natural gas supplied is free of liquids, which may be present from the liquid hydrocarbons in the gas stream, liquids from the lubrication systems used in the pumping stations, and water condensation in the pipeline, great care should be used in fuel handling system at the plants.

Superheating is the only sure method for eliminating all liquids at the inlet to the fuel gas control module of the turbine, since it prevents the formation of liquids and reduces the vaporization time for liquid droplets; this ensures that liquids are removed. ASME "Gas Turbine Fuels," ANSI/ASME B133.7M, 1992, recommends that 45 °F to 54 °F (25 °C–30 °C) of superheat be used for combustion turbine gaseous fuel. Calculations show the 50 °F (28 °C) minimum superheat requirement will prevent liquid formation downstream from the control valves and is verified by field experience. Meeting this requirement requires heating the gas. Some margin must be provided to cover daily variations in dew point. In many applications the gas is heated to about 350 °F–400 °F (177 °C–205 °C), well above the 45 °F–54 °F (7.2 °C–30 °C) recommended by ASME and also by many manufacturers who use the ASME standard.

Vaporization time for liquid droplets decreases as superheat temperature increases. Figure 12-11 shows the dew point temperatures of the Table 12-7 indicates that at the intake pressure of the gas around 490 psia (28 bar) the superheated moisture minimum temperature requirement as per ASME B133.7M is 42 °F (5.55 °C), and the superheated hydrocarbon minimum temperature is −7 °F (−14 °C). At the recommended temperature of the fuel gas at 350 °F to 400 °F (177 °C–205 °C), there is a large enough

Table 12-6 Gas Fuel Specification

Fuel Properties	Max	Min	Notes
Lower heating value, Btu/lb	1,150	300	Guidelines only
Modified Wobbe Index range	+5%	−5%	$WI = LHV/\sqrt{(Sp.GrxT_f)}$
Superheat, °F	–	45 °F to 54 °F	ANSI/ASME B133.7M
Flammability		>2.2:1	Rich to lean fuel to air ratio, volume basis
Gas Constituents Limits, % by Volume:			
Methane	100	85	% of reactant species
Ethane	15	0	% of reactant species
Propane	15	0	% of reactant species
Butane + Paraffin (C_4+)	5	0	% of reactant species
Hexane (C_6)	0.5	0	
Hydrogen	0	0	% of reactant species
Carbon monoxide	15	0	% of reactant species
Oxygen	10	0	% of reactant species
Carbon dioxide	15	0	% total (reactants + inerts)
Nitrogen	30	0	% total (reactants + inerts)
Sulfur	<1%	–	
Total inerts ($N_2 + CO_2 + AR$) Aromatics (Benzene, Toluene, etc.)	30	0	$T_f > 300$ °F possibility of gum formation if excess aromatics are present
Gas fuel supply pressure		50–100 psia above compressor discharge	Minimum and maximum gas fuel supply are furnished by manufacturer

Contaminants	Fuel Limits ppm (weight)		Notes
	Diffusion Combustors	Dry Low NO_x Combustors	
Total particulate above 10 microns	32–35 0.3–0.4	23 0.2	
Trace metals Sodium plus potassium (from salt water)	0.8		When formed into alkali metasulfate
Liquids	0		No liquids allowed, see superheat requirements

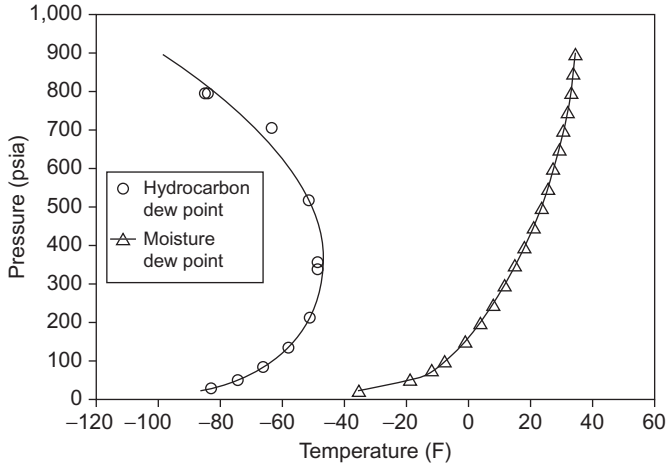


Figure 12-11 Hydrocarbon and moisture dew point.

Table 12-7 Superheat Requirements for Natural Gas to Ensure Liquid Removal

Maximum allowable supply pressure	490 psia	28 bar
Hydrocarbon dew point	−49 °F	−44 °C
Required hydrocarbon superheat	42 °F	5.5 °C
Required minimum temperature for HC	−7 °F	−14 °C
Moisture dew point	23 °F	−5 °C
Required moisture superheat	18 °F	−7.8 °C
Required minimum temperature for moisture	42 °F	5.5 °C
Required minimum gas temperature	42 °F	5.5 °C

temperature margin to should prevent liquid formation downstream from the control valves, where expansion takes place.

The variation in the composition of the gas has a small impact on the gas turbine operation (e.g., emissions); the principal point of concern is the formation of condensates as the composition of C_6 + compounds. Depending on the hexanes + species, this constituent of the natural gas could lead to liquid hydrocarbon condensation in the gas stream supplied to the gas turbine, resulting in serious damage to the unit.

Particulates in the fuel gas can cause:

- Fuel nozzle plugging
- Erosion
- Deposition

Fuel nozzles are more prone to plugging, especially in DLN combustion systems, due to the smaller fuel nozzle holes than those used in diffusion flame combustor

fuel nozzles. Plugging will result in poor fuel distribution from nozzle to nozzle, and combustor to combustor. This will result in increasing emissions and exhaust temperature spreads. Plugging could also lead to fuel flow split deviations between gas manifolds, which could lead to poor emissions and, in the worst case, to auto ignition and flashback problems in DLN combustors.

Erosion rates are exponentially proportional to particle velocity, and areas that experience high gas velocities, such as orifices and valve seats, are more susceptible to erosion. Particles that are smaller than about 10 microns tend to follow the gas stream, thus resulting in a decrease in the rate of erosion. All the OEM fuel specifications call for removal of particulates greater in size than approximately 10 microns to prevent erosion and deposition.

Erosion problems on the leading edge of the turbine nozzle vanes and blades will cause erosion of the thermal barrier coating (TBC). Turbine nozzle vanes and blades even are affected by those of less than 10 microns in diameter. For this reason, many of the OEM specifications limit the concentration of particulates from all sources and sizes to no more than 600 ppb at the first stage nozzle vane inlet.

Equipment for Removal of Particulates and Liquids from Fuel Gas Systems

Clean-up equipment must address both solids and liquids removal processes. It is better to be on the safe side by *always* assuming that liquids will be present in all fuel gas, since liquids in the fuel gas, if injected into the combustion system, would cause major damage to the gas turbine. The cost of additional protective equipment such as knock-out drums or vertical coalescing systems is less than half of one percent of the plant costs; therefore there should be no excuse for not placing equipment that would remove liquids from the fuel gas. DLN combustors have no tolerance for liquids in the fuel gas.

The recommended particulate removal equipment is a filter system that is designed with an absolute removal rating of three microns or less. The equipment is normally available in a vertical configuration and consists of a series of parallel filter elements attached to a tube sheet. The elements are changed once a predetermined pressure drop is reached for a given volumetric flow rate of gas. Duplexed arrangements are recommended since this permits isolation of one vessel for maintenance while the other is in operation. Under no circumstances should a bypass line be installed with the intention of using the bypass line for maintenance purposes. If the gas is to be heated prior to filtration, then the filter elements must meet the maximum gas temperature requirements.

The clean-up system for liquid removal should include the following equipment in the following order:

- Pressure-reducing station
- Dry scrubber
- Filter/separator
- Superheater

Many of the gas pipelines have high pressures above approximately 1,000 psia (69 bar), and have a high moisture content; the gas would require upstream heating to avoid the formation of hydrates and slugging of condensed hydrocarbons after the expansion valves that would otherwise remain in the gas phase throughout the liquids removal process. This heater, most likely, will not provide sufficient energy to meet the 50 °F (10 °C) minimum superheat requirement at the gas control module inlet, but may prevent collection of free liquids.

For *all* sites a vertical gas separator followed by either duplex multitube filters or a filter separator and superheater is recommended. Each of the duplex units must be designed for 100% of the system flow rate so that one can stay on-line while maintenance is being performed on the other. The concept that if the "*gas is wet and slugging is present in the incoming gas supply, a dry scrubber may be required upstream from the pressure reducing station*" which should be changed as all fuel gas systems must be treated as if they will be contaminated with liquids.

Fuel gas conditioning requires the removal of both liquid and solid contaminants from the gas stream. These dry scrubbers and coalescing filters must be located as close as possible to the gas turbine. Dry scrubbers are multiple-cyclone (multiclones) inertial separators that remove both liquids and solid materials without the use of scrubbing oils or liquids. They are virtually maintenance-free except for blow down of the drain tank.

Dry scrubbers should be combined with coalescing filters in order to provide protection over the entire operating range of the gas turbine. Typically, vertical units are used, and in multiple gas turbine plants it is recommended that one unit per turbine is required. Figure 12-12 shows such a typical arrangement. Each gas turbine in the plant should have its own clean-up system, and there should be at a minimum one knockout drum at the gas transfer location. It is recommended that a similar system as that located at the individual gas turbines should be installed at the transfer station. A filter separator is also required to provide protection over 100% of the flow range and to minimize any liquid carry-over to the heater. A dry scrubber and heater are usually required upstream from the pressure-reducing station. A filter/separator and superheater are required as before. The heat input can be minimized upstream, heating to a level that avoids hydrate formation and allows the downstream filter/separator to remove liquids by physical separation.

Coalescing filters are normally used in conjunction with a dry scrubber to remove all liquid droplets. Coalescing filters should always be preceded by a stage 1 liquid and solid removal device to prevent the entry of gross amounts of contamination. Typically, coalescing filters will remove all droplets and solids larger than about 0.3 microns. The filter unit consists of a vertical pressure vessel that contains a number of parallel tubular filter cartridges. The wet gas containing fine droplets flows though the filter where the droplets collide with the fibrous filter material. The droplets coalesce with others and form larger droplets that are then removed from the filter element by gravity and collected in the sump.

The filter separator combines changeable filter elements along with vane mist eliminators in a single vessel. The gas first passes through the filter elements, enabling smaller liquid particles to be coalesced while the solids are removed. Because of the

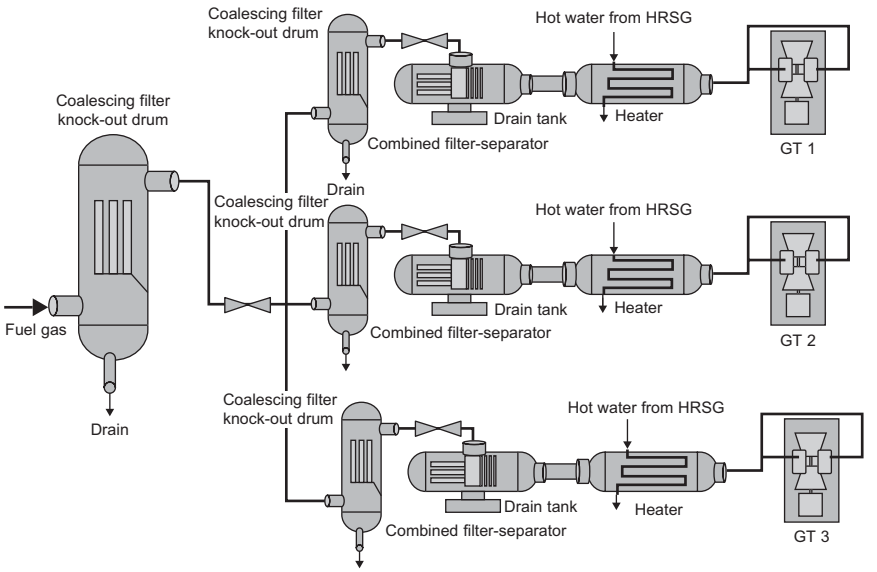


Figure 12-12 Natural gas fuel handling system.

coalescing effect, the vane is able to remove more free liquid particles than either the dry scrubber or the vertical gas separator alone. This combines the efficiency of the vane separator with that of the coalescing filter in one vessel.

As with the coalescing filter just described, the filter separator maintains its guaranteed separation efficiency from 0% to 100% of its design flow capacity. Filter separators are often used in lieu of filters when high liquid rates are expected. The filter separator also removes solids from the gas stream, but must be taken off-line periodically in order to replace the dirty filter elements. For this reason, base-loaded units require a duplex arrangement that permits maintenance to be performed on one unit while the other is in service.

Fuel Heating

Fuel heating to raise the temperature of the gas to 50 °F/28 °C above the hydrocarbon dew point may be required. Three basic types of heater are available; each has economic, maintenance, and operating advantages and disadvantages.

Electrical heaters are the most convenient type of fuel heater to use and install. A simple control system can maintain a constant exit temperature or a constant temperature rise within the capacity limits of the equipment as fuel flow rate varies. Thermal efficiency is close to 100% in that all of the electricity used is converted into heat and is used to raise the gas temperature, neglecting losses to the ambient surroundings. The electricity used to power the equipment, however, is being produced at 30% to 40%

efficiency for simple-cycle machines; the overall energy efficiency is approximately one-half, or less than that of gas- or oil-fired heaters.

The capital cost is the lowest of the three types, but the operating expense is, therefore, the highest, whereas maintenance costs are relatively low. The electrical heater is simple in construction, compact, and requires a smaller foundation. Heating elements can be easily replaced and no intermediate heat transfer fluid is required, a concern in freezing climates, which reduces maintenance costs.

Gas- or oil-fired heaters of this type are readily available and already in use throughout the world. An intermediate heat transfer fluid is generally used for safety purposes.

In cold climates, a mixture of ethylene glycol and water or equivalent prevents freezing, elevates the boiling temperature of the water, and reduces the heat exchanger surface area. The thermal efficiency of these units is reasonably high; about 80% of the heat generated is transferred to the gas and the remainder is discharged in the flue gas. Heat added to the gas fuel, however, reduces the quantity of fuel required by the gas turbine and offsets the fuel required by the heater to some extent.

Larger foundations are required for this type of heater, and several burners may be required in order to provide improved thermal response and turndown capabilities. Operating costs are significantly lower than an electrical heater, but maintenance and capital costs are higher. Difficulty in tracking rapid fuel demand changes of the gas turbine may be an issue for peaking units or during start-up.

Waste-heat-fired fuel heaters are an option for combined cycle units where low-grade heat (hot water) may be readily available. The advantage of this type of heater is that no fuel penalty is incurred and the overall thermal efficiency of the power plant may be increased. Disadvantages are higher capital cost, increased maintenance, and installation costs for larger foundations.

This type of a system is more suited for base-loaded units because of lack of heating during start-up. Usually a small supplementary boiler is used for start-up conditions. Construction is of the tube and shell type and is heavier than the indirect-fired heater to accommodate the 400 + psia/28 + bar pressurized water supply.

The gas clean-up systems described here are a minimum. The specific needs of each individual site must be carefully assessed, and the equipment and system design selected accordingly. It is not sufficient, however, to independently select equipment based on claimed high efficiency alone; the entire system must be evaluated and preferably modeled to determine the overall system sensitivity to changes in gas composition, pressure, temperature, and mass flow rate. It is important to remember that this is not a place where cost savings should be considered.

Cleaning of Turbine Components

A fuel treatment system will effectively eliminate corrosion as a major problem, but the ash in the fuel plus the added magnesium does cause deposits in the turbine. Intermittent operation of 100 hours or less offers no problem, since the character of the deposit is such that most of it sheds upon refiring, and no special cleaning is required.

However, the deposit does not reach a steady-state value with continuous operation and gradually plugs the first-stage nozzle area at a rate of between 5% and 12% per 100 hours. Thus, at present, residual oil use is limited to applications where continuous operation of more than 1,000 hours is not required.

If the need exists to increase running time between shutdowns, the turbine can be cleaned by the injection of a mild abrasive into the combustion system. Abrasives include walnut shells, rice, and spent catalyst. Rice is a very poor abrasive, since it tends to shatter into small pieces. Usually, a 10% maximum blockage of the first-stage nozzle is tolerated before abrasive cleaning is initiated. Abrasive cleaning will restore 20–40% of the lost power by removing 50% of the deposits. If the frequency of abrasive injection becomes unacceptable and cannot prevent the nozzle blockage from becoming more than 10%, water washing becomes necessary. Water or solvent washing can effectively restore 100% of the lost power. A typical operating plot is shown in Figure 12-13.

Hot Section Wash

The water washing of the hot section of the turbine is required for fuels with high vanadium contents. The addition of magnesium salts to encounter the corrosive action of the vanadium creates ash, which deposits on the blades reducing the flow area. This ash must be removed and in many cases this means that the hot section blades and nozzles must be washed every 100–120 hours. This is done by bringing the turbine down and running it on turning gear till the turbine blade temperatures are around 200 °F (93.3 °C), in most cases this is reached in about six to eight hours. The turbine hot expander section is then blasted by steam and most of the ash is removed. The turbine is then brought up to speed after the turbine blade section is dried. This whole process takes about 20 hours.

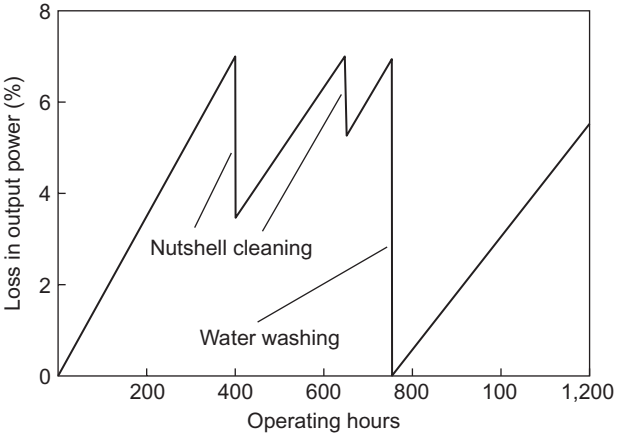


Figure 12-13 Effect of cleaning on power output.

Compressor Washing

Compressor washing is also a very important part of turbine operations. Two approaches to compressor cleaning are abrasion and solvent cleaning. The use of abrasive cleaning has diminished due to erosion problems, liquid washing is primarily used. The new high-pressure compressors are very susceptible to dirt on the blades that not only can lead to a reduction in performance but can also lead to compressor surge. Washing efficacy is site-specific due to the different environmental conditions at each plant. There are many excellent techniques and systems for water washing. Operators must often determine the best approach for their gas turbines. This includes what solvents if any should be used, and the frequencies of wash. Many operators have found that water wash without any solvent is as effective as with the use of solvents. This is a complex technical-economical problem also depending on the service that the gas turbines are in and the plant surroundings. However the use of non-demineralized water could result in more harm than good.

Water washing (with or without detergents) cleans by water impact and by removing the water-soluble salts. The effect of water cleaning is usually not very effective after the first few stages. It is most important that the manufacturer's recommendations be followed with respect to water wash quality, detergent/water ratio, and other operating procedures. Water washing using a water–soap mixture is an efficient method of cleaning. This cleaning is most effective when carried out in several steps, which involve the application of a soap and water solution, followed by several rinse cycles. Each rinse cycle involves the acceleration of the machine to approximately 50 percent of the starting speed, after which the machine is allowed to coast to a stop. A soaking period follows during which the soapy water solution may work on dissolving the salt.

A fraction of airborne salt always passes through the filter. The method recommended for determining whether or not the foulants have a substantial salt base is to soap wash the turbine and collect the water from all drainage ports available. Dissolved salts in the water can then be analyzed.

On-line washing is being widely used as a means to control fouling by keeping the problem from developing. Techniques and wash systems have evolved to a point where this can be done effectively and safely. Washing can be accomplished by using water, water-based solvents, petroleum-based solvents, or surfactants. The solvents work by dissolving the contaminants while surfactants work by chemically reacting with the foulants. Water-based solvents are effective against salt, but fare poorly against oily deposits. Petroleum-based solvents do not effectively remove salty deposits. With solvents, there is a chance of foulants being re-deposited in the latter compressor stages.

Even with good filtration, salt can collect in the compressor section. During the collection process of both salt and other foulants, an equilibrium condition is quickly reached, after which re-ingestion of large particles occurs. This re-ingestion has to be prevented by the removal of salt from the compressor prior to saturation. The rate at which saturation occurs is highly dependent on filter quality. In general, salts can safely pass through the turbine when gas and metal temperatures are less than 1000 °F.

Aggressive attacks will occur if the temperatures are much higher. During cleaning, the actual instantaneous rates of salt passage are very high together with greatly increased particle size.

The following are some tips that should be followed by operators during water washes:

- The water used should be demineralized. The use of non-demineralized water would harm the turbine.
- On-line wash should be done whenever compressor performance diminishes by 2–3%. It would be imprudent to let foulants build up before commencing water wash.
- Stainless steel for tanks, nozzles, and manifolds are recommended to reduce corrosion problems.
- Spray nozzles should be placed where proper misting of the water would occur, and minimize the downstream disturbance of the flow. Care should be taken that a nozzle would not vibrate loose and enter the flow passage.
- After numerous water washes, the compressor performance will deteriorate and a crank wash will be necessary.

Fuel Economics

Because gas turbine fuel properties are not the ones that determine cost, in some instances the better gas turbine fuel will sell for less than the poorer one. The selection of the most economical fuel depends on many considerations, of which fuel cost is but one. However, users should always burn the most *economical* fuel, which may not be the cheapest fuel.

Fuel properties must be known and economics considered before a fuel is selected. The properties of a fuel greatly affect the cost of a fuel treatment facility. A doubling of viscosity roughly doubles the cost of desalting equipment, and having a specific gravity of greater than .96 greatly complicates the washing system and raises costs. Trying to remove the last trace of a metallic element affects the cost of fuel washing approximately as shown in Table 12-8. The high cost of fuel treatment systems is the fuel washing system, since the ignition system costs about 10% of that amount. The fuel flow rate as well as the fuel type affect the fuel treatment system investment cost as shown in Figure 12-14.

Gas turbines, like other mechanical devices, require inspection, maintenance, and service. Maintenance costs include the combustion system, hot-gas path, and major

Table 12-8 Effect of Washed Fuel Quality on System Cost

Sodium Reduction	Washing System Cost
100 → 5 ppm Na	x dollars
100 → 2 ppm Na	2x dollars
100 → 1 ppm Na	4x dollars
100 → ½ ppm Na	8x dollars

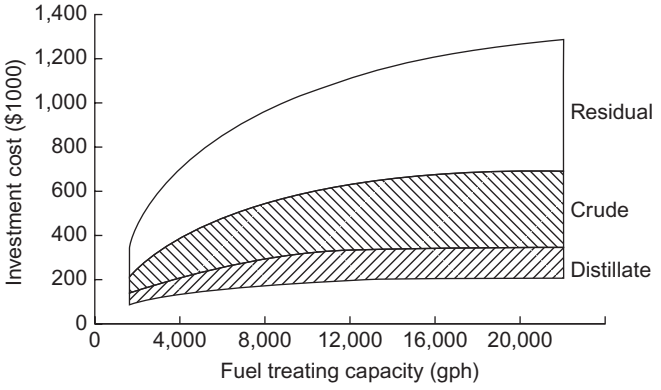


Figure 12-14 Gas turbine fuel treatment plant investment costs (Courtesy of General Electric Company).

Table 12-9 Average Total Maintenance and Cost Factor for a Gas Turbine

Fuel	Expected Actual Maintenance Cost (mils/kWh)	Expected Maintenance Cost Factor
Natural gas	0.3	1:0 = Base line
No. 2 distillate oil	0.4	1.25
Typical crude oil	0.6	2.0
No. 6 residual oil	1.0	3.33

Table 12-10 Economic Factors Influencing Fuel Selection

I.	*Fuel Cost*
II.	*Operation*
	1. Power output for given turbine
	2. Efficiency degradation
	3. Outstage (Downtime)
III.	*Capital Investment*
	1. Fuel washing and inhibition
	2. Fuel quality monitoring
	3. Turbine wash and cleaning
IV.	*Duty Cycle*
	1. Continuous duty required
	2. Total annual operation
	3. Starts and stops

inspections (See Chapter 21). The effect of fuel type on maintenance costs is shown in Table 12-9. A cost factor is shown using natural gas as unity. The cost of maintenance is subject to great variations. Recognizing the great difficulty in establishing expected

maintenance costs for different applications, Table 12-10 should be used as a rough guide in estimating costs. These data are based on actual maintenance costs for heavy-duty gas turbines.

As has been shown, the selection of the most economical fuel can depend on many factors besides cost. Table 12-9 summarizes the major economic considerations in fuel selection.

Operating Experience

Early US experience in residual operation dates back to the early 1950s. Several companies adapted gas turbines to run on residual fuel for locomotive application. Operating with a low inlet temperature 1350 °F (732 °C), low-sulfur residual corrosion was limited; however, it was noted that any increase in firing temperature was accompanied by serious corrosion. Because of the advantage of increased firing temperatures, research on fuel treatment was initiated. Eventually, the corrosion-causing materials were discovered, and a fuel treatment system to limit corrosion was developed.

Power plants in both peaking and standby modes achieved 30,000 hours between major overhauls. It was during these operations that the deposit problem on the turbine nozzles became apparent. Also, deposits developed on the fuel nozzles, a situation that could cause deviation in the fuel spray angle and related combustion problems. Therefore, both turbine and fuel nozzles needed frequent cleaning.

As discussed earlier, economic situations heavily dictate fuel selection. After the surge of interest in gas turbines in the early 1950s, use in the 1960s dwindled because of the cost, problems, and availability of natural gas. The 1990s have seen a tremendous growth in gas turbine usage with the advent of the high-efficiency gas turbines (40–45%), being used in Combined Cycle Power Plants, which have plant efficiencies between 55–60%. Most of these turbines were all driven by natural gas in 2000–2001, gas turbines were backordered for the next three to five years. All this growth in the turbine has been fueled by cheap natural gas at $3.50/mmBTU ($3.32/mmkJ). The cost of natural gas in late 2001 reached $9.0/mmBTU ($8.53/mmkJ), this helped to make alternative fuels interesting once again. Table 12-11 is an estimate of the world

Table 12-11 Typical Manufacturer's Fuel Data on Total Installed Horsepower

Fuel	Units %	% Hours of Operation	% Total hp
Natural gas	60	80	90
Dual fuel	22.5	8	4.0
Distillate oil	15	6	0.6
Residual oil	2.0	5	5
Crude oil	.2	.5	0.4
Other	0.3	.5	–

population of gas turbines, and it reflects the growth of natural gas driven gas turbines in the late 1990s and early 2000s.

Heat Tracing of Piping Systems

As mentioned earlier, heavy fuels need to be kept at a temperature where the viscosity of the fuel is limited to 20 centistokes at the fuel nozzles. Heat tracing is used to maintain pipes and the material that pipes contain at temperatures above the ambient temperature. Two common uses of heat tracing are preventing water pipes from freezing and maintaining fuel oil pipes at high enough temperatures such that the viscosity of the fuel oil will allow easy pumping. Heat tracing is also used to prevent the condensation of a liquid from a gas.

A study on a heat-tracing system is often more expensive on an installed cost basis than the piping system it is protecting, and it will also have significant operational costs. A study on heat-tracing costs showed installed costs of $31/ft ($95/meter) to $142/ft ($430/meter) and yearly operating cost of $1.40/ft ($4.35/meter) to $16.66/ft ($50/meter). In addition to being a major cost, the heat-tracing system is an important component of the reliability of a piping system. A failure in the heat-tracing system will often render the piping system inoperable. For example, with a water freeze protection system; the piping system may be destroyed by the expansion of water as it freezes if the heat-tracing system fails.

The vast majority of heat-traced pipes are insulated to minimize heat loss to the environment. A heat input of two to 10 watts per foot (six to 30 watts per meter) is generally required to prevent an insulated pipe from freezing. With high wind speeds, an un-insulated pipe could require well over 100 watts per foot (300 watts per meter) to prevent freezing. Such a high heat input would be very expensive.

Heat tracing for insulated pipes is generally only required for the period when the material in the pipe is not flowing. The heat loss of an insulated pipe is very small compared to the heat capacity of a flowing fluid. Unless the pipe is extremely long (several thousands of feet or meters), the temperature drop of a flowing fluid will not be significant.

The three major methods of avoiding heat tracing are:

1. Changing the ambient temperature around the pipe to a temperature that will avoid low-temperature problems. Burying water pipes below the frost line or running them through a heated building are the two most common examples of this method.
2. Emptying a pipe after it is used. Arranging the piping such that it drains itself when not in use can be an effective method of avoiding the need for heat tracing. Some infrequently used lines can be pigged or blown out with compressed air. This technique is not recommended for commonly used lines due to the high labor requirement.
3. Arranging a process such that some lines have continuous flow can eliminate the need for tracing these lines. This technique is generally not recommended because a failure that causes a flow stoppage can lead to blocked or broken pipes.

Some combination of these techniques may be used to minimize the quantity of traced pipes. However, the majority of pipes containing fluids that must be kept above the minimum ambient temperature are generally going to require heat tracing.

Types of Heat-Tracing Systems

Industrial heat-tracing systems are generally fluid systems or electrical systems. In fluid systems, a pipe or tube called the tracer is attached to the pipe being traced, and a warm fluid is put through it. The tracer is placed under the insulation. Steam is by far the most common fluid used in the tracer, although ethylene glycol and more exotic heat-transfer fluids are used. In electrical systems, an electrical heating cable is placed against the pipe under the insulation.

Stream Tracing Systems

Steam tracing is the most common type of industrial pipe tracing. In 1960, over 95 percent of industrial tracing systems were steam traced. By 1995, improvements in electric heating technology increased the electric share from 30 to 40 percent, but steam tracing is still the most common system. Fluid systems other than steam are rather uncommon and account for less than 5% of tracing systems.

Half-inch (12.7 mm) copper tubing is commonly used for steam tracing. Three-eighths-inch (9.525 mm) tubing is also used, but the effective circuit length is then decreased from 150 feet (50 meters) to about 60 feet (20 meters). In some corrosive environments, stainless steel tubing is used, and occasionally standard carbon steel pipe ($\frac{1}{2}$–1 inch) is used as the tracer.

In addition to the tracer, a steam tracing system as seen in Figure 12-15, consists of steam supply lines to transport steam from the existing steam lines to the traced pipe, a steam trap to remove the condensate and hold back the steam, and in most

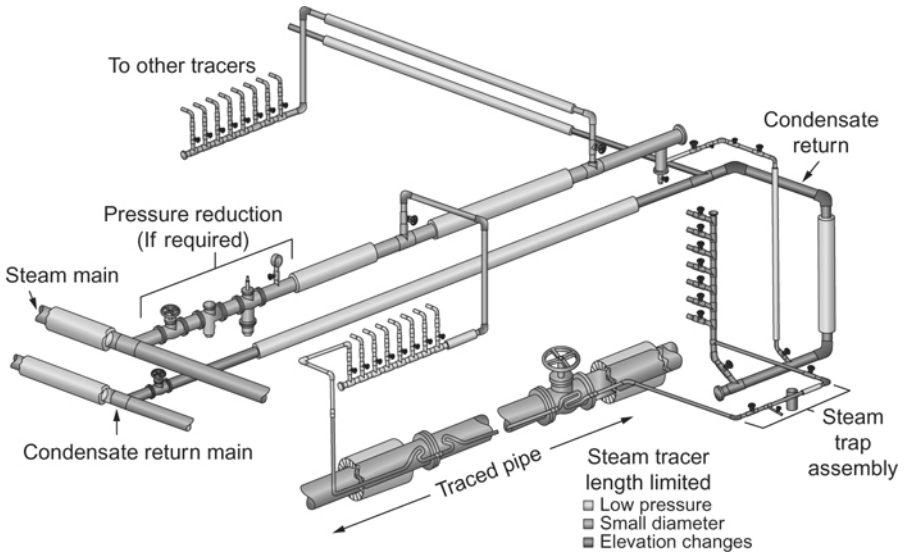


Figure 12-15 Steam tracing system.

cases a condensate return system to return the condensate to the existing condensate return system. In the past, a significant percentage of condensate from steam tracing was simply dumped to drains, but increased energy cost and environmental rules have caused almost all condensate from new steam tracing systems to be returned. This has significantly increased the initial cost of steam tracing systems.

Applications requiring accurate temperature control are generally limited to electric tracing. For example, chocolate lines cannot be exposed to steam temperatures or the product will degrade, and if caustic soda is heated above 150 °F (66 °C), it becomes extremely corrosive to carbon steel pipes.

For some applications, either steam or electricity is simply not available and this makes the decision. It is rarely economical to install a steam boiler just for tracing. Steam tracing is generally considered only when a boiler already exists or is going to be installed for some other primary purpose. Additional electric capacity can be provided in most situations for reasonable costs. It is considerably more expensive to supply steam from a long distance than it is to provide electricity. Unless steam is available close to the pipes being traced, the automatic choice is usually electric tracing.

Electric Tracing

An electric tracing system as seen in Figure 12-16 consists of an electric heater placed against the pipe under the thermal insulation, the supply of electricity to the tracer, and any control or monitoring system that may be used (optional). The supply of electricity to the tracer usually consists of an electrical panel and electrical conduit or cable trays. Depending on the size of the tracing system and the capacity of the existing electrical system, an additional transformer may be required.

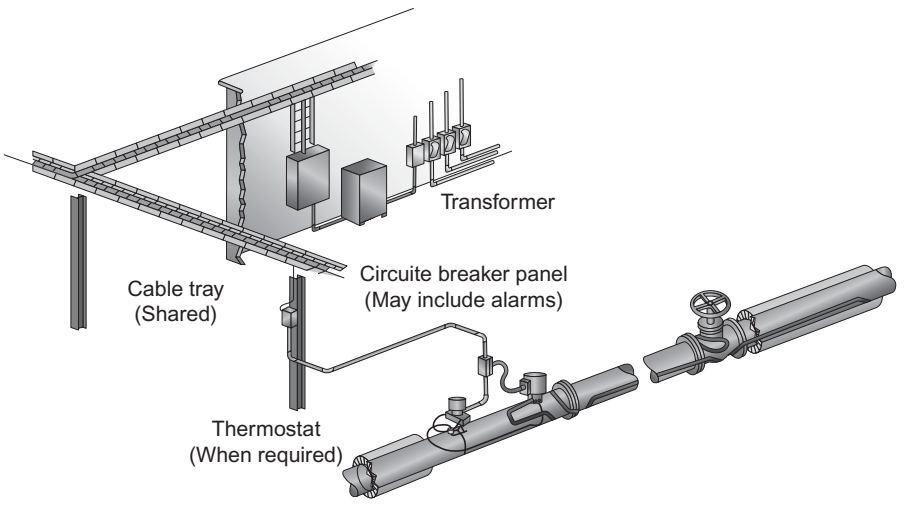


Figure 12-16 Electric heat tracing system.

Storage of Liquids

Atmospheric Tanks

The term atmospheric tank as used here applies to any tank that is designed to be used within plus or minus a few pounds per square foot (a few tenths of a Bar) of atmospheric pressure. It may be either open to the atmosphere or enclosed. Minimum cost is usually obtained with a vertical cylindrical shape and a relatively flat bottom at ground level.

Elevated Tanks

These can supply a large flow when required, but pump capacities need be only for average flow. Thus, they may save on pump and piping investment. They also provide flow after pump failure, an important consideration for fire systems.

Open Tanks

These may be used to store materials that will not be harmed by water, weather, or atmospheric pollution. Otherwise, a roof, either fixed or floating, is required. Fixed roofs are usually either domed or coned. Large tanks have coned roofs with intermediate supports. Since negligible pressure is involved, snow and wind are the principal design loads. Local building codes often give required values.

Fixed Roof Tanks

Atmospheric tanks require vents to prevent pressure changes, which would otherwise result from temperature changes and the withdrawal or the addition of liquid. API Standard 2000, venting atmospheric and Low Pressure Storage Tanks, gives practical rules for vent design. The principals of this standard can be applied to fluids other than petroleum products. Excessive losses of volatile liquids, particularly those with flash points below 100 °F (38 °C), may result from the use of open vents on fixed roof tanks. Sometimes vents are manifolded and led to a vent tank, or the vapor may be extracted by a recovery system.

An effective way of preventing vent loss is to use one of the many types of variable-volume tanks. These are built under API Standard 650. They may have floating roofs of the double-deck or the single-deck type. There are lifter-roof types in which the roof either has a skirt moving up and down in an annular liquid seal or is connected to the tank shell by a flexible membrane. A fabric expansion chamber housed in a compartment on top of the tank roof also permits variation in volume.

Floating Roof Tanks

These tanks must have a seal between the roof and the tank shell. If not protected by a fixed roof, they must have drains for the removal of water, and the tank shell must have a “wind girder” to avoid distortion. An industry has developed to retrofit

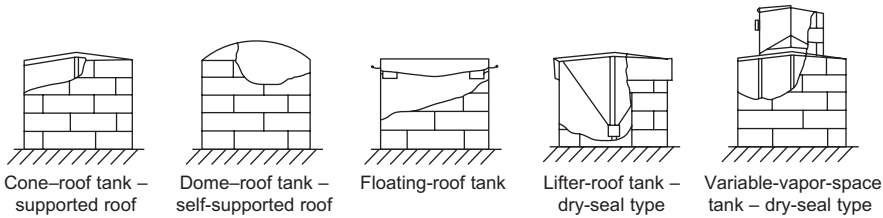


Figure 12-17 Some types of atmospheric storage tanks.

existing tanks with floating roofs. Much detail on the various types of tank roofs is given in manufacturers' literature. Figure 12-17 shows types. These roofs cause less condensation buildup and are highly recommended.

Pressure Tanks

Vertical cylindrical tanks constructed with domed or coned roofs, which operate at pressures above 15 psia (1 Bar) but are still relatively close to atmospheric pressure, can be built according to API Standard 650. The pressure force acting against the roof is transmitted to the shell, which may have sufficient weight to resist it. If not, the uplift will act on the tank bottom. The strength of the bottom, however, is limited, and if it is not sufficient, an anchor ring or a heavy foundation must be used. In the larger sizes, uplift forces limit this style of tank to very low pressures.

Bibliography

Bahr, D.-W., Smith, J.R., and Kenworthy, N.J., "Development of Low Smoke Emission Combustors for Large Aircraft Turbine Engines," AIAA Paper Number 69–493, 1969.

Boyce, M.P., "Chapter 10. Transport and Storage of Fluids-Process-Plant Piping," *Perm's Chemical Engineers' Handbook*, 7th Edition, 1997.

Boyce, M.P., Trevillion, W., and Hoehing, W.W., "A New Gas Turbine Fuel," *Diesel & Gas Turbine Progress*, March 1978 (Reprint).

Boyce, M.P., Trevillion, W., and Hoehing, W.W., "A New Gas Turbine Fuel," *Diesel & Gas Turbine Progress*, March 1978 (Reprint).

Brown Boveri Turbomachinery, Inc., "MEGA PAK CT, The simple cycle combustion turbine plant designed for today's energy needs," Pub. No. 4875-BIO-7610.

"Characterization and Measurement of Natural Gas Trace Constituents, Vol II: Natural Gas Survey," Gas Research Institute Report GRI-94/0243.2.

Combustors for Large Aircraft Turbine Engines, AIAA Paper Number 69-4931. Federal Energy, 1969.

C. Wilkes, "Gas Fuel Clean-Up System Design Considerations for GE Heavy Duty Gas Turbines," GER 3942 GE Power, 1996.

Deaton and Frost, "Apparatus for Determining the Dew Point of Gases Under Pressure," Bureau of Mines, May 1938.

"Gas Sampling for Accurate Btu, Specific Gravity and Compositional Analysis Determination," Welker, Natural Gas Quality and Energy Measurement Symposium, 5–6 Feb, 1996, published by The Institute of Gas Technology.

"Gas Turbine Fuels," ANS1/ASME B133.7M, 1985, reaffirmed in 1992. An American National Standard published by the American Society of Mechanical Engineers, United Engineering Center, New York.

GE Power "Process Specification: Fuel Gases for Combustion in Heavy-Duty Gas Turbines," GEI41040E, GE, 1994.

"GPA Method for Standard Gas Analysis, C1-C6+," GPA 2261-95.

"Method for Analysis of Natural Gas by Gas Chromatography," ASTM method D1945-81, 1945.

"Method for Extended Gas Analysis Cl-C14," GPA 2286-95 GPA.

"Obtaining Natural Gas Samples for Analysis by Gas Chromatography," GPA Standard 2166-85, 1992.

"Variability of Natural Gas Composition in Select Major Metropolitan Areas of the United States," Liss, Thrasher, Steinmetz, Chowdiah and Attari, Gas Research Institute Report, GRI-92/0123, 1992.

Copyrighted Materials
Copyright © 2012 Elsevier Retrieved from www.knovel.com

Part IV

Auxiliary Components and Accessories

13 Bearings and Seals

Bearings

The bearings in gas and steam turbines provide support and positioning for the rotating components. Radial support is generally provided by journal, or roller bearings, and axial positioning is provided by thrust bearings. Some engines, mainly aircraft jet engines, use ball or roller bearings for radial support, but nearly all-industrial gas turbines use journal bearings.

A long service life, a high degree of reliability, and economic efficiency are the chief aims when designing bearing arrangements. To reach these criteria, design engineers examine all the influencing factors:

1. Load and speed
2. Lubrication
3. Temperatures
4. Shaft arrangements
5. Life
6. Mounting and dismounting
7. Noise
8. Environmental conditions

Rolling Bearings

The aero-derivative gas turbine design, with its low-supported weight rotors – for example, the LM 5,000 HP rotor weights 1,230 lbs (558 kg) – incorporates roller bearings throughout. These do not require the large lube oil reservoirs, coolers and pumps, or the pre- and post-lube cycle associated with journal bearing designs. Roller bearings have proven to be extremely rugged and have demonstrated excellent life in industrial service. Most bearings provide reliable service for over 100,000 hours. In practice, it is advisable to replace bearings when exposed during major repairs, estimated at 50,000 hours for gas generators and 100,000 hours for power turbines.

There are many roller bearing types. They are differentiated according to the direction of the main radial loads (radial bearings) or axial loads (thrust bearings), and the type of rolling elements used, balls or rollers. Figure 13-1 shows the different types of bearings. The essential difference between ball bearings and roller bearings are that ball bearings have a lower carrying capacity and higher speeds, while roller bearings have higher load carrying capacity and lower speeds.

Gas Turbine Engineering Handbook, Fourth Edition. DOI: 10.1016/B978-0-12-383842-1.00013-5
Copyright © 2012 Elsevier Inc. All rights reserved.

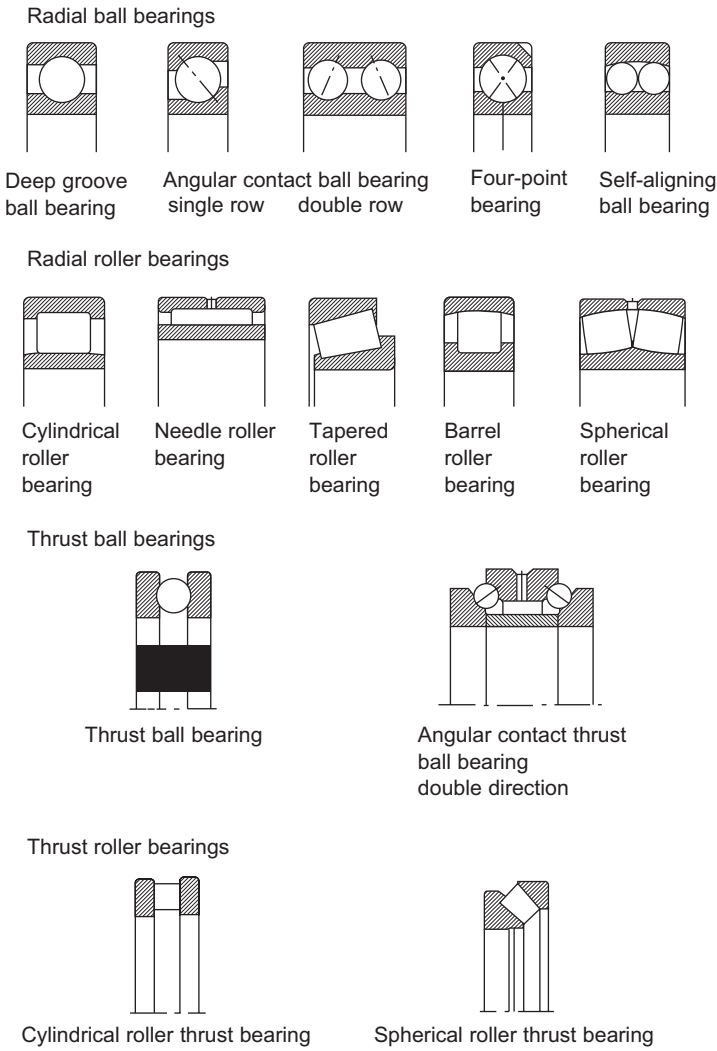


Figure 13-1 Types of rolling bearings (courtesy FAG bearings).

The rolling elements transmit loads from one bearing ring to the other in the direction of the contact lines. The contact angle α is the angle formed by the contact lines and the radial plane of the bearing. α refers to the nominal contact angle, i.e., the contact angle of the load-free bearing as seen in Figure 13-2. Under axial loads, the contact angle of deep groove ball bearings, angular contact ball bearings, etc., increases. Under a combined load it changes from one rolling element to the next. These changing contact angles are taken into account when calculating the pressure distribution within the bearing. Ball bearings and roller bearings with symmetrical rolling elements have identical contact angles at their inner rings and outer rings. In roller bearings with asymmetrical rollers,

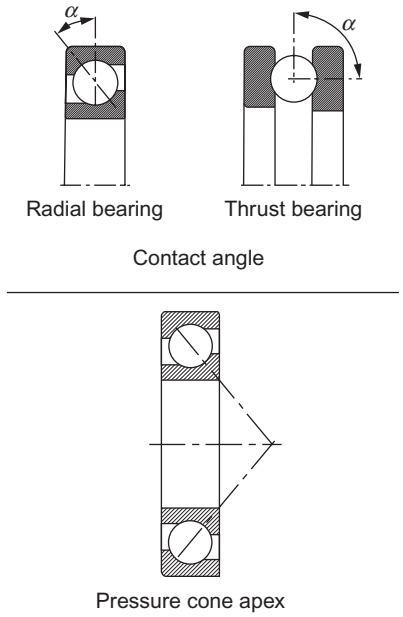
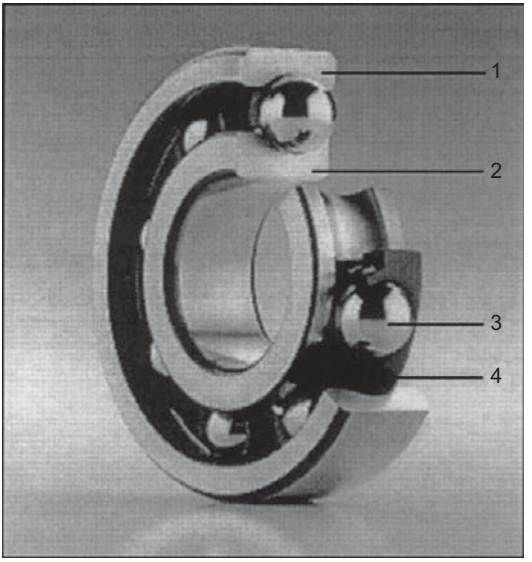


Figure 13-2 Rolling bearing terminology (courtesy FAG bearings).

the contact angles at the inner rings and outer rings are not identical. The equilibrium of forces in these bearings is maintained by a force component, which is directed towards the lip. The pressure cone apex is that point on the bearing axis where the contact lines of an angular contact bearing (i.e., an angular contact ball bearing, a tapered roller bearing, or a spherical roller thrust bearing) intersect. The contact lines are the generatrices of the pressure cone apex. In angular contact bearings, the external forces act, not at the bearing center, but at the pressure cone apex.

Rolling bearings generally consist of bearing rings, inner ring and outer ring, rolling elements that roll on the raceways of the rings, and a cage that surrounds the rolling elements as seen in Figure 13-3. The rolling elements are classified according to their shapes, into: balls, cylindrical rollers, needle rollers, tapered rollers, and barrel rollers as shown in Figure 13-4.

The rolling elements' function is to transmit the force acting on the bearing from one ring to the other. For a high load carrying capacity it is important that as many rolling elements as possible, which are as large as possible, are accommodated between the bearing rings. Their number and size depend on the cross section of the bearing. It is just as important for load ability that the rolling elements within the bearing are of identical size. Therefore, they are sorted according to grades. The tolerance of one grade is very slight. The generatrices of cylindrical rollers and tapered rollers have a logarithmic profile. The center part of the generatrix of a needle roller is straight, and the ends are slightly crowned, this profile prevents edge stressing when under load.



(1) Outer ring (2) Inner ring (3) Rolling element and (4) Cage

Figure 13-3 Roller bearing showing the various components (courtesy FAG Bearings).

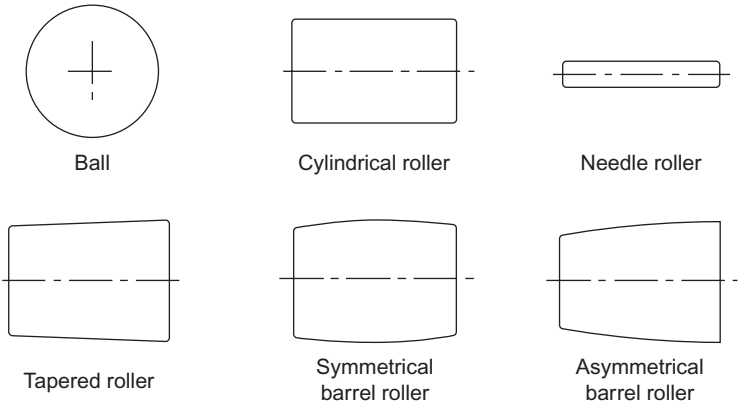


Figure 13-4 Various types of rollers used in a rolling bearing (courtesy FAG bearings).

The bearing rings comprise an inner ring and an outer ring to guide the rolling elements in the direction of rotation. Raceway grooves, lips, and inclined running areas guide the rollers and transmit axial loads in a transverse direction as seen in Figure 13-5. Cylindrical roller bearings and needle roller bearings, which need to accommodate shaft expansions have lips only on one bearing ring and are commonly known as floating bearings.

The functions of a cage are to keep the rolling elements apart so that they do not rub against each other, to keep the rolling elements evenly spaced for uniform load

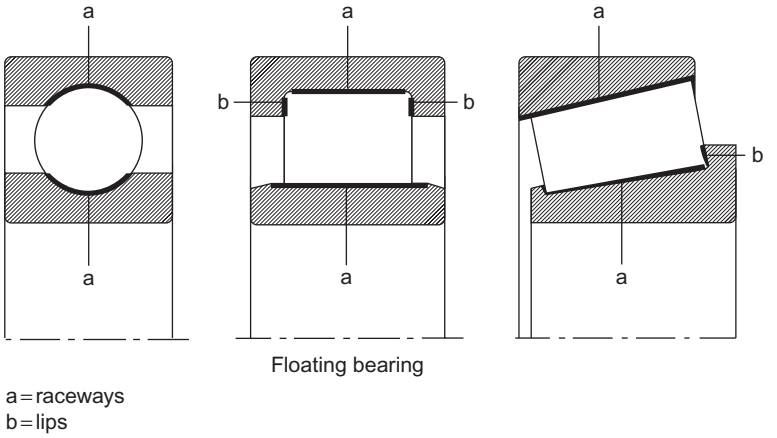


Figure 13-5 Raceway grooves and lips for typical roller bearings (courtesy FAG bearings).

distribution, to prevent rolling elements from falling out of separable bearings and bearings that are swiveled out, and to guide the rolling elements in the unloaded zone of the bearing. The transmission of forces is not one of the cage's functions.

Cages are classified into pressed cages, machined cages, and molded cages. Pressed cages are usually made of steel, but sometimes of brass too. They are lighter than machined metal cages. Since a pressed cage barely closes the gap between the inner ring and outer ring, lubricant can easily penetrate into the bearing.

Machined cages of metal and textile laminated phenolic resin are made from tubes of steel, light metal or textile laminated phenolic resin, or cast brass rings. To obtain the required strength, large, heavily loaded bearings are fitted with machined cages. Machined cages are also used where lip guidance of the cage is required. Lip-guided cages for high-speed bearings are, in many cases, made of light materials such as light metal or textile laminated phenolic resin to keep the forces of gravity low.

Molded cages using injection molding techniques can realize designs with an especially high-load carrying capacity. The elasticity and low weight of the cages are of advantage where shock-type bearing loads, great accelerations and decelerations as well as tilting of the bearing rings relative to each other have to be accommodated. Polyamide cages feature very good sliding and dry running properties.

There are a number of special rolling bearing designs and some series of cylindrical roller bearings without cages. By omitting the cage the bearing can accommodate more rolling elements. This yields an increased load rating, but, due to the increased friction, the bearing is suitable for lower speeds only.

Load ratings

The load rating of a bearing reflects its load carrying capacity and is an important factor in the dimensioning of rolling bearings. It is determined by the number and size of the rolling elements, the curvature ratio, the contact angle, and the pitch circle

diameter of the bearing. Due to the larger contact area between rollers and raceways the load ratings of roller bearings are higher than those of ball bearings.

The load rating of a radial bearing is defined by radial loads whereas that of a thrust bearing is defined by axial loads. Every rolling bearing has a dynamic load rating and a static load rating. The terms "dynamic" and "static" refer to the movement of the bearing but not to the type of load.

In all rolling bearings with a curved raceway profile, the radius of the raceway is slightly larger than that of the rolling elements. This curvature difference in the axial plane is defined by the curvature ratio x. The curvature ratio is the curvature difference between the rolling element radius and the slightly larger groove radius:

$$\text{radius curvature ratio } x = (\text{groove radius} - \text{rolling element})/\text{rolling element radius}$$

Thrust ball bearings are used where purely axial loads have to be accommodated. The single direction (= single row) design is designed for loads from one direction, the double direction one (= double row) for reversing loads. Besides the design with flat washers, designs with spherical housing washers and seating washers are also available that can compensate for misalignment.

Spherical roller thrust bearings can accommodate high axial loads. They are suitable for relatively high speeds. The raceways, which are inclined toward the bearing axis, allow the bearings to accommodate radial loads as well. The radial load must not exceed 55% of the axial load.

The bearings have asymmetrical barrel rollers and compensate for misalignment. As a rule, spherical roller thrust bearings have to be lubricated with oil.

Wear

The life of rolling bearings can be terminated, apart from fatigue, as a result of wear. The clearance of a worn bearing gets too large.

One frequent cause of wear is that foreign particles penetrate into a bearing due to insufficient sealing and have an abrasive effect. Wear is also caused by starved lubrication and when the lubricant is used up.

Therefore, wear can be considerably reduced by providing good lubrication conditions (viscosity ratio $x > 2$ if possible) and a good degree of cleanliness in the rolling bearing. Where $x \leq 0.4$ wear will dominate in the bearing if it is not prevented by suitable additives (EP additives).

The kinematically permissible speed may be higher or lower than the thermal reference speed. The basis of the thermal reference speed is for cases where the operating conditions (load, oil viscosity, or permissible temperature) deviate from the reference conditions. Decisive criteria for the kinematically permissible speed are the strength limit of the bearing parts and the permissible sliding velocity of rubbing seals. Kinematically permissible speeds, which are higher than the thermal reference speeds, can be reached, for example, with specially designed lubrication, bearing clearance

adapted to the operating conditions, and accurate machining of the bearing seats with special regard to heat dissipation.

The thermal reference speed is a new index of the speed suitability of rolling bearings. It is defined as the speed at which the reference temperature of 160 °F (70 °C) is established. For high temperature rolling bearings, the steel used for bearing rings and rolling elements is generally heat-treated so that it can be used at operating temperatures of up to 300 °F (150 °C). At higher temperatures, dimensional changes and hardness reductions result. Therefore, operating temperatures over 300 °F (150 °C) require special heat treatment.

Journal Bearings

The heavy frame type gas turbines use journal bearings. Journal bearings may be either full round or split; the lining may be heavy as used in large-size bearings for heavy machinery, or thin, as used in precision insert-type bearings in internal combustion engines. Most sleeve bearings are of the split type for convenience in servicing and replacement. Often in split bearings, where the load is entirely downward, the top half of the bearing acts only as a cover to protect the bearing and to hold the oil fittings. Figure 13-6 shows a number of different types of journal bearings. A description of a few of the pertinent types of journal bearings is given here:

1. *Plain journal.* Bearing is bored with equal amounts of clearance (on the order of 1½ to two thousands of an inch per inch of journal diameter) between the journal and bearing.
2. *Circumferential grooved bearing.* Normally has the oil groove at half the bearing length. This configuration provides better cooling, but reduces load capacity by dividing the bearing into two parts.
3. *Cylindrical bore bearings.* Another common bearing type used in turbines. It has a split construction with two axial oil-feed grooves at the split.
4. *Pressure or pressure dam.* Used in many places where bearing stability is required, this bearing is a plain journal bearing with a pressure pocket cut in the unloaded half. This pocket is approximately 1/32 of an inch (.8 mm) deep with a width 50% of the bearing length. This groove or channel covers an arc of 135 ° and terminates abruptly in a sharp-edge dam. The direction of rotation is such that the oil is pumped down the channel toward the sharp edge. Pressure dam bearings are for one direction of rotation. They can be used in conjunction with cylindrical bore bearings as shown in Figure 13-6.
5. *Lemon bore or elliptical.* This bearing is bored with shims at the split line, which are removed before installation. The resulting bore shape approximates an ellipse with the major axis clearance approximately twice the minor axis clearance. Elliptical bearings are for both directions of rotation.
6. *Three-lobe bearing.* The three-lobe bearing is not commonly used in turbomachines. It has a moderate load-carrying capacity and can be operated in both directions.
7. *Offset halves.* In principle, this bearing acts very similar to a pressure dam bearing. Its load-carrying capacity is good. It is restricted to one direction of rotation.
8. *Tilting-pad bearings.* This bearing is the most common bearing type in today's machines. It consists of several bearing pads posed around the circumference of the shaft. Each pad is able to tilt to assume the most effective working position. Its most important feature is

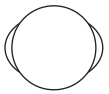
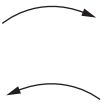
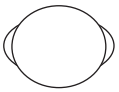
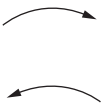
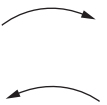
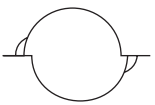
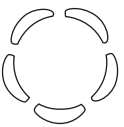
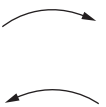
Bearing type	Load capacity	Suitable direction of rotation	Resistance to half-speed whirl	Stiffness and damping
Cylindrical bore 	Good		Worst	Moderate
Cylindrical bore with dammed groove 	Good			Moderate
Lemon bore 	Good			Moderate
Three lobe 	Moderate		Increasing	Good
Offset halves 	Good			Excellent
Tilting pad 	Moderate		Best	Good

Figure 13-6 Comparison of general bearing types.

self-alignment when spherical pivots are used. This bearing also offers the greatest increase in fatigue life because of the following advantages:

a. Self-aligning for optimum alignment and minimum limit.

b. Thermal conductivity backing material to dissipate heat developed in oil film.

c. A thin babbitt layer can be centrifugally cast with a uniform thickness of about 0.005 of an inch (0.127 mm). Thick babbitts greatly reduce bearing life. Babbitt thickness in the neighborhood of .01 in. (.254 mm) reduce the bearing life by more than half.
d. Oil film thickness is critical in bearing stiffness calculations. In a tilting-pad bearing, one can change this thickness in a number of ways: (1) changing the number of pads; (2) directing the load on or in between the pads; (3) and changing axial length of pad.

The previous list contains some of the most common types of journal bearings. They are listed in the order of growing stability. All of the bearings designed for increased stability are obtained at higher manufacturing costs and reduced efficiency. The antiwhirl bearings all impose a parasitic load on the journal, which causes higher power losses to the bearings, and in turn, requires higher oil flow to cool the bearing. Many factors enter into the selection of the proper design for bearings. Some of the factors that affect bearing design follow:

1. Shaft speed range.
2. Maximum shaft misalignment that can be tolerated.
3. Critical speed analysis and the influence of bearing stiffness on this analysis.
4. Loading of the compressor impellers.
5. Oil temperatures and viscosity.
6. Foundation stiffness.
7. Axial movement that can be tolerated.
8. Type of lubrication system and its contamination.
9. Maximum vibration levels that can be tolerated.

Bearing Design Principles

The journal bearing is a fluid-film bearing. This description means that a full film of fluid completely separates the stationary bushing from the rotating journal – the two components that make up the bearing system. This separation is achieved by pressurizing the fluid in the clearance space to the extent that the fluid forces a balance in the bearing load. This balance requires the fluid to be continuously introduced into and pressurized in the film space. Figure 13-7 shows the four modes of lubrication in a fluid-film bearing. The hydrodynamic mode bearing is the most common bearing type used and is also often called the "self-acting" bearing.

As can be seen in Figure 13-7 (a), the pressure is self-induced by the relative motion between the two bearing member surfaces. The film is wedge-shaped in this type of lubrication mode. Figure 13-7 (b) shows the hydrostatic mode of lubrication. In this type of a bearing, the lubricant is pressurized externally and then introduced in the bearing. Figure 13-7 (c) shows the squeeze-film lubrication mode. This type of a bearing derives its load-carrying capacity and separation from the fact that a viscous fluid cannot be instantaneously squeezed out between two surfaces that are approaching each other. Figure 13-7 (d) shows a hybrid-type bearing that combines the previous modes. The most common hybrid type combines the hydrodynamic and hydrostatic modes.

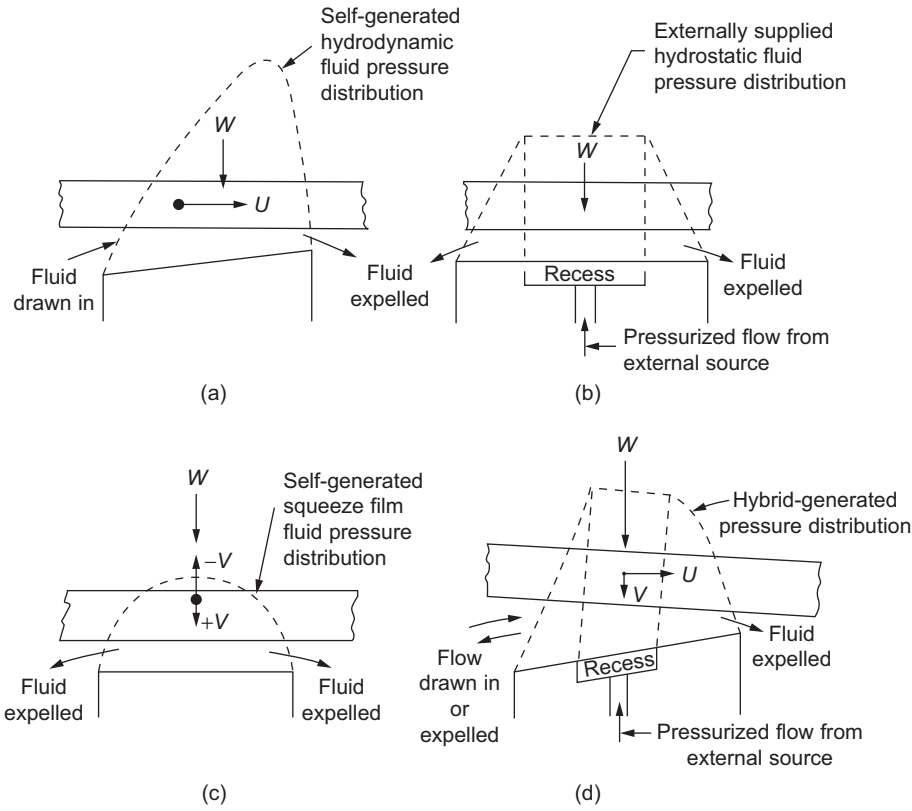


Figure 13-7 Modes of fluid-film lubrication: (a) hydrodynamic, (b) hydrostatic, (c) squeeze film, (d) hybrid.

A further investigation of the hydrodynamic mode is warranted, since it is the most common type of lubrication mode employed. This type of lubrication depends on the bearing member velocity as well as the existence of a wedge-shaped configuration. The journal bearing forms a natural wedge as seen in Figure 13-8, which is inherent in its design. Figure 13-3 also shows the pressure distribution in the bearing. Fluid-film thickness depends on the mode, lubrication, and application and varies from .0001 to .01 inches (.00254–.254 mm). For hydrostatic oil-lubricated bearings, the film thickness is .008 of an inch (.203 mm). In the special case of oil-squeeze film bearings where the capacity must be provided to take extremely high-revising loads with no bearing harm, the oil-film thickness could be below .0001of an inch (.00254 mm). Since the film thickness is so very important, an understanding of the surface is also vital.

All surfaces, regardless of their finish, are made up of peaks and valleys, and in general, the average asperity height may be 5–10 times the RMS surface finish reading. When the surface is abraded, an oxide film will form almost immediately.

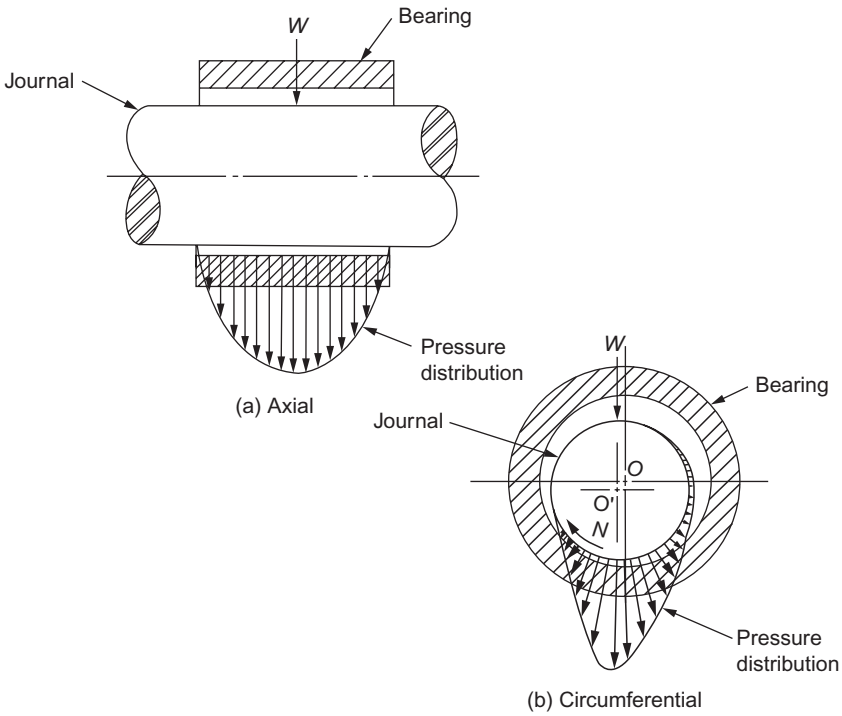


Figure 13-8 Pressure distribution in a full journal bearing.

Figure 13-9 (a) shows the relative separation of the full-film, mixed-film, and boundary. If a full-film exists, the bearing life is almost infinite. The limitation in the case of full-film is due to lubricant breakdown, shock load, bearing surface erosion, and fretting of bearing components. Figures 13-9 (b) and 13-9 (c) are cross sections showing the various contamination types. Oil additives are contaminants that form beneficial surface films.

The bearing health can be best described by plotting a *ZN/P* versus coefficient of friction curve. Figure 13-10 shows such a curve where *Z* is the lubricant viscosity in centipoise, *N* the rpm of the journal, and *P* is the projected area unit loading.

As the bearing speed is increased for a given lubricant and loading, the friction is at its lowest when full-film is achieved, after which the increase is due to the increasing lubricant shear force.

The bearing fluid film acts like a spring that is nonlinear. Figure 13-11 shows a curve of bearing load versus film thickness and eccentricity ratio. The bearing stiffness can then be obtained at any load value by drawing a line tangent to the curve at the load point. The film stiffness can then be used in determining the critical speed of the rotor.

With higher speeds and unusual fluid lubricants, turbulence in the fluid film is no longer rare. Normally, thin film is thought of as being laminar, but with high speeds,

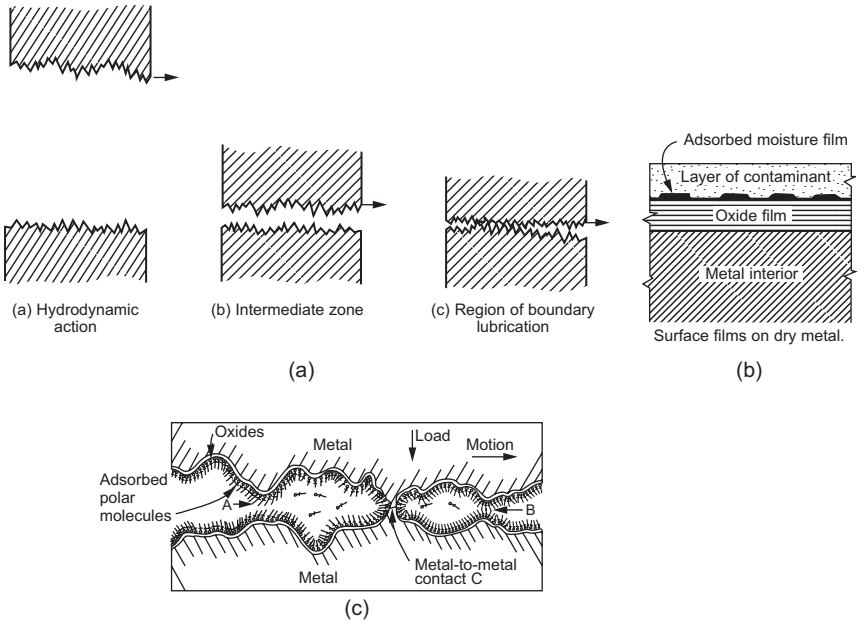


Figure 13-9 Enlarged views of bearing surfaces.

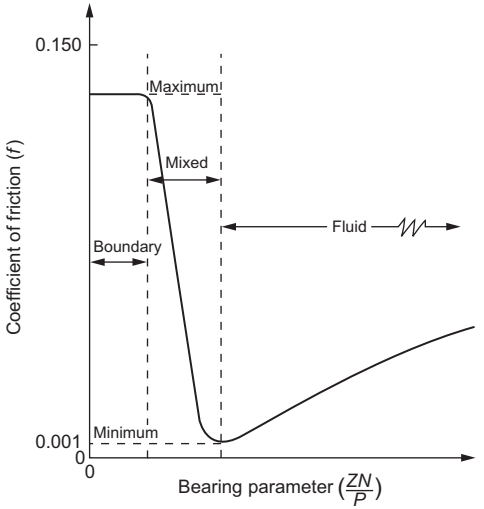


Figure 13-10 Classic *ZN/P* curve.

low viscosity, and sometimes high-density fluids, the lubricant can be turbulent in the film space. This turbulence manifests itself as an abnormal increase in power loss. As compared to laminar-flow conditions, a Reynolds number, even in the transition region, can double the power and, deep in the turbulent region, can increase the power tenfold. Although this phenomenon, because of its random nature, is difficult to

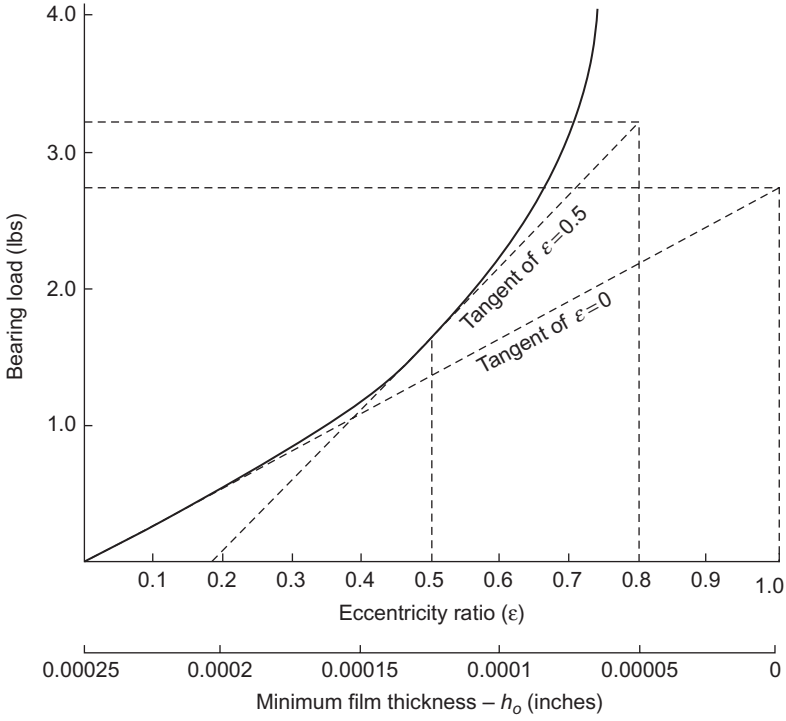


Figure 13-11 Journal bearing load capacity versus minimum film thickness and eccentricity ratio.

analyze, there is an unusual amount of theoretical work that has been done and some experimental work that is available. Just as a guide, one can assume that the transition point will occur at a Reynolds number of about 800. As to film thickness, there is evidence indicating that under turbulent conditions it is actually greater than calculated, based on laminar-flow theory.

Tilting-Pad Journal Bearings

Normally, the tilting-pad journal bearing is considered when shaft loads are light because of its inherent ability to resist oil whirl vibration. However, this bearing, when properly designed, has a very high load-carrying capacity. It has the ability to tilt to accommodate the forces being developed in the hydrodynamic oil film, and therefore operates with an optimum oil-film thickness for the given load and speed. This ability to operate over a large range of loads is especially useful in high-speed gear reductions with various combinations of input and output shafts.

Another important advantage of the tilting-pad journal bearing is its ability to accommodate shaft misalignment. Because of its relatively short length-to-diameter ratio, it can accommodate minor misalignment quite easily.

As shown earlier, bearing stiffness varies with the oil-film thickness so that the critical speed is directly influenced to a certain degree by oil-film thickness. Again, in the area of critical speeds, the tilting-pad journal bearing has the greatest degree of design flexibility. There are sophisticated computer programs that show the influence of various load and design factors on the stiffness of tilting-pad journal bearings. The following variations are possible in the design of tilting-pad bearings:

1. The number of pads can be varied from three to any practical number.
2. The load can be placed either directly on a pad or to occur between pads.
3. The unit loading on the pad can be varied by either adjusting the arc length or the axial length of the bearing pad.
4. A parasitic pre-load can be designed into the bearing by varying the circular curvature of the pad with respect to the curvature of the shaft.
5. An optimum support point can be selected to obtain a maximum oil-film thickness.

On a high-speed rotor system, it is necessary to use tilting-pad bearings because of the dynamic stability of these bearings. A high-speed rotor system operates at speeds above the first critical speed of the system. It should be understood that a rotor system includes the rotor, the bearings, the bearing support system, seals, couplings, and other items attached to the rotor. The system's natural frequency is therefore dependent on the stiffness and damping effect of these components.

Commercial multipurpose tilting-pad bearings are usually designed for multidirectional rotation so that the pivot point is at pad midpoint. However, the design criteria generally applied for producing maximum stability and load-carrying capacity locates the pivot at two-thirds of the pad arc in the direction of rotation.

Bearing pre-load is another important design criterion for tilting-pad bearings. Bearing pre-load is bearing assembly clearance divided by machined clearance:

$$\text{Pre-load ratio} = C'/C = \frac{\text{Concentric pivot film thickness}}{\text{Machined clearance}}$$

A pre-load of 0.5–1.0 provides for stable operation because a converging wedge is produced between the bearing journal and the bearing pads.

The variable C' is an installed clearance and is dependent upon the radial pivot position. The variable C is the machine clearance and is fixed for a given bearing. Figure 13-7 shows two pads of a five-pad tilting-pad bearing where the pads have been installed such that the pre-load ratio is less than one, and Pad 2 has a pre-load ratio of 1.0. The solid line in Figure 13-7 represents the position of the journal in the concentric position. The dashed line represents the journal in a position with a load applied to the bottom pads.

From Figure 13-12, Pad 1 is operating with a good converging wedge, while Pad 2 is operating with a completely diverging film, thus indicating that the pad is completely unloaded. Therefore, bearings with pre-load ratios of 1.0 or greater will be operating with some of their pads completely unloaded, thus reducing the overall stiffness of the bearing and decreasing its stability, since the upper pads do not aid in resisting cross-coupling influences.

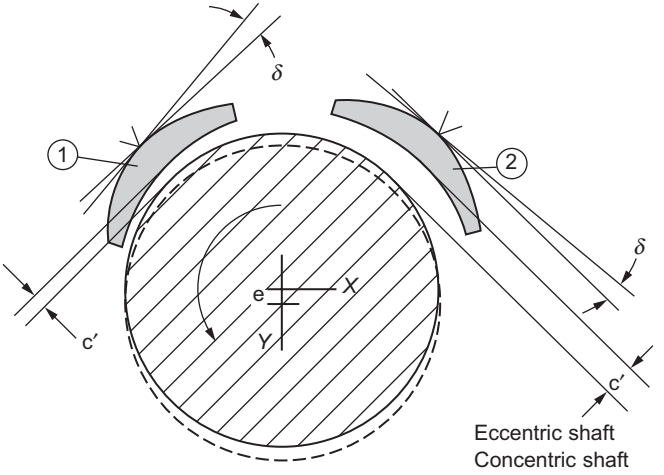


Figure 13-12 Tilting-pad bearing pre-load.

Unloaded pads are also subject to flutter, which leads to a phenomenon known as "leading-edge lock-up." Leading-edge lock-up causes the pad to be forced against the shaft, and it is then maintained in that position by the frictional interaction of the shaft and the pad. Therefore, it is of prime importance that the bearings be designed with pre-load, especially for low-viscosity lubricants. In many cases, manufacturing reasons and the ability to have two-way rotation cause many bearings to be produced without pre-load.

Bearing designs are also affected by the transition of the film from a laminar to a turbulent region. The transition speed (N_t) can be computed using the following relationship:

$$N_t = 1.57 \times 10^3 \frac{v}{\sqrt{DC^3}}$$

where:

v = viscosity of the fluid

D = diameter (inches)

C = diametrical clearance (inches)

Turbulence creates more power absorption, thus increasing oil temperature that can lead to severe erosion and fretting problems in bearings. It is desirable to keep the oil discharge temperature below 170 °F (77 °C), but with high-speed bearings, this ideal may not be possible. In those cases, it is better to monitor the temperature difference between the oil entering and leaving as shown in Figure 13-13.

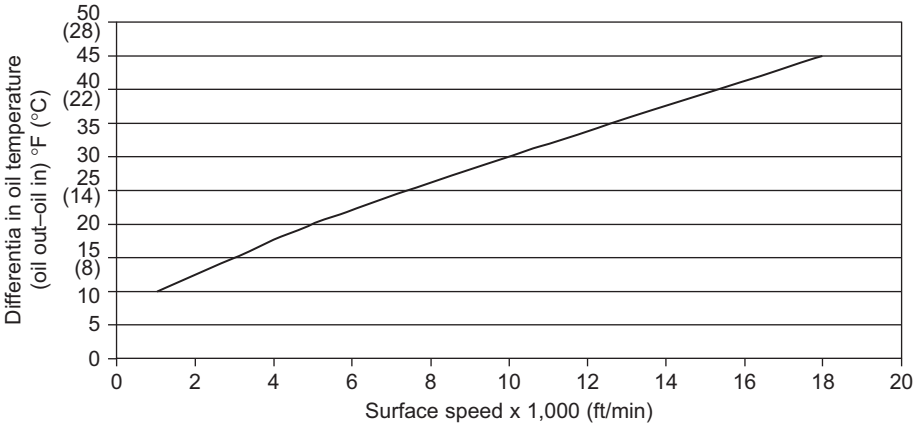


Figure 13-13 Oil discharge characteristics.

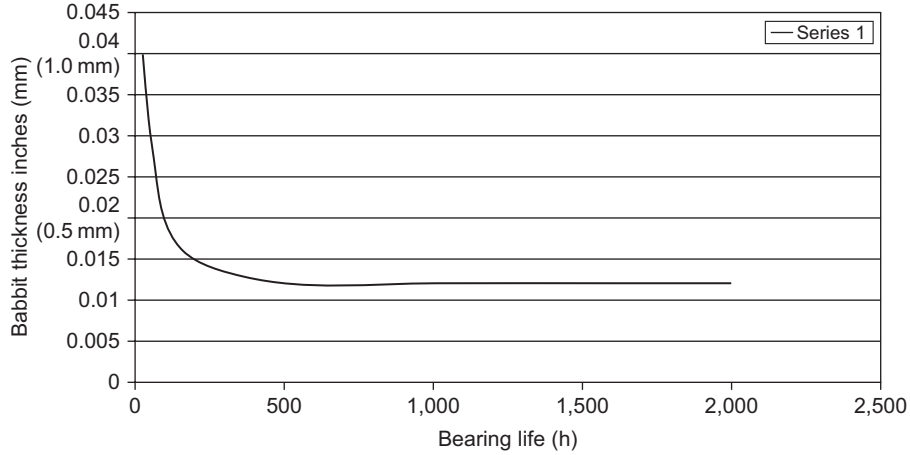


Figure 13-14 Babbitt fatigue characteristics.

Bearing Materials

In all the time since Issaac Babbitt patented his special alloy in 1839, nothing has been developed that encompasses all of its excellent properties as an oil-lubricated bearing surface material. Babbitts have excellent compatibility and non-scoring characteristics and are outstanding in embedding dirt and conforming to geometric errors in machine construction and operation. They are, however, relatively weak in fatigue strength, especially at elevated temperatures and when the babbitt is more than about 0.015 of an inch (.381 mm) thick as seen in Figure 13-14. In general, the selection of a bearing material is always a compromise, and no single composition can include all desirable properties. Babbitts can tolerate momentary rupture of the oil film, and

may well minimize shaft or runner damage in the event of a complete failure. Tin babbitts are more desirable than the lead-based materials, since they have better corrosion resistance, less tendency to pickup on the shaft or runner, and are easier to bond to a steel shell.

Application practices suggest a maximum design temperature of about 300 °F (149 °C) for babbitt, and designers will set a limit of about 50 °F (28 °C) less. As temperatures increase, there is a tendency for the metal to creep under the softening influence of the rising temperature. Creep can occur with generous film thickness and can be observed as ripples on the bearing surface where flow took place. With tin babbitts, observation has shown that creep temperature ranges from 375 °F (190 °C) for bearing loads below 200 psi (13.79 Bar) to about 260–270 °F (127–132 °C) for steady loads of 1,000 psi (69 Bar). This range may be improved by using very thin layers of babbitt such as in automotive bearings.

Bearing and Shaft Instabilities

One of the most serious forms of instability encountered in journal bearing operation is known as ‘‘half-frequency whirl.” It is caused by self-excited vibration and characterized by the shaft center orbiting around the bearing center at a frequency of approximately half of the shaft rotational speed as shown in Figure 13-15.

As the speed is increased, the shaft system may be stable until the “whirl” threshold is reached. When the threshold speed is reached, the bearing becomes unstable, and further increase in speed produces more violent instability until eventual seizure results. Unlike an ordinary critical speed, the shaft cannot “pass through,” and the instability frequency will increase and follow that half ratio as the shaft speed is increased. This type of instability is associated primarily with high-speed, lightly loaded bearings. At present, this form of instability is well understood, can be theoretically predicted with accuracy, and avoided by altering the bearing design.

It should be noted that the tilting-pad journal bearing is almost completely free from this form of instability. However, under certain conditions, the tilting pads themselves can become unstable in the form of shoe (pad) flutter, as mentioned previously.

All rotating machines vibrate when operating, but the failure of the bearings is mainly caused by their inability to resist cyclic stresses. The level of vibration a unit can tolerate is shown in the severity charts in Figure 13-16. These charts are modified by many users to reflect the critical machines in which they would like to maintain much lower levels. Care must always be exercised when using these charts, since different machines have different size housings and rotors. Thus, the transmissibility of the signal will vary.

Thrust Bearings

The most important function of a thrust bearing is to resist the unbalanced force in a machine’s working fluid and to maintain the rotor in its position (within prescribed limits). A complete analysis of the thrust load must be conducted. As mentioned

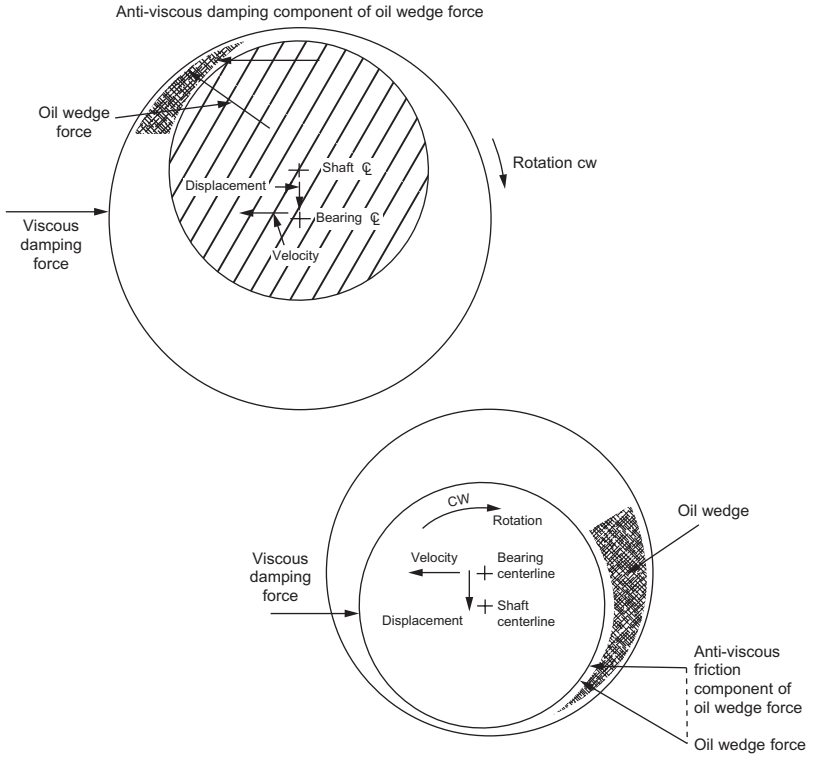


Figure 13-15 Oil whirl.

earlier, compressors with back-to-back rotors reduce this load greatly on thrust bearings. Figure 13-17 shows a number of thrust-bearing types. Plain, grooved thrust washers are rarely used with any continuous load, and their use tends to be confined to cases where the thrust load is of very short duration or possibly occurs at a standstill or low speed only. Occasionally, this type of bearing is used for light loads (less than 50 lb/in^2 [3.5 bar]), and in these circumstances the operation is probably hydrodynamic due to small distortions present in the nominally flat bearing surface.

When significant continuous loads have to be taken on a thrust washer, it is necessary to machine into the bearing surface a profile to generate a fluid film. This profile can be either a tapered wedge or occasionally a small step.

The tapered-land thrust bearing, when properly designed, can take and support a load equal to a tilting-pad thrust bearing. With perfect alignment, it can match the load of even a self-equalizing tilting-pad thrust bearing that pivots on the back of the pad along a radial line. For variable-speed operation, tilting-pad thrust bearings, as shown in Figure 13-18, are advantageous when compared to conventional taper-land bearings. The pads are free to pivot and form a proper angle for lubrication over a wide

speed range. The self-leveling feature equalizes individual pad loadings and reduces the sensitivity to shaft misalignments that may occur during service. The major drawback of this bearing type is that standard designs require more axial space than a non-equalizing thrust bearing.

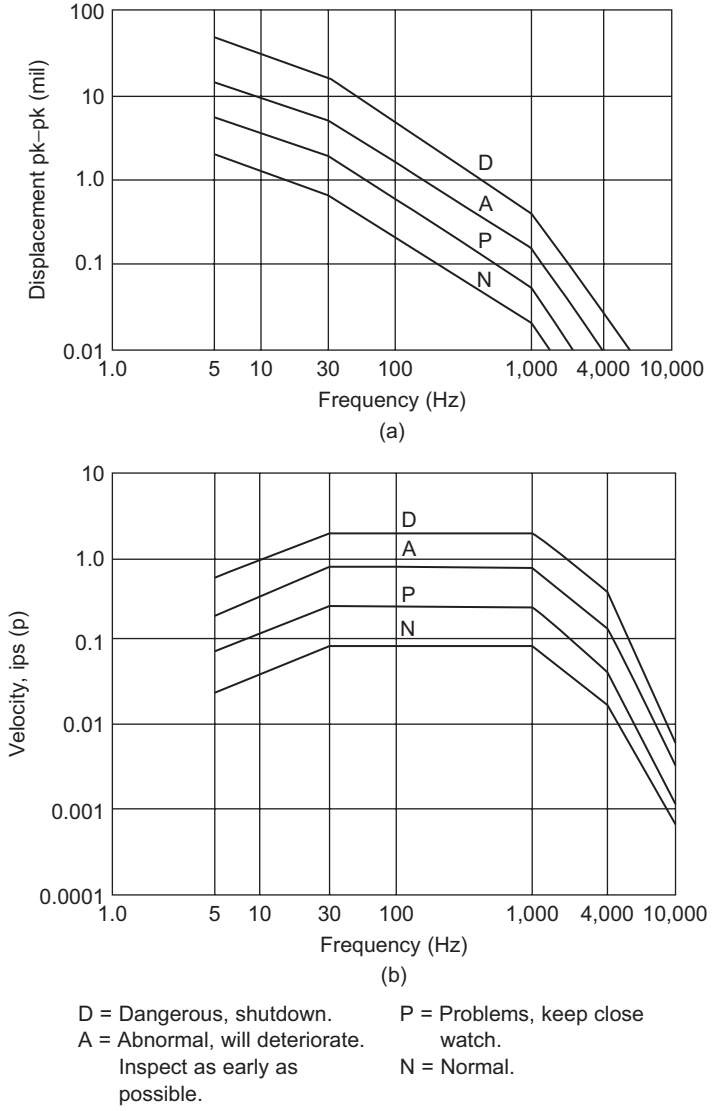
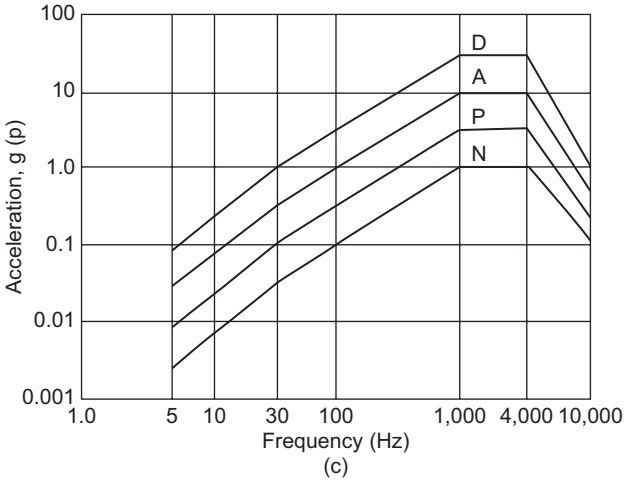


Figure 13-16 Severity charts: (a) displacement, (b) velocity. Severity chart: (c) acceleration.



D = Dangerous, shutdown.
A = Abnormal, will deteriorate. Inspect as early as possible.
P = Problems, keep close watch.
N = Normal.

Figure 13-16 *continued*

Bearing type	Load capacity	Suitable direction of rotation	Tolerance of changing load/speed	Tolerance of misalignment	Space requirement
Plain washer	Poor		Good	Moderate	Compact
Taper land — Bidirectional	Moderate		Poor	Poor	Compact
Taper land — Unidirectional	Good		Poor	Poor	Compact
Tilting pad — Bidirectional	Good		Good	Good	Greater
Tilting pad — Unidirectional	Good		Good	Good	Greater

Figure 13-17 Comparison of thrust-bearing types.

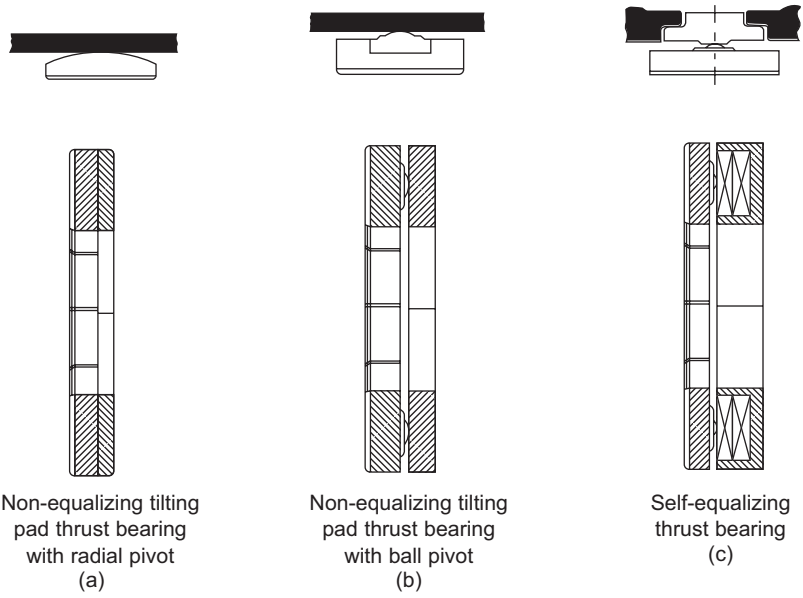


Figure 13-18 Various types of thrust-bearings.

Factors Affecting Thrust-Bearing Design

The principal function of a thrust bearing is to resist the thrust unbalance developed within the working elements of a turbomachine and to maintain the rotor position within tolerable limits.

After an accurate analysis has been made of the thrust load, the thrust bearing should be sized to support this load in the most efficient method possible. Many tests have proven that thrust bearings are limited in load capacity by the strength of the babbitt surface in the high load and temperature zone of the bearing. In normal steel-backed babbitted tilting-pad thrust bearings, this capacity is limited to between 250 and 500 psi (17 and 35 Bar) average pressure. It is the temperature accumulation at the surface and pad crowning that cause this limit.

The thrust-carrying capacity can be greatly improved by maintaining pad flatness and by removing heat from the loaded zone. By the use of high thermal conductivity backing materials with proper thickness and proper support, the maximum continuous thrust limit can be increased to 1,000 psi or more. This new limit can be used to increase either the factor of safety and improve the surge capacity of a given size bearing or reduce the thrust bearing size and consequently the losses generated for a given load.

Since the higher thermal conductivity material (copper or bronze) is a much better bearing material than the conventional steel backing, it is possible to reduce the babbitt thickness to .010–.030 of an inch (.254–.762 mm). Embedded thermocouples and RTDs will signal distress in the bearing if properly positioned. Temperature

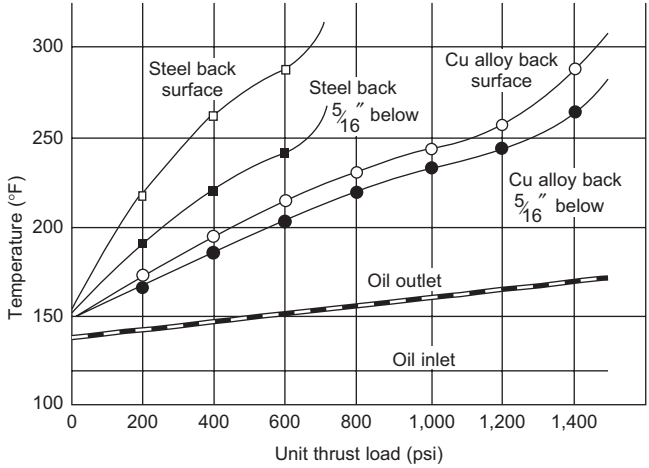


Figure 13-19 Thrust-bearing temperature characteristics.

monitoring systems have been found to be more accurate than axial position indicators, which tend to have linearity problems at high temperatures.

In a change from steel-backing to copper-backing a different set of temperature limiting criteria should be used. Figure 13-19 shows a typical set of curves for the two backing materials. This chart also shows that drain oil temperature is a poor indicator of bearing operating conditions because there is very little change in drain oil temperature from low load to failure load.

Thrust-Bearing Power Loss

The power consumed by various thrust bearing types is an important consideration in any system. Power losses must be accurately predicted so that turbine efficiency can be computed and the oil supply system properly designed.

Figure 13-20 shows the typical power consumption in thrust bearings as a function of unit speed. The total power loss is usually about 0.8–1.0% of the total rated power of the unit. New vectored lube bearings that are being tested show preliminary figures of reducing the power loss by as much as 30%.

Seals

Seals are very important and often critical components in turbomachinery, especially on high-pressure and high-speed equipment. This chapter covers the principal sealing systems used between the rotor and stator elements of turbomachinery. They fall into two main categories: (1) non-contacting seals, and (2) face seals.

Since these seals are an integral part of the rotor system, they affect the dynamic operating characteristics of the machine; for instance, both the stiffness and damping

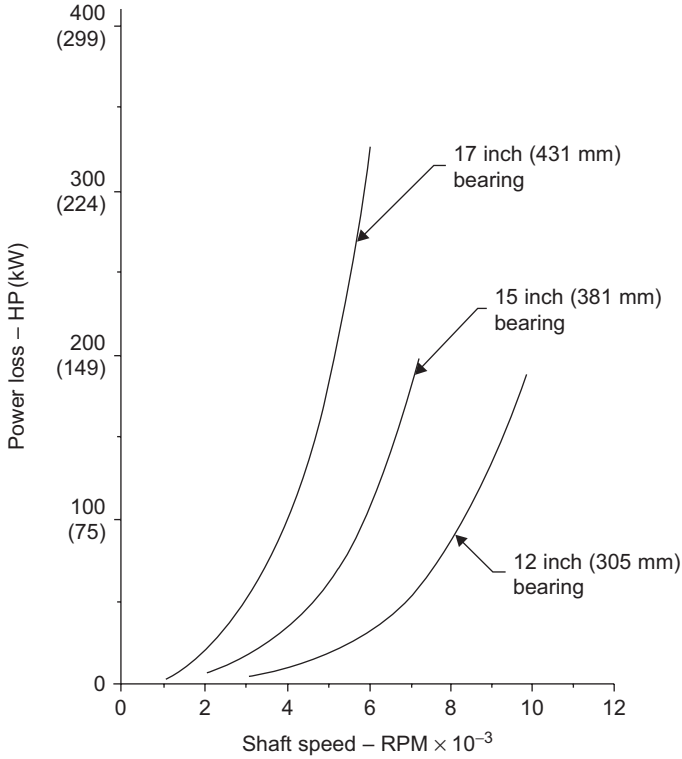


Figure 13-20 Total power loss in thrust bearings.

factors will be changed by seal geometry and pressures. Hence, these effects must be carefully evaluated and factored in during the design of the seal system.

Non-contacting Seals

These seals are used extensively in high-speed turbomachinery and have good mechanical reliability. They are not positive sealing. There are two types of non-contacting seals (or clearance seals): labyrinth seals and ring seals.

Labyrinth Seals

The labyrinth is one of the simplest of sealing devices. It consists of a series of circumferential strips of metal extending from the shaft or from the bore of the shaft housing to form a cascade of annular orifices. Labyrinth seal leakage is greater than that of clearance bushings, contact seals, or film-riding seals. Consequently, labyrinth seals are utilized when a small loss in efficiency can be tolerated. They are sometimes a valuable adjunct to the primary seal.

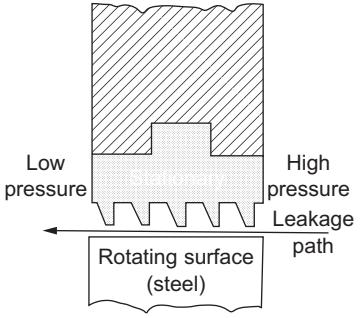
In large gas turbines labyrinth seals are used in static as well as dynamic applications. The essentially static function occurs where the casing parts must remain unjoined to allow for differences in thermal expansion. At this junction location, the labyrinth minimizes leakage. Dynamic labyrinth applications for both turbines and compressors are inter-stage seals, shroud seals, balance pistons, and end seals.

The major advantages of labyrinth seals are: their simplicity; reliability, tolerance to dirt, system adaptability, very low shaft power consumption, material selection flexibility, minimal effect on rotor dynamics, back diffusion reduction, integration of pressure, lack of pressure limitations, and tolerance to gross thermal variations. The major disadvantages are the high leakage, loss of machine efficiency, increased buffering costs, tolerance to ingestion of particulates with resulting damage to other critical items such as bearings, the possibility of the cavity clogging due to low gas velocities or back diffusion, and the inability to provide a simple seal system that meets OSHA or EPA standards. Because of some of the foregoing disadvantages, many machines are being converted to other types of seals.

Labyrinth seals are simple to manufacture and can be made from conventional materials. Early designs of labyrinth seals used knife-edge seals and relatively large chambers or pockets between the knives. These relatively long knives are easily subject to damage. The modern, more functional, and more reliable labyrinth seals consist of sturdy, closely spaced lands. Some labyrinth seals are shown in Figure 13-21. Figure 13-21 (a) is the simplest form of the seal. Figure 13-21 (b) shows a grooved seal is more difficult to manufacture but produces a tighter seal. Figures 13-21 (c) and 13-21 (d) are rotating labyrinth-type seals. Figure 13-21 (e) shows a simple labyrinth seal with a buffered gas for which pressure must be maintained above the process gas pressure and the outlet pressure (which can be greater than or less than the atmospheric pressure). The buffered gas produces a fluid barrier to the process gas. The eductor sucks gas from the vent near the atmospheric end. Figure 13-21 (f) shows a buffered, stepped labyrinth. The step labyrinth gives a tighter seal. The matching stationary seal is usually manufactured from soft materials such as babbitt or bronze, while the stationary or rotating labyrinth lands are made from steel. This composition enables the seal to be assembled with minimal clearance. The lands can therefore cut into the softer materials to provide the necessary running clearances for adjusting to the dynamic excursions of the rotor.

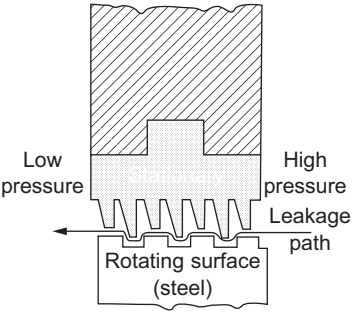
To maintain maximum sealing efficiency, it is essential that the labyrinth lands maintain sharp edges in the direction of the flow. This requirement is similar to that in orifice plates. A sharp edge provides for maximum vena contracta effect, and hence maximum restriction for the leakage flows (Figure 13-22).

High fluid velocities are generated at the throats of the constrictions, and the kinetic energy is then dissipated by turbulence in the chamber beyond each throat. Thus, the labyrinth is a device wherein there is a multiple loss of velocity head. With a straight labyrinth, there is some velocity carry-over that results in a loss of effectiveness, especially if the throats are closely spaced. To maximize the aerodynamic blockage effect of this carry-over, the diameters can be stepped or staggered to cause impingement of the expanding orifice jet on a solid, transverse surface. The leakage is approximately inversely proportional to the square root of the number of labyrinth lands. Thus, if



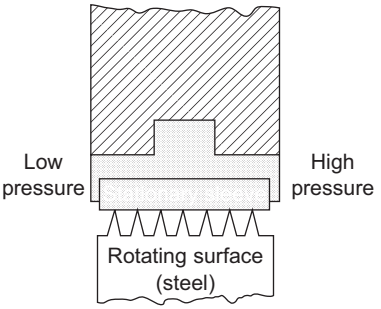
Simplest design (labyrinth materials: aluminum, bronze, babbitt or steel).

(a)



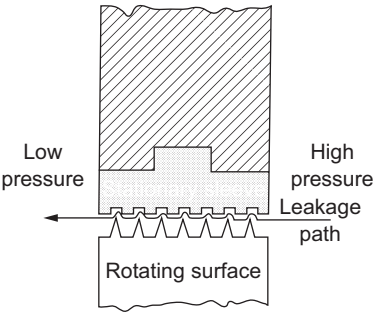
More difficult to manufacture but produces a tighter seal (same material as in (a)).

(b)



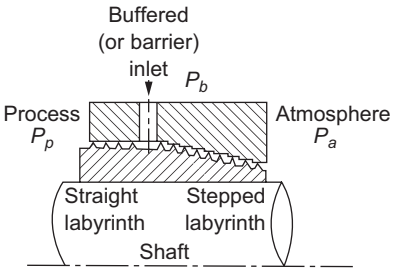
Rotating labyrinth type, before operation (sleeve material: babbitt, aluminum, nonmetallic or other soft material).

(c)



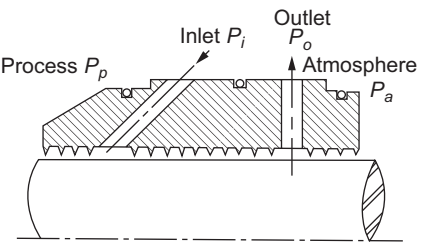
Rotating labyrinth, after operation. Radial and axial movement of rotor cuts grooves in sleeve material to simulate staggered type shown in (b).

(d)



Buffered combination labyrinth

(e)



Buffered-vented straight labyrinth

(f)

Figure 13-21 Various configurations of labyrinth seals.

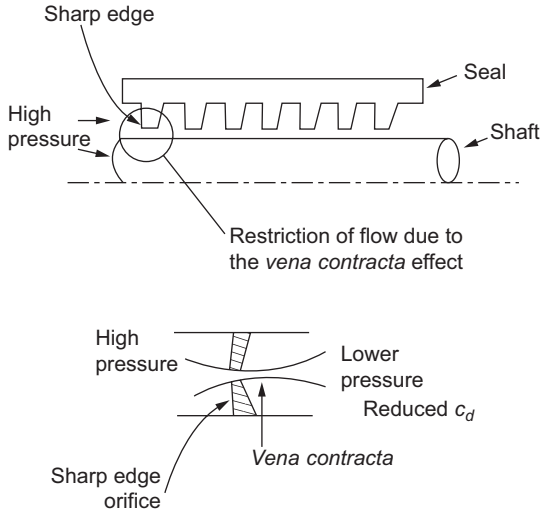


Figure 13-22 Theory behind the knife-edge arrangement.

leakage is to be cut in half at a four-point labyrinth, the number of lands would have to be increased to 16. The Elgi leakage formulae can be modified and written as:

$$\dot{m}_1 = 0.9A\left[\frac{\frac{g}{V_o}(P_o - P_n)}{n + ln\frac{P_n}{P_o}}\right]^{1/2}$$

For staggered labyrinths, the equation can be written as:

$$\dot{m}_1 = 0.75A\left[\frac{\frac{g}{V_o}(P_o - P_n)}{n + ln\frac{P_n}{P_o}}\right]^{1/2}$$

where

$\dot{m}_1 =$ leakage, lb/sec
$A =$ leakage area of single throttling, sq ft
$P_o =$ absolute pressure before the labyrinth, lb/sq ft
$V_o =$ specific volume before the labyrinth, cu ft/lbm
$P_n =$ absolute pressure after the labyrinth, lb_f/sq ft
$n =$ number of lands

The leakage of a labyrinth seal can be kept to a minimum by providing: (1) minimum clearance between the seal lands and the seal sleeve, (2) sharp edges on the lands to reduce the flow discharge coefficient, and (3) grooves or steps in the flow path for reducing dynamic head carry-over from stage to stage.

The labyrinth sleeve can be flexibly mounted to permit radial motion for self-aligning effects. In practice, a radial clearance of under 0.008 is difficult to achieve, except with very small high-precision machines. On larger turbines, clearances of 0.015–0.02 are generally used. During machine construction, it is important to measure and record these clearances because mechanical seizure or loss in aerodynamic efficiency can often be traced to incorrect labyrinth seal clearances.

The windback seal closely resembles the labyrinth but has an entirely different operational principle. A screw-thread device winds the oil, which is carried around the bore by the windage of the shaft, into an internal drain for return to the system as shown in Figure 13-23 (a).

Windback structures are extremely simple. Clearances about the shaft are ample, and the device has high reliability. When shaft speeds extend into the low regions where windage contributions are inadequate for effective operation, augmentation of windage can be achieved by special configurations of the shaft surface. Windbacks are also used as adjuncts to other types of seals, as shown in Figure 13-23 (b). With circumferential seals, windbacks can be used to keep oil splash from reaching the seal carbons when coking problems exist. In oil-buffered seals for compressors they are used to direct the small internal leakage into a pressurized drain to effect practically complete recovery of the leakage.

Ring (Bushing) Seals

The restrictive ring seal is essentially a series of sleeves in which the bores form a small clearance around the shaft. Thus, leakage is limited by the flow resistance in the restricted area and controlled by the laminar or turbulent friction. The API 617 codes characterize this type of seal. Most of the restrictive-type seals are of the floating type rather than the fixed type. The floating rings permit a much smaller leakage, and they can be of either the segmented type as shown in Figure 13-24 (a) or the rigid type as shown in Figure 13-24 (b).

Because of the minimal contact between the stationary ring and the rotor, these seals, when properly designed, are ideal for high-speed rotating machinery.

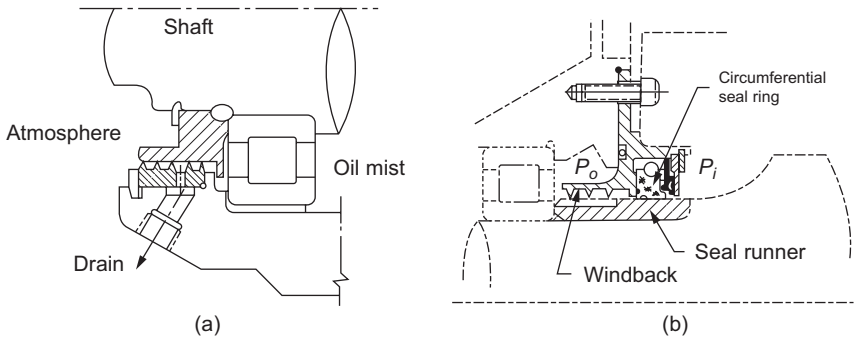


Figure 13-23 Windback seal.

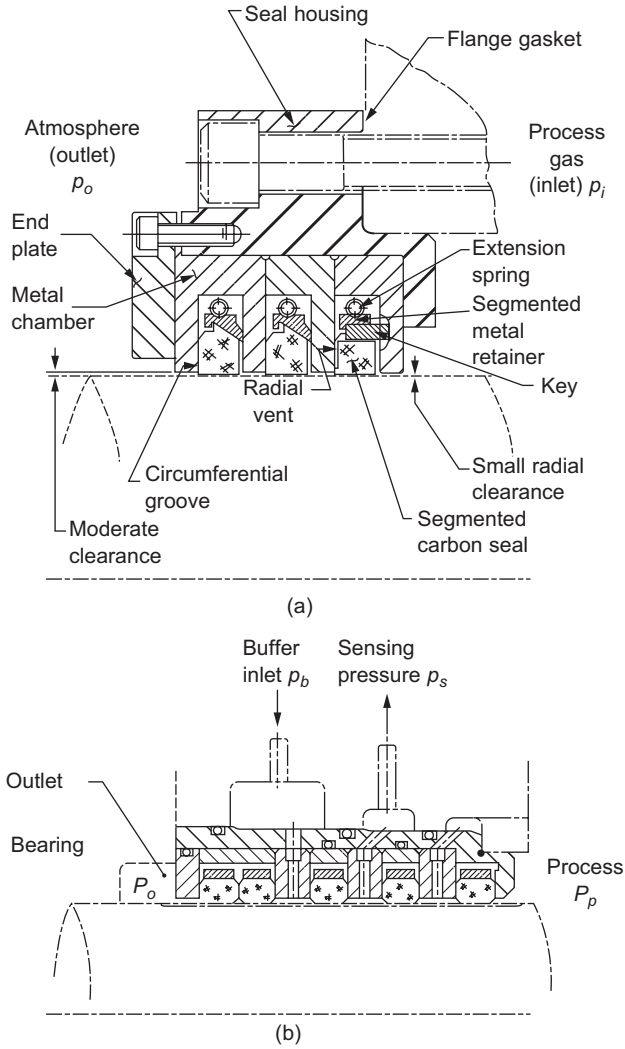


Figure 13-24 Floating-type restrictive ring seal.

When adequate lubrication and cooling fluid is available, the seal ring, manufactured from babbitt-lined steel, bronze, or carbon, will function satisfactorily. When the medium to be sealed is air or gas, carbon seal rings must be used. Carbon has self-lubricating properties. Cooling of the seal is provided by the leakage flow through the seal. Depending on the operating temperature and environment, aluminum alloys and silver are also used in the manufacture of the seal rings. Leakage limitation depends upon the type of flow and type of bushing. There are four types of flow: compressible and incompressible, each of which may be either laminar or turbulent. Ring seals are divided into two categories: fixed breakdown rings and floating breakdown rings, according to whether or not they are fixed with respect to the stationary housing.

Fixed seal rings

The fixed seal ring consists of a long sleeve affixed to a housing in which the shaft rotates with small clearance. It is an inexpensive assembly. However, since it is fixed, the seal behaves like a redundant bearing when rubbing occurs and, like the labyrinth, requires large clearances. Therefore, long assemblies must be used to keep leakage within reasonable limits. Since long seal assemblies aggravate alignment and rubbing problems, sturdier shafts are required to keep operating speeds in a subcritical region. The fixed-bushing seal almost always operates with appreciable eccentricity. This, plus the combination of a large clearance and a large eccentricity ratio, produces large leakages per unit length. Fixed-seal rings are therefore impractical where leakage is undesirable.

Floating seal rings

Clearance seals, which are free to move in a radial direction relative to the shaft and machine housing, are known as floating seals. These seals have advantages that very close annular clearance-type seals do not possess. The floating characteristic permits them to move freely with shaft motions and deflections, thereby avoiding the effects of severe rubbing.

Differential thermal expansion is a problem at high temperatures where the shaft and bushing are of dissimilar materials, or where there is any substantial temperature gradient between them. For example, the grades of carbon used commonly have a linear thermal expansion coefficient of one-third to one-fifth that of steel, necessitating the design of thermal expansion control into the carbon bushing. This is achieved by shrinking the carbon into a metallic retaining ring with a coefficient of expansion that equals or exceeds that of the shaft material.

It is good practice in critical applications to use bushings of a material with a slightly higher coefficient of thermal expansion than that of the shaft. Here, incipient seizure causes the bushings to grow away from the shaft. The large torque associated with high shearing intensity may necessitate locking the bushings against rotation if the unbalanced pressure forces seating them against the housing walls are insufficient to prevent rotation.

Build up of dirt or other foreign material between the seal ring and seat will result in damage to the journal and excessive seal spin on a floating seal ring unit. Soft materials, such as babbitt and silver, are notorious for trapping contaminants and causing shaft damage.

Mechanical (Face) Seals

This device forms a running seal between flat precision-finished surfaces. Its primary function is to prevent leakage. When used on rotating shafts, the sealing surfaces are in a plane perpendicular to the shaft, and the forces that hold the contact faces together will consequently be parallel to the shaft axis. For a seal to work properly, four sealing points must function as shown in Figure 13-25. They are: (1) the stuffing-box face must be sealed, (2) leakage down the shaft must be sealed, (3) the mating ring in the

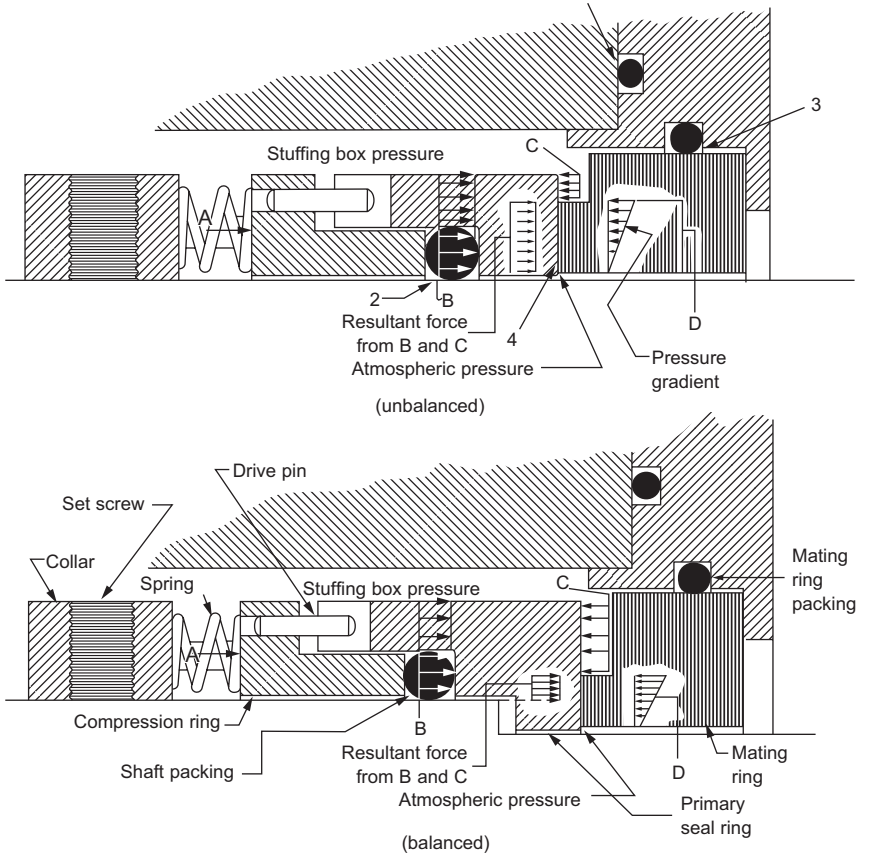


Figure 13-25 Unbalanced seal and balanced seal with step in shaft.

gland plate must be sealed in a floating design, and (4) the dynamic faces (rotary to stationary) must seal. Basically, most mechanical seals have the following components:

1. Rotating seal ring
2. Stationary seal ring
3. Spring devices to provide pressure
4. Static seals

A complete seal has two basic units: the seal head unit and the seal seat. The seal head unit consists of the housing, the end-face member, and the spring assembly. The seal seat is the mating member that completes the precision-lapped face combination that provides the seal.

The seal head may either rotate or remain stationary (attached to the body). Either one (head or seat) may rotate, while the other remains stationary. The movement of the sealing action depends on the direction of the pressure. This is illustrated in Figure 13-26, which shows rotating and stationary heads.

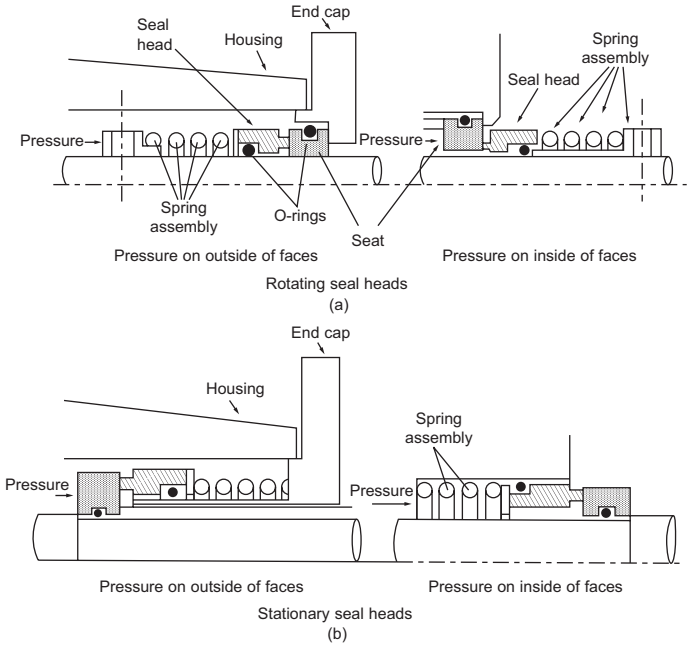


Figure 13-26 Rotating and stationary seal heads.

Some form of mechanical loading device, usually a spring, is needed to ensure that, in the event of a loss of hydraulic pressure, the sealing surfaces are kept closed. The amount of load on the sealing area is determined by the degree of "seal balance." Figure 13-27 shows what is meant by seal balance. A completely balanced combination occurs when the only force exerted on the sealing surfaces is the spring force, i.e., hydraulic pressure does not act on the sealing surfaces. The kind of spring that should be used depends upon a variety of factors: the space available, the loading characteristics required, the environment in which the seal is to operate, amongst others. Based on these considerations, either a single-spring or a multiple-spring design can be utilized. When a very small axial space is available, belleville springs, finger washers, or curved washers may be used.

A somewhat recent development is the use of magnetic force to obtain a face-loading action. Magnetic seals have provided reliable service under a variety of fluids and severe operating conditions. Some of the design advantages claimed are that magnetic seals are compact and lighter, provide an even distribution of sealing force, and are easy to assemble. Figure 13-28 shows a simple magnetic seal.

Shaft sealing elements can be split up into two groups. The first may be called pusher-type seals and includes the O-ring, V-ring, U-cup, and wedge configurations. The second group are Bellow-type seals, which differ from the pusher-type seals in that they form a static seal between themselves and the shaft. Figure 13-29 shows some typical pusher-type seals.

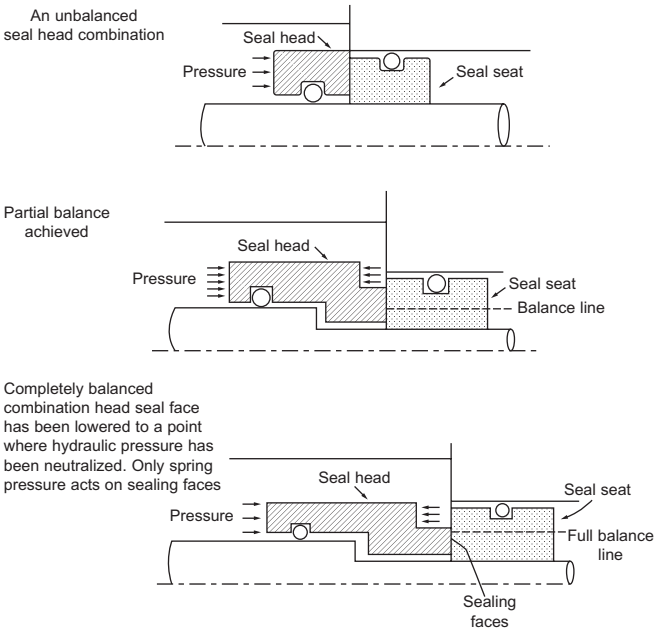


Figure 13-27 The seal balance concept.

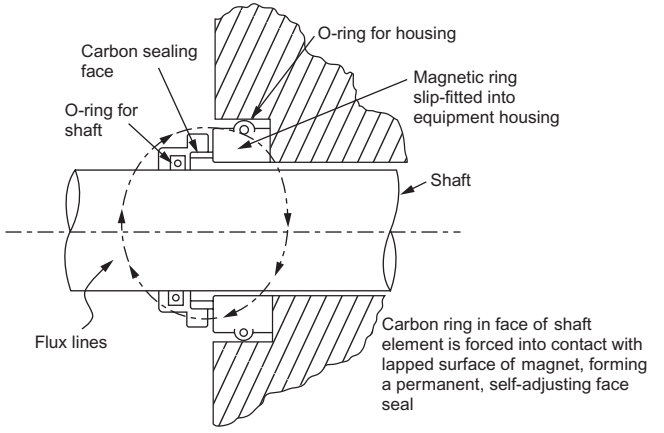


Figure 13-28 Simple magnetic-type seal.

A typical mechanical contact shaft seal has two major elements, as seen in Figure 13-30. These are the oil-to-pressure-gas seal and the oil-to-uncontaminated-seal-oil-drain seal or breakdown bushing. This type of seal will normally have buffering via a single ported labyrinth located inboard of the seal and a positive shutdown device, which will attempt to maintain gas pressure in the casing when the compressor

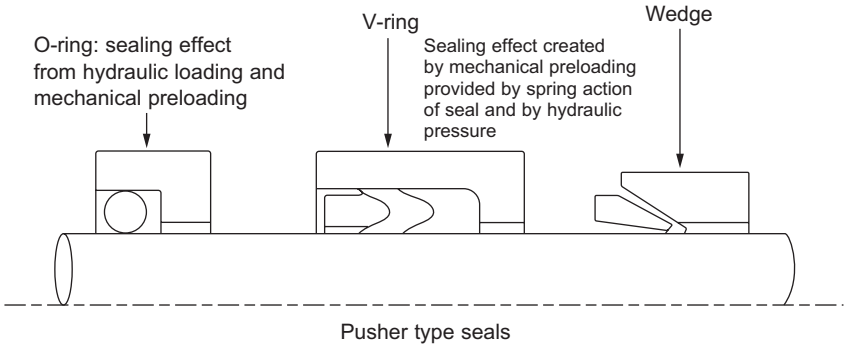


Figure 13-29 Various types of shaft sealing elements.

is at rest and seal oil is not being applied. For shutdown, the carbon ring is kept tightly sandwiched between the rotating seal ring and stationary sleeve with gas pressure to prevent gas from leaking out when no oil pressure is available.

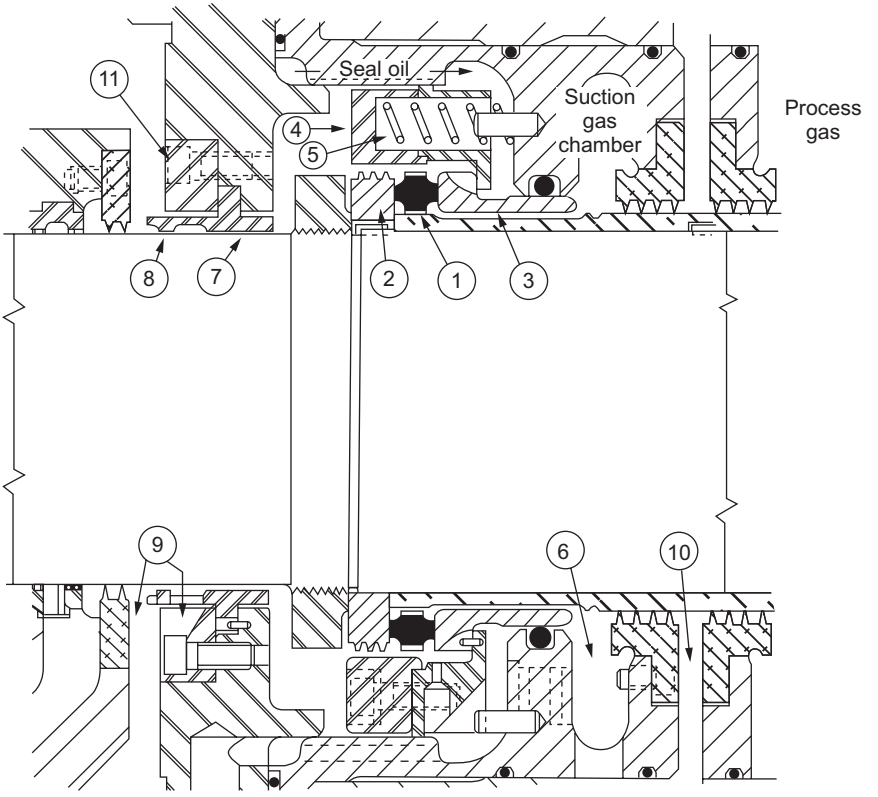
In operation, seal oil pressure is held at a differential of 35–50 psi (2.4–3.5 Bar) over the process gas pressure which the seal is sealing against. This high-pressure oil can be seen entering in the top in Figure 13-30 and completely fills the seal cavity. Some of the oil (a relatively small percentage, ranging from two to eight gpd per seal depending on machine size) is forced across the carbon ring seal faces, which are sandwiched between the rotating seal ring (rotating at shaft velocity) and the stationary sleeve (non-rotating and forced against the carbon ring by a series of peripheral springs). Therefore, the actual rotative speed of the carbon ring can be anywhere between zero rpm and full rotational speed. Oil crossing these seal faces contacts the process gas and is, thus, "contaminated oil."

The majority of the oil flows out of the uncontaminated seal oil drain after taking a pressure drop from design seal oil pressure to atmospheric pressure across the breakdown bushing. An orifice is placed in parallel with the breakdown bushing to meter the proper amount of oil flow for cooling. The contaminated oil leaves through the drain to a degasifier for purification. The bearing oil drain can be either combined with the uncontaminated seal oil drain or kept separate; however, a separate system will increase bearing span and lower critical speeds.

Mechanical Seal Selection and Application

The following is a list of factors that have proven to be helpful in seal system design and selection:

1. Product
2. Seal environment
3. Seal arrangement
4. Equipment



1. Rotating carbon ring
2. Rotating seal ring
3. Stationary sleeve
4. Spring retainer
5. Spring
6. Gas and contaminated oil drain
7. Floating babbitt-faced steel ring
8. Seal wiper ring
9. Seal oil drain line
10. Buffer gas injection port
11. Bypass orifice

Figure 13-30 Mechanical contact shaft seal.

5. Secondary packing
6. Seal-face combinations
7. Seal gland plate
8. Main seal body

Product

The physical and chemical properties of the liquid being sealed will place constraints upon the type of seal arrangement, the materials of construction, and the seal design that can be used.

Pressure

The relative pressures of the material to be sealed affect the decision of whether to use a balanced or unbalanced seal design. Pressure also affects the choice of face material because of the seal-face loading.

If the service happens to be below atmospheric pressure, then special considerations are required to seal the material effectively. Most unbalanced seal designs are applicable up to 100 psig (7 Bar) stuffing-box pressure. At more than 100 psig (7 Bar), balanced seals should be used.

Seal manufacturers base their seal-face combination designs on *PV* ratings. These are the multiple of the face load (*P*) and the sliding velocity (*V*) of the faces. The maximum *PV* rating for an unbalanced seal is about 200,000 and about 2,250,000 for a balanced seal.

Temperature

The temperature of the liquid being pumped is important because it affects the seal-face material selection as well as face wear life. This is primarily a result of changes in lubricity of the fluid with changes in temperature.

Common seal designs may handle fluid temperatures in the 0 °F to +200 °F (−17 °C to 93 °C) range. When temperatures are above the +200 °F (93 °C) range, special metal bellows seals may be used up to the +650 °F (343 °C) range. Low temperature (−100 °F to 0 °F) (−73 °C to −17 °C) also requires special arrangements, since most hydrocarbons have little lubricity in this range.

The most important consideration concerning temperature is to avoid operating close to a temperature which will allow flashing of the liquid. Mechanical seals work well on many liquids; they work poorly on most gases.

Lubricity

In any mechanical seal design there is rubbing motion between the dynamic seal faces. This rubbing motion is most often lubricated by the fluid being pumped. Therefore, the lubricity of the pumped liquid at the given operating temperature must be considered to determine if the chosen seal design and face combination will perform satisfactorily.

Most seal manufacturers limit the speed of their seals to 90 fps (27.4 mps) with good lubrication of the faces. This is primarily due to the centrifugal forces acting on the seal which tend to restrict its axial flexibility.

Abrasion

When evaluating the possibility of installing a seal in a liquid that has entrained solids, several factors must be considered. Is the seal constructed in such a way that the dynamic motion will be restricted by fouling of the seal parts? The seal arrangement that is usually preferred when abrasives are present is a flushed single inside type with a face combination of very hard material. However, factors such as toxicity or corrosiveness of the material may dictate that other arrangements be used.

Corrosion

When considering the corrosiveness of the material being pumped, one must determine what metals will be acceptable for the seal body, what spring material may be used, what face material will be compatible with the liquid being pumped (that is, whether the binder or the carbon or tungsten carbide will be attacked, or whether the base metal of the plated seal face will be attacked), and what type of elastomer or gasket material can be used. The corrosion rate will affect the decision of whether to use a single- or multiple-spring design because the spring can tolerate a greater amount of corrosion without weakening it appreciably.

Toxicity

This factor is becoming an increasingly important consideration in the design of mechanical seals. Since the rubbing seal faces require liquid penetration to cool and lubricate them, it is reasonable to expect that there will be some vapor passing across the faces. This is in fact the case. A normal seal can be expected to "leak" from a few ppm to 10 cc/min. It is also generally accepted that the seal leakage rate will increase with speed.

Additional Product Considerations

1. Is the product thermosensitive? The heat generated by the seal faces may cause polymerization.
2. Is the product shear sensitive, i.e., will it harden due to turbulence?
3. If the product is highly flammable, be aware of possible ignition sources.
4. In-hazardous services plan for personnel protection in the event of seal leakage.
5. Products with dissolved gas must be properly vented. In most cases, vent the stuffing box back to the pump action.
6. Seals in cold services are extremely sensitive to moisture. There must be a way to "dry out the system" after repair.
7. Consideration must be given to the pressure and temperature that the seal will see during normal operation, start-up, shutdown, and upset conditions.
8. Vapor pressure of the product must be known to prevent vaporization in the stuffing box.

Seal Environment

Once an adequate definition of the product is made, the design of the seal environment can be selected. There are four general parameters that an environmental system may regulate or change:

1. Pressure control
2. Temperature control
3. Fluid replacement
4. Atmospheric air elimination

The most common environmental control systems include flushing, barrier fluids, quenching, and heating/cooling systems. Each has its use in regulating the parameters mentioned previously.

Seal Arrangement Considerations

There are four considerations:

1. Double seals have been the standard with toxic and lethal products, but maintenance problems and the seal design contribute to poor reliability. The double face-to-face seal should be looked at more closely.
2. Do not use a double seal in dirty service – the inside seal will hang up.
3. The API standard is a good guide to the use of balanced and unbalanced seals. Application of a balanced seal at too low a pressure may encourage face lift-off.
4. The number of arrangements and auxiliary features are more than 100. Regardless of the seal vendor, the arrangement will generally determine success.

Equipment

Too few people consider the equipment with the seal selection. In most cases, poor equipment will give poor seal performance, regardless of the seal or arrangement chosen. Also, beware that different pumps with the same shaft diameter and TDH may present different sealing problems (note: these same considerations may be used for troubleshooting).

Secondary Packing

More emphasis should be placed on secondary packing than it receives, especially if these members involve Teflon. Most seal designs using an O-ring for shaft packing give similar performance. A wide variation in performance is seen between various seal vendor designs when Teflon shaft packing is used. Depending on the seal arrangement, there can be a difference in mating-ring (stationary) packing performance when Teflon is used.

Seal-Face Combinations

Choices of seal-face combinations have come a long way in the last eight to 10 years. Stellite is being phased out in petroleum and petrochemical seal applications. Better grades of ceramic are being offered as the standard material. The cost of tungsten carbide has decreased considerably. Relapping services for tungsten are available near most industrial areas. Silicon carbide is gaining a hold on the market, especially in abrasive services. The technology of manufacturing tungsten carbide in a composite or overlay arrangement is offered by all of the major seal manufacturers. The dynamics of seal faces are better understood today.

Seal Gland Plate

The seal gland plate is an item that is caught in between the pump vendor and the seal vendor. The pump vendors can furnish good, reasonably priced alloy glands, but they are also limited because the gland is cast and must fit several seal designs. There are also some glands furnished by pump vendors that can be easily distorted by bolting.

Special glands requiring heating, quench, and drain with a floating-throat bushing on ANSI pumps should be furnished by the seal vendor. Gland designs on several ANSI pumps are not that impressive.

Main Seal Body

Designs differ considerably from one manufacturer to another. The term "seal body" makes reference to all rotating parts on a pusher seal, excluding shaft packing and the seal ring. The configuration or options offered on the seal body may be the chief reason to avoid the design for that particular service.

Seal Systems

In recent years, these systems have become more sophisticated to meet modern chemical process requirements and government restrictions. A simple seal system is the buffered and educted restrictive-ring seal system. This type of system, as shown in Figure 13-31, must operate with buffering pressure greater than the process and eductor pressure. The eductor pressure must in turn be below the atmospheric pressure. Problems with these systems are common because the eductor system does not have a large enough capacity, the buffered gas pressure is not higher than the process pressure, and in many cases the rings are installed backward.

The complex seal systems incorporate many different types of components to provide the most efficient sealing. Figure 13-32 shows a system that includes three different types of seals. The labyrinth seal initially provides the restriction that prevents the polymers contained in the process gas from clogging the seal rings. The labyrinth seal is followed by the two segmented circumferential contact seals and the four segmented restrictive-ring seals, which are primary seals in this combination. The primary restrictive-ring seals are followed by four circumferential segmented seal

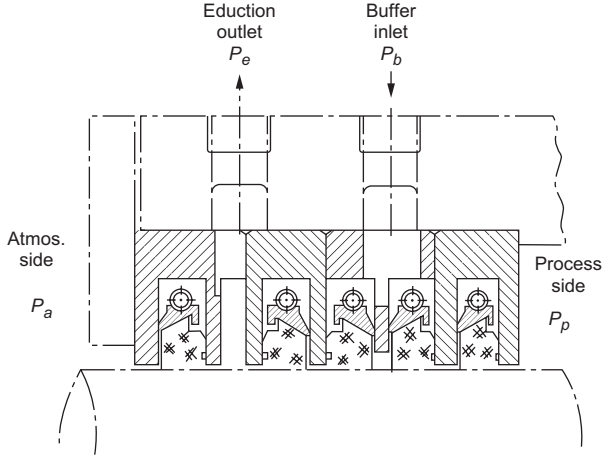


Figure 13-31 Restrictive ring seal system with both buffer and eduction cavities.

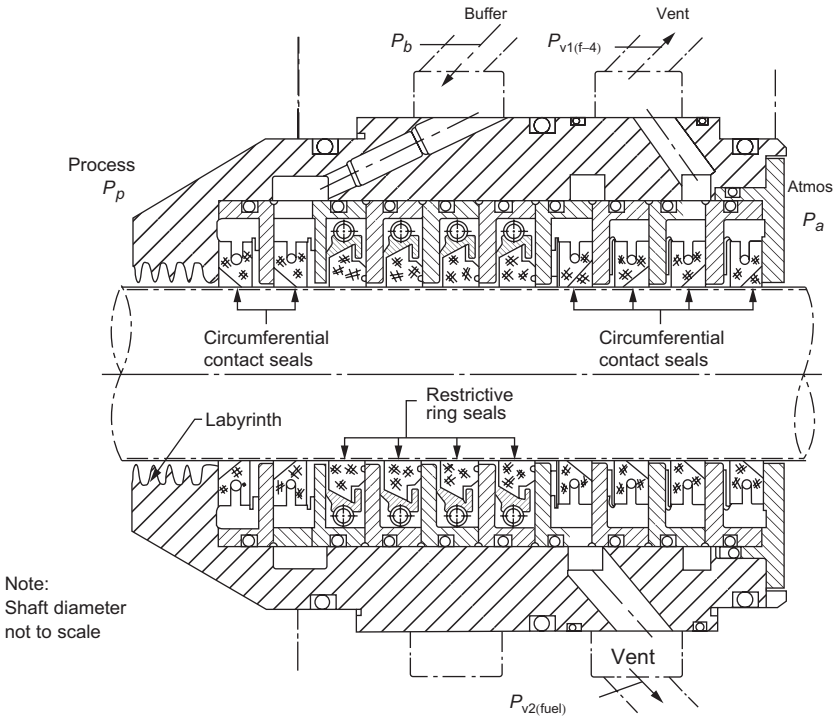


Figure 13-32 Multiple combination segmented gas seal system.

rings. A buffer gas is also introduced at the first set of circumferential contact seals, and an eductor is situated in the middle of the rear circumferential seals. Thus, this sealing system is very efficient in preventing any leakage and also for utilizing educted gas in the process.

Gas compressors operating on highly toxic or flammable gases may require redundant systems to assure no leakages. In many applications, such as refrigeration gas, buffer seals are required with the liquid-buffered face seal. A popular technique is to use a buffered labyrinth seal with a liquid seal.

Associated Oil System

One of the advantages of mechanical contact seals is that the associated seal oil supply system may be relatively simple compared to the system required with other types of seals, as seen in Figure 13-33. The relatively high oil-to-gas differential and wide allowable range allow simple differential regulators to be used to control the oil supply system rather than a complex overhead tank arrangement. The dark lines in Figure 13-34 represent the seal oil system used for this type of seal. Seal oil is taken from a controlled header "A" and dropped to the required ΔP via a relatively inexpensive regulator control. The sensing point for this ΔP control is off the contaminated drain cavity on the high-pressure end of the compressor. By sensing off the

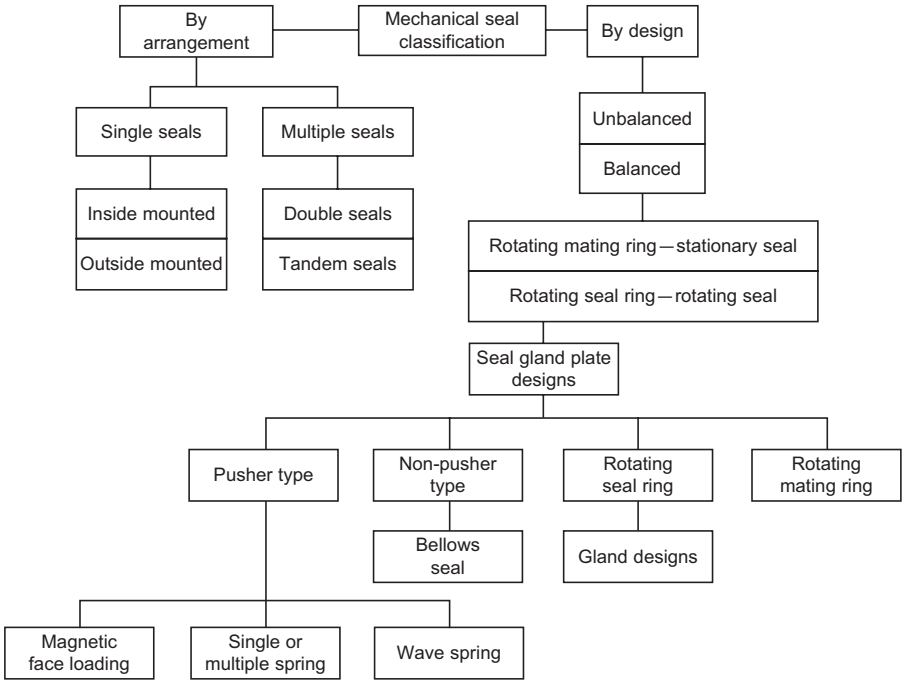


Figure 13-33 Mechanical seal classifications.

high-pressure end, a minimum of ΔP of oil to gas is always held on both ends of the compressor. Any pressurizing of the contaminated drain cavity due to buffer gas being used is also automatically followed by using a sensing point located in the contaminated drain oil cavity. In the system shown, the "uncontaminated oil" combines immediately with lube oil and returns to the reservoir where the "contaminated oil" can be trapped by a drainer and automatically drained to be optionally discarded or returned to the reservoir via a degasing tank.

Dry Gas Seals

The use of dry gas seals in process gas centrifugal compressors has increased over the last 30 years, replacing traditional oil film seals in most applications. Over 85% of centrifugal gas compressors manufactured today are equipped with dry gas seals.

Dry gas seals are basically mechanical face seals, consisting of a mating ring, which rotates and a primary ring, which is stationary. A cross-sectional view of a dry gas seal is shown in Figure 13-35. The rotating assembly consists of the mating ring (with spiral grooves) mounted on a shaft sleeve held in place axially with a clamp sleeve and a locknut. It is typically pin driven. The mating ring with spiral grooves and the primary ring are held within the retainer assembly. The stationary assembly consists of the primary ring mounted in a retainer assembly held stationary within the compressor

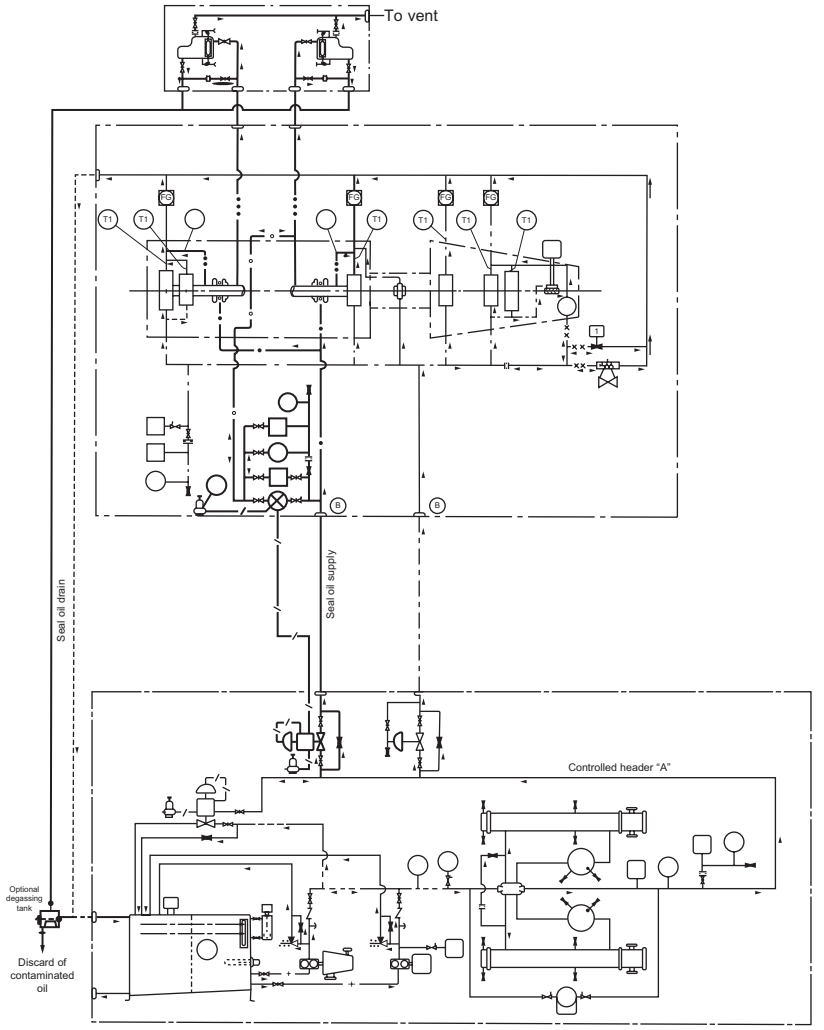


Figure 13-34 Mechanical contact seal and lube oil system.

housing. Under static conditions, the primary and mating rings are held in contact due to the spring load on the primary ring.

The spiral groove pattern, for a clockwise rotation, on the mating ring is shown in Figure 13-36. The operating principle of the spiral grooved gas seal is that of a hydrostatic and hydrodynamic force balance. As gas enters the grooves, it is sheared towards the center. The sealing dam acts as a restriction to the gas outflow, thereby raising the pressure upstream of the dam. This increased pressure causes the flexibly mounted, primary ring to separate from the mating ring. During normal operation, the running gap is approximately three microns. Under pressurization, the forces exerted on the

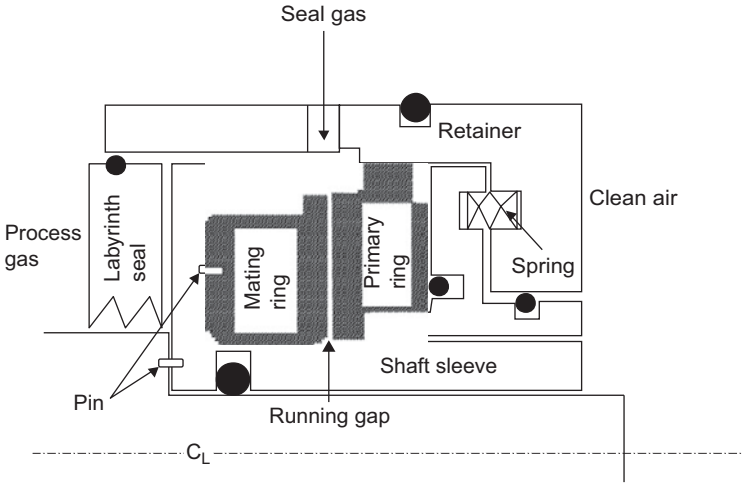


Figure 13-35 Single dry gas seal.

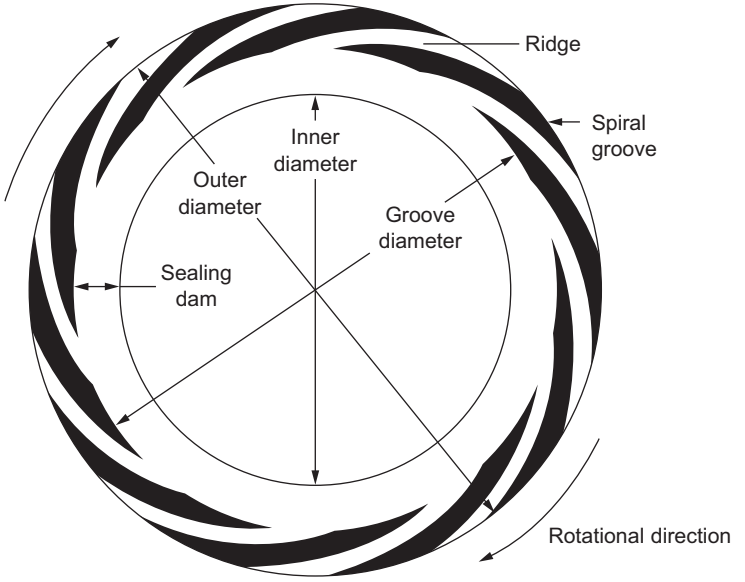


Figure 13-36 Spiral grooved mating ring (courtesy Proceedings Seventeenth Turbomachinery Symposium, Dry Gas Compressor Seals by Piyush Shah, John Crane Inc.).

seal are hydrostatic and are present whether the mating ring is stationary or rotating. Hydrodynamic forces are generated only upon rotation. The mating ring consisting of the logarithmic spiral grooves is the key to generating these hydrodynamic forces.

During operation, the grooves in the mating ring generate a hydrodynamic force that causes the primary ring to separate from the mating ring creating a "running gap" between the two rings, which effectively seals against the process gas. During normal operation, the running gap is approximately three microns. A sealing gas is injected into the seal, providing the working fluid, which establishes the running gap.

Tandem Dry Gas Seals

The tandem dry gas seal as seen in Figure 13-37 relates to applications where small product leakages of process gas are admissible. The seal on the atmosphere side acts as a safety seal. The tandem arrangement provides a particularly high degree of operational safety. The seal on the product side and the seal on the atmosphere side are able to absorb the complete pressure differential. Under normal operating conditions the full pressure is reduced only by the seal on the product side. The space between the seal on the product side and the seal on the atmosphere side is cleared by a connection to the flare. The pressure differential to be sealed by the seal on the atmosphere side equals the flare pressure, so leakage to the atmosphere side or to the vent is very low. If the main seal fails, the second seal acts as a safety seal.

Tandem Dry Gas Seal with Labyrinth

A tandem seal with intermediate labyrinth is shown in Figure 13-38. This seal is used in applications where the product leakages to the atmosphere as well as buffer gas leakages to the product are inadmissible, for example, on H2, ethylene or propylene compressors. In this type of seal the product pressure to be sealed is reduced via the seal on the product side. The entire process gas leakage is discharged via connection

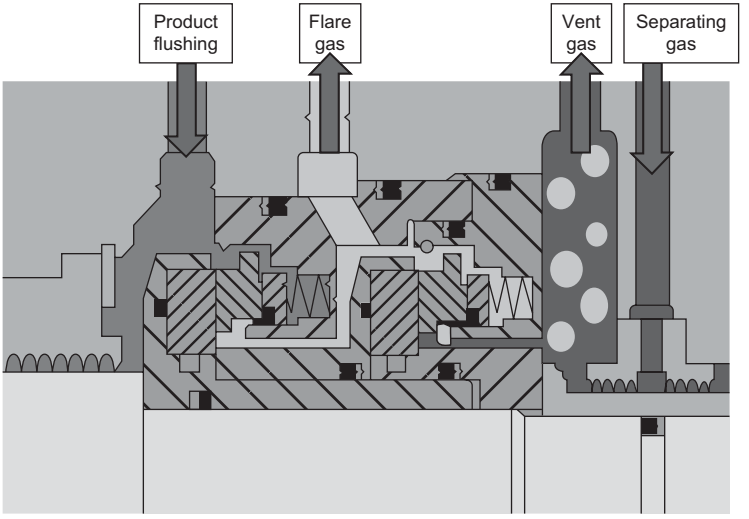


Figure 13-37 Tandem seal (courtesy Eagle Burgmann Germany GmbH & Co. KG).

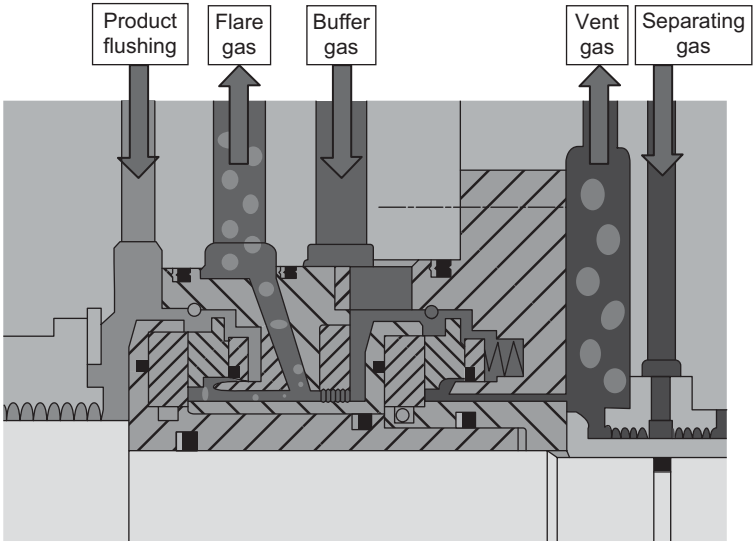


Figure 13-38 Tandem seal with intermediate labyrinth (courtesy Eagle Burgmann Germany GmbH & Co. KG).

to the flare. The seal on the atmosphere side is pressurized with a buffer gas such as nitrogen via connection to the buffer gas. The pressure of the buffer gas ensures that a current flows via the labyrinth to the primary vent outlet.

Double Gas Seals

A double gas seal, as shown in Figure 13-39, is used where product leakages to the atmosphere are inadmissible and tandem arrangements are not suitable because of too small product gas pressures. Buffer gas leakages into the product must be admissible and the buffer gas pressure must be higher than the product pressure. This seal is used when a neutral buffer gas of suitable pressure is available. Typical applications are to be found mainly in the chemical industry, for example, on HC gas compressors. A buffer gas, for example, nitrogen, is fed between the seals at a higher pressure than the product pressure. One part of the buffer gas leakage escapes to the atmosphere side and the other part to the product side.

Operating Range of Dry Gas Seals

Gases ranging from inert gases such as nitrogen to highly toxic gaseous mixtures of natural gas and hydrogen sulfide can be sealed utilizing the optimum seal arrangements. The operating range of the spiral grooved dry gas seals is as follows:

Sealed Pressure: 2400 psi (165 Bar)
Temperature: 500 °F (260 °C)
Surface Speed: 500 ft/sec (152 m/sec)
M.W.: 2–60

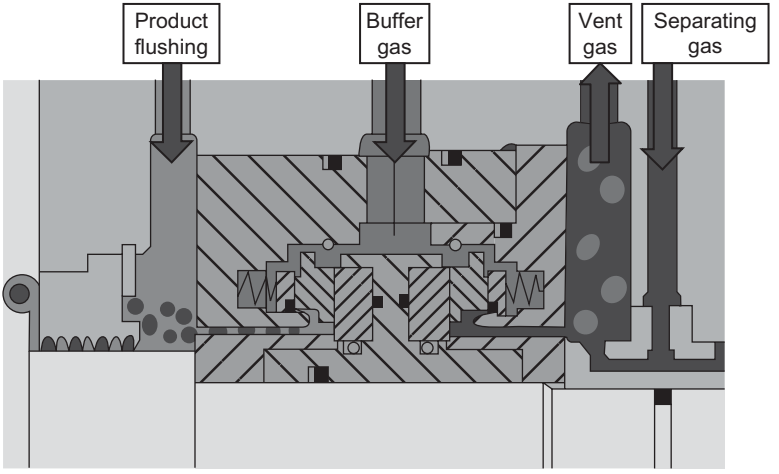


Figure 13-39 Double seal (courtesy Eagle Burgmann Germany GmbH & Co. KG).

Dry Gas Seal Materials

The gas composition, contaminants in the gas stream, operating temperatures, and process conditions dictate the choice of materials. The most common materials of construction are as follows:

Mating Ring: Tungsten Carbide, Silicon Carbide
Primary Ring: Carbon, Silicon Carbide
O-Rings: Elastomers (Viton, "Kalrez")
Hardware: 300 or 400 series ss (Sleeves, discs, retainer rings)
Coil Springs: 316 ss, Hastelloy

Dry Gas Seal Systems

The use of dry gas seals requires a system designed to supply sealing gas to the seal as a working fluid for the running gap. These gas seal systems are normally supplied by the compressor OEM mounted on the compressor base plate. There are two basic types of gas seal systems, differential pressure (ΔP) control and flow control. Differential control systems control the supply of seal gas to the seal by regulating the seal gas pressure to a pre-determined value typically 15 psi (1 Bar) above the sealing pressure. This is accomplished through the use of a differential pressure control valve. Flow control systems control the supply of seal gas to the seal by regulating the seal gas flow through an orifice upstream of the seal. This is accomplished through the use of a differential pressure control valve monitoring pressures on either side of the orifice.

Dry Gas Seal Degradation

Contamination of the seal by foreign objects leads to seal failures. The running gap between the primary and mating gas seal rings is typically around three microns.

Injection of any type of solids or liquids into this very narrow seal running gap can cause degradation of seal performance. This would create excessive gas leakage to the vent and eventual failure of the seal.

Since the typical operating gaps between the two sealing surfaces range from 0.0001 in to 0.0003 in, the resultant leakage is very small in magnitude. Under conditions of static pressurization beyond 50–75 psi (3.4–5.17 Bar), the seal leaks a very small amount. This leakage increases with increasing pressure and reduces with increasing temperature. Increased viscosity of gases at higher temperatures reduces the amount of seal leakage. For example, a 4-in (101.6 mm) shaft seal on a natural gas compressor statically pressurized to 1000 psi (69 bar) will leak about 1 scfm (0.03 scmm). Under dynamic condition, due to the pumping effect of the spiral grooves, the leakage increases as well.

The power loss can also be increased along with seal contamination. The seal surfaces being non-contacting under dynamic conditions the power loss associated with dry gas seals is very small. The power loss for a 10-in. (254 mm) seal operating at 1,000 psi (69 Bar) and 10,000 rpm is about 12–14 kW. With damage seal surfaces, these losses can be increased by 20–30%.

Foreign material within the seal results in increased shearing forces between the primary and mating rings, causing overheating of the seal components, leading to O-ring extrusion or some other mechanical form of seal failure. The major areas from which gas seals contamination occurs are:

- Process gas leakages from the inboard or high-pressure side of the seal.
- Bearing lubrication oil from the outboard or low-pressure side of the seal.
- The seal gas injected into the seal being contaminated upstream of the injection.

Contamination from Process Gas

Contamination from process gas can occur when there is insufficient supply of sealing gas into the seal, allowing process gas to come into direct contact with the seal ring faces. Contaminants existing within the process gas can then damage the seal.

Contamination from Bearing Lubrication Oil

A barrier seal is required on the outboard side of the dry gas seal, between the gas seal and the compressor bearing. The primary function of the barrier seal, typically buffered with air or nitrogen, is to prohibit the flow of bearing lubrication oil into the gas seal. Contamination of the dry gas seal from lube oil can occur when the barrier seal fails to function as intended.

Contamination from Seal Gas Supply

Contamination from the seal gas supply occurs when the sealing gas is not properly treated upstream of the dry gas seal. Gas seal manufacturers have stringent requirements for seal gas quality. Typically, the sealing gas must be dry and filtered of particles three microns and larger. Filters are normally provided in the gas seal system to meet this requirement.

Dry gas seals operate under extremely tight tolerances, which demand that special care be taken in the design of the gas seal environment, and in the operation of the compressor and gas seal system. While the threat of seal degradation and reduced seal life due to outside influences is real, the detrimental effects of these factors can be minimized.

The replacement of mechanical seals by dry gas seals must be closely examined. There have been many cases where the replacement has caused the compressor to operate in an unstable manner. This is due to the fact that removal of the mechanical seal causes a change in the damping of the rotor and can cause the rotor to operate closer to its critical speed.

Bibliography

Abramovitz, S., "Fluid Film Bearings, Fundamentals and Design Criteria, and Pitfalls," Proceedings of the 6th Turbomachinery Symposium, December 1977, pp. 189–204.

Childs, D.W., and Vance, J.M., "Annular Gas Seals and Rotordynamics of Compressors and Turbines," Proceedings of the 26th Turbomachinery Symposium, Texas A&M University, 1997, p. 201.

"Effects of Compressible Annular Seals," Proceedings of the 24th Turbomachinery Symposium, Texas A&M University, 1995, p. 175.

Egli, T., "The Leakage of Steam through Labyrinth Seals," Trans. ASME, 1935, pp. 115–122.

Evenson, R.S., Mason, B., Frederick, D.V., St. Onge, and Alain, G., "Development and Field Application of a Single Rotor Design Dry Gas Seal," Proceedings of the 24th Turbomachinery Symposium, Texas A&M University, 1995, p. 107.

FAG "Rolling Bearing Damage," Publication No. WL 82 102/2 Esi, 1995.

FAG "Rolling Bearings, Fundamentals, Types, Design," Publication No. WL 43 1190 EA, 1996.

Garner, D.R., and Leopard., A.J., "Temperature Measurements in Fluid Film Bearings," Proceedings of the 13th Turbomachinery Symposium, Texas A&M University, 1984, p. 133.

Herbage, B., "High Efficiency Fluid Film Thrust Bearings for Turbomachinery," 6th Proceedings of the Turbomachinery Symposium, Texas A&M University, December 1977, pp. 33–38.

Herbage, B.S., "High Speed Journal and Thrust Bearing Design," Proceedings of the 1st Turbomachinery Symposium, Texas A&M University, October 1972, pp. 56–61.

Jackson, C., "Radial and Thrust Bearing Practices with Case Histories," Proceedings of the 14th Turbomachinery Symposium, Texas A&M University, 1985, p. 73.

King, T.L., and Capitao, J.W., "Impact on Recent Tilting Pad Thrust Bearing Tests on Steam Turbine Design and Performance," Proceedings of the 4th Turbomachinery Symposium, Texas A&M University, October 1975, pp. 1–8.

Leopard, A.J., "Principles of Fluid Film Bearing Design and Application," Proceedings of the 6th Turbomachinery Symposium, Texas A&M University, December 1977, pp. 207–230.

Mayeux, T., Paul, Feltman Jr., and Paul, L., "Design Improvements Enhance Dry Gas Seal's Ability to Handle Reverse Pressurization," Proceedings of the 25th Turbomachinery Symposium, Texas A&M University, 1996, p. 149.

Richards, R.L., Vance, J.M., Paquette, D.J., and Zeidan, F.Y., "Using a Damper Seal to Eliminate Subsynchronous Vibrations in Three Back-to-Back Compressors," Proceedings of the 24th Turbomachinery Symposium, Texas A&M University, 1995, p. 59.

Salamone, D.J., "Journal Bearing Design Types and Their Applications to Turbomachinery," Proceedings of the 13th Turbomachinery Symposium, Texas A&M University, 1984, p. 179.

Scharrer, J.K., Pelletti, and Joseph, M., "Leakage and Rotordynamic Effects of Compressible Annular Seals," Proceedings of the 24th Turbomachinery Symposium, Texas A&M University, 1995, p. 175.

Shah, P., "Dry Gas Compressor Seals," Proceedings of the 17th Turbomachinery Symposium, Texas A&M University, 1988, p. 133.

Shapiro, W., and Colsher, R., "Dynamic Characteristics of Fluid Film Bearings," Proceedings of the 6th Turbomachinery Symposium, Texas A&M University, December 1977, pp. 39–53.

Southcott, J.F., Sweeney, J.M., Feltrnan Jr., and Paul, L., "Dry Gas Seal Retrofit," Proceedings of the 24th Turbomachinery Symposium, Texas A&M University, 1995, p. 221.

Takeuchi, Takao, Kataoka, Tadashi, Nagasaka, Hiroshi, Kakutani, Momoko, Ito, Masanobu, Muraki, and Ryoji "Advanced Dry Gas Seal by the Dynamic Ion Beam Mixing Technique," Proceedings of the 27th Turbomachinery Symposium, Texas A&M University, 1998, p. 39.

Copyrighted Materials
Copyright © 2012 Elsevier Retrieved from www.knovel.com

Part IV

Auxiliary Components and Accessories

13 Bearings and Seals

Bearings

The bearings in gas and steam turbines provide support and positioning for the rotating components. Radial support is generally provided by journal, or roller bearings, and axial positioning is provided by thrust bearings. Some engines, mainly aircraft jet engines, use ball or roller bearings for radial support, but nearly all-industrial gas turbines use journal bearings.

A long service life, a high degree of reliability, and economic efficiency are the chief aims when designing bearing arrangements. To reach these criteria, design engineers examine all the influencing factors:

1. Load and speed
2. Lubrication
3. Temperatures
4. Shaft arrangements
5. Life
6. Mounting and dismounting
7. Noise
8. Environmental conditions

Rolling Bearings

The aero-derivative gas turbine design, with its low-supported weight rotors – for example, the LM 5,000 HP rotor weights 1,230 lbs (558 kg) – incorporates roller bearings throughout. These do not require the large lube oil reservoirs, coolers and pumps, or the pre- and post-lube cycle associated with journal bearing designs. Roller bearings have proven to be extremely rugged and have demonstrated excellent life in industrial service. Most bearings provide reliable service for over 100,000 hours. In practice, it is advisable to replace bearings when exposed during major repairs, estimated at 50,000 hours for gas generators and 100,000 hours for power turbines.

There are many roller bearing types. They are differentiated according to the direction of the main radial loads (radial bearings) or axial loads (thrust bearings), and the type of rolling elements used, balls or rollers. Figure 13-1 shows the different types of bearings. The essential difference between ball bearings and roller bearings are that ball bearings have a lower carrying capacity and higher speeds, while roller bearings have higher load carrying capacity and lower speeds.

Gas Turbine Engineering Handbook, Fourth Edition. DOI: 10.1016/B978-0-12-383842-1.00013-5
Copyright © 2012 Elsevier Inc. All rights reserved.

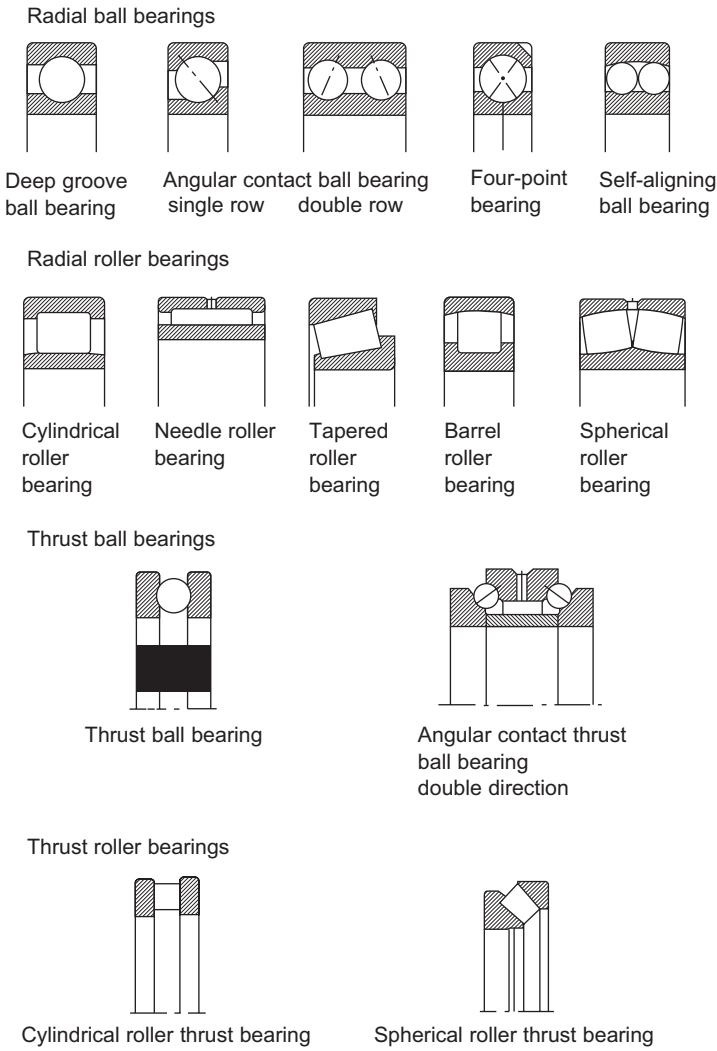


Figure 13-1 Types of rolling bearings (courtesy FAG bearings).

The rolling elements transmit loads from one bearing ring to the other in the direction of the contact lines. The contact angle α is the angle formed by the contact lines and the radial plane of the bearing. α refers to the nominal contact angle, i.e., the contact angle of the load-free bearing as seen in Figure 13-2. Under axial loads, the contact angle of deep groove ball bearings, angular contact ball bearings, etc., increases. Under a combined load it changes from one rolling element to the next. These changing contact angles are taken into account when calculating the pressure distribution within the bearing. Ball bearings and roller bearings with symmetrical rolling elements have identical contact angles at their inner rings and outer rings. In roller bearings with asymmetrical rollers,

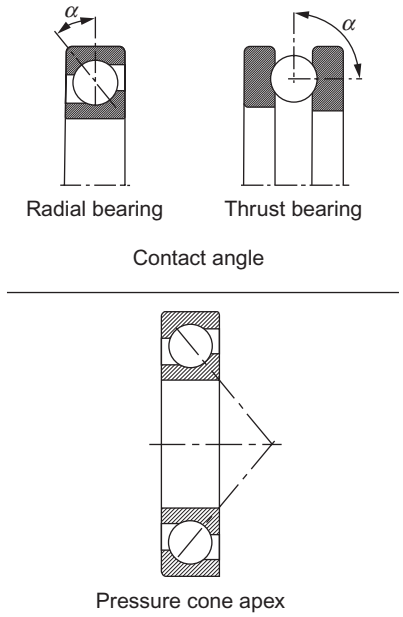
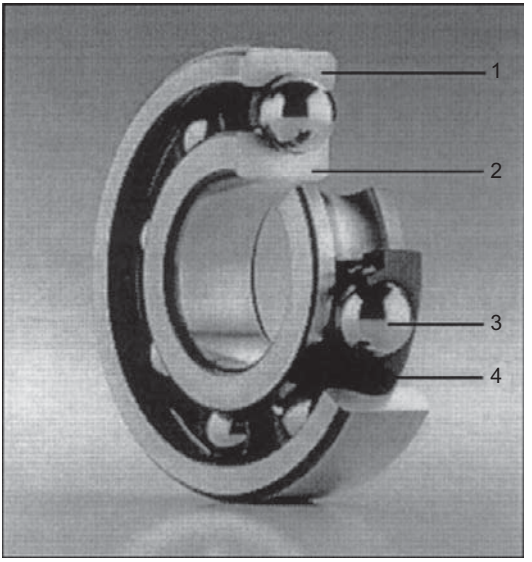


Figure 13-2 Rolling bearing terminology (courtesy FAG bearings).

the contact angles at the inner rings and outer rings are not identical. The equilibrium of forces in these bearings is maintained by a force component, which is directed towards the lip. The pressure cone apex is that point on the bearing axis where the contact lines of an angular contact bearing (i.e., an angular contact ball bearing, a tapered roller bearing, or a spherical roller thrust bearing) intersect. The contact lines are the generatrices of the pressure cone apex. In angular contact bearings, the external forces act, not at the bearing center, but at the pressure cone apex.

Rolling bearings generally consist of bearing rings, inner ring and outer ring, rolling elements that roll on the raceways of the rings, and a cage that surrounds the rolling elements as seen in Figure 13-3. The rolling elements are classified according to their shapes, into: balls, cylindrical rollers, needle rollers, tapered rollers, and barrel rollers as shown in Figure 13-4.

The rolling elements' function is to transmit the force acting on the bearing from one ring to the other. For a high load carrying capacity it is important that as many rolling elements as possible, which are as large as possible, are accommodated between the bearing rings. Their number and size depend on the cross section of the bearing. It is just as important for load ability that the rolling elements within the bearing are of identical size. Therefore, they are sorted according to grades. The tolerance of one grade is very slight. The generatrices of cylindrical rollers and tapered rollers have a logarithmic profile. The center part of the generatrix of a needle roller is straight, and the ends are slightly crowned, this profile prevents edge stressing when under load.



(1) Outer ring (2) Inner ring (3) Rolling element and (4) Cage

Figure 13-3 Roller bearing showing the various components (courtesy FAG Bearings).

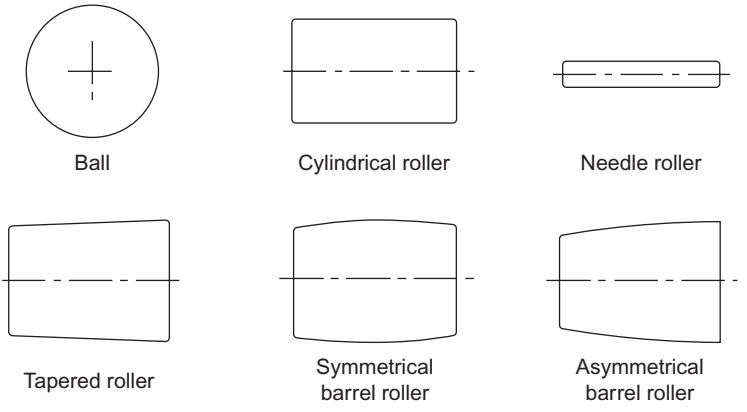


Figure 13-4 Various types of rollers used in a rolling bearing (courtesy FAG bearings).

The bearing rings comprise an inner ring and an outer ring to guide the rolling elements in the direction of rotation. Raceway grooves, lips, and inclined running areas guide the rollers and transmit axial loads in a transverse direction as seen in Figure 13-5. Cylindrical roller bearings and needle roller bearings, which need to accommodate shaft expansions have lips only on one bearing ring and are commonly known as floating bearings.

The functions of a cage are to keep the rolling elements apart so that they do not rub against each other, to keep the rolling elements evenly spaced for uniform load

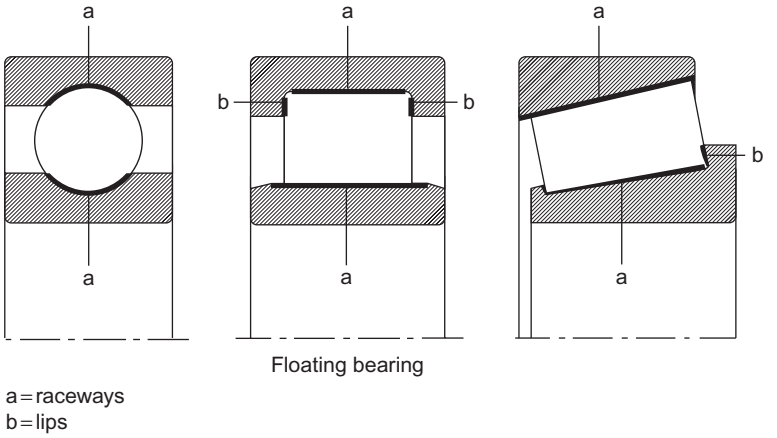


Figure 13-5 Raceway grooves and lips for typical roller bearings (courtesy FAG bearings).

distribution, to prevent rolling elements from falling out of separable bearings and bearings that are swiveled out, and to guide the rolling elements in the unloaded zone of the bearing. The transmission of forces is not one of the cage's functions.

Cages are classified into pressed cages, machined cages, and molded cages. Pressed cages are usually made of steel, but sometimes of brass too. They are lighter than machined metal cages. Since a pressed cage barely closes the gap between the inner ring and outer ring, lubricant can easily penetrate into the bearing.

Machined cages of metal and textile laminated phenolic resin are made from tubes of steel, light metal or textile laminated phenolic resin, or cast brass rings. To obtain the required strength, large, heavily loaded bearings are fitted with machined cages. Machined cages are also used where lip guidance of the cage is required. Lip-guided cages for high-speed bearings are, in many cases, made of light materials such as light metal or textile laminated phenolic resin to keep the forces of gravity low.

Molded cages using injection molding techniques can realize designs with an especially high-load carrying capacity. The elasticity and low weight of the cages are of advantage where shock-type bearing loads, great accelerations and decelerations as well as tilting of the bearing rings relative to each other have to be accommodated. Polyamide cages feature very good sliding and dry running properties.

There are a number of special rolling bearing designs and some series of cylindrical roller bearings without cages. By omitting the cage the bearing can accommodate more rolling elements. This yields an increased load rating, but, due to the increased friction, the bearing is suitable for lower speeds only.

Load ratings

The load rating of a bearing reflects its load carrying capacity and is an important factor in the dimensioning of rolling bearings. It is determined by the number and size of the rolling elements, the curvature ratio, the contact angle, and the pitch circle

diameter of the bearing. Due to the larger contact area between rollers and raceways the load ratings of roller bearings are higher than those of ball bearings.

The load rating of a radial bearing is defined by radial loads whereas that of a thrust bearing is defined by axial loads. Every rolling bearing has a dynamic load rating and a static load rating. The terms "dynamic" and "static" refer to the movement of the bearing but not to the type of load.

In all rolling bearings with a curved raceway profile, the radius of the raceway is slightly larger than that of the rolling elements. This curvature difference in the axial plane is defined by the curvature ratio x. The curvature ratio is the curvature difference between the rolling element radius and the slightly larger groove radius:

$$\text{radius curvature ratio } x = (\text{groove radius} - \text{rolling element})/\text{rolling element radius}$$

Thrust ball bearings are used where purely axial loads have to be accommodated. The single direction (= single row) design is designed for loads from one direction, the double direction one (= double row) for reversing loads. Besides the design with flat washers, designs with spherical housing washers and seating washers are also available that can compensate for misalignment.

Spherical roller thrust bearings can accommodate high axial loads. They are suitable for relatively high speeds. The raceways, which are inclined toward the bearing axis, allow the bearings to accommodate radial loads as well. The radial load must not exceed 55% of the axial load.

The bearings have asymmetrical barrel rollers and compensate for misalignment. As a rule, spherical roller thrust bearings have to be lubricated with oil.

Wear

The life of rolling bearings can be terminated, apart from fatigue, as a result of wear. The clearance of a worn bearing gets too large.

One frequent cause of wear is that foreign particles penetrate into a bearing due to insufficient sealing and have an abrasive effect. Wear is also caused by starved lubrication and when the lubricant is used up.

Therefore, wear can be considerably reduced by providing good lubrication conditions (viscosity ratio $x > 2$ if possible) and a good degree of cleanliness in the rolling bearing. Where $x \leq 0.4$ wear will dominate in the bearing if it is not prevented by suitable additives (EP additives).

The kinematically permissible speed may be higher or lower than the thermal reference speed. The basis of the thermal reference speed is for cases where the operating conditions (load, oil viscosity, or permissible temperature) deviate from the reference conditions. Decisive criteria for the kinematically permissible speed are the strength limit of the bearing parts and the permissible sliding velocity of rubbing seals. Kinematically permissible speeds, which are higher than the thermal reference speeds, can be reached, for example, with specially designed lubrication, bearing clearance

adapted to the operating conditions, and accurate machining of the bearing seats with special regard to heat dissipation.

The thermal reference speed is a new index of the speed suitability of rolling bearings. It is defined as the speed at which the reference temperature of 160 °F (70 °C) is established. For high temperature rolling bearings, the steel used for bearing rings and rolling elements is generally heat-treated so that it can be used at operating temperatures of up to 300 °F (150 °C). At higher temperatures, dimensional changes and hardness reductions result. Therefore, operating temperatures over 300 °F (150 °C) require special heat treatment.

Journal Bearings

The heavy frame type gas turbines use journal bearings. Journal bearings may be either full round or split; the lining may be heavy as used in large-size bearings for heavy machinery, or thin, as used in precision insert-type bearings in internal combustion engines. Most sleeve bearings are of the split type for convenience in servicing and replacement. Often in split bearings, where the load is entirely downward, the top half of the bearing acts only as a cover to protect the bearing and to hold the oil fittings. Figure 13-6 shows a number of different types of journal bearings. A description of a few of the pertinent types of journal bearings is given here:

1. *Plain journal.* Bearing is bored with equal amounts of clearance (on the order of 1½ to two thousands of an inch per inch of journal diameter) between the journal and bearing.
2. *Circumferential grooved bearing.* Normally has the oil groove at half the bearing length. This configuration provides better cooling, but reduces load capacity by dividing the bearing into two parts.
3. *Cylindrical bore bearings.* Another common bearing type used in turbines. It has a split construction with two axial oil-feed grooves at the split.
4. *Pressure or pressure dam.* Used in many places where bearing stability is required, this bearing is a plain journal bearing with a pressure pocket cut in the unloaded half. This pocket is approximately 1/32 of an inch (.8 mm) deep with a width 50% of the bearing length. This groove or channel covers an arc of 135 ° and terminates abruptly in a sharp-edge dam. The direction of rotation is such that the oil is pumped down the channel toward the sharp edge. Pressure dam bearings are for one direction of rotation. They can be used in conjunction with cylindrical bore bearings as shown in Figure 13-6.
5. *Lemon bore or elliptical.* This bearing is bored with shims at the split line, which are removed before installation. The resulting bore shape approximates an ellipse with the major axis clearance approximately twice the minor axis clearance. Elliptical bearings are for both directions of rotation.
6. *Three-lobe bearing.* The three-lobe bearing is not commonly used in turbomachines. It has a moderate load-carrying capacity and can be operated in both directions.
7. *Offset halves.* In principle, this bearing acts very similar to a pressure dam bearing. Its load-carrying capacity is good. It is restricted to one direction of rotation.
8. *Tilting-pad bearings.* This bearing is the most common bearing type in today's machines. It consists of several bearing pads posed around the circumference of the shaft. Each pad is able to tilt to assume the most effective working position. Its most important feature is

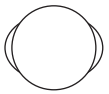
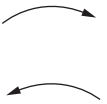
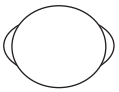
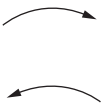
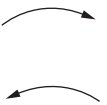
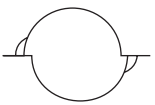
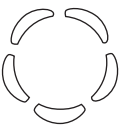
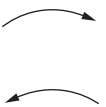
Bearing type	Load capacity	Suitable direction of rotation	Resistance to half-speed whirl	Stiffness and damping
Cylindrical bore 	Good		Worst	Moderate
Cylindrical bore with dammed groove 	Good			Moderate
Lemon bore 	Good			Moderate
Three lobe 	Moderate		Increasing	Good
Offset halves 	Good			Excellent
Tilting pad 	Moderate		Best	Good

Figure 13-6 Comparison of general bearing types.

self-alignment when spherical pivots are used. This bearing also offers the greatest increase in fatigue life because of the following advantages:

a. Self-aligning for optimum alignment and minimum limit.

b. Thermal conductivity backing material to dissipate heat developed in oil film.

c. A thin babbitt layer can be centrifugally cast with a uniform thickness of about 0.005 of an inch (0.127 mm). Thick babbitts greatly reduce bearing life. Babbitt thickness in the neighborhood of .01 in. (.254 mm) reduce the bearing life by more than half.
d. Oil film thickness is critical in bearing stiffness calculations. In a tilting-pad bearing, one can change this thickness in a number of ways: (1) changing the number of pads; (2) directing the load on or in between the pads; (3) and changing axial length of pad.

The previous list contains some of the most common types of journal bearings. They are listed in the order of growing stability. All of the bearings designed for increased stability are obtained at higher manufacturing costs and reduced efficiency. The antiwhirl bearings all impose a parasitic load on the journal, which causes higher power losses to the bearings, and in turn, requires higher oil flow to cool the bearing. Many factors enter into the selection of the proper design for bearings. Some of the factors that affect bearing design follow:

1. Shaft speed range.
2. Maximum shaft misalignment that can be tolerated.
3. Critical speed analysis and the influence of bearing stiffness on this analysis.
4. Loading of the compressor impellers.
5. Oil temperatures and viscosity.
6. Foundation stiffness.
7. Axial movement that can be tolerated.
8. Type of lubrication system and its contamination.
9. Maximum vibration levels that can be tolerated.

Bearing Design Principles

The journal bearing is a fluid-film bearing. This description means that a full film of fluid completely separates the stationary bushing from the rotating journal – the two components that make up the bearing system. This separation is achieved by pressurizing the fluid in the clearance space to the extent that the fluid forces a balance in the bearing load. This balance requires the fluid to be continuously introduced into and pressurized in the film space. Figure 13-7 shows the four modes of lubrication in a fluid-film bearing. The hydrodynamic mode bearing is the most common bearing type used and is also often called the "self-acting" bearing.

As can be seen in Figure 13-7 (a), the pressure is self-induced by the relative motion between the two bearing member surfaces. The film is wedge-shaped in this type of lubrication mode. Figure 13-7 (b) shows the hydrostatic mode of lubrication. In this type of a bearing, the lubricant is pressurized externally and then introduced in the bearing. Figure 13-7 (c) shows the squeeze-film lubrication mode. This type of a bearing derives its load-carrying capacity and separation from the fact that a viscous fluid cannot be instantaneously squeezed out between two surfaces that are approaching each other. Figure 13-7 (d) shows a hybrid-type bearing that combines the previous modes. The most common hybrid type combines the hydrodynamic and hydrostatic modes.

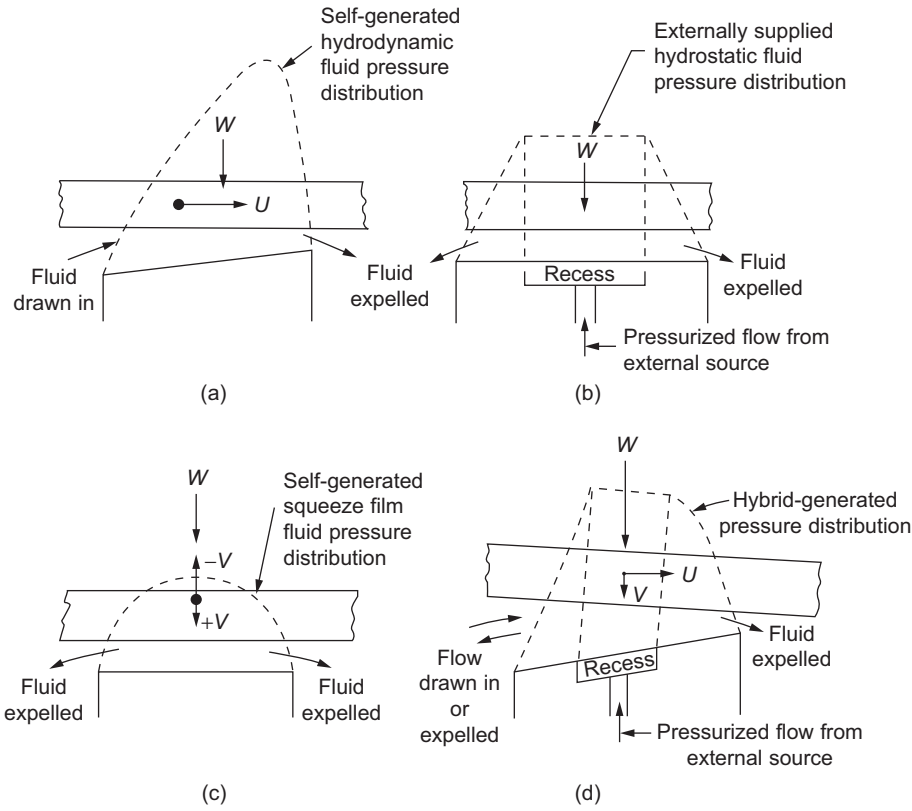


Figure 13-7 Modes of fluid-film lubrication: (a) hydrodynamic, (b) hydrostatic, (c) squeeze film, (d) hybrid.

A further investigation of the hydrodynamic mode is warranted, since it is the most common type of lubrication mode employed. This type of lubrication depends on the bearing member velocity as well as the existence of a wedge-shaped configuration. The journal bearing forms a natural wedge as seen in Figure 13-8, which is inherent in its design. Figure 13-3 also shows the pressure distribution in the bearing. Fluid-film thickness depends on the mode, lubrication, and application and varies from .0001 to .01 inches (.00254–.254 mm). For hydrostatic oil-lubricated bearings, the film thickness is .008 of an inch (.203 mm). In the special case of oil-squeeze film bearings where the capacity must be provided to take extremely high-revising loads with no bearing harm, the oil-film thickness could be below .0001of an inch (.00254 mm). Since the film thickness is so very important, an understanding of the surface is also vital.

All surfaces, regardless of their finish, are made up of peaks and valleys, and in general, the average asperity height may be 5–10 times the RMS surface finish reading. When the surface is abraded, an oxide film will form almost immediately.

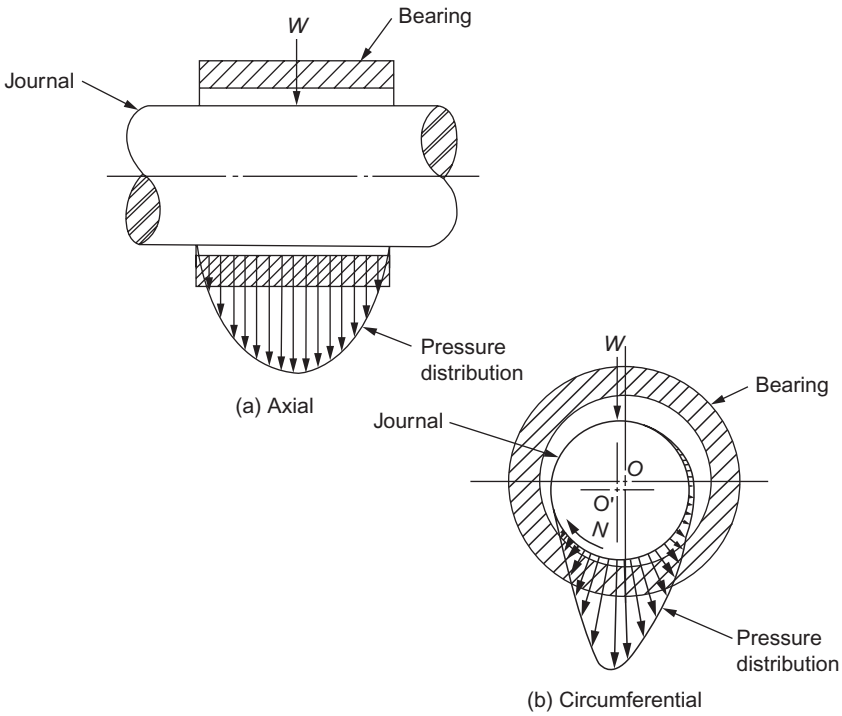


Figure 13-8 Pressure distribution in a full journal bearing.

Figure 13-9 (a) shows the relative separation of the full-film, mixed-film, and boundary. If a full-film exists, the bearing life is almost infinite. The limitation in the case of full-film is due to lubricant breakdown, shock load, bearing surface erosion, and fretting of bearing components. Figures 13-9 (b) and 13-9 (c) are cross sections showing the various contamination types. Oil additives are contaminants that form beneficial surface films.

The bearing health can be best described by plotting a *ZN/P* versus coefficient of friction curve. Figure 13-10 shows such a curve where *Z* is the lubricant viscosity in centipoise, *N* the rpm of the journal, and *P* is the projected area unit loading.

As the bearing speed is increased for a given lubricant and loading, the friction is at its lowest when full-film is achieved, after which the increase is due to the increasing lubricant shear force.

The bearing fluid film acts like a spring that is nonlinear. Figure 13-11 shows a curve of bearing load versus film thickness and eccentricity ratio. The bearing stiffness can then be obtained at any load value by drawing a line tangent to the curve at the load point. The film stiffness can then be used in determining the critical speed of the rotor.

With higher speeds and unusual fluid lubricants, turbulence in the fluid film is no longer rare. Normally, thin film is thought of as being laminar, but with high speeds,

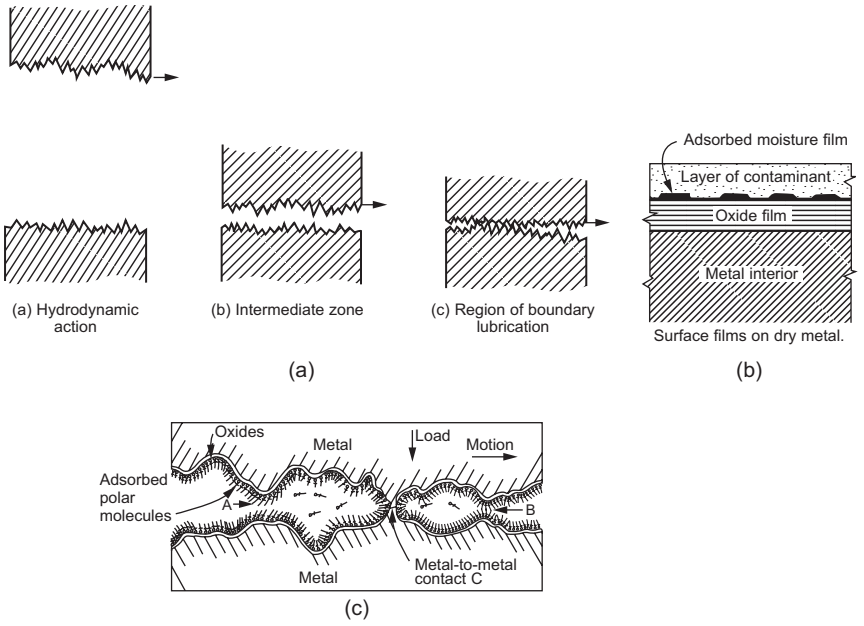


Figure 13-9 Enlarged views of bearing surfaces.

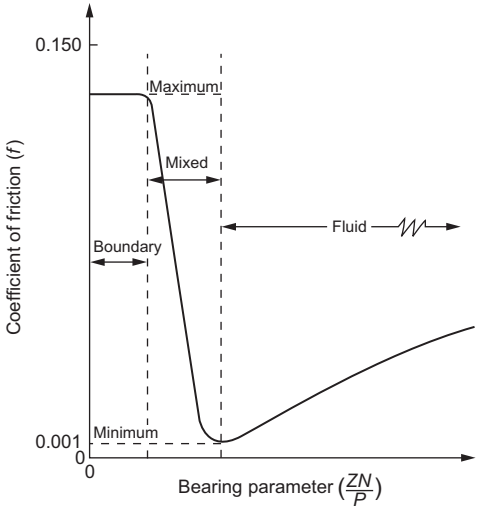


Figure 13-10 Classic *ZN/P* curve.

low viscosity, and sometimes high-density fluids, the lubricant can be turbulent in the film space. This turbulence manifests itself as an abnormal increase in power loss. As compared to laminar-flow conditions, a Reynolds number, even in the transition region, can double the power and, deep in the turbulent region, can increase the power tenfold. Although this phenomenon, because of its random nature, is difficult to

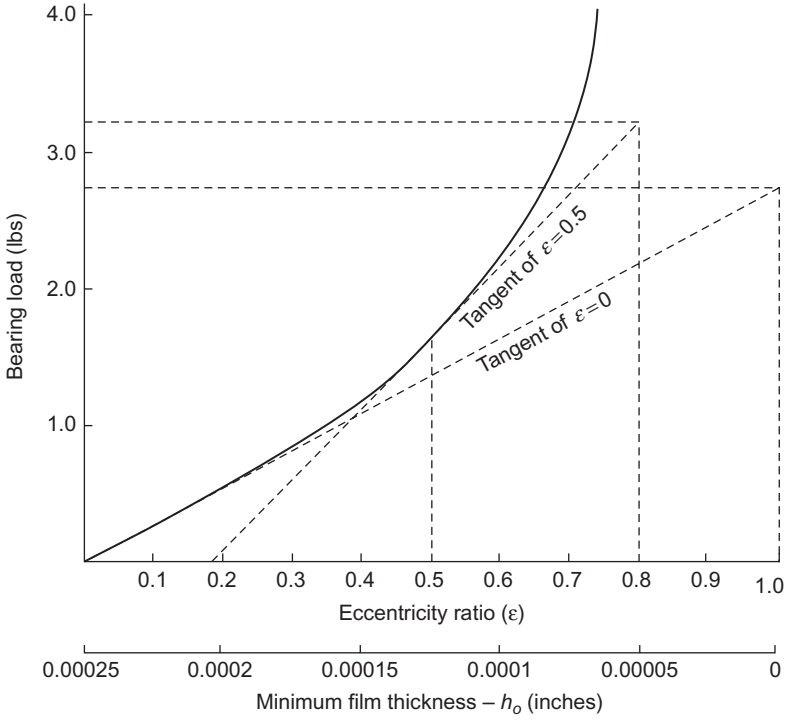


Figure 13-11 Journal bearing load capacity versus minimum film thickness and eccentricity ratio.

analyze, there is an unusual amount of theoretical work that has been done and some experimental work that is available. Just as a guide, one can assume that the transition point will occur at a Reynolds number of about 800. As to film thickness, there is evidence indicating that under turbulent conditions it is actually greater than calculated, based on laminar-flow theory.

Tilting-Pad Journal Bearings

Normally, the tilting-pad journal bearing is considered when shaft loads are light because of its inherent ability to resist oil whirl vibration. However, this bearing, when properly designed, has a very high load-carrying capacity. It has the ability to tilt to accommodate the forces being developed in the hydrodynamic oil film, and therefore operates with an optimum oil-film thickness for the given load and speed. This ability to operate over a large range of loads is especially useful in high-speed gear reductions with various combinations of input and output shafts.

Another important advantage of the tilting-pad journal bearing is its ability to accommodate shaft misalignment. Because of its relatively short length-to-diameter ratio, it can accommodate minor misalignment quite easily.

As shown earlier, bearing stiffness varies with the oil-film thickness so that the critical speed is directly influenced to a certain degree by oil-film thickness. Again, in the area of critical speeds, the tilting-pad journal bearing has the greatest degree of design flexibility. There are sophisticated computer programs that show the influence of various load and design factors on the stiffness of tilting-pad journal bearings. The following variations are possible in the design of tilting-pad bearings:

1. The number of pads can be varied from three to any practical number.
2. The load can be placed either directly on a pad or to occur between pads.
3. The unit loading on the pad can be varied by either adjusting the arc length or the axial length of the bearing pad.
4. A parasitic pre-load can be designed into the bearing by varying the circular curvature of the pad with respect to the curvature of the shaft.
5. An optimum support point can be selected to obtain a maximum oil-film thickness.

On a high-speed rotor system, it is necessary to use tilting-pad bearings because of the dynamic stability of these bearings. A high-speed rotor system operates at speeds above the first critical speed of the system. It should be understood that a rotor system includes the rotor, the bearings, the bearing support system, seals, couplings, and other items attached to the rotor. The system's natural frequency is therefore dependent on the stiffness and damping effect of these components.

Commercial multipurpose tilting-pad bearings are usually designed for multidirectional rotation so that the pivot point is at pad midpoint. However, the design criteria generally applied for producing maximum stability and load-carrying capacity locates the pivot at two-thirds of the pad arc in the direction of rotation.

Bearing pre-load is another important design criterion for tilting-pad bearings. Bearing pre-load is bearing assembly clearance divided by machined clearance:

$$\text{Pre-load ratio} = C'/C = \frac{\text{Concentric pivot film thickness}}{\text{Machined clearance}}$$

A pre-load of 0.5–1.0 provides for stable operation because a converging wedge is produced between the bearing journal and the bearing pads.

The variable C' is an installed clearance and is dependent upon the radial pivot position. The variable C is the machine clearance and is fixed for a given bearing. Figure 13-7 shows two pads of a five-pad tilting-pad bearing where the pads have been installed such that the pre-load ratio is less than one, and Pad 2 has a pre-load ratio of 1.0. The solid line in Figure 13-7 represents the position of the journal in the concentric position. The dashed line represents the journal in a position with a load applied to the bottom pads.

From Figure 13-12, Pad 1 is operating with a good converging wedge, while Pad 2 is operating with a completely diverging film, thus indicating that the pad is completely unloaded. Therefore, bearings with pre-load ratios of 1.0 or greater will be operating with some of their pads completely unloaded, thus reducing the overall stiffness of the bearing and decreasing its stability, since the upper pads do not aid in resisting cross-coupling influences.

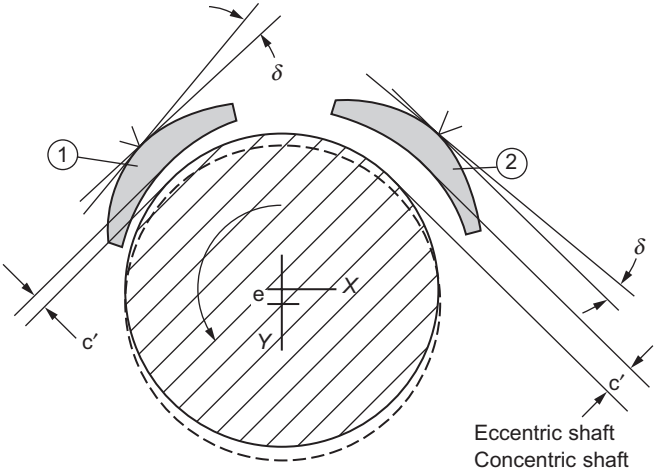


Figure 13-12 Tilting-pad bearing pre-load.

Unloaded pads are also subject to flutter, which leads to a phenomenon known as "leading-edge lock-up." Leading-edge lock-up causes the pad to be forced against the shaft, and it is then maintained in that position by the frictional interaction of the shaft and the pad. Therefore, it is of prime importance that the bearings be designed with pre-load, especially for low-viscosity lubricants. In many cases, manufacturing reasons and the ability to have two-way rotation cause many bearings to be produced without pre-load.

Bearing designs are also affected by the transition of the film from a laminar to a turbulent region. The transition speed (N_t) can be computed using the following relationship:

$$N_t = 1.57 \times 10^3 \frac{v}{\sqrt{DC^3}}$$

where:

v = viscosity of the fluid

D = diameter (inches)

C = diametrical clearance (inches)

Turbulence creates more power absorption, thus increasing oil temperature that can lead to severe erosion and fretting problems in bearings. It is desirable to keep the oil discharge temperature below 170 °F (77 °C), but with high-speed bearings, this ideal may not be possible. In those cases, it is better to monitor the temperature difference between the oil entering and leaving as shown in Figure 13-13.

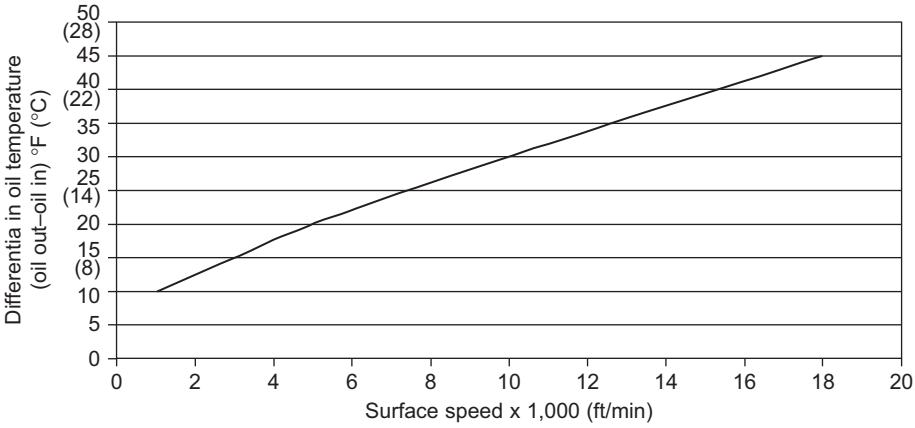


Figure 13-13 Oil discharge characteristics.

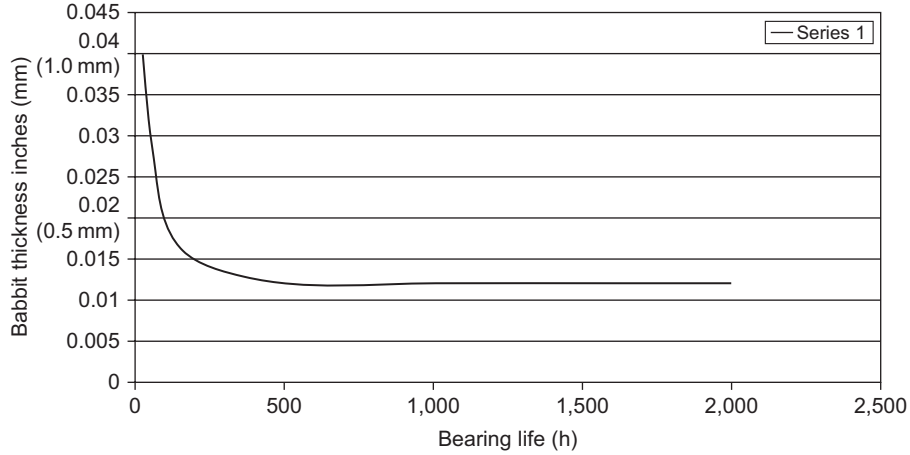


Figure 13-14 Babbitt fatigue characteristics.

Bearing Materials

In all the time since Issaac Babbitt patented his special alloy in 1839, nothing has been developed that encompasses all of its excellent properties as an oil-lubricated bearing surface material. Babbitts have excellent compatibility and non-scoring characteristics and are outstanding in embedding dirt and conforming to geometric errors in machine construction and operation. They are, however, relatively weak in fatigue strength, especially at elevated temperatures and when the babbitt is more than about 0.015 of an inch (.381 mm) thick as seen in Figure 13-14. In general, the selection of a bearing material is always a compromise, and no single composition can include all desirable properties. Babbitts can tolerate momentary rupture of the oil film, and

may well minimize shaft or runner damage in the event of a complete failure. Tin babbitts are more desirable than the lead-based materials, since they have better corrosion resistance, less tendency to pickup on the shaft or runner, and are easier to bond to a steel shell.

Application practices suggest a maximum design temperature of about 300 °F (149 °C) for babbitt, and designers will set a limit of about 50 °F (28 °C) less. As temperatures increase, there is a tendency for the metal to creep under the softening influence of the rising temperature. Creep can occur with generous film thickness and can be observed as ripples on the bearing surface where flow took place. With tin babbitts, observation has shown that creep temperature ranges from 375 °F (190 °C) for bearing loads below 200 psi (13.79 Bar) to about 260–270 °F (127–132 °C) for steady loads of 1,000 psi (69 Bar). This range may be improved by using very thin layers of babbitt such as in automotive bearings.

Bearing and Shaft Instabilities

One of the most serious forms of instability encountered in journal bearing operation is known as ‘‘half-frequency whirl.” It is caused by self-excited vibration and characterized by the shaft center orbiting around the bearing center at a frequency of approximately half of the shaft rotational speed as shown in Figure 13-15.

As the speed is increased, the shaft system may be stable until the “whirl” threshold is reached. When the threshold speed is reached, the bearing becomes unstable, and further increase in speed produces more violent instability until eventual seizure results. Unlike an ordinary critical speed, the shaft cannot “pass through,” and the instability frequency will increase and follow that half ratio as the shaft speed is increased. This type of instability is associated primarily with high-speed, lightly loaded bearings. At present, this form of instability is well understood, can be theoretically predicted with accuracy, and avoided by altering the bearing design.

It should be noted that the tilting-pad journal bearing is almost completely free from this form of instability. However, under certain conditions, the tilting pads themselves can become unstable in the form of shoe (pad) flutter, as mentioned previously.

All rotating machines vibrate when operating, but the failure of the bearings is mainly caused by their inability to resist cyclic stresses. The level of vibration a unit can tolerate is shown in the severity charts in Figure 13-16. These charts are modified by many users to reflect the critical machines in which they would like to maintain much lower levels. Care must always be exercised when using these charts, since different machines have different size housings and rotors. Thus, the transmissibility of the signal will vary.

Thrust Bearings

The most important function of a thrust bearing is to resist the unbalanced force in a machine’s working fluid and to maintain the rotor in its position (within prescribed limits). A complete analysis of the thrust load must be conducted. As mentioned

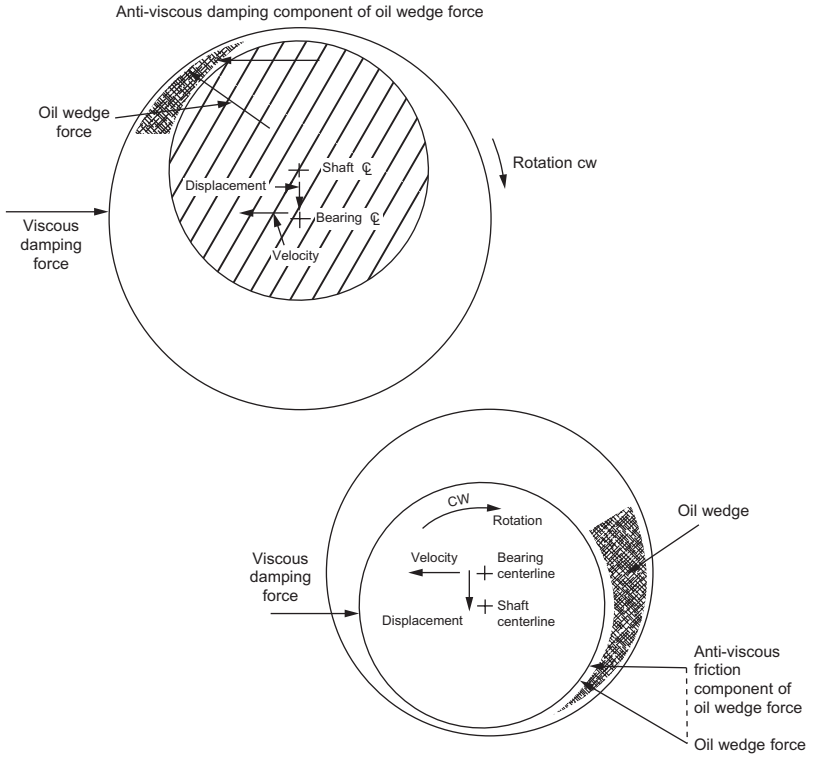


Figure 13-15 Oil whirl.

earlier, compressors with back-to-back rotors reduce this load greatly on thrust bearings. Figure 13-17 shows a number of thrust-bearing types. Plain, grooved thrust washers are rarely used with any continuous load, and their use tends to be confined to cases where the thrust load is of very short duration or possibly occurs at a standstill or low speed only. Occasionally, this type of bearing is used for light loads (less than 50 lb/in^2 [3.5 bar]), and in these circumstances the operation is probably hydrodynamic due to small distortions present in the nominally flat bearing surface.

When significant continuous loads have to be taken on a thrust washer, it is necessary to machine into the bearing surface a profile to generate a fluid film. This profile can be either a tapered wedge or occasionally a small step.

The tapered-land thrust bearing, when properly designed, can take and support a load equal to a tilting-pad thrust bearing. With perfect alignment, it can match the load of even a self-equalizing tilting-pad thrust bearing that pivots on the back of the pad along a radial line. For variable-speed operation, tilting-pad thrust bearings, as shown in Figure 13-18, are advantageous when compared to conventional taper-land bearings. The pads are free to pivot and form a proper angle for lubrication over a wide

speed range. The self-leveling feature equalizes individual pad loadings and reduces the sensitivity to shaft misalignments that may occur during service. The major drawback of this bearing type is that standard designs require more axial space than a non-equalizing thrust bearing.

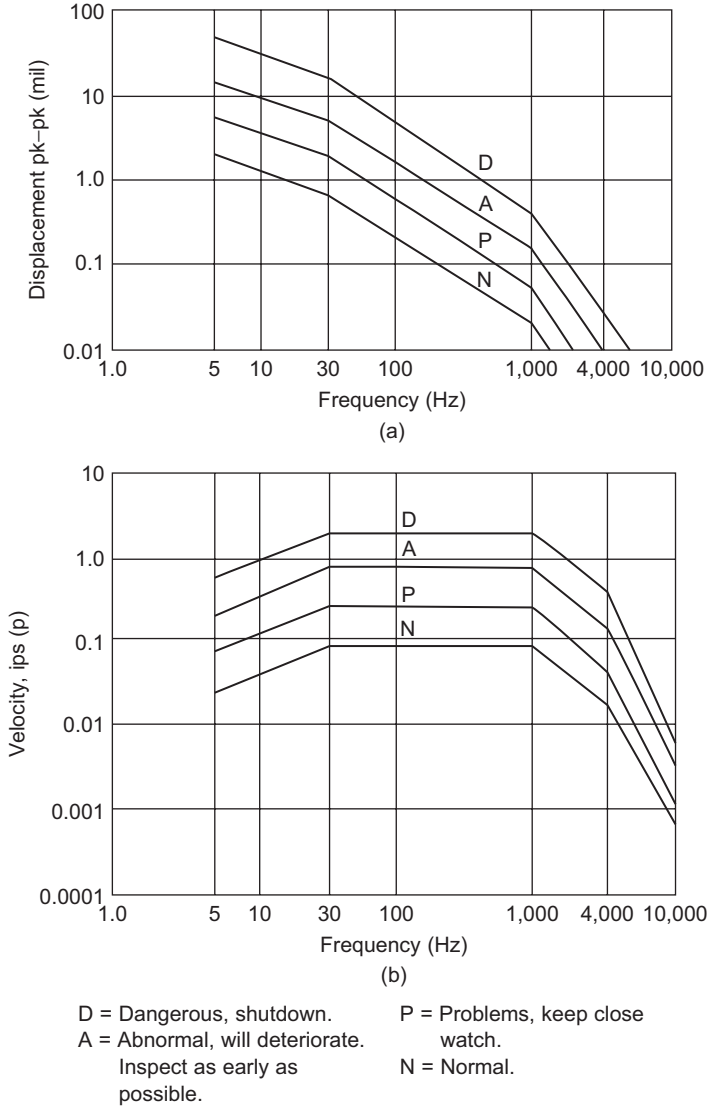
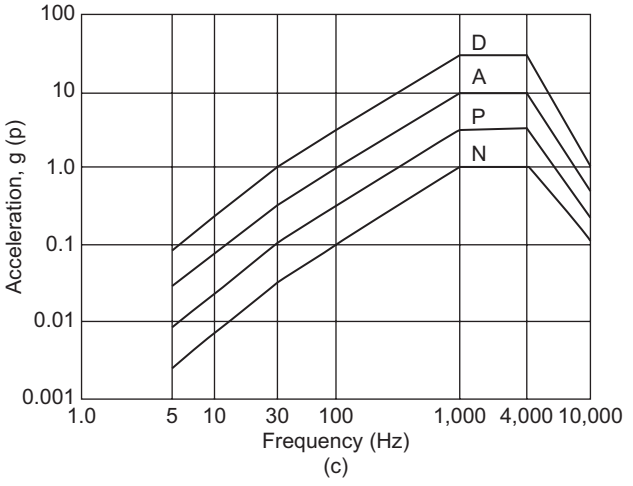


Figure 13-16 Severity charts: (a) displacement, (b) velocity. Severity chart: (c) acceleration.



D = Dangerous, shutdown.
A = Abnormal, will deteriorate. Inspect as early as possible.
P = Problems, keep close watch.
N = Normal.

Figure 13-16 *continued*

Bearing type	Load capacity	Suitable direction of rotation	Tolerance of changing load/speed	Tolerance of misalignment	Space requirement
Plain washer	Poor		Good	Moderate	Compact
Taper land — Bidirectional	Moderate		Poor	Poor	Compact
Taper land — Unidirectional	Good		Poor	Poor	Compact
Tilting pad — Bidirectional	Good		Good	Good	Greater
Tilting pad — Unidirectional	Good		Good	Good	Greater

Figure 13-17 Comparison of thrust-bearing types.

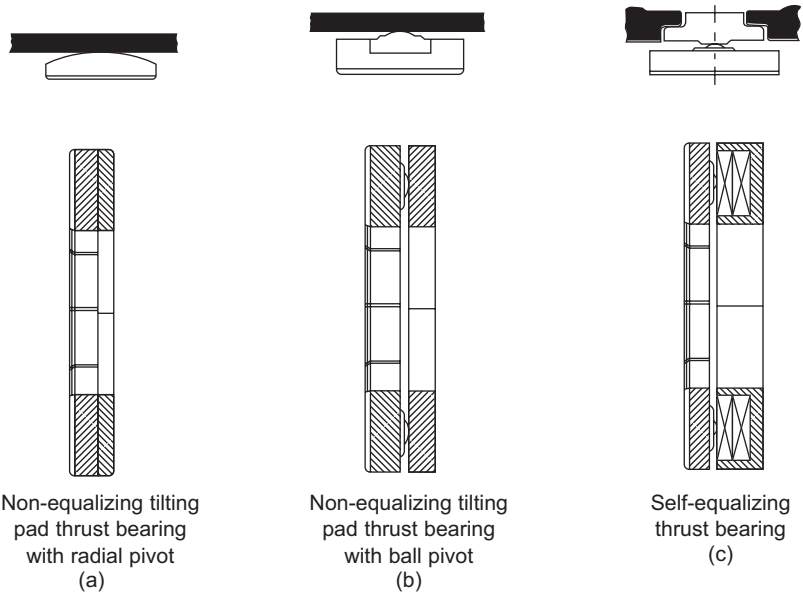


Figure 13-18 Various types of thrust-bearings.

Factors Affecting Thrust-Bearing Design

The principal function of a thrust bearing is to resist the thrust unbalance developed within the working elements of a turbomachine and to maintain the rotor position within tolerable limits.

After an accurate analysis has been made of the thrust load, the thrust bearing should be sized to support this load in the most efficient method possible. Many tests have proven that thrust bearings are limited in load capacity by the strength of the babbitt surface in the high load and temperature zone of the bearing. In normal steel-backed babbitted tilting-pad thrust bearings, this capacity is limited to between 250 and 500 psi (17 and 35 Bar) average pressure. It is the temperature accumulation at the surface and pad crowning that cause this limit.

The thrust-carrying capacity can be greatly improved by maintaining pad flatness and by removing heat from the loaded zone. By the use of high thermal conductivity backing materials with proper thickness and proper support, the maximum continuous thrust limit can be increased to 1,000 psi or more. This new limit can be used to increase either the factor of safety and improve the surge capacity of a given size bearing or reduce the thrust bearing size and consequently the losses generated for a given load.

Since the higher thermal conductivity material (copper or bronze) is a much better bearing material than the conventional steel backing, it is possible to reduce the babbitt thickness to .010–.030 of an inch (.254–.762 mm). Embedded thermocouples and RTDs will signal distress in the bearing if properly positioned. Temperature

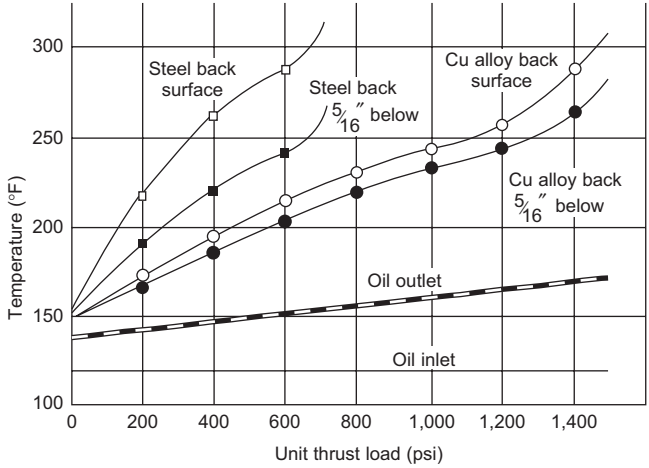


Figure 13-19 Thrust-bearing temperature characteristics.

monitoring systems have been found to be more accurate than axial position indicators, which tend to have linearity problems at high temperatures.

In a change from steel-backing to copper-backing a different set of temperature limiting criteria should be used. Figure 13-19 shows a typical set of curves for the two backing materials. This chart also shows that drain oil temperature is a poor indicator of bearing operating conditions because there is very little change in drain oil temperature from low load to failure load.

Thrust-Bearing Power Loss

The power consumed by various thrust bearing types is an important consideration in any system. Power losses must be accurately predicted so that turbine efficiency can be computed and the oil supply system properly designed.

Figure 13-20 shows the typical power consumption in thrust bearings as a function of unit speed. The total power loss is usually about 0.8–1.0% of the total rated power of the unit. New vectored lube bearings that are being tested show preliminary figures of reducing the power loss by as much as 30%.

Seals

Seals are very important and often critical components in turbomachinery, especially on high-pressure and high-speed equipment. This chapter covers the principal sealing systems used between the rotor and stator elements of turbomachinery. They fall into two main categories: (1) non-contacting seals, and (2) face seals.

Since these seals are an integral part of the rotor system, they affect the dynamic operating characteristics of the machine; for instance, both the stiffness and damping

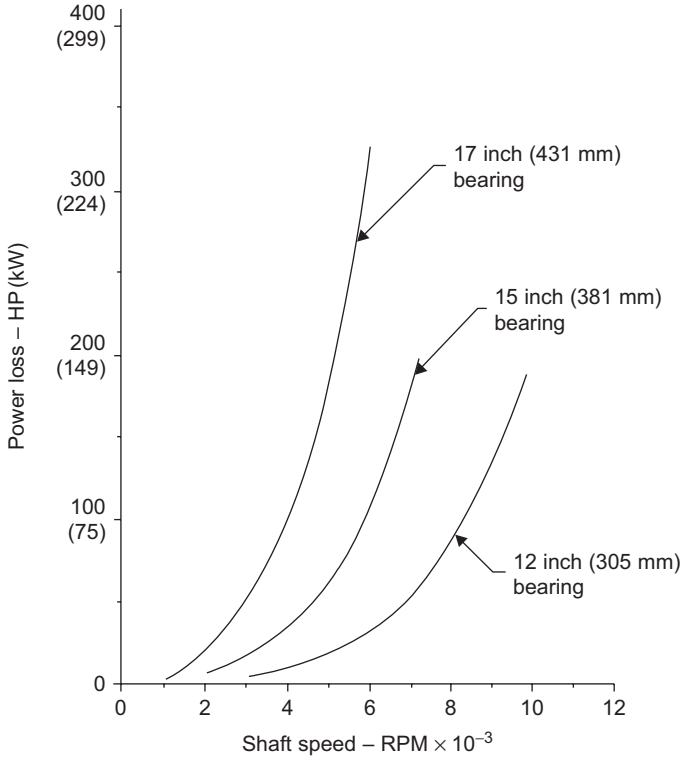


Figure 13-20 Total power loss in thrust bearings.

factors will be changed by seal geometry and pressures. Hence, these effects must be carefully evaluated and factored in during the design of the seal system.

Non-contacting Seals

These seals are used extensively in high-speed turbomachinery and have good mechanical reliability. They are not positive sealing. There are two types of non-contacting seals (or clearance seals): labyrinth seals and ring seals.

Labyrinth Seals

The labyrinth is one of the simplest of sealing devices. It consists of a series of circumferential strips of metal extending from the shaft or from the bore of the shaft housing to form a cascade of annular orifices. Labyrinth seal leakage is greater than that of clearance bushings, contact seals, or film-riding seals. Consequently, labyrinth seals are utilized when a small loss in efficiency can be tolerated. They are sometimes a valuable adjunct to the primary seal.

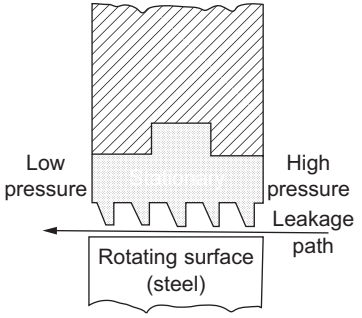
In large gas turbines labyrinth seals are used in static as well as dynamic applications. The essentially static function occurs where the casing parts must remain unjoined to allow for differences in thermal expansion. At this junction location, the labyrinth minimizes leakage. Dynamic labyrinth applications for both turbines and compressors are inter-stage seals, shroud seals, balance pistons, and end seals.

The major advantages of labyrinth seals are: their simplicity; reliability, tolerance to dirt, system adaptability, very low shaft power consumption, material selection flexibility, minimal effect on rotor dynamics, back diffusion reduction, integration of pressure, lack of pressure limitations, and tolerance to gross thermal variations. The major disadvantages are the high leakage, loss of machine efficiency, increased buffering costs, tolerance to ingestion of particulates with resulting damage to other critical items such as bearings, the possibility of the cavity clogging due to low gas velocities or back diffusion, and the inability to provide a simple seal system that meets OSHA or EPA standards. Because of some of the foregoing disadvantages, many machines are being converted to other types of seals.

Labyrinth seals are simple to manufacture and can be made from conventional materials. Early designs of labyrinth seals used knife-edge seals and relatively large chambers or pockets between the knives. These relatively long knives are easily subject to damage. The modern, more functional, and more reliable labyrinth seals consist of sturdy, closely spaced lands. Some labyrinth seals are shown in Figure 13-21. Figure 13-21 (a) is the simplest form of the seal. Figure 13-21 (b) shows a grooved seal is more difficult to manufacture but produces a tighter seal. Figures 13-21 (c) and 13-21 (d) are rotating labyrinth-type seals. Figure 13-21 (e) shows a simple labyrinth seal with a buffered gas for which pressure must be maintained above the process gas pressure and the outlet pressure (which can be greater than or less than the atmospheric pressure). The buffered gas produces a fluid barrier to the process gas. The eductor sucks gas from the vent near the atmospheric end. Figure 13-21 (f) shows a buffered, stepped labyrinth. The step labyrinth gives a tighter seal. The matching stationary seal is usually manufactured from soft materials such as babbitt or bronze, while the stationary or rotating labyrinth lands are made from steel. This composition enables the seal to be assembled with minimal clearance. The lands can therefore cut into the softer materials to provide the necessary running clearances for adjusting to the dynamic excursions of the rotor.

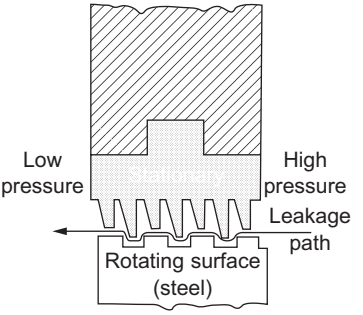
To maintain maximum sealing efficiency, it is essential that the labyrinth lands maintain sharp edges in the direction of the flow. This requirement is similar to that in orifice plates. A sharp edge provides for maximum vena contracta effect, and hence maximum restriction for the leakage flows (Figure 13-22).

High fluid velocities are generated at the throats of the constrictions, and the kinetic energy is then dissipated by turbulence in the chamber beyond each throat. Thus, the labyrinth is a device wherein there is a multiple loss of velocity head. With a straight labyrinth, there is some velocity carry-over that results in a loss of effectiveness, especially if the throats are closely spaced. To maximize the aerodynamic blockage effect of this carry-over, the diameters can be stepped or staggered to cause impingement of the expanding orifice jet on a solid, transverse surface. The leakage is approximately inversely proportional to the square root of the number of labyrinth lands. Thus, if



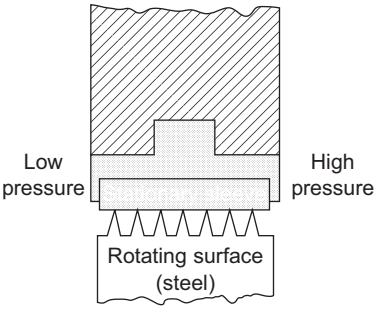
Simplest design (labyrinth materials: aluminum, bronze, babbitt or steel).

(a)



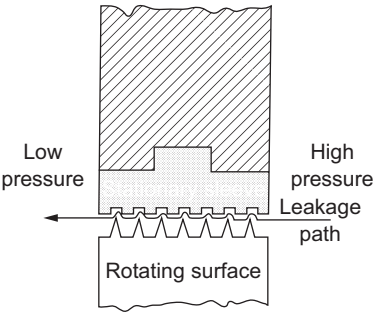
More difficult to manufacture but produces a tighter seal (same material as in (a)).

(b)



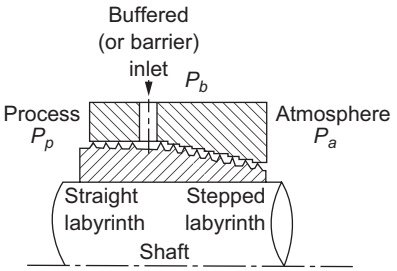
Rotating labyrinth type, before operation (sleeve material: babbitt, aluminum, nonmetallic or other soft material).

(c)



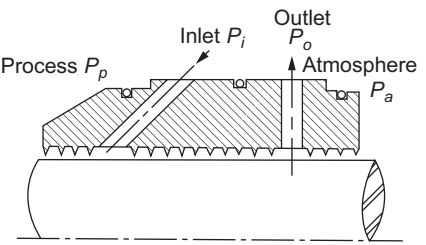
Rotating labyrinth, after operation. Radial and axial movement of rotor cuts grooves in sleeve material to simulate staggered type shown in (b).

(d)



Buffered combination labyrinth

(e)



Buffered-vented straight labyrinth

(f)

Figure 13-21 Various configurations of labyrinth seals.

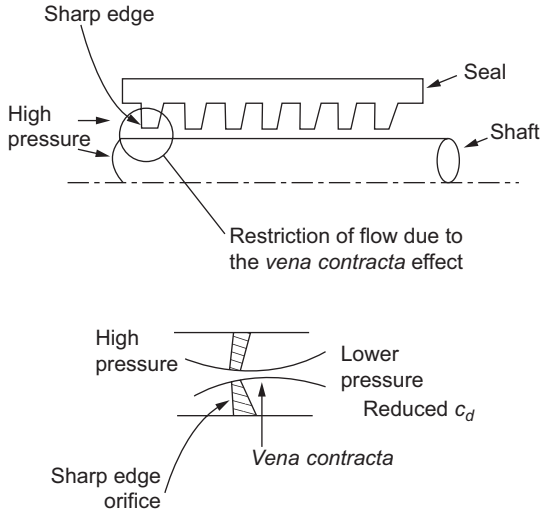


Figure 13-22 Theory behind the knife-edge arrangement.

leakage is to be cut in half at a four-point labyrinth, the number of lands would have to be increased to 16. The Elgi leakage formulae can be modified and written as:

$$\dot{m}_1 = 0.9A\left[\frac{\frac{g}{V_o}(P_o - P_n)}{n + ln\frac{P_n}{P_o}}\right]^{1/2}$$

For staggered labyrinths, the equation can be written as:

$$\dot{m}_1 = 0.75A\left[\frac{\frac{g}{V_o}(P_o - P_n)}{n + ln\frac{P_n}{P_o}}\right]^{1/2}$$

where

$\dot{m}_1 =$ leakage, lb/sec
$A =$ leakage area of single throttling, sq ft
$P_o =$ absolute pressure before the labyrinth, lb/sq ft
$V_o =$ specific volume before the labyrinth, cu ft/lbm
$P_n =$ absolute pressure after the labyrinth, lb_f/sq ft
$n =$ number of lands

The leakage of a labyrinth seal can be kept to a minimum by providing: (1) minimum clearance between the seal lands and the seal sleeve, (2) sharp edges on the lands to reduce the flow discharge coefficient, and (3) grooves or steps in the flow path for reducing dynamic head carry-over from stage to stage.

The labyrinth sleeve can be flexibly mounted to permit radial motion for self-aligning effects. In practice, a radial clearance of under 0.008 is difficult to achieve, except with very small high-precision machines. On larger turbines, clearances of 0.015–0.02 are generally used. During machine construction, it is important to measure and record these clearances because mechanical seizure or loss in aerodynamic efficiency can often be traced to incorrect labyrinth seal clearances.

The windback seal closely resembles the labyrinth but has an entirely different operational principle. A screw-thread device winds the oil, which is carried around the bore by the windage of the shaft, into an internal drain for return to the system as shown in Figure 13-23 (a).

Windback structures are extremely simple. Clearances about the shaft are ample, and the device has high reliability. When shaft speeds extend into the low regions where windage contributions are inadequate for effective operation, augmentation of windage can be achieved by special configurations of the shaft surface. Windbacks are also used as adjuncts to other types of seals, as shown in Figure 13-23 (b). With circumferential seals, windbacks can be used to keep oil splash from reaching the seal carbons when coking problems exist. In oil-buffered seals for compressors they are used to direct the small internal leakage into a pressurized drain to effect practically complete recovery of the leakage.

Ring (Bushing) Seals

The restrictive ring seal is essentially a series of sleeves in which the bores form a small clearance around the shaft. Thus, leakage is limited by the flow resistance in the restricted area and controlled by the laminar or turbulent friction. The API 617 codes characterize this type of seal. Most of the restrictive-type seals are of the floating type rather than the fixed type. The floating rings permit a much smaller leakage, and they can be of either the segmented type as shown in Figure 13-24 (a) or the rigid type as shown in Figure 13-24 (b).

Because of the minimal contact between the stationary ring and the rotor, these seals, when properly designed, are ideal for high-speed rotating machinery.

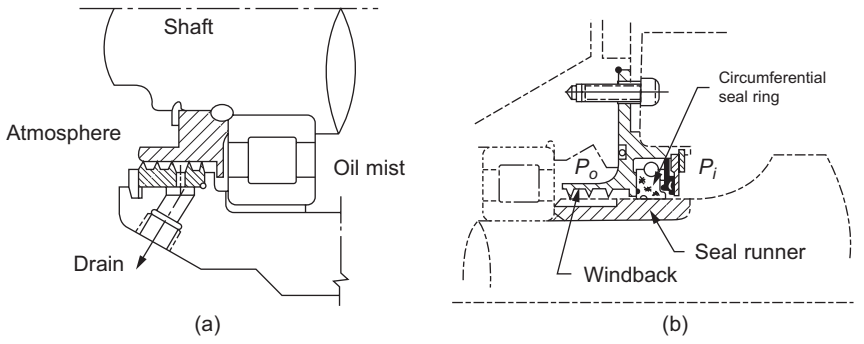


Figure 13-23 Windback seal.

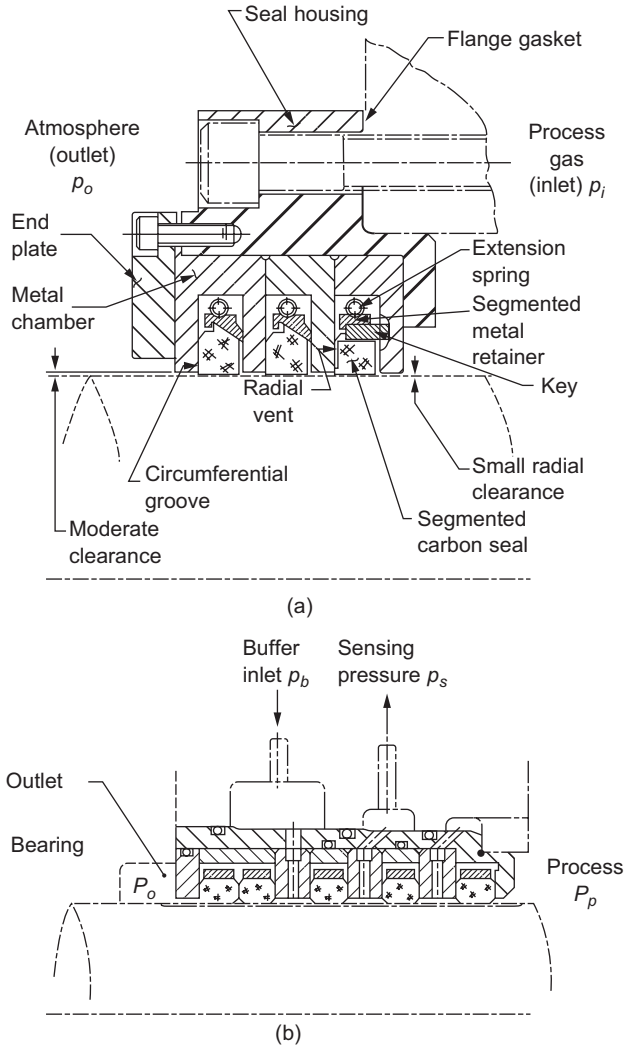


Figure 13-24 Floating-type restrictive ring seal.

When adequate lubrication and cooling fluid is available, the seal ring, manufactured from babbitt-lined steel, bronze, or carbon, will function satisfactorily. When the medium to be sealed is air or gas, carbon seal rings must be used. Carbon has self-lubricating properties. Cooling of the seal is provided by the leakage flow through the seal. Depending on the operating temperature and environment, aluminum alloys and silver are also used in the manufacture of the seal rings. Leakage limitation depends upon the type of flow and type of bushing. There are four types of flow: compressible and incompressible, each of which may be either laminar or turbulent. Ring seals are divided into two categories: fixed breakdown rings and floating breakdown rings, according to whether or not they are fixed with respect to the stationary housing.

Fixed seal rings

The fixed seal ring consists of a long sleeve affixed to a housing in which the shaft rotates with small clearance. It is an inexpensive assembly. However, since it is fixed, the seal behaves like a redundant bearing when rubbing occurs and, like the labyrinth, requires large clearances. Therefore, long assemblies must be used to keep leakage within reasonable limits. Since long seal assemblies aggravate alignment and rubbing problems, sturdier shafts are required to keep operating speeds in a subcritical region. The fixed-bushing seal almost always operates with appreciable eccentricity. This, plus the combination of a large clearance and a large eccentricity ratio, produces large leakages per unit length. Fixed-seal rings are therefore impractical where leakage is undesirable.

Floating seal rings

Clearance seals, which are free to move in a radial direction relative to the shaft and machine housing, are known as floating seals. These seals have advantages that very close annular clearance-type seals do not possess. The floating characteristic permits them to move freely with shaft motions and deflections, thereby avoiding the effects of severe rubbing.

Differential thermal expansion is a problem at high temperatures where the shaft and bushing are of dissimilar materials, or where there is any substantial temperature gradient between them. For example, the grades of carbon used commonly have a linear thermal expansion coefficient of one-third to one-fifth that of steel, necessitating the design of thermal expansion control into the carbon bushing. This is achieved by shrinking the carbon into a metallic retaining ring with a coefficient of expansion that equals or exceeds that of the shaft material.

It is good practice in critical applications to use bushings of a material with a slightly higher coefficient of thermal expansion than that of the shaft. Here, incipient seizure causes the bushings to grow away from the shaft. The large torque associated with high shearing intensity may necessitate locking the bushings against rotation if the unbalanced pressure forces seating them against the housing walls are insufficient to prevent rotation.

Build up of dirt or other foreign material between the seal ring and seat will result in damage to the journal and excessive seal spin on a floating seal ring unit. Soft materials, such as babbitt and silver, are notorious for trapping contaminants and causing shaft damage.

Mechanical (Face) Seals

This device forms a running seal between flat precision-finished surfaces. Its primary function is to prevent leakage. When used on rotating shafts, the sealing surfaces are in a plane perpendicular to the shaft, and the forces that hold the contact faces together will consequently be parallel to the shaft axis. For a seal to work properly, four sealing points must function as shown in Figure 13-25. They are: (1) the stuffing-box face must be sealed, (2) leakage down the shaft must be sealed, (3) the mating ring in the

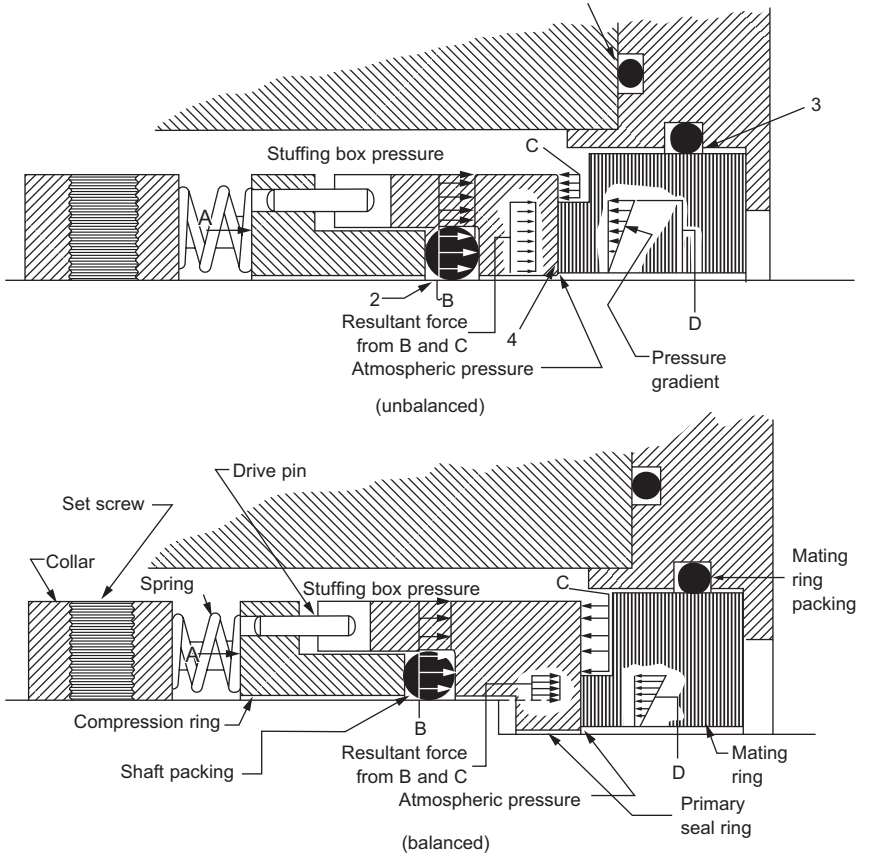


Figure 13-25 Unbalanced seal and balanced seal with step in shaft.

gland plate must be sealed in a floating design, and (4) the dynamic faces (rotary to stationary) must seal. Basically, most mechanical seals have the following components:

1. Rotating seal ring
2. Stationary seal ring
3. Spring devices to provide pressure
4. Static seals

A complete seal has two basic units: the seal head unit and the seal seat. The seal head unit consists of the housing, the end-face member, and the spring assembly. The seal seat is the mating member that completes the precision-lapped face combination that provides the seal.

The seal head may either rotate or remain stationary (attached to the body). Either one (head or seat) may rotate, while the other remains stationary. The movement of the sealing action depends on the direction of the pressure. This is illustrated in Figure 13-26, which shows rotating and stationary heads.

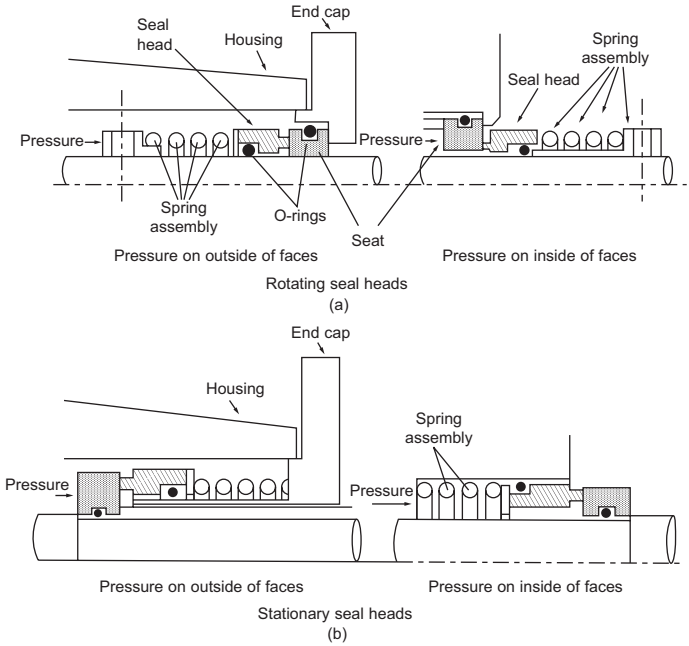


Figure 13-26 Rotating and stationary seal heads.

Some form of mechanical loading device, usually a spring, is needed to ensure that, in the event of a loss of hydraulic pressure, the sealing surfaces are kept closed. The amount of load on the sealing area is determined by the degree of "seal balance." Figure 13-27 shows what is meant by seal balance. A completely balanced combination occurs when the only force exerted on the sealing surfaces is the spring force, i.e., hydraulic pressure does not act on the sealing surfaces. The kind of spring that should be used depends upon a variety of factors: the space available, the loading characteristics required, the environment in which the seal is to operate, amongst others. Based on these considerations, either a single-spring or a multiple-spring design can be utilized. When a very small axial space is available, belleville springs, finger washers, or curved washers may be used.

A somewhat recent development is the use of magnetic force to obtain a face-loading action. Magnetic seals have provided reliable service under a variety of fluids and severe operating conditions. Some of the design advantages claimed are that magnetic seals are compact and lighter, provide an even distribution of sealing force, and are easy to assemble. Figure 13-28 shows a simple magnetic seal.

Shaft sealing elements can be split up into two groups. The first may be called pusher-type seals and includes the O-ring, V-ring, U-cup, and wedge configurations. The second group are Bellow-type seals, which differ from the pusher-type seals in that they form a static seal between themselves and the shaft. Figure 13-29 shows some typical pusher-type seals.

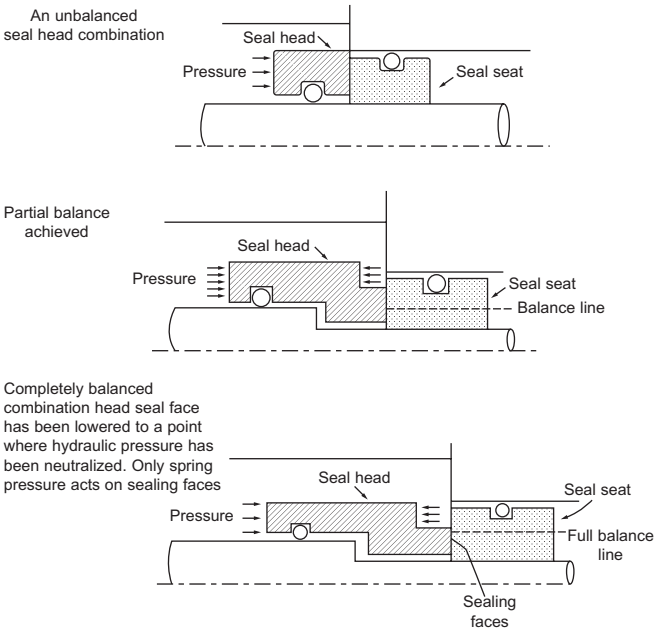


Figure 13-27 The seal balance concept.

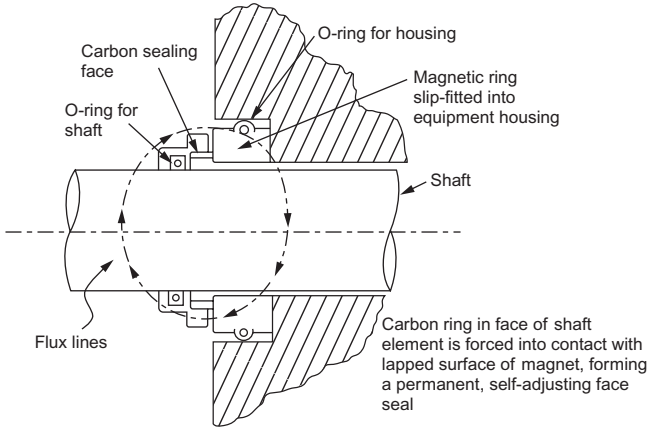


Figure 13-28 Simple magnetic-type seal.

A typical mechanical contact shaft seal has two major elements, as seen in Figure 13-30. These are the oil-to-pressure-gas seal and the oil-to-uncontaminated-seal-oil-drain seal or breakdown bushing. This type of seal will normally have buffering via a single ported labyrinth located inboard of the seal and a positive shutdown device, which will attempt to maintain gas pressure in the casing when the compressor

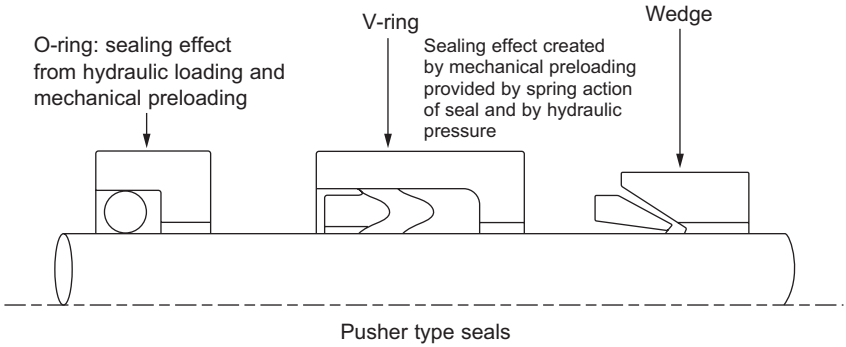


Figure 13-29 Various types of shaft sealing elements.

is at rest and seal oil is not being applied. For shutdown, the carbon ring is kept tightly sandwiched between the rotating seal ring and stationary sleeve with gas pressure to prevent gas from leaking out when no oil pressure is available.

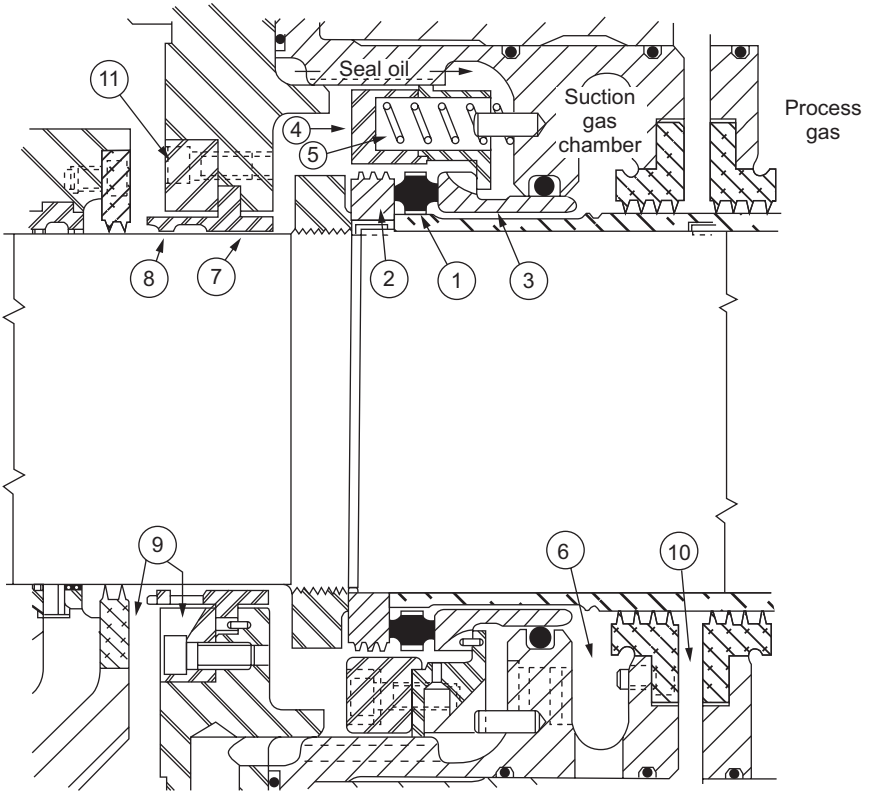
In operation, seal oil pressure is held at a differential of 35–50 psi (2.4–3.5 Bar) over the process gas pressure which the seal is sealing against. This high-pressure oil can be seen entering in the top in Figure 13-30 and completely fills the seal cavity. Some of the oil (a relatively small percentage, ranging from two to eight gpd per seal depending on machine size) is forced across the carbon ring seal faces, which are sandwiched between the rotating seal ring (rotating at shaft velocity) and the stationary sleeve (non-rotating and forced against the carbon ring by a series of peripheral springs). Therefore, the actual rotative speed of the carbon ring can be anywhere between zero rpm and full rotational speed. Oil crossing these seal faces contacts the process gas and is, thus, "contaminated oil."

The majority of the oil flows out of the uncontaminated seal oil drain after taking a pressure drop from design seal oil pressure to atmospheric pressure across the breakdown bushing. An orifice is placed in parallel with the breakdown bushing to meter the proper amount of oil flow for cooling. The contaminated oil leaves through the drain to a degasifier for purification. The bearing oil drain can be either combined with the uncontaminated seal oil drain or kept separate; however, a separate system will increase bearing span and lower critical speeds.

Mechanical Seal Selection and Application

The following is a list of factors that have proven to be helpful in seal system design and selection:

1. Product
2. Seal environment
3. Seal arrangement
4. Equipment



1. Rotating carbon ring
2. Rotating seal ring
3. Stationary sleeve
4. Spring retainer
5. Spring
6. Gas and contaminated oil drain
7. Floating babbitt-faced steel ring
8. Seal wiper ring
9. Seal oil drain line
10. Buffer gas injection port
11. Bypass orifice

Figure 13-30 Mechanical contact shaft seal.

5. Secondary packing
6. Seal-face combinations
7. Seal gland plate
8. Main seal body

Product

The physical and chemical properties of the liquid being sealed will place constraints upon the type of seal arrangement, the materials of construction, and the seal design that can be used.

Pressure

The relative pressures of the material to be sealed affect the decision of whether to use a balanced or unbalanced seal design. Pressure also affects the choice of face material because of the seal-face loading.

If the service happens to be below atmospheric pressure, then special considerations are required to seal the material effectively. Most unbalanced seal designs are applicable up to 100 psig (7 Bar) stuffing-box pressure. At more than 100 psig (7 Bar), balanced seals should be used.

Seal manufacturers base their seal-face combination designs on *PV* ratings. These are the multiple of the face load (*P*) and the sliding velocity (*V*) of the faces. The maximum *PV* rating for an unbalanced seal is about 200,000 and about 2,250,000 for a balanced seal.

Temperature

The temperature of the liquid being pumped is important because it affects the seal-face material selection as well as face wear life. This is primarily a result of changes in lubricity of the fluid with changes in temperature.

Common seal designs may handle fluid temperatures in the 0 °F to +200 °F (−17 °C to 93 °C) range. When temperatures are above the +200 °F (93 °C) range, special metal bellows seals may be used up to the +650 °F (343 °C) range. Low temperature (−100 °F to 0 °F) (−73 °C to −17 °C) also requires special arrangements, since most hydrocarbons have little lubricity in this range.

The most important consideration concerning temperature is to avoid operating close to a temperature which will allow flashing of the liquid. Mechanical seals work well on many liquids; they work poorly on most gases.

Lubricity

In any mechanical seal design there is rubbing motion between the dynamic seal faces. This rubbing motion is most often lubricated by the fluid being pumped. Therefore, the lubricity of the pumped liquid at the given operating temperature must be considered to determine if the chosen seal design and face combination will perform satisfactorily.

Most seal manufacturers limit the speed of their seals to 90 fps (27.4 mps) with good lubrication of the faces. This is primarily due to the centrifugal forces acting on the seal which tend to restrict its axial flexibility.

Abrasion

When evaluating the possibility of installing a seal in a liquid that has entrained solids, several factors must be considered. Is the seal constructed in such a way that the dynamic motion will be restricted by fouling of the seal parts? The seal arrangement that is usually preferred when abrasives are present is a flushed single inside type with a face combination of very hard material. However, factors such as toxicity or corrosiveness of the material may dictate that other arrangements be used.

Corrosion

When considering the corrosiveness of the material being pumped, one must determine what metals will be acceptable for the seal body, what spring material may be used, what face material will be compatible with the liquid being pumped (that is, whether the binder or the carbon or tungsten carbide will be attacked, or whether the base metal of the plated seal face will be attacked), and what type of elastomer or gasket material can be used. The corrosion rate will affect the decision of whether to use a single- or multiple-spring design because the spring can tolerate a greater amount of corrosion without weakening it appreciably.

Toxicity

This factor is becoming an increasingly important consideration in the design of mechanical seals. Since the rubbing seal faces require liquid penetration to cool and lubricate them, it is reasonable to expect that there will be some vapor passing across the faces. This is in fact the case. A normal seal can be expected to "leak" from a few ppm to 10 cc/min. It is also generally accepted that the seal leakage rate will increase with speed.

Additional Product Considerations

1. Is the product thermosensitive? The heat generated by the seal faces may cause polymerization.
2. Is the product shear sensitive, i.e., will it harden due to turbulence?
3. If the product is highly flammable, be aware of possible ignition sources.
4. In-hazardous services plan for personnel protection in the event of seal leakage.
5. Products with dissolved gas must be properly vented. In most cases, vent the stuffing box back to the pump action.
6. Seals in cold services are extremely sensitive to moisture. There must be a way to "dry out the system" after repair.
7. Consideration must be given to the pressure and temperature that the seal will see during normal operation, start-up, shutdown, and upset conditions.
8. Vapor pressure of the product must be known to prevent vaporization in the stuffing box.

Seal Environment

Once an adequate definition of the product is made, the design of the seal environment can be selected. There are four general parameters that an environmental system may regulate or change:

1. Pressure control
2. Temperature control
3. Fluid replacement
4. Atmospheric air elimination

The most common environmental control systems include flushing, barrier fluids, quenching, and heating/cooling systems. Each has its use in regulating the parameters mentioned previously.

Seal Arrangement Considerations

There are four considerations:

1. Double seals have been the standard with toxic and lethal products, but maintenance problems and the seal design contribute to poor reliability. The double face-to-face seal should be looked at more closely.
2. Do not use a double seal in dirty service – the inside seal will hang up.
3. The API standard is a good guide to the use of balanced and unbalanced seals. Application of a balanced seal at too low a pressure may encourage face lift-off.
4. The number of arrangements and auxiliary features are more than 100. Regardless of the seal vendor, the arrangement will generally determine success.

Equipment

Too few people consider the equipment with the seal selection. In most cases, poor equipment will give poor seal performance, regardless of the seal or arrangement chosen. Also, beware that different pumps with the same shaft diameter and TDH may present different sealing problems (note: these same considerations may be used for troubleshooting).

Secondary Packing

More emphasis should be placed on secondary packing than it receives, especially if these members involve Teflon. Most seal designs using an O-ring for shaft packing give similar performance. A wide variation in performance is seen between various seal vendor designs when Teflon shaft packing is used. Depending on the seal arrangement, there can be a difference in mating-ring (stationary) packing performance when Teflon is used.

Seal-Face Combinations

Choices of seal-face combinations have come a long way in the last eight to 10 years. Stellite is being phased out in petroleum and petrochemical seal applications. Better grades of ceramic are being offered as the standard material. The cost of tungsten carbide has decreased considerably. Relapping services for tungsten are available near most industrial areas. Silicon carbide is gaining a hold on the market, especially in abrasive services. The technology of manufacturing tungsten carbide in a composite or overlay arrangement is offered by all of the major seal manufacturers. The dynamics of seal faces are better understood today.

Seal Gland Plate

The seal gland plate is an item that is caught in between the pump vendor and the seal vendor. The pump vendors can furnish good, reasonably priced alloy glands, but they are also limited because the gland is cast and must fit several seal designs. There are also some glands furnished by pump vendors that can be easily distorted by bolting.

Special glands requiring heating, quench, and drain with a floating-throat bushing on ANSI pumps should be furnished by the seal vendor. Gland designs on several ANSI pumps are not that impressive.

Main Seal Body

Designs differ considerably from one manufacturer to another. The term "seal body" makes reference to all rotating parts on a pusher seal, excluding shaft packing and the seal ring. The configuration or options offered on the seal body may be the chief reason to avoid the design for that particular service.

Seal Systems

In recent years, these systems have become more sophisticated to meet modern chemical process requirements and government restrictions. A simple seal system is the buffered and educted restrictive-ring seal system. This type of system, as shown in Figure 13-31, must operate with buffering pressure greater than the process and eductor pressure. The eductor pressure must in turn be below the atmospheric pressure. Problems with these systems are common because the eductor system does not have a large enough capacity, the buffered gas pressure is not higher than the process pressure, and in many cases the rings are installed backward.

The complex seal systems incorporate many different types of components to provide the most efficient sealing. Figure 13-32 shows a system that includes three different types of seals. The labyrinth seal initially provides the restriction that prevents the polymers contained in the process gas from clogging the seal rings. The labyrinth seal is followed by the two segmented circumferential contact seals and the four segmented restrictive-ring seals, which are primary seals in this combination. The primary restrictive-ring seals are followed by four circumferential segmented seal

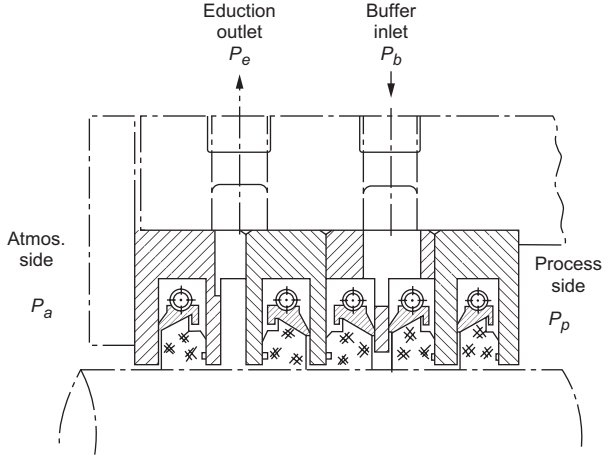


Figure 13-31 Restrictive ring seal system with both buffer and eduction cavities.

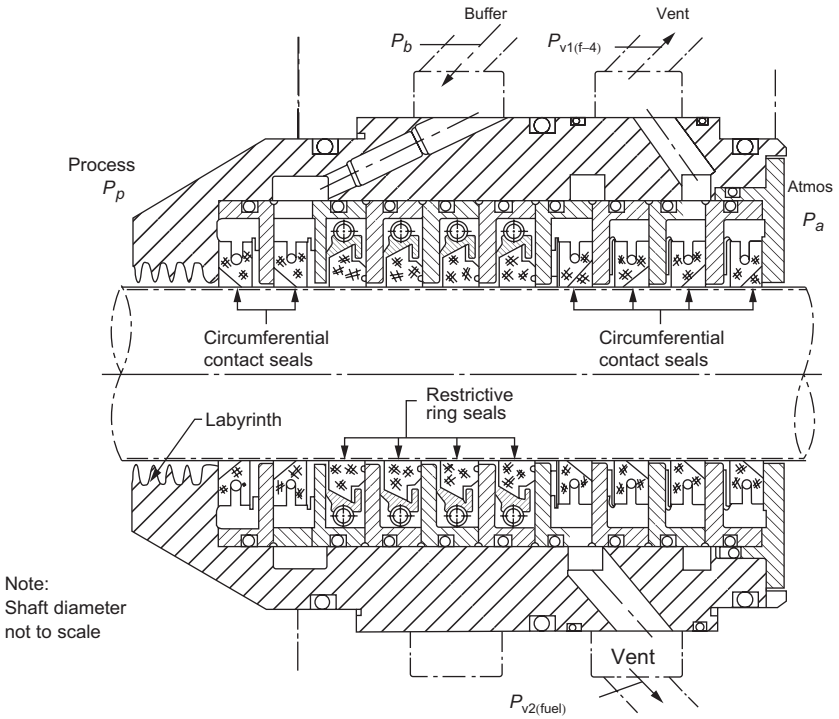


Figure 13-32 Multiple combination segmented gas seal system.

rings. A buffer gas is also introduced at the first set of circumferential contact seals, and an eductor is situated in the middle of the rear circumferential seals. Thus, this sealing system is very efficient in preventing any leakage and also for utilizing educted gas in the process.

Gas compressors operating on highly toxic or flammable gases may require redundant systems to assure no leakages. In many applications, such as refrigeration gas, buffer seals are required with the liquid-buffered face seal. A popular technique is to use a buffered labyrinth seal with a liquid seal.

Associated Oil System

One of the advantages of mechanical contact seals is that the associated seal oil supply system may be relatively simple compared to the system required with other types of seals, as seen in Figure 13-33. The relatively high oil-to-gas differential and wide allowable range allow simple differential regulators to be used to control the oil supply system rather than a complex overhead tank arrangement. The dark lines in Figure 13-34 represent the seal oil system used for this type of seal. Seal oil is taken from a controlled header "A" and dropped to the required ΔP via a relatively inexpensive regulator control. The sensing point for this ΔP control is off the contaminated drain cavity on the high-pressure end of the compressor. By sensing off the

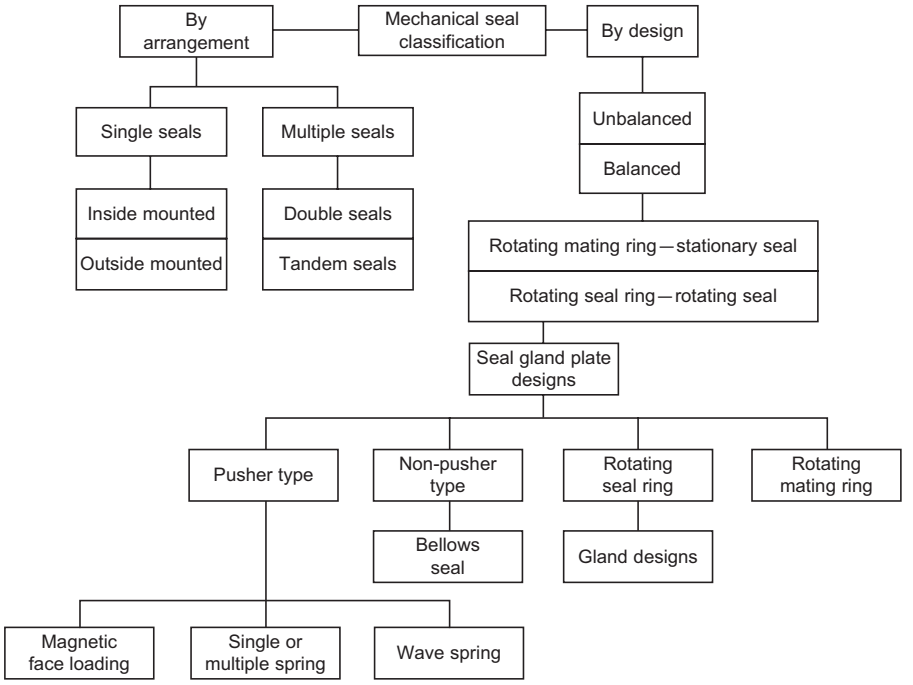


Figure 13-33 Mechanical seal classifications.

high-pressure end, a minimum of ΔP of oil to gas is always held on both ends of the compressor. Any pressurizing of the contaminated drain cavity due to buffer gas being used is also automatically followed by using a sensing point located in the contaminated drain oil cavity. In the system shown, the "uncontaminated oil" combines immediately with lube oil and returns to the reservoir where the "contaminated oil" can be trapped by a drainer and automatically drained to be optionally discarded or returned to the reservoir via a degasing tank.

Dry Gas Seals

The use of dry gas seals in process gas centrifugal compressors has increased over the last 30 years, replacing traditional oil film seals in most applications. Over 85% of centrifugal gas compressors manufactured today are equipped with dry gas seals.

Dry gas seals are basically mechanical face seals, consisting of a mating ring, which rotates and a primary ring, which is stationary. A cross-sectional view of a dry gas seal is shown in Figure 13-35. The rotating assembly consists of the mating ring (with spiral grooves) mounted on a shaft sleeve held in place axially with a clamp sleeve and a locknut. It is typically pin driven. The mating ring with spiral grooves and the primary ring are held within the retainer assembly. The stationary assembly consists of the primary ring mounted in a retainer assembly held stationary within the compressor

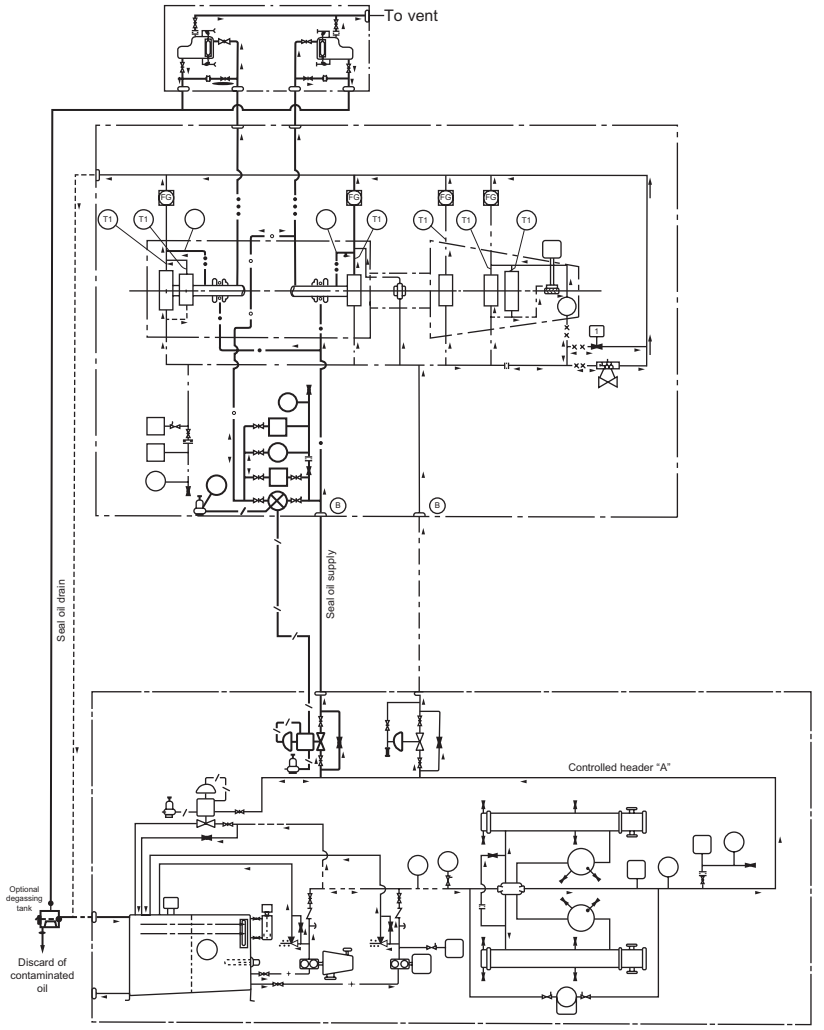


Figure 13-34 Mechanical contact seal and lube oil system.

housing. Under static conditions, the primary and mating rings are held in contact due to the spring load on the primary ring.

The spiral groove pattern, for a clockwise rotation, on the mating ring is shown in Figure 13-36. The operating principle of the spiral grooved gas seal is that of a hydrostatic and hydrodynamic force balance. As gas enters the grooves, it is sheared towards the center. The sealing dam acts as a restriction to the gas outflow, thereby raising the pressure upstream of the dam. This increased pressure causes the flexibly mounted, primary ring to separate from the mating ring. During normal operation, the running gap is approximately three microns. Under pressurization, the forces exerted on the

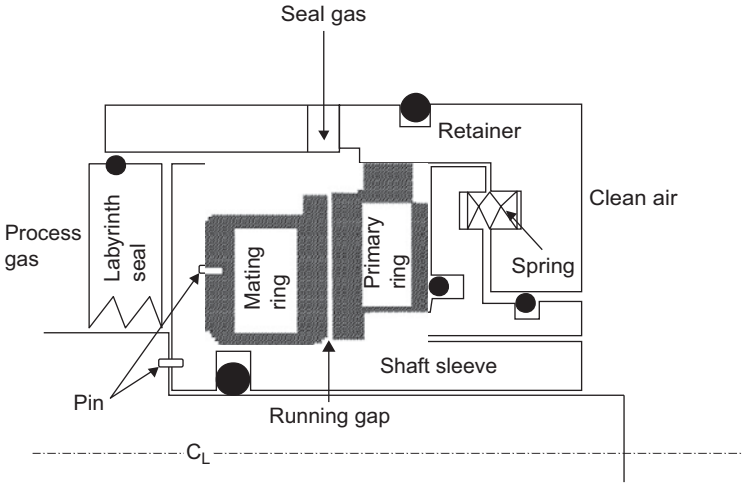


Figure 13-35 Single dry gas seal.

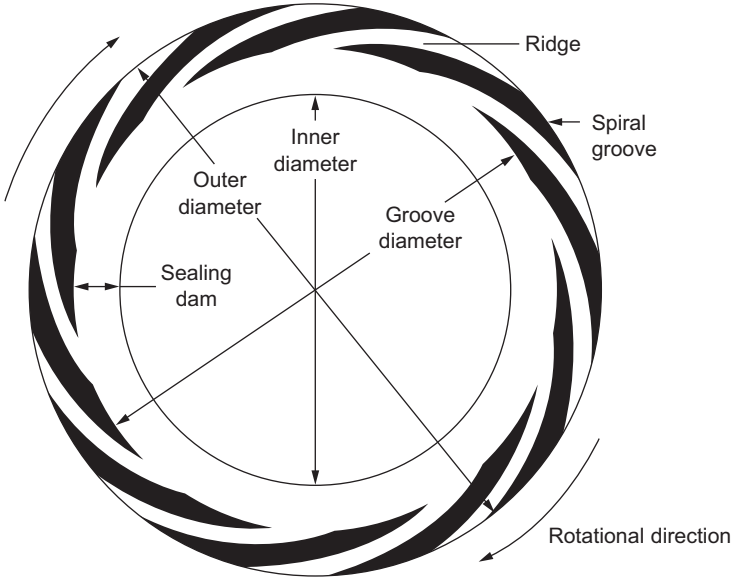


Figure 13-36 Spiral grooved mating ring (courtesy Proceedings Seventeenth Turbomachinery Symposium, Dry Gas Compressor Seals by Piyush Shah, John Crane Inc.).

seal are hydrostatic and are present whether the mating ring is stationary or rotating. Hydrodynamic forces are generated only upon rotation. The mating ring consisting of the logarithmic spiral grooves is the key to generating these hydrodynamic forces.

During operation, the grooves in the mating ring generate a hydrodynamic force that causes the primary ring to separate from the mating ring creating a "running gap" between the two rings, which effectively seals against the process gas. During normal operation, the running gap is approximately three microns. A sealing gas is injected into the seal, providing the working fluid, which establishes the running gap.

Tandem Dry Gas Seals

The tandem dry gas seal as seen in Figure 13-37 relates to applications where small product leakages of process gas are admissible. The seal on the atmosphere side acts as a safety seal. The tandem arrangement provides a particularly high degree of operational safety. The seal on the product side and the seal on the atmosphere side are able to absorb the complete pressure differential. Under normal operating conditions the full pressure is reduced only by the seal on the product side. The space between the seal on the product side and the seal on the atmosphere side is cleared by a connection to the flare. The pressure differential to be sealed by the seal on the atmosphere side equals the flare pressure, so leakage to the atmosphere side or to the vent is very low. If the main seal fails, the second seal acts as a safety seal.

Tandem Dry Gas Seal with Labyrinth

A tandem seal with intermediate labyrinth is shown in Figure 13-38. This seal is used in applications where the product leakages to the atmosphere as well as buffer gas leakages to the product are inadmissible, for example, on H2, ethylene or propylene compressors. In this type of seal the product pressure to be sealed is reduced via the seal on the product side. The entire process gas leakage is discharged via connection

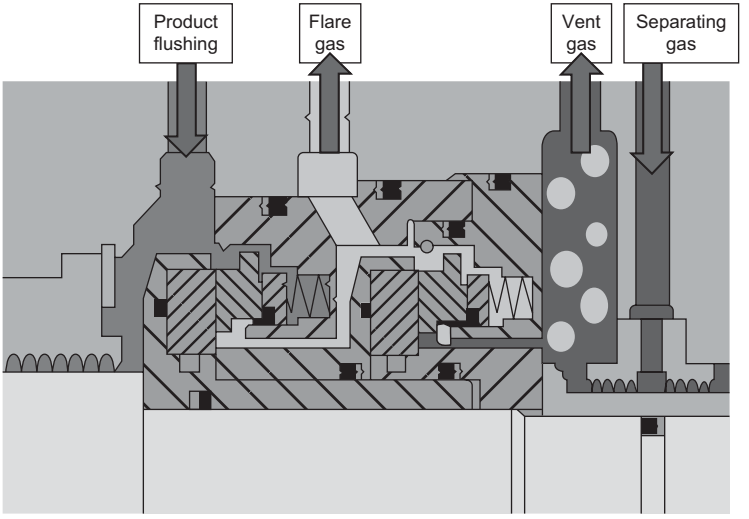


Figure 13-37 Tandem seal (courtesy Eagle Burgmann Germany GmbH & Co. KG).

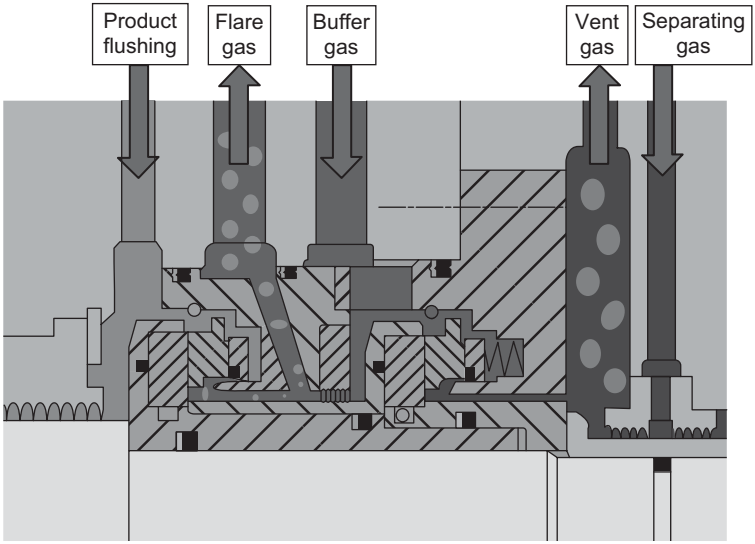


Figure 13-38 Tandem seal with intermediate labyrinth (courtesy Eagle Burgmann Germany GmbH & Co. KG).

to the flare. The seal on the atmosphere side is pressurized with a buffer gas such as nitrogen via connection to the buffer gas. The pressure of the buffer gas ensures that a current flows via the labyrinth to the primary vent outlet.

Double Gas Seals

A double gas seal, as shown in Figure 13-39, is used where product leakages to the atmosphere are inadmissible and tandem arrangements are not suitable because of too small product gas pressures. Buffer gas leakages into the product must be admissible and the buffer gas pressure must be higher than the product pressure. This seal is used when a neutral buffer gas of suitable pressure is available. Typical applications are to be found mainly in the chemical industry, for example, on HC gas compressors. A buffer gas, for example, nitrogen, is fed between the seals at a higher pressure than the product pressure. One part of the buffer gas leakage escapes to the atmosphere side and the other part to the product side.

Operating Range of Dry Gas Seals

Gases ranging from inert gases such as nitrogen to highly toxic gaseous mixtures of natural gas and hydrogen sulfide can be sealed utilizing the optimum seal arrangements. The operating range of the spiral grooved dry gas seals is as follows:

Sealed Pressure: 2400 psi (165 Bar)
Temperature: 500 °F (260 °C)
Surface Speed: 500 ft/sec (152 m/sec)
M.W.: 2–60

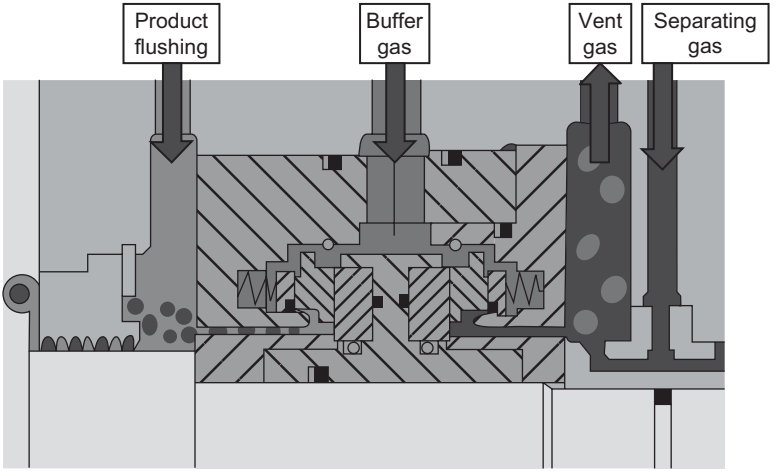


Figure 13-39 Double seal (courtesy Eagle Burgmann Germany GmbH & Co. KG).

Dry Gas Seal Materials

The gas composition, contaminants in the gas stream, operating temperatures, and process conditions dictate the choice of materials. The most common materials of construction are as follows:

Mating Ring: Tungsten Carbide, Silicon Carbide
Primary Ring: Carbon, Silicon Carbide
O-Rings: Elastomers (Viton, "Kalrez")
Hardware: 300 or 400 series ss (Sleeves, discs, retainer rings)
Coil Springs: 316 ss, Hastelloy

Dry Gas Seal Systems

The use of dry gas seals requires a system designed to supply sealing gas to the seal as a working fluid for the running gap. These gas seal systems are normally supplied by the compressor OEM mounted on the compressor base plate. There are two basic types of gas seal systems, differential pressure (ΔP) control and flow control. Differential control systems control the supply of seal gas to the seal by regulating the seal gas pressure to a pre-determined value typically 15 psi (1 Bar) above the sealing pressure. This is accomplished through the use of a differential pressure control valve. Flow control systems control the supply of seal gas to the seal by regulating the seal gas flow through an orifice upstream of the seal. This is accomplished through the use of a differential pressure control valve monitoring pressures on either side of the orifice.

Dry Gas Seal Degradation

Contamination of the seal by foreign objects leads to seal failures. The running gap between the primary and mating gas seal rings is typically around three microns.

Injection of any type of solids or liquids into this very narrow seal running gap can cause degradation of seal performance. This would create excessive gas leakage to the vent and eventual failure of the seal.

Since the typical operating gaps between the two sealing surfaces range from 0.0001 in to 0.0003 in, the resultant leakage is very small in magnitude. Under conditions of static pressurization beyond 50–75 psi (3.4–5.17 Bar), the seal leaks a very small amount. This leakage increases with increasing pressure and reduces with increasing temperature. Increased viscosity of gases at higher temperatures reduces the amount of seal leakage. For example, a 4-in (101.6 mm) shaft seal on a natural gas compressor statically pressurized to 1000 psi (69 bar) will leak about 1 scfm (0.03 scmm). Under dynamic condition, due to the pumping effect of the spiral grooves, the leakage increases as well.

The power loss can also be increased along with seal contamination. The seal surfaces being non-contacting under dynamic conditions the power loss associated with dry gas seals is very small. The power loss for a 10-in. (254 mm) seal operating at 1,000 psi (69 Bar) and 10,000 rpm is about 12–14 kW. With damage seal surfaces, these losses can be increased by 20–30%.

Foreign material within the seal results in increased shearing forces between the primary and mating rings, causing overheating of the seal components, leading to O-ring extrusion or some other mechanical form of seal failure. The major areas from which gas seals contamination occurs are:

- Process gas leakages from the inboard or high-pressure side of the seal.
- Bearing lubrication oil from the outboard or low-pressure side of the seal.
- The seal gas injected into the seal being contaminated upstream of the injection.

Contamination from Process Gas

Contamination from process gas can occur when there is insufficient supply of sealing gas into the seal, allowing process gas to come into direct contact with the seal ring faces. Contaminants existing within the process gas can then damage the seal.

Contamination from Bearing Lubrication Oil

A barrier seal is required on the outboard side of the dry gas seal, between the gas seal and the compressor bearing. The primary function of the barrier seal, typically buffered with air or nitrogen, is to prohibit the flow of bearing lubrication oil into the gas seal. Contamination of the dry gas seal from lube oil can occur when the barrier seal fails to function as intended.

Contamination from Seal Gas Supply

Contamination from the seal gas supply occurs when the sealing gas is not properly treated upstream of the dry gas seal. Gas seal manufacturers have stringent requirements for seal gas quality. Typically, the sealing gas must be dry and filtered of particles three microns and larger. Filters are normally provided in the gas seal system to meet this requirement.

Dry gas seals operate under extremely tight tolerances, which demand that special care be taken in the design of the gas seal environment, and in the operation of the compressor and gas seal system. While the threat of seal degradation and reduced seal life due to outside influences is real, the detrimental effects of these factors can be minimized.

The replacement of mechanical seals by dry gas seals must be closely examined. There have been many cases where the replacement has caused the compressor to operate in an unstable manner. This is due to the fact that removal of the mechanical seal causes a change in the damping of the rotor and can cause the rotor to operate closer to its critical speed.

Bibliography

Abramovitz, S., "Fluid Film Bearings, Fundamentals and Design Criteria, and Pitfalls," Proceedings of the 6th Turbomachinery Symposium, December 1977, pp. 189–204.

Childs, D.W., and Vance, J.M., "Annular Gas Seals and Rotordynamics of Compressors and Turbines," Proceedings of the 26th Turbomachinery Symposium, Texas A&M University, 1997, p. 201.

"Effects of Compressible Annular Seals," Proceedings of the 24th Turbomachinery Symposium, Texas A&M University, 1995, p. 175.

Egli, T., "The Leakage of Steam through Labyrinth Seals," Trans. ASME, 1935, pp. 115–122.

Evenson, R.S., Mason, B., Frederick, D.V., St. Onge, and Alain, G., "Development and Field Application of a Single Rotor Design Dry Gas Seal," Proceedings of the 24th Turbomachinery Symposium, Texas A&M University, 1995, p. 107.

FAG "Rolling Bearing Damage," Publication No. WL 82 102/2 Esi, 1995.

FAG "Rolling Bearings, Fundamentals, Types, Design," Publication No. WL 43 1190 EA, 1996.

Garner, D.R., and Leopard., A.J., "Temperature Measurements in Fluid Film Bearings," Proceedings of the 13th Turbomachinery Symposium, Texas A&M University, 1984, p. 133.

Herbage, B., "High Efficiency Fluid Film Thrust Bearings for Turbomachinery," 6th Proceedings of the Turbomachinery Symposium, Texas A&M University, December 1977, pp. 33–38.

Herbage, B.S., "High Speed Journal and Thrust Bearing Design," Proceedings of the 1st Turbomachinery Symposium, Texas A&M University, October 1972, pp. 56–61.

Jackson, C., "Radial and Thrust Bearing Practices with Case Histories," Proceedings of the 14th Turbomachinery Symposium, Texas A&M University, 1985, p. 73.

King, T.L., and Capitao, J.W., "Impact on Recent Tilting Pad Thrust Bearing Tests on Steam Turbine Design and Performance," Proceedings of the 4th Turbomachinery Symposium, Texas A&M University, October 1975, pp. 1–8.

Leopard, A.J., "Principles of Fluid Film Bearing Design and Application," Proceedings of the 6th Turbomachinery Symposium, Texas A&M University, December 1977, pp. 207–230.

Mayeux, T., Paul, Feltman Jr., and Paul, L., "Design Improvements Enhance Dry Gas Seal's Ability to Handle Reverse Pressurization," Proceedings of the 25th Turbomachinery Symposium, Texas A&M University, 1996, p. 149.

Richards, R.L., Vance, J.M., Paquette, D.J., and Zeidan, F.Y., "Using a Damper Seal to Eliminate Subsynchronous Vibrations in Three Back-to-Back Compressors," Proceedings of the 24th Turbomachinery Symposium, Texas A&M University, 1995, p. 59.

Salamone, D.J., "Journal Bearing Design Types and Their Applications to Turbomachinery," Proceedings of the 13th Turbomachinery Symposium, Texas A&M University, 1984, p. 179.

Scharrer, J.K., Pelletti, and Joseph, M., "Leakage and Rotordynamic Effects of Compressible Annular Seals," Proceedings of the 24th Turbomachinery Symposium, Texas A&M University, 1995, p. 175.

Shah, P., "Dry Gas Compressor Seals," Proceedings of the 17th Turbomachinery Symposium, Texas A&M University, 1988, p. 133.

Shapiro, W., and Colsher, R., "Dynamic Characteristics of Fluid Film Bearings," Proceedings of the 6th Turbomachinery Symposium, Texas A&M University, December 1977, pp. 39–53.

Southcott, J.F., Sweeney, J.M., Feltrnan Jr., and Paul, L., "Dry Gas Seal Retrofit," Proceedings of the 24th Turbomachinery Symposium, Texas A&M University, 1995, p. 221.

Takeuchi, Takao, Kataoka, Tadashi, Nagasaka, Hiroshi, Kakutani, Momoko, Ito, Masanobu, Muraki, and Ryoji "Advanced Dry Gas Seal by the Dynamic Ion Beam Mixing Technique," Proceedings of the 27th Turbomachinery Symposium, Texas A&M University, 1998, p. 39.

Copyrighted Materials
Copyright © 2012 Elsevier Retrieved from www.knovel.com

14 Gears

Gearing is one of the most important components between prime movers and driven units. If gearing is not selected properly, it can cause many problems. Gearing transmits great power at high rotational speeds. Recent advances in turbomachinery technology, especially in turbines, compressors, couplings, and bearings, have required gearing to withstand high external forces. To design problem-free equipment, it is important to consider the effect of the external system on gearing. Thus, all the factors that influence design, application, and operation of gear drives should be considered in the design phase.

Since problems encountered with gears are complex, it is unfair to blame the gear manufacturers alone. The gear supplier is much less-informed about the package than any other group. Problems should be handled as a team effort between manufacturers and users. One factor causing problems is that the system is not timed in terms of spring constants and masses. The gear is usually the only item required to operate with metal parts in such close contact with other components. This setup can result in early failure. Gearing is also subjected to cyclic loading varying from 0 to 55,000 cycles/min.

With current materials and heat-treating techniques, the use of high-hardness gearing with tooth loads up to 5,000 psi (34,474 kPa) of face at pitch line velocities of 20,000–30,000 ft/min (6,096–9,144 m/min) is not at all uncommon. In turbine-driven test equipment, gear drives have been built with pitch line velocities as high as 55,000 ft/min (16,764 m/min) and rotational speeds approaching 100,000 rpm. The magnitude of internal forces and material stresses coupled with the high speeds has resulted in gear drives that are dynamically complicated and sensitive to influences from other components in the system.

The system characteristics of the entire train must be known, so that the selection of the gear will be proper. The major points affecting the system are as follows: (1) couplings, (2) external vibration, (3) operating conditions, (4) thrust loads, and (5) mounting type.

Couplings are a constant source of unbalance vibration, and critical speed changes can be attributed to spacer shift and wear. Coupling keys can also cause severe housing vibration, whereas shaft vibration can remain low. Therefore, it is important to monitor vibration with accelerometers in addition to proximity probes. Gear failure from high vibration is common when the gear and pinion teeth operate within a distance of few hundred microinches between each other. Accelerometers can also monitor gear

Gas Turbine Engineering Handbook, Fourth Edition. DOI: 10.1016/B978-0-12-383842-1.00014-7
Copyright © 2012 Elsevier Inc. All rights reserved.

mesh frequencies and thus act as early warning devices. Operating conditions must be known in detail.

In many cases, the gear manufacturer is provided with only the design horsepower of the machine. Actual transmitted loads can be much higher due to the proximity of torsional or lateral critical speeds. Surge in centrifugal compressors can cause severe overload and result in failures.

External thrust loads are another major problem, and in many cases, they lead to double-helical gear selection as shown in Figure 14-1. The gear housing and the mounting type of the gear train are very important considerations in the overall life of the unit, since improper mounting and expansion of the gear housing can lead to misalignment problems.

A substantial structure to support the gear drive weight, thrust, and torque reactions with minimum load deflections must be provided. At least two dowels for locating each gear housing are required, and it is necessary to minimize housing vibration from any source. Ideally, the structures should be reinforced concrete or steel filled with grout. The inclusion of oil reservoirs in the structure supporting major train components should be avoided, since unavoidable thermal changes will have adverse effects on the alignment. If a reinforced concrete or a filled structure cannot be provided,

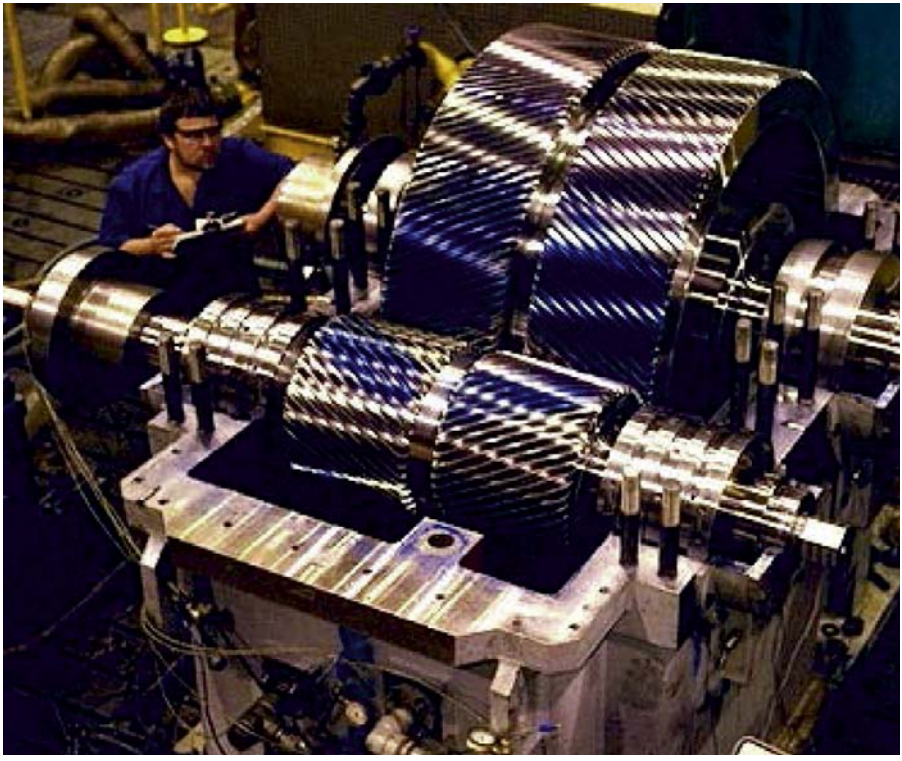


Figure 14-1 A double helical 54,000-HP (40 MW) gearbox (courtesy Lufkin Industries, Inc.).

resonance due to train component mass and structure stiffness at system rotational frequencies or harmonies should be avoided.

Gear Types

The choice between single- and double-helical gearing is sometimes difficult. Both gearing types can be made to equal limits of accuracy. Control of the gearing accuracy is only a function of the gear generating machines, which need maintenance, and operator skill for machining techniques. A hobbed gear is generated in a continuous process by a simple and easily maintained rack-form cutter, which will produce gearing of extremely high-profile accuracy with virtually immeasurable spacing errors and uniform lead. When both helices of a double-helical gear are cut at the same time, or sequentially without a change in setup, apex position error will be virtually unobservable in operation, and axial vibration excitation from the mesh will be negligible. The same basic equipment can be used for generating either single- or double-helical gears. Most gas turbine application gearing, whether single or double helical, is finished with a grinding process, to achieve the necessary tooth accuracy and surface finish.

Thrust loading is a significant problem in the design of any gear unit, and its effects differ based on the choice of single- or double-helical gearing. In either case, an accurate estimate of the thrust loading is required to make an intelligent compensation for it. With double-helical gearing, continuous axial loading can be accommodated by a slight increase in capacity to account for the helix load imbalance. American Petroleum Institute (API) 613 and 617 specifications require that single-helical gears must have a thrust bearing. It is also recommended (but not required) that double-helical gears must have thrust bearings.

The increase in cost and the reduction of efficiency thus caused is only a fraction of that incurred when a large diameter and high-velocity thrust bearing must be mounted on a single-helical pinion shaft.

Intermittent loading, such as that from gear couplings mounted on thermally expanding shafting, is a different problem. This problem is accommodated in a double-helical unit by judicious selection of helix angle and coupling size, so that axial coupling forces resulting from the transmission of torque are less than the thrust force produced by each helix of the gear. This design assures that the coupling will slip to relieve any axial loading and that the power balance on the two helices will be maintained.

High-speed gear couplings are selected in which the pitch diameter is substantially smaller than that of the pinion. Axial forces produced will be high, and the combination should be examined very closely as a potential trouble source. Diaphragm and disc couplings may help avoid a gear coupling-induced axial force.

Double-helical gearing is usually the first choice in providing the accuracy of loading and smoothness of operation. Predictable performance renders unnecessary complex deviations from easily defined and measured geometry. These gear sets will be more efficient and have unmatched reliability if properly applied. Reasonable

intelligence must be exercised in coupling selection. This discretion will assure vibration and noise levels that are often indistinguishable from that of the connected machinery.

In single-helical gearing, all forces externally generated must be added to the thrust produced by the gear itself, and the total force is used on each shaft to select the high-speed shaft thrust bearing. An error in thrust or bearing capacity estimation will result in frequent failures of the thrust bearing or the associated shafting. Single-helical gearing, due to asymmetrical loading from the helix, has two sources of design difficulty that do not exist in double-helical gear sets. The effective center of tooth pressure oscillates back and forth across the face, putting substantial alternating loads on the shaft bearings. This oscillation results in peak-bearing loads substantially greater than those calculated, which can lead to early bearing failure. In addition, the helix-induced thrust force causes the gearing to try to skew in the housing, unbalancing the bearing loading and forcing the gearing to run out of parallel. Crowning of single-helical gearing is used to counter the effects of shaft misalignment.

Factors Affecting Gear Design

A transverse section through a gear and pinion mesh is shown in Figure 14-2 with some of the major points in gear and pinion interaction. Figure 14-3 shows the terminology used to describe helical gears. The major factors affecting gear performance are as follows: (1) pressure angle, (2) helix angle, (3) tooth hardness, (4) scuffing

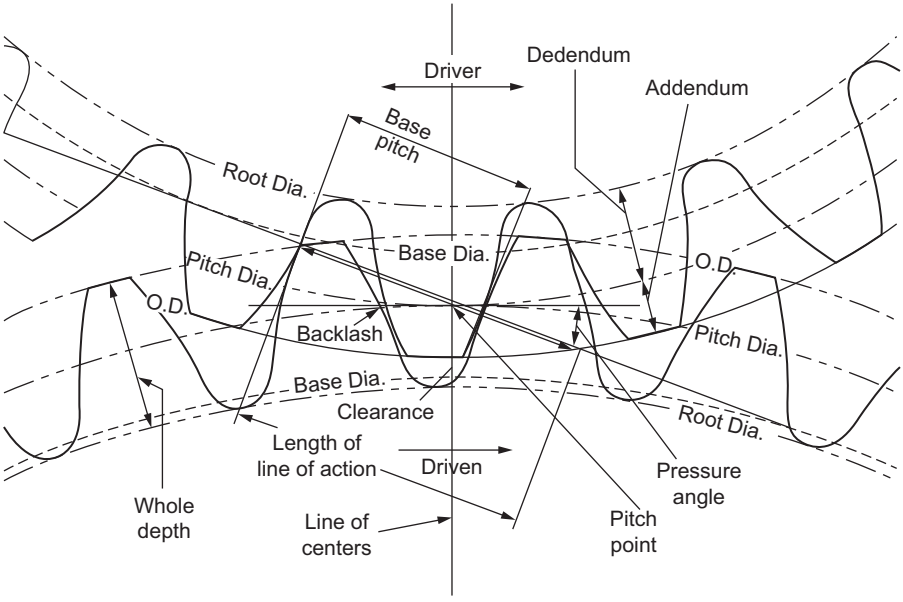


Figure 14-2 Transverse section through gear and pinion mesh.

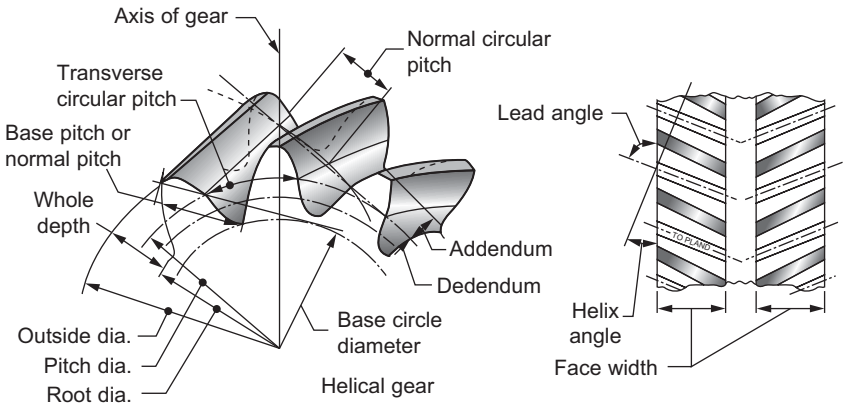


Figure 14-3 Helical gear terminology.

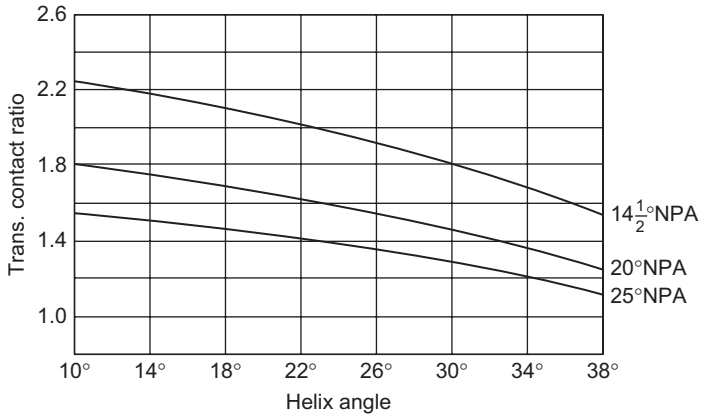


Figure 14-4 Variation of gear tooth geometry with pressure angle and helix angle (courtesy Lufkin Industries, Inc.).

prediction, (5) gear accuracy, (6) bearing types, (7) service factor, (8) gear housing, and (9) lubrication.

Pressure Angle

The decision regarding the pressure angle is one which the designer has to make early in the design stage. Conventionally, pressure angles ranged between 14.5° and 25°. Changes in the pressure angle affect both the contact ratio and the length of line of action. As the pressure angle increases, the contact ratio and the length of line of action decrease as shown in Figures 14-4 and 14-5, respectively. The contact ratio is an indication of the number of teeth in contact. As a general rule, the higher the contact ratio, the lesser the noise the gears generate.

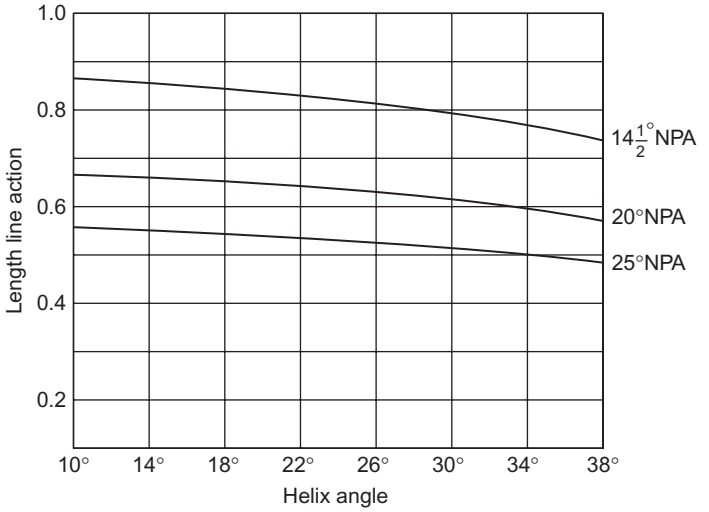


Figure 14-5 Length of line of action change with pressure angle and helix angle (courtesy Lufkin Industries, Inc.).

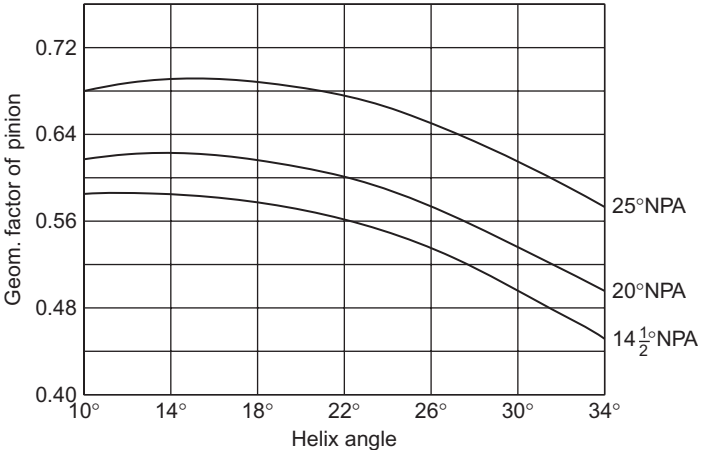


Figure 14-6 Variation of gear tooth geometry with pressure angle and helix angle (courtesy Lufkin Industries, Inc.).

The strength of the tooth is an important factor in the selection of the pressure angle. Figure 14-6 shows the variation of gear tooth geometry and pressure angle. The higher the pressure angle, the higher the tooth strength. The noise that the gears generate decreases with an increase in the contact ratio. Thus, the selection of pressure angle involves many factors. Normal pressure angles in use today are between 17.5° and 22.5°. Higher pressure angles increase the bearing loadings, but this increase is not a determining factor when selecting pressure angles.

Helix Angle

Helix angles vary from 5° to 45°. Single-helical angles fall between 5° and 20°, and double-helical angles fall between 20° and 45°. Helix angles are selected to obtain a minimum overlap ratio and to provide good load sharing. Figure 14-7 shows the effect on overlap ratio with an increasing helix angle. The thrust generated is also a function of the helix angle as shown in Figure 14-8. An increase in the helix angle increases the thrust; thus, this increase is the main reason for the lower helix angles in single-helical gearing.

Both single- and double-helical gearings have advantages and disadvantages. The advantages of single-helical gearing are greater accuracy, less sensitivity to coupling thrust, no apex runout, and less-expensive tooth cutting. The disadvantages of

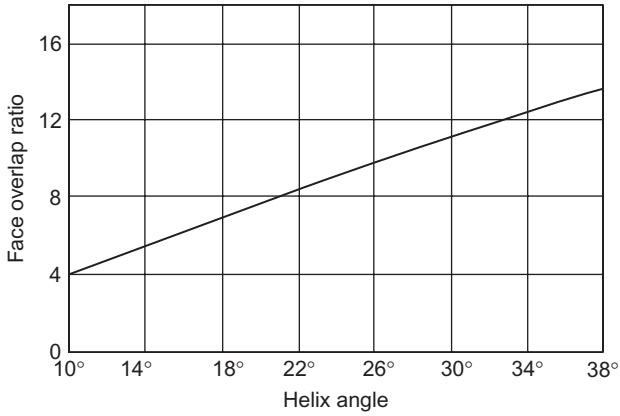


Figure 14-7 Face overlap (contact) ratio variation with helix angle (courtesy Lufkin Industries, Inc.).

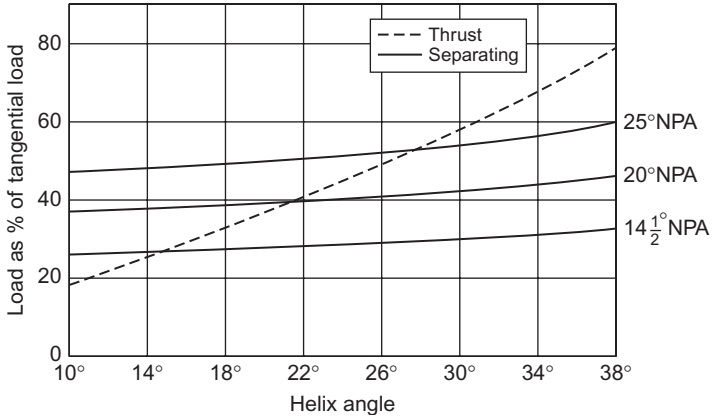


Figure 14-8 Thrust and separating load as a percentage of transmitted tangential load (courtesy Lufkin Industries, Inc.).

single-helical gears are that they require expensive thrust bearings and/or thrust faces and are less-efficient due to heat load on the thrust bearings.

Advantages of double-helical gears are that they are very simple to design and manufacture because of the absence of thrust faces and thrust bearings, very little thrust is produced by gearing, and they are generally more efficient than single-helical gears, which are subject to thrust-bearing losses. Some disadvantages of double-helical gears are as follows: they are sensitive to coupling lockup, they are slightly more expensive to cut teeth for because of setup and tool change, and they usually have a slightly wider gear box to accommodate the gap between helices.

Tooth Hardness

Gears available today have varying hardness, ranging from 225 BHN to 60 Rc. Each gear has its own advantages and disadvantages, so factors determining hardness must be carefully evaluated. Medium-range hardness gears are not too sensitive to operational errors and wear slightly before failing. Also, very hard gears are more susceptible to scuffing due to high-load intensity and sliding velocities. The noise levels on medium-hard gears increase with wear and give warning of gear failure. Heat treatment on medium-hard gears is simple when compared with that on surface-hardened gearing. Hardened gearing is used in turbomachinery applications to provide more power density in a smaller package. When case hardened, gearing must be subjected to a grinding operation to provide the finish. Figure 14-9 shows parts during the carburizing process. Carburizing is a process used to harden low-carbon steels that normally would not respond to quenching and tempering. This is done to provide a tough part with good wear characteristics and high load-carrying capability. Carburizing introduces carbon into a solid ferrous alloy by heating the metal in contact with



Figure 14-9 Parts during the carburizing process (courtesy Lufkin Industries, Inc.).

a carbonaceous material to a temperature above the transformation range and holding at that temperature. The depth of penetration of carbon is dependent on temperature, time at temperature, and the composition of the carburizing agent.

Nitriding is a process that is also used as a case-hardening method for gears. This process provides more load-carrying capability than hardening, but not as much as case carburizing. Other methods of hardening are available, but not in common use for this class of gearing.

Scuffing

For high-speed or high-load intensity, scuffing must be evaluated. One method to predict the probability of scuffing is by using the flash temperature index, calculated from American Gear Manufacturers Association (AGMA) 217. If the index value is less than 275, it is considered to be a low-scuffing risk. Values between 275 and 335 are considered high risks. Scuffing can usually be controlled by using optimum combinations of tooth pitch, lubrication choice, surface finish, and tooth loading.

Figure 14-10 shows the effect of speed and load intensity on the flash temperature index. These curves are general in nature, since scuffing is a function of pressure angle, lubrication, and tooth size.

Gear Accuracy

Turbomachinery gears normally require gear tooth accuracies per ANSI/AGMA ISO 1328-1 of Grade 4 or more. Grinding methods allow close control of tooth lead and profile modification to compensate for rotor and tooth deflections. This provides better load-carrying capabilities by creating more even load distribution. ANSI/AGMA

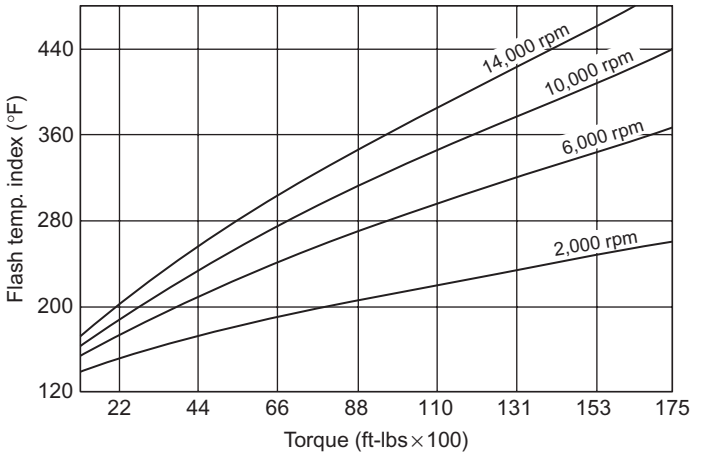


Figure 14-10 Scoring based on flash temperature index related to speed and torque (courtesy Lufkin Industries, Inc.).

ISO 1328-1 provides gear accuracy requirements for individual gears. Care should be taken for high-speed/high-power gears to evaluate the results of mating the measured profiles and leads of the gear and pinion. As a general rule, manufacturers of high-speed gearing monitor the gears and pinions for involute, lead, runout, tooth spacing, and surface finish. Light-load blue transfer checks are conducted to prove the accuracy of the system.

Types of Bearings

Bearings of all types can be used to support gears. Normally, gear drives proposed for turbine-driven applications, whether they are single or double helical, will be supported in hydrodynamic journal bearings.

The most basic type used is plain journal bearings. They have good load carrying capacity, but they can also have oil whirl problems. To prevent oil whirl problems, pressure dam or tilting pad journal bearings are used. Gear motors have imposed operating loads, and do not require the same degree of no-load bearing stability as compressor turbines, which have only the rotor weight applied to the bearings.

The exclusion of rolling-type bearings from drives of this class may be unwarranted. In the low-horsepower ranges, bearing ratings can be easily provided so that race and roller fatigue can be ignored as a source of failure. Drives using rolling element bearings may sometimes provide additional design latitude for the gear manufacturer. The extensive use of rolling element bearings in contemporary light-weight gas turbine designs bears strong testimony for this point.

Thrust bearings vary from the ball bearing to the self-equalizing tilting pad type. The most common type is the babbitt-lined, flat-face thrust bearing. The flat-face bearing is sometimes modified to add tapered lands that double the load-carrying capacity. Tilting pad bearings are becoming more popular because of their high-thrust capacity and misalignment capabilities. Also, the tilting pad thrust bearing is more efficient because of the higher allowable loading and lower rubbing speeds.

Service Factor

When selecting gears, two major areas to consider are the service factor and type of drive to be employed. The service factor is defined as the minimum ratio between calculated capacity and average transmitted load for any component of the system. In general, one of the three criteria will be the controlling influence in gear drives. These are failures due to tooth surface pitting, wear, or physical loss of teeth from breakage. Consequences of the three failure modes differ, particularly in regard to the length of the time involved. Wear can continue for a long period of time without affecting machinery serviceability or reliability. Pitting, if progressive, will eventually destroy the working profile of the teeth, altering their thermal characteristics, and often rendering the drive unsuitable because of high vibration levels long before the teeth are incapable of carrying load. Loss of a portion of a tooth by breakage has immediate

consequences. The balance is immediately and drastically affected and, with major tooth breakage, the gear will be incapable of further operation. Any evaluation of a service factor should determine which of the three modes is involved.

Current practice includes the provision of an additional margin when designing for gear tooth bending. The intent of applying this margin is to eliminate gear tooth breakage as a primary cause of failure, except with severe and unforeseen overloads.

Design against failure by wear under heavy tooth loads will result in the selection of heavy-bodied lubricants, generally 150 SSU or more at supply temperature. Pitting failures are the most difficult to provide a margin for, as increasing gear size or hardness are the only means of improving capacity, and both entail an increase in cost.

The service factor itself is not an overload capacity per se, as it includes either empirical or theoretical estimates of the effect of factors such as length of service life, torque fluctuations, and reliability level required. The service factors as established by the AGMA and the API, along with other organizations, and published in their standards, are intended for application to transmitted load requirements; if substantial overload capacity is planned or allowed (an oversize driver), additional gear rating must be included to provide for operation at those levels. Similarly, torque loads resulting from torsional oscillations or faulty operation are outside the scope of normally applied service factors and must be evaluated and provided for separately. Any torque fluctuations which result in a separation of gear teeth at speed will be most difficult to provide for. Impact loads occur during re-engagement, and very short service life is a frequent result of operation under these conditions, if these loads have not been considered and the gear adequately sized for them.

Gear Housings

Gear housings are made from materials such as cast iron, steel, or aluminum. Before final matching, the gear housing must be stress relieved for dimensional stability. Housing should also be rigid enough to resist misalignment. A sufficient clearance should be provided around the gears to prevent oil choking. To prevent thermal distortion, the design should be able to maintain uniform case temperatures. Gear housings can cause alignment problems from thermal distortion.

Lubrication

The oil furnished to high-speed gears has a dual purpose: tooth and bearing lubrication and cooling. Usually, only 10%–30% of the oil is used for lubrication and 70%–90% is used for cooling.

Turbine oil with rust and oxidation inhibitors is preferred. This oil must be kept clean, cooled, and have the correct viscosity. Synthetic oils are gaining popularity. If their use is anticipated, it is important that the gear manufacturer is informed, so the gear can be designed to be compatible with the synthetic oil.

When 150 SSU at 100°F (38°C) oil is necessary, inlet temperatures should be limited to 110–120°F (43–49°C), if possible, to maintain an acceptable viscosity. Higher

inlet temperatures require more detailed analysis to ensure adequate lubrication to gears. Oil should be supplied in the temperature and pressure range specified by the manufacturer. Up to a pitch line speed of approximately 15,000 ft/min (4,572 m/min), the oil should be sprayed into the outmesh (the side of the mesh where the teeth are disengaging). Spraying the outmesh allows maximum cooling time for the gear blanks and applies the oil at the highest temperature area of the gears. Also, a negative pressure is formed when the teeth come out of the mesh, pulling the oil into the tooth spaces.

At more than approximately 15,000 ft/min (4,572 m/min), 90% of the oil may also be sprayed into the outmesh and 10% into the inmesh. This procedure is a safety precaution to assure that the amount of oil required for lubrication is available at the mesh. When the speed ranges from 25,000 to 40,000 ft/min (7,620–12,192 m/min), oil may be sprayed on the sides and gap area (on double helical) of the gears to minimize thermal distortion.

Manufacturing Processes

Gear manufacturers use several methods for manufacturing good high-speed gearing. The most common are precision hobbing, hobbing and shaving, and hobbing and grinding.

High-speed gearing requires a finishing operation after cutting that involves honing, shaving, or grinding. Typically, gears of this class are hobbed and ground.

Hobbing

Hobbing produces good tooth spacing and accurate lead. Figure 14-11 shows a gear undergoing a hobbing process. It cannot economically achieve a surface finish better than 40 microinches. The cutting tool, called the "hob gear," is basically a worm gear that has been fluted and has form-relieved teeth as shown in Figure 14-12. These flutes provide the cutting edges and can be sharpened to retain the original tooth profile. As the workpiece meshes with the hob, the teeth are formed by a series of cuts known as the generating process. To cut the helix angle, the rotation of the work is slightly retarded or advanced in relationship to the hob rotation, and the feed is held in a definite relationship with the work and hob. Very accurate gearing can be produced by this process.

Hobbing and Shaving

The shaving process improves surface finish, involute profile, lead, and can be used to crown the teeth. Shaving with inaccurate cutters will reduce hobbed accuracy, and it cannot improve spacing or pitch line runout. The shaving cutter has involute teeth and meshes with the part being shaved, thus improving the finish.



Figure 14-11 The hobbing process for gear manufacture (courtesy Lufkin Industries, Inc.).



Figure 14-12 The hob used in the hobbing process for gear manufacture (courtesy Lufkin Industries, Inc.).

Hobbing and Lapping

Hobbing and lapping was used extensively in the past for this gear class; however, technology has progressed and as the gear materials have become harder in order to carry more load, grinding has replaced lapping as the preferred finishing operation.

Grinding

Grinding produces the best values of lead and involute profile. Figures 14-13 and 14-14 represent a typical grinding machine and a form of grinder, respectively. As a general rule, tooth spacing is good and surface finish can be 24-microinch R_a or more. Current grinding technology includes form grinding, which may be performed with a cubic boron nitride (CBN), aluminum oxide, or ceramic wheel. The advantage of this type of grinder over generating-type grinders is better speed, tooth spacing, and tooth finish, along with highly controllable lead and involute. One drawback of grinding is that the process must be carefully performed and controlled to prevent grinding burns and cracks.



Figure 14-13 Gleason Pfauter form grinder (courtesy Lufkin Industries, Inc.).

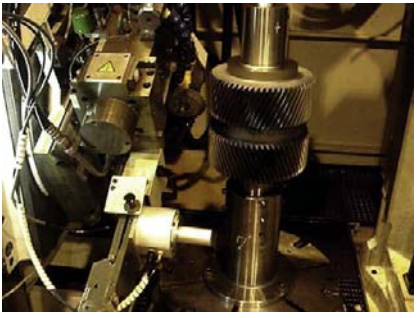


Figure 14-14 A form grinder (courtesy Lufkin Industries, Inc.).

Gear Rating

API 613 "Special Purpose Gear Units for Petroleum, Chemical and Gas Industry Services", currently Fifth Edition, February 2003, has been used as a worldwide guide for building reliable gears for the turbomachinery market. API 613 provides a simplified gear rating, based on and consistent with ANSI/AGMA 2101-D02. The API 613 rating method is generally more conservative than AGMA methods. A common procedure for comparing and sizing gear is based on the tooth pitting index, the K factor (in U.S. Customary units):

$$\text{Allowable}\, K = \frac{\text{Material index number}}{\text{Service factor}}$$

The material index is based on hardness. The service factor takes into account the driving and the driven equipment characteristics.

$$K = \frac{126{,}000 \times P_g}{N_p \times d^2 \times F_w} \times \frac{R+1}{R}$$

where

P_g = transmitted horsepower
R = gear ratio
N_p = pinion rpm
d = pinion pitch diameter in inches
F_w = net face width of narrowest mating gears, or the sum of the face width of each helix of double helical (inches)

The strength rating based on API 613 is:

$$S = \frac{\mathrm{W}_t \times P_n \times \mathrm{SF}}{F_w} \times \frac{1.8 \cos \gamma}{J}$$

where,

S = bending stress number
γ = helix angle
J = geometry factor
SF = service factor
P_n = normal diameter pitch
W_t = transmitted tangential load at operating pitch diameter

Gear Noise

Noise from an operating gear set is a function of roundness and concentricity of operating elements (both gearing and shafting), accurate balance, and, in particular, control of tooth spacing errors and uniformity of mesh stiffness to reduce meshing

frequency excitation. Some factors causing gear noise can be attributed to, but not limited to, the following:

- Tooth spacing or involute error
- Contact ratio
- Surface finish
- Wear on tooth flanks or pitting
- Excessive or too little backlash
- Gear, shaft, or housing resonance
- Tooth deflections
- Pitch line runout
- Load intensity on gearing
- Clutches and couplings
- Lube oil pump and piping
- Transmitted noise from driven or driving machinery.

Installation and Initial Operation

The mounting of a gearbox into machinery trains is a precision job and should be done carefully. Gear unit installation is one of the most important factors to be considered for long, trouble-free operation, thus careful testing of the gear box should be undertaken. Figure 14-15 is a gear box under test. No matter how accurately the gear unit is manufactured, it can be destroyed in a few hours of operation when improperly installed. The same care should be taken when installing a gearbox as with any high-speed machinery. The mounting surface should be a flat-level, single-plane surface of finished steel at a height that will permit the shimming necessary to align the gear unit



Figure 14-15 Gas turbine gear drive (courtesy Lufkin Industries, Inc.).

properly to connecting shafts. The shims should be of a size at least equal to the width of the unit foot pad. Then, the gear unit should be placed on the foundation in the approximate required position. Uneven supports can distort the gearbox and adversely affect the gear tooth contact.

Shaft alignment is very important for long gear life. Poor alignment can cause unequal distribution of tooth loads and distortion of the gear elements from overhung moments. A 0.002 inch (0.05 mm) shaft vibration level on the gear unit produced by misalignment is equivalent to a gear pitch line runout of 0.002 inch (0.05 mm).

The gear housing must be properly supported to maintain proper internal gear alignment. When a gear unit is installed, the support pads must be maintained in the same plane as used by the manufacturer during assembly when gear face contact was obtained in the plant. Before startup, gear face contact should be checked using high-spot bluing and rotating or rocking the pinion or lighter element back and forth sharply within the confines of the backlash. Inspection of this blued area should show approximately 90% face contact. If this contact is not obtained, the gear housing can be shimmed under the proper corner until an acceptable face contact is achieved.

Many large, high-hardness or wide-face width gears are manufactured with helix angle modifications to account for torsional and bending deflection. When the helix angle has been modified, 90% face contact will not be obtained under light load. In this case, the gear supplier should furnish data on percent of face contact versus the load to be used as a guide during installation and startup. Also, many gears have a short area of ease-off on each end of the teeth to prevent end loading, and this area usually will not show contact under a light load.

The larger the gear unit, the more important this check becomes, since large housings tend to be more flexible. Also, the use of baseplates furnished by the original equipment manufacturer does not eliminate face contact problems, and these inspection procedures should be carried out.

After the gear checks have been made, the foundation bolts should be uniformly tightened and the alignment should be re-checked. It may be necessary to repeat the shimming and tightening of foundation bolts to obtain final and correct cold alignment.

Alignment of high-speed gear units should always be hot checked and adjustments made as necessary. Temperatures vary so greatly throughout the housing and shafting that it is impossible to calculate a thermal growth accurately and, therefore, an alignment check must be made in the hot condition.

When the alignment is complete, the baseplate or bed should be grouted in as close to the gear housing as possible. Journal bearings are used on the gear shafts and proper oil flow must be maintained. The oil system should therefore be checked thoroughly prior to startup. The gear lube system is normally flushed prior to any operations. Gear mesh spray nozzles should be checked to be sure that dirt was not pumped through the system by observing the sprays or by introducing high-pressure air into the spray nozzle manifold during installation.

When possible, gears should be run-in on initial startup. Speeds and loads should be increased in percentage increments. Lube oil temperature and pressure and bearing temperatures should be observed and adjustments made to the lube system as required.

The number of adjustments made will depend on the complexity of the system. Oil pressure is of primary importance. When an auxiliary pump has been provided, oil should be circulated before the actual start. If not, the pump should be primed, and the journals wetted with oil. Primer holes are sometimes provided as an alternative, and journals can be oiled through the holes provided for bearing temperature detectors.

It is recommended that warning devices be provided to eliminate as much human error as possible, and the set points should be checked carefully. As with any startup, vibrations should be monitored and recorded. The vibration monitoring system should include at least one accelerometer to detect any vibrations generated at gear mesh frequency. The recorded data should be saved to provide baseline vibration data for future reference.

Shutdowns, as well as startups, require care and attention. Shutdown of a unit, which has been operating in a humid atmosphere, can result in considerable condensation and subsequent rusting of the gears, shaft journals, and housing in a very short time. When water contacts the clean steel, it begins to etch the steel immediately. When shutdowns are necessary in such conditions, provisions to prevent condensation must be furnished.

Under normal operating conditions, the oil should be changed every 2,500 operating hours or every 6 months, whichever occurs first. Oil analysis at regular intervals greatly extends the time between oil changes, if utilized correctly. When operating conditions warrant, this period may be extended; conversely, severe operating conditions may make it necessary to change oil at more frequent intervals. Such conditions may occur with the rapid rise and fall in temperature that produces condensation, when operating in moist or dusty atmospheres, or in the presence of chemical fumes. In any case, the lubrication supplier should be consulted when determining a lubricant maintenance program.

Gear Failures

Gears, due to their metal to metal contact, are the most susceptible to problems in many gas turbine trains. Gear teeth can undergo very high pressures that can be further enhanced due to misalignment and loss of lubrication properties of the oil, such as loss of viscosity, due to a mixture of water with the oil or on increased particle count in the oil.

Careful analysis of gear tooth failure evidence may result in valuable information about the mode of failure, which may be used to prevent a recurrence. This analysis may include: visual observation, at the site or in the laboratory; metallurgical examination of microstructure and material properties, physical specimen testing for mechanical properties, testing for chemical properties, load analysis, investigation of installation results, and lubrication analysis, among others.

Figure 14-16 shows a sectional view of a sub-case fatigue that initiated at the case–core interface of a carburized part. This failure was caused by high tooth loading that initiated fatigue failure at a non-metallic inclusion.

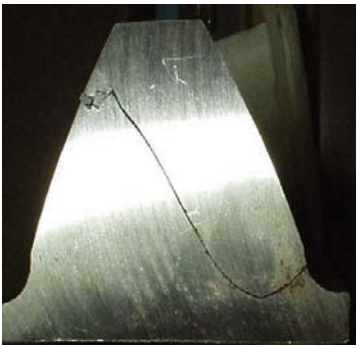


Figure 14-16 Damage to gear tooth due to high tooth loads (courtesy Lufkin Industries, Inc.).



Figure 14-17 Plan view of tooth loss due to sub-case fatigue failure.

Figures 14-17 and 14-18 are examples of fatigue failure, where a failure may begin when a crack initiates at an area of structural discontinuity or at a localized area of stress concentration. The crack then propagates as the cycles continue, until the fracture ultimately occurs.

Case crushing, shown in Figure 14-19, can result when the carburized case has insufficient strength to withstand the loading. This may also occur because of insufficient hardness and/or strength in the material core.

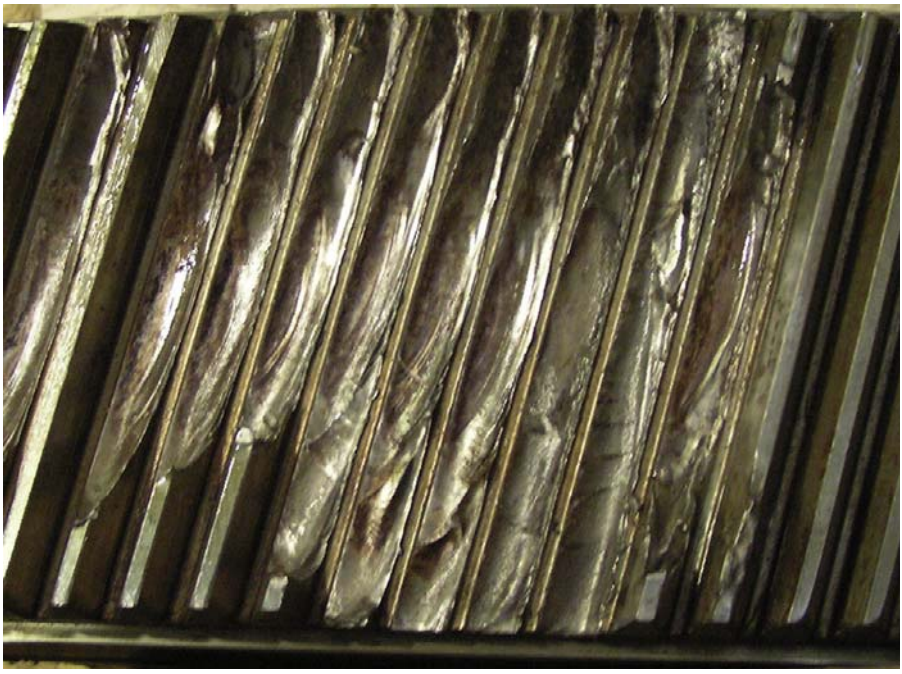


Figure 14-18 Root bending fatigue failures of multiple teeth.

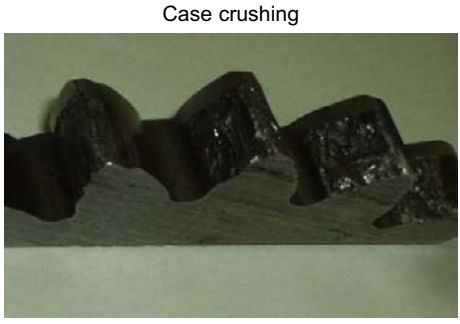


Figure 14-19 Case crushing of carburized part due to insufficient case depth and soft core.

The ANSI/AGMA publication, ANSI/AGMA 1010-E95, *Appearance of Gear Teeth-Terminology of Wear and Failure*, provides valuable information on gear tooth failure modes and their identifying features.

Acknowledgement

The author wishes to acknowledge and thank Ms. Lisa Ford, Director of Engineering, Lufkin Industries, for her knowledge, and helpful suggestions in this chapter.

Bibliography

API 617, *Axial and Centrifugal Compressors and Expandor-Compressors for Petroleum, Chemical and Gas Industry Services*, 7th edition, Washington DC, AIP, 2002.

API 613, *Special Purpose Gear Units for Petroleum, Chemical and Gas Industry Services*, 5th edition, Washington, DC, AIP, 2003.

Partridge, J.R. High-Speed Gears-Design and Application, *Proceedings of the 6th Turbomachinery Symposium,* Texas A&M Univ., December 1977, pp. 133–142.

AGMA/ISO 1328-1, *Cylindrical Gears-ISO System of Accuracy-Part 1*, 1999.

Phinney, J.M. Selection and Application of High-Speed Gear Drives, *Proceedings of the 1st Turbomachinery Symposium*, Texas A&M Univ., October 1972, pp. 62–66.

AGMA 2101/2001-DO4 *Fundamental Rating Factors and Calculation Methods for Involute Spur and Helical Gear Teeth*, 2010.

ANSI/AGMA 1010-E95, *Appearance of Gear Teeth Terminology of Wear and Failure*, 1995.

Copyrighted Materials
Copyright © 2012 Elsevier Retrieved from www.knovel.com

Part V

Installation, Operation, and Maintenance

15 Lubrication

For reliable turbomachine performance, it is vital to have a properly designed, installed, operated, and maintained lubrication system. The lubrication system of a turbomachine is the "lifeblood" for this complex and finely tuned piece of machinery. The oil must be pumped in continuous circulation, conditioned, drained, and returned to be pumped again. In some units there are independent and dedicated turbine lube oil, compressor lube oil, and turbine control oil systems. There are combined systems with turbine lube oil and control oil from one system and compressor lube oil from another, or with turbine and compressor lube oil from one system and turbine control oil from another. In most cases, one system will supply all lube and control oil.

This chapter deals with the principles involved in the operation and maintenance of a lubrication system, and it describes the main components of such a system, including the lubricant itself. The following topics are discussed:

1. Basic oil system
2. Lubricant selection
3. Oil contamination
4. Filter selection
5. Cleaning and flushing
6. Oil sampling and testing
7. Test profiles
8. Gearboxes
9. Clean oil systems
10. Coupling lubrication

Basic Oil System

API Standard 614 covers in detail the minimum requirements for lubrication systems, oil-type shaft-sealing systems, and control oil supply systems for special-purpose applications.

Lubrication Oil System

A typical lubrication oil system is shown in Figure 15-1. Oil is stored in a reservoir to feed the pumps and is then cooled, filtered, distributed to the end users, and returned to the reservoir. The reservoir can be heated for start-up purposes and is provided with local temperature indication, a high-temperature alarm and high/low-level alarm in the

Gas Turbine Engineering Handbook, Fourth Edition. DOI: 10.1016/B978-0-12-383842-1.00015-9
Copyright © 2012 Elsevier Inc. All rights reserved.

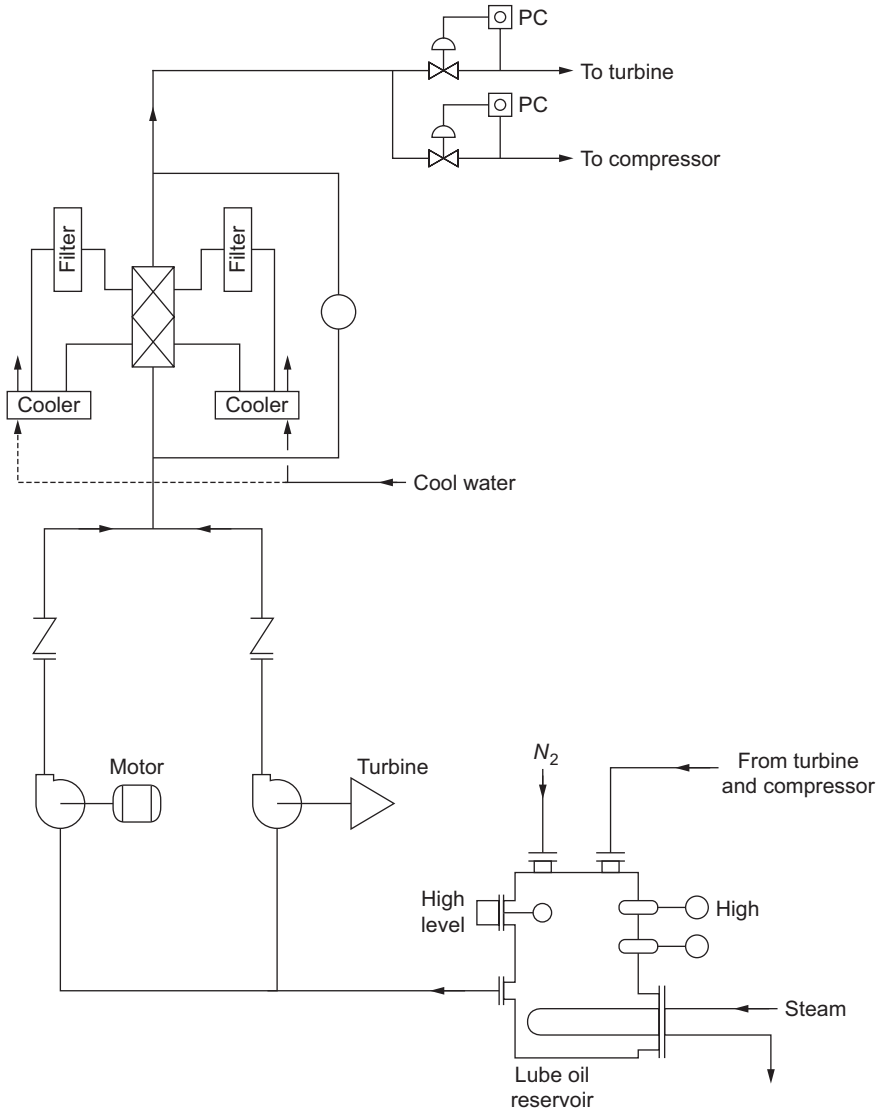


Figure 15-1 A typical lube oil system.

control room, a sight glass, and a controlled dry nitrogen purge blanket to minimize moisture intake.

The reservoir shown in Figure 15-2 should be separate from the equipment base plate and sealed against the entrance of dirt and water. The bottom should be sloped to the low drain point, and the return oil lines should enter the reservoir away from the oil pump suction to avoid disturbances of the pump suction. The working capacity should be at least five minutes based on normal flow. Reservoir retention time should be

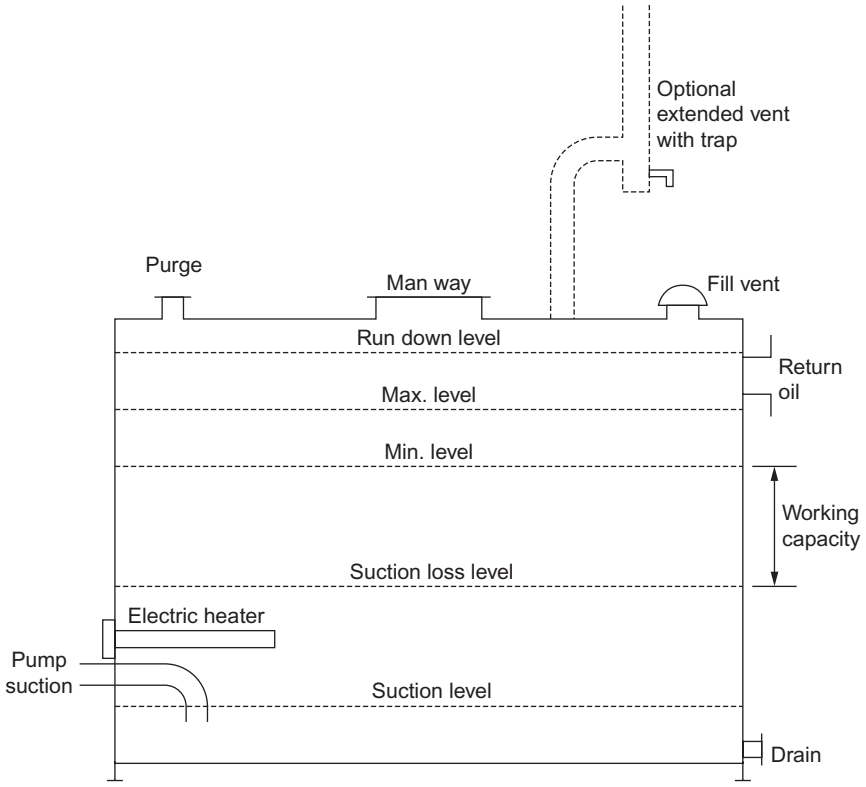


Figure 15-2 Lube oil reservoir.

10 minutes, based on normal flow and total volume below minimum operating level. Heating for the oil should also be provided. If thermostatically controlled electrical emersion heating is provided, the maximum watt density should be 15 watts per square inch (2.33 w/cm^2). When steam heating is used, the heating element should be external to the reservoir.

The rundown level, which is the highest level the oil in the reservoir may reach during system idleness, is computed by considering the oil contained in all components, bearing and seal housings, control elements, and furnished piping that drains back to the reservoir. The rundown capacity should also include a 10% minimum allowance for the interconnecting piping.

The capacity between the minimum and the maximum operating levels in an oil system that discharges seal oil from the unit should be enough for a minimum operation of three days with no oil being added to the reservoir. The free surface should be a minimum of 0.25 sq ft/gpm (0.023 m^2/gpm) of normal flow.

The reservoir interior should be smooth to avoid pockets and provide an unbroken finish for any interior protection. Reservoir wall-to-top junctions may be welded from the outside by utilizing full-penetration welds.

Each reservoir compartment should be provided with two three-quarter-inch minimum size plugged connections above the rundown oil level. These connections may be used for such services as purge gas, makeup, oil supply, and clarifier return. One connection should be strategically located to ensure an effective sweep of purge gas toward the vents.

The oil system should be equipped with a main oil pump, a standby, and, for critical machines, an emergency pump. Each pump must have its own driver, and check valves must be installed on each pump discharge to prevent reverse flow through idle pumps. The pump capacity of the main and standby pumps should be 10–15% greater than maximum system usage. The pumps should be provided with different prime movers.

The main pumps are usually steam turbine driven with an electric motor–driven backup pump. A small mechanical-drive turbine is highly reliable as long as it is running, but it is undependable when starting automatically after long idle periods. A motor is thus the preferred backup pump driver. A "ready-to-run" status light is usually provided for the motor in the control room to give visible evidence that the electrical circuit is viable. Starting the backup pump is initiated by multiple and redundant sources. The turbine drivers should be maintained against failure, by either low-speed or low-steam chest pressure, or both.

Low oil pressure switches are provided on the pumps and discharge header ahead of the coolers and filters, sometimes after the cooler and filters, and always at the end of the line where the reduced oil pressure feeds the various users. A signal from any of these should start the motor-driven pump and all alarms should be activated in the control room. The emergency oil pump can be driven with an AC motor but from a power source that is different to the standby pump. When Dc power is available, DC electric motors can also be used. Process gas or air-driven turbines and quick-start steam turbines are often used to drive the emergency pumps.

The pump capacities for lube and control oil systems should be based upon the particular system's maximum usage (including transients) plus a minimum of 15%. The pump capacity for a seal oil system should be based upon the system's maximum usage plus either 10 gpm or 20%, whichever is greater. Maximum system usage should include allowance for normal wear. Check valves should be provided on each pump discharge to prevent reverse flow through the idle pump.

The pumps can be either centrifugal or positive displacement types. The centrifugal pumps should have a head curve continuously rising toward the shut-off point. The standby pump should be piped into the system in a manner that permits checking of the pump while the main pump is in operation. To achieve this, a restriction orifice is required with a test bleeder valve piped to the return oil line or the reservoir.

Twin oil coolers (Figure 15-3) should be provided and piped in parallel using a single multiport transflow valve to direct the oil flow to the coolers. The water should be on the tube side and the oil on the shell side. The oil-side pressure should be greater than the water-side pressure. This ratio is no assurance that water will not enter the system in the event of a tube leak, but it does reduce the risk. The oil system should be equipped with twin full-flow oil filters located downstream from the oil coolers. Since the filters are located downstream from the oil coolers, only one multiport transflow valve is required to direct the oil flow to the cooler-filter combinations. Do not pipe the

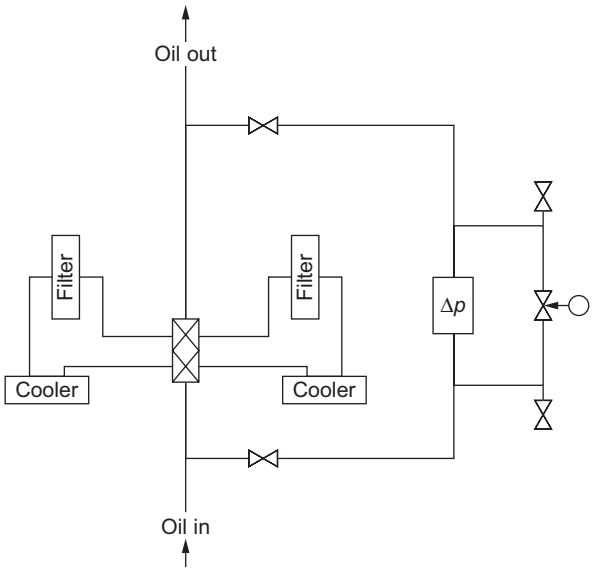


Figure 15-3 Cooler-filter arrangement.

filters and coolers with separate inlet and outlet block valves. Separate block valves can cause loss of oil flow from the possible human error of flow blockage during a filter switching operation.

Filtration should be 10 μm nominal. For hydrocarbon and synthetic oils, the pressure drop for clean filters should not exceed five psi at 100°F (38°C) operating temperature at normal flow. Cartridges will have a minimum collapsing differential pressure of 50 psi (3.447379 Bars).

The system should have an accumulator to maintain sufficient oil pressure while the standby pump accelerates from an idle condition. An accumulator becomes a must if a steam turbine drives the standby pump. Overhead tanks are specified by many users to assure flow to critical machinery components. The sizing of the tanks varies depending on the application. In some gas turbine applications, the bearings reach maximum temperature as long as 20 minutes after shutdown.

The oil coolers and filters are controlled by a local temperature control loop with remote control room indication and high/low alarm. The coolers and filters also have an indicating differential pressure alarm. These usually feed into a common high alarm to pre-warn a need for switching and filter element replacement.

To ensure the required constant pressure, a local pressure control loop is provided on each system – turbine lube oil, compressor lube oil, and control oil. Each oil pressure system should be recorded in the control room to provide trouble-shooting information. The success of the oil system depends upon not only the instrumentation, but upon proper instrument location.

The minimum alarms and trips recommended for each major driver and driven machine should be: a low oil pressure alarm; a low oil pressure trip (at some point

lower than the alarm point), a low oil level alarm (reservoir), a high oil filter differential pressure alarm, a high bearing metal temperature alarm, and a metal chip detector. See Table 15-1.

Each pressure- and temperature-sensing switch should be in a separate housing. The switch type should be single-pole, double-throw, furnished as "open" (de-energized) to alarm and "close" (energize) to trip. The pressure switches for alarms should be installed with a "T"-connection pressure gauge and bleeder valve for testing the alarm.

Thermometers should be mounted in the oil piping to measure the oil at the outlet of each radial and thrust bearing and into and out of the coolers. It is also advisable to measure bearing metal temperatures.

Pressure gauges should be provided at the discharge of the pumps, the bearing header, the control oil line, and the seal oil system. Each atmospheric oil drain line should be equipped with steel nonrestrictive bull's-eye-type flow indicators positioned for viewing through the side. Viewports in oil lines can be very useful in providing a visual check for oil contamination.

In the piping arrangement and layout it is very important to eliminate air pockets and trash collectors. Before starting a new or modified oil system, every foot of the entire system – right up to the final connection at the machine – should be methodically cleaned, flushed, drained, refilled, and all instruments thoroughly checked.

Seal Oil System

The compressor seal oil system is designed and furnished with instrumentation similar to the lube oil system shown in Figure 15-4. The only essential difference is how the end-supply control is handled. Since much higher pressures (1,500–2,500 psi) (103.4214–172.3689 Bars) are often involved, the pumps are usually a positive displacement-type. This requires a pressure control valve spilling oil back to the reservoir. This oil supply is available to an elevated head tank that is provided for each shaft seal. The head tank is pressured by its own process-seal pressure connection, so the seal oil supply system pressure must be maintained at a level to supply the highest pressure seal. The oil rate to each seal is maintained by tank level control from the supply system. The tanks are provided with a high/low-level alarm to the control room. The low alarm warns of excessive oil consumption by the seal and also calls for

Table 15-1 Alarms and Trips

	Alarm	Trip
Low oil pressure	x	x
Low oil level	x	
High oil filter	x	
High thrust bearing metal temperature	x	
High thrust bearing oil temperature	x	
Metal chip detector	x	

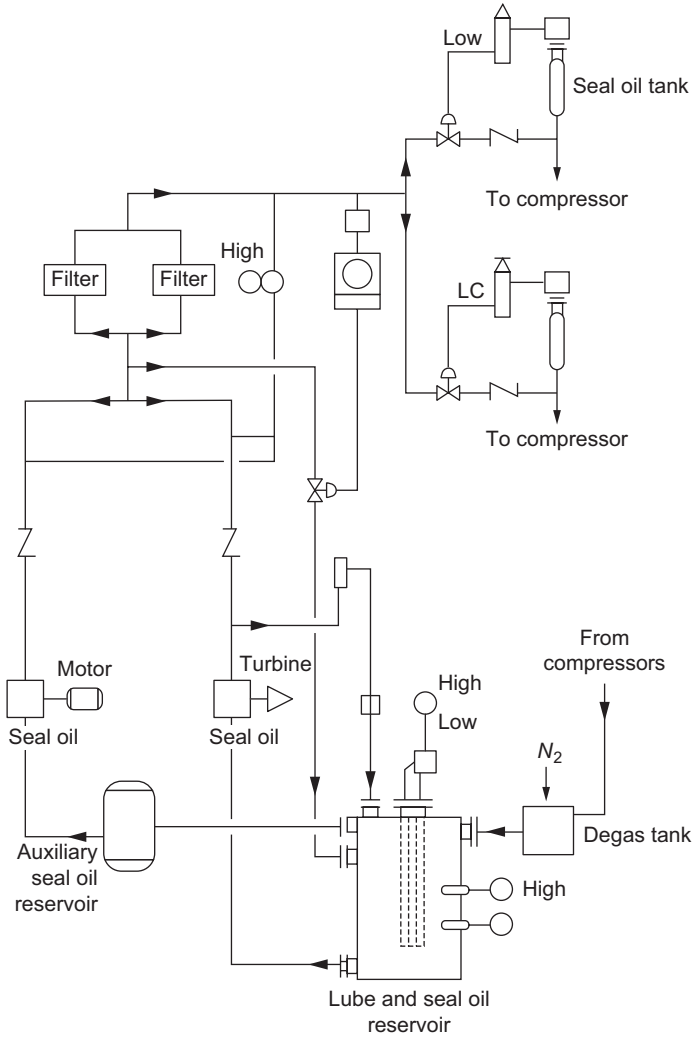


Figure 15-4 Seal oil system.

backup pump start along with the various pressure switches and the high-level alarm warns of primary pump turbine failure in a similar manner to the lube oil system.

A degassing facility is also provided to separate gas contaminants from the seal oil. Figure 15-5 shows a typical degassing drum arrangement. A gas-tight baffle and a liquid seal should divide the degassing drum into two sections to confine the separated gas to one side of the drum. The gas side of the drum should be vented and provided with an inert-gas purge. To assist in degassing the oil, the drum will be heated by electricity or steam.

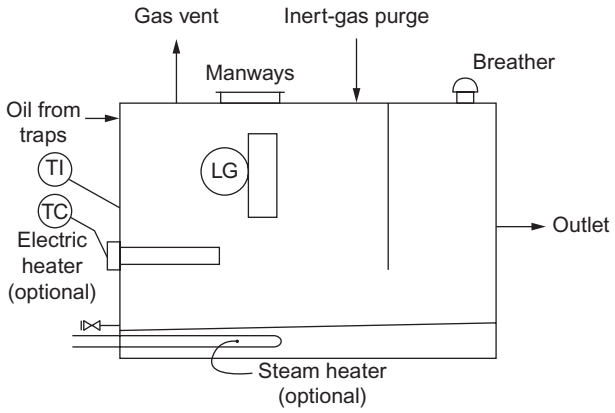


Figure 15-5 Typical degassing drum arrangement.

Lubrication Management Program

A well-planned and managed lubrication program is an important factor in the overall maintenance plan of a plant. A lubrication program includes developing a lubrication period maintenance program, sampling and testing oil, and developing specific procedures to apply lubricants. The initial step in developing a comprehensive plant lubrication program is to conduct a plant survey to determine existing lubrication practices. The survey should utilize machine drawings and external machinery inspections.

A detailed list of lubricant types and their points of application can be compiled from the results of the survey. Combining the list of lubrication types and a current schedule, a master plant lubrication schedule can be published.

A monthly lubrication schedule can then be issued to the appropriate maintenance personnel to serve as a reminder. The issuing of the lubrication schedule does not ensure its compliance and supervisors should check to see that required lubrication is performed.

As a part of the lubrication program, oil should be periodically tested. The testing requires drawing oil from the system for a laboratory analysis. The usual tests conducted to determine the condition of oils include viscosity, pH and neutralization number, precipitation, color and odor, and a check for foreign particles in the oil. The results should be reviewed and compared with new oil characteristics to determine the life characteristics of the oil.

A program for evaluating any new lubrication products can be used to indicate the possible replacement of current lubricants. The general characteristics of new lubricants can be obtained from specifications provided by the suppliers or from testing the lubricant. The final selection of new lubricants should be made only after close observation of the lubricant in several typical plant applications. During the monthly inspections, new lubricants should be checked especially closely to ensure that they are retaining their desired properties. Although, all lubrication applications are important to machinery health, gear couplings present special critical lubrication problems and

require special attention as explained previously. Operating experience has proven that unless a continuous program of required lubrication is followed, even the most well-designed units are sure to fail. A proper lubrication management program must incorporate a monthly lubrication schedule, an evaluation of new lubrication products, and supervision to ensure the prescribed procedures are carried out by maintenance personnel.

In the event of failures due to lubrication problems, the failures should be thoroughly analyzed to determine if they were indeed caused by lubricant failure or incorrect maintenance procedures. Once the problem has been isolated, corrective action can be initiated to prevent subsequent similar failures – whether it requires changing lubricants or procedures.

Lubricant Selection

A good turbomachinery oil must have a rust and oxidation inhibitor, good demulsibility and the correct viscosity, and be both nonsludging and form resistant. Besides lubrication, the oil has to cool bearings and gears, prevent excessive metal-to-metal contact during starts, transmit pressure in control systems, carry away foreign materials, reduce corrosion, and degrade resin. For gas turbines, especially the more advanced high-temperature gas turbines, the oil of choice should be synthetic oil, since synthetic oils have a high flash point. Gas turbine lubrication systems should be run for about 20 minutes after shutdown, since maximum temperatures are reached 10–15 minutes after shutdown, especially in the bearing area. Most gas turbines are also on turning gear to avoid sagging in the shaft. Mineral oils can be used for the compressor. It is not uncommon to have two types of oil in a petrochemical plant, since mineral oil costs much less than the synthetic oil.

The selection of the correct lubricant must begin with the manufacturer. The operator's instruction manual can be referred for the oil required and the recommended viscosity range. The local environmental conditions should be seriously considered, including exposure to outside element conditions, acid gas, or steam leaks. As a general rule, most turbomachines are lubricated with premium-quality turbine-grade oil. However, under certain environmental conditions, it may be advantageous to consider an alternative oil. For example, if a machine is subject to exposure to low concentrations of chlorine or anhydrous hydrochloric acid gases, it may be better to select an oil that will outperform the premium turbine oil. Good results have been recorded using oil containing alkaline additives. Certain automotive or diesel engine oils contain the optimum amount and type of alkaline additives to protect the base oil from reaction with chlorine and HCl. In services where attack on the lubricant by the gas is unknown, laboratory tests are suggested.

Oil Contamination

Oil contamination in a turbomachine is one of the major problems maintenance crews face. However, although contamination is a continuous problem, the levels of contamination are what cause the most concern. The greatest source of contamination

is extraneous matter. Atmospheric dirt, for example, is always a serious threat. It can enter the oil system through vents, breathers, and seals. Its primary effect is equipment wear, but plugging of oil lines and ports, and reduced oxidation stability of the oil are also serious effects. Metal particles from wear, and rust particles from reservoir and oil piping corrosion, can lead to premature equipment failure and oil deterioration. It is important to provide suitable filtering equipment to remove these particles from the system.

Water contamination is a constant threat. The sources of water are many – atmospheric condensation, steam leaks, oil coolers, and reservoir leaks. Rusting of machine parts and the effects of rust particles in the oil system are the major results of water in oil. In addition, water forms an emulsion and, combined with other impurities, such as wear metal and rust particles, acts as a catalyst to promote oil oxidation.

Contamination from process gas can be a serious problem, particularly during startup. Every effort must be exercised to prevent and detect this type of contamination. Most hydrocarbon gases are more soluble in cold oil than in hot oil and may lower the viscosity to a dangerous level. The problems of thrust bearing failures during startup, due to low-viscosity oil, can be eliminated by equipping the reservoir with oil heaters to raise the oil to the normal operating temperatures before starting the machine.

Equipment in HCl and chlorine service must be protected against the exposure of these acid gases to the oil. Obviously, the first line of defense is to eliminate seal failures. However, as a secondary protection, these machines could be lubricated with an alkaline oil. The alkaline additives react to the low concentrations of the acid gases, thus eliminating the addition of these acids to the oil molecule.

Filter Selection

Various types of full-flow filters can be used for the removal of insoluble contaminants. Two general types are usually selected: surface filters and depth filters. Both types of filters are effective for the removal of particulate matter.

Surface filters, if manufactured from the correct material, will not be affected by water in the oil. Water-resistant pleated paper elements have much greater surface areas than the depth-type element and yield a much lower differential pressure when used as replacement elements in filters originally equipped with depth-type elements. Pleated paper elements are available that will remove particle sizes down to a nominal one-half micron.

The depth-type filter elements are used when the oil is free from water, and when particle sizes to be removed are in the 5-μm range and greater. Generally, the depth-type element is water-sensitive, and when oil is contaminated with moisture, this element type will absorb the water and produce a rapid increase in differential pressure across the filter. The desired maximum differential pressure across a filter with clean elements is 5 psig at normal operating temperature.

The filter elements should remove particles of 5 μm, must be water-resistant, have a high flow rate capability with low pressure drop, possess high dirt-retention capacity,

and be rupture-resistant. The clean pressure drop should not exceed 5 psig at 100°F (38°C). The elements must have a minimum collapse differential pressure of 50 psig. Pleated paper elements are preferred – provided they meet these requirements. Usually, the pleated paper element will yield the 5 psig clean drop when used in a filter that was sized to use depth-type elements. This result is due to the greater surface area of the pleated element, more than twice the area of a conventional stacked disc-type or other depth-type elements.

A differential pressure switch is set to alarm when the pressure drop reaches a predetermined point protects against the loss of oil flow. In addition to the differential pressure switch, a two-way, three-port valve with a pressure gauge is piped in parallel with the differential pressure switch for accurate indication of inlet and outlet oil filter pressure. When a single transflow valve is used with a cooler–filter installation, the differential pressure switch and pressure gauge assembly should span the cooler–filter system.

Water contamination in the oil system can cause serious damage to turbomachinery, and every reasonable effort should be made to, first, prevent its entrance into the system, and second, provide suitable removal equipment if water cannot be effectively kept out. Experience indicates that designers and equipment operators can be more effective in keeping water out of the system. Since the main sources of contamination are atmospheric condensation, steam leaks, and faulty oil coolers, preventive measures should be taken.

Condensation will occur in the atmospheric vented oil system whenever the temperature in the vapor space areas drops below the dew point. This effect can take place in the return oil piping as well as the reservoir. Consoles installed in unprotected locations are more vulnerable to climatic changes than those installed inside buildings. Outside locations will be adversely affected by temperature cycles between day and night operations, by showers and sudden temperature drops due to other weather changes, especially in the fall and winter seasons.

There has been great success in "drying up" oil systems by making a few simple alterations. The first step is to check the reservoir unit. The vent should be located in the very top of the reservoir. It should be free of baffles that can collect and return condensate to the reservoir, and the length should be kept as short as possible to provide a minimum of surface areas on which condensate can form. If it is necessary to run the vent up and away from the reservoir, a water trap should be provided as close to the reservoir as possible to remove any condensate formed in the vent stack. The next step is to provide and maintain an inert gas or dry-air purge on the reservoir. Only 2–5 ft^3/h (cfh) (0.057–0.1415 m^3/h (cmh)) is required. The reservoir purge system will not substitute for the elimination of other water sources.

Steam and condensate leaks are the most difficult water sources to prevent in turbomachinery; however, it can be done, and every effort should be made to eliminate these sources. Obviously, the first means of prevention is to maintain the steam packing in perfect condition. Experience has shown that eventually the steam packings will leak, and steam condensate will enter the system through the bearing seals. There has also been great success in "drying up" a wet oil system. The procedure is to purge the bearing labyrinths with inert gas or dry air. One method is to drill a one-eighth-inch

hole through the bearing cap and intersect the labyrinth. A one-quarter-inch diameter tube is connected to the hole in the bearing cap and to a rotometer. The labyrinth is then purged with 15 cfh (0.43 cmh) dry air or inert gas.

Another method is to install an external labyrinth with purge provisions on the bearing housings of a machine that has the necessary space to accommodate the external seal.

Removal of free water from oil systems is usually done with centrifuges or coalescer separators. Centrifuging is the most costly method in both capital outlay and operating cost. The centrifuges usually are the conventional disc-type with manual cleaning. The discs must be cleaned at least once a week with one hour required per cleaning. The coalescer separators usually require much less attention. Some separators only require element changes once a year while others may require changes at six or three months, and in some instances once a month. The frequency appears to be related to the amount of water in the oil system. In many instances, coalescer element changes have been reduced by the use of a prefilter in the system. This element removes the particulates (usually rust) that would restrict the 2-μm coalescer element. The time required to change both the prefilter element and coalescer separator elements is less than one hour.

Cleaning and Flushing

Serious mechanical damage to turbomachinery can result from operation with dirty oil systems. It is essential that an oil system is thoroughly cleaned prior to the initial startup of a new machine, and after each overhaul of an existing machine.

Preliminary steps for the initial startup and startup after the overhaul are similar, except for the reservoir and oil requirements of the machine after an overhaul. For an overhauled machine, the oil is drained and tested for condition. If there is no water or metal change, the oil may be used again.

Inspect the reservoir interior for rust and other deposits. Remove any rust with scrapers and wire brushes, wash down the interior with a detergent solution, and flush with clean water. Dry the interior by blowing the surfaces with dry air and use a vacuum cleaner to remove trapped liquids.

Install all new 5-μm pleated paper elements in the filters. Connect steam piping to the water side of the oil coolers for heating the oil during the flush. Remove the orifice and install jumpers at the bearings, coupling, controls, governor, and other critical parts to prevent damage from debris during the flush. Make provisions for 40-mesh telltale screens at each jumper. The conical-shaped screen is preferred, but a flat screen is acceptable. Adjust all control valves in the full open position to allow maximum flushing flow. The effectiveness of the flush depends to a large extent on high flow velocities through the system to carry the debris into the reservoir and filters. It may be necessary to sectionalize the system to obtain maximum velocities by alternately blocking off branch lines during the flush.

Fill the reservoir with new or clean used oil. Begin the flush without telltale screens by running the pump or pumps to provide the highest possible flow rate. Heat the oil to 160°F (71°C) with steam on the oil cooler. Cycle the temperature between 110°F (43°C) and 160°F (71°C) to thermally exercise the pipe. Tap the piping to dislodge

debris, especially along the horizontal sections. Flush through one complete temperature cycle, shutdown and install the telltale screens, and flush for an additional 30 minutes. Remove screens and check for the amount and type of debris. Repeat the preceding procedure until the screens are clean after two consecutive inspections. Observe the pressure drop across the filters during the consecutive operation. Do not allow the pressure drop to exceed 20 psig (1.4 Bar).

When the system is considered clean, empty the oil reservoir, and clean out all debris by washing with a detergent solution followed by a freshwater rinse. Dry the interior by blowing with dry air, and vacuum any freestanding water. Replace the filter elements. Remove jumpers and replace orifices. Return controls to their normal settings. Refill the oil reservoir with the same oil used in the flush if lab tests indicate it is satisfactory; otherwise, refill with new oil.

Because of the high flow velocities obtained during the flush, the previous procedure will allow the fastest possible cleanup of the oil system. The objective is to carry the debris into the reservoir and filters. The turbulence from the high flows, along with the thermal and mechanical exercising of the piping, are the main factors necessary for a fast and effective system cleanup.

Oil Sampling and Testing

Oils from turbomachinery should be tested periodically to determine their suitability for continued use. Oil sample should be withdrawn from the system and analyzed in the laboratories on-site and off-site. The usual simple tests of the used oil in the past included: (1) viscosity, (2) pH and neutralization number, and (3) precipitation. However, new tests as outlined below are needed now for high-temperature machinery such as gas turbines. The test results will indicate changes from the original specifications and, depending on how extensive these changes are, whether the oil can or cannot be reused in the machines.

Oil Analysis Tests

An important aspect of oil analysis is the ability of testing oil to ensure that its lubricant quality is maintained. Oil analysis must be conducted to meet the different types of applications. There is no single set of oil analysis which can serve all the needs of all the different types of oil-lubricated machines in a plant. Knowledge of what different oil analysis tests can provide is invaluable in determining which set of tests can be used for various different types of equipment.

Oil analysis can provide a warning of imminent breakdown, in a properly designed predictive maintenance program. Another view is that oil analysis is a metric of the overall health of a machine, or the proactive approach. Oil analysis can fulfill both of these roles admirably, if used correctly. “Used correctly” means that the correct tests are chosen for the machine to serve its reliability profile.

It is important to determine the correct series of tests for any machine that depends on the environment where the machine is deployed and applied. There are many tests available, but some are appropriate for a given application. Having an idea about what

the various tests are, what they can accomplish, and taking into account the maintenance philosophy being practiced, a series of tests can easily be drawn up to accomplish the desired results. The method used is of secondary importance to consistency in method in performing the test from sample to sample, and it is the trend that is ultimately most important.

On-site laboratories are available at most large and newer power plants and petrochemical facilities. These laboratories are capable of conducting the following tests:

1. Particle counting tests
2. Water (Crackle) test
3. Viscosity
4. Filter analysis
5. Acid number
6. Patch test

Particle Counting

Online analysis such as a magnetic probe is used in the lubrication tank and is used to determine metal content in the oil. This type of probe gives a count of the ferrous material suspended in the oil. Offline particle counters produces a count, in different size ranges, of particles per milliliter of oil. This type of contamination is mainly from environmental sources though some is from internally generated wear of the machine. With most particle counters differentiating internal and external wear is impossible, but there are new technologies available which are addressing this.

A particle counter produces a number for each of the different size ranges, as shown in Table 15-2. Various different types of machines are used to generate these counts and different reporting structures are used. Table 15-2 probably represents the most common type of report.

Each column, except the last, reports the number of particles bigger than a certain size in microns per milliliter of fluid. A summary of the particle count is presented in the last column. The summary reports an index related to the number of particles in each of the following different size ranges: larger than 4 μm; larger than 6 μm, and larger than 14 μm. Increasing numbers as evaluated on a trend basis indicate the fluid is getting dirtier and decreasing numbers indicate the fluid is becoming cleaner.

There are interferences that can cause anomalies in the results. The interferences depend on the technology being used, but can include water droplets, air bubbles, and heavily discolored oil. If significant differences in particle counts are noticed, the first course of action should be to ensure, as much as possible, that interferences have been

Table 15-2 A Typical Particle Count Analysis of Oil

4	**6**	**10**	**14**	**20**	**50**	**75**	**100**	**4/6/14**
1,752	517	144	55	25	1.3	0.27	0.08	18/16/13

dealt within the testing process and that other significant test results have not changed, such as water contamination.

Particle counters are not inexpensive, but the results they provide are generally seen as being important enough to warrant their inclusion in many on-site oil analysis laboratories.

Water (Crackle) Test

The crackle test is one of the simplest tests that can be performed on an oil sample and is an absolute must for any on-site laboratory. The test addresses the contamination aspect of oil analysis and involves heating the oil up to between the boiling point of oil and water. At this temperature, water in the oil will boil and produce noticeable bubbles. In practice, it involves putting a drop of oil onto a hotplate and watching for water bubbles in the drop. It is accurate to approximately 500 parts per million (ppm), or 0.05% water content.

Interferences are few, but probably the most significant is the presence of contaminants, such as refrigerant gas. The crackle test will suffice for most moisture content determination needs. If it passes the crackle test, moisture levels are acceptable. A failed crackle test should, in most cases, be followed up by a test to determine the exact water content. Various options are available, the most common being the Karl Fischer test.

Viscosity

Viscosity is a fluid's resistance to flow. It is an important indicator of the condition of the oil and can also be negatively affected by contamination. There are various means of carrying out the viscosity test and it can be reported at temperatures of 104°F (40°C) or 212°F (100°C). For most industrial applications a viscosity measurement at 104°F (40°C) is required.

Many on-site laboratory instruments do not carry out the test at 104°F (40°C), but rather perform the test at room temperature and then estimate a 104°F (40°C) measurement.

Filter Analysis

Filter analysis is a visual analysis of solid contaminants removed from the filter. It involves washing out a piece of the filter membrane and depositing the contents onto a filter patch for microscopic analysis. The debris can be separated into magnetic and nonmagnetic components if desired, but unlike analytical ferrography, the particles are not separated according to size. Like ferrography, the test is time-consuming, expensive, and subjective. It provides better resolution of nonmagnetic debris than analytical ferrography. This test should be carried out on filtered systems as an exception test, possibly generated by an out-of-specification elemental analysis, ferrous density, or particle count.

Filter analysis can be successfully performed in an on-site laboratory; however, more advanced diagnoses will probably be available from a commercial laboratory.

Acid Number

The acid number (AN) test measures the acid content of a sample. The AN is an indication of how much the fluid has oxidized or degraded. AN also is used to determine the rate of depletion of the anti-oxidant additive. It is primarily focused on the condition of the oil, although some contaminants can also affect the AN. Units are mg KOH/g oil. An increasing AN indicates increasing oxidation of the oil. Unlike some conditions, like contamination, which can be reversed, a high AN cannot be.

AN can be easily and inexpensively carried out in an on-site laboratory.

Patch Test

Like the crackle test, the patch test is one of the easiest and most inexpensive tests to perform and is a must for an on-site laboratory. The test involves filtering oil through a filter patch and then examining the filtergram through a microscope. This test focuses on the contamination and wear aspects of oil analysis. If desired, the contents of the oil sample can be separated into magnetic and nonmagnetic components and each part examined individually. It is worth attaching a camera to the microscope to record the resulting images on a computer for comparison purposes.

Other tests which require a larger or commercial laboratory to supplement the online tests can be complemented by the following tests:

1. Water (Karl Fischer)
2. Ferrous density
3. Analytical ferrography
4. Fourier transform infrared (FTIR) spectroscopy
5. Elemental analysis

Water (Karl Fischer)

The Karl Fischer method is used to determine the exact water content of an oil sample. It reports results as ppm water. It is most commonly used as an exception test generated by the crackle test, but should absolutely be run as a routine test in situations where water content below 1,000 ppm is important, such as electrical transformers. In most industrial applications Karl Fischer as an exception test from the crackle test should suffice.

Ferrous Density

Ferrous density is a determination of the content of magnetic debris in the oil. As most wear metals are iron-based, this test is, in most cases, a good indicator of the amount of wear debris in the oil. It does not have a particle size bias, as does the elemental analysis test, but generally does not have good sensitivity at very low levels of wear metal contamination. As such, the nature of the test puts it squarely into the realm of predictive maintenance rather than being a proactive maintenance tool.

There are several different instruments for performing the test, ranging from portable to desktop units, and each instrument reports its results differently. Once

again, the particular instrument used to perform the test is of secondary importance compared to the consistency of method from sample to sample.

Analytical Ferrography

Analytical ferrography is the visual analysis of solid contaminants removed from the oil sample. As the name suggests, it is biased toward contaminants of a ferrous nature, that is, wear metal, but some nonmagnetic debris gets trapped as well. The test uses magnetic fields to separate the ferrous debris into different size ranges on a microscope slide, then it is examined under a compound microscope. It is an expensive test to perform and the results are subjective, so this test is usually only performed as an exception test.

On filtered systems, the results of the test may be misleading due to the possibility of abnormal wear particles being filtered out. It can be used on filtered systems and on systems which are filtered by portable filtration units, but preferably a filter analysis should be carried out in such systems.

The high cost of equipment and the complexity of interpretation make it unlikely that analytical ferrography will be found in most on-site laboratories.

Fourier Transform Infrared (FTIR) Spectroscopy

FTIR spectroscopy uses infrared light of varying frequencies to search for the presence or absence of certain compounds in the oil. The scope of the test can range from very simple, or inexpensive, to very complex and expensive, depending on the desired results. FTIR examines both the condition and contamination of the sample.

For most industrial applications the simple tests can give sufficient information. The primary property sought here is oxidation.

FTIR is seldom found in on-site laboratories due to its high costs and moderate complexity of operation. It is worth noting that prices on the spectrometers are decreasing and the feasibility of including one of the devices in an on-site laboratory is increasing. A number of large power plants are using aspect spectrometers to calculate online fuel analysis to determine the heating value of the fuel.

Elemental Analysis

Arguably the most important test in the oil analysis arsenal is elemental analysis and it provides information on all three aspects of oil analysis: the condition of the fluid (levels of some additives), contamination, and machine wear.

The commonly used method is inductively coupled plasma (ICP) spectroscopy, which utilizes light in the visible and ultraviolet ranges. It reports results in ppm of various elements.

The major drawback of this test is the size of the particles it can detect. Particles larger than 5–8 μm in size are not detected by this test. However, in most wear situations, there will be an increase in wear particle sizes across the range, so elemental analysis can still provide excellent results. Knowledge of the metallurgy of the machine is vital in the interpretation of the results. It is also important to employ exception tests when anomalies in the elemental analysis are detected.

Due to the high capital costs and complexity of operation, ICP spectrometers are found in only the most sophisticated on-site laboratories.

Test Profiles

The test profiles can be divided into three categories: screening, predictive, and proactive.

A screening test can be run in a few different applications. It might be used on small and non-critical pieces of equipment where regular full-slate oil analyses are not cost-effective. Screening tests also can be run on any piece of equipment where a problem is suspected. The benefits of a screening test should be its low cost and high-speed turnaround. Because of those reasons, a screening test would be performed at an on-site laboratory. A screening test should be seen as an enhancement to a routine oil analysis test slate rather than a replacement.

The routine oil analyses have been divided into two categories: predictive and proactive. Ideally, one wants to be performing proactive maintenance as much as possible, but there are times when performing predictive maintenance is the correct course of action. Such occasions might include low replacement costs or low criticality of particular pieces of equipment, when more complex maintenance strategies are unwarranted. Proactive maintenance strategies would typically be performed on newer, more expensive equipment and where criticality of operation makes the high reliability desirable.

The predictive and proactive test profiles have two types of tests indicated, routine and exception. Routine tests are performed each and every time the sample is tested. The screening profile has no exception tests indicated – the exception test for a failed screening test is a full routine analysis.

The profiles presented are designed to serve as guidelines only to help with creating a series of test for the most common industrial applications. There are instances when criticality of operation, cost, safety factors, environmental factors, or fluid selection, make changes to the suggested test slates desirable. In all instances the previously mentioned factors need to be taken into account in deciding the final series of tests. Knowledge of what oil analysis can provide in conjunction with the reliability goals is essential when making the final choice.

Gearboxes

Gearboxes, because of their metal-to-metal contact, are very conducive of failures and thus require to be closely monitored by vibration, Chapter 16, and various oil analyses. There is more emphasis on abnormal wear in the predictive series of tests, and more emphasis on contamination and oil condition in the proactive series of tests. As an example, although ferrous density and patch tests are suggested as routine tests in the predictive series of tests, they are only exceptions in the proactive series of tests. It can also be seen that the AN test is included in the proactive series of tests

more to monitor abnormal additive depletion rather than oxidation. Some suggested test profiles for gearboxes are presented in Table 15-3.

Clean Oil Systems

Clean oil systems include machines such as compressors, hydraulics, and circulating systems, such as turbines. As shown in Table 15-4, there is more emphasis placed on contamination in clean oil systems than with gearboxes. Due to the nature of these machines they are generally less tolerant of contamination than gearboxes.

Oil analysis can serve many goals, including failure prediction and overall health monitoring. But it is only able to do its job when the correct series of tests are chosen to

Table 15-3 Gearbox Test Profiles

Item	Test	Screening	Predictive	Proactive
1	Particle Counting			□
2	Water (crackle test)	□	□	□
3	Water (Karl Fischer)			E(2)
4	Viscosity	□	□	□
5	Ferrous Density		□	E(1)
6	Analytical Ferrography		E(5)	E(5, 10)
7	Filter Analysis			
8	Acid Number			□
9	FTIR (oxidation)		□	□
10	Patch Test	□	□	E(1, 5, 11)
11	Elemental Analysis		□	□

R = routine and E = exception (triggering tests in parentheses).

Table 15-4 Clean Oil Systems

Item	Test	Screening	Predictive	Proactive
1	Particle Counting	□	□	□
2	Water (crackle test)	□	□	
3	Water (Karl Fischer)		E(2)	
4	Viscosity	□	□	□
5	Ferrous Density			E(1, 11)
6	Analytical Ferrography			
7	Filter Analysis			E(1, 10, 11)
8	Acid Number		□	□
9	FTIR (oxidation)		□	□
10	Patch Test		E(1)	E(1, 11)
11	Elemental Analysis		□	□

serve the goals. A series of tests chosen must take into consideration both the reliability profile of the machine and have a thorough understanding of the basic tests. Once this has been done the user can confidently select a series of oil analysis tests to accomplish the task.

Coupling Lubrication

Couplings are a very critical part of any turbomachinery. When lubrication fails, bearings fail. Fifty percent of premature bearing failures are due to bad lubrication practices. In addition, bad lubrication practices lead to inefficient lubrication, such as relubricating more frequently than needed, resulting in high grease consumption.

Couplings and their lubricating systems must be carefully designed and proper lubrication must be applied. Storage is very important and care must be taken to ensure that shelf-life is not exceeded and high ambient temperatures must be avoided. High ambient temperatures cause changes in the grease chemical properties, such as excessive oil separation and oxidation, that effect lubrication properties and efficiency.

Operating and ambient temperatures strongly influence grease selection and degradation. While high temperatures promote grease oxidation and base oil loss, low temperatures might stiffen the grease, promoting lubricant starvation. Figure 15-6 (a) shows the failure due to grease starvation, whereas Figure 15-6 (b) shows the failure due to thermal grease degradation after 48 hours of operation.

The grease base oil viscosity is an important parameter. Lubricant film formation might not be sufficient to separate surfaces and metal-to-metal contacts which occur at low speeds (in the boundary lubrication regime). The lubricating film may also become too thick under high speeds and viscous forces, as well as the friction increases (upper end of the hydrodynamic lubrication regime). Grease viscosity can change during operation, especially when base oil is lost due to grease degradation.



(a) (b)

Figure 15-6 Effect on bearings due to grease starvation and degradation.

The most common methods of lubricating gear-type couplings are: (1) grease-packed, (2) oil-filled, or (3) continuous oil flow. The lubricant of a gear coupling must withstand severe service from forces in the coupling which exceed 8,000 g.

The grease-packed and oil-filled couplings offer similar advantages and disadvantages. The main advantage is simplicity of operation. They are also economical, easy to maintain, and the grease type resists the entry of contaminants. In addition, high tooth leading can be accommodated, since lubricants with heavy-bodied oil can be used. Care must be taken to verify the grease suitability, lubrication intervals, and the quantity used. Important properties like consistency changes, oil bleeding properties and contamination should be checked.

For grease-filled couplings, special-quality grease is required to prevent mating teeth wear while operating at high 'g' loads in a sliding load environment. This severe operating condition causes grease separation at high speeds and results in excessive wear. Tests indicate that grease separation is a function of g levels and time. Therefore, grease coupling is not considered suitable for high-speed service, except when approved high-speed coupling grease is used, and then only for up to one year of continuous operation. Presently, new greases on the market do not separate at high speeds and may not deteriorate for three years of continuous operation.

An important requisite for the oil-filled type is that the coupling must have an adequate static oil capacity to provide the required amount of oil to submerge the teeth when the coupling is in operation. The greatest disadvantage of these couplings is the possible loss of lubricants during operation due to defective flange gaskets, loose flange bolts, lubricant plugs, and flaws in the coupling flanges and spacers.

The continuous oil flow method is used primarily in high-speed rotating machinery. This method provides the potential for maximum continuous periods of operation at high operating speeds. The oil flow also provides cooling by carrying away heat generated within the coupling. Another important advantage is maximum reliability, since the oil supply is constant, and the loss of oil from within the coupling is not a problem as it is with oil-filled or grease-packed.

Bibliography

API-614, *Lubrication, Shaft-Sealing and Oil-Control Systems and Auxiliaries*, 5th edition (ISO 10438:2008, Modified), Includes Errata, 2008.

Noordover, Alain. "*Grease Analysis in the Field: Helps to Improve Lubrication*," February 2010.

ExxonMobil Corp., *Outlook for Energy: A View to 2030*, December 2009.

Hinrichs, R., and Kleinbach, M. *Energy: Its Use and the Environment*, Thomsen Brooks/Cole Corp., 2006.

U.S. Department of Energy, "*Compressed Air Tip Sheet #6*," August 2004.

Lubrication Engineers, Inc., ZAP flyer, www.le-inc.com/documents/Zap_Flyer.pdf.

U.S. Department of Energy, "*Energy Efficiency and Renewable Energy*," accessed 1 April, 2010, www.eere.energy.gov/industry/bestpractices/compressed_ air_ma.html.

Clapp, A.M., 1972. "Fundamentals of Lubricating Relating to Operating and Maintenance of Turbomachinery," *Proceedings of the 1st Turbomachinery Symposium*, Texas A&M University.

Fuller, D.D., 1956. *Theory & Practice of Lubrication for Engineers*, Wiley Interscience.

O'Connor, J.J., and Boyd, J., eds, 1968. *Standard Handbook of Lubrication Engineering*, McGraw-Hill Book Co.

Copyrighted Materials
Copyright © 2012 Elsevier Retrieved from www.knovel.com

Part V

Installation, Operation, and Maintenance

15 Lubrication

For reliable turbomachine performance, it is vital to have a properly designed, installed, operated, and maintained lubrication system. The lubrication system of a turbomachine is the "lifeblood" for this complex and finely tuned piece of machinery. The oil must be pumped in continuous circulation, conditioned, drained, and returned to be pumped again. In some units there are independent and dedicated turbine lube oil, compressor lube oil, and turbine control oil systems. There are combined systems with turbine lube oil and control oil from one system and compressor lube oil from another, or with turbine and compressor lube oil from one system and turbine control oil from another. In most cases, one system will supply all lube and control oil.

This chapter deals with the principles involved in the operation and maintenance of a lubrication system, and it describes the main components of such a system, including the lubricant itself. The following topics are discussed:

1. Basic oil system
2. Lubricant selection
3. Oil contamination
4. Filter selection
5. Cleaning and flushing
6. Oil sampling and testing
7. Test profiles
8. Gearboxes
9. Clean oil systems
10. Coupling lubrication

Basic Oil System

API Standard 614 covers in detail the minimum requirements for lubrication systems, oil-type shaft-sealing systems, and control oil supply systems for special-purpose applications.

Lubrication Oil System

A typical lubrication oil system is shown in Figure 15-1. Oil is stored in a reservoir to feed the pumps and is then cooled, filtered, distributed to the end users, and returned to the reservoir. The reservoir can be heated for start-up purposes and is provided with local temperature indication, a high-temperature alarm and high/low-level alarm in the

Gas Turbine Engineering Handbook, Fourth Edition. DOI: 10.1016/B978-0-12-383842-1.00015-9
Copyright © 2012 Elsevier Inc. All rights reserved.

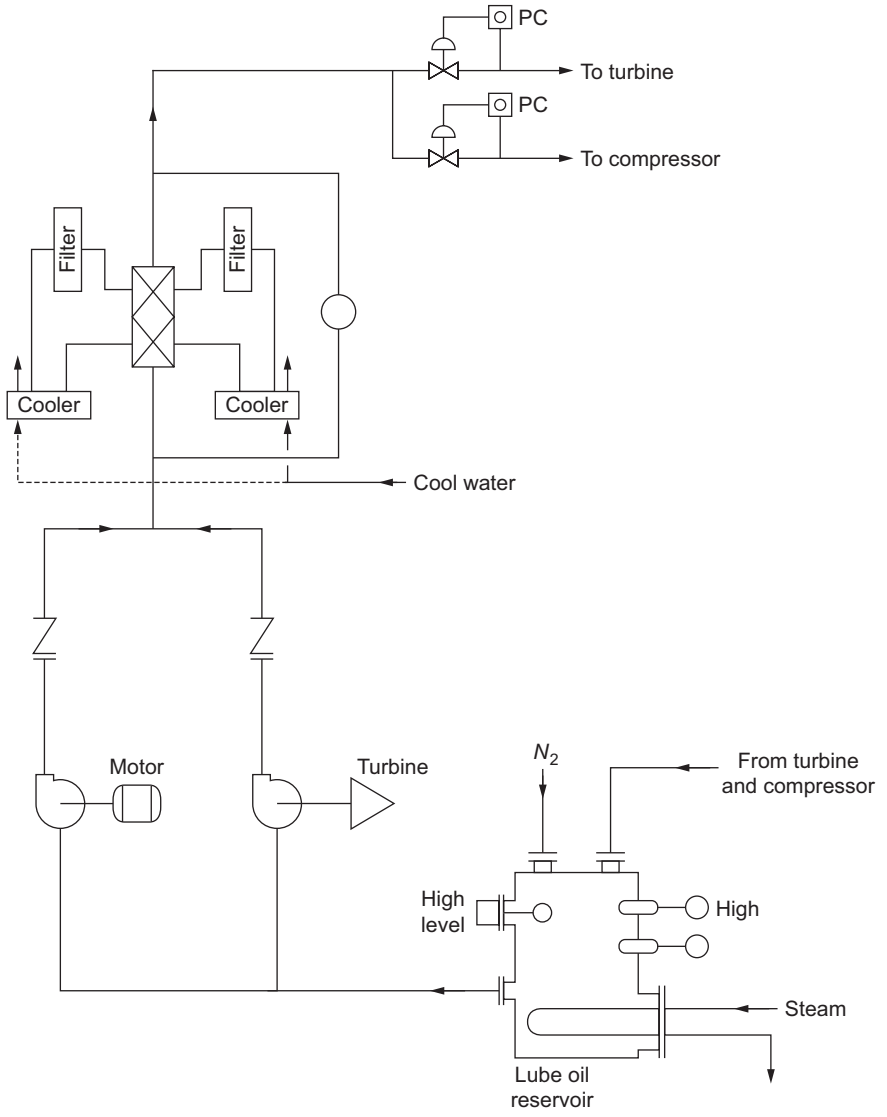


Figure 15-1 A typical lube oil system.

control room, a sight glass, and a controlled dry nitrogen purge blanket to minimize moisture intake.

The reservoir shown in Figure 15-2 should be separate from the equipment base plate and sealed against the entrance of dirt and water. The bottom should be sloped to the low drain point, and the return oil lines should enter the reservoir away from the oil pump suction to avoid disturbances of the pump suction. The working capacity should be at least five minutes based on normal flow. Reservoir retention time should be

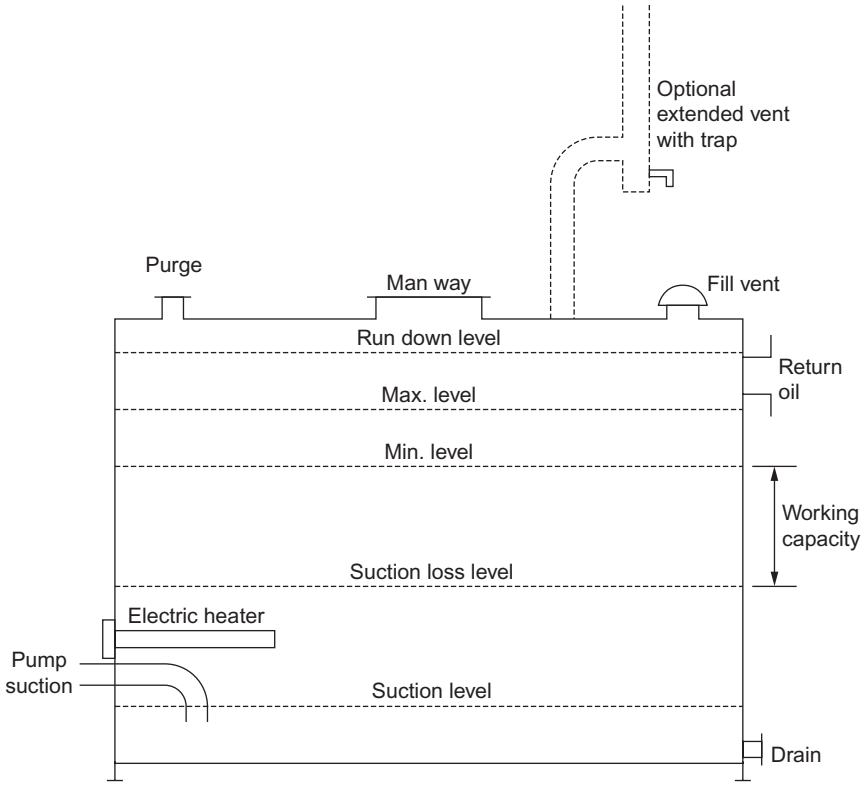


Figure 15-2 Lube oil reservoir.

10 minutes, based on normal flow and total volume below minimum operating level. Heating for the oil should also be provided. If thermostatically controlled electrical emersion heating is provided, the maximum watt density should be 15 watts per square inch (2.33 w/cm^2). When steam heating is used, the heating element should be external to the reservoir.

The rundown level, which is the highest level the oil in the reservoir may reach during system idleness, is computed by considering the oil contained in all components, bearing and seal housings, control elements, and furnished piping that drains back to the reservoir. The rundown capacity should also include a 10% minimum allowance for the interconnecting piping.

The capacity between the minimum and the maximum operating levels in an oil system that discharges seal oil from the unit should be enough for a minimum operation of three days with no oil being added to the reservoir. The free surface should be a minimum of 0.25 sq ft/gpm (0.023 m^2/gpm) of normal flow.

The reservoir interior should be smooth to avoid pockets and provide an unbroken finish for any interior protection. Reservoir wall-to-top junctions may be welded from the outside by utilizing full-penetration welds.

Each reservoir compartment should be provided with two three-quarter-inch minimum size plugged connections above the rundown oil level. These connections may be used for such services as purge gas, makeup, oil supply, and clarifier return. One connection should be strategically located to ensure an effective sweep of purge gas toward the vents.

The oil system should be equipped with a main oil pump, a standby, and, for critical machines, an emergency pump. Each pump must have its own driver, and check valves must be installed on each pump discharge to prevent reverse flow through idle pumps. The pump capacity of the main and standby pumps should be 10–15% greater than maximum system usage. The pumps should be provided with different prime movers.

The main pumps are usually steam turbine driven with an electric motor–driven backup pump. A small mechanical-drive turbine is highly reliable as long as it is running, but it is undependable when starting automatically after long idle periods. A motor is thus the preferred backup pump driver. A "ready-to-run" status light is usually provided for the motor in the control room to give visible evidence that the electrical circuit is viable. Starting the backup pump is initiated by multiple and redundant sources. The turbine drivers should be maintained against failure, by either low-speed or low-steam chest pressure, or both.

Low oil pressure switches are provided on the pumps and discharge header ahead of the coolers and filters, sometimes after the cooler and filters, and always at the end of the line where the reduced oil pressure feeds the various users. A signal from any of these should start the motor-driven pump and all alarms should be activated in the control room. The emergency oil pump can be driven with an AC motor but from a power source that is different to the standby pump. When Dc power is available, DC electric motors can also be used. Process gas or air-driven turbines and quick-start steam turbines are often used to drive the emergency pumps.

The pump capacities for lube and control oil systems should be based upon the particular system's maximum usage (including transients) plus a minimum of 15%. The pump capacity for a seal oil system should be based upon the system's maximum usage plus either 10 gpm or 20%, whichever is greater. Maximum system usage should include allowance for normal wear. Check valves should be provided on each pump discharge to prevent reverse flow through the idle pump.

The pumps can be either centrifugal or positive displacement types. The centrifugal pumps should have a head curve continuously rising toward the shut-off point. The standby pump should be piped into the system in a manner that permits checking of the pump while the main pump is in operation. To achieve this, a restriction orifice is required with a test bleeder valve piped to the return oil line or the reservoir.

Twin oil coolers (Figure 15-3) should be provided and piped in parallel using a single multiport transflow valve to direct the oil flow to the coolers. The water should be on the tube side and the oil on the shell side. The oil-side pressure should be greater than the water-side pressure. This ratio is no assurance that water will not enter the system in the event of a tube leak, but it does reduce the risk. The oil system should be equipped with twin full-flow oil filters located downstream from the oil coolers. Since the filters are located downstream from the oil coolers, only one multiport transflow valve is required to direct the oil flow to the cooler-filter combinations. Do not pipe the

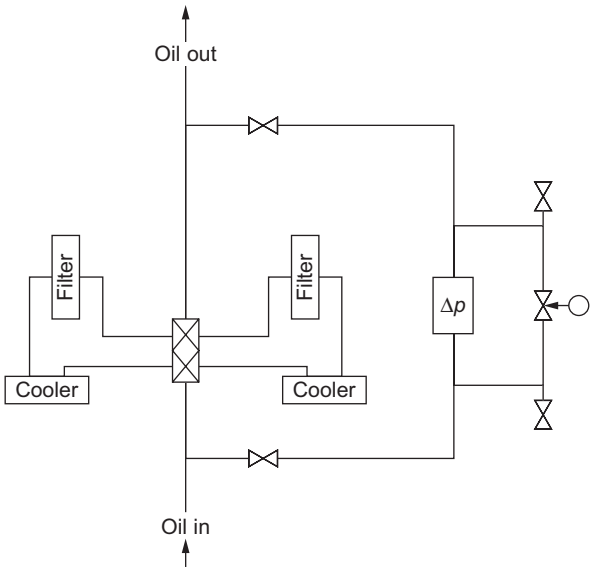


Figure 15-3 Cooler-filter arrangement.

filters and coolers with separate inlet and outlet block valves. Separate block valves can cause loss of oil flow from the possible human error of flow blockage during a filter switching operation.

Filtration should be 10 μm nominal. For hydrocarbon and synthetic oils, the pressure drop for clean filters should not exceed five psi at 100°F (38°C) operating temperature at normal flow. Cartridges will have a minimum collapsing differential pressure of 50 psi (3.447379 Bars).

The system should have an accumulator to maintain sufficient oil pressure while the standby pump accelerates from an idle condition. An accumulator becomes a must if a steam turbine drives the standby pump. Overhead tanks are specified by many users to assure flow to critical machinery components. The sizing of the tanks varies depending on the application. In some gas turbine applications, the bearings reach maximum temperature as long as 20 minutes after shutdown.

The oil coolers and filters are controlled by a local temperature control loop with remote control room indication and high/low alarm. The coolers and filters also have an indicating differential pressure alarm. These usually feed into a common high alarm to pre-warn a need for switching and filter element replacement.

To ensure the required constant pressure, a local pressure control loop is provided on each system – turbine lube oil, compressor lube oil, and control oil. Each oil pressure system should be recorded in the control room to provide trouble-shooting information. The success of the oil system depends upon not only the instrumentation, but upon proper instrument location.

The minimum alarms and trips recommended for each major driver and driven machine should be: a low oil pressure alarm; a low oil pressure trip (at some point

lower than the alarm point), a low oil level alarm (reservoir), a high oil filter differential pressure alarm, a high bearing metal temperature alarm, and a metal chip detector. See Table 15-1.

Each pressure- and temperature-sensing switch should be in a separate housing. The switch type should be single-pole, double-throw, furnished as "open" (de-energized) to alarm and "close" (energize) to trip. The pressure switches for alarms should be installed with a "T"-connection pressure gauge and bleeder valve for testing the alarm.

Thermometers should be mounted in the oil piping to measure the oil at the outlet of each radial and thrust bearing and into and out of the coolers. It is also advisable to measure bearing metal temperatures.

Pressure gauges should be provided at the discharge of the pumps, the bearing header, the control oil line, and the seal oil system. Each atmospheric oil drain line should be equipped with steel nonrestrictive bull's-eye-type flow indicators positioned for viewing through the side. Viewports in oil lines can be very useful in providing a visual check for oil contamination.

In the piping arrangement and layout it is very important to eliminate air pockets and trash collectors. Before starting a new or modified oil system, every foot of the entire system – right up to the final connection at the machine – should be methodically cleaned, flushed, drained, refilled, and all instruments thoroughly checked.

Seal Oil System

The compressor seal oil system is designed and furnished with instrumentation similar to the lube oil system shown in Figure 15-4. The only essential difference is how the end-supply control is handled. Since much higher pressures (1,500–2,500 psi) (103.4214–172.3689 Bars) are often involved, the pumps are usually a positive displacement-type. This requires a pressure control valve spilling oil back to the reservoir. This oil supply is available to an elevated head tank that is provided for each shaft seal. The head tank is pressured by its own process-seal pressure connection, so the seal oil supply system pressure must be maintained at a level to supply the highest pressure seal. The oil rate to each seal is maintained by tank level control from the supply system. The tanks are provided with a high/low-level alarm to the control room. The low alarm warns of excessive oil consumption by the seal and also calls for

Table 15-1 Alarms and Trips

	Alarm	Trip
Low oil pressure	x	x
Low oil level	x	
High oil filter	x	
High thrust bearing metal temperature	x	
High thrust bearing oil temperature	x	
Metal chip detector	x	

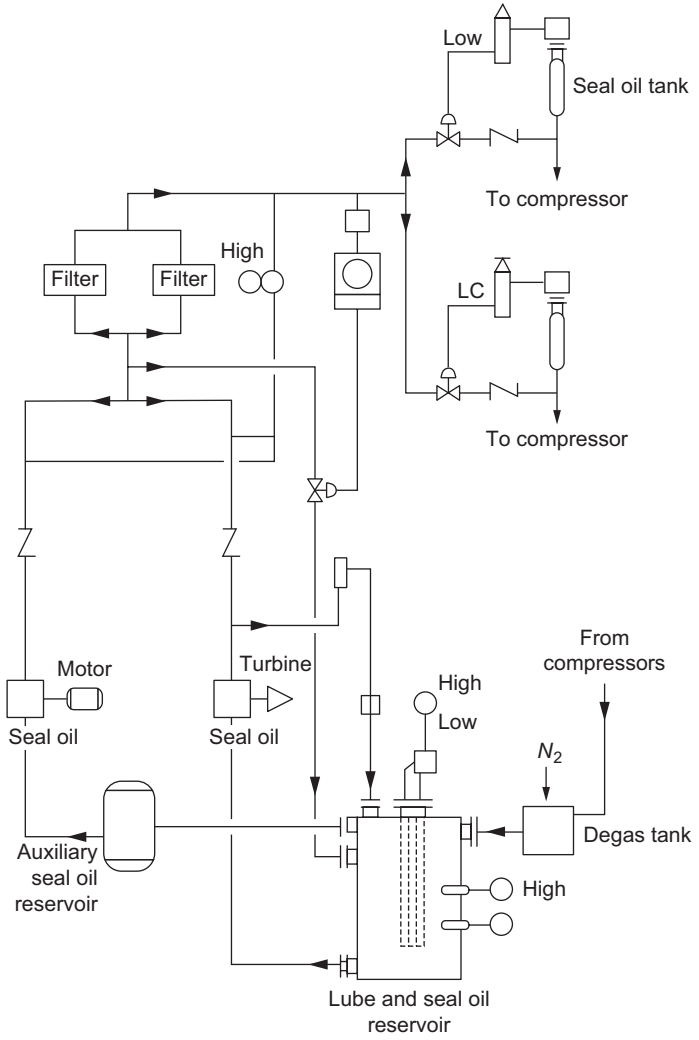


Figure 15-4 Seal oil system.

backup pump start along with the various pressure switches and the high-level alarm warns of primary pump turbine failure in a similar manner to the lube oil system.

A degassing facility is also provided to separate gas contaminants from the seal oil. Figure 15-5 shows a typical degassing drum arrangement. A gas-tight baffle and a liquid seal should divide the degassing drum into two sections to confine the separated gas to one side of the drum. The gas side of the drum should be vented and provided with an inert-gas purge. To assist in degassing the oil, the drum will be heated by electricity or steam.

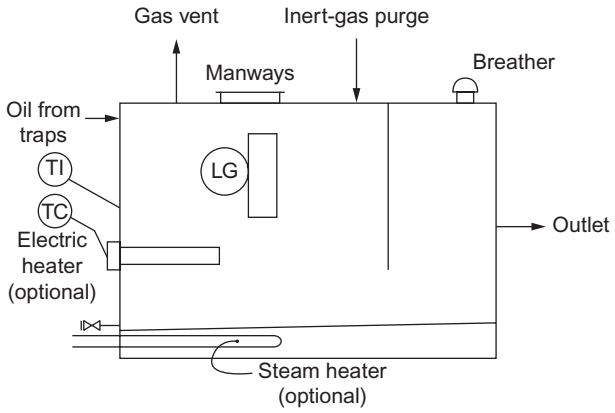


Figure 15-5 Typical degassing drum arrangement.

Lubrication Management Program

A well-planned and managed lubrication program is an important factor in the overall maintenance plan of a plant. A lubrication program includes developing a lubrication period maintenance program, sampling and testing oil, and developing specific procedures to apply lubricants. The initial step in developing a comprehensive plant lubrication program is to conduct a plant survey to determine existing lubrication practices. The survey should utilize machine drawings and external machinery inspections.

A detailed list of lubricant types and their points of application can be compiled from the results of the survey. Combining the list of lubrication types and a current schedule, a master plant lubrication schedule can be published.

A monthly lubrication schedule can then be issued to the appropriate maintenance personnel to serve as a reminder. The issuing of the lubrication schedule does not ensure its compliance and supervisors should check to see that required lubrication is performed.

As a part of the lubrication program, oil should be periodically tested. The testing requires drawing oil from the system for a laboratory analysis. The usual tests conducted to determine the condition of oils include viscosity, pH and neutralization number, precipitation, color and odor, and a check for foreign particles in the oil. The results should be reviewed and compared with new oil characteristics to determine the life characteristics of the oil.

A program for evaluating any new lubrication products can be used to indicate the possible replacement of current lubricants. The general characteristics of new lubricants can be obtained from specifications provided by the suppliers or from testing the lubricant. The final selection of new lubricants should be made only after close observation of the lubricant in several typical plant applications. During the monthly inspections, new lubricants should be checked especially closely to ensure that they are retaining their desired properties. Although, all lubrication applications are important to machinery health, gear couplings present special critical lubrication problems and

require special attention as explained previously. Operating experience has proven that unless a continuous program of required lubrication is followed, even the most well-designed units are sure to fail. A proper lubrication management program must incorporate a monthly lubrication schedule, an evaluation of new lubrication products, and supervision to ensure the prescribed procedures are carried out by maintenance personnel.

In the event of failures due to lubrication problems, the failures should be thoroughly analyzed to determine if they were indeed caused by lubricant failure or incorrect maintenance procedures. Once the problem has been isolated, corrective action can be initiated to prevent subsequent similar failures – whether it requires changing lubricants or procedures.

Lubricant Selection

A good turbomachinery oil must have a rust and oxidation inhibitor, good demulsibility and the correct viscosity, and be both nonsludging and form resistant. Besides lubrication, the oil has to cool bearings and gears, prevent excessive metal-to-metal contact during starts, transmit pressure in control systems, carry away foreign materials, reduce corrosion, and degrade resin. For gas turbines, especially the more advanced high-temperature gas turbines, the oil of choice should be synthetic oil, since synthetic oils have a high flash point. Gas turbine lubrication systems should be run for about 20 minutes after shutdown, since maximum temperatures are reached 10–15 minutes after shutdown, especially in the bearing area. Most gas turbines are also on turning gear to avoid sagging in the shaft. Mineral oils can be used for the compressor. It is not uncommon to have two types of oil in a petrochemical plant, since mineral oil costs much less than the synthetic oil.

The selection of the correct lubricant must begin with the manufacturer. The operator's instruction manual can be referred for the oil required and the recommended viscosity range. The local environmental conditions should be seriously considered, including exposure to outside element conditions, acid gas, or steam leaks. As a general rule, most turbomachines are lubricated with premium-quality turbine-grade oil. However, under certain environmental conditions, it may be advantageous to consider an alternative oil. For example, if a machine is subject to exposure to low concentrations of chlorine or anhydrous hydrochloric acid gases, it may be better to select an oil that will outperform the premium turbine oil. Good results have been recorded using oil containing alkaline additives. Certain automotive or diesel engine oils contain the optimum amount and type of alkaline additives to protect the base oil from reaction with chlorine and HCl. In services where attack on the lubricant by the gas is unknown, laboratory tests are suggested.

Oil Contamination

Oil contamination in a turbomachine is one of the major problems maintenance crews face. However, although contamination is a continuous problem, the levels of contamination are what cause the most concern. The greatest source of contamination

is extraneous matter. Atmospheric dirt, for example, is always a serious threat. It can enter the oil system through vents, breathers, and seals. Its primary effect is equipment wear, but plugging of oil lines and ports, and reduced oxidation stability of the oil are also serious effects. Metal particles from wear, and rust particles from reservoir and oil piping corrosion, can lead to premature equipment failure and oil deterioration. It is important to provide suitable filtering equipment to remove these particles from the system.

Water contamination is a constant threat. The sources of water are many – atmospheric condensation, steam leaks, oil coolers, and reservoir leaks. Rusting of machine parts and the effects of rust particles in the oil system are the major results of water in oil. In addition, water forms an emulsion and, combined with other impurities, such as wear metal and rust particles, acts as a catalyst to promote oil oxidation.

Contamination from process gas can be a serious problem, particularly during startup. Every effort must be exercised to prevent and detect this type of contamination. Most hydrocarbon gases are more soluble in cold oil than in hot oil and may lower the viscosity to a dangerous level. The problems of thrust bearing failures during startup, due to low-viscosity oil, can be eliminated by equipping the reservoir with oil heaters to raise the oil to the normal operating temperatures before starting the machine.

Equipment in HCl and chlorine service must be protected against the exposure of these acid gases to the oil. Obviously, the first line of defense is to eliminate seal failures. However, as a secondary protection, these machines could be lubricated with an alkaline oil. The alkaline additives react to the low concentrations of the acid gases, thus eliminating the addition of these acids to the oil molecule.

Filter Selection

Various types of full-flow filters can be used for the removal of insoluble contaminants. Two general types are usually selected: surface filters and depth filters. Both types of filters are effective for the removal of particulate matter.

Surface filters, if manufactured from the correct material, will not be affected by water in the oil. Water-resistant pleated paper elements have much greater surface areas than the depth-type element and yield a much lower differential pressure when used as replacement elements in filters originally equipped with depth-type elements. Pleated paper elements are available that will remove particle sizes down to a nominal one-half micron.

The depth-type filter elements are used when the oil is free from water, and when particle sizes to be removed are in the 5-μm range and greater. Generally, the depth-type element is water-sensitive, and when oil is contaminated with moisture, this element type will absorb the water and produce a rapid increase in differential pressure across the filter. The desired maximum differential pressure across a filter with clean elements is 5 psig at normal operating temperature.

The filter elements should remove particles of 5 μm, must be water-resistant, have a high flow rate capability with low pressure drop, possess high dirt-retention capacity,

and be rupture-resistant. The clean pressure drop should not exceed 5 psig at 100°F (38°C). The elements must have a minimum collapse differential pressure of 50 psig. Pleated paper elements are preferred – provided they meet these requirements. Usually, the pleated paper element will yield the 5 psig clean drop when used in a filter that was sized to use depth-type elements. This result is due to the greater surface area of the pleated element, more than twice the area of a conventional stacked disc-type or other depth-type elements.

A differential pressure switch is set to alarm when the pressure drop reaches a predetermined point protects against the loss of oil flow. In addition to the differential pressure switch, a two-way, three-port valve with a pressure gauge is piped in parallel with the differential pressure switch for accurate indication of inlet and outlet oil filter pressure. When a single transflow valve is used with a cooler–filter installation, the differential pressure switch and pressure gauge assembly should span the cooler–filter system.

Water contamination in the oil system can cause serious damage to turbomachinery, and every reasonable effort should be made to, first, prevent its entrance into the system, and second, provide suitable removal equipment if water cannot be effectively kept out. Experience indicates that designers and equipment operators can be more effective in keeping water out of the system. Since the main sources of contamination are atmospheric condensation, steam leaks, and faulty oil coolers, preventive measures should be taken.

Condensation will occur in the atmospheric vented oil system whenever the temperature in the vapor space areas drops below the dew point. This effect can take place in the return oil piping as well as the reservoir. Consoles installed in unprotected locations are more vulnerable to climatic changes than those installed inside buildings. Outside locations will be adversely affected by temperature cycles between day and night operations, by showers and sudden temperature drops due to other weather changes, especially in the fall and winter seasons.

There has been great success in "drying up" oil systems by making a few simple alterations. The first step is to check the reservoir unit. The vent should be located in the very top of the reservoir. It should be free of baffles that can collect and return condensate to the reservoir, and the length should be kept as short as possible to provide a minimum of surface areas on which condensate can form. If it is necessary to run the vent up and away from the reservoir, a water trap should be provided as close to the reservoir as possible to remove any condensate formed in the vent stack. The next step is to provide and maintain an inert gas or dry-air purge on the reservoir. Only 2–5 ft^3/h (cfh) (0.057–0.1415 m^3/h (cmh)) is required. The reservoir purge system will not substitute for the elimination of other water sources.

Steam and condensate leaks are the most difficult water sources to prevent in turbomachinery; however, it can be done, and every effort should be made to eliminate these sources. Obviously, the first means of prevention is to maintain the steam packing in perfect condition. Experience has shown that eventually the steam packings will leak, and steam condensate will enter the system through the bearing seals. There has also been great success in "drying up" a wet oil system. The procedure is to purge the bearing labyrinths with inert gas or dry air. One method is to drill a one-eighth-inch

hole through the bearing cap and intersect the labyrinth. A one-quarter-inch diameter tube is connected to the hole in the bearing cap and to a rotometer. The labyrinth is then purged with 15 cfh (0.43 cmh) dry air or inert gas.

Another method is to install an external labyrinth with purge provisions on the bearing housings of a machine that has the necessary space to accommodate the external seal.

Removal of free water from oil systems is usually done with centrifuges or coalescer separators. Centrifuging is the most costly method in both capital outlay and operating cost. The centrifuges usually are the conventional disc-type with manual cleaning. The discs must be cleaned at least once a week with one hour required per cleaning. The coalescer separators usually require much less attention. Some separators only require element changes once a year while others may require changes at six or three months, and in some instances once a month. The frequency appears to be related to the amount of water in the oil system. In many instances, coalescer element changes have been reduced by the use of a prefilter in the system. This element removes the particulates (usually rust) that would restrict the 2-μm coalescer element. The time required to change both the prefilter element and coalescer separator elements is less than one hour.

Cleaning and Flushing

Serious mechanical damage to turbomachinery can result from operation with dirty oil systems. It is essential that an oil system is thoroughly cleaned prior to the initial startup of a new machine, and after each overhaul of an existing machine.

Preliminary steps for the initial startup and startup after the overhaul are similar, except for the reservoir and oil requirements of the machine after an overhaul. For an overhauled machine, the oil is drained and tested for condition. If there is no water or metal change, the oil may be used again.

Inspect the reservoir interior for rust and other deposits. Remove any rust with scrapers and wire brushes, wash down the interior with a detergent solution, and flush with clean water. Dry the interior by blowing the surfaces with dry air and use a vacuum cleaner to remove trapped liquids.

Install all new 5-μm pleated paper elements in the filters. Connect steam piping to the water side of the oil coolers for heating the oil during the flush. Remove the orifice and install jumpers at the bearings, coupling, controls, governor, and other critical parts to prevent damage from debris during the flush. Make provisions for 40-mesh telltale screens at each jumper. The conical-shaped screen is preferred, but a flat screen is acceptable. Adjust all control valves in the full open position to allow maximum flushing flow. The effectiveness of the flush depends to a large extent on high flow velocities through the system to carry the debris into the reservoir and filters. It may be necessary to sectionalize the system to obtain maximum velocities by alternately blocking off branch lines during the flush.

Fill the reservoir with new or clean used oil. Begin the flush without telltale screens by running the pump or pumps to provide the highest possible flow rate. Heat the oil to 160°F (71°C) with steam on the oil cooler. Cycle the temperature between 110°F (43°C) and 160°F (71°C) to thermally exercise the pipe. Tap the piping to dislodge

debris, especially along the horizontal sections. Flush through one complete temperature cycle, shutdown and install the telltale screens, and flush for an additional 30 minutes. Remove screens and check for the amount and type of debris. Repeat the preceding procedure until the screens are clean after two consecutive inspections. Observe the pressure drop across the filters during the consecutive operation. Do not allow the pressure drop to exceed 20 psig (1.4 Bar).

When the system is considered clean, empty the oil reservoir, and clean out all debris by washing with a detergent solution followed by a freshwater rinse. Dry the interior by blowing with dry air, and vacuum any freestanding water. Replace the filter elements. Remove jumpers and replace orifices. Return controls to their normal settings. Refill the oil reservoir with the same oil used in the flush if lab tests indicate it is satisfactory; otherwise, refill with new oil.

Because of the high flow velocities obtained during the flush, the previous procedure will allow the fastest possible cleanup of the oil system. The objective is to carry the debris into the reservoir and filters. The turbulence from the high flows, along with the thermal and mechanical exercising of the piping, are the main factors necessary for a fast and effective system cleanup.

Oil Sampling and Testing

Oils from turbomachinery should be tested periodically to determine their suitability for continued use. Oil sample should be withdrawn from the system and analyzed in the laboratories on-site and off-site. The usual simple tests of the used oil in the past included: (1) viscosity, (2) pH and neutralization number, and (3) precipitation. However, new tests as outlined below are needed now for high-temperature machinery such as gas turbines. The test results will indicate changes from the original specifications and, depending on how extensive these changes are, whether the oil can or cannot be reused in the machines.

Oil Analysis Tests

An important aspect of oil analysis is the ability of testing oil to ensure that its lubricant quality is maintained. Oil analysis must be conducted to meet the different types of applications. There is no single set of oil analysis which can serve all the needs of all the different types of oil-lubricated machines in a plant. Knowledge of what different oil analysis tests can provide is invaluable in determining which set of tests can be used for various different types of equipment.

Oil analysis can provide a warning of imminent breakdown, in a properly designed predictive maintenance program. Another view is that oil analysis is a metric of the overall health of a machine, or the proactive approach. Oil analysis can fulfill both of these roles admirably, if used correctly. “Used correctly” means that the correct tests are chosen for the machine to serve its reliability profile.

It is important to determine the correct series of tests for any machine that depends on the environment where the machine is deployed and applied. There are many tests available, but some are appropriate for a given application. Having an idea about what

the various tests are, what they can accomplish, and taking into account the maintenance philosophy being practiced, a series of tests can easily be drawn up to accomplish the desired results. The method used is of secondary importance to consistency in method in performing the test from sample to sample, and it is the trend that is ultimately most important.

On-site laboratories are available at most large and newer power plants and petrochemical facilities. These laboratories are capable of conducting the following tests:

1. Particle counting tests
2. Water (Crackle) test
3. Viscosity
4. Filter analysis
5. Acid number
6. Patch test

Particle Counting

Online analysis such as a magnetic probe is used in the lubrication tank and is used to determine metal content in the oil. This type of probe gives a count of the ferrous material suspended in the oil. Offline particle counters produces a count, in different size ranges, of particles per milliliter of oil. This type of contamination is mainly from environmental sources though some is from internally generated wear of the machine. With most particle counters differentiating internal and external wear is impossible, but there are new technologies available which are addressing this.

A particle counter produces a number for each of the different size ranges, as shown in Table 15-2. Various different types of machines are used to generate these counts and different reporting structures are used. Table 15-2 probably represents the most common type of report.

Each column, except the last, reports the number of particles bigger than a certain size in microns per milliliter of fluid. A summary of the particle count is presented in the last column. The summary reports an index related to the number of particles in each of the following different size ranges: larger than 4 μm; larger than 6 μm, and larger than 14 μm. Increasing numbers as evaluated on a trend basis indicate the fluid is getting dirtier and decreasing numbers indicate the fluid is becoming cleaner.

There are interferences that can cause anomalies in the results. The interferences depend on the technology being used, but can include water droplets, air bubbles, and heavily discolored oil. If significant differences in particle counts are noticed, the first course of action should be to ensure, as much as possible, that interferences have been

Table 15-2 A Typical Particle Count Analysis of Oil

4	**6**	**10**	**14**	**20**	**50**	**75**	**100**	**4/6/14**
1,752	517	144	55	25	1.3	0.27	0.08	18/16/13

dealt within the testing process and that other significant test results have not changed, such as water contamination.

Particle counters are not inexpensive, but the results they provide are generally seen as being important enough to warrant their inclusion in many on-site oil analysis laboratories.

Water (Crackle) Test

The crackle test is one of the simplest tests that can be performed on an oil sample and is an absolute must for any on-site laboratory. The test addresses the contamination aspect of oil analysis and involves heating the oil up to between the boiling point of oil and water. At this temperature, water in the oil will boil and produce noticeable bubbles. In practice, it involves putting a drop of oil onto a hotplate and watching for water bubbles in the drop. It is accurate to approximately 500 parts per million (ppm), or 0.05% water content.

Interferences are few, but probably the most significant is the presence of contaminants, such as refrigerant gas. The crackle test will suffice for most moisture content determination needs. If it passes the crackle test, moisture levels are acceptable. A failed crackle test should, in most cases, be followed up by a test to determine the exact water content. Various options are available, the most common being the Karl Fischer test.

Viscosity

Viscosity is a fluid's resistance to flow. It is an important indicator of the condition of the oil and can also be negatively affected by contamination. There are various means of carrying out the viscosity test and it can be reported at temperatures of 104°F (40°C) or 212°F (100°C). For most industrial applications a viscosity measurement at 104°F (40°C) is required.

Many on-site laboratory instruments do not carry out the test at 104°F (40°C), but rather perform the test at room temperature and then estimate a 104°F (40°C) measurement.

Filter Analysis

Filter analysis is a visual analysis of solid contaminants removed from the filter. It involves washing out a piece of the filter membrane and depositing the contents onto a filter patch for microscopic analysis. The debris can be separated into magnetic and nonmagnetic components if desired, but unlike analytical ferrography, the particles are not separated according to size. Like ferrography, the test is time-consuming, expensive, and subjective. It provides better resolution of nonmagnetic debris than analytical ferrography. This test should be carried out on filtered systems as an exception test, possibly generated by an out-of-specification elemental analysis, ferrous density, or particle count.

Filter analysis can be successfully performed in an on-site laboratory; however, more advanced diagnoses will probably be available from a commercial laboratory.

Acid Number

The acid number (AN) test measures the acid content of a sample. The AN is an indication of how much the fluid has oxidized or degraded. AN also is used to determine the rate of depletion of the anti-oxidant additive. It is primarily focused on the condition of the oil, although some contaminants can also affect the AN. Units are mg KOH/g oil. An increasing AN indicates increasing oxidation of the oil. Unlike some conditions, like contamination, which can be reversed, a high AN cannot be.

AN can be easily and inexpensively carried out in an on-site laboratory.

Patch Test

Like the crackle test, the patch test is one of the easiest and most inexpensive tests to perform and is a must for an on-site laboratory. The test involves filtering oil through a filter patch and then examining the filtergram through a microscope. This test focuses on the contamination and wear aspects of oil analysis. If desired, the contents of the oil sample can be separated into magnetic and nonmagnetic components and each part examined individually. It is worth attaching a camera to the microscope to record the resulting images on a computer for comparison purposes.

Other tests which require a larger or commercial laboratory to supplement the online tests can be complemented by the following tests:

1. Water (Karl Fischer)
2. Ferrous density
3. Analytical ferrography
4. Fourier transform infrared (FTIR) spectroscopy
5. Elemental analysis

Water (Karl Fischer)

The Karl Fischer method is used to determine the exact water content of an oil sample. It reports results as ppm water. It is most commonly used as an exception test generated by the crackle test, but should absolutely be run as a routine test in situations where water content below 1,000 ppm is important, such as electrical transformers. In most industrial applications Karl Fischer as an exception test from the crackle test should suffice.

Ferrous Density

Ferrous density is a determination of the content of magnetic debris in the oil. As most wear metals are iron-based, this test is, in most cases, a good indicator of the amount of wear debris in the oil. It does not have a particle size bias, as does the elemental analysis test, but generally does not have good sensitivity at very low levels of wear metal contamination. As such, the nature of the test puts it squarely into the realm of predictive maintenance rather than being a proactive maintenance tool.

There are several different instruments for performing the test, ranging from portable to desktop units, and each instrument reports its results differently. Once

again, the particular instrument used to perform the test is of secondary importance compared to the consistency of method from sample to sample.

Analytical Ferrography

Analytical ferrography is the visual analysis of solid contaminants removed from the oil sample. As the name suggests, it is biased toward contaminants of a ferrous nature, that is, wear metal, but some nonmagnetic debris gets trapped as well. The test uses magnetic fields to separate the ferrous debris into different size ranges on a microscope slide, then it is examined under a compound microscope. It is an expensive test to perform and the results are subjective, so this test is usually only performed as an exception test.

On filtered systems, the results of the test may be misleading due to the possibility of abnormal wear particles being filtered out. It can be used on filtered systems and on systems which are filtered by portable filtration units, but preferably a filter analysis should be carried out in such systems.

The high cost of equipment and the complexity of interpretation make it unlikely that analytical ferrography will be found in most on-site laboratories.

Fourier Transform Infrared (FTIR) Spectroscopy

FTIR spectroscopy uses infrared light of varying frequencies to search for the presence or absence of certain compounds in the oil. The scope of the test can range from very simple, or inexpensive, to very complex and expensive, depending on the desired results. FTIR examines both the condition and contamination of the sample.

For most industrial applications the simple tests can give sufficient information. The primary property sought here is oxidation.

FTIR is seldom found in on-site laboratories due to its high costs and moderate complexity of operation. It is worth noting that prices on the spectrometers are decreasing and the feasibility of including one of the devices in an on-site laboratory is increasing. A number of large power plants are using aspect spectrometers to calculate online fuel analysis to determine the heating value of the fuel.

Elemental Analysis

Arguably the most important test in the oil analysis arsenal is elemental analysis and it provides information on all three aspects of oil analysis: the condition of the fluid (levels of some additives), contamination, and machine wear.

The commonly used method is inductively coupled plasma (ICP) spectroscopy, which utilizes light in the visible and ultraviolet ranges. It reports results in ppm of various elements.

The major drawback of this test is the size of the particles it can detect. Particles larger than 5–8 μm in size are not detected by this test. However, in most wear situations, there will be an increase in wear particle sizes across the range, so elemental analysis can still provide excellent results. Knowledge of the metallurgy of the machine is vital in the interpretation of the results. It is also important to employ exception tests when anomalies in the elemental analysis are detected.

Due to the high capital costs and complexity of operation, ICP spectrometers are found in only the most sophisticated on-site laboratories.

Test Profiles

The test profiles can be divided into three categories: screening, predictive, and proactive.

A screening test can be run in a few different applications. It might be used on small and non-critical pieces of equipment where regular full-slate oil analyses are not cost-effective. Screening tests also can be run on any piece of equipment where a problem is suspected. The benefits of a screening test should be its low cost and high-speed turnaround. Because of those reasons, a screening test would be performed at an on-site laboratory. A screening test should be seen as an enhancement to a routine oil analysis test slate rather than a replacement.

The routine oil analyses have been divided into two categories: predictive and proactive. Ideally, one wants to be performing proactive maintenance as much as possible, but there are times when performing predictive maintenance is the correct course of action. Such occasions might include low replacement costs or low criticality of particular pieces of equipment, when more complex maintenance strategies are unwarranted. Proactive maintenance strategies would typically be performed on newer, more expensive equipment and where criticality of operation makes the high reliability desirable.

The predictive and proactive test profiles have two types of tests indicated, routine and exception. Routine tests are performed each and every time the sample is tested. The screening profile has no exception tests indicated – the exception test for a failed screening test is a full routine analysis.

The profiles presented are designed to serve as guidelines only to help with creating a series of test for the most common industrial applications. There are instances when criticality of operation, cost, safety factors, environmental factors, or fluid selection, make changes to the suggested test slates desirable. In all instances the previously mentioned factors need to be taken into account in deciding the final series of tests. Knowledge of what oil analysis can provide in conjunction with the reliability goals is essential when making the final choice.

Gearboxes

Gearboxes, because of their metal-to-metal contact, are very conducive of failures and thus require to be closely monitored by vibration, Chapter 16, and various oil analyses. There is more emphasis on abnormal wear in the predictive series of tests, and more emphasis on contamination and oil condition in the proactive series of tests. As an example, although ferrous density and patch tests are suggested as routine tests in the predictive series of tests, they are only exceptions in the proactive series of tests. It can also be seen that the AN test is included in the proactive series of tests

more to monitor abnormal additive depletion rather than oxidation. Some suggested test profiles for gearboxes are presented in Table 15-3.

Clean Oil Systems

Clean oil systems include machines such as compressors, hydraulics, and circulating systems, such as turbines. As shown in Table 15-4, there is more emphasis placed on contamination in clean oil systems than with gearboxes. Due to the nature of these machines they are generally less tolerant of contamination than gearboxes.

Oil analysis can serve many goals, including failure prediction and overall health monitoring. But it is only able to do its job when the correct series of tests are chosen to

Table 15-3 Gearbox Test Profiles

Item	Test	Screening	Predictive	Proactive
1	Particle Counting			□
2	Water (crackle test)	□	□	□
3	Water (Karl Fischer)			E(2)
4	Viscosity	□	□	□
5	Ferrous Density		□	E(1)
6	Analytical Ferrography		E(5)	E(5, 10)
7	Filter Analysis			
8	Acid Number			□
9	FTIR (oxidation)		□	□
10	Patch Test	□	□	E(1, 5, 11)
11	Elemental Analysis		□	□

R = routine and E = exception (triggering tests in parentheses).

Table 15-4 Clean Oil Systems

Item	Test	Screening	Predictive	Proactive
1	Particle Counting	□	□	□
2	Water (crackle test)	□	□	
3	Water (Karl Fischer)		E(2)	
4	Viscosity	□	□	□
5	Ferrous Density			E(1, 11)
6	Analytical Ferrography			
7	Filter Analysis			E(1, 10, 11)
8	Acid Number		□	□
9	FTIR (oxidation)		□	□
10	Patch Test		E(1)	E(1, 11)
11	Elemental Analysis		□	□

serve the goals. A series of tests chosen must take into consideration both the reliability profile of the machine and have a thorough understanding of the basic tests. Once this has been done the user can confidently select a series of oil analysis tests to accomplish the task.

Coupling Lubrication

Couplings are a very critical part of any turbomachinery. When lubrication fails, bearings fail. Fifty percent of premature bearing failures are due to bad lubrication practices. In addition, bad lubrication practices lead to inefficient lubrication, such as relubricating more frequently than needed, resulting in high grease consumption.

Couplings and their lubricating systems must be carefully designed and proper lubrication must be applied. Storage is very important and care must be taken to ensure that shelf-life is not exceeded and high ambient temperatures must be avoided. High ambient temperatures cause changes in the grease chemical properties, such as excessive oil separation and oxidation, that effect lubrication properties and efficiency.

Operating and ambient temperatures strongly influence grease selection and degradation. While high temperatures promote grease oxidation and base oil loss, low temperatures might stiffen the grease, promoting lubricant starvation. Figure 15-6 (a) shows the failure due to grease starvation, whereas Figure 15-6 (b) shows the failure due to thermal grease degradation after 48 hours of operation.

The grease base oil viscosity is an important parameter. Lubricant film formation might not be sufficient to separate surfaces and metal-to-metal contacts which occur at low speeds (in the boundary lubrication regime). The lubricating film may also become too thick under high speeds and viscous forces, as well as the friction increases (upper end of the hydrodynamic lubrication regime). Grease viscosity can change during operation, especially when base oil is lost due to grease degradation.



(a) (b)

Figure 15-6 Effect on bearings due to grease starvation and degradation.

The most common methods of lubricating gear-type couplings are: (1) grease-packed, (2) oil-filled, or (3) continuous oil flow. The lubricant of a gear coupling must withstand severe service from forces in the coupling which exceed 8,000 g.

The grease-packed and oil-filled couplings offer similar advantages and disadvantages. The main advantage is simplicity of operation. They are also economical, easy to maintain, and the grease type resists the entry of contaminants. In addition, high tooth leading can be accommodated, since lubricants with heavy-bodied oil can be used. Care must be taken to verify the grease suitability, lubrication intervals, and the quantity used. Important properties like consistency changes, oil bleeding properties and contamination should be checked.

For grease-filled couplings, special-quality grease is required to prevent mating teeth wear while operating at high 'g' loads in a sliding load environment. This severe operating condition causes grease separation at high speeds and results in excessive wear. Tests indicate that grease separation is a function of g levels and time. Therefore, grease coupling is not considered suitable for high-speed service, except when approved high-speed coupling grease is used, and then only for up to one year of continuous operation. Presently, new greases on the market do not separate at high speeds and may not deteriorate for three years of continuous operation.

An important requisite for the oil-filled type is that the coupling must have an adequate static oil capacity to provide the required amount of oil to submerge the teeth when the coupling is in operation. The greatest disadvantage of these couplings is the possible loss of lubricants during operation due to defective flange gaskets, loose flange bolts, lubricant plugs, and flaws in the coupling flanges and spacers.

The continuous oil flow method is used primarily in high-speed rotating machinery. This method provides the potential for maximum continuous periods of operation at high operating speeds. The oil flow also provides cooling by carrying away heat generated within the coupling. Another important advantage is maximum reliability, since the oil supply is constant, and the loss of oil from within the coupling is not a problem as it is with oil-filled or grease-packed.

Bibliography

API-614, *Lubrication, Shaft-Sealing and Oil-Control Systems and Auxiliaries*, 5th edition (ISO 10438:2008, Modified), Includes Errata, 2008.

Noordover, Alain. "*Grease Analysis in the Field: Helps to Improve Lubrication*," February 2010.

ExxonMobil Corp., *Outlook for Energy: A View to 2030*, December 2009.

Hinrichs, R., and Kleinbach, M. *Energy: Its Use and the Environment*, Thomsen Brooks/Cole Corp., 2006.

U.S. Department of Energy, "*Compressed Air Tip Sheet #6*," August 2004.

Lubrication Engineers, Inc., ZAP flyer, www.le-inc.com/documents/Zap_Flyer.pdf.

U.S. Department of Energy, "*Energy Efficiency and Renewable Energy*," accessed 1 April, 2010, www.eere.energy.gov/industry/bestpractices/compressed_ air_ma.html.

Clapp, A.M., 1972. "Fundamentals of Lubricating Relating to Operating and Maintenance of Turbomachinery," *Proceedings of the 1st Turbomachinery Symposium*, Texas A&M University.

Fuller, D.D., 1956. *Theory & Practice of Lubrication for Engineers*, Wiley Interscience.

O'Connor, J.J., and Boyd, J., eds, 1968. *Standard Handbook of Lubrication Engineering*, McGraw-Hill Book Co.

Copyrighted Materials
Copyright © 2012 Elsevier Retrieved from www.knovel.com

16 Spectrum Analysis

A total analysis of high-speed rotating equipment requires a complex blend of performance and vibration data. The trend toward total analysis is growing with the problems of an energy shortage and the need for maximum plant utilization. Performance analysis is essential in the efficient utilization of turbomachinery and, when coupled with vibration analysis, is an unbeatable tool as a total diagnostic system.

The real-time analyzer plays a very important role in presenting vibratory data in a manner that can lend itself to a trending data system. This important role of the spectrum analyzer will be explored in detail in this chapter. Also, the role of the spectrum analyzer will increase with a better understanding of statistical techniques in vibration analysis.

Basically, spectrum analysis transforms a displacement/time chart into an amplitude/frequency chart known as a spectrum. This analysis consists of decomposing a time-varying signal into its component pure tones. Pure tones are sinusoidal wave forms of constant frequency and amplitude. This decomposition is done digitally upon a signal by a minicomputer using Fourier transformation or by filtering the signal.

Signals generated by high-speed machinery are very complex in nature and are generated by several forces with a net effect that masks the pure tones. The random portion of the signal, which is blended with the pure tones, is called noise. The ratio of the total amplitude (area under spectrum) to that of the noise is called the signal-to-noise (S/N) ratio. Sometimes this ratio is expressed in decibels, or db, as follows:

$$\text{S/N ratio in db} = 20\log_{10}\frac{\text{S}}{\text{N}} \tag{16-1}$$

For example:

$$6\,\text{db} = 2$$
$$10\,\text{db} = 3.16$$
$$20\,\text{db} = 10$$
$$40\,\text{db} = 100$$

If the S/N ratio is less than 10 db, it becomes difficult to differentiate the periodic part of the spectrum from noise.

Gas Turbine Engineering Handbook, Fourth Edition. DOI: 10.1016/B978-0-12-383842-1.00016-0
Copyright © 2012 Elsevier Inc. All rights reserved.

Several types of analyzers exist today that allow a time-domain signal to be converted to a frequency-domain spectrum. The resulting spectrum of all spectrum analyzers is equivalent to the amplitude/frequency plot, which is obtained by passing the given signal across a set of constant bandwidth filters and noting the output of each filter at its center frequency.

Unfortunately, such a simple procedure cannot be used because, for adequate resolution each filter can cover only a very narrow frequency band, and because of the cost involved. In the so-called "wave analyzer" or "tracking filter" one filter is utilized by manually incrementing the filter across the time input to determine which frequencies exhibit a large amplitude. In time-compression real-time analyzers (RTA) the filter is swept electronically across the input. The term "real time" as applied here means the instrument takes the time-domain signal and converts it to a frequency domain while the event is actually taking place. In technical terms, real time is viewed when the rate of sampling is equal to or greater than the bandwidth of the filters taking the measurements. RTAs use an analog-to-digital converter and digital circuits to speed up the data signal effectively and improve the sweeping filter scan rate, thus creating an apparent time compression. Both of the previous analyzers are basically analog instruments and, because of the characteristics of analog filtering, may be quite slow at lower frequencies.

The Fourier analyzer is a digital device based on the conversion of time-domain data to a frequency domain by the use of fast Fourier transform analyzers. The fast Fourier transform (FFT) analyzers employ a minicomputer to solve a set of simultaneous equations by matrix methods.

Time domains and frequency domains are related through Fourier series and Fourier transforms. By Fourier analysis, a variable expressed as a function of time may be decomposed into a series of oscillatory functions (each with a characteristic frequency), which, when superpositioned or summed at each time, will equal the original expression of the variable. This process is shown graphically in Figure 16-1. Since each of the oscillatory signals has a characteristic frequency, the frequency domain reflects the amplitude of the oscillatory function at that corresponding frequency.

The breakdown of a given signal into a sum of oscillatory functions is accomplished by the application of Fourier series techniques or by Fourier transforms. For a periodic function $F(t)$ with a period t, a Fourier series may be expressed as:

$$F(t) = \frac{a_0}{2} + \sum_{n=1}^{\infty} (a_n \cos n\omega t + b_n \sin n\omega t) \tag{16-2}$$

Here a and b are amplitudes of the oscillatory functions $\cos(n\omega t)$ and $\sin(n\omega t)$, respectively. The value of ω is related to the characteristic frequency f by:

$$\omega = 2\pi f \tag{16-3}$$

The previous function may also be written in a complex form as:

$$F(t) = \int_{-\infty}^{\infty} G(\omega) e^{i\omega t} d\omega \tag{16-4}$$

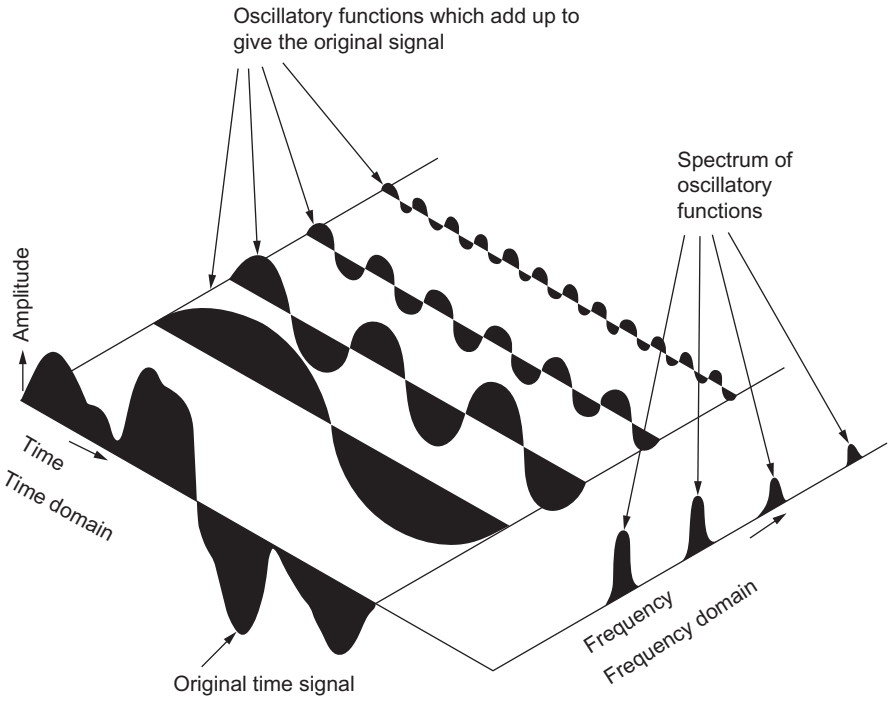


Figure 16-1 Decomposition of a time signal into a sum of oscillatory functions from which a spectrum can be obtained.

where

$$G(\omega) = \frac{1}{2\pi} \int_{-\infty}^{\infty} F(t) e^{-i\omega t} dt \tag{16-5}$$

The function $G(\omega)$ is the exponential Fourier transform of $F(t)$ and is a function of the circular frequency ω. In practice the function $F(t)$ is not given over the entire time domain but is known from time zero to some finite time T, as shown in Figure 16-2. The time span T may be divided into K equal increments of Δt each. For computational reasons, let $K = 2^p$ where p is an integer. Also, let the circular frequency span ω_n be divided into N parts where $N = 2^q$ (in practice, N is often set equal to K). By setting $f = K/NT$, the frequency interval $\Delta\omega$ becomes:

$$\Delta\omega = 2\pi\,\Delta f = \frac{2\pi K}{NT} \tag{16-6}$$

Now, discrete equations analogous to Equations (16-3) and (16-4) may be defined:

$$F(t_k) = \Delta\omega \sum_{n=0}^{N-1} G(\omega_n) e^{i\omega_{n'_k}} \tag{16-7}$$

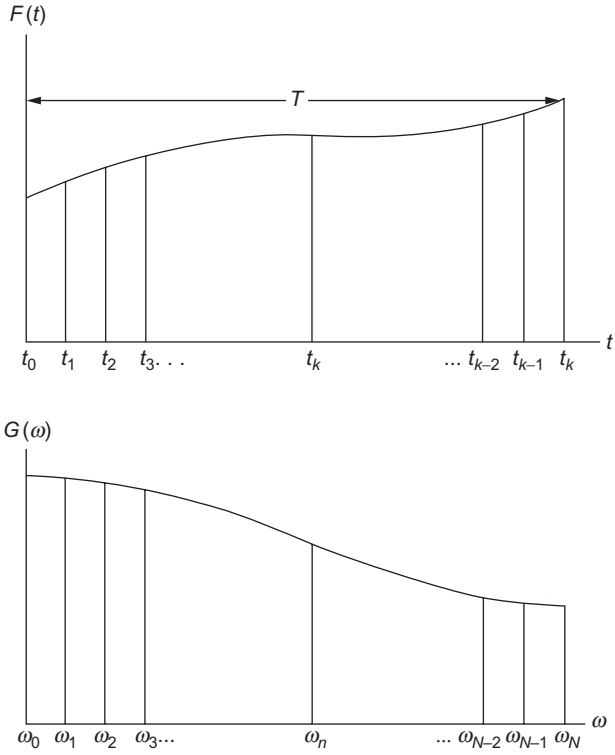


Figure 16-2 Discrete Fourier transform representation.

and

$$G(\omega_n) = \frac{\Delta t}{2\pi} \sum_{k=0}^{k-1} F(t_k) e^{i\omega_{n'_k}} \tag{16-8}$$

where the limits are set at 0 and $N - 1$ for computational reasons.

By using Euler identities, Equations (16-6) and (16-7) can be written:

$$G(\omega_n)_{\text{real}} = \sum_{n=0}^{n-1} F(t_k) \cos(\omega_n t_k) \tag{16-9}$$

$$G(\omega_n)_{\text{imaginary}} = \sum_{n=0}^{n-1} F(t_k) \sin(\omega_n t_k) \tag{16-10}$$

$$F(t_k) = \Delta\omega \sum_{n=0}^{n-1} (G(\omega_n)_{\text{real}} \cos(\omega_n t_k) + G(\omega_n)_{\text{imaginary}} \sin(\omega_n t_k)) \tag{16-11}$$

Comparison of the previous equations with Equations (16-6) and (16-7) reveal that the Fourier transform is really just a Fourier series constructed over a finite interval.

The equations may be rewritten in a simpler form by making the following definitions:

$$\bar{F}_k = F(t_k) \tag{16-12}$$

$$G_n = G(\omega_n) \tag{16-13}$$

$$\omega_n = n\Delta\omega = \frac{2\pi nK}{NT} \tag{16-14}$$

$$t_k = K\Delta t \tag{16-15}$$

so that Equations (16-6) and (16-7) become:

$$\bar{F}_k = \Delta\omega \sum_{n=0}^{n-1} G_n e^{(2\pi i/N)(nk)} \tag{16-16}$$

$$G_n = \frac{T}{2\pi K} \sum_{k=0}^{k-1} \bar{F}_k e^{(-2\pi i/N)(nk)} \tag{16-17}$$

If we further define:

$$F_k = \frac{T}{2\pi K} \bar{F}_k \tag{16-18}$$

and

$$W = e^{-2\pi i/N}$$

we have

$$G_n = \sum_{k=0}^{k-1} F^{nk} \tag{16-19}$$

or in matrix form

$$[G_n] = [W^{(nk)}][F_k] \quad n = 0, 1, 2, \ldots, N-1 \quad k = 0, 1, 2, \ldots, K-1 \tag{16-20}$$

The matrices $[G]$ and $[F]$ are column matrices with row numbers n and k, respectively. The matrix solution is simplified by special properties of the symmetric matrix and because the resulting values of G_n occur in complex conjugate pairs.

In general, we may write:

$$G_n = a_n + ib_n = |G_n|e^{i\alpha}{}_n \tag{16-21}$$

where

$$|G_n| = a^2{}_n + b^2{}_n \tag{16-22}$$

$$\alpha_n = \tan^{-1}(b_n/a_n) \tag{16-23}$$

From the time function $F(t)$ and the calculation of $[W]$, the values of G_n may be found. One way to calculate the G matrix is by a fast Fourier technique called the Cooley-Tukey method. It is based on an expression of the matrix as a product of q square matrices, where q is again related to N by $N = 2^q$. For large N, the number of matrix operations is greatly reduced by this procedure. In recent years, more advanced high-speed processors have been developed to carry out the fast Fourier transform analysis. The calculation method is basically the same for both the discrete Fourier transform and the fast Fourier transform. The difference in the two methods lies in the use of certain relationships to minimize calculation time prior to performing a discrete Fourier transform.

Finding the values of G_n allows the determination of the frequency-domain spectrum. The power-spectrum function, which may be closely approximated by a constant times the square of $G(f)$, is used to determine the amount of power in each frequency spectrum component. The function that results is a positive real quantity and has units of volts squared. From the power spectra, broadband noise may be attenuated so that primary spectral components may be identified. This attenuation is done by a digital process of ensemble averaging, which is a point-by-point average of a squared-spectra set.

Vibration Measurement

Successful measurement of machine vibration requires more than a transducer randomly selected, installed, and a piece of wire to carry the signal to the analyzer. When the decision to monitor vibration is made, three choices of measurement are available: (1) displacement, (2) velocity, and (3) acceleration. These three measurement types emphasize different parts of the spectrum. To understand this peculiarity, it is necessary to consider the different characteristics of each type. Consider a simple harmonic vibration. The displacement, x, is given by:

$$x = A\sin\omega t$$

Successive differentiation gives the expressions for velocity ($\dot{x}$) and acceleration ($\ddot{x}$):

$$x = A\sin\omega t$$

$$\dot{x} = A\omega\cos\omega t$$

$$\ddot{x} = -A\omega^2\sin\omega t$$

In actual practice, these are specified:

$$\text{Displacement: peak-to-peak measure} = 2A$$
$$\text{Velocity: maximum measure} = A\omega$$
$$\text{Acceleration: maximum measure} = A\omega^2$$

It can be observed that displacement is independent of frequency, velocity is proportional to frequency, and acceleration is proportional to the square of the frequency. If the displacement and frequency are known, the velocity and acceleration can be calculated.

To measure any of the signals, a vibration transducer is used. A transducer is a device that translates some aspect of machine vibration into a time-varying voltage output that can be analyzed. The frequency range to be analyzed should be carefully considered before selecting a transducer. It should be kept in mind, however, that there is no one best sensor, and several kinds may be needed to analyze a given machine. Also, in many cases, signal conditioning of the transducer signal may be required prior to analysis.

Displacement Transducers

Eddy-current proximity probes are primarily used as displacement transducers. Eddy probes generate an eddy-current field, which is absorbed by a conducting material at a rate proportional to the distance between the probe and the surface. They are often used to sense shaft motion relative to a bearing (by mounting them within the bearing itself) or to measure thrust motions. They are generally indifferent to hostile environments, including temperatures up to 250 °F (121 °C) and are not expensive. One drawback is that shaft surface conditions and electrical runout can result in false signals. Also, the smallest displacement that can be successfully measured is limited by the S/N ratio of the system. In practice, it is difficult to measure values less than 0.0001 of an inch. If shaft displacement is being measured, the shaft runout (measured with the same pickup) should be less than the smallest measurable value. To achieve the proper shaft runout, it is necessary that the shaft be precision ground, polished, and demagnetized.

Velocity Transducers

Usual types of velocity transducers are made up of an armature mounted in a magnet. The motion of the armature in the magnet creates a voltage output proportional to the velocity of the armature. Usually, the forces being measured must be relatively great to cause a signal output. However, if the signal is quite strong when mounted on the machine bearings, amplification is usually not needed. They are very rugged but are also large and cost roughly 10 times as much as a proximity probe.

Because of damping, transfer function characteristics of the armature-magnet construction generally limit the low-frequency response to approximately 10 Hz. At the high end of the frequency range, the resonant peak of the pickup itself is the limiting

factor. Thus, the useful linear bandwidth is limited. The main advantage of the velocity pickup is that it is a high-output/low-impedance device, and hence, it provides an excellent S/N ratio–even under less than ideal conditions. The major disadvantage of the velocity pickup is its sensitivity to placement. The probe is directional so that if the same force is applied horizontally or vertically, the probe will give different readings.

Acceleration Transducers

Most accelerometers consist of some small mass mounted on a piezo-electric crystal. A voltage is produced when accelerations acting on the mass create a force acting on the crystal. Accelerometers have a wide frequency response and are not excessively costly. They also are temperature resistant. Accelerometers have two main limitations. First, they are extremely low-output/high-impedance devices requiring loading impedances of at least one MΩ. Such requirements rule out the use of long cables. One solution has been to have an amplifier built into the pickup to provide a low-impedance/amplified signal. A power supply is required, and the weight is increased. The second limitation of this pickup is illustrated by an example. Acceleration of one g at 0.5 Hz represents a displacement of 100 inches. It is obvious that in spite of its wide-band response (sometimes 0.1–15 kHz), it is severely limited at the low end by a poor S/N ratio.

The transducer type used should be matched to the machine being analyzed. A knowledge of the types of problems normally encountered will benefit this selection. For instance, the non-contacting shaft displacement probe helps to correct misalignment and balancing problems but is inappropriate in analyzing gear mesh problems and blade passage frequencies. Also, if signal integration or double integration is to be carried out, the lowpass filters used to attenuate high-frequency spectra also have a highpass filter, which effectively creates a lower frequency limit (often as high as five Hz). As mentioned before, one main criterion in deciding which transducer to use is the frequency range to be analyzed. Figure 16-3 shows the frequency limitations placed on the three types of transducers discussed previously.

Dynamic Pressure Transducers

The use of dynamic pressure transducers gives early warning of problems in the compressor. The very high pressure in most advanced gas turbines causes these compressors to have a very narrow operating range between surge and choke. Thus, these units are very susceptible to dirt and blade vane angles. Dynamic pressure transducers are used to obtain a spectrum where the blade and vane passing frequency are monitored. As the compressor approaches surge, the second order of the blade passing frequency ($2 \times$ number of blades $\times$ running speed) approaches the magnitude of the first order of the blade passing frequency. The early warning provided by the use of dynamic pressure measurement at the compressor exit can save major problems encountered due to tip stall and surge phenomenon.

The use of the dynamic pressure transducer in the combustor section, especially in low NO_x combustors, ensures that each combustor can is burning evenly. This is

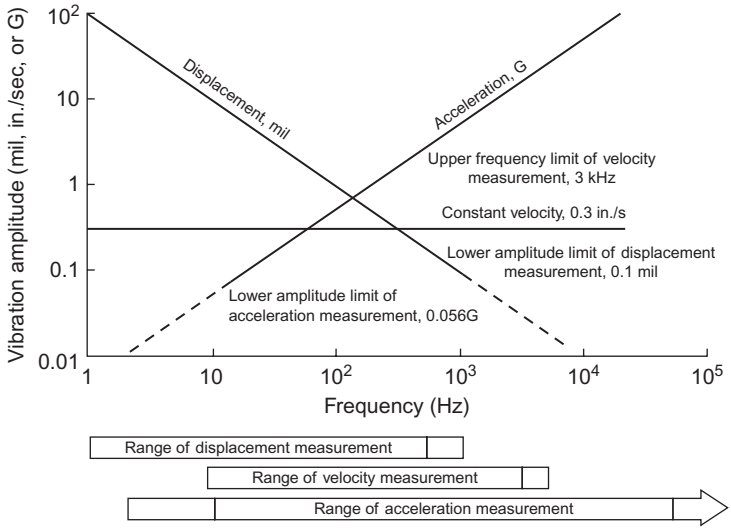


Figure 16-3 Limitations on machinery vibrations analysis systems and transducers.

achieved by controlling the fuel flow to each combustor can till the spectrums obtained from each combustor can are close to being identical. The dynamic pressure transducers when used in this application must be mounted so that the probes are not exposed to the full combustor temperatures. This can be done by the use of buffer gases. This technique has been used and found to be very effective and ensures smooth operation of the turbine.

Taping Data

For many reasons, it may be inconvenient to take the spectrum analyzer to the field each time an analysis is to be made. Often, several machines are to be analyzed at various locations. Also, a hostile environment may exist at the test site, which might result in damage to the analyzer. A way of overcoming these problems is offered by data taping. With a tape, a permanent record is made. Since each channel of the tape offers a place for data to be stored, this record may be a condensation of several inputs either from different transducers or from the same transducer at various locations. A continuous tape monitor is very beneficial. In the event of machine failure, an analysis of the playback will help to diagnose the problem.

The choice of what kind of tape recorder to use is an important decision. AM tape recorders are much less expensive than FM recorders and usually have a voltage saturation limit of 20 or more volts. An FM recorder may be saturated by as little as one volt. A drawback to AM recorders is a rather high roll-off frequency of about 50 Hz (3,000 rpm). Data below the roll-off frequency is attenuated and appears to be lessened in magnitude. An FM recorder has no lower frequency limit; however, it may require

careful signal conditioning (attenuation or amplification) to prevent tape saturation. Usually, if the problems lie at high frequencies, an AM recorder is the best selection. Regardless of the recorder type, a calibration of input signals is recommended using a known oscillating signal and is usually best done by following manufacturer's instructions.

The use of computers has, in many cases, replaced the taping of the data. High speed digital acquisition signals are put directly into the memory for further storing to a hard disk, and then processing through a fast Fourier transform program.

Interpretation of Vibration Spectra

The spectrum analyzer correctly depicts the frequency content of each time-domain instant; however, the time-domain picture as well as its frequency-domain counterpart of a continuous signal, change with time. Averaging is used to show which amplitudes predominate in a continuous signal. For the most part, machinery vibrations result in "stationary" signals. A stationary signal has statistical properties that do not change with time. In other words, the average of a set of time-history records is the same regardless of when that average is taken. A stationary signal is demonstrated by a machine running at constant speed and load. Averages are also used in diagnosing startups and load changes of machinery. In this usage, averages of successive time intervals show the change in vibration levels and frequencies taking place.

Averaging is a technique to improve the S/N ratio. Two or more successive spectra made up of both periodic and random (noise) signals are added together and then averaged. This combination results in a spectrum with a periodic component that is much the same as when viewed in instantaneous signals, but with random peaks of much less amplitude. This result occurs because the period peak stays at a fixed frequency in the spectrum, while the noise peak is fluctuating in frequency over the spectrum.

The fact that averaging removes noise-related signals is demonstrated by the instantaneous and averaged spectra shown in Figure 16-4 (a) taken from the taped signal of a machine being diagnosed. A representation of the normal instantaneous spectra is shown in the second spectrum. An instantaneous signal clearly caused by noise was exhibited at one point in the tape and is shown in the upper spectrum. Note that the contribution of the instantaneous noise signal does not appear in the averaged signal. The large peak on the plots is the running frequency. Lesser harmonics of the running speed also appear. The importance of the instantaneous signal should not be overlooked. During startups, a long-term average may eliminate important parts of the spectra, which change because of the change in rpm. Also, nonperiodic impulses such as those caused by random impulsive loading may be masked by an average. Short averages can be used in "waterfall" graphs to show the growth of certain frequency patterns at run-up as shown in Figure 16-4 (b).

The frequencies of a spectrum can be divided into two parts: sub-harmonic and harmonic (i.e., frequencies below and above the running speed). The sub-harmonic part of the spectrum may contain oil whirl in the journal bearings. Oil whirl is identifiable at about one-half the running speed (as are several components) due to structural

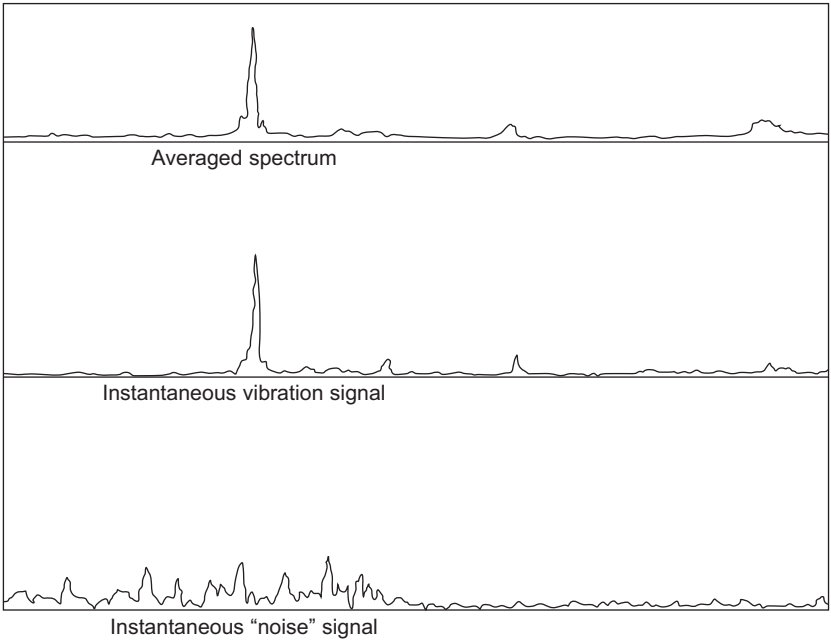


Figure 16-4 (a) Noise attenuation by averaging.

resonances of the machine with the rest of the system in which it is operating and hydrodynamic instabilities in its journal bearings. Almost all sub-harmonic components are independent of the running speed.

The harmonic part of the spectrum may contain multiples of running speed, blade passage frequencies (given by number of blades times the running speed), gear mesh frequencies (given by number of teeth times the running speed), and finally, solid-disc resonant frequencies of the gear discs (independent of the running speed). Roller contact bearings may add another component based on the number of rolling elements present. In addition, a once-per-revolution or first harmonic frequency is caused by mechanical imbalance. Table 16-1 shows more of the major diagnostics. To identify these frequencies with the various machine components, a baseline signature should be obtained.

To be able to do effective trouble-shooting on any particular machine, it is necessary that the baseline signature of the machine be available and thoroughly analyzed. A baseline signature is the spectrum of machine vibration when the machine is operating under "normal conditions." Generally, "normal conditions" are difficult to define and are judgmental in nature. When a machine is first installed, or after it has undergone an overhaul, a vibration spectrum should be taken and stored to serve as a "baseline" for evaluating future spectra. When a baseline signature is determined, it should be carefully evaluated, and every component should be identified as far as possible.

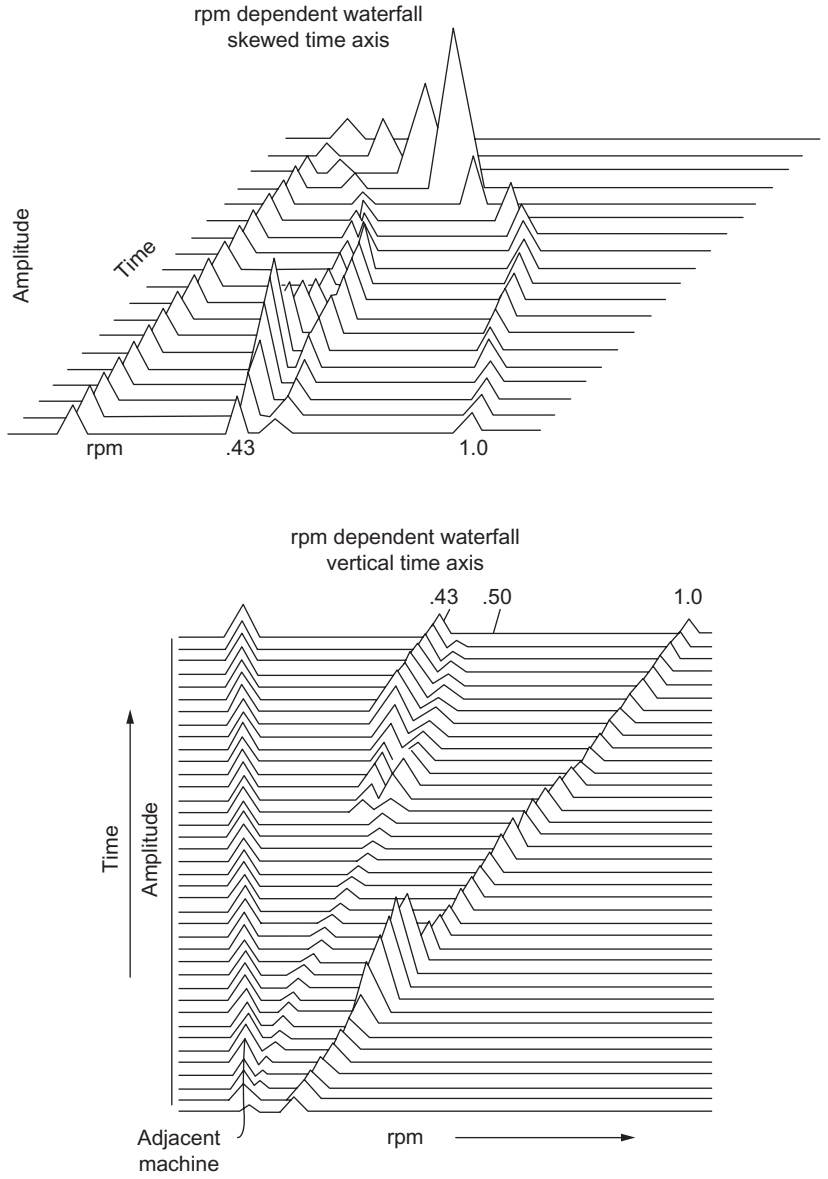


Figure 16-4 (b) Waterfall graph of increasing rpm.

First, and the most important factor to determine, is the primary or fundamental excitation frequency (i.e., frequency of the forcing function). In certain machines more than one excitation corresponds to the running speed of the machine. In split-shaft and multispool machines there is more than one running speed.

Table 16-1 Vibration Diagnosis

Usual Predominant Frequency*	Cause of Vibration
Running frequency at 0–40%	Loose assembly of bearing liner, bearing casing, or casing and support Loose rotor shrink fits Friction-induced whirl thrust bearing damage
Running frequency at 40–50%	Bearing-support excitation Loose assembly of bearing liner, bearing case, or casing and support Oil whirl Resonant whirl Clearance induced vibration
Running frequency	Initial unbalance Rotor bow Lost rotor parts Casing distortion Foundation distortion Misalignment Piping forces Journal & bearing eccentricity Bearing damage Rotor-bearing system critical Coupling critical Structural resonances Thrust bearing damage
Odd frequency	Loose casing and support Pressure pulsations Vibration transmission Gear inaccuracy Valve vibration
Very high frequency	Dry whirl Blade passage

*Occurs in most cases predominantly at this frequency; harmonics may or may not exist.

The relationships in Table 16-1 help to further identify excitations. This information in conjunction with the baseline signature can identify the causes of sudden changes in the spectrum. However, this method runs into difficulty when a new machine is being brought up to speed. No baseline signature is available. Normal operation of the machine is not known. Information about similar machines is of limited value because of the wide variation between different samples of the same machine. This lack of knowledge is the most challenging aspect of machine vibration analysis.

For a new machine, the harmonic part of the spectrum is approximately known in its frequency content due to its relationship with the running speed. The amplitudes at these frequencies are not known. The sub-harmonic part, with a lot of information

unrelated to the running speed, is unknown both in frequency and amplitude content. To predict some characteristics of the sub-harmonic spectrum, transfer-function analysis is employed.

Transfer-function analysis consists of providing an external excitation of a known variable frequency by means of a vibrator. This excitation is applied to the machine while it is stopped. The observed vibration response is a measure of the machine's structural characteristics. It helps in identifying various structural resonance frequencies and thus provides some information about the sub-harmonic spectrum.

During the start-up of a new machine, one should try to identify all the major peaks in the real-time spectrum. If unidentifiable peaks appear, then perhaps the speed should be held constant until a cause for the peak is identified. When a completely new component shows up on the spectrum, a baseline signature is of limited help in pinpointing the cause of such a component. Generally, such an occurrence is a warning of future disaster. If the new component is erratically changing in time, it almost certainly spells trouble. On the other hand, a low-amplitude, a broad-band peak, or a set of peaks that gradually build-up over years of operation may be the result of normal aging or the settling-down process and may be completely harmless. The identification problem area is again a matter of judgment. Some insight can be gained by studying published case histories, but many times, even after a major failure, the cause of the failure cannot be positively identified. To properly utilize spectrum data as an analysis tool, one must use it in conjunction with performance factors.

Performance and vibration monitoring should be properly interfaced to achieve a level of operation free from excessive maintenance and downtime and to maximize operating efficiency at every possible point in the system. Compressor and turbine sections can be analyzed effectively by combining vibration spectra with changes in performance data. Major problem areas in each of these components can be identified with proper monitoring and analysis.

Subsynchronous Vibration Analysis Using RTA

High-speed, flexible-shaft rotor systems, especially those that operate at more than twice the first critical speed, are prone to subsynchronous instabilities. These instabilities can be induced by various elements in the rotor system from fluid-film bearings, bushing and labyrinth seals, to aerodynamic components such as impellers, shrink fits, and shaft hysteresis. With vibration instability, the rotor's provides the energy and source of rotation. In high-speed rotor systems sub-synchronous instabilities are a major cause of catastrophic failures of rotor and bearing systems. The application of high-pressure reinjection in recent years has resulted in a very high incidence of problems and failures due to sub-synchronous vibration. The causes of many of these problems were not identified because the conventional analog-tuned filter vibration analyzer was incapable of analyzing the problem–except when catastrophic levels of sub-synchronous vibrations were reached. At this condition, machine failure was very rapid.

In the early-to-marginal stages of sub-synchronous vibration the phenomenon is highly intermittent, and requires the rapid analysis and high-resolution capability of the real-time analyzer for its identification.

This study shows the analysis and identification of sub-synchronous instability on a high-pressure centrifugal compressor operating at more than the first critical speed of the unit. The test plots given in Figures 16-5 through 16-8 show the vibration spectra. The bearing journal displacement in peak-to-peak mils, on the *Y* axis, is on a logarithmic scale. This scale enables identification of the low levels of sub-synchronous vibrations which occur during the marginal conditions of sub-synchronous instability.

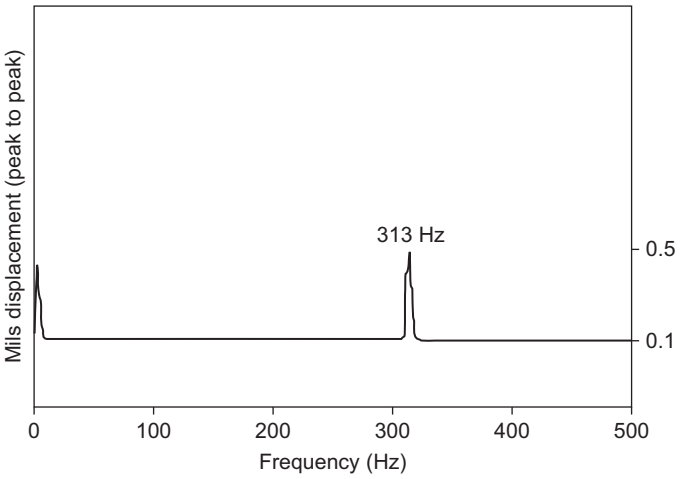


Figure 16-5 Vibration spectrum (rpm = 20,000, p_d = 1,200 psig).

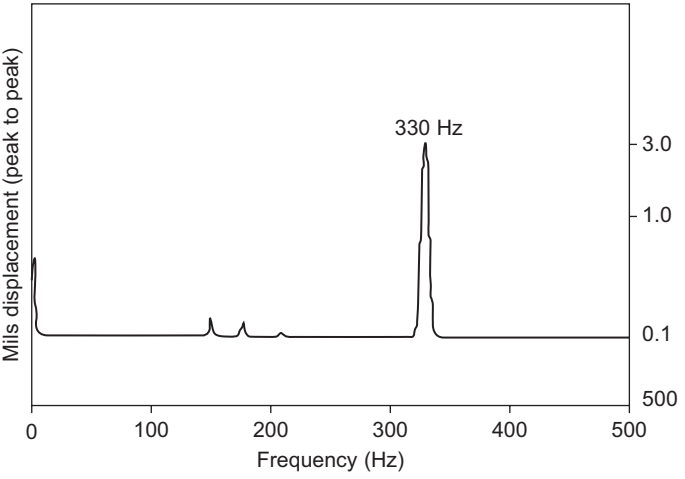


Figure 16-6 Vibration spectrum (rpm = 20,000, p_d = 1,250 psig).

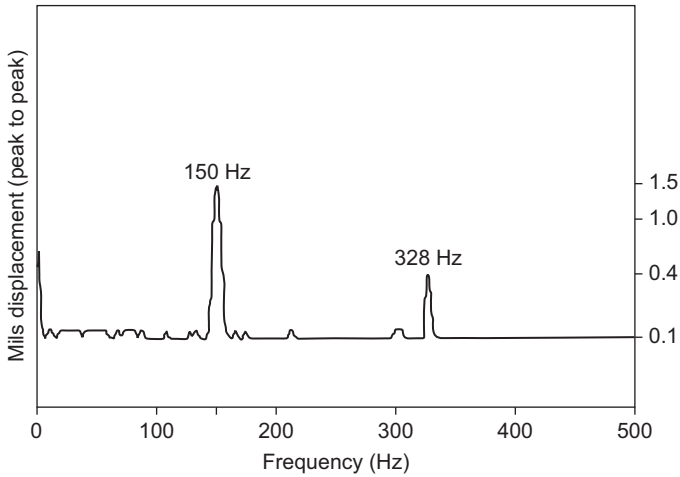


Figure 16-7 Vibration spectrum (rpm = 20,000, p_d = 1,270 psig).

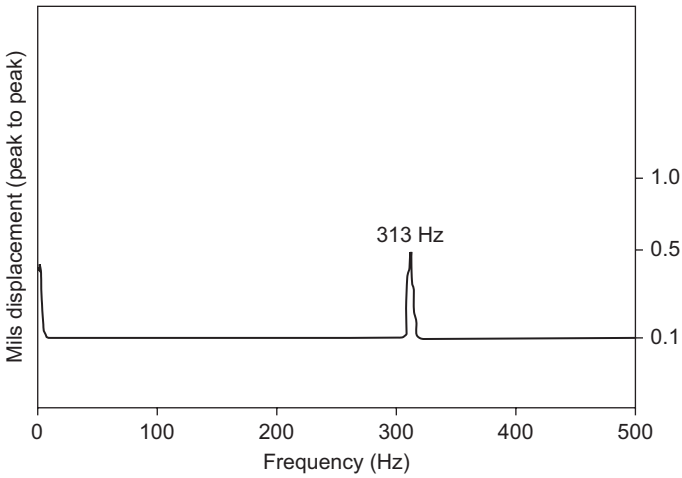


Figure 16-8 Vibration spectrum (rpm = 20,000, p_d = 1,320 psig).

Figure 16-5 shows the vibration spectrum with the machine operating at 20,000 rpm, 500 psig (34.5 Bar) suction pressure, and 1,200 psig (82.7 Bar) discharge pressure. Here a synchronous peak of 0.5 mil (0.0127 mm) at 20,000 rpm, due to rotor system unbalance, is the only component that shows up on the spectrum plot. Figure 16-6 shows the vibration spectrum with the machine operating at 20,000 rpm and suction pressure of 500 psig (34.5 Bar) while the discharge pressure has been raised to 1,250 (86.2 Bar) psig. Observe on the plot the 0.2 mil (0.00508 mm) sub-synchronous component at 9,000 rpm. Using the analyzer in the continuous real-time

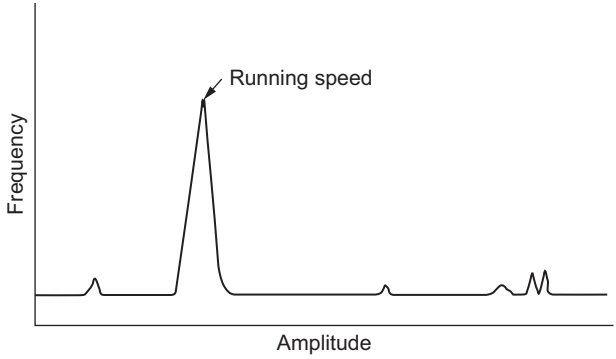


Figure 16-9 A typical unbalance signature plot.

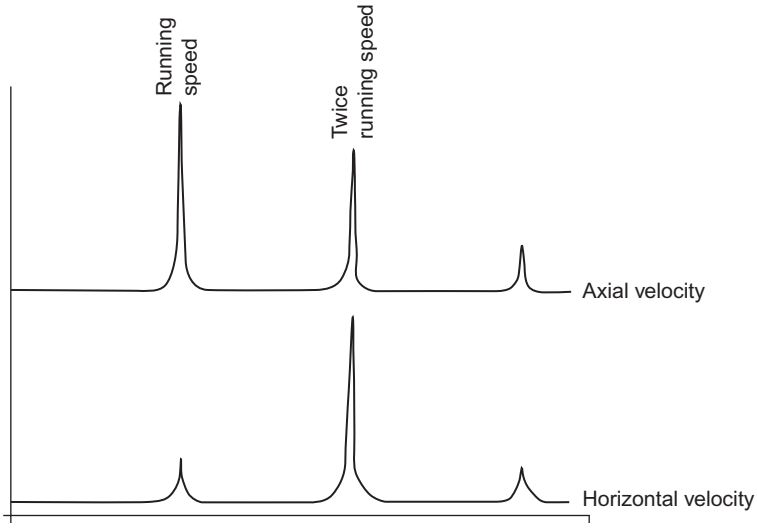


Figure 16-10 A typical misalignment signature plot.

mode, this 9,000 rpm component was very intermittent and was captured by setting the real-time analyzer controls to the "peak hold" mode.

Figure 16-7 shows the vibration spectrum with the speed and suction pressure kept constant but with a small 20 psig increase in discharge pressure. Notice the large increase in the 9,000 rpm component from 0.2 to 1.5 mil (0.0127−0.0381 mm). A further small increase in discharge pressure would have increased the sub-synchronous vibrations to more than 1.0 mil (0.0254 mm) and wrecked the unit.

When the suction pressure was raised by some 50 psig (3.45 Bar) while maintaining the same discharge pressure, the unit regained its stability with the elimination of the sub-synchronous component as shown in Figure 16-8. The sub-synchronous instability

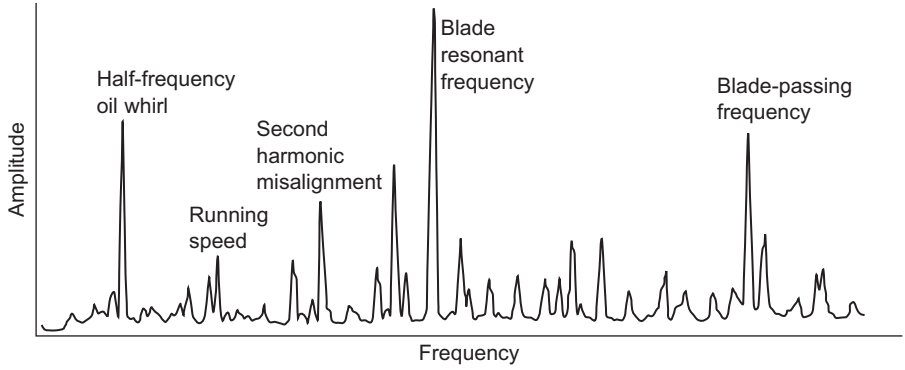


Figure 16-11 Real-time plot for a compressor shows details of critical frequencies.

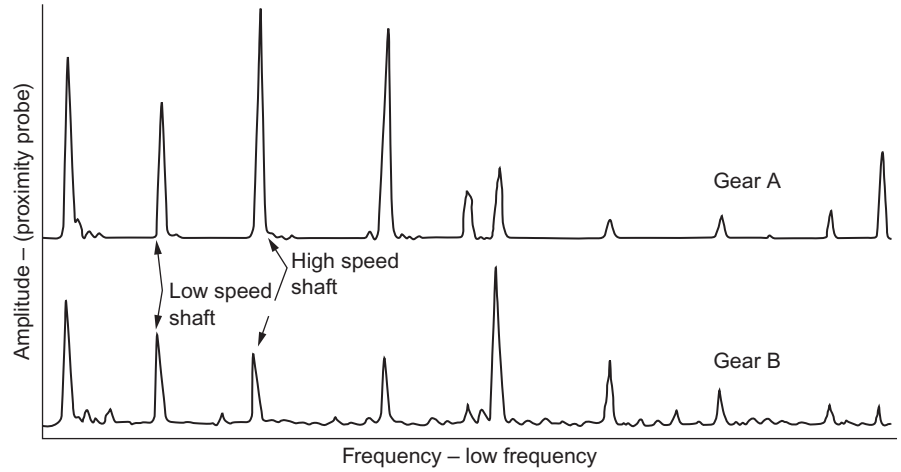


Figure 16-12 Gear box signature (low-frequency end).

in this machine was the result of aerodynamic excitation of the rotor systems occurring at a critical pressure rise across the machine of 770 psi differential (500–1,270 psig).

Synchronous and Harmonic Spectra

The spectrum signature plots at synchronous speeds and high-frequency spectra reveal an interesting set of information. A high running speed amplitude can indicate problems such as unbalance. The spectrum showing this unbalance is in Figure 16-9. Misalignment problems can be also analyzed. Figure 16-10 shows a plot obtained from a casing-mounted pickup and the classical, high twice-per-revolution radial vibration. A high axial vibration also exists that is usually more prominent in diaphragm-type

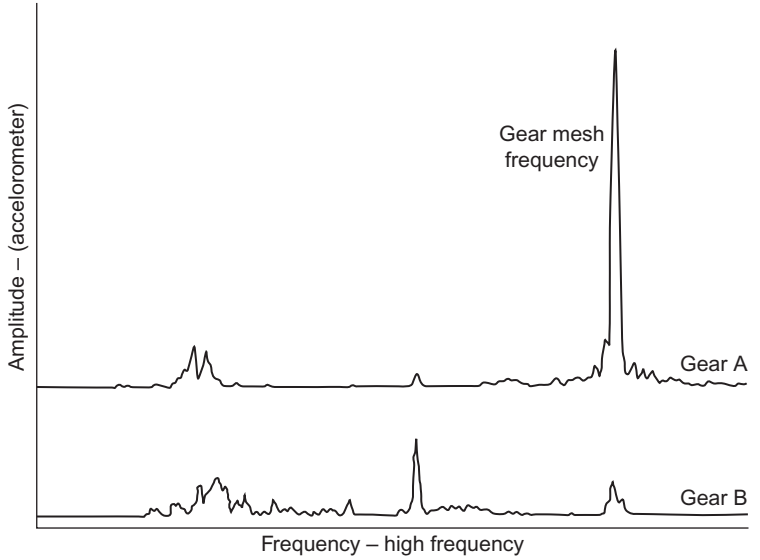


Figure 16-13 Gear box signature (high-frequency end).

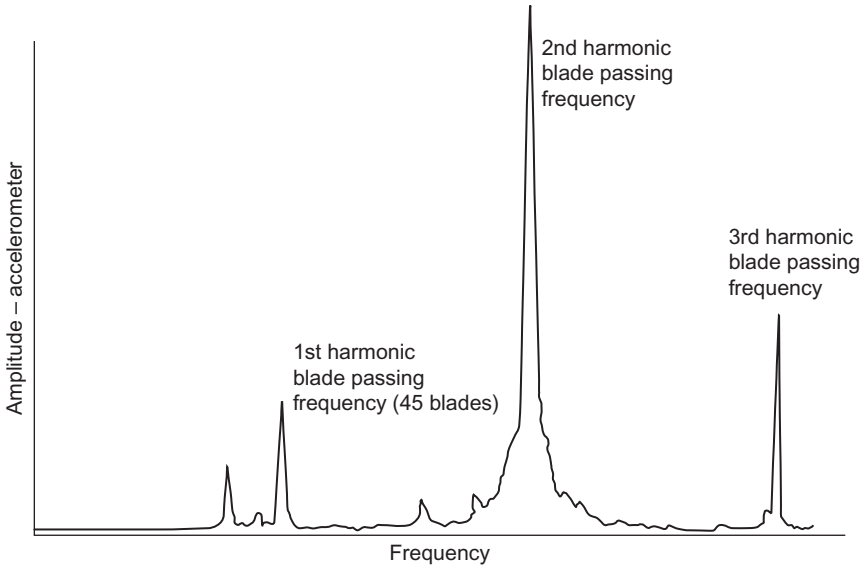


Figure 16-14 Axial-flow compressor spectrum showing blade passing frequency.

couplings. A high-speed machinery plot is shown in Figure 16-11. To determine what the various frequency components represent, a detailed analysis of the machinery components must be known. This information consists of the number of blades in

the impeller, the number of diffusers or nozzle blades, the number of gear teeth, the resonant frequencies of the blades or casing (for antifriction bearings), the number of balls or rollers, and (for tilting-pad hydrodynamic bearings) the number of pads.

The use of accelerometers for diagnosing problems is very effective, since in many cases the high-frequency spectra give much more information than the low-frequency spectra obtained from proximity probes. An example can be seen in Figure 16-12,

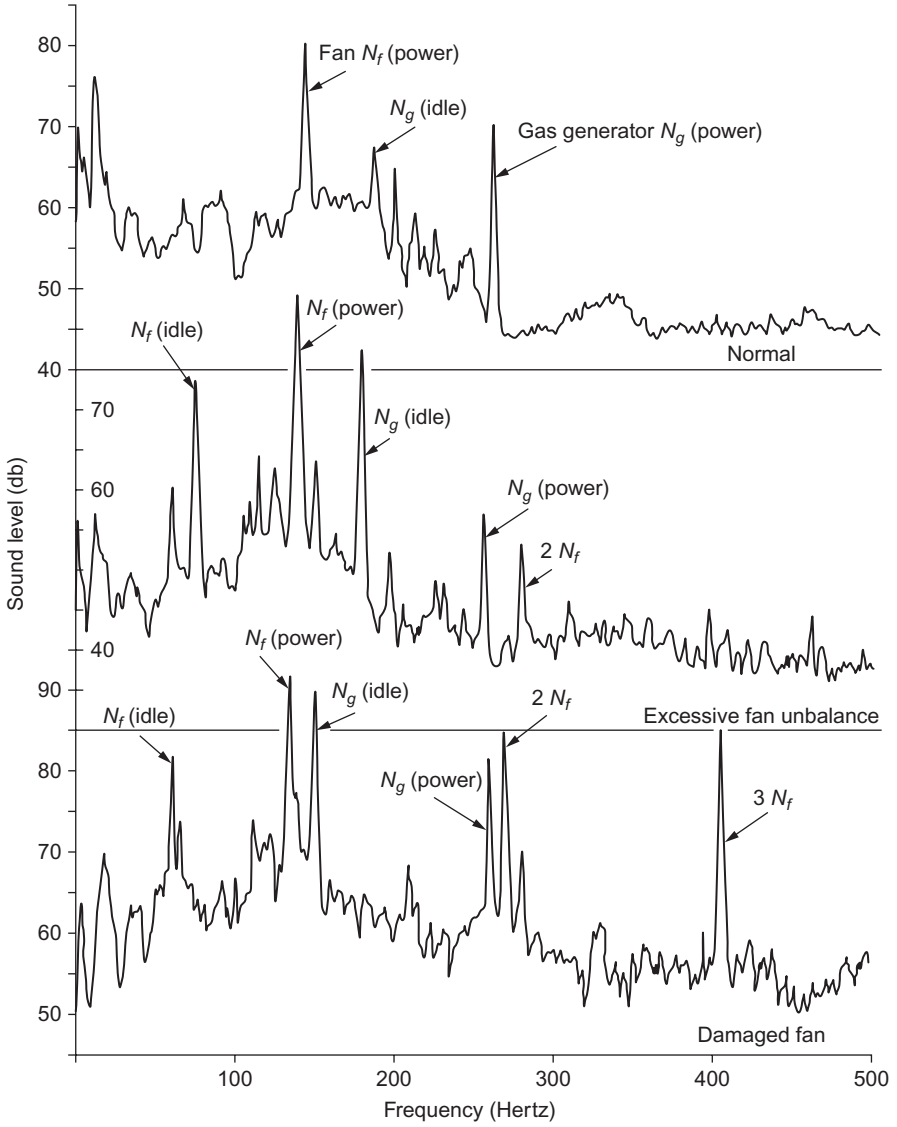


Figure 16-15 Jet engine acoustic signature.

which shows that the two gear drives are in good mechanical condition. Figure 16-13 shows the high-frequency accelerometer signatures. These indicate a problem with gear A (a cracked or chipped tooth).

Accelerometers can also be used to detect problems with stator angles or tip stalls in axial-flow compressors. The analysis from proximity probes indicates that there is a high running-speed vibration, which can be acceptable. An analysis of the accelerometer spectrum (Figure 16-14) shows a strong frequency component of the first, second, and third harmonic of the fifth-stage stator blade. An inspection of the blades indicated cracks caused by low-stress high-cycle fatigue.

Figure 16-15 shows acoustic signatures of three jet engines of the same type installed in three different aircraft. The data were recorded with the aircraft at altitude, one engine at power and the other at flight idle. The top signature is the normal signature for this engine configuration. In the middle signature the once-per-revolution or unbalance components of the fans on both engines are considerably greater than normal, indicating a poor fan balance. On the other hand, the once-per-revolution component of the gas generator at power is less than the norm, indicating better balance. The bottom plot shows a third engine with a fan damaged by ingesting a bird on takeoff. The damaged fan has a large unbalance as shown by the size of the once-per-revolution component. In addition, the second-and third-order fan harmonics are very prominent compared to the other two signatures.

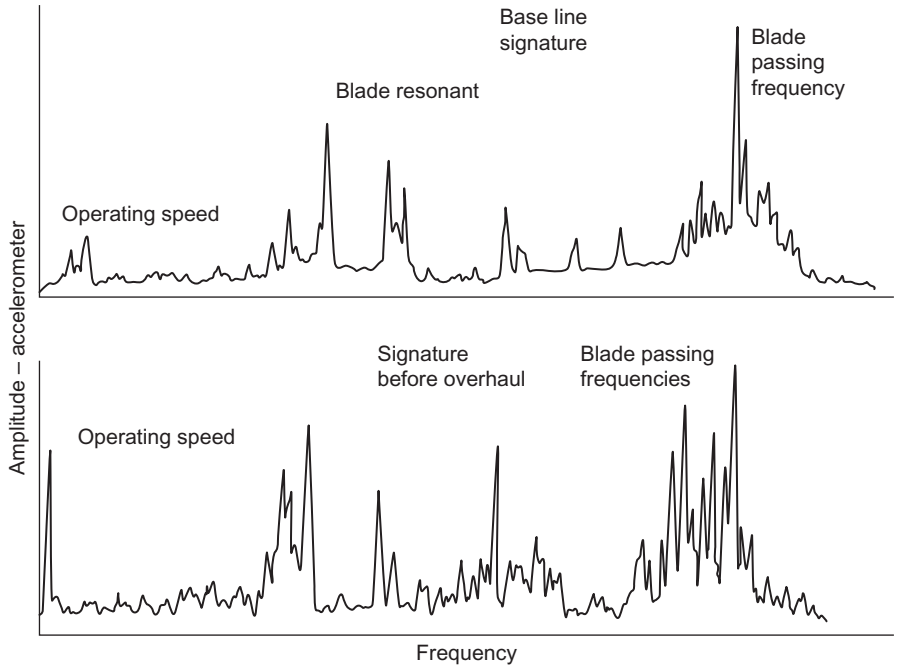


Figure 16-16 Machinery analyses showing comparison of baseline signature to signature before overhaul.

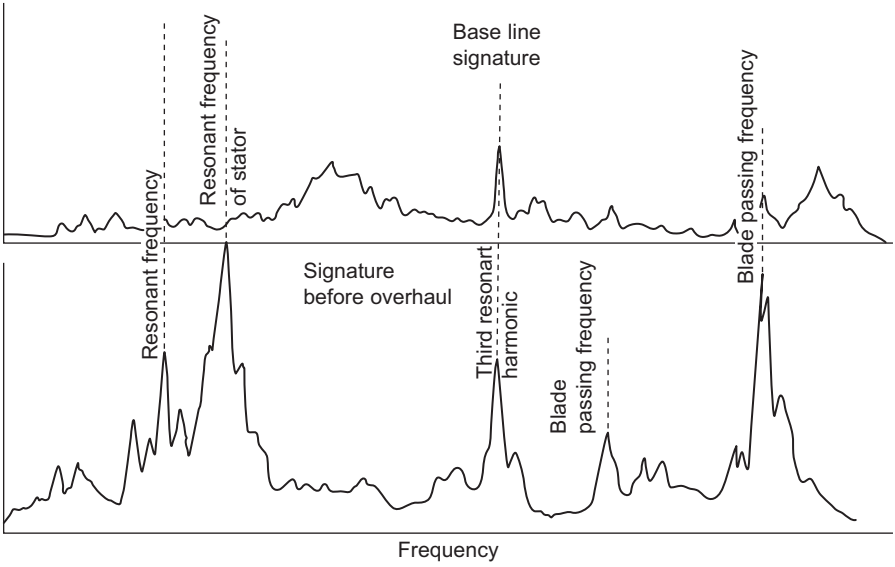


Figure 16-17 Machinery analyses showing the comparison of baseline signature to signature before overhaul.

Obtaining baseline signatures is a very useful tool for detecting deterioration of an engine with time. Figure 16-16 compares the signatures of the machine when installed and after a couple of years of operation. The spectrum shows an increase in level at the high-frequency range, indicating blade flutter problems. Inspection of the unit indicated a number of cracked blades. Another example (Figure 16-17) shows the increase over time of a stator resonant frequency, indicating a high flutter of the blades. Inspection indicated cracks on that stage blade.

Spectrum analysis is a very useful tool in analyzing machinery problems; spectra in both sub-harmonic and high frequencies are needed to evaluate machinery problems fully.

Bibliography

Bickel, H.J., "Calibrated Frequency Domain Measurements Using the Ubiquitous Spectrum Analyzer," *Federal Scientific Monograph* 2, January 1970.

Bickel, H.J., and Rothschild, R.S., "Real-Time Signal Processing in the Frequency Domain," *Federal Scientific Monograph* 3, March 1973.

Borhaug, J.E., and Mitchell, J.S., "Applications of Spectrum Analysis to Onstream Condition Monitoring and Malfunction Diagnosis of Process Machinery," Proceedings of the 1st Turbomachinery Symposium, Texas A&M University, 1972, pp. 150–162.

Boyce, M.P., Morgan, E., and White, G., "Simulation of Rotor Dynamics of High-Speed Rotating Machinery," Proceedings of the First International Conference in Centrifugal Compressor Technology, Madras, India, 1978, pp. 6–32.

Lang, G.F., "The Fourier Transform . . . What It Is and What It Does," *Informal Nicolet Scientific Corporation Monograph*, December 1973.

Lubkin, Y.J., "Lost in the Forest of Noise," *Sound and Vibration Magazine*, November 1968.

Mitchell, H.D., and Lynch, G.A., "Origins of Noise," *Machine Design Magazine*, May 1969.

Copyrighted Materials
Copyright © 2012 Elsevier Retrieved from www.knovel.com

17 Balancing

Vibration problems in present-day turbomachinery are as pressing and important as those encountered in their design, manufacture, and general maintenance. Considerable amounts of precious energy go unused during machinery breakdowns, and the associated costs of machine downtime add to unproductive overheads. The modern trend of building high-speed engines requires new, dependable techniques to reduce vibrations.

Rotor Imbalance

Of the several factors that can cause vibrations in turbomachines, an unbalanced rotor stands at the top of the list. The lack of balance in a rotor may be caused by internal nonhomogeneity and/or external action. The general sources which can cause this problem are classified in the following categories:

1. Dissymmetry
2. Nonhomogeneous material
3. Eccentricity
4. Bearing misalignment
5. Shifting of parts due to plastic deformation of rotor parts
6. Hydraulic or aerodynamic unbalance
7. Thermal gradients

A certain amount of the unbalance from factors such as misalignment, aerodynamic coupling, and thermal gradients may be corrected at running speeds using modern balancing techniques; however, in most cases, they are basic problems that must be initially corrected before any balancing can be done. Rotor mass unbalance from dissymmetry, nonhomogeneous material, distortion, and eccentricity can be corrected so that the rotor can run without exerting undue forces on the bearing housings. In balancing procedures only the synchronous vibrations (vibration in which the frequency is the same as the rotor rotating speed) are considered.

In a real rotor system the amount and location of unbalances cannot always be found. The only way to detect them is with the study of rotor vibration. Through careful operation, the amount and the phase angle of vibration amplitude can be precisely recorded by electronic equipment. The relation between vibration amplitude and its

Gas Turbine Engineering Handbook, Fourth Edition. DOI: 10.1016/B978-0-12-383842-1.00017-2
Copyright © 2012 Elsevier Inc. All rights reserved.

generating force for an uncoupled mass station is:

$$\bar{F}(t) = \bar{F}e^{i\omega t} \tag{17-1}$$

$$\bar{Y}(t) = \bar{A}e^{i(\omega t - \phi)} \tag{17-2}$$

$$\bar{A} = \frac{\bar{F}/K}{1 - \left(\frac{\omega}{\omega_n}\right)^2 + i2\xi\left(\frac{\omega}{\omega_n}\right)} \tag{17-3}$$

$$\phi = \tan^{-1}\frac{2\xi\left(\frac{\omega}{\omega_n}\right)}{1 - \left(\frac{\omega}{\omega_n}\right)^2} \tag{17-4}$$

where

$\bar{Y}(t)$ = vibration amplitude
$\bar{F}$ = generating force
$\bar{A}$ = amplification factor
ϕ = phase lag between force and amplitude

From Equation (17-4), one will find that the phase lag is a function of the relative rotating speed ω/ω_n and the damping factor ξ (see Figure 17-1). The force direction is not the same as the maximum amplitude. Thus, for maximum benefit, the correction weight must be applied in an opposite direction to the force.

The existence of unbalance in a rotor system may be in continuous form or discrete form, as shown in Figure 17-2. Ascertaining an exact distribution is an extremely difficult, if not impossible, task by today's techniques.

For a perfectly balanced rotor, not only should the center of gravity be located at the axis of rotation, but also the inertial axis should coincide with the axis of rotation shown in Figure 17-3. This condition is almost impossible to achieve. Balancing may be defined as a procedure for adjusting the mass distribution of a rotor so that the once-per-revolution vibration motion of the journals or forces on the bearings is reduced or controlled. Balancing functions can be separated into two major areas: (1) determining the amount and location of the unbalance and (2) installing a mass or masses equal to the unbalance to counteract its effects or removing the mass of the unbalance exactly at its location.

Static techniques to determine unbalance can be performed by setting a rotor on a set of frictionless supports; the heavy point of the rotor will have a tendency to roll down. Noting the location of this point, the resultant unbalance force can be found, and the rotor can be statically balanced. Static balancing makes the center of gravity of the rotor approach the centerline of two end supports.

Dynamic balancing can be achieved by rotating the rotor either on its own supports or on an external stand. Unbalance can be detected by studying rotor vibration with

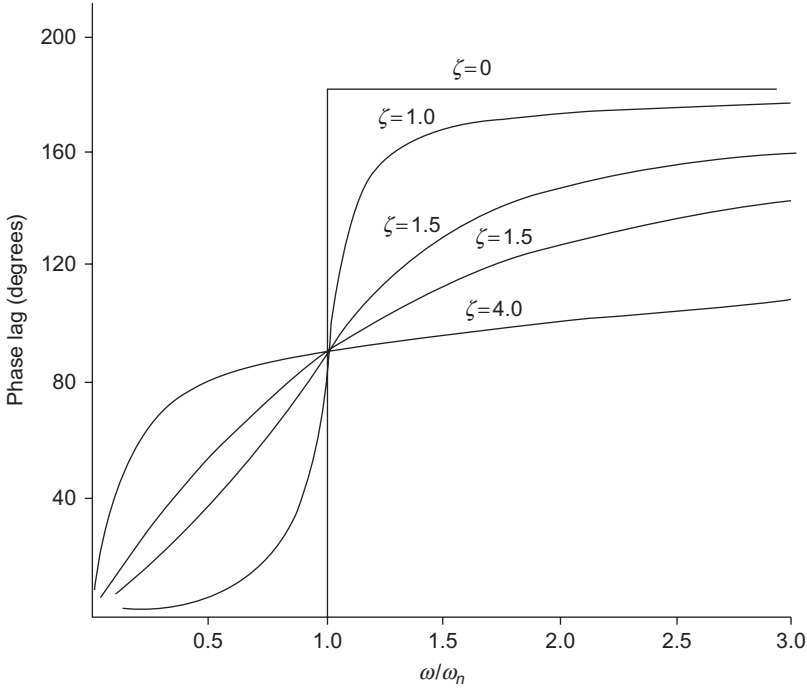


Figure 17-1 Typical phase lag between force and vibration amplitude chart.

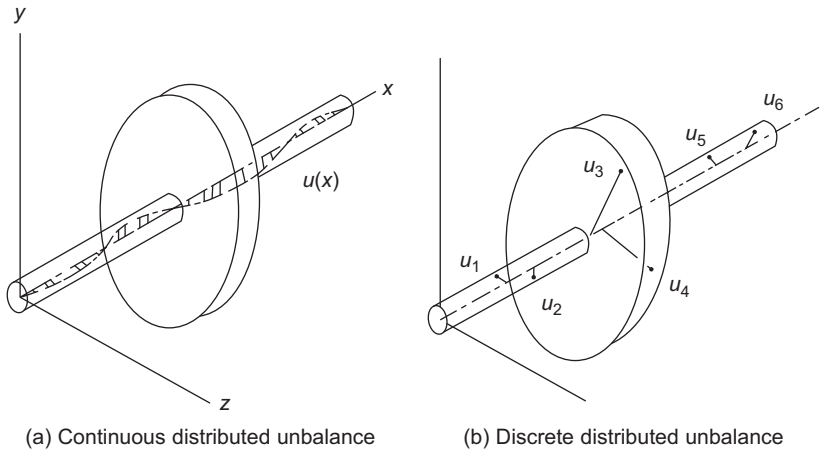


Figure 17-2 Distribution of unbalance in a rotor.

various types of probes or sensors. Balancing is then achieved by placing correction weights in various planes that are perpendicular to the rotor axis. The weights reduce both the unbalanced forces and unbalanced moments. Placing the correction weights in

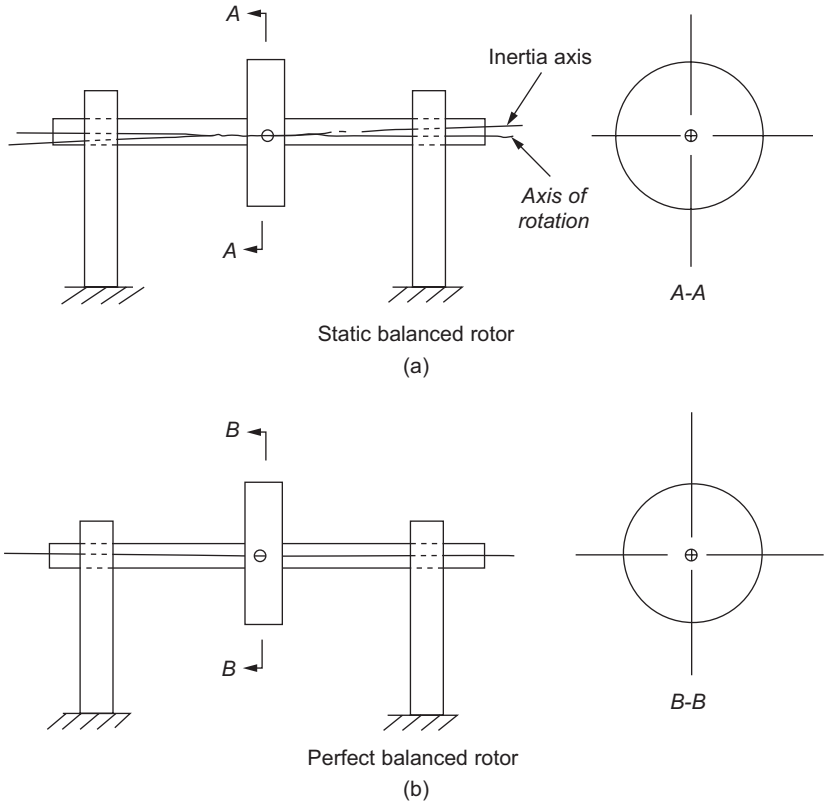


Figure 17-3 Balanced rotor.

as many planes as possible minimizes the bending moments along the shaft introduced by the original unbalance and/or the balance correction weights.

Flexible rotors are designed to operate at speeds above those corresponding to their first natural frequencies of transverse vibrations. The phase relation of the maximum amplitude of vibration experiences a significant shift as the rotor operates above a different critical speed. Hence, the unbalance in a flexible rotor cannot simply be considered in terms of a force and moment when the response of the vibration system is in-line (or in-phase) with the generating force (the unbalance). Consequently, the two-plane dynamic balancing usually applied to a rigid rotor is inadequate to assure the rotor is balanced in its flexible mode.

The best balance technique for high-speed flexible rotors is to balance them, not in low-speed machines, but at their rated speed. This is not always possible in the shop; therefore, it is often done in the field. New facilities are being built that can run a rotor in an evacuated chamber at running speeds in a shop. Figure 17-4 shows the evacuation chamber, and Figure 17-5 shows the control room.

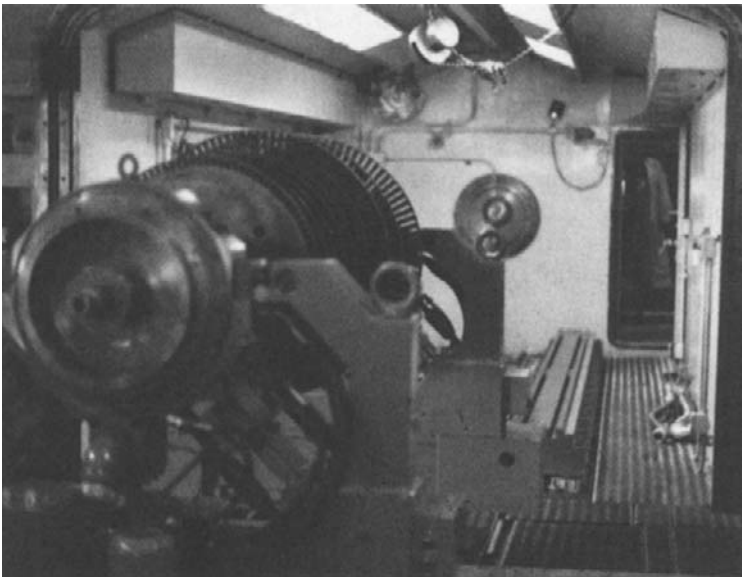


Figure 17-4 Evacuation chamber for a high-speed balancing rig (courtesy of Transamerica Delaval, Inc.).



Figure 17-5 Control room for a high-speed balancing rig (courtesy of Transamerica Delaval, Inc.).

High-speed balancing should be considered for one or more of the following reasons:

1. The actual field rotor operates with characteristic mode shapes significantly different than those that occur during a standard production balance.
2. Flexible rotor balancing must be performed with the rotor whirl configuration approximating the mode in question. The operating speed(s) is in the vicinity of a major flexible mode resonance (damped critical speed). As these two speeds approach one another, a tighter balance tolerance will be required. Those designs that have a low rotor-bearing stiffness ratio or bearings in the vicinity of mode nodal points are of special concern.
3. The predicted rotor response of an anticipated unbalance distribution is significant. This type of analysis may indicate a sensitive rotor which should be balanced at rated speed. It will also indicate which components need to be carefully balanced prior to assembly.
4. The available balance planes are far removed from locations of expected unbalance and are thus relatively ineffective at the operating speed. The rule of balancing is to compensate in the planes of unbalance when possible. A low-speed balance using inappropriate planes has an adverse effect on the high-speed operation of the rotor. In many cases, implementation of an incremental low-speed balance as the rotor is assembled will provide an adequate balance, since compensations are being made in the planes of unbalance. This is particularly effective with designs incorporating solid-rotor construction.
5. A very low-production balance tolerance is needed to meet rigorous vibration specifications. Vibration levels below those associated with a standard production-balanced rotor are often best obtained with a multiple-plane balance at the operating speed(s).
6. The rotors on other similar designs have experienced field vibration problems. Even a well-designed and constructed rotor may experience excessive vibrations from improper or ineffective balancing. This situation can often occur when the rotor has had multiple rebalances over a long service period and thus contains unknown balance distributions. A rotor originally balanced at high speed should not be rebalanced at low speed.

A wealth of technical literature concerning balancing has been published. Various phases of a variety of balancing procedures have been discussed in these papers. Jackson and Bently discuss in detail the orbital techniques. Bishop and Gladwell, as well as Lindsey, discuss the modal method of balancing. Thearle, Legrow, and Goodman discuss early forms of influence coefficient balancing. The author, Tessarzik, and Badgley have presented improved forms of the influence coefficient method that provide for the balancing of flexible rotors over a wide speed range and multiple-bending critical speeds.

Practical applications of the influence coefficient method to multiplane, multispeed balancing are presented by Badgley and the author. The separate problem of choosing balancing planes is discussed at some length by Den, Hartog, Kellenberger, and Miwa for the $(N + 2)$-plane method, and by Bishop and Parkinson in the N-plane method.

Balancing Procedures

There are three basic rotor balancing procedures: (1) orbital balancing, (2) modal balancing, and (3) multiplane balancing. These methods are subject to certain conditions that determine their effectiveness.

Orbital Balancing

This procedure is based on the observation of the orbital movement of the shaft centerline. Three signal pickups are employed, of which two probes measure the vibration amplitudes of the rotor in two mutually perpendicular directions. These two signals trace the orbit of the shaft centerline. The third probe is used to register the once-per-revolution reference point and is called the *keyphazor*. A schematic arrangement of these probes is shown in Figure 17-6.

The three signals are fed into an oscilloscope as vertical-, horizontal-, and external-intensity marker input. The keyphazor appears as a bright spot on the screen. In cases where the orbit obtained is completely circular, the maximum amplitude of vibration occurs in the direction of the keyphazor. To estimate the magnitude of the correction mass, a trial-and-error process is initiated. With the rotor perfectly balanced, the orbit finally shrinks to a point. In the event of an elliptic orbit, a simple geometric construction allows for the establishment of the phase location of the unbalance (force). Through the keyphazor spot, a perpendicular is dropped on the major axis of the ellipse to intersect its circumcircle as shown in Figure 17-7. This intersecting point defines the desired phase angle. Correction mass is found as described earlier. It is important to note that for speeds above the first critical, the keyphazor will appear opposite the heavy point.

In the orbital method, the damping is not taken into account. Therefore, in reality, this method is effective only for very lightly damped systems. Further, as no distinction is made between the deflected mass and the centrifugal unbalance due to its rotation, the balance weights are meaningful only at a particular speed. The optimum balancing plane considered is the plane containing the center of gravity of the rotor system or, alternately, any convenient plane that allows for the orbit to be shrunk to a spot.

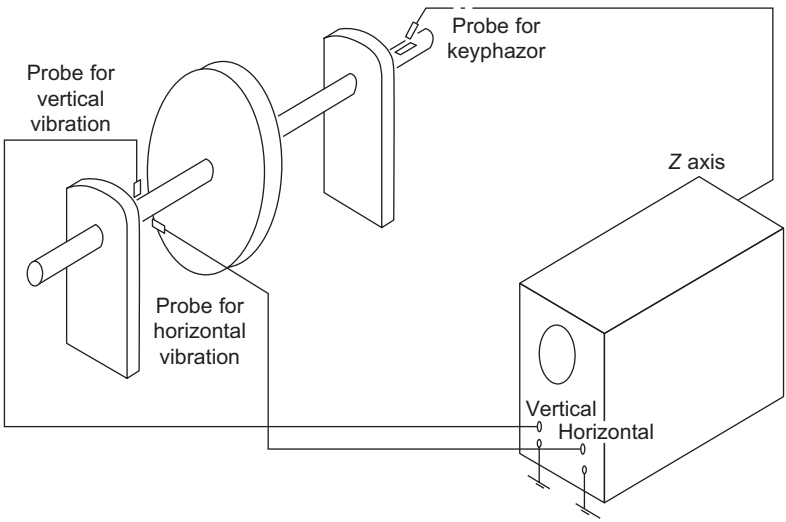


Figure 17-6 Typical arrangement for orbit.

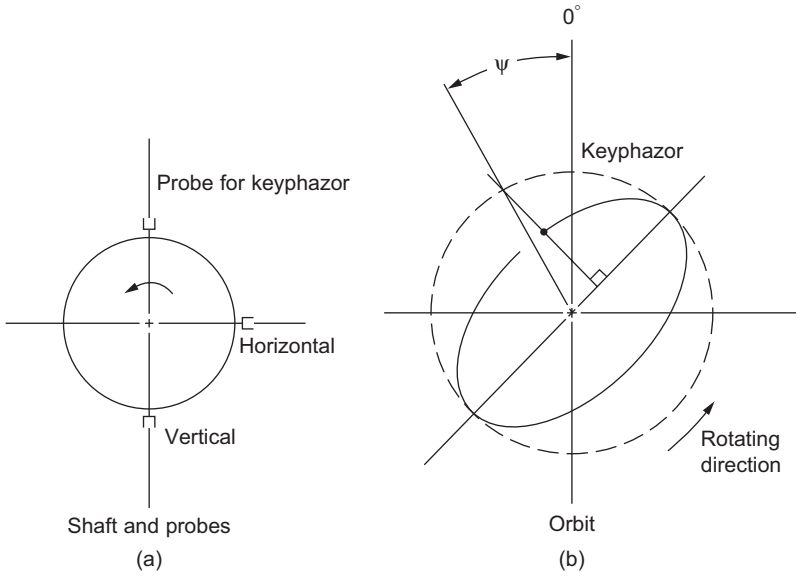


Figure 17-7 Typical probe positions and the phase angle in an elliptic orbit.

Modal Balancing

Modal balancing is based on the fact that a flexible rotor may be balanced by eliminating the effect of the unbalance distribution in a mode-by-mode sequence. Typical principal modes of a symmetric, uniform shaft are shown in Figure 17-8. The deflections of a rotor at any speed may be represented by the sum of various modal deflections multiplied by constants dependent on speed:

$$\bar{Y}(x,\omega) = \sum_{r=1}^{\infty} \bar{B}_r(\omega) \times \eta_r(x) \tag{17-5}$$

where $\bar{Y}(x,\omega)$ represents the amplitude of transverse vibrations, as a function of the distance along the shaft at a rotational speed ω. $\bar{B}_r(\omega)$ and $\eta_r(x)$ express, respectively, the complex coefficient at rotating speed ω and the rth principal mode.

Thus, a rotor, which has been balanced at all critical speeds, is also balanced at any other speed. For end-bearing rotors, the recommended procedure is: (1) balance the shaft as a rigid body, (2) balance for each critical speed in the operating range, and (3) balance out the remaining noncritical modes as far as possible at the running speed. Balance planes picked are the ones wherein the maximum amplitudes of vibration occur.

Modal balancing is one of the proven methods for flexible rotor balancing. Modal balancing has also been applied to problems of dissimilar lateral stiffness, hysteretic whirl, and to complex shaft-bearing problems. In many discussions on modal balancing fluid-film damping is not included. In other instances rolling-element

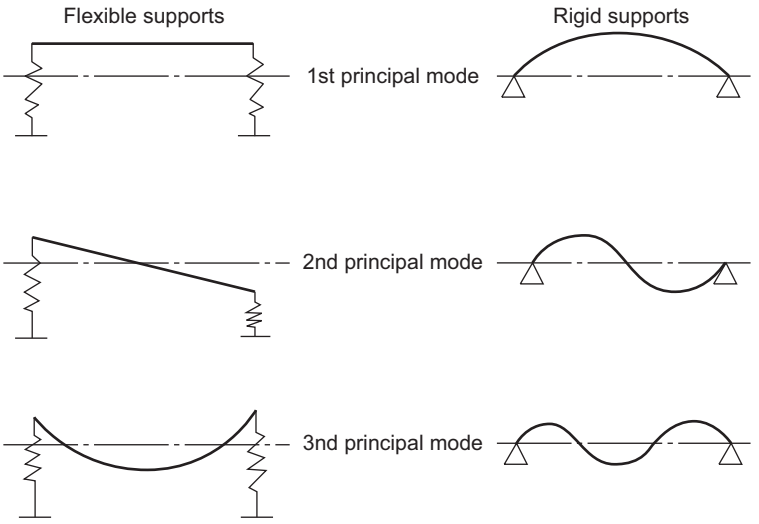


Figure 17-8 Typical principal modes for a symmetric and uniform shaft.

bearing effects are neglected. In such cases, the practical usefulness of the modal method is not fully defined.

Several problems hinder the application of the modal technique to more complex systems. To use the technique, calculated information is required on the mode shapes and natural frequencies of the system to be balanced. The accuracy of the computed results depends on the capabilities of the computer program used and on the input data (dimension, coefficients, system model effectiveness) used in the calculations. In turbomachinery where system damping is significant, as with fluid-film bearings, problems arise. The mode shapes and resonant frequencies of heavily damped systems often bear little resemblance to undamped mode shapes and frequencies. The reliance of modal balancing on predicted modes and frequencies is at least an inconvenience and, without proper response programs, can be a significant disadvantage.

At present, no general-purpose modal balancing computer programs exist that are comparable in nature to the programs developed for the influence coefficient (multiplane) method. Such a program would require calculated modal amplitudes and phase angles, and that the measured amplitudes and phase angles of the rotor bearing system be balanced. The program would then be run for each separate rotor whirl mode, including the full-speed residual balance correction. At present, no general analysis suitable for programming exists.

Multiplane Balancing (Influence Coefficient Method)

Modal balancing came into being to alleviate the problems of the supercritical rotor unbalance of the steam turbine-generator industry. It combined the then available techniques for calculating response amplitudes for the various rotor vibrational modes with the available instruments for measuring actual installed vibration levels. In recent

years, more systems have been designed for supercritical operation. Newer types of sensors and instruments are becoming available, making it feasible to obtain precision in amplitude and phase measurement. Minicomputers for operation on the shop floor or in balancing pits, and time-sharing terminals for in-the-field access to large computers, are now commonly available. The newest multiplane balancing techniques owe their success to advancement in these areas.

The influence coefficient method is simple to apply, and data are now easily obtainable. Consider a rotor with n discs. The method of influence coefficients provides the means for measuring the compliance characteristics of the rotor.

Let $P_1, \ldots, P_j, \ldots, P_n$ be the forces acting on the shaft. Then the deflection Z_i in the i-plane is given by:

$$Z_i = \sum_{j=1}^{n} e_{ij} P_j, i = 1, \ldots, n \tag{17-6}$$

This equation defines the compliance matrix $[e_{ij}]$, and the elements of the matrix are called the influence coefficients. The compliance matrix is obtained by making:

$$P_j = \delta_{ij} \tag{17-7}$$

where δ_{ij} is the Kronecker delta, and measuring the deflections Z_i. As j is varied from 1 to n, each column of the compliance matrix is obtained. Once the compliance matrix is obtained, knowing the initial vibration level in each plane q_i, the system of equations:

$$\sum_{j=1}^{n} e_{ij} F_j = q_1, i = 1, \ldots, n \tag{17-8}$$

is solved for the correction forces, F_j. The correction weights can be computed from the correction forces.

In general, $2N$ sets of amplitude and phase are all that is required by the exact-point speed-balancing method. In balancing with the influence coefficient method: (1) initial unbalance amplitudes and phases are recorded, (2) trial weights are inserted sequentially at selected locations along the rotor, (3) resultant amplitudes and phases are measured at convenient locations, and (4) required corrective weights are computed and added to the system. Balance planes are obviously where the trial weights are inserted. The influence coefficients (or system parameters) can be stored for future trim balance. The method requires no foreknowledge of the system dynamic response characteristics (although such knowledge is helpful in selecting the most effective balance planes, readout locations, and trial weights).

The influence coefficient method examines relative displacements rather than absolute displacements. No assumptions about perfect balancing conditions are made. Its

effectiveness is not influenced by damping, by motions of the locations at which readings are taken, or by initially bent rotors. The least-square technique for data processing is applied to find an optimum set of correction weights for a rotor that has a range of operating speeds.

A number of investigations have concerned themselves with the optimum selections of the number of balancing planes necessary to balance a flexible rotor. To perform an ideal balance on a flexible rotor, as many balancing planes as possible are needed. The perfect balance is either impractical or uneconomical. Two substitute approaches for deciding the number of balancing planes have been proposed.

One is the so-called *N*-plane approach. This approach states that only *N*-planes are necessary for a rotor system running over *N* critical speeds. The other technique, called the $(N+2)$-plane approach, requires two additional planes. These two additional planes are for the two-bearing system and are necessary in this school of balancing.

The *N*-plane is based on the concepts of the modal technique. From Equation (17-5), there are *N* principal modes that need to be zero for the perfect balance of a rotor, which runs through *N*th critical speed. Thus, *N*-planes located at the peaks of the principal modes will be enough for cancelling these modes. From the point of view of residual forces and moments at the support bearings, $(N+2)$-planes are better than *N*-planes.

If one can balance at design speed, that point is ideal, but there may be problems while trying to go through the various criticals. Thus, it is best to balance the unit through the entire operation range. The number of speeds to be selected is also very important. Tests conducted show that when the points were taken at the critical speed and at a point just after the critical speed, the best balance results throughout the operating range were obtained, as seen in Figure 17-9.

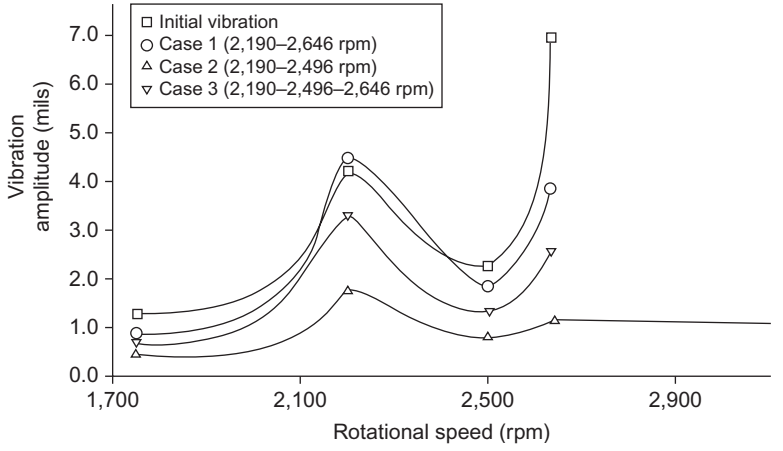


Figure 17-9 Rotor amplitude for least-square balance.

Application of Balancing Techniques

Using the influence coefficient technique for multiplane balancing is simply an extension of the logic, which is "hardwired" into the standard balancing machine. This extension has been made possible by the availability of better electronics and easier access to computers.

Practical balancing may now be performed in any reasonable number of planes at virtually any reasonable number of speeds. The one-plane, low-speed balancing operation is perhaps the simplest application of the method, where a known weight at a known radial location (often in the form of wax added by hand) is used to determine balance sensitivity of the part to be balanced in a spin-up fixture. This procedure can effectively remove an unbalance force from a component. Two-plane balancing is simply an extension to permit unbalance moments as well as forces to be removed. In several instances, the sensitivities associated with these types of machines can be predetermined (the machine may be calibrated) and the values stored to permit one-start balancing. Balancing a fully assembled rotor operating in its running environment, whether rigid or flexible in nature, represents the ultimate application.

The balancing process must be in accord with the rotor dynamics, as specified by the operating environment. Unfortunately, the dynamic characteristics are often not properly recognized when the balancing procedure is specified. As a result, the unbalance distribution problem may not be identified; not enough planes may be provided, sensors may be located at nonoptimum positions, or critical speeds may be overlooked entirely. It is the responsibility of the machinery end user to satisfy himself that the manufacturer has considered:

1. The locations of the critical speeds in the running-speed range for the entire rotor system.
2. The mode shapes (problem unbalance distributions) of the rotor at the criticals.
3. The most probable distribution of unbalance in the finally installed rotor, considering manufacturing tolerances, balancing residuals after low-speed balance, assembly tolerances, etc.
4. The response of the entire rotor-bearing system to this unbalance, considering damping in bearings, joints, dampers, etc.
5. Provisions for eliminating "unbalance distribution problems" at each manufacturing step, whether by machining, low-speed balancing, or high-speed balancing.
6. Provisions for future balancing of the final rotor assembly, when and if necessary.

All of the previous steps are now commercially available at a small fraction of the cost of a replacement rotor.

Component balancing in the factory is required for a very simple reason: the mass center of the component design (or the mass center of each section of long components) does not lie on the intended axis of rotation. The problem occurs because of machining tolerances, void inclusions in the metal, etc. As a result, the component is subjected to one or more balancing steps. In the balancing operation, rotor unbalance sensitivities (interference coefficients) are determined for a sampling of rotors and stored.

Design of the production-rotor balancing process begins with an analytical optimization process, usually best conducted during system design. An unbalance-response computer program is coupled with a balancing computer program to calculate

vibration amplitude as a function of unbalance. These programs yield the optimum location of vibration sensors, correction planes, and optimum balance speeds. Multiplane balancing of the rotor assembly may be done conveniently in a balancing fixture that simulates dynamically the actual environment in which the rotor will operate. A drive motor is required, and possibly a vacuum system, depending on rotor configuration and balancing speed.

It is important that final balancing corrections should not be made on any components that are later to be replaced under field operation conditions. Items such as turbine wheels, which are to be replaced as balanced items during field maintenance, obviously cannot be removed and replaced without altering the assembly balance if they have been utilized for balance corrections. The balancing process design should therefore also be integrated with the maintainability design for best results.

Once the rotor system has been installed, downtime is the key cost associated with vibration. For example, it is not unusual for lost production costs to be measured in tens of thousands of dollars per day for a chemical plant compressor. Obviously, shutting down the machine to rebalance the rotor is a decision not taken lightly. The optimum approach is to determine corrections while the machine is running, and shut down only for long enough to install the trim balance weights. The multiplane balancing procedure permits this to be done with ease after the rotor sensitivities have been measured.

In field balancing (trim balancing), however, rotor speed and system temperatures are the key considerations. It will often be difficult to control speed because of process considerations; system temperatures may require hours, or even days, to stabilize. Vibration should be recorded each time the unit is stopped for trial weight insertion to determine the length of time required for thermal stabilization. Consideration of critical speed locations, vibratory mode shapes and the like, obtained by a separate rotor dynamics study, can also greatly improve the results by providing better guidance to the best sensor and balancing plane locations.

Minimization of the number of startups is an important consideration because the number of starts reduces engine life. The critical aspect in this minimization is the correct selection of balance planes at the start of the process. This selection is essential because the rotor to be balanced often consists of a number of units (turbine, compressor) connected by couplings and has a great number of available correction planes. Usually, balancing is required only in one "zone" (on the turbine or at the coupling) at a particular speed. The critical location can be pinpointed almost exactly by reference to a prior analytical unbalance-response sensitivity study. Such a study, which involves the entire rotor and couplings, will indicate those planes where particular unbalance distributions, if present, will cause vibration at a particular speed. For example, a machinery train, consisting of a precisely balanced compressor with a precisely balanced coupling, will sometimes vibrate excessively at one or more speeds. This vibration usually results because the rotor assembly has one or more bending critical speeds in the running range where the mode shapes are forced by the residual unbalances left in the precision-balanced subassemblies. It must be stressed that a balanced rotor subassembly does not have zero unbalance. In reality, it has a residual unbalance distribution, which does not excite the subassembly under the balance conditions.

If an analytical study does not exist, the balancing engineer must depend on vibration readings from available sensors and, ultimately, on judgment or past experience for selection of correction locations.

Once the critical zones along the rotor axis have been identified, the sensitivity factors of those planes must be calculated. If unbalance sensitivity factors are not available for the balance planes and sensors at the speeds of interest, trial weight runs are required. Thermal stabilization times become important, since the process can consume significant periods of time. If the sensitivities are available, then corrections may be calculated based on vibration levels measured in-service just before shutdown, and the unit can be balanced and restarted very rapidly.

It is often tempting to try to shortcut the sensitivity factor gathering process by inserting correction weights in available planes one at a time based on hunches or one-plane vector plots. Occasionally, this shortcut will result in a balanced rotor; but more often, the opposite result is achieved. This unbalance results because the trial weights in later planes are then not the only perturbation from the "as-is" condition. Data Sheets A, B, and C show a typical process for field balancing with a computer program that employs this balancing technique.

The balancing engineer must try to maintain a balance record for each machine he or she balances, since in most cases the machinery system itself will often contain some nonrepeatable element. Components sensitive to thermal variations, such as dampers and bearing alignments, etc., may often cause problems. When a nonrepeatability is present, the engineer must first determine whether or not another corrective action is indicated. If not, then the balance quality that may be obtained is limited strictly by the range of the nonrepeatable element's variability. This level of quality is difficult to ascertain without experience, either on the individual machine or on a family of similar machines. The balance engineer must balance each rotor by using mean values for each parameter, and he or she must keep a detailed record of the different results. This record consists, essentially, of residual unbalance experience in each case. From the standpoint of the multiplane balancing procedure, the record consists of sensitivity parameters for each machine, which are obtained as a matter of due course in the trial weight procedure.

User's Guide for Multiplane Balancing

The following are suggested steps for balancing a rotor using a multiplane balancing technique. The steps are applicable to a specific program; however, other programs will require about the same information:

1. Choose the number of balancing planes and install an equal or greater number of proximity probes. Install a tachometer that gives a once-per-revolution pulse anywhere on the rotor. Feed the tach signal and the probe signal from one plane at a time into a phase meter to indicate the rotating speed in rpm, the vibration amplitude in peak-to-peak mils, and the phase angle of the maximum amplitude in degrees from the tach pulse.
2. Note the number of balancing planes and the balancing speed in rpm on Data Sheet A. Next, rotate the machine at a slow speed (less than 25% of balancing speed), and measure the initial runout amplitude and phase in each plane. Now, rotate the machine at the balancing

speed, and measure the final vibration amplitude and phase in each plane. Record all this data on Data Sheet A.

3. Take a blank Data Sheet B. Enter the plane number. Place a trial weight at any radius and any angle in that plane. Enter these values on the sheet. Now, operate the machine at the balancing speed, and measure the vibration amplitude and phase in each plane. Repeat the procedure for each plane (place only one trial weight in only one plane at a time). When finished, you should have as many Data Sheets B as the number of planes.
4. Data Sheet C describes the options available to the user. Enter the proper choice for each option.

Data Sheet A

Number of Balancing Planes		Speed in rpm	
		Amplitude	Phase
Initial Run-Out Amplitude and Phase-In-Plane	1		
	2		
	3		
	4		
	5		
Final Vibration Amplitude and Phase Before Balancing In-Plane	1		
	2		
	3		
	4		
	5		

Data Sheet B

Plane ____

Trial Weight	Radius	Angle

		Amplitude	Phase
Vibration Amplitude and Phase-In-Plane	1		
	2		
	3		
	4		
	5		

Data Sheet C

Options

1. If the same weight as the trial weight is to be used for balancing, then the program will locate radius ($NS1 = 1$). For computing the weight at a fixed radius, $NS1 = 2$.

$NS1 =$ ____

2. Radius at which balancing weights will be placed. If $NS1 = 2$, give the locating radius in each plane (this is not applicable if $NS1 = 1$).

Plane No.	1	2	3	4	5
Radius					

3. If balancing is to be done to the initial run-out, then $NS2 = 1$.
If balancing is to be done to zero amplitude, $NS2 = 2$.
$NS2 =$ ____

4. If add-on weights will be used, $NS3 = 1$.
If holes will be drilled, $NS3 = 2$. $NS3 =$ ____

5. If weights can only be placed or removed at a certain number of evenly spaced locations, $NS4 = 1$.
If they can be placed anywhere, $NS4 = 2$. $NS4 =$ ____

6. If $NS4 = 1$, then give the number of holes and the angle to the first hole in each plane.

Plane No.	No. of Holes	Angle of First Hole
1		
2		
3		
4		
5		

Bibliography

Badgley, R.H., "Recent Development in Multiplane-Multispeed Balancing of Flexible Rotors in the United States," Presented at the Symposium on Dynamics of Rotors, IUTAM, Lyngby, Denmark, 12 August, 1974.

Bently Nevada Corp., "Balancing Rotating Machinery," Report 1970, Minden, Nevada.

Bishop, R.E.D., and Gladwell, G.M.L., "The Vibration and Balancing of an Unbalanced Flexible Rotor," *Journal of Mechanical Engineering Society*, Vol. 1, 1959, pp. 66–77.

Bishop, R.E.D., and Parkinson, A.G., "On the Use of Balancing Machines for Flexible Rotors," ASME Paper No. 71-Vibr-73 1971.

Boyce, M.P., "Multiplane, Multispeed Balancing of High Speed Machinery," Keio University, Tokyo, Japan, July 1977.

Boyce, M.P., White, G., and Morgan, E., "Dynamic Simulation of a High Speed Rotor," International Conference on Centrifugal Compressors at Madras, India, February 1978.

Den Hartog, J.P., "The Balancing of Flexible Rotors," *Air, Space, and Industr.*, McGraw-Hill, New York, 1963.

East, J.R., "Turbomachinery Balancing Considerations," Proceedings of the 20th Turbomachinery Symposium, Texas A&M University, p. 209, 1991.

Goodman, T.P., "A Least-Squares Method for Computing Balance Corrections," ASME Paper No. 63-WA-295 1963.

Jackson, C., "Using the Orbit to Balance," *Mechanical Engineering*, pp. 28–32, February 1971.

Kellenberger, W., "Should a Flexible Rotor Be Balanced in N or $(N + 2)$ Planes?" *Trans. ASME Journal of Engineering for Industry*, pp. 548–560, May 1972.

Legrow, J.V., "Multiplane Balancing of Flexible Rotors—A Method of Calculating Correction Weights," ASME Paper No. 71-Vibr-52 1971.

Lindsey, J.R., "Significant Developments in Methods for Balancing High-Speed Rotors," ASME Paper No. 69-Vibr-53.

Miwa, S., "Balancing of a Flexible Rotor (3rd Report)," *Bulletin of the ASME*, Vol. 16, No. 100, October 1973, pp. 1562–1572.

Stroh, C.G., MacKenzie, J.R., Rebstock, and Jordan, "Options for Low Speed and Operating Speed Balancing of Rotating Equipment," Proceedings of the 25th Turbomachinery Symposium, Texas A&M University, p. 253, 1996.

Tessarzik, J.M., Badgley, R.H., and Anderson, W.J., "Flexible Rotor Balancing by the Exact-Point Speed Influence Coefficient Method," Transactions ASME, Inst. of Engineering for Industry, Vol. 94, Series B, No. 1, p. 148, February 1972.

Thearle, E.L., "Dynamic Balancing of Rotating Machinery in the Field," Trans. ASME Vol. 56, pp. 745–753, 1934.

Copyrighted Materials
Copyright © 2012 Elsevier Retrieved from www.knovel.com

18 Couplings and Alignment

Couplings in most turbomachines attach the driver to the driven piece of machinery. High-performance flexible couplings used in turbomachines must perform three major functions: (1) efficiently transmit mechanical power directly from one shaft to another with constant velocity, (2) compensate for misalignment without inducing high stress and with minimum power loss, and (3) allow for axial movement of either shaft without creating excessive thrust on the other. There are three basic types of flexible couplings that satisfy these requirements. The first type is the mechanical-joint coupling. In this coupling, flexibility is accomplished by a sliding and rolling action. Mechanical-joint couplings include gear tooth couplings, chain and sprocket couplings, and slider or Oldham couplings.

The second type is the resilient-material coupling. In resilient-material couplings flexibility is a function of flexing of material. Resilient-material couplings include those that use elastomer in compression (pin and bushing, block, spider, and elastomer-annulus, metal-insert types); elastomer in shear (sandwich type, tire type), steel springs (radial leaf, peripheral coil types) and steel-disc and diaphragm couplings.

The third type is the combined mechanical and material couplings where flexibility is provided by sliding, or rolling and flexing. Combination couplings include continuous and interrupted metallic-spring grid couplings, non-metallic gear couplings, non-metallic chain couplings, and slider couplings that have non-metallic sliding elements.

In choosing a coupling, the loading and speed must be known. Figure 18-1 shows the relation between coupling type, peripheral velocity coupling size, and speed. The loadings in these high-performance flexible couplings are as follows:

1. *Centrifugal force*. Varies in importance, depending on the system speed.
2. *Steady transmitted torque*. Smooth non-fluctuating torque in electric motors, turbines, and a variety of smooth torque-absorbing load (driven) machines.
3. *Cyclically transmitted torque*. Pulsating or cyclic torque in reciprocating prime movers and load machines such as reciprocating compressors, pumps, and marine propellers.
4. *Additional cyclic torque*. Caused by machining imperfections of drive components (particularly gearing) and imbalance of rotating drive components.
5. *Peak torque (transience)*. Caused by starting conditions, momentary shock, or overload.
6. *Impact torque*. A function of system looseness or backlash. Generally, mechanical-joint flexible couplings have inherent backlash.
7. *Misalignment loads*. All flexible couplings generate cyclic or steady moments within themselves when misaligned.
8. *Sliding velocity*. A factor in mechanical-joint couplings only.

Gas Turbine Engineering Handbook, Fourth Edition. DOI: 10.1016/B978-0-12-383842-1.00018-4
Copyright © 2012 Elsevier Inc. All rights reserved.

9. *Resonant vibration*. Any of the forced vibration loads, such as cyclic or misalignment loads, may have a frequency that coincides with a natural frequency of the rotating-shaft system, or any component of the complete power plant and its foundation, and may, thus, excite vibration resonance.

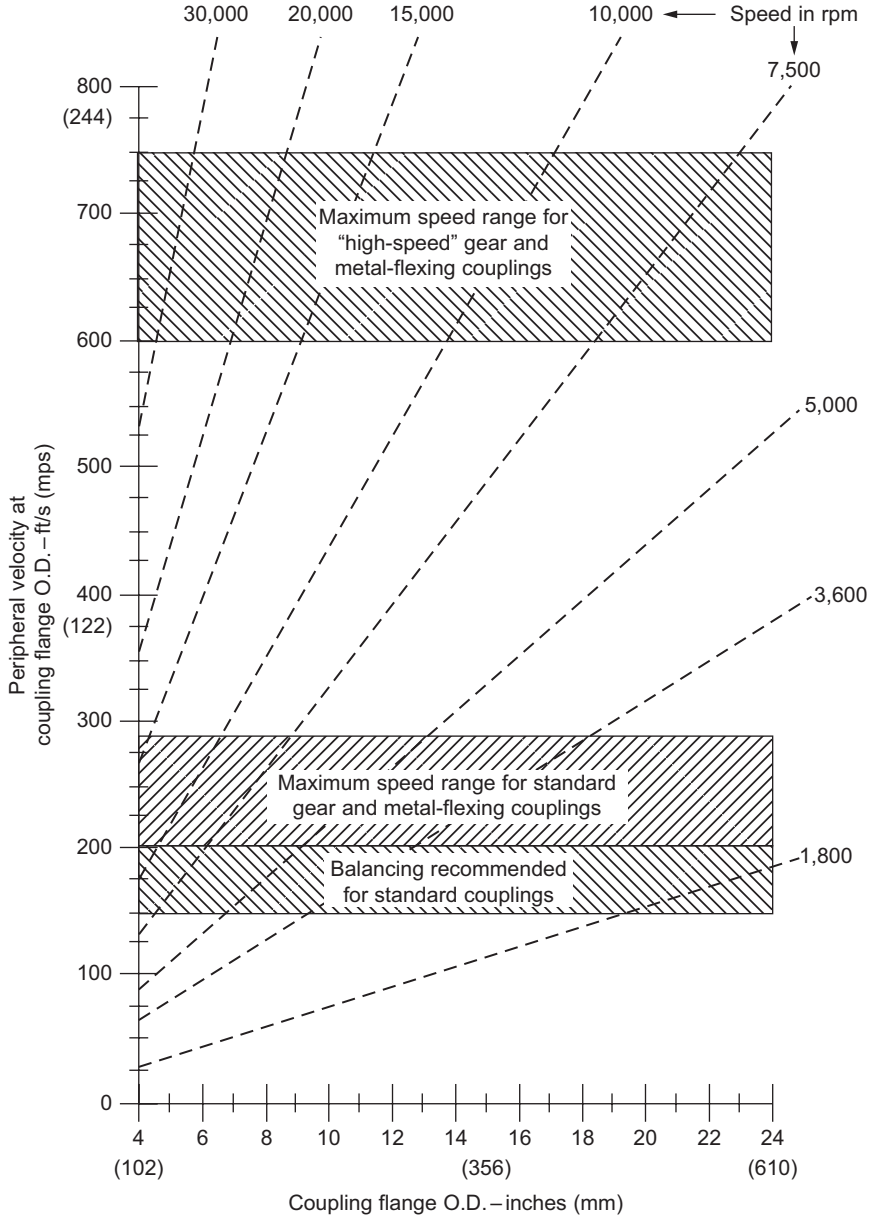


Figure 18-1 Flexible coupling operating spectrum.

Table 18-1 Disc, Diaphragm, and Gear Couplings*

	Disc	Diaphragm	Gear
Speed capacity	High	High	High
Power-to-weight ratios	Moderate	Moderate	High
Lubrication required	No	No	Yes
Misalignment capacity at high speed	Moderate	High	Moderate
Inherent balance	Good	Very good	Good
Overall diameter	Low	High	Low
Normal failure mode	Abrupt (fatigue)	Abrupt (fatigue)	Progressive (wear)
Overhung moment on machine shafts	Moderate	Moderate	Very low
Generated moment, misaligned, with torque	Moderate	Low	Moderate
Axial movement capacity	Low	Moderate	High
Resistance to axial movement			
Suddenly applied	High	Moderate	High
Gradually applied	High	Moderate	Low

*This table is intended as a rough guide only.

The gas turbine is a high-speed, high-torque drive and requires that its coupling has the following characteristics:

1. Low-weight, low-overhung moment
2. High-speed, capacity-acceptable centrifugal stresses
3. High balancing potential
4. Misalignment capability

Gear couplings, disc couplings, and diaphragm-type couplings are best suited for this type of service. Table 18-1 shows some of the major characteristics of these types of couplings.

Gear Couplings

A gear coupling consists of two sets of meshing gears. Each mesh has an internal and external gear with the same number of teeth. There are two major types of gear couplings that are used in turbomachinery. The first type of gear coupling has the male teeth integral with the hub as seen in Figure 18-2. In this coupling type the heat generated at the teeth flows in a different way into the shaft than it does through the sleeve to the surrounding air. The sleeve will therefore heat up and expand more than the hub. This expansion plus the centrifugal force acting on the sleeve will cause it to grow rapidly – as much as 3–4 mils more than the hub – causing an eccentricity, which can lead to a large, unbalanced force. Thus, this coupling type is more useful in low-horsepower units.

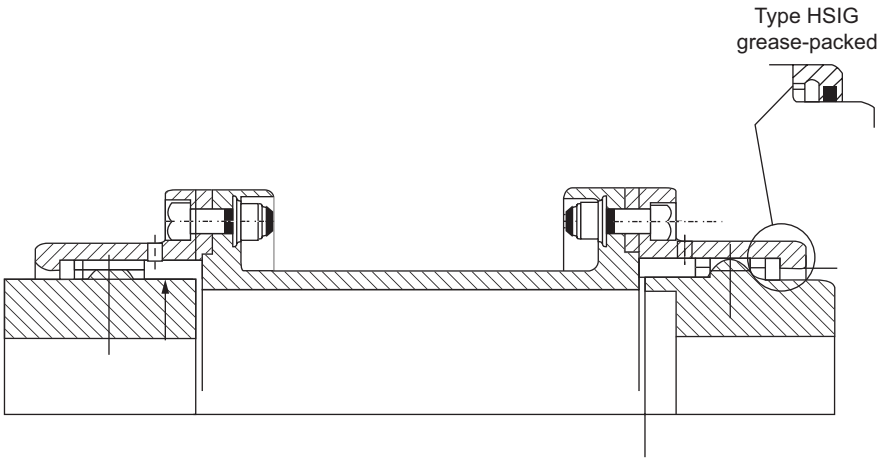


Figure 18-2 Gear coupling (male teeth integral with the hub).

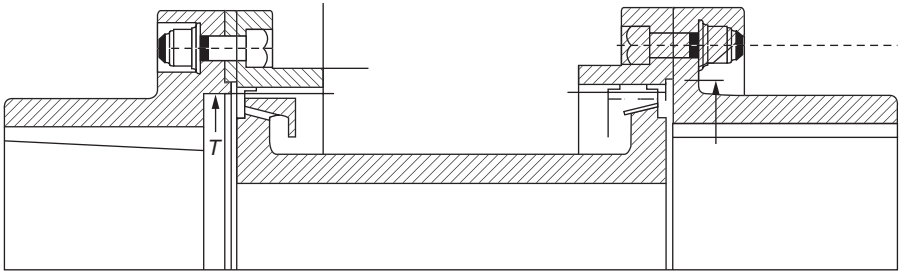


Figure 18-3 Gear coupling (male teeth integral with the spool).

The second type of coupling, shown in Figure 18-3, has the male teeth integral with the spool. In this coupling type the same amount of heat is produced, but the hollow-bored spool will accept heat in a manner similar to the sleeve so that no differential growth occurs.

Gear couplings have a pilot incorporated into the male tooth form to support the loose member of the coupling in a concentric manner at speed, as shown in Figure 18-4.

The sliding friction coefficient is another area of evaluation in gear couplings. It produces a resistance to the necessary axial movement as rotors heat and expand. This relative sliding motion between the coupling elements takes care of the misalignment problem in gear couplings.

Relative motion between meshing gears is oscillatory in the axial direction and has a low amplitude and a relatively high frequency. Some of the major advantages of the gear couplings are:

1. They can transmit more power per pound of steel, or per inch of diameter, than any other coupling.

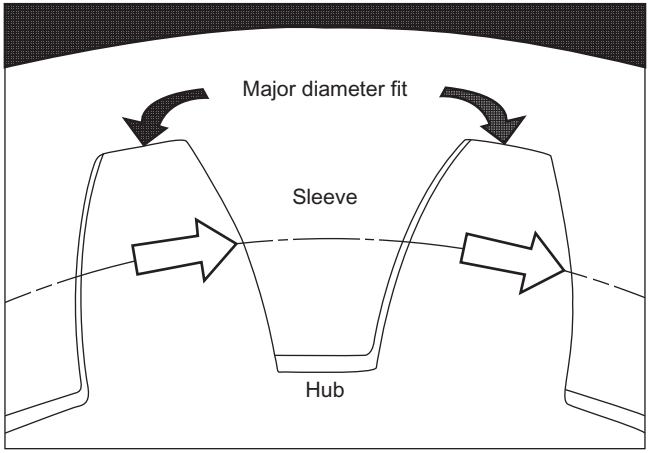


Figure 18-4 Schematic of gear used in coupling applications.

2. They are forgiving; they accept errors in installation and mistreatment more readily than other types of couplings.
3. They are reliable and safe; they do not throw around pieces of metal or rubber even when they fail, and they can work longer in corrosive conditions than many other couplings.

A major disadvantage in gear couplings is the misalignment problem. Tooth-sliding velocity is directly proportional to the tooth-mesh misalignment angle and the rotational speed. Therefore, misalignment of high-speed drives must be kept to a minimum to limit sliding velocity to an acceptable value.

The coupling must be able to accommodate misalignment caused by cold start-up. The physical misalignment capability of a gear-type coupling should never be considered an acceptable running condition for high-speed applications. The limits of misalignment versus operating speed are best stated on the basis of a constant, relative sliding velocity between the gear teeth.

Figure 18-5 gives recommended limits of misalignment with the system at operating temperature. The graph is based on a maximum constant sliding velocity of 1.3 inches per second and includes coupling size, speed, and the axial distance between gear meshes. Gear couplings can be more tolerant of axial growth than other coupling types.

In the disc-type couplings, the axial growth is limited by the disc deflection range, so the equipment must be adjusted with more axial accuracy than with gear couplings.

High-speed couplings must be balanced very carefully and, with a low overhung moment. The effect of the coupling overhung moment is felt not only in the machine bearing load but in the shaft vibration.

The advantage of a reduction in overhung moment is not only to reduce bearing loads, but also to minimize shaft deflection, which results in a reduction of the vibration amplitude. The reduction of the coupling overhung moment produces an upward

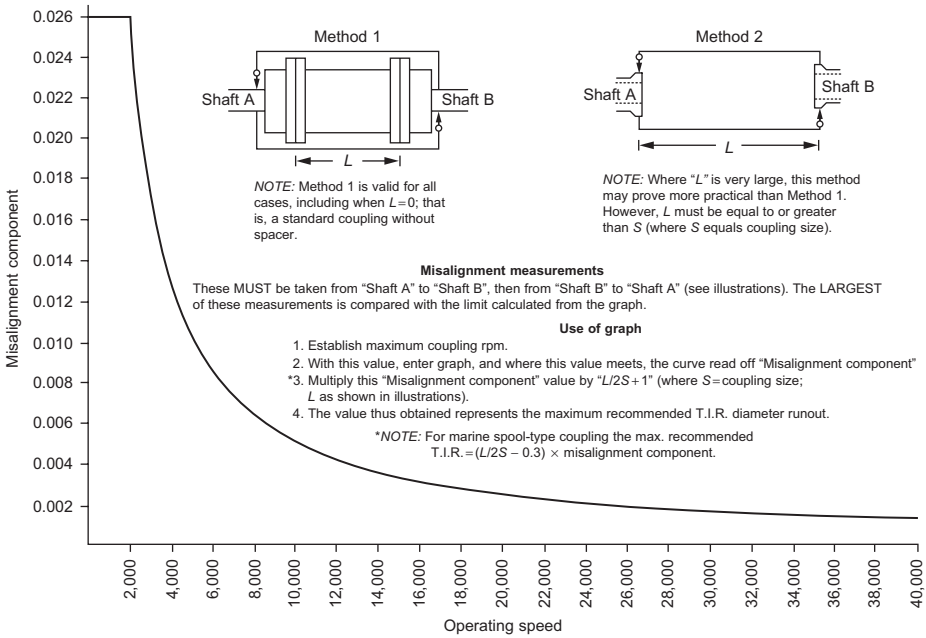


Figure 18-5 Recommended limits of misalignment vs. operating speed (Reference 3).

shift in shaft critical speeds. This change in natural frequencies results in an increase in the spread between natural frequencies. For many applications, reduced overhung moment is an absolute necessity to enable the system to operate satisfactorily at the required operating speed.

The high-speed couplings have five components – usually two hubs, two sleeves, and a spacer. To obtain a proper balance, each hub should be balanced separately, then the spacer should be balanced, and finally the full coupling should be assembly balanced.

The couplings should be carefully match-marked before removal from the balancing mandrels.

Lubrication problems are a major consideration in the use of gear couplings. Relative sliding between the teeth of the hub and the sleeve requires proper lubrication to assure long component life. This sliding motion is alternative and is characterized by small amplitudes and relatively high frequencies.

Gear couplings can be either packed with lubricant or continuously lubricated. Each system has advantages and disadvantages, and the choice depends on the conditions under which the coupling works.

Oil-Filled Couplings

Very few high-performance couplings use this system because it requires large-volume couplings. It is, however, the best method of lubrication and, incidentally, the first

used. Its major disadvantage is that it may leak lubricant from defective flange gaskets, etc.

Grease-Packed Couplings

Besides enabling the user to select a good lubricant, grease-packing has the advantage of sealing the coupling from the environment. The high-performance coupling works under very small misalignment and usually generates very little heat. In most cases, the couplings receive more heat from the shafts than they generate. Very few greases can work in temperatures of more than 250 °F (121 °C), and for this reason grease-packed couplings cannot be installed within an enclosure that prevents the heat from dissipating. Greases also separate under large centrifugal forces. In many high-speed couplings forces exceed 8,000 g's. New lubricants are appearing on the market that do not separate under high loadings.

A second disadvantage of grease lubrication is the maintenance requirement. Coupling manufacturers generally recommend re-lubrication every six months. There are known cases, however, where grease-packed couplings were found to be in excellent condition after two years of maintenance-free service.

Continuously Lubricated Couplings

Lubrication by continuous oil flow can represent an ideal method if there is:

1. Freedom to select the type of oil.
2. An independent lube circuit.

From the user's point of view, neither condition is acceptable, not only because of the added cost of an independent lube circuit, but because it is almost impossible to prevent mixing of the oil from this circuit with the lube system for the rest of the equipment.

In practice, continuously lubricated couplings are supplied with oil from the main lube system. The oil is not the best type for couplings, and also brings a large quantity of impurities to the coupling. The accumulated sludge shortens coupling life.

Sludge accumulates within a coupling for two reasons: (1) because the lubricant is not pure, and (2) because the coupling centrifuges and retains the impurities.

Very little can be done to prevent the coupling from retaining the impurities. The g forces in a coupling are very high, and the oil dam built in the sleeve configuration prevents the impurities from going over it.

Some manufacturers now offer couplings without a dam, or with sleeves provided with radial holes. Experience has shown that such couplings accumulate no sludge. The dam has, however, two useful purposes:

1. It maintains an oil level high enough to submerge the teeth completely.
2. It retains a quantity of oil within the coupling even if the lube system fails.

Removing the oil dam defeats both these features. To maintain the same performance for a damless coupling, the oil flow to the coupling should be re-evaluated. Nothing can be done, however, to retain oil in the damless coupling, and some users

will not accept them for this reason. A proper decision can only be made by weighing a possible coupling failure because of sludge accumulation against an accidental failure of the lube system.

Gear Coupling Failure Modes

The main causes of failure in gear couplings are wear or surface fatigue caused by lack of lubricant, incorrect lubrication, or excessive surface stresses. Component fracture caused by overload or fatigue is generally of secondary importance.

High speeds require relatively lightweight gear elements. All case-hardening procedures produce distortion – to keep this distortion to a minimum, nitriding is the preferred hardening method. This method is employed after all machinery operations are complete and no further corrections are to be made to the tooth geometry.

Nitriding permits increased tooth loading. The amount of increased capacity is not exactly known, but a 20% increase in load at 10,000–12,000 rpm has proven reliable. A further advantage of the nitrided coupling is that the coefficient of friction is lower than that for through-hardened parts. The heat from friction in the coupling decreases. More important, the transmission of axial forces is decreased by the reduced friction.

In many cases, gear shaving prior to nitriding has been used to correct or minimize small errors of tooth geometry caused by the shaping or hobbing processes.

A method of assuring nearly perfect tooth contact is to match-lap the gear teeth after nitriding. Lapping eliminates the break-in period, which otherwise takes from 70 to 120 hours. It is during the break-in period, that tooth surface distress usually occurs.

For maximum reliability, it is recommended that nitrided gear teeth be specified. Experience indicates that the extra cost of match lapping is justified.

The major failure in gear couplings is the fretting on the gear teeth. Fretting can be caused by improper lubrication. Lubrication problems can be categorized by the type of lubrication system being used. The two types of lubrication systems are the batch type and the continuous lubrication type. Table 18-2 shows some of the common problems that affect gear couplings, depending on the lube system used. Misalignment is another problem with gear couplings. Excessive misalignment can lead to any of the following problems, such as: tooth breakage, scoring, cold flow, wear, and pitting. Fasteners are another problem source in couplings.

Table 18-2 Types of Typical Gear Coupling Failures

Standard or Sealed Lube	Continuous Lube
Wear	Wear
Fretting corrosion	Corrosive wear
Worm tracking	Coupling contamination
Cold flow	Scoring and welding
Lube separation	Worm tracking

Table 18-3 Diagnostic Analysis of Gear Couplings

Damage or Stress Signs	Cause
Gear tooth surface deterioration (high rate of wear, scoring, and worm tracking)	Low oil viscosity and/or excessive misalignment
Gear tooth surface deterioration and overheating	Misalignment, high sliding velocity
Tooth breakage and wear	High misalignment angle
Broken hub, keys sheared	Too much shrink fit on shaft
Lockup-worn and broken teeth	Contaminated lubrication system, excessive misalignment
Worm tracking	Misalignment, separation of lubricant, low oil viscosity
Broken end or seal ring	Too much shaft-to-shaft spacing and misalignment
Galled bores	Improper removing techniques, insufficient or incorrect heating, excessive interference fit
Discolored bores	Improper hydraulic fit, contamination between shaft and hub
Fracture of components	Overload or fatigue, shock loading
Cold flow, wear, and fretting	High vibration
Bolt shearing, bolt hole elongation	Nut bottoming out on threads
Separation of lubricant ingredients	Centrifugal force
Retention of moisture impurities	Centrifugal force
Lubricant deterioration	High ambient temperature

Coupling fasteners should be properly heat-treated to withstand the large forces they experience in high-speed coupling applications. Fasteners should be properly torqued and, after four-to-six disassemblies, the entire fastener set should be replaced. Bolt shearing or bolt-hole elongation results from the nut bottoming out on the threads before the coupling flanges are tight, thus transmitting force through the bolt rather than through the flange faces. Bolts and nuts should be weight-balanced to very close tolerances. Table 18-3 is a diagnostic analysis of gear coupling failures.

Metal Diaphragm Couplings

The metal diaphragm coupling is relatively new in turbomachinery applications. Although the first recorded use of such a coupling dates back to 1922 on a condensing steam turbine locomotive, the contoured diaphragm did not come into wide use until the late 1950s.

Diaphragm couplings accommodate system misalignment through flexing. Fatigue resistance is the main performance criterion. The life expectancy of a diaphragm

coupling that operates within its design limits is theoretically infinite. Figure 18-6 is a photograph of a typical metal diaphragm coupling.

Figure 18-7 shows a section through a diaphragm coupling. The coupling has only five parts: two rigid hubs, one spool piece, and two alignment rings. These five parts are solidly bolted together, and misalignment is accommodated through flexing of the two diaphragms of the spool. The spool piece is made up of three separate parts: two diaphragms and a spacer tube. These parts are welded together by an electron beam.

The heart of these couplings is the flexing disc; it is manufactured from vacuum-degassed alloy steel, forged with a radial-grain orientation, and has a contoured profile machined on high-precision equipment.

The contoured profile is shown in Figure 18-8. The diaphragm undergoes axial deflection. The forces acting on the disc that are generating the stresses are caused by the torque effects, centrifugal forces, and axial deflection. Standard methods for calculating centrifugal forces in a rotating disc show that both tangential and radial stresses increase rapidly with a decrease in the radius.

The stresses imposed by axial deflection are much greater at the hub than at the rim, as seen in Figure 18-9. Therefore, to maintain uniform stresses in the diaphragm when all the various forces acting on the diaphragm are at their maximum, the diaphragm must be used to connect the contoured profile at both the hub and the rim to reduce stresses.

Diaphragm couplings are more susceptible to axial movement problems than gear couplings, since the diaphragm has a maximum deflection that cannot be exceeded.

Theoretically, a diaphragm coupling will have no problems or failures as long as it is operated within "design limits." The diaphragm fails from excessive torque. Two distinct modes of failure can be found – one at a zero axial displacement and the other at a large axial displacement. Zero axial displacement is characterized by a circular crackline that goes through the thinnest portion of the diaphragm. The crack

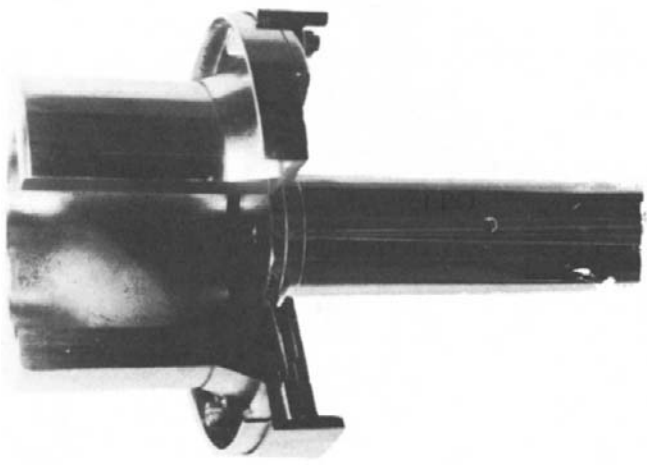


Figure 18-6 Metal diaphragm coupling, one end shown (Courtesy of Kóppers Company, Inc.).

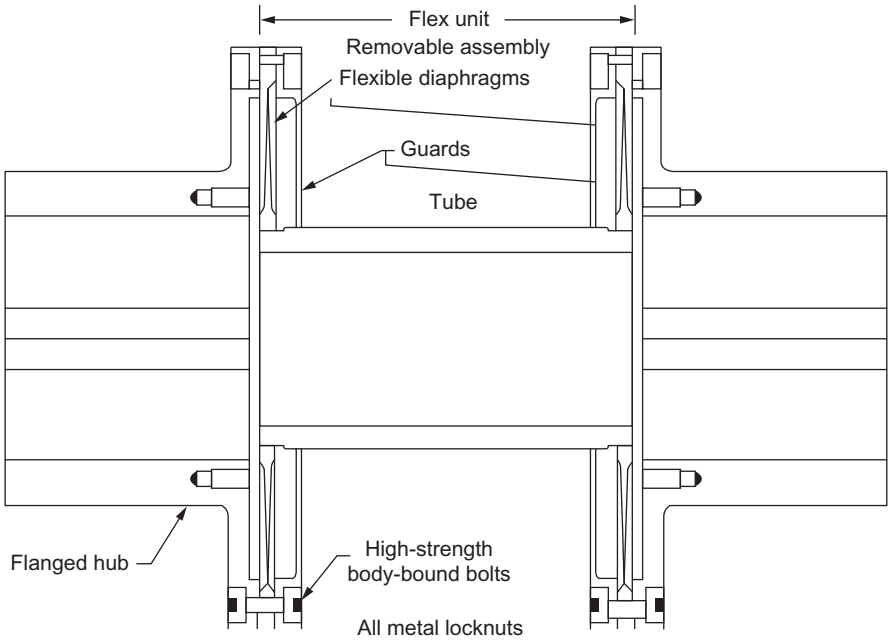


Figure 18-7 Schematic of atypical diaphragm coupling (Courtesy of Kóppers Company, Inc.).

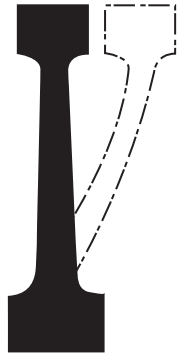


Figure 18-8 Axial deflection in a disc.

is relatively smooth, and there is no buckling of the disc. The large axial movement and angular misalignment, which lead to disc failure, are characterized by a crackline that follows a random path from the thinnest to the thickest portion of the disc. The crackline is very irregular, and there is severe buckling of the unfailed part of the disc. Failure in this mode shows that the crackline propogates some 270° before disc buckling takes place, indicating that the torque load makes only a small contribution to the total stresses in the disc. Metal diaphragm couplings can also have problems due to corrosive action on the diaphragms. Thus, care must be taken to apply coating to protect against damage from a harsh environment.

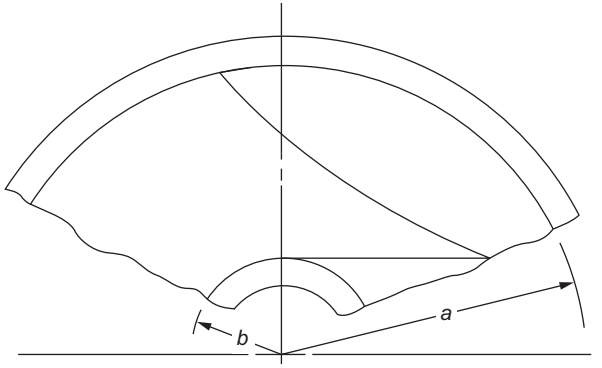


Figure 18-9 Stress distribution under axial deflection.

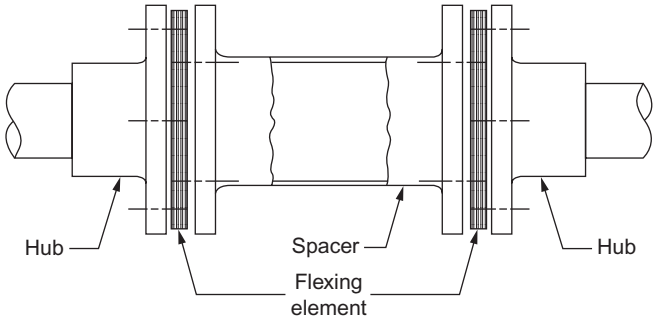


Figure 18-10 Typical metal-flexing disc coupling.

Metal Disc Couplings

The main difference between the metal diaphragm coupling and the typical metal-flexing disc coupling is that a number of discs replace the single diaphragm between the hubs and the spacer. Figure 18-10 shows a schematic of this type of coupling. A typical metal-flexing disc coupling consists of two hubs rigidly attached by interference fit or flange bolting to the driving and driven shaft of the connected equipment. Laminated disc sets are attached to each hub to compensate for the misalignment. A spacer spans the gap between the shafts and is attached to the flexing elements at each end.

The functional requirements and characteristics of the flexing elements are to transmit rated torque as well as any system overloads without buckling or permanent deformation. In other words, they must possess torsional rigidity. However, under conditions of parallel, angular, and axial misalignment, the flexing element must have sufficient flexibility to accommodate these conditions without imposing excessive forces and moments on equipment shafts and bearings. Both of the previous requirements must be met while maintaining stress levels that are safely within the fatigue

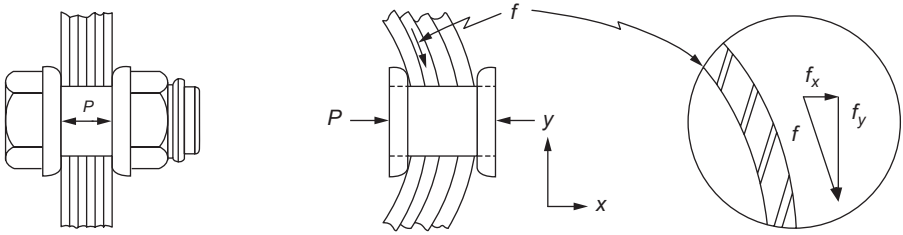


Figure 18-11 Frictional damping in a metal-disc coupling.

limit of the flexing material. Metal-flexing couplings have been known to exhibit occasional large-amplitude vibrations in the axial direction when excited at the natural frequency of the coupling.

The amount of damping present in a metal-flexing coupling is thought to be relatively small, although it is known to be greater for the laminated disc-type construction than for a coupling consisting of a single-piece membrane. The reason for the greater damping in the laminate disc configuration is that under conditions of axial movement, a microscopic amount of motion takes place between adjacent lamina, as shown in Figure 18-11. Since the element is clamped together under a bolt preload, there is a frictional force, which resists sliding.

Field experience by manufacturers and users of turbomachinery has shown that resonant axial vibration of a metal-flexing coupling can cause problems at times that are reflected through the entire drive train. With laminated disc couplings, problems occurs only when an external forcing function exists. This condition could be a result of aerodynamic or hydraulic fluctuations in the machine train, out-of-square thrust collars, gearing inaccuracies, or electrical excitations of motor-driven equipment. It is usually possible to avoid operating the couplings at or near resonance if the condition is anticipated during the system design stage. However, such problems do not always occur until after a machine is in service. More information is needed on the nature and magnitude of external excitations.

Turbomachinery Uprates

If an existing coupling is to be replaced with a new type of coupling because of a machinery uprate, or for any other reason, there is good justification to review, with the latest techniques, the nature of the rotating system to be coupled. Couplings, whether gear or disc-type, should not be simply picked from a catalog. Some installations are very old, and some have been revised in other ways in the field. Unfortunately, such engineering reviews are not easy to arrange with busy equipment suppliers.

Therefore, the tendency is to match the obvious characteristics of the existing coupling and see what happens. Many older designs have relatively heavy and larger-diameter shafts, and retrofits have been very successful and trouble-free. Part of

this success is due to the consideration given to the retrofit by cooperating engineers of the coupling manufacturer and the rotating equipment manufacturer. A large part of the success is due to the dedication and extra effort of the first companies offering the disc coupling to ensure success.

If retrofits and new installations consume the available time of these engineers, the potential for omission increases. Therefore, more time should be allowed for the work.

Coupling application is an engineering effort involving the coupling and rotating equipment designers. The user, by the purchasing technique he employs, can aid or hinder this effort, since he chooses the basic coupling style his operations and maintenance people will work with.

In either case a good purchase specification should designate that the selection and design of the coupling must follow the rotor design work and exclude the coupling from becoming involved in competitive bids. It is simply too important an item to risk reliability for initial cost savings.

Disc couplings are used as replacements for gear couplings for two reasons: (1) the disc couplings do not require lubrication, and (2) the machinery ratings can be uprated with disc couplings.

Compressor and driver shafts often prove to be overstressed in equipment uprate situations; however, a change from conventional gear-type couplings to the more recent diaphragm coupling design can lower the shaft stress enough to avoid shaft replacement during power uprates of compressors or compressor drivers.

A close examination of how the equipment vendor arrived at his maximum allowable stress levels may frequently show that such shaft replacements can be avoided without undue risk if the coupling selection is optimized. This situation is based on the fact that gear-type couplings have the potential of inducing both torsional stresses and bending stresses in a shaft, whereas diaphragm couplings tend to induce primarily torsional stresses and insignificant bending stresses at best.

To determine if a machine's performance can be uprated without installing a large shaft, the forces acting on the shaft must be computed. The forces acting on a shaft can be put into three separate categories: (1) torsional, (2) axial, and (3) bending forces. Torsional forces are a function of the shaft rotational speed and horsepower transmitted. They can be calculated from:

$$T = \frac{63{,}000\ (\text{hp})}{\text{rpm}} \tag{18-1}$$

and the torsional stress τ_T can be computed with:

$$\tau_T = \frac{16T}{\pi d^3} \tag{18-2}$$

It is a generally accepted assumption that the axial stress will not exceed 20% of the torsional stress. τ_a can therefore be obtained by $\tau_a = 0.20\,\tau_T$. These two stresses

will be the same for either type of coupling; however, the bending stress will vary depending on which type of coupling is used.

There are three relevant bending moments caused by a gear coupling when transmitting torque with angular or parallel misalignment:

1. *Moment caused by contact-point shift*. This moment acts in the angular misalignment plane and tends to straighten the coupling. It can be expressed:

$$M_c = \frac{T}{D_p/2} \times \frac{X}{2} \tag{18-3}$$

where

T = shaft torque
D_p = gear coupling pitch diameter
X = tooth face length (Figure 18-12)

2. *Moment caused by coupling friction.* This moment acts in a plane at a right angle relative to the angular misalignment. It has the magnitude:

$$M_f = T_\mu \tag{18-4}$$

where μ is the friction coefficient.

3. Moment caused by turning torque through a misalignment angle α. It acts in the same direction as the friction moment M_f and can be expressed as:

$$M_T = T \sin \alpha \tag{18-5}$$

The total moment is the vector sum of the individual moments:

$$M_{\text{total}} = \sqrt{M_c^2 + (M_f + M_T)^2} \tag{18-6}$$

The contoured diaphragm coupling causes two bending moments:

1. *Moment caused by angular misalignment.* This results in bending of the diaphragm:

$$M_B = k_B^\alpha \tag{18-7}$$

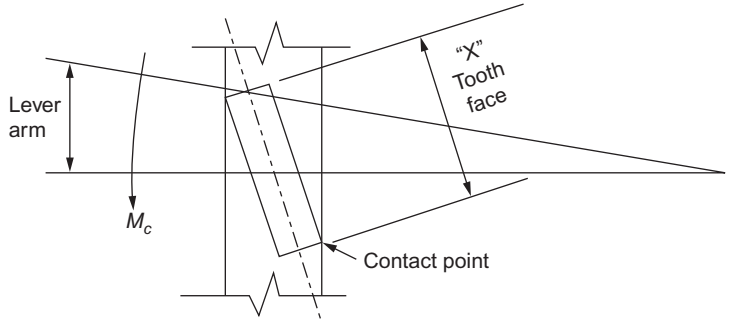


Figure 18-12 Shift in contact point.

In this expression k_B equals the angular spring rate of the diaphragm (lb-in/degree) and α is the misalignment angle. This moment acts in the angular misalignment plane, as did M_c in the gear-coupling analysis.

2. *Moment caused by turning the torque through a misalignment angle* α. It can be expressed:

$$M_T = T\sin\alpha \tag{18-8}$$

The total moment is now:

$$M_{\text{total}} = \sqrt{M_B{}^2 + M_T{}^2} \tag{18-9}$$

Comparing the bending moments caused by gear couplings with those resulting from contoured diaphragm couplings shows the former to be significant and the latter virtually negligible.

The cyclic bending stress imposed on a gear coupling-equipped shaft can be computed from:

$$\sigma_a = \frac{M_{\text{total}} \times C}{I} \tag{18-10}$$

where

$C =$ shaft radius

$I =$ shaft area moment of inertia

In addition, there is a mean tensile stress acting on the shaft cross-sectional area. This effect means stress equates to:

$$\sigma_m = \frac{T\mu}{(D_p/2)(\pi C^2)\cos\Theta} \tag{18-11}$$

where Θ is the pressure angle assumed for the gear teeth.

The cycle bending stress seen by the diaphragm coupling-equipped shaft can be obtained by a rapid ratio calculation:

$$\frac{\sigma_a\,(\text{diaphragm coupling})}{\sigma_a\,(\text{gear coupling})} = \frac{M_{\text{total}}\,(\text{diaphragm coupling})}{M_{\text{total}}\,(\text{gear coupling})} \tag{18-12}$$

The mean tensile stress acting on the cross-sectional area of the diaphragm coupling-equipped shaft depends on how far the diaphragm is displaced axially from its neutral rest position and the axial spring rate of the diaphragm.

For combined bending and torsion, the factor of safety can be calculated by the following relationships:

$$n = \frac{1}{\sqrt{\left(k_f \dfrac{\sigma_a}{\sigma_e} + \dfrac{\sigma_m}{\sigma_{y.p.}}\right)^2 + 3\left(k_f' \dfrac{\tau_a}{\sigma_e} + \dfrac{\tau_m}{\sigma_{y.p.}}\right)^2}} \tag{18-13}$$

where

σ_e = endurance limit in tension

σ_{yp} = minimum yield strength in tension

The stress concentration factor k_f results from the keyway and must be used in torsional stress calculations. Factor k_f' takes into account the shaft step; it must be used in the bending stress calculation.

Curvic Couplings

In essence, the curvic coupling is a ring of precision ground face splines that are meshed after index. The splines, or radial teeth, are ground in such a manner that on one member the sides of the teeth surfaces that meshed are convex and on the other member the sides are concave. The result is that after these members are clamped together, perfect index location is achieved, and further, the turret is perfectly on the center.

The other important advantage of the curvic coupling is that its accuracy in both axes actually improves with use, rather than degrades. Care should be taken in the necessity of guarding against the entry of chips or other debris into the seating area. Figure 18-13 shows one-half of a typical curvic coupling, and Figure 18-14 shows a typical wheel in a gas turbine with curvic coupling machined into the disk.

Figure 18-15 shows a typical cross section of a gas turbine.

Many gas turbine's rotors are of bolted construction with a positive torque incorporating such features as radial pins and curvic couplings, respectively. The rotor is supported by two-element tilting pad bearings and an upper-half fixed bearing. The thrust bearing is a double-acting type that uses the leading-edge groove lubrication system, as shown in Figure 18-15.



Figure 18-13 A typical curvic coupling.



Figure 18-14 A typical disc with a curvic coupling.

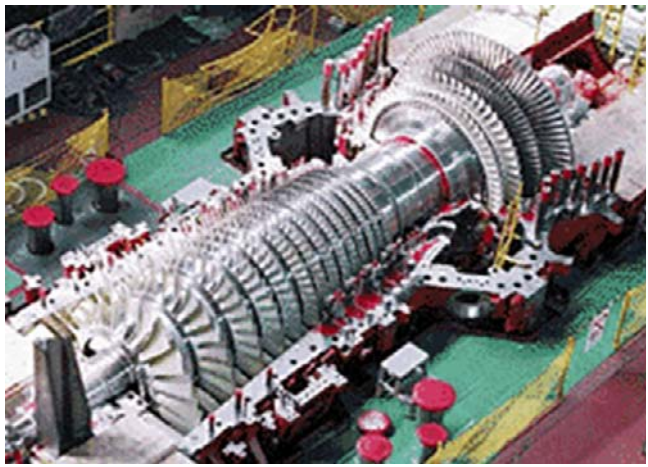


Figure 18-15 Cross section of a gas turbine.

Figure 18-16 shows a schematic of how the axial compressor disks in the gas turbine are put together by the use of bolts and curvic couplings. These couplings transmit loads over 200 MW and are commonly used in many gas turbines.

Shaft Alignment

The successful alignment of a gas turbine to the unit it is driving is of great importance. A major portion of operating problems experienced in the field can often be attributed to faulty misalignment. Operating problems caused by misalignment include excessive vibration, coupling overheat, wear, and bearing failures.

Typically, misalignment problems will show up at two times rpm frequencies with axial vibrations at one and two times rpm. With diaphragm-type flexible couplings,

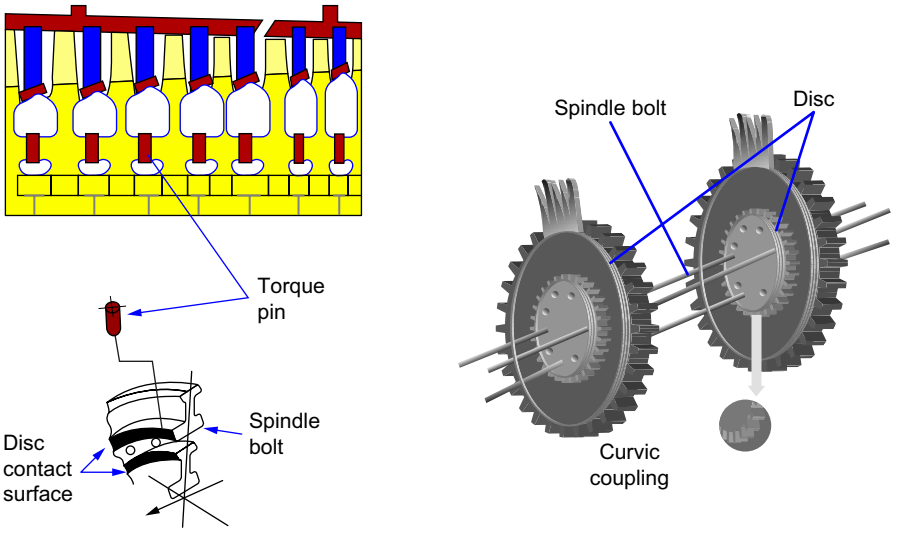


Figure 18-16 Assembly mechanism of turbine disks using a curvic coupling.

vibrations may be somewhat suppressed, and consequently, trains using these couplings should be monitored periodically to ensure they are in alignment.

Perfect alignment – exact shaft colinearity under operating conditions – is difficult and uneconomical to attain. The degree of tolerable misalignment is a function of coupling length, size, and speed. Some companies are now specifying a minimum coupling spacer length of 18 inches, since longer coupling lengths can tolerate more misalignment.

The amount of misalignment that can be tolerated by the machine also depends on the types of journal and thrust bearings used. Tilting-pad-type bearings greatly reduce the misalignment problem. Figure 18-17 shows misalignment in both the journal and thrust bearings. The effect of misalignment on a journal bearing causes the shaft to contact the end of the bearing. Thus, journal length is a criterion in the amount of misalignment a bearing can tolerate; a shorter length obviously can tolerate more misalignment. The effect on the thrust bearing is to load up one segment of the thrust bearing arc and unload the opposite segment. This effect is more pronounced with higher loads and less flexible bearings.

The Shaft Alignment Procedure

In essence, there are three steps in any alignment procedure. These are: (1) the prealignment survey, (2) cold alignment, and (3) the hot alignment check.

The Prealignment Survey

This survey is carried out well ahead of the cold alignment. In this survey; piping, grouting, foundation bolts, shim packs, etc., are studied and ascertained to be appropriately done and of good quality. Again, casing distortion, piping strain, misalignment

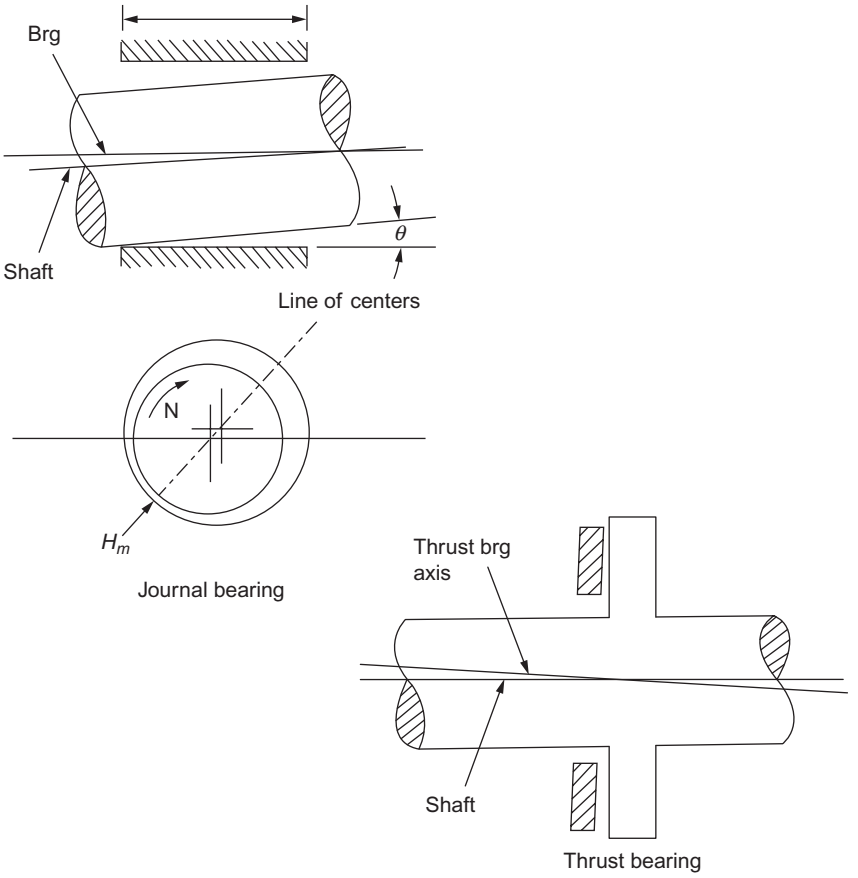


Figure 18-17 Misalignment in both journal and thrust bearings.

of machine supports relative to the sole plate, etc. are determined, and corrections are made to ensure that these problems will not cause problems with the alignment.

Piping strain is by far the greatest problem causer, and so piping should be carefully reviewed to ensure that it is properly done according to the code. Piping strains as high as 0.22 inches (0.5588 cm) have been observed.

A typical cause of piping strain occurs when two flanges do not meet and pipefitters force them together. Pipe hangers that are poorly placed or tensioned can also cause significant piping stress problems.

Cold Alignment

There are two predominant techniques used for cold alignment. These are: (1) the face-OD method, and (2) the reverse-dial indicator method. Both these techniques utilize dial indicators. For high-speed turbomachinery, the reverse-dial indicator method is the superior method and should be used.

Figure 18-18 shows a face-OD indicator setup. As the name indicates, an alignment bracket is attached to one coupling hub, and face-OD readings are taken on the adjacent hub. The face and OD dial indicator readings give an indication of the angularity and offset of the shafts, respectively. The problems with this method are numerous. First, there is the problem of shaft axial float, which makes consistent readings difficult to obtain. Second, inaccuracies in the geometry of the coupling hub have to be taken into account. Third, the face diameter on which the readings are taken is relatively small, and errors are magnified over the length of the machine. The reverse-dial indicator method is shown in Figure 18-19. This method measures just the OD of the coupling hubs or shaft and eliminates the problem of shaft axial float. By spanning the entire coupling, angular misalignment is greatly magnified. For both the face-OD and reverse-dial indicator methods, it is important that sag in the alignment bracket be determined. Figure 18-20 shows a method for the determination of sag. Once the sag is determined, it must be permanently stamped on the bar. The alignment bracket should be considered an important precision tool and must be stored and handled with care so that it may be reused when realignment is required.

Once the dial indicator readings are taken, a graphic plot of the two-shaft centerlines can be made on graph paper. It is at this stage that anticipated thermal growths are used in determining the shimming required to obtain shaft colinearity when the units are in the hot condition. Unfortunately, the values supplied by the manufacturers may not be accurate, and pipe strain and other external forces come into play. It is for this reason that the hot alignment check is conducted.

A simple graphic plotting exercise for the reverse-dial indicator method shows the basic principles involved. A steam turbine compressor train is shown in Figure 18-21. Assume this train is a new installation and the manufacturer's estimated thermal growths are as indicated in Figure 18-21. Reverse-dial indicator readings are taken to determine the relative shaft positions. Once readings are taken, the estimated thermal growths are incorporated by shimming, in the hope that a good, hot alignment can be achieved.

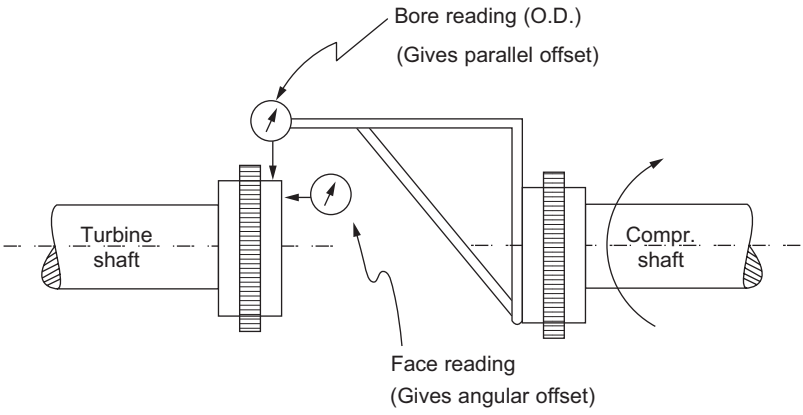


Figure 18-18 Face-OD indicator setup.

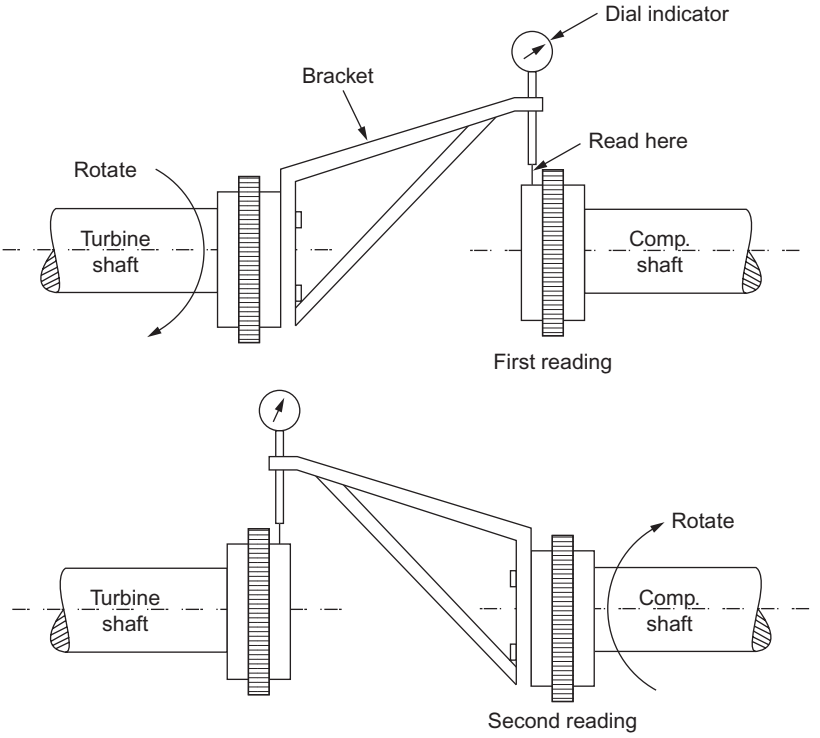


Figure 18-19 Reverse-dial indicator setup.

The hot alignment check is used to determine the actual thermal growth, and then the final shim changes are made if needed. This example addresses only vertical movements. Horizontal movements are obtained in a similar fashion. The graphic plot uses an amplified scale on the vertical *Y* axis of one inch equals five mils vertical growth, while the *X* axis has a scale of one inch equals 10 inches (25 cm) of train length.

In this example, it is assumed that Machine A is to be fixed, and all moves are to be conducted on Machine B. As shown in Figure 18-21, a "hot running line" is first drawn. This line is where the shafts should be when the machines are operating.

Now, using estimated thermal growth of Machines A and B, a "cold target B" line is drawn. This line is where shaft B should lie so that when hot it will be colinear with shaft A on the hot running line.

The next step is to use the dial indicator readings to determine where the shafts actually lie relative to each other. The B-to-A readings show that shaft B lies below shaft A by three mils (half-dial indicator readings) and the A-to-B reading shows that shaft A is above shaft B by five mils. Once these two points are located, shaft B can be plotted. This line is the "actual shaft B" line. Once this procedure is done, the shim changes needed can be easily found and "desired" indicator readings can be given to the millwrights.

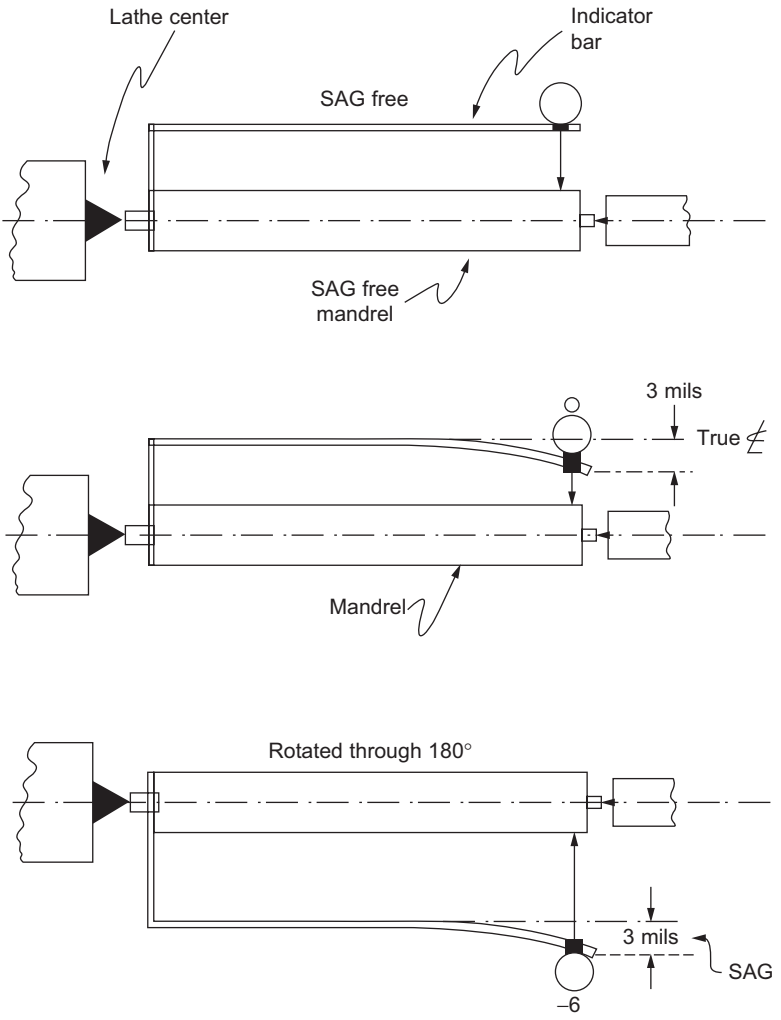


Figure 18-20 Method for determining sag.

A similar procedure is followed for horizontal movements. If the hot alignment check indicates a significant deviation from expected thermal growths and an unacceptable amount of misalignment, further shim changes can be achieved by similar plotting.

Hot Alignment Check

This technique attempts to determine actual alignment status when the machines are hot. When the machines are running, it is impossible to use dial indicator techniques on the shafts.

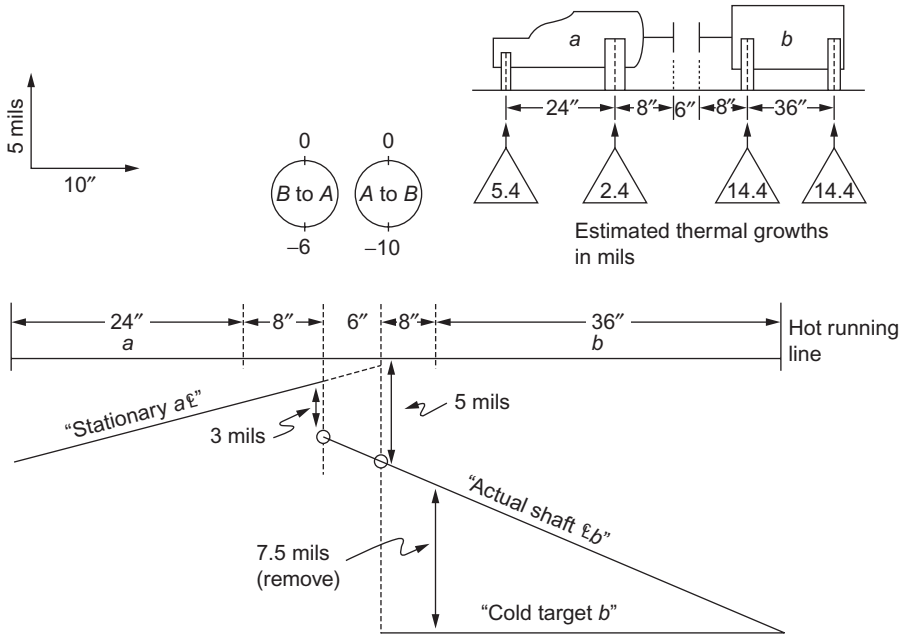


Figure 18-21 Graphic plotting for reverse-dial indicator method.

The old concept of a "hot check" – in which the units were shut down and the coupling disassembled as quickly as possible to allow indicator readings to be taken – should not be used. Currently used, continuously lubricated couplings require significant time to disassemble during which considerable cooling occurs. Because of this factor, a number of hot alignment techniques have been developed. Optical and laser methods, proximity probe methods, and a purely mechanical means using dial indicators may be used for hot alignment checks. In all these methods, an attempt is made to use the cold position of the shaft as a benchmark and then to measure the shaft movement (or bearing housings) from the cold position to the hot position. The objective is to find the change in vertical and horizontal positions at each shaft end. Once this procedure is done along the train, the machines can be shut down and appropriate shim changes made to attain acceptable hot alignment.

Basically, the optical method uses equipment such as alignment telescopes, jig transits, and sight levels. Instruments with built-in optical micrometers for measuring displacements from a referenced line of sight enable an accurate determination of target movements, which are mounted on the machine.

Optical alignment reference points are located on the bearing housings of the units. A jig transit is then set up at some distance from the train, and readings are taken and recorded in the vertical plane for each reference point in the train. Then the transit is moved, and a similar set of readings are taken in the horizontal plane. This procedure should be done at the same time as the reverse-dial indicator readings are taken. Then, when the train is in its operating condition, another set of readings are taken. The two

data sets and the cold alignment dial indicator readings enable the determination of vertical and horizontal growths of each point.

The advantages of this system are that it is accurate and, once the reference marks are on the machine, there is no need to approach the machine. However, the equipment involved is expensive and delicate, and great care has to be taken during its use. Moreover, heat waves often cause some problems in taking readings. Alignment with laser techniques has also been used, but the equipment is expensive and can be applied only in certain situations such as for a bearing alignment check. It is used primarily by manufacturers of turbomachinery during fabrication and assembly of their units.

Proximity probes have also been used to measure machine movements. Proximity probes are mounted in special water-cooled columns and aimed at "targets" mounted on bearing housings or on other parts of the unit. Changes in the gap distances are then displayed on electrical meters. The Dodd bar system utilizes proximity probes mounted on an air-cooled bar attached between the bearings of the two machines to be aligned. The Dodd bar system allows continuous monitoring of the relative positions of the two shafts. Another system uses proximity probes located within the coupling to continuously monitor the alignment. Digital readouts of misalignment angles, etc., are available from this system.

A purely mechanical, hot alignment system utilizing dial indicators has also been developed. The system uses permanently mounted tooling balls made of stainless steel attached to the bearing housing and to the machine foundation. A spring-loaded device with a dial indicator is provided to determine accurately the distance between the two tooling balls. An inclinometer is also provided to give a measure of the angularity. Figure 18-22 shows a typical configuration. Cold readings are taken at the time when the reverse-dial indicator readings are taken, and hot readings are taken when the machine is on-line. These two sets of readings are enough to determine the vertical and horizontal movement of the shaft. The same procedure is followed at each end of the units in the train. Computations can be made either graphically or by a calculator with preprogrammed cards. Direct outputs are the degree of misalignment and the shim changes needed to correct the misalignment.

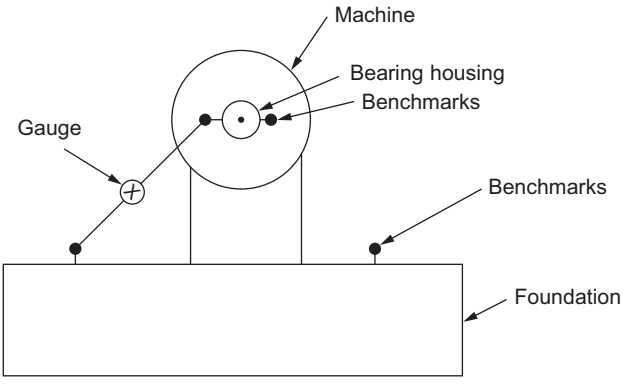


Figure 18-22 Hot alignment system with dial indicator.

It must be realized that correct alignment is of great importance in attaining high unit availability. Alignment procedures must be carefully planned, tools must be checked carefully, and, in general, great care must be taken during the alignment. The time, effort, and money spent on good alignment is well worth it.

Bibliography

Bendix Fluid Power Corp, "Contoured Diaphragm Couplings," *Technical Bulletin*.

Bloch, H.P., "Less Costly Turboequipment Uprates through Optimized Coupling Section," Proceedings of the 4th Turbomachinery Symposium, Texas A&M University, 1975, pp. 149–152.

Calistrat, M.M., "Gear Coupling Lubrication," American Society of Lubrication Engineers, 1974.

Calistrat, M.M., "Grease Separation under Centrifugal Forces, American Society of Mechanical Engineers, Pub. 75-PTG-3 1975.

Calistrat, M.M., "Metal Diaphragm Coupling Performance," Proceedings of the 5th Turbomachinery Symposium, Texas A&M University, October 1976, pp. 117–123.

Calistrat, M.M., and Leaseburge, G.G., "Torsional Stiffness of Interference Fit Connections," American Society of Mechanical Engineers, Pub. 72-PTG-37, 1972.

Calistrat, M.M., and Webb, S.G., "Sludge Accumulation in Continuously Lubricated Couplings," American Society of Mechanical Engineers, 1972.

Campbell, A.J., "Optical Alignment of Turbomachinery," Proceedings of the 2nd Turbomachinery Symposium, Texas A&M Univ., 1973, pp. 8–12.

Dodd, R.N., "Total Alignment Can Reduce Maintenance and Increase Reliability," Proceedings of the 9th Turbomachinery Symposium, Texas A&M University, 1980, pp. 123–126.

Essinger, J.N., "Benchmark Gauges for Hot Alignment of Turbomachinery," Proceedings of the 9th Turbomachinery Symposium, Texas A&M University, 1980, pp. 127–133.

Finn, A.E., "Instrumented Couplings: The What, the Why, and the How of the Indikon Hot Alignment Measuring System," Proceedings of the 9th Turbomachinery Symposium, Texas A&M University, 1980, pp. 135–136.

Jackson, C.J., "Alignment Using Water Stands and Eddy-Current Proximity Probes," Proceedings of the 9th Turbomachinery Symposium, Texas A&M University, 1980, pp. 137–146.

Jackson, C.J., "Cold and Hot Alignment Techniques of Turbomachinery," Proceedings of the 2nd Turbomachinery Symposium, Texas A&M University, 1973, pp. 1–7.

Kramer, K., "New Coupling Applications or Applications of New Coupling Designs," Proceedings of the 2nd Turbomachinery Symposium, Texas A&M University, October 1973, pp. 103–115.

Massey, C.R., and Campbell, A.J., "Reverse Alignment-Understanding Centerline Measurement," Proceedings of the 21st Turbomachinery Symposium, Texas A&M University, 1992, p. 189.

Peterson, R.E., *Stress Concentration Factors*, John Wiley & Son, 1953.

Timoshenko, S., *Strength of Materials: Advanced Theory & Problems,* 3rd ed. Van Nostrand Reinhold Pub., 1956.

Webb, S.G., and Calistrat, M.M., "Flexible Couplings," 2nd Symposium on Compressor Train Reliability, Manufacturing Chemists Association, April 1972.

Wilson, C.E., Jr., "Mechanisms – Design Oriented Kinematics," American Technical Society, 1969.

Wright, J., "A Practical Solution to Transient Torsional Vibration in Synchronous Motor Drive Systems," American Society of Mechanical Engineers, Pub. 75-DE-15, 1975.
Wright, J., "Which Flexible Coupling?" *Power Transmission & Bearing Handbook*, Industrial Publishing Co., 1971.
Wright, J., "Which Shaft Coupling Is Best – Lubricated or Non-Lubricated?" *Hydrocarbon Processing*, April 1975, pp. 191–196.

Copyrighted Materials
Copyright © 2012 Elsevier Retrieved from www.knovel.com

19 Control Systems and Instrumentation

Gas turbines operate over a large range of applications, primarily as drivers for generators in a power complex or drivers for large compressors and pumps in petrochemical complexes and offshore platforms. The power and the process requirements control the operations of the plant. In the case of power plants they are usually part of a major grid and they need to meet the demands of the grid, both in power and frequency. Control systems are also closely tied up with the distributed control systems (DCS) and condition monitoring systems (CMS) with plant optimization software.

The traditional concept of maintenance in the petrochemical and the utilities industries has been undergoing a major change; to ensure that equipment is the best available, but also is operating at its maximum efficiency. There is a consistent trend in these industries throughout the world to improve maintenance strategy from fix-as-fail to total performance-based planned maintenance. In practice, this calls for online monitoring and condition management of all major equipment in the plant. To reach the Utopian goal of just-in-time, maintenance with minor disruption in the operation of the plant, requires a very close understanding of the thermodynamic and mechanical aspects of plant equipment to be able to implement predictive maintenance programs.

Total performance-based planned maintenance not only ensures the best and lowest cost maintenance program but also makes sure that the plant is operated at its most efficient standard. An important supplementary effect is that the plant will be operating consistently within its environmental constraints.

Gas turbine instrumentation has expanded in the past few years from simple control systems to more complex diagnostic and monitoring systems that are designed to avert major catastrophes and operate a unit at its peak performance.

Control Systems

All gas turbines are provided with a control system by the manufacturer. The control system has three fundamental functions: start-up and shutdown sequencing, steady control when the unit is in operation, and protection of the gas turbine.

Control systems can be an open-loop or closed-loop system. The open-loop system positions the manipulated variable either manually or on a programmed basis, without

Gas Turbine Engineering Handbook, Fourth Edition. DOI: 10.1016/B978-0-12-383842-1.00019-6
Copyright © 2012 Elsevier Inc. All rights reserved.

using any process measurements. A closed-loop control system is one that receives one or more measured process variables and then uses it to move the manipulated variable to control a device. Most combined cycle power plants have a closed-loop control system.

Closed-loop systems include either a feedback or feedforward, control loop, or both to control the plant. In a feedback control loop, the controlled variable is compared with a set point. The difference between the controlled variable and the set point is the deviation for the controller to act and minimize the deviation. A feedforward control system uses the measured load or set point to position the manipulated variable in such a manner to minimize any resulting deviation.

In many cases, the feedforward control is usually combined with a feedback system to eliminate any offset resulting from inaccurate measurements and calculations. The feedback controller can either bias or multiply the feedforward calculation.

A controller has tuning parameters related to proportional, integrated, derivative, lag, deadtime, and sampling functions. A negative control loop will oscillate if the controller gain is too high, but if it is too low it will be ineffective. The controller must be properly related to the process parameters to ensure closed-loop stability while still providing effective control. This is accomplished first by the proper selection of control modes to satisfy the requirements of the process and second by the appropriate tuning of those modes. Figure 19-1 shows a typical block diagram for forward and feedback controls.

Computers have been used in the new systems to replace analog PID controllers, either by setting set points or lower level set points in supervisory control or by driving valves in direct digital control. Single-station digital controllers perform PID control in one or two loops, including computing functions such as mathematical operations, with digital logic and alarms. DCS provides all the functions, with the digital processor shared among many control loops. A high-level computer may be introduced to provide condition monitoring, optimizing, and maintenance scheduling.

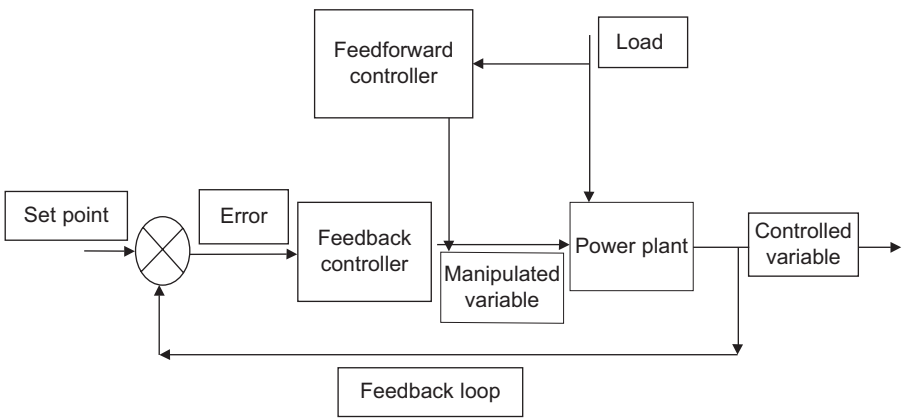


Figure 19-1 Feedforward and feedback control loop.

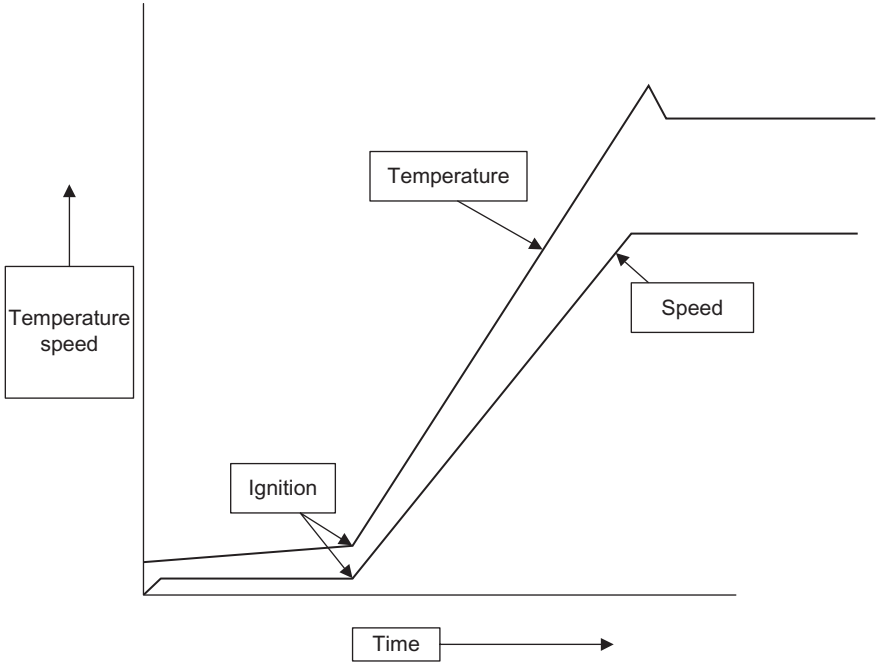


Figure 19-2 Start-up characteristics of a gas turbine.

The gas turbine control systems are fully automated, and ensure the safe and proper start-up of the gas turbine. The gas turbine control system is complex and has a number of safety interlocks to ensure the safe start-up of the turbine.

The start-up speed and temperature acceleration curves as shown in Figure 19-2 are examples of one such safety measure. If the temperature or the speed is not reached in a certain time span from ignition, the turbine will be shut down. In the early days when these acceleration and temperature curves were not used, the fuel which was not ignited, was carried from the combustor and then deposited at the first or second turbine nozzle, where the fuel combusted which resulted in the burnout of the turbine nozzles. After an aborted start, the turbine must be fully purged of any fuel before the next start is attempted. To achieve the purge of any fuel residual from the turbine, there must be about seven times the turbine volume of air that must be exhausted before combustion is once again attempted. The gas turbine is a complex system. A typical control system with hierarchic levels of automation is shown in Figure 19-3. The control system at the plant level consists of a DCS, which in many new installations is connected to a condition monitoring system and an optimization system. The DCS is considered to be a plant-level system and is connected to the three machine-level systems. In some cases, it can also be connected to functional level systems such as lubrication systems and fuel-handling systems. In those cases, it would give a signal of readiness from those systems to the machine-level systems. The condition

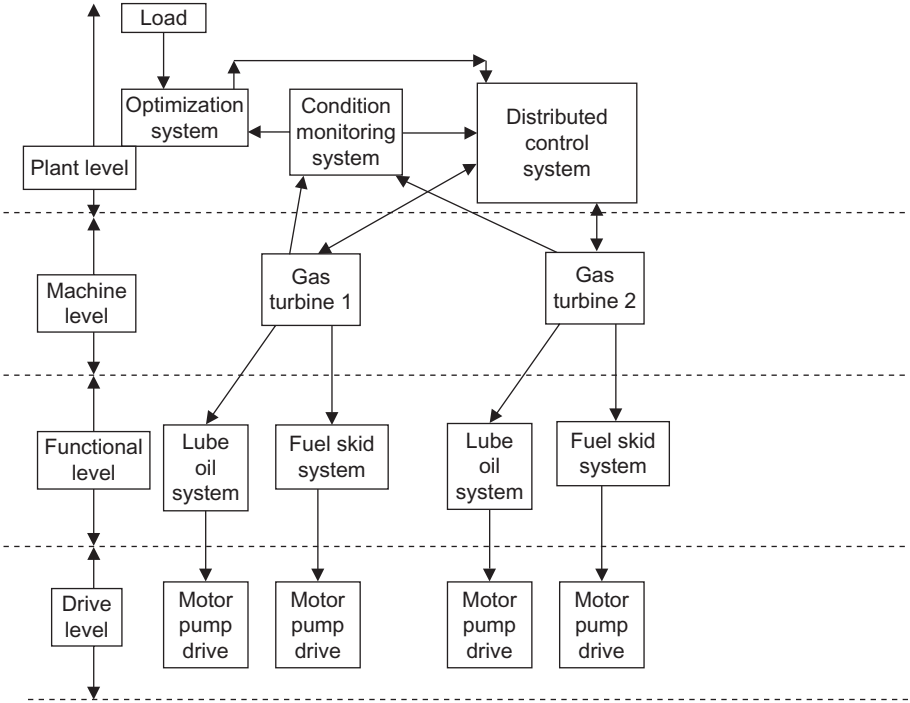


Figure 19-3 Hierarchic levels of automation.

monitoring system and the control system receive all their inputs from the DCS, and from the steam and gas turbine controllers. The signals are checked initially for their accuracy and then a full machinery performance analysis is provided. The new performance curves produced by the condition monitoring system are then provided to the optimization system. The optimization system, usually used where multiple turbines are used, receives the load and then sends a signal to the DCS system, which in turn sends the signal to the gas turbine for the best settings of the gas turbine to meet the load.

The gas turbine has a number of systems it controls such as the following:

1. *Lubrication skid.* The gas turbine lubrication skid is usually independent of the steam turbine skid as the lubrication oil is usually synthetic due to the high temperatures in the gas turbine. Another reason is due to water contamination of the lubrication oil from the steam turbine. It is advisable for the lubrication system to be totally independent. The gas turbine lubrication skid would report to the gas turbine controller. Since the lubrication system is also used for providing cooling, it is usually operated at about 20° minimum after the gas turbine is shutdown. The lubrication skid contains at least three pumps: two pumps in which each can provide the head required and a third pump that is usually recommended to be a DC drive for emergency use. These pumps and their control fall under the drive level hierarchy.
2. *The fuel skid.* This could contain a gas compressor if the fuel gas pressure is low and a knockout drum for any liquid contamination that the gas may have. The requirement of fuel

gas pressure is that it should be operated at a minimum of 50–70° psi (3.5–4.83° Bar) above the compressor discharge pressure. The compressor and its motor drive fall under the drive-level hierarchy. In the case of liquid fuels, the skid may also contain a fuel treatment plant, which would have centrifuges, electrostatic precipitators, fuel additive pumps, and other equipments. These could be directly controlled by the DCS system, which would then report its readiness to the gas turbine controller.

The control system requires inputs for speed determination, temperature control, flame detection, and vibration. The speed monitoring system receives an input from magnetic transducers in the form of an AC voltage with a frequency proportional to the rotational speed of the shaft. A frequency-to-voltage converter provides a voltage proportioned to speed, which is then compared with a set value. If the measured voltage is different from the reference voltage, a speed change is made. Typically, the desired speed can be manually set to a range between 80% and 105% of the design speed.

The temperature control receives its signals from a series of thermocouples mounted in the exhaust. The thermocouples are normally iron-constantan or chromel-alumel fully enclosed in magnesium oxide sheaths to prevent erosion. The thermocouples are frequently mounted with one for each combustion can. The output of the thermocouples is generally averaged into two independent systems with half of the thermocouples in each group. The output of the two systems is compared and used for decisions requiring a temperature input. This redundancy protects the system against tripping if a thermocouple fails.

The protective system is independent of the control system and provides protection from overspeed, over-temperature, vibration, loss of flame, and loss of lubrication. The overspeed protection system generally has a transducer mounted on the accessory gear or shaft and trips the gas turbine at approximately 10% of the maximum design speed. The over-temperature system has thermocouples similar to the normal temperature controls with a similar redundant system. The flame detection system consists of at least two ultraviolet flame detectors to sense a flame in the combustion cans.

In gas turbines with multiple cans, the detectors are mounted in cans not equipped with spark plugs to assure flame propagation between cans during start-up. Once the unit is running, more than one indicator must indicate a loss of flame to trip the machine, although the loss of flame in only one can is indicated on the annunciator panel.

Vibration protection can be based on either of the three measurement modes – acceleration, velocity, or displacement – but velocity is frequently used to provide constant trip levels throughout the operating speed range. Due to the problems encountered by velocimeters, many manufacturers, especially in aero-engines, have started using accelerometers. Two transducers are normally located on the gas turbine with additional transducers on the driven component. Vibration monitors are set to provide a warning at one vibration level with a trip at a higher level. Normally, the control system is designed to provide a warning in the event of an open circuit, ground, or short circuit

The gas turbine control loop controls the inlet guide vanes (IGV) and the gas turbine inlet temperature (TIT). The TIT is defined as the temperature at the inlet of

the first-stage turbine nozzle. Presently, in 99% of the units, the inlet temperature is controlled by an algorithm, which relates; the turbine exhaust temperature, or the turbine temperature after the gasifier turbine; the compressor pressure ratio, the compressor exit temperature, and the air mass flow to the turbine inlet temperature. New technologies are being developed to measure the TIT directly by the use of pyrometers and other specialized probes, which could last in these harsh environments. The TIT is controlled by the fuel flow and the IGV, which controls the total air mass flow to the gas turbine. In a combined-cycle power plant application, the turbine exhaust temperature is maintained at or near a constant, down to about 40% of the load.

All power plants are synchronized to the overall grid, and thus the operation of the plant at the given frequency is very important. The grid cannot stand many fluctuations of the plant frequency. It is, therefore, very important to operate the plant at its assigned frequency, which is 60 Hz in the United States as well as many countries in the Middle East. Europe and most of Asia are operating at a frequency of 50 Hz. If there is a frequency change, this must be taken care of in seconds.

Frequency response will be needed outside a dead band of ±0.1 Hz. The dead band is essential for stable operation of a plant; otherwise the plant could oscillate and plant failures have occurred due to a lack of a dead band. Frequency droop is a major problem in plants due to machinery degradation. The standard droop setting is about 5%, which means that a grid frequency drop of 5% would cause an increase in the load by 100%. Gas turbines can easily take swings of 20–30%, but large swings cause changes in firing temperature, which places a large strain on the hot section of the turbine. Gas turbines are rated for peak operation at about 10%–15% of their base load. It is therefore suggested that the gas turbine be operated at about 95% of the base load so that there is room for adjustment

Figure 19-4 shows the behavior of the gas turbine for changes in frequency as a standalone and also for changes as part of acombined cycle plant. The figure shows

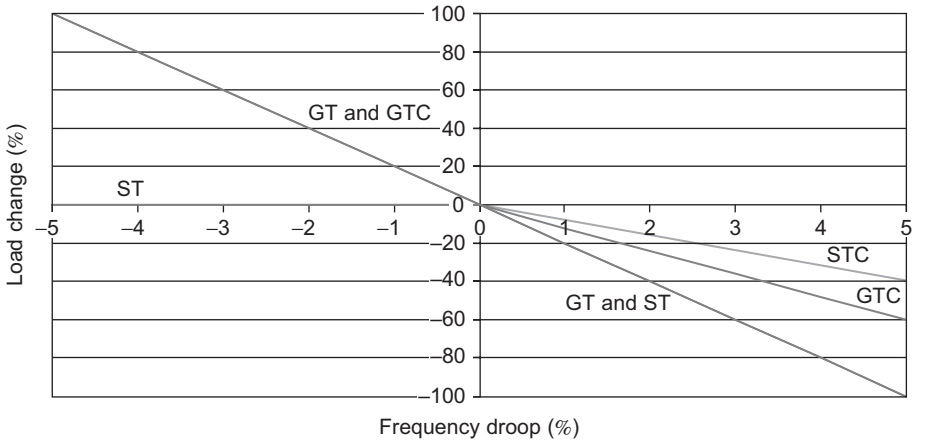


Figure 19-4 Droop curves for combined cycle power plants.

changes in the gas turbine plant (GT), the steam turbine plant (ST), and the gas turbine (GTC) and the steam turbine (STC) as part of a steam turbine plant. In a combined-cycle power plant, the falling frequency is usually taken up by the GTC, by a fast change in increasing the load, since the steam turbine cannot respond quickly enough. For an increasing frequency, both the gas turbine and the steam turbine can respond, thus, as shown in the figure, the gas turbine (60% load) and the steam turbine (40% load) take their appropriate change in load.

The start-up and shutdown of a typical gas turbine is shown in Figures 19-5 and 19-6, respectively. The time and percentages are approximate values and will vary depending on the turbine design.

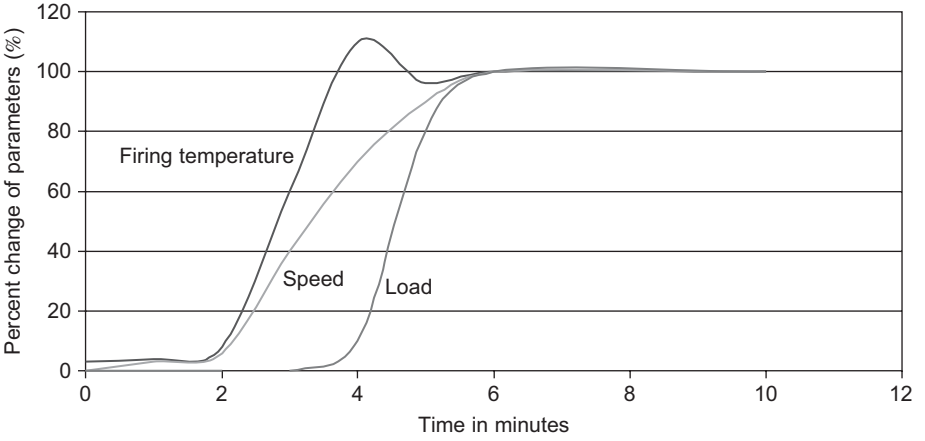


Figure 19-5 A typical start-up curve for a gas turbine.

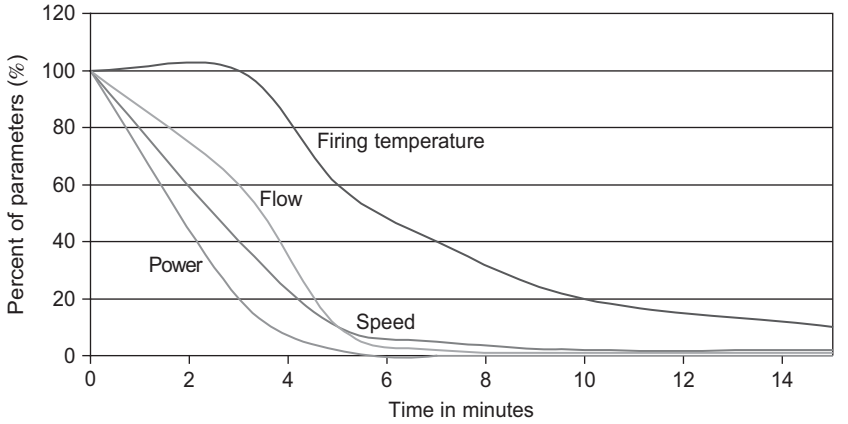


Figure 19-6 A typical shutdown curve for a gas turbine.

The gas turbine during the start-up is on an auxiliary drive; initially, it is brought to a speed of about 1,200–1,500 rpm when ignition takes place and the turbine speed and temperature rise very rapidly. The bleed valves are open to prevent the compressor from surging. As the speed reaches about 2,300–2,500 rpm, the turbine is de-clutched from its start-up motor, the first set of bleed valves are closed, and then as the turbine has reached near full speed, the second set of bleed valves are closed. If the turbine is a two- or three-shaft turbine as is the case with aero-derivative turbines, the power turbine shaft will "break loose" at a speed of about 60% of the rated speed of the turbine.

The turbine temperature, flow, and speed increase in a very short time of about 3–5 min to the full-rated parameters. There is usually a short period of time where the temperature may overshoot. If supplementary firing or steam injection for power augmentation is part of the plant system, these should be turned on only after the gas turbine has reached full flow. The injection of steam for power augmentation, if done before full load, could cause the gas turbine compressor to surge.

The shutdown of a gas turbine first requires the shutdown of the steam injection and then the opening of the bleed valves to prevent the compressor from surging as the speed is reduced. The gas turbine, especially for frame-type units, must be put on a turning gear to ensure that the turbine rotor does not bow. The lubrication systems must be on so that the lubrication can cool the various components; this usually takes about 30–60 min.

Start-up Sequence

One of the major functions of the combined control-protection system is to perform the start-up sequence. This sequence ensures that all subsystems of the gas turbine perform satisfactorily, and the turbine does not heat too rapidly or overheat during start-up. The exact sequence will vary for each manufacturer's engine, and the owner's and operator's manual should be consulted for details.

The gas turbine control is designed for remote operations to start from rest, accelerate to synchronous speed, automatically synchronize with the system, and be loaded in accordance with the start selector button depressed. The control is designed to automatically supervise and check as the unit proceeds through the starting sequence to load condition. A typical start-up sequence for a large gas turbine follows.

Starting Preparations

The steps necessary to prepare the services and apparatus for a typical start-up are as follows:

1. Close all associated control and service breakers.
2. If the computer has been de-energized, close the computer breaker, start the computer, and enter time of day. Under normal conditions, the computer is left running continuously.
3. Place maintenance switches to "Auto."
4. Acknowledge any alarm condition.
5. Check that all lockout relays are reset.
6. Position "Remote-Local" switch to desired position.

Start-up Description

When the unit is prepared to start, the "Ready to Start" lamp will be lit. With local control, operating one of the following push buttons will initiate a start:

1. Load minimum start.
2. Load base-start.
3. Load peak-start.

The master contactor function will accomplish the following:

1. Secondary auxiliary lube pump starter energized.
2. Instrument air solenoid valve energized.
3. Combustor-shell pressure transducer line drain solenoid valve energized.

When the auxiliary lube pump builds up sufficient pressure, the circuit to close the turbine gear starter will be completed. Thirty seconds are allowed for the lube pressure to build up or the unit will shut down. With the signal that the turning-gear line-starter is picked up, the sequence will continue. Next, the starting-device circuit is energized if lube oil pressure is sufficient. The turning-gear motor will be turned off at about 15% speed. When the turbine has reached the firing speed, the turbine overspeed trip solenoid and vent solenoid will be energized to reset. With the build up of overspeed trip oil pressure, the ignition circuit is energized.

The ignition will energize or initiate the following:

1. Ignition transformers.
2. Ignition time function (30 s allowed for establishing flame on both detectors or the unit will be shut down after several tries).
3. Appropriate fuel circuits (as determined from mode of fuel selected).
4. Atomizing air.
5. Ignition time function (to de-energize ignition at the proper time).

At approximately 50% speed, as sensed by the speed channel, the starting device is stopped. The bleed valves are closed near synchronous speed, each at a particular combustor-shell pressure. After fuel is introduced and ignition confirmed, the speed reference is increased at a preset variable rate and will determine the fuel valve position set point. The characterized speed reference and compressor inlet temperature will provide a feed-forward signal that will approximately position the fuel valves to maintain the desired acceleration. The speed reference will be compared with the shaft-speed signal and any error provides a calibration signal to ensure that the desired acceleration is maintained. This mode of control will be limited by the maximum blade path and exhaust temperatures corresponding to the desired turbine inlet temperatures. If desired acceleration is not maintained, the unit must be shut down. This control avoids many major turbine failures.

With the advance of the turbine to idle speed, the turbine is ready to synchronize, and control is considered in synchronization. Both manual and automatic synchronizings are available locally. The unit is synchronized and the main breaker is closed. The speed reference will be switched to become a load reference. The speed or load reference will be automatically increased at a predetermined rate so that the fuel valve will be at the approximate position required for the desired load. For maintenance

scheduling, the computer will count the number of normal starts and accumulate the number of hours at the various load levels.

Shutdown

Normal shutdown shall proceed in an orderly fashion. Either a local or a remote request for shutdown will first reduce the fuel at a predetermined rate until minimum load is reached. The main and field breakers and the fuel valves will be tripped. In an emergency shutdown, the main and field breakers and fuel valves will be tripped immediately without waiting for the load to be reduced to minimum. All trouble shutdowns are emergency shutdowns. The turbine will coast down and as the oil pressure from the motor-driven pump drops, the DC auxiliary lube oil pump will come on. At about 15% speed, the turning-gear motor will be restarted, and when the unit coasts to turning-gear speed (about 5 rpm), the turning-gear overrunning clutch will engage, allowing the turning-gear motor to rotate the turbine slowly. Below ignition speed, the unit may be restarted; however, the unit must be purged completely of any fuel. This is accomplished by moving through the turbine at least five times its total volume flow.

If left on turning gear, it will continue until the turbine exhaust temperature decreases to 150 °F (66 °C), and a suitable amount of time (up to 60 hours) has elapsed. At this point, the turning gear and auxiliary lube oil pump will stop, and the shutdown sequence is complete. On recognition of a shutdown condition, various contact status and analog values are saved (frozen) for display if desired.

Generator Protection

The generator protective relays are mounted in a switchboard, which usually houses the wattmeter and various transducers, unit cost teleductors, and optional watt-hour meters.

The basic generator protection equipment has the following items:

1. Generator differential
2. Negative sequence
3. Reverse power
4. Lockout relays
5. Generator ground relay
6. Voltage-controlled overcurrent relay

Condition Monitoring Systems

Predictive performance-based condition monitoring is emerging as a major maintenance technique, with large reduction in maintenance costs as shown in Figure 19-7. The histogram shows that although an approximate one-third reduction in operating and maintenance (O&M) costs was achieved by moving from a “corrective,” more realistically termed a “breakdown” or “fix-as-fail” repair strategy to a “preventive” regime, this yielded only approximately half of the maximum cost savings. Although more difficult to introduce than the simple scheduling of traditional maintenance activities required for preventive action, the Electric Power Research Institute (EPRI)

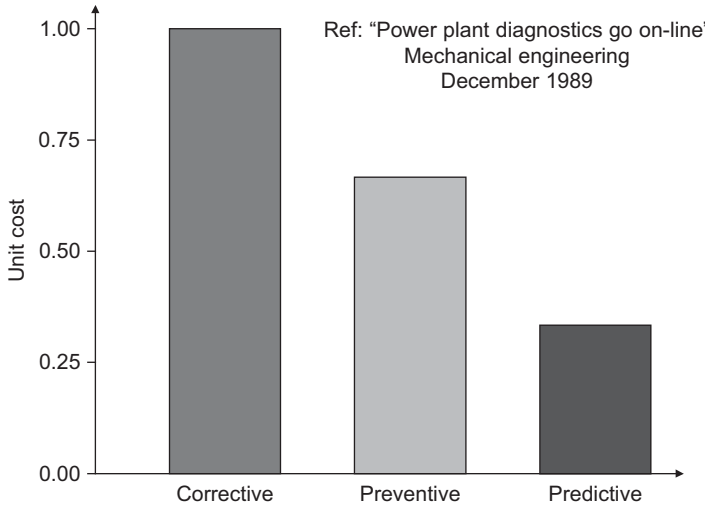


Figure 19-7 Comparison between various maintenance techniques (Rosen, 1989) .

research showed that the introduction of "predictive" maintenance strategies could yield a further one-third reduction in O&M costs.

The introduction of the total maintenance condition monitoring system means the use of composite condition monitoring systems, which combine mechanical and performance-based analysis with corrosion monitoring. These three components are the primary building blocks that enable the introduction of a comprehensive plant-wide condition management strategy. Numerous case studies have shown that many turbomachinery operational problems can only be diagnosed and resolved by correlating the representative performance parameters with mechanical parameters.

In plant health terms, monitoring and measurement both cost money and are only halfway to the real objective, which is the avoidance of cost and plant damage. Condition management makes proper use of both activities and exploits information derived from them to generate money for the plant operator. Good plant condition management, therefore, should be the objective of materials and machine health specialists.

The change has further implications: in the past, corrosion and condition monitoring were considered to be service activities, providing only a *reactive* strategy. Condition *management* embodies a *proactive* stance on plant health. This fundamental understanding should not go unrecognized by the materials and condition monitoring specialists. Condition management is a huge opportunity for technical specialists to provide the best possible service to clients, whether internal or external. The same specialists will also be able to derive the maximum direct benefit from their expertise.

Conventional alloy selection, coating specification, and failure investigation skills will always be required, as will inspection services to confirm the condition of the plant. However, the phenomenon labeled corrosion should no longer be regarded as a necessary evil as it is only a problem when out of control. The electrochemical

behavior characterizing corrosion is also the means by which online plant health management can be achieved.

Major power plant complexes contain various types of large machinery. Examples include many types of machinery, in particular gas and steam turbines, pumps and compressors with their effect on the heat recovery steam generators (HRSG), condensers, cooling towers, and other major plant equipment. Thus, the logical trend in condition monitoring is to multimachine train monitoring. To accomplish this goal, an extensive database, which contains data from all machine trains along with many composite multimachine analysis algorithms, is implemented in a systematic and modular form in a central system.

Implementation of advanced performance degradation models necessitate the inclusion of advanced instrumentation and sensors such as pyrometers for monitoring hot section components, dynamic pressure transducers for the detection of surges and other flow instabilities such as combustion, especially in the new dry low NO_x combustors. To fully round out a condition monitoring system the use of expert systems in determining faults and the life cycle of various components is a necessity.

Total performance-based planned maintenance not only ensures the best and lowest cost maintenance program but also makes sure that the plant is operated at its most efficient standard. An important supplementary effect is that the plant will be operating consistently within its environmental constraints.

The new purchasing mantra for the new utility plants is "life cycle cost" and to properly ensure that this is achieved a "total performance condition monitoring" strategy should be implemented.

To avoid excessive downtime and maintain availability, a turbine should be closely monitored and all data analyzed for major problem areas.

To achieve effective monitoring and diagnostics of turbomachinery, it is necessary to gather and analyze both the mechanical and aerothermal operating data from the machines. The instrumentation and diagnostics must also be custom tailored to suit the individual machines in the system and also to meet the requirements of the end users. The reason for this is that there can be significant differences in machines of the same type or manufacturer because of differences in installation and operation.

Requirements for an Effective Diagnostic System

1. The system must produce diagnostic and failure prediction information in a timely manner before serious problems occur on the machines monitored.
2. When equipment shutdown becomes necessary, diagnostics must be precise enough to accomplish problem identification and rectification with minimal downtime.
3. The system should be useable and understood well enough by production personnel so that an engineer is not always necessary when urgent decisions need to be made.
4. The system should be simple and reliable and cause negligible downtime for repairs, routine calibration, and checks.
5. The system must be cost effective; namely, it should cost less to operate and maintain than the expenses resulting from loss of production and machinery repairs that would have resulted if the machinery was not under monitoring and predictive surveillance.
6. System flexibility to incorporate improvements in the state of the art is desirable.

7. System expansion capabilities to accept projected increases in installed machinery or increases in the number of channels must be considered.
8. The use of excess capacity in a computer system available at the plant can result in considerable equipment cost savings. System components that mate with the existing computer system may, therefore, be a necessary prerequisite.

A condition monitoring system designed to meet these needs must comprise hardware and software designed by engineers with experience in machinery and energy system design, operation, and maintenance. Each system needs to be carefully tailored to individual plant and machinery requirements. The systems must obtain real-time data from the plant DCS and if required from the gas and steam turbine control systems. Dynamic vibration data are taken from the existing vibration analysis system into a data acquisition system. The system can comprise several high-performance networked computers depending on plant size and layout. The data must be presented using a graphic user interface (GUI) and include the following:

1. *Aerothermal analysis*. This pertains to a detailed thermodynamic analysis of the full power plant and individual components. Models are created of individual components, including the gas turbine, steam turbine heat exchangers, and distillation towers. Both the algorithmic and statistical approaches are used. Data are presented in a variety of performance maps, bar charts, summary charts, and baseline plots.
2. *Combustion analysis*. This includes the use of pyrometers to detect metal temperatures of both stationary and rotating components such as turbine blades. The use of dynamic pressure transducers is to detect flame instabilities in the combustor, especially in the new dry low NO_x applications.
3. *Vibration analysis*. This includes an online analysis of the vibration signals, FFT spectral analysis, transient analysis, and diagnostics. A wide variety of displays are available including orbits, cascades, bode and Nyquist plots, and transient plots.
4. *Mechanical analysis*. This includes detailed analysis of the bearing temperatures, lube, and seal oil systems and other mechanical subsystems.
5. *Corrosion analysis*. Online electrochemical sensors are being used to monitor changes in the corrosivity of flue gases, especially in exhaust stacks. The progressive introduction of ever-more stringent regulations to reduce NO_x emissions has resulted in an increase in the risk of water wall tube wastage in large power boilers, refinery process heaters, and municipal waste incinerators.
6. *Diagnosis*. This includes several levels of machinery diagnosis assistance available via expert systems. These systems must integrate both mechanical and aerothermal diagnostics.
7. *Trending and prognosis*. This includes sophisticated trending and prognostic software. These programs must clearly provide users with the ability to understand underlying causes of operating problems.
8. *"What-if" analysis*. This program should allow the user to do various studies of plant operating scenarios to ascertain the expected performance level of the plant due to environmental and other operational conditions.

Monitoring Software

The monitoring software for each system will be different. However, all software are there to achieve one goal – it must gather data, ensure that they are correct, and then

analyze and diagnose the data. Presentations must be in a convenient form and should be easily understood by plant operational personnel. All priorities must be to the data collection process. This process must not be hampered in any manner since it is the cornerstone of the whole system.

A convenient *framework* within which to categorize the software could be as follows:

1. *Graphic User Interface* (*GUI*). This consists of screens, which would enable the operator to easily interrogate the system and to visually see where the instruments are installed and their values at any point of time. By carefully designed screens, the operator will be able to view at a glance the relative positions of all values, thus fully understanding the operation of the machinery.
2. *Alarm/system logs*. To fully understand a machine we have to have various types of alarms. The following are some of the suggested types of alarms:
   - **(a)** *Instrument alarms*. These alarms are based on the instrumentation range.
   - **(b)** *Value range alarms*. These alarms are based on operating values of individual points both measured and calculated. These alarms should be variable in that they would change with operating conditions.
   - **(c)** *Rate of change alarms*. These alarms must be based on any rapid change in values in a given time range. This type of alarm is very useful to detect bearing problems, surge problems, and other instabilities.
   - **(d)** *Prognostic alarms*. These alarms must be based on trends and the prognostics based on those trends. It is advisable not to have prognostics which project more than the time of data that is trended.
3. *Performance maps*. These are performance maps based on design or initial tests (base lines) of the various machinery parameters. These maps, for example, present how power output varies with ambient conditions, properties of the fuel, or the condition of the filtration system; or how close to the surge line a compressor is operating. On these maps, the present value is displayed, thus allowing the operator to determine the degradation in performance occurring in the units.
4. *Analysis programs*. These include aerothermal and mechanical analysis programs, with diagnostics and optimization programs.
   - **(a)** *Aerothermal analysis*. Typical aerothermal performance calculations involve the evaluation of component unit power, polytropic and adiabatic head, pressure ratio, temperature ratio, polytropic and adiabatic efficiencies, temperature profiles, and a host of other machine-specific conditions under steady state as well as during transients – start-ups and shutdowns. This program must be tailored to individual machinery and to the instrumentation available. Data must be corrected to a base condition, so that it can be compared and trended. The base condition can vary from ISO ambient conditions to design conditions of a compressor or pump if those conditions are very different from ISO ambient conditions. To analyze off-design operation, it is necessary to transpose values from the operating points back to the design point for comparison of unit degradation.
   - **(b)** *Mechanical analysis*. This program must be tailored to the mechanical properties of the machine train under consideration. It should include bearing analysis, seal analysis, lubrication analysis, rotor dynamics, and vibration analysis. This includes the evaluation and correlation of bearing metal temperatures, shaft orbits, vibration velocity, spectrum snapshots, waterfall plots, stress analysis, and material properties.

(c) *Diagnostic analysis*. This program can be a part of an expert system or consist of an operational matrix, which can point to various problems. The program must include comparison of both performance and mechanical health parameters to a machine-specific fault matrix to identify if a fault exists. Expert analysis modules can in many cases aid to faster fault identification but are usually more difficult to integrate into the system.

(d) *Optimization analysis*. Optimization programs take into account many variables, such as deterioration rate, overhaul costs, interest, and utilization rates. These programs may also be dependent on more than one machine train if the process is interrelated between various trains.

(e) *Life cycle analysis*. The determination of the effect of the material, the temperature excursions, the number of start-ups and shut downs, and the type of fuel all relate to the life of hot section components.

5. *Historical data management*. This includes the data acquisition and storage capabilities. Present-day prices of storage mediums have been dropping rapidly, and systems with 80 GB hard disks are available.

These disks could store a minimum of 5 years of 1-min data for most plants. One-minute data are adequate for most steady state operation, while startups and shutdowns or other nonsteady state operation should be monitored and stored at an interval of 1 s. To achieve these time rates, data for steady state operation can be obtained from most plant-wide DCSs, and for unsteady state conditions, data can be obtained from control systems.

Implementation of a Condition Monitoring System

The implementation of a condition monitoring system in a major utilities plant requires a great deal of forethought. A major utilities plant will have a number of varied, large, rotating equipment. This will consist usually of various types of prime movers such as large gas turbines, steam turbines, compressors, pumps, electric generators, and motors. The following are some of the major steps that need to be undertaken to ensure a successful system installation:

1. The first decision is to decide on what equipment should be monitored online and what systems should be monitored off-line. This requires an assessment of the equipment in terms of both first cost and operating costs, redundancy, reliability, efficiency, and criticality.

2. Obtain all pertinent data of the equipment to be monitored. This would include details of the mechanical design and the performance design. Some of this information may be difficult to obtain from the manufacturer and will have to be calculated from data being obtained in the field or after installation during commissioning tests in a new installation. Obtaining baseline data is critical in the installation of any condition monitoring system. In most systems, it is the rate of change of parameters that are being trended and not the absolute values of these points. It is also important to decide what type of alarms will be attached to the various points. Rate of change alarms must be for bearing metal temperatures, especially for thrust bearings where temperature changes are critical. Prognostic alarms should be applied to critical points. Alarms randomly applied tend to slow down the system and do not provide added protection.

The following are some of the basic data that would be necessary in setting up a system:

(a) Type of gases and fluids used in the various processes: the equation of state and other thermodynamic relationships which govern these gases and fluids.

(b) Type of fuel used in the prime movers: if the fuel analysis is available including the fuel composition and the heating values of the fuel.

(c) Materials used in various hot sections such as combustor liners, turbine nozzles, and blades: this includes stress and strain properties, as well as Larson–Miller parameters.

(d) Performance maps of various critical parameters such as power and heat consumption as a function of ambient conditions, pressure drop in filters, and the effect of backpressure. Compressor surge, efficiency, and head maps.

3. Determine the instrumentation and its actual location. Location of the instrumentation from the inlet or exit of the machinery is important so that proper and effective compensation may be provided for the various measured parameters. In some cases, additional instrumentation will be needed. Experience indicates that older plants require 10–20% more instrumentation depending on the age of the plant.

4. Once the data points have been decided, limits and alarm must be set. This is a long and challenging task, as the limits on many points are not given in the operation manuals. In some cases, the criticality of the equipment may necessitate that the alarm threshold on certain points be lowered to give early warning of any deterioration of the system. It should be noted that since this is a condition monitoring system, early alarm warnings are desirable in most cases.

5. Types of reports and summary charts should be planned to optimize the data and to present it in the most useful manner to the plant operations and maintenance personnel.

6. The types of DCS and the control systems available in the plant: the protocol of these systems and their relationships to the condition monitoring system. The slave or master relationship is important in setting up the protocols.

7. Diagnostics for the system require noting any unusual characteristics of the machinery, especially in older plants, which have a history of operation inspections and overhauls.

8. Costs of operations, such as fuel costs, labor costs, downtime costs, overhaul hours, and interest rates, are necessary in computing parameters such as time of major inspections, off-line cleaning, and overhauls.

Plant Power Optimization

Online optimization processes for large utility plants are gaining tremendous favor. Plant optimization is gaining importance with combined-cycle power plants, as these plants are operated over a wide range of power in day-to-day running. Online optimization may be defined as the place where economics, operation, and maintenance meet. At first sight, it may be imagined that process integration is not connected to condition management or inspection, and this has been the case in the past. However, there is every incentive for complete integration of all these production-related technologies, since the condition monitoring of the various components in a plant are upgraded constantly; thus, the operational curves with degradation of each unit are no longer stagnant.

Process integration was developed initially as a means of optimizing the design of chemical and petrochemical process plants. Process optimization is still only a pre-construction or pre-production exercise. This is surprising because many process

plants are designed for batch manufacture of a range of products, each of which will require continuously changing optimization parameters. Process optimization and re-optimization "on the fly" can enable companies to meet variations in market demand and maximize production efficiency and overall profitability.

When embodied in a modern integrated plant environment, dynamic plant health assessment, process modeling, and process integration provide the means to augment plant reliability, availability, and safety with maximum capacity and flexibility.

Online Optimization Process

Figure 19-8 shows how online systems are configured. The system gathers data in real time. The data are gathered from either the DCS or the control system. Data for start-ups and transients are needed from the control system since the data from the

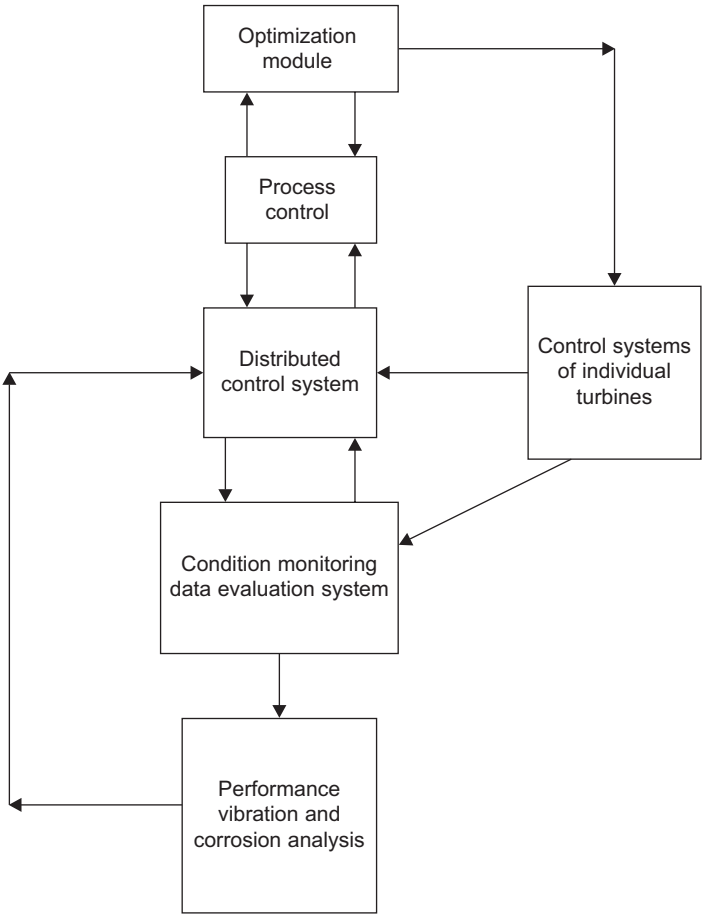


Figure 19-8 A block diagram for an online condition monitoring system.

DCS are usually updated every 3–4 s, while the control system can have very rapid loops, which are updated as often as 40 times/s. To ensure that performance data are taken at a steady state condition, since most models of the plant are at steady state, the system must observe some key parameters and ensure that they are not varying. In turbine parameters, such as turbine wheel space, temperatures should be observed to be constant. These data are then checked for accuracy and errors are removed. This involves simple checks against instrument operational ranges and system operation parameter ranges. The data are then fully analyzed, and various performance data checks are made. New operational and performance maps are then plotted and the system can then optimize itself against an operational model. The operational goal is to maximize the efficiency of the plant at all loads, thus the new performance maps, which show degradation of the plant, are then used in the plant model to ensure that the control is at the right setting for the operation of the plant at any given time. Many maintenance practices are also based on the rate of economic return. These operational maintenance practices, such as an off-line compressor wash, would contribute to the operations of the plant.

Many plants use off-line optimization. Off-line optimization is an open-loop control system. Instead of the closed-loop system, which controls the plant settings, data are provided to the operator so that he or she can make the decisions based on the findings of the operational data. Off-line systems are also used by engineers to design plants and by maintenance personnel to plan plant maintenance. Comparisons of the online systems with off-line systems is given in Table 19-1.

Performance evaluation is also important initially in determining that a plant meets its guarantee points and, subsequently, to ensure that it continues to be operated at or near its design operating condition. Maintenance practices are being combined ever more closely with operational practices to ensure that plants have the highest reliability with maximum efficiency. When a new plant is built, its cost amounts to only about 7–10% of the life cycle cost. Maintenance costs represent approximately

Table 19-1 Comparisons of Online and Off-Line Plant Optimization System Use

	Online Systems	**Off-Line Systems**
Objectives	Maximize economic benefit, operate the plant at its maximum efficiency at all operation points	Maximize economic benefit, operate the plant at its maximum efficiency at all operation points Optimize overall facilities design and investment
Target	Existing operating plant	Existing operating plant New facilities Facility expansion
Prime use	Process and maintenance operations	Process and maintenance operations Design modifications
Users	Operation and maintenance engineers	Operation and maintenance engineers Project and design engineers

15–20% overall. However, operating costs, which in the case of a power plant, for example, consist essentially of energy costs, make up the remainder, and amount to between 70% and 80% of the life cycle costs of the facility. This brings performance monitoring to the forefront as an essential tool in any type of plant condition monitoring system. Operating a plant as close as possible to its design conditions will guarantee that its operating costs will be reduced. As an illustration of the cost, this represents large fossil power plants currently being commissioned ranging from 600 to 2,800 MW. The fuel costs for these plants will amount between US$72 million and US$168 million per annum. Therefore, savings of 1–3% of these costs can amount to an overall cost reduction of upward of US$1 million per annum.

A change in approach is clearly necessary in order that the full benefit of integrated plant condition management and control can be recognized and exploited. Improved control and enhanced performance monitoring will enable shutdown intervals to be extended without increasing the risk of premature or unexpected failure. In turn, this will increase the confidence of operations, inspection, and management personnel in the effectiveness of unified plant administration.

Life Cycle Costs

The life cycle costs of any machinery are dependent on the life expectancy of the various components and the efficiency of its operation throughout its life. Figure 19-9 shows the cost distribution by the three major categories, initial costs, maintenance costs, and operating or energy costs. This figure indicates that the initial costs are about 7–10% of the life cycle costs, while maintenance costs are approximately 15–20% of the life cycle costs, and operating costs, which essentially consist of energy costs, make up the remainder; between 70% and 80% of the life cycle costs of any major machinery in a utilities plant. It is therefore clear why the new purchasing mantra for a utility plant, or for that matter, for any major plant operating large machinery, is "life cycle cost."

This brings performance monitoring to the forefront as an essential tool in any type of plant condition monitoring system. The major cost in a life cycle is the cost of energy. Thus, operating the plant as close to its design conditions guarantees that the plant will reduce its operating costs. This can be achieved by ensuring that the turbine compressor is kept clean and that the driven compressor is operating close to its maximum efficiency, which in many cases is close to the surge line. Thus knowing

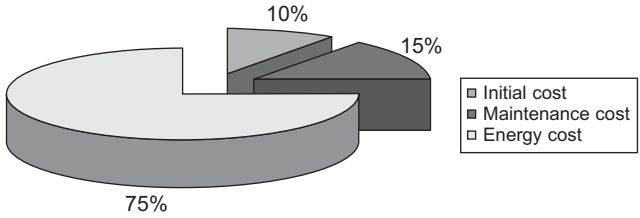


Figure 19-9 Life cycle costs for combined cycle power plants.

where the compressor is operating with respect to its surge line is a very critical component in plant operating efficiency.

The life expectancy of most hot section parts is dependent on various parameters and is usually measured in terms of equivalent engine hours. The following are some of the major parameters that effect the equivalent engine hours in most machinery, especially gas turbines:

1. Type of fuel.
2. Firing temperature.
3. Materials stress and strain properties.
4. Effectiveness of cooling systems.
5. Number of starts.
6. Number of trips.

Maintenance practices are being combined more and more with operational practices to ensure that plants have the highest reliability with maximum efficiency. This has led to the importance of performance condition monitoring as a major tool in the operation and maintenance of a plant. Life cycle costs, rightly so, now drive the entire purchasing cycle and thus the operation of the plant. Life cycle costs, based on a 25-year life, indicate that the following are the major cost parameters:

1. Initial purchase cost of equipment is 7–10% of the overall life cycle cost.
2. Maintenance costs are about 15–20% of the overall life cycle cost.
3. Energy costs are about 70–80% of the life cycle costs.

This distribution in life cycle costs indicates that component efficiency throughout the life period of the plant is the most important factor affecting the cost of a particular train. Thus, monitoring the efficiency of the train and ensuring that degradation rates are slowed down ensures that the predicted life cycle costs are achieved. Performance monitoring of the entire train is a must for plants operating on life cycle cost strategies.

Performance monitoring also plays a major role in extending life, diagnosing problems, and increasing time between overhauls. Online performance monitoring requires an in-depth understanding of the equipment being measured. Most trains are very complex in nature and thus require very careful planning in installation of these types of systems. The development of algorithms for a complex train needs careful planning and understanding of the machinery and process characteristics. In most cases, help from the manufacturer of the machinery would be a great asset. For new equipment, this requirement can be a part of the bid requirements. For plants with already installed equipment, a plant audit to determine the plant machinery status is the first step.

To sum up, total performance condition monitoring systems will help the plant engineers to achieve their following goals:

1. Maintaining high availability of their machinery.
2. Minimizing degradation and maintaining operation near design efficiencies.
3. Diagnosing problems, and avoiding operating in regions, which could lead to serious malfunctions.
4. Extending time between inspections and overhauls.
5. Reducing life cycle costs.

Diagnostic System Components and Functions

1. Instrumentation and instrumentation mountings
2. Signal conditioning and amplifiers for instrumentation
3. Data transmission system (cables, telephone link-up, or microwave)
4. Data integrity checking, data selection, data normalization, and storage
5. Baseline generation and comparison
6. Problem detection
7. Diagnostics generation
8. Prognoses generation
9. On-site display
10. Systems for curve plotting, documentation, and reporting

Data Inputs

Obtaining good data inputs is a fundamental requirement, since any analysis system is only as good as the inputs to the system. A full audit of the various trains to be monitored must be made to obtain optimum instrumentation selection. The factors that need to be considered are: the instrument type, its measurement range, accuracy requirements, and the operational environmental conditions. These factors must be carefully evaluated to select instruments of optimum function and cost to match the total requirements of the system. For instance, the frequency range of the vibration sensor should be adequate for monitoring and diagnostics and should match with the frequency range of analysis equipment. Sensors should be selected to operate reliably and accurately within the environmental conditions that prevail (e.g., when used on high-temperature turbine casings). Resistance temperature sensors, with their higher accuracy and reliability compared with thermocouples, may be necessary for analysis accuracy and reliability. Calibration of instrumentation should be conducted on a schedule established after reliability factors have been analyzed.

All data should be checked for validity and to determine whether they are within reasonable limits. Data that are beyond predetermined limits should be discarded and flagged for investigation. An unreasonable result or analysis should set up a routine for identification of possible discrepant input data.

Instrumentation Requirements

It is essential that instrumentation requirements be tailored to the requirements of the machine being monitored. However, the instrumentation requirements should exist to cover the requirements for both vibration and aerothermal monitoring.

Any existing instrumentation should be used if found to be adequate. Although there are advantages in the use of non-contacting sensors built into the machine for measurement of journal displacements, this instrumentation is often impossible to install in existing machinery. Suitably selected and located accelerometers can adequately cover the vibration monitoring requirements of machinery. Accelerometers are often an essential supplement to displacement sensors to cover the higher frequencies generated by gear mesh, blade passing, rubs, and other conditions.

Typical Instrumentation (Minimum Requirements for Each Machine)

(*Note*: Locations and type of sensors depend on the type of machine under consideration.)

1. Accelerometer
   - **(a)** At machine inlet bearing case, vertical
   - **(b)** At the machine discharge bearing case, vertical
   - **(c)** At machine inlet bearing case, axial
2. Process pressure
   - **(a)** Pressure drop across filter
   - **(b)** Pressure at compressor and turbine inlet
   - **(c)** Pressure at compressor and turbine discharge
3. Process temperature
   - **(a)** Temperature at compressor and turbine inlet
   - **(b)** Temperature at compressor and turbine discharge
4. Machine speed
   - **(a)** Machine speed of all shafts
5. Thrust-bearing temperature
   - **(a)** Thermocouples or resistance temperature elements embedded in front and rear thrust bearing

Desirable Instrumentation (Optional)

1. Non-contacting eddy-current vibration displacement probe adjacent to the following:
   - **(a)** Inlet bearing, vertical
   - **(b)** Inlet bearing, horizontal
   - **(c)** Discharge bearing, vertical
   - **(d)** Discharge bearing, horizontal
2. Non-contacting eddy-current gap-sensing probe adjacent to the following:
   - **(a)** Forward face of thrust-bearing collar
   - **(b)** Rear face of thrust-bearing collar (*Note*: The non-contacting sensor in its role of measurement of gap DC voltage is sensitive to probe and driver temperature variations. Careful evaluation must be conducted on sensor type, its mounting, and location for this measurement.)
3. Process flow measurement at inlet or discharge of machine
4. Radial-bearing temperature thermocouple or resistance temperature element embedded in each bearing, or temperature at lube oil discharge of each bearing.
5. Lube oil pressure, temperature, and corrosion probe
6. Dynamic pressure transducer at compressor discharge for indication of flow instability
7. Fuel system (water capacitance probe, corrosion probe, and BTU detector)
8. Exhaust gas analysis
9. Torque measurement

Figures 19-10 and 19-11 show possible instrument locations for an industrial gas turbine and centrifugal compressor.

Criteria for the Collection of Aerothermal Data

Turbomachinery operating pressures, temperatures, and speeds are very important parameters. Obtaining accurate pressures and temperatures will depend not only on

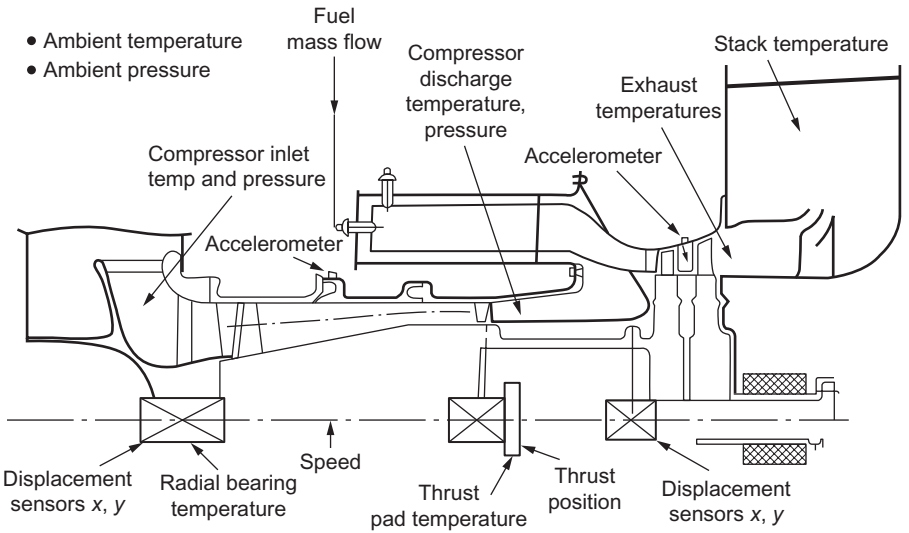


Figure 19-10 Instrumentation for monitoring and diagnostics on a gas turbine engine.

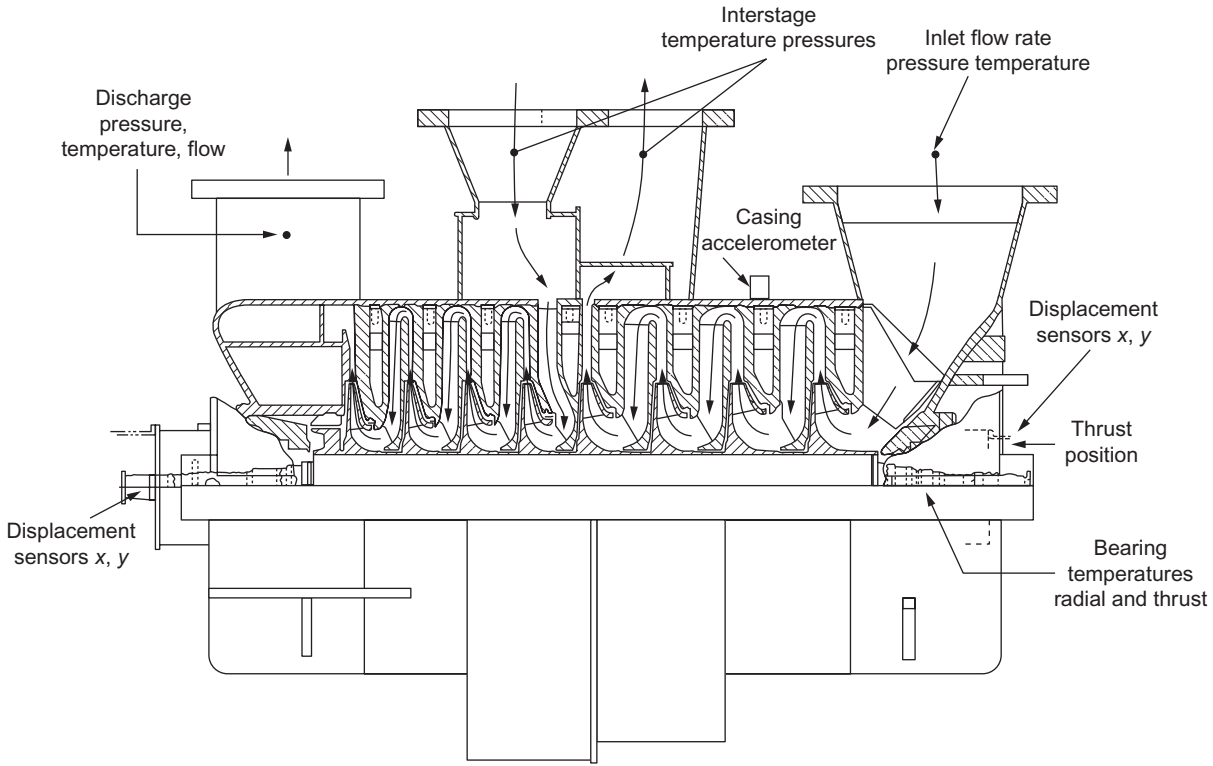


Figure 19-11 Instrumentation for monitoring and diagnostics on a centrifugal compressor.

Table 19-2 Criteria for Selection of Pressure and Temperature Sensors for Compressor Efficiency Measurements

Compressor Pressure Ratio P_2/P_1	P_2 Sensitivity (%)	T_2 Sensitivity (%)
6	0.704	0.218
7	0.750	0.231
8	0.788	0.240
9	0.820	0.250
10	0.848	0.260
11	0.873	0.265
12	0.895	0.270
13	0.906	0.277
14	0.933	0.282
15	0.948	0.287
16	0.963	0.290

Tabulation showing percent changes in P_2 and T_2 needed to cause 50% change in air compressor efficiency. Ideal gas equations are used.

the type and quality of the transducers selected but also on their location in the gas path of the machine. These factors should be carefully evaluated. The accuracy of pressure and temperature measurements required will depend on the analysis and diagnostics that need to be performed. Table 19-2 presents some criteria for selection of aerothermal instrumentation of pressure and temperature sensors for measurement of compressor efficiency. Note that the percentage accuracy requirements are more critical for temperature sensors than pressure sensors. The requirements are also dependent on the compressor pressure ratio.

Pressure Drop in Filter System

The prime design objective of the filter system is to protect the gas turbine. The performance of the gas turbine inlet-air filter system has important and far-reaching influences on overall maintenance costs, reliability, and availability of gas turbines. There are three major results of improper air filtration: (1) erosion, (2) fouling of the axial-flow compressor, and (3) corrosion of the gas turbine hot-gas path inlets. The importance of the inlet-air filter, as it relates to each of these three phenomena, can be appreciated if one considers that the gas turbine ingests about 7,000–9,000 cf (198.2179–254.8516 cm) of air per minute for every megawatt of power produced.

Temperature and Pressure Measurement for Compressors and Turbines

Temperature and pressure represent two of the major parameters measured and evaluated in a monitoring system. All gas turbine engines are equipped with sensors of this type; however, the exact number, as well as their location, varies considerably among manufacturers.

At each of the measurement locations, pressure probes may be attached to a harness, and these probes will direct the air flow to external pressure transducers for measurement while serving as a sheath for the appropriate thermocouple at that location (each thermocouple will be seated inside a pressure probe).

The electrical output of the thermocouple varies with temperature. This output is fed through a flexible cable to an external signal-conditioner circuit to amplify and condition the signal for interfacing to the monitoring system.

Temperature Measurement

Temperature measurement is important to gas turbine performance. Exhaust gas temperature should be monitored to avoid overheating turbine components. Most gas turbines are equipped with a series of thermocouples in their exhausts. Measuring turbine inlet temperature directly is very useful, but because of the turbine damage that results if a thermocouple breaks and passes through the turbine blades, thermocouples are not generally installed upstream of the turbine. Bearing oil temperature is normally monitored at the discharge to ensure proper oil characteristics; however, this temperature is not an accurate indication of bearing conditions, since bearings may develop localized hot spots during operation. To measure bearing temperature accurately, transducers should be located in the bearings themselves. The temperature will indicate problems in either journal or thrust bearings prior to damage. In addition to turbine exhaust temperatures, compressor inlet and discharge temperature measurement is necessary to evaluate compressor performance.

For most points requiring temperature monitoring, either thermocouples or resistive thermal detectors (RTDs) can be used. Each type of temperature transducer has its own advantages and disadvantages, and both should be considered when temperature is to be measured. Since there is considerable confusion in this area, a short discussion of the two types of transducers is necessary.

Thermocouples

The various types of thermocouples provide transducers suitable for measuring temperatures from −330 to 5000 °F (−201 to 2760 °C). The useful ranges for the various types are shown in Figure 19-12. Thermocouples function by producing a voltage proportional to the temperature difference between two junctions of dissimilar metals. By measuring this voltage, the temperature difference can be determined. It is assumed that the temperature is known at one of the junctions; therefore, the temperature at the other junction can be determined. Since the thermocouples produce a voltage, no external power supply is required to the test junction; however, for accurate measurement, a reference junction is required. For a temperature monitoring system, reference junctions must be placed at each thermocouple or similar thermocouple wire installed from the thermocouple to the monitor where there is a reference junction. Properly designed thermocouple systems can be accurate to approximately ±2 °F (±1 °C).

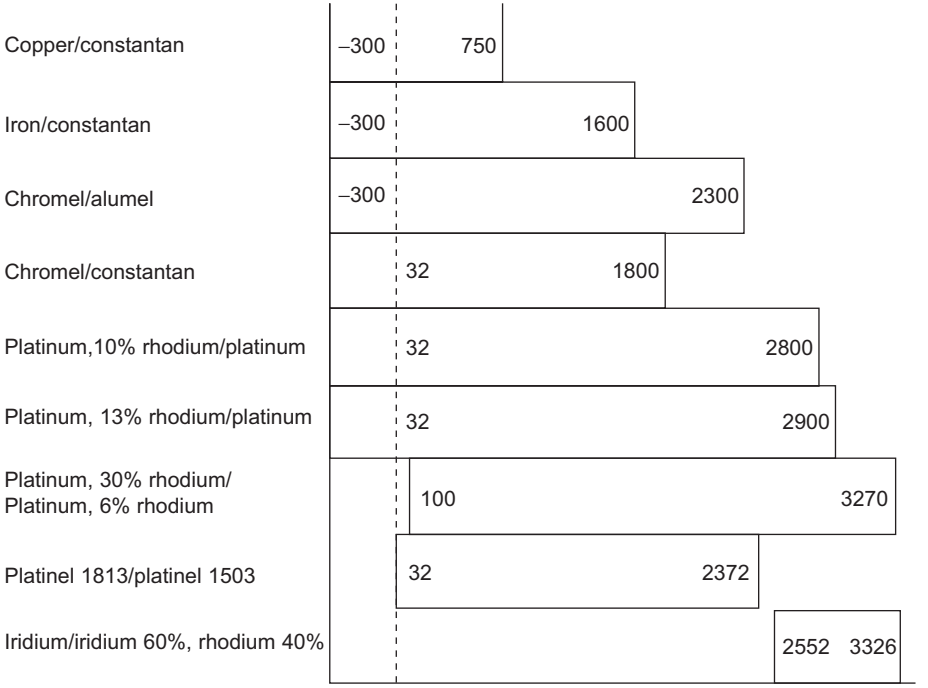


Figure 19-12 Ranges of various thermocouples.

Resistive Thermal Detectors

RTDs determine temperature by measuring the change in resistance of an element due to temperature. Platinum is generally utilized in RTDs, because it is mechanically and electrically stable, resists contamination, and can be highly refined. The useful range of platinum RTDs is −454 to 1832 °F (−270 to 1000 °C). Since the temperature is determined by the resistance in the element, any type of electrical conductor can be utilized to connect the RTD to the indicator; however, an electrical current must be provided to the RTD. A properly designed temperature monitoring system utilizing RTDs can be accurate to ±0.02 °F (±0.01 °C).

Pyrometers

The use of pyrometers in control of the advanced gas turbines is being investigated. Presently, all turbine controls are based on gasifier turbine exit temperatures or power turbine exit temperatures. By measuring the blade metal temperatures of the first-stage nozzles and blades, the gas turbine is being controlled at its most important parameter. In this manner, the turbine is being operated at its real maximum capability.

Gas turbines can be ordered with ports for pyrometer measurements of the first-stage nozzles and blades. Pyrometers have been able to detect which blade is running hot. In a particular case, a blade was found to be running about 50 °F (28 °C) hotter

than the rest of the blades. The blade on inspection was found to have its cooling passages blocked. This led the manufacturer to change its inspection techniques.

Pressure Measurement

Almost all gas turbines are equipped with pressure-measuring devices of some type, although the number and location may vary. These transducers consist of a diaphragm and strain gauges. When pressure is applied, the deformation of the diaphragm is measured by the strain gauges. The resulting output signal varies linearly with pressure changes over the operating range.

Because of temperature constraints, the transducers, which usually do not operate above 350 °F (177 °C), are located outside the engine. A probe is then located inside to direct the air into the transducer. Most manufacturers provide probes to measure the compressor inlet pressure, compressor exit pressure, and the turbine exhaust pressure. These probes are usually located along the shroud of the machine, and therefore, the pressure readings may be slightly in error due to boundary-layer effects.

In addition to these standard locations, it is recommended that probes be located at each bleed chamber in the compressor and on each side of the air filter. These new locations are not intended to measure the unit performance but are used to diagnose problem areas.

By using dynamic pressure probes in the bleed chamber, it is possible to detect tip stall. A pressure rake at the compressor exit enables accurate readings of exit pressure and is also helpful in the diagnosis of compressor stall.

Pressure transducers must be located outside of the engine because of temperature constraints. A pressure transducer can typically withstand temperatures up to 350 °F (177 °C), which is quite low with respect to the temperature of the points to be measured. The electrical output of the transducer will be in the millivolt/volt range and therefore must be amplified and conditioned for interfacing to the monitor system. The locations are as follows:

1. *Compressor inlet*. Unit is constructed of chromel-alumel (nickel alloy) and characterized by an exposed junction consisting of a bare wire with ceramic insulation. One unit is required here.
2. *Compressor discharge*. Same as compressor inlet thermocouples; one or two units required in this area.
3. *Turbine inlet temperature*. Thermocouple is constructed of platinum–platinum rhodium with the junction enclosed with ceramic insulation. Typically, 9–12 units are required at this stage.
4. *Turbine exhaust*. Thermocouple is constructed of chromel-alumel with an exposed junction. About 9–12 units are required at this stage.

Vibration Measurement

Vibration measurement is described in detail in Chapter 16. To monitor a machine for vibration problems, the use of displacement probes, velocity pickups, and accelerometers must be used to fully describe the mechanical behavior of a machine.

Displacement probes measure the movement of the shaft at the location of the probe. They cannot be used very successfully to measure a shaft bending away from the probe location. Displacement probes can indicate problems such as unbalance, misalignment, and some sub-synchronous vibration instabilities such as oil whirl and hysteretic whirl. Accelerometers, since they are mounted on the casing, pick up the spectrum vibration problems that are transmitted from the shaft to the casing. Accelerometers are used to diagnose many problems, especially those that have a high frequency response, such as blade flutter, dry frictional whirl, surge, and gear-teeth wear. Velocity pickups are used for their flat response of amplitude as a function of frequency as a go/no-go device. This means that the setting to alert the operator can be the same regardless of the speed of the unit. The role of velocity probes as diagnostic tools is somewhat limited. The velocity pickups are very directional – they read different values for the same force if the probe is placed in a different direction.

Charts are available to convert from one type of measurement to another as shown in Figure 19-13. Many of these charts also show approximate vibration limits. The charts demonstrate the independence of velocity measurements relative to frequency,

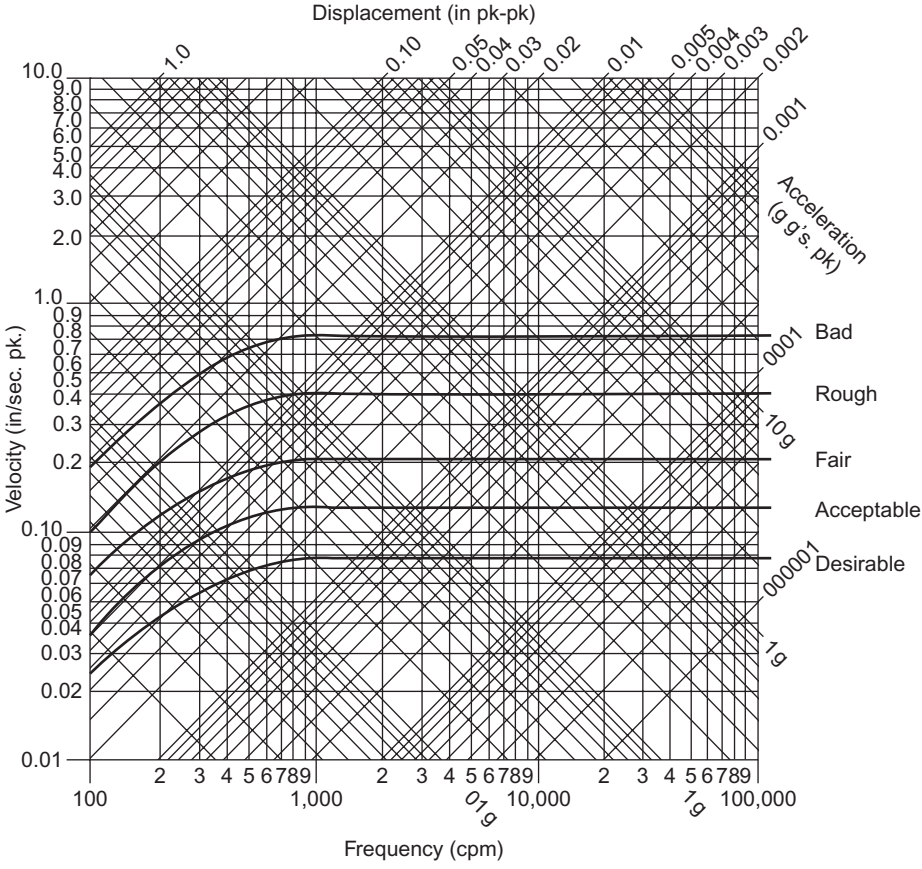


Figure 19-13 Vibration nomograph and severity chart (courtesy of IRD Mechanalysis, Inc.).

except at very low and very high frequencies where the amplitude limits are constant throughout the operating speed range. These limits are approximate – the type of machinery, casing, foundation, and bearings must be considered to determine final vibration limits.

Vibration Instrumentation Selection

The type of vibration instrumentation, its frequency ranges, its accuracy, and its location within, or on the machine, must be carefully analyzed with respect to the diagnostics required to be achieved. These guidelines have been previously discussed.

The displacement non-contacting eddy-current sensor is most effective for monitoring and measuring vibrations near rotational and sub-rotational speeds. Although the displacement sensor is capable of measuring vibration frequencies of more than 2 kHz, the amplitude of vibrational displacement levels that occur at frequencies above 1 kHz is extremely small and is usually lost or buried in the noise level of the readout system. The acceleration sensor is best suited for measurements at high frequencies, such as blade-passing and gear-meshing frequencies; however, the signals at one rotational speed are usually at low acceleration levels and may be lost in the noise level of the measurement system monitoring.

Low-pass filtering and additional amplification stages may, therefore, be necessary to bring out the rotational speed signals when measurements are made with accelerometers.

Velocity sensors, because of their limited operational frequency range (usually) from 10 Hz to 2 kHz, are not recommended for application in a diagnostic system for high-speed machinery. Velocity sensors have moving elements and are subject to reliability problems at operational temperatures of more than 250 °F (121 °C). Gas turbine engine casing temperatures are usually in the 500 °F (200 °C) level or above; hence, sensor locations must be carefully examined for temperature levels. Accelerometers for these higher temperatures are more easily available than velocity sensors. At these elevated operational temperatures, high-frequency accelerometers (20 kHz and above) are available from only a few selected manufacturers.

Selection of Systems for Analyses of Vibration Data

The overall vibration level on a machine is satisfactory for an initial or rough check. However, when a machine has a seemingly acceptable overall level of vibration, there may be some small hidden levels of vibrations under this level at discrete frequencies that are known to be dangerous. An example of this is sub-synchronous instabilities in a rotor system.

In the analysis of vibration data, there is often the need to transform the data from the time domain to the frequency domain or, in other words, to obtain a spectrum analysis of the vibration. The original and inexpensive system to obtain this analysis is the tunable swept-filter analyzer. Because of inherent limitations of this system, this process, despite the use of automated sweep, is time consuming when analyzing low frequencies. When the spectra data need to be digitized for computer inputing, there are further limitations in the capability of tunable filter-analysis systems.

Real-time spectrum analyzers using "time compression" or the "fast Fourier transform" (FFT) techniques are used extensively for performing vibration spectrum analysis in computerized diagnostic systems. The FFT analyzers use digital-signal processing and hence are easier to integrate with the modern digital computer. FFT analyzers are often hybrids using microprocessors and FFT-dedicated circuitry.

The FFT can be implemented in a computer using the FFT algorithm for obtaining a pure mathematical computation. Although this computation is an error-free process, its implementation in a digital computer can introduce several errors. To avoid these errors, it is essential to provide signal conditioning upstream of the computer. Such signal conditioning minimizes the errors, such as aliasing and signal leakage introduced in sampling and digitizing the time domain. Such signal conditioning systems will introduce considerable expense and complexity in effecting the mathematical FFT in a computer. The computerized FFT is also slower than a dedicated FFT analyzer. It also has limitations in frequency resolution. Hence, the use of a dedicated FFT analyzer is considered to be the most reliable and cost-effective means for performing frequency spectrum analysis and plots in a computerized system for machinery diagnostics.

Careful analysis must be made of the type of spectrum analysis systems and the computational techniques used in vibrational analysis. There are several factors that must be considered, some of which are as follows:

1. Frequency analysis ranges
2. Single or multichannel analysis
3. Dynamic range
4. Accuracy of measurements necessary
5. Speed at which analyses are required to be made
6. System portability, especially if the analysis system is required for both laboratory and field use
7. Ease of integration with the host computer system

Auxiliary System Monitoring

Fuel System

Since the reliability of gas turbines in the power industry has been lower than desired in recent years because of hot-corrosion problems, techniques have been developed to detect and control the parameters that cause these problems. By monitoring the water content and corrosive contaminant in the fuel line, any changes in fuel quality can be noted and corrective measures initiated. The concept here is that Na contaminants in the fuel are caused from external sources such as seawater; thus, by monitoring water content, Na content is automatically being monitored. This online technique is adequate for lighter distillate fuels. For heavier fuels, a more complete analysis of the fuel should be carried out at least once a month using the batch-type system. The data should be input directly to the computer. The water- and corrosion-detecting systems also operate in conjunction with the batch analysis for the heavier fuels.

A BTU meter may be used as an aid in determining turbine system efficiency in the fuel-quality system. A water capacitance probe is used for detection of water in the fuel line. A water-detecting device can be incorporated into the corrosion-monitoring system. This monitoring device is based on the detection of changes in the dielectric constant of unknown fluid components passing through the probe. This device provides continuous and instantaneous monitoring of the percentage of water suitable for quality or process control.

The sensor itself is based on a balanced capacitance bridge detection principle, utilizing a high-frequency oscillator with a closed-loop servo-amplitude control to assure that loading or variation in supply voltage does not affect the stability and accuracy of this instrument. Output from the bridge is directly coupled to a preamplifier to step up the detected signal to a desired level and, also, to correct for nonlinear characteristics of the water measurement. This measurement is achieved through a nonlinear feedback loop.

The corrected and amplified output is then directly coupled to a constant current amplifier, which can provide 0–5 mA or 4–20 mA output. This type of signal termination allows the detector system to be located at a distance from the measuring point for ease of usage. This water detection system offers (1) an accurate means of water measurement, (2) an easy installation and minimum maintenance, (3) a simple two-step calibration procedure, and (4) a long-term stability and dependable service.

A corrosion probe is used to monitor the corrosive condition of the fuel. This can be accomplished with a special probe that can detect metal in the lubricant. A BTU meter is used to determine the fuel heating rate. The BTU meter is a capacitance device ideally suited to real-time online BTU measurement of gas turbine liquid fuel, such as naphtha, that is a valuable asset in determining turbine efficiency.

Torque Measurement

This measurement can be accomplished by using a mechanical system or various types of electronic systems. All these systems are expensive and in many cases require repeated calibration. The mechanical system (Figure 19-14) is a three-gear, phase-related system that measures the displacement between two gears and the proportionate shaft twist. A third gear is situated so that any variations other than shaft twist will occur in the first two gears. This signal is used to eliminate errors caused by these variations.

Baseline for Machinery

Mechanical Baseline

The vibration baseline for a machine can be defined as the normal or average operating condition of a machine. It can be represented on a vibration spectrum plot showing vibration frequency on the *X*-axis and vibration amplitude (peak-to-peak displacement, peak velocity, or peak acceleration) on the *Y*-axis. Since the vibration spectrum will be different at different positions, the spectrum must be associated with a specific

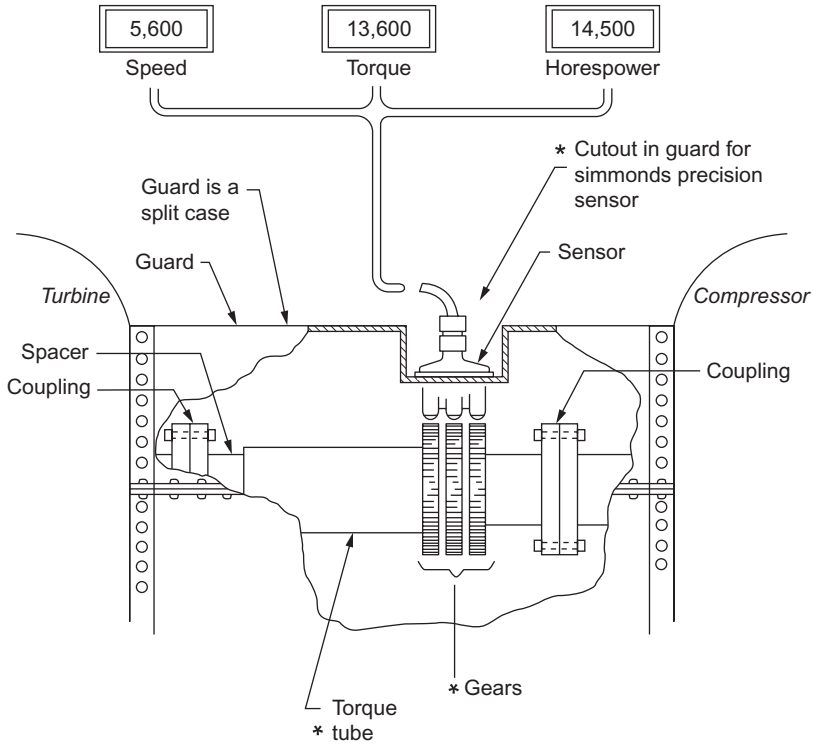


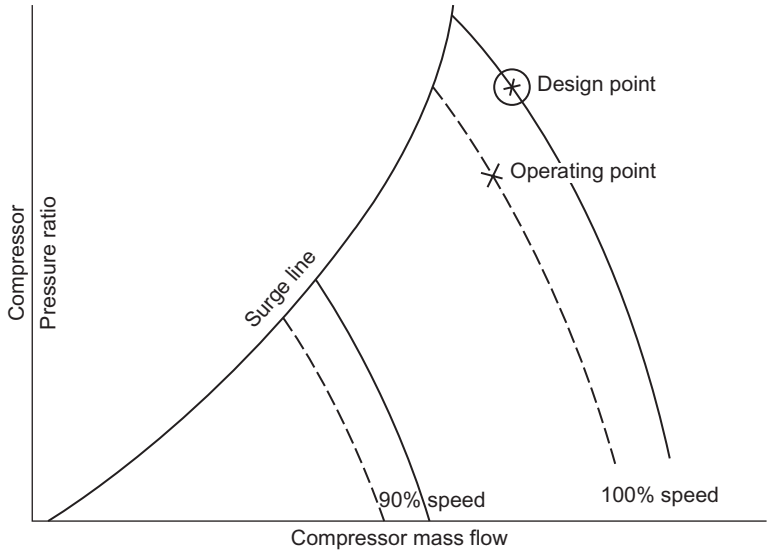
Figure 19-14 Torque meter for a gas turbine.

measurement position or sensor location on the machine. When portable vibration measurement equipment is used, it is essential to ensure that the sensor is relocated at exactly the same point on the machine each time vibration readings are taken. Changes of baseline with machine speed and process conditions should be investigated and, where necessary, baseline should be generated for set ranges of speeds and process conditions. When the operating vibration levels exceed the baseline levels beyond set values, an alert signal should be activated for investigation of this condition.

Aerothermal Baseline

In addition to the vibration baseline spectrum, a machine also has an aerothermal performance baseline or its normal operating point on the aerothermal characteristic. Significant deviation of the operating point beyond its base point should generate alert signals.

When a compressor operates beyond its surge margin, a danger alert should be activated. A typical compressor characteristic is presented in Figure 19-15. Some of the other monitoring and operating outputs are: loss in compressor flow, loss in pressure ratio, and increase in operating fuel cost due to, for instance, operating at off-design conditions or with a dirty compressor.



DATA INPUT

Ambient pressure
Compressor inlet pressure
Compressor discharge pressure
Compressor inlet temperature
Compressor discharge temperature
Compressor speed
Compressor inlet or discharge flow if available

DIAGNOSTICS OUTPUTS

Compressor efficiency lower than design
Compressor approaching surge conditions
Compressor approaching choke conditions
Dirty compressor

CONDITION MONITORING OUTPUTS

Loss in compressor flow through-put
Loss in compressor pressure ratio
Fuel cost penalty
Projected increase in fuel cost after one month operation
Surge point deterioration trend and anticipated outage date

Figure 19-15 Aerothermal condition monitoring for compressors.

Since aerothermal performance of compressors and turbines is very sensitive to inlet temperature and pressure variations, it is essential to normalize the aerothermal performance parameters such as flow, speed, horsepower, and so on, to standard-day conditions. When these corrections to standard conditions are not applied, a performance degradation may appear to occur when in fact it was a performance change resulting merely from ambient pressure and temperature changes. Some of the equations for obtaining correction to standard-day conditions are given in Table 19-3.

Data Trending

The data received should first be corrected for sensing errors. This usually consists of sensor calibration correction.

The trending technique essentially involves evaluating the slope of a curve derived from the received data. The slope of the curve is calculated for both a long-term trend,

Table 19-3 Gas Turbine Aerothermal Performance Equations for Correction to Standard-Day Conditions

Factors for Correction to Standard-Day Temperature and Pressure Conditions	
Assumed standard-day pressure	14.7 psia
Assumed standard-day temperature	60 °F (520 °R)
Conditions of test	
Inlet temperature	T_i °R
Inlet pressure	P_i psia

$$\text{Corrected compressor discharge temperature} = (\text{Observed temperature})\ (520/T_i)$$

$$\text{Corrected compressor discharge pressure} = (\text{Observed pressure})\ (14.7/P_i)$$

$$\text{Corrected speed} = (\text{Observed speed})\ \sqrt{520/T_i}$$

$$\text{Corrected air flow} = (\text{Observed flow})\ (14.7/P_i)\ \sqrt{T_i/520}$$

$$\text{Corrected horsepower} = (\text{Observed power})\ (14.7/P_i)\ \sqrt{T_i/520}$$

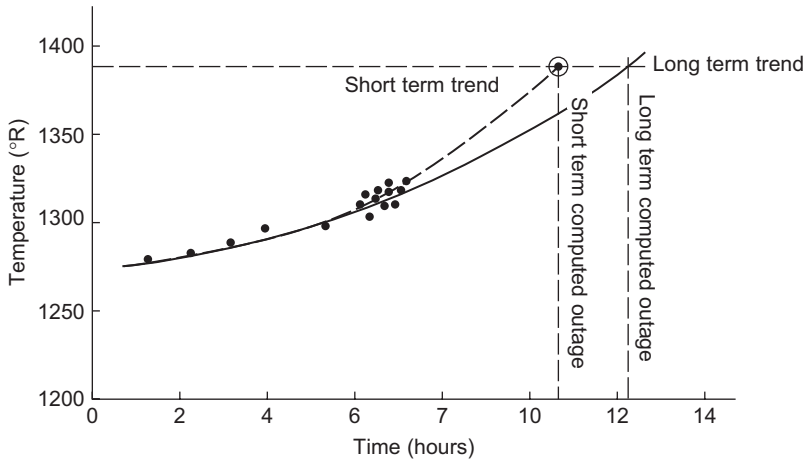


Figure 19-16 Temperature versus expected outage time.

about 168 hours, and a short-term trend, based on the last 24 hours. If the short-term slope deviates from the long-term slope beyond a set limit, it means that the rate of deterioration is changed and the maintenance schedule will be affected. Thus, the program might take into account the biasing of the long-term slope by the short-term slope. Figure 19-16 shows a schematic of this type of trending. Numerous statistical techniques are available for trending.

Trended data are used to obtain predictions that are helpful in the scheduling of maintenance. Referring to Figure 19-17, for example, it is possible to estimate when compressor cleaning will be necessary. This figure was prepared by recording the compressor exit temperature and pressure each day. These points are then joined, and a

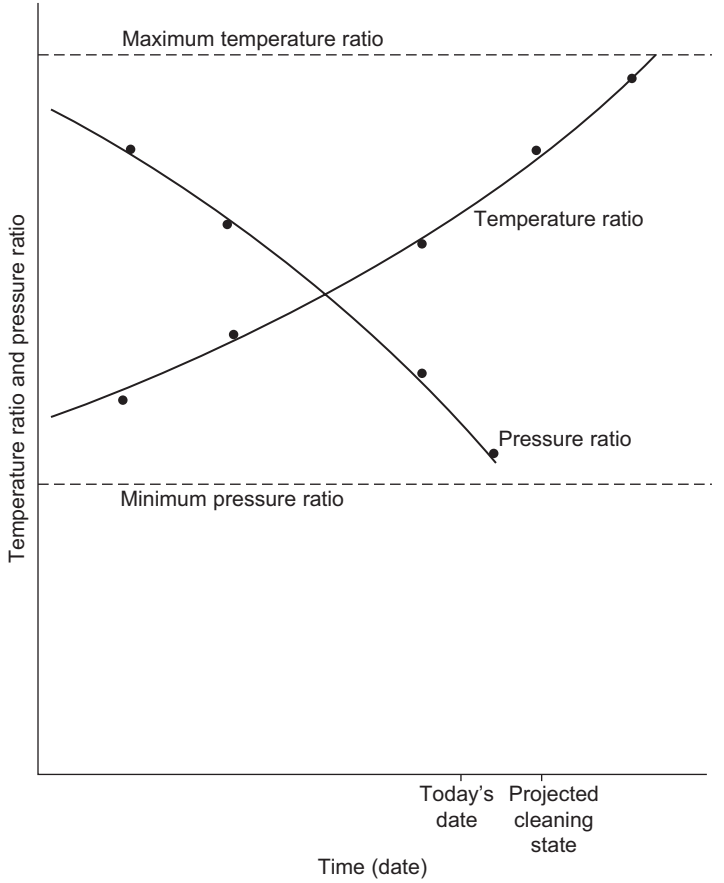


Figure 19-17 Data trending to predict maintenance schedules.

dotted line is projected to predict when cleaning will be required. In this case, two parameters were monitored, but since their rates differed, the cleaning was based on the first parameter to reach the critical point.

However, using a trend of both temperature and pressure provides a cross check on the validity of the diagnostics.

The Gas Turbine

The new gas turbines are the cornerstone of the rise of the combined cycle as the power source of the new millennium and for many other drives for petrochemical plants. The new gas turbines have a very high-pressure ratio, a high-firing temperature, and in some cases, a reheat burner in the gas turbine. The gas turbines also have new

dry low NO_x combustors. The combination of all these components has dramatically increased the thermal efficiency of the gas turbine. The gas turbine since the early 1960s has gone from efficiencies as low as 15–17% to around 45%. This has been due to the pressure ratio increase from around 7:1 to as high as 30:1 and an increase in the firing temperature from about 800 °C to about 1350 °C. With these changes, we have also seen the efficiency of the major components in the gas turbine increase dramatically. The gas turbine compressor efficiency increased from around 78% to 87%; the combustor efficiency from about 94% to 98%, and the turbine expander efficiency from about 84% to 92%.

The increase in compressor pressure ratio decreases the operating range of the compressor. The operating range of the compressor stretches from the surge line at the low flow end of the compressor speed line to the choke point at the high flow end. As shown in Figure 19-18, the lower pressure speed line has a larger operational range than the higher pressure speed line. Therefore, the higher pressure ratio compressors are subject to fouling and can result in surge problems or blade-excitation problems, which lead to blade failure.

The drop in pressure ratio at the turbine inlet due to filter fouling amounts to a substantial loss in the turbine overall efficiency and the power produced. An increase in the pressure drop of about 1 in. (25 mm) WC amounts to a drop of about 0.3% reduction in power. Table 19-4 shows the approximate changes that would occur for changes in ambient conditions; the fouling of the inlet filtration system, and the increase in backpressure on the gas turbine in a combined-cycle mode. These modes were selected because these are the most common changes that occur on a system in the field. It must be remembered that these are just approximations and will vary for individual power plants.

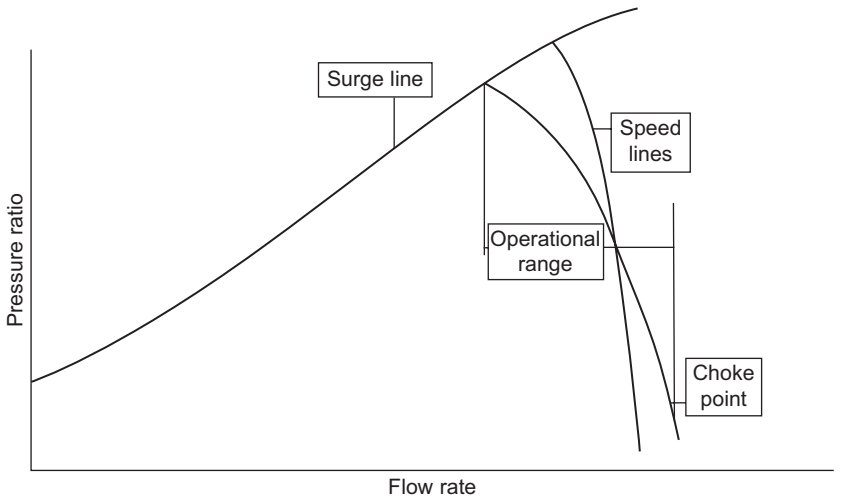


Figure 19-18 Performance map of an axial-flow compressor used in most gas turbines.

Table 19-4 Effect of Various Parameters on the Output and Heat Rate

Parameters	Parameter Change	Power Output (%)	Heat Rate Change (%)
Ambient temperature	20 °F (11 °C)	−6.5	2
Ambient pressure	4 in. H_2O 0.15 psi 10 mbar	0.9	0.9
Ambient relative humidity	10%	−0.0002	0.0005
Pressure drop in filter	1 in (25 mm) WC	−0.5	−0.3
Increase in gas turbine Backpressure	1 in WC 25 mm WC	−0.25	−0.08

The gas turbine has to be operated at a constant speed since this is used for power generation, and any slight variation in speed could result in major problems for the grid. Thus, the control of the load has to be done by controlling the fuel input, therefore the turbine firing temperature, and the inlet guide vane position, thus controlling the airflow. The effect of this is to try and maintain the exhaust temperature from the gas turbine at a relatively high value, especially in combined-cycle or cogeneration plants, since this gas is used in the HRSG, the effectiveness of the HRSG is dependent on maintaining this temperature.

The effect of compressor fouling is also very important on the overall performance of the gas turbine since it uses nearly 60% of the work generated by the gas turbine. Therefore, a 1% drop in compressor efficiency equates to nearly a 0.5% drop in the gas turbine efficiency and about a 0.3% drop in the overall cycle efficiency. The cleaning of these blades by online water washing is a very important operational requirement. In many plants, this operational procedure has contributed literally hundreds of thousands of dollars to the bottom line of the plant. It has been the experience of many plants that washing using demineralized water is as effective as using a detergent in online water wash. The practice of using abrasive cleaning by injecting walnut shells, rice, or spent catalyst is being suspended in most new plants. Where it is used, it must be carefully evaluated; rice for instance is a very poor abrasive since it shatters and tends to get into seals and bearings and into the lubrication system. Walnut shells should never be used since they tend to collect inside the HRSG system, and in some cases, have been noted to catch fire. Online water washing is not the answer to all the problems since after each wash the full power is not regained; therefore, a time comes when the unit needs to be cleaned off-line. The time for off-line cleaning must be determined by calculating the loss of income in power, as well as the cost of labor to do so, and equating it against the extra energy costs. The cleaning of the hot section turbine nozzles is a major problem in turbines, which use heavy liquid fuels with high vanadium content. To counteract the vanadium, the fuel is treated with the addition of magnesium, which is supposed to mix with the vanadium and results in harmless fly ash. The problem occurs when the fly ash gets collected in the turbine nozzles and reduces the turbine nozzle areas. This can be a very major problem since it collects at the rate of 5–12% per 100 hours of operation.

The life of the various hot section components of the gas turbine depends on the following operational parameters:

1. *Type of fuel.* Natural gas is the base fuel against which all other fuels are measured. The use of diesel fuel reduces the average life by about 25%, and the use of residual fuel reduces life by as much as 65%.
2. *Type of service.* Peaking service tends to reduce life by as much as 20% as compared with base load operation.
3. *Number of starts.* Each start is equivalent to about 50 hours of operation.
4. *Number of full-load trips.* This is very hard on the turbine and is nearly equivalent to about 400–500 hours of operation.
5. *Type of material.* The properties of the blade and nozzle vanes are a very important factor. The new blade materials, which are the single crystal structures, have done much to help the life of these blades in the higher temperatures, which are used in these new turbines. It must be remembered that if more than about 8% of the air is used in cooling then the advantage of going to higher temperatures is lost. The Larson–Miller parameters, which describe an alloy's stress rupture characteristics over a wide range of temperature, life, and stress, are very useful in comparing the elevated temperature capabilities of many alloys.
6. *Types of coatings.* The use of coatings in both compressor and turbines has extended the life of most of the components. Coatings are also being used on combustor liners. The new overlay coatings are more corrosion resistant as compared with the old diffusion coatings. The coatings of the compressor are now more prevalent, especially since some of the new compressors are operating at very high-pressure ratios, which translate into high exit temperatures from the compressor. Compressor coatings also tend to reduce the frictional losses and can have a very rapid payback.

Identification of Losses

The losses that are encountered in a plant can be divided into two groups: uncontrollable losses and controllable losses. The uncontrollable losses are usually environmental conditions, such as temperature, pressure, humidity, and turbine aging. The controllable losses are those that the operator can have some degree of control over and can take corrective actions:

1. *Pressure drop across the inlet filter.* This can be remedied by cleaning or replacing the filter.
2. *Compressor fouling.* Online water cleaning can restore part of the drop encountered.
3. *Fuel lower heating value.* In many plants, online fuel analyzers have been introduced not only to monitor the turbine performance but also to calculate the fuel payments, which are usually based on the energy content of the fuel.
4. *Turbine backpressure.* In this case, the operator is relatively limited since he/she cannot do anything about the downstream design if there is some obstruction in the ducting to the HRSG that can be removed or if the duct has collapsed in an area the duct could be replaced.

Compressor Aerothermal Characteristics and Compressor Surge

Figure 19-19 shows a typical performance map for a centrifugal compressor, showing efficiency islands and constant aerodynamic speed lines. The total pressure ratio can be seen to change with flow and speed. Usually, compressors are operated on a working line separated by some safety margin from the surge line. Compressor surge is

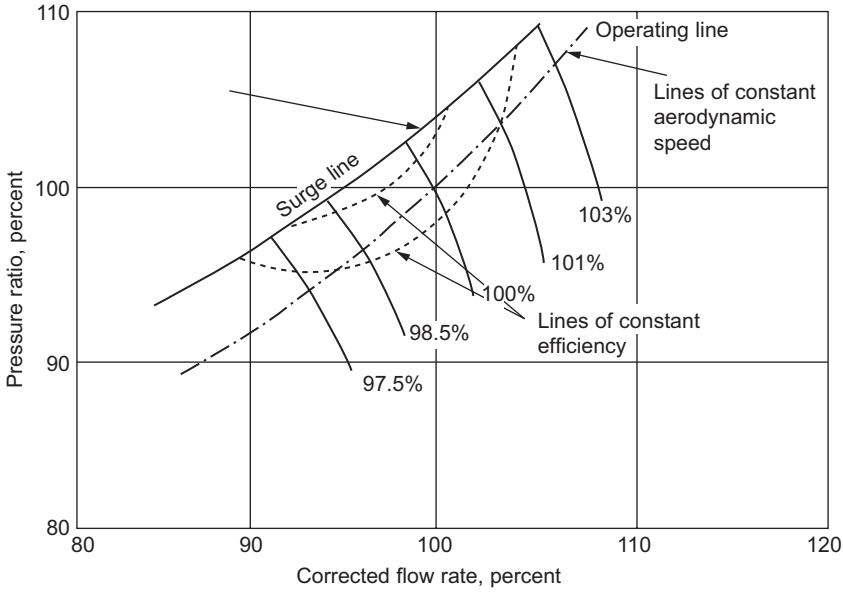


Figure 19-19 Typical compressor map.

essentially a situation of unstable operation and should, therefore, be avoided in both design and operation. Surge has been traditionally defined as the lower limit of stable operation of a compressor and involves the reversal of flow. This reversal of flow occurs because of some kind of aerodynamic instability within the system. Usually, it is a part of the compressor that is the cause of the aerodynamic instability, although it is possible that the system arrangement could be capable of magnifying this instability.

Usually, surge is linked with excessive vibration and an audible sound; yet, there have been cases in which surge problems, which are not audible, have caused failures.

Failure Diagnostics

Problem evaluation in turbomachinery is complex, but with the aid of performance and mechanical signals, solutions can be found to diagnose various types of failures. This is done by using several inputs and a matrix. Samples of some of the problems are given in the next few sections.

Compressor Analysis

Compressor analysis is done by monitoring the inlet and exit pressures and temperatures, the ambient pressure, vibration at each bearing, and the pressure and temperature of the lubrication system. Table 19-5 shows the effect various parameters have on some of the major problems encountered in a compressor. Monitoring these parameters allows the detection of the following:

1. *Clogged air filter.* A clogged air filter may be detected by noting an increase in the pressure drop through the filter.
2. *Compressor surging.* Surge may be detected by noting a rapid increase in shaft vibration, along with a discharge pressure instability. If more than one stage is present, the probes located within the bleed air chambers are useful in locating the problem stage by checking for pressure fluctuations.
3. *Compressor fouling.* This is indicated by a decrease in pressure ratio and flow accompanied by an increase in exit temperature with time. The change in the temperature and pressure ratio tends to show a decrease in efficiency. If a change in vibration has occurred, the fouling is critical, since it indicates excessive buildup of deposits on the rotor.
4. *Bearing failure.* Symptoms of bearing trouble include a loss of lubrication pressure, an increase in the temperature difference across the bearing, and an increase in vibration. If oil whirl or other bearing instabilities are present, there will be a vibration at sub-synchronous frequency.

Combustor Analysis

In the combustor, the only two parameters that can be measured are fuel pressure and evenness of combustion noise. Turbine inlet temperatures are not usually measured due to very high temperatures and limited probe life. Table 19-6 shows the effect of various parameters on important functions of the combustor.

Table 19-5 Compressor Diagnostics

	η_c	P_2/P_1	T_2/T_1	Mass Flow	Vibration	T Bearing	Bearing Pressure	Bleed Chamber Pressure
Clogged filter		↓		↓				
Surge	↑	Variable		↓	Highly fluctuating	↑	↑	Highly fluctuating
Fouling	↓	↓	↑	↓	↑			
Damaged blade	↓	↓	↑	↓	↑			Highly fluctuating
Bearing failure					↑	↑	↓	

Table 19-6 Combustor Diagnostics

	Fuel Pressure	Unevenness of Combustion (Sound)	Exhaust Temperature Spread	Exhaust Temperature
Clogging	↑	↑	↑	↑
Combustor fouling	↑ or ↓	↑	↑	↑
Crossover tube failure	↑ or ↓	–	$\uparrow^{+}$	–
Detached or cracked liner	↑ or ↓	↑	↑	–

The measurement of the two parameters allows the detection of the following:

1. *Plugged nozzle.* This is indicated by an increase in fuel pressure in conjunction with increased combustion unevenness. This is a common problem when residual fuels are used.
2. *Cracked or detached liner.* This is indicated by an increase in an acoustic meter reading and a large spread in exhaust temperature.
3. *Combustor inspection or overhaul.* This is based on equivalent engine hours, which are based on the number of starts, fuel, and temperature. Figure 19-20 shows the effect of these parameters on the life of the unit. Note the strong effect that fuel and number of starts has on the life cycle.

Turbine Analysis

To analyze a turbine, it is necessary to measure pressures and temperatures across the turbine, shaft vibration, and the temperature and pressure of the lubrication system. Table 19-7 shows the effect various parameters have on important functions of the turbines. Analysis of these parameters will aid in the prediction of the following:

1. *Turbine fouling.* This is indicated by an increase in turbine exhaust temperature. Change in vibration amplitude will occur when fouling is excessive and causes rotor imbalance.
2. *Damaged turbine blades.* This results in a large vibration increase accompanied by an increase in the exhaust temperature.
3. *Bowed nozzle.* The exhaust temperature will increase, and there may be an increase in turbine vibration.
4. *Bearing failure.* The symptoms of bearing problems for a turbine are the same as that for a compressor.

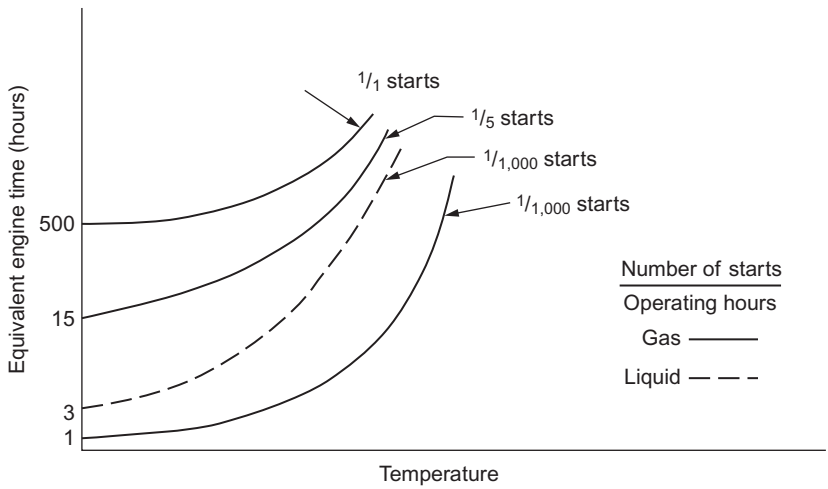


Figure 19-20 Equivalent engine time in the combustor section.

Table 19-7 Turbine Diagnosis

	η_c	P_3/P_4	T_3/T_4	Vibration	T Bearing	Cooling Air Pressure	Wheel Space Temperature	Bearing Pressure
Fouling	↓		↓	↑			↑	
Damaged blade	↓		↓	↑				
Bowed nozzle	↓	↓	↓	↑			↑	
Bearing failure				↑	↑			↓
Cooling air failure					↑	↓	↑	

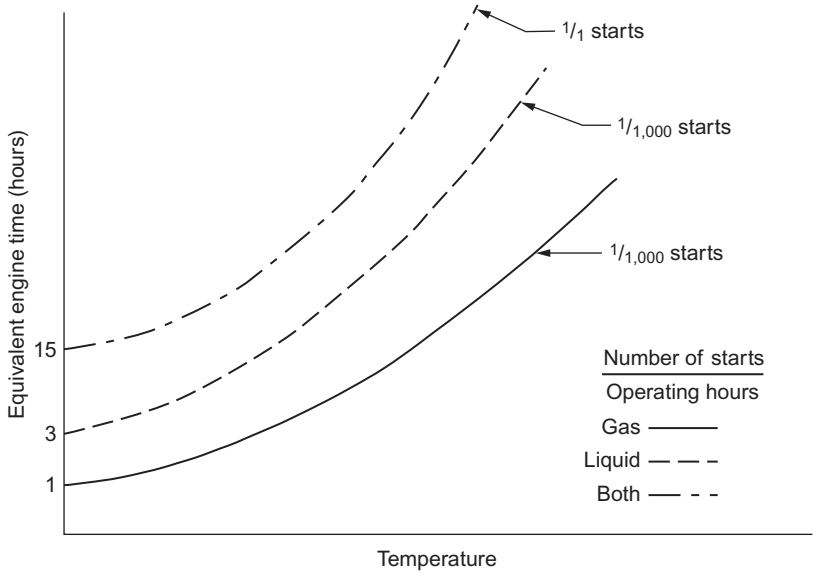


Figure 19-21 Equivalent engine time in the turbine section.

5. *Cooling air failure.* Problems associated with the blade cooling system may be detected by an increase in the pressure drop in the cooling line.
6. *Turbine maintenance.* This should be based on "equivalent engine time," which is the function of temperature, type of fuel used, and number of starts. Figure 19-21 shows the correction that can be applied to running hours for intermittent-duty units with high-start/stop operation.

Turbine Efficiency

1. With the current high cost of fuel, very significant savings can be achieved by monitoring equipment operating efficiencies and correcting for operational inefficiencies. Some of these operational inefficiencies may be very simple to correct, such as the washing or cleaning of the compressor on a gas turbine unit. In other cases, it may be necessary to develop a load-distribution program that achieves maximum overall efficiency of the plant equipment for a given load demand.
2. Figure 19-22 shows the significant dollar cost penalties that occur when operating a turbine at a very small percentage efficiency degradation.
3. Table 19-8 shows a load-distribution program for an 87.5-MW power station of steam turbines and gas turbines. The selection of equipment and their loading for the most efficient operation can be programmed when the efficiency of individual units is monitored. The program selects the units that should be operated to provide the power-load demand at the maximum overall efficiency of the combination of units.

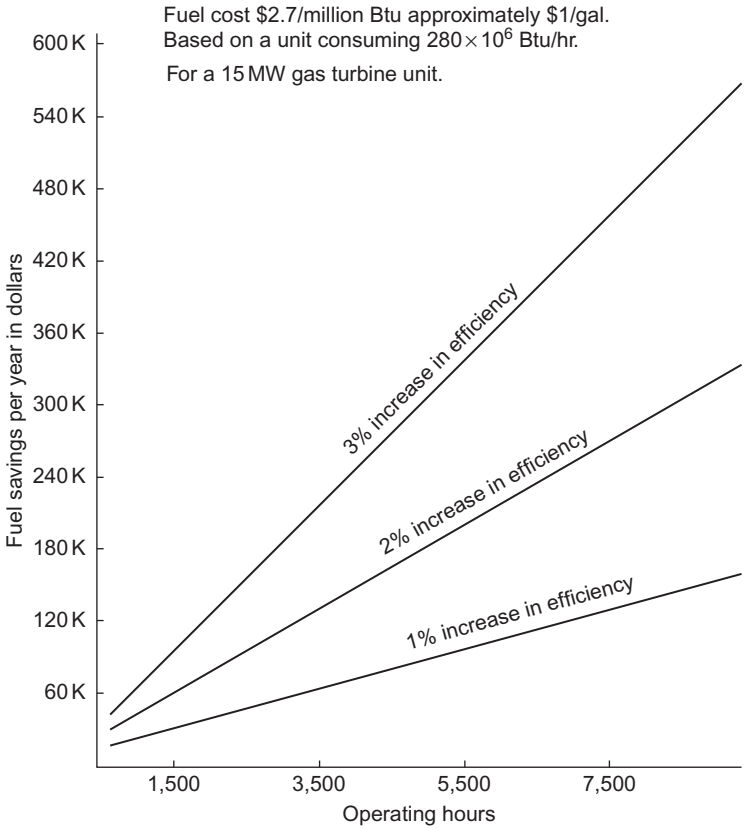


Figure 19-22 Savings versus efficiency.

Table 19-8 Load-Sharing Program Description of Utility Plant Units

Unit #	Design MW	Turbine Type	Efficiency at Design Output Point
1	2.5	Steam	22
2	2.5	Steam	22
3	5.0	Steam	24
4	5.0	Steam	24
5	5.0	Steam	24
6	7.5	Steam	25
7	15.0	Steam	30
8	15.0	Steam	23
9	15.0	Gas	21
10	15.0	Gas	21

Combination of Units of Yield Efficient Power-Load Distribution for Different Demand Loads

Total Demand = 30.00 MW			**Total Demand = 50.00 MW**		
Total Output Supplied = 30.00 MW			**Total Output Supplied = 50.00 MW**		
Units not working = 1,490			**Units not working = 1,400**		
Unit 1	0.00	0.00	Unit 1	0.00	0.00
Unit 2	0.00	0.00	Unit 2	2.50	22.01
Unit 3	2.50	21.00	Unit 3	5.00	24.50
Unit 4	0.00	0.00	Unit 4	0.00	0.00
Unit 5	5.00	24.50	Unit 5	5.00	24.50
Unit 6	7.50	25.19	Unit 6	7.50	25.19
Unit 7	15.00	29.91	Unit 7	15.00	29.81
Unit 8	0.00	0.00	Unit 8	0.00	0.00
Unit 9	0.00	0.00	Unit 9	0.00	0.00
Unit 10	0.00	0.00	Unit 10	15.00	21.00
Maximum Overall Efficiency = 27.04			Maximum Overall Efficiency = 25.02		
Power Demands = MW (Maximum demand = 87.5)					

Mechanical Problem Diagnostics

The advent of new, more reliable, and sensitive vibration instrumentation such as the eddy-current sensor and the accelerometer coupled with modern technology analysis equipment (the real-time vibration spectrum analyzer and low-cost computers) gives the mechanical engineer very powerful aids in achieving machinery diagnostics.

Table 19-9 Vibration Diagnosis

Usual Predominant Frequency*	Cause of Vibration
Running frequency at 0–40%	Loose assembly of bearing liner, bearing casing, or casing and support Loose rotor shrink fits Friction-induced whirl Thrust bearing damage
Running frequency at 40–50%	Bearing-support excitation Loose assembly of bearing liner, bearing case, or casing and support Oil whirl Resonant whirl Clearance-induced vibration
Running frequency	Initial unbalance Rotor bow Lost rotor parts Casing distortion Foundation distortion Misalignment Piping forces Journal and bearing eccentricity Bearing damage Rotor-bearing system critical Coupling critical Structural resonances Thrust-bearing damage
Odd frequency	Loose casing and support Pressure pulsations Vibration transmission Gear inaccuracy Valve vibration
Very high frequency	Dry whirl Blade passage

*Occurs in most cases predominantly at this frequency; harmonics may or may not exist.

A chart for vibration diagnosis is presented in Table 19-9. Although this is a general criterion or rough guideline for diagnosis of mechanical problems, it can be developed into a very powerful diagnostic system when specific problems and their associated frequency domain vibration spectra are logged and correlated in a computerized system. With the extensive memory capability of the computer system, case histories can be recalled and efficient diagnostics achieved.

Data Retrieval

In addition to being valuable as a diagnostic and analysis tool, a data retrieval program also provides an extremely flexible method of data storage and recovery. By careful design of a health monitoring system, an engineer or technician can compare the present operation of a unit with the operation of the same machine, or of another machine, under similar conditions in the past. This can be done by selecting one or several limiting parameters and defining the other parameters that are to be displayed when the limiting parameters are met. This eliminates the necessity of sifting through large amounts of data. Examples of how this system is used are as follows:

1. *Retrieval by time.* In this mode, the computer retrieves data taken during a specified time period, thus enabling the user to evaluate the period of interest.
2. *Retrieval by ambient temperature.* The failure of a gas turbine may occur during an unusually hot or cold period, and the operator may wish to determine how the unit functioned at this temperature in the past.
3. *Retrieval by turbine exhaust temperature.* The exhaust temperature can be an important parameter in failure investigations. An analysis of this parameter can verify the existence of a problem with either the combustor or turbine.
4. *Retrieval by vibration levels.* Inspection of data provided by this mode can be useful in determining compressor fouling, compressor or turbine blade failure, nozzle bowing, uneven combustion, and bearing problems.
5. *Retrieval by output power.* In this mode, the user should input the output power range of interest and thus obtain only data applying to that particular power setting. In this manner, he or she has only to consider the pertinent data to pinpoint the problem areas.
6. *Retrieval by two or more limiting parameters.* By retrieving data with limits on several parameters, the data can be evaluated and will be even further reduced. Diagnostic criteria can then be developed.

Summary

1. The monitoring of turbomachinery mechanical characteristics, such as vibrations, has been applied extensively over the past decade. The advent of the accelerometer and the real-time vibration spectrum analyzer has required a computer to match and utilize the extensive analysis and diagnostic capability of these instruments.
2. The high cost for machinery replacements and downtime makes machinery operational reliability very important; however, with the current and projected increases in fuel costs, aerothermal monitoring has become very important. Aerothermal monitoring can provide not merely increased operational efficiency for turbomachinery, but when combined with mechanical monitoring, it provides an overall, more effective system than one that monitors only the mechanical functions or aerothermal functions.
3. Although there had been concern about the reliability of computer systems, they are currently receiving wide acceptance and are fast replacing analog systems.
4. The systematized application of modern technology (instrumentation, both mechanical and aerothermal, and low-cost computers) and turbomachinery engineering experience will result in the development and application of cost-effective systems.

Bibliography

ASME, *Gas Turbine Control and Protection Systems*, B133.4 Pub. 1978 (Reaffirmed year: 1997).

Boyce, M.P., "Condition Monitoring of Combined Cycle Power Plants," Asian Electricity, July/August 1999, pp. 35–36.

Boyce, M.P., "Control and Monitoring an Integrated Approach," Middle East Electricity, December 1994, pp. 17–20.

Boyce, M.P., "How to Identify and Correct Efficiency Losses through Modeling Plant Thermodynamics," Proceedings of the CCGT Generation Power Conference, London, United Kingdom, March, 1999.

Boyce, M.P., "Improving Performance with Condition Monitoring" – Power Plant Technology Economics and Maintenance, March/April 1996, pp. 52–55.

Boyce, M.P., and Cox, W.M., "Condition Monitoring Management-Strategy," The Intelligent Software Systems in Inspection and Life Management of Power and Process Plants in Paris, France, August 1997.

Boyce, M.P., Gabriles, G.A., and Meher-Homji, C.B., "Enhancing System Availability and Performance in Combined Cycle Power Plants by the Use of Condition Monitoring," European Conference and Exhibition Cogeneration of Heat and Power, Athens, Greece, 3–5 November, 1993.

Boyce, M.P., Gabriles, G .A., Meher-Homji, C.B., Lakshminarasimha, A.N., and Meher-Homji, F.J., "Case Studies in Turbomachinery Operation and Maintenance Using Condition Monitoring," Proceeding of the 22nd Turbomachinery Symposium, Dallas, Texas. 14–16 September, 1993, pp. 101–112.

Boyce, M.P., and Herrera, G., "Health Evaluation of Turbine Engines Undergoing Automated FAA Type Cyclic Testing," Presented at the SAE International Ameritech '93, Costa Mesa, California, 27–30 September, 1993, SAE Paper No. 932633.

Boyce, M.P., and Venema, J., "Condition Monitoring and Control Center," Power Gen Europe in Madrid, Spain, June 1997.

Meher-Homji, C.B., Boyce, M.P., Lakshminarasimha, A.N., Whitten, J.A., and Meher-Homji, F.J., "Condition Monitoring and Diagnostic Approaches for Advanced Gas Turbines," Proceedings of ASME Cogen Turbo Power 1993, 7th Congress and Exposition on Gas Turbines in Cogeneration and Utility, Sponsored by ASME in participation of BEAMA, IGTI-Vol. 8 Bournemouth, United Kingdom, 21–23 September, 1993, pp. 347–355.

Rosen, J., "Power Plant Diagnostics Go On-Line," Mechanical Engineering, December 1989.

Copyrighted Materials
Copyright © 2012 Elsevier Retrieved from www.knovel.com

20 Gas Turbine Performance Test

Introduction

The performance analysis of the new generation of gas turbines is complex and presents new problems, which have to be addressed. Performance acceptance tests, which are required to be conducted for contractual guarantees, require that the turbine be cleaned before the test. The average commissioning time for the advanced gas turbine (G Type) units is longer than the F and FA Type units. This is usually due to the increased number of starts and trips during commissioning, because a lot of fine tuning is required for the DLN combustors, cooling systems, and complicated control systems, which increase the number of equivalent engine hours. It is recommended that contractually the maximum number of equivalent engine hours be limited to about 600–800 hours regardless of the actual equivalent operating hours. If this is not done then the power output will be corrected to a larger corrected output, reducing the actual power the plant will produce. There have been many cases of 2,000–6,500 equivalent operating hours recorded during commissioning, which in many cases amounts to the power and heat rate being corrected by 2–5%. This affects the profitability of the plant.

The new units operate at very high turbine firing temperatures. Thus, variation in this firing temperature significantly affects the performance and life of the components in the hot section of the turbine. The compressor pressure ratio is high which leads to a very narrow operation margin, thus making the turbine very susceptible to compressor fouling. The turbines are also very sensitive to backpressure exerted on them when used in combined cycle or cogeneration duty. The pressure drop through the air filter also results in major deterioration of the performance of the turbine.

If a life cycle analysis were conducted the new costs of a plant are about 7–10% of the life cycle costs. Maintenance costs are approximately 15–20% of the life cycle costs. Operating costs, which essentially consist of energy costs, make up the remainder, between 70–80% of the life cycle costs, of any major power plant. Thus, performance evaluation of the turbine is one of the most important parameters in the operation of a plant.

Total performance monitoring on- or off-line is important for the plant engineers to achieve their goals of:

1. Maintaining high availability of their machinery.
2. Minimizing degradation and maintaining operation near design efficiencies.

Gas Turbine Engineering Handbook, Fourth Edition. DOI: 10.1016/B978-0-12-383842-1.00020-2
Copyright © 2012 Elsevier Inc. All rights reserved.

3. Diagnosing problems, and avoiding operating in regions which could lead to serious malfunctions.
4. Extending time between inspections and overhauls.
5. Reducing life cycle costs.

To determine the deterioration in component performance and efficiency, the values must be corrected to a reference plane. These corrected measurements will be referenced to different reference planes depending upon the point which is being investigated. Corrected values can further be adjusted to a transposed design value to properly evaluate the deterioration of any given component. Transposed data points are very dependent on the characteristics of the component's performance curves. To determine the characteristics of these curves, raw data points must be corrected and then plotted against representative non-dimensional parameters. It is for this reason that we must evaluate the turbine train while its characteristics have not been altered due to component deterioration. If component data were available from the manufacturer, the task would be greatly reduced.

Performance Codes

Performance analysis is not only extremely important in determining overall performance of the cycle but also in determining life cycle considerations of various critical hot section components.

In this chapter, a detailed technique with all the major equations governing a Gas Turbine Power Plant is presented based on the various ASME Test Codes. The following three ASME Test Codes govern the test of a Gas Turbine Power Plant:

1. ASME, Performance Test Code on Overall Plant Performance, ASME PTC 46 1996, American Society of Mechanical Engineers 1996
2. ASME, Performance Test Code on Test Uncertainty: Instruments and Apparatus PTC 19.1, 1988
3. ASME, Performance Test Code on Gas Turbines, ASME PTC 22 1997, American Society of Mechanical Engineers 1997.

The ASME, Performance Test Code on Overall Plant Performance, ASME PTC 46, was designed to determine the performance of the entire heat cycle as an integrated system. This code provides explicit procedures for the determination of power plant thermal performance and electrical output.

The ASME, Performance Test Code on Test Uncertainty: Instruments and Apparatus PTC 19.1 specifies procedures for the evaluation of uncertainties in individual test measurements, arising from both random errors and systematic errors, and for the propagation of random and systematic uncertainties into the uncertainty of test results. The various statistical terms involved are defined. The end result of a measurement uncertainty analysis is to provide numerical estimates of systematic uncertainties, random uncertainties, and the combination of these into a total uncertainty with an approximate confidence level. This is especially very important when computing guarantees in plant output and plant efficiency.

Table 20-1 Instrumentation Accuracy

Measurement	Bias Uncertainty
Temperature below 200 °F (93.3 °C)	0.5 °F (0.27 °C)
Temperature above 200 °F (93.3 °C)	1.0 °F (0.56 °C)
Pressure	0.1%
Vacuum pressure	Absolute pressure transmitters recommended
Mass flow of fuel gas	0.8%

The PTC 22 establishes a limit of uncertainty of each measurement required; the overall uncertainty must then be calculated in accordance with the procedures defined in ASME PTC 19.1 Measurement Uncertainty. The code requires that the typical uncertainties be within a 1.1% for the Power Output, and 0.9% in the heat rate calculations. It is very important that the post-test uncertainty analysis should also be performed to assure the parties that the actual test has met the requirement of the code.

The instrumentation will be calibrated as per the requirements of the test codes. All the instrumentation must be calibrated before a test and certified that they meet the code requirements. The ASME PTC 19 series outlines the governing requirements of all instrumentation for an ASME Performance Test to be within the governing band of uncertainty.

Table 20-1 is a very short abstract of the test measurement requirements for the performance tests; the ASME PTC 19 series should be the final governing document.

Flow Straighteners

Minimum lengths of straight pipe are required for flow-measuring devices and for certain pressure measurements. Flow straighteners and/or equalizers should be used in the vicinity of throttle valves and elbows, as shown in Figure 20-1.

Pressure Measurement

The following types of instruments are used to make pressure measurements:

1. Bourdon tube gauges
2. Dead-weight gauges (used for calibration purposes only)
3. Liquid manometers
4. Impact tubes
5. Pitot-static tubes
6. Pressure transmitters
7. Pressure transducers
8. Barometers

Good-quality Bourdon tube test gauges are highly suitable for pressure measurements of more than 20 psi. They should be calibrated against a deadweight tester in

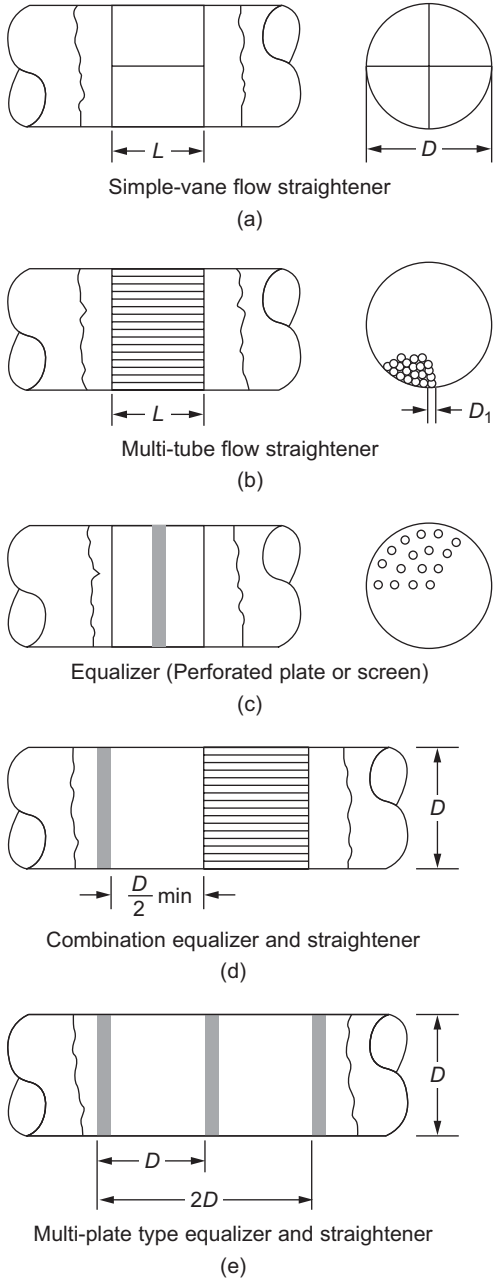


Figure 20-1 Flow equalizers and straighteners (Power Test Code 10, *Compressors and Exhausters*, American Society of Mechanical Engineers, 1965).

their normal operating range. When selecting a pressure gauge, it is important to see that the measure value is above midpoint on the scale.

Differential pressures and sub-atmospheric pressures should be measured by manometers with a fluid that is chemically stable when in contact with the test gas. Mercury traps should be used where necessary to prevent the manometer fluid from entering the process piping. Errors in these instruments should not exceed 0.25%.

A common failure in pressure measurement is the uncertainty of the configuration of static-pressure taps penetration through the pipe wall. This failure is another early-planning concern, since proper taps are easy to provide prior to placing the machine in service, but inspection of the taps after operation has commenced is a luxury rarely afforded the test team.

Another pitfall in pressure measurement, particularly important in flow measurement, is the potential for liquids in gauge lines. All too often gauge lines coming from overhead pipes have no provision for maintaining a liquid-free status, even though the flowing fluid may be condensible at gauge-line temperatures.

Calibration of the pressure-measuring device presents another pitfall for test crews. All too often a test is conducted through the field calculation step before bad data reveal that gauges, possibly with too large a minimum increment, were removed from the shipping carton and installed, relying on the vendor's calibration. On-site calibration of all instruments is always good insurance against a bad test.

Frequently, new machines are put into service with a "start-up screen" in the compressor inlet piping to guard against the inevitable weld slag and construction debris that will remain in a new or rebuilt piping system after construction. Regardless of the age of the installation, care must be exercised to ensure that measurements defining suction or discharge conditions are not influenced by such devices.

Inlet and discharge pressures are defined as the stagnation pressures at the inlet and discharge, which are the sum of static and velocity pressures at the corresponding points. Static pressures should be measured at four stations in the same plane of the pipe as shown in the piping arrangements. Velocity pressure, when less than 5% of the pressure rise, can be computed by the formula:

$$P_v = \frac{(V_{av})^2 \rho}{2g_c \times 144} = \frac{(V_{av})^2 \rho}{9266.1} \tag{20-1}$$

where V_{av} is the ratio of measured volume flow rate to the cross-sectional area of the pipe.

When the velocity pressure is more than 5% of the pressure rise, it should be determined by a pitot-tube traverse of two stations. For each station, the traverse consists of 10 readings at positions representing equal areas of the pipe cross section, as shown in Figure 20-2. The average velocity pressure P_v is given by:

$$P_v = \frac{\rho \Sigma V_p^3}{288 g_c n_t V_{av}} \tag{20-2}$$

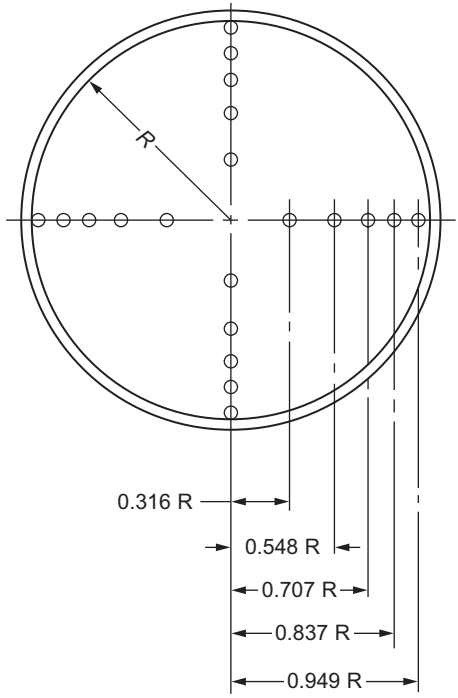


Figure 20-2 Traverse points in pipe (Power Test Code 10, *Compressors and Exhausters*, American Society of Mechanical Engineers, 1965).

where at each traverse point

$$V_p = \sqrt{\frac{9266.1 p_v}{\rho}} \tag{20-3}$$

and n_t equals the number of traverse points.

Barometric pressure should be measured at the test site at 30-minute intervals during the test.

Temperature Measurement

Temperature may be measured by any of the following instruments:

1. Mercury-in-glass thermometers
2. Thermocouples
3. Resistance thermometers
4. Thermometer wells

Thermocouples are the preferred type of instruments because of the simplicity in basic design and operation. They can attain a high level of accuracy, are suitable for remote reading, and are robust and relatively inexpensive.

Regardless of the temperature-measuring device to be used, on-site calibration of the entire measurement system is desirable. Usually, a two-point check can be made by employing frozen and boiling water. At the very least, all devices can be checked at a common temperature, preferably in the midrange of expected temperatures so that any deviant devices can be discarded. This check is particularly desirable for low-head machines where the temperature rise will be slight.

Test plans frequently are prepared on the assumption that a laboratory thermometer can replace an operating instrument in an existing thermometer well. While this change may be satisfactory, the prudent tester needs to be aware that because of the propensity of thermowells to break off and perhaps enter the machine or cause a hazardous leak, their design is compromised such that true gas temperature determination is impossible. The compromise may be to make the well short and/or to make it thick-walled. In either event the mass of metal exposed to ambient temperature may exceed that exposed to the gas, resulting in significant error if the gas temperature is much different from the ambient temperature. High-pressure systems requiring thick-wall pipe are particularly susceptible to this fault. However, the use of a good heat-transfer fluid can minimize the error. The best gas temperature reading is attained by a calibrated fine-wire thermocouple with the junction directly exposed to the gas near the center of the flow. As deviations from this ideal are made, the potential for error is increased.

Inlet and discharge temperatures are the stagnation temperatures at the respective points and should be measured within an accuracy of 1 °F (0.55 °C). When the velocity of the gas stream is more than 125 fps (36.6 mps), the velocity effect should be included in the temperature measurement with a total temperature probe. This probe is a thermocouple with its hot junction provided with a shielded cup. The cup opening points upstream. A trade-off has to be made in a field test situation where the gas is not clean.

Flow Measurement

Gas flow through the compressor is measured by flow nozzles or other devices installed in the piping. Among the various devices are:

1. *Orifice plates.* Either the concentric orifice, eccentric orifice, or segmented orifice-type. Choice depends on the quality of the fluid handled.
2. *Venturi tubes.* These consist of a well-rounded convergent section at the entrance, a throat of constant diameter, and a divergent section. Their accuracy is high; however, installation, unless planned for in advance, is very difficult in the field.
3. *ASME flow nozzles.* These nozzles provide for accurate measurements. Their use is limited because they are not easily placed in a process plant; however, they are excellent for shop tests. Venturi meters and nozzles can handle about 60% more flow than orifice plates with varied pressure losses.
4. *Elbow flow meters.* The principle of centrifugal force at the bend is used to obtain the difference in pressure at the inside and outside of the elbow, which is then related to the discharge pressure.
5. *Turbine flow meters.* The principle of this flow meter is the computation of the revolutions of the turbine wheel in a given time frame.

Other techniques for measuring flow through the compressor include:

1. Calibrated pressure drops from the inlet flange to the eye of the first stage impeller in centrifugal compressors, when such data are available from the manufacturer.
2. A flow trace technique in which Freon is injected into the constream, and the flight time between two detection points is measured.
3. Velocity traverse techniques must be used when, due to the configuration in piping, nozzles, or orifice plates, etc., cannot be used.

These techniques have been described previously in the pressure measurement section. Usually, one of the flow-measuring devices and the required instrumentation is incorporated as a part of the plant piping. The choice of technique depends on the allowable pressure drop, flow type, accuracy required, and cost.

Nozzle arrangements for various applications vary considerably. For subcritical flow measurement at the outlet end, where nozzle differential pressure p is less than

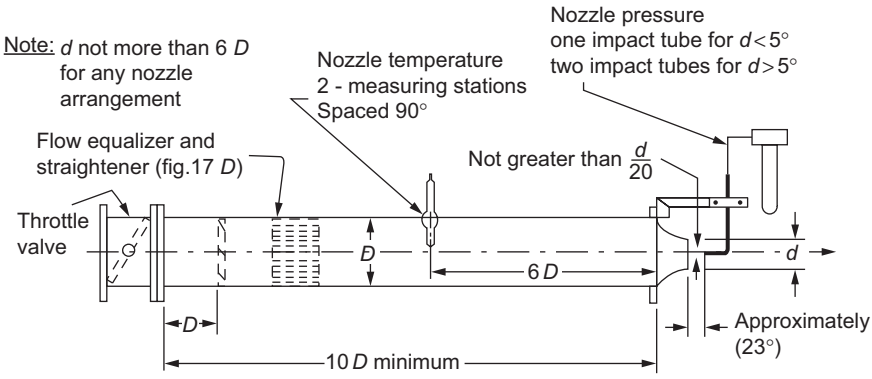


Figure 20-3 Flow nozzle for subcritical flow (Power Test Code 10, *Compressors and Exhausters*, American Society of Mechanical Engineers, 1965).

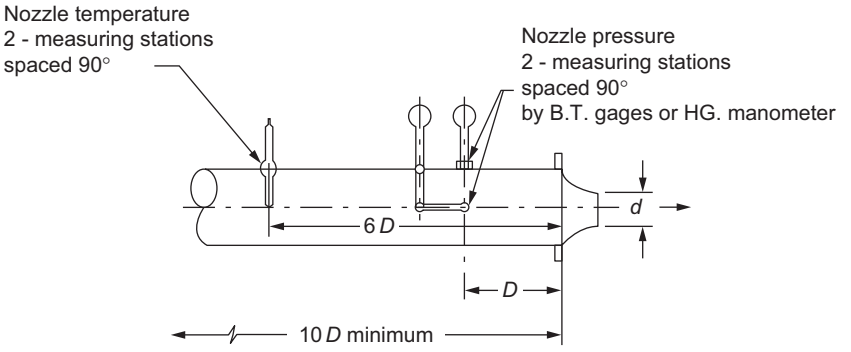


Figure 20-4 Flow nozzle for critical flow (Power Test Code 10, *Compressors and Exhausters*, American Society of Mechanical Engineers, 1965).

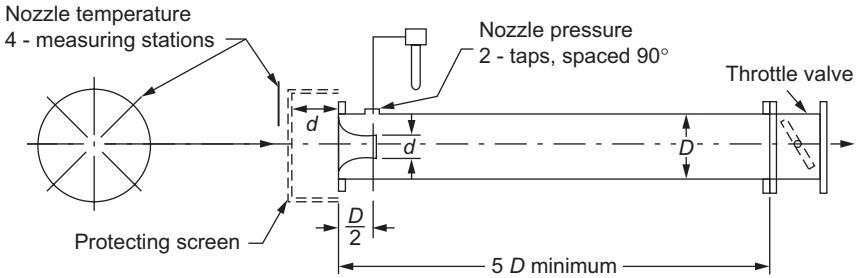


Figure 20-5 Flow nozzle for exhausters (Power Test Code 10, *Compressors and Exhausters*, American Society of Mechanical Engineers, 1965).

the barometric pressure, flow should be measured with impact tubes and manometers as shown in Figure 20-3.

For critical measurement, where the drop p is more than the barometric pressure, flow should be measured with static-pressure taps upstream from the nozzle as illustrated in Figure 20-4. For exhaust measurements, differential pressure is measured at two static taps located downstream from the nozzle at the inlet as shown in Figure 20-5.

Gas Turbine Test

Before starting any performance test the gas turbine shall be run until stable conditions have been established. Stability conditions will be achieved when continuous monitoring indicates the readings have been within the maximum permissible limits. The ASME PTC–22-test code requires that the performance test will be run as much as possible to the design test conditions as specified in the contract. The maximum permissible variation in a test run shall not vary from the computed average for that operating condition during the complete run by more than the values specified in Table 20-2. If operation conditions vary during any test run by more than the prescribed values in Table 20-2 then the results of that test run shall be discarded. The test run should not exceed 30 minutes and during that time the interval between readings should not exceed 10 minutes. There should be three to four test runs performed, which then could be averaged to get the final guarantee test points.

Correction factors are also provided in ASME PTC Test Code-46. The correction factors for ambient temperature, ambient pressure, and relative humidity are presented in this chapter.

The equations and performance parameters for all the major components of a power train must be corrected for ambient conditions and certain parameters must be further corrected to design conditions to accurately compute the degradation. Therefore, to fully compute the performance, and degradation of the plant and all its components, the actual, corrected, and transposed reference conditions of critical parameters must be computed.

Table 20-2 Maximum Permissible Variation in Test Conditions

Variables	Variation of Any Station During the Test Run
Power output (electrical)	±2%
Power factor	±2%
Rotating speed	±1%
Barometric pressure at site	±0.5%
Inlet air temperature	±4.0 °F (±2.2 °C)
Heat valve – gaseous fuel per unit volume	±1%
Pressure – gaseous fuel as supplied to engine	±1%
Absolute exhaust backpressure at engine	±0.5%
Absolute inlet air pressure at engine	±0.5%
Coolant temperature – outlet [Note (2)]	±5.0 °F (±2.8 °C)
Coolant temperature – rise [Note (2)]	±5.0 °F (±2.8 °C)
Turbine control temperature [Note (3)]	±5.0 °F (±2.8 °C)
Fuel mass flow	±0.8%

The overall plant needs the following parameters to be computed. The most important two parameters from an economic point of view are the computation of the power delivered and the fuel consumed to deliver the power. The following are the parameters that need to be computed to fully understand the macro picture of the plant:

1. Overall plant system
2. Gross unit heat rate
   a. Net unit heat rate
   b. Gross output
   c. Net output
   d. Auxiliary power

Gas Turbine

The ASME, Performance Test Code on Gas Turbines, ASME PTC 22 examines the overall performance of the gas turbine. The ASME PTC 22 only examines the overall turbine and many turbines in the field are better instrumented for computation of the detail characteristics of the gas turbine. Figure 20-6 shows the desired location of the measurement points for a fully instrumented turbine. The following are the various computations required to calculate the gas turbine overall performance based on the code:

1. Gas turbine overall computation
2. Gas turbine output
3. Inlet air flow
4. First stage nozzle cooling flow rate
5. Total cooling flow rate
6. Heat rate

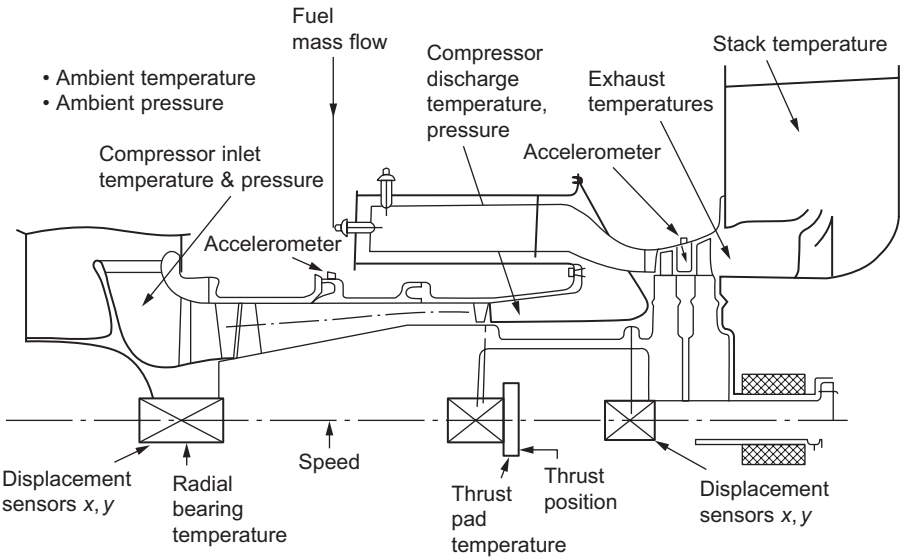


Figure 20-6 Gas turbine suggested measurement points.

7. Expander efficiency
8. Gas turbine efficiency
9. Exhaust flue gas flow
10. Specific heat of exhaust flue gas

To further analyze, the gas turbine must be examined in its four major categories:

1. Air inlet filter
2. Compressor
3. Combustor
4. Expander turbine

Air Inlet Filter Module

Loss computation enables the operator to ensure that the filters are clean and that no additional losses than necessary reduce the performance of the gas turbine. The following parameters are necessary to monitor the filter:

1. Time to replace each stage of filters
2. Filter plugged index to monitor the condition of each stage of filters
3. Inlet duct air leak

Compressor Module

The compressor of a gas turbine is one of the most important components. It consumes between 50–65% of the energy produced in a gas turbine. Thus fouling of the compressor can cause large losses in power and efficiency for the gas turbine. Furthermore,

the fouling of the compressor also creates surge problems, which not only affects the performance of the compressor but also creates bearing problems and flame-outs. The following are some of the major characteristics that need to be calculated:

Overall Parameters of the Compressor

1. Efficiency
2. Surge map
3. Compressor power consumption
4. Compressor fouling index
5. Compressor deterioration index
6. Humidity effects on the fouling
7. Stage deterioration

Compressor Losses

These losses are divided into two sections:

1. *Controllable Losses.* Losses which can be controlled by the action of the operator such as:
   a. Compressor fouling
   b. Inlet pressure drop
2. *Uncontrollable Losses.* Losses which cannot be controlled by the operator such as:
   a. Ambient pressure
   b. Ambient temperature, that, in cases of refrigerated inlets, could be controlled but in most applications is uncontrolled.
   c. Ambient humidity
   d. Ageing

Compressor Wash

When the compressor should be washed on-line, and when an off-line compressor wash should be considered.

On-Line Wash

This wash is done by many plants as the pressure drop decreases by more than 2%. Some plants do it on a daily basis. The water for these washes must be treated.

Off-Line Wash

Figure 20-7 shows that on-line water wash will not return the power to normal, thus, after a number of these washes, an off-line water wash must be planned. This is a very expensive maintenance program and must be fully evaluated before it is undertaken. Chapter 12 deals with the various washes in detail.

Combustor Module

The calculation of the firing temperature is one of the most important calculations in the combined cycle performance computation. The temperature is computed using two techniques: (1) Fuel Heat Rate and (2) Power Balance. The following are the important parameters that need to be computed:

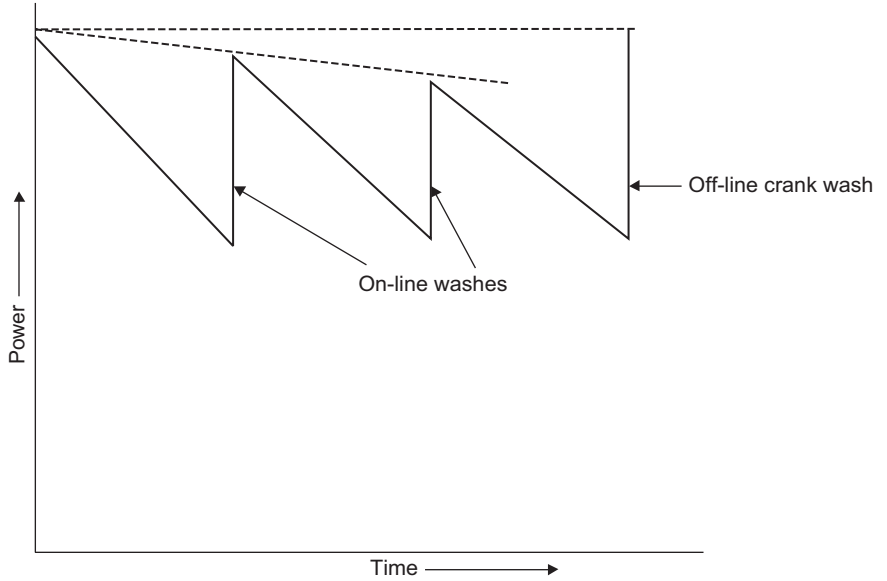


Figure 20-7 Compressor water wash characteristics.

1. Combustor efficiency
2. Deterioration of combustor
3. Turbine inlet temperature (first stage nozzle inlet temperature)
4. Flashback monitor (for dry low NO_x combustors)
5. Specific fuel consumption

Expander Module

The calculation of the turbine expander module depends on whether or not this is a single shaft gas turbine or a multiple shaft gas turbine. In aero-derivative turbines, there are usually two or more shafts. In the latest aero-derivative turbines, there are usually two compressor sections, the LP compressor section, and the HP compressor section. This means that the turbine has three shafts; the third shaft is the power shaft. The turbines that drive the compressor section are known as the gasifier turbines, and the turbine which drives the generator is the power turbine.

The parameters which must be computed are:

1. Expander efficiency
2. Fouled expander parameter
3. Eroded turbine nozzle monitor parameter
4. Expander power produced
5. Deterioration monitor parameter
6. Plugged turbine nozzle monitor parameter

Life Cycle Consideration of Various Critical Hot Section Components

The life expectancy of most hot section parts is dependent on various parameters and is usually measured in terms of equivalent engine hours. The following are some of the major parameters that affect the equivalent engine hours in most machinery, especially gas turbines:

1. Type of fuel
2. Firing temperature
3. Materials stress and strain properties
4. Effectiveness of cooling systems
5. Number of starts
6. Number of trips
7. Expander Losses
   a. Controllable losses
      1) Firing temperature
      2) Backpressure
      3) Turbine fouling (combustion deposits)
   b. Uncontrollable (degradation) losses
      1) Turbine ageing (increasing clearances)

Performance Curves

It is very important to form a baseline for the entire power plant. This would enable the operator to determine if the section of the plant is operating below design conditions. The following performance curves should be obtained either from the manufacturer or during acceptance testing so that the in-depth study of the parameters and their interdependency with each other can be defined:

1. Gas turbine compressor inlet bell-mouth pressure differential versus air flow rate
2. Gas turbine output versus compressor inlet temperature
3. Heat rate versus compressor inlet temperature
4. Fuel consumption versus compressor inlet temperature
5. Exhaust temperature versus compressor inlet temperature
6. Exhaust flow versus compressor inlet temperature
7. The NO_x water injection rate for oil firing versus gas turbine compressor inlet temperature
8. Gas turbine generator power output and heat rate correction as a result of water injection
9. Effect of water injection on generator output as a function of compressor inlet temperature
10. Effect of water injection rate on heat rate as a function of compressor inlet temperature
11. Ambient humidity corrections to generator output and heat rate
12. Power factor correction
13. Losses in generation due to fuel restriction resulting in operational constraints (e.g., temperature spread, problems on fuel stroke valve, etc.)

Performance Computations

This section deals with the equations and techniques used to compute and simulate the various performance and mechanical parameters for the gas turbine power plant. The goals have been to be able to operate the entire power plant at its maximum design

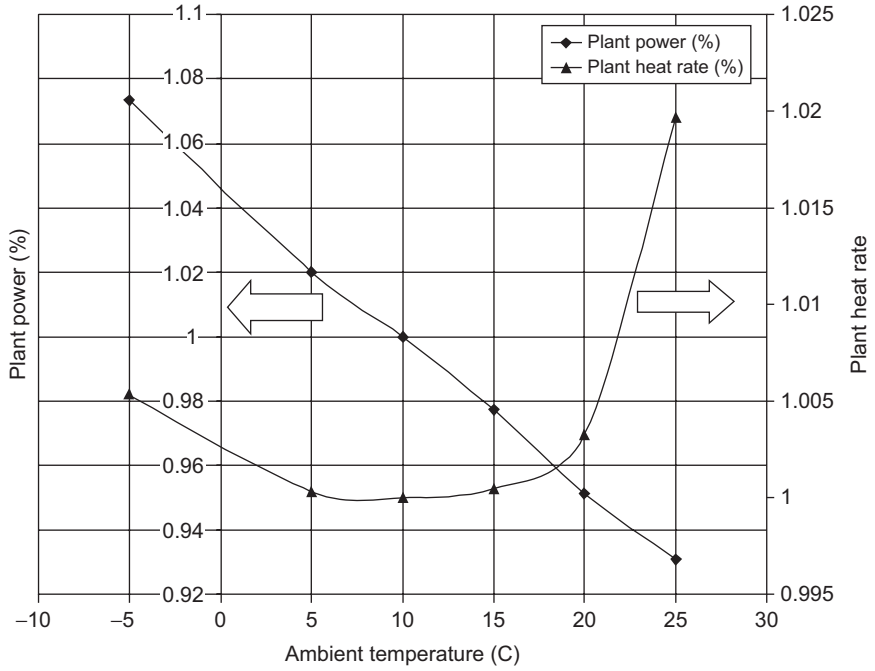


Figure 20-8 Plant conditions as a function of inlet ambient temperature.

efficiency, and at the maximum power that can be obtained by the turbine without degrading the hot section life.

Gas turbine power adjustments in a utility application require that the mechanical speed must remain constant due to unacceptable consequences of frequency fluctuations. The control is obtained by IGV adjustments to reduce the flow at off-design loads and to maintain the high exhaust gas temperature.

The gas turbine efficiency drops off quickly at part load as would be expected, as the gas turbine is very dependent on turbine firing temperature and mass flow of the incoming air. The gas turbine heat rate increases rapidly at part load conditions.

The plant overall power and the heat rate are very dependent on the inlet conditions as seen in Figure 20-8, which is based on a typical gas turbine plant. The effect of temperature is the most critical component in the ambient condition variations of temperature, pressure, and humidity.

General Governing Equations

The four fundamental equations, which govern the properties of the combined cycle, are the equation of state, conservation of mass, momentum, and energy equations.

Equation of state:

$$\frac{P}{\rho} = Z\frac{R}{MW}T \tag{20-4}$$

which can also be written as:

$$\frac{P}{\rho^n} = C \tag{20-4a}$$

Where n varies from $0 \rightarrow \infty; n = 0, P = C$ (constant pressure process); $n = 1, T = C$ (constant temperature process); $n = \gamma (\gamma = \frac{C_p}{C_v}), S = C$ (constant entropy process); $n = \infty, V = C$ (constant volume process).

Conservation of mass:

$$m = \rho AV \tag{20-5}$$

Momentum equation for a calorically and thermally perfect gas, and one in which the radial and axial velocities do not contribute to the forces generated on the rotor the Adiabatic Energy (E_{ad}) per unit mass is given as follows (Euler Turbine Equation):

$$E_{\text{ad}} = \frac{1}{g_c}(U_1 V_{\theta 1} - U_2 V_{\theta 2}) \tag{20-6}$$

Energy equation for a calorically and thermally perfect gas the Work (W) can be written as follows:

$$Q_{\text{rad}} + \Delta UE + \Delta PV + \Delta KE + \Delta PE = W \tag{20-7}$$

where ΔUE is the change in the internal energy, ΔPV is the change in the flow energy, ΔKE is the change in kinetic energy, and ΔPE is the change in Potential Energy. The total enthalpy is given by the following relationship:

$$H = U + PV + KE \tag{20-8}$$

neglecting the changes in potential energy (ΔPE) and heat losses due to radiation (Q_{rad}); the work is equal to the change in total enthalpy:

$$W = H_2 - H_1 \tag{20-9}$$

In the gas turbine (Brayton cycle), the compression and expansion processes are adiabatic and isentropic processes. Thus, for an isentropic adiabatic process $\gamma = \frac{C_p}{C_v}$; where c_p and c_v are the specific heats of the gas at constant pressure and volume respectively and can be written as:

$$c_p = c_v = R \tag{20-10}$$

where

$$c_p = \frac{\gamma R}{\gamma - 1} \quad \text{and} \quad c_v = \frac{R}{\gamma - 1} \tag{20-11}$$

Values for air and products of combustion (400% theoretical air) are given in Appendix B. It is important to note that the pressure measured can be either Total or Static however, only Total Temperature can be measured. The relationship between total and static conditions for pressure and temperature are as follows:

$$T = T_s + \frac{V^2}{2c_p} \tag{20-12}$$

where T_s = static temperature, and V = gas stream velocity and

$$P = P_s + \rho \frac{V^2}{2g_c} \tag{20-13}$$

where P_s = static pressure and the acoustic velocity in a gas is given by the following relationship:

$$a^2 = \left(\frac{\partial P}{\partial \rho}\right)_{s=c} \tag{20-14}$$

For an adiabatic process (s = entropy = constant) the acoustic speed can be written as follows:

$$a = \sqrt{\frac{\gamma g_c R T_s}{MW}} \tag{20-15}$$

where T_s = static Temperature.
The Mach Number is defined as:

$$M = \frac{V}{a} \tag{20-16}$$

it is important to note that the Mach No. is based on static temperature.

The turbine compressor efficiency and pressure ratio are closely monitored to ensure that the turbine compressor is not fouling. Based on these computations the turbine compressor is water washed with mineralized water, and if necessary adjustment of Inlet Guide Vanes (IGV) is carried out to optimize the performance of the compressor, which amounts to between 60–65% of the total work produced by the gas turbine.

The turbine firing temperature, which affects the life and power output, as well as the overall thermal efficiency of the turbine, must be calculated very accurately. To ensure the accuracy of this calculation, the turbine firing temperature is computed using two techniques. These techniques are based firstly on the fuel heat input and secondly on the turbine heat balance. Turbine expander efficiencies are computed and deterioration noted.

Gas Turbine Performance Calculation

Increase in pressure ratio and increase in the firing temperature are the two most important factors in the increase of gas turbine efficiency as can be seen from Figure 20-9. Today the large gas turbines have pressure ratios ranging from 15:1 to as high as 30:1, and firing temperatures as high as 2500 °F (2071 °C). These high-pressure ratios lead to a very narrow operational margin in the gas turbine compressor. The operating margin, between the surge line and the choke region, is reduced with the increasing pressure ratio. This means, in a practical sense, that the new compressors on these gas turbines are very susceptible to any fouling of the compressor, indicating that the inlet filters must be very efficient and the turbines must be performance monitored to ensure maximum operational efficiency.

The overall compressor work is calculated using the following relationship:

$$W_c = (H_{2a} - H_1) = c_{\text{pavg}} T_1 \left\{ \left(\frac{P_2}{P_1} \right)^{\left(\frac{\gamma-1}{\gamma}\right)} - 1 \right\} \tag{20-17}$$

The work per stage is calculated assuming the energy per stage is equal and this has been found to be a better assumption than assuming the pressure ratio per stage to be

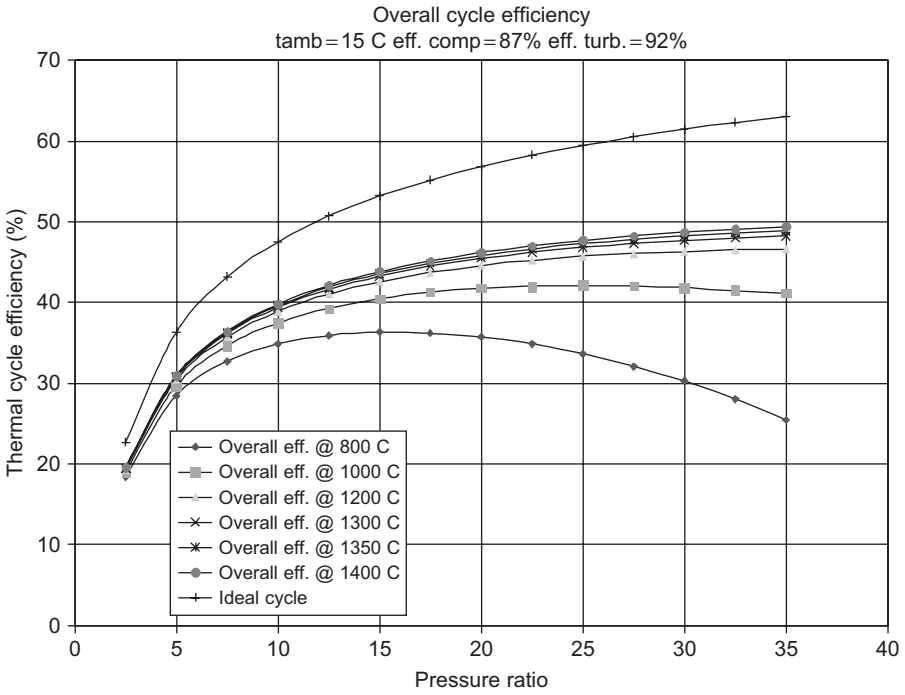


Figure 20-9 Effect of pressure ratio and firing temperature on the performance of a gas turbine.

equal. It is necessary to know the work per stage if there is inter-stage bleed of the air for cooling or other reasons.

$$W_{\text{stg}} = \frac{(H_{2a} - H_1)}{n_{\text{stg}}} \tag{20-18}$$

where n_{stg} = number of compressor stages. The computation of the compressor total energy requirements can now be computed.

$$Pow_{\text{c}} = m_a w_{\text{stg}} n_1 + (m_a - m_{b1}) w_{\text{stg}} n_2 + (m_a - m_{b1} - m_{b2}) w_{\text{stg}} n_3 \ldots \tag{20-19}$$

The work of the compressor under ideal conditions occurs at constant entropy. The actual work occurs with an increase in entropy thus the adiabatic efficiency can be written in terms of the total changes in enthalpy:

$$\eta_{\text{ac}} = \frac{\text{Isentropic work}}{\text{Actual work}} = \frac{H_{2T1} - H_{1T}}{H_{2a} - H_{1T}} \tag{20-20}$$

where H_{2T1} = total enthalpy of the gas at isentropic exit conditions, and H_{2a} = total enthalpy of the gas at actual exit conditions, and H_1 = total enthalpy of the gas at inlet conditions for a calorically perfect gas the equation can be written as:

$$\eta_{\text{ac}} = \frac{\left[\left(\frac{P_2}{P_1}\right)^{\left(\frac{\gamma-1}{\gamma}\right)} - 1\right]}{\left[\frac{T_{2a}}{T_1} - 1\right]} \tag{20-21}$$

The gas turbine compressor which produces the high-pressure gas at elevated temperature uses a very large part of the turbine power produced by the gas turbine, this can amount to about 60% of the total power produced. Figure 20-10 shows the distribution of the gasifier power required as a function of the gas turbine load of a typical large gas turbine. The fouling of the compressor therefore is a large parasitic load on the gas turbine. Figure 20-11 shows the effect on the compressor efficiency at part load conditions. The flow and the firing temperature affect the turbine expander.

The calculation of the turbine firing temperature (T_{tit}) is based firstly on the fuel injected into the turbine and the fuel's lower heating value (*LHV*). The lower heating value of the gas is one in which the H_2O in the products has not condensed. The lower heating value is equal to the higher heating value minus the latent heat of the condensed water vapor.

$$H_{\text{tit}} = \frac{(m_a - m_b) H_{2a} + m_f \eta_b LHV}{(m_a + m_f - m_b)} \tag{20-22}$$

where H_{tit} = enthalpy of the combustion gas at the firing temperature; m_a = mass of air; m_b = bleed air; m_f = mass of fuel; η_b = combustor efficiency (usually between 97–99%).

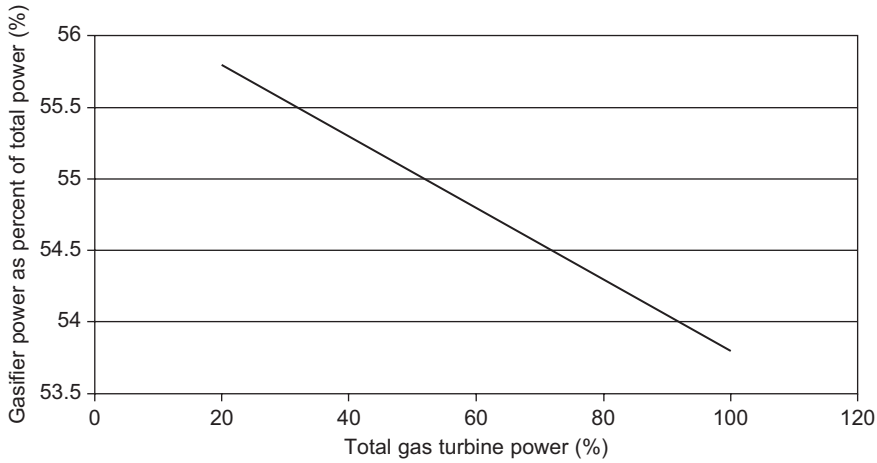


Figure 20-10 Gasifier power as a function of total gas turbine power.

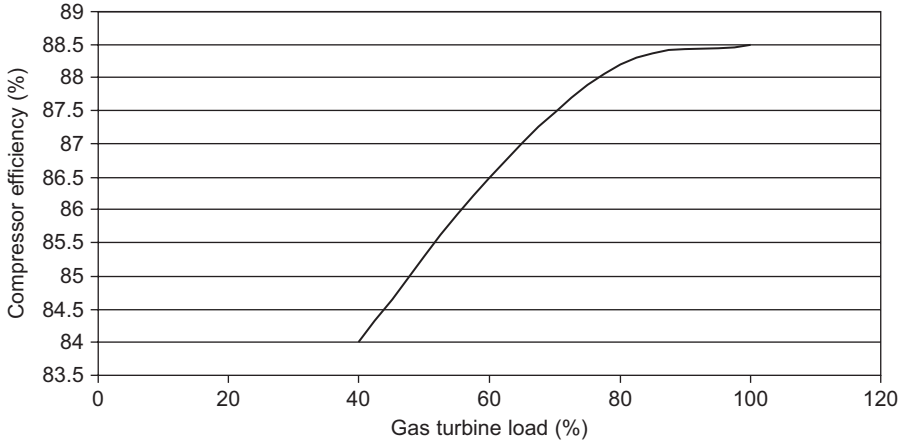


Figure 20-11 Gas turbine compressor efficiency as a function of temperature load.

The turbine firing temperature should be computed by knowing the gas characteristics of the combustion gas. If these characteristics are known then one can use the combustion gas equations given in the ASME performance test codes 4.4 (1991) for gas turbine HRSG. Usually the gas constituents are not known so it is not a bad assumption to use the 400% theoretical air tables in the Keenan and Kaye gas tables. The following equations for specific heat at constant pressure and the ratio of specific heats have been obtained based on the air tables based on a fuel with a mole weight of the combustion gas to be 28.9553 lb_m/pmole (kg/kgmole).

$$c_p = (-2.76 * 10^{(-10)} T^2 + 1.1528 * 10^{(-5)} T + 0.237) * C1 \tag{20-23}$$

where $C1 = 1.0$ in the U.S. units and $C1 = 4.186$ in the SI units and

$$\gamma = \frac{c_p}{\left(c_p - \frac{\frac{R}{778.16}}{MW}\right)} \tag{20-24}$$

The turbine firing temperature based on the heat balance can be also computed and must be within about 2–6 °F (1–3 °C) of each other. The heat balance relationships as they apply to the gas turbine are:

$$H_{\text{tit}} = \frac{\frac{Pow_{\text{c}}}{\eta_{\text{mc}}} + \frac{Pow_{\text{g}}}{\eta_{\text{mt}}} + (m_a + m_f)H_{\text{exit}}}{(m_a + m_f - \Sigma m_b)} \tag{20-25}$$

where Pow_{c} = work of the gas turbine compressor (Btu/sec, kJ/sec); Pow_{g} = generator output; η_{mc} = mechanical loss in the turbine compressor drive; η_{mt} = mechanical loss in the turbine process compressor drive; and H_{exit} = enthalpy at turbine exit.

Split shaft gas turbines usually have temperature measurements at the gasifier turbine exit and also at the power turbine exit. From experience and also based on theoretical relationships, the temperature ratio of the temperature at the gasifier inlet (T_{tit}) and the temperature of the power turbine inlet (T_{pit}) for a given geometry remains constant even though the load and ambient conditions change. It is because of this that most manufacturers limit the engine based on the power turbine inlet temperature.

$$Tr = \frac{T_{\text{tit}}}{T_{\text{pit}}} \tag{20-26}$$

This also enables Equation (20-19) for the case of a split shaft turbine to be rewritten as:

$$H_{\text{tit}} = \frac{\frac{Pow_{\text{c}}}{\eta_{\text{mc}}} + (m_a + m_f - 0.6m_b)H_{\text{pit}}}{(m_a + m_f - m_b)} \tag{20-27}$$

where an assumption of 40% of the bleed flow was assumed to have entered the turbine through the cooling mechanisms of the first few stages of the turbine.

To ensure that the heat balance is accurate the following relationship indicates the accuracy of the computations. This heat balance ratio can be written as follows:

$$HB_{\text{ratio}} = \frac{\frac{Pow_{\text{c}}}{\eta_{\text{mc}}} + (m_a + m_f)H_{\text{exit}} - m_a H_{\text{inlet}}}{m_f * LHV} \tag{20-28}$$

this ratio should be between 0.96 and 1.04.

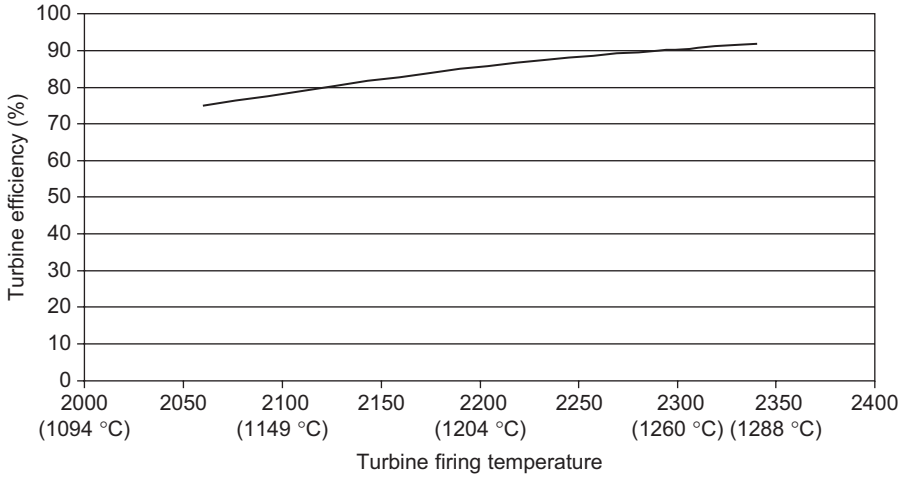


Figure 20-12 Gas turbine efficiency as a function of firing temperature.

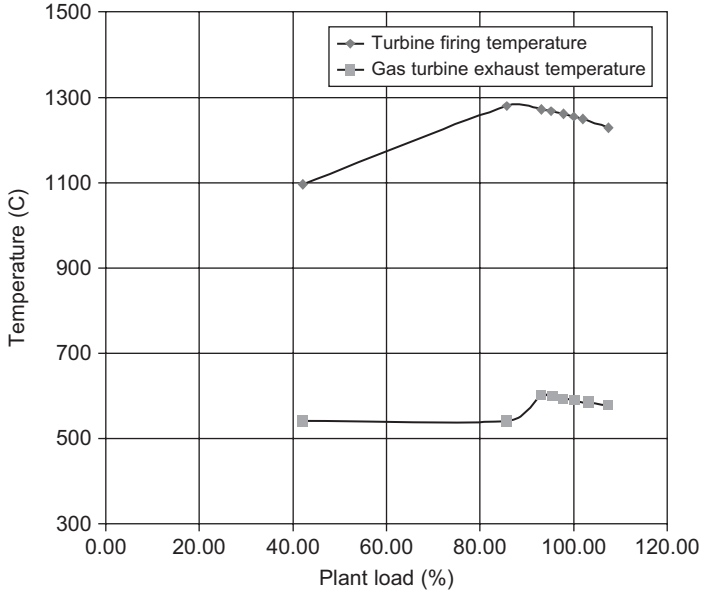


Figure 20-13 Effect of the plant load on turbine firing temperature and the turbine exhaust.

Figure 20-12 shows the effect of the turbine firing temperature on the turbine expander efficiency. The decrease in firing temperature reduces the absolute velocity, as also does the reduction in the mass flow, both of which occur at part load conditions. Figure 20-13 shows the variation in the firing temperature and the exhaust gas temperature as a function of the load. It is interesting to note that the firing temperature of

the turbine is greatly reduced while the exhaust temperature remains nearly constant accounting for the steam turbine producing more work at low part loads.

The work produced by the gasifier turbine (W_{gt}) is equal to the gas turbine compressor work (W_c):

$$Pow_{gt} = \frac{Pow_c}{\eta_{mc}} \tag{20-29}$$

The gasifier turbine efficiency (η_{gt})

$$\eta_{gt} = \frac{H_{tit} - H_{pita}}{H_{tit} - H_{piti}} 100 \tag{20-30}$$

where H_{pita} is the enthalpy of the gas based on the actual temperature at the exit of the gasifier turbine; H_{piti} is the enthalpy of the gas based on the ideal temperature at the exit of the gasifier turbine. To obtain this ideal enthalpy, the pressure ratio across the gasifier turbine must be known.

The pressure ratio (P_{grt}) across the turbine depends on the pressure drop (ΔP_{cb}) through the combustor. This varies in various combustor designs where there is a pressure drop of between 1–3% of the compressor discharge.

$$P_{grt} = \frac{P_{dc}(1 - \Delta P_{cb})}{P_{dgt}} \tag{20-31}$$

where P_{dgt} is the pressure at the gasifier turbine exit. Thus, the ideal enthalpy at the gasifier turbine exit is given by:

$$H_{piti} = \frac{H_{tit}}{\frac{C_{p_{tit}}}{C_{p_{pit}}}\left(P_{grt}\left(\frac{\gamma - 1}{\gamma}\right)\right)} \tag{20-32}$$

where γ is based on an average temperature across the gasifier turbine based on Equation (20-24). The power turbine efficiency can be computed using Equations (20-30) and (20-32).

The overall thermal efficiency of the gas turbine in a simple cycle (varies between 25–45% depending on the turbine) is computed to determine deterioration of the turbine:

$$\eta_{ovt} = \frac{\frac{Pow_g}{\eta_{mt}}}{m_f LHV} 100 \tag{20-33}$$

The heat rate can now be easily computed:

$$HR = \frac{2544}{\frac{\eta_{th}}{100}}\left(\frac{\text{Btu}}{HP - hr}\right) = \frac{3600}{\frac{\eta_{th}}{100}}\left(\frac{\text{kJ}}{kW - hr}\right) \tag{20-34}$$

Gas Turbine Performance Calculations

The performance of the gas turbine is based on the basic equations in the prior section. To relate these relationships to the turbine concerned and to calculate the deterioration of different sections of the gas turbine, the values obtained must be corrected to design conditions and in some cases values would have to be transposed from off-design conditions to the design conditions. The corrected values define the engine corrected performance values. Geometric similarity such as blade characteristics, clearances, nozzle areas, and guide vane settings do not change when geometric similarity is constant. Dynamic similarity, which relates to such parameters as gas velocities, and turbine speeds, when maintained together with the geometric similarity ensures that these corrected parameters will maintain the engine performance in all operating conditions.

Corrected mass flow:

$$m_{\text{acorr}} = \frac{m_a \sqrt{\dfrac{T_{\text{inlet}}}{T_{\text{std}}}}}{\dfrac{P_{\text{inlet}}}{P_{\text{std}}}} \tag{20-35}$$

where m_{acorr} is the corrected mass flow of the air entering the gas turbine inlet. These corrections are from the ambient conditions to usually the ISO conditions (14.7 psia, 60 °F, RH = 60%), (1.01 Bar, 15 °C, RH = 60%).

The corrected speed for both the gasifier and power turbine defines the corrected engine performance.

Corrected speed:

$$N_{\text{corr}} = \frac{N_{\text{act}}}{\sqrt{\dfrac{R_a T_a}{(RT)_{\text{std}}}}} \tag{20-36}$$

Corrected temperature:

$$T_{\text{corr}} = \frac{T_a}{\dfrac{T_{\text{inlet}}}{T_{\text{std}}}} \tag{20-37}$$

Corrected fuel flow:

$$m_{\text{fcorr}} = \frac{m_f}{\left(\dfrac{P_{\text{inlet}}}{P_{\text{std}}}\right) \Big/ \left(\sqrt{\dfrac{T_{\text{inlet}}}{T_{\text{std}}}}\right)} \tag{20-38}$$

Corrected power:

$$HP_{\text{corr}} = \frac{HP_{\text{act}} \dfrac{T_{\text{inlet}}}{T_{\text{std}}}}{\dfrac{P_{\text{inlet}}}{P_{\text{std}}}} \tag{20-39}$$

The above relationship has to be further modified to take into account the pressure drop in the inlet ducting, the increase in backpressure due to exhaust ducting, and the off-design operation due to decrease in turbine firing temperature and decrease in speed of the power turbine. These modifications are used to calculate the transposed power (HP_{pt}) by transposing from the off-design output power at operating conditions of the turbine to the design conditions.

Transpose power output:

$$HP_{\text{tp}} = HP_{\text{corr}} + (\Delta P_c(PW_i)) + (\Delta P_e(PW)_e) + (T_{\text{dtit}} - T_{\text{atit}})c_p(m_d - m_a)\eta_{\text{at}} + \left[1 + 0.45\left(1 - \frac{N_{\text{ptcorr}}}{N_{\text{ptdes}}}\right)^m\right] HP_{\text{act}} \tag{20-40}$$

where ΔP_c is the pressure drop at the inlet due to the filters and evaporator in the inlet ducting, P_{wi} the power loss per inch of H_2O (mm H_2O) drop, ΔP_e is the backpressure at the discharge due to the exhaust ducting, and P_{we} the power loss per inch of H_2O (mm H_2O) drop. The last term of the equation only applies to split shaft turbines. The power factor (m) to which the speed ratio is raised will vary with turbines; in the case of this turbine the value was $m = 0.4$.

Correction Factors for Gas Turbines

Correction factors for the gas turbine ambient conditions depend on individual gas turbines, and should be provided by the gas turbine manufacturer. In this section average correction factors have been assembled to give you an approximate value within (1–2% accuracy) the effect of the different ambient conditions on the performance of the gas turbine.

The base conditions for these graphs are based on ISO standard conditions, which are pressure = 14.7 psia, temperature = 59.4 °F (15 °C), and a relative humidity of 0%.

The sensors for the ambient conditions should be located in a stable environment, not susceptible to engine inlet and outlet effects. Correction factors for ambient inlet pressure for the thrust power are given in Figure 20-14. The ambient pressure variation is due to the altitude where the plant is located. At high altitude the power of the plant is greatly reduced. It should be noted that these values are average, and engine-specific values should be obtained from the engine manufacturer. It is not a value that varies greatly from day to day.

Ambient temperature affects the power and heat rate produced by an engine. It is one of the most important parameters in day-to-day operation. Correction factors for ambient inlet temperature for the thrust power are given in Figure 20-15. It should be noted that these values are average, and engine-specific values should be obtained from the engine manufacturer.

Heat rate is also affected by the changes in operational temperature as seen in Figure 20-16. The heat rate is increased as the temperature increases. Therefore changes in temperature that occur daily and that can range over 30 °F–50 °F in a single

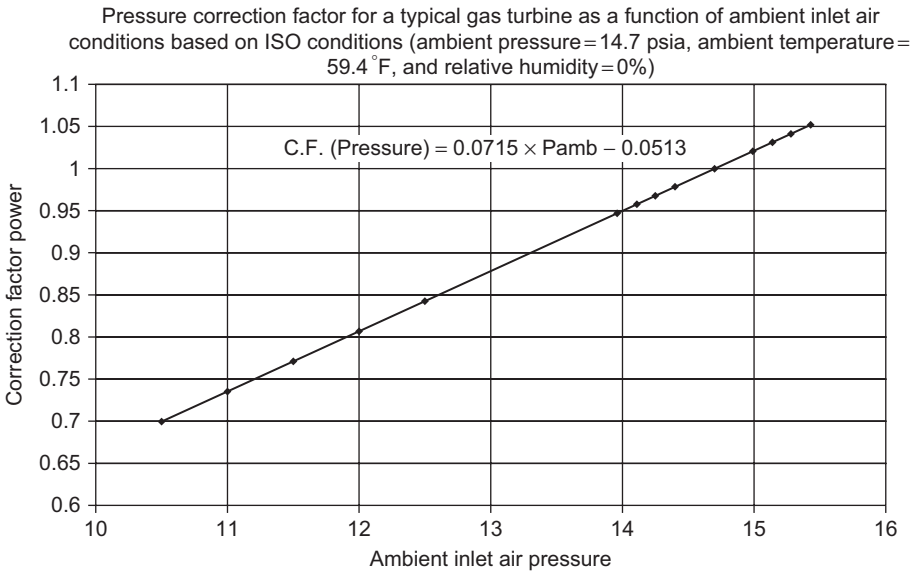


Figure 20-14 Correction factor for power as a function of inlet ambient pressure.

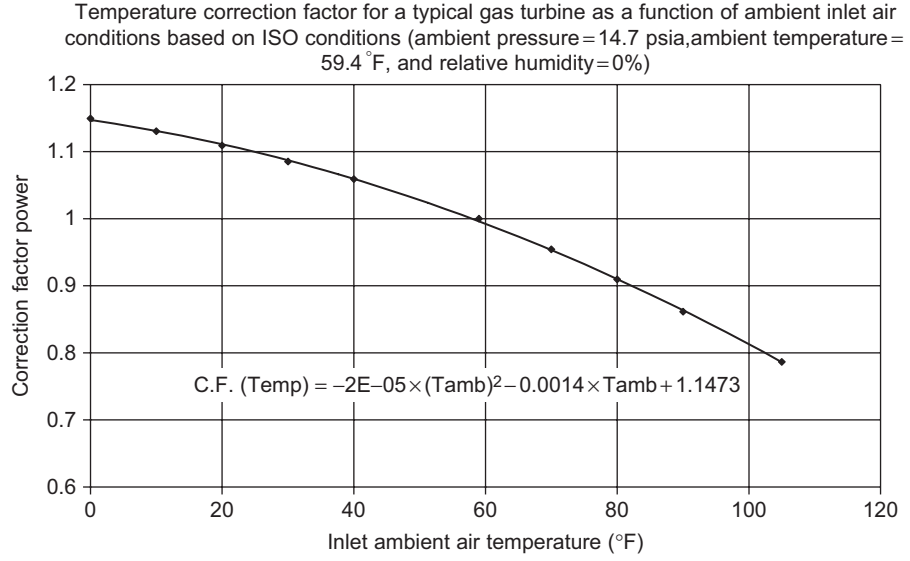


Figure 20-15 Correction factor for power as a function of inlet ambient air temperature.

24-hour period are the most significant factor that affects the daily operation of the gas turbine, affecting the power and the heat rate.

Water vapor contained in the air influences the engine and its performance. Although the consequences are complex, they fall into two major categories: engine

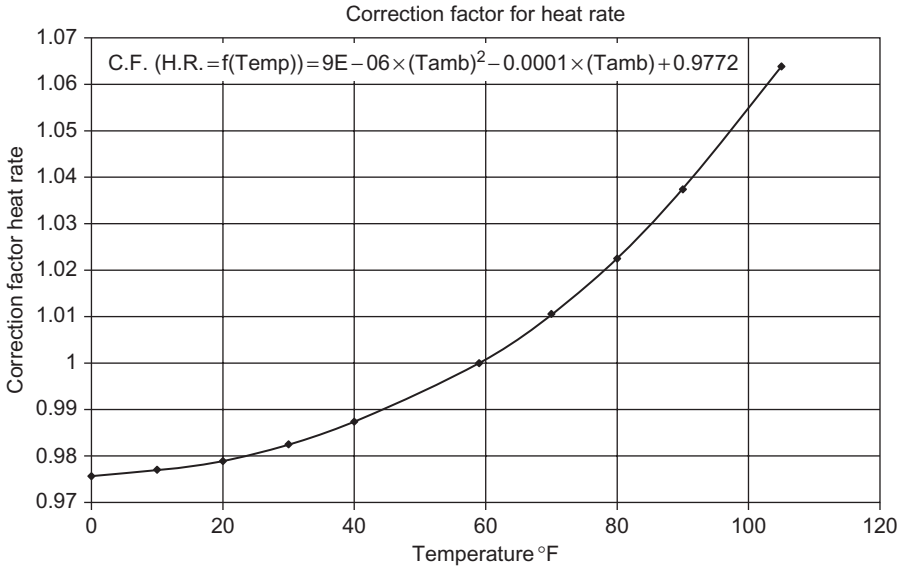


Figure 20-16 Correction factor for heat rate as a function of inlet ambient air temperature.

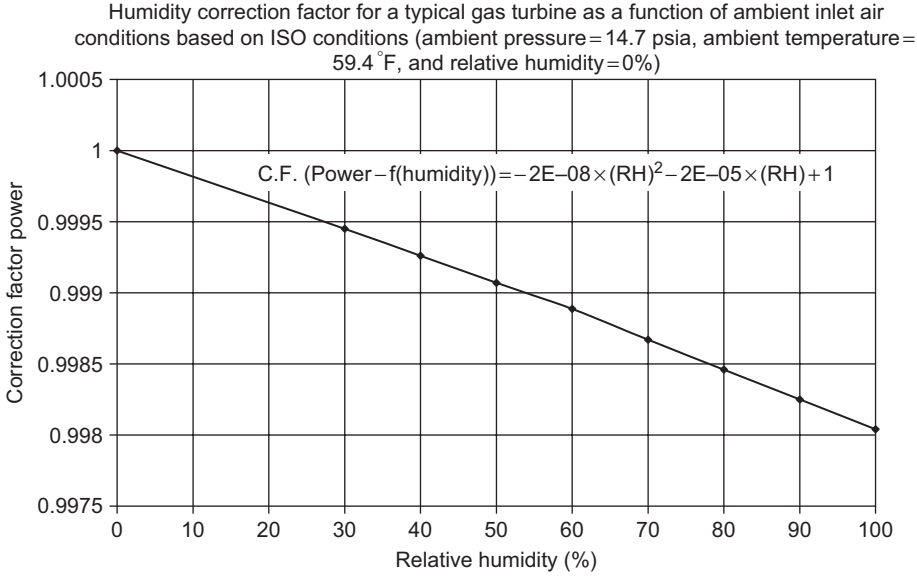


Figure 20-17 Correction factor for power as a function of inlet ambient air relative humidity.

inlet condensation and changes in engine gas properties. The relative humidity is related to the extent of engine inlet condensation, whereas the absolute or specific humidity affects the gas properties of the engine cycle and, hence, the performance elements.

Humidity has an impact on performance and should be considered when accurate performance measurements are required. Changes in humidity do affect the power and heat rate of the turbine, but this is a very insignificant change as compared to the changes due to temperature variation. Correction factors for ambient inlet humidity for the thrust power are given in Figure 20-17. It should be noted that these values are average and engine-specific values should be obtained from the engine manufacturer.

Vibration Measurement

Rotor Dynamics

The characteristics of the high speed rotor system are very important to define in evaluating the performance of the gas turbine. The vendor should provide a damped unbalanced response analysis for the prototype of each gas turbine model. The damped unbalance response analysis should be based on but not limited to the following considerations of the turbine characteristics:

1. Support (base, frame, and bearing housing) stiffness, mass, and damping characteristics, including effects of rotational speed variation. The vendor should state the support system values and the basis of these values.
2. Bearing stiffness and damping values used in the analysis. The basis of these values and the assumptions made in calculating these values.
3. Rotational speeds, including various starting speeds, operating speeds, critical speeds, and the trip speed. Start-up and coast down conditions indicating bleed valve closures and openings, respectively, must be fully documented.
4. Rotor masses including the mass moment of coupling halves, stiffness, and damping effects (such as accumulated fit tolerances, damping, frame effects).
5. Rotor system response to trim balancing in the field.

The analysis should consist of the following charts and tables:

1. A Nyquist and Bode chart showing the frequency phase and amplitude through the entire range of operation.
2. Identification of each critical speed from zero to trip.
3. Identification of mode shapes at each critical speed from zero to trip.
4. Tables showing the acceptable vibration level at various frequencies.
5. A detailed description of the rotor system including the number of stages, number of vanes and blades at each stage, number of gear teeth, and other geometric components that would affect the rotor characteristics of the turbine.

Vibration Measurements

Vibration measurements as part of a performance test should be measuring the pk-pk amplitude at the bearings, and with the use of accelerometers mounted on the casing of the gas turbine, the forces generated by the entire rotor system. It is recommended that a minimum of two accelerometers be placed on the casing of the gas turbine – one near the compressor section and the other near the turbine section. The turbine

Table 20-3 Acceptable Vibration Limits

	RPM	Acceleration (ft/sec^2)	Velocity (ft/sec)	Displacement pk-pk (mils)
Gas generator Frame type	<10,000 rpm (200 Hz)	2.0 g (ft/sec^2)	0.75 (in/sec)	1.5
Gas generator Aircraft type	>10,000 rpm (200 Hz)	3.0 g (ft/sec^2)	0.75 (in/sec)	1.0

section accelerometer will have to be a high-temperature accelerometer. The values of the accelerometer will be in G's (ft/sec^2); however, many users prefer to use readings in velocity (ft/sec), or in displacement pk-pk (mils-.001 inch). It is also recommended that the signals be analyzed by the use of FFTs of the data gathered by the proximity probes, and accelerometers and major frequencies such as sub-harmonic frequencies in the 40–60% range of running speed, multiples of running speed, gear mesh frequencies, and blade passing frequencies should be monitored and logged.

Table 20-3 shows some of the recommended limits of vibration levels that are considered acceptable.

Emission Measurements

Emissions

Emissions from gas turbines cover a wide range of greenhouse gases including particulates such as:

- Carbon dioxide (CO_2)
- Water vapor (H_2O)
- Nitrogen Oxides (NO_x)
- Unburnt Hydrocarbons (UHC)
- Carbon monoxide (CO)
- Particulate matter (PM)
- Sulfur Oxides (SO_x)
- Volatile Organic Compounds (VOCs)

The concentration levels of pollutants produced in gas turbine exhausts can be related to various factors that include the pressure ratio and temperature, and time and concentration histories of the combustor. Carbon monoxide and unburned hydrocarbons are highest at low-power conditions and decrease with increased power. In contrast, oxides of nitrogen and smoke are fairly insignificant at lower power settings and attain maximum values at the highest temperature and pressure.

The main reason for the production of CO and UHC is the incomplete combustion. If the primary zone is fuel rich then large amounts of CO are formed due to lack of oxygen for the reaction to produce CO_2. If the primary zone mixture is stochiometric or slightly fuel lean, then again a significant amount of CO is produced due to the

dissociation of CO_2. Incomplete combustion could be caused by one or more of these factors:

- Inadequate burning rates in the primary zone (too short residence time)
- Poor mixing of fuel and air
- Local chilling of the flame leading to the quenching of post flame products
- Poor fuel injection design
- Poor atomization of the fuel

At high power conditions, UHC and CO decreases due to improved fuel atomization, which happens due to high-pressure and temperature that enhances chemical reaction rate in the primary zone as seen in Figures 20-18 and 20-19. Both these figures indicate that the levels of UHC and CO are low at full load and high at idling conditions.

To reduce the UHC and CO emissions the following points are suggested:

- Improved fuel atomization
- Redistribution of the airflow to bring the primary zone equivalence ratio closer to the optimal value (0.7)
- Increase in the primary zone volume or residence time
- Reduction of film cooling air
- Compressed air-bleed
- Fuel staging

Smoke is produced due to the production of finely divided soot particles in fuel-rich regions of the flame and can be produced anywhere in the combustion zone where mixing is inadequate. Most of the soot produced in the primary zone is consumed in

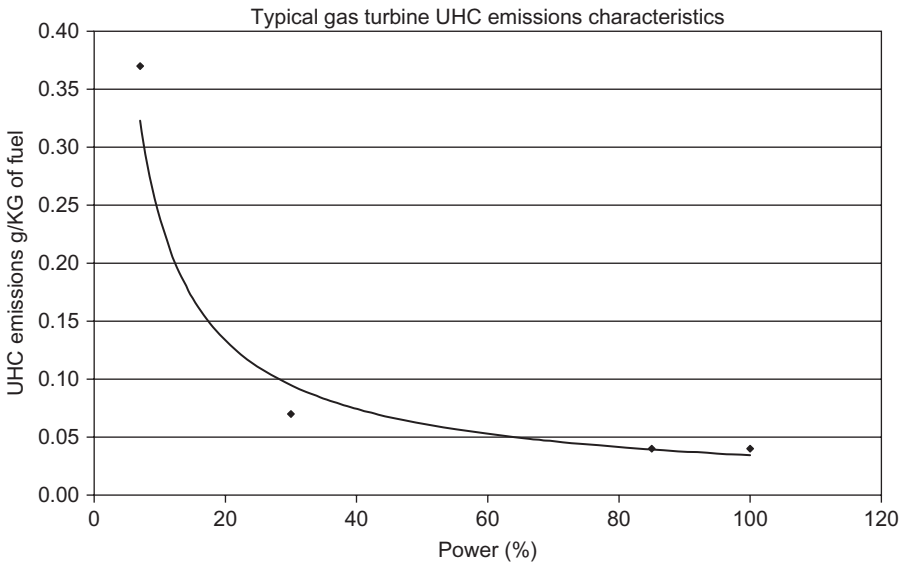


Figure 20-18 UHC emissions for a typical gas turbine.

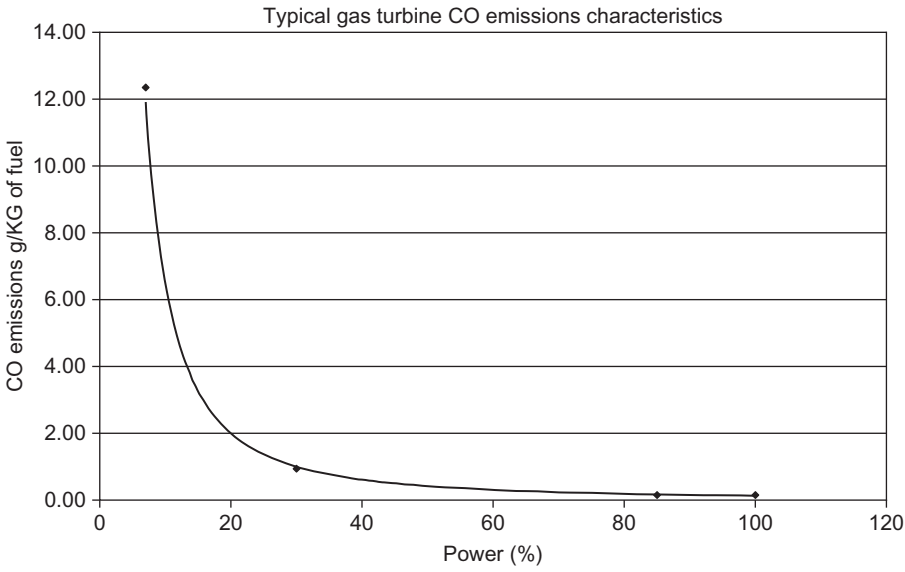


Figure 20-19 CO emissions for a typical gas turbine.

the high temperature regions downstream. Soot is formed only in the fuel-rich regions of the flame and is affected by temperature, pressure, fuel/air ratio, fuel-air mixing, and the process of atomization.

The main governing factor for smoke formation is atomization and fuel-air mixing. Therefore techniques to eliminate fuel-rich areas would minimize smoke but would have adverse effects of producing CO and UHC. Smoke can be eliminated by:

- Water injection
- Any technique to eliminate fuel-rich areas

The main governing factor for NO_x emissions is the firing temperature. Therefore to reduce the levels of NO_x the following steps need to be followed:

1. A lower reaction temperature
2. Elimination of the hotspots from the reaction zone
3. Better wall cooling techniques
4. Better fuel injection system
5. Water injection
6. Exhaust-gas recirculation
7. Lean primary zone
8. Changes in liner geometry and airflow distribution
9. Maintaining the combustion history farther away from stochiometric conditions

Figure 20-20 is the NO_x curve for a typical engine as a function of the engine power. As seen in the figure, the NO_x emission increases with load as the firing temperature is increased.

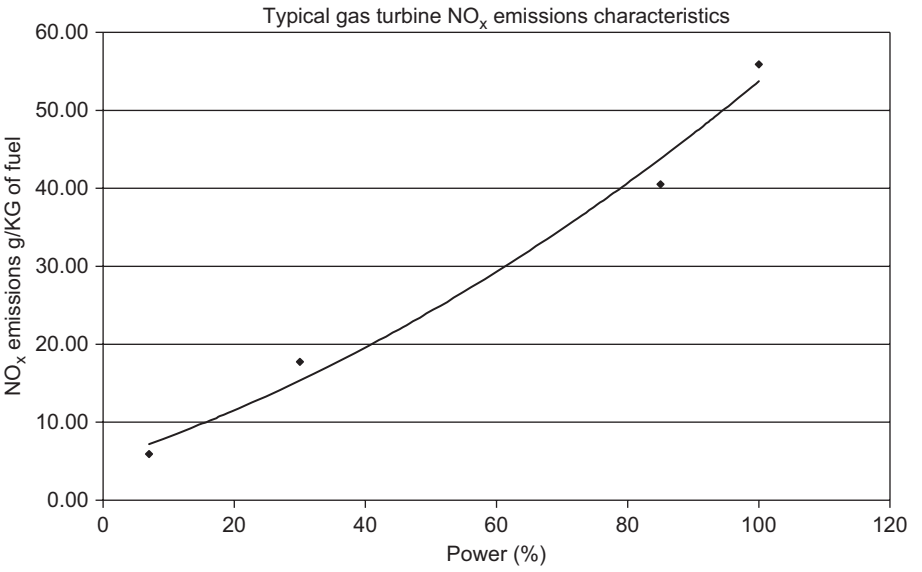


Figure 20-20 NO_x emissions for a typical gas turbine.

Reduction in both the flame temperature and the residence time decrease the production of NO_x but at the same time increases CO and UHC. Thus a compromise must be found to reduce all of them simultaneously.

The other approaches that are stated and being studied actively are:

- Lean premixed prevaporized (DLN Combustors)
- Variable geometry
- Staged (controlled) combustion, for example, rich burn, quick quench, lean burn combustor
- Catalytic oxidation

Measurements of the emissions should be taken from the exhaust duct at various operational speeds. Temperature and pressure readings are taken at the exit at a minimum of three different locations at any given time. Probes are connected to the various sections at the exhaust of the engine so that representative readings can be taken, and then to a manifold from which we can choose to open the required valve to get the various different emissions or pressure readings.

Plant Losses

The losses that are encountered in a plant can be divided into two groups, uncontrollable losses, and controllable losses. The uncontrollable losses are usually environmental conditions, such as temperature, pressure, humidity, and the turbine aging. Table 20-4 shows the approximate changes that would occur. It must be remembered that these are just approximations and will vary for individual power plants.

Table 20-4 Effect of Uncontrollable Losses on the Output and Heat Rate

Parameters	Parameter Change	Power Output	Heat Rate Change
Increase in ambient temperature	20 °F (11 °C)	−8.3%	2.2%
Decrease in ambient pressure	1 psi (6.895 KPa) Elevation = 2,000 ft.	−7%	−0.0001%
Increase in ambient Relative humidity	10%	−0.0002%	−0.0005%
Pressure drop in filter	1 inch (25 mm)WC	−0.5%	0.3%
Increase in gas turbine backpressure	1 inch (25 mm)WC	−.25%	.08%
Turbine age	First 10,000 hrs	−0.34/1,000 hrs	0.5/1,000 hrs
Turbine age	More than 10,000 hrs	−0.03/1,000 hrs	0.08/1,000 hrs

Table 20-5 Effect of Controllable Losses on the Output and Heat Rate

Parameters	Parameter Change	Power Output (%)	Heat Rate Change (%)
Compressor fouling	2%	−1.5	0.65
Pressure drop in filter	1 in H_2O (25 mm H_2O)	−0.5	−0.3
Increase in gas turbine backpressure	1 in H_2O (25 mm H_2O)	−0.25	−0.08
Lower heating value	−430 Btu/lb (−1,000 kJ/kg)	0.4	−1.0
Power factor	−0.05	−0.14	0.15

The controllable losses are those that the operator can have some degree of control over and can take corrective actions:

1. Pressure drop across the inlet filter. This can be remedied by cleaning or replacing the filter.
2. Compressor fouling. On-line water cleaning can restore part of the drop encountered.
3. Fuel lower heating value. In many plants on-line fuel analyzers have been introduced to not only monitor the turbine performance but to also calculate the fuel payments, which are usually based on the energy content of the fuel.
4. Turbine backpressure. In this case, the operator is relatively limited since the operator cannot do anything about the downstream design. Unless there is some obstruction in the ducting, which can be removed, or if the duct has collapsed in a section the duct could be replaced.

Table 20-5 shows the effect of controllable losses in the output and heat rate of a typical Combined Cycle Power Plant. The gas turbine has to be operated at a constant speed for power generation, and any slight variation in speed could result in major problems for the grid. Thus, the control of the load has to be by controlling the fuel input, therefore, the turbine firing temperature, and the inlet guide vane position, thus controlling the airflow. The effect of this is to try and maintain the exhaust temperature from the gas turbine at a relatively high value since this gas is used in the HRSG, and the effectiveness of the HRSG is dependent on maintaining this temperature.

Bibliography

ASME, Power Test Code 10 (PTCIO), 1965.

ASME, Performance Test Code on Steam Condensing Apparatus, ASME PTC 12.2, 1983, American Society of Mechanical Engineers, 1983.

ASME, Performance Test Code on Test Uncertainty: Instruments and Apparatus PTC 19.1, 1988.

ASME, Performance Test Code on Gas Turbine Heat Recovery Steam Generators, ASME PTC 4.4, 1981, American Society of Mechanical Engineers, Reaffirmed 1992.

ASME, Gas Turbine Fuels B 133.7M Published: 1985 Reaffirmed 1992.

ASME, Performance Test Code on Overall Plant Performance, ASME PTC 46, 1996.

ASME, Performance Test Code on Steam Turbines, ASME PTC 6, 1996.

ASME, Performance Test Code on Atmospheric Water Cooling Equipment PTC 23, 1997.

ASME, Performance Test Code on Gas Turbines, ASME PTC 22, 1997, American Society of Mechanical Engineers, 1997.

Boyce, M.P., Bayley, R.D., Sudhakar, V., and Elchuri, V., "Field Testing of Compressors," Proceedings of the 5th Turbomachinery Symposium, Texas A&M University, pp. 149–160, 1976.

Boyce, M.P., "Performance Monitoring of Large Combined Cycle Power Plants," Proceedings of the ASME 1999 International Joint Power Generation Conference, San Francisco, California. Vol. 2, pp. 183–190, July 1999.

Boyce, M.P., "Performance Characteristics of a Steam Turbine in a Combined Cycle Power Plant," Proceedings of the 6th EPRI Steam Turbine Generator/ Workshop, August 1999.

Canjar, L.N., "There's a Limit to Use of Equations of State," Petroleum Refiner, p. 113, February 1956.

Edmister, W.C., *Applied Hydrocarbon Dynamics*, Vol. 1, Gulf Publishing Co., Houston, Texas, pp. 1–3, 1961.

Gas Producers Association, Table of Physical Constants of Paraffin Hydrocarbons and Other Components of Natural Gas, Standard 2145–94.

Gonzalez, F., Boyce, M.P., "Solutions to Field Problems of a Gas Turbine-Axial-Flow Chemical Process Compressor Train Based on Computer Simulation of the Process," Proceedings of the 28th Turbomachinery Symposium, Texas A&M University, p. 77, 1999.

ISO, Natural Gas—Calculation of Calorific Value, Density and Relative Density International Organization for Standardization ISO 6976-1983(E).

Copyrighted Materials
Copyright © 2012 Elsevier Retrieved from www.knovel.com

21 Maintenance Techniques

Philosophy of Maintenance

Maintenance, defined as the "upkeep of property," is one of the most important operations in a plant. The manufacture and maintenance of turbomachinery are totally different. The first involves the shaping and assembly of various parts to required tolerances, while the second, maintenance, involves restoration of these tolerances through a series of intelligent compromises. The crux of maintenance technique is in keeping the compromises intelligent.

Maintenance is not a glamorous procedure; however, its importance is second to none. Maintenance procedures are always controversial, since the definition of "upkeep" varies with the individual interpretation of each maintenance supervisor. The latitude of maintenance ranges from strict planning and execution, inspection and overhaul, accompanied by complete reports and accounting of costs, to the operation of machinery until some failure occurs, and then making the necessary repairs.

Modern day turbomachinery is built to last between 30–40 years. Thus, the keeping of basic maintenance records and critical data is imperative for a good maintenance program. Economic justification is always the controlling factor for any program, and maintenance practices are not different.

Maintenance costs can be minimized by, and are directly related to, good operation; likewise, better operating results can be obtained when the equipment is under the control of a planned maintenance program. Improper operation of mechanical equipment can be as much or more of the cause of its deterioration and failure as is actual, normal mechanical wear. Thus, operation and maintenance go together.

Combining the practice of preventive maintenance and total quality control and total employee involvement results in an innovative system for equipment maintenance that optimizes effectiveness, eliminates breakdowns, and promotes autonomous operator maintenance through day-to-day activities. This concept known as Total Productive Maintenance (TPM) was conceived by Seiichi Nakajima and is well documented in his book "Introduction of TPM" and is highly recommended reading for all involved in the maintenance area.

A new maintenance system is introduced based on the new mantra for the selection of all equipment "Life Cycle Cost." This new system especially for major power plants is based on the combination of total condition monitoring, and the maintenance principles of total productive maintenance, and is called the "Performance Based Total Productive Maintenance System."

Gas Turbine Engineering Handbook, Fourth Edition. DOI: 10.1016/B978-0-12-383842-1.00021-4
Copyright © 2012 Elsevier Inc. All rights reserved.

The general maintenance system is fragmented and can be classified into many maintenance concepts. The following are the five P's of maintenance for major power plants, petro-chemical corporations, and other process-type industries leading to the ultimate maintenance system:

1. Panic maintenance based on breakdowns
2. Preventive maintenance
3. Performance based maintenance
4. Performance productive maintenance
5. Performance-based total productive maintenance (PTPM).

Performance-based total productive maintenance consists of the following elements:

1. Performance-based total productive maintenance aims to maximize equipment efficiency and time between overhaul (overall performance effectiveness).
2. Performance-based total productive maintenance aims to maximize equipment effectiveness (overall effectiveness).
3. Performance-based total productive maintenance establishes a thorough system of PM for the equipment's entire life span.
4. Performance-based total productive maintenance is implemented by various departments (engineering, operations, maintenance).
5. Performance-based total productive maintenance involves every single employee, from top management to workers on the floor.
6. Performance-based total productive maintenance is based on the promotions of PM through *motivation management*: autonomous small group activities.

The word "total" in "performance-based *total* productive maintenance" has four meanings that describe the principal features of PTPM:

1. *Total overall performance effectiveness* indicates PTPM's pursuit of maximum plant efficiency and minimum downtime.
2. *Total overall performance effectiveness* indicates PTPM's pursuit of economic efficiency or profitability.
3. *Total maintenance system* includes maintenance prevention (MP) and maintainability improvement (MI) as well as preventive maintenance.
4. *Total participation of all employees* includes autonomous maintenance by operators through small group activities.

Table 21-1 shows the relationship between PTPM, productive maintenance, and preventive maintenance.

Performance-based total productive maintenance eliminates the following seven major losses:

Down time:

1. Loss of time – due to unnecessary overhauls based only on time intervals.
2. Equipment failure – from breakdowns.
3. Loss of time – due to spare part unsuitability or insufficient spares.
4. Idling and minor stoppages – due to the abnormal operation of sensors or other protective devices.
5. Reduced output – due to discrepancies between designed and actual operating conditions.

Table 21-1 Benefits of Various Maintenance Systems Maintenance

	Performance-Based Total Productive Maintenance	Performance Productive Maintenance	Performance-Based Maintenance	Preventive Maintenance	Panic Maintenance
Economic efficiency	Yes	Yes	Yes	Yes	No
Economic and time efficiency	Yes	Yes	Yes	No	No
Total system efficiency	Yes	Yes	No	No	No
Autonomous maintenance by operators	Yes	No	No	No	No

Defect:

1. Process defects – due to improper process conditions that do not meet machinery design requirements.
2. Reduced yield – from machine start-up to stable production due to the inability of the machine to operate at proper design conditions.

Maximization of Equipment Efficiency and Effectiveness

High machine efficiency and availability can be attained by maintaining the health of the equipment. Total performance condition monitoring can play a major part here as it provides early warnings of potential failures and performance deterioration. Figure 21-1 shows the concept of a total performance condition monitoring system.

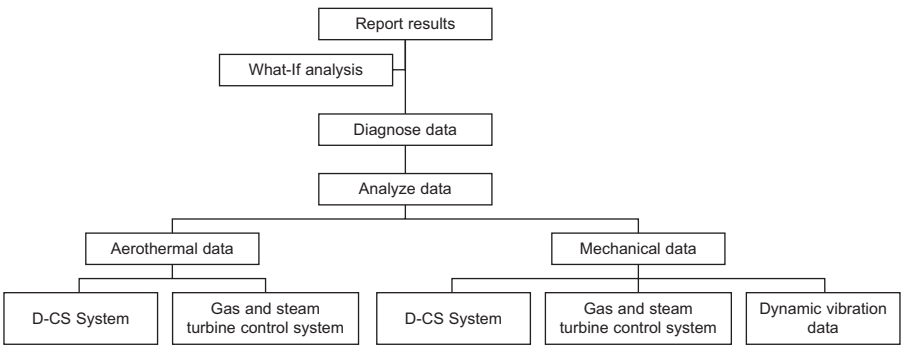
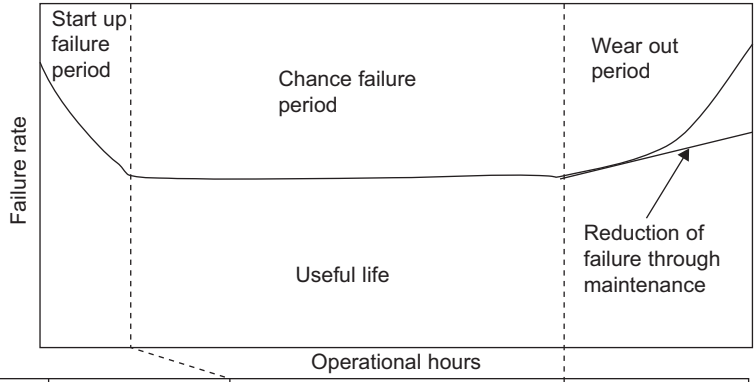


Figure 21-1 Total performance-based condition monitoring system.



Category	Start up failure	Chance failure	Wear out failure
Cause	Design manufacturing errors	Operational errors	Wear out
Counter measures	Trial runs at acceptance and startup controls	Proper operation	Preventive and maintainability improvement
	Maintenance prevention		

Figure 21-2 Machinery life cycle characteristics.

Pure preventive maintenance alone cannot eliminate breakdowns. Breakdowns occur due to many factors such as design and/or manufacturing errors, operational errors, and wearing out of various components. Thus, changing components at fixed intervals does not solve the problems and in some cases adds to the problem. A study at a major nuclear power station indicated that nearly 35% of the failures occurred within a month of a major turnaround. Figure 21-2 shows the life characteristics of a major piece of turbomachinery.

The goal of any good maintenance program is "Zero Breakdown." To achieve this goal, there are five countermeasures. These are listed below:

1. Maintaining well-regulated basic conditions (cleaning, lubricating, and bolting).
2. Adhering to proper operating procedures.
3. Total condition monitoring (performance, mechanical, and diagnostic based).
4. Improving weaknesses in design.
5. Improving operation and maintenance skills.

The interrelationship between these five items is shown in Figure 21-3.

The division of labor between operations and maintenance is shown in Figure 21-4. It is the primary responsibility of the production department to establish and regulate basic operating conditions, and it is the primary responsibility of the maintenance department to improve defects in design. The other tasks are shared between the two departments.

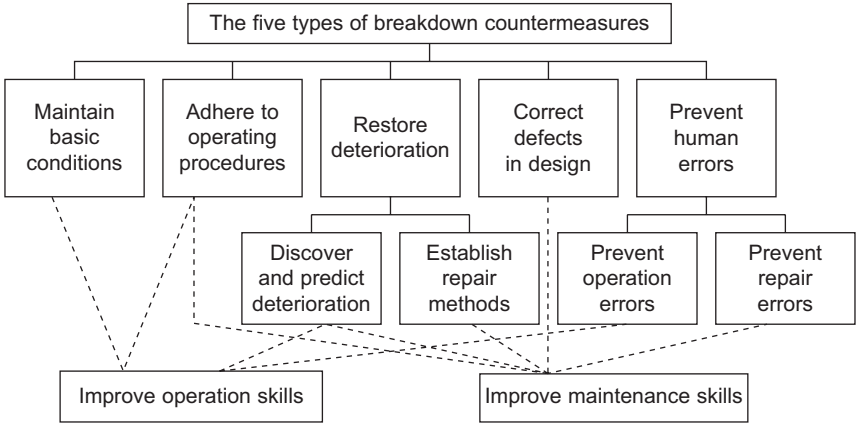


Figure 21-3 Breakdown countermeasures.

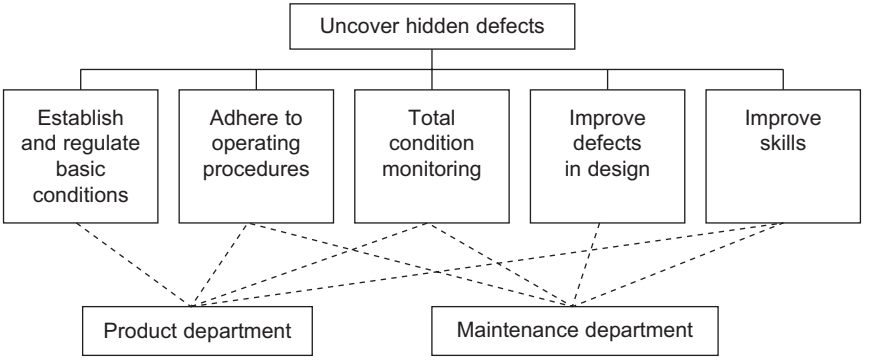


Figure 21-4 Responsibilities of the operations and maintenance departments.

The successful implementation of total productive maintenance requires:

1. Elimination of the six big losses to improve equipment effectiveness
2. An autonomous maintenance program with total condition monitoring
3. A scheduled maintenance program for the maintenance department
4. Increased skills of operations and maintenance personnel
5. An initial equipment management program

Organization Structures for a Performance-Based Total Productive Maintenance Program

Typically successful implementation of PTPM in a large plant takes three years. Implementation calls for:

1. Changing people's attitudes
2. Increasing motivation

3. Increasing competency
4. Improving the work environment

The four major categories in developing a Performance-Based Total Productive Maintenance program are:

1. Preparation for the PTPM program
2. Preliminary implementation
3. PTPM implementation
4. Stabilization of the program

Implementation of a Performance-Based Total Productive Maintenance

There are several steps involved in implementation of a PTPM program.

1. *Announcement of decision to implement PTPM.* A formal presentation must be made by top management introducing the concepts, goals, and benefits of PTPM. Management commitment must be made clear to all levels of the organization.
2. *Educational campaign.* The training and promotion of PTPM philosophy is a must. This is useful to reduce the resistance to change. The education should cover how PTPM will be beneficial to both the corporation and the individuals.
3. *Creation of organization to promote PTPM.* The PTPM promotional structure is based on an organizational matrix. Obviously, the optimal organizational structure would change from organization to organization.

   In large corporations, PTPM promotional headquarters must be formed and staffed. Thus, any questions can be addressed here on a corporate level.
4. *Establishment of basic PTPM goals.* Establishing mottos and slogans can do this. All goals must be quantifiable and precise specifying:
   a. Target (what)
   b. Quantity (how much)
   c. Time Frame (when)
5. *Master plan development for PTPM.* A master plan must be created. Total condition monitoring equipment should be designed, and equipment should be purchased.
6. *Initiation of PTPM.* This represents a "kickoff" stage. At this point, the whole staff must start to get involved.
7. *Improvement of equipment effectiveness.* This should start with a detailed design review of the plant machinery. A performance analysis of the plant could point to a specific area known to have problems (i.e., section of plant) must be selected and focused on, project teams should be formed and assigned to each train. An analysis should be conducted that addresses the following:
   a. *Define the problem.* Examine the problem (loss) carefully; compare its symptoms, conditions, affected parts, and equipment with those of similar cases.
   b. *Do a physical analysis of the problem.* A physical analysis clarifies ambiguous details and consequences. All losses can be explained by simple physical laws. For example, if scratches are frequently produced in a process, friction or contact between two objects should be suspected, (of the two objects, scratches will appear in the object with the weaker resistance). Thus, by examining the points of contact, specific problem areas and contributing factors are revealed.

c. *Isolate every condition that might cause the problem.* A physical analysis of breakdown phenomena reveals the principles that control their occurrence and uncovers the conditions that produce them. Explore all possible causes.
d. *Evaluate equipment, material, and methods.* Consider each condition identified in relation to the equipment, jigs and tools, material, and operating methods involved, and draw up a list of factors that influence the conditions.
e. *Plan the investigation.* Carefully plan the scope and direction of investigation for each factor. Decide what to measure and how to measure it and select the datum plane.
f. *Investigate malfunctions.* All items planned in step 5 must be thoroughly investigated. Keep in mind optimal conditions to be achieved and the influence of slight defects. Avoid the traditional factor analysis approach; do not ignore malfunctions that might otherwise be considered harmless.
g. *Formulate improvement plans.* Define consultants who could re-design the given piece of equipment. Discuss your plans with manufacturers.

8. *Establishment of autonomous maintenance program for operators.* This is focused against the classic "Operations" versus "Maintenance" battle. *Operators here must be convinced that they should maintain their own equipment.* For example, *an attitude has to be developed for operators to understand* and *act* on the reports produced by the on-line performance condition monitoring systems.
9. *Setup of scheduled maintenance program.* Scheduled maintenance conducted by the maintenance department must be smoothly coordinated with autonomous maintenance done by the plant operators. This can be done by frequent meetings and plant audits. In most plants an undeclared conflict exists between the operations and maintenance groups. This arises from the false perception that these two groups having conflicting goals. The PTPM philosophy will go a long way in bringing these groups together.
10. *Training for improvement of operation and maintenance skills.* This is a key part of PTPM. Ongoing training in advanced maintenance techniques, tools, and methods must be done. This could cover areas such as:
a. Bearings and seals
b. Alignment
c. Balancing
d. Vibration
e. Troubleshooting
f. Failure analysis
g. Welding procedures
h. Inspection procedures
i. NDT
11. *Equipment management program.* Start-up problems, solutions, and design changes should be clearly documented and available for a good equipment management plan. All items that can reduce Life Cycle Costs (LCC) should be considered. These include:
a. Economic evaluation at the equipment-investment stage
b. Consideration of MP or maintenance-free design and economic LCC
c. Effective use of accumulated MP data
d. Commissioning control activities
e. Thorough efforts to maximize reliability and maintainability
12. Final implementation of PTPM. This stage involves the refinement of PTPM and the formulation of new goals that meet specific corporate needs.

Maintenance Department Requirements

To ensure the success of the PTPM program, the maintenance department must be well equipped and trained. The following six basic categories are prerequisite to the proper functioning of the Maintenance Department under the PTPM:

1. Training of personnel
2. Tools and equipment
3. Condition and life assessment
4. Spare parts inventory
5. Redesign for higher machinery reliability
6. Maintenance scheduling
7. Maintenance communication
8. Inspections

Training of Personnel

Training must be the central theme. The days of the mechanic armed with a ball-peen hammer, screwdriver, and a crescent wrench are gone. More and more complicated maintenance tools must be placed in the hands of the mechanic, and he must be trained to utilize them.

People must be trained, motivated, and directed so that they gain experience and develop, not into mechanics, but into highly capable technicians. While good training is expensive, it yields great returns. Machinery has grown more complex, requiring more knowledge in many areas. The old, traditional craft lines must yield before complicated equipment maintenance needs. A joint effort by craftsmen is necessary to accomplish this.

I. Type of Personnel

a. Maintenance Engineer

In most plants, the maintenance engineer is a mechanical engineer with training in the turbomachinery area. His needs are to convert what he has learned in the classroom into actual hands-on solutions. He must be well versed in a number of areas such as performance analysis, rotor dynamics, metallurgy, lubrication systems, and general shop practices. His training must be well planned so that he can pick up these various areas in steps. His training must be a combination of a hands-on approach coupled with the proper theoretical background. He should be well versed in the various ASME power test codes. Table 21-2 is a listing of some of the applicable codes for gas turbine power plants. Attendance at various symposiums where users of machinery get together to discuss problems should be encouraged. It is not uncommon to find a solution to a problem at these types of round table discussions.

b. Foreperson and Lead Machinist

These people are the key to a good maintenance program. They should be sent frequently to training schools to enhance their knowledge. Some plants have one

Table 21-2 Performance Test Codes

1. ASME, Performance Test Code on Overall Plant Performance, ASME PTC 46 1996, American Society of Mechanical Engineers, 1996
2. ASME, Performance Test Code on Test Uncertainty: Instruments and Apparatus PTC 19.1, 1988
3. ASME, Performance Test Code on Gas Turbines, ASME PTC 22 1997, American Society of Mechanical Engineers, 1997
4. ASME, Performance Test Code on Gas Turbine Heat Recovery Steam Generators, ASME PTC 4.4 1981, American Society of Mechanical Engineers, Reaffirmed 1992
5. ASME Gas Turbine Fuels B 133.7M Published: 1985 (Reaffirmed year: 1992)
6. ISO, Natural Gas—Calculation of Calorific Value, Density and Relative Density International Organization for Standardization ISO 6976-1983(E)

foreperson who is an "in-house serviceperson;" he or she supervises no personnel, but acts as an in-house consultant on maintenance jobs.

c. Machinist/Millwright

The machinist should be encouraged to operate most of the machinery in the plant maintenance shop. By rotating among various jobs, learning and development is accelerated. He or she should then become as familiar with a large compressor as a small pump. Encouragement should be given to the machinist to learn balancing operations and to participate in the solution of problems.

Spreading around the hardest jobs develops more competent people and is the basis of any PTPM program. Restricting people to one type of work will probably make them an expert in that area, but curiosity and initiative, prime motivators, will eventually fade.

II. Types of Training

a. Update Training

This training is mandatory for all maintenance personnel, so that they may keep abreast of this high technology industry. Personnel must be sent to manufacturer-conducted schools. These schools, in turn, should be encouraged to cover some basic machinery principles as well as their own machinery. In-house seminars should be provided with in-house personnel and consultants at the plant. Engineers should be sent to various schools so that they may be exposed to the latest technology.

An in-house website, cataloging experiences and special maintenance techniques, should be updated and available for the entire corporation especially maintenance and operation personnel. These websites should be full of illustrations, short, and to the point.

A small library should be adjacent to the shop floor, with field drawings, written histories of equipment, catalogs, API specifications, and other literature pertinent to the machine maintenance field. Drawings and manuals should be transferred to the electronic digital media as soon as possible. Access to the Internet on the maintenance and

Table 21-3 Mechanical Specifications

ASME Basic Gas Turbines B133.2 Published: 1977 (Reaffirmed year: 1997).
ASME Gas Turbine Control and Protection Systems B133.4 Published: 1978 (Reaffirmed year: 1997).
ASME Gas Turbine Installation Sound Emissions B133.8 Published: 1977 (Reaffirmed: 1989).
ASME Measurement of Exhaust Emissions from Stationary Gas Turbine Engines B133.9 Published: 1994.
ASME Procurement Standard for Gas Turbine Electrical Equipment B133.5 Published: 1978 (Reaffirmed year: 1997).
ASME Procurement Standard for Gas Turbine Auxiliary Equipment B133.3 Published: 1981 (Reaffirmed year: 1994).
ANSI/API Std 610 Centrifugal Pumps for Petroleum, Heavy Duty Chemical and Gas Industry Services, 8th Edition, August 1995.
API Std 613 Special Purpose Gear Units for Petroleum, Chemical and Gas Industry Services, 4th Edition, June 1995.
API Std 614, Lubrication, Shaft-Sealing, and Control-Oil Systems and Auxiliaries for Petroleum, Chemical and Gas Industry Services, 4th Edition, April 1999.
API Std 616, Gas Turbines for the Petroleum, Chemical and Gas Industry Services, 4th Edition, August 1998.
API Std 617, Centrifugal Compressors for Petroleum, Chemical and Gas Industry Services, 6th Edition, February 1995.
API Std 618, Reciprocating Compressors for Petroleum, Chemical and Gas Industry Services, 4th Edition, June 1995.
API Std 619, Rotary-Type Positive Displacement Compressors for Petroleum, Chemical, and Gas Industry Services, 3rd Edition, June 1997.
ANSI/API Std 670 Vibration, Axial-Position, and Bearing-Temperature Monitoring Systems, 3rd Edition, November 1993.
API Std 671, Special Purpose Couplings for Petroleum Chemical and Gas Industry Services, 3rd Edition, October 1998.

production area computers is a must as many manufacturers post helpful operational and maintenance hints on their websites. API specifications, which govern mechanical machinery, are listed in Table 21-3.

Manufacturer instruction books are often inadequate and need to be supplemented. The rewriting of maintenance manuals on such subjects as mechanical seals, vertical pumps, hot-tapping machines, and gas and steam turbines is not uncommon. The turbine overhaul manuals transferred on CD's could consist of (1) step-by-step overhaul procedures, developed largely from the manufacture's training school, (2) hundreds of photographs, illustrating the step-by-step procedures on various types of gas and steam turbines, (3) an arrow diagram showing the sequences of the procedures, and (4) typical case histories.

Detailed drawings on CD's are developed to aid in maintenance, such as a contact seal assembly, because the "typical" dimensionless drawing supplied by the OEM is not adequate to correctly assemble the compressor seals. Many other assembly drawings should be developed to facilitate the overall maintenance program. Videotaped programs are being developed on seals, bearings, and rotor dynamics, which will be a tremendous asset to most company maintenance programs.

b. Practical Training

The engineers in the maintenance group should be encouraged to gather pertinent vibration and aerothermal data and analyze the machinery. ASME performance specifications, which govern all types of power plants and other critical equipment, are listed in Table 21-2. They should be encouraged to work closely at the various maintenance schedules and turnarounds so that they are familiar with the machinery. They should be sent to special training sessions where hands-on experience can be gained.

After the completion of basic machinist training, the machinist should continue training with on-the-job experiences. His or her skills should be tested, and the machinist should be encouraged to take on different tasks.

To develop the skills of in-house personnel, as much repair work as possible should utilize plant personnel. Encouraging the participation of the machinist in the solution of difficult problems often results in the machinist seeking information on his or her own. References to API and ASME specifications should not be uncommon on the shop floor. Today's machinist and mechanic must be computer literate. Internet training must be provided with some basic training on word processing and spreadsheet programs.

c. Basic Machinist Training

Most of the basic training can be developed and conducted by in-plant personnel. This training can be highly detailed and tailored precisely to meet individual plant requirements. Training must be carefully planned and administered to fit the requirements of different machinery in the plant.

Many plants have a full-time training program, and personnel for conducting training at this basic level. Good maintenance practices should be inculcated into the young machinist from the beginning. He or she should be taught that all clearances should be carefully checked and noted both before and after reassembly. The machinist should learn the proper care in the handling of instrumentation, and the care in placing and removing seals and bearings. A base course on the major turbomachinery principles is a must, so there is basic understanding of what these machines do and how they function. The young machinist should also be exposed to basic machinery-related courses such as:

1. Reverse indicator alignment
2. Gas and steam turbine overhaul
3. Compressor overhaul

4. Mechanical seal maintenance
5. Bearing maintenance
6. Lubrication system maintenance
7. Single plane balancing

Tools and Shop Equipment

A mechanic must be supplied with the proper tools to facilitate the job. Many special tools are required for different machines, so as to ensure proper disassembly and reassembly. Torque wrenches should be an integral part of the tools, as well as of the vocabulary.

The concepts of "finger tight" and "hand tight" can no longer be applied to high-speed, high-pressure machinery. A major explosion at an oxygen plant, which resulted in a death, was traced back to gas leakage due to improper torquing. A good dial indicator and special jigs for taking reverse indicator dial readings is a must. The jigs must be specially made for the various compressor and turbine trains. Special gear and wheel pullers are usually necessary.

Equipment for heating wheels in the field for assembly and disassembly are needed; specially designed gas rings are often used for this purpose.

A maintenance shop should have the traditional horizontal and vertical lathes, mills, drill presses, slotters, bores, grinders, and a good balancing machine. A balancing machine can pay for itself in a very short time in providing a fast turnaround and accurate dynamic balance. Techniques to check the balance of gear-type couplings for the large high-speed compressors and turbine drives as a unit should be developed. This leads to the solving of many vibration related problems. High-speed couplings should be routinely check-balanced.

By dynamically balancing most parts, seal life and bearing life are greatly improved, even on smaller equipment. Dynamic balancing is needed on pump impellers, as the practice of static balance is woefully inadequate. Vertical pumps must be dynamically balanced; the long, slender shafts are highly susceptible to any unbalance-induced vibration.

This assembly and disassembly of rotors must be in a clean area. Horses or equivalents should be available to hold the rotor. The rotor should rest on the bearing journals, which must be protected by soft packing, or the equivalent, to avoid any marring of the journals. To accomplish uniform shrink fits, the area should have provisions for heating and/or cooling. A special rotor-testing fixture should be provided; this is very useful in checking for wheel wobbles, wheel roundness, and shaft trueness. Rotors in long-term storage should be stored in a vertical position in temperature-controlled warehouses.

Spare Parts Inventory

The problem of spare parts is an inherent phase of the maintenance business. The high costs of replacement parts, delivery, and in some instances, poor quality, are problems

faced daily by everyone in the maintenance field. The cost of spare parts for a major power plant or refinery runs into many millions of dollars.

The inventory of these plants can run into over 20,000 items, including over 100 complete rotor systems. The field of spare parts is changing rapidly and is much more complex than in the past. A group of plants have got together in a given region and formed "Part Banks."

Many pieces of equipment are made up of unitized components from several different vendors. The traditional attitude has been to look to the packaging vendor as the source of supply. Many vendors refuse to handle requests for replacement parts on equipment not directly manufactured by them. More and more specialty companies are entering the equipment parts business; some are supplying parts directly to OEM companies for resale as their "own" brand. Others supply parts directly to the end user. The end user must develop multiple sources of supply for as many parts as possible.

Gaskets, turbine carbon packing, and mechanical seal parts can be purchased from local sources. Shafts, sleeves, and cast parts can be purchased from local sources. Shafts, sleeves, and cast parts such as impellers, are becoming increasingly available from specialty vendors. All this competition is causing the OEM's to alter their spare parts system to improve service and reduce prices, which is definitely a bright spot in the picture. The quality control of both OEM and some specialty houses leaves much to be desired. In turn, this causes many plants to have an in-house quality control person checking all incoming parts, a concept highly recommended.

Condition and Life Assessment

Condition and life assessment is significant for all types of plants, and especially Combined Cycle Power Plants. The most important aspect of a plant is high availability, and reliability, in some cases even more significant than higher efficiency.

Availability and Reliability

The Availability of a gas turbine is the percent of time the gas turbine is available to generate power in any given period at its acceptance load. The Acceptance Load or the Net Established Capacity would be the net electric power generating capacity of the gas turbine at design or reference conditions established as a result of the Performance Tests conducted for acceptance of the plant. The actual power produced by the gas turbine would be corrected to the design or reference conditions and is the actual net available capacity of the gas turbine. Thus it is necessary to calculate the effective forced outage hours, which are based on the maximum load the plant can produce in a given time interval when the plant is unable to produce the power required of it. The effective forced outage hours are based on the following relationship:

$$EFH = HO_x \frac{(MW_d - MW_a)}{MW_d} \tag{21-1}$$

where

MW_d = Desired output corrected to the design or reference conditions. This must be equal to or less than the gas turbine load measured and corrected to the design or reference conditions at the acceptance test.
MW_a = Actual maximum acceptance test produced and corrected to the design or reference conditions.
HO = Hours of operation at reduced load.

The Availability of a gas turbine can now be calculated by the following relationship, which takes into account the stoppage due to both forced and planned outages, as well as the forced effective outage hours:

$$A = \frac{(PT - PM - FO - EFH)}{PT} \tag{21-2}$$

where

PT = Time period (8760 hrs/year)
PM = Planned maintenance hours
FO = Forced outage hours
EFH = Equivalent forced outage hours

The Reliability of the gas turbine is the percentage of time between planned overhauls and is defined as:

$$R = \frac{(PT - FO - EFH)}{PT} \tag{21-3}$$

Availability and Reliability have a very major impact on the plant economy. Reliability is essential in that when the power is needed it must be there. When the power is not available it must be generated or purchased and can be very costly in the operation of a plant. Planned outages are scheduled for nonpeak periods. Peak periods are when the majority of the income is generated, as usually there are various tiers of pricing depending on the demand. Many power purchase agreements have clauses, which contain capacity payments, thus making plant availability critical in the economics of the plant. A 1% reduction in plant availability could cost $500,000 in loss of income on a 100 MW plant.

Reliability of a plant depends on many parameters, such as the type of fuel, the preventive maintenance programs, the operating mode, the control systems, and the firing temperatures. Another very important factor in a gas turbine is the Starting Reliability (SR). This reliability is a clear understanding of the successful starts that have taken place and is given by the following relationship:

$$SR = \frac{number\ of\ starting\ successes}{(number\ of\ starting\ successes + number\ of\ starting\ failures)} \tag{21-4}$$

The insurance industry concerns itself with the risks of equipment failure. For advanced gas turbines, the frequencies of failures and the severity of failures are major concerns. In engineering terms, however, risk is better defined as:

$$Risk = Probability\ of\ Failure \times Consequences\ of\ Failure \tag{21-5}$$

where

the consequences of failure include the repair/replacement costs and the lost revenue from the down time to correct the failure.

Actions taken, which reduce the probability and/or consequences of failure, tend to reduce risk and generally enhance insurability. Because of the high risks associated with insuring advanced gas turbines, demonstrated successful operation is important to the underwriting process.

Gas turbines with the new technology, higher pressure ratio, and higher firing temperature, have led to the building of large gas turbines producing nearly 300 MW and reaching gas turbine efficiencies in the mid-forties. The availability factor for units with mature technology, below 100 MW, are between 94–97%, while the bigger units above 100 MW have availability factors of 85–89%. The bigger units produce twice the output, but the availability factor has decreased from 95% to 85%. A decrease of 7–10 points for all manufacturers. Part of this decrease may be related to larger machinery taking more time to repair. It is also due to the high temperature and pressure.

The increase in unit size and complexity together with the higher turbine inlet temperature and higher pressure ratio has led to an increase in overall gas turbine efficiency. The increase in efficiency of 7–10% has in many cases led to an availability decrease of the same amount or even more as seen in Figure 21-5. A 1% reduction in plant availability could cost $500,000 a year in income on a 100 MW plant, thus in many cases offsetting gains in efficiency.

Reliability of a plant depends on many parameters, such as the type of fuel, the preventive maintenance programs, the operating mode, the control systems, and the firing temperatures.

Redesign for Higher Machinery Reliability

Low reliability of units gives rise to high maintenance costs. Low reliability is usually a greater economic factor than the high maintenance costs. In many large power plants, refineries, and petrochemical complexes, about one-third of the failures are due to machinery failure; it is therefore necessary to redesign parts of a machine to improve reliability.

The maintenance practice of one large refinery is to replace gas turbine control systems with state-of-the-art electronics and “plug-in” concepts for ease of maintenance. These installations have been highly successful in that maintenance has been minimal, and can usually be accomplished on-stream. Another replaces all journal bearings with tilting pad bearings.

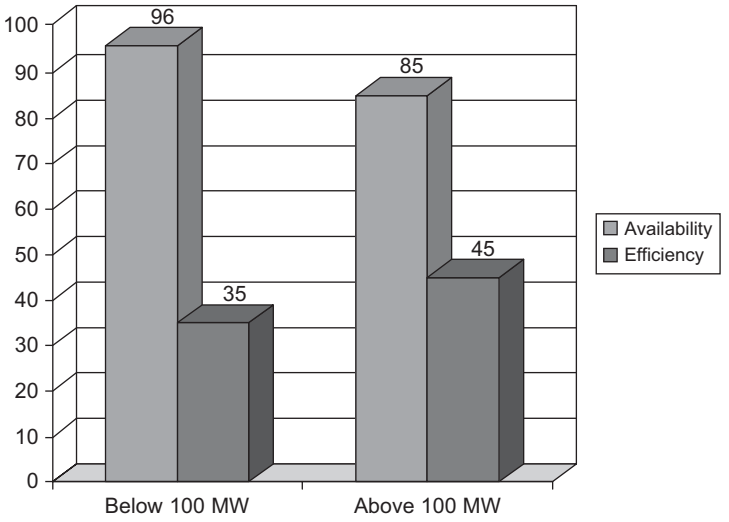


Figure 21-5 Comparison of availability and efficiency for large frame–type gas turbines.

In addition, the new control systems increase turbine performance, while speed control and flexibility are greatly improved. The original design has been supplemented to include a self-contained alarm system, a semiautomatic sequential start system, and a complete trip and protection system, as well as the electronic controls. The cost of this system is substantially less than the cost of a similar device offered by the OEM on new machines.

The gas turbine's major limitations are the life of the combustor cans, first-stage turbine nozzles, and first-stage turbine blades as seen in Figure 21-6. The effect of dry Low NO_x combustors has been very negative on the availability of Combined Cycle Power Plants, especially those with dual fuel capability. Flashback problems are a very major disruption as they tend to create burning in the pre-mix section of the combustor, and cause failure of the pre-mix tubes. These pre-mix tubes are also very susceptible to resonance vibrations.

Bearing failures are one of the major causes of failures in turbomachinery. The changing of various types of radial bearings from cylindrical and/or pressure dam babbitted sleeve bearings to tilting pad journal bearings is becoming common in the industry. In most cases, this gives better stability, eliminates oil whirl, and under misalignment condition, is more forgiving.

Thrust bearing changes, from the simple, tapered land thrust bearings to tilting pad thrust bearings with leveling links (Kingsbury type) are another area of common change. These types of bearings absorb sudden load surges and liquid slugs. Many users have changed out the inactive thrust bearing to carry the same load as the active thrust bearings. This has been the case in older gas turbines where traditionally the load carrying capacity of the inactive thrust bearing was 1/3 of the active thrust bearing. As

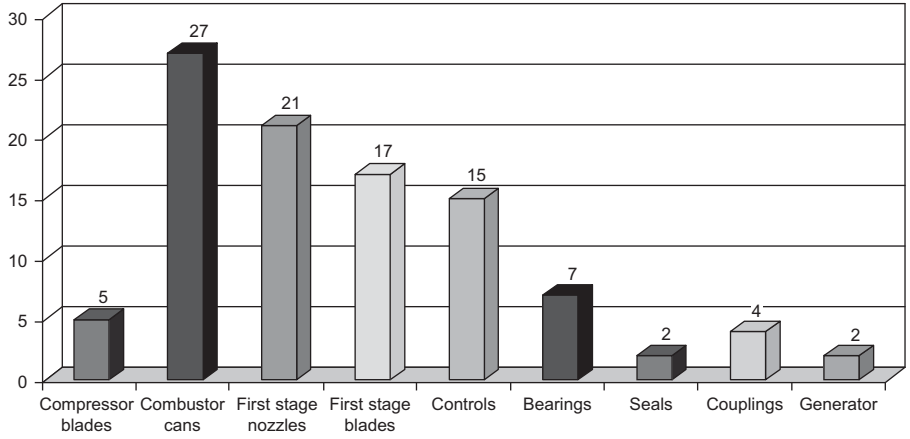


Figure 21-6 Contributions of various major components to gas turbine down time.

gas turbines got older the leakages increased and the thrust forces were altered greatly leading to failures in the inactive thrust bearings.

A major plant replaces the entire large journal and thrust bearings in their main machinery to tilting pad bearings in their plant as a matter of practice.

Material changes of the babbit are sometimes undertaken. Changing from the more common steel backed babbitted bearings to the copper alloys, with babbitted pads, conducts surface heat away at a faster rate, thus increasing the load carrying capacity. In some instances, a 50–100% load carrying capacity improvement can be achieved. Some equipment manufacturers are offering bearing-upgrading kits for their machine in service.

Design of turbine blades to obtain higher efficiency and damping has been done. In some cases, this has improved efficiency by 8–10%, and stopped failures in these blades. Steam injection has been utilized in gas turbines to improve efficiency and to increase the power output. Redesign of various bleed-off ports has reduced tip stalls and their accompanying blade failures.

Today's machinery, which is pushing the state-of-the-art in design, needs more than "simple fixes." This is one major reason why so much redesign takes place in the field. Maintenance engineers are no longer just required to repair, they are required in many cases to make revisions. Continual improvements and updating of the machinery is required to obtain the long runs and high efficiencies desirable in today's turbomachinery.

Gas Turbine Start-up

Many problems Gas Turbines encounter during their operation can be traced to improper start-up procedures. It is recommended that good baseline data should be

obtained during the start-up procedure. The following are some guidelines that should be followed during the start-up:

1. Before start-up, become familiar with the gas turbine and its driven equipment. If the gas turbine is a power generation unit it operates at a constant speed; however, if it is a mechanical drive turbine the turbine would have to operate over a wide range of speed. The following are some of the critical operating parameters that should be considered:
   - **a.** Operating speeds of the gas turbine – if the gas turbine has more than one shaft, operating speeds of all the shafts
   - **b.** Operating speeds of the driven train (compressors, pumps)
   - **c.** Critical speeds of the gas turbine
   - **d.** Critical speeds of the driven train
   - **e.** Operating temperatures, and pressures of the gas turbine
   - **f.** Operating temperatures, and pressures of the driven equipment; surge flow and pressure of the driven compressor
   - **g.** For multiple shaft gas turbines, the speed of the gasifier turbine, when the power turbine will commence turning
   - **h.** If all vibration monitoring systems are functioning, and what the alert and danger limits are
   - **i.** Assurance that the turbine turning gear is operational
   - **j.** Assurance that the internal alignment and external alignment is accurate as per the growth of the various bearing pedestals
2. To ensure that the gas turbine has no shaft bow the following steps should be undertaken:
   - **a.** Slow roll (from one-half to three hours, depending on operational experience of the type of gas turbine) to relieve rotor bow and allow for system warm-up
   - **b.** At a slow-roll speed of less than 800 rpm, take the applicable slow-roll data:
     - **i.** Gap voltages
     - **ii.** Probe identification
     - **iii.** Total electrical and mechanical run-out
     - **iv.** Keyphazor relationships
     - **v.** Vibration values in mils, displacement, velocity, and acceleration
     - **vi.** Observation of all meters, gauges, sight glasses, oil temperatures, discharge temperatures, balance-line pressures, surface condenser temperature, and so on
3. Bring the machine *through* the first critical, and observe the machine's performance for 15 minutes. It is good practice that the unit be outfitted with a signature analyzer using Fast Fourier Transform (FFT) to analyze the start-up data. This data should be stored and analyzed thoroughly and stored for future reference.
4. Bring the machine midway between the first critical and minimum governor. Observe performance for 15 minutes.
5. Go quickly to minimum governor to ensure that the rotors go through any other criticals as easily as possible.
6. At minimum governor, another set of vibration readings must be recorded.
7. Bearing temperatures should be monitored at both the journal and thrust bearings.
8. Oil samples should be taken to ensure that metallic elements are not present.
9. Checks must be made to ensure that auxiliary oil pumps are operational. Also the DC pump needs to be examined and the control system permissive needs to be checked out to ensure that the system is never permitted to operate if the DC pump is not operational.

10. Oil systems must be programmed so that oil flows throughout the turbine for a minimum of 20 to 30 minutes after shutdown, as in many cases maximum temperature is reached 15 to 20 minutes after shutdown.
11. For DLN combustion systems the combustors require tuning. In many cases the tuning equipment, which also consists of an FFT analyzer analyzing the signal from the dynamic pressure transducers which measure the combustion pressure dynamics, is removed after start-up, but it is recommended that this equipment should be left fully operational as another protection device.
12. The fuel system should be checked to ensure that there are no liquids in the system and that the fuel pressure is remaining constant.
13. NO_x emission readings should be taken; an increase in NO_x data may indicate problems in the combustion system.
14. Wheel space temperature data should be measured and logged. These temperatures should remain constant at given power levels.
15. Exhaust gas temperatures should be recorded. A minimum of 10 exhaust temperature probes should be used to ensure that the combustion is even. Difference between maximum and minimum temperature should not exceed over 60 °F–80 °F (37 °C–50 °C) for Natural gas systems, and between 90 °F and 110 °F (57 °C–69 °C) for liquid fuel systems. Adjacent exhaust temperatures should not vary more than 25 °F–35 °F (16 °C–22 °C). Excess variations would indicate combustion problems.
16. Gas turbine compressor pressure ratio and exhaust compressor temperature should be recorded.
17. Gas turbine power and heat rate with power variation should be recorded.
18. Data should be recorded in D-CS systems, and then stored for future reference. Care should be taken that the start-up data is not overwritten.

These are some major points that should be carefully monitored to ensure trouble free operation.

Redesign for Higher Machinery Reliability

Advanced Gas Turbines

The new advanced gas turbines are pushing the technology envelope in pressure (up to 588 psia, 40 Bar), temperature (2700 °F, 1482 °C), low NO_x combustion systems (less than 9 ppm), and material technology (single crystal blades). The benefits of advanced gas turbines and their technologies are easily quantified. The gas turbines produce more power, use less fuel, provide higher combined cycle efficiencies, and reduce emission levels significantly. The advanced gas turbines have developed very high efficiencies of between 40–45% due to high pressure ratio (30:1 for frame and 40:1 for aero-engines) and high firing temperatures (2700 °F, 1482 °C). The advantages of advanced gas turbines have been eclipsed by the following major problems experienced in the operation of these turbines:

- Lower availability (up to 10% lower)
- Lower life of nozzles and blades (averaging 15,000 hours)
- Higher degradation rate (5–7% in the first 10,000 hours of operation)
- Instability of low NO_x combustors

Meetings with users have indicated that the users are satisfied with the efficiency of these turbines but would like to see an improvement in the overall operation and maintenance of the turbines. The survey of users indicated that the following were the major concerns of the users, regarding the operation of gas turbines:

- Low availability and reliability
- Repair of single crystal blades
- Stability of low NO_x combustors
- Surge in compressors, and excessive tip rubs
- Bearings and seal problems

From an availability and reliability point of view, there is a significant down-side to today's new turbines. New advanced turbines are run at higher firing temperatures, are physically larger in size, have larger throughput (airflows and fuel flows), and have higher loadings (pressure and expansion ratios, fewer airfoils, larger diameters) than previous gas turbine designs. The large size of these gas turbines is one inherent cause of a lower availability and reliability as it takes much longer to do the various inspections and overhauls.

New advanced turbines are run at higher pressure ratios (as high as 30:1). This creates a very narrow operating margin (surge-choke). Thus any deposits on the blade could lead to degraded performance and surge in the compressors. The close tolerances between the casing and the compressor blades lead sometimes to excessive rubs.

New advanced gas turbines are pushing the temperature envelope. The technologies (design, materials, and coatings) required to achieve the benefits are more complex to concurrently meet gas turbine performance, emissions, and life requirements.

The design margins with these technologies tend to be reduced or unvalidated. Although analytical models may be extrapolated to evaluate the new designs, full-scale verification of new designs is an absolute necessity. Similarly, the materials being used are either relatively new or are being pushed to new limits. This leads to temperature problems in the turbine nozzle vanes and the turbine blades, causing a reduction in the life of these components.

There is no reliability record for the new designs. Although component rig testing (scale or sector) may help validate some component's performance, the first time the unit reaches design conditions is in the owner's plant. Essentially, the units are considered prototype or unproven designs for the first three years of operation or until the entire major design problems are identified and corrected. Most of the advanced gas turbine nozzle vanes and blades have had to be redesigned as excessive hot spots were being located after short field operations.

The cost of hardware and subsequent cost of ownership have increased due to the complex designs, increased size, and higher throughput in the advanced machines. Gas turbine operation has become more complex and computer driven, thus requiring new and different skill sets for staffing in plants.

Axial-Flow Compressor

The axial-flow compressor with high pressure ratios in the advanced gas turbine is a multistage compressor (17–22 stages). The more stages there are, the smaller the

operating margin between the surge and choke regions of the compressor (2.5–3.5% as compared to 4–5% in previous models).

The trends for compressors are toward airfoils that are fewer (30–35 first-stage blades as compared to 40 earlier), thinner (thickness to chord ratio has decreased from 0.1 to 0.08), larger (airfoil diameter has increased from five to six ft to eight to 10 ft), and three-dimensional and controlled diffusion-shaped (3D/CDA). These blades have smaller clearances and higher loading per stage (pressure ratio per stage from 1.14 to 1.18). There are also trends toward water injection at the inlet or between compressor sections that will likely affect airfoil erosion life. The smaller clearances (20–50 mils) and high pressure ratios tend to increase the probability of encountering rubs. These tip rubs usually occur near the bleed flow sections of the turbines where there are inner diameter changes and the compressor casing is not a perfect circle.

The advanced compressor blades also usually have squealer sections on the blade tips, which are designed to wear in a safe manner if the blades are in contact with the casing. These rubs, if severe, can lead to tip fractures and overall destruction of the downstream blades and diffuser vanes due to Domestic Object Damage (DOD).

The high temperature at the exit of the compressor, which in some cases exceeds 1000 °F °C, causes a hot compression section. This requires the cooling of the bleed flows before they can be used for cooling the turbine section. This also limits the downtime between start-ups of the turbines.

Table 21-4 indicates the changes in the compressor blades that are now prevalent on the advanced gas turbines. The first column represents previous gas turbine designs, the second column represents new gas turbine designs, and the last column indicates the change in risk (↑ represents higher) for the design differences. Most of the comparisons are self-explanatory.

Design margins are set by Finite Element Modeling (FEM) at the element level, which results in lower safety margins than previous designs. The costs of these larger, thinner, less-rub tolerant, and more twisted-shape airfoils are usually higher. When several of the major characteristics of advanced gas turbines are examined from a risk viewpoint (i.e., probability and consequences of failure), there are no characteristics that reduce the probability of failure, and/or decrease the consequence of failure, thus careful inspection of the compressor section is a must.

Dry Low NO_x Combustors

The advanced gas turbines all have Dry Low NO_x combustors. Advances in combustion technology now make it possible to control the levels of NO_x production at source, removing the need for *wet* controls. This, of course, opened up the market for the gas turbine to operate in areas with limited supplies of suitable quality water; for example, deserts or marine platforms. Although water injection is still used, *dry* control combustion technology has become the preferred method for the major players in the industrial power generation market. DLN (Dry Low NO_x) was the first acronym to be coined, but with the requirement to control NO_x without increasing carbon monoxide and unburned hydrocarbons, has changed to DLE (Dry Low Emissions).

Table 21-4 Technology Changes in Axial-Flow Compressors

Previous Designs	New Designs	Risk
• 2D double circular arc or NACA 65 profiles	• 3D or Controlled Diffusion Airfoil (CDA) profiles	↑
• Large number of airfoils	• Reduced airfoil count	↑
• Repeating stages/shorter chords	• Stages unique/longer chords	↑
• Low/modest aspect ratios	• High aspect ratios	↑
• Large clearances	• Smaller clearances	↑
• Low/modest pressure ratios (R_c)	• Much higher pressure ratios (R_c)	↑
• Low/modest blade loading per stage	• High blade loading per stage	↑
• Wider operating margin	• Narrow operating margin	↑
• Thicker leading edges	• Thinner leading edges	↑
• Dry operation	• Wet operation	↑
• Bulk safety margins	• Safety margins by FEM	↑
• Lower costs	• Higher costs	↑

The typical stable, simple, diffusion flame combustor has been replaced with barely stable, staged-combustion systems with multiple injection locations that vary with gas turbine load. These combustors have greatly reduced the NO_x output. New units under development have goals, which would reduce NO_x levels below 9 ppm. This, however, increases combustion instability and flashback problems, which lead to major problems in the combustor.

In 1977 it was recognized that there were a number of ways to control oxides of nitrogen:

1. Use of a rich primary zone in which little NO_x formed, followed by rapid dilution in the secondary zone.
2. Use of a very lean primary zone to minimize peak flame temperature by dilution.
3. Use of water or steam admitted with the fuel for cooling the small zone downstream from the fuel nozzle.
4. Use of inert exhaust gas recirculated into the reaction zone.
5. Catalytic exhaust cleanup.

Wet control became the preferred method in the 1980s and most of 1990s since *dry* controls and catalytic cleanup were both at the very early stages of development. The catalytic converters were used in the 1980s and are still being widely used; however the cost of rejuvenating the catalyst is very high.

The management of air for combustion and cooling of the combustor is particularly critical; this requires that DLN combustors have complex fuel nozzle, cooling, and TBC coating systems to provide adequate life for both the canannular and annular combustion systems.

The important parameters in the reduction of NO_x are the temperature of the flame, the nitrogen and oxygen content, and the resident time of the gases in the combustor.

Reduction of any and all of these parameters will reduce the amount of NO_x emitted from the turbine.

The DLE approach seeks to reduce NO_x without increasing CO by burning most (at least 75%) of the fuel at cool, fuel-lean conditions. The principal features of such a combustion system are the premixing of the fuel and air before the mixture enters the combustion chamber and leanness of the mixture strength in order to lower the flame temperature and reduce NO_x emission.

Controlling CO emissions can thus be difficult. Rapid engine off-loads bring the problem of avoiding flame extinction. If the flame gets extinguished it cannot safely be re-established without bringing the engine to rest and going through the restart procedure. With the flame temperature being much closer to the lean limit than in a conventional combustion system, some action has to be taken when the engine load is reduced to prevent flame out. If no action is taken, flame out would occur since the mixture strength would become too lean to burn. The major problem with DLE combustors is the flash back problem in which the flame moves from the main combustor to the premix chambers. This causes the burn out of those chambers as well as damage to the main section of the combustor can.

The Dry Low NO_x combustor system has to be monitored and tuned precisely for stability from starting to full load while maintaining low emissions and avoiding flashback and high pressure pulsations that could damage combustor and turbine components. The principal features of such a combustion system are the premixing of the fuel and air before the mixture enters the combustion chamber and leanness of the mixture strength in order to lower the flame temperature and reduce NO_x emission. The fuel nozzles are more complicated and larger in number due to the multiple injection locations. When dual fuel is involved or water injection is used to further reduce emissions, the purge systems for the multiple injection points are complex and can be a significant source of problems with fuel nozzle plugging and localized hot section damage. As with new design compressors and turbines, the costs and the risks of these complex combustion systems are high as shown in Table 21-5.

The majority of the NO_x produced in the combustion chamber is called *thermal* NO_x. It is produced by a series of chemical reactions between the nitrogen (N_2) and the oxygen (O_2) in the air that occurs at the elevated temperatures, and pressures in gas turbine combustors. The reaction rates are highly temperature dependent, and the NO_x production rate becomes significant above flame temperatures of about 3300 °F (1815 °C).

The important parameters in the reduction of NO_x are the temperature of the flame, the nitrogen and oxygen content, and the resident time of the gases in the combustor.

The DLE approach is to burn most (at least 75%) of the fuel at cool, fuel-lean conditions to avoid any significant production of NO_x. The principal features of such a combustion system are the premixing of the fuel and air before the mixture enters the combustion chamber and leanness of the mixture strength in order to lower the flame temperature and reduce NO_x emission. Controlling CO emissions thus can be difficult and rapid engine off-loads bring the problem of avoiding flame extinction, which if it

Table 21-5 State of Gas Turbine Technology—Combustors

Previous Designs	New Designs	Risk
• NO_x, high emissions	• Very low emissions on gas	↑
• Diffusion flame with stable combustion	• Premix/DLN with instability (pulsations)	↑
• Single injection points/fuel nozzles simpler	• Multiple injection points/fuel nozzles more complex	↑
• Simple operation with simple controls	• Staged operation with complex controls/tuning	↑
• Combustor construction/cooling designs simpler	• Combustor construction/cooling designs complex	↑
• Combustion thermal life long with or without TBC	• TBC required but life reduced from flashback/distortion damage	↑
• Dry, water, and steam injected	• Dry and wet injected	↑
• Low costs	• High costs	↑

occurs cannot be safely re-established without bringing the engine to rest and going through the restart procedure.

In the DLE combustor swirlers are used to create the required flow conditions in the combustion chamber to stabilize the flame. The DLE fuel injector is much larger because it contains the fuel/air premixing chamber and the quantity of air being mixed is large, approximately 50–60% of the combustion air flow.

The DLE injector has two fuel circuits. The main fuel, approximately 97% of the total, is injected into the air stream immediately downstream of the swirler at the inlet to the premixing chamber. The pilot fuel is injected directly into the combustion chamber with little if any premixing. With the flame temperature being much closer to the lean limit than in a conventional combustion system, some action has to be taken when the engine load is reduced to prevent flame out. If no action were taken, flame out would occur since the mixture strength would become too lean to burn. A small proportion of the fuel is always burned richer to provide a stable *piloting* zone, and the remainder is burned lean. In both cases a swirler is used to create the required flow conditions in the combustion chamber to stabilize the flame.

The major problem with DLE combustors is the flashback problem in which the flame moves from the main combustor to the premix chambers. This causes the burn out of those chambers as well as damage to the main section of the combustor can.

Axial-Flow Turbine

The advanced gas turbines have been encountering temperature problems such as failures in turbine nozzle vanes and blades. The failures have been occurring at blade tips, and at the base of the turbine nozzle vanes. Air temperatures in the first-stage nozzle vanes are in the range of 2100 °F–2300 °F (1149 °C–1260 °C) and the cooling of these blades is very important. The nozzle vanes are facing problems at their base due to these high temperatures.

Design changes have been carried out by all OEMs to overcome these problems. These include new cooling patterns for the nozzle vane base, further cooling of the compressor bleed air with external cooling heat exchangers, and the use of steam for cooling purposes in combined cycle applications.

The first-stage turbine blades are usually impulse turbines, and the second to the third and fourth stages are reaction type (30–60%) and usually have tip shrouds. These tip shrouds give the blade more support so that they do not suffer from resonance problems. The development of new materials as well as new cooling schemes has made the rapid growth of the turbine firing temperature possible leading to high turbine efficiencies. The first-stage blades must withstand the most severe combination of temperature, stress, and environment; it is generally the limiting component in the machine. Since 1950, turbine bucket material temperature capability has advanced approximately 850 °F (472 °C), approximately 20 °F (10 °C) per year. The importance of this increase can be appreciated by noting that an increase of 100 °F (56 °C) in turbine firing temperature can provide a corresponding increase of 8–13% in output power and 2–4% improvement in simple-cycle efficiency. Advances in alloys and processing, although expensive and time consuming, provide significant incentives through increased power density and improved efficiency.

In the first and second stages of the turbine, complex multipath serpentine cooling designs are utilized. Higher strength single crystal (SC) blade materials coupled with oxidation resistant coatings and/or thermal barrier coatings (TBC) are used in the first-stage blades, and directionally solidified (DS) blade materials with TBC are used in the second- and third-stage blades to meet turbine life requirements. TBC is composed of two layers, a bond coat of NiCrAlY and a top coat of Yttria stabilized Zirconia (this coating reduces the blade metal temperature of cooled components). Most blades have 12–25 mil thickness of TBC, which allows for an 8 °F–16 °F (5 °C–10 °C) reduction per mil of coating.

Design margins are set by FEM at the element level, but the long-term creep strength characteristics of the turbine materials are not well defined. The costs of these larger, complex-cooled, more twisted-shape airfoils with more sophisticated materials and coatings are substantially higher per airfoil stage (cost of first-stage turbine blades has increased from $3,000 to $30,000). In addition, the turbine materials utilized typically have reduced temperature margin to melting as compared to previous designs. As with compressors, the smaller clearances and higher expansion ratios associated with the new design turbines tend to increase the probability of encountering rubs.

The trends for the advanced turbines are similar to the compressor with fewer 40–60 first-stage blades now as compared to 90 before, larger, 3D airfoils with smaller clearances and higher expansion ratios (R_e) being used. As with compressors, the smaller clearances and higher expansion ratios associated with the new design turbines tend to increase the probability of encountering rubs. Table 21-6 shows the difference between the older turbines and the new advanced gas turbines.

Maintenance Scheduling

The scheduling of maintenance inspections and overhauls is an essential part of the total maintenance philosophy. As we move from “Breakdown” or “Panic”

Table 21-6 State of Gas Turbine Technology—Turbines

Previous Designs	New Designs	Risk
• 2D reaction-type airfoil profiles	• 3D airfoil profiles	↑
• More airfoils/shorter chords	• Fewer airfoils/longer chords	↑
• Larger clearances	• Smaller clearances	↑
• Low/modest expansion ratios (R_e)	• Much higher R_e's	↑
• Uncooled/simple cooling designs	• Complex cooling designs	↑
• Air as the only cooling medium	• Air and steam as cooling mediums	↑
• Equi-axed castings	• DS and SC castings	↑
• Oxidation coatings and/or TBC used for extending life	• Oxidation coatings and/or TBC needed to meet life	↑
• Bulk safety margins	• Safety margins by FEM	↑
• Margin to melting larger	• Margin to melting smaller	↑
• Lower costs/stage	• Ultra-high costs/stage	↑

maintenance towards a *performance-based total productive maintenance system*, total condition monitoring and diagnostics become an integral part of both operation and maintenance. Total condition monitoring examines both the mechanical system and performance of the machinery and then carries out diagnostics. Condition monitoring systems, which are only mechanical systems without performance inputs give less than half of the picture and can be very unreliable. Unscheduled maintenance is very costly and should be avoided. To properly schedule overhauls, both mechanical and performance data must be gathered and evaluated. As indicated earlier, we want to consider repairs during a planned "turnaround" not "random" repairs, which are frequently done on an "emergency" basis and where, due to time restraints, techniques are sometimes used, which are questionable and should only be used in emergencies.

To plan for a "turnaround," one must be guided by the operating history of the given plant and, if it is the first "turnaround," by conditions found in other plants utilizing the same or a closely similar process and machinery. This is how the time between subsequent "turnarounds" has been extended to three years or more in many instances. By utilizing the operating history and inspection at previous "turnarounds" at this or similar installations, one can get a fair idea of what parts are most likely to be found deteriorated and, therefore, must be replaced and/or repaired, and what other work should be done to the unit while it is down. It should be pointed out that, with modern turbomachinery, items such as bearings, seals, filters, and certain instrumentation, which are precision made, are seldom, if ever, repaired except in an emergency; such items are replaced with new parts.

This means that parts must be ordered in advance for the "turnaround" and other work must be planned so that the whole operation may proceed smoothly and without holdups that could have been foreseen. This usually means close collaboration with the manufacturer or consultant and the OEM (or specialty service shop) so that handling facilities, service-people, parts, cleaning facilities, inspection facilities, chrome plating

and/or metalizing facilities, balancing facilities, and in some cases even heat treatment facilities, are available and will be open for production at the proper time required. This is the planning which must be done in detail before the shutdown with sufficient lead-time available in order to have replacement parts available at the job site.

The old maxim "if it ain't broke don't fix it" is very applicable in today's machinery. A study conducted at a major nuclear power facility found that 35% of the failures occurred after a major turnaround. This is why total condition monitoring is necessary in any performance-based total productive maintenance system and leads to overhauls being planned on proper data evaluation of the machinery rather than on a fixed interval.

Maintenance Communications

It is not uncommon to hear the complaint that the maintenance department has "never been informed as to what is happening in the plant." If this is a common complaint, the maintenance manager needs to examine the communications in his department. The following are seven practical suggestions for improving communications:

1. Operation and service manuals
2. Continuous updating of drawing and print files
3. Updating of training materials
4. Pocket guides
5. Written memos, interoffice E-mails
6. Seminars
7. Website postings

Each of these items listed, if properly employed, can transmit knowledge to the person who must keep the plant's machinery running. How well the information is transmitted depends entirely on the communication skills applied to the preparation of the materials.

Operation and Service Manuals

To be of real value to the mechanic, an operation and service manual must be indexed to permit the quick location of necessary information. The manual must be written in simple, straightforward language, have illustrations, sketches, or exploded views adjacent to pertinent text, and have minimum references to another page or section. Major sections or chapters should be tabbed for quick location.

Most often a mechanic or service-person refers to a manual because of a problem. Problems seem to happen during a production run. It is essential, therefore, that he or she be able to find the necessary information quickly. The mechanic should not be delayed by wordy, irrelevant text. The objective of any manual is to be an effective, immediate source of service information.

The assignment of a nontechnical person to write a manual is short-sighted and more costly in the long run. A well-written manual is continuously in use. Good manuals need not be complicated. In fact, the simpler the better. Manuals should be readable and understandable, whether they are compiled in-house or outside.

Drawing and Print File

A good print file is a vital tool for any maintenance organization. Reference files in a large or multi-plant company can be particularly burdensome for several reasons:

1. Prints are bulky and difficult to store properly
2. Control of use is necessary
3. Files must be kept up to date
4. Handling and distribution of new or revised prints is usually expensive.

A practical solution is to digitize the drawings and place them on CDs available to the maintenance and operation department. A good digital file reduces search time and helps the departments do a better job of keeping the machinery operating at its peak efficiency with minimal downtime.

Training Materials

Like any other written or audio-visual maintenance tool, training materials of all kinds are basically communication devices, and to be effective, should be presented in a simple straightforward, attractive, and professional manner.

Once the need for specific maintenance training has been determined, a program must be developed. If the training need applies to a proprietary machine or one that is unique to a very few industries, it might be necessary to contact companies who specialize in custom digital programs on CDs, slide/tape, movies, videotape, or written training programs. The cost may shock the uninitiated, but after shopping around, the company may find that it can recover far more than the initial cost in tangible benefits over a relatively short period.

Pocket Guide

When a new maintenance form or procedure is introduced, a quick reference pocket guide can promote understanding and accuracy. The key to effectiveness is a deliberate design to provide maximum illustrations or examples in simple language. If it cannot be prepared in-house, outside help should be sought. Professionalism is essential to good communications.

Written Memos

One of the most effective devices for improving maintenance communications is a newsletter or internal memo. The memo's success depends heavily on communicating formal tips and techniques in the mechanic's language and using photos, sketches, and drawings generously to get the message across.

Everyone in the maintenance department should be encouraged to contribute ideas on a better way to do a task or a solution to a nagging problem related to the maintenance or operation of production equipment. Each contributor should be given credit by name and location for his or her effort. Very few workers can resist a bit of pride in seeing their names attached to an article that is seen by virtually everyone in the company.

Seminars and Workshops

College or industry-sponsored seminars, continuing education courses, and workshops are means of upgrading or sharpening skills of maintenance people. Such an approach serves a twofold purpose. First, it communicates the company's good faith in the person's ability to benefit from the experience, and by acceptance, the worker shows willingness to improve his or her usefulness to the company. The seminars are very useful in disseminating knowledge. They also provide a forum for gripes and meaningful solutions. Discussion groups in these seminars and workshops are very important as participants share experiences and solutions to problems. The knowledge gained from these seminars is very useful.

Inspection

As with any power equipment, gas turbines require a program of planned inspections with repair or replacement of damaged components. A properly designed and conducted inspection and preventive maintenance program can do much to increase the availability of gas turbines and reduce unscheduled maintenance. Inspections and preventive maintenance can be expensive, but not as costly as forced shutdowns. Nearly all manufacturers emphasize and describe preventive maintenance procedures to ensure the reliability of their machinery, and any maintenance program should be based on manufacturers' recommendations. Inspection and preventive maintenance procedures can be tailored to individual equipment application with references such as the manufacturer's instruction book, the operator's manual, and the preventive maintenance checklist.

Inspections range from daily checks made while the unit is operating to major inspections that require almost total disassembly of the gas turbine. Daily inspections should include (but are not limited to) the following checks:

1. Lubrication oil level
2. Oil leakage around the engine
3. Loose fasteners, pipe and tube fittings, and electrical connections
4. Inlet filters
5. Exhaust system
6. Control and monitoring system indicator lights

The daily inspection should require less than an hour to perform properly and can be made by the operator.

The interval between more thorough inspections will depend on the operating conditions of the gas turbine. Manufacturers generally provide guidelines for determining inspection intervals based on exhaust gas temperatures, type and quality of fuel utilized, and number of starts. Table 12-2 shows time intervals for various inspections based on fuels and startups. Minor inspections should be performed after about 3,000–6,000 hours of operation, or after approximately 200 starts, whichever comes first. This inspection requires a shutdown for two to five days, depending on availability of parts and extent of repair work to be done. During this inspection, the combustion system and turbine should be checked.

The first minor inspection or overhaul of a turbine forms the most important datum point in its maintenance history, and it should always be made under the supervision of an experienced engineer. All data should be carefully taken and compared with the turbine erection information to ascertain if any setting changes, misalignment, or excessive wear has occurred during operation. Subsequent inspections are also of great importance, since they verify manufacturers' recommendations or help to establish maintenance trends for particular operating conditions.

When the established time for major maintenance approaches, a meeting should be arranged between the operating department and the manufacturer's engineer to discuss and arrange for the date of turbine outage. A short time before taking the turbine out of service a complete operational test should be made at zero, one-half, and normal maximum loads, preferably in the presence of the manufacturer's engineer. These tests are for reference temperatures and pressures, which will serve as a means of comparison with identical tests that should be made immediately after the unit is overhauled. The operational tests should end with an over-speed trip test to indicate whether attention should be given to the governor or tripping mechanism during the shutdown. These specific data will also serve together with the logged operational data or case history (which should be reviewed with the manufacturer's engineer) to determine the focal point or items requiring special attention or investigation:

1. Increase or change in vibration
2. Decrease in air compressor discharge pressure
3. Change in lube oil temperatures or pressure
4. Air or combustion gases blowing out at the shaft seals
5. Incorrectly reading thermocouples
6. Change in wheel space temperatures
7. Fuel oil or gas leakage
8. Fuel control valves operate satisfactorily
9. Hydraulic control oil pressures changed
10. The turbine governor "hunts"
11. Change in sound level of gear boxes
12. Over-speed devices operate satisfactorily
13. Babbitt or other material found on lubricating oil screens
14. Lube oil analysis shows corrosion factor increase
15. Change in pressure drop across heat exchangers
16. Turbogenerator reaches rated load at design ambient and exhaust temperature conditions

Preparation for shutdown should be made as complete as possible to eliminate lost time and confusion at the beginning of the job.

A list should be made of all major items that are to be inspected or repairs to be made if they are known at the time. This list should be prepared with the manufacturer's engineer present. A detailed schedule should be formulated from this list including the time allotted for the shutdown and the maintenance crew available. Plan the work with the expectation of finding the worst conditions – the unexpected work found after the machine is opened will then be compensated. This procedure will greatly reduce the possible need for costly overtime.

Tools on-site should be reviewed by the manufacturer's engineer. All special or regular equipment not on hand that is necessary or required to do any part of the work should be ordered and on-site before shutdown.

Exact outage time should be arranged, and the turbine prepared for the contracting crew or plant maintenance crew. All personnel should be on the job or available to meet the starting date.

Facilities, such as convenient air and electrical connections, should be prearranged for operating tools, and other things. Sufficient hose lengths and connectors are required as well as electrical extension cords. Install air driers or water separators in the air system, since dry air is necessary for successful grit blasting of turbine parts.

Before removing turbine flange bolts or disturbing the normal turbine setting, clearance readings between the last row of turbine rotating blades and its wheel shroud should be made at both horizontal and vertical positions. Evidence of the main turbine flange spreading or warping should be checked with feeler gauges between each of the flange bolts. Elevation checks at each of the turbine supports should be made for comparison with original readings to determine if there has been movement at these points. When all outside checks have been made, structural beam supports should be placed under the turbine at the mid-points between the normal turbine supports. Screw jacks must then be used to bring pressure under the turbine until a slight deflection on the dial has been reached. For this purpose, use only screw jacks, not hydraulic or lift jacks. Flange bolts can then be removed as well as the top half of the turbine casing.

Long-Term Service Agreements

Long-Term Service Agreements (LTSA), sometimes also known as Contractual Service Agreements, for the long-term equipment maintenance and service programs at large plants (especially for advanced gas turbines) have become the norm, due to, in most cases, the insistence of the long-term note holder. Plant operators and owners worldwide have to deal with these complex contracts. LTSAs typically commit the original equipment manufacturer (OEM) to providing, on a relatively "fixed-priced" basis, maintenance services for the complex and sometimes untested advanced gas turbines. These gas turbines are pushing the limits of technology thus the LTSAs give the lender a sense of comfort in knowing their long-term exposure. By their very nature, long-term service agreements are going to be a significant part of owners' businesses for a very long time, thus fully understanding these complex agreements is very important.

LTSAs offer many advantages to owners and operators of large advanced gas turbine combined cycle power plants:

1. Fixed long-term maintenance costs.
2. Availability of parts due to incentives for OEM support.
3. Contractually guaranteed availability and reliability of the plant.
4. Performance power and heat rate guarantees with bonuses.

The LTSAs, due to their very complex and legalistic language, are hard for many operators to fully fathom. Some of the disadvantages of LTSAs are:

1. High maintenance costs.
2. Long-term relationship that cannot easily be dissolved.
3. Owner to bear an inordinate amount of risk if contract is not properly negotiated.
4. Lengthy litigation if contracts are not analyzed properly.
5. Plant operators often come in after the contract has been negotiated and do not fully understand the scope of the contract, which may result in costly and time-consuming disputes with the OEM.

LTSAs are negotiated contracts, thus no two of them are alike but they must cover some of the following basic important points:

1. Fixed scheduled maintenance on the equipment, to include replacement of all hot parts at a relatively fixed price such as:
   a. Combustor liners
   b. Fuel nozzles
   c. Transition pieces
   d. Turbine nozzle vanes and blades
2. Unscheduled maintenance work on the equipment, on a relatively fixed price basis.
3. Clearly defined responsibilities between unscheduled maintenance and warranty obligations.
4. Extra work as may be requested by the owner, on a unit-price basis.
5. Defining what is covered under warranty and what is covered by the LTSA.
6. Defining clearly what are inspect-only parts and which are replacement parts.
7. Availability and reliability guarantees, to protect the owner in ensuring the outage is minimal.
8. Performance power and heat rate guarantees.
9. End-of-term quality of replacement parts.
10. Early cancellation policy.
11. Liquidated damages.
12. Limits of liability.

Although LTSAs can offer many advantages to owners, these very complex agreements can often contain pitfalls for the unwary – pitfalls that can cause an owner to bear an inordinate amount of risk, or that may result in costly and time-consuming disputes with the OEM. The majority of the LTSAs were signed in the 1990s bubble, which was a sellers market, thus the LTSAs of that period were mostly beneficial to the OEM. Things have now changed to a buyers market, and the OEMs are getting competition from other large non-OEM maintenance groups in the area of providing LTSAs.

The plant developers in those days were assuming that the plants would be used in base load operation but have found that their plants are operating in cyclic conditions where the load, at off-prime time, could be as low as 40–50% of the base load. Many of these plants now shut down for the weekends. These changes in operation in many cases require maintenance and inspection changes. Maintenance of most gas turbines depends on equivalent engine hours, and the number of starts as shown in Table 21-7.

Table 21-7 Typical Gas Turbine Inspection Interval

Equivalent Operating Hours	8,000	16,000	24,000	32,000	40,000	48,000
Type of inspection	Combustor inspection	Combustor and first-stage nozzle vanes and blades	Hot gas path inspection	Combustor inspection	Combustor and first-stage nozzle vanes and blades	Full turbine maintenance
Fired starts	400	800	1,200	1,600		
Inspection	Combustor inspection	Hot gas path inspection	Combustor inspection	Full turbine maintenance		

The most common problem encountered in LTSAs is the lack of a clearly defined scope of the OEM's responsibilities for providing scheduled maintenance on the equipment. The risks an owner faces from such a lack of clarity can be very costly, especially in the context of an LTSA that contains fixed-pricing for scheduled maintenance work.

Availability and reliability requirements in the LTSAs give the owner a large advantage since the OEM would have financial penalties to ensure that the equipment is capable of achieving commercially operational performance levels in the shortest time possible.

The most important question on every owner's mind when entering into an LTSA (especially merchant plant owners) is whether the pricing inherent in the LTSA will remain competitive over time as compared to a self-maintenance program. As the availability of after-market parts continues to develop, a self-maintenance program or programs with major third-party maintenance providers will be an alternative to LTSAs.

Finally the *long-term* nature of LTSAs creates an atmosphere where owners do not focus on the problems that will occur in the distant future. At the completion of the last major inspection at the end of the LTSA's term, a number of important issues arise such as the quality of parts to be installed into the equipment at that time. Addressing these issues at the time of signing the contract would be extremely beneficial to the operator.

Borescope Inspection

A borescope is a device used to examine components inside a cavity that cannot be visually examined directly. A flexible fiberscope lets you see inside spaces and can offer the additional benefit of articulation, which is the ability to remotely control the

tip of the scope so that it bends in two or four directions to look around a cavity. Before you can see anything in a dark cavity, you need some light on the subject. The borescope contains its own light source throughout the engine's internal passages; borescopes usually use fiber optic illumination, where glass fibers carry light from an external light source through a flexible light guide, then through the borescope, to the distal end. Once inserted, the flexible borescope can be maneuvered to inspect the complete hot-section flow path. The results of the visual inspection can be used to assist in planning scheduled disassembly of the gas turbine. It must be remembered that a borescope is a monocular device, and it is extremely difficult to estimate size or distance. A borescope has a very large depth of field often from infinity down to an inch or less; this makes it easy to use without constant refocusing. The closer an object is to the lens of a borescope, the greater the magnification. To calculate magnification you must know the distance of the subject from the lens. The field-of-view on a borescope is the cone coming from the borescope tip, so that anything within the cone is visible. The cone may be very wide (90° included angle around the sight of view) to a narrow telephoto (30° included angle around the sight of view). The field-of-view of a slim borescope is close to a narrow telephoto view. The field-of-view is dictated by the distance from the distal end of the borescope to the subject being inspected. The wider the field, the lower the magnification, and vice versa. If you have plenty of space to move inside the cavity, but want to see both detailed close-ups and big picture views you might choose a 67° moderate wide angle. If the space is more confined but you still need to see most of it at one time, try a 90° extreme wide angle. On the other hand, if you can't get close enough to show the detail you need, a 30° telephoto might be required. Figure 21-7 shows the magnification at various distances of the distal end to the subject.

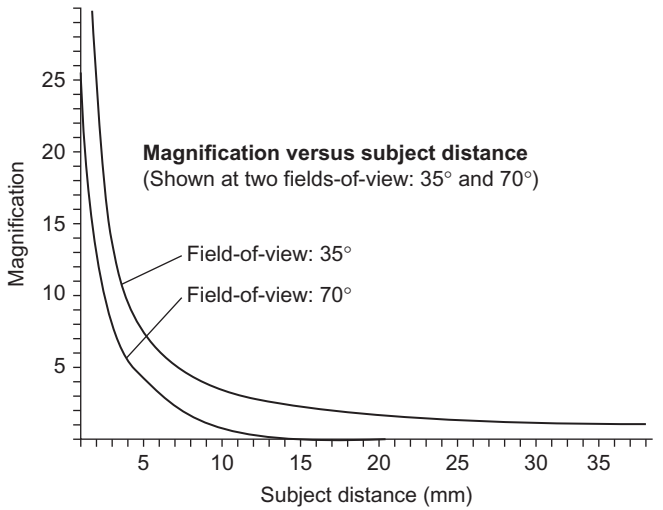


Figure 21-7 Borescope magnification.

Use of the borescope for condition monitoring requires knowledge of the specific gas turbine's internal design as well as experience with the borescope. To be of maximum value, borescope probes with specific field-of-views and angles of vision and magnification must be used, depending on the areas to be inspected. It is of little value to use a probe that is not capable of focusing on the most critical internal areas of interest. It is also important the user knows the diameter of the access ports, where they are located, as well as the depth of probe insertion required for optimum viewing. The current pattern of inspection most frequently followed is to periodically scan selected areas of stationary components with a 35 ° field of vision probe of 1:1 magnification at 18 cm. If no evidence of degradation is identified, the remaining stationary components within view of borescope ports are inspected semi-annually. If, however, significant degradation is identified, all stationary components should be inspected depending upon the specific defect. Selected rotating hot section components should also be inspected periodically by viewing those stages where the most degradation has been identified in the past. One or more additional stages are inspected semi-annually and, depending upon the type and extent of degradation, other stages may be inspected. Inspection of rotating components usually requires more than one pass to accomplish complete coverage. A 60°–65° field-of-view probe with 1:1 magnification at five cm is recommended. Blade tips and concave surfaces should be scanned in the first pass. Blade leading edges and blade platforms should be scanned in the second pass. In the third pass the convex surfaces at the platform, the trailing edges, and tips from the adjacent borescope port. Each pass is accomplished by slowly rotating the rotor at an optimum viewing rate. When an area of particular interest is identified, the inspection sequence is stopped and the component and probe are positioned for optimum viewing. A variety of probes should be available for detail inspection and magnification as necessary. With the use of digital cameras we can see the results immediately so that magnification, lighting, and distance to object are corrected to get optimum results. It is also suggested that the photographs be taken at the maximum pixel resolution the camera provides so that magnification of sections can be done with minimal distortion.

Maintenance personnel should be well trained to use a borescope effectively. When an overall record of engine condition is desirable, DVDs and videotapes (especially colored) can be utilized as a reference on the history of a machine, and are available for immediate conference viewing at the home office via the Internet, where they can be evaluated by a group of engineering specialists. The benefit is to observe and document the physical condition of critical internal components for identification and analysis of conditions that may require future repair/overhaul. As frequently happens, the first indication of trends may be identified visually before sufficient operational sensor data are available. Condition monitoring using the borescope is extremely helpful in learning to predict degradation rates, and detect abnormal conditions early enough so that corrective action can be taken, thereby minimizing (or eliminating) potential engine failures. In addition to performing inspections while the gas turbine is not operating, some research has been conducted to develop methods for inspection during operations by providing a film of cooling air around the borescope tube. If this system

is developed, it will enable visual inspections of the hot sections up to the first-stage turbine blades without shutting down the unit.

Borescope inspection is carried out because of the following benefits it can provide in the maintenance program:

1. Perform internal on-site visual checks without disassembly.
2. Detect abnormal conditions early to avoid failures.
3. Determine degradation rates.
4. Extend periods between scheduled inspections.
5. Allow accurate planning and scheduling of maintenance actions.
6. Monitor condition of internal components.
7. Provide increased ability to predict required parts, special tools, and skilled manpower.

Figure 21-8 shows the time savings we may obtain by the proper use of borescopic inspection for planned maintenance. The borescope system must be capable of enough resolution, depth of field, focus, and magnification to first permit identification of defects and then permit close-up inspection and evaluation of such minute features as cracks, penetrations, deposits, and corrosion/erosion and burning.

Figure 21-9 shows the deterioration of the High Pressure Turbine (HPT) blades, with the turbine operating hours. Figure 21-9 (a) is a borescope view of the new blades; to the casual observer they appear in mint condition. However, there is a leading edge

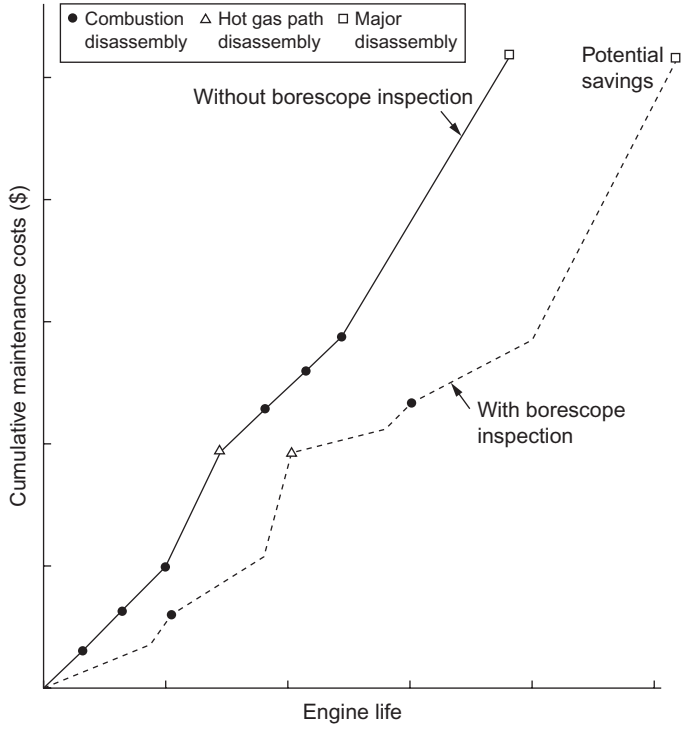
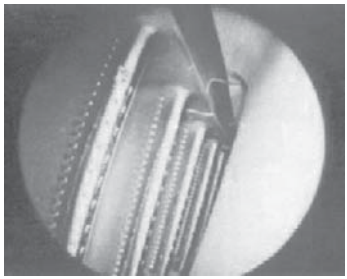


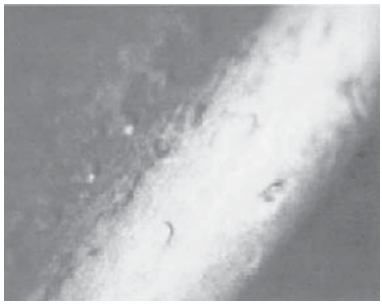
Figure 21-8 Effect of planned maintenance with usage of borescope.



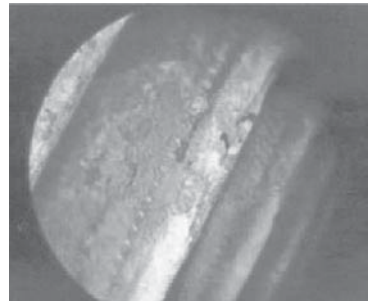
(a) New HPT blades



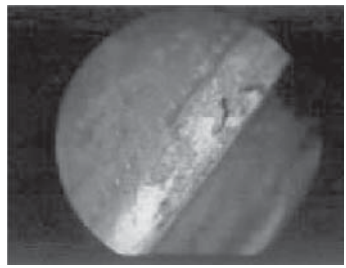
(b) Erosion after 3,960 hrs



(c) Cooling holes plugged



(d) Leading edge penetration (5,591 hrs)



(e) Magnified leading edge penetration

Figure 21-9 Borescope view of high pressure turbine blades at various stages of life.

defect on all visible blades adjacent to the first cooling hole. Additional magnification would permit evaluation to determine the seriousness of the defect. Figure 21-9 (b) shows HPT stage 1 blades after 3,960 hours of operation. In this view the leading edge of the right-hand blade is eroding in local areas centered between the first and second cooling holes. Figure 21-9 (c) shows a close-up view of the leading edge. The cooling holes are plugged and the local erosion seen resulted from loss of adequate blade leading edge cooling. Figure 21-9 (d) shows these same blades after 5,591 operating hours. The erosion has progressed to the point of leading edge penetration, a magnification of this area is seen in Figure 21-9 (e). Determining the size of the penetration in this area of heavy local erosion is calculated by knowing the diameter of the cooling holes and the distance between them. In this particular illustration, cooling

holes are .017 inches diameter and are approximately .116 inches between centers. It is this type of detail resolution that is required to analyze engine condition. The same philosophy may also be followed for a variety of other conditions that can be observed and photographed using the borescope.

Table 21-8 lists some of the more common types of degradation that can be visually observed and analyzed before built-in condition and performance monitoring sensors identify degradation.

Figure 21-10 (a) shows the HPT stage one nozzle guide vanes from a port through the combustor can area using a 50 mm adapter between the camera and the probe. The vane details are difficult to distinguish, however we can note that the vane concave

Table 21-8 Inspection for Degradation

Type of Damage	Location	Source of the Damage
Heavy oxide deposits	HPT vanes, blades	Environment, fuel
Penetration	HPT vanes, blades	Corrosion, erosion
Blade tips missing	HPT and compressors	Clearance, DOD/FOD
Distortion	Combustor	Uneven combustion
Coking	Fuel nozzle assembly	Uneven combustion
Penetration	Combustor	Uneven combustion
Cracks	Combustor liners	Thermal stress, Wobbe number change
Heavy corrosion	HPT vanes, blades	Coating defect
Heavy erosion	HPT vanes, blades	Loss of film cooling
Hot streaking	Combustor	Faulty fuel nozzle
Dents	Vanes, blades	DOD/FOD
Hot spots	HPT vanes, blades	Faulty fuel spray pattern, liquid hydrocarbons in NG fuel
TBC coating flaking	HPT blades	Tips rubbing, blocked cooling passages
Gouge	HPT blades	DOD/FOD
Pieces missing	Blades	DOD/FOD
Seal cracks	Transition piece	Uneven combustion



(a) Stage 1 turbine nozzle vanes 50 mm adapter

(b) Stage 1 turbine nozzle vanes 100 mm adapter

(c) Stage 1 turbine nozzle vanes 100 mm adapter plus 2X magnifier

Figure 21-10 Effect of adapters and magnifiers on borescope investigations.

surfaces are not clean and smooth. Figure 21-10 (b) shows the same HPT stage one nozzle guide vane through a 100 mm adapter; much more detail such as the rows of cooling holes at the leading edge can be seen. It is also possible to distinguish the trailing edge cooling slots and to ascertain that some leading edge holes are partially plugged. In Figure 21-10 (c), a 100 mm adapter plus a 2X magnifier were used, making it possible to count .020 inch diameter leading edge cooling holes.

These same techniques may be employed throughout the inspection of other gas turbine components wherever access ports are available and detail inspection is required. The value of this type of condition monitoring is the identification of conditions that do not show up on built-in sensors such as the deposit build-up conditions as seen on these nozzle vanes and blades. Once identified, the source must be found and rectified immediately in order to prevent overheating of metal surfaces, accelerated erosion, and premature failures.

It is frequently necessary to employ special techniques to enhance the object being viewed in order to evaluate various engine conditions. This is done by using a miniature high intensity remote light. The light is small enough to fit through an adjacent borescope port and can be remotely positioned to back-light specific surfaces or to provide proximity lighting. By positioning the remote light adjacent to a vane surface, deposit build-up conditions can be seen. An alternate method of evaluating vane surfaces is to position the remote light behind the component so that the light shines across the concave surfaces, while the borescope light is then turned off for additional contrast.

One of the other requirements of borescope photography is to obtain a true representation of the colors and hues as seen internally. Because of spectral shifts resulting from failure of the reciprocity law when making time exposures, color compensating filters must be used on exposures of one second or longer. These filters provide a truer representation of actual colors. They also provide additional contrast of various shades of the same color.

Maintenance of Gas Turbine Components

Performance degradation in a gas turbine can be categorized as recoverable and non-recoverable. Recoverable performance is the deterioration in a gas turbine performance that can be recovered by engine cleaning, otherwise known as an on-line and off-line water wash. Non-recoverable degradation is the performance deterioration of a gas turbine caused by internal engine component wear. The only way to recover the non-recoverable degradation is by performing a shop inspection and engine overhaul.

The rate at which a gas turbine deteriorates is primarily affected by the amount of contaminants that enter the turbine through the inlet air filters, ducts, water from evaporative coolers, fuel, and the frequency as well as the thoroughness of engine water washing. At times unusual site conditions exist that accelerate gas turbine degradation. Unusual airborne contaminants from process mists, smoke, oil, and chemical releases, dust storms, sugar cane burning smoke, and other sources have been documented to accelerate engine degradation. A site-specific test program should therefore be conducted in order to optimize the effectiveness of

a turbine water wash program. Deterioration in turbine performance is indicated by one or more of the following conditions:

- Slower engine acceleration
- Engine compressor surge or stall
- Lower power output
- Loss of engine compressor discharge pressure
- Increase in compressor discharge temperature

Figure 21-11 is a typical non-recoverable power and heat rate degradation curve as a function of equivalent engine operating hours (EOH). With an increase in equivalent engine operating hours there is a sharp drop in delivered power and an increase in the turbine heat rate during the first 5,000 equivalent operating hours. These losses are non-recoverable in most cases, and would require the turbine to be returned to the shop, and outfitted with most new components.

The following section is designed to guide you through some of the major problems that are encountered in gas turbines. A set of tables have been designed to aid you in solving some of your day-to-day problems in the three main components of the gas turbine. The following are the major components of the gas turbine, which are examined here from a maintenance point of view.

1. Axial-flow compressor
   - **a.** On-line cleaning
   - **b.** Fouling indicators
   - **c.** Cleaning techniques
2. Combustors

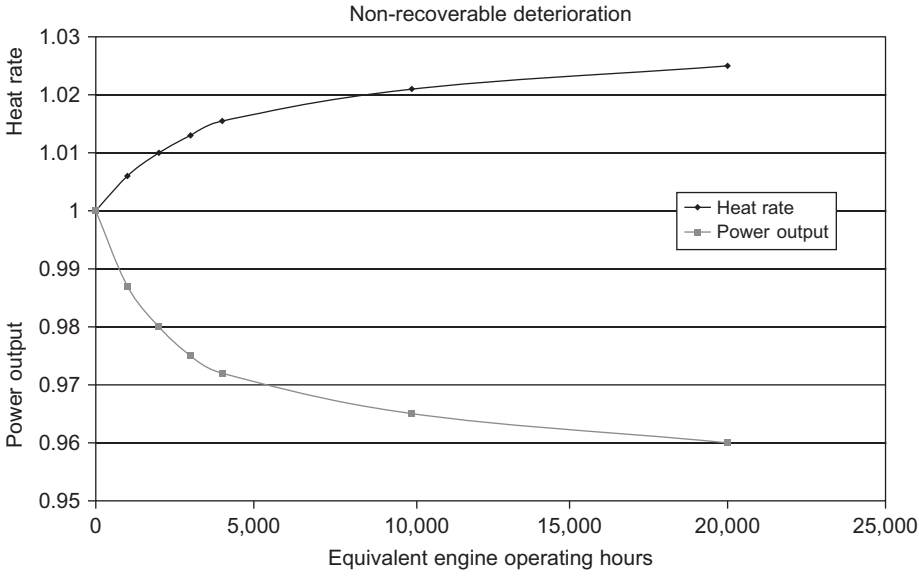


Figure 21-11 Non-recoverable losses in a gas turbine as a function of equivalent operating hours.

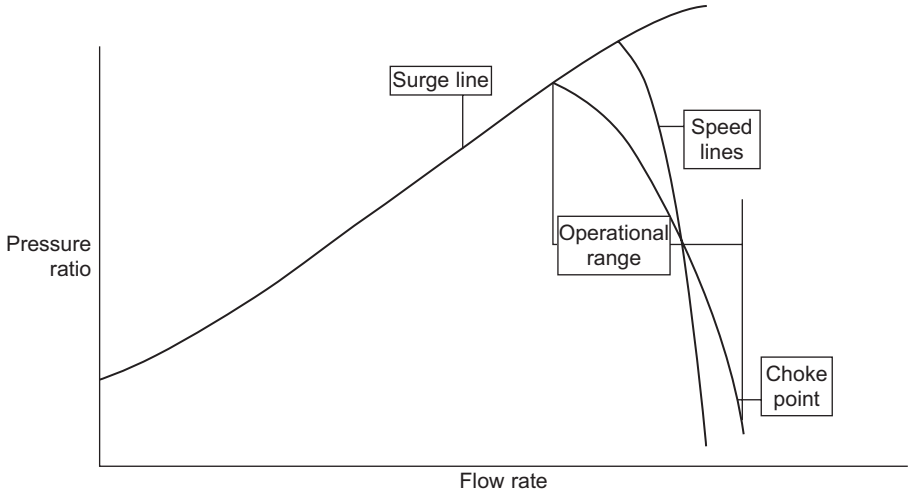


Figure 21-12 Compressor performance map.

3. Turbine
   a. Rejuvenation of used turbine blades
4. Accessories
   a. Bearings
      i. Journal bearings
      ii. Thrust bearings
5. Repair and rehabilitation of gas turbine foundation

Compressors

The advanced gas turbines operate at very high pressure ratios. Pressure ratios have increased from about 7:1 in the 1950s to as high as 30:1 in the late 1990s. This increase in compressor pressure ratio decreases the operating range of the compressor. The operating range of the compressor stretches from the surge line at the low-flow end of the compressor speed line to the choke point at the high-flow end. As seen in Figure 21-12, the lower pressure speed line has a larger operational range than the higher pressure speed line. Therefore, the higher pressure ratio compressors are more susceptible to fouling, and can result in surge problems or blade excitation problems, which can lead to blade failures.

The drop in pressure ratio at the turbine inlet, due to filter fouling, amounts to a substantial loss in the turbine overall efficiency and the power produced. An increase in the pressure drop of about one inch (25 mm.) WC causes a drop of about 0.3% reduction in power. Table 21-9 shows the approximate changes that would occur for changes in ambient conditions; the fouling of the inlet filtration system and the increase in backpressure on the gas turbine in a combined cycle mode. These modes were selected because these are the most common changes that occur on a system in the field. It must be remembered that these are just approximations and will vary for individual power plants.

Table 21-9 Effect of Various Parameters on the Output and Heat Rate

Parameters	Parameter Change	Power Output	Heat Rate Change
Increase in Ambient Temperature	20 °F (11 °C)	−8.3%	2.2%
Decrease in Ambient Pressure	1 psi (6.895 KPa) Elevation = 2,000 ft.	−7%	−0.0001%
Increase in Ambient Relative Humidity	10%	−.0002%	.0005%
Pressure Drop in Filter	1 inch (25 mm) WC	−0.5%	0.3%
Increase in Gas Turbine Backpressure	1 inch (25 mm) WC	−.25%	.08%

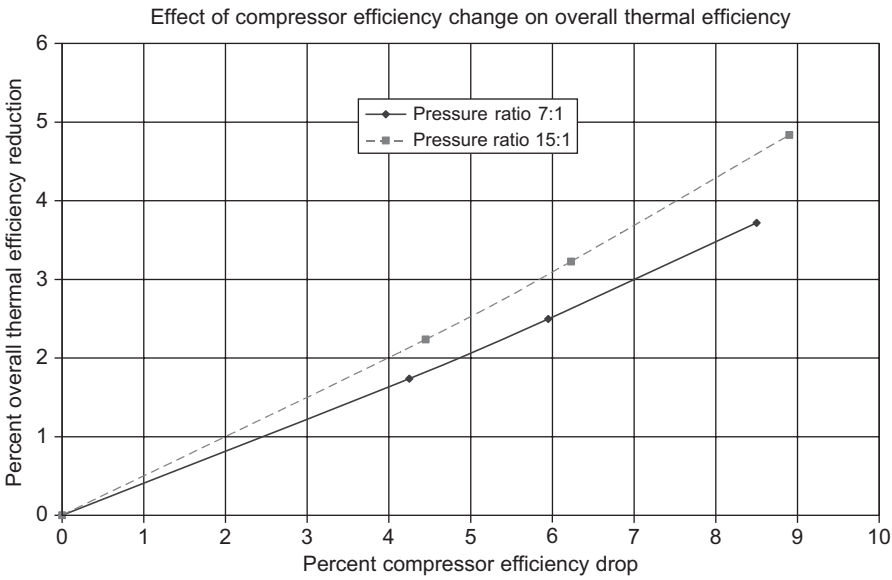


Figure 21-13 Effect of compressor efficiency drop on the overall thermal efficiency reduction.

The compressor of a gas turbine consumes over 55–60% of the power generated by the turbine, thus problems with the compressor can be very costly as to power produced and the loss of overall thermal efficiency of the gas turbine. Figure 21-13 shows the effect of compressor fouling on overall cycle efficiency. The effect of fouling the compressor that reduces compressor efficiency leads to a reduction in the overall efficiency. The higher the pressure ratio of the compressor, the greater the reduction in the overall thermal efficiency of the turbine, as can also be seen.

The compressor inspection should be conducted to determine the mechanical and aerodynamic condition of the compressor. Most axial-flow compressors have stacked rotors with bolts extending through the discs, as seen in Figure 21-14. These

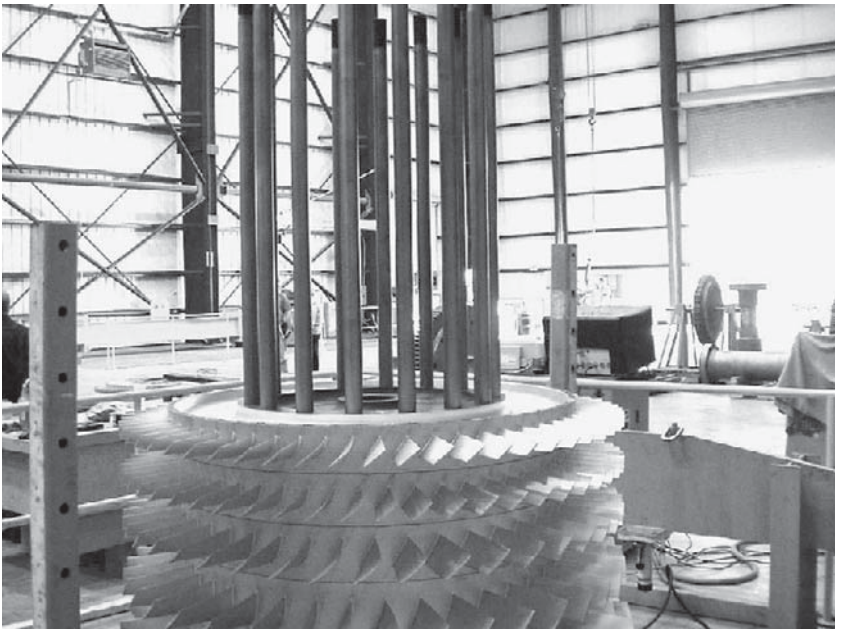


Figure 21-14 Compressor rotor stack (note the long bolts that position the disks).

bolts keep the entire compressor section under the proper compressive force. The bolts should be inspected and, if any are loose, the stretch on the bolts should be determined.

Table 21-10 indicates the various fouling mechanisms that affect the compressor section of the gas turbine. The table indicates the effect that various types of fouling mechanisms have on the entire compressor section from the inlet guide vanes to the exhaust guide vanes. The table deals with the effects on the variable and fixed compressor stator vanes, and the rotating blades.

Axial-flow compressor performance is sensitive to the condition of the rotor blades. The compressor's major problems are caused by dirt on the blades, due to poor filtration and maintenance practices. On-line water washing recovers the majority of the performance deterioration. During a major inspection, all blades should be cleaned and checked for cracks with a penetrant test. If cracks are found in any blade, that blade should be replaced. Occasionally, small cracks can be blended out, but this procedure should be approved by the manufacturer.

The amount of wear on an axial-flow compressor blade is usually a function of foreign particle ingestion. Dust is the most common foreign particle. The maximum and minimum chord lengths should be recorded and reported to the manufacturer, who in turn should be able to report the performance loss occasioned by wear and the decrease in structural strength.

Many of the new high performance compressors suffer from tip rubs. These tip rubs can lead to blade failures at the trailing edge. Most of these tip rubs usually

Table 21-10 Axial-Flow Compressor

Failure Mechanism	General Description	IGV	Compressor Blades	Variable Compressor Stator	Fixed Compressor Stator	EGV
Clogged Filters	This increases the pressure drop at the inlet; causes a reduction in the available power. Small particulates start to bypass the filter pitting the blades.	Pitting of the guide vane.	First stages should be coated. Usually covered with dirt.	First stages should be coated. Usually covered with dirt.	First stages should be coated. Usually covered with dirt.	Minimal effect.
Evaporative Coolers	Water, droplets from the evaporative coolers must be less than 15 microns. Water should be treated, otherwise major damage to the compressor blades and vanes occurs.	Erosion of the leading edge. Vanes should be coated.	Erosion of the first few stages mostly at leading edge and blade tips. Blades should be coated.	Erosion of the first stages. Vanes should be coated.	Erosion of the first stages. Vanes should be coated.	Minimal effect.
Compressor Surge	Reversal of flow in the compressor.	Could lead to vane failure.	Flow separates and surge occurs, usually at the later stages of the turbines. Can lead to blade failures due to excitation of the blade resonance.	Gives a larger margin for operation at various speeds.	Smaller margin for operation at various speeds.	Surge could lead to failure of the EGV blades.

Compressor Tip Stall	This is the separation of the flow at the blade tip.	Minimal effect.	This usually occurs toward the later stages. Tip stalls often lead to a full compressor surge.	Minimal effect as usually variable stators are in the first few stages.	Tip stall at later stages.	Minimal effect.
Rotating Stall	Cells move from one blade to the other in the direction of rotation.	Tends to activate the blades resonance leading to high frequency fatigue failure.	Tends to activate the blades resonance leading to high frequency fatigue failure.	Tends to activate the blades resonance leading to high frequency fatigue failure.	Mostly occurs in the early stages.	Minimal effect.
Blade Tip Rub	Excessive rubs take place on blade tips usually near the bleed ports.	No damage.	Failure of the blade tip at the trailing edge.	Damage due to impact from the failed pieces of blades (DOD).	Damage due to impact from the failed pieces of blades (DOD).	Damage due to impact from the failed pieces of blades (DOD).
Blade Fouling	Deposits on the blades, on-line water wash cleans only the first few stages.	Heavy fouling in the front stages. On-line compressor water wash is usually successful.	Heavy fouling. On-line compressor water wash is usually successful in the first three to four stages.	Fouling can lead to jamming the movement of the stator blades, could cause surge.	Heavy fouling. On-line compressor water wash is usually successful in the first three to four stages.	Minimal fouling, but this can be also very detrimental due to small cross-sectional area.

(*Continued*)

Table 21-10 Axial-Flow Compressor (*continued*)

Failure Mechanism	General Description	IGV	Compressor Blades	Variable Compressor Stator	Fixed Compressor Stator	EGV
Foreign Object Damage	Foreign objects that get past the filter.	Impact damage severe.	Damage due to failed upstream blades. DOD damage.	Damage due to failed upstream blades. DOD damage.	Damage due to failed upstream blades. DOD damage.	Damage due to failed upstream blades. DOD damage.
Aspect Ratios	The new blades have high aspect ratios, which require higher pretwist angles, increasing blade stress.	No effect.	Most of the effect of high aspect ratio occurs in the first few stages. High pretwist angle leads to flow separation at the blade tip.	No effect.	No effect.	No effect.
Pressure Ratio	Pressure ratio has increased from about 7:1, to about 30:1 for industrial gas turbines. The higher the pressure ratio the smaller the operation range (Surge-Choke).	Guide vanes in the newer units are variable, wrong angles have caused failure of the IGVs.	Flow reversal at the higher stages. Higher blade loading per stage.			Some units have encountered failures of the EGT.

Number Stages	Increased number of stages causes the reduction of the operation range of a compressor.		Increased chance of surge.		Increased chance of damage.	Increased chance of damage.
Blade Profile	Older gas turbines have mostly double circular arc blades. The advanced blades are 3D, or controlled diffusion blades. Blade shapes vary from stage to stage.	New blades are transonic. Transonic blades have position of max. thickness toward the rear of the blades (65–70% of the blade chord from the leading edge).	First stages especially at the tip section would have transonic flow.	Minimal effect.	Minimal effect.	Minimal effect.

occur near the bleed sections, which are usually positioned around the fourth to sixth compressor stages. Measurements should be taken to determine blade tip clearances at four points on the circumference. Comparison of these clearance readings with those at installation or at some previous time will indicate if rubs have occurred and whether or not the casing is warped and out of round. It will also indicate whether or not the rotor is below its original position and requires further investigation at the overhaul period.

If the air inlet is subjected to salt-water contamination, the rotor and stator blades should be checked for pitting. Severe pitting near the blade roots may lead to structural failures. The manufacturer should be informed of severe pitting.

Stator blades are as important as rotor blades. All the same cleaning, inspection, and non-destructive test procedures should apply. It should be noted that the wear pattern is somewhat different on the stator blades. Again, the manufacturer should be informed of the wear conditions and should in turn make recommendations concerning continuous operation or replacement.

On completion of required repair and replacement, the gas turbine should be reassembled. This reassembly should be done under careful and experienced supervision to ensure all work meets established criteria. Blade clearances, bearing clearances, and spacing should be checked and recorded during assembly. Special care should be taken to ensure that the machinist uses the proper torque when tightening bolts and nuts. There is a very strong tendency for machinists to apply a torque that "feels" right rather than using a torque wrench. Torque is a very important aspect of assembly. Improper torqueing can cause component warpage and distortion, especially in those components subject to high temperatures during operation.

Compressor Cleaning

There are at least three major reasons for maintaining the cleanliness of the compressor. The first is to restore the gas turbine's capability. If the unit is a driver, its maximum power will decrease as it becomes dirty. Cleaning will restore the majority of the power. Compressor fouling leads to reduction of the pressure ratio and the reduction of the flow through the turbine.

The second reason is to restore the turbine's efficiency. Fouling will increase the fuel required for a given load. Deposits of dirt on the blades change the flow contours. Removal of the deposits will restore the blades to their original profiles and thus restore their efficiency.

The third reason is that removing the build-up on the blades prevents failures due to abnormal operating modes. Fouling of the rotor blades on turbines can also cause thrust-bearing failures. Deposits on turbine governor valves and trip and throttle valves are suspected of causing overspeed failures. Fouling of balance piston labyrinths and balance lines has caused thrust-bearing failures. Deposits on rotor blades can cause vibration from unbalance as these deposits are never uniform, which will cause failure of a unit.

Degradation of power and increase in heat rates is a good indicator that there may be excess build-up on the compressor blades and vanes.

Fouling indicators include:

1. Gas turbine exhaust temperature.
2. Compressor discharge pressure and temperature.
3. The compressor adiabatic and polytropic efficiency.
4. The pressure ratio in the compressor section of the turbine relative to the turbine section.
5. Thrust loading usually indicated by a rise in the thrust bearing metal temperature.
6. Changes in the differential pressure between the suction pressure and the balance piston, which regulates the position of the turbine shaft.
7. High vibration readings at the bearings.

Compressor Water Wash

There are two basic approaches to on-line cleaning: abrasive cleaning, and solvent cleansing. On-line cleaning is a very important operational requirement. On-line cleaning is not the answer to all compressor fouling problems since after each cleaning cycle full power is not regained, therefore a time comes when the unit needs to be cleaned off-line, as seen in Figure 21-15.

The time for off-line cleaning must be determined by calculating the loss of income in power as well as the cost of labor to do so and equate it against the extra energy costs. In the trade-off between performance and availability, we must consider the fact that the reduction in power should also be treated as equivalent forced outage hours, thus reducing the plant availability.

The use of abrasive cleaning has diminished due to erosion problems; liquid washing is now primarily being used. The more common abrasives are 1/64 inch nut shells or spent catalyst. The abrasive must have sufficient mass to achieve the momentum required to dislodge the dirt. However, high-mass particles do not follow the gas stream. Also, they are hit by the leading edge of the moving wheels and blades. Consequently, the trailing edges are not abraded. The closer the dirt is to the injection point the less significant the asymmetrical distribution.

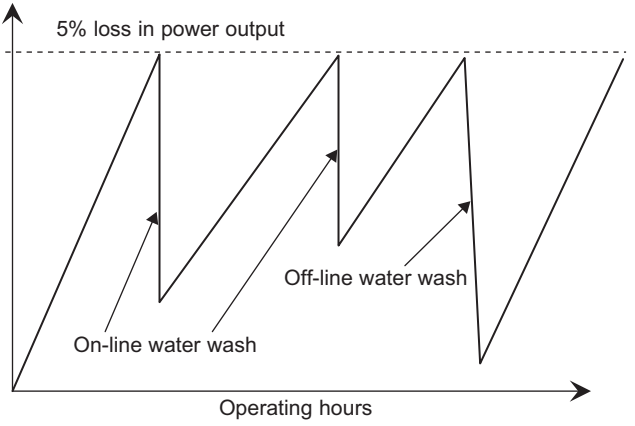


Figure 21-15 Effect of compressor water wash on power output.

The abrasive must also be sufficiently tough to resist breakage on impact. Rice is a poor substitute, since it tends to shatter on impact and small particles lodge themselves in bearings and seals. Another problem with abrasives is what happens to them after they have done the cleaning. In a simple-cycle gas turbine they will probably be burnt. However, in a regenerative unit they can deposit in the regenerator. Some regenerator burnouts have been attributed to these deposits. In steam systems they will probably plug up traps throughout the system. During discussions about abrasive cleaning, the possibility of causing labyrinth damage is always raised. In fact, these apprehensions have proven groundless. No one knows why, but it could be that the particles are too big to enter the clearance space.

On-line water wash and off-line compressor washing was an important part of gas turbine operations in the late 1990s. High pressure compressors are very susceptible to dirt on the blades, which can not only lead to a reduction in performance but also to compressor surge. Washing efficacy is site-specific due to the different environmental conditions at each plant. There are many excellent techniques and systems for water washing. Operators must often determine the best approach for their gas turbines. This includes what solvents, if any, should be used, and the frequencies of wash. This is a complex technical-economical problem also depending on the service that the gas turbines are in and the plant surroundings.

Off-line water washing (with or without detergents) cleans by water impact and by removing the water-soluble salts. It is important that the water used should be demineralized water. The detergent/water ratio is also another important parameter. Water washing using a water-soap mixture is an efficient method of cleaning. This cleaning is most effective when carried out in several steps, which involve the application of a soap and water solution, followed by several rinse cycles. Each rinse cycle involves the acceleration of the machine to approximately 20–50% of the starting speed, after which the machine is allowed to coast to a stop. A soaking period follows, during which the soapy water solution may work on dissolving the salt.

A fraction of airborne salt always passes through the filter. The method recommended for determining whether or not the foulants have a substantial salt base, is to soap wash the turbine and collect the water from all drainage ports available. Dissolved salts in the water can then be analyzed.

On-line washing is being widely used as a means to control fouling by keeping the problem from developing. Water cleaning is not usually very effective after the first few stages. Techniques and wash systems have evolved to a point where on-line washing can be done effectively and safely. Washing can be accomplished by using water, water-based solvents, and petroleum-based solvents or surfactants. The solvents work by dissolving the contaminants, whereas surfactants work by chemically reacting with the foulants. Water-based solvents are effective against salt, but fare poorly against oily deposits. Petroleum-based solvents do not effectively remove salty deposits. With solvents, there is a chance of foulants being re-deposited in the latter compressor stages.

Even with good filtration, salt can collect in the compressor section. During the collection process of both salt and other foulants, an equilibrium condition is quickly reached, after which re-ingestion of large particles occurs. This re-ingestion has to be prevented by the removal of salt from the compressor prior to saturation. The rate

at which saturation occurs is highly dependent on filter quality. In general, salts can safely pass through the turbine when gas and metal temperatures are less than 1000 °F (538 °C). Aggressive attacks will occur if the temperatures are much higher. During cleaning, the actual instantaneous rates of salt passage are very high together with greatly increased particle size.

Different Wash Systems

There are primarily three different types of wash systems: on-line wash system, off-line crank wash system, and manual handheld crank wash system. These cleaning systems are primarily designed to maintain the engine compressor at its maximum efficiency. The effectiveness of a system will greatly depend on its proper use. In order to evaluate the effectiveness of these systems it is strongly recommended to link the use of these systems to engine performance parameters.

For the most part, the on-line wash system is intended as a supplement to the off-line crank wash system and not a substitute. In general, it is extremely important to implement a turbine crank wash program in order to recover most of the recoverable performance deterioration. At times when turbine crank washes are put off due to operating constraints, there may be the need to manually clean the turbine compressor blades, as a large buildup of dirt will be on the blades. In order to manually clean the compressor blades the turbine compressor case has to be inspected and hand scrubbed in the field. Testing has revealed that an additional five efficiency points were recovered in a turbine when an off-line water wash was performed.

On-Line Wash Cleaning System

The on-line wash cleaning system is used while the turbine operating parameters are stable. The system can be used without disturbing the operational unit, thus it does not matter if the turbine is operating at part or full load. Cleaning the turbine compressor with the on-line wash system should be a routine and scheduled maintenance function. The on-line water wash system is based on injecting atomized cleaning fluid thus avoiding any problems that could be associated with abrasive cleaning methods that could erode blades and damage component coatings.

The typical on-line wash system consists of a wash ring located outside of the turbine inlet air plenum as seen in Figure 21-16. The wash ring has several pigtails that are connected to atomizing type water nozzles as seen in Figure 21-17.

Off-Line Crank Wash Cleaning System

The off-line crank wash system is used while the turbine is out of service. The off-line wash is performed when the turbine is cranked manually by the engine starter with the fuel and ignition system deactivated. This type of wash is more effective in recovering the performance degradation that the turbine experiences. Before performing this procedure most of the low drain piping, igniter, torch and pilot gas, and so on is removed in order to avoid liquid pockets in the turbine fuel igniter piping. The effectiveness of

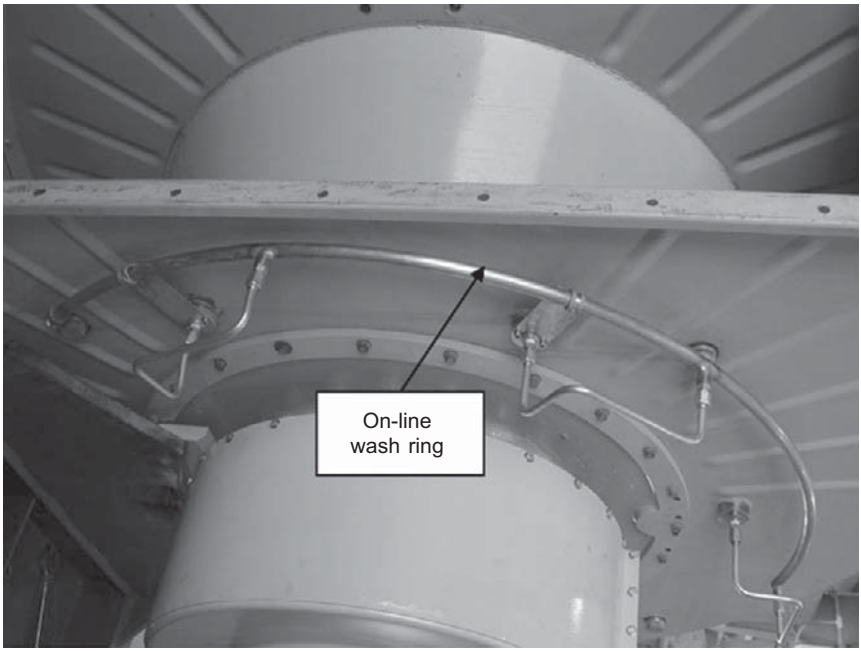


Figure 21-16 Gas turbine plenum showing the on-line wash ring on the outside of the plenum.

this cleaning method is enhanced by the use of different wash fluids. Manufacturers recommend different water and solvent base wash fluids, and field technicians have exhausted many different combinations of relatively available household agents.

Many turbines are configured with a crank wash ring with nozzles that do not atomize the water. The wash fluid is mixed and stored in an SS holding tank. The tank is equipped with a pressure connection and outlet connection. Plant air is used to force the mixed fluid into the turbine inlet air plenum through the stainless steel piping and valves.

A preferred method used to perform a crank wash is through the use of a handheld wash wand. Several of the turbine inlet air inspection covers have to be removed in order to obtain access to the compressor inlet. A handheld wand is rotated around the inlet turbine screen in order to spray the compressor air inlet evenly.

Hand scrubbing the compressor blades is another method of recovering the performance of an engine compressor. A routine off-line crank wash is performed before the compressor case is open for inspection and cleaning. This is a very labor-intensive method that helps recover an additional level of performance. Not all gas turbine compressor blades can be accessed in the field, and the economic incentives have to be evaluated before this method is undertaken. The expected engine compressor polytropic efficiency improvement is about 0.5 to 1.0 efficiency points. In an engine that has to run for 11 months without a crank wash the extra efficiency point is an added boost in fuel savings and additional power delivered.

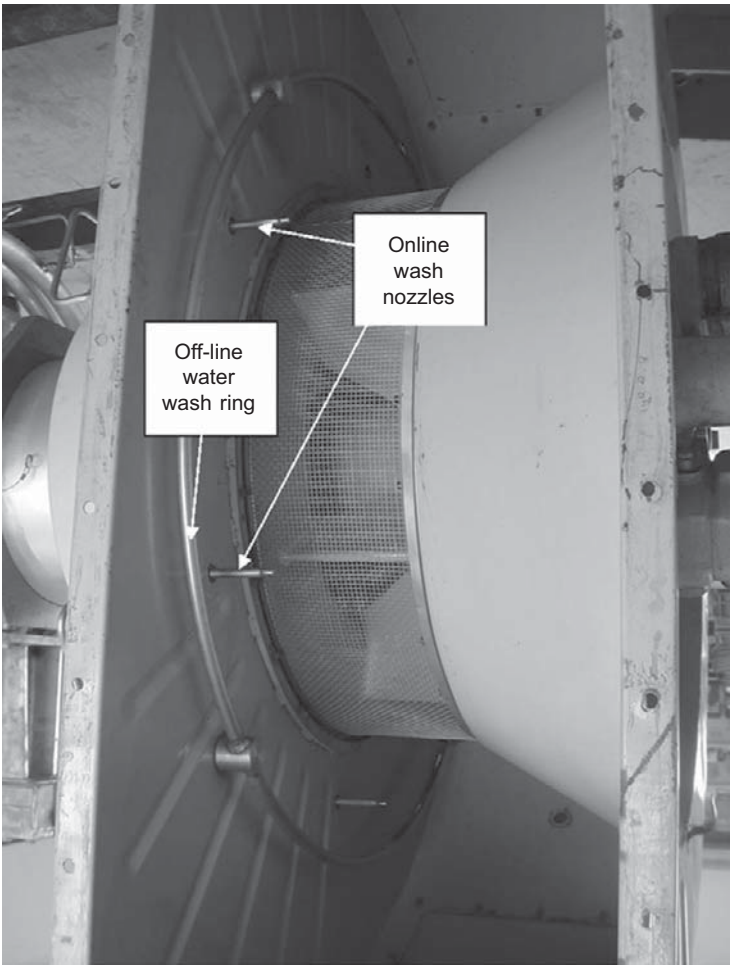


Figure 21-17 Inside view of air plenum showing the off-line water wash ring and the on-line water wash nozzles.

Water quality for both on-line and off-line water washes must be stringent, so as to ensure that impurities are not introduced. Table 21-11 gives a detailed specification of the quality of the water required to complete a successful water wash.

Testing the quality of the water is critically essential before performing a routine on-line water wash. A common problem with demineralized water sources is the occasional fluid channeling in the catalyst beds. A demineralized water-polishing skid after the demineralized water is recommended for the turbine water wash in order to ensure good water quality. Since the water wash of each turbine is a batch mode, the polishing skid is designed for small batch rates, thus water consistency is maintained. Effectiveness of every on-line water wash has greatly improved by incorporating a test of the water quality. A detailed analysis of the water for every water wash would

Table 21-11 Water Quality for Compressor Wash

Water Specification	
Sodium and Fluorine	<1.9 ppmw
Chlorine	<40 ppmw
Lead	<0.7 ppmw
Vanadium	<0.35 ppmw
Iron, Tin, Silicon, Aluminum, Copper, Manganese, Phosphorous, Calcium, and Magnesium	<3.8 ppmw
Dissolved Solids	<5 ppmw
pH	6–9

be time consuming and expensive; an alternative would be to use a handheld conductivity/total dissolved solids/pH meter. The meter readings should indicate a water conductivity of <0.5 μmhos, total dissolved solids of <1.0 ppmw, and pH between seven and nine.

On-Line and Off-Line Water Wash Fluids

Many solvents are used for turbine on-line and off-line water washing. Water base, solvent base, industrial cleaners, and demineralized water are just a few of the different types of agents used to clean gas turbine engine compressors.

There are several types of water base agents used for compressor cleaning. The most popular water base solvents contain low metal contents, and are derived from highly active natural oils and surfactants. The water base agents are environmentally safe and contain no solvents that are capable of dissolving and removing engine deposits that accumulate with time. Common industrial cleaning agents work well in combination with water base agents and solvent base agents. Most turbine manufacturers offer an approved list of soaps that can be used with their turbines. It is extremely important not to use an agent that the OEM does not approve or has not reviewed.

Many different types of solvent base agents also are used for on-line and off-line turbine washes. Most solvents are derived from hydrocarbon base stocks, and contain very little metals. Most of these solvents are not considered fully environmentally friendly, but with the proper procedures these agents can be used in a safe manner. These solvents are predominantly used during off-line crank washes.

By far the most common agent used for water washing is demineralized water. Demineralized water systems are very effective if the filtration system effectively filters out the majority of airborne particles and oily substances.

Before implementing a water wash procedure, the procedure should be discussed with the turbine manufacturer and soap supplier. Their expertise in the subject at hand will contribute to your success with the proposed program.

Obtain demineralized water sampled to meet the specifications required. If a water wash agent is used, mix the fluids in the tank per the soap vendor's specifications. The

water quantity required depends on the recommended soap-to-water ratio and the size of the gas turbine.

Water washes are done with the turbine operating at steady conditions, and ambient temperatures above 40 °F (4 °C). Special procedures must be applied if ambient temperatures are below 40 °F (4 °C).

Connect the outlet of the water wash cart to the turbine water wash piping. Connect the air hose supply to the tank air inlet valve; adjust the air pressure from your supply header to obtain 85 to 100 psig.

Open the tank water wash fluid outlet valve and the turbine water wash inlet valve, which is connected to the water wash manifold. The wash fluid will be forced into the turbine by the air pressure in the tank. Observe the turbine performance; the Compressor Discharge Pressure (CDP) will rise and firing temperature will drop when the water is injected. Power will increase, but will not affect process variables. The turbine will have adequate power to maintain its set points.

- Observe the time it takes to ingest a fixed amount of fluid.
- If the time to ingest the fluid increases with time, then the injection nozzles are getting plugged.
- When the wash fluid ends, the turbine operation will continue without any problems.
- If a wash solvent is used, follow this same procedure with a water-only rinse.

Off-Line Crank Wash Procedure

Shut down the turbine and allow sufficient time for the turbine to cool to below 150 °F (66 °C). This is extremely important if solvent base agents will be used for cleaning. Disconnect the lower case drain plug and igniter torch tubing, remove all low point tubing components such as the gas line to the fuel manifold, and install caps to all the open lines.

Remove the turbine inlet inspection covers. Fill a handheld pump sprayer with the appropriate crank wash solution, water, or solvent base agent with its appropriate water mixture. Initiate manual crank mode on the turbine engine. Spray the crank wash solution into turbine inlet air bell mouth. Continue this process until the wash solution is almost finished. Shut down the manual crank mode and continue to spray the solution during the engine coast down. Let the solution sit in the turbine for 10–15 minutes.

Introduce 10 gallons of demineralized water into the crank wash water tank. Start manual crank mode, and inject the water into the crank wash manifold. For better results use the handheld injection wand. Care must be taken to make sure foreign objects are not sucked into the turbine air inlet, and that the protective foreign object screens are in place before starting this procedure.

Inject a recommended detergent during the turbine's crank mode and during coast down. Let the solution sit for about 10–15 minutes. Fill injection cart with 20–30 gallons of demineralized water. Start manual turbine crank mode and inject water into the turbine inlet bell mouth. You can use either the hand injection wand or the water injection ring.

Continue to inject demineralized water until you obtain a clean water stream out of the turbine drains.

Combustors

Combustion chambers have seen considerable change as the new advanced gas turbines have moved from a diffusion type wet combustor to the Dry Low NO_x, sometimes known as Dry Low Emission combustors. The new DLN or DLE combustors have stability problems and are very susceptible to any liquids in the system. There are also four different arrangements of the combustor systems:

- Can-annular combustors
- Annular combustors
- Silo combustors
- Side combustors

Can-annular combustors and the small side combustors can be removed and the combustion liners and nozzles are easily inspected for cracks and burned areas without having to remove the turbine casing. Silo combustors can also be examined easily after they have cooled, and technicians can enter the combustors to examine the combustor tiles. The best way to examine the annular combustors is with the use of borescopes. Short, individual cracks are not uncommon and need no immediate attention. However, if the cracks are grouped such that their continuance or the beginning of another crack could cause the loss of a piece of metal, then a repair should be made. Cracks of this nature normally can be welded with a type of welding rod recommended by the manufacturer, depending on the kind of metal involved. Burned or warped areas in combustion chambers or baskets can be cut out and new sections welded. However, burned areas should be studied with regard to location, pattern, or repetition in all chambers to determine the cause of the burning.

Table 21-12 indicates the various fouling mechanisms that affect the combustor section of the gas turbine. The table indicates the effect that various types of fouling mechanisms have on the entire combustor section including diffusion and DLN combustors, fuel nozzles, cross-over-tubes, and the transition pieces. The table deals with the effects on can-annular and annular combustors.

Individual burned areas may indicate a dirty or faulty fuel burner nozzle or misalignment of the combustion chamber. Similar burned areas in various chambers may indicate abnormally high firing temperatures during starting due to excessive fuel use. They may also be the result of "slugs" of liquids entering with the fuel gas, excessively rapid starts, or overloading of the turbine. In the case of DLN combustors problems with flashbacks due to liquids in the fuel gas destroy the fuel premix nozzles.

The combustion chamber positions as well as the actual chambers or baskets should be permanently numbered, and a complete record should be made for each basket regarding hours of service, repairs, or replacements made, and their location in the turbine at each inspection date. The basket ends, or at places where they are supported, should be inspected for excessive wear from vibration or expansion and contraction movement. Repair of these parts should be made by cutting out and welding in new materials or replacing spring seals if necessary.

Table 21-12 Combustor Section

	Can-Annular Combustors					Annular Combustor			Transition Piece
Failure Mechanism	**General Description**	**Diffusion Combustor**	**Dry Low NO_x Combustor**	**Cross Over Tubes**	**Fuel Nozzles**	**Diffusion Combustor**	**Dry Low NO_x Combustor**	**Fuel Nozzles**	**Transition Piece**
Uneven combustion	Many causes such as clogged fuel nozzles, improper injection of water or steam, flame stability.	High temperature on the combustor can walls. Spalling of TBC.	Improper mix.	Burnt out cross over tubes.	Heavy carbon buildup on the fuel nozzles.	Cracks noted on tiles. Problems noted at tile joints. Spalling of TBC.	High pulsations leading to high vibration.	Heavy carbon build-up on the fuel nozzles.	Vibration could cause seal failure where the transition piece connects with the first-stage nozzle.
Variation in heating value	This effects the Wobee Index (WI) (LHV/$\sqrt{}$ (Sp.Gr. $*$ T)) High WI causes the flame to burn closer to the liner. Low WI can cause pulsation.	Cracks on the combustor liner. Spalling of TBC.	Flashback-problems.	Burnt-out cross over tubes.	Burnt premix fuel nozzles.	Cracks on the combustor liner. Spalling of TBC.	Flashback problems	Burnt premix fuel nozzles.	Cracks on the inner surface. Spalling of TBC. Seal problems due to vibration.
Low Btu Fuel Gas <500 Btu/cu.ft.	Can-annular combustors are not recommended for low BTU gas, because more air is needed in the primary zone so less air available. More surface area to cool than an annular combustor.	Good stable operation for low BTU gas. Cooling of combustor liners must be carefully monitored.	Not suited for low Btu gas.	If uneven combus-tion occurs the cross tubes could be burnt out.	Coking on fuel nozzles.	Best suited for low BTU gas fuel. Less surface area to cool.	Not suited for low Btu gas.	Coking on fuel nozzles.	Unsteady com-bustion can lead to seal problems.

(*Continued*)

Table 21-12 Combustor Section (*continued*)

	Can-Annular Combustors					Annular Combustor			Transition Piece
Failure Mechanism	**General Description**	**Diffusion Combustor**	**Dry Low NO_x Combustor**	**Cross Over Tubes**	**Fuel Nozzles**	**Diffusion Combustor**	**Dry Low NO_x Combustor**	**Fuel Nozzles**	**Transition Piece**
High Emissions	High temperature in the primary zone high NO_x.	Incomplete combustion leading to UHC.	Combustion pulsation, flashback.	Burnt-out cross over tubes.	Burnt-out fuel nozzles.	High temperature in the primary zone high NO_x. Incomplete combustion leading to UHC.	Combustion pulsation, flashback.	Burnt-out fuel nozzles.	Vibration could cause seal failure where the transition piece connects with the first-stage nozzle.
Flashback	This is a phenomenon common in DLN combustors, and is accelerated if there is any liquids in the fuel gas.	No problem in diffusion combustors.	Major problem in these types of combustors. High vibration and pulsation.	Burnt-out cross over tubes.	Melting of premix nozzles.	No problem in diffusion combustors.	Major problem in these types of combus-tors. High vibration and pulsation.	Melting of premix nozzles.	Vibration could cause seal failure where the transition piece connects with the first-stage nozzle.
Dual fuel	Liquid fuel and natural gas. Operation at various percent mixture settings.	Good operation at all percent mixture settings. Changes of percent on-line possible.	Best operation on natural gas. Poor tolerance for any liquids. Flashback problems during transition from NG to liquid fuel.	If there is uneven combus-tion, tube burnout is possible.	Diffusion combustor fuel nozzles encounter vibration problems. Melting of premix DLN nozzles could take place during transition.	Good operation at all percent mixture settings. Changes of percent on-line possible.	Best operation on natural gas. Poor tolerance for any liquids.	Diffusion combustor fuel nozzles encounter vibration problems. Melting of premix DLN nozzles could take place during transition.	Vibration could cause seal failure where the transition piece connects with the first-stage nozzle.

The transition pieces should be inspected for cracking and wear at points of contact. Transition pieces are now being coated with a TBC. Wear usually occurs between the transition piece and the combustion liner sleeve, and also at the first-stage nozzle fit. The cylindrical section of the transition piece may be replaced if the wear is excessive; wear at the nozzle-end of the transition piece is more serious because it allows excessive vibration of the transition piece, which might lead to cracking. Transition pieces should be replaced if 50% of the inner or outer seal is reduced to half the original thickness. If the transition piece is in otherwise excellent condition, the seals may be ground off and replaced. The new floating seals have been found to be more reliable than the old fixed seals. Transition pieces should be replaced if cracks are found in the body.

Turbines

The first-stage turbine nozzle vanes can be superficially inspected by the use of a borescope for bowing by entering the turbine through the combustion chamber areas or by removing inspection plates. In certain size turbines (and by somewhat difficult maneuvering) the last row of turbine rotating blades can be inspected by entering through the turbine discharge duct. The opportunity should be taken to measure, if possible, the blade tip clearance at four points on the circumference. Comparison of these clearance readings with those at installation or at some previous time will indicate if rubs have occurred and whether or not the seal ring is warped and out of round. It will also indicate whether or not the rotor is below its original position and requires further investigation at the overhaul period.

Table 21-13 indicates the various fouling mechanisms that affect the turbine section of the gas turbine. The table indicates the effect that various types of fouling mechanisms and corrosion have on the entire turbine section from the first-stage nozzle vanes to the third- or fourth-stage blades.

As the hot sections become exposed, preliminary inspection for cracks or bowings should be undertaken to estimate work to be done. The bearings require inspection for wear and alignment for the same reason.

Turbine blades should be inspected closely for erosion and cracks. The most critical areas in the turbine rotor are the fir-tree section, where the blades are attached to the rotor, and the trailing edge of the blade near the hub. The trailing edge of the turbine blade is usually the hottest section of the blade, and cracks usually start at the trailing edge at about 1/3 the height of the blade from the base. These areas should be carefully cleaned and checked for cracks with spray penetrant. First-stage inlet vanes and rotating blades should be removed and blasted clean with a No. 200 grit aluminum oxide or other approved blasting material. The coatings should be stripped. They should then be inspected minutely for cracks by means of red dye or black light. The first-stage nozzle vanes will probably need attention, which can be done on the job. In older design vanes bowing on the trailing edge, if any, can be taken out by inserting a spacer piece of correct cross-sectional area between the vanes, heating the top vane to red heat with a torch, and forging the vane edge flat with a hammer and flatter. The cracks, if less than 1.5 inches long, can be grooved out and welded, providing the crack does not run under the end-supporting rings. In this case the vane

Table 21-13 Axial-Flow Turbine

Failure Mechanism	General Description	First-Stage Nozzles	First-Stage Blades	Second-Stage Nozzles	Second-Stage Blades	Third- & Fourth-Stage Nozzles	Third- & Fourth-Stage Blades
Nozzle vane bowing	Reduction in passage area. High temperature, improper cooling, high wheel space temperature.	Vanes can suffer from hot corrosion. Spallation of TBC.	Spallation of TBC coating.	Vanes can suffer from hot corrosion. Spallation of TBC.	In some units these blades are not cooled and may be affected by excessive temperatures.	These vanes are usually not affected, except for DOD.	These blades are usually not affected, except for DOD.
Burnt nozzle vanes	Uneven combustion creates various hot spots, which lead to melting of vanes.	Trailing edge melted. Damage to vane platforms is usually due to improper cooling.	Damage due to DOD.	These are usually due to fuel gathering in the vanes due to incomplete combustion and then combusting in the vane passage.	Damage due to DOD.	These vanes are usually not affected, except for DOD.	These blades are usually not affected, except for DOD.
Incomplete combustion or excess fuel	During start-up the fuel is not combusted and collects in the stationary vanes, which act as flame holders. Ensure that the control system has a rate of acceleration shutdown mode.	Vanes totally melted.	Blades are cut as if by a flame torch. Damage due to DOD.	DOD due to impact of upstream component failures. Vanes totally melted. The case where the second-stage vanes are melted while the first-stage vanes are relatively intact is caused by fuel accumulating in the second-stage nozzle during start-up.	DOD due to impact of upstream component failures.	DOD due to impact of upstream component failures.	DOD due to impact of upstream component failures.

Hot corrosion type I (over 1500 °F)	Rapid form of oxidation, caused by the reaction of Na in the air or fluid; sulfur, which is usually in the fluid; and oxygen. Intergranular attack, sulfide particles, and a denuded zone of base metal.	Damage to the leading edge. Erosion of the TBC coating, attack on the base coating.	Thinned down LE or TE. Cracks experienced in the platform area.	Damage to the leading edge from erosion from first-stage nozzles and blades.	DOD damage.	Minimal effect.	Minimal effect.
Hot corrosion type II (between 1100 °F–1450 °F)	Caused by low melting eutectic compounds resulting from the contamination of sodium sulfate and some of the alloy constituents such as nickel and cobalt. Layered type of corrosion scale.			Typically damage to the coating, layered type of corrosion.	Typically damage to the coating, layered type of corrosion.	Not usually found in the lower temperature stages but in some advanced turbines, these stages may have high temperature.	
Hot gas erosion oxidation	Caused by small solids in the air or the fuel. By poor combustor pattern, excessive EGT pattern.	Failure of TBC on nozzle vane or platforms. Not even around circumference.	Damaged coating.	Erosion of coating and oxidation.	Minimal effect.	Minimal effect.	Minimal effect.

(*Continued*)

Table 21-13 Axial-Flow Turbine (*continued*)

Failure Mechanism	General Description	First-Stage Nozzles	First-Stage Blades	Second-Stage Nozzles	Second-Stage Blades	Third- & Fourth-Stage Nozzles	Third- & Fourth-Stage Blades
Blade tip rubs	Due to very small tip clearance, and high metal temperatures in the blades.		This can lead to failure of the squealer section, and also of the blade trailing edge.	Damage due to DOD.	Blade failure can be caused by shroud tips coming into contact with the casing.	Damage due to DOD.	Blade failure can be caused by shroud tips coming into contact with the casing.
Blade fretting erosion	Fretting in the dove tails/ fir trees is caused by the rocking action of the blades. Peaking turbines are highly susceptible to this problem.	Severe attack on TE and LE, and on concave side of the airfoil.	Reddish brown debris of iron oxide and cracks can be found in the blade attachment region.		Reddish brown debris of iron oxide and cracks can be found in the blade attachment region.		Usually not susceptible to this problem.
Blade and wheel rupture failure	This failure occurs in high temperature and highly loaded blades (highly stressed) and disks. Disk failure can be catastrophic. Caused by inadequate cooling due to blockage of cooling passages.	Creep distortion usually at trailing edge.	Wheel space tempera-tures can be very high if seal leakages occur, or cooling holes are blocked.				

Foreign object damage/ domestic object damage	FOD occurs from materials coming from an external source to the gas turbine, and DOD occurs from failure of internal components.	Most damage from this point forward.					
Low Cycle Fatigue (LCF)	Turbine disks, and first-stage turbine suffering from low steady state stress, also due to thermo-mechanical fatigue problems. Peaking turbines more susceptible.	Cracks in the vanes. Single vane segments suffer less than multiple vane segments.	Thermo-mechanical fatigue.	Coatings can become rumpled.		Coatings can become rumpled.	
High cycle fatigue	Can occur in any blades or vanes due to blade resonance frequency being excited. This usually occurs in blades where there are no tip or mid-span shrouds.	Not applicable in most designs.	Nicks and cracks act as initiators and usually failure occurs around 1/3 of the blade height from the platform.	Not applicable in most designs.	Nicks and cracks act as initiators and usually failure occurs around 1/3 of the blade height from the platform.	Not applicable in most designs.	Failure in these blades may be due to support spars at the exit, the resonance frequency of the blades.

must be removed and welded or a new vane fitted in place. As the vanes are welded, they must be continually checked for new cracks, which in turn must be grooved and welded and checked again. The new advanced nozzle vanes, because of the complex cooling sections, may not be able to be repaired.

While repairing the first-stage nozzle vanes, the upper and lower vane section should be bolted or clamped together, and the entire ring should be placed on a flat, level surface, or sufficiently supported in the horizontal plane to prevent heat warpage or bowing of the ring due to heating the vanes during their repair.

After straightening or taking out any bowing in the trailing edges of the vanes (partitions), perpendicular distances between the trailing edges of each vane and the surface of the next should be carefully measured. An average of these distances should be made and then corrected to a plus or minus percentage approved by the manufacturer. This method will help to assure equal distribution of gas flow to the first-stage rotating blades for the elimination of blade vibration.

Turbine rotating blades cannot be field repaired if they are cracked. If one or two blades are damaged mechanically, the manufacturer may recommend field repair or replacement of the damaged blades. However, if several blades are fatigue cracked, it is recommended that the entire set be replaced, since the remaining blades have been exposed to the same operating conditions and, therefore, have little fatigue life left.

Both top and bottom halves of the journal bearings should be inspected for misalignment wear as well as excessive *in-line* wear, which can occur in peaking turbines that have frequent starts. An indication of the condition of the thrust bearings can be made by removing a small section of the turbine shaft, usually on the governor end, and axially moving or bumping the shaft. The amount of axial shaft movement will indicate the thrust clearance and, if it is found to be between 0.012 to 0.015 inches, it can be considered normal.

If the turbine is not out of alignment, or the shaft bowed as determined by the vertical and horizontal clearance checks or the appearance of the bearing surfaces, it is not recommended that the rotor be removed. Some turbine designs, however, may require removal of the rotor to facilitate the removal of some bottom sections of the diaphragms or inlet vanes. If the rotor is removed, special care must be taken when separating the couplings. Coupling flanges must be marked and run-out checks made for alignment so that they can be properly reassembled. However, the work should always be done under the manufacturer's supervision.

Work should be made to progress strictly in accordance with the planned flow charts, which must be constantly kept updated. Extra work and delays will probably be encountered; however, a well-planned program will include certain allowances, and little change should be required. If any significant change is encountered, the program should be revised to show the extra outage time and possible extra personnel required.

Rejuvenation of Used Turbine Blades

Two distinct types of damage can be recognized: surface damage and internal degradation. Surface damage may be due to either mechanical impact or corrosion and

generally is confined to the blade airfoil. In both cases light damage can be removed by blending or dressing, and then applying coating for surface smoothness and temperature protection. Blades with severe surface damage or cracks are scrapped. When properly applied, these coatings can increase the life of the blades considerably, in some cases even more than when they were new. Recent advances in high temperature coatings for severe hot corrosion service have resulted in the low unit cost feature of pack cementation and the economy of electroplating to yield multiple element coatings containing precious metal aluminides. These coatings are available in several combinations of platinum, rhodium, and aluminum for application to cobalt- and nickel-based vanes and blades. Most of the newer first two stages of blades are coated with TBC coating. These coatings were optional on the old turbines but they are now necessary to maintain the blade metal temperature below 1350 °F (732 °C).

Internal degradation is caused by micro-structural changes, which result from extended exposure at high temperature under stress. The micro-structural changes are responsible for the reduction in mechanical properties. Three forms of internal degradation have been verified: (1) precipitate coarsening or overaging, (2) changes in grain boundary carbides, and (3) cavitation or void formation.

A considerable fraction of the intermediate temperature strength of nickel-based turbine blade alloys results from the fine γ' precipitate Ni_3 (Al, Ti). The γ' particles generally coarsen as a function of time to the one-third power growth law, with a corresponding decrease in strength. Grain boundary carbide morphology and amount can also change with time. Since the alloy heat treatments that cause carbide formation are generally optimized for short-term properties, long-term changes in carbide structure are usually detrimental, particularly with respect to such properties as ductility and notch sensitivity. Cavitation represents the initial step in creep failure. It consists of the nucleation and growth of voids on grain boundaries. With time, the isolated voids link up to form cracks. It appears that blade material has to be near or in tertiary creep before cavitation can readily be detected by optical microscopy.

It is not known to what extent each of the previous mechanisms contributes to turbine blade degradation during service. It is also probable that each alloy will respond differently to a particular temperature/stress combination. Figure 21-18 shows the typical variation in stress/rupture life determined at 1350 °F (375 °C) with service time for forged Inconel X-750 blades.

Internal service damage due to precipitate coarsening and changes in grain boundary carbides should generally be reversible with conventional heat treatment involving complete solutioning followed by controlled precipitation at lower temperatures. For creep voids, it is not clear if cavitation damage can be removed by conventional heat treatment.

Normal reheat treatment can partially restore blade properties; however, it does not appear to be capable of full property recovery, although the micro-structures are comparable to new blades. This shortcoming implies that cavitation may be present and was not removed by conventional reheat treatment. Hot isostatic pressure (HIP) processing is an alternative that ensures void removal. It has demonstrated its ability to remove even gross internal shrinkage porosity in investment castings. The results of HIP treatment, as seen in Figure 21-19, clearly show that the HIP processed material

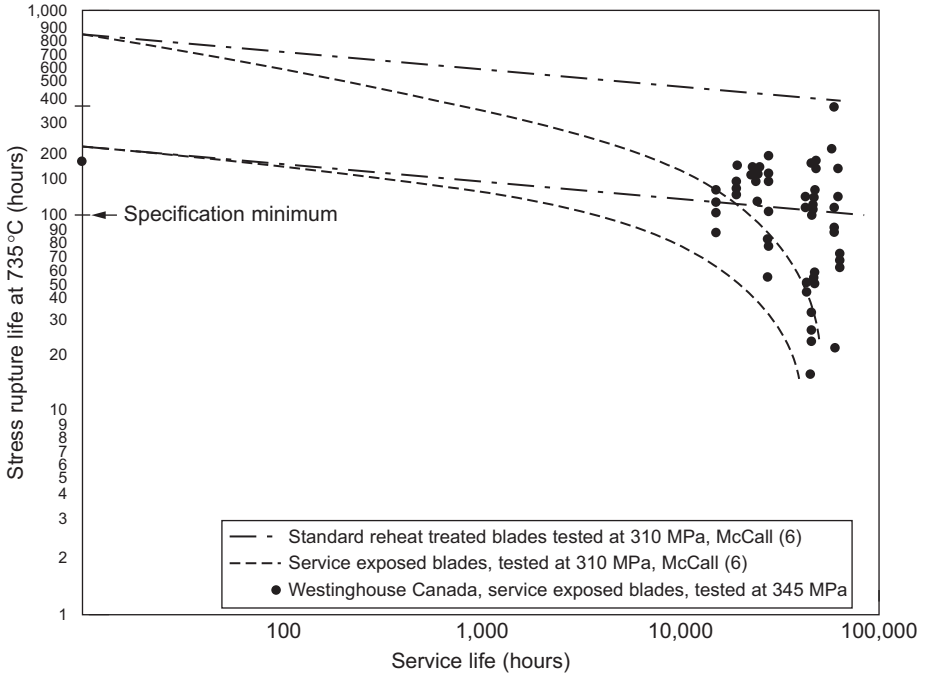


Figure 21-18 The variation of remaining stress rupture life at 1350 °F (735 °C) with service time in forged Inconel alloy X-750 turbine blades (Courtesy of Westinghouse Electric Corp., Gas Turbine Div.).

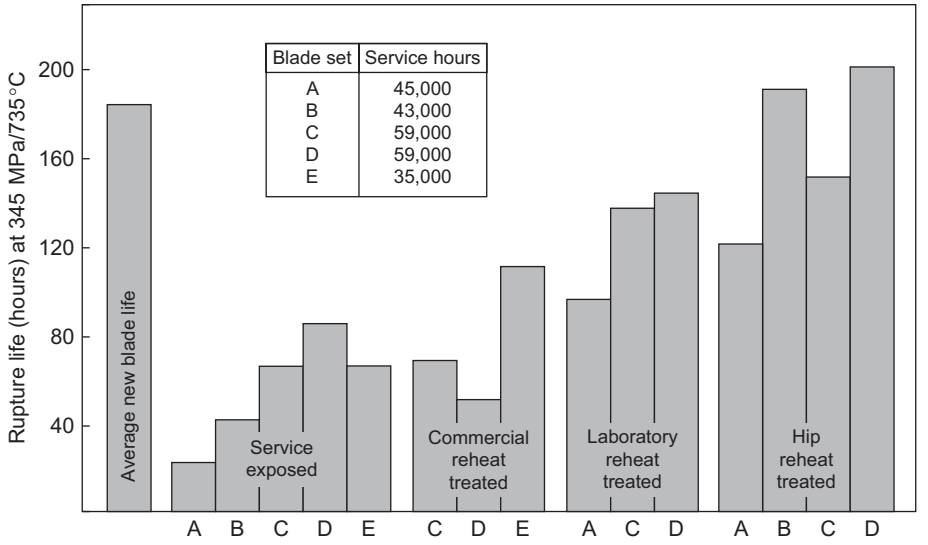


Figure 21-19 Comparison of stress rupture life at 50 ksi/1350 °F (345 MPa/735 °C) in service exposed, commercially reheat-treated, laboratory reheat-treated, and HIP reheat-treated used Inconel X-750 turbine blades (Courtesy of Westinghouse Electric Corp., Gas Turbine Div.).

is superior to both commercial and laboratory conventional reheat-treated material. Cost estimates indicate that used blades can be rejuvenated at a fraction of the cost of a new set of blades.

Rotor Dynamic System Characteristics

Gas turbines operate at high speeds and therefore require a complex blend of aero-thermal performance and rotor dynamic characteristics. Total analysis is needed to ensure maximum plant utilization. In the previous sections in this chapter we have discussed many of the aero-thermal performance parameters. In this section, we discuss the rotor dynamic characteristics of gas turbines.

The rotor dynamic characteristics in present-day gas turbines and especially in advanced gas turbines are very critical and must be fully understood. It is important to understand the various causes of the rotor dynamic characteristics and the vibration signatures experienced by the gas turbine. To properly maintain advanced gas turbines, an in-depth understanding of the causes of rotor dynamic characteristics and their associated vibration signals generated must be made. Of the several factors that can cause vibrations in gas turbines, rotor-bearing systems head the list. The following are some of the major elements that contribute to these signals:

1. Rotor Unbalance
   - **a.** Dissymmetry
   - **b.** Non-homogeneous material
   - **c.** Eccentricity
   - **d.** Thermal gradients
   - **e.** Shrink fits
2. Rotor bow
3. Bearing misalignment
4. Hydraulic or aerodynamic unbalance
5. Shifting of parts due to plastic deformation of rotor parts
6. Rotor rub
7. Journal bearings
8. Thrust bearings
9. Casing deformation
10. Whirling motion
    - **a.** Oil whirl
    - **b.** Friction induced whirl
    - **c.** Aerodynamic whirl

The spectrum of a vibration signal, which is composed of a time domain signal converted by the use of Fast Fourier Transform techniques to a frequency domain signal, is the basis of most analysis of vibration signals. This signal correctly depicts the frequency content of each time-domain instant; however, the time-domain picture as well as its frequency-domain counterpart is a continuous signal changing with time. Averaging concepts are used to show which amplitudes predominate in a continuous signal. For the most part, machinery vibrations result in stationary signals. A stationary signal has statistical properties that do not change with time. In other words, the average of a set of time-history records is the same regardless of when that average is

taken. A stationary signal is demonstrated by a machine running at constant speed and load. Averages are also used in diagnosing start-ups and load changes of machinery. In this usage averages of successive time intervals show the change in vibration levels and frequencies taking place.

To be able to do effective troubleshooting on any particular gas turbine, it is necessary that the baseline signature of the machine be available and thoroughly analyzed. A baseline signature is the spectrum of machine vibration when the machine is operating under normal conditions. Generally, normal conditions are difficult to define and are judgmental in nature. When a machine is first installed, or after it has undergone an overhaul, a vibration spectrum should be taken and stored to serve as a baseline for evaluating future spectra. When a baseline signature is determined, it should be carefully evaluated, and every component should be identified as far as possible.

Table 21-14 indicates the various rotor bearing system characteristics that generate various types of vibrations in a gas turbine. The table studies the effect that the entire rotor bearing system, which includes the rotor, bearings, seals, gears, couplings, casing, and foundation, has on the operation of the gas turbine. It examines the various vibration signals that describe the rotor dynamics of this system.

Bearing Maintenance

With high-speed machines, simple bearing failures are rare unless they are caused by faulty alignment, distortion, wrong clearance, or dirt. More common are failures caused by vibrations and rotor whirls. Some of these originate in the bearings, others can be amplified or attenuated by the bearings, the bearing cases, and the bearing support structure.

During inspection, all journal bearings should be closely inspected. If the machine has not suffered from excessive vibrations or lubrication problems, the bearings can be reinstalled and utilized.

Four places should be checked for wear during inspection periods:

1. Babbitted shoe surface
2. Pivoting shoe surface and seat in retaining ring
3. Seal ring bore or end plates
4. The shoe thickness at the pivot point or across ball *and* socket; all shoes should be within 0.0005% of the same thickness

While being inspected, the following checks should be made:

1. All leading edges of shoes must have a uniform radius for the full length across the shoe. File the radii if necessary to obtain proper size.
2. Light scratches in the babbitt face do not necessarily require shoe replacement. If no wear is detected, scrape lightly with a sharp straight-edged scraper (plate type) to remove any upsetting caused by scratches.
3. Shoes should be replaced as sets only if:
   a. Radial clearance has increased more than one mil over nominal design clearance.
   b. Leading or lagging edges of shoes show signs of wear.

Table 21-14 Rotor Bearing System Characteristics for a Gas Turbine

Cause of Vibration	Direction of Force			Location of Force					Predominant Frequencies Indicated									Comments
	Vertical	Horizontal	Axial	Shaft	Brgs.	Casing	Foundation	Coupling	0–40%	40–50%	50–100%	1×R. F.	2×R. F.	Higher Multiples	1/2 R. F.	1/4 R. F.	Lower Multiples	Odd Frequency	Very High Frequency	
Initial unbalance	40	50	10	90	10							90	5	5						High-speed rotors often require field-balancing (trim balancing) at full speed to make adjustments for rotor deflection and final bearing stiffness and damping conditions. Trim balancing is done at gas turbine balance planes in the forward and aft sections of the gas turbine.
Rotor bow	40	50	10	90	10							90	5	5						Bowed rotors can sometimes be straightened by "hot spot" procedure, but this should be regarded only as a temporary solution because bow will come back in time, and several rotor failures have resulted from this practice. If blades, vanes, or disks are lost or cracked, check for corrosion fatigue, stress-corrosion, resonance, and off-design operation. Straighten the bow slowly, by running on turning gear or at low speed. If rubbing occurs, trip unit immediately and keep rotor turning 90° by shaft-wrench every 5 minutes until rub clears. Then resume slow run. This may take 24 hours.
Casing distortion	40	50	10	90	10					10		80	5	5						Casing distortion is often caused by thermal shock. Compressor section casing deforms near the bleed ports causing rubs with the blades. Usually requires rework of the inner case.
Foundation distortion	40	50	10	40	30	10		10		20		50	20					10		Usually caused by poor mat under the foundation, or thermal stress (hot spots), or unequal shrinkage. Usually requires extensive and costly repairs.

(*Continued*)

Table 21-14 Rotor Bearing System Characteristics for a Gas Turbine (*continued*)

Cause of Vibration	Direction of Force			Location of Force					Predominant Frequencies Indicated											Comments
	Vertical	Horizontal	Axial	Shaft	Brgs.	Casing	Foundation	Coupling	0–40%	40–50%	50–100%	1×R. F.	2×R. F.	Higher Multiples	1/2 R. F.	1/4 R. F.	Lower Multiples	Odd Frequency	Very High Frequency	
Seal rub	30	40	30	80	10	10			10	10	10	20	10	10			10	10	10	Slight rubs may clear, but trip unit immediately if a high-speed rub gets worse. Turn by hand until clear.
Rotor rub axial	30	40	30	70	10	20				20		30	10	10			10	10	10	Unless thrust bearing has failed this is caused by rapid changes of load and temperature. Machine should be opened and inspected.
Misalignment	20	30	50	80	10	10						40	50	10						Usually caused by excessive pipe strain and/or inadequate mounting and foundation, but sometimes also by local heat from pipes or sun on base and foundation.
Journal & bearing eccentricity	40	50	10	90	10							80	20							Bearing may get distorted from heat especially near the turbine section. Some gas turbines have three bearings and the bearing in the vicinity of combustor section runs at elevated temperatures. Make hub-check, if possible, check contact.
Journal bearing damage	30	40	30	70	20	10				20		40	20						20	Watch for brown discoloration which often precedes recurring failure. This indicates very high local oil-film temperatures. Check rotor for vibration. Check bearing design and hot clearances.
Bearing & support excited vibration (oil whirl, etc.)	40	50	10	50	20	20	20		10	70					10	10				Replace with tilting-pad bearings if possible, if not machine internal bearing creating a dammed groove. Check clearances and roundness of journal, as well as contact and tight bearing fit in case.

Unequal bearing stiffness horizontal-vertical	40	50	10	40	30	30						80	20				Can excite resonances and criticals and combinations thereof at twice the running frequency. Usually difficult to field-balance because as horizontal vibration gets better, vertical gets worse and vice versa. It may be necessary to increase horizontal bearing support stiffness (or mass) if the problem is severe.
Thrust bearing damage	20	30	50	60	20	20				90						10	This is a result of increased clearances resulting in the imbalance of the thrust forces. Can also be the result of compressor surge.
Loose rotor (shrink fits)	40	50	10	60	20	20		40	40	10					10		Disks and sleeves may have lost their interference fit on the shaft by rapid temperature change. The disks have higher temperatures, thus grow at a faster rate than the shaft and therefore get loose and walk on the shaft. Parts usually are not loose at standstill. It is not recommended that shrink fits be used where the disk is transmitting over 5,000 HP, and the velocity is over 1,000 ft/sec.
Loose rotor bearing liner	40	50	10	80	10	10			90						10		Often confused with oil whirl because characteristics are essentially the same. Before suspecting any whirl make sure everything in bearing assembly is absolutely tight with interference fit.
Loose bearing case	40	50	10	70	20	10			90						10		This is rare, but should always be checked as a matter of routine.
Loose casing & support	40	50	10	50	20	30			50						50		Check that feet are properly anchored. Soft feet (improper shimming) can lead to major problems. Check that there are no gas leakages occurring on one side increasing the temperature of one foot.

(*Continued*)

Table 21-14 Rotor Bearing System Characteristics for a Gas Turbine (*continued*)

Cause of Vibration	Direction of Force			Location of Force				Predominant Frequencies Indicated									Comments
	Vertical	Horizontal	Axial	Shaft	Brgs.	Casing	Foundation	Coupling	0–40%	40–50%	50–100%	1×R. F.	2×R. F.	Higher Multiples	1/2 R. F.	1/4 R. F.	Lower Multiples	Odd Frequency	Very High Frequency	
Gear inaccuracy	30	50	20	80	10	10								20				20	60	Gear passing frequency (R.F. × number of teeth) would be predominant. Accelerometers should be used to measure gear-related problems.
Coupling inaccuracy & Damage	30	40	30	70	20			10	10	20	10	20	30	10						Couplings are cantilevered and thus loose coupling sleeves can cause major problems. This is especially true if the spacer is long and heavy. Use hollow spacers and make sure hubs are tightly bolted. In gear couplings check tooth fit by placing indicators on top, then lift with hand or jack and note looseness. This should not be more than 1–2 mils. at rest.
Rotor & bearing system critical	40	50	10	70	30							100								Change the bearing dampness by turning the bearing if it is a tilting pad bearing. Field balancing; use of more viscous oil, longer bearings with minimum clearance and tight fit; stiffening bearing supports and other structures between bearing and ground are some of the ways to solve this problem. Adding mass at the bearing case helps considerably, especially at speeds exceeding 8,000 rpm. This is a problem that is difficult to correct in the field, it is basically a design problem.
Critical speed	40	50	10	60	40							100								Most gas turbines have flexible shafts and thus operate over the first critical. Operational speed of the gas turbine must be at least 10–15% away from any criticals. Basically this is a design problem, often aggravated by poor balancing and poor foundation. To reduce the problem field balance rotor at operating speed, lower oil temperature, and use larger and tighter bearings to increase the damping effect and move the critical speed.

Resonant vibration	40	40	20	20	10	20	30					100						Add mass or change stiffness to change frequency. Add damping. Reduce excitation. Improve system isolation. Reducing mass or stiffness can leave the amplitude the same even if resonant frequency shifts. Check mobility.
Coulomb or dry friction whirl (rotor - bearing system)	40	50	10	80	20				80	10	10							A rub between the bearing and the rotor. This can be a very serious problem. To alleviate this problem use tilting pad bearings, larger bearings, and better foundation. If the problem is intermittent look into temperature variations.
Coulomb or dry friction whirl (rotor-blade-casing system)	30	40	30	40	20	20	10	10									100	This can be a very serious problem with the rotor blades contacting the casing. The blade tip velocities are about 1,200–1,500 ft/sec and thus the outcome can lead to major failures, especially of the trailing edge of the blades. There can be possibilities of an axial movement.
Oil whirl	40	50	10	80	20					80			10	5	5			Change to tilting-pad bearings if possible. Add pressure dams to simple journal bearings if replacement to tilting pad type bearings is not possible. Stiffen foundation or bearing structure, add mass at bearing, increase critical speed.
Resonant whirl	40	50	10	20	20	20	20			100								Similar to oil whirl, but with additional resonance of rotor, stator, and foundation. Tilting pad bearings are the answer to most of these whirl-type motions. Isolate the resonant members and sources of excitation.

(*Continued*)

Table 21-14 Rotor Bearing System Characteristics for a Gas Turbine (*continued*)

Cause of Vibration	Direction of Force			Location of Force					Predominant Frequencies Indicated									Comments
	Vertical	Horizontal	Axial	Shaft	Brgs.	Casing	Foundation	Coupling	0–40%	40–50%	50–100%	1×R. F.	2×R. F.	Higher Multiples	1/2 R. F.	1/4 R. F.	Lower Multiples	Odd Frequency	Very High Frequency	
Aerodynamic cross coupling whirl	40	50	10	70	10	10		10	10	80	10									Due to casing out of roundness. Frequencies are often below running frequency. Can create some very strong forces on the blades and the bearings. The critical speed acts as a catalyst to initiate the whirling motion.
Blade resonant frequency	Tangential																		100	Excitation of the blade resonant frequency occurs due to the various aerodynamic forces on the blades. These frequencies are very high and do not change with the speed of the gas turbine. Once the resonant frequency is excited failure of that blade occurs in a few hours.
Surge characteristics of the gas turbine compressor	Tangential		60											80					20	As the compressor proceeds to surge it is usually preceded with a tip stall. Surge also reverses the thrust forces on the turbine rotor shaft and can damage the thrust bearing.
Combustor pulsations	Affect the combustor liner and the transition piece			Dynamic pressure pulsations in the combustor													100			Combustion pulsations are common in DLE combustors. The combustors are finely tuned so that all the combustor cans are synchronized. Often at high loads the vibration amplitude increases to an unacceptable level and the power of the unit has to be reduced. Failure to do so will crack the combustor liner and the seals between the transition piece and the first-stage nozzles.

4. The tilting-pad and support-ball combination spare parts should be lapped together, making them an integral unit. When a new or used bearing is disassembled for cleaning and inspection, care should be taken not to mix the tilting-pad and support-ball combinations.
5. On reassembly, care should be taken to return the tilting-pad and support-ball combination to the original location in the support ring. Changes in clearance and concentricity can result if the tilting-pad and support-ball combination is not returned to the same location. An eccentricity of as little as one mil can cause severe vibration problems.

Clearance Checks

1. Check housing OD and ID to be sure it is round.
2. Check bore and face-end plates for nicked edges, deep scratches, or scoring. Stone or scrape if necessary, and polish with very fine aluminum oxide polishing paper.
3. Check parting-line surfaces for full contact. Stone or lap if burrs or raised edges exist.
4. Check pivoting surfaces of shoe and housing ring for scratches, scoring, or erosion. Stone if necessary.
5. For tilting-pad bearings, blue-shoe the pivot surface, and check for contact area and position. The contacting surface must be in the center only and at the bottom portion of the pivot bore in the retainer.
6. Check to be sure that pins do not bottom-out in pads.
7. For ball-and-socket designs, check to be sure the ball seats properly and solidly in the counter bore.
8. Check for shaft clearance as follows:
   a. Select a stub mandrel in which the minimum diameter is the journal diameter plus minimum desired clearance (about one mil per inch of shaft diameter) and the larger diameter is journal diameter plus desired clearance (about two mils per inch of shaft diameter).
   b. Assemble the bearing halves.
   c. Slip the assembled bearing over the smaller diameter of the mandrel.
   d. Tap the bearing lightly on the back of the housing and slide the bearing down on the next larger diameter.
   e. The mandrel should be rotated and the OD of housing indicated.

Thrust-Bearing Failure

A thrust-bearing failure is one of the worst things that can happen to a machine, since it often wrecks the machine, sometimes completely. To evaluate the reliability of a thrust-bearing arrangement, we must first consider how a failure is initiated and evaluate the merits of the various designs.

Failure Initiation

Failures caused by bearing overload during normal operation (design error) are rare today, but still far more thrust failures occur than one would expect, considering all the precautions taken by the bearing designer. The causes in the following list are roughly in sequence of importance:

1. *Fluid slugging.* Passing a slug of fluid through a turbine or compressor can increase the thrust to many times its normal level – even if only a few gallons are involved. Instantaneous failures of the downstream bearing may result from fluid slugging.

2. *Build-up of solids in rotor and/or stator passages ("plugging" of turbine buckets).* This problem should be noticed from performance or pressure distribution in the machine (first-stage pressure) long before the failure occurs.
3. *Off-design operation.* Especially from backpressure (vacuum), inlet pressure, extraction pressure, and moisture. Many failures are caused by overload, and off-design speed.
4. *Compressor surging.* Especially in double-flow machines.
5. *Gear coupling thrust.* A frequent cause of failure, especially of upstream thrust bearings. Thrust is high when alignment is perfect (friction coefficient 0.4–0.6), decreasing to a minimum when a small misalignment is present (about 0.1 at 25 ° angular misalignment). Friction increases rapidly again to 0.5 or more with an increase in misalignment (these are rough numbers only, to show basic relationships). The thrust is caused by friction in the loaded teeth that opposes thermal expansion. Therefore, thrust can get very high, since it has no relation to the normal thrust caused by pressure distribution inside the machine (for which the thrust bearing may have been dimensioned). The coupling thrust may act either way, adding to or subtracting from normal thrust. Much depends on tooth geometry and coupling quality. A straight-sided tooth can take misalignment only when the tooth fit has enough clearance to permit slanting of the male tooth inside the female teeth. For example, with vertical misalignment, the teeth on both sides will bind when the clearance is insufficient to allow for slanting. This can cause very high thrust, sometimes one can hear a "metallic sound" building up until the rotors finally slip with a very noticeable "bump." Then the noise and vibration are gone, at least for a while. This phenomenon, of course, is torture for the thrust bearings, and it may cause failure in either direction. Dirt in the coupling can aggravate this situation or even cause it.
6. *Dirt in oil.* A common cause of failures, especially when combined with other factors. The oil film at the end of the oil wedge is only a small fraction of a thousandth thick. If dirt goes through, it can cause the film to rupture, and the bearing may burn out. Therefore, very fine filtering of the oil is required. But the best filter is no good if maintenance personnel leave the filter or bearing case open after inspection, and the rain and sand blow in, or if they put the wet filter elements on the sandy floor, or accidentally knock holes in the elements. It happens far too often. Once a machine is wrecked, it is difficult to reconstruct.
7. *Momentary loss of oil pressure.* Sometimes encountered while switching filters or coolers.

Failure Protection

Fortunately, accurate and reliable instrumentation is now available to monitor thrust bearings well enough to assure safe continuous operation and to prevent catastrophic failure in the event of an upset to the system.

Temperature sensors, such as RTDs (Resistance Temperature Detectors), thermocouples, and thermistors, can be installed directly in the thrust bearing to measure metal temperature. The installation shown in Figure 21-20 has the RTD embedded in the babbitted surface. It is in the most sensitive zone of the shoe – 70% from the leading edge and 50% radially. The position of the sensor is critical in establishing the safe operating limits. As long as the probe is generally in the zone of maximum temperature, it will be highly sensitive to load, although the level of temperature may vary considerably as can be seen in Figure 21-21. The temperature is also dependent on the pad-backing material. At 500 psi load, the center sensor at A-II registers 200 °F while the sensor at B-I registers 280 °F in a steel-backed bearing. Again, these temperatures are typical and will vary with size, type, speed, and lubrication from bearing

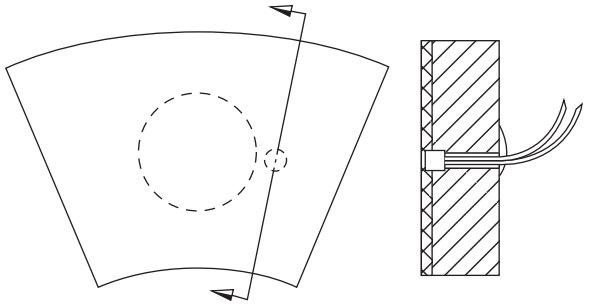
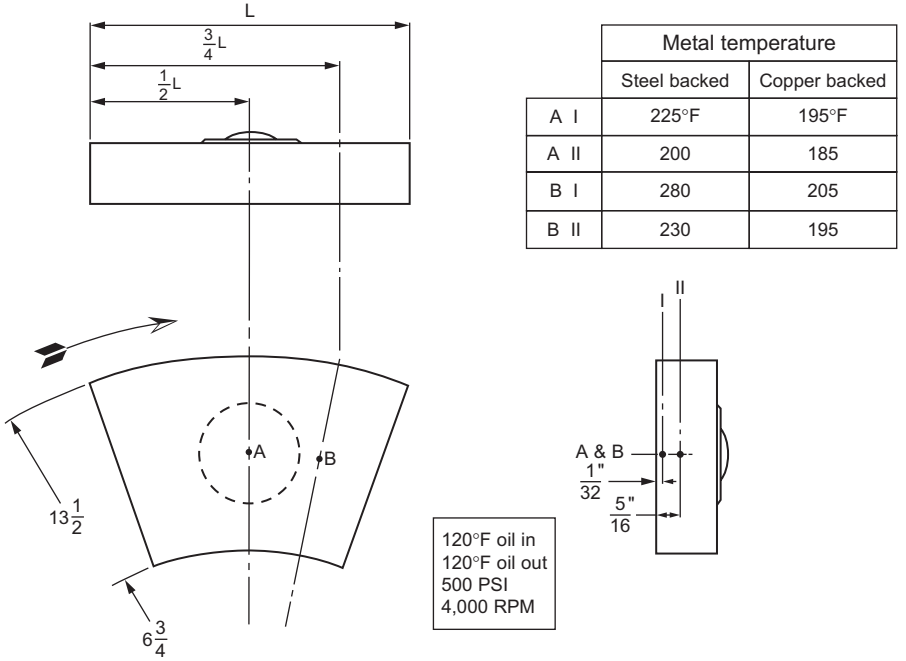


Figure 21-20 RTD embedded in bearing surface.



	Metal temperature	
	Steel backed	Copper backed
A I	225°F	195°F
A II	200	185
B I	280	205
B II	230	195

Figure 21-21 Temperature distribution in bearing surfaces.

to bearing. The difference in a copper-backed bearing can be seen to be quite significant, with A-II reading 185 °F and B-I reading 205 °F. The position of the sensor with respect to the surface is less significant in this bearing than in the steel-backed bearing. Again, position in the sensitive zone is important in establishing safe operating limits with respect to temperature.

Axial proximity probes are another means of monitoring rotor position and the integrity of the thrust bearing. A typical installation is shown in Figure 21-22. In this case two positions are being monitored: one at the thrust runner, and one at the end of the shaft near the centerline. This method detects thrust-collar runout and also rotor

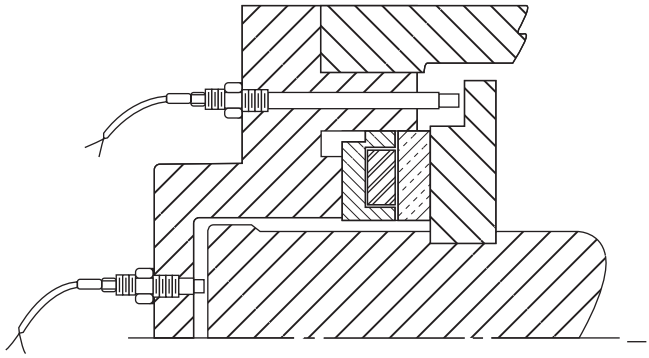


Figure 21-22 Actual probes for thrust-bearing monitoring.

movement. In most cases this ideal positioning of the probes is not possible. Often the probes are indexed to the rotor or other convenient locations and thus do not truly show the movement of the rotor with respect to the thrust bearing.

A critical installation should have the metal temperature sensors in the thrust pad. Axial proximity probes may be used as a backup system. If metal temperatures are high and the rate of change of those temperatures begins to alter rapidly, thrust-bearing failure should be anticipated.

Coupling Maintenance

The major inspections should also include detailed inspections of any couplings in the train. Gear couplings should be disassembled and teeth inspected for indications of problems. The most common failures encountered with continuous lubrication-type gear couplings are:

1. Wear
2. Corrosive wear
3. Coupling contamination
4. Scoring and welding

Couplings with sealed lubrication systems tend to have wear problems similar to couplings with continuous lubrication, but they must also be checked for fretting corrosion and cold flow. These problems result from normal coupling operation. If for some reason excessive misalignment exists, additional damage can be revealed by tooth breakage, scoring, and pitting.

Disc couplings should be checked to ensure there are no cracks in the discs or connecting shaft. If damage does not exist, the coupling should be rebalanced prior to installation.

Repair and Rehabilitation of Turbomachinery Foundations

In many instances, vibration problems in turbomachinery can be attributed to faulty support. Once the problem areas have been identified, correcting defects can be a

logical procedure. What is novel is that this result can often be accomplished through the proper selection and application of adhesives.

Most turbomachinery is mounted on structural steel platforms sometimes referred to as base plates or skids. These platforms are then installed on a mass of concrete at the jobsite (either by direct grouting or mounting on sole plates) to become the machinery foundation. Platforms should always be considered as part of the foundation rather than as part of the machinery.

Problems with platforms fall into one or both of the following categories:

1. Improper installation
2. Insufficient mass and/or rigidity

Improper installation is not a design weakness. This defect can be corrected rather easily in the field at any time after installation. Insufficient mass or rigidity is a design weakness brought about by the complexity of the origin of vibration in high-speed rotating machinery and its sensitivity of vibration. Nevertheless, mass and rigidity can be increased in the field, but it is more of a task to do so than the mere correcting of installation defects.

Installation Defects

A typical compressor train containing a turbine and two compressor stages are shown in Figure 21-23. The I-beams on the platform are grouted to the concrete structure. When proper grouting techniques are carried out during the original installation, the grout should contact the entire lower surfaces of all longitudinal and transverse I-beams.

Cement-based grouts will not bond well to the platform load-bearing surfaces. Over a period of time, lubricating oils will severely degrade both cement groups and concrete. This problem is further aggravated because most platforms are not designed with oil drains. On several occasions, as much as 6–8 inches of oil has been found trapped within the platform cavities. This condition not only provides head-pressure for an increased rate of oil penetration, but also creates a severe fire hazard.

All platforms, regardless of the type of grout to be used, should be designed with oil drains. Epoxy grouts are recommended on platform installations because they provide

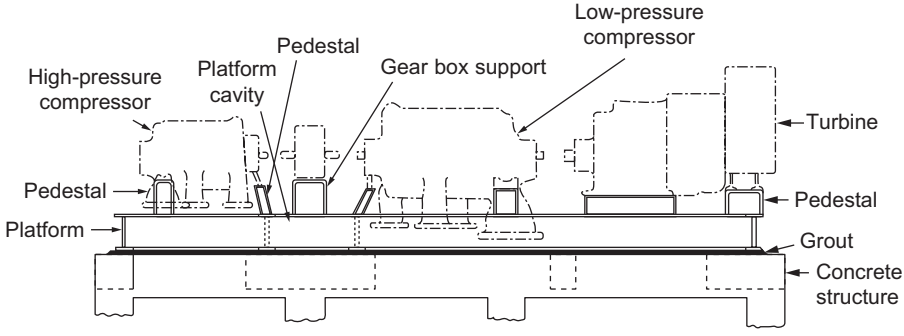


Figure 21-23 Typical compressor train containing a turbine and two compressor stages.

an excellent oil barrier for the concrete below. Cement grouts should only be used for temporary installations.

When differences in vibration amplitudes can be detected between the lower flange of the platform beams and the concrete structure, the decision to bond the entire lower surfaces of the platform to the concrete structure should be made. Bonding can be accomplished using a technique known as pressure-grouting. With this technique, holes are drilled through the lower flange at locations near the web on centers of approximately 18 inches. These holes are then tapped, and ordinary grease fittings are installed. Pressure-grouting can then be carried out with either automatic injection equipment or with conventional grease guns.

Some manufacturers recommend that their platforms be installed on rails or sole plates, which have been grouted to the concrete foundation. Occasionally, the installation will be either poorly designed or the contractor will fail to clean the plates before grouting. Loss of adhesion may result in excessive vibration or movement of the plate in the grout. When this problem occurs, pressure-grouting can be accomplished with a relatively high degree of success if proper techniques are used. The following are some main points to consider when designing and grouting a sole plate:

1. Check to see that the block between the equipment base and the sole plate is adequate to transmit the load.
2. Corners on the edges of the sole plate should have at least a two-inch radius to prevent the creation of stress risers and subsequent cracking of the corners.
3. There should be a sufficient amount of aggregate in the epoxy mixture. Insufficient quantities of aggregate will lead to a layer of unfilled epoxy on the surface of the mortar. The linear coefficient of thermal expansion of the unfilled epoxy can be expected to be in the order of magnitude of 6–8 $\times$ 10^{-5} inches per inch of thickness per °F. The linear coefficient of thermal expansion for the epoxy mortar below can be expected to be in the order of magnitude of 2 $\times$ 10^{-5} inches per inch of thickness per °F. This difference in thermal expansion rates will encourage crack propagation, particularly on cooling when the system is subjected to cyclic temperatures such as between day and night.
4. Make sure that a foamy surface does not exist immediately below the sole plate. A foamy surface is caused by an insufficient quantity of aggregate in preparing the epoxy mortar. The epoxy adhesive has a density of about nine pounds per gallon. The aggregate has a bulk density of about 14 pounds per gallon, which assumes about 25–30% voids. In preparing an epoxy mortar, the resin and hardener components are always mixed together before the addition of aggregate. When the aggregate is added to the mix, it obviously falls to the bottom and introduces air into the mix. If a soupy mortar is prepared, the air will simply rise to create a weak, foamy surface.

Increasing Mass and Rigidity

When excessive vibration is detected in the gear box of a compressor train (Figure 21-14) and is transferred to the platform below, a dampening effect can be created by increasing the rigidity of the support below. This effect can be accomplished by first filling the platform cavity and then the gear-box support with epoxy mortar.

In the case where the turbine and supports have a minimal cross section, the ability to increase the stiffness of these pedestals is minimized. Consequently, the objective is

to concentrate on increasing the mass of the pedestals. This increase is accomplished by filling the cavities with a special mortar prepared with epoxy and steel shot. The density of this special mortar can be in excess of 300 pounds per cubic foot. To inject this special mortar, a pipe has been installed in the access hole that was drilled in the side of the pedestal near the top. These same techniques can be employed to stabilize the foundations under much smaller equipment.

Bibliography

Boyce, M.P., "Managing Power Plant Life Cycle Costs," International Power Generation, pp. 21–23, July 1999.

Herbage, B.S., "High Efficiency Film Thrust Bearings for Turbomachinery," Proceedings of the 6th Turbomachinery Symposium, Texas A&M University, pp. 33–38, 1977.

Meher-Homji C.B., and Gabriles G.A., "Gas Turbine Blade Failures—Causes, Avoidance, and Troubleshooting," Proceedings of the 27th Turbomachinery Symposium, Texas A&M University, p. 129, 1998.

Nakajima, S., "Total Productive Maintenance," Productivity Press, Inc 1988.

Nelson, E., "Maintenance Techniques for Turbomachinery," Proceedings of the 2nd Turbomachinery Symposium, Texas A&M University, 1973.

Renfro, E.M., "Repair and Rehabilitation of Turbomachinery Foundation," Proceedings of the 6th Turbomachinery Symposium, Texas A&M University, pp. 107–112, 1977.

Sohre, J., "Operating Problems with High-Speed Turbomachinery—Causes and Correction," 23rd Annual Petroleum Mechanical Engineering Conference, September 1968.

Sohre, J., "Reliability Evaluation for Trouble-Shooting of High-Speed Turbo-machinery," ASME Petroleum Mechanical Engineering Conference, Denver, Colorado.

VanDrunen, G., and Liburdi, J., "Rejuvenation of Used Turbine Blades by Host Isostatic Processing," Proceedings of the 6th Turbomachinery Symposium, Texas A&M University, pp. 55–60, 1977.

Copyrighted Materials
Copyright © 2012 Elsevier Retrieved from www.knovel.com

22 Case Histories

There are many types of failures associated with a gas turbine, since these units are very complex in their overall makeup. Gas turbines are used in many different applications, from driving compressors and pumps, in process plants and offshore platforms, to generating power as peaking units, and as part of large combined-cycle power plants. The gas turbines in the process and offshore platforms are usually below 30 MW and are operated 24 hours a day, 365 days of the year. The peaking units operate about 1,300–1,500 hours a year and about 5–12 hours a day. Combined-cycle power plants were originally designed to operate as base-loaded units; however, in 2005 most of these units operated five days a week and during the day the plants were cycled from about 40% to 100% power load. Most operators and OEMs work on an equivalent hour basis, which takes into account the number of starts and the percentage load and time at which they are operated. The gas turbine failures range from control system problems, which are the most frequent although the downtime accompanying these failures usually is the smallest, averaging a few hours; the problems with combustors, rotors, and blade failures are less frequent; however, the downtime and costs accompanying those failures could extend to several weeks and several million dollars in costs. The hot section failures far outnumber the problems in the compressor due to the high temperatures associated with the hot section; however, a blade failure in the compressor can cause extensive downstream failures.

This chapter deals with the failures and problems that have been encountered in the various components of gas turbines. This chapter has been written not as a criticism of any manufacturer but as a guide to the end user of these gas turbines on what they should be looking for to ensure that they would not suffer the same problems. The last 20 years have seen a large growth in gas turbine technology. The growth is spearheaded by the increase in compressor pressure ratio, advanced combustion techniques, the growth of materials technology, new coatings, and new cooling schemes. In other words, the technology envelope is being pushed, so that many of the components are operating in uncharted waters.

The aerospace engines have been the leaders in most of the technology in the gas turbine over the past half-century. The design criteria for these engines were high reliability and high performance, with many starts and flexible operation throughout the flight envelope. The engine life of about 3,500 hours between major overhauls was considered good. The performance of aerospace engine has always been rated primarily on its thrust-to-weight ratio. Increase in engine thrust-to-weight ratio is achieved by the development of high aspect ratio blades in the compressor as well as optimizing

Gas Turbine Engineering Handbook, Fourth Edition. DOI: 10.1016/B978-0-12-383842-1.00022-6
Copyright © 2012 Elsevier Inc. All rights reserved.

the pressure ratio and firing temperature of the turbine for maximum work output per unit flow.

The industrial gas turbine has always emphasized long life and this conservative approach has often resulted in the industrial gas turbine giving up high performance for rugged operation. The industrial gas turbine has been conservative in the pressure ratio and the firing temperatures. This has all changed in the last 10 years; spurred on by the introduction of the aero-derivative gas turbine, the industrial gas turbine has dramatically improved its performance in all operational aspects. This has resulted in dramatically reducing the performance gap between these two types of gas turbines.

Another area of concern is the Dry Low NO_x (DLN) combustors. The development of new DLN combustors has been a very critical component in reducing the NO_x output, as the gas turbine firing temperature is increased. The new low NO_x combustors increase the number of fuel nozzles and the complexity of the control algorithms. These combustors often experience problems with combustion instability and flashback problems, which lead to the destruction of the combustor, and consequently the failure of turbine nozzles and blades due to domestic object damage (DOD) from components that dislodge and move downstream.

The new gas turbines have seen a great increase in the technology in the following components over the past few years:

- The axial-flow compressor
- The combustors
- The materials used in the high-temperature region of the gas turbine
- The controls

Axial-Flow Compressors

Axial-flow compressors are the most common type of compressors in gas turbines of one MW or more. Most of these compressors are multistage units with the number of stages between seven and 22. Most axial-flow compressors have a set of inlet guide vanes that are located in front of the first-stage rotor blade. An axial-flow compressor stage consists of a set of rotating blades followed by a set of stationary diffusion blades. A set of stationary row of blades, which follow the last stage of a stationary diffusion set of blades, are known as the exhaust guide vanes. The pressure ratio of the axial-flow compressor varies from about 7:1 to as high as 40:1 and the problems faced by these units differ.

The axial-flow compressor in the advanced gas turbines is a multistage compressor (17–22 stages) with an exceedingly high pressure ratio. It is common to see pressure ratios in industrial gas turbines in the 17–20:1 range; some units have pressure ratios in the 30:1 range. The more stages and higher pressure ratios result in the smaller operational margin between the surge and choke regions of the compressor as shown in Figure 22-1.

Dirt in a gas turbine compressor section causes several problems such as reduction in the efficiency of compressor, distortion of the air flow leading to an early surge,

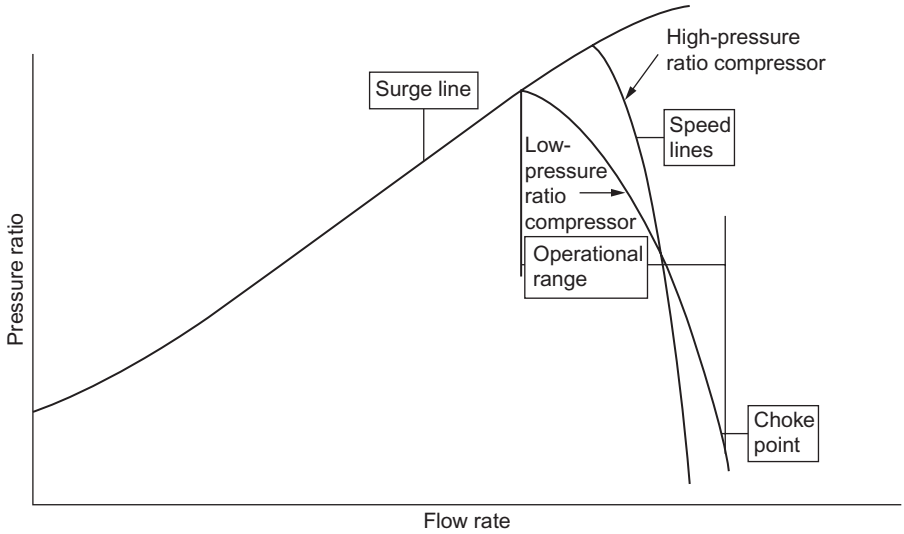


Figure 22-1 Compressor performance map.

erosion and corrosion of the blades, blockages of the cooling air passages, unbalance, and foreign object damage. To minimize these types of problems in the compressor section of a gas turbine, a high-efficiency filter should be used to reduce the deposits on the blades and to reduce blade erosion. The high-efficiency filters usually come in three stages. The first stage is an inertia filter, which usually is composed of vanes to remove large particles and water droplets. In areas where there is a high moisture content, a rain shield should be used in front of the vanes. The second stage usually is a prefilter; it is usually regarded as a medium-efficiency filter and usually is made from spun glass fibers. It is usually used to extend the life of the bag- or barrier-type high-efficiency filters by removing the smaller particles of dirt.

Compressor problems are minimized due to the less-hostile environment in which they operates as compared with the hot section of the turbine. It is common to see a very high rate of erosion at the blade tips of compressors operating in sandy regions with poor or no filtration as shown in Figure 22-2. The erosion of the blade tips leads to inefficiency and compressor surge.

Gas turbines often use evaporative cooling or water fogging techniques to cool the inlet and thus get more work out of the gas turbine (see the Power Augmentation section). Figure 22-3 shows the water nozzles at the inlet of the filter housing of the gas turbine.

Inlet air fogging systems operate at very high pressures, around 200 bars (3,000 psia). These nozzles are designed to create a very fine spray as shown in Figure 22-4 in which the size of droplet should be between 15 and 30 μm.

Evaporative cooling leads to erosion of the first few stages of the compressor blades as shown in Figure 22-5. In this figure, we can see the leading edge of the compressor blades where the coating is eroded. Evaporative cooling will cause some erosion

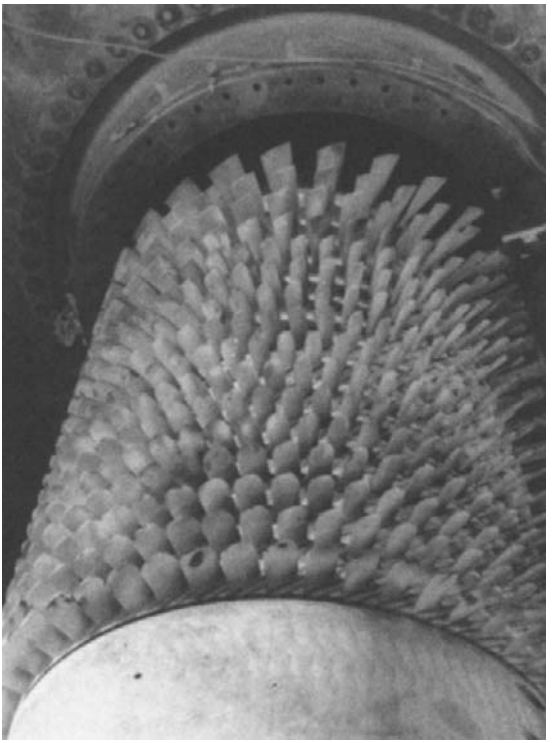


Figure 22-2 Compressor with high erosion at blade tips due to improper filtration system.



Figure 22-3 Water nozzles at the gas turbine inlet.



Figure 22-4 Inlet spray from evaporative cooling water nozzles.



Figure 22-5 Coating erosion found at the leading edge of the first stages of the compressor.

of the first stages of the compressor blades; however, in most cases (hot and low-humidity regions) where evaporative cooling is used, the benefit far outweighs the erosion damage to the blades.

The trends for the advanced axial-flow compressors are toward fewer, thinner, larger, three-dimensional, and controlled diffusion-shaped airfoils (3D/CDA), with smaller clearances and higher loading per stage. Some of these blades, because of

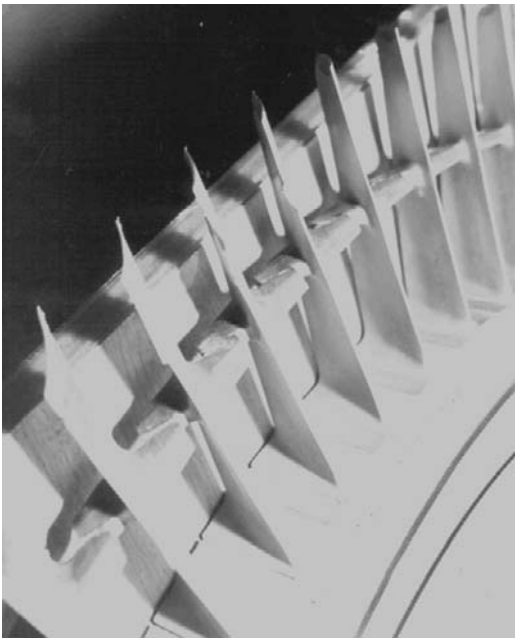


Figure 22-6 Mid-span shrouds on compressor blades.

their length, require mid-span shrouds as shown in Figure 22-6, to prevent the blades from exciting their resonance frequencies. The figure also shows some of the blades with foreign object damage.

The smaller clearances (20–50 mils) and high pressure ratios tend to increase the probability of encountering tip rubs. These tip rubs usually occur near the bleed flow sections, as shown in Figure 22-7, of the turbines where there are inner diameter changes, and the compressor casing could be out of round.

Heavy tip rubs in that section cause damage to the compressor blades, as shown in Figure 22-8, and cause a loss of the blade coating. These tip rubs can also cause the trailing edge to break and cause extensive damage downstream. Scratch marks can be seen on the rotor from the stator blades being in contact with the rotor, which could lead to the failure of the stator diffuser vanes.

The advanced compressor blades also usually have squealer sections on the blade tips, as shown in Figure 22-9, which are designed to wear in a safe manner if the blades are in contact with the casing; however, if the rubbing is severe, even with blade tip squealers, failures of the blades would occur as shown in Figure 22-10. These rubs, if severe, can lead to tip fractures and overall destruction of the downstream blades and diffuser vanes due to domestic object damage (DOD).

Figure 22-11 indicates typical blade failures in blades around the fourth to seventh stage of a typical axial-flow compressor in an advanced gas turbine. Note the number of blades downstream that have suffered from DOD.

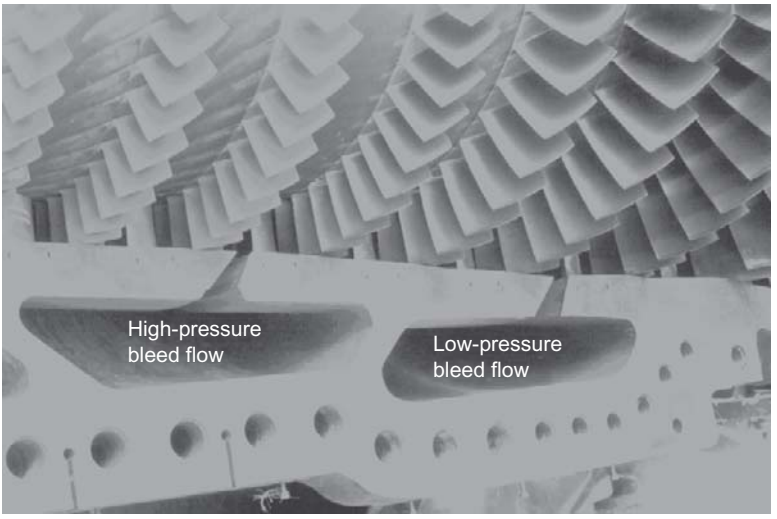


Figure 22-7 Axial-flow compressor showing bleed-flow ports.

The very high temperature at the exit of the compressor, which in some cases exceeds 1000 °F, causes a very hot compression section that also requires the cooling of the bleed flows before they can be used for cooling the turbine section. This also limits the downtime between start-ups of the turbines.

The high compressor exit temperatures leads in many cases to the use of external air coolers for the gas turbine cooling air. These coolers can be water–compressor air, fuel–compressor air, or ambient air–compressor air-based systems. Great care must be taken, so that the cooling air-cooler and the connecting pipes are clean, and do not have any residue from welding or adherent rust.

The cooling coils should be made of stainless steel to avoid corrosion and the connecting pipes also preferably should be made of stainless steel; if not, the inner side of the pipes should be coated to reduce the chances of adherent rust entering the cooling blade passages. The entrance of particulates from the cooling air system could lead to major damage to the turbine blades.

Blade flutter, rotating stall, and surge are the problems encountered in the compressor due to deposits of foreign matter on the blades, which results in air angles leaving the blade to be skewed and have a high incidence angle on the following set of blades, causing flow separation. Regular on-line water washing of the compressor followed by off-line water washes will usually restore the blade surface and thus create the original design angle. In some cases, blade flutter problems are initiated due to bleed-off valves; excessive bleed-off can result in a compressor surge in the latter stages. The amount of bleed-off that can be tolerated in most units is between 12% and 17%.

Monitoring the compressor for both performance and vibration is recommended for safe operation of the units. In the area of performance monitoring, pressure ratios and compressor efficiencies should be monitored. Vibration spectrums are an important

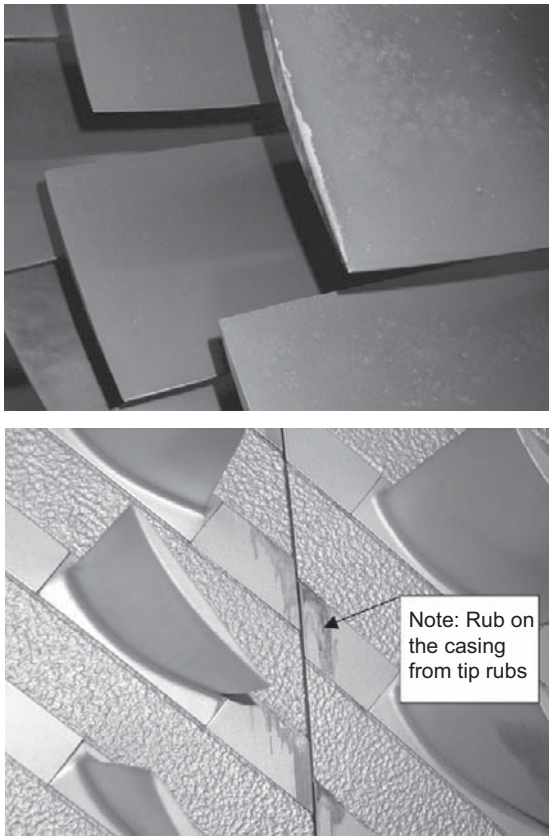


Figure 22-8 Compressor blade tips and compressor casing showing heavy rub.

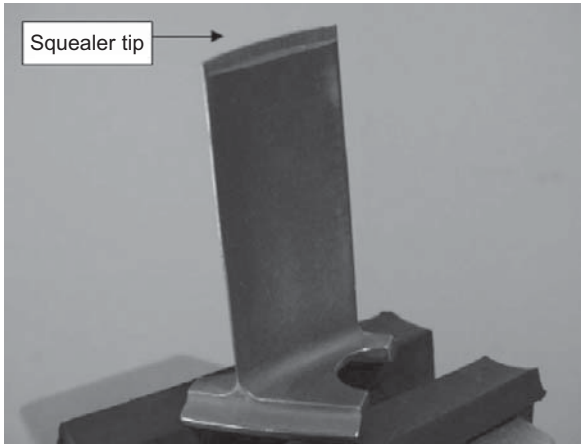


Figure 22-9 Compressor blade showing the blade tip squealer.

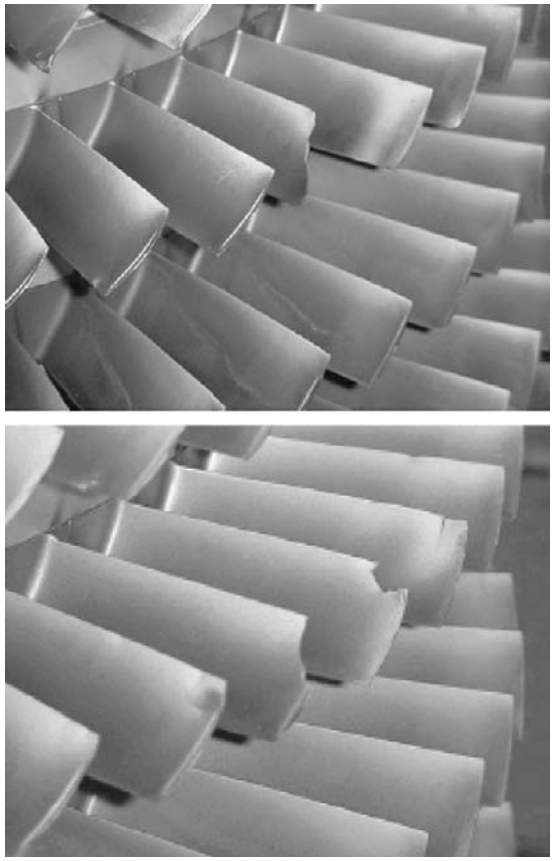


Figure 22-10 Blade failures due to excessive tip rubs.

tool in the monitoring of the compressor. Monitoring running speed frequencies with blade passing frequencies (rpm × number of blades) is highly recommended. This includes first- and second-order blade pass frequencies for many of the stages.

Figure 22-12 is a photograph of a failed first-stage compressor blade of an axial-flow compressor. Figure 22-13 shows a spectrum obtained during this period of time. In this case, the compressor operating speed was 6,937 rpm. Vibration spectra taken at the same time indicated a rise of an unknown frequency at 78,000 cpm (1,300 Hz) in the spectrum. Since this frequency was not identifiable to any known ratios, a concern was raised that it could be an individual blade resonance frequency. The frequency did not fluctuate with speed. This confirmed further the suspicion that this was a blade resonance frequency. In that same period of time it was also noted that the second-order blade passing frequencies (2 × blade passing frequency) kept increasing, which led us to believe that the axial-flow compressor was reaching a surge scenario. This phenomenon of the increase of the second-order blade passing frequencies has been noted in many axial-flow compressors (see Chapter 7). The unit surged and after the

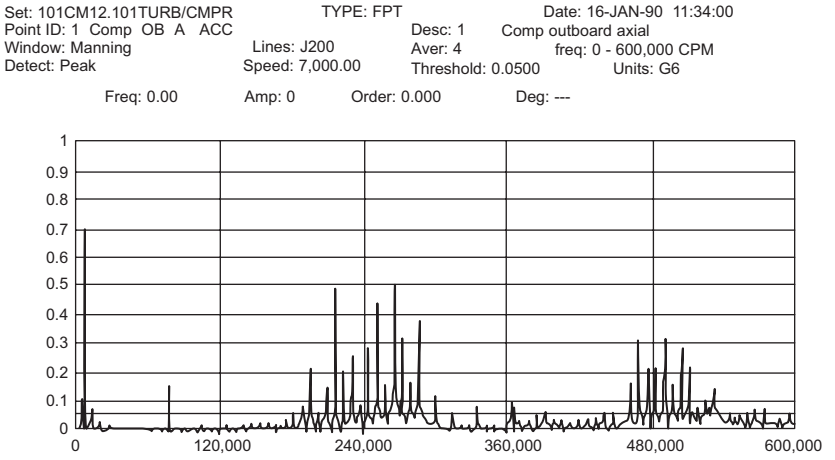


Figure 22-11 Compressor blade damage due to domestic object damage (DOD).



Figure 22-12 Failure of the first-stage compressor.

surge it was noted that there was a deterioration of the performance of the first section of the compressor, as shown in Figure 22-14. The compressor was never able to return to the pressure ratio before the surge. The pressure ratio in the forward stages was lower after the surge. Reviewing this data in conjunction with the spectra data, it was concluded that a significant flow disturbance was occurring in the front section of the compressor. This instability was exciting the blade's fundamental frequency. Therefore, it was concluded that during the surge event one or more blades in the first few stages of Section one were damaged. The compressor was operated, due to plant process considerations, till the blade resonance frequency reached 0.4 in/s and the second-order blade passing frequencies was half the magnitude of the first-order blade passing frequencies. On opening the unit, one of the first-stage blades was found to have failed at about two-thirds the height from the base, as shown in Figure 22-12.



IDENTIFICATION OF SPECTRAL PEAKS ABOVE THRESHOLD

No.	Amp.	Freq.	Order	No.	Amp.	Freq.	Order
1.	0.7018	6,937.5	0.991	9.	0.5049	266,250.0	30.036
2.	0.4532	217,125.0	31.018	10.	0.3324	266,625.0	38.089
3.	0.4801	217,500.0	31.071	11.	0.3169	273,187.5	39.027
4.	0.2561	231,187.5	33.027	12.	0.3786	287,250.0	41.036
5.	0.2832	245,250.0	35.036	13.	0.3027	469,312.5	67.045
6.	0.4373	252,187.0	36.027	14.	0.3224	490,687.5	70.090
7.	0.3636	252,562.0	36.080	15.	0.2846	504,760.0	72.107
8.	0.2345	265,500.0	37.929	16.	0.2245	511,607.5	73.098

Figure 22-13 Vibration spectra.

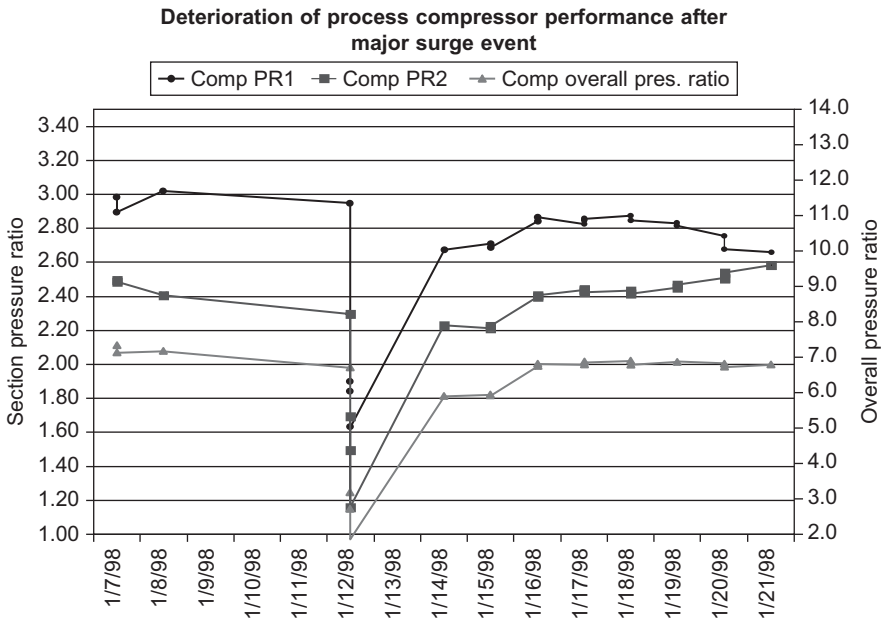


Figure 22-14 Deterioration of the axial-flow compressor.

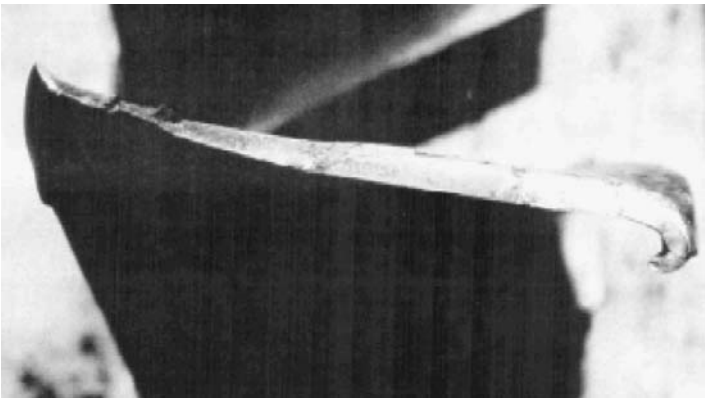


Figure 22-15 Cross section of the failed first-stage compressor blade.

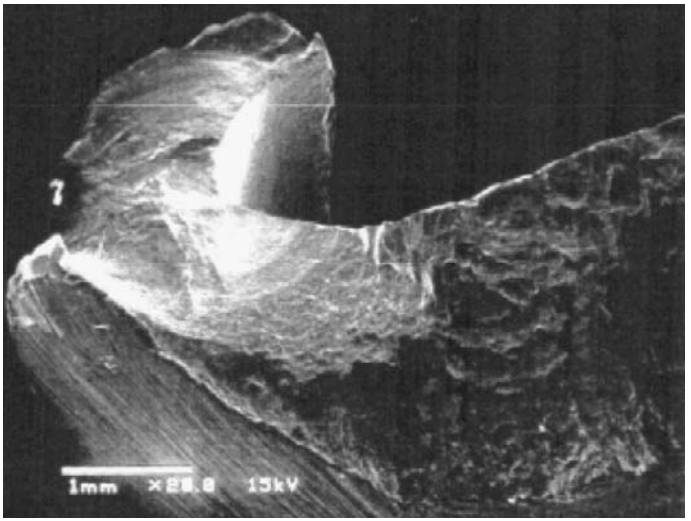


Figure 22-16 Electron microscope photograph of the first-stage failed blade.

Figure 22-15 is a photograph of the failure of the cross section of the first-stage rotor blade. The blade was deflected when initial contact with the inlet guide vanes occurred during the surge event. This contact deformed the first-stage blade to induce turbulent flow over the blade, resulting in a high cycle fatigue situation. This is amply illustrated in the spectrum as shown in Figure 22-13. Figure 22-16 is a photograph of the same blade as seen under an electron microscope. Note the chevron-type markings near the trailing edge of the blade indicating a high cycle fatigue failure at that point and then a subsequent tear and propagation of the crack.

Subsequent damage to the rotor blades from this point indicated that with time the stage blade began to fatigue and fracture. This failure of the first-stage blade inflicted the bulk of the damage downstream. A severe gouge was cut into the leading edge of



Figure 22-17 Damaged blades due to domestic object damage (DOD).

the downstream third-stage blade, as shown in Figure 22-17. This served as a stress riser and an initiation point for a fatigue crack and subsequent propagation. The failure of this blade was also a fatigue failure, although some of the features were masked due to the initial contact damage.

Combustion Systems

Combustor problems and case histories are divided into two major areas: diffusion flame combustors and premixed dry low NO_x combustors. Furthermore, in each of these categories, they are divided into annular and can-annular combustors.

The diffusion-type combustor is one in which the fuel is injected directly into the combustor, where it is burnt with about 8–10% air in the primary zone; the rest of the air is used for cooling purposes. The can-annular combustors are connected to each other through the cross-over tubes, as shown in Figure 22-18. Cross-over tubes are used in can-annular combustors to assure combustion in all chambers and to equalize pressure.

Many times the flow of hot gases through the cross-over tubes is increased due to blocked fuel nozzles, which can lead to cross-over tube failures as shown in Figure 22-19. A typical water injection fuel nozzle is shown in Figure 22-20. This type of fuel nozzle is used to decrease the NO_x emissions by injecting water or steam into the primary zone of the combustor.

This injection of steam reduces the temperature in the hot section, thus reducing the amount of NO_x produced. When sprayed through the fuel nozzle, this steam can impinge on the liner, thus creating a temperature gradient that can lead to cracks. Steam injection – whether it is required for NO_x, control, or for extra power (5% steam by weight will produce 12% more work and increase efficiency a few percentage) – must inject steam into the compressor diffuser to be safe and effective. This process will allow the steam to be fully mixed with the air before it enters the combustor, reducing the incidence of liner failures due to steam injection.

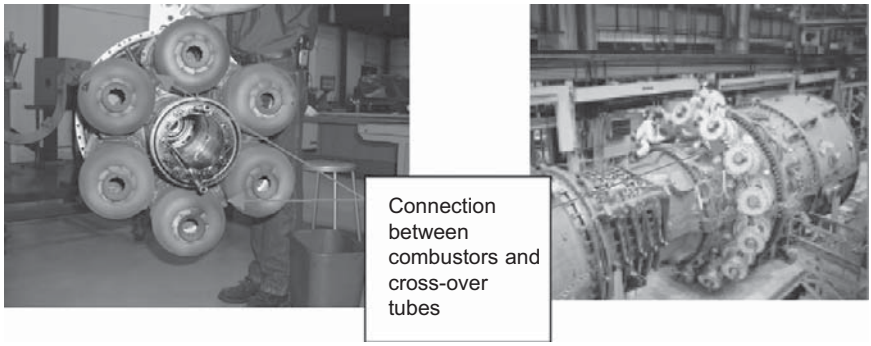


Figure 22-18 A typical can-annular combustion arrangement.

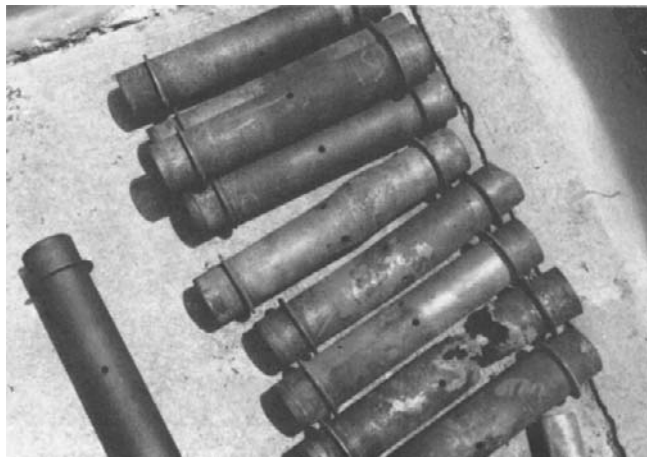


Figure 22-19 Damaged cross-over tubes.

Liner cracks can be caused by liquids in the fuel or blocked nozzles, which can create hot sections in the liner as shown in Figure 22-21. In many turbines, when the injection of steam or water in the combustor can been used to meet NO_x, emission requirements, impingement of the water, or steam on the combustor liner would tend to create cracks as shown in Figure 22-21.

Figure 22-22 shows the combustor liner with heavy carbonizing due to operation on crude oil. Some hot spots can also be seen near the primary zone region of the combustor. These cans do not have thermal barrier coating.

Figure 22-23 shows the same type of combustor with thermal barrier coating. It is greatly recommended that the combustors have thermal barrier coating. These coatings are necessary especially when used in the new high-temperature combustors.

Figure 22-24 shows the combustor liner plates used in an annular combustor. Several of the combustor liner plates had thermal barrier coating failure along the edges. The coating had failed in such a manner that the base metal appears to have

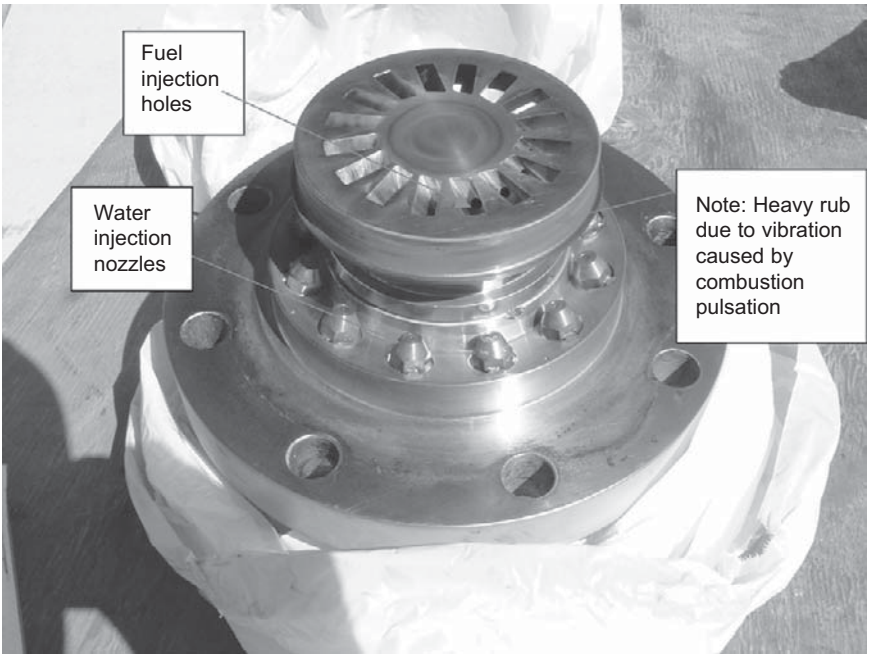


Figure 22-20 Fuel nozzle with water injection system.

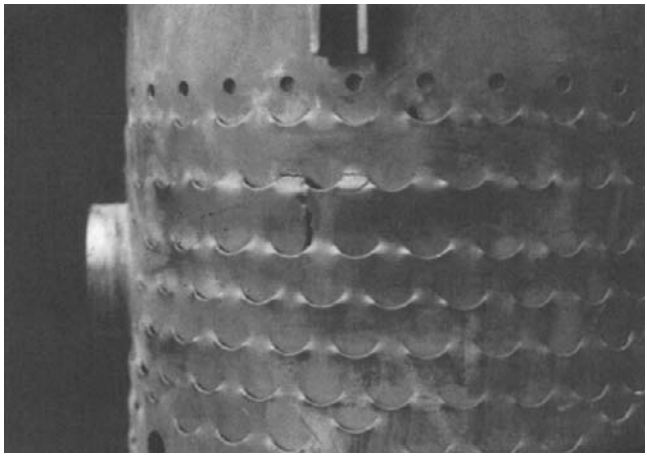


Figure 22-21 Cracks in a combustor liner.

been affected. This was caused by flashback problems, which cause a high frequency of combustor pulsations.

DLN combustors in their attempt to burn very lean are subject to problems in their combustion characteristics leading to flame destabilization and combustion pulsation.

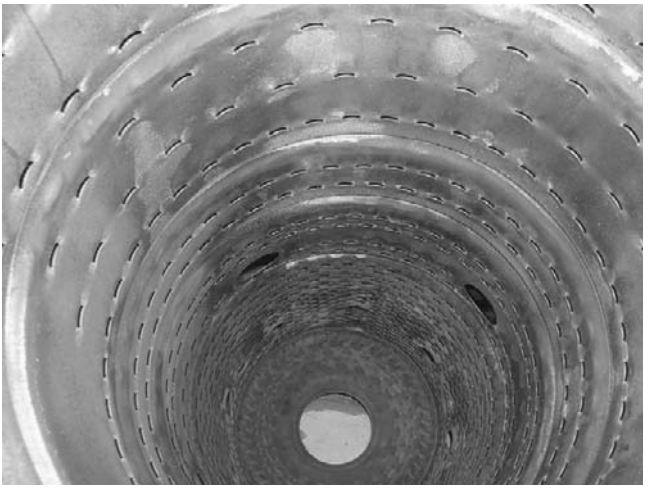


Figure 22-22 Can-annular combustor used in a crude oil application.

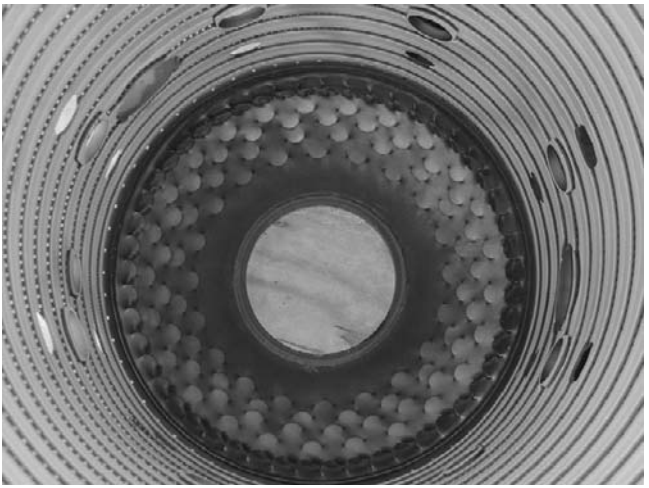


Figure 22-23 Can-annular combustor with TBC.

These problems lead to flashback problems in DLN combustors, usually under transient operation conditions when the flame moves backward and then attaches itself in the recirculation zone and not in the primary combustion zone. The recirculation zone is not designed to withstand the very high temperatures resulting from the combustion of the gases and the presence of the flame.

Accompanied with the flashback is also combustion pulsation due to the unsteady dynamics of the combustion, which can lead to vibration and the failure of the liner. Damage due to the flashback can be seen on a typical can-annular combustor as shown in Figure 22-25. The failure of the liner due to vibration caused by high-frequency

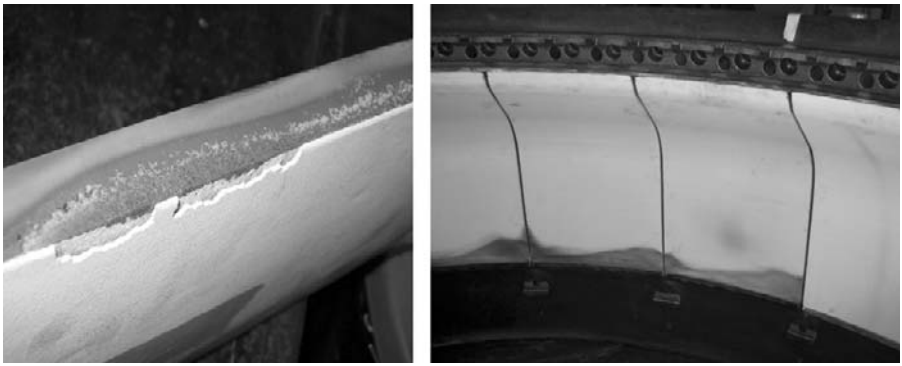


Figure 22-24 Combustor liner plates from an annular combustor.

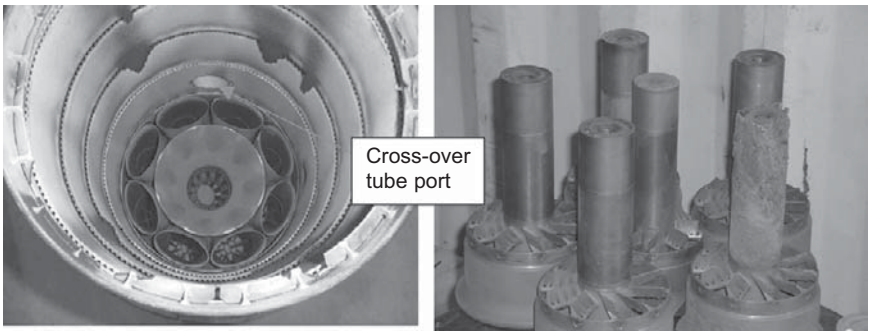


Figure 22-25 Damage to DLN combustor liners and fuel nozzles.

combustion pulsations is a common problem on nearly all dry low NO_x (DLN) combustors regardless of the manufacturer. To avoid flashback, the fuel for these combustors must be totally free of any liquid hydrocarbons. This usually means that at the entrance of the fuel to the turbines, all steps to ensure that dry gas must be taken such as vertical knockout drums and heating of the fuel to a temperature at a minimum of 50 °F (28 °C) of superheat at the inlet fuel valve. The details of treatment of fuels are given in Chapter 12.

Figure 22-26 shows other designed DLN fuel nozzles damaged due to flashback problems. These nozzles show that some of the premix nozzles are burnt due to the fact that in a flashback the combustion takes place in the recirculation area. To prevent these types of problems, the fuel must be closely monitored and it is highly recommended that online combustion monitoring devices that monitor the pulsations in the combustor be installed on all makes of DLN combustors.

Liquids in the fuel supply, especially liquid hydrocarbons, can lead to problems downstream of the combustor. Impingement of liquid hydrocarbons on the turbine nozzle vanes and blades creates hot spots, which lead to turbine coating blistering and spalling, and in some cases, it can attack the base material as shown in Figure 22-26; thus, the fuel gas must be dry and all traces of liquid hydrocarbons removed. This

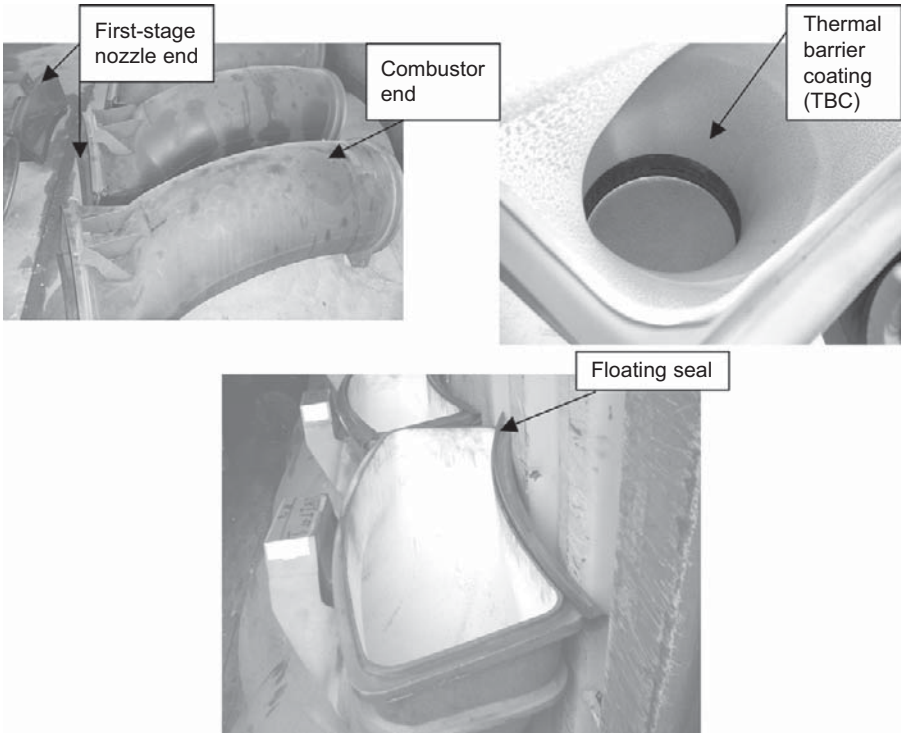


Figure 22-26 Transition pieces.

requires the operator of the turbine to take steps such as use of vertical knockout drums and heating of the fuel to a temperature at a minimum of 50 °F (28 °C) of superheat.

Transition Piece

A typical transition piece connects the combustor to the first-stage nozzle vanes, as shown in Figure 22-26. The circular end connects to the combustor can and the rectangular end connects to the first-stage nozzle vanes. These transition pieces have problems with the floating seals at the nozzle end due to the combustion dynamics that set up a vibratory stress. These seal failures can occur after about 6,000–8,000 equivalent operating hours of service. Most of the newer transition pieces also have a thermal barrier coating to give them a longer life. Some of these newer transition pieces used in advanced gas turbines have an impingement shield to direct cooling air, and some have steam jackets for cooling.

Axial-Flow Turbines

The turbine section of the gas turbine operates at extremely high temperatures. The first-stage turbine nozzles and blades experience gas temperatures as high as 2500 °F

(1370 °C). This requires that the nozzles and blades have adequate coatings and the first stages have additional thermal barrier coatings. The first stages of the turbine also have very extensive cooling systems to ensure that the base metal temperatures do not reach the high corrosion region (1450 °F, 788 °C). The turbine nozzles and blades are also very susceptible to fuel properties and can suffer from erosion and temperature gradients in the combustor due to the combustion process. Liquid hydrocarbons, which are entrained in gaseous fuels, impinge on the turbine, causing hot spots and leading to cracked vanes and blades. Figure 22-27 shows a first-stage nozzle with leading edge failure due to high temperatures and liquid impingement. The thermal barrier coating has been eroded and in some regions the base coating has also melted due to high temperatures.

Fuel nozzles can easily carbonize and clog, especially with liquid fuels. In gas turbines, especially the pre-1990 models, when operating on both liquid and gaseous fuels, vibration can occur, loosening the fuel nozzle, which causes liquid fuel to leak into the combustor, which usually then ignites downstream of the combustor in sections where it can accumulate. These sections are not designed to experience flame temperatures, which can reach about 3500 °F (1927 °C); this leads to severe burning of the nozzles and blades. A number of such cases have occurred in dual-fuel units. In most of these cases, the fuel nozzle loosens and comes off. Because of design constraints, the nozzle does not go through the turbine, but allows a very large amount of fuel to enter the combustor can. This fuel is then transported to the transition piece and toward the first-stage nozzles. The first-stage nozzles act as flame holders, causing the fuel to ignite and create a large flame, which burns out the first-stage nozzle and rotor blades. Figure 22-28 shows the burnt first-stage rotor blades, due to such a failure. In this case, the fuel combusted in the first-stage nozzle area and the flame emitting from that combustion cut the blades as they rotated past, just like a high-powered acetylene torch aimed at the blades at an angle of 45° from the base.

Figure 22-29 shows the damage on the first-stage nozzles, which acted as a flame holder for the combustion of the liquid fuel collected there. The nozzles have been totally burnt due to the extreme heat generated by the flame. This also melted the retainer disc due to the intense heat generated.

Bowing of the first-stage turbine nozzles is a common problem. Bowing can be caused by uneven combustion or loss of cooling air to the nozzle and it can decrease



Figure 22-27 First-stage nozzle vanes.

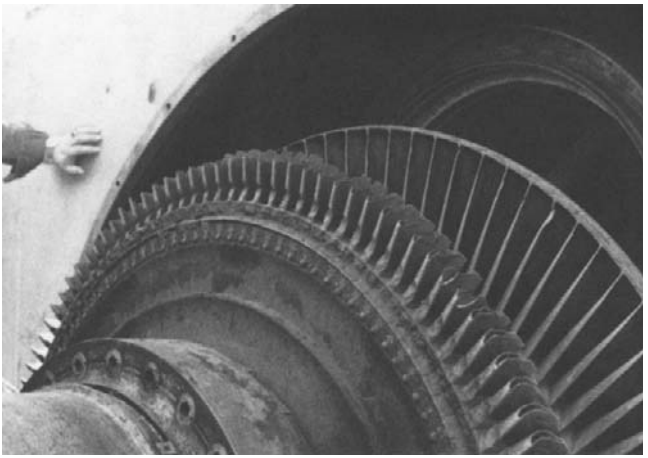


Figure 22-28 Burnt first-stage turbine blades (note evenness of burn).



Figure 22-29 Burnt first-stage nozzle.

turbine efficiency by changing the air velocity and angles leaving the nozzles. In this case, the turbine nozzle areas vary from one nozzle vane to the other due to the high temperatures encountered as shown in Figure 22-30.

Another problem with turbine nozzles occurs with the second or downstream nozzles. This problem is due to liquids entrained in the downstream nozzle area due to the failure of the fuel to fully ignite during start-up. The raw unburnt fuel is carried downstream and is deposited in the second- or downstream-stage nozzle area, where it ignites. When combustion finally occurs, it creates an explosion and/or fire where the fuel is trapped. This trapping of the fuel occurs in the areas where the velocity is lower and the blades act as flame holders. Thus, the second-stage nozzles are ideal



Figure 22-30 Bowed turbine nozzle vanes.

candidates for this problem. The problem is often caused by the fuel migrating downstream after a failure of the turbine to ignite, and the attempt of the operator to start the turbine again, without a proper purge of the turbine. The purging function can be automatic or manual. Usually, a five-minute interval is required and at least five times the total air volume must be changed before another start-up can be attempted.

Another reason for this type of a failure is that the turbine fails to accelerate at or near design rate, signifying that all the fuel injected was not ignited. The fuel that was not ignited is carried downstream where it collects in a downstream nozzle stage and then ignites inside the nozzle vanes. This problem is common in control systems that do not check the acceleration rate from the time of flame start to the time the turbine reaches its full speed. A clue that this phenomenon is occurring in the turbine is when the first-stage turbine nozzle vanes are showing very little distress and the second-stage or other downstream nozzle vanes are totally burnt due to the fire inside that region. Figure 22-31 shows the first- and second-stage nozzle vanes of the turbine that failed due to ignition of the carried over fuel in the downstream (second)-stage nozzle vanes.

Further examination of the turbine rotor in Figure 22-32 shows that the first-stage turbine rotor blades were very slightly damaged but the second- and third-stage blades were heavily damaged due to debris from the second-stage nozzle vanes.

The first-stage turbine blades are usually impulse-type (zero-percentage reaction) blades and the second- to the third- and fourth-stage blades are of reaction type (30–60%); the reaction percentage is higher in the latter stages and these latter stage

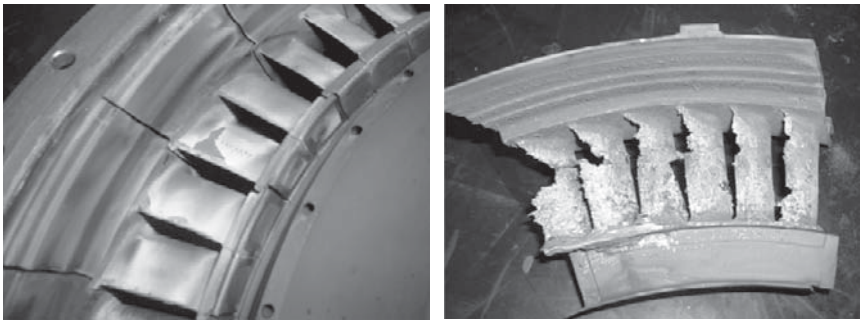


Figure 22-31 Failed nozzle vanes due to fuel ignition in the second-stage vane.



Figure 22-32 Turbine rotor shaft.

blades usually have shroud tips. These shroud tips are there to give the blade more support, so that the blades do not suffer from blade resonance problems. Figure 22-33 is a typical large industrial gas turbine. Note that the first-stage blades are short and stubby (low aspect ratio) and have a "bucket" shape, whereas the second- and third-stage blades are more airfoil-shaped and have a larger aspect ratio, and have tip shrouds. The second- and third-stage blades are also more impulse type at the hub and have an increasing reaction as they reach the tip.

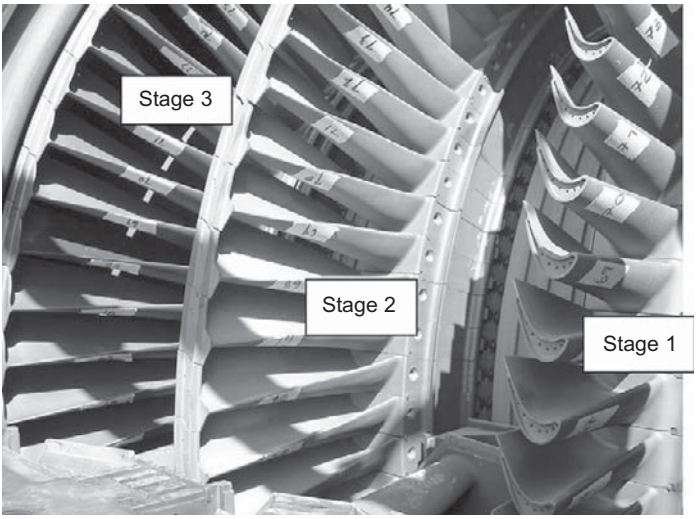


Figure 22-33 A typical turbine section of an industrial-type gas turbine.

The second-stage buckets/blades are precision cast and have integral tip shrouds as can also be seen in the same figure. This reduces tip leakage losses and provides damping of the buckets/blades leading to higher mechanical integrity. The shroud tips must be very carefully examined at turnarounds to ensure that no lift of the shroud is occurring. These tips in most cases are interlocked with each other. Figure 22-34 shows a close-up of a typical blade tip shroud showing a slight shroud lift.

The tip shroud lift can lead to major problems especially if the there is contact with the casing, which can tend to rip out the shroud. Figure 22-35 is the same turbine as shown in Figure 22-33; however, note that the stages two and three no longer have the tip shrouds. The tip shrouds due to a shroud lift were in contact with the casing and were then torn off due to the contact. This is the reason that tip shrouds should be closely examined. Tip shroud lift occurs due to the fact that blades are undergoing loss of strength and the blades are being stretched due to high temperatures and centrifugal forces acting on the blade.

The very high firing temperatures in advanced gas turbines have led to failures in the turbine nozzle vanes and blades. The first-stage nozzle vanes are encountering gas temperatures in the range of 2100–2400 °F (1149–1315 °C); therefore, proper cooling techniques and coatings for the nozzle vanes and blades are very important. These high temperatures require cooling at the base and the trailing edge of these turbine nozzle vanes and blades. As noted in Chapter 9, maximum temperature is encountered at the airfoil profile at both the leading and trailing edges of the airfoil; however, at these very high temperatures, cooling often also is required at the base platform of these blades. The nozzle vanes are especially encountering problems at their base with these high temperatures. Design changes have been carried out by all OEMs; these include new cooling patterns for the nozzle vane base, further cooling of the

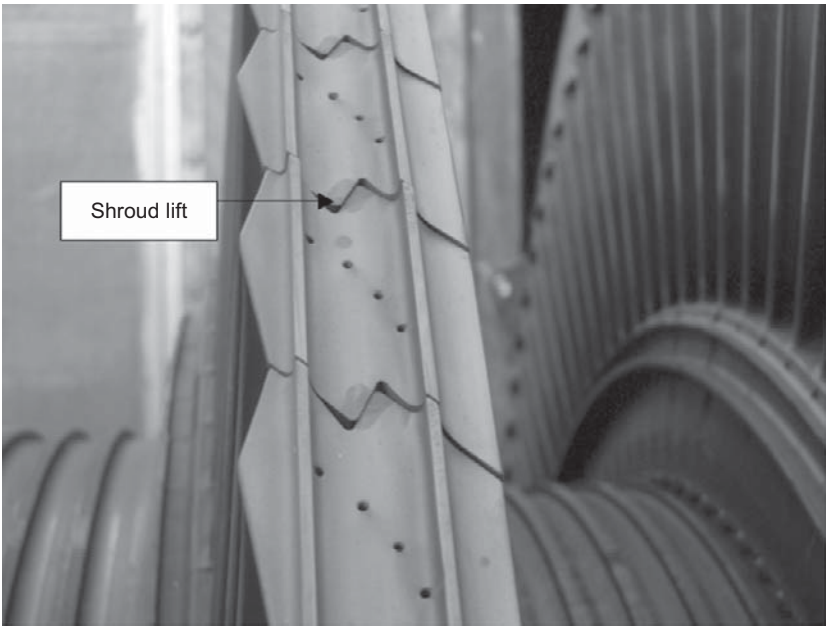


Figure 22-34 Tip shrouds showing a slight shroud lift.

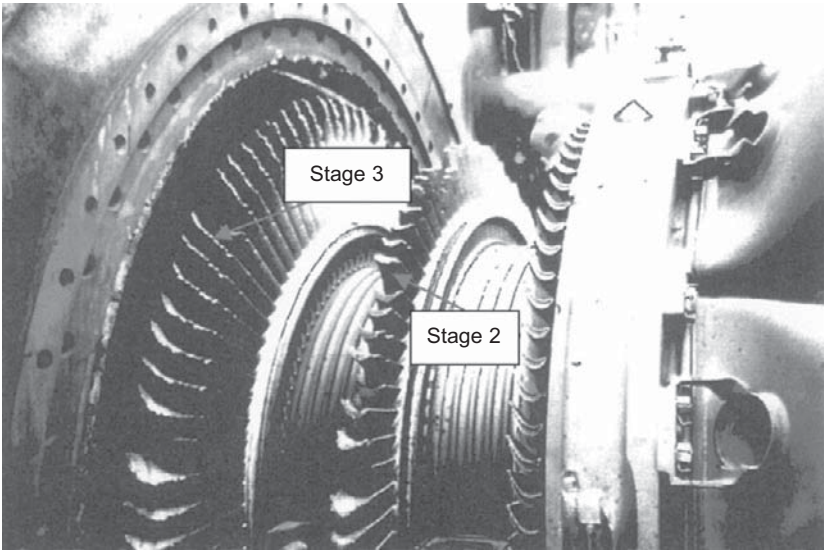


Figure 22-35 Damaged turbine rotor.

compressor bleed air with external cooling heat exchangers, and in some cases, the use of steam for cooling purposes in combined-cycle applications. These nozzles are under very high temperatures and failures occur at the trailing edge where the highest

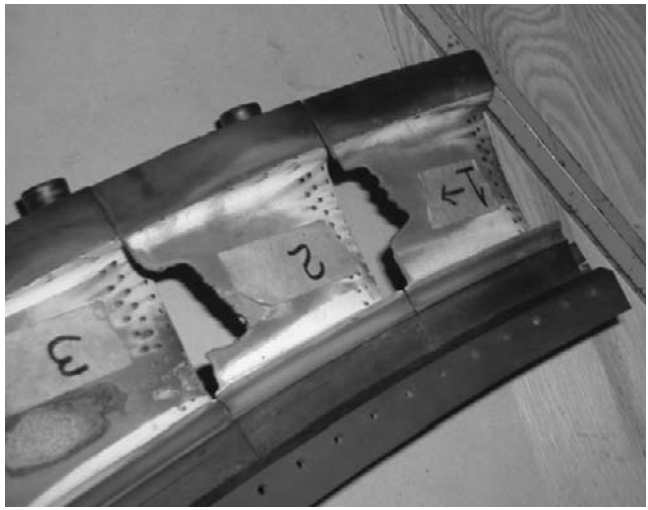


Figure 22-36 Advanced gas turbine failed nozzle vanes due to high temperatures.



Figure 22-37 Nozzle vanes showing damage to the nozzle vane base due to high temperature.

gas temperatures are found and the amount of metal is minimum. Figure 22-36 shows a typical first-stage nozzle suffering from high temperatures, due to lack of cooling.

Many of the advanced gas turbine nozzle vanes require additional cooling and cooling at the base and shroud of the nozzles. Figure 22-37 shows a typical turbine nozzle vane with damage at the base due to high temperatures in this platform area of the nozzle vanes. Many of the advanced gas turbine OEMs are adding more cooling to the base and shroud regions to avoid similar types of damage.

The failures have been occurring at blade tips and at the base of the turbine nozzle vanes. Figure 22-38 shows a typical failure of the blade shroud tips on the second through the fourth stages in an advanced gas turbine. It should be noted that some of the second-stage blades have been mowed down at their base by impact from the failed nozzles and blades upstream of them.

The first-stage blades also are in very high-temperature regions and have to be provided with proper cooling, which is further aided by TBC. The additions of cooling



Figure 22-38 A typical gas turbine failure tip; shrouds are missing from Stages two–four.

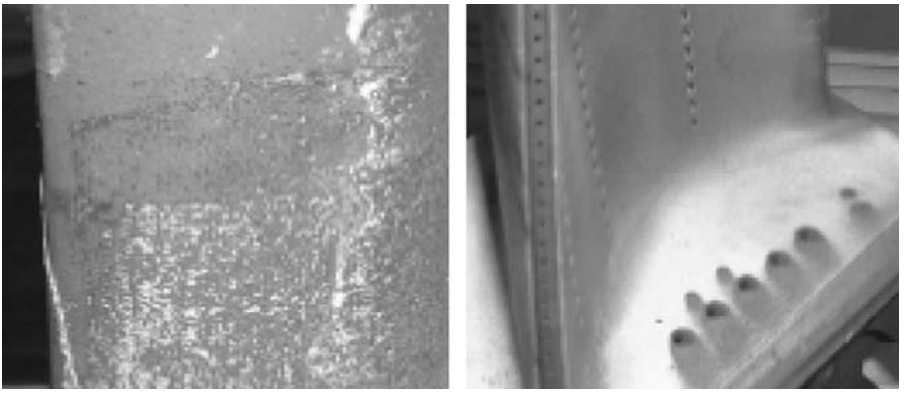


Figure 22-39 Typical first-stage blades (note the erosion of the TBC from the leading edge and the cooling holes needed at the base of the blades).

holes in the base are now a requirement at these very high temperatures to prevent cracks at the base as shown in Figure 22-39. The older turbines, which operate at lower temperatures, have not had to have cooling at the blade platforms. The advanced turbine, due to the very high-temperature type, requires cooling at the turbine blade

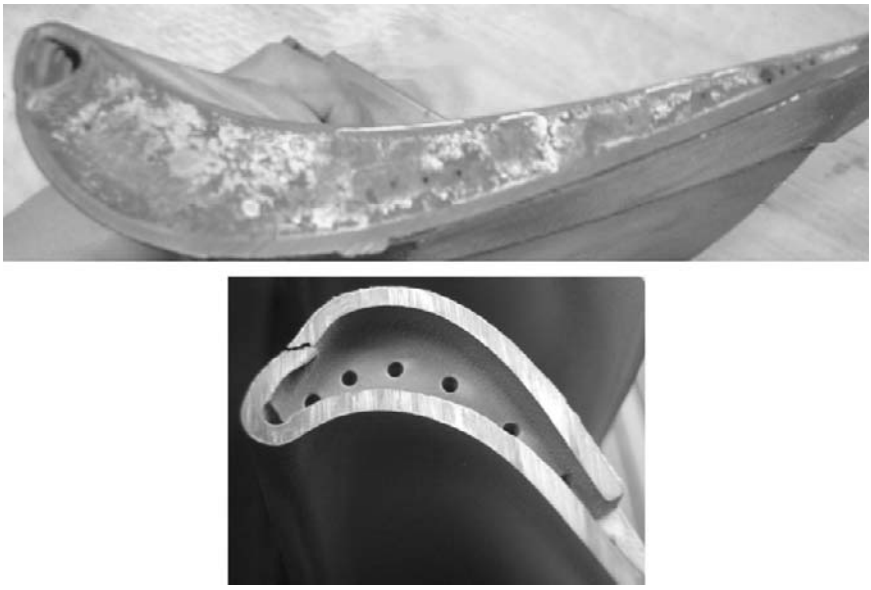


Figure 22-40 Blade tip rubs.

base. Many OEMs have had to increase the amount of cooling at the base to achieve the turbine blade life goals.

The high efficiency requires that close casing clearances be maintained between the rotating elements (blades) and the stationary shroud ring. This, in many cases, causes extensive rubbing at the blade tips leading to blade failures as shown in Figure 22-40.

The first-stage tip shroud ring also encounters excessive high temperatures and requires cooling. It is not unusual to see sections of the shroud ring burnt. Figure 22-41 shows one such turbine stator vane section. The extreme left of the picture is the first-stage shroud ring. Note that this ring has cooling holes; also note the sections that are discolored due to high temperatures. The second section is the honeycomb seal, which is there to reduce the leakage between the wheel and the base of stationary nozzle vanes. Honeycomb seals in that region have been much more successful than labyrinth seals.

Figure 22-42 shows second- and third-stage nozzle vanes. These have labyrinth seals for the reduction of leakage between the wheel and the base of stationary nozzle vanes.

Figure 22-43 shows a shroud ring burnt due to the high temperatures encountered in that region. Shroud ring problems to the first-stage ring are common and these rings have to be replaced on the more advanced gas turbines after 12,000–15,000 hours.

Another area where the blades have problems is in the region where they are attached to the wheel disk. Turbine blades are designed to be loosely fitted at room temperature in the wheel disks, so that they can expand at the high temperatures and with the centrifugal force acting on them. This means that these blades rock in their

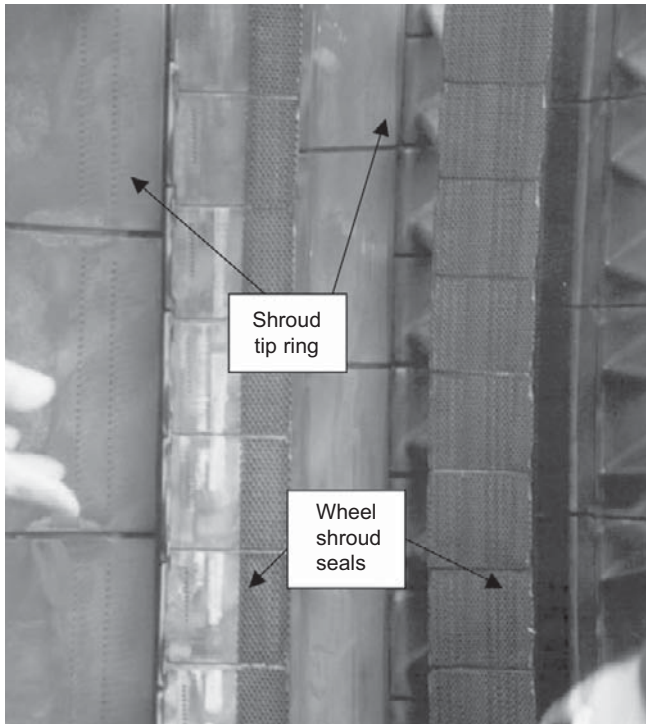


Figure 22-41 Turbine casing and vane sections.

wheel sockets and often suffer from erosion at the attachment region as shown in Figure 22-44.

There are many different types of attachments of the blades. Figure 22-45 shows the different types of blade attachments, which vary from the simple T attachment to the complex fir tree attachments.

Wheel space temperatures are measured in between the turbine wheels usually at forward and aft regions of each wheel, and at two locations on the left and right sides at each position along the axial positioning of each wheel. A disk failure can lead to a very massive failure in the gas turbine. When the disk fails, the blades will also fail and in many cases would seriously damage the gas turbine casing. A typical disk failure is a tri-hub failure, which leads to the disk breaking into three sections. Figure 22-46 shows a typical failure of the disk, the fir tree section containing the blades, and the base of the blade.

Bearing problems are one of the most common failures that occur in gas turbines. Journal-type rotor bearings usually experience a type of instability called oil whirl. This phenomenon has been described in detail in Chapter 5. In some cases, this problem is alleviated by a change of oil temperature, otherwise the problem requires a change in bearing design such as going to a pressure-dam bearing, or in excessive cases, to a tilting-pad bearing. Figure 22-47 shows the failed bearing with most of the

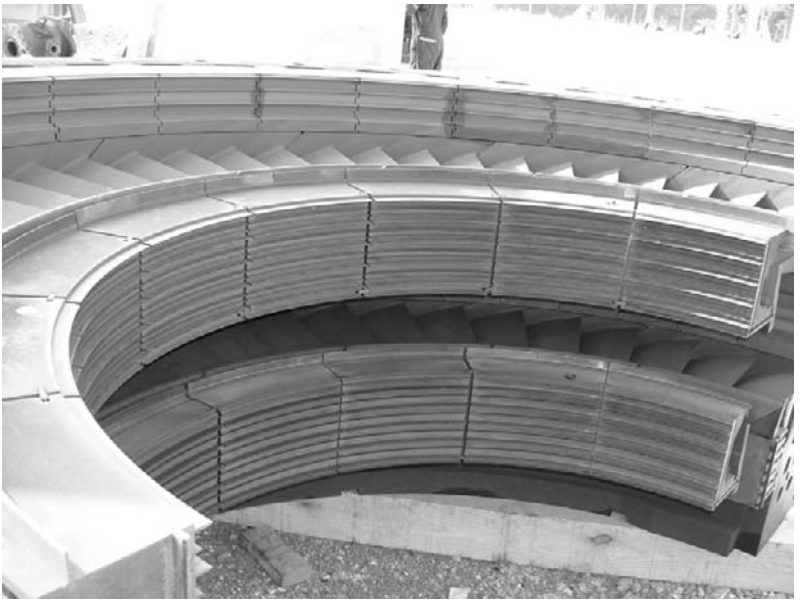


Figure 22-42 Turbine casing and vane sections with labyrinth seals.



Figure 22-43 First-stage shroud ring heavily burnt.

babbitt destroyed. This indicates that there was considerable rub between the bearing and the journal. Babbitt is a soft metallic covering with excellent properties as an oil-lubricated bearing surface material. Babbitt has excellent compatibility and

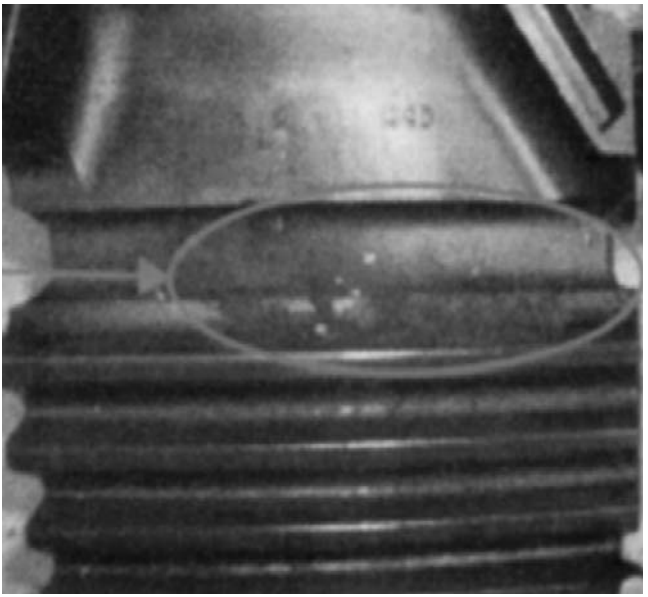


Figure 22-44 Erosion and corrosion in the blade fir tree region.

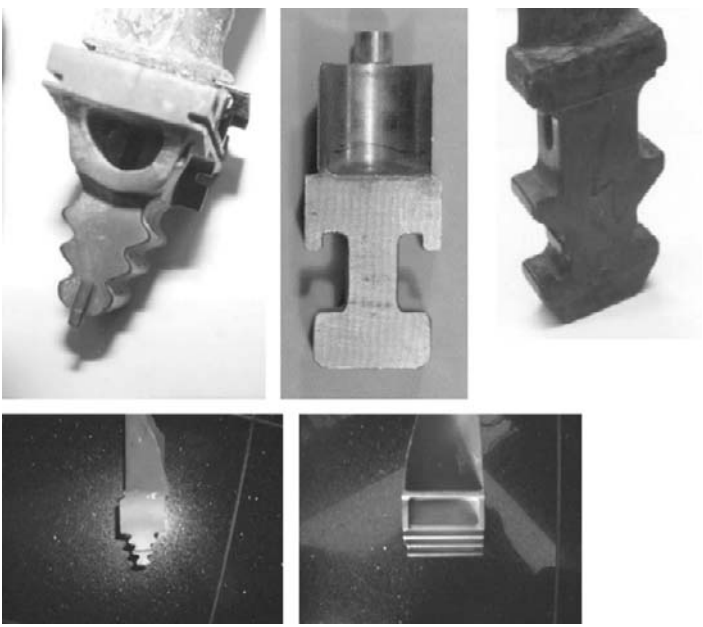


Figure 22-45 Various attachment types for turbine blades.

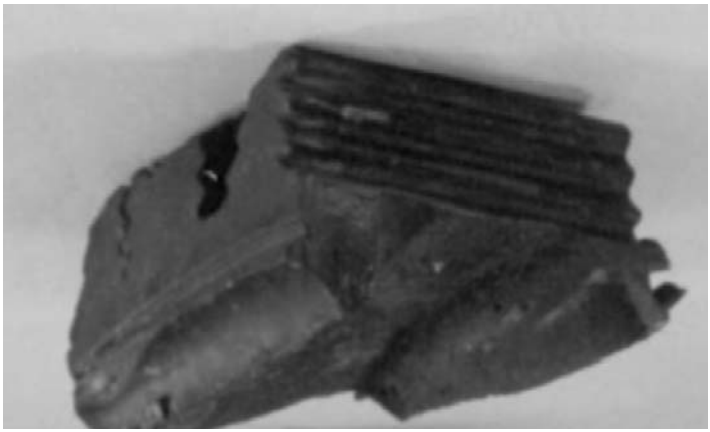


Figure 22-46 Failed disk component.

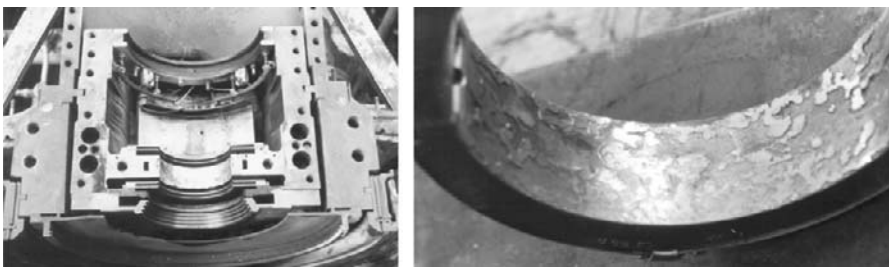


Figure 22-47 Journal bearing babbitt has been mainly wiped out due to excessive rub.

non-scoring characteristics, and it is outstanding in embedding dirt and conforming to geometric errors in machine construction and operation. However, it is relatively weak in fatigue strength, especially at elevated temperatures.

Figure 22-48 is a view of a tilting-pad journal bearing. These types of bearing are greatly recommended, as they do not suffer from oil whirl problems. The bearing shows minor rubs.

Figure 22-49 shows the journal that was also seen with heavy rubs. The journal has the thrust shoulder, which has on it a number of drilled and tapped screw holes into which bolts can be screwed to trim balance the turbine in the field. Kingsbury-type self-aligning tilting-pad thrust bearings are used in most gas turbines, as shown in Figure 22-50. Most gas turbines have an active and inactive thrust bearing; the shaft shoulder is running very close to the active thrust surface on a very thin film of lubricating oil. Under normal operating loads, the turbine operates against the active thrust bearing. To compensate for the thrust force caused by the aerodynamics of the air and gas, a balance force is introduced by providing bleed flow from the gas turbine compressor to the turbine exit disk. This force acting on the shaft and disks compensates for the aerodynamic thrust caused by the gas flow. The active thrust bearing

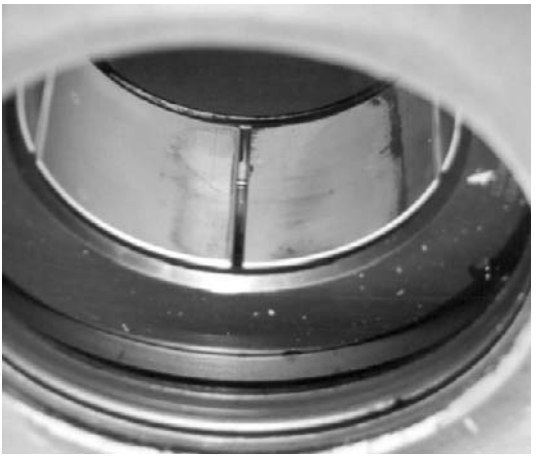


Figure 22-48 Tilting-pad thrust bearing.

on most units is designed to carry the load. Under upset conditions or when the turbine has many operating hours, excessive clearances in the unit occur and the thrust load moves to the inactive side. This not only damages the thrust bearings but also causes the rotating blades to come in contact with the stationary blades leading to a massive failure. In the older gas turbines, the inactive side thrust bearings are usually taper-land-type bearings and have the ability of carrying less than 50% of the load; thus they fail during an upset and cause severe damage to the turbine. It is recommended that in those instances where taper-land thrust bearings are used, they may be replaced with self-aligning Kingsbury-type tilting-pad thrust bearings capable of carrying the same load as the active side. This would involve machining the turbine case to accommodate the larger axial thickness of the self-aligning-type tilting-pad bearings. Figure 22-49 shows a typical self-aligning-type thrust bearing. The rocker pushes on the tilting pad to ensure equal forces on the entire bearing.

Figure 22-51 shows a tilting-pad bearing that has been blued for inspection. In the same figure are tilting pads from another bearing that has had a massive thrust failure. Note the deep rings that have been cut into the bearing pads. Moreover, note that the ends between the pads are broken and have suffered major damage due to the heat generated in the rub. Many thrust-bearing problems are due to internal and external misalignments. Internal misalignment problems are critical and must be solved for the smooth operation of the gas turbine. Due to large differences in temperatures at the compressor- and turbine-end bearing, pedestals grow at different rates and thus it is critical that their growth may be properly evaluated to obtain proper alignment at the rated speed and load. External alignment between the turbine and the driven equipment is also of great importance. The complexity of this alignment is greater if the drive is from the hot end, than from the cold end. It must be remembered that forces due to misalignment are very great and can lead to major failures of both the gas turbine and the driven equipment. Misalignment problems in the system can often be aggravated

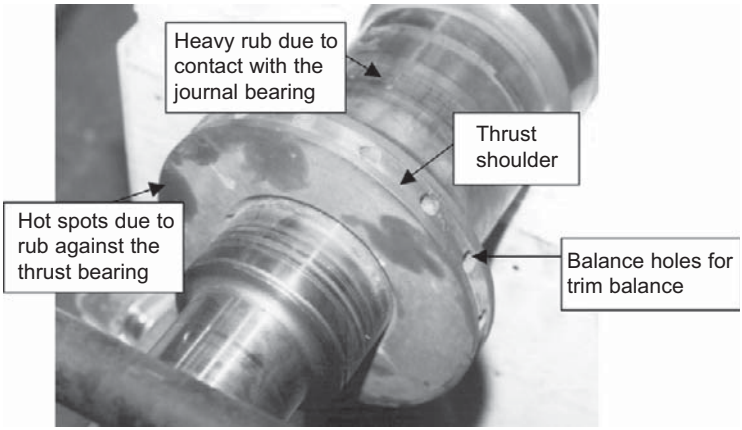


Figure 22-49 Journal shaft with thrust shoulder.

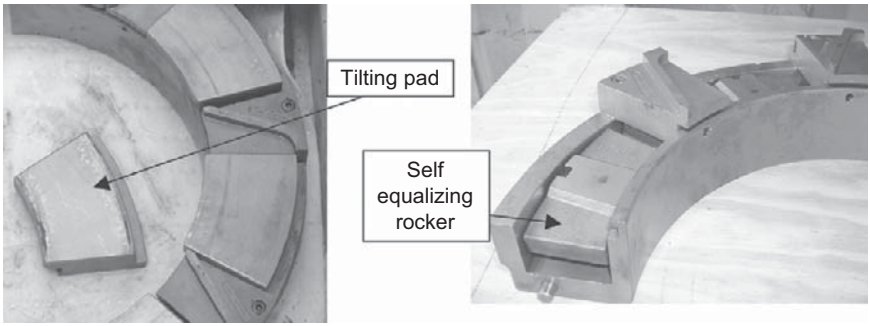


Figure 22-50 Kingsbury-type self-aligning thrust bearing.



Figure 22-51 A failed thrust bearing.

by the piping to the system, especially in mechanical drive turbines. Pipe stresses can run very high and the forces generated by the piping can move the driven compressor, thus causing high misalignments in the system.

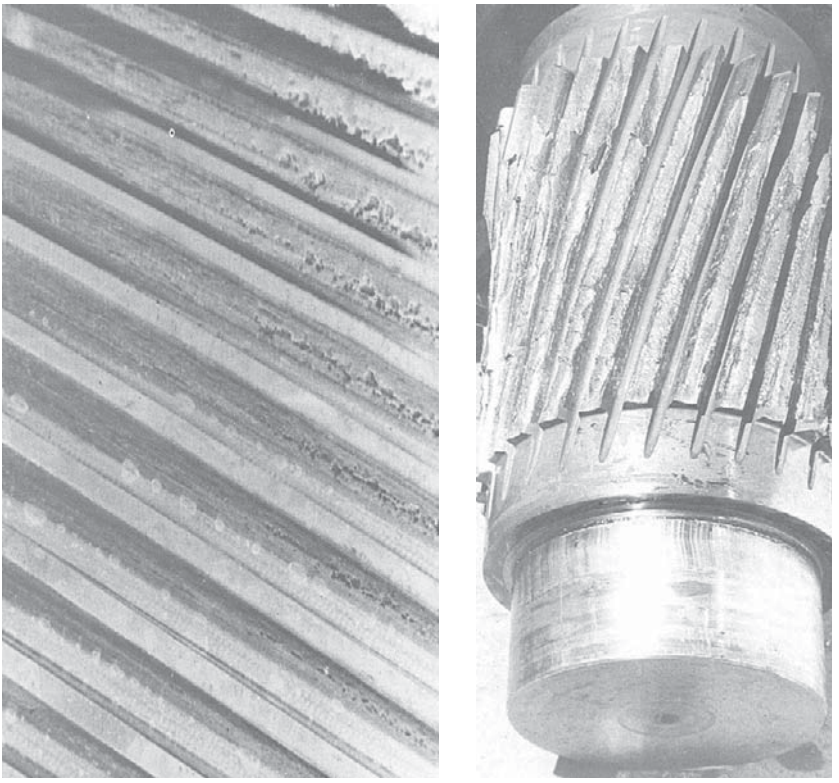


Figure 22-52 Pitted and broken gear teeth.

Seal problems can give rise to high leakages and thrust problems. The high leakages reduce the efficiency of the unit and can also lead to contamination of the lubricant. Thrust problems are created by air leakage past seals, causing an unbalance of the thrust forces on the system. Figure 22-52 shows a typical labyrinth seal in a gas turbine.

Shaft problems are usually not very common, but shafts will shear due to high torque, excessive loads, and the number of starts and full load trips. In combined-cycle plants, the problem results when the type of driver is changed from a turbine drive to a synchronous electric-motor drive, especially on boiler feedwater pumps. With the latter drive, very high torsional stresses are produced, which can lead to shaft failures when the unit is brought from rest to design speed in seconds.

Other problems experienced in gas turbines occur in regenerators/recuperators, gearing, and couplings. Problems with regenerators often occur due to a leak in the system. Abrasive cleaning of compressors that have led to erosion problems and hot spots or a fire that will burn through the wall in regenerators should be discontinued.

Water washing has been proven to be safe and successful as compared to using spent catalyst or other abrasive cleaners.

Gear failures can be attributed to the following major causes:

- Pitting or surface failure,
- Teeth failures, and
- Lubrication failure.

Pitting occurs due to surface fatigue. Gear teeth under load are subjected to high compressive stresses, and if the endurance limit of the material of the gear is exceeded then pits or cavities are formed on the surface of the teeth. Pitting usually occurs in a small band around the pitch line of the teeth. Failure and breakage of the gear teeth is the most serious of all forms of gear failure. If a small part of the gear tooth is broken, heavier loads are transferred to the remainder of the tooth with the risk of complete failure. Figure 22-52 shows gear teeth with pitting and gear teeth failure. Lubrication forms a thin oil film that prevents metal-to-metal contact when gear teeth slide. Gear teeth are subject to a rolling action with sliding added. Pure rolling occurs at the pitch diameters, and sliding takes place above and below this location. Thus, with lubrication failure and under the high pressure of gear teeth loading the contact procedures alternate welding and tearing in the direction of sliding. This causes the materials to be displaced over the tips of the teeth causing a "feather edge." This destroys the tooth profile and the gears run with severe vibration and noise.

Other gearing problems are due to case distortion, improper gear cooling, or high backlash on the gears. Misalignment also is a great contributor to this problem. Gears should be checked for proper fit; in some cases, lapping is advised. Care is always needed to prevent the lapping compound from entering the lubrication system and bearings. Cooling of the high-speed gears is accomplished by directing a jet of lubrication oil on the gears, as they become unmeshed. In very high-speed applications, oil should be directed at the casing to reduce thermal distortion of the casing.

Coupling problems are also directly or indirectly caused by improper lubrication or a high level of misalignment. Couplings of the gear type should have a continuous lubrication system rather than be grease packed. Grease tends to separate at high speeds; however, new greases being developed may change the whole coupling picture. In many cases, gear couplings are being replaced by disc-type couplings. This type of coupling is more forgiving of angular alignment problems and also does not require any type of lubrication. However, these couplings can suffer from sand or other contaminants getting between the various metal disks and causing high vibration. Most of these types of couplings have now been placed in enclosures to prevent contamination. In these enclosures, due to turbulence of the air caused by the bolts and air shearing forces, very high temperatures can be reached, above 500 °F (260 °C). In some cases, oil has to be injected to keep the area cool.

The previous problems are some of the more common types encountered on a gas turbine train. Regular and preventive maintenance is the key to a successful operation. Problems will arise, but by proper monitoring of the aerothermal and mechanical problems, preventive maintenance can often avert major or catastrophic failures.

Recent reports published based on information from "Moderne Gas Turbinen-Technologie, Risiken und Schaden," Dr. J. Stoiber, Allianz Zentrum Fur Technik Gmbh, VGB PowerTech 2/2002, divides the problems for gas turbines into sizes larger than 220 MW and gas turbines less than 170 MW. Figures 22-53 and Figures 22-54 show the major problem areas experienced in gas turbines less than 220 MW and larger than 220 MW, respectively. In the smaller turbines, the problems are concentrated in the hot section, as has been traditionally experienced. The interesting point, as shown in Figure 22-54, is that the compressor problems are greatly increased, as the turbine ratings increase. In fact, the turbine compressor problems are slightly larger than the turbine problems. This is related to the high flow and high pressure in the larger turbines, and the air coolers for compressor air used for turbine cooling.

The failures of the gas turbine in the compressor section are usually in the inlet guide vanes, at the transition between the low-pressure and high-pressure compressors and due to rubbing in stages usually upstream of the bleed flow sections. The larger units have very high pressure ratios and have both low-pressure and high-pressure

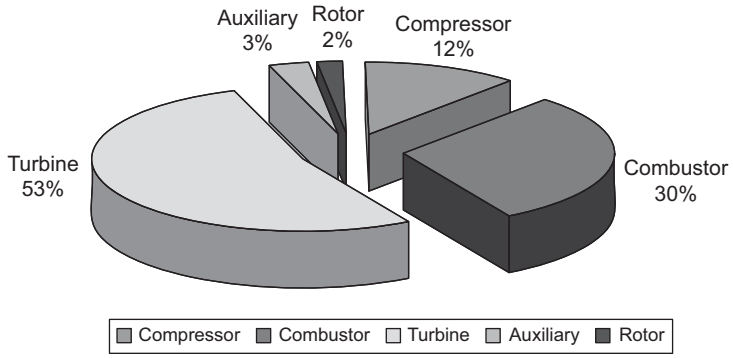


Figure 22-53 Major failures in gas turbines less than 170 MW.

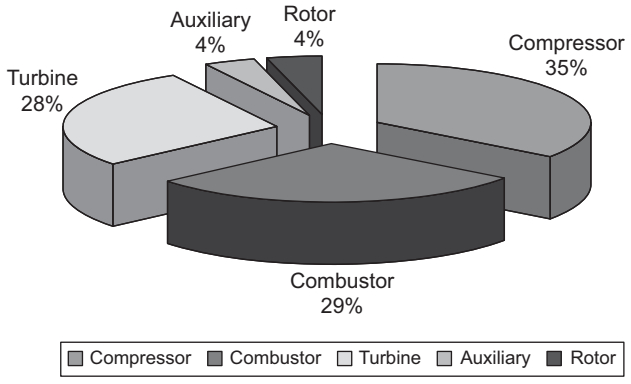


Figure 22-54 Major failures in gas turbines larger than 220 MW.

compressors and have high exit temperatures, all leading to problems in the compressor section. The compressor exhaust air coolers in some systems are part of the heat recovery steam generator systems (HRSG), adding further complexity to the system.

The risks and costs of these new design technologies present real problems for investment bankers, insurers, OEMs, and owners. The providing of long-term service agreements (LTSA) has spawned a new profit center within all OEMs. The LTSA is the fastest and most profitable growth sector for the OEMs. The owners in most cases cannot get the investment or insurance without an LTSA with the OEMs for these advanced gas turbines. Insurer's appetite for new designs is limited. The advanced gas turbines, such as the later F, plus the G, and H technology designs and the new reheat GT 24 and 26 have had poor early reliability experience. There have been problems with these designs from all OEMs, as they push the design envelope to its limit. Problems such as failure and/or major rubs of compressor blades and vanes; oxidation damage and failure of turbine airfoils and nozzle vanes and coating failures; failure of DLN combustors due to flashback, pulsation, distortion and/or control systems, and transition sections have plagued these new advanced turbines. Insurance companies consider some of these to be prototype designs with few spares that can only be validated at the owner's site. Insurers typically cover sudden and accidental damage and do not want to insure design deficiencies. When these designs are insured, the insurers try to spread the risk to other insurers and reinsurers to minimize the amount of potential loss. This does increase the operational costs but is a comfort factor for both investors and insurance companies. Insurance is mandatory for new projects as well as for subsequent ownership and commercial operation. However, with no track record of the designs to quantify risk for insurance, investors, and cost of ownership, the handling of the risk is difficult during the first three years of operation – that is, until the design is proven.

Advanced gas turbines over the past few years have seen considerable improvement in the design of the major components. These changes have increased the availability and reliability of these units and increased the life of some of these parts. Therefore, with the advancements of various components in the last few years, the operation of these turbines has greatly improved, and in conjunction with the high overall turbine efficiency, the new advanced gas turbines are here to stay.

Copyrighted Materials
Copyright © 2012 Elsevier Retrieved from www.knovel.com

Appendix: Equivalent Units

Abbreviations. A = angstrom, atm = standard atmosphere, 760 mm of Hg at 0 °C, cal = calorie (gram), cm = centimeter, deg = degree, gal = gallon, U.S. liquid, gm (and g) = gram, gmole = gram-mole, J = joule, kcal = kilocalorie, kg = kilogram, kJ = kilojoule, km = kilometer, kW = kilowatt, l = liter, lb = avoirdupois pound, m = meter, mi = mile (U.S.) mm = millimeter, N = newton, oz = avoirdupois ounce, pmole = pound mole, pt = pint, rad = radian, rev = revolution, s = second, ton = short U.S. ton, V = volt, W = watt. Others are as usual.

Length

$$12\frac{\text{in}}{\text{ft}} \quad 6080.2\frac{\text{ft}}{\text{naut.mi}} \quad 5280\frac{\text{ft}}{\text{mi}} \quad 0.3937\frac{\text{in}}{\text{cm}} \quad 30.48\frac{\text{cm}}{\text{ft}} \quad 10^4\frac{\text{microns}}{\text{cm}}$$

$$3\frac{\text{ft}}{\text{yd}} \quad 1.152\frac{\text{mi}}{\text{naut.mi}} \quad 10^{10}\frac{\text{A}}{\text{m}} \quad 2.54\frac{\text{cm}}{\text{in}} \quad 3.28\frac{\text{ft}}{\text{m}} \quad 1.609\frac{\text{km}}{\text{mi}}$$

Area

$$144\frac{\text{in}^2}{\text{ft}^2} \quad 43{,}560\frac{\text{ft}^2}{\text{acre}} \quad 640\frac{\text{acres}}{\text{mi}^2} \quad 10.76\frac{\text{ft}^2}{\text{m}^2} \quad 929\frac{\text{cm}^2}{\text{ft}^2} \quad 6.452\frac{\text{cm}^2}{\text{in}^2}$$

Volume

$$1728\frac{\text{in}^3}{\text{ft}^3} \quad 7.481\frac{\text{gal}}{\text{ft}^3} \quad 43{,}560\frac{\text{ft}^3}{\text{acre}-\text{ft}} \quad 3.7854\frac{1}{\text{gal}} \quad 28.317\frac{1}{\text{ft}^3} \quad 35.31\frac{\text{ft}^3}{\text{m}^3}$$

$$231\frac{\text{in}^3}{\text{gal}} \quad 8\frac{\text{pt}}{\text{gal}} \quad 10^3\frac{1}{\text{m}^3} \quad 61.025\frac{\text{in}^3}{1} \quad 10^3\frac{\text{cm}^3}{1} \quad 28{,}317\frac{\text{cm}^3}{\text{ft}^3}$$

Density

$$1728\frac{\text{lb/ft}^3}{\text{lb/in}^3} \quad 32.174\frac{\text{lb/ft}^3}{\text{slug/ft}^3} \quad 0.51538\frac{\text{gm/cm}^3}{\text{slug/ft}^3} \quad 16.018\frac{\text{kg/m}^3}{\text{lb/ft}^3} \quad 1000\frac{\text{kg/m}^3}{\text{gm/cm}^3}$$

Angular

$$2\pi = 6.2832\frac{\text{rad}}{\text{rev}} \quad 57.3\frac{\text{deg}}{\text{rad}} \quad \frac{1}{2\pi}\frac{\text{rpm}}{\text{rad/min}} \quad 9.549\frac{\text{rpm}}{\text{rad/sec}}$$

Time

$$60\frac{\text{s}}{\text{min}} \quad 3600\frac{\text{s}}{\text{hr}} \quad 60\frac{\text{min}}{\text{hr}} \quad 24\frac{\text{hr}}{\text{day}}$$

Speed

$$88\frac{\text{fpm}}{\text{mph}} \quad 0.6818\frac{\text{mph}}{\text{fps}} \quad 0.5144\frac{\text{m/s}}{\text{knot}} \quad 0.3048\frac{\text{m/s}}{\text{fps}} \quad 0.44704\frac{\text{m/s}}{\text{mph}}$$

$$1.467\frac{\text{fps}}{\text{mph}} \quad 1.152\frac{\text{mph}}{\text{knot}} \quad 1.689\frac{\text{fps}}{\text{knot}} \quad 152.4\frac{\text{cm/min}}{\text{ips}}$$

Force, Mass

$$16\frac{\text{oz}}{\text{lb}_\text{m}} \quad 32.174\frac{\text{lb}_\text{m}}{\text{slug}} \quad 444{,}820\frac{\text{dynes}}{\text{lb}_\text{f}} \quad 2.205\frac{\text{lb}_\text{m}}{\text{kg}} \quad 9{,}080{,}665\frac{\text{N}}{\text{kg}_\text{f}}$$

$$1000\frac{\text{lb}_\text{f}}{\text{kip}} \quad 32.174\frac{\text{poundals}}{\text{lb}_\text{f}} \quad 980.665\frac{\text{dynes}}{\text{gm}_\text{f}} \quad 14.594\frac{\text{kg}}{\text{slug}} \quad 4.4482\frac{\text{N}}{\text{lb}_\text{f}}$$

$$2000\frac{\text{lb}_\text{m}}{\text{ton}} \quad 7000\frac{\text{grains}}{\text{lb}_\text{m}} \quad 453.6\frac{\text{gm}}{\text{lb}_\text{m}} \quad 10^5\frac{\text{dynes}}{\text{N}} \quad 1\frac{\text{kilopond}}{\text{kg}}$$

$$14.594\frac{\text{kg}}{\text{slug}} \quad 28.35\frac{\text{gm}}{\text{oz}} \quad 453.6\frac{\text{gmole}}{\text{pmole}} \quad 907.18\frac{\text{kg}}{\text{ton}} \quad 1000\frac{\text{kg}}{\text{metric ton}}$$

Pressure

$$14.696\frac{\text{psi}}{\text{atm}} \quad 101{,}325\frac{\text{N/m}^2}{\text{atm}} \quad 13.6\frac{\text{kg}}{\text{mm Hg}(0\,^\circ\text{C})}$$

$$51.715\frac{\text{mm Hg}(0\,^\circ\text{C})}{\text{psi}} \quad 47.88\frac{\text{N/m}^2}{\text{psf}}$$

$$29.921\frac{\text{in Hg}(0\,^\circ\text{C})}{\text{atm}} \quad 10^5\frac{\text{N/m}^2}{\text{bar}} \quad 13.57\frac{\text{in}\,\text{H}_2\text{O}(60\,^\circ\text{F})}{\text{in Hg}(60\,^\circ\text{F})}$$

$$703.07\frac{\text{kg/m}^2}{\text{psi}} \quad 6894.8\frac{\text{N/m}^2}{\text{psi}}$$

$$33.934\frac{\text{ft}\,\text{H}_2\text{O}(60\,^\circ\text{F})}{\text{atm}} \quad 14.504\frac{\text{psi}}{\text{bar}} \quad 0.0361\frac{\text{psi}}{\text{in}\,\text{H}_2\text{O}(60\,^\circ\text{F})}$$

$$0.0731\frac{\text{kg/cm}^2}{\text{psi}} \quad 760\frac{\text{torr}}{\text{atm}}$$

$$1.01325\frac{\text{bar}}{\text{atm}} \quad 10^6\frac{\text{dynes/cm}^2}{\text{bar}} \quad 0.4898\frac{\text{psi}}{\text{in Hg}(60\,^\circ\text{F})}$$

$$\frac{9.869}{10^7}\frac{\text{atm}}{\text{dyne/cm}^2} \quad 133.3\frac{\text{N/m}^2}{\text{torr}}$$

$$33.934\frac{\text{ft}\,\text{H}_2\text{O}(60\,^\circ\text{F})}{\text{atm}} \quad 760\frac{\text{mm Hg}(0\,^\circ\text{C})}{\text{atm}} \quad 406.79\frac{\text{in}\,\text{H}_2\text{O}(39.2\,^\circ\text{F})}{\text{atm}}$$

$$0.1\frac{\text{dyne/cm}^2}{\text{N/m}^2} \quad 1.0332\frac{\text{kg/cm}^2}{\text{atm}}$$

Energy and Power

$$778.16\frac{\text{ft}-\text{lb}}{\text{Btu}} \quad 2544.4\frac{\text{Btu}}{\text{hp}-\text{hr}} \quad 5050\frac{\text{hp}-\text{hr}}{\text{ft}-\text{lb}} \quad 1\frac{\text{J}}{\text{W}-\text{s}}\frac{\text{J}}{\text{N}-\text{m}} \quad 0.01\frac{\text{bar}-\text{dm}^3}{\text{J}}$$

$$550\frac{\text{ft}-\text{lb}}{\text{hp}-\text{s}} \quad 42.4\frac{\text{Btu}}{\text{hp}-\text{min}} \quad 1.8\frac{\text{Btu/lb}}{\text{cal/gm}} \quad 1\frac{\text{kW}-\text{s}}{\text{kJ}} \quad \frac{16.021}{10^{12}}\frac{\text{J}}{\text{Mev}} \quad .948\frac{\text{Btu}}{\text{kW}-\text{s}}$$

$$33{,}000\frac{\text{ft}-\text{lb}}{\text{hp}-\text{min}} \quad 3412.2\frac{\text{Btu}}{\text{kW}-\text{hr}} \quad 1800\frac{\text{Btu/pmole}}{\text{kcal/gmole}} \quad 1\frac{\text{V}-\text{amp}}{\text{W}-\text{s}} \quad \frac{1.6021}{10^{12}}\frac{\text{erg}}{\text{eV}}$$

$$737.562\frac{\text{ft}-\text{lb}}{\text{kW}-\text{s}} \quad 56.87\frac{\text{Btu}}{\text{kW}-\text{min}} \quad 2.7194\frac{\text{Btu}}{\text{atm}-\text{ft}^3} \quad 10^7\frac{\text{ergs}}{\text{J}} \quad \frac{11.817}{10^{12}}\frac{\text{ft}-\text{lb}}{\text{MeV}}$$

$$1.3558\frac{\text{J}}{\text{ft}-\text{lb}} \quad 251.98\frac{\text{cal}}{\text{Btu}} \quad 4.1868\frac{\text{kJ}}{\text{kcal}} \quad 3600\frac{\text{kJ}}{\text{kW}-\text{hr}} \quad 0.746\frac{\text{kW}}{\text{hp}}$$

$$1.055\frac{\text{kJ}}{\text{Btu}} \quad 101.92\frac{\text{kg}-\text{m}}{\text{kJ}} \quad 0.4300\frac{\text{Btu/pmole}}{\text{J/gmole}} \quad 860\frac{\text{cal}}{\text{W}-\text{hr}}$$

$$1.8\frac{\text{Btu}}{\text{chu}} \quad 3.969\ \frac{\text{Btu}}{\text{kcal}}$$

Entropy, Specific Heat, Gas Constant

$$1\frac{\text{Btu/pmole}-{}^{\circ}\text{R}}{\text{cal/gmole}-\text{K}} \quad 1\frac{\text{Btu/lb}-{}^{\circ}\text{R}}{\text{gal/cm}-\text{K}} \quad 1\frac{\text{Btu/lb}-{}^{\circ}\text{R}}{\text{kcal/kg}-\text{K}}$$

$$0.2389\frac{\text{Btu/pmole}-{}^{\circ}\text{R}}{\text{J/gmole}-\text{K}} \quad 4.187\frac{\text{kJ/kg}-\text{K}}{\text{Btu/lb}-{}^{\circ}\text{R}}$$

Universal Gas Constant

$$1545.32\frac{\text{ft}-\text{lb}}{\text{pmole}-{}^{\circ}\text{R}} \quad 8.3143\frac{\text{kJ}}{\text{kmole}-\text{K}}$$

$$0.7302\frac{\text{atm}-\text{ft}^3}{\text{pmole}-{}^{\circ}\text{R}} \quad 82.057\frac{\text{atm}-\text{cm}^3}{\text{gmole}-\text{K}}$$

$$1.9859\frac{\text{Btu}}{\text{pmole}-{}^{\circ}\text{R}} \quad 1.9859\frac{\text{cal}}{\text{gmole}-\text{K}}$$

$$10.731\frac{\text{psi}-\text{ft}^3}{\text{pmole}-{}^{\circ}\text{R}} \quad 83.143\frac{\text{bar}-\text{cm}^3}{\text{gmole}-\text{K}}$$

$$8.3143\frac{\text{J}}{\text{gmole}-\text{K}} \quad 8.3149\times 10^7\frac{\text{erg}}{\text{gmole}-\text{K}}$$

$$0.08206\frac{\text{atm}-\text{m}^3}{\text{kgmole}-\text{K}} \quad 0.083143\frac{\text{bar}-1}{\text{gmole}-\text{K}}$$

Newton's proportionality constant k (as a conversion unit)

$$32.174\,\text{fps}^2\left[\frac{\text{lb}}{\text{slug}}\right] \quad 386.1\,\text{ips}^2\left[\frac{\text{lb}}{\text{p sin}}\right]$$

$$9.80665\frac{\text{m}}{\text{s}^2}\left[\frac{\text{N}}{\text{kg}}\right] \quad 980.665\frac{\text{cm}}{\text{s}^2}\left[\frac{\text{dynes}}{\text{gm}}\right]$$

Miscellaneous Constants

Speed of light	Avogadro Constant	Planck Constant
$c = 2.9979 \times 10^{8} \frac{m}{s}$	$N_A = 6.02252 \times 10^{23} \frac{\text{molecules}}{\text{gmole}}$	$h = 6.6256 \times 10^{-34} J - s$
Boltzmann Constant	**Gravitational Constant**	**Normal mole volume**
$k = 1.38054 \times 10^{-23} \frac{J}{K}$	$G = 6.670 \times 10^{-11} \frac{N - m^2}{kg^2}$	$2.24136 \times 10^{-2} \frac{m^3}{\text{gmole}}$

Copyrighted Materials
Copyright © 2012 Elsevier Retrieved from www.knovel.com

INDEX

Index Terms **Links**

Page numbers with "*t*" denote tables; those with "*f*" denote figures.

A

A-286 alloy 507
ABB turbine 20*f* 21
Abrasives, for turbine cleaning 544 851
Absolute velocity 155 387
Absorption cooling systems 126 127*f*
Accelerated oxidation 501
Acceleration transducers 658
Accelerometers 87 247 248*f* 605 658 670 741 749 750
ACCPPs, *see* Advanced combined-cycle power plants
Acid number (AN) test 644
Adiabatic efficiency
  description of 279
  of axial-flow compressors 329 341
Adiabatic thermal efficiency 90 91*f* 93*f* 158
  Carnot cycle 97
  overall cycle work and 112
  regeneration effect 94 94*f*
  simple-cycle 99

This page has been reformatted by Knovel to provide easier navigation.

Index Terms	Links			
Advanced combined-cycle power plants (ACCPPs)				
efficiency of	5*f*			
heat rate of	5*f*			
Advanced gas turbines				
benefits of	821			
concerns regarding	822			
pressure ratios for	821	843		
redesign of, for reliability improvements	821			
Aeroderivative gas turbine	9	30	50*f*	180
benefits of	39			
Aerodynamic cross-coupling effect	242			
Aerodynamic theory	368			
Aerodynamic whirl	241	246*t*		
Aerospace engines	8	885		
Aerothermal				
analysis	733	734		
baseline	753			
condition monitoring	754*f*			
data	742			
Aerothermal equations				
continuity equation	153			
energy equation	156			
momentum equation	154			
Aerothermodynamics, turbomachinery				
compressibility effect	150			
dry- and wet-bulb temperatures				
dew point	144			
psychrometers	145			

This page has been reformatted by Knovel to provide easier navigation.

Index Terms	Links	
Aerothermodynamics, turbomachinery (*Cont.*)		
psychrometric chart	145	145*f*
RTDs vs thermocouples	148	
temperature measurement devices	146	
Eulerian motion	139	
ideal flow	139	
ideal gas	140	149
Lagrangian motion	139	
optical and radiation pyrometers	148	
Air atomization system	531	533*f*
Air bypass valves	469	
Air filtration	779	
Air inlet angle	308	
Air-cooling schemes	401	403*f*
Aircraft propulsion gas turbines	177	
Aircraft-derivative gas turbines	15	30
Airfoils		
description of	307	823
elementary theory of	309	
laminar-flow	311	312*f*
NACA 65 series of	325	326*f*
zero-camber	322*f*	
AIT, *see* Auto ignition temperatures		
Alarm/system logs	734	
Alloy 706 nickel-based alloy	505	
Alloy 718 nickel-based alloy	505	
Alloys	493	
A-286	507	
Cr	507	

This page has been reformatted by Knovel to provide easier navigation.

Index Terms	Links			
Alloys (*Cont.*)				
Cr–Mo–V	507			
high-temperature	504*t*			
Alstom GT24/26 gas turbine	25	33	34*f*	
Aluminum-alloy impellers	299			
AM recorder	659			
Ambient temperature	793			
American Gear Manufacturers Association (AGMA)	613			
American Petroleum Institute, mechanical specifications	812			
American Society of Mechanical Engineers				
flow nozzle	775	776*f*		
performance test codes				
description of	770			
list of	811*t*			
on overall plant performance	770			
on test uncertainty	770			
Amplitude factor	225*f*			
AN test, *see* Acid number test				
Analytical ferrography	645			
Angular misalignment	707			
Annular combustors	72	73*f*	429	858
ANSI/API Std 670 Vibration, Axial Position and Bearing-Temperature Monitoring Systems	195			
API Std 613 Special Purpose Gear Units for Petroleum, and Gas Industry Services	194			

This page has been reformatted by Knovel to provide easier navigation.

Index Terms	Links	
API Std 614 Lubrication, Shaft-Sealing and Control-Oil Systems and Auxiliaries for Petroleum Chemical, and Gas Industry Services	194	
API Std 616 Gas Turbines for the Petroleum, Chemical, and Gas Industry Services	194	
API Std 618, Reciprocating Compressors for Petroleum, Chemical, and Gas Industry Services	195	
API Std 619, Rotary-Type Positive Displacement Compressors for Petroleum, Chemical, and Gas Industry Services	195	
API Std 671, Special Purpose Couplings for Petroleum, Chemical, and Gas Industry Services	195	
API Std 677, General-Purpose Gear Units for Petroleum, Chemical, and Gas Industry Services	196	
Approach temperature	85	119
ASME B 133.2 Basic Gas Turbines	192	
ASME B 133.7M Gas Turbine Fuels	193	
ASME B133.3 Procurement Standard for Gas Turbine Auxiliary Equipment	192	
ASME B133.4 Gas Turbine Control and Protection Systems	192	

This page has been reformatted by Knovel to provide easier navigation.

Index Terms	Links		
ASME B133.5 Procurement Standard for Gas Turbine Electrical Equipment	193		
ASME B133.8 Gas Turbine Installation Sound Emissions	193		
ASME B133.9 Measurement of Exhaust Emissions from Stationary Gas Turbine Engines	193		
ASME Measurement of Exhaust Emissions from Stationary Gas Turbine Engines B133.9	190		
ASME PTC 19.11: Steam and Water Sampling, Conditioning, and Analysis in the Power Cycle	187		
ASME PTC 19.1: Test Uncertainty	185		
ASME PTC 19.23: Guidance Manual for Model Testing	188		
ASME PTC 19.3: Temperature Measurement Instruments and Apparatus	185		
ASME PTC 19.5: Flow Measurement	186		
ASME PTC 36 Measurement of Industrial Sound (ASME B133.8)	191		
ASME PTC 46: Performance Test Code on Overall Plant Performance	188		
Aspect ratio	344	354	848*t*
Atmospheric tanks, for liquid fuel storage	552		
Atomization air system	532	533*f*	
Auto ignition temperatures (AIT)	537		

This page has been reformatted by Knovel to provide easier navigation.

Index Terms	Links			
Auto-ignition	69	70	479	
classification of	70			
flashback, *see* Flashback				
Auxiliary system monitoring				
aerothermal baseline	753			
data trending	754			
fuel system	751			
mechanical baseline	752			
torque measurement	752			
Availability	815			
AVCO Lycoming's AGT-1500 gas turbine	49	49*f*		
Averaging	660			
Axial deflection	702	703*f*		
Axial proximity probes	879			
Axial velocity	315			
Axial-flow compressors	2	35	54	54*f*
	166	168*f*	891*f*	
accelerometers for detecting problems with	671			
adiabatic efficiency of	329			
airfoils in				
description of	307	823		
elementary theory of	309			
laminar-flow	11	312*f*		
aspect ratio of	344	354		
blades				
advancements in	344*f*			
coatings on	354			
description of	306			
hand scrubbing of	854			

This page has been reformatted by Knovel to provide easier navigation.

Index Terms	Links		
Axial-flow compressors (*Cont.*)			
materials used in	351	353*t*	
profile of	345	849*t*	
squealer sections on	823		
stall of	332	332*f*	
stators	305	305*f*	
with tip rub	343*f*	845	847*t*
transonic	350		
wear on	845		
cascades, tests of	345		
casing treatments	347	349*f*	
centrifugal compressors vs.	253		
characteristics of	304*t*		
choke of	331		
in cylindrical coordinate system	306		
degree of reaction in	315		
description of	307		
design point for	329		
deterioration of	895*f*		
deviation rule	323		
diffusion factor	320		
efficiencies of	313		
energy increase in	313		
enthalpy in	306	307*f*	
evaporative cooling	887		
exit guide vanes for	303		
failure mechanisms for	846*t*	849*t*	
first-stage rotor blade	886		
gas turbines	887		
high-pressure axial-flow turbine			

This page has been reformatted by Knovel to provide easier navigation.

Index Terms	Links			
Axial-flow compressors (*Cont.*)				
rotor	55	55*f*		
incidence rule	321			
inlet air fogging systems	887			
interstage cooling of	350			
losses in	340			
new developments in	342			
operation of	303	328		
performance				
blade condition and	845			
losses	340			
map of	330	757*f*		
parameters for	337			
radial equilibrium	319			
redesign of, for reliability improvements	822			
research of	344			
rotor	304	305*f*		
stages of				
asymmetrical	318			
description of	303			
symmetrical	317			
stall				
description of	332			
flutter	333	336*f*		
individual blade	332			
propagating	332	332*f*		
rotating	332	332*f*	334	335*t*
	847*t*			
tip	846*t*			

This page has been reformatted by Knovel to provide easier navigation.

Index Terms	Links		
Axial-flow compressors (*Cont.*)			
stators	305	305*f*	
surge of	328	846*t*	
technology changes in	824*t*		
trends for	889		
velocity			
diagram for	319		
triangles	313		
Axial-flow turbines	78	79*f*	383
first-stage nozzles	903		
fuel nozzles	903		
impulse turbine	78	394	
reaction turbine	79		
redesign of	826	828*t*	
second-stage nozzle vanes	904		
thermodynamic and aerodynamic theory			
absolute velocity	387		
axial-flow turbine	387		
degree of reaction	391		
Euler turbine equation	390		
fluid velocity	387		
Reynolds number	387		
utilization factor	391		
work factor	392		
turbine blade cooling concepts	401		
turbine geometry	385		
velocity diagrams	393		

B

Babbitt	572	819	

This page has been reformatted by Knovel to provide easier navigation.

Index Terms	Links			
Backward-curved vanes	256	257*f*	259	259*f*
	272	286		
Balancing				
component	686			
high-speed	679*f*	680		
modal	682			
multiplane	683	687		
one-plane	686			
orbital	681			
production-rotor	686			
rule of	680			
techniques, application of	686			
trim	687			
two-plane	686			
Barrel-type centrifugal compressor	296*f*			
Baseline signatures	672	671	672*f*	
BBC/Alstom GT 11N2 gas turbine	23	25	26*f*	
Bearing(s)				
clearance checks for	877			
design of	557	565		
failure of	818			
fluid-film lubrication for	565	566*f*		
functions of	557			
hydrodynamic mode	565			
journal				
circumferential grooved	563			
cylindrical bore	563			
description of	563			
design principles for	565			
elliptical	563			

This page has been reformatted by Knovel to provide easier navigation.

Index Terms	Links		
Bearing(s) (*Cont.*)			
fluid-film principles of	565		
half-frequency whirl	573		
inspection of	870		
instabilities in	573		
lemon bore	563		
load capacity for	569*f*		
maintenance of	870		
materials used in	572		
offset halves	563		
pressure dam	563	564*f*	
three-lobe	563		
tilting-pad	563	569	711
maintenance of	870		
pre-load	570		
radial ball			
illustration of	558*f*		
load rating of	562		
rolling			
cages of	561		
components of	559	560*f*	
cylindrical	560		
description of	557		
load ratings of	561		
rollers used in	560*f*		
rolling elements	558		
terminology for	559*f*		
types of	557	558*f*	
wear of	562		
“self-acting”	565		

This page has been reformatted by Knovel to provide easier navigation.

Index Terms	Links		
Bearing(s) (*Cont.*)			
sleeve	563		
surfaces of	568*f*		
thrust			
carrying capacity of	577		
changing of	818		
design of	577		
failure of	877		
function of	573	577	
plain washer	574	576*f*	
power loss	578	579*f*	
resistance temperature detectors for monitoring of	878		
tapered-land	574	576*f*	
temperature characteristics of	578*f*		
types of	574	577*f*	
"Bending critical speed"	229		
Blade(s)			
axial-flow compressors			
advancements in	344*f*		
coatings on	354		
description of	306		
hand scrubbing of	854		
materials used in	351		
profile of	345	849*t*	
squealer sections on	823		
stall of	332*f*		
with tip rub	343*f*	845	847*t*
transonic	350		
wear on	845		

This page has been reformatted by Knovel to provide easier navigation.

Index Terms	Links		
Blade(s) (*Cont.*)			
borescope inspection of	838	839*f*	
coatings	509		
compressor	507		
cooling diagrams	417*f*		
efficiency of	819		
failures	893*f*		
flutter	891		
fouling	847*t*		
geometry loss	423	423*f*	
high pressure turbine	839*f*	840	
impeller	256	257*f*	
IN-738	503		
inlet angle for	308		
loading	380		
nomenclature for	308*f*		
single-crystal	505		
stall of	332*f*		
stress levels	246		
tip rubs	845	847	911*f*
turbine			
description of	861		
failure of	861	867	
internal degradation of	867		
surface damage to	866		
used, rejuvenation of	866		
Borescope inspection	835		
Boundary-layer development, in centrifugal compressors	269	270*f*	
Bourdon tube gauges	771		

This page has been reformatted by Knovel to provide easier navigation.

Index Terms	Links			
Bowed turbine nozzle vanes	905*f*			
Boyle's gas law	146			
Brake-specific fuel combustion (BSFC)	44			
Brayton cycle	89	90*f*		
description of	784			
Brayton–Rankine cycle	12*f*	110	113*f*	176
Breakdown	807*f*			
Brittle fracture	497			
BSFC, *see* Brake-specific fuel combustion				
BTU meter	752			
Burnt first-stage turbine blades	904*f*			
C				
CAES, *see* Compressed air energy storage				
Cages, of rolling bearings	561			
Campbell diagram	244			
Can-annular combustors	23	72	429	452*f*
	858	897		
TBC with	900*f*			
Can-annular gas turbine combustion system	464*f*			
Cantilever-type radial-inflow turbines	362			
velocity triangles	363*f*			
Carbon monoxide	443	797	825	
Carbon residue	520			
Carnot cycle	97			
inter-cooled regenerative reheat cycle	105			
Carter's rule	323			
Cascade	307			
Casing accelerometers	292			
Casing force	234	235*t*		

This page has been reformatted by Knovel to provide easier navigation.

Index Terms	Links			
Casing(s)				
in axial-flow compressors	347			
in process centrifugal compressors	292	349*f*		
Catalyst surface temperatures	481			
Catalytic combustion	481			
features of	481			
Catalytic combustor, design of	483			
Catalytic converters	428	444		
Catalytic reactor	484			
Catastrophic corrosion	523			
Catastrophic oxidation	501			
CCGT, *see* Combined-cycle gas turbine				
CCPP, *see* Combined-cycle power plant				
CDA, *see* Controlled diffusion airfoil				
Centrifugal compressors, gas	43	45	48	55
	56*f*	744*f*		
axial-flow compressors vs.	253			
barrel-type	296*f*			
boundary-layer development in	269	270*f*		
casing types	292			
components of				
description of	254			
diffusers	274	275*f*		
double-entry inducer	256	257*f*		
entry-inducer systems	256	257*f*		
inducer	264			
inlet guide vanes	254	260		
scroll	275			
volute	275			
configuration of	295			

This page has been reformatted by Knovel to provide easier navigation.

Index Terms	Links	
Centrifugal compressors, gas (*Cont.*)		
description of	253	
flow in	268*f*	
forces in	268*f*	
high-pressure-ratio	274	
horizontally split	293	295*f*
industrial applications of	295	
leakage in	270	
losses in		
clearance	280	282*f*
description of	278	
diffusion-blading	280	
disc friction	280	281*f*
incidence	280	
recirculating	281	
rotor	279	
skin friction	281	
stator	281	
wake-mixing	282	
low-pressure	294	
map of	255*f*	
multistage	294	294*f*
operating principles of	253	
performance of		
description of	278	
losses in, *see* Centrifugal compressors losses in		
map	284	
pressure ratios of	253	
process	292	

This page has been reformatted by Knovel to provide easier navigation.

Index Terms	Links			
Centrifugal compressors, gas (*Cont.*)				
schematic diagram of	255*f*			
slip in, causes of	269			
Stanitz slip factor	273			
Stodola slip factor	272			
vaneless diffuser				
description of	287			
flow trajectory in	287*f*			
loss in	282			
stall of	285			
surge in	285			
vanes				
inlet guide	254	260		
number of	271			
thickness of	271			
Centrifugal force	693			
Centrifugal oil pump	632			
Centrifuging	640			
Ceramics	508			
Choke				
axial flow compressor, stone wall	331			
centrifugal compressor	284			
Circular arc camber lines	265			
Circumferential grooved bearings	563			
Clean oil systems	647	647*t*		
Clearance loss	280	282*f*	342	380
Clearance seals	585			
Clogged filter	761			
Clogged filters	846*t*			
Closed impeller	256*f*			

This page has been reformatted by Knovel to provide easier navigation.

Index Terms	Links
Closed-loop systems	722
CMS, *see* Condition monitoring systems	
Coalescer separators	640
Coalescing filters	541
Coatings	759
on axial-flow compressors blades	354
blade	509
developments of	511*f*
diffusion	512
duplex type	354
future of	513
plasma-sprayed	512
shroud	513
thermal barrier	83 512
types of	83 512
Cold alignment	712
Coloumb damping	218
Combined-cycle gas turbine (CCGT)	121
Combined-cycle plants	
overview of	114 115*f* 116*f* 117*f* 118*f* 123*f*
CAES	121
Combined-cycle power plant (CCPP)	726*f*
efficiency of	5*f*
heat rate of	5*f*
life cycle costs for	739*f*
Combustion analysis	733

This page has been reformatted by Knovel to provide easier navigation.

Index Terms	Links			
Combustion chamber				
linear metallic as	534			
positions of	858			
Combustion chamber liner, metallic tiles as	534			
Combustion instability	480			
Combustion liners	439			
Combustion process	441			
Combustion systems				
diffusion-type combustor	897			
dry low NO_x (DLN) combustors	901			
Combustor(s)	14	61	75*f*	77*f*
air pollution issues, unburnt hydrocarbons	797	799*f*		
analysis	761			
annular	72	73*f*	858	
arrangements of	72			
can-annular	23	72	858	
catalytic combustion and	481			
cross-sectional area	438			
description of	536	823		
diagnostics	761*t*			
diffusion flame	824			
diffusion type	63			
dry low emission nitrous oxide				
flashback	860*t*			
dynamic pressure transducers in	658			
external	73			
failure mechanisms for	859	860*t*		
fuel nozzles	539			

This page has been reformatted by Knovel to provide easier navigation.

Index Terms	Links		
Combustor(s) (*Cont.*)			
length	438		
liner	899*f*		
film cooling of	453		
fuel nozzles and	901*f*		
plates	898	901*f*	
liner plates	901*f*		
maintenance of	858		
monitoring of	825		
performance of	780		
potassium effects on	525*f*		
redesign of	826*t*		
reliability of	440		
side	72		
silo-type	23	72	74*f*
sodium effects on	525*f*		
vanadium effects on	525*f*		
Combustor-exit temperature	427		
Combustor-inlet temperature	427		
Commissioning time	769		
Component balancing	686		
Compressed air energy storage (CAES)	121		
Compressed air injection	124		
of humidified and heated	129	131*f*	133*f*
Compressor cleaning			
reasons for	850		
water washing			
abrasive cleaning	544	851	
fluids used in	856		

This page has been reformatted by Knovel to provide easier navigation.

Index Terms	Links		
Compressor cleaning (*Cont.*)			
off-line	853		
on-line	853		
solvent base agents for	856		
systems for	850		
water quality for	855	856*t*	
Compressor performance characteristics			
axial-flow compressor	166	168*f*	
efficiency islands	166		
gas turbine performance computation			
Brayton–Rankine cycle	176		
compressor and turbine efficiencies	172*f*		
gas turbine load	175	176*f*	
part-load turbine efficiencies	168		
turbine efficiency	174		
turbine inlet temperature	168	172*f*	
stone walling	166		
turbine performance characteristics	167		
typical compressor map	166	169*f*	
Compressor surge			
axial-flow compressors	328	846*t*	
blade stall	332		
compressor stall	331		
rotating stall	332	334	335
stall flutter	333		
surge margin	329		
vibration and	329	335	
boundary-layer prediction of	292	293*f*	
control system for	291*f*	291	292*f*
definition of	284		

This page has been reformatted by Knovel to provide easier navigation.

Index Terms	Links		
Compressor surge (*Cont.*)			
description of	283		
detection of	291		
dynamic surge detectors	291		
external causes of	290		
gas consumption effects	289		
impeller blades and	287		
initiation of	285		
internal causes of	290		
signs of	284		
static surge detectors	291		
Compressor(s)			
aerothermal characteristics	759		
analysis	760		
blades	507		
categories of	51		
characteristics of	52	53*f*	53*t*
choke	331		
diagnostics	761*t*		
discharge	748		
efficiency	53	785	
measurements	745	745*t*	
fouling	758	759	761
effects on	843		
inlet	748		
inspection of	844	845*f*	
losses	780		
maintenance of	843		
map	164	164*f*	
performance, testing of	779		

This page has been reformatted by Knovel to provide easier navigation.

Index Terms	Links	
Compressor(s) (*Cont.*)		
stall	331	
surge	759	
surging	761	
types of	52*f*	
Condition management	731	
Condition monitoring systems (CMS)	730	
borescope	837	
description of	828	
implementation of	735	
online optimization process	737	
plant power optimization	736	
Conservation of mass equation	784	
Contact-point shift	707	
Continuity equation	153	
Continuous oil-flow couplings	649	
Continuously lubricated couplings	699	
Control systems	137	
closed-loop systems	722	
combined cycle power plants	726	726*f*
DCS	722	723
feedback control loop	722	722*f*
feedforward control system	722	722*f*
flame detection system	725	
gas turbine	724	
negative control loop	722	
open-loop system position	721	
start-up sequence	728	
thermocouples	725	
TIT	725	

This page has been reformatted by Knovel to provide easier navigation.

Index Terms	Links		
Control systems (*Cont.*)			
vibration monitors	725		
Control-vortex pre-whirl	261		
Controllable losses	759	801	
Controlled diffusion airfoil (CDA) blading	26		
Convection cooling	405		
design	406		
Convection-cooled blade	409*f*		
Conventional equiaxed investment casting process	403		
Cooled turbine			
aerodynamics	412		
blade	416*f*		
Cooley-Tukey method	656		
Coriolis circulation	269	269*f*	
Correction factors	793		
Corrosion			
analysis	733		
catastrophic	523		
fuel-related	520		
hot	499	510	862*t*
probe	752		
sulfidation	499		
Counter-rotation	289		
Counteract vanadium	182		
Coupling(s)	605		
application of	706		
characteristics of	695		
continuous oil-flow	649		

This page has been reformatted by Knovel to provide easier navigation.

Index Terms	Links	
Coupling(s) (*Cont.*)		
continuously lubricated	699	
description of	693	
diaphragm	701	
fasteners	701	
flexible	693	
friction	707	
gear		
advantages of	696	
description of	695	
failure of	700	
fretting on gear teeth	700	
high-speed	697	698
lubrication problems with	698	
maintenance of	880	
thrust	878	
grease-packed	649	699
high-performance flexible	693	
keys	605	
lubrication of	648	
maintenance of	880	
mechanical-joint	693	
metal diaphragm	701	
metal disc	704	
oil-filled	649	698
resilient-material	693	
Cr–Mo–V alloy	507	
Crackle test	643	
Creep	496	
life experiments	416*t*	

This page has been reformatted by Knovel to provide easier navigation.

Index Terms	Links			
Critical shaft speed	224			
Critical speed				
calculations, for rotor bearing systems	230			
definition of	231			
map of	228			
Critically damped systems	220			
Cross-flow recuperator	58*f*			
Curtis turbine	395	396*f*		
Cycle analysis				
Brayton–Rankine cycle	110	113*f*		
evaporative regenerative cycle	109	109*f*	111*f*	
inter-cooled regenerative reheat cycle	106*f*			
inter-cooled simple cycle	96*f*	102	104*f*	
regenerative cycle	101	102*f*	103*f*	
reheat cycle	97*f*	103	105*f*	
simple-cycle	98	98*f*	99*f*	
split-shaft simple cycle	100	100*f*	101*f*	
steam injection cycle	105	107*f*	108*f*	109*f*
summation of	113	114*f*		
Cyclic bending stress	708			
Cyclic fatigue	498			
Cylindrical bore bearings	563			
Cylindrical coordinate system	306*f*			

D

Damped systems	
critically damped systems	220
description of	218
overdamped systems	220
underdamped systems	221

This page has been reformatted by Knovel to provide easier navigation.

Index Terms	Links			
Damping	218	657	681	705
Data inputs	741			
Data retrieval	767			
Data trending	754			
DCS, *see* Distributed control systems				
Deaeration	118	119		
Degassing drum arrangement	635	636*f*		
Degradation				
inspection for	840*t*			
nonrecoverable	841			
recoverable	841			
Degree of reaction	370	391		
in axial-flow compressors	315			
Demulsifier	524			
Depth filters	638			
Design point	376			
of axial-flow compressors	329			
Dew point	144			
Diagnostic analysis	735			
Diaphragm couplings	701			
Differential pressure class meters	186			
Differential pressure switch	533	639		
Differential thermal expansion	585			
Diffusers	274	275*f*		
Diffusion coatings	512			
Diffusion combustor				
air pollution problems in				
nitrogen oxides	443			
oxides of nitrogen	445			
smoke	443			

This page has been reformatted by Knovel to provide easier navigation.

Index Terms	Links			
Diffusion combustor (*Cont.*)				
design consideration	438			
simple straight-walled duct combustor	448	449*f*		
velocity	449			
Diffusion factor	320			
Diffusion flame combustors	824			
Diffusion loss	380			
Diffusion type combustor	63	65*f*	432	897
air distribution in	65*f*			
Diffusion blading loss	280			
Dilution	452			
Dimensional analysis	166			
compressor map	164	164*f*		
Reynolds number	166			
turbine map	164	165*f*		
turbomachines	163			
Direct inlet fogging method	124			
Directional solidification (DS)	82	403	503	
Disc couplings	697	704		
Disc friction loss	280	281*f*	341	422
Displacement probes	749			
Displacement transducers	657			
Distributed control systems (DCS)	722	723		
DLE, *see* Dry low emission				
Dodd bar system	717			
Domestic object damage (DOD)	886	897*f*		
Double gas seals	600	601*f*		
Double-entry inducer	256	257*f*		
Double-helical gearing	607			
Dresser-Rand KG2-3E gas turbine	43	44*f*		

This page has been reformatted by Knovel to provide easier navigation.

Index Terms	Links			
Driver shafts	706			
Dry gas seals				
degradation of	601			
description of	596			
double	600	601*f*		
materials for	601			
operating range of	600			
schematic diagram of	598*f*			
spiral groove pattern used in	597	598*f*		
systems	601			
tandem	599	600*f*		
Dry low NO_x (DLN)	108			
combustion system	23			
combustors	886	901		
Dry low emission (DLE)	108			
combustors	68*f*	72	455	460*f*
operation of	479			
problems with	69			
staging of	70*f*			
frame-type gas turbine with	68*f*			
injector	66	826		
Dry low emission nitrous oxide combustor				
description of	536	823		
flashback	860*t*			
monitoring of	825			
Dry low NOx (DLN)	108			
Dry scrubbers	541			
Dry-bulb temperature	144			
Dry-friction whirl	240	242*f*	246*t*	
DS, *see* Directional solidification				

This page has been reformatted by Knovel to provide easier navigation.

Index Terms	Links		
Ductile fracture	497		
Ductility	497		
Duplex type coating	354		
Dynamic fluid system	141	141*f*	
Dynamic pressure transducers	87	658	
Dynamic surge detectors	291		
Dynamic vibration data	733		
E			
Eddy probes	657		
Effective diagnostic system requirements of	732		
Effective forced outage hours	815		
Efficiencies			
adiabatic	279		
cleaning of compressor and	850		
factors that affect	786		
firing temperature and	10	11*f*	790*f*
maximization of	805		
of power plants	5*f*		
pressure ratio and	10	11*f*	
pressure ratio effects on	786		
Efficiency islands	166		
Elbow flow meters	775		
Electric Power Research Institute (EPRI)	730		
Electrical heaters, for fuel heating	542		
Electrical tracing	551	551*f*	
Electromagnetic flow meters	187		
Electron microscope	896*f*		

This page has been reformatted by Knovel to provide easier navigation.

Index Terms	Links	
Electrostatic separators	528	
Elemental analysis, oil	645	
Elevated tanks, for liquid fuel storage	552	
Elliptical arc	265	
Elliptical bearings	563	
Emissions		
carbon monoxide	797	825
measurement of	797	
nitrous oxide		
factors that affect	799	
dry control of	823	
wet control of	823	
smoke	798	
types of	797	
unburnt hydrocarbons	797	798*f*
End-wall losses	422	
Energy equation	156	784
Enthalpy		
changes in	787	
in axial-flow compressors	306	307*f*
multistage turbine	374*f*	
radial-inflow turbines	370*f*	
Entropy		
multistage turbine	374*f*	
radial-inflow turbines	370*f*	
Entry-inducer systems	256	257*f*
Environmental (EV) burner technology	27	
EPRI, *see* Electric Power Research Institute		
Equation of state	783	

This page has been reformatted by Knovel to provide easier navigation.

Index Terms	Links			
Equations				
energy	784			
Euler	258	260		
Euler turbine	314	317	339	
momentum	784			
performance computation	783			
Equivalence ratio	439			
Equivalent engine time				
in combustor section	762*f*			
in turbine section	763*f*			
Euler equation	258	260	397	399
Euler turbine equation	155	156	314	317
	339	368		
Eulerian motion	139			
Evacuation chamber	679*f*			
Evaporative and refrigerated inlet systems				
combination of	122	127	128*f*	
Evaporative cooling	887			
and steam injection, combination of	131	134*f*		
failure of	846*t*			
of turbine	125			
Evaporative methods	122			
Evaporative regenerative cycle	109	109*f*	111*f*	
Evaporators	85			
Excitations				
frequency of	662			
identification of	663	663*t*		
Exducer	367			
fatigue	378			
Exit guide vanes	303			

This page has been reformatted by Knovel to provide easier navigation.

Index Terms	Links	
Exit loss	283	381
Exit velocity diagrams for, radial-inflow turbine	377*f*	
Expander module	781	
Expander stage	136	
External combustors	73	
External thrust loads	606	
F		
Face-OD method, of cold alignment	713	
Failure		
axial-flow compressor	846	
bearings		
description of	819	
thrust	877	
combustor	859	860*t*
gear couplings	700	
lubrication as cause of	637	
thrust bearings	877	
Failure diagnostics		
combustor analysis	761	
compressor analysis	760	
turbine analysis	762	
turbine efficiency	764	
Fast Fourier transform (FFT)	751	
Feedback control loop	722	722*f*
Feedforward control system	722	722*f*
Ferrography, analytical	645	
Ferrous density	644	
FFT, *see* Fast Fourier transform		

This page has been reformatted by Knovel to provide easier navigation.

Index Terms	Links		
Film convection-cooled design	410*f*		
Film cooling	405		
design	406		
Film-cooled blade	409*f*		
Filter analysis	643		
Filtration, oil	633	638	
Finite element modeling	823		
Firing temperature			
calculation of	786	787	
description of	10	10*f*	
efficiencies and	790*f*		
efficiency and	10	11*f*	
life cycle and	769		
First law of thermodynamics	89	110	
First turbine stage, nozzle area of	136		
First-stage compressor			
blade	893	896*f*	
failure of	894*f*		
First-stage nozzle vanes	903*f*		
Five-stage power turbine, design of	21		
Fixed roof tanks, for liquid fuel storage	552		
Fixed seal rings	585		
Flame detection system	70	725	
Flame stabilization	450*f*	452	
Flame tubes	451		
Flash point	521		
Flashback	70	479	860*t*
Flexible supports	227*f*	228	
Floating roof tanks, for liquid fuel storage	552		

This page has been reformatted by Knovel to provide easier navigation.

Index Terms	Links			
Floating seal rings	585			
Flow conditioning	186			
Flow measurement	775	777*f*		
Flow nozzle	775	776*f*		
Flow straighteners	771	772*f*		
Fluid pressure	140			
Fluid velocity	387			
FM recorder	659			
Force(s)				
casing	234	235*t*		
foundation	234	235*t*		
on rotor bearing system	233			
rotor motion-generated	234	235*t*		
rotor-applied	236	236*t*		
Force-current analogy	232	234*f*		
Force-voltage system	233*f*			
Forced circulation system	85			
Forced vibrations				
characteristics of	237*t*			
description of	222	237		
stimuli	237			
with viscous damping	233*f*			
Forced-vortex pre-whirl	261			
Ford gas turbine	48*f*			
Ford turbine engine	49			
Foremen	810			
Forgings	508			
Forward-curved vanes	256	257*f*	259*f*	260
	287			

This page has been reformatted by Knovel to provide easier navigation.

Index Terms	Links		
Fouling			
blade	847*t*	850	
description of	520	531	
indicators of	851		
on-line washing to control	852		
turbine	861	862*t*	864*t*
Foundation forces	234	235*t*	
Foundations			
improper installation of	880		
mass and rigidity increases	882		
vibration problems caused by	880		
Fourier analyzer	652		
Fourier transform infrared (FTIR) spectroscopy	645		
Fourier transforms	652	654*f*	
Fracture	497		
Frame type heavy-duty gas turbines	15		
advantages of	18		
axial flow compressors in	17		
schematic diagram of	18		
Frame-type gas turbine	80*f*		
blade cooling in	79*f*		
Francis turbine	357	360*f*	
cross section of	359*f*		
Free-power gas turbine	35*f*		
Free-vortex pre-whirl	261		
Fretting	700	864*t*	
Friction damping	219		
Frictional flow losses	364		
Frictional loss	380		

This page has been reformatted by Knovel to provide easier navigation.

Index Terms	Links	
FT8 gas turbine	38	39*f*
FTIR, *see* Fourier transform infrared spectroscopy		
Fuel	59	
atomization	453	
availability of	520	
blended	515	
cleanliness of	520	
corrosion by	520	
deposition tendencies of	520	
fouling of	520	531
gaseous	515	
heating value of	61	518
heavy	531	
high-ash crudes and residuals	515	
liquid		
air atomization system	531	533*f*
ash content of	520	521*t*
characteristics of	522*t*	
description of	515	516*t*
flash point of	521	
handling of	523	
luminosity of	523	
pour point of	523	
properties of	521	522*t*
specific gravity of	523	
specifications of	520	521*t*
storage of	552	
tank storage of	552	
treatment of	523	

This page has been reformatted by Knovel to provide easier navigation.

Index Terms	Links	
Fuel (*Cont.*)		
vaporized fuel oil system	530	
viscosity of	523	
maintenance costs based on	546	547*t*
operating experience regarding	548	
overview of	515	
skid	724	
specifications for	519	
system	751	
turbine cleaning after using	543	
types of	180	516*t*
vaporized fuel oil system	530	
viscosity of	520	529*f*
Fuel blending	527	528*f*
Fuel economics	546	547*t*
Fuel gas		
auto ignition temperatures	537	
characteristics of	537	538*t*
conditioning of	541	
contaminants in		
construction debris	536	
liquids	536	
description of	517	
handling of	535	
heating value of	518	537
particulates in		
effects of	539	
equipment for removal of	540	
superheating of	537	539*t*
treatment of	535	

This page has been reformatted by Knovel to provide easier navigation.

Index Terms	Links	
Fuel gas (*Cont.*)		
vaporized fuel oil system	530	
Fuel heating	542	
Fuel nozzles	899*f*	903
combustors	539	
Fuel oil	526	
Fuel washing		
definition of	524	
inhibitors	529	
sludge from	527	531
systems for	528	530*t*
types of	525	
Fuel–bound nitrogen (FBN)	445	
Fuel/air ratio, effect of	66*f*	

G

Gage pressure	141	
Galvanic corrosion	502	
Gas		
compressor surge and	289	
fuel characteristic of	61	
heavy	289	
hydrogen-rich	289	
Gas generator	30	
Gas thermometer	146	
Gas turbine		
aerothermal performance equations	755*t*	
availability of	815	
axial-flow compressor, performance map of	757*f*	

This page has been reformatted by Knovel to provide easier navigation.

Index Terms	Links		
Gas turbine (*Cont.*)			
categories of	15		
combined-cycle mode	757		
combustion chambers	64	64*f*	
combustors	427		
annular combustors	429		
can-annular combustors	429		
silo-type	431		
commissioning time for	769		
components, compressors	51		
compressor			
aerothermal characteristics and surge	759		
fouling	758		
control	728		
loop	725		
correction factors for	793		
cycle, reheat	33*f*		
deterioration of	841		
efficiency of	303		
electrical power generation unit production	17*f*		
engine	743*f*		
environmental effects	62		
exhaust gases from	3		
firing temperature for	10	10*f*	
generation technologies of	3	4*t*	
heavy-duty	509		
limitations of	818		
losses, identification of	759		
materials	80	82*f*	503

This page has been reformatted by Knovel to provide easier navigation.

Index Terms	Links	
Gas turbine (*Cont.*)		
metallurgical behaviors in	496	
operational parameters	759	
performance of	6	
pressure ratio for	10	10*f*
refrigerated inlet for	125	
reliability of	815	
sales, distribution	16*f*	
start-up characteristics of	723*f*	
starting reliability of	816	
torque meter for	753*f*	
turbines used in	76	
walnut shells	758	
Gas turbine adiabatic thermal efficiency	158	
Gas turbine applications	177	
ASME PTC 22	190	190
enclosures of	183	
mechanical standards to	196	
size and efficiency	180	
start-up techniques of	184	
types of	177	
variables	177	
Gas turbine blade	404*f*	
Gas turbine cycle	159*f*	
in cogeneration mode	3	
in combined cycle mode	3	
Gas turbine design		
auxiliary systems	15	
availability	13	
considerations for	11	

This page has been reformatted by Knovel to provide easier navigation.

Index Terms	Links			
Gas turbine design (*Cont.*)				
criteria for	11			
environmental considerations	14			
firing temperature	10	10*f*		
lubrication systems	15			
pressure ratio	10	10*f*		
reliability	14			
serviceability	14			
Gas turbine gear drive	620*f*			
Gas turbine load	175	176*f*		
Gas turbine performance computation				
Brayton–Rankine cycle	176			
compressor and turbine efficiencies	172*f*			
gas turbine load	175	176*f*		
part-load turbine efficiencies	168			
thermocouples	174			
turbine efficiency	174			
turbine inlet temperature	168	172*f*		
Gas turbine power plant	157	158*f*		
Gas turbines	721	724	747	756
	885			
Gas-fired heaters, for fuel heating	543			
Gaseous fuel	472			
Gasifier turbine	41			
GE H gas turbine	19	19*f*		
GE industrial-type gas turbine	18*f*			
GE LM 6,000 engine	36*f*			
GE LMS 100 turbine	19	20*f*	21	22*f*
Gear	203			
advantages of	696			

This page has been reformatted by Knovel to provide easier navigation.

Index Terms	Links	
Gear (*Cont.*)		
description of	695	
design considerations		
accuracy	613	
bearings	614	
gear housings	615	
helix angle	611	
lubrication	615	
pressure angle	609	
scuffing	613	
service factor	614	
tooth hardness	612	
failures of	622	
high-speed	697	698
installation and initial operation of	620	
lubrication problems with	698	
manufacturing of	616	
types of	607	
Gear accuracy	613	
Gear couplings		
description of	695	
failure of	700	
fretting on gear teeth	700	
maintenance of	880	
thrust	878	
Gear failures	605	622
Gear housings	615	621
Gear noise	619	
Gear rating	619	

This page has been reformatted by Knovel to provide easier navigation.

Index Terms	Links			
Gear selection				
couplings	605			
external thrust loads	606			
operating conditions	606			
Gearbox	620			
signature spectra for	668*f*			
Gearboxes	646	647*t*		
Generator power output capacity	136			
Generator protective	730			
Graphic user interface (GUI)	734			
Grease-packed couplings	649	699		
Grinding process	618			
GT24/26 gas turbine	27	29		
GTD-111	503			
GUI, *see* Graphic user interface				

H

Half-frequency whirl	573			
Harmonic frequencies of spectrum	661	663	668	
Harmonic motion	216	217*f*		
Harmonic vibration	656			
Heat balance ratio	789			
Heat loss	381			
Heat rate				
controllable losses effect on	801*t*			
description of	793			
of power plants	5*f*			
Heat recovery steam generator (HRSG)	35	37*f*	83	84*f*
	116	117	118*f*	119
	121	183	921	

This page has been reformatted by Knovel to provide easier navigation.

Index Terms	Links	
Heat recovery steam generator (HRSG) (*Cont.*)		
approach temperature	85	
evaporators	85	
power augmentation system summation of	132	
Heat recovery steam generator systems (HRSG)	921	
Heat recovery systems	83	
supplemental firing of	85	87*f*
Heat tracing		
costs of	549	
electrical	551	551*f*
for insulated pipes	549	
how to avoid	549	
stream	550	550*f*
uses of	549	
Heating value	518	
Heavy fuels		
description of	531	
heat tracing of piping systems for	549	
Helix angle	611	611*f*
Helmholtz law	272	
Hero's turbine	357	
High cycle fatigue	864*t*	
High pressure turbine blades	839*f*	840
High-nickel alloy	502	
High-performance flexible couplings	693	
High-pressure burners for gas turbines	70	480
High-pressure compressor (HPC)	21	
High-pressure-ratio centrifugal compressor	274	

This page has been reformatted by Knovel to provide easier navigation.

Index Terms	Links		
High-speed balancing	679*f*	680	
High-speed couplings	607	697	698
Highpass filter	658		
Historical data management	735		
Hobbing process	616	617*f*	
Horizontally split centrifugal compressors	293	295*f*	
Hot alignment	715		
Hot corrosion	499	510	862*t*
Hot gas erosion oxidation	862*t*		
Hot section wash	544		
HPC, *see* High-pressure compressor			
HRSG, *see* Heat recovery steam generator			
Hub-to-shroud plane	377		
Humidity	796		
Hydraulic fracturing	59		
Hydrocarbon liquids	537		
Hydrocarbon radicals	448		
Hydrodynamic mode bearing	565		
Hydrogen-rich gases	289		
Hysteretic whirl	240	241*f*	246*t*

I

ICP, *see* Inductively coupled plasma spectroscopy			
Ideal gas	140	149	
Ideal isentropic process	372		
Ignition	453		
IGV, *see* Inlet guide vanes			
Impact torque	693		

This page has been reformatted by Knovel to provide easier navigation.

Index Terms	Links			
Impeller centrifugal				
backward-curved vanes	256	257*f*	259	259*f*
	272	286		
blading of	256	257*f*	264	
centrifugal section of	267			
closed	256*f*			
components of	262			
description of	248	248*f*		
Euler work distribution at exit of	263*f*			
fabrication of	298			
flow in	264			
forward-curved vanes	256	257*f*	259*f*	260
	287			
function of	262			
open-faced	257*f*			
radial vanes	256	257*f*	258*t*	259*f*
shrouded	298			
velocity profiles through	266*f*			
Impeller efficiency	365			
Impingement cooling	405			
Impulse diagram	394			
Impulse turbine	78	394		
IN-738 blades	503			
Incidence loss	280	342	381	
Incidence rule	321			
Inducer	264			
Inductively coupled plasma (ICP) spectroscopy	645			
Industrial turbines	405			

This page has been reformatted by Knovel to provide easier navigation.

Index Terms	Links			
Industrial-type gas turbines	9	15	39	40*f*
	42*f*			
description of	304			
pressure ratios in	304			
Influence coefficient method	683			
Injection pressure	136			
Inlet air fogging systems	887			
Inlet cooling	122			
evaporative and refrigerated inlet systems, combination of	127			
evaporative cooling of turbine	124	125*f*		
gas turbine, refrigerated inlet for	125			
thermal energy storage systems	131			
Inlet guide vanes (IGV)	116			
in axial-flow compressors	303			
in centrifugal compressors	260			
Inspection				
borescope	835			
compressor	844	845*f*		
degradation-based	840*t*			
description of	831			
journal bearings	870			
long-term service agreements for	833			
turbine	861	866		
Instabilities				
rotor bearing system	236			
self-excited, *see* Self-excited instabilities				
Instrument alarms	734			

This page has been reformatted by Knovel to provide easier navigation.

Index Terms	Links		
Instrumentation			
accuracy of	771*t*		
and controls	87		
pressure measurement	771		
temperature measurement	774		
Inter-cooled regenerative reheat cycle	105	106*f*	
Inter-cooled simple cycle	96*f*	102	104*f*
Interconnecting piping	631		
Intercooling and reheating effects	95	96*f*	97*f*
Inward-flow radial turbine	76	78	79*f*
Isentropic adiabatic process	142		
Isentropic efficiency	370	372	374
relationship between polytropic and	373*f*		
Isentropic flow	149	150	157
Isentropic process	89	142	
Isobaric process	89		
J			
Jet engine	178	178*f*	
Journal bearings			
babbitt	913		
circumferential grooved	563		
cylindrical bore	563		
description of	563		
design principles for	565		
elliptical	563		
fluid-film principles of	565		
half-frequency whirl	573		
inspection of	870		
instabilities in	573		

This page has been reformatted by Knovel to provide easier navigation.

Index Terms	Links		
Journal bearings (*Cont.*)			
lemon bore	563		
load capacity for	569*f*		
materials used in	572		
offset halves	563		
pressure dam	563	564*f*	
three-lobe	563		
tilting-pad	563	569	711
K			
Karl Fischer test	643	644	
Karman vortices	333		
Kawasaki gas turbines	43		
Keyphazor	681		
Kingsbury-type tilting-pad thrust bearings	916		
Kongsberg gas turbine	43		
Kronecker delta	684		
L			
Labyrinth seals			
advantages and disadvantages of	580		
description of	579		
dynamic applications of	580		
knife-edge arrangement	580	582*f*	
leakage of	579	582	
materials for	580		
staggered labyrinth	582		
static applications of	580		
straight labyrinth	580		

This page has been reformatted by Knovel to provide easier navigation.

Index Terms	Links			
Labyrinth seals (*Cont.*)				
tandem seal with	599	600*f*		
types of	580	581*f*		
Lagrangian motion	139			
Laminar-flow airfoils	311			
Lapping process	618	700		
Large power turbines	179			
Larson–Miller parameters	497	497*f*	505	759
Lead machinist	810			
Leading-edge lock-up	571			
Leak(s)				
in centrifugal compressors	270			
condensate	639			
labyrinth seal	579	582		
steam	639			
steam leaks in	639			
Lean–lean modes	468			
Lemon bore bearings	563			
Life cycle				
analysis	735			
characteristics of	806*f*			
costs	732	769		
aerothermal data	742			
for combined cycle power plants	739*f*			
compressors and turbines, temperature and pressure measurement for	745			
data inputs	741			
desirable instrumentation	742			
diagnostic system components and functions	741			

This page has been reformatted by Knovel to provide easier navigation.

Index Terms	Links	
Life cycle (*Cont.*)		
filter system, pressure drop in	745	
instrumentation requirements	741	
performance monitoring	740	
total performance condition monitoring systems	740	
typical instrumentation	742	
parameters that affect	782	
Liner holes	439	
Liner combustion chamber metallic tiles as	534	
Lip-guided cages	561	
Liquid fuel		
air atomization system	531	533*f*
ash content of	520	521*t*
characteristics of	522*t*	
description of	515	516*t*
flash point of	521	
handling of	523	
luminosity of	523	
pour point of	523	
properties of	521	522*t*
specific gravity of	523	
specifications of	520	521*t*
tank storage of	552	
treatment of	523	
viscosity of	523	
Ljungström turbine	357	
Load-distribution program	764	765*t*
Long-term service agreements (LTSA)	833	921

This page has been reformatted by Knovel to provide easier navigation.

Index Terms	Links		
Losses			
in axial-flow compressors	340		
in centrifugal compressors	278		
clearance	280	282*f*	
controllable	801		
description of	278		
diffusion-blading loss	280		
disc friction	280	281*f*	341
exit	283		
incidence	280		
performance based total productive maintenance system for	804		
recirculating	281		
rotor	279		
skin friction	281		
stator	281		
uncontrollable	800	801*t*	
wake-mixing	282		
Low-cycle fatigue (LCF)	505	864*t*	
Low-pressure centrifugal compressors	294		
Low-pressure compressor (LPC)	21		
Low-temperature hot corrosion	501		
Lower heating value	439		
LP fuel injector	67		
LPC, *see* Low-pressure compressor			
Lubricants, selection of	636		
Lubrication	615		
coupling	648		
failure	637	919	
gear couplings	698		

This page has been reformatted by Knovel to provide easier navigation.

Index Terms	Links	
Lubrication (*Cont.*)		
grease	699	
management program for	636	
scheduling of	636	
skid	724	
Lubrication systems	205	
design of	15	
oil reservoir	629	631*f*
oil systems, *see* Oil systems		
M		
Mach number	150	423
description of	260	
incidence angle affected by	322	
Machined cages	561	
Machinery		
breakdown of	807*f*	
condensate leaks in	639	
description of	629	
diagnosis	733	
foundations for		
improper installation of	880	
mass and rigidity increases	882	
vibration problems caused by	880	
life cycle of	806*f*	
uprates	705	
Machinist		
description of	811	
training of	813	
Magnesium sulfate	526	529

This page has been reformatted by Knovel to provide easier navigation.

Index Terms	Links	
Magnesium/vanadium ratio	529	
Magnetic bearings	382	
turbo expanders with	382*f*	
Magnetic seals	587	588*f*
Main fuel injector	484	
Maintenance		
bearing	870	
combustors	858	
communications regarding	829	
compressor	843	
costs	769	803
coupling	880	
definition of	803	
description of	841	
fuel effects on	546	546*t*
importance of	803	
inspection		
borescope	835	
degradation-based	840*t*	
description of	831	
long-term service agreements for	833	
performance based total productive maintenance system		
description of	804	
development of	808	
elements of	804	
equipment efficiency and effectiveness	805	
features of	804	
implementation of	808	

This page has been reformatted by Knovel to provide easier navigation.

Index Terms	Links			
Maintenance (*Cont.*)				
losses eliminated using	804			
organization structures for	807			
personnel training for	810			
shop equipment	814			
tools	814			
philosophy of	803			
rotor dynamic system	869	871	872*t*	874*t*
	876*t*			
scheduling of				
description of	827			
setup of	809			
total productive	803			
training materials	830			
turbines	861			
turnaround of	828			
Maintenance engineer	810			
Manometers	773			
Materials	493			
axial-flow compressor blades	351			
gas turbine	80	82*f*	503	
Mean tensile stress	708			
Mechanical analysis	733	734		
Mechanical baseline	752			
Mechanical contact shaft seal	588	590*f*		
Mechanical drive gas turbines	179	179		
Mechanical meters	187			
Mechanical parameters	191	192		
Mechanical problem diagnostics	765			
Mechanical refrigeration system	125	126*f*		

This page has been reformatted by Knovel to provide easier navigation.

Index Terms	Links	
Mechanical seals		
classification of	596*f*	
components of	586	
equipment considerations	593	
material to be sealed and	591	
oil system associated with	595	597*f*
product considerations	590	
seal arrangement considerations	593	
“seal balance”	587	588*f*
“seal body”	594	
seal environment and	592	
seal gland plate	593	
seal head unit	586	587*f*
seal seat	586	
seal-face combinations	593	
secondary packing	593	
selection of	589	
Mechanical-joint couplings	693	
Medium-sized gas turbines	179	
Memos	830	
Mercury thermometer, bimetallic element	146	
Meridional cross section, radial- and mixed-flow impellers	363*f*	
Meridional velocity distribution	379*f*	
Metal diaphragm couplings	701	
Metal disc couplings	704	
Metallurgical behaviors		
corrosion	499	
creep	496	
ductility	497	

This page has been reformatted by Knovel to provide easier navigation.

Index Terms	Links		
Metallurgical behaviors (*Cont.*)			
fatigue			
cyclic	498		
thermal	498		
fracture	497		
rupture	496		
Meter installation	186		
Microturbines	15	50	51
cogeneration system using	52*f*		
Millwright	811		
Mitsubishi's M501 J rotor gas turbine	32	32*f*	
Mitsubishis M501 G gas turbine	31*f*		
Mixed-flow radial-inflow turbine	363		
nomenclature	364*f*		
Mixed-flow turbine	77	78*f*	
Modal balancing	682		
Molded cages	561		
Momentum equation	154	368	784
Monitoring software	733		
Motion			
periodic	216		
rotor	234		
vibration-related	217		
Multi-nozzle combustors	428		
Multi-venturi tube (MVT)	484		
Multiplane balancing	683	687	
Multiple small-hole			
design	408	414*f*	
transpiration-cooled blade	413*f*		
Multipressure steam generators	84		

This page has been reformatted by Knovel to provide easier navigation.

Index Terms	Links	
Multistage turbine, enthalpy–entropy diagram for	374*f*	
N		
N-plane	685	
NACA 65 series	325	326*f*
Natural frequency	224	
Natural gas	59	
auto ignition temperatures	537	
characteristics of	537	538*t*
combustion of	64	
conditioning of	541	
consumption	60*f*	
contaminants in		
construction debris	536	
liquids	536	
description of	517	
handling of	542*f*	
heating value of	518	
particulates in		
effects of	539	
equipment for removal of	540	
superheating of	537	539*t*
vaporized fuel oil system	531	
Negative control loop	722	
Negative pre-swirl	289	
Neutral-strain axis	240	
Neutral-stress axis	240	
Nitriding	700	

This page has been reformatted by Knovel to provide easier navigation.

Index Terms	Links		
Nitrous oxide emissions	136		
reductions	63*f*		
dry control of	823		
wet control of	823		
Noise	380		
Non-destructive testing	508		
Nozzle vanes	414	418*f*	909*f*
failure of	862*t*		
repairing of	866		
Nozzle, combustors	539		

O

O&M, *see* Operating and maintenance			
Off-design performance	85		
Off-line optimization	738	738*t*	
Oil			
contamination of	637		
dirt in	878		
heating of	631		
rust and oxidation inhibitor	637		
sampling and testing of	641		
water contamination of	637		
Oil analysis tests	641		
Oil coolers	632		
Oil filters	634		
depth-type	638		
selection of	638		
surface-type	638		
Oil pressure switches	632		
Oil pump	632		

This page has been reformatted by Knovel to provide easier navigation.

Index Terms	Links			
Oil reservoir	629	631*f*	641	
Oil systems				
basic	629			
cleaning of	640	647	647*t*	
condensation in	639			
flushing of	640			
lubrication	629			
mechanical contact seal and	595	597*f*		
seal	634	635*f*		
Oil whirl	240	243*f*	246*t*	574*f*
	660			
Oil-filled couplings	49	698		
Oil-fired heaters, for fuel heating	543			
Oil-to-pressure-gas seal	588			
Oil-to-uncontaminated-seal-oil-drain seal	588			
On-line washing	545			
Once through steam generators (OTSG)	35	84	84*f*	
One-plane balancing	686			
Online condition monitoring system	737*f*			
Online optimization process	736			
Open tanks, for liquid fuel storage	552			
Open-faced impeller	257*f*			
Open-faced radial-inflow impeller	368*f*			
Open-loop system position	721			
Operating and maintenance (O&M)	730			
Operating conditions	606			
Operation manual	829			
Optical pyrometers	148			
Optimization analysis	735			

This page has been reformatted by Knovel to provide easier navigation.

Index Terms	Links	
Optimum pressure ratio	92	93*f*
regenerative cycle	102	
Orbital balancing	681	
Organic NO_x	445	
Oscillatory functions	652	
OTSG, *see* Once through steam generators		
Overdamped systems	220	
P		
Palladium oxide	483	
Part-load turbine efficiencies	168	
Particle counting tests	642	642*t*
Patch test	644	
Performance analysis	769	
Performance based total productive maintenance system		
description of	804	
development of	808	
elements of	804	
equipment efficiency and effectiveness	805	
features of	804	
implementation of	808	
losses eliminated using	804	
organization structures for	807	
personnel training for	810	
shop equipment	814	
tools	814	
Performance codes	770	

This page has been reformatted by Knovel to provide easier navigation.

Index Terms	Links	
Performance computations		
equations	783	785
overview of	782	
Performance curves	782	
Performance evaluation	738	
Performance maps	734	
of centrifugal compressors	284	
of axial-flow compressors	330	
of regenerative gas turbine cycle	13*f*	
of simple-cycle gas turbine	12*f*	
Performance monitoring	87	740
importance of	769	
Performance test(s)		
air inlet fillter module	778	
codes		
description of	770	
list of	811*t*	
on overall plant performance	770	
on test uncertainty	770	
combustor module	780	
compressor module	779	
computations used in	778	
description of	778	
emission measurements	797	
expander module	781	
measurement points for	778	779*f*
vibration measurements	796	
Performance, calculations	786	
Periodic loading	238	
Periodic motion	216	

This page has been reformatted by Knovel to provide easier navigation.

Index Terms	Links		
Personnel			
foremen	810		
lead machinist	810		
machinist	811		
maintenance engineer	810		
millwright	811		
Personnel training			
borescope	837		
description of	810	810	
machinist	813		
practical	813		
update	811		
Phase angles	217	226*f*	
Phase lag	676	677*f*	
Piloted premix modes	468		
Piloting zone	826		
Pinch point	85	119	
Piping strain	712		
Pitting	919		
Plant location	179		
Plant operation mode	184		
Plant power optimization	736		
Plasma-sprayed coatings	512		
Pocket guide	830		
Pollutants	62		
Polytropic compression process	96*f*		
Polytropic efficiency	161	372	373
Power augmentation system	122		
summation of	132	135*t*	
Power generation turbines	179		

This page has been reformatted by Knovel to provide easier navigation.

Index Terms	Links		
Power plants			
availability of	13		
complexes	732		
economic and operation characteristics of	7*t*		
heat rate of	5*f*		
reliability of	13	14	
Power turbine	48		
Pre-whirl			
control-vortex	261		
forced-vortex	261		
free-vortex	261		
Preburner	484		
Predictive test	646		
Premix modes	469		
Premix transfer modes	468		
Pressed cages	561		
Pressure angle	609		
Pressure dam bearings	563	564*f*	
Pressure drop	439	791	
Pressure gauges	634		
Pressure measurement	748		
instrumentation for	771		
Pressure ratio			
advanced gas turbines	821	843	
axial-flow compressor and	848*t*		
description of	10	10*f*	
development of	304	304*f*	
efficiency and	10	11*f*	785
pressure drop effects on	791		

This page has been reformatted by Knovel to provide easier navigation.

Index Terms	Links		
Pressure tanks, for liquid fuel storage	553		
Pressure transducers	748		
Pressure-sensing switch	634		
Primary modes	467		
Proactive test	646		
Probes			
accelerometers	658		
axial proximity	879		
dynamic pressure	658		
eddy	657		
velocity	657		
Process centrifugal compressors	292		
Process integration	736		
Production-rotor balancing	686		
Profile factor	438		
Prognostic alarms	734	735	
Propagating stall	332	332*f*	
Proximity probes	717		
Psychrometers	145		
Psychrometric chart	145	145*f*	
PTC 19.10: Flue and Exhaust Gas Analyses	187		
Pure tones	651		
Pusher-type seals	587	589*f*	
Pyrometers	87	148	747

R

Radial ball bearings	558*f*		
Radial equilibrium	319		
Radial roller bearings	558*f*		

This page has been reformatted by Knovel to provide easier navigation.

Index Terms	Links			
Radial turbine scallops, types of	365*f*			
Radial vanes	256	257*f*	258*t*	259*f*
Radial-flow turbine and compressor	51*f*			
Radial-inflow gas turbine	43*f*			
Radial-inflow impeller	366			
boundary-layer formation in	380*f*			
Radial-inflow turbines	76	357	358*f*	358
advantage	359	361		
applications	381			
characteristic	376*f*			
configurations	361			
deep scallops	366*f*			
design	374			
efficiency of	370			
enthalpy	371*f*			
entropy	371*f*			
for gas applications	358			
losses in	380			
N_s versus D_s diagram	362*f*			
noise problems in	379			
nomenclature	364*f*	370*f*		
numerical positions for components of	370*f*			
performance of	376			
rotor/impeller of	367			
shrouded	367*f*			
thermodynamic and aerodynamic theory	368			
two dimensional surfaces for flow analysis	378*f*			
velocity triangles for	375*f*			
Radiation pyrometers	148			

This page has been reformatted by Knovel to provide easier navigation.

Index Terms	Links			
Ratteau turbine	396	397*f*		
Raw material costs, comparison of	494*f*			
RB 211 gas turbine	36	37*f*		
Reaction turbine	79	398	399*f*	401
Real-time analyzers				
description of	652			
subsynchronous vibration analysis using	664			
Recirculating loss	281			
Recuperative gas turbine (RGT)	41*f*			
efficiency of	5*f*			
heat rate of	5*f*			
Recuperative heat exchanger	57	95		
Recuperators	13	57		
cross-flow	58*f*			
Reference velocity	438			
Refrigerated inlet cooling system	122			
Regeneration effect	92	93*f*	94*f*	
Regenerative cycle	101	102*f*	103*f*	
Regenerative gas turbine cycle, performance maps of	13*f*			
Regenerative heat exchanger	57	94		
Regenerators	13	47*f*	57	
advantages of	59			
disadvantage of	59			
Reheat cycle	97*f*	103	105*f*	
Reheat factor	374			
Reheat gas turbine cycle	33*f*			
Relative velocity	155			
distribution	379*f*			

This page has been reformatted by Knovel to provide easier navigation.

Index Terms	Links			
Reliability				
description of	815			
redesigns to improve				
advanced gas turbines	821			
axial-flow compressor	822			
axial-flow turbine	826	828*t*		
overview of	817			
Resilient-material couplings	693			
Resistance temperature detectors (RTDs)	147	148	878	
Resistive thermal detectors (RTDs)	747			
Resonant vibrations	237	237*t*		
Restrictive-ring seals	594	594*f*		
Reverse-dial indicator method, of cold alignment	713			
Reynolds number	149	166	361	387
description of	339			
on turbine stage efficiency	361*f*			
Rigid supports	226			
Ring seals				
cooling of	584			
description of	583			
fixed	585			
floating	585			
restrictive	583	584*f*		
Rolling bearings				
cages of	561			
components of	559	560*f*		
cylindrical	560			
description of	557			
load ratings of	561			

This page has been reformatted by Knovel to provide easier navigation.

Index Terms	Links			
Rolling bearings (*Cont.*)				
rollers used in	560*f*			
rolling elements	558			
terminology for	559*f*			
types of	557	558*f*		
wear of	562			
Rolls-Royce aero-derivative gas turbines	35			
Rotary generator	58*f*			
Rotary regenerator	57			
Rotating machines				
flexible supports	227*f*	228		
rigid supports	226			
Rotating shaft	230			
Rotating stall	332	332*f*	334	335*t*
Rotor				
assembly and disassembly of	814			
balanced	678*f*			
dynamic balancing of	676			
flexible	678			
high-speed balancing of	679*f*	680		
imbalance				
causes of	675			
correction of	675			
distribution of	677			
vibration measurements	796			
Rotor bearing system				
forces acting on	233			
instabilities of	236			
Routine oil analyses	646			

This page has been reformatted by Knovel to provide easier navigation.

Index Terms	Links	
RTDs, *see* Resistance temperature detectors		
Rumble	71	
Runner	357	
S		
Salt	545	852
SCGT, *see* Simple-cycle gas turbine		
Screening test	646	
Scroll	275	
Scuffing	613	
Seal oil system	634	635*f*
Seal systems		
buffered	594*f*	
description of	594	
restrictive-ring	594*f*	
Seal(s)		
bearing lubrication oil contamination	602	
clearance	585	
contamination of	602	
description of	578	
dry gas		
degradation of	601	
description of	596	
double	600	601*f*
materials for	601	
operating range of	600	
schematic diagram of	598*f*	
spiral groove pattern used in	597	598*f*
systems	601	

This page has been reformatted by Knovel to provide easier navigation.

Index Terms	Links	
Seal(s) (*Cont.*)		
gland plate	593	
labyrinth		
advantages and disadvantages of	580	
description of	579	
dynamic applications of	580	
knife-edge arrangement	580	582*f*
leakage of	579	582
materials for	580	
staggered labyrinth	582	
static applications of	580	
straight labyrinth	580	
tandem seal with	599	600*f*
types of	580	581*f*
windback	583	583*f*
magnetic	587	588*f*
mechanical		
classification of	596*f*	
components of	586	
equipment considerations	593	
material to be sealed and	591	
oil system associated with	595	597*f*
product considerations	590	
seal arrangement considerations	593	
“seal balance”	587	588*f*
“seal body”	594	
seal environment and	592	
seal gland plate	593	
seal head unit	586	587*f*
seal seat	586	

This page has been reformatted by Knovel to provide easier navigation.

Index Terms	Links		
Seal(s) (*Cont.*)			
seal-face combinations	593		
secondary packing	593		
selection of	589		
noncontacting	579		
oil pressure	589		
oil-to-pressure-gas seal	588		
oil-to-uncontaminated-seal-oil-drain	588		
process gas contamination of	602		
pusher-type	587	589*f*	
ring (bushing)			
cooling of	584		
description of	583		
fixed	585		
floating	585		
restrictive	583	584*f*	
seal gas supply contamination of	602		
Second-stage nozzle vanes	904		
Secondary loss	380		
Selective catalytic reactor	485		
“Self-acting” bearing	565		
Self-excited instabilities			
aerodynamic whirl	241	246*t*	
characteristics of	239*f*	239	246*t*
dry-friction whirl	240	242*f*	246*t*
hysteretic whirl	240	241*f*	246*t*
oil whirl	240	243*f*	246*t*
whirl from fluid trapped in the rotor	244	245*f*	
Service manual	829		
SEV burners	27		

This page has been reformatted by Knovel to provide easier navigation.

Index Terms	Links
Severity chart	749*f*
Shaft alignment	621
cold alignment	712
description of	710
hot alignment check	715
prealignment survey	711
procedure for	711
Shaving process	616
Shock, in rotor losses	279
Shop equipment, spare parts inventory for	814
Shroud coatings	513
Shrouded impeller	298
Shutdown, preparation for	832
Side combustors	72
Siemen's V94.2 gas turbine	27*f*
Siemen's V94.3 gas turbine, DLN annular combustor in	73*f*
Siemen's W501 G gas turbine	29 30f
Siemens combustors, fuel injector for	472*f*
Siemens W501 F gas turbine	23 29*f*
Siemens/KWU gas turbine	23 24*f*
Siemens V94.2 gas turbine	28*f*
Signal-to-noise ratio	
averaging effects on	660
description of	651
Silo-type combustors	23 72 74*f* 431 432*f* 477
Simple straight-walled duct combustor	448 449*f*

This page has been reformatted by Knovel to provide easier navigation.

Index Terms	Links		
Simple-cycle	98	98*f*	99*f*
gas turbine	95	96*f*	97*f*
split-shaft	100	100*f*	101*f*
Simple-cycle gas turbine (SCGT)			
classification of	15		
efficiency of	5*f*		
heat rate of	5*f*		
performance map of	12*f*		
Single-crystal alloys	83		
Single-crystal blades	404	505	
Single-entry inducer	256	257*f*	
Single-helical gearing	608		
Single-nozzle combustors	428		
Single-stage impulse turbine	395	395*f*	
Site configuration	179		
Skin friction loss	281	342	
Sleeve bearings	563		
Sliding friction coefficient	696		
Slip	269		
Sludge	699		
Small gas turbines	15	42	
Small standby power turbines	179		
Smoke	62	534	798
Sodium sulfate	501	510	
Solvent cleaning	545		
Sonic flow nozzles	187		
Spare parts inventory	814		
Spectrum analysis	651		
analyzers for	651		
Fourier transforms	652	654*f*	

This page has been reformatted by Knovel to provide easier navigation.

Index Terms	Links			
Spectrum analysis (*Cont.*)				
harmonic spectra	668			
signal-to-noise ratio	651			
spectra interpretation	660			
subsynchronous vibration analysis	664			
synchronous spectra	668			
taping data	659			
time-domain instant	660			
velocity transducers for	657			
vibration measurements				
acceleration transducers for	658			
displacement transducers for	657			
dynamic pressure transducers for	658			
overview of	656			
Split-shaft simple cycle	100	100*f*	101*f*	
Split-shaft turbines	789			
Staging ratio (SR)	475			
Stall				
description of	331			
flutter	333	336*f*		
individual blade	332			
propagating	332	332*f*		
rotating	332	334	335*t*	847*t*
tip	846*t*			
Standby pump	632			
Stanitz slip factor	273			
Start-up sequence				
gas turbine control	728			
generator protective	730			
shutdown	730			

This page has been reformatted by Knovel to provide easier navigation.

Index Terms	Links			
Start-up sequence (*Cont.*)				
start-up description	729			
Starting reliability	816			
Startup, guidelines for	819			
Static pressure	141	143*f*		
Static surge detectors	291			
Static temperature	144			
Stationary guide vanes	289			
Stationary signal	660			
Stator losses	281	342		
Steady-state oscillation	222			
Steam cooling	405			
Steam generators	84			
Steam injection	124	132	133*f*	387
	412			
cycle	105	107*f*	108*f*	109*f*
Steam tracing	550	550*f*		
Steam turbine (ST) plant				
efficiency of	5*f*			
heat rate of	5*f*			
Steam-cooled turbine blades	412			
Stodola slip factor	272			
Stoichiometric proportions	438			
Stokes flow	149			
Stone walling	166	284	331	
Straight-wall conical diffuser	275*f*			
Straight-wall rectangular diffuser	275*f*			
Strut insert				
blade	407*f*			
design	406	408*f*		

This page has been reformatted by Knovel to provide easier navigation.

Index Terms	Links		
Strut-supported porous shell	408		
Subcritical operation	225		
Subharmonic frequencies of spectrum	660		
Sulfidation corrosion	499		
Supercritical operation	225		
Superheating	537	539*t*	
Surface filters	638		
Surge control	136		
Surge margin	329		
Surge, compressor			
axial-flow compressors	331		
boundary-layer prediction of	292	293*f*	
control system for	291	291*f*	292*f*
definition of	284	328	
description of	283	328	
detection of	291		
dynamic surge detectors	291		
external causes of	290		
gas consumption effects	289		
impeller blades and	287		
initiation of	285		
internal causes of	290		
signs of	284		
static surge detectors	291		
vibration and	329		
Surging	328		
Swirler	66	67	
Symmetrical diagram	394		
Synchronous spectra	668		

This page has been reformatted by Knovel to provide easier navigation.

Index Terms	Links			
T				
Tandem dry gas seals	599	599*f*		
with labyrinth	599	600*f*		
Tandem inducers	265	268*f*		
Tapered-land thrust bearings	574	576*f*		
Teeth failures	919			
Temperature				
energy	86*f*			
firing				
calculation of	786	787		
life cycle and	769			
measurement	746			
instruments for	774			
transducer	746			
Temperature measurement				
devices	146			
Temperature-sensing switch	634			
Tertiary full-speed no load (FSNL) modes	469			
Thermal barrier coating (TBC)	25	72	83	487
	512			
Thermal energy storage systems	122	129*f*	131	
Thermal fatigue	498			
Thermal nitrous oxide	825			
Thermal NO_x	444			
Thermal reference speed	563			
Thermocouples	146	725	746	774
	747*f*			
Thermodynamic theory	368			
and aerodynamic theory				
absolute velocity	387			

This page has been reformatted by Knovel to provide easier navigation.

Index Terms	Links		
Thermodynamic theory (*Cont.*)			
axial-flow turbine	387		
degree of reaction	391		
Euler turbine equation	390		
fluid velocity	387		
Reynolds number	387		
utilization factor	391		
work factor	392		
Thermometers	634		
Thrust bearings	614		
carrying capacity of	577		
changing of	818		
design of	577		
failure of	877		
function of	573	577	
plain washer	574	576*f*	
power loss in	578	579*f*	
resistance temperature detectors for monitoring of	878		
schematic diagram of	558*f*		
tapered-land	574	576*f*	
temperature characteristics of	578*f*		
types of	574	577*f*	
Tilting pad bearings	381		
Tilting-pad journal bearings	563	569	711
Tilting-pad thrust bearing	915	916*f*	
Tip rubs	845	847*t*	
Tip shrouds	908*f*		
Tip stall	846*t*		
Tip-shrouded blocks/rings	420	421*f*	

This page has been reformatted by Knovel to provide easier navigation.

Index Terms	Links		
Tips-shrouded blades	420*f*		
TIT, *see* Turbine inlet temperature			
Titanium impellers	299		
Tools			
overview of	814		
spare parts inventory	814		
Tooth hardness	612		
Tooth-sliding velocity	697		
Torque			
description of	693		
measurement	752		
Torsional forces	706		
Tracer methods	187		
Transducers			
acceleration	658		
displacement	657		
dynamic pressure	658		
velocity	657		
Transfer-function analysis	664		
Transition piece	487	902	902*f*
Transonic blades	350		
Transpiration cooling	405		
design	408	412*f*	
Transpiration-cooled blade	411*f*		
Trim balancing	687		
Truck engines	45	46*t*	
Truck gas turbine, specification of	46*t*		
Turbine blade cooling			
concepts	401		
design			

This page has been reformatted by Knovel to provide easier navigation.

Index Terms	Links			
Turbine blade cooling (*Cont.*)				
convection and impingement				
cooling/strut insert design	406			
cooled-turbine aerodynamics	412			
film and convection cooling design	406			
multiple small-hole design	408			
steam-cooled turbine blades	412			
transpiration cooling design	408			
turbine losses	420			
water-cooled turbine blades	410			
Turbine car	47*f*			
Turbine inlet temperature (TIT)	168	172*f*	725	748
Turbine(s)				
analysis	762			
axial-flow	78	79*f*		
backpressure	759			
blades	416	494	911	
blades of				
failure of	861	866		
internal degradation of	867			
surface damage to	866			
used, rejuvenation of	866			
bucket material’s temperature	495			
car	47*f*			
casing	912*f*			
cleaning of	543	546		
efficiency	74	417*f*	764	
exhaust	748			
temperature	767			
firing temperature	136			

This page has been reformatted by Knovel to provide easier navigation.

Index Terms	Links			
Turbine(s) (*Cont.*)				
flow meters	775			
fouling of	762	861	862*t*	
geometry	385			
inspection of	866			
inward-flow radial	76	78	79*f*	
losses	420			
maintenance of	763	861		
map	164	165*f*		
mixed-flow	77	78*f*		
oil	615			
performance characteristics	167			
performance map	425*f*			
radial-inflow	76			
rotor shaft	906*f*			
salt collection in	545			
velocity triangles	393*f*			
wheel alloys	505	506*f*		
Turbo expanders	382*f*			
applications of	382	383		
Turbo-compressors	54			
Turbochargers	381			
cross section of	381*f*			
Turbomachines	139	163	493	732
aerothermodynamics of				
compressibility effect	150			
dry- and wet-bulb temperatures	144			
Eulerian motion	139			
ideal flow	139			
ideal gas	140	149		

This page has been reformatted by Knovel to provide easier navigation.

Index Terms	Links	
Turbomachines (*Cont.*)		
Lagrangian motion	139	
optical and radiation pyrometers	148	
condensate leaks in	639	
description of	629	
efficiencies	57	
adiabatic thermal efficiency	158	
gas turbine power plant	157	
gasturbine power plant	158*f*	158
polytropic efficiency	161	
foundations for		
improper installation of	880	
mass and rigidity increases	882	
vibration problems caused by	880	
gears	613	
steam leaks in	639	
uprates	705	
Turboprop engine	178	179*f*
Twin oil coolers	632	
Two-plane balancing	686	
Two-stage intermediate-pressure turbine		
design of	21	
Two-stage power turbine	38*f*	
Typical compressor map	166	169*f*
Typical performance map	759	760*f*
U		
Ultrasonic flow meters	187	
Unbalance	224	
sensitivity factors	688	

This page has been reformatted by Knovel to provide easier navigation.

Index Terms	Links			
Unburnt hydrocarbons	443	797	798*f*	
Uncontrollable losses	759	800	801*t*	
Underdamped systems	221			
US Main Battle tank	49			
Utilization factor	391	396	398*f*	399
	400*f*			
V				
Value range alarms	734			
Vanadium	515	525*f*	528	
Vane cooling diagrams	417*f*			
Vaned diffuser				
loss caused by	283			
schematic diagram of	288*f*			
vanes used in	288			
Vaneless diffuser				
description of	287			
flow trajectory in	287*f*			
loss in	282			
stall of	285			
surge in	285			
Vaneless nozzle configurations	364			
Vaporized fuel oil system (VFO)	530			
Vehicular gas turbines	16	44		
Velocity diagrams	393	394*f*		
Velocity pressure	773			
Velocity sensors	750			
Velocity transducers	657			

This page has been reformatted by Knovel to provide easier navigation.

Index Terms	Links		
Velocity triangles			
in axial-flow compressors	313		
in centrifugal compressor	259*f*	260	272*f*
Velocity vectors	154	154*f*	
Vent valves	534		
Venturi tubes	775		
VFO, *see* Vaporized fuel oil system			
Vibration			
signal	869		
Vibration measurements	206		
Vibration systems			
classification of	215		
damped			
critically damped systems	220		
description of	218		
overdamped systems	220		
underdamped systems	221		
degree of freedom	215	216*f*	218*f*
free			
description of	215		
undamped	217		
Vibration(s)			
acceptable limits for	797*t*		
amplitude	675		
analysis	733		
baseline	752		
compressor surge and	329		
data	750		
diagnosis of	663*t*	765	766*t*
forced	222		

This page has been reformatted by Knovel to provide easier navigation.

Index Terms	Links	
Vibration(s) (*Cont.*)		
instrumentation selection	750	
measurement of	748	
acceleration transducers for	658	
displacement transducers for	657	
dynamic pressure transducers for	658	
overview of	656	
rotor dynamics	796	
subsynchronous analysis of	664	
velocity transducers for	657	
monitors	725	
motion caused by	216	
nomograph	749*f*	
protection	725	
resonant	237	237*t*
signal	869	
spectra	893	895*f*
theory	215	
Viscosity	149	
blending	527	529*f*
oil analysis test	643	
Viscous damping		
description of	218	
forced vibration with	233*f*	
Volumetric heat-release rate	439	
Volute	275	

W

Wake-mixing loss	282	342
Walnut shells	758	

This page has been reformatted by Knovel to provide easier navigation.

Index Terms	Links		
Washable fuel	524		
Waste-heat recovery system	83		
back pressure considerations	85		
Waste-heat-fired heaters, for fuel heating	543		
Water (crackle) test	643		
Water contamination, of oil system	637		
Water cooling	405		
Water injection	113	124	132*f*
mid-compressor flashing of	128		
Water nozzles	888*f*		
inlet spray from	889*f*		
Water test (Karl Fischer method)	644		
Water washing of compressor			
abrasive cleaning	544	851	
description of	780		
fluids used in	856		
off-line	853		
on-line	853		
solvent base agents for	856		
systems for	850		
water quality for	855	856*t*	
Water-cooled turbine blades	410	415*f*	
Water-detecting device	752		
Wave analyzer	652		
Westinghouse gas turbines	23		
Wet-bulb temperature	144		
Whirl	239		
aerodynamic	241	246*t*	
dry-friction	240	242*f*	246*t*
from fluid trapped in the rotor	244	245*f*	

This page has been reformatted by Knovel to provide easier navigation.

Index Terms	Links			
Whirl (*Cont.*)				
half-frequency	573			
hysteretic	240	241*f*	246*t*	
oil	240	243*f*	246*t*	574*f*
	660			
velocity				
ratio of	375			
Whirling	239			
Whittle gas turbine	6	9*f*		
Windback seal	583	583*f*		
Wobbe index (WI)	61			
Wobbe number	61	62	439	
Work factor	392			

Z

Zeldovich mechanism	447			
Zero axial displacement	702			
Zero-camber airfoils	322*f*			
Zero-exit swirl diagram	393			

This page has been reformatted by Knovel to provide easier navigation.

Mechanical Engineering / Turbomachinery

GAS TURBINE ENGINEERING HANDBOOK

FOURTH EDITION

MEHERWAN P. BOYCE

The most widely-used and comprehensive reference available for those working with gas turbines

- A one-stop resource for industrial gas turbine engineers, including vital background theory, maintenance information, legislative details and day-to-day calculations
- Includes hard-won information from industry experts in the form of case studies that offer practical trouble-shooting guidance and solutions
- Suitable for use as a training companion or a reliable dip-in reference for experienced engineers

Written by one of the field's most well-known experts, the ***Gas Turbine Engineering Handbook*** has long been the standard for engineers involved in the design, selection, maintenance and operation of gas turbines. With far reaching, comprehensive coverage across a range of topics from design specifications to maintenance troubleshooting, this new edition has been fully updated with new legislation and emerging topics to ensure it remains the most widely referenced resource in the field.

With its all-in-one approach, the book covers not only the underlying principles of gas turbine operation, but also the economic considerations and implications of operating these machines. It provides newcomers to the industry with all the essentials in one place to help them learn and fill knowledge gaps, and gives established practicing gas turbine engineers a reliable and comprehensive go-to reference.

Also available from Butterworth-Heinemann

Soares – *Gas Turbines: A Handbook of Air, Land and Sea Applications*
ISBN: 9780750679695

Woodyard – *Pounder's Marine Diesel Engines and Gas Turbines, 9th edition*
ISBN: 9780750689847

Childs – *Rotating Flow* – ISBN: 9780123820983

ELSEVIER

Butterworth-Heinemann
An imprint of Elsevier
elsevierdirect.com

ISBN: 978-0-12-383842-1
90000
9 780123 838421